



NUREG/KM-0017

# **Seismic Hazard Evaluations for U.S. Nuclear Power Plants: Near-Term Task Force Recommendation 2.1 Results**

Office of Nuclear Reactor Regulation

## AVAILABILITY OF REFERENCE MATERIALS IN NRC PUBLICATIONS

### NRC Reference Material

As of November 1999, you may electronically access NUREG-series publications and other NRC records at the NRC's Library at [www.nrc.gov/reading-rm.html](http://www.nrc.gov/reading-rm.html). Publicly released records include, to name a few, NUREG-series publications; *Federal Register* notices; applicant, licensee, and vendor documents and correspondence; NRC correspondence and internal memoranda; bulletins and information notices; inspection and investigative reports; licensee event reports; and Commission papers and their attachments.

NRC publications in the NUREG series, NRC regulations, and Title 10, "Energy," in the *Code of Federal Regulations* may also be purchased from one of these two sources:

#### 1. The Superintendent of Documents

U.S. Government Publishing Office  
Washington, DC 20402-0001  
Internet: [www.bookstore.gpo.gov](http://www.bookstore.gpo.gov)  
Telephone: (202) 512-1800  
Fax: (202) 512-2104

#### 2. The National Technical Information Service

5301 Shawnee Road  
Alexandria, VA 22312-0002  
Internet: [www.ntis.gov](http://www.ntis.gov)  
1-800-553-6847 or, locally, (703) 605-6000

A single copy of each NRC draft report for comment is available free, to the extent of supply, upon written request as follows:

Address: **U.S. Nuclear Regulatory Commission**  
Office of Administration  
Digital Communications and Administrative  
Services Branch  
Washington, DC 20555-0001  
E-mail: [distribution.resource@nrc.gov](mailto:distribution.resource@nrc.gov)  
Facsimile: (301) 415-2289

Some publications in the NUREG series that are posted at the NRC's Web site address [www.nrc.gov/reading-rm/doc-collections/nuregs](http://www.nrc.gov/reading-rm/doc-collections/nuregs) are updated periodically and may differ from the last printed version. Although references to material found on a Web site bear the date the material was accessed, the material available on the date cited may subsequently be removed from the site.

### Non-NRC Reference Material

Documents available from public and special technical libraries include all open literature items, such as books, journal articles, transactions, *Federal Register* notices, Federal and State legislation, and congressional reports. Such documents as theses, dissertations, foreign reports and translations, and non-NRC conference proceedings may be purchased from their sponsoring organization.

Copies of industry codes and standards used in a substantive manner in the NRC regulatory process are maintained at—

#### The NRC Technical Library

Two White Flint North  
11545 Rockville Pike  
Rockville, MD 20852-2738

These standards are available in the library for reference use by the public. Codes and standards are usually copyrighted and may be purchased from the originating organization or, if they are American National Standards, from—

#### American National Standards Institute

11 West 42nd Street  
New York, NY 10036-8002  
Internet: [www.ansi.org](http://www.ansi.org)  
(212) 642-4900

Legally binding regulatory requirements are stated only in laws; NRC regulations; licenses, including technical specifications; or orders, not in NUREG-series publications. The views expressed in contractor prepared publications in this series are not necessarily those of the NRC.

The NUREG series comprises (1) technical and administrative reports and books prepared by the staff (NUREG-XXXX) or agency contractors (NUREG/CR-XXXX), (2) proceedings of conferences (NUREG/CP-XXXX), (3) reports resulting from international agreements (NUREG/IA-XXXX), (4) brochures (NUREG/BR-XXXX), and (5) compilations of legal decisions and orders of the Commission and the Atomic and Safety Licensing Boards and of Directors' decisions under Section 2.206 of the NRC's regulations (NUREG-0750).

**DISCLAIMER:** This report was prepared as an account of work sponsored by an agency of the U.S. Government. Neither the U.S. Government nor any agency thereof, nor any employee, makes any warranty, expressed or implied, or assumes any legal liability or responsibility for any third party's use, or the results of such use, of any information, apparatus, product, or process disclosed in this publication, or represents that its use by such third party would not infringe privately owned rights.

# **Seismic Hazard Evaluations for U.S. Nuclear Power Plants: Near-Term Task Force Recommendation 2.1 Results**

**Manuscript Completed: June 2021  
Manuscript Published: December 2021**

**Prepared by:**

**Cliff Munson  
Jon Ake  
John Stamatakos  
Miriam Juckett**



## ABSTRACT

This document represents the current best knowledge and practices for characterizing the site-specific seismic hazards for each nuclear power plant (NPP) in the United States. The U.S. Nuclear Regulatory Commission (NRC) staff will use the hazard characterizations provided in this NUREG/KM as a benchmark to evaluate new data, models, and methods consistent with the staff's process for ongoing assessment of natural hazard information provided in Staff Requirements Memorandum (SRM)-SECY-16-0144, "Staff Requirements—SECY-16-0144—Proposed Resolution of Remaining Tier 2 and 3 Recommendations Resulting from the Fukushima Dai-ichi Accident," dated May 3, 2017 (NRC, 2017). This document builds on the hazard assessments performed by the U.S. NPP licensees in response to the letter issued by the NRC under Title 10 of the *Code of Federal Regulations* (10 CFR) 50.54(f) [50.54(f) letter] and associated information requests (NRC, 2012) following the March 11, 2011, Great East Japan Earthquake and tsunami and resulting accident at the Fukushima Dai-ichi NPP.

The seismic hazard evaluations performed by U.S. NPP licensees used Senior Seismic Hazard Analysis Committee (SSHAC) Level 3 seismic source and ground motion studies to develop probabilistic seismic hazard curves and ground motion response spectra for comparison with the plant design Safe Shutdown Earthquake Ground Motion (SSE). These SSHAC Level 3 studies incorporated the latest data, models, and methods that have been developed over the past 30 to 40 years and also systematically incorporated parametric and modeling uncertainty. As described in the 50.54(f) letter and Electric Power Research Institute (EPRI) Report 1025287, "Seismic Evaluation Guidance: Screening, Prioritization, and Implementation Details (SPID) for the Resolution of Fukushima NTF Recommendation 2.1: Seismic," dated November 27, 2012 (EPRI, 2012), the ground motion response spectra (GMRS) developed by each of the licensees was compared to the plant SSE to determine (screen) which plants needed to perform new seismic risk evaluations. Section 1 of this NUREG/KM presents the ADAMS accession numbers for the NRC staff assessments of the Seismic Hazard and Screening Reports (SHSRs) for all operating U.S. NPPs and holders of construction permits in active or deferred status. Although the individual plant screening assessments are complete for the relevant NPP sites, the NRC staff was able to gather additional geologic data subsequent to its reviews of the licensees' 50.54(f) SHSRs. The NRC staff used this additional information to refine and augment its analyses and provide a more representative characterization of the hazard for many of the NPP sites. However, it is important to note that the results contained within this report did not invalidate or change the conclusions documented in the NRC's staff assessment for each NPP or the subsequent screening determinations made by the NRC staff.

In summary, this NUREG/KM presents a seismic hazard characterization for each U.S. NPP and compares the licensee's hazard characterization and the NRC staff's confirmatory analyses. This document also provides a comprehensive description of the probabilistic methods used by the U.S. NPP licensees and the NRC staff and summarizes spectral shapes and amplification functions for each NPP site.



# TABLE OF CONTENTS

<b>ABSTRACT</b>		<b>iii</b>
<b>LIST OF FIGURES</b>		<b>xiii</b>
<b>LIST OF TABLES</b>		<b>xliv</b>
<b>EXECUTIVE SUMMARY</b>		<b>xlix</b>
<b>ACKNOWLEDGMENTS</b>		<b>li</b>
<b>ABBREVIATIONS AND ACRONYMS</b>		<b>liii</b>
<b>1</b>	<b>INTRODUCTION</b>	<b>1-1</b>
1.1	Seismic Hazard Reevaluations Under Generic Issue-199	1-1
1.2	Post-Fukushima Near-Term Task Force Recommendation 2.1, the 50.54(f) Letter, and Subsequent Actions	1-2
1.3	Purpose and Overview of This Report	1-5
1.4	References	1-7
<b>2</b>	<b>CENTRAL AND EASTERN UNITED STATES SITES</b>	<b>2-1</b>
2.1	CEUS Seismic Hazard Methodology	2-1
2.1.1	Background	2-1
2.1.2	Seismic Source Characterization Model	2-2
2.1.3	Ground Motion Model	2-4
2.1.4	Site Response Evaluation	2-6
2.1.4.1	Input Motions	2-7
2.1.4.2	Site Profile Development	2-8
2.1.4.3	Site Kappa	2-10
2.1.4.4	Nonlinear Dynamic Properties	2-13
2.1.4.5	Analysis Methodology	2-13
2.1.5	Hazard Calculations	2-15
2.2	Region I Sites	2-17
2.2.1	Beaver Valley	2-19
2.2.1.1	Reference Rock Hazard	2-19
2.2.1.2	Site Response Evaluation	2-19
2.2.1.3	Control Point Hazard Results	2-21
2.2.2	Calvert Cliffs	2-26
2.2.2.1	Reference Rock Hazard	2-26
2.2.2.2	Site Response Evaluation	2-26
2.2.2.3	Control Point Hazard	2-28
2.2.3	Ginna	2-33
2.2.3.1	Reference Rock Hazard	2-33
2.2.3.2	Site Response Evaluation	2-33
2.2.3.3	Control Point Hazard	2-35
2.2.4	Hope Creek and Salem	2-40
2.2.4.1	Reference Rock Hazard	2-40
2.2.4.2	Site Response Evaluation	2-40
2.2.4.3	Control Point Hazard	2-42
2.2.5	Indian Point	2-48

	2.2.5.1	Reference Rock Hazard .....	2-48
	2.2.5.2	Site Response Evaluation .....	2-48
	2.2.5.3	Control Point Hazard .....	2-50
2.2.6		FitzPatrick and Nine Mile Point .....	2-55
	2.2.6.1	Reference Rock Hazard .....	2-55
	2.2.6.2	Site Response Evaluation .....	2-55
	2.2.6.3	Control Point Hazard .....	2-57
2.2.7		Limerick .....	2-63
	2.2.7.1	Reference Rock Hazard .....	2-63
	2.2.7.2	Site Response Evaluation .....	2-63
	2.2.7.3	Control Point Hazard .....	2-65
2.2.8		Millstone .....	2-71
	2.2.8.1	Reference Rock Hazard .....	2-71
	2.2.8.2	Site Response Evaluation .....	2-71
	2.2.8.3	Control Point Hazard .....	2-73
2.2.9		Oyster Creek .....	2-78
	2.2.9.1	Reference Rock Hazard .....	2-78
	2.2.9.2	Site Response Evaluation .....	2-78
	2.2.9.3	Control Point Hazard .....	2-80
2.2.10		Peach Bottom .....	2-86
	2.2.10.1	Reference Rock Hazard .....	2-86
	2.2.10.2	Site Response Evaluation .....	2-86
	2.2.10.3	Control Point Hazard .....	2-88
2.2.11		Pilgrim .....	2-93
	2.2.11.1	Reference Rock Hazard .....	2-93
	2.2.11.2	Site Response Evaluation .....	2-93
	2.2.11.3	Control Point Hazard .....	2-94
2.2.12		Seabrook .....	2-100
	2.2.12.1	Reference Rock Hazard .....	2-100
	2.2.12.2	Site Response Evaluation .....	2-100
	2.2.12.3	Control Point Hazard .....	2-100
2.2.13		Susquehanna .....	2-104
	2.2.13.1	Reference Rock Hazard .....	2-104
	2.2.13.2	Site Response Evaluation .....	2-104
	2.2.13.3	Control Point Hazard .....	2-106
2.2.14		Three Mile Island .....	2-111
	2.2.14.1	Reference Rock Hazard .....	2-111
	2.2.14.2	Site Response Evaluation .....	2-111
	2.2.14.3	Control Point Hazard .....	2-113
2.3		Region II Sites .....	2-118
	2.3.1	Bellefonte .....	2-121
		2.3.1.1 Reference Rock Hazard .....	2-121
		2.3.1.2 Site Response Evaluation .....	2-121
		2.3.1.3 Control Point Hazard .....	2-123
	2.3.2	Browns Ferry .....	2-128
		2.3.2.1 Reference Rock Hazard .....	2-128
		2.3.2.2 Site Response Evaluation .....	2-128
		2.3.2.3 Control Point Hazard .....	2-130
	2.3.3	Brunswick .....	2-136
		2.3.3.1 Reference Rock Hazard .....	2-136
		2.3.3.2 Site Response Evaluation .....	2-136



2.3.3.3	Control Point Hazard.....	2-138
2.3.4	Catawba .....	2-144
2.3.4.1	Reference Rock Hazard.....	2-144
2.3.4.2	Site Response Evaluation .....	2-144
2.3.4.3	Control Point Hazard .....	2-145
2.3.5	Farley.....	2-151
2.3.5.1	Reference Rock Hazard.....	2-151
2.3.5.2	Site Response Evaluation .....	2-151
2.3.5.3	Control Point Hazard.....	2-153
2.3.6	Harris .....	2-159
2.3.6.1	Reference Rock Hazard.....	2-159
2.3.6.2	Site Response Evaluation .....	2-159
2.3.6.3	Control Point Hazard.....	2-161
2.3.7	Hatch .....	2-167
2.3.7.1	Reference Rock Hazard.....	2-167
2.3.7.2	Site Response Evaluation .....	2-167
2.3.7.3	Control Point Hazard.....	2-169
2.3.8	McGuire .....	2-175
2.3.8.1	Reference Rock Hazard.....	2-175
2.3.8.2	Site Response Evaluation .....	2-175
2.3.8.3	Control Point Hazard.....	2-176
2.3.9	North Anna.....	2-182
2.3.9.1	Reference Rock Hazard.....	2-182
2.3.9.2	Site Response Evaluation .....	2-182
2.3.9.3	Control Point Hazard.....	2-183
2.3.10	Oconee .....	2-189
2.3.10.1	Reference Rock Hazard.....	2-189
2.3.10.2	Site Response Evaluation .....	2-189
2.3.10.3	Control Point Hazard.....	2-190
2.3.11	H.B. Robinson.....	2-196
2.3.11.1	Reference Rock Hazard.....	2-196
2.3.11.2	Site Response Evaluation .....	2-196
2.3.11.3	Control Point Hazard.....	2-197
2.3.12	Sequoyah .....	2-203
2.3.12.1	Reference Rock Hazard.....	2-203
2.3.12.2	Site Response Evaluation .....	2-203
2.3.12.3	Control Point Hazard.....	2-205
2.3.13	St. Lucie.....	2-210
2.3.13.1	Reference Rock Hazard.....	2-210
2.3.13.2	Site Response Evaluation .....	2-210
2.3.13.3	Control Point Hazard.....	2-212
2.3.14	Summer .....	2-218
2.3.14.1	Reference Rock Hazard.....	2-218
2.3.14.2	Site Response Evaluation .....	2-218
2.3.14.3	Control Point Hazard.....	2-219
2.3.15	Surry .....	2-225
2.3.15.1	Reference Rock Hazard.....	2-225
2.3.15.2	Site Response Evaluation .....	2-225
2.3.15.3	Control Point Hazard.....	2-227
2.3.16	Turkey Point.....	2-232
2.3.16.1	Reference Rock Hazard.....	2-232

	2.3.16.2	Site Response Evaluation .....	2-232
	2.3.16.3	Control Point Hazard .....	2-234
	2.3.17	Vogtle .....	2-240
	2.3.17.1	Reference Rock Hazard .....	2-240
	2.3.17.2	Site Response Evaluation .....	2-240
	2.3.17.3	Control Point Hazard .....	2-242
	2.3.18	Watts Bar .....	2-247
	2.3.18.1	Reference Rock Hazard .....	2-247
	2.3.18.2	Site Response Evaluation .....	2-247
	2.3.18.3	Control Point Hazard .....	2-249
2.4		Region III Sites .....	2-254
	2.4.1	Braidwood .....	2-257
	2.4.1.1	Reference Rock Hazard .....	2-257
	2.4.1.2	Site Response Evaluation .....	2-257
	2.4.1.3	Control Point Hazard .....	2-259
	2.4.2	Byron .....	2-265
	2.4.2.1	Reference Rock Hazard .....	2-265
	2.4.2.2	Site Response Evaluation .....	2-265
	2.4.2.3	Control Point Hazard .....	2-267
	2.4.3	Clinton .....	2-273
	2.4.3.1	Reference Rock Hazard .....	2-273
	2.4.3.2	Site Response Evaluation .....	2-273
	2.4.3.3	Control Point Hazard .....	2-275
	2.4.4	Davis Besse .....	2-281
	2.4.4.1	Reference Rock Hazard .....	2-281
	2.4.4.2	Site Response Evaluation .....	2-281
	2.4.4.3	Control Point Hazard .....	2-283
	2.4.5	Donald C. Cook .....	2-288
	2.4.5.1	Reference Rock Hazard .....	2-288
	2.4.5.2	Site Response Evaluation .....	2-288
	2.4.5.3	Control Point Hazard .....	2-290
	2.4.6	Dresden .....	2-296
	2.4.6.1	Reference Rock Hazard .....	2-296
	2.4.6.2	Site Response Evaluation .....	2-296
	2.4.6.3	Control Point Hazard .....	2-298
	2.4.7	Duane Arnold .....	2-304
	2.4.7.1	Reference Rock Hazard .....	2-304
	2.4.7.2	Site Response Evaluation .....	2-304
	2.4.7.3	Control Point Hazard .....	2-306
	2.4.8	Fermi .....	2-311
	2.4.8.1	Reference Rock Hazard .....	2-311
	2.4.8.2	Site Response Evaluation .....	2-311
	2.4.8.3	Control Point Hazard .....	2-312
	2.4.9	LaSalle .....	2-318
	2.4.9.1	Reference Rock Hazard .....	2-318
	2.4.9.2	Site Response Evaluation .....	2-318
	2.4.9.3	Control Point Hazard .....	2-320
	2.4.10	Monticello .....	2-325
	2.4.10.1	Reference Rock Hazard .....	2-325
	2.4.10.2	Site Response Evaluation .....	2-325
	2.4.10.3	Control Point Hazard .....	2-327

2.4.11	Palisades .....	2-332
2.4.11.1	Reference Rock Hazard .....	2-332
2.4.11.2	Site Response Evaluation .....	2-332
2.4.11.3	Control Point Hazard .....	2-334
2.4.12	Perry .....	2-340
2.4.12.1	Reference Rock Hazard .....	2-340
2.4.12.2	Site Response Evaluation .....	2-340
2.4.12.3	Control Point Hazard .....	2-342
2.4.13	Prairie Island .....	2-347
2.4.13.1	Reference Rock Hazard .....	2-347
2.4.13.2	Site Response Evaluation .....	2-347
2.4.13.3	Control Point Hazard .....	2-349
2.4.14	Point Beach .....	2-355
2.4.14.1	Reference Rock Hazard .....	2-355
2.4.14.2	Site Response Evaluation .....	2-355
2.4.14.3	Control Point Hazard .....	2-357
2.4.15	Quad Cities .....	2-363
2.4.15.1	Reference Rock Hazard .....	2-363
2.4.15.2	Site Response Evaluation .....	2-363
2.4.15.3	Control Point Hazard .....	2-365
2.5	Region IV Sites .....	2-370
2.5.1	Arkansas .....	2-372
2.5.1.1	Reference Rock Hazard .....	2-372
2.5.1.2	Site Response Evaluation .....	2-372
2.5.1.3	Control Point Hazard .....	2-374
2.5.2	Callaway .....	2-380
2.5.2.1	Reference Rock Hazard .....	2-380
2.5.2.2	Site Response Evaluation .....	2-380
2.5.2.3	Control Point Hazard .....	2-382
2.5.3	Comanche Peak .....	2-388
2.5.3.1	Reference Rock Hazard .....	2-388
2.5.3.2	Site Response Evaluation .....	2-388
2.5.3.3	Control Point Hazard .....	2-390
2.5.4	Cooper .....	2-396
2.5.4.1	Reference Rock Hazard .....	2-396
2.5.4.2	Site Response Evaluation .....	2-396
2.5.4.3	Control Point Hazard .....	2-398
2.5.5	Fort Calhoun .....	2-404
2.5.5.1	Reference Rock Hazard .....	2-404
2.5.5.2	Site Response Evaluation .....	2-404
2.5.5.3	Control Point Hazard .....	2-406
2.5.6	Grand Gulf .....	2-412
2.5.6.1	Reference Rock Hazard .....	2-412
2.5.6.2	Site Response Evaluation .....	2-412
2.5.6.3	Control Point Hazard .....	2-414
2.5.7	River Bend .....	2-419
2.5.7.1	Reference Rock Hazard .....	2-419
2.5.7.2	Site Response Evaluation .....	2-419
2.5.7.3	Control Point Hazard .....	2-421
2.5.8	South Texas .....	2-426
2.5.8.1	Reference Rock Hazard .....	2-426

	2.5.8.2	Site Response Evaluation .....	2-426
	2.5.8.3	Control Point Hazard .....	2-428
	2.5.9	Waterford .....	2-434
	2.5.9.1	Reference Rock Hazard .....	2-434
	2.5.9.2	Site Response Evaluation .....	2-434
	2.5.9.3	Control Point Hazard .....	2-436
	2.5.10	Wolf Creek .....	2-441
	2.5.10.1	Reference Rock Hazard .....	2-441
	2.5.10.2	Site Response Evaluation .....	2-441
	2.5.10.3	Control Point Hazard .....	2-443
2.6		References .....	2-449
<b>3</b>		<b>WESTERN UNITED STATES SITES .....</b>	<b>3-1</b>
	3.1.	Background .....	3-1
	3.1.1.	Overview of Senior Seismic Hazard Analysis Committee Level 3 Studies .....	3-1
	3.1.2.	Conduct of the NRC Staff Review .....	3-3
	3.2.	Palo Verde Nuclear Generating Station .....	3-5
	3.2.1.	Seismotectonic and Geologic Setting .....	3-8
	3.2.2.	Senior Seismic Hazard Analysis Committee Process .....	3-9
	3.2.3.	Seismic Source Characterization .....	3-10
	3.2.3.1.	Earthquake Catalog .....	3-11
	3.2.3.2.	Areal Source Zones .....	3-11
	3.2.3.3.	Fault Sources .....	3-15
	3.2.4.	Ground Motion Characterization .....	3-19
	3.2.4.1.	Ground Motion Databases and Seed Model Selection .....	3-19
	3.2.4.2.	Median Ground Motion Models .....	3-20
	3.2.4.3.	Ground Motion Variability .....	3-22
	3.2.4.4.	Implementation of Ground Motion Characterization Model .....	3-22
	3.2.5.	Probabilistic Seismic Hazard Analysis .....	3-23
	3.2.6.	Staff Confirmatory Evaluation of the Probabilistic Seismic Hazard Analysis .....	3-23
	3.2.7.	Site Response Analysis .....	3-26
	3.2.7.1.	Site Basecase Profiles .....	3-26
	3.2.7.2.	Dynamic Material Properties .....	3-29
	3.2.7.3.	Input Spectra .....	3-29
	3.2.7.4.	Site Response Methods and Results .....	3-29
	3.2.8.	Control Point Hazard Results .....	3-30
	3.3.	Diablo Canyon Power Plant .....	3-33
	3.3.1.	Seismotectonic Setting .....	3-34
	3.3.2.	Senior Seismic Hazard Analysis Committee Process .....	3-38
	3.3.3.	Seismic Source Characterization .....	3-39
	3.3.3.1.	Data and Supporting Studies .....	3-39
	3.3.3.2.	Complex Fault Sources and Fault Ruptures .....	3-40
	3.3.3.3.	Seismic Source Characterization Modeling Approach .....	3-41
	3.3.3.4.	The Hosgri Fault Source .....	3-42
	3.3.3.5.	NRC Staff Independent Evaluation of the Hosgri Slip Rate .....	3-43
	3.3.3.6.	Shoreline Fault .....	3-48
	3.3.3.7.	Areal Sources .....	3-49

3.3.3.8.	Time Dependency Model .....	3-51
3.3.4.	Ground Motion Characterization.....	3-51
3.3.4.1.	Median Ground Motion Models .....	3-52
3.3.4.2.	Ground Motion Variability.....	3-54
3.3.5.	Probabilistic Seismic Hazard Analysis.....	3-55
3.3.6.	NRC Staff Confirmatory Evaluation of the Probabilistic Seismic Hazard Analysis.....	3-56
3.3.7.	Site Response Analysis.....	3-58
3.3.7.1.	Data for Empirical and Analytical Approaches .....	3-59
3.3.7.2.	Empirical Site Term Approach .....	3-61
3.3.7.3.	Analytical Site Response Evaluation.....	3-62
3.3.7.4.	NRC Staff Confirmatory Evaluation.....	3-64
3.3.8.	Control Point Hazard .....	3-66
3.4.	Columbia Generating Station .....	3-68
3.4.1.	Seismotectonic and Geologic Setting.....	3-69
3.4.2.	Senior Seismic Hazard Analysis Committee Process .....	3-70
3.4.3.	Seismic Source Characterization.....	3-71
3.4.3.1.	Crustal Fault Sources.....	3-71
3.4.3.2.	Cascadia Subduction Zone Sources.....	3-78
3.4.3.3.	Areal Source Zones .....	3-79
3.4.4.	Ground Motion Characterization.....	3-82
3.4.4.1.	Median Models.....	3-82
3.4.4.2.	Ground Motion Characterization Median Adjustment Factors .....	3-83
3.4.4.3.	Aleatory Variability .....	3-84
3.4.4.4.	Implementation in the Ground Motion Characterization Logic Tree .....	3-85
3.4.5.	Probabilistic Seismic Hazard Analysis.....	3-86
3.4.6.	Staff Confirmatory Evaluations of the Hanford Probabilistic Seismic Hazard Analysis .....	3-86
3.4.6.1.	Evaluation of the Baserock Probabilistic Seismic Hazard Analysis Results.....	3-86
3.4.6.2.	Evaluation of Fault Source Geometries .....	3-89
3.4.6.3.	Evaluation of Cascadia Subduction Zone Hazard.....	3-92
3.4.6.4.	Evaluation of Areal Source Zone Hazard .....	3-92
3.4.7.	Site Response Evaluation.....	3-93
3.4.7.1.	Site Basecase Profiles .....	3-93
3.4.7.2.	Dynamic Material Properties and Site Kappa .....	3-96
3.4.7.3.	Site Response Method and Results.....	3-96
3.4.8.	NRC Staff Confirmatory Evaluation of Site Response Analysis .....	3-97
3.4.9.	Control Point Hazard Results .....	3-97
3.5.	References .....	3-102
<b>4</b>	<b>SITE AMPLIFICATION FACTORS AND SPECTRAL SHAPES.....</b>	<b>4-1</b>
4.1	Background .....	4-1
4.1.1	Amplification Factor Distributions .....	4-1
4.1.2	Spectral Shapes .....	4-2
4.2	NEHRP Class A Nuclear Power Plant Sites.....	4-2
4.3	NEHRP Class B Nuclear Power Plant Sites.....	4-5
4.4	NEHRP Class C Nuclear Power Plant Sites.....	4-8
4.5	NEHRP Class D Nuclear Power Plant Sites.....	4-11

4.6	References .....	4-14
<b>5</b>	<b>Summary .....</b>	<b>5-1</b>
5.1	References .....	5-3

## LIST OF FIGURES

Figure 2.1-1	CEUS NPPs within the 500 Km [311 Mi] Radius of the Charleston Rlme (Charleston Regional Source Configuration).....	2-5
Figure 2.1-2	Input Fourier Amplitude Spectra and Corresponding Acceleration Response Spectra Developed Using RVT.....	2-9
Figure 2.1-3	Models 1 And 3 (M1 And M3) from Campbell (2009) Compared to Models from Cabas and Rodriguez-Marek (Crmb) (2017) and PNNL (2014), Demonstrating Correlation Between $Q_{ef}$ and $V_s$ .....	2-12
Figure 2.1-4	Example Randomized Velocity Profiles about Lower (Red), Basecase (Black), and Upper (Blue) Profiles .....	2-14
Figure 2.2-1	Location Map Showing NPPs (Red Triangles) in Region I; Seismotectonic Source Zones, Indicated by Solid Black Lines (from NUREG-2115), with Acronym Defined in Table 2.1-1 of this Report; And Physiographic Provinces, Identified by Underlined Italicized Labels, with Water Bodies Represented in Gray. Earthquake Epicenters (from NUREG-2115) are Shown with Open Gray Circles.....	2-18
Figure 2.2-2	Low-Frequency (1 Hz, Left) and High-Frequency (10 Hz, Right) Reference Rock Hazard Curves for Beaver Valley. Total Hazard is Shown as a Bold Black Line; Individual Contributions to the Hazard for Each of the CEUS-SSC Sources are Shown as Colored Lines Defined in the Legend. See Table 2.1-1 for Source Name Definitions .....	2-22
Figure 2.2-3	Shear Wave Velocity ( $V_s$ ) Profiles for Beaver Valley. Basecase (BC) Profile Shown as Solid Bold Line; Lower and Upper Range (LR and UR) Profiles Shown as Dashed Lines. Profiles Terminate at Reference Rock Velocity of 2,831 m/sec [9,285 ft/sec] per EPRI GMM (2013).....	2-23
Figure 2.2-4	Overall Weighted Median Site Amplification Factor (SAF) (Upper) and Log Standard Deviation of the SAF (Lower) as a Function of Input Acceleration for EPRI GMM (2013) Spectral Frequencies .....	2-24
Figure 2.2-5	Mean Control Point Hazard Curves (Left) for EPRI GMM (2013) Spectral Frequencies, and Ground Motion Response Spectrum/Spectra (GMRS) and UHRS (Right) for Beaver Valley .....	2-25
Figure 2.2-6	Low-Frequency (1 Hz, Left) and High-Frequency (10 Hz, Right) Reference Rock Hazard Curves for Calvert Cliffs. Total Hazard is Shown as a Bold Black Line; Individual Contributions to the Hazard for Each of the CEUS-SSC Sources are Shown as Colored Lines Defined in the Legend. See Table 2.1-1 for Source Name Definitions .....	2-29
Figure 2.2-7	Shear Wave Velocity ( $V_s$ ) Profiles for Calvert Cliffs. Basecase (BC) Profile Shown as Solid Bold Line; Lower and Upper Range (LR and UR) Profiles Shown as Dashed Lines. Profiles Terminate at Reference Rock Velocity of 2,831 m/sec [9,285 ft/sec] per EPRI GMM (2013) .....	2-30

Figure 2.2-8	Overall Weighted Median Site Amplification Factor (SAF) (Upper) and Log Standard Deviation of the SAF (Lower) as a Function of Input Acceleration for EPRI GMM (2013) Spectral Frequencies .....	2-31
Figure 2.2-9	Mean Control Point Hazard Curves (Left) for EPRI GMM (2013) Spectral Frequencies, and GMRS and UHRS (Right) for Calvert Cliffs .....	2-32
Figure 2.2-10	Low-Frequency (1 Hz, Left) and High-Frequency (10 Hz, Right) Reference Rock Hazard Curves for Ginna. Total Hazard is Shown as a Bold Black Line; Individual Contributions to the Hazard for Each of the CEUS-SSC Sources are Shown as Colored Lines Defined in the Legend. See Table 2.1-1 for Source Name Definitions .....	2-36
Figure 2.2-11	Shear Wave Velocity ( $V_s$ ) Profiles for Ginna. Basecase (BC) Profile Shown as Solid Bold Line; Lower and Upper Range (LR and UR) Profiles Shown as Dashed Lines. Profiles Terminate at Reference Rock Velocity of 2,831 m/sec [9,285 ft/sec] per EPRI GMM (2013) .....	2-37
Figure 2.2-12	Overall Weighted Median Site Amplification Factor (SAF) (Upper) and Log Standard Deviation of the SAF (Lower) as a Function of Input Acceleration for EPRI GMM (2013) Spectral Frequencies .....	2-38
Figure 2.2-13	Mean Control Point Hazard Curves (Left) for EPRI GMM (2013) Spectral Frequencies, and GMRS and UHRS (Right) for Ginna .....	2-39
Figure 2.2-14	Low-Frequency (1 Hz, Left) and High-Frequency (10 Hz, Right) Reference Rock Hazard Curves for Hope Creek-Salem. Total Hazard is Shown as a Bold Black Line; Individual Contributions to the Hazard for Each of the CEUS-SSC Sources are Shown as Colored Lines Defined in the Legend. See Table 2.1-1 for Source Name Definitions .....	2-44
Figure 2.2-15	Shear Wave Velocity ( $V_s$ ) Profiles for Hope Creek-Salem. Basecase (BC) Profile Shown as Solid Bold Line; Lower and Upper Range (LR and UR) Profiles Shown as Dashed Lines. Profiles Terminate at Reference Rock Velocity of 2,831 m/sec [9,285 ft/sec] per EPRI GMM (2013) .....	2-45
Figure 2.2-16	Overall Weighted Median Site Amplification Factor (SAF) (Upper) and Log Standard Deviation of the SAF (Lower) as a Function of Input Acceleration for EPRI GMM (2013) Spectral Frequencies .....	2-46
Figure 2.2-17	Mean Control Point Hazard Curves (Left) for EPRI GMM (2013) Spectral Frequencies, and GMRS and UHRS (Right) for Hope Creek-Salem .....	2-47
Figure 2.2-18	Low-Frequency (1 Hz, Left) and High-Frequency (10 Hz, Right) Reference Rock Hazard Curves for Indian Point. Total Hazard is Shown as a Bold Black Line; Individual Contributions to the Hazard for Each of the CEUS-SSC Sources are Shown as Colored Lines Defined in the Legend. See Table 2.1-1 for Source Name Definitions .....	2-51



Figure 2.2-19	Shear Wave Velocity ( $V_s$ ) Profiles for Indian Point. Basecase (BC) Profile Shown as Solid Bold Line; Lower and Upper Range (LR and UR) Profiles Shown as Dashed Lines. Profiles Terminate at Reference Rock Velocity of 2,831 m/sec [9,285 ft/sec] per EPRI GMM (2013).....	2-52
Figure 2.2-20	Overall Weighted Median Site Amplification Factor (SAF) (Upper) and Log Standard Deviation of the SAF (Lower) as a Function of Input Acceleration for EPRI GMM (2013) Spectral Frequencies .....	2-53
Figure 2.2-21	Mean Control Point Hazard Curves (Left) for EPRI GMM (2013) Spectral Frequencies, and GMRS and UHRS (Right) for Indian Point.....	2-54
Figure 2.2-22	Low-Frequency (1 Hz, Left) and High-Frequency (10 Hz, Right) Reference Rock Hazard Curves for Fitzpatrick and Nine Mile Point. Total Hazard is Shown as a Bold Black Line; Individual Contributions to the Hazard for Each of the CEUS-SSC Sources are Shown as Colored Lines Defined in the Legend. See Table 2.1-1 for Source Name Definitions .....	2-59
Figure 2.2-23	Shear Wave Velocity ( $V_s$ ) Profiles for FitzPatrick and Nine Mile Point. Basecase (BC) Profile Shown as Solid Bold Line; Lower and Upper Range (LR and UR) Profiles Shown as Dashed Lines. Profiles Terminate at Reference Rock Velocity of 2,831 m/sec [9,285 ft/sec] per EPRI GMM (2013).....	2-60
Figure 2.2-24	Overall Weighted Median Site Amplification Factor (SAF) (Upper) and Log Standard Deviation of the SAF (Lower) as a Function of Input Acceleration for EPRI GMM (2013) Spectral Frequencies .....	2-61
Figure 2.2-25	Mean Control Point Hazard Curves (Left) for EPRI GMM (2013) Spectral Frequencies, and GMRS and UHRS (Right) for FitzPatrick and Nine Mile Point.....	2-62
Figure 2.2-26	Low-Frequency (1 Hz, Left) and High-Frequency (10 Hz, Right) Reference Rock Hazard Curves for Limerick. Total Hazard is Shown as a Bold Black Line; Individual Contributions to the Hazard for Each of the CEUS-SSC Sources are Shown as Colored Lines Defined in the Legend. See Table 2.1-1 for Source Name Definitions .....	2-67
Figure 2.2-27	Shear Wave Velocity ( $V_s$ ) Profiles for Limerick. Basecase (BC) Profile Shown as Solid Bold Line; Lower and Upper Range (LR and UR) Profiles Shown as Dashed Lines. Profiles Terminate at Reference Rock Velocity of 2,831 m/sec [9,285 ft/sec] per EPRI GMM (2013).....	2-68

Figure 2.2-28	Overall Weighted Median Site Amplification Factor (SAF) (Upper) and Log Standard Deviation of the SAF (Lower) as a Function of Input Acceleration for EPRI GMM (2013) Spectral Frequencies .....	2-69
Figure 2.2-29	Mean Control Point Hazard Curves (Left) for EPRI GMM (2013) Spectral Frequencies, and GMRS and UHRS (Right) for Limerick .....	2-70
Figure 2.2-30	Low-Frequency (1 Hz, Left) and High-Frequency (10 Hz, Right) Reference Rock Hazard Curves for Millstone. Total Hazard is Shown as a Bold Black Line; Individual Contributions to the Hazard for Each of the CEUS-SSC Sources are Shown as Colored Lines Defined in the Legend. See Table 2.1-1 for Source Name Definitions .....	2-74
Figure 2.2-31	Shear Wave Velocity ( $V_s$ ) Profiles for Millstone. Basecase (BC) Profile Shown as Solid Bold Line; Lower and Upper Range (LR and UR) Profiles Shown as Dashed Lines. Profiles Terminate at Reference Rock Velocity of 2,831 m/sec [9,285 ft/sec] per EPRI GMM (2013).....	2-75
Figure 2.2-32	Overall Weighted Median Site Amplification Factor (SAF) (Upper) and Log Standard Deviation of the SAF (Lower) as a Function of Input Acceleration for EPRI GMM (2013) Spectral Frequencies .....	2-76
Figure 2.2-33	Mean Control Point Hazard Curves (Left) for EPRI GMM (2013) Spectral Frequencies, and GMRS and UHRS (Right) for Millstone.....	2-77
Figure 2.2-34	Low-Frequency (1 Hz, Left) and High-Frequency (10 Hz, Right) Reference Rock Hazard Curves for Oyster Creek. Total Hazard is Shown as a Bold Black Line; Individual Contributions to the Hazard for Each of the CEUS-SSC Sources are Shown as Colored Lines Defined in the Legend. See Table 2.1-1 for Source Name Definitions .....	2-82
Figure 2.2-35	Shear Wave Velocity ( $V_s$ ) Profiles for Oyster Creek. Basecase (BC) Profile Shown as Solid Bold Line; Lower and Upper Range (LR and UR) Profiles Shown as Dashed Lines. Profiles Terminate at Reference Rock Velocity of 2,831 m/sec [9,285 ft/sec] per EPRI GMM (2013).....	2-83
Figure 2.2-36	Overall Weighted Median Site Amplification Factor (SAF) (Upper) and Log Standard Deviation of the SAF (Lower) as a Function of Input Acceleration for EPRI GMM (2013) Spectral Frequencies .....	2-84
Figure 2.2-37	Mean Control Point Hazard Curves (Left) for EPRI GMM (2013) Spectral Frequencies, and GMRS and UHRS (Right) for Oyster Creek .....	2-85
Figure 2.2-38	Low-Frequency (1 Hz, Left) and High-Frequency (10 Hz, Right) Reference Rock Hazard Curves for Peach Bottom. Total Hazard is Shown as a Bold Black Line; Individual Contributions to the Hazard for Each of the CEUS-SSC Sources are Shown as Colored Lines Defined in the Legend. See Table 2.1-1 for Source Name Definitions .....	2-89

Figure 2.2-39	Shear Wave Velocity ( $V_s$ ) Profiles for Peach Bottom. Basecase (BC) Profile Shown as Solid Bold Line; Lower and Upper Range (LR and UR) Profiles Shown as Dashed Lines. Profiles Terminate at Reference Rock Velocity of 2,831 m/sec [9,285 ft/sec] per EPRI GMM (2013).....	2-90
Figure 2.2-40	Overall Weighted Median Site Amplification Factor (SAF) (Upper) and Log Standard Deviation of the SAF (Lower) as a Function of Input Acceleration for EPRI GMM (2013) Spectral Frequencies .....	2-91
Figure 2.2-41	Mean Control Point Hazard Curves (Left) for EPRI GMM (2013) Spectral Frequencies, and GMRS and UHRS (Right) for Peach Bottom .....	2-92
Figure 2.2-42	Low-Frequency (1 Hz, Left) and High-Frequency (10 Hz, Right) Reference Rock Hazard Curves for Pilgrim. Total Hazard is Shown as a Bold Black Line; Individual Contributions to the Hazard For Each of the CEUS-SSC Sources are Shown as Colored Lines Defined in the Legend. See Table 2.1-1 for Source Name Definitions .....	2-96
Figure 2.2-43	Shear Wave Velocity ( $V_s$ ) Profiles for Pilgrim. Basecase (BC) Profile Shown as Solid Bold Line; Lower and Upper Range (LR and UR) Profiles Shown as Dashed Lines. Profiles Terminate at Reference Rock Velocity of 2,831 m/sec [9,285 ft/sec] per EPRI GMM (2013).....	2-97
Figure 2.2-44	Overall Weighted Median Site Amplification Factor (SAF) (Upper) and Log Standard Deviation of the SAF (Lower) as a Function of Input Acceleration for EPRI GMM (2013) Spectral Frequencies .....	2-98
Figure 2.2-45	Mean Control Point Hazard Curves (Left) for EPRI GMM (2013) Spectral Frequencies, and GMRS and UHRS (Right) for Pilgrim.....	2-99
Figure 2.2-46	Low-Frequency (1 Hz, Left) and High-Frequency (10 Hz, Right) Reference Rock Hazard Curves for Seabrook. Total Hazard is Shown as a Bold Black Line; Individual Contributions to the Hazard for Each of the CEUS-SSC Sources are Shown as Colored Lines Defined in the Legend. See Table 2.1-1 for Source Name Definitions .....	2-102
Figure 2.2-47	Mean Control Point Hazard Curves (Left) for EPRI GMM (2013) Spectral Frequencies, and GMRS and UHRS (Right) for Seabrook .....	2-103
Figure 2.2-48	Low-Frequency (1 Hz, Left) and High-Frequency (10 Hz, Right) Reference Rock Hazard Curves for Susquehanna. Total Hazard is Shown as a Bold Black Line; Individual Contributions to the Hazard for Each of the CEUS-SSC Sources are Shown as Colored Lines Defined in the Legend. See Table 2.1-1 for Source Name Definitions .....	2-107
Figure 2.2-49	Shear Wave Velocity ( $V_s$ ) Profiles for Susquehanna. Basecase (BC) Profile Shown as Solid Bold Line; Lower and Upper Range (LR and UR) Profiles Shown as Dashed Lines. Profiles Terminate at Reference Rock Velocity of 2,831 m/sec [9,285 ft/sec] per EPRI GMM (2013) .....	2-108

Figure 2.2-50	Overall Weighted Median Site Amplification Factor (SAF) (Upper) and Log Standard Deviation of the SAF (Lower) as a Function of Input Acceleration for EPRI GMM (2013) Spectral Frequencies .....2-109
Figure 2.2-51	Mean Control Point Hazard Curves (Left) for EPRI GMM (2013) Spectral Frequencies, and GMRS and UHRS (Right) for Susquehanna.....2-110
Figure 2.2-52	Low-Frequency (1 Hz, Left) and High-Frequency (10 Hz, Right) Reference Rock Hazard Curves for Three Mile Island. Total Hazard is Shown as a Bold Black Line; Individual Contributions to the Hazard for Each of the CEUS-SSC Sources are Shown as Colored Lines Defined in the Legend. See Table 2.1-1 for Source Name Definitions .....2-114
Figure 2.2-53	Shear Wave Velocity ( $V_s$ ) Profiles for Three Mile Island. Basecase (BC) Profile Shown as Solid Bold Line; Lower and Upper Range (LR and UR) Profiles Shown as Dashed Lines. Profiles Terminate at Reference Rock Velocity of 2,831 m/sec [9,285 ft/sec] per EPRI GMM (2013).....2-115
Figure 2.2-54	Overall Weighted Median Site Amplification Factor (SAF) (Upper) and Log Standard Deviation of the SAF (Lower) as a Function of Input Acceleration for EPRI GMM (2013) Spectral Frequencies .....2-116
Figure 2.2-55	Mean Control Point Hazard Curves (Left) for EPRI GMM (2013) Spectral Frequencies, and GMRS and UHRS (Right) for Three Mile Island .....2-117
Figure 2.3-1	Location Map Showing NPPs (Red Triangles) in Region II; RLMEs, Indicated by Solid Red Lines, and Seismotectonic Source Zones, Indicated by Solid Black Lines (from NUREG-2115), with Acronyms Defined in Table 2.1-1 of this Report; and Physiographic Provinces, Identified by Underlined Italicized Labels, with Water Bodies Represented in Gray. Earthquake Epicenters (from NUREG-2115) are Shown with Open Gray Circles.....2-120
Figure 2.3-2	Low-Frequency (1 Hz, Left) and High-Frequency (10 Hz, Right) Reference Rock Hazard Curves for Bellefonte. Total Hazard Is Shown as a Bold Black Line; Individual Contributions to the Hazard for Each of the CEUS-SSC Sources are Shown as Colored Lines Defined in the Legend. See Table 2.1-1 for Source Name Definitions .....2-124
Figure 2.3-3	Shear Wave Velocity ( $V_s$ ) Profiles for Bellefonte. Basecase (BC) Profile Shown as Solid Bold Line; Lower and Upper Range (LR and UR) Profiles Shown as Dashed Lines. Profiles Terminate at Reference Rock Velocity of 2,831 m/sec [9,285 ft/sec] per EPRI GMM (2013).....2-125
Figure 2.3-4	Overall Weighted Median Site Amplification Factor (SAF) (Upper) and Log Standard Deviation of the SAF (Lower) as a Function of Input Acceleration for EPRI GMM (2013) Spectral Frequencies ..... 2-126

Figure 2.3-5	Mean Control Point Hazard Curves (Left) for EPRI GMM (2013) Spectral Frequencies, and GMRS and UHRS (Right) for Bellefonte .....	2-127
Figure 2.3-6	Low-Frequency (1 Hz, Left) and High-Frequency (10 Hz, Right) Reference Rock Hazard Curves for Browns Ferry. Total Hazard is Shown as a Bold Black Line; Individual Contributions to the Hazard for each of the CEUS-SSC Sources are Shown as Colored Lines Defined in the Legend. See Table 2.1-1 for Source Name Definitions .....	2-132
Figure 2.3-7	Shear Wave Velocity ( $V_s$ ) Profiles for Browns Ferry. Basecase (BC) Profile Shown as Solid Bold Line; Lower and Upper Range (LR and UR) Profiles Shown as Dashed Lines. Profiles Terminate at Reference Rock Velocity of 2,831 m/sec [9,285 ft/sec] per EPRI GMM (2013).....	2-133
Figure 2.3-8	Overall Weighted Median Site Amplification Factor (SAF) (Upper) and Log Standard Deviation of the SAF (Lower) as a Function of Input Acceleration for EPRI GMM (2013) Spectral Frequencies .....	2-134
Figure 2.3-9	Mean Control Point Hazard Curves (Left) for EPRI GMM (2013) Spectral Frequencies, and GMRS and UHRS (Right) for Browns Ferry .....	2-135
Figure 2.3-10	Low-Frequency (1 Hz, Left) and High-Frequency (10 Hz, Right) Reference Rock Hazard Curves for Brunswick. Total Hazard is Shown as a Bold Black Line; Individual Contributions to the Hazard for Each of the CEUS-SSC Sources are Shown as Colored Lines Defined in the Legend. See Table 2.1-1 for Source Name Definitions .....	2-140
Figure 2.3-11	Shear Wave Velocity ( $V_s$ ) Profiles for Brunswick. Basecase (BC) Profile Shown as Solid Bold Line; Lower and Upper Range (LR and UR) Profiles Shown as Dashed Lines. Profiles Terminate at Reference Rock Velocity of 2,831 m/sec [9,285 ft/sec] per EPRI GMM (2013).....	2-141
Figure 2.3-12	Overall Weighted Median Site Amplification Factor (SAF) (Upper) and Log Standard Deviation of the SAF (Lower) as a Function of Input Acceleration for EPRI GMM (2013) Spectral Frequencies .....	2-142
Figure 2.3-13	Mean Control Point Hazard Curves (Left) for EPRI GMM (2013) Spectral Frequencies, and GMRS and UHRS (Right) for Brunswick .....	2-143
Figure 2.3-14	Low-Frequency (1 Hz, Left) and High-Frequency (10 Hz, Right) Reference Rock Hazard Curves for Catawba. Total Hazard is Shown as a Bold Black Line; Individual Contributions to the Hazard for Each of the CEUS-SSC Sources are Shown as Colored Lines Defined in the Legend. See Table 2.1-1 for Source Name Definitions .....	2-147
Figure 2.3-15	Shear Wave Velocity ( $V_s$ ) Profiles for Catawba. Basecase (BC) Profile Shown as Solid Bold Line; Lower and Upper Range (LR and UR) Profiles Shown as Dashed Lines. Profiles Terminate at Reference Rock Velocity of 2,831 m/sec [9,285 ft/sec] per EPRI GMM (2013) .....	2-148

Figure 2.3-16	Overall Weighted Median Site Amplification Factor (SAF) (Upper) and Log Standard Deviation of the SAF (Lower) as a Function of Input Acceleration for EPRI GMM (2013) Spectral Frequencies .....	2-149
Figure 2.3-17	Mean Control Point Hazard Curves (Left) for EPRI GMM (2013) Spectral Frequencies, and GMRS and UHRS (Right) for Catawba.....	2-150
Figure 2.3-18	Low-Frequency (1 Hz, Left) and High-Frequency (10 Hz, Right) Reference Rock Hazard Curves for Farley. Total Hazard is Shown as a Bold Black Line; Individual Contributions to the Hazard for Each of the CEUS-SSC Sources are Shown as Colored Lines Defined in the Legend. See Table 2.1-1 for Source Name Definitions .....	2-155
Figure 2.3-19	Shear Wave Velocity ( $V_s$ ) Profiles for Farley. Basecase (BC) Profile Shown as Solid Bold Line; Lower and Upper Range (LR and UR) Profiles Shown as Dashed Lines. Profiles Terminate at Reference Rock Velocity of 2,831 m/sec [9,285 ft/sec] per EPRI GMM (2013) .....	2-156
Figure 2.3-20	Overall Weighted Median Site Amplification Factor (SAF) (Upper) and Log Standard Deviation of the SAF (Lower) as a Function of Input Acceleration for EPRI GMM (2013) Spectral Frequencies .....	2-157
Figure 2.3-21	Mean Control Point Hazard Curves (Left) for EPRI GMM (2013) Spectral Frequencies, and GMRS and UHRS (Right) for Farley .....	2-158
Figure 2.3-22	Low-Frequency (1 Hz, Left) and High-Frequency (10 Hz, Right) Reference Rock Hazard Curves for Harris. Total Hazard is Shown as a Bold Black Line; Individual Contributions to the Hazard for Each of the CEUS-SSC Sources are Shown as Colored Lines Defined in the Legend. See Table 2.1-1 for Source Name Definitions .....	2-163
Figure 2.3-23	Shear Wave Velocity ( $V_s$ ) Profiles for Harris. Basecase (BC) Profile Shown as Solid Bold Line; Lower and Upper Range (LR and UR) Profiles Shown as Dashed Lines. Profiles Terminate at Reference Rock Velocity of 2,831 m/sec [9,285 ft/sec] per EPRI GMM (2013) .....	2-164
Figure 2.3-24	Overall Weighted Median Site Amplification Factor (SAF) (Upper) and Log Standard Deviation of the SAF (Lower) as a Function of Input Acceleration for EPRI GMM (2013) Spectral Frequencies .....	2-165
Figure 2.3-25	Mean Control Point Hazard Curves (Left) for EPRI GMM (2013) Spectral Frequencies, and GMRS and UHRS (Right) for Harris .....	2-166
Figure 2.3-26	Low-Frequency (1 Hz, Left) and High-Frequency (10 Hz, Right) Reference Rock Hazard Curves for Hatch. Total Hazard is Shown as a Bold Black Line; Individual Contributions to the Hazard for Each of the CEUS-SSC Sources are Shown as Colored Lines Defined in the Legend. See Table 2.1-1 for Source Name Definitions .....	2-171

Figure 2.3-27	Shear Wave Velocity ( $V_s$ ) Profiles for Hatch. Basecase (BC) Profile Shown as Solid Bold Line; Lower and Upper Range (LR and UR) Profiles Shown as Dashed Lines. Profiles Terminate at Reference Rock Velocity of 2,831 m/sec [9,285 ft/sec] per EPRI GMM (2013).....	2-172
Figure 2.3-28	Overall Weighted Median Site Amplification Factor (SAF) (Upper) and Log Standard Deviation of the SAF (Lower) as a Function of Input Acceleration for EPRI GMM (2013) Spectral Frequencies .....	2-173
Figure 2.3-29	Mean Control Point Hazard Curves (Left) for EPRI GMM (2013) Spectral Frequencies, and GMRS and UHRS (Right) for Hatch .....	2-174
Figure 2.3-30	Low-Frequency (1 Hz, Left) and High-Frequency (10 Hz, Right) Reference Rock Hazard Curves for McGuire. Total Hazard is Shown as a Bold Black Line; Individual Contributions to the Hazard for Each of the CEUS-SSC Sources are Shown as Colored Lines Defined in the Legend. See Table 2.1-1 for Source Name Definitions .....	2-178
Figure 2.3-31	Shear Wave Velocity ( $V_s$ ) Profiles for McGuire. Basecase (BC) Profile Shown as Solid Bold Line; Lower and Upper Range (LR and UR) Profiles Shown as Dashed Lines. Profiles Terminate at Reference Rock Velocity of 2,831 m/sec [9,285 ft/sec] per EPRI GMM (2013).....	2-179
Figure 2.3-32	Overall Weighted Median Site Amplification Factor (SAF) (Upper) and Log Standard Deviation of the SAF (Lower) as a Function of Input Acceleration for EPRI GMM (2013) Spectral Frequencies .....	2-180
Figure 2.3-33	Mean Control Point Hazard Curves (Left) for EPRI GMM (2013) Spectral Frequencies, and GMRS and UHRS (Right) for McGuire .....	2-181
Figure 2.3-34	Low-Frequency (1 Hz, Left) and High-Frequency (10 Hz, Right) Reference Rock Hazard Curves for North Anna. Total Hazard is Shown as a Bold Black Line; Individual Contributions to the Hazard for Each of the CEUS-SSC Sources are Shown as Colored Lines Defined in the Legend. See Table 2.1-1 for Source Name Definitions. ....	2-185
Figure 2.3-35	Shear Wave Velocity ( $V_s$ ) Profiles for North Anna. Basecase (BC) Profile Shown as Solid Bold Line; Lower and Upper Range (LR and UR) Profiles Shown as Dashed Lines. Profiles Terminate at Reference Rock Velocity of 2,831 m/sec [9,285 ft/sec] per EPRI GMM (2013).....	2-186
Figure 2.3-36	Overall Weighted Median Site Amplification Factor (SAF) (Upper) and Log Standard Deviation of the SAF (Lower) as a Function of Input Acceleration for EPRI GMM (2013) Spectral Frequencies .....	2-187

Figure 2.3-37	Mean Control Point Hazard Curves (Left) for EPRI GMM (2013) Spectral Frequencies, and GMRS and UHRS (Right) for North Anna.....	2-188
Figure 2.3-38	Low-Frequency (1 Hz, Left) and High-Frequency (10 Hz, Right) Reference Rock Hazard Curves for Oconee. Total Hazard is Shown as a Bold Black Line; Individual Contributions to the Hazard for Each of the CEUS-SSC Sources are Shown as Colored Lines Defined in the Legend. See Table 2.1-1 for Source Name Definitions .....	2-192
Figure 2.3-39	Shear Wave Velocity ( $V_s$ ) Profiles for Oconee. Basecase (BC) Profile Shown as Solid Bold Line; Lower and Upper Range (LR and UR) Profiles Shown as Dashed Lines. Profiles Terminate at Reference Rock Velocity of 2,831 m/sec [9,285 ft/sec] per EPRI GMM (2013) .....	2-193
Figure 2.3-40	Overall Weighted Median Site Amplification Factor (SAF) (Upper) and Log Standard Deviation of the SAF (Lower) as a Function of Input Acceleration for EPRI GMM (2013) Spectral Frequencies .....	2-194
Figure 2.3-41	Mean Control Point Hazard Curves (Left) for EPRI GMM (2013) Spectral Frequencies, and GMRS and UHRS (Right) for Oconee .....	2-195
Figure 2.3-42	Low-Frequency (1 Hz, Left) and High-Frequency (10 Hz, Right) Reference Rock Hazard Curves For Robinson. Total Hazard is Shown as a Bold Black Line; Individual Contributions to the Hazard for Each of the CEUS-SSC Sources are Shown as Colored Lines Defined in the Legend. See Table 2.1-1 for Source Name Definitions .....	2-199
Figure 2.3-43	Shear Wave Velocity ( $V_s$ ) Profiles for Robinson. Basecase (BC) Profile Shown as Solid Bold Line; Lower and Upper Range (LR and UR) Profiles Shown as Dashed Lines. Profiles Terminate at Reference Rock Velocity of 2,831 m/sec [9,285 ft/sec] per EPRI GMM (2013).....	2-200
Figure 2.3-44	Overall Weighted Median Site Amplification Factor (SAF) (Upper) and Log Standard Deviation of the SAF (Lower) as a Function of Input Acceleration for EPRI GMM (2013) Spectral Frequencies .....	2-201
Figure 2.3-45	Mean Control Point Hazard Curves (Left) for EPRI GMM (2013) Spectral Frequencies, and GMRS and UHRS (Right) for Robinson.....	2-202
Figure 2.3-46	Low-Frequency (1 Hz, Left) and High-Frequency (10 Hz, Right) Reference Rock Hazard Curves for Sequoyah. Total Hazard is Shown as a Bold Black Line; Individual Contributions to the Hazard for Each of the CEUS-SSC Sources are Shown as Colored Lines Defined in the Legend. See Table 2.1-1 for Source Name Definitions .....	2-206
Figure 2.3-47	Shear Wave Velocity ( $V_s$ ) Profiles for Sequoyah. Basecase (BC) Profile Shown as Solid Bold Line; Lower and Upper Range (LR and UR) Profiles Shown as Dashed Lines. Profiles Terminate at Reference Rock Velocity of 2,831 m/sec [9,285 ft/sec] per EPRI GMM (2013).....	2-207



Figure 2.3-48	Overall Weighted Median Site Amplification Factor (SAF) (Upper) and Log Standard Deviation of the SAF (Lower) as a Function of Input Acceleration for EPRI GMM (2013) Spectral Frequencies .....	2-208
Figure 2.3-49	Mean Control Point Hazard Curves (Left) for EPRI GMM (2013) Spectral Frequencies, and GMRS and UHRS (Right) for Sequoyah.....	2-209
Figure 2.3-50	Low-Frequency (1 Hz, Left) and High-Frequency (10 Hz, Right) Reference Rock Hazard Curves for St. Lucie. Total Hazard is Shown as a Bold Black Line; Individual Contributions to the Hazard for Each of the CEUS-SSC Sources are Shown as Colored Lines Defined in the legend. See Table 2.1-1 for Source Name Definitions .....	2-214
Figure 2.3-51	Shear Wave Velocity ( $V_s$ ) Profiles for St. Lucie. Basecase (BC) Profile Shown as Solid Bold Line; Lower and Upper Range (LR and UR) Profiles Shown as Dashed Lines. Profiles Terminate at Reference Rock Velocity of 2,831 m/sec [9,285 ft/sec] per EPRI GMM (2013).....	2-215
Figure 2.3-52	Overall Weighted Median Site Amplification Factor (SAF) (Upper) and Log Standard Deviation of the SAF (Lower) as a Function of Input Acceleration for EPRI GMM (2013) Spectral Frequencies .....	2-216
Figure 2.3-53	Mean Control Point Hazard Curves (Left) for EPRI GMM (2013) Spectral Frequencies, and GMRS and UHRS (Right) for St. Lucie.....	2-217
Figure 2.3-54	Low-Frequency (1 Hz, Left) and High-Frequency (10 Hz, Right) Reference Rock Hazard Curves for Summer. Total Hazard is Shown as a Bold Black Line; Individual Contributions to the Hazard for Each of the CEUS-SSC Sources are Shown as Colored Lines Defined in the Legend. See Table 2.1-1 for Source Name Definitions .....	2-221
Figure 2.3-55	Shear Wave Velocity ( $V_s$ ) Profiles for Summer. Basecase (BC) Profile Shown as Solid Bold Line; Lower and Upper Range (LR and UR) Profiles Shown as Dashed Lines. Profiles Terminate at Reference Rock Velocity of 2,831 m/sec [9,285 ft/sec] per EPRI GMM (2013).....	2-222
Figure 2.3-56	Overall Weighted Median Site Amplification Factor (SAF) (Upper) and Log Standard Deviation of the SAF (Lower) as a Function of Input Acceleration for EPRI GMM (2013) Spectral Frequencies .....	2-223
Figure 2.3-57	Mean Control Point Hazard Curves (Left) for EPRI GMM (2013) Spectral Frequencies, and GMRS and UHRS (Right) for Summer .....	2-224
Figure 2.3-58	Low-Frequency (1 Hz, Left) and High-Frequency (10 Hz, Right) Reference Rock Hazard Curves for Surry. Total Hazard is Shown as a Bold Black Line; Individual Contributions to the Hazard for Each of the CEUS-SSC Sources are Shown as Colored Lines Defined in the Legend. See Table 2.1-1 for Source Name Definitions .....	2-228

Figure 2.3-59	Shear Wave Velocity ( $V_s$ ) Profiles for Surry. Basecase (BC) Profile Shown as Solid Bold Line; Lower and Upper Range (LR and UR) Profiles Shown as Dashed Lines. Profiles Terminate at Reference Rock Velocity of 2,831 m/sec [9,285 ft/sec] per EPRI GMM (2013).....	2-229
Figure 2.3-60	Overall Weighted Median Site Amplification Factor (SAF) (Upper) and Log Standard Deviation of the SAF (Lower) as a Function of Input Acceleration for EPRI GMM (2013) Spectral Frequencies .....	2-230
Figure 2.3-61	Mean Control Point Hazard Curves (Left) for EPRI GMM (2013) Spectral Frequencies, and GMRS and UHRS (Right) for Surry .....	2-231
Figure 2.3-62	Low-Frequency (1 Hz, Left) and High-Frequency (10 Hz, Right) Reference Rock Hazard Curves for Turkey Point. Total Hazard is Shown as a Bold Black Line; Individual Contributions to the Hazard for Each of the CEUS-SSC Sources are Shown as Colored Lines Defined in the Legend. See Table 2.1-1 for Source Name Definitions .....	2-236
Figure 2.3-63	Shear Wave Velocity ( $V_s$ ) Profiles for Turkey Point. Basecase (BC) Profile Shown as Solid Bold Line; Lower and Upper Range (LR and UR) Profiles Shown as Dashed Lines. Profiles Terminate at Reference Rock Velocity of 2,831 m/sec [9,285 ft/sec] per EPRI GMM (2013).....	2-237
Figure 2.3-64	Overall Weighted Median Site Amplification Factor (SAF) (Upper) and Log Standard Deviation of the SAF (Lower) as a Function of Input Acceleration for EPRI GMM (2013) Spectral Frequencies .....	2-238
Figure 2.3-65	Mean Control Point Hazard Curves (Left) for EPRI GMM (2013) Spectral Frequencies, and GMRS and UHRS (Right) for Turkey Point.....	2-239
Figure 2.3-66	Low-Frequency (1 Hz, Left) and High-Frequency (10 Hz, Right) Reference Rock Hazard Curves for Vogtle. Total Hazard is Shown as a Bold Black Line; Individual Contributions to the Hazard for Each of the CEUS-SSC Sources are Shown as Colored Lines Defined in the Legend. See Table 2.1-1 for Source Name Definitions .....	2-243
Figure 2.3-67	Shear Wave Velocity ( $V_s$ ) Profiles for Vogtle. Basecase (BC) Profile Shown as Solid Bold Line; Lower and Upper Range (LR and UR) Profiles Shown as Dashed Lines. Profiles Terminate at Reference Rock Velocity of 2,831 m/sec [9,285 ft/sec] per EPRI GMM (2013).....	2-244
Figure 2.3-68	Overall Weighted Median Site Amplification Factor (SAF) (Upper) and Log Standard Deviation of the SAF (Lower) as a Function of Input Acceleration for EPRI GMM (2013) Spectral Frequencies .....	2-245
Figure 2.3-69	Mean Control Point Hazard Curves (Left) for EPRI GMM (2013) Spectral Frequencies, and GMRS and UHRS (Right) for Vogtle.....	2-246

Figure 2.3-70	Low-Frequency (1 Hz, Left) and High-Frequency (10 Hz, Right) Reference Rock Hazard Curves for Watts Bar. Total Hazard as Shown as a Bold Black Line; Individual Contributions to the Hazard for Each of the CEUS-SSC Sources are Shown as Colored Lines Defined in the Legend. See Table 2.1-1 for Source Name Definitions....	2-250
Figure 2.3-71	Shear Wave Velocity ( $V_s$ ) Profiles for Watts Bar. Basecase (BC) Profile Shown as Solid Bold Line; Lower and Upper Range (LR and UR) Profiles Shown as Dashed Lines. Profiles Terminate at Reference Rock Velocity of 2,831 m/sec [9,285 ft/sec] per EPRI GMM (2013).....	2-251
Figure 2.3-72	Overall Weighted Median Site Amplification Factor (SAF) (Upper) and Log Standard Deviation of the SAF (Lower) as a Function of Input Acceleration for EPRI GMM (2013) Spectral Frequencies .....	2-252
Figure 2.3-73	Mean Control Point Hazard Curves (Left) for EPRI GMM (2013) Spectral Frequencies, and GMRS and UHRS (Right) for Watts Bar .....	2-253
Figure 2.4-1	Location Map Showing NPPs (Red Triangles) in Region III; RLMs, Indicated by Solid Red Lines, and Seismotectonic Source Zones, Indicated by Solid Black Lines (from NUREG-2115), with Acronyms Defined in Table 2.1-1 of this Report; and Physiographic Provinces, Identified by Underlined Italicized Labels, with Water Bodies Represented in Gray. Earthquake Epicenters (from NUREG-2115) are Shown by Open Gray Circles .....	2-256
Figure 2.4-2	Low-Frequency (1 Hz, Left), and High-Frequency (10 Hz, Right) Reference Rock Hazard Curves for Braidwood. Total Hazard is Shown as a Bold Black Line; Individual Contributions to the Hazard for Each of the CEUS-SSC Sources are Shown as Colored Lines Defined in the Legend. See Table 2.1-1 for Source Name Definitions .....	2-261
Figure 2.4-3	Shear Wave Velocity ( $V_s$ ) Profiles for Braidwood. Basecase (BC) Profile Shown as Solid Bold Line; Lower and Upper Range (LR and UR) Profiles Shown as Dashed Lines. Profiles Terminate at Reference Rock Velocity of 2,831 m/sec [9,285 ft/sec] per EPRI GMM (2013).....	2-262
Figure 2.4-4	Overall Weighted Median Site Amplification Factor (SAF) (Upper) and Log Standard Deviation of the SAF (Lower) as a Function of Input Acceleration for EPRI GMM (2013) Spectral Frequencies .....	2-263
Figure 2.4-5	Mean Control Point Hazard Curves (Left) for EPRI GMM (2013) Spectral Frequencies, and GMRS and UHRS (Right) for Braidwood.....	2-264
Figure 2.4-6	Low-Frequency (1 Hz, Left), and High-Frequency (10 Hz, Right) Reference Rock Hazard Curves for Byron. Total Hazard is Shown as a Bold Black Line; Individual Contributions to the Hazard for Each of the CEUS-SSC Sources are Shown as Colored Lines Defined in the Legend. See Table 2.1-1 for Source Name Definitions .....	2-269

Figure 2.4-7	Shear Wave Velocity ( $V_s$ ) Profiles for Byron. Basecase (BC) Profile Shown as Solid Bold Line; Lower and Upper Range (LR and UR) Profiles Shown as Dashed Lines. Profiles Terminate at Reference Rock Velocity of 2,831 m/sec [9,285 ft/sec] per EPRI GMM (2013).....	2-270
Figure 2.4-8	Overall Weighted Median Site Amplification Factor (SAF) (Upper) and Log Standard Deviation of the SAF (Lower) as a Function of Input Acceleration for EPRI GMM (2013) Spectral Frequencies .....	2-271
Figure 2.4-9	Mean Control Point Hazard Curves (Left) for EPRI GMM (2013) Spectral Frequencies, and GMRS and UHRS (Right) for Byron .....	2-272
Figure 2.4-10	Low-Frequency (1 Hz, Left), and High-Frequency (10 Hz, Right) Reference Rock Hazard Curves for Clinton. Total Hazard is Shown as a Bold Black Line; Individual Contributions to the Hazard for Each of the CEUS-SSC Sources are Shown as Colored Lines Defined in the Legend. See Table 2.1-1 for Source Name Definitions .....	2-277
Figure 2.4-11	Shear Wave Velocity ( $V_s$ ) Profiles for Clinton. Basecase (BC) Profile Shown as Solid Bold Line; Lower and Upper Range (LR and UR) Profiles Shown as Dashed Lines. Profiles Terminate at Reference Rock Velocity of 2,831 m/sec [9,285 ft/sec] per EPRI GMM (2013).....	2-278
Figure 2.4-12	Overall Weighted Median Site Amplification Factor (SAF) (Upper) and Log Standard Deviation of the SAF (Lower) as a Function of Input Acceleration for EPRI GMM (2013) Spectral Frequencies .....	2-279
Figure 2.4-13	Mean Control Point Hazard Curves (Left) for EPRI GMM (2013) Spectral Frequencies, and GMRS and UHRS (Right) for Clinton.....	2-280
Figure 2.4-14	Low-Frequency (1 Hz, Left), and High-Frequency (10 Hz, Right) Reference Rock Hazard Curves for Davis Besse. Total Hazard is Shown as a Bold Black Line; Individual Contributions to the Hazard for Each of the CEUS-SSC Sources are Shown as Colored Lines Defined in the Legend. See Table 2.1-1 for Source Name Definitions .....	2-284
Figure 2.4-15	Shear Wave Velocity ( $V_s$ ) Profiles for Davis Besse. Basecase (BC) Profile Shown as Solid Bold Line; Lower and Upper Range (LR and UR) Profiles Shown as Dashed Lines. Profiles Terminate at Reference Rock Velocity of 2,831 m/sec [9,285 ft/sec] per EPRI GMM (2013).....	2-285
Figure 2.4-16	Overall Weighted Median Site Amplification Factor (SAF) (Upper) and Log Standard Deviation of the SAF (Lower) as a Function of Input Acceleration for EPRI GMM (2013) Spectral Frequencies .....	2-286
Figure 2.4-17	Mean Control Point Hazard Curves (Left) for EPRI GMM (2013) Spectral Frequencies, and GMRS and UHRS (Right) for Davis Besse.....	2-287

Figure 2.4-18	Low-Frequency (1 Hz, Left), and High-Frequency (10 Hz, Right) Reference Rock Hazard Curves for Cook. Total Hazard is Shown as a Bold Black Line; Individual Contributions to the Hazard for Each of the CEUS-SSC Sources are Shown as Colored Lines Defined in the Legend. See Table 2.1-1 for Source Name Definitions .....2-292
Figure 2.4-19	Shear Wave Velocity ( $V_s$ ) Profiles for Cook. Basecase (BC) Profile Shown as Solid Bold Line; Lower and Upper Range (LR and UR) Profiles Shown as Dashed Lines. Profiles Terminate at Reference Rock Velocity of 2,831 m/sec [9,285 ft/sec] per EPRI GMM (2013) .....2-293
Figure 2.4-20	Overall Weighted Median Site Amplification Factor (SAF) (Upper) and Log Standard Deviation of the SAF (Lower) as a Function of Input Acceleration for EPRI GMM (2013) Spectral Frequencies .....2-294
Figure 2.4-21	Mean Control Point Hazard Curves (Left) for EPRI GMM (2013) Spectral Frequencies, and GMRS and UHRS (Right) for Cook .....2-295
Figure 2.4-22	Low-Frequency (1 Hz, Left), and High-Frequency (10 Hz, Right) Reference Rock Hazard Curves for Dresden. Total Hazard is Shown as a Bold Black Line; Individual Contributions to the Hazard for Each of the CEUS-SSC Sources are Shown as Colored Lines Defined in the Legend. See Table 2.1-1 for Source Name Definitions .....2-300
Figure 2.4-23	Shear Wave Velocity ( $V_s$ ) Profiles for Dresden. Basecase (BC) Profile Shown as Solid Bold Line; Lower and Upper Range (LR and UR) Profiles Shown as Dashed Lines. Profiles Terminate at Reference Rock Velocity of 2,831 m/sec [9,285 ft/sec] per EPRI GMM (2013).....2-301
Figure 2.4-24	Overall Weighted Median Site Amplification Factor (SAF) (Upper) and Log Standard Deviation of the SAF (Lower) as a Function of Input Acceleration for EPRI GMM (2013) Spectral Frequencies .....2-302
Figure 2.4-25	Mean Control Point Hazard Curves (Left) for EPRI GMM (2013) Spectral Frequencies, and GMRS and UHRS (Right) for Dresden .....2-303
Figure 2.4-26	Low-Frequency (1 Hz, Left), and High-Frequency (10 Hz, Right) Reference Rock Hazard Curves for Duane Arnold. Total Hazard is Shown as a Bold Black Line; Individual Contributions to the Hazard for Each of the CEUS-SSC Sources are Shown as Colored Lines Defined in the Legend. See Table 2.1-1 for Source Name Definitions .....2-307
Figure 2.4-27	Shear Wave Velocity ( $V_s$ ) Profiles for Duane Arnold. Basecase (BC) Profile Shown as Solid Bold Line; Lower and Upper Range (LR and UR) Profiles Shown as Dashed Lines. Profiles Terminate at Reference Rock Velocity of 2,831 m/sec [9,285 ft/sec] per EPRI GMM (2013).....2-308
Figure 2.4-28	Overall Weighted Median Site Amplification Factor (SAF) (Upper) and Log Standard Deviation of the SAF (Lower) as a Function of Input Acceleration for EPRI GMM (2013) Spectral Frequencies .....2-309

Figure 2.4-29	Mean Control Point Hazard Curves (Left) for EPRI GMM (2013) Spectral Frequencies, and GMRS and UHRS (Right) for Duane Arnold .....	2-310
Figure 2.4-30	Low-Frequency (1 Hz, Left), and High-Frequency (10 Hz, Right) Reference Rock Hazard Curves for Fermi. Total Hazard is Shown as a Bold Black Line; Individual Contributions to the Hazard for Each of the CEUS-SSC Sources are Shown as Colored Lines Defined in the Legend. See Table 2.1-1 for Source Name Definitions .....	2-314
Figure 2.4-31	Shear Wave Velocity ( $V_s$ ) Profiles for Fermi. Basecase (BC) Profile Shown as Solid Bold Line; Lower and Upper Range (LR and UR) Profiles Shown as Dashed Lines. Profiles Terminate at Reference Rock Velocity of 2,831 m/sec [9,285 ft/sec] per EPRI GMM (2013) .....	2-315
Figure 2.4-32	Overall Weighted Median Site Amplification Factor (SAF) (Upper) and Log Standard Deviation of the SAF (Lower) as a Function of Input Acceleration for EPRI GMM (2013) Spectral Frequencies .....	2-316
Figure 2.4-33	Mean Control Point Hazard Curves (Left) for EPRI GMM (2013) Spectral Frequencies, and GMRS and UHRS (Right) for Fermi.....	2-317
Figure 2.4-34	Low-Frequency (1 Hz, Left), and High-Frequency (10 Hz, Right) Reference Rock Hazard Curves for LaSalle. Total Hazard is Shown as a Bold Black Line; Individual Contributions to the Hazard for Each of the CEUS-SSC Sources are Shown as Colored Lines Defined in the Legend. See Table 2.1-1 for Source Name Definitions .....	2-321
Figure 2.4-35	Shear Wave Velocity ( $V_s$ ) Profiles for LaSalle. Basecase (BC) Profile Shown as Solid Bold Line; Lower and Upper Range (LR and UR) Profiles Shown as Dashed Lines. Profiles Terminate at Reference Rock Velocity of 2,831 m/sec [9,285 ft/sec] per EPRI GMM (2013) .....	2-322
Figure 2.4-36	Overall Weighted Median Site Amplification Factor (SAF) (Upper) and Log Standard Deviation of the SAF (Lower) as a Function of Input Acceleration for EPRI GMM (2013) Spectral Frequencies .....	2-323
Figure 2.4-37	Mean Control Point Hazard Curves (Left) for EPRI GMM (2013) Spectral Frequencies, and GMRS and UHRS (Right) for LaSalle.....	2-324
Figure 2.4-38	Low-Frequency (1 Hz, Left), and High-Frequency (10 Hz, Right) Reference Rock Hazard Curves for Monticello. Total Hazard is Shown as a Bold Black Line; Individual Contributions to the Hazard for Each of the CEUS-SSC Sources are Shown as Colored Lines Defined in the Legend. See Table 2.1-1 for Source Name Definitions .....	2-328
Figure 2.4-39	Shear Wave Velocity ( $V_s$ ) Profiles for Monticello. Basecase (BC) Profile Shown as Solid Bold Line; Lower and Upper Range (LR and UR) Profiles Shown as Dashed Lines. Profiles Terminate at Reference Rock Velocity of 2,831 m/sec [9,285 ft/sec] per EPRI GMM (2013).....	2-329

Figure 2.4-40	Overall Weighted Median Site Amplification Factor (SAF) (Upper) and Log Standard Deviation of the SAF (Lower) as a Function of Input Acceleration for EPRI GMM (2013) Spectral Frequencies .....2-330
Figure 2.4-41	Mean Control Point Hazard Curves (Left) for EPRI GMM (2013) Spectral Frequencies, and GMRS and UHRS (Right) for Monticello.....2-331
Figure 2.4-42	Low-Frequency (1 Hz, Left), and High-Frequency (10 Hz, Right) Reference Rock Hazard Curves for Palisades. Total Hazard is Shown as a Bold Black Line; Individual Contributions to the Hazard for Each of the CEUS-SSC Sources are Shown as Colored Lines Defined in the Legend. See Table 2.1-1 for Source Name Definitions ....2-336
Figure 2.4-43	Shear Wave Velocity ( $V_s$ ) Profiles for Palisades. Basecase (BC) Profile Shown as Solid Bold Line; Lower and Upper Range (LR and UR) Profiles Shown as Dashed Lines. Profiles Terminate at Reference Rock Velocity of 2,831 m/sec [9,285 ft/sec] per EPRI GMM (2013).....2-337
Figure 2.4-44	Overall Weighted Median Site Amplification Factor (SAF) (Upper) and Log Standard Deviation of the SAF (Lower) as a Function of Input Acceleration for EPRI GMM (2013) Spectral Frequencies .....2-338
Figure 2.4-45	Mean Control Point Hazard Curves (Left) for EPRI GMM (2013) Spectral Frequencies, and GMRS and UHRS (Right) for Palisades .....2-339
Figure 2.4-46	Low-Frequency (1 Hz, Left), and High-Frequency (10 Hz, Right) Reference Rock Hazard Curves for Perry. Total Hazard is Shown as a Bold Black Line; Individual Contributions to the Hazard for Each of the CEUS-SSC Sources are Shown as Colored Lines Defined in the Legend. See Table 2.1-1 for Source Name Definitions .....2-343
Figure 2.4-47	Shear Wave Velocity ( $V_s$ ) Profiles for Perry. Basecase (BC) Profile Shown as Solid Bold Line; Lower and Upper Range (LR and UR) Profiles Shown as Dashed Lines. Profiles Terminate at Reference Rock Velocity of 2,831 m/sec [9,285 ft/sec] per EPRI GMM (2013) .....2-344
Figure 2.4-48	Overall Weighted Median Site Amplification Factor (SAF) (Upper) and Log Standard Deviation of the SAF (Lower) as a Function of Input Acceleration for EPRI GMM (2013) Spectral Frequencies .....2-345
Figure 2.4-49	Mean Control Point Hazard Curves (Left) for EPRI GMM (2013) Spectral Frequencies, and GMRS and UHRS (Right) for Perry .....2-346
Figure 2.4-50	Low-Frequency (1 Hz, Left), and High-Frequency (10 Hz, Right) Reference Rock Hazard Curves for Prairie Island. Total Hazard is Shown as a Bold Black Line; Individual Contributions to the Hazard for Each of the CEUS-SSC Sources are Shown as Colored Lines Defined in the Legend. See Table 2.1-1 for Source Name Definitions ....2-351

Figure 2.4-51	Shear Wave Velocity ( $V_s$ ) Profiles for Prairie Island. Basecase (BC) Profile Shown as Solid Bold Line; Lower and Upper Range (LR and UR) Profiles Shown as Dashed Lines. Profiles Terminate at Reference Rock Velocity of 2,831 m/sec [9,285 ft/sec] per EPRI GMM (2013).....	2-352
Figure 2.4-52	Overall Weighted Median Site Amplification Factor (SAF) (Upper) and Log Standard Deviation of the SAF (Lower) as a Function of Input Acceleration for EPRI GMM (2013) Spectral Frequencies .....	2-353
Figure 2.4-53	Mean Control Point Hazard Curves (Left) for EPRI GMM (2013) Spectral Frequencies, and GMRS and UHRS (Right) for Prairie Island .....	2-354
Figure 2.4-54	Low-Frequency (1 Hz, Left), and High-Frequency (10 Hz, Right) Reference Rock Hazard Curves for Point Beach. Total Hazard is Shown as a Bold Black Line; Individual Contributions to the Hazard for Each of the CEUS-SSC Sources are Shown as Colored Lines Defined in the Legend. See Table 2.1-1 for Source Name Definitions .....	2-359
Figure 2.4-55	Shear Wave Velocity ( $V_s$ ) Profiles for Point Beach. Basecase (BC) Profile Shown as Solid Bold Line; Lower and Upper Range (LR and UR) Profiles Shown as Dashed Lines. Profiles Terminate at Reference Rock Velocity of 2,831 m/sec [9,285 ft/sec] per EPRI GMM (2013).....	2-360
Figure 2.4-56	Overall Weighted Median Site Amplification Factor (SAF) (Upper) and Log Standard Deviation of the SAF (Lower) as a Function of Input Acceleration for EPRI GMM (2013) Spectral Frequencies .....	2-361
Figure 2.4-57	Mean Control Point Hazard Curves (Left) for EPRI GMM (2013) Spectral Frequencies, and GMRS and UHRS (Right) for Point Beach .....	2-362
Figure 2.4-58	Low-Frequency (1 Hz, Left), and High-Frequency (10 Hz, Right) Reference Rock Hazard Curves for Quad Cities. Total Hazard is Shown as a Bold Black Line; Individual Contributions to the Hazard for Each of the CEUS-SSC Sources are Shown as Colored Lines Defined in the Legend. See Table 2.1-1 for Source Name Definitions .....	2-366
Figure 2.4-59	Shear Wave Velocity ( $V_s$ ) Profiles for Quad Cities. Basecase (BC) Profile Shown as Solid Bold Line; Lower and Upper Range (LR and UR) Profiles Shown as Dashed Lines. Profiles Terminate at Reference Rock Velocity of 2,831 m/sec [9,285 ft/sec] per EPRI GMM (2013).....	2-367
Figure 2.4-60	Overall Weighted Median Site Amplification Factor (SAF) (Upper) and Log Standard Deviation of the SAF (Lower) as a Function of Input Acceleration for EPRI GMM (2013) Spectral Frequencies .....	2-368
Figure 2.4-61	Mean Control Point Hazard Curves (Left) for EPRI GMM (2013) Spectral Frequencies, and GMRS and UHRS (Right) for Quad Cities .....	2-369



Figure 2.5-1	Location Map Showing NPPs (Red Triangles) in Region IV; RLMEs, Indicated by Solid Red Lines, and Seismotectonic Source Zones, Indicated by Solid Black Lines (from NUREG-2115), with Acronyms Defined in Table 2.1-1 of this Report; and Physiographic Provinces, Identified by Underlined Italicized Labels, with Water Bodies Represented in Gray. Earthquake Epicenters (from NUREG-2115) are Shown with Open Gray Circles.....	2-371
Figure 2.5-2	Low-Frequency (1 Hz, Left), and High-Frequency (10 Hz, Right) Reference Rock Hazard Curves for Arkansas. Total Hazard is Shown as a Bold Black Line; Individual Contributions to the Hazard for Each of the CEUS-SSC Sources are Shown as Colored Lines Defined in the Legend. See Table 2.1-1 for Source Name Definitions .....	2-376
Figure 2.5-3	Shear Wave Velocity ( $V_s$ ) Profiles for Arkansas. Basecase (BC) Profile Shown as Solid Bold Line; Lower and Upper Range (LR and UR) Profiles Shown as Dashed Lines. Profiles Terminate at Reference Rock Velocity of 2,831 m/sec [9,285 ft/sec] per EPRI GMM (2013).....	2-377
Figure 2.5-4	Overall Weighted Median Site Amplification Factor (SAF) (Upper) and Log Standard Deviation of the SAF (Lower) as a Function of Input Acceleration for EPRI GMM (2013) Spectral Frequencies .....	2-378
Figure 2.5-5	Mean Control Point Hazard Curves (Left) for EPRI GMM (2013) Spectral Frequencies, and GMRS and UHRS (Right) for Arkansas.....	2-379
Figure 2.5-6	Low-Frequency (1 Hz, Left), and High-Frequency (10 Hz, Right) Reference Rock Hazard Curves for Callaway. Total Hazard is Shown as a Bold Black Line; Individual Contributions to the Hazard for Each of the CEUS-SSC Sources are Shown as Colored Lines Defined in the Legend. See Table 2.1-1 for Source Name Definitions .....	2-384
Figure 2.5-7	Shear Wave Velocity ( $V_s$ ) Profiles for Callaway. Basecase (BC) Profile Shown as Solid Bold Line; Lower and Upper Range (LR and UR) Profiles Shown as Dashed Lines. Profiles Terminate at Reference Rock Velocity of 2,831 m/sec [9,285 ft/sec] per EPRI GMM (2013).....	2-385
Figure 2.5-8	Overall Weighted Median Site Amplification Factor (SAF) (Upper) and Log Standard Deviation of the SAF (Lower) as a Function of Input Acceleration for EPRI GMM (2013) Spectral Frequencies .....	2-386
Figure 2.5-9	Mean Control Point Hazard Curves (Left) for EPRI GMM (2013) Spectral Frequencies, and GMRS and UHRS (Right) for Callaway .....	2-387
Figure 2.5-10	Low-Frequency (1 Hz, Left), and High-Frequency (10 Hz, Right) Reference Rock Hazard Curves for Comanche Peak. Total Hazard is Shown as a Bold Black Line; Individual Contributions to the Hazard for Each of the CEUS-SSC Sources are Shown as Colored Lines Defined in the Legend. See Table 2.1-1 for Source Name Definitions .....	2-392

Figure 2.5-11	Shear Wave Velocity ( $V_s$ ) Profiles for Comanche Peak. Basecase (BC) Profile Shown as Solid Bold Line; Lower and Upper Range (LR and UR) Profiles Shown as Dashed Lines. Profiles Terminate at Reference Rock Velocity of 2,831 m/sec [9,285 ft/sec] per EPRI GMM (2013).....	2-393
Figure 2.5-12	Overall Weighted Median Site Amplification Factor (SAF) (Upper) and Log Standard Deviation of the SAF (Lower) as a Function of Input Acceleration for EPRI GMM (2013) Spectral Frequencies .....	2-394
Figure 2.5-13	Mean Control Point Hazard Curves (Left) for EPRI GMM (2013) Spectral Frequencies, and GMRS and UHRS (Right) for Comanche Peak.....	2-395
Figure 2.5-14	Low-Frequency (1 Hz, Left), and High-Frequency (10 Hz, Right) Reference Rock Hazard Curves For Cooper. Total Hazard is Shown as a Bold Black Line; Individual Contributions to the Hazard for Each of the CEUS-SSC Sources are Shown as Colored Lines Defined in the Legend. See Table 2.1-1 for Source Name Definitions .....	2-400
Figure 2.5-15	Shear Wave Velocity ( $V_s$ ) Profiles for Cooper. Basecase (BC) Profile Shown as Solid Bold Line; Lower and Upper Range (LR and UR) Profiles Shown as Dashed Lines. Profiles Terminate at Reference Rock Velocity of 2,831 m/sec [9,285 ft/sec] per EPRI GMM (2013) .....	2-401
Figure 2.5-16	Overall Weighted Median Site Amplification Factor (SAF) (Upper) and Log Standard Deviation of the SAF (Lower) as a Function of Input Acceleration for EPRI GMM (2013) Spectral Frequencies .....	2-402
Figure 2.5-17	Mean Control Point Hazard Curves (Left) for EPRI GMM (2013) Spectral Frequencies, and GMRS and UHRS (Right) for Cooper .....	2-403
Figure 2.5-18	Low-Frequency (1 Hz, Left), and High-Frequency (10 Hz, Right) Reference Rock Hazard Curves for Ft. Calhoun. Total Hazard is Shown as a Bold Black Line; Individual Contributions to the Hazard for Each of the CEUS-SSC Sources are Shown as Colored Lines Defined in the Legend. See Table 2.1-1 for Source Name Definitions .....	2-408
Figure 2.5-19	Shear Wave Velocity ( $V_s$ ) Profiles for Ft. Calhoun. Basecase (BC) Profile Shown as Solid Bold Line; Lower and Upper Range (LR and UR) Profiles Shown as Dashed Lines. Profiles Terminate at Reference Rock Velocity of 2,831 m/sec [9,285 ft/sec] per EPRI GMM (2013).....	2-409
Figure 2.5-20	Overall Weighted Median Site Amplification Factor (SAF) (Upper) and Log Standard Deviation of the SAF (Lower) as a Function of Input Acceleration for EPRI GMM (2013) Spectral Frequencies .....	2-410
Figure 2.5-21	Mean Control Point Hazard Curves (Left) for EPRI GMM (2013) Spectral Frequencies, and GMRS and UHRS (Right) for Ft. Calhoun .....	2-411

Figure 2.5-22	Low-Frequency (1 Hz, Left), and High-Frequency (10 Hz, Right) Reference Rock Hazard Curves for Grand Gulf. Total Hazard is Shown as a Bold Black Line; Individual Contributions to the Hazard for Each of the CEUS-SSC Sources are Shown as Colored Lines Defined in the Legend. See Table 2.1-1 for Source Name Definitions .....2-415
Figure 2.5-23	Shear Wave Velocity ( $V_s$ ) Profiles for Grand Gulf. Basecase (BC) Profile Shown as Solid Bold Line; Lower and Upper Range (LR and UR) Profiles Shown as Dashed Lines. Profiles Terminate at Reference Rock Velocity of 2,831 m/sec [9,285 ft/sec] per EPRI GMM (2013).....2-416
Figure 2.5-24	Overall Weighted Median Site Amplification Factor (SAF) (Upper) and Log Standard Deviation of the SAF (Lower) as a Function of Input Acceleration for EPRI GMM (2013) Spectral Frequencies .....2-417
Figure 2.5-25	Mean Control Point Hazard Curves (Left) for EPRI GMM (2013) Spectral Frequencies, and GMRS and UHRS (Right) for Grand Gulf .....2-418
Figure 2.5-26	Low-Frequency (1 Hz, Left), and High-Frequency (10 Hz, Right) Reference Rock Hazard Curves for River Bend. Total Hazard is Shown as a Bold Black Line; Individual Contributions to the Hazard for Each of the CEUS-SSC Sources are Shown as Colored Lines Defined in the Legend. See Table 2.1-1 for Source Name Definitions .....2-422
Figure 2.5-27	Shear Wave Velocity ( $V_s$ ) Profiles for River Bend. Basecase (BC) Profile Shown as Solid Bold Line; Lower and Upper Range (LR and UR) Profiles Shown as Dashed Lines. Profiles Terminate at Reference Rock Velocity of 2,831 m/sec [9,285 ft/sec] per EPRI GMM (2013).....2-423
Figure 2.5-28	Overall Weighted Median Site Amplification Factor (SAF) (Upper) and Log Standard Deviation of the SAF (Lower) as a Function of Input Acceleration for EPRI GMM (2013) Spectral Frequencies .....2-424
Figure 2.5-29	Mean Control Point Hazard Curves (Left) for EPRI GMM (2013) Spectral Frequencies, and GMRS and UHRS (Right) for River Bend .....2-425
Figure 2.5-30	Low-Frequency (1 Hz, Left), and High-Frequency (10 Hz, Right) Reference Rock Hazard Curves for South Texas. Total Hazard is Shown as a Bold Black Line; Individual Contributions to the Hazard for Each of the CEUS-SSC Sources are Shown as Colored Lines Defined in the Legend. See Table 2.1-1 for Source Name Definitions .....2-430
Figure 2.5-31	Shear Wave Velocity ( $V_s$ ) Profiles for South Texas. Basecase (BC) Profile Shown as Solid Bold Line; Lower and Upper Range (LR and UR) Profiles Shown as Dashed Lines. Profiles Terminate at Reference Rock Velocity of 2,831 m/sec [9,285 ft/sec] per EPRI GMM (2013).....2-431

Figure 2.5-32	Overall Weighted Median Site Amplification Factor (SAF) (Upper) and Log Standard Deviation of the SAF (Lower) as a Function of Input Acceleration for EPRI GMM (2013) Spectral Frequencies .....2-432
Figure 2.5-33	Mean Control Point Hazard Curves (Left) for EPRI GMM (2013) Spectral Frequencies, and GMRS and UHRS (Right) for South Texas.....2-433
Figure 2.5-34	Low-Frequency (1 Hz, Left), and High-Frequency (10 Hz, Right) Reference Rock Hazard Curves for Waterford. Total Hazard is Shown as a Bold Black Line; Individual Contributions to the Hazard for Each of the CEUS-SSC Sources are Shown as Colored Lines Defined in the Legend. See Table 2.1-1 for Source Name Definitions ....2-437
Figure 2.5-35	Shear Wave Velocity ( $V_s$ ) Profiles for Waterford. Basecase (BC) Profile Shown as Solid Bold Line; Lower and Upper Range (LR and UR) Profiles Shown as Dashed Lines. Profiles Terminate at Reference Rock Velocity of 2,831 m/sec [9,285 ft/sec] per EPRI GMM (2013).....2-438
Figure 2.5-36	Overall Weighted Median Site Amplification Factor (SAF) (Upper) and Log Standard Deviation of the SAF (Lower) as a Function of Input Acceleration for EPRI GMM (2013) Spectral Frequencies .....2-439
Figure 2.5-37	Mean Control Point Hazard Curves (Left) for EPRI GMM (2013) Spectral Frequencies, and GMRS and UHRS (Right) for Waterford .....2-440
Figure 2.5-38	Low-Frequency (1 Hz, Left), and High-Frequency (10 Hz, Right) Reference Rock Hazard Curves for Wolf Creek. Total Hazard is Shown as a Bold Black Line; Individual Contributions to the Hazard for Each of the CEUS-SSC Sources are Shown as Colored Lines Defined in the Legend. See Table 2.1-1 for Source Name Definitions ....2-445
Figure 2.5-39	Shear Wave Velocity ( $V_s$ ) Profiles for Wolf Creek. Basecase (BC) Profile Shown as Solid Bold Line; Lower and Upper Range (LR and UR) Profiles Shown as Dashed Lines. Profiles Terminate at Reference Rock Velocity of 2,831 m/sec [9,285 ft/sec] per EPRI GMM (2013).....2-446
Figure 2.5-40	Overall Weighted Median Site Amplification Factor (SAF) (Upper) and Log Standard Deviation of the SAF (Lower) as a Function of Input Acceleration for EPRI GMM (2013) Spectral Frequencies .....2-447
Figure 2.5-41	Mean Control Point Hazard Curves (Left) for EPRI GMM (2013) Spectral Frequencies, and GMRS and UHRS (Right) for Wolf Creek .....2-448
Figure 3.1-1	Digital Elevation Model of the Western United States Showing the Location of the Plant Sites Relative to the Major Tectonic Features of Western North America. The Base Digital Elevation Model is Derived from the USGS National Elevation Dataset .....3-2

Figure 3.2-1	Digital Topographic Map of Northern Mexico (Including the Northern Baja Peninsula and the Northern Gulf of California), Western Arizona, and Southern California Showing the Location of the PVNGS Relative to Geographic and Tectonic Features. The Base Digital Elevation Model is Derived from the USGS National Elevation Dataset .....	3-6
Figure 3.2-2	Map of the United States Southwest Showing the Distribution of Earthquakes Relative to Physiographic Provinces, Quaternary Faults, and Other Tectonic Features. The Earthquake Epicenters are from the U.S. Geological Survey (USGS) Advanced National Seismic System Catalog, Spanning the Period 1900–2018.....	3-7
Figure 3.2-3	Map of Faults in the California Strike-Slip Boundary, Redrafted from Dorsey and Umhoefer (2012). The PVNGS Site is Just Off the Right Edge of the Map .....	3-9
Figure 3.2-4	Map Showing the Two-Zone (Top Panel) and Six-Zone (Bottom Panel) Areal Source Alternatives. The Large Circle is the Area Within a Radius of 400 km [250 mi] of the PVNGS (Star). Redrafted from Figures 9-2 and 9-7 in APS (2015).....	3-13
Figure 3.2-5	Final 18 Fault Sources Included in PVNGS Hazard Calculations. The Black Star Shows the Location of the PVNGS Site. Redrafted from Figure 11-1 in APS (2015).....	3-16
Figure 3.2-6	Example Map of 2,000 Sampled Models in Sammon’s Space, for 100 Hz (0.01 Second Period). Model A and Model B Represent Two Alternative Distance Measures Used in the Common Functional Form. The Red Dots Show the Location of the Candidate or Seed GMPEs Used to Develop the Ground Motion Distributions. The Magenta and Cyan Dots Show Plus and Minus Two Standard Deviations in Epistemic Uncertainty, Respectively, about the Seed GMPEs. Modified from Figure 6.4.3-3 in the SWUS GMC Report (GeoPentech, 2015) .....	3-21
Figure 3.2-7	Total Mean Site-Specific Rock Hazard Curves Showing Seven Spectral Frequencies, Based on the Data in Table 2 in Cadogan (2015a) .....	3-24
Figure 3.2-8	(a) Site-Specific Rock Hazard Curves Showing Total Mean Hazard and Contributions from Area Sources and Faults for 10 Hz Spectral Acceleration (from Figure 10 in Cadogan, 2015a) and (b) Site-Specific Rock Hazard Curves Showing Total Mean Hazard and Contributions from Area Sources and Faults for 1 Hz Spectral Acceleration (Redrafted from Figure 11 in Cadogan, 2015a).....	3-25
Figure 3.2-9	Location of the Virtual Faults for the SBR (Blue) and TZ (brown) Areal Source Zones (Outlined in Black) Relative to the PVNGS Site (Red Triangle).....	3-27

Figure 3.2-10	Mean Hazard Curves for the SBR (Blue Lines) and TZ (Brown Lines) Areal Sources Showing the Staff’s PSHA Confirmatory Analysis Results (Solid Heavy Lines) and the Licensee’s Results (Dashed Heavy Lines).....	3-28
Figure 3.2-11	Basecase Profile for (a) Surface Response Spectra and (b) Site Amplification Factors for $10^{-5}$ High Frequency Input Motion (Reference Rock Spectral Amplitudes of 0.01–1.50g) Using The EPRI Soil Material Model, and a Single Reference Rock to Local Rock Adjustment Function, Showing Spectra for 60 Individual Randomized Profiles (Green Lines), Median (Black Solid Line), and $\pm 1\sigma_{in}$ (Black Dashed Lines). Redrafted from Figure 41 in Cadogan (2015a). Basecase Profile for (c) Median Amplification Factors and (d) Log Standard Deviation as a Function of Spectral Acceleration. Redrafted from Figure 42 in Cadogan (2015a).....	3-31
Figure 3.2-12	(a) Total Mean Site-Specific Control Point Hazard Curves Plotted for Seven Spectral Frequencies, Based on the Data in Table 10 in Cadogan (2015a), (b) Uniform Hazard Response Spectra and the GMRS are Plotted Based on the Data from Table 11 in Cadogan (2015a).....	3-32
Figure 3.3-1	Simplified Geologic Map of the Central California Coast Showing the Location of the DCP, Reprinted from Figure 2.01 in PG&E (2015a). The Inset Image on the Left is an Aerial Photograph Showing the Power Plant on Top of the Late Quaternary Marine Terrace.....	3-34
Figure 3.3-2	Control Point Design Spectra for the DCP, Replotted from the Data Provided in PG&E (2015a) .....	3-35
Figure 3.3-3	Regional Seismicity Patterns from Recorded Earthquakes Between 1987 and 2013 Relative to the Mapped Traces of Known Faults, Redrafted from Figure 5-16 in PG&E (2015b) .....	3-36
Figure 3.3-4	Seismicity Patterns and Focal Mechanisms for the Central California Coastal Region Based on Hardebeck (2010) for Events Between 1987 and 2008. Redrafted from Figure 5-24 in PG&E (2015b) .....	3-37
Figure 3.3-5	Slip-Rate Estimates for the Hosgri Fault from the SSC Model Showing (a) the Locations of the Four Sites with Cumulative Slip-Rate Probabilities and (b) the Mean Cumulative Slip-Rate Curve. Both Figures were Derived from Figures 8-13 and 8-33 in PG&E (2015b) .....	3-44
Figure 3.3-6	Location Map of the Half Graben Fault, Modified from Figure 1.2-1 in PG&E (2014), Showing Full Trace of the Half Graben Fault with Respect to the Hosgri Fault Trace.....	3-45

Figure 3.3-7	Map View of the Principal Geometric Elements of the Hosgri and Half Graben Faults Showing how the Magnitude and Slip Rate of Hosgri-Parallel Slip are Calculated from the Extension with the Half Graben Pull-Apart Basin. Heave is the Measured Horizontal Offset of the Fault.....	3-46
Figure 3.3-8	An Example Seismic Reflection Line from the USGS 2008–2009 High-Resolution Sparker Tracklines, Showing (a) the Initial Unconformity Horizon and Fault Interpretations, along with the Four Regional Unconformities (H10, H30, H40 East, and UNCON2) and (b) the Modeled Half Graben Fault Geometry and Attributes .....	3-47
Figure 3.3-9	Calculated Horizontal Slip Rate for the Hosgri Fault Over Time. Black Line Connects Each Slip Rate for Seismic Lines that Contain All Four Unconformities. The Inset Chart Shows the Average Slip Rate Based on Each Age Unconformity .....	3-48
Figure 3.3-10	Shaded Relief Image of the Bedrock Surface Interpreted from 3D Seismic-Reflection Data in the San Luis Obispo Bay Study Area. The Image Shows a Series of Paleochannels Now Buried Offshore. The Shoreline Fault Cuts Across these Paleochannels with Little or No Detectable Offset. Redrafted from Figure 8-35 in PG&E (2015b).....	3-50
Figure 3.3-11	Example Sammon’s Map for 100 Hz Spectral Acceleration, Redrafted from Figure 6.4.4-1 of the SWUS GMC Report (GeoPentech, 2015), Showing the 2,000 Models Derived from the Common-Form Models (Gray Dots), the Common-Form Models that Fit to the Candidate or Seed GMPEs (Red Dots), and the Common-Form Models that Fit to the Candidate GMPEs, Including Plus and Minus Epistemic Uncertainty (Magenta and Cyan Dots, Respectively). The Solid Black Line Shows the Smallest Shape that Encloses these Points .....	3-53
Figure 3.3-12	Total Mean Site-Specific Rock Hazard Curves for Seven Spectral Frequencies, Redrafted from Figure 2.2.2-3 in PG&E (2015a) .....	3-55
Figure 3.3-13	Reference Rock Hazard by Source for 1 Hz and 10 Hz Spectral Accelerations, Redrafted from Figures 2.2.2-1 and 2.2.2-2 in PG&E (2015a) .....	3-56
Figure 3.3-14	Results of the NRC Staff’s Confirmatory Analysis for the Hosgri Fault, Showing the Individual Analyses, Assuming Median Slip Rate, for each GMPE (Thin Light-Blue Lines); Staff Mean Confirmatory Results for Three Fault Slip Rates (Dashed Blue Lines); the Licensee’s Mean Result (Orange Line); and the Licensee’s Total Mean Result (Red Line).....	3-58
Figure 3.3-15	Results of the NRC Staff’s Confirmatory Analysis for the Shoreline Fault, Showing the Individual Analyses, Assuming Median Slip Rate, for Each GMPE (Thin Light-Blue Lines); Staff Mean Confirmatory Results for Three Fault Slip Rates (Dashed Blue Lines); the Licensee’s Mean Result (Green Line); and the Licensee’s Total Mean Result (Red Line).....	3-59

Figure 3.3-16	Results of the NRC Staff’s Confirmatory Analysis for the Virtual Faults Showing the Mean Hazard Curves for Each of the Virtual Faults (Thin Light-Blue Lines), the Overall Mean Result (Dashed Blue Line), the Licensee’s Mean Result (Green Line), and the Licensee’s Total Mean Result (Red Line).....	3-60
Figure 3.3-17	Aerial View of the DCPD Site Location, Basemap (from Google Maps). Red Squares Indicate Location of ESTA27 (South of Turbine Building) and ESTA28 (North of the Turbine Building) .....	3-61
Figure 3.3-18	(a) Shear Wave Velocity Profiles (Colored Lines) Beneath the DCPD Powerblock and Turbine Building Region. Heavy Black Curves Show the Central, Upper, and Lower Profiles from Figure 2.2 in PG&E (2015c). (b) Comparison of the Host $V_s$ Profile (Labeled Reference 760) and the Central, Upper, and Lower Profiles for the Target, from Figure 2.3 in PG&E (2015c).....	3-63
Figure 3.3-19	Empirical Site Term for the DCPD, Showing the results of NRC Staff’s Confirmatory Analyses (Red Lines) and the Licensee’s Analyses in PG&E (2015c) .....	3-65
Figure 3.3-20	Comparison of the NRC and Licensee Amplification Factors Using the Analytical Site Terms for SWUS Reference Rock {760 m/sec [2,493 ft/sec]} with 0.2g and 1.07g PGA .....	3-66
Figure 3.3-21	(a) Total Mean Site-Specific Control Point Hazard Curves Plotted for Seven Spectral Frequencies, Based on the Data in PG&E (2015c). (b) UHRS and GMRS are Plotted Based on the Data from Table 6-1 in PG&E (2015c).....	3-67
Figure 3.4-1	Tectonic Setting of the Hanford Site Modified from Figure 1 of Blakely et al. (2014). Cascade Volcanic Peaks in Washington: Mount Rainier (MR), Mount Adams (MA), and Mount Saint Helens (MSH) .....	3-68
Figure 3.4-2	Map of the Pacific Northwest Showing the Distribution of Earthquakes Relative to the Physiographic Provinces, Quaternary Faults, and Other Tectonic Features. The Earthquake Epicenters are from the USGS Advanced Nation Seismic System Catalog Spanning 1900–2018.....	3-70
Figure 3.4-3	The 20 Fault Sources the SSC TI Team Identified for Inclusion in the SSC Model: Ahtanum Ridge (AR), Arlington (AF), Cleman Mountain (CM), Columbia Hills (CH), Frenchman Hills (FH), Horn Rapids (HR), Horse Heaven Hills (HHH), Laurel (LF), Luna Butte (LB), Manastash Ridge (MR), Maupin (MF), Rattles of the Rattlesnake-Rallula (RAW) Alignment, Rattlesnake Hills (RH), Rattlesnake Mountain (RM), Saddle Mountains (SM), Seattle Fault Zone (SFZ), Selah Butte (SB), Toppenish Ridge (TR), Umtanum Ridge (UM), and Wallula Fault (WF). The Figure was Adapted from Figure 8.43 in PNNL (2014) .....	3-72



Figure 3.4-4	Block Diagram Showing the Seismic Sources Related to the Cascadia Subduction Zone, Modified from Dzurisin et al. (2014). The Subduction Interface Source is Labeled “Seismogenic Zone.” The Episodic Tremor and Slip (ETS) Zone Approximates the Fore-Arc Mantle Corner of McCrory et al. (2014), which is the Line of Intersection of the Fore-Arc Moho with the Plate Interface. Example Focal Mechanisms for Historic Earthquakes are Identified to Represent the Kind of Seismicity Typical for Each Zone. The Volcanic Arc Forms the Axis of the Cascade Range. The CGS Site is Right (East) of the Cascade Range and would be Located Off the Image to the Right .....	3-79
Figure 3.4-5	Seismic Source Zones Characterized in the SSC Model and Earthquake Epicenters in the Hanford PSHA Crustal Catalog with $M \geq 1.85$ . Red Lines Indicate Fault Sources. The Figure was Adapted from Figure 8.1 of PNNL (2014). E[M] is the Expected Moment Magnitude as Defined in NUREG-2115 (NRC, 2012b).....	3-80
Figure 3.4-6	Range of Magnitude Scaling Produced by Crustal Footwall GMPEs. The Illustration is for PGA, and for the Reverse Faulting Case with the Site Located on the Footwall of the Fault. The Different Site-To-Source Distances are in Terms of the Parameter Rx, which is the Perpendicular (to Fault Strike) Distance to the Site from the Fault Line (Surface Projection of Top of Rupture), Positive in the Downdip Direction (in km). The Four NGA-West2 GMPEs are Shown by Colored Lines, the Nine Scaled Backbone Models are Solid Black Lines, and the Total Range in Epistemic Uncertainty is Indicated by the Gray Shaded Area. To Convert km to Miles, Divide by 1.61 .....	3-84
Figure 3.4-7	(a) The Reference Baserock Probabilistic Seismic Hazard Curves for the CGS Site for PGA and Six Spectral Accelerations, Based on the Data in Table 2.2.2-2a in Swank (2015a). (b) The Mean UHRS for the $10^{-4}$ , $10^{-5}$ , and $10^{-6}$ Annual Exceedance Frequencies, Based on the Data in Table 2.2.2-1 in Swank (2015a) .....	3-87
Figure 3.4-8	Generalized Stratigraphy of the Hanford Site and Vicinity Showing the Location of the Reference Baserock Horizon, which is Atop the Uppermost Low in the Wanapum Basalt. The Figure was Adapted from Figure 2.1 in Barnett et al. (2007).....	3-88
Figure 3.4-9	(a) The NRC Staff’s Confirmatory Calculation for the Rattlesnake Mountain Fault, which uses 27 of the 189 Crustal Earthquake GMPEs (Light-Blue Lines). Hazard Curves (Blue Dashed Lines) Result from Using the 5th and 95th Percentile Slip Rates for the Rattlesnake Mountain Fault. The NRC Staff’s Confirmatory Results (Solid Blue Line) Closely Match the Licensee’s Results (Solid Green Line), for 1 Hz (b) and 10 Hz (c) .....	3-89

Figure 3.4-10	(a) Observed (Black Line) and Modeled (Colored Lines) Topography Using the SSC TI Team’s Fault-Source Parameters and the NRC Staff’s Elastic Dislocation Model for the Saddle Mountain Fault. (b) Observed (Black Line) Topography and Differences in Modeled (Colored Lines) Topography Generated by Increasing the Fault Slip-Rate by 30 to 50 Percent in the Staff’s Elastic Dislocation Model .....	3-91
Figure 3.4-11	The NRC Staff’s Deterministic Models of the 84 <sup>th</sup> Percentile Spectral Acceleration at the CGS Site from an <i>M</i> 9.1 Earthquake Occurring 320 km [200 mi] (Upper Dashed Line) and 350 km [218 mi] (Lower Dashed Line) from the Site in the Cascadia Subduction Zone, Showing a SSE and Operating-Basis Earthquake for the CGS Plant for Comparison .....	3-92
Figure 3.4-12	(a) The NRC Staff’s Confirmatory Analysis Showing the Location of Virtual Faults for the YFTB Source Zone in the Vicinity of the CGS Site (Red Triangle). The NRC Staff’s Hazard Curves for Each of the 324 YFTB Virtual Faults (Light-Blue Lines) are Shown with Staff’s (Thick Blue Line) and PNNL (2014) (Dashed Blue Line) Mean Hazard Curves for 1 Hz (b) and 10 Hz (c).....	3-94
Figure 3.4-13	Geologic Profile and Estimated Layer Thicknesses for the Strata Beneath the CGS Site, Compiled from the Data in Section 2.3 in Swank (2015a). To Convert Depth and <i>V<sub>s</sub></i> Values (m to ft), Multiply the Values by 3.28. To Convert from Density Values (g/cm <sup>3</sup> to lb/ft <sup>3</sup> ), Multiply the Values by 62.48.....	3-95
Figure 3.4-14	Measured Shear Wave Velocities and the NRC Staff’s Shear Wave Profiles in Upper Strata. WNP (Red Lines) Represents <i>V<sub>s</sub></i> Measurements Made for WNP Site Investigations (PNNL, 2014). In Earlier Licensing Documentation, the CGS Plant was Referred to as the Washington Public Power Supply System Nuclear Project (WNP) .....	3-98
Figure 3.4-15	Comparison of the NRC staff’s Confirmatory Analyses with the Licensee’s Amplification Functions and Amplification Function Log Standard Deviation for (a) 1 Hz Amplification, (b) 10 Hz Amplification, (c) 1 Hz Log Standard Deviation, and (d) 100 Hz Log Standard Deviation.....	3-99
Figure 3.4-16	Comparison of the Licensee’s and the NRC Staff’s Hazard Curves at (a) 1 Hz Spectral Acceleration and (b) 100 Hz Spectral Acceleration .....	3-100
Figure 3.4-17	(a) Total Mean Site-Specific Control Point Hazard Curves Plotted for Seven Spectral Frequencies, Based on the Data in Tables 2.3.7-1 through 2.3.7.7 in Swank (2015a). (b) Uniform Hazard Response Spectra and the GMRS are Plotted Based on the Data from Table 2.4-1 in Swank (2015a).....	3-101

Figure 4.2-1	Amplification Factors as a Function of Frequency for Class A NPP Sites. Upper Panel Results are for Low Input Loading Level (PGA = 0.06g), and Lower Panel Results are for Intermediate Input Loading Level (PGA = 0.58g) .....	4-4
Figure 4.2-2	Normalized GMRS Results for Class A Sites. Average Normalized Spectral Shape is Shown by Red Curve, and Individual Sites are Shown by Thin Black Lines.....	4-5
Figure 4.3-1	Amplification Factors as a Function of Frequency for Class B NPP Sites. Upper Panel Results are for Low Input Loading Level (PGA = 0.06g), and Lower Panel Results are for Intermediate Input Loading Level (PGA = 0.58g) .....	4-7
Figure 4.3-2	Normalized GMRS Results for Class B Sites. Average Normalized Spectral Shape is Shown by Red Curve, and Individual Sites are Shown by Thin Black Lines.....	4-8
Figure 4.4-1	Amplification Factors as a Function of Frequency for Class C NPP Sites. Upper Panel Results are for Low Input Loading Level (PGA = 0.06g), and Lower Panel Results are for Intermediate Input Loading Level (PGA = 0.58g) .....	4-10
Figure 4.4-2	Normalized GMRS Results for Class C Sites. Average Normalized Spectral Shape is Shown by Red Curve, and Individual Sites are Shown by Thin Black Lines.....	4-11
Figure 4.5-1	Amplification Factors as a Function of Frequency for Class D NPP Sites. Upper Panel Results are for Low Input Loading Level (PGA = 0.06g), and Lower Panel Results are for Intermediate Input Loading Level (PGA = 0.58g) .....	4-13
Figure 4.5-2	Normalized GMRS Results for Class D Sites. Average Normalized Spectral Shape is Shown by Red Curve, and Individual Sites are Shown by Thin Black Lines.....	4-14



## LIST OF TABLES

Table 1.2-1	Nuclear Power Plant SHSR and NRC Staff Assessments .....	1-3
Table 1.3-1	Nuclear Power Plant SPRAs and NRC Staff Assessments .....	1-5
Table 2.1-1	CEUS Seismic Sources in NUREG-2115 .....	2-5
Table 2.2-1	Region I Plant Names, Site Names, States, Geology, Physiographic Provinces, and Co-Located ESPs/COLs .....	2-17
Table 2.2-2	Layer Depths, Shear Wave Velocities ( $V_s$ ), Unit Weights, and Dynamic Properties for Beaver Valley .....	2-21
Table 2.2-3	Layer Depths, Shear Wave Velocities ( $V_s$ ), Unit Weights, and Dynamic Properties for Calvert Cliffs .....	2-28
Table 2.2-4	Layer Depths, Shear Wave Velocities ( $V_s$ ), Unit Weights, and Dynamic Properties for Ginna .....	2-35
Table 2.2-5	Layer Depths, Shear Wave Velocities ( $V_s$ ), Unit Weights, and Dynamic Properties for Hope Creek-Salem .....	2-43
Table 2.2-6	Layer Depths, Shear Wave Velocities ( $V_s$ ), Unit Weights, and Dynamic Properties for Indian Point .....	2-50
Table 2.2-7	Layer Depths, Shear Wave Velocities ( $V_s$ ), Unit Weights, and Dynamic Properties for Fitzpatrick and Nine Mile Point .....	2-58
Table 2.2-8	Layer Depths, Shear Wave Velocities ( $V_s$ ), Unit Weights, and Dynamic Properties for Limerick .....	2-66
Table 2.2-9	Layer Depths, Shear Wave Velocities ( $V_s$ ), Unit Weight, and Dynamic Properties for Millstone .....	2-73
Table 2.2-10	Layer Depths, Shear Wave Velocities ( $V_s$ ), Unit Weights, and Dynamic Properties for Oyster Creek .....	2-81
Table 2.2-11	Layer Depths, Shear Wave Velocities ( $V_s$ ), Unit Weights, and Dynamic Properties for Peach Bottom .....	2-88
Table 2.2-12	Layer Depths, Shear Wave Velocities ( $V_s$ ), Unit Weights, and Dynamic Properties for Pilgrim .....	2-95
Table 2.2-13	Layer Depths, Shear Wave Velocities ( $V_s$ ), Unit Weights, and Dynamic Properties for Susquehanna .....	2-106
Table 2.2-14	Layer Depths, Shear Wave Velocities ( $V_s$ ), Unit Weights, and Dynamic Properties for Three Mile Island .....	2-113

Table 2.3-1	Region II CEUS Plant Names, Site Names, States, Geology, Physiographic Provinces, and Co-Located ESPs/COLs.....	2-119
Table 2.3-2	Layer Depths, Shear Wave Velocities ( $V_s$ ), Unit Weights and Dynamic Properties for Bellefonte .....	2-123
Table 2.3-3	Layer Depths, Shear Wave Velocities ( $V_s$ ), Unit Weights, and Dynamic Properties for Browns Ferry .....	2-131
Table 2.3-4	Layer Depths, Shear Wave Velocities ( $V_s$ ), Unit Weights, and Dynamic Properties for Brunswick.....	2-139
Table 2.3-5	Layer Depths, Shear Wave Velocities ( $V_s$ ), Unit Weights, and Dynamic Properties for Catawba .....	2-146
Table 2.3-6	Layer Depths, Shear Wave Velocities ( $V_s$ ), Unit Weights, and Dynamic Properties for Farley .....	2-154
Table 2.3-7	Layer Depths, Shear Wave Velocities ( $V_s$ ), Unit Weights, and Dynamic Properties for Harris.....	2-162
Table 2.3-8	Layer Depths, Shear Wave Velocities ( $V_s$ ), Unit Weights, and Dynamic Properties for Hatch.....	2-169
Table 2.3-9	Layer Depths, Shear Wave Velocities ( $V_s$ ), Unit Weights, and Dynamic Properties for McGuire.....	2-177
Table 2.3-10	Layer Depths, Shear Wave Velocities ( $V_s$ ), Unit Weights, and Dynamic Properties for North Anna .....	2-184
Table 2.3-11	Layer Depths, Shear Wave Velocities ( $V_s$ ), Unit Weights, and Dynamic Properties for Oconee.....	2-191
Table 2.3-12	Layer Depths, Shear Wave Velocities ( $V_s$ ), Unit Weights, and Dynamic Properties for Robinson .....	2-198
Table 2.3-13	Layer Depths, Shear Wave Velocities ( $V_s$ ), Unit Weights, and Dynamic Properties for Sequoyah .....	2-205
Table 2.3-14	Layer Depths, Shear Wave Velocities ( $V_s$ ), Unit Weights, and Dynamic Properties for St. Lucie .....	2-212
Table 2.3-15	Layer Depths, Shear Wave Velocities ( $V_s$ ), Unit Weights, and Dynamic Properties for Summer.....	2-220
Table 2.3-16	Layer Depths, Shear Wave Velocities ( $V_s$ ), Unit Weights, and Dynamic Properties for Surry.....	2-227
Table 2.3-17	Layer Depths, Shear Wave Velocities ( $V_s$ ), Unit Weights, and Dynamic Properties for Turkey Point.....	2-234

Table 2.3-18	Layer Depths, Shear Wave Velocities ( $V_s$ ), Unit Weights, and Dynamic Properties for Vogtle .....	2-242
Table 2.3-19	Layer Depths, Shear Wave Velocities ( $V_s$ ), Unit Weights, and Dynamic Properties for Watts Bar .....	2-249
Table 2.4-1	Region III CEUS Plant Names, Site Names, States, Geology, Physiographic Provinces, and Co-Located ESPs/COLs .....	2-254
Table 2.4-2	Layer Depths, Shear Wave Velocities ( $V_s$ ), Unit Weights, and Dynamic Properties for Braidwood .....	2-260
Table 2.4-3	Layer Depths, Shear Wave Velocities ( $V_s$ ), Unit Weights, and Dynamic Properties for Byron .....	2-268
Table 2.4-4	Layer Depths, Shear Wave Velocities ( $V_s$ ), Unit Weights, and Dynamic Properties for Clinton .....	2-276
Table 2.4-5	Layer Depths, Shear Wave Velocities ( $V_s$ ), Unit Weights, and Dynamic Properties for Davis Besse .....	2-283
Table 2.4-6	Layer Depths, Shear Wave Velocities ( $V_s$ ), Unit Weights, and Dynamic Properties for Cook .....	2-291
Table 2.4-7	Layer Depths, Shear Wave Velocities ( $V_s$ ), Unit Weights, and Dynamic Properties for Dresden .....	2-299
Table 2.4-8	Layer Depths, Shear Wave Velocities ( $V_s$ ), Unit Weights, and Dynamic Properties for Duane Arnold .....	2-306
Table 2.4-9	Layer Depths, Shear Wave Velocities ( $V_s$ ), Unit Weights, and Dynamic Properties for Fermi .....	2-313
Table 2.4-10	Layer Depths, Shear Wave Velocities ( $V_s$ ), Unit Weights, and Dynamic Properties for LaSalle .....	2-320
Table 2.4-11	Layer Depths, Shear Wave Velocities ( $V_s$ ), Unit Weights, and Dynamic Properties for Monticello .....	2-327
Table 2.4-12	Layer Depths, Shear Wave Velocities ( $V_s$ ), Unit Weights, and Dynamic Properties for Palisades .....	2-335
Table 2.4-13	Layer Depths, Shear Wave Velocities ( $V_s$ ), Unit Weights, and Dynamic Properties for Perry .....	2-342
Table 2.4-14	Layer Depths, Shear Wave Velocities ( $V_s$ ), Unit Weights, and Dynamic Properties for Prairie Island .....	2-350
Table 2.4-15	Layer Depths, Shear Wave Velocities ( $V_s$ ), Unit Weights, and Dynamic Properties for Point Beach .....	2-358

Table 2.4-16	Layer Depths, Shear Wave Velocities ( $V_s$ ), Unit Weights, and Dynamic Properties for Quad Cities .....	2-365
Table 2.5-1	Region IV CEUS Plant Names, Site Names, States, Geology, Physiographic Provinces, and Co-Located ESPs/COLs.....	2-370
Table 2.5-2	Layer Depths, Shear Wave Velocities ( $V_s$ ), Unit Weights, and Dynamic Properties for Arkansas .....	2-375
Table 2.5-3	Layer Depths, Shear Wave Velocities ( $V_s$ ), Unit Weights, and Dynamic Properties for Callaway.....	2-383
Table 2.5-4	Layer Depths, Shear Wave Velocities ( $V_s$ ), Unit Weights, and Dynamic Properties for Comanche Peak.....	2-391
Table 2.5-5	Layer Depths, Shear Wave Velocities ( $V_s$ ), Unit Weights, and Dynamic Properties for Cooper .....	2-399
Table 2.5-6	Layer Depths, Shear Wave Velocities ( $V_s$ ), Unit Weights, and Dynamic Properties for Ft. Calhoun.....	2-407
Table 2.5-7	Layer Depths, Shear Wave Velocities ( $V_s$ ), Unit Weights, and Dynamic Properties for Grand Gulf.....	2-414
Table 2.5-8	Layer Depths, Shear Wave Velocities ( $V_s$ ), Unit Weights, and Dynamic Properties for River Bend .....	2-421
Table 2.5-9	Layer Depths, Shear Wave Velocities ( $V_s$ ), Unit Weights, and Dynamic Properties for South Texas .....	2-429
Table 2.5-10	Layer Depths, Shear Wave Velocities ( $V_s$ ), Unit Weights, and Dynamic Properties for Waterford .....	2-436
Table 2.5-11	Layer Depths, Shear Wave Velocities ( $V_s$ ), Unit Weights, and Dynamic Properties for Wolf Creek .....	2-443
Table 3.2-1	Source Characterization Parameters for the Two-Zone Areal Source Alternative.....	3-14
Table 3.2-2	Source Characterization Parameters for the Six-Zone Areal Source Alternative.....	3-14
Table 3.2-3	Summary of Seismic Hazard Characteristics for the 18 Fault Sources in the PVNGS SSC Model .....	3-17
Table 3.4-1	Summary of Fault Characterization Data for Fault Sources in the Yakima Fold and Thrust Belt .....	3-77
Table 3.4-2	Summary of Source Characterization Parameters for Areal Sources .....	3-82
Table 4.1-1	NEHRP Site Classifications .....	4-1



Table 4.2-1	NEHRP Class A Nuclear Power Plant Sites .....	4-3
Table 4.3-1	NEHRP Class B Nuclear Power Plant Sites .....	4-6
Table 4.4-1	NEHRP Class C Nuclear Power Plant Sites .....	4-9
Table 4.5-1	NEHRP Class D Nuclear Power Plant Sites .....	4-12
Table 5.1-1	Nuclear Power Plant Data File References in ADAMS .....	5-2



## EXECUTIVE SUMMARY

Following the accident at the Fukushima Dai-ichi nuclear power plant (NPP), and in response to Commission direction, the U.S. Nuclear Regulatory Commission (NRC) established the Near-Term Task Force to reevaluate U.S. nuclear plant safety. Near-Term Task Force Recommendation 2.1 and subsequent NRC staff requirements memoranda instructed the NRC staff to issue requests for information to licensees pursuant to Title 10 of the *Code of Federal Regulations* (10 CFR) 50.54(f) [50.54(f) letter]. The 50.54(f) letter (NRC, 2012a) requested that licensees perform a reevaluation of the seismic hazards at their sites using present-day NRC requirements and guidance to develop a ground motion response spectrum (GMRS) for comparison with the plant Safe Shutdown Earthquake Ground Motion (SSE) in order to determine whether further plant risk assessments were warranted. Present-day NRC requirements and guidance with respect to characterizing seismic hazards use a probabilistic approach in order to develop a risk-informed performance-based GMRS for the site. In response to the 50.54(f) letter, licensees submitted Seismic Hazard and Screening Reports (SHSRs) for each of their plant sites. The individual plant screening assessments performed by the NRC staff subsequent to its evaluation of the SHSRs are complete, and plants that screened in for further risk evaluations have completed their assessments. Section 1 of this NUREG/KM presents the ADAMS accession numbers for the NRC staff assessments of the SHSRs for all operating U.S. NPPs and holders of construction permits in active or deferred status. Therefore, this NUREG/KM does not provide further comparisons between the NRC staff's confirmatory GMRS and the plant SSEs, but documents for reference the NRC staff's processes and analyses.

The purpose of this report is to capture in a single document the information used by the NRC staff to evaluate the updated probabilistic seismic hazard analyses at U.S. NPPs. This includes a compilation and synthesis of information provided by the licensees in the SHSRs, information collected by the NRC staff during its confirmatory reviews of the SHSRs, and information subsequently collected by the NRC staff from the scientific and engineering literature. As such, this report provides the current best estimate of site-specific seismic hazards at each NPP that can be used in the future to assess the implications of new data, models, and methods on facility safety, consistent with the NRC staff's process for ongoing assessment of natural hazard information (NRC 2016, 2017).

This report summarizes the seismic hazard characterization for each U.S. NPP and compares the licensee's hazard characterization and the NRC staff's confirmatory analyses. The NRC has published the plant-specific data files developed by the NRC staff and presented in this report in the NRC's Agencywide Documents Access and Management System (ADAMS) online library along with an explanatory file [ADAMS Accession No. ML21133A274 (package)]. Section 1 of this report provides background information and introduces the contents of the NUREG/KM. Section 2 of the NUREG/KM provides hazard curves for each NPP in the central and eastern United States (CEUS), organized alphabetically within NRC region subsections (i.e., Regions 1–4). The CEUS studies conducted by licensees and the NRC staff relied on the updated regional Electric Power Research Institute (EPRI) ground motion characterization (GMC) (EPRI, 2013) and seismic source characterization (SSC) models in NUREG-2115, "Central and Eastern United States Seismic Source Characterization for Nuclear Facilities," issued January 2012 (NRC, 2012b), to develop the hazards.

Section 3 of this report presents the hazard information for the three NPPs in the western United States (WUS). The document describes WUS plants separately because the 50.54(f) letter specified that WUS licensees should develop SSC and GMC models using the Senior Seismic

Hazard Advisory Committee (SSHAC) Level 3 process. These site-specific SSHAC Level 3 studies were necessary for the WUS sites because these sites could not use the models that were previously approved by the NRC staff for the licensees in the CEUS. As a result, Section 3 describes the SSHAC processes conducted by each of the WUS licensees, the resulting SSC and GMC models, and confirmatory studies conducted by the NRC staff. For the WUS sites, the NRC staff also reviewed the site-specific site response analyses and the final GMRS. Section 4 of this report contains site amplification factors and response spectra classified by the type of site (i.e., the types of rock and soil), and Section 5 provides the document conclusion and path forward for future use of this report.

## **References**

Electric Power Research Institute (EPRI). "EPRI Ground Motion Model Review Final Report." Palo Alto, CA. June 3, 2013. ADAMS Accession No. ML13155A553.

U.S. Nuclear Regulatory Commission (NRC). "Proposed Resolution of Remaining Tier 2 and 3 Recommendations Resulting from the Fukushima Dai-ichi Accident." SECY-16-0144. Washington, DC. December 26, 2016. ADAMS Accession No. ML16286A552.

NRC. "Staff Requirements—SECY-16-0144—Proposed Resolution of Remaining Tier 2 and 3 Recommendations Resulting from the Fukushima Dai-ichi Accident." SRM-SECY-16-0144. Washington, DC. May 3, 2017.

NRC. Letter from Eric J. Leeds, Director, Office of Nuclear Reactor Regulation, and Michael R. Johnson, Director, Office of New Reactors, to All Power Reactor Licensees and Holders of Construction Permits in Active or Deferred Status. Washington, DC. March 12, 2012a. ADAMS Accession No. ML12053A340.

NRC. NUREG-2115, "Central and Eastern United States Seismic Source Characterization for Nuclear Facilities." Washington, DC. January 2012b.

## ACKNOWLEDGMENTS

The authors wish to acknowledge and extend our sincere appreciation to some of the many individuals who contributed to the results presented in this document.

Developing the framework for conducting the post-Fukushima Near-Term Task Force seismic re-evaluations was the product of lengthy discussions between the U.S. Nuclear Regulatory Commission (NRC) staff and many nuclear industry and seismic experts. The authors especially thank Nilesh Chokshi, Scott Flanders, Bob Kennedy, John Richards, Greg Hardy, Robin McGuire, Jeff Kimball, and Walt Silva.

We also thank all our current and former NRC colleagues who participated in the NRC's independent evaluations as well as the review of all licensee submittals: Diane Jackson, Scott Stovall, Thomas Weaver, Dogan Seber, David Heeszal, Vladimir Graizer, Stephanie Devlin-Gill, Rasool Anooshehpour, Lisa Schleicher, Zuhan Xi, Yong Li, Tianqing Cao, Sarah Tabatabai, Laurel Bauer, Brittain Hill, LUISSETTE Candelario-Quintana and Gerry Stirewalt.

Staff from the Center for Nuclear Waste Regulatory Analyses (Ronnie McGinnis, Alan Morris, Kristin Ulmer, and Nora Naukam) provided outstanding technical and administrative support.

Scott Stovall and Dogan Seber were instrumental in the conduct of this project and facilitated the technical and contractual support.

Luisette Candelario-Quintana oversaw the final edits and guided the document to publication.



## ABBREVIATIONS AND ACRONYMS

2D	two dimensional
3D	three dimensional
ADAMS	Agencywide Documents Access and Management System
ac	acre
AF	amplification factor
AFE	annual frequency of exceedance
APS	Arizona Public Service
BSSC	Building Seismic Safety Council
CCCSIP	Central Coastal California Seismic Imaging Project
CEUS	central and eastern United States
CEUS-SSC	CEUS seismic source characterization
CFR	<i>Code of Federal Regulations</i>
CGS	Columbia Generating Station
COL	combined license
CRADA	Cooperative Research and Development Agreement
DCCP	Diablo Canyon Power Plant
DOE	U.S. Department of Energy
ECC-AM	Extended Continental Crust—Atlantic Margin
ECC-GC	Extended Continental Crust—Gulf Coast
EPR	equivalent Poisson ratios
EPRI	Electric Power Research Institute
ESP	early site permit
ETS	episodic tremor and slip
FAS	Fourier amplitude spectra
FSAR	final safety analysis report
ft	foot/feet
g	acceleration due to gravity
GI	Generic Issue
GMC	ground motion characterization
GMM	ground motion model
GMPE	ground motion prediction equations
GMRS	ground motion response spectrum/spectra
GPS	Global Positioning System
Hz	Hertz
IBEB	Illinois Basin Extended Basement
in.	inch
ISFSI	independent spent fuel storage installation

ka	<i>kilo annum</i>
KM	knowledge management
km	kilometer(s)
LTSP	Long-Term Seismic Program
m	meter(s)
<b>M</b>	magnitude
Ma	<i>mega annum</i>
mi	mile(s)
MIDC-A	Midcontinent Craton (Geometry A)
mm	millimeter
msec	millisecond(s)
MSIV	main stream isolation valve
MSL	mean sea level
NEI	Nuclear Energy Institute
NGA-West2	Next Generation Attenuation
NMFS	New Madrid Fault System
NPP	nuclear power plant
NRC	U.S. Nuclear Regulatory Commission
NTTF	Near-Term Task Force
pcf	pounds per cubic foot
PEER	Pacific Earthquake Engineering Research
PEZ-N	Paleozoic Extended Crust (Narrow Geometry)
PG&E	Pacific Gas and Electric Company
PGA	peak ground acceleration
PNNL	Pacific Northwest National Laboratory
POANHI	Process for Ongoing Assessment of Natural Hazard Information
PPRP	participatory peer review panel
PSEG	Public Service Enterprise Group
PSHA	probabilistic seismic hazard analysis
PTC	Pennsylvania Turnpike Commission
PVNGS	Palo Verde Nuclear Generating Station
R2.1	Near-Term Task Force Recommendation 2.1
RG	regulatory guide
RLME	repeated large-magnitude earthquake
RQD	rock quality designation
RVT	random vibration theory
SAF	site amplification factor
SASW	spectral analysis of surface waves
SBR	Southern Basin and Range
SCE&G	South Carolina Electric & Gas
sec	second(s)
SHSR	Seismic Hazard and Screening Reports
SLPB	San Luis Pismo Block
SLR	St. Lawrence Rift
SPID	Screening, Prioritization, and Implementation Details



SPT	Standard Penetration Test
SRM	Staff Requirements Memoranda
SRM	staff requirements memorandum/memoranda
SSC	seismic source characterization
SSE	Safe Shutdown Earthquake Ground Motion
SSHAC	Senior Seismic Hazard Analysis Committee
SWUS	southwestern United States
TI	Technical Integration
TVA	Tennessee Valley Authority
TZ	Transition Zone
UCERF3	Uniform California Earthquake Rupture Forecast model
UFSAR	Updated Final Safety Analysis Reports
UHRS	uniform hazard response spectrum/spectra
USGS	U.S. Geological Survey
WAACY	Wooddell, Abrahamson, Acevedo-Cabrera, and Youngs
WUS	western United States
YFTB	Yakima Fold and Thrust Belt
yr	year



# 1 INTRODUCTION

U.S. Nuclear Regulatory Commission (NRC) regulations and associated regulatory guidance provide a robust regulatory approach for the evaluation of site hazards associated with natural phenomena. However, this framework has evolved over time as new information on site hazards and potential consequences has become available. As a result, while all plants are adequately protected against seismic events, the licensing basis, design, and level of protection from natural phenomena differ among the existing operating reactors in the United States, depending on when the plant was constructed and licensed for operation. Additionally, the assumptions and factors that were considered in determining the level of protection necessary at these sites vary depending on a number of contributing factors. The state of knowledge of external hazards has evolved significantly since the licensing of many of the plants within the United States.

On March 11, 2011, the Great East Japan Earthquake and tsunami, which struck off the east coast of the island of Honshu, triggered an accident at the Fukushima Dai-ichi nuclear power plant (NPP). This accident demonstrated significant consequences with respect to the potential impacts of beyond-design-basis events at NPP sites. The NRC conducted many assessments and lessons-learned activities following this event to ensure the safety of U.S. NPPs. The NRC has posted information about these actions on the NRC's Web site at <https://www.nrc.gov/reactors/operating/ops-experience/japan-info.html>. Specific to the topic of this NUREG/KM, to assess the potential impacts of beyond-design-basis events, the NRC requested information and analysis from licensees that reevaluated the hazards assumed for U.S. plants and the ability of plants to cope with and protect against such hazards using current techniques and models. This document provides background information about seismic hazard evaluations before the Fukushima accident and summarizes information specific to seismic hazard reevaluations for U.S. NPPs in response to the Fukushima accident.

## 1.1 Seismic Hazard Reevaluations Under Generic Issue-199

Nearly a decade before the accident at the Fukushima NPP, in support of early site permits for new reactors, the NRC staff<sup>1</sup> reviewed updates to seismic source models and ground motion models (GMMs) provided by applicants. The updated seismic information included new models to estimate earthquake ground motion and updated models for earthquake sources in seismic regions around Charleston, South Carolina, and New Madrid, Missouri. The staff reviewed and evaluated this new information along with recent U.S. Geological Survey seismic hazard estimates for the central and eastern United States (CEUS). From this review, the staff determined that the estimated seismic hazard levels at some current CEUS operating NPP sites might be higher than the seismic hazard values used in design and previous evaluations and concluded that this issue should be evaluated under the Generic Issue process. The NRC staff conducted screening analyses and further evaluations and issued the August 2010 document, "Generic Issue 199 (GI-199): Implications of Updated Probabilistic Seismic Hazard Estimates in Central and Eastern United States on Existing Plants, Safety/Risk Assessment" [Agencywide Documents Access and Management System (ADAMS) Accession No. ML100270582] (NRC, 2010a), which discusses updates to estimates of the seismic hazard in the CEUS and the safety implications thereof. In addition, the NRC staff issued Information Notice 2010-18, "Generic Issue 199, 'Implications of Updated Probabilistic Seismic Hazard Estimates in Central and

---

<sup>1</sup> The term "NRC staff" refers in this document to staff of the NRC or NRC staff supplemented by staff from the Center for Nuclear Waste Regulatory Analyses (CNWRA®).

Eastern United States on Existing Plants,” dated September 2, 2010 (ADAMS Accession No. ML101970221) (NRC, 2010b).

## **1.2 Post-Fukushima Near-Term Task Force Recommendation 2.1, the 50.54(f) Letter, and Subsequent Actions**

On March 11, 2011, a magnitude 9 (*M*9) earthquake struck Japan and was followed by a 14-meter (m) [45-foot (ft)] tsunami, resulting in extensive damage to the nuclear power reactors at the Fukushima Dai-ichi facility. The accident had a profound impact on the nuclear power industry. Nuclear regulators and NPP operators worldwide immediately began evaluating the accident to identify whether there was a need for action to ensure continued safe operation of their facilities. As a result, the process for resolving GI-199 was incorporated into the NRC’s lessons-learned activities and updated seismic hazard evaluations.

Following the accident at the Fukushima NPP, the NRC established the Near-Term Task Force (NTTF) in response to Commission direction. The NTTF charter, dated March 30, 2011, tasked the NTTF with conducting a systematic and methodical review of NRC processes and regulations and determining whether the agency should make additional improvements to its regulatory system. In SECY-11-0093, “Near-Term Report and Recommendations for Agency Actions Following the Events in Japan,” dated July 12, 2011 (NRC, 2011a), the NRC staff recommended a set of actions to clarify and strengthen the regulatory framework for protection against natural hazards. In particular, NTTF Recommendation 2.1, and subsequent staff requirements memoranda (SRM) associated with Commission papers SECY-11-0124, “Recommended Actions To Be Taken Without Delay from the Near-Term Task Force Report,” dated September 9, 2011 (NRC, 2011b), and SECY-11-0137, “Prioritization of Recommended Actions To Be Taken in Response to Fukushima Lessons Learned,” dated October 3, 2011 (NRC, 2011c), instructed the NRC staff to issue requests for information to licensees pursuant to Title 10 of the *Code of Federal Regulations* (10 CFR) 50.54(f). By letter dated March 12, 2012 (NRC, 2012a), the NRC issued a request for information to all power reactor licensees and holders of construction permits in active or deferred status, pursuant to 10 CFR 50.54(f) on conditions of license [referred to as the “50.54(f) letter”]. Enclosure 1 to the 50.54(f) letter requested that addressees reevaluate the seismic hazards at their sites using present-day NRC requirements and guidance to develop a ground motion response spectrum (GMRS). Finally, the 50.54(f) letter requested that licensees compare the GMRS with the plant Safe Shutdown Earthquake Ground Motion (SSE) in order to determine whether further plant risk assessments were warranted.

Present-day NRC requirements and guidance with respect to characterizing seismic hazards use a probabilistic approach in order to develop a risk-informed, performance-based GMRS for the site. Regulatory Guide 1.208, “A Performance-Based Approach To Define the Site-Specific Earthquake Ground Motion,” issued March 2007 (NRC, 2007), describes an acceptable approach for estimating the site hazard and a GMRS.

By letter dated November 27, 2012 (NEI, 2012), the Nuclear Energy Institute (NEI) submitted Electric Power Research Institute (EPRI) Report 1025287, “Seismic Evaluation Guidance: Screening, Prioritization and Implementation Details (SPID) for the Resolution of Fukushima NTTF Recommendation 2.1 Seismic” (EPRI, 2012) (hereafter called the SPID). The SPID provided guidance to support licensees in responding to the 50.54(f) letter in a manner that addressed the requested information items in the letter’s Enclosure 1. By letter dated February 15, 2013 (NRC, 2013a), the NRC staff endorsed the SPID.

The required response section of Enclosure 1 to the 50.54(f) letter specified that CEUS licensees must provide their Seismic Hazard and Screening Reports (SHSRs) within 1.5 years of issuance of the 50.54(f) letter. However, in order to complete its update of the EPRI seismic GMMs for the CEUS (EPRI, 2013), the industry proposed a 6-month extension, to March 31, 2014, for submitting the SHSRs. By letter dated May 7, 2013 (NRC, 2013b), the NRC determined that the modified schedule was acceptable, and by letter dated August 28, 2013 (NRC, 2013c), the NRC determined that the updated GMM (EPRI, 2013) was acceptable for use by CEUS plants in developing a site-specific GMRS. By letter dated April 9, 2013 (Pietrangelo, 2013), the industry committed to following the SPID to develop the SHSRs for existing NPPs.

For NPPs in the western United States (WUS), the required response section of Enclosure 1 to the 50.54(f) letter specified that WUS licensees provide their SHSRs within 2.5 years of the letter's issuance. The NRC granted the WUS licensees an additional year to submit the SHSRs because the sites could not use the updated EPRI seismic GMMs and seismic source characterization (SSC) models that CEUS licensees were able to rely upon (NRC, 2012b; EPRI, 2013). As specified in Enclosure 1 to the 50.54 (f) letter, the WUS licensees used the Senior Seismic Hazard Analysis Committee (SSHAC) Level 3 process to develop the ground motion characterization (GMC) and SSC models necessary for each of the WUS sites.

All CEUS sites submitted their SHSRs by March 2014, and all WUS sites submitted their SHSRs by March 2015. By December 2017, the NRC staff completed its assessment of the SHSRs for all operating U.S. NPPs and holders of construction permits in active or deferred status. For plants that were in the process of ceasing operations, the NRC staff verified that certifications were docketed and the licenses no longer authorized operation of the reactors or placement or retention of fuel in the reactor vessels. Therefore, these plants ultimately received relief from responding to the 50.54(f) letter (i.e., the plants did not submit an SHSR and are not included in Table 1.2-1). Subsequent to the NRC's reviews of the hazard reevaluations, several other operating plants have ceased operation or have made plans to do so. For completeness, this document includes all of the plants evaluated by the NRC staff. Individual staff assessments document the NRC staff's evaluations of the SHSR submittals, as shown in Table 1.2-1.

<b>Plant Name</b>	<b>SHSR</b>	<b>Staff Assessment</b>
Arkansas Nuclear 1 and 2	ML14092A021	ML15344A109
Beaver Valley 1 and 2	ML14092A203	ML15274A307
Bellefonte 1 and 2*	ML14098A478	ML15180A366
Braidwood 1 and 2	ML14091A005	ML16014A188
Browns Ferry 1, 2, and 3	ML14098A478	ML15090A745
Brunswick 1 and 2	ML14090A236	ML16041A435
Byron 1 and 2	ML14091A010	ML16027A045, Supplemental Staff Assessment ML16070A116
Callaway	ML14090A448	ML15063A517
Calvert Cliffs 1 and 2	ML14099A196	ML15153A073
Catawba 1 and 2	ML14093A052	ML15096A513
Clinton	ML14091A011	ML15281A226
Columbia	ML15078A243	ML16285A410

**Table 1.2-1 Nuclear Power Plant SHSR and NRC Staff Assessments (cont.)**

<b>Plant Name</b>	<b>SHSR</b>	<b>Staff Assessment</b>
Comanche Peak 1 and 2	ML14099A197	ML16014A125
Cooper	ML14094A040	ML15240A030
D.C. Cook 1 and 2	ML14092A329	ML15097A196
Davis-Besse	ML14092A203	ML15230A289
Diablo Canyon 1 and 2	ML15071A046	ML16341C057
Dresden 2 and 3	ML14091A012	ML15097A519
Duane Arnold <sup>†</sup>	ML14092A331	ML15324A176
Farley 1 and 2	ML14092A020	ML15287A092
Fermi 2	ML14090A326	ML15077A028
FitzPatrick	ML14090A243	ML16043A411
Fort Calhoun <sup>†</sup>	ML14097A087	ML15329A181
Ginna	ML14099A196	ML15153A026
Grand Gulf 1	ML14090A098	ML15348A379
Harris 1	ML14090A441	ML15349A149
Hatch 1 and 2	ML14092A017	ML15097A424
Hope Creek 1	ML14087A436	ML16049A609
Indian Point 2 and 3 <sup>†</sup>	ML14099A110, ML14099A111	ML15096A340
LaSalle 1 and 2	ML14091A013	ML15013A132
Limerick 1 and 2	ML14090A236	ML15296A492
McGuire 1 and 2	ML14098A421	ML15182A067
Millstone 2 and 3	ML14092A417	ML15328A268, Supplemental Staff Assessment ML16057A785
Monticello	ML14136A288	ML15175A336
Nine Mile Point 1 and 2	ML14099A196	ML15153A660
North Anna 1 and 2	ML14092A416	ML15057A249
Oconee 1, 2, and 3	ML14092A024	ML15201A008
Oyster Creek <sup>†</sup>	ML14090A241	ML15350A353
Palisades	ML14090A069	ML15098A032
Palo Verde 1, 2, and 3	ML15076A073	ML16221A604
Peach Bottom 2 and 3	ML14090A247	ML15051A262
Perry 1	ML14092A203	ML15208A034
Pilgrim 1 <sup>†</sup>	ML14092A023	ML15051A336
Point Beach 1 and 2	ML14090A275	ML15211A593
Prairie Island 1 and 2	ML14086A628	ML15341A162
Quad Cities 1 and 2	ML14090A526	ML15309A493
River Bend 1	ML14091A426	ML15295A186
Robinson 2	ML14099A204	ML15280A199
Saint Lucie 1 and 2	ML14099A106	ML15352A053
Salem 1 and 2	ML14090A043	ML16041A033
Seabrook 1	ML14092A413	ML15208A049
Sequoyah 1 and 2	ML14098A478	ML15098A641
South Texas 1 and 2	ML14099A235	ML15287A077
Surry 1 and 2	ML14092A414	ML15335A093
Susquehanna 1 and 2	ML14086A163	ML15356A247

<b>Plant Name</b>	<b>SHSR</b>	<b>Staff Assessment</b>
Three Mile Island 1 <sup>†</sup>	ML14090A271	ML15223A215
Turkey Point 3 and 4	ML14106A032	ML16013A472
V.C. Summer Unit 1 <sup>†</sup>	ML14092A250	ML15194A055
Vogtle 1 and 2	ML14092A019	ML15054A296
Waterford 3	ML14086A427	ML15335A050
Watts Bar 1 and 2	ML14098A478	ML15055A543 (Unit 1) ML15111A377 (Unit 2)
Wolf Creek 1	ML14097A020	ML15216A320
*Plant is not operational.		
†Plant was shut down or has subsequently shut down.		

### **1.3 Purpose and Overview of This Report**

The purpose of this report is to capture in a single document the information used to develop probabilistic seismic hazard analyses at U.S. NPPs to date. This includes a compilation and synthesis of (1) information provided by the licensees in the SHSRs, (2) information collected by the NRC staff during its reviews, and (3) information subsequently collected by the NRC staff from the scientific and engineering literature.

As described in the 50.54(f) letter and Section 3 of the SPID, the GMRS each of the licensees developed was compared to the plant SSE to determine (screen) which plants needed to perform new seismic risk evaluations. The individual plant screening assessments are complete and are not redone in this NUREG/KM. Plants that screened in for further risk evaluations have completed their assessments. It is important to note that the site GMRS itself is not an indication of plant safety. Rather, the NRC staff used the GMRS as an input to characterize the seismic demand on the facility relative to the plant structural capacity, as represented by the SSE. It is also important to note that the results contained within this report do not supersede or change the conclusions documented in the staff assessment for each NPP. Individual staff assessments document the NRC staff's evaluations of the SPRAs submittals, as shown in Table 1.3-1.

<b>Plant Name</b>	<b>No. of Units</b>	<b>SPRA</b>	<b>Staff Assessment</b>
Beaver Valley	2	ML17213A014	ML18092A837
Browns Ferry	3	ML19351E391	ML20255A000
Callaway	1	ML19225D321	ML20210L323
Columbia	1	ML19273A907	ML20076A547
DC Cook	2	ML19310D805	ML20232A894
Diablo Canyon	2	ML18120A201	ML18254A040
Dresden	2	ML19304B567	ML20105A507
North Anna	2	ML18093A445	ML19052A522
Oconee	3	ML19004A127	ML19267A022
Peach Bottom	2	ML18240A065	ML19053A469
Robinson	1	ML20084P290	ML20156A093
Sequoyah	2	ML19291A003	ML20143A175
VC Summer	1	ML18271A109	ML19199A696
Vogtle	2	ML17088A130	ML17293A427
Watts Bar	2	ML17181A485	ML18115A138

The information compiled in this document represents current best knowledge and practices for characterizing site-specific seismic hazards that evolved as new data, models, and methods were developed. As such, this document provides the current best estimate of site-specific seismic hazard at each NPP that can be used in the future to assess the implications of new data, models, and methods on facility safety, consistent with the NRC staff's process for ongoing assessment of natural hazard information. Because new data continue to become available and methodologies for assessing hazards continue to evolve, the NRC will use the information gained through recent hazard reevaluations as a baseline to facilitate proactive and systematic risk-informed assessments of the implications of new natural hazards information. In SECY-16-0144, "Proposed Resolution of Remaining Tier 2 and 3 Recommendations Resulting from the Fukushima Dai-ichi Accident," dated December 29, 2016 (NRC, 2016), the NRC staff describes a dedicated process to ensure the ongoing aggregation and assessment of new natural hazard information. Consistent with the direction provided in SRM-SECY-16-0144, dated May 3, 2017 (NRC, 2017), the NRC staff continues to collect information in order to assess the potential hazard implications for individual NPP sites. In this way, new information will further refine and enhance confidence in the site-specific hazard estimates that would be used in future site-specific evaluations. The NRC refers to this as the Process for Ongoing Assessment of Natural Hazard Information (POANHI).

The updated assessments for each of the CEUS plants are presented in Section 2 of this report and include revised site profiles, amplification factors, hazard curves, uniform hazard response spectra (UHRS), and GMRS. These results are presented in graphical and tabular format for each of the NPP sites, along with a description of the local site geology and any updates or refinements made to the previous confirmatory analyses in the NRC's staff assessments.

Section 3 of this report contains information about the NRC staff assessments conducted for the power plants in the WUS. The WUS submittals were reviewed by NRC staff with contract support from the Center for Nuclear Waste Regulatory Analyses (CNWRA<sup>®</sup>) at Southwest Research Institute<sup>®</sup> (SwRI<sup>®</sup>) (hereafter referred to as "the NRC staff"). In contrast to the CEUS, each of the WUS plants conducted new probabilistic seismic hazard analysis studies that included new site-specific SSC and GMC models and new site-specific site response analyses. As a result, Section 3 describes the SSHAC processes conducted, the seismic SSC and GMC model development, and confirmatory studies conducted by the NRC staff. For the WUS sites, the NRC staff reviewed the SSHAC Level 3 studies used to develop the SSC and GMC models, the resulting reference point hazards, the site-specific site response analyses, and the final control point hazards, emphasizing how the NRC staff identified and evaluated the most significant contributors to the resulting seismic hazards.

Section 4 of this report contains site amplification factors and response spectra classified by the type of site (i.e., the types of rock and soil). These spectra show distinct shapes that are typical for soil and rock sites and can be used to develop seismic design response spectra. Section 5 provides the document conclusion and path forward for future use of this report. This section includes a table that references an ADAMS archive of the hazard results discussed throughout this report.



## 1.4 References

*Code of Federal Regulations* (CFR), "Domestic licensing of production and utilization facilities." Part 50, Chapter 1, Title 10, "Energy." Washington, DC. September 2019.

Electric Power Research Institute (EPRI). "EPRI Ground Motion Model Review Final Report." Palo Alto, CA. June 3, 2013. ADAMS Accession No. ML13155A553.

EPRI. "Seismic Evaluation Guidance, Screening, Prioritization and Implementation Details (SPID) for the Resolution of Fukushima Near-Term Task Force Recommendation 2.1: Seismic." EPRI Report 1025287. Palo Alto, CA. November 27, 2012. ADAMS Accession No. ML12333A170.

Nuclear Energy Institute (NEI). Letter from Kimberly Keithline, Senior Project Manager, to David L. Skeen, Director, Japan Lessons Learned Project Directorate, U.S. Nuclear Regulatory Commission, Final Draft of Industry Seismic Evaluation Guidance (EPRI 1025287). Washington, DC. November 27, 2012. ADAMS Accession No. ML12333A168.

U.S. Nuclear Regulatory Commission (NRC). "Proposed Resolution of Remaining Tier 2 and 3 Recommendations Resulting from the Fukushima Dai-ichi Accident." SECY-16-0144. Washington, DC. December 29, 2016. ADAMS Accession No. ML16286A552.

NRC. "Staff Requirements—SECY-16-0144—Proposed Resolution of Remaining Tier 2 and 3 Recommendations Resulting from the Fukushima Dai-ichi Accident." SRM-SECY-16-0144. Washington, DC. May 3, 2017b.

NRC. Letter from David L. Skeen, Director, Japan Lessons-Learned Directorate, to Joseph E. Pollock, Executive Director, NEI, Endorsement of Electric Power Research Institute Draft Report 1025287, "Seismic Evaluation Guidance." Washington, DC. February 15, 2013a. ADAMS Accession No. ML12319A074.

NRC. Letter from Eric J. Leeds to Joseph Pollock, Executive Director, NEI, Acceptance Letter for NEI Submittal of Augmented Approach, Ground Motion Model Update Project, and 10 CFR 50.54(f) Schedule Modifications Related to the NTF Recommendation 2.1, Seismic Reevaluations. Washington, DC. May 7, 2013b. ADAMS Accession No. ML13106A331.

NRC. Letter from D.L. Skeen to K.A. Keithline, NEI, Approval of Electric Power Research Institute Ground Motion Model Review Project Final Report for Use by Central and Eastern United States Nuclear Power Plants. Washington, DC. August 28, 2013c. ADAMS Accession No. ML13233A102.

NRC. Letter from Eric J. Leeds, Director, Office of Nuclear Reactor Regulation, and Michael R. Johnson, Director, Office of New Reactors, to All Power Reactor Licensees and Holders of Construction Permits in Active or Deferred Status. Washington, DC. March 12, 2012a. ADAMS Accession No. ML12053A340.

NRC. "Near-Term Report and Recommendations for Agency Actions Following the Events in Japan." SECY-11-0093. Washington, DC. July 12, 2011a. ADAMS Accession No. ML11186A950.

NRC. "Recommended Actions To Be Taken Without Delay from the Near-Term Task Force Report." SECY-11-0124. Washington, DC. September 9, 2011b. ADAMS Accession No. ML11245A158.

NRC. "Prioritization of Recommended Actions To Be Taken in Response to Fukushima Lessons Learned." SECY-11-0137. Washington, DC. October 3, 2011c. ADAMS Accession No. ML11272A111.

NRC. "Results of Safety/Risk Assessment Results for Generic Issue 199, Implications of Updated Probabilistic Seismic Hazard Estimates in Central and Eastern United States on Existing Plants." Washington, DC. 2010a. ADAMS Accession No. ML100270582.

NRC. "Generic Issue 199, 'Implications of Updated Probabilistic Seismic Hazard Estimates in Central and Eastern United States on Existing Plants.'" Information Notice 2010-18. Washington, DC. September 2, 2010b. ADAMS Accession No. ML101970221.

NRC. "A Performance-Based Approach To Define the Site-Specific Earthquake Ground Motion." Regulatory Guide 1.208. Washington, DC. March 2007. ADAMS Accession No. ML070310619.

Piترangelo, A.R. Letter from NEI to D.L. Skeen, NRC, Proposed Path Forward for NTTF Recommendation 2.1: Seismic Reevaluations. Washington, DC. April 9, 2013. ADAMS Accession No. ML13101A254.

## 2 CENTRAL AND EASTERN UNITED STATES SITES

### 2.1 CEUS Seismic Hazard Methodology

#### 2.1.1 Background

As described more fully in Section 1 of this report, on March 12, 2012, the U.S. Nuclear Regulatory Commission (NRC) issued a request for information to all power reactor licensees and holders of construction permits (NRC, 2012a) to provide updated seismic hazard assessments under Title 10 of the *Code of Federal Regulations* (10 CFR) 50.54(f). This “50.54(f) letter” (NRC, 2012a) specified that licensees in the central and eastern United States (CEUS) use the following models to develop seismic hazard curves at the reference rock horizon:

- CEUS Seismic Source Characterization (CEUS-SSC) model in NUREG-2115, “Central and Eastern United States Seismic Source Characterization for Nuclear Facilities,” issued January 2012 (NRC, 2012b)
- Electric Power Research Institute (EPRI) (2004, 2006) ground motion model (GMM) for the CEUS, which was subsequently updated (EPRI, 2013).

The 50.54(f) letter also asked licensees to evaluate the local site response to develop site-specific hazard curves and a ground motion response spectrum (GMRS) for comparison with the plant Safe Shutdown Earthquake Ground Motion (SSE).

The regional CEUS-SSC model (NRC, 2012b) was developed as a Senior Seismic Hazard Analysis Committee (SSHAC) Level 3 study. EPRI developed the GMM (EPRI, 2013) as a SSHAC Level 2 update of the earlier SSHAC Level 3 EPRI GMM (EPRI, 2004, 2006). The NRC staff had reviewed and endorsed these studies before the licensees submitted responses to the 50.54(f) letter for individual nuclear power plants (NPPs). Therefore, both the NRC staff and the licensees were able to use these two regional studies to develop updated reference horizon hazards. Because these regional models were already developed and approved, the licensees’ hazard assessment primarily focused on characterizing the dynamic properties of the materials beneath their sites that may amplify or deamplify ground motions as they propagate from the reference horizon at depth to the ground surface.

Recognizing the challenge of a timely review of over 60 submittals from sites across the United States, the NRC staff adopted a phased review strategy. First, the NRC staff interacted with industry during development of the guidance in EPRI Report 1025287, “Seismic Evaluation Guidance: Screening, Prioritization and Implementation Details (SPID) for the Resolution of Fukushima Near-Term Task Force Recommendation 2.1: Seismic,” dated November 27, 2012 (EPRI, 2012) (hereafter called the SPID). The NRC staff subsequently endorsed the SPID. Second, while licensees were developing Seismic Hazard and Screening Reports (SHSRs) in response to the 50.54(f) letter, the NRC staff developed initial independent site response models for all CEUS sites. Third, the NRC staff developed a preliminary probabilistic seismic hazard analysis (PSHA) for all sites that combined the CEUS-SSC (NRC, 2012b), the EPRI GMM (EPRI, 2013), and facility-specific site amplification factors. This approach provided important technical insights that enhanced the efficiency and effectiveness of the NRC staff’s review of the subsequent licensee submittals. After receiving the submittals, the NRC staff refined its preliminary results based on site information in the SHSRs and each licensee’s Updated Final Safety Analysis Report (UFSAR). The NRC staff used these refined confirmatory

reviews to calculate a GMRS for comparison with the licensees' GMRS for each NPP site. The staff assessment produced for each site (Table 1.2-1) documents the results of the NRC staff reviews of the licensee submittals and the NRC staff's determination about the licensee path forward.

This section presents the methodology for the NRC staff's independent review for each CEUS site that responded to the 50.54(f) letter; a staff assessment for each site documents this review. Because the NRC staff reviewed the 50.54(f) letter responses within a compressed timeline, the analyses presented in this section benefitted from additional research by the NRC staff to obtain more detailed information related to the site geology and dynamic properties. In addition, the NRC staff has been able to further assess and refine the site response guidance in Appendix B to the SPID (EPRI, 2012). Consequently, the resulting control point<sup>1</sup> hazard curves and final GMRS presented in this section may differ from the NRC staff's initial assessments; however, these differences are not significant. Even though the NRC staff was able to further refine the stratigraphic profiles for many of the plant sites based on additional research, there is still considerable uncertainty in determining the deeper portion of the site profiles beneath the plant foundations for many of the older plants. For these older plants, the geologic and geophysical investigations focused primarily on the uppermost layers and the stability of the rock or soil layers supporting the plant foundations. As such, the NRC staff's refined site geologic profiles provide a more likely but not definitive interpretation of the site geology. To address the uncertainty in the site geologic profiles, the licensees and NRC staff used the guidance in Appendix B to the SPID, which specifies use of logic trees to capture alternative data and models. Appropriate and systematic consideration of uncertainty is a key component of the SSHAC process and is an important part of demonstrating the reasonable assurance of safety.

In summary, the site-specific control point hazard curves and response spectra presented in this section represent the NRC staff's most complete and thorough characterization of the hazard for each of the NPP sites and will be used as the baseline to evaluate future data, models, and methods on facility safety. However, these updated seismic hazard curves and spectra developed by the NRC staff should not be considered definitive due to the inherent uncertainties in defining subsurface soil and rock properties; characterizing the location, size, and frequency of future earthquakes associated with each seismic source; and predicting the ground motions resulting from these seismic sources. In conclusion, the results presented in this NUREG/KM for each U.S. NPP do not invalidate the NRC staff's conclusions in the staff assessment for each site nor the NRC staff's subsequent screening determinations.

### **2.1.2 Seismic Source Characterization Model**

This section describes the NRC staff's implementation of the CEUS-SSC model for its seismic hazard evaluations of the CEUS NPP sites. As described in NUREG-2115 (NRC, 2012b), the purpose of the CEUS-SSC model is to develop a seismic source model for the CEUS that includes consideration of an updated geologic database, full assessment and incorporation of uncertainties, and the range of diverse technical interpretations from the larger technical community. The primary uses of the model have been for regional seismic source

---

<sup>1</sup> In accordance with the 50.54(f) letter, the GMRS comparison screening was completed using the licensing-basis definition of the Safe Shutdown Earthquake Ground Motion (SSE) control point. The SSE control point is a specific location (elevation) beneath the NPP foundation where the SSE ground motions are computed. For many NPP sites, the control point is defined in the licensee's Final Safety Analysis Report (FSAR). For NPP sites that don't have an SSE control point defined in the FSAR, the SSE control point is defined using the criteria in EPRI (2013), Section 2.4.2.

characterizations for early site permit (ESP) and combined license (COL) applications as well as updated hazard assessments for existing NPPs in the CEUS. Because the CEUS-SSC model was developed in accordance with the SSHAC guidelines, all credible data and interpretations were appropriately considered in the development of seismic source geometries and parameters, including earthquake magnitude distributions, rates of activity, and characteristics of earthquake faulting.

The CEUS-SSC is a regional model, developed to calculate seismic hazard at potential or existing nuclear facilities. As described in Chapter 9 of NUREG-2115 (NRC, 2012b), for site-specific applications, local data sets (including local geologic structures or local seismic sources) that were not captured in the CEUS-SSC model should be reviewed for potential site-specific refinements to the model. However, for the purposes of Near-Term Task Force (NTTF) Recommendation 2.1 (R2.1) seismic hazard reevaluations, the NRC staff and industry determined that the use of the CEUS-SSC regional model as published was adequate, as documented in the SPID (EPRI, 2012). The NRC staff and industry based this determination on recognition that the NRC completed NUREG-2115 just before the Fukushima event. The NRC staff's confirmatory analyses presented in this Section 2 of this document have focused on incorporating additional local geologic information to better characterize the dynamic properties for each site response analysis. For this report, the NRC staff continued to implement the CEUS-SSC model without refinements. However, future reevaluations of the seismic hazard at existing nuclear facilities will need to consider potential updates to the source geometries and parameters of the model.

The CEUS-SSC model defines two types of seismic sources. The first type of seismic source characterizes the contribution to hazard from repeated large-magnitude earthquakes (RLMEs). RLMEs are defined based on paleoseismic evidence for the occurrence of two or more earthquakes with moment magnitudes ( $M$ ) that are greater than or equal to  $M6.5$  that occur in approximately the same location over periods of a few thousand years. The second type of seismic source characterizes the contribution to hazard from distributed seismicity and serves as background zones to the RLME sources. For the distributed seismicity sources, the developers of the CEUS-SSC model implemented two alternative approaches:

- (1) The first approach defines seismic source boundaries based on differences in the degree of Mesozoic crustal extension. Wheeler (2009) summarizes the various analytical and statistical methods used to derive the maximum magnitude ( $M_{max}$ ) for source zones in the CEUS. His work identified marginal differences in estimates of  $M_{max}$  depending on whether the underlying continental crust experienced significant extension of North America following the breakup of the Pangea supercontinent during the Mesozoic Era. The Bayesian approach to estimating  $M_{max}$  described in Section 5.2.1.1 of NUREG-2115 (NRC, 2012b) uses a prior distribution that is defined based on a statistical analysis of the updated global Stable Continental Region database.
- (2) The second approach defines seismic sources based on their different seismotectonic characteristics (e.g., depth of seismicity, style of faulting, and  $M_{max}$ ). For its hazard evaluations, the NRC staff used a radius of 320 kilometers (km) [200 miles (mi)] around the site for the distributed seismicity sources and a radius of 500 km [310 mi] for the RLMEs, with the exception of the New Madrid Fault System (NMFS) and Charleston RLMEs. For these two RLMEs, which have higher recurrence rates, the NRC staff used a radius of 800 km [500 mi]. Figure 2.1-1 shows the Charleston RLME (Charleston regional source configuration) and the NPP sites that included this RLME for their respective hazard characterizations.

In summary, the NRC staff fully implemented the CEUS-SSC logic tree branches, as described in the Hazard Input Document (HID) in NUREG-2115, Appendix H (NRC, 2012b), to develop mean hazard curves for each site. Table 2.1-1 lists the CEUS-SSC distributed seismicity sources (seismotectonic and  $M_{\max}$  zones) and the RLMEs.

### **2.1.3 Ground Motion Model**

This section describes the NRC staff's implementation of the updated EPRI GMM (2013) for its seismic hazard evaluations of the CEUS NPP sites. The purpose of the 2013 EPRI study was to develop an updated CEUS GMM for use by licensees to respond to the NRC's 50.54(f) letter (EPRI, 2013). The EPRI GMM (2013) is an update to an earlier GMM (EPRI, 2004, 2006) and was carried out as a SSHAC Level 2 study, conducted in two phases. Phase 1 assembled an up-to-date database and determined whether the existing EPRI GMM (2004, 2006) needed to be updated. Based on the affirmative outcome of Phase 1, Phase 2 updated the EPRI GMM (2004, 2006) by integrating up-to-date data, models, and methods. The licensees have used the updated EPRI GMM (2013) primarily to evaluate the seismic hazards in response to the NRC's 50.54(f) letter and for siting applications for potential new nuclear facilities in the CEUS. Since the development of the 2013 updated EPRI GMM, the NRC staff reviewed the implementation of the SSHAC process and determined that all relevant data, models, and methods were evaluated and integrated and appropriate uncertainties included. Thus, the model was appropriate for use in evaluating hazards at NPPs.

The EPRI GMM (2013) is a regional model, developed to calculate seismic hazard at potential and existing nuclear facilities. The GMM region includes two subregions: the midcontinent region and the Gulf region. In addition, the GMM consists of four clusters. Each cluster represents a similar approach for modeling ground motions in the CEUS, including within-cluster epistemic uncertainty. The 2013 EPRI GMM update included more recent ground motion prediction equations (GMPEs) within some of the clusters and removed many of the GMPEs used for the earlier version of the GMM (EPRI, 2004, 2006). The final version of the EPRI GMM (2013) provides a set of 12 median ground motion prediction models (three for each of the four clusters) and a model for the aleatory variability about each of the median models. For the CEUS-SSC distributed seismic sources, EPRI GMM (2013) clusters 1–3 are recommended for use. For the CEUS-SSC RLME sources, all four of the clusters should be used. The NRC staff fully implemented the EPRI GMM (2013) logic tree branches, as described in the HID, to develop mean hazard curves for each site.

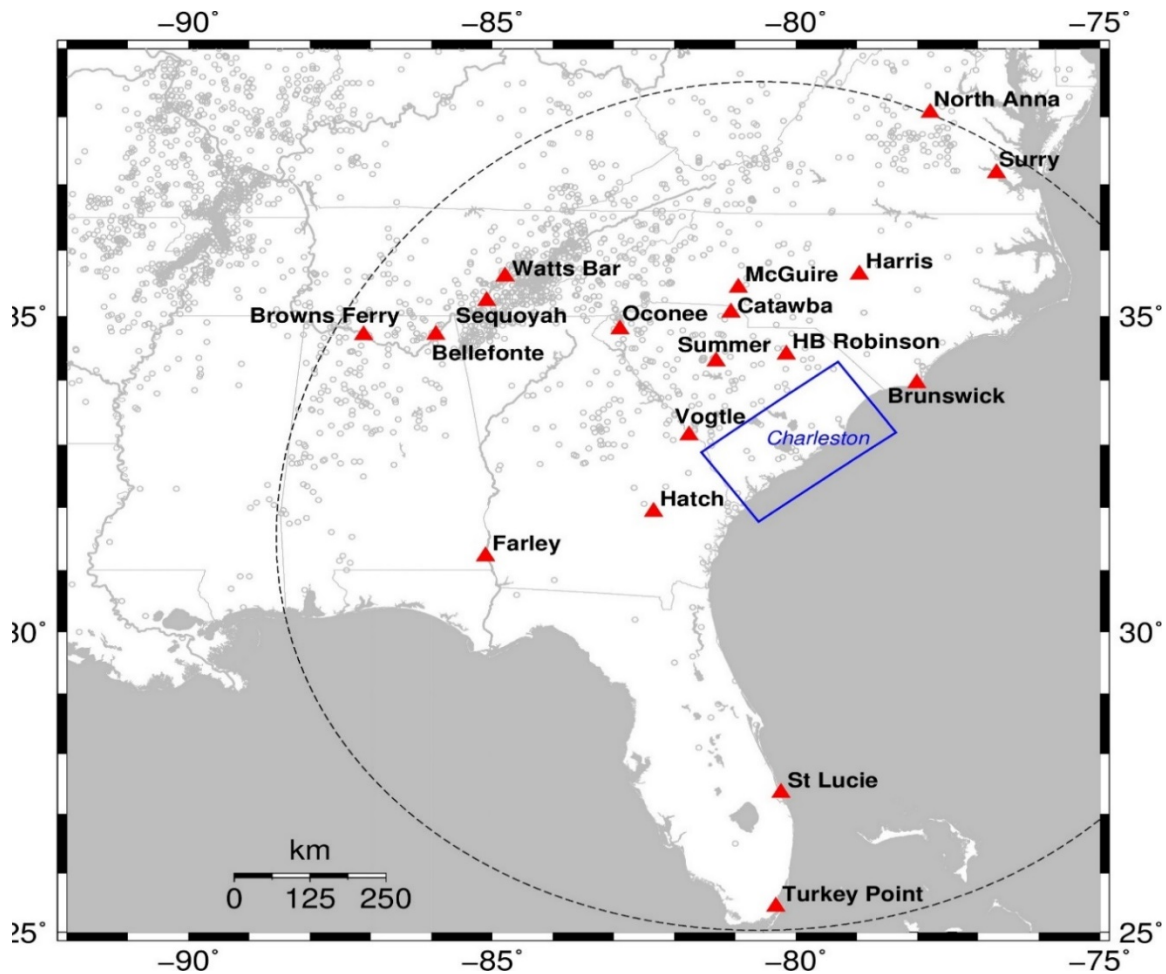


Figure 2.1-1 CEUS NPPS within the 500 Km [311 Mi] Radius of the Charleston RLME (Charleston Regional Source Configuration)

Table 2.1-1 CEUS Seismic Sources in NUREG-2115	
Source	Acronym or Abbreviation as Used in Figures
<b>RLME Sources</b>	
Charlevoix	none
Charleston	none
Cheraw Fault	Cheraw
Meers Fault	Meers
New Madrid Fault System	NMFS
Reelfoot Rift—Eastern Rift Margin North	ERM_N
Reelfoot Rift—Eastern Rift Margin South	ERM_S
Reelfoot Rift—Marianna	Marianna
Reelfoot Rift—Commerce Fault System	Commerce
Wabash Valley	none
<b>M<sub>max</sub> Zones</b>	
Mesozoic and Younger Extended Zone—Narrow	MESE_N
Mesozoic and Younger Extended Zone—Wide	MESE_W

<b>Table 2.1-1 CEUS Seismic Sources in NUREG-2115 (cont.)</b>	
<b>Source</b>	<b>Acronym or Abbreviation as Used in Figures</b>
<b>RLME Sources</b>	
Non-Mesozoic and Younger Extended Zone—Narrow	NMESE_N
Non-Mesozoic and Younger Extended Zone—Wide	NMESE_W
Study Region	STUDY_R
<b>Seismotectonic Zones</b>	
Atlantic Highly Extended Crust	AHEX
Extended Continental Crust—Atlantic Margin	ECC_AM
Extended Continental Crust—Gulf Coast	ECC_GC
Gulf Coast Highly Extended Crust	GHEX
Great Meteor Hotspot	GMH
Illinois Basin Extended Basement	IBEB
Midcontinent Craton (Geometries A, B, C, D)	MIDC_A,B,C,D
Northern Appalachian	NAP
Oklahoma Aulacogen	OKA
Paleozoic Extended Crust (Geometries Narrow and Wide)	PEZ_N and PEZ_W
Reelfoot Rift, Reelfoot Rift with Rough Creek Graben	RR and RR_RCG
St. Lawrence Rift	SLR

#### **2.1.4 Site Response Evaluation**

The purpose of the site response evaluation is to determine how the bedrock ground motions are modified as they propagate upward through the soil/rock column to the surface. The critical parameters that determine the frequencies of ground motion that are affected by the upward propagation of bedrock motions are (1) the layering of soil and soft rock, (2) the thicknesses of these layers, (3) the shear-wave velocities and low-strain damping of the layers, and (4) the degree to which the shear modulus and damping change with increasing input bedrock amplitude. For the CEUS NPP sites, the above- and below-grade topographic effects are generally minimal, and the geologic layers generally dip at shallow angles. Therefore, the NRC staff and licensees used one-dimensional ground response analysis to represent the wave propagation conditions, for which the response is assumed to be dominated by vertically propagating and horizontally polarized shear waves. In addition, based on the expected intensity range of the input motions for CEUS NPP sites, the NRC staff considers that the use of the equivalent linear site response method yields valid results.

Enclosure 1 of the 50.54(f) letter requested that, after completing PSHA calculations for reference rock site conditions, licensees provide a GMRS developed from the site-specific seismic hazard curves at the control point elevation. Enclosure 1 further requested that licensees develop site-specific hazard curves and a GMRS at the control point elevation by first performing a site response analysis. Detailed site response analyses were not typically performed for many of the older operating plants; therefore, Appendix B to the SPID has guidance on developing site-specific amplification factors (including the treatment of uncertainty) for sites that do not have detailed, measured soil and rock parameters to extensive depths. In addition, the SPID specifies that the subsurface site response model, for both soil and rock sites, should extend to sufficient depth to reach the reference or base rock conditions as defined by the GMMs used in the PSHA.



The approach outlined in the SPID was generally followed by the licensees for developing the hazard estimates in response to the 50.54(f) letter, and by the NRC staff for its confirmatory reviews. Based on lessons learned from completing these assessment and review activities, the NRC staff found that the suggested ranges of uncertainty for shear-wave velocity recommended in the SPID may be overly broad and, in addition, the methods for estimating the site component of kappa (i.e., spectral decay factor) could be improved. These observations were one reason for developing this NUREG/KM. The subsequent sections of this report capture the NRC staff's experience in evaluating the CEUS NPP sites collectively and across a broad range of site conditions. The assessments in this report include previously used information supplemented by available regional information (e.g., from State geological surveys, State water commissions, oil and gas exploration, and the open literature). Sections 2.2 through 2.5 give detailed descriptions of the supplemental information used for each site.

The NRC staff used the following procedure for performing a probabilistic site response analysis for the CEUS NPP sites described in the next subsections:

1. Develop input motions consistent with the seismic hazard at the GMM reference horizon.
2. Develop basecase profiles and associated material properties.
3. Determine site kappa (i.e., low-strain attenuation).
4. Characterize nonlinear dynamic properties.
5. Perform profile randomization and apply Random Vibration Theory (RVT) to compute site amplification factor distributions.

#### 2.1.4.1 *Input Motions*

For the site response evaluation, the NRC staff developed input (bedrock outcrop) motions at the horizon corresponding to the base of the modeled geologic profile. These input motions are consistent with the reference shear wave velocity and site kappa specified by the EPRI GMM (2013) as well as the range of ground motions used to determine the hazard at the reference horizon. To determine the appropriate range for the input motions, the NRC staff evaluated deaggregation results for the low and high frequency [i.e., 1 and 10 Hertz (Hz)] reference rock hazard at annual frequencies of exceedance (AFE) of  $10^{-4}$ ,  $10^{-5}$ , and  $10^{-6}$  at several representative CEUS sites.

To generate the input motions for the site response evaluations, the NRC staff developed Fourier amplitude spectra (FAS) based on seismological source theory (i.e., a single-corner frequency Brune source spectrum) and regional attenuation parameters appropriate for the CEUS. Tables B-4 through B-7 in Appendix B to the SPID specify these parameters. Although the SPID recommends implementing both single-corner and double-corner frequency source spectra to capture the uncertainty in the development of the input motions, the NRC staff found minimal to no difference between the two types of source spectra on the 1 Hz and 10 Hz hazard curves at either the  $10^{-4}$  and  $10^{-5}$  AFE levels. Therefore, the NRC staff developed input FAS using only single-corner source spectra with appropriate attenuation parameters for the CEUS. To capture an appropriate range of input motions, the NRC staff developed 12 FAS using *M*6.5 and peak ground acceleration (PGA) levels ranging from 0.01 to 2.1g (1 to 210 percent of the acceleration due to earth's gravity). This range of PGA values covers the set of source epicentral distances and depths in Table B-4 in Appendix B to the SPID and also spans the

reference rock amplitudes from the deaggregation results for each of the CEUS NPP sites. As described in Appendix B to the SPID and verified by the NRC staff through its initial confirmatory site response evaluations, the shape of the input FAS resulting from multiple magnitudes and source-to-site distances has a relatively minor effect on the resulting site amplification factor (*AF*) distributions and hazard curves. In contrast, the amplitude of the input motions has a significant impact on the resulting *AFs*. As such, the NRC staff concluded that a single *M*6.5 with a wide range of PGA levels would appropriately characterize the potential range of reference rock input motions and simultaneously the potential nonlinear response of the soil and soft rock to these input motions. As described in Section 2.1.4.5, the NRC staff used RVT to develop acceleration response spectra consistent with the input FAS as well as the FAS at the control point elevation. Figure 2.1-2 shows the input FAS developed by the NRC staff and the corresponding acceleration response spectra developed using RVT.

#### 2.1.4.2 Site Profile Development

Before developing a site basecase profile, the NRC staff evaluated the licensee's SHSR descriptions of the local geologic subsurface structure, including descriptions of the soil and rock types, subsurface layer geometry and thickness, compression and shear wave velocities, unit weights, and strain-dependent dynamic shear modulus reduction and material damping ratio relations for each of the layers. In addition, the NRC staff reviewed the licensee's site-specific field and laboratory investigations for the NPP and geologic descriptions in the plant UFSARs. If available, the NRC staff also reviewed the descriptions and investigations for Independent Spent Fuel Storage Installations (ISFSIs), ESP, or COL applications for facilities located adjacent to the site. Frequently, the geologic descriptions and siting investigations for older NPPs focused on the stability of the foundation-bearing soil or rock layer, so the investigations of deeper subsurface layers were limited. To augment the limited information for older facilities, the NRC staff gathered new information from State geological surveys, State water commissions, oil and gas exploration, and the open literature where available.

To develop a best-estimate basecase profile for each site, the NRC staff defined a median profile in terms of layer thickness (*h*), low-strain shear wave velocity ( $V_s$ ), unit weight ( $\gamma$ ), and strain-dependent relationship of shear modulus ( $G/G_{max}$ ) reduction and material damping ratio ( $\xi$ ) relations. For this report, the NRC staff used the licensee's control point elevations as specified in each of the licensee's SHSRs.

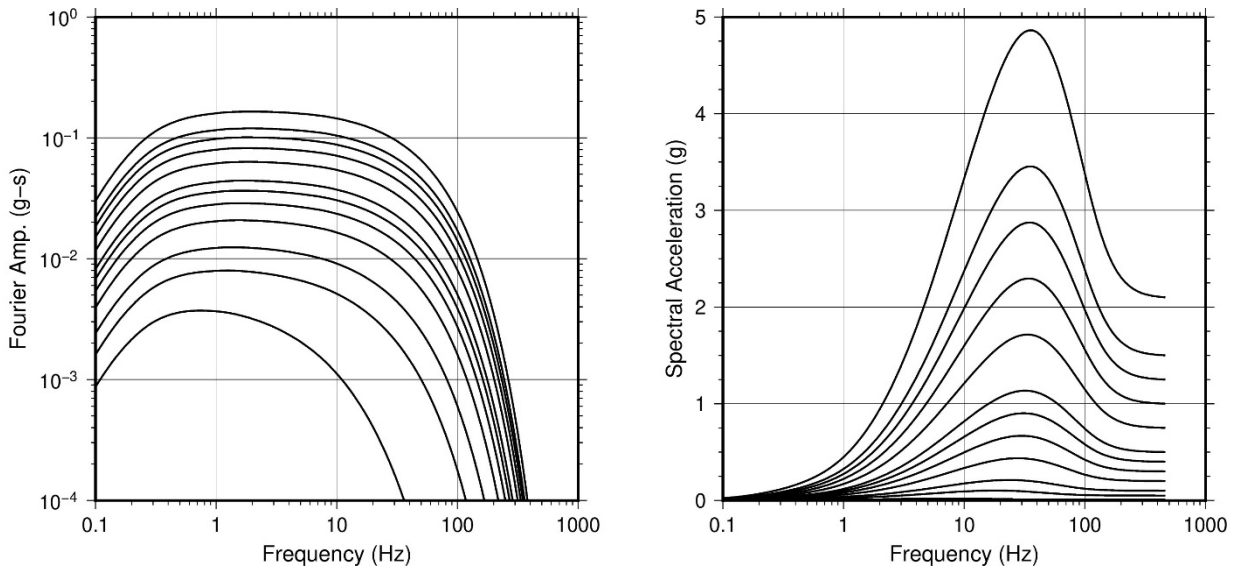


**Figure 2.1-2 Input Fourier Amplitude Spectra and Corresponding Acceleration Response Spectra Developed Using RVT**

Based on the extent of the geologic descriptions and field explorations described in the licensee’s SHSRs and UFSARs as well as supplemental descriptions, if available, from nearby ISFSIs, ESPs, or COL applications, the NRC staff developed a median basecase profile for each site. For each of the CEUS sites described in Sections 2.2 to 2.5, the NRC staff briefly summarizes the licensee’s basecase profile and the NRC staff’s confirmatory profile. For the sites where the NRC staff’s basecase profile differs from the licensee’s, Sections 2.2 to 2.5 provide the rationale for the differences.

To capture the uncertainty in the basecase profile due to the limited amount of data for most of the sites, the NRC staff developed lower ( $BC_L$ ) and upper ( $BC_U$ ) basecase profiles using an epistemic logarithmic standard deviation ( $\sigma_{\ln V_S, ep}$ ) based on the estimated uncertainty in the in situ  $V_S$  structure:

$$BC_L = BC_M \exp(-1.282\sigma_{\ln V_S, ep}) \quad \text{Eq. 2-1}$$

$$BC_U = BC_M \exp(1.282\sigma_{\ln V_S, ep}) \quad \text{Eq. 2-2}$$

where  $BC_M$  is the best-estimate median basecase profile. Typically, the NRC staff selected a logarithmic standard deviation of either 0.15 or 0.20 to develop the lower and upper profiles. The NRC staff concluded that logarithmic standard deviation values in this range provide reasonable alternative lower and upper profiles that are consistent with typical ranges in  $V_S$  for the identified soil type or rock lithology. Based on its initial site response confirmatory evaluations, the NRC staff concluded that use of the larger logarithmic standard deviation values (e.g., 0.35 and 0.50) recommended in the SPID have the potential to flatten out prominent site  $AF$ s at the fundamental frequency of the profile.

The NRC staff also incorporated the uncertainty in the depth to the reference rock horizon through the development of lower and upper basecase profiles. In particular, for many of the

sites, the lower basecase profile captures the potential for a deeper reference rock horizon, while the upper basecase profile assumes a shallower depth to the reference horizon. Sections 2.2 to 2.5 describe the NRC staff's basecase profiles for each of the CEUS sites, summarized in tables and figures.

#### 2.1.4.3 Site Kappa

Recent studies have shown that the sole use of geotechnical material damping estimates for site response analyses generally does not capture the overall crustal attenuation of a geologic profile (Stewart et al., 2017; Ktenidou et al., 2015; Cabas and Rodriguez-Marek, 2017). Consequently, recent site response evaluations have first estimated the site component ( $\kappa_0$ ) of the high-frequency spectral decay parameter, kappa ( $\kappa$ ), which captures both intrinsic and scattering attenuation. This site attenuation parameter is then used to constrain the amount of material damping used for each of the layers in the basecase profiles. Site kappa can be partitioned into a regional component and a site profile component:

$$\kappa_0 = \kappa_{ref} + \kappa_{profile} \quad \text{Eq. 2-3}$$

where, for the CEUS, the regional component is the reference value ( $\kappa_{ref}$ ) of 6 milliseconds (msec) specified by the EPRI GMM (2013) and the site profile component ( $\kappa_{profile}$ ) is estimated either from onsite or nearby seismic records, if available, or from empirical correlations with site parameters (Campbell, 2009; Laurendeau et al., 2013). Because none of the CEUS NPPs have at-site seismic recordings, Appendix B to the SPID provides multiple approaches to estimate  $\kappa_0$ . These approaches are based on empirical correlations with site parameters that depend on general site classifications.

The first approach is used for sites classified as deep rock, {i.e., sites with at least 1,000 meters (m) [3,000 feet (ft)]} of firm sedimentary strata. This approach estimates  $\kappa_0$  using a correlation with the single parameter  $V_{S30}$  {average  $V_S$  over the upper 30 m [100 ft] of the profile}. However, several recent studies (e.g., Cabas and Rodriguez-Marek, 2017) have shown that the correlation between  $V_{S30}$  and  $\kappa_0$  is weak to nonexistent and neglects the deeper portion of the profile, which provides an important contribution to  $\kappa_0$ .

The second approach is used for sites classified as shallow to intermediate rock or soil over rock. For this site type, the SPID recommends first estimating  $\kappa_{profile}$  by using the minimum low-strain damping ratio value from the damping curves specified for the upper layers of the profile and then assuming a damping seismic quality factor ( $Q_d$ ) value of 40. This value of  $Q_d$  corresponds to a damping ratio value ( $\xi$ ) of 1.25 percent for the lower rock layers of the profile. The profile component of site kappa due solely to damping ( $\kappa_{prof,d}$ ) is then determined by

$$\kappa_{prof,d} = \sum_{i=1}^L \frac{h_i}{V_{S_i} Q_{d_i}} \quad \text{Eq. 2-4}$$

where  $L$  is the number of layers in the site profile. However, using assumed material damping values from the profile to estimate  $\kappa_0$  is inconsistent with using  $\kappa_0$  to provide a constraint on the amount of material damping assigned to each layer. In addition, this approach neglects the scattering contribution to  $\kappa_0$ . Finally,  $\kappa_0$  values for intermediate rock sites tend to be very large if, as recommended in the SPID, EPRI (1993) rock damping curves are used for the upper 152 m

[500 ft] of the profile. This is due to the minimum low-strain damping value of about 3 percent for these damping curves.

The third approach is used for sites with less than 1,000 m [3,000 ft] of soil. For these site types, the SPID recommends using a simple correlation from Campbell (2009) between the total profile thickness ( $H$ ) and  $\kappa_0$ . The limitation with this approach is that it estimates  $\kappa_0$  based on only a single site parameter.

For deep soil sites, (i.e., those sites with soils deeper than 1,000 m [3,000 ft]), the SPID recommends using a  $\kappa_0$  of 40 msec as a maximum value. However, Chapman and Conn (2016) estimated  $\kappa_0$  values of about 160 msec for locations near the coast of Texas, Louisiana, and Mississippi, which rest atop about 12 km [40,000 ft] of sediments.

Rather than using these multiple approaches specified in the SPID, for each of the CEUS sites, the NRC staff used one of the relationships between the frequency-independent effective seismic quality factor of shear waves ( $Q_{ef}$ ) and  $V_S$  from Campbell (2009). Specifically, the NRC staff used Model 1 from Campbell (2009) to first estimate  $Q_{ef}$ , which captures attenuation from both damping and scattering, for each of the profile layers. The NRC staff then estimated  $\kappa_0$  by determining the profile component of site kappa using

$$\kappa_{prof,T} = \sum_{i=1}^L \frac{h_i}{V_{S_i} Q_{ef_i}} \quad \text{Eq. 2-5}$$

and then adding the 6 msec contributed by the regional component,  $\kappa_{ref}$ , of site kappa. This is in contrast to the second approach (Equation 2-4), which estimates the kappa profile ( $\kappa_{prof,d}$ ) based only on damping ( $Q_d$ ). The benefits of the NRC staff's approach are that (1) it uses multiple site parameters for estimating  $\kappa_0$ , rather than just a single parameter, and (2) Model 1 from Campbell (2009) has been shown to provide reasonable results for estimating  $\kappa_0$  by Pacific Northwest National Laboratory [(PNNL), 2014] and Cabas and Rodriguez-Marek (2017) (Figure 2.1-3).

Further, because Gulf Coast sites in the CEUS have  $\kappa_0$  values that greatly exceed 40 msec (Chapman and Conn, 2016), the NRC staff decided not to constrain  $\kappa_0$  to be less than or equal to 40 msec for any of the CEUS soil sites. Also, the NRC staff concluded that using a maximum value of 40 msec does not produce realistic spectral shapes for these soil sites.

After estimating a  $\kappa_0$  value for each of the basecase profiles, the NRC staff used a multistep process to evaluate the total amount of material damping within the profile. The NRC staff first converted the material damping ratio ( $\xi$ ), expressed as a percentage, to  $Q_d$  for each layer within the profile using the following equation:

$$Q_d = \frac{100}{2\xi} \quad \text{Eq. 2-6}$$

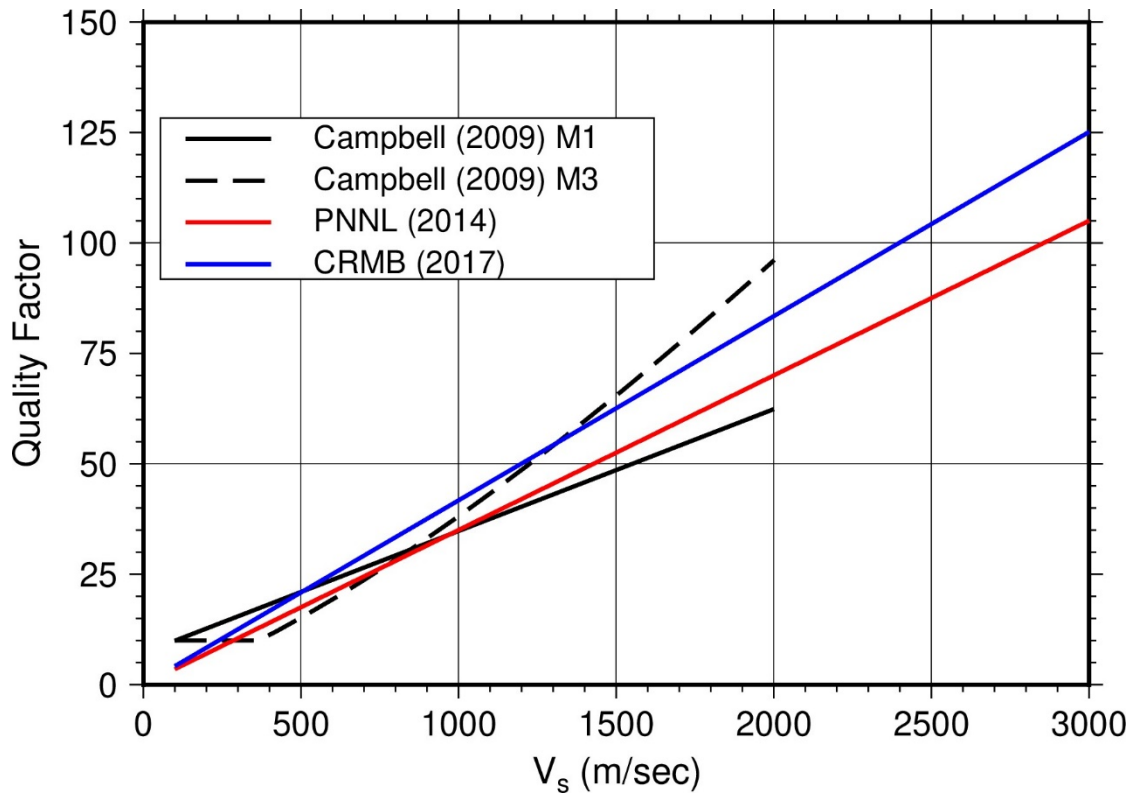


**Figure 2.1-3 Models 1 And 3 (M1 And M3) from Campbell (2009) Compared to Models from Cabas and Rodriguez-Marek (Crmb) (2017) and PNNL (2014), Demonstrating Correlation Between  $Q_{ef}$  and  $V_s$**

Next, the NRC staff used Equation 2-4 to sum the total material damping contribution to estimate  $\kappa_{prof,d}$ . The NRC staff then ensured that this estimate of  $\kappa_{prof,d}$  did not exceed the  $\kappa_{prof,T}$  estimated using Equation 2-5. Finally, the NRC staff either increased or decreased the damping ratio ( $\xi$ ) assigned to each layer until  $\kappa_{prof,d}$  matched  $\kappa_{prof,T}$  for each of the basecase profiles. This approach provides a mechanism to account for the contribution to  $\kappa_0$  due to scattering as well as damping. Most importantly, this approach provides a way to capture the overall crustal attenuation of a geologic profile, which recent studies (Stewart et al., 2017; Ktenidou et al., 2015; Cabas and Rodriguez-Marek, 2017) have shown to be greater than the attenuation achieved from the sole use of geotechnical material damping measurements.

Although the NRC staff's approach to estimating  $\kappa_0$  differed from the multiple approaches recommended in the SPID, the overall effect on the resulting control point hazard curves and GMRS is generally not that significant below 10 Hz and, therefore, does not produce screening results substantively different than those documented in each of the staff assessments.

In summary, the NRC staff found that incorporating  $\kappa_0$  into the site response evaluation is important to produce realistic spectral shapes. The NRC staff's approach captures the overall crustal attenuation of the geologic profile and also informs the amount of damping assigned to each of the layers. Without available site recordings, this important site attenuation parameter is difficult to estimate accurately. However, the approach adopted by the NRC provides a consistent method that relies on multiple site parameters to estimate  $\kappa_0$ .

The next sections of this report compare  $\kappa_0$  values estimated for each CEUS site, based on the approaches outlined in the SPID and the NRC approach.

#### 2.1.4.4 *Nonlinear Dynamic Properties*

For equivalent linear site response analysis, nonlinearity is incorporated through the use of strain-compatible site properties (i.e., shear modulus and damping ratio) for each layer. In this type of analysis, these soil properties are modified to be consistent with the shear strains generated in each layer by the vertically propagating shear waves. The strain-compatible properties model both the shear modulus reduction and the increased damping that is expected as the intensity of the shaking increases.

Appendix B to the SPID recommends the use of both the EPRI (1993) and Peninsular Range (Silva et al., 1996) shear modulus and damping curves for soil sites to capture the epistemic uncertainty in the nonlinear material properties. The Peninsular Range curves reflect a more linear cyclic shear strain dependency than the EPRI (1993) curves; therefore, the use of both sets of curves accommodates the range in nonlinearity expected for the CEUS sites. The two sets of curves are appropriate for cohesionless soils (sands, gravels, silts, and low-plasticity clays). For rock sites, the SPID recommends use of the EPRI rock curves to accommodate the potential nonlinear behavior of sedimentary rocks such as shale, sandstone, or siltstone. As an alternative to the EPRI rock curves, the SPID recommends assuming a linear response with a  $\xi$  value of 3 percent.

For this report, the NRC staff followed the SPID recommendations by using both the EPRI (1993) and Peninsular Range curves for soil sites and the EPRI rock curves and a linear alternative for rock sites. However, due to their larger nonlinearity, the NRC staff limited the use of the EPRI rock curves to only the very uppermost weathered rock layers that have a  $V_S$  generally less than 1,500 meters per second (m/sec) [5,000 feet per second (ft/sec)]. This limited use of these curves is based upon the approach described in this section, which imposes a constraint on the amount of damping based on the  $\kappa_0$  value that the NRC staff first estimated for each of the basecase profiles. Sections 2.2 to 2.5 describe the NRC staff's approach to capturing the nonlinear material properties for each of the CEUS sites.

#### 2.1.4.5 *Analysis Methodology*

The NRC staff used the RVT approach to develop site amplification factors in terms of the median and logarithmic standard deviation for each of the 12 input spectra for all seven spectral frequencies specified by the EPRI GMM (2013). To account for the aleatory variability in  $V_S$ , the NRC staff developed 60 random profiles for each of the three median profiles (basecase, lower, and upper) using the Toro (1995) model. This model assumes that the  $V_S$  at the midpoint of each layer is described by a lognormal distribution and is correlated between adjacent layers. The interlayer correlation ( $\rho$ ) between the  $V_S$  of each layer proposed by Toro (1995) depends on layer thickness ( $h$ ) and depth ( $d$ ) and their respective interlayer correlations ( $\rho_h$  and  $\rho_d$ ). As specified in the SPID, the NRC staff used a logarithmic standard deviation value of 0.25 for the uppermost layers and a value of 0.15 for the layers below. The remaining parameters used by the NRC staff to determine the interlayer correlations are based on the U.S. Geological Survey (USGS)  $V_{S30} > 760$  m/sec [2,500 ft/sec] site category, for which Toro (1995) provides the required parameters. In addition to randomizing the shear wave velocity, the NRC staff captured the variability in the total thickness of the three profiles by randomizing by  $\pm 15$  percent. Figure 2.1-4 shows an example of the randomized profiles for each of the three basecase profiles, which also includes the randomized depth to the reference horizon. In contrast to the

recommendation in the SPID, the NRC staff did not truncate the randomized profiles at the reference  $V_s$  of 2,830 m/sec [9,280 ft/sec] to avoid artificially low aleatory variabilities about the upper basecase profile, as shown in Figure 2.1-4.

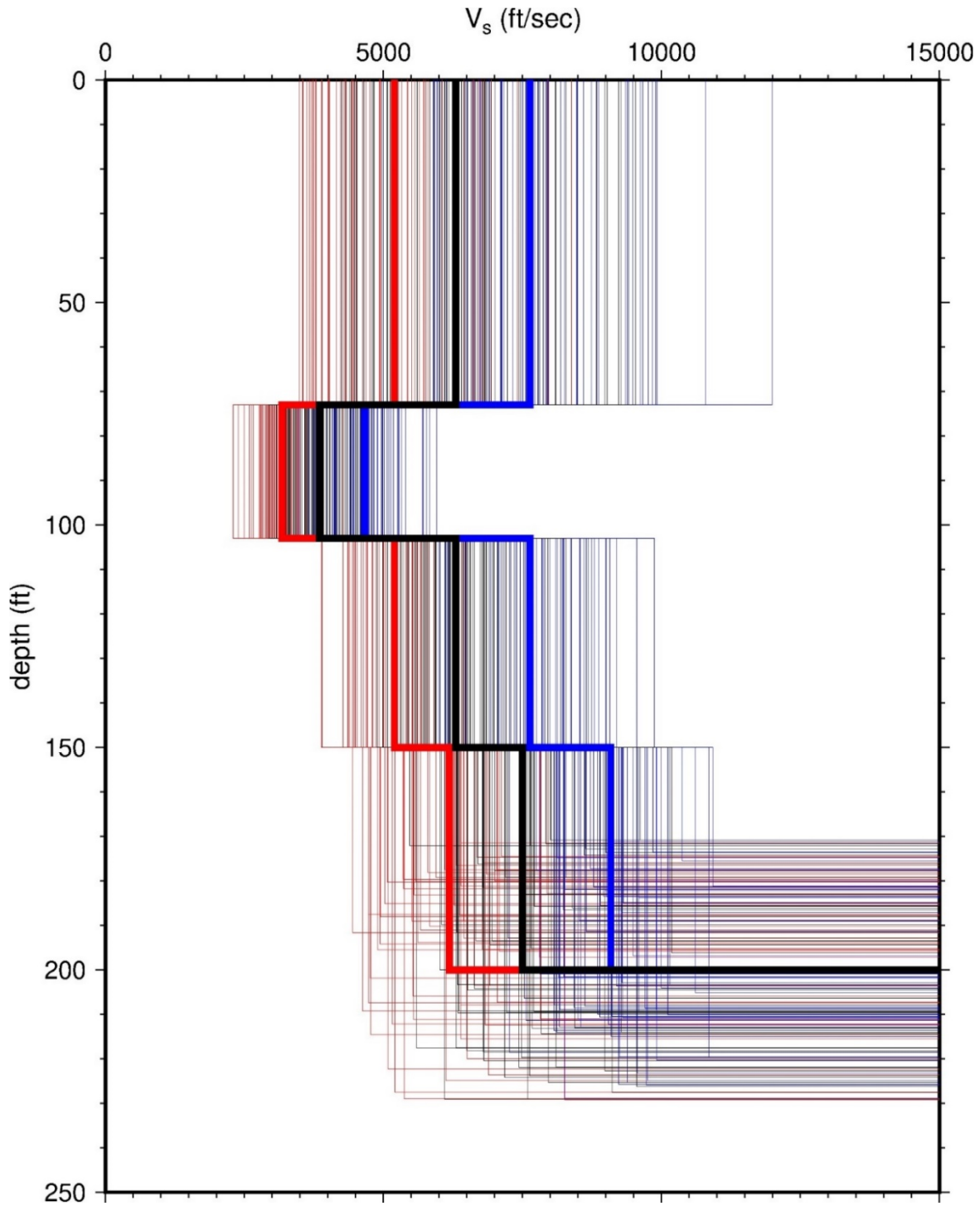


**Figure 2.1-4 Example Randomized Velocity Profiles about Lower (Red), Basecase (Black), and Upper (Blue) Profiles**



In summary, the NRC staff developed three basecase profiles, with each profile having a single  $\kappa_0$  estimate and two alternative sets of shear modulus and damping curves for a total of six unique logic tree branches. For each of the unique logic tree branches, the NRC staff calculated the frequency-dependent site  $AF$ .  $AF$  is defined by

$$AF(f) = SA_{cp}(f) / SA_{ref}(f) \quad \text{Eq. 2-7}$$

where  $f$  is frequency, and  $SA_{cp}$  and  $SA_{ref}$  are the 5-percent damped spectral accelerations at the profile control point and reference rock horizon, respectively. Based on the 60 random profiles, the NRC staff determined the median ( $\overline{AF}$ ) and logarithmic standard deviation ( $\sigma_{\ln AF}$ ) of  $AF$  for each of the unique combinations of the site response logic tree. In contrast to the SPID recommendation that the  $AF$  should always be greater than 0.5, for the purpose of this NUREG, the NRC staff allowed  $AF$  to be less than 0.5. The NRC staff considers that a minimum  $AF$  value of 0.5 may impose an artificial constraint based on the material properties of some sites.

### 2.1.5 Hazard Calculations

The NRC staff calculated mean reference rock hazards through implementation of the CEUS-SSC model (NRC, 2012b) combined with the EPRI GMM (2013). The NRC staff then performed a site response evaluation for each of the CEUS NPP sites and developed a mean control point hazard curve for each site. To develop fully probabilistic mean hazard curves at the control point elevation, the NRC staff implemented Approach 3 using the convolution of the reference rock hazard curves with distribution parameter estimates for the  $AF$ s developed from the site response analysis (Bazzurro and Cornell, 2004; Rodriguez-Marek et al., 2014). Using the convolution approach and assuming that  $AF$  is primarily a function of the spectral acceleration at the reference rock horizon ( $SA_{ref}$ ), the hazard at the control point ( $\lambda_{cp}$ ) is given by

$$\lambda_{cp}(z) = \sum_{x_j} P \left[ AF > \frac{z}{x_j} \mid x_j \right] p_{SA_{ref}}(x_j) \quad \text{Eq. 2-8}$$

in which  $z$  is the ground motion level at the control point,  $P \left[ AF > \frac{z}{x_j} \mid x_j \right]$  is the probability that  $AF$  is greater than  $\frac{z}{x_j}$  given  $SA_{ref} = x_j$ , and  $p_{SA_{ref}}(x_j)$  is the annual probability of occurrence for  $SA_{ref} = x_j$ . This probability is approximated by differencing the rates from the computed reference rock hazard curve ( $\lambda_{ref}$ ) in discrete form about  $SA_{ref} = x_j$

$$p_{SA_{ref}}(x_j) \approx \lambda_{ref}(x_k) - \lambda_{ref}(x_{k+1}) \quad \text{Eq. 2-9}$$

where

$$x_j = \frac{x_k + x_{k+1}}{2} \quad \text{Eq. 2-10}$$

Assuming that  $AF$  is lognormally distributed, the  $P \left[ AF > \frac{z}{x_j} \mid x_j \right]$  is given by

$$P \left[ AF > z/x_j | x_j \right] = \hat{\Phi} \left( \frac{\ln \frac{z}{x_j} - \ln \bar{AF} | x_j}{\sigma_{\ln AF} | x_j} \right) \quad \text{Eq. 2-11}$$

where estimates of the distribution parameters of  $AF$  ( $\bar{AF}$  and  $\sigma_{\ln AF}$ ) are based on the 60 random profiles for each of the unique combinations of the site response logic tree and  $\hat{\Phi}(\cdot)$  is the standard complementary Gaussian cumulative distribution function.

In summary, the NRC staff performed site response analyses to determine the distribution of site  $AF$ s for each spectral frequency and for a range of input ground motion levels. To the extent possible, the NRC staff selected the input ground motions for these analyses to span the reference rock hazard curves and to cover the motions indicated by the deaggregation magnitudes and distances for the low- and high-frequency (i.e., 1 Hz and 10 Hz) reference rock hazard at AFEs of  $10^{-4}$ ,  $10^{-5}$ , and  $10^{-6}$ . The NRC staff then propagated these input motions through multiple realizations about each of the site response tree logic branches (i.e.,  $V_S$  profiles and shear modulus and damping curves) to account for the uncertainty and spatial variability in the dynamic properties across each site. Next, the NRC staff implemented the estimates of the distribution parameters of  $AF$  using Approach 3 to develop mean control point hazard curves. For the CEUS sites, the NRC staff used the median and logarithmic standard deviation of  $AF$  ( $\bar{AF}$  and  $\sigma_{\ln AF}$ ) from each of the terminal branches of the site response logic tree along with the mean reference rock hazard for its implementation of Approach 3. Section 4.1.1 of this report summarizes the  $AF$  distributions for each site.

The NRC staff completed its hazard characterization for each of the CEUS NPP sites by using the mean control point hazard curves developed for each of the seven spectral frequencies specified in the EPRI GMM (2013) to determine mean uniform hazard response spectra (UHRS) at AFEs of  $10^{-4}$  and  $10^{-5}$  and, finally, a GMRS. For each of the CEUS NPP site hazard characterizations, Sections 2.2 through 2.4 show the mean control point hazard curves, UHRS, and GMRS, as determined by the NRC staff, along with the GMRS submitted in the SHSRs by each of the licensees.

## 2.2 Region I Sites

The NRC staff characterized the seismic hazard for the 14 Region I NPP sites shown in Table 2.2-1 and Figure 2.2-1. As shown in Table 2.2-1, 9 of the 14 Region I NPPs are founded on rock, 3 on soil, and 2 on till over rock. Table 2.2-1 also shows the State, the physiographic province, and whether there is a co-located ESP or COL application for each site. Figure 2.2-1 shows each Region I site overlain on the physiographic provinces, the highest weighted CEUS-SSC (NRC, 2012b) seismotectonic source zone configuration, and the CEUS-SSC earthquake epicenters.

The following subsections describe the NRC staff's development of reference rock hazard curves, site response analyses, and use of Approach 3 to develop control point seismic hazard curves and a GMRS for each Region I site.

<b>Plant Name</b>	<b>Site Name</b>	<b>State</b>	<b>Geology</b>	<b>Physiographic Province</b>	<b>ESP/COL (Y/N)</b>
Millstone Power Station	Millstone	CT	Rock	New England	N
Calvert Cliffs Nuclear Power Plant	Calvert Cliffs	MD	Soil	Coastal Plain	Y
Pilgrim Nuclear Power Station*	Pilgrim	MA	Till over rock	New England	N
Seabrook Station	Seabrook	NH	Rock	New England	N
Hope Creek Generating Station and Salem Nuclear Generating Station	Hope Creek and Salem	NJ	Soil	Coastal Plain	Y
Oyster Creek Nuclear Generating Station*	Oyster Creek	NJ	Soil	Coastal Plain	N
James A. FitzPatrick Nuclear Power Plant and Nine Mile Point Nuclear Station	FitzPatrick and Nine Mile Point	NY	Rock	Central Lowland	Y
R.E. Ginna Nuclear Power Plant	Ginna	NY	Rock	Central Lowland	N
Indian Point Energy Center*	Indian Point	NY	Rock	New England	N
Beaver Valley Power Station	Beaver Valley	PA	Till over rock	Appalachian Plateau	N
Limerick Generating Station	Limerick	PA	Rock	Piedmont	N
Peach Bottom Atomic Power Station	Peach Bottom	PA	Rock	Piedmont	N
Susquehanna Steam Electric Station	Susquehanna	PA	Rock	Valley and Ridge	Y

Table 2.2-1 Region I Plant Names, Site Names, States, Geology, Physiographic Provinces, and Co-Located ESPs/COLs (cont.)					
Plant Name	Site Name	State	Geology	Physiographic Province	ESP/COL (Y/N)
Three Mile Island Nuclear Station*	Three Mile Island	PA	Rock	Piedmont	N

\*Plant was shut down or has subsequently been shut down.

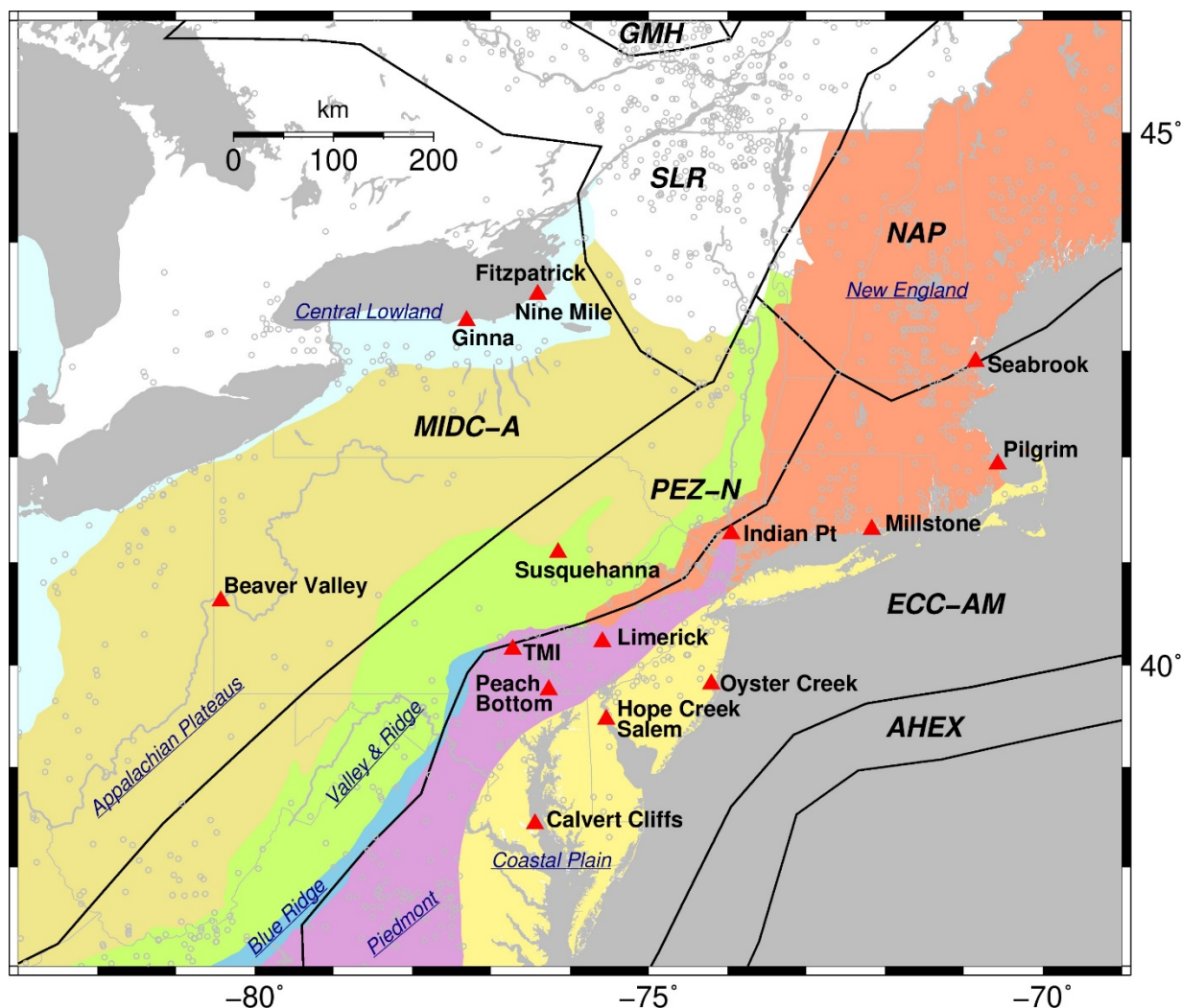


**Figure 2.2-1** Location Map Showing NPPs (Red Triangles) in Region I; Seismotectonic Source Zones, Indicated by Solid Black Lines (from NUREG-2115), with Acronym Defined in Table 2.1-1 of this Report; And Physiographic Provinces, Identified by Underlined Italicized Labels, with Water Bodies Represented in Gray. Earthquake Epicenters (from NUREG-2115) are Shown with Open Gray Circles

## 2.2.1 Beaver Valley

The Beaver Valley Power Station site is located along the Ohio River in western Pennsylvania within the Appalachian Plateau physiographic province and is founded on approximately 30 m [100 ft] of alluvial terrace deposits overlying about 3,354 m [11,000 ft] of sedimentary rock (shale, sandstone, limestone and dolomite). The horizontal SSE response spectrum for Beaver Valley has a Newmark spectral shape and is anchored at a PGA of 0.125g.

### 2.2.1.1 Reference Rock Hazard

For the reference rock PSHA, the NRC staff selected the 12 CEUS-SSC (NRC, 2012b) background seismic source zones that are located within 320 km [200 mi] of the Beaver Valley site. In addition, the NRC staff selected the Charleston, New Madrid Fault System (NMFS), and Wabash Valley CEUS-SSC RLME sources, which are all within 1,000 km [625 mi] of the site. To develop the reference rock seismic hazard curves for the Beaver Valley site, the NRC staff used the GMPEs in the updated EPRI GMM (2013). As shown in Figure 2.2-2, the NMFS RLME is the largest contributor to the 1 Hz reference rock total mean hazard curve at the  $10^{-4}$  AFE level. For the 10 Hz reference rock total mean hazard curve, the Midcontinent Craton-A (MIDC-A) seismotectonic source zone is the largest contributor at the  $10^{-4}$  AFE level.

### 2.2.1.2 Site Response Evaluation

#### 2.2.1.2.1 Site Profiles

To develop a basecase profile, the NRC staff used the geologic information in the NTTF R2.1 SHSR (Sena, 2014a) submitted by FirstEnergy Nuclear Operating Company (hereafter referred to as “the licensee” within this plant section). As described in the SHSR, the Beaver Valley site consists of about 30 m [100 ft] of alluvial granular terraces that formed during the Pleistocene overlying a sequence of flat-lying shale and sandstone strata that is occasionally interbedded with coal seams. The major Beaver Valley plant structures are founded on relatively dense and incompressible sand and gravel. In Table 2-2 of the SHSR, the licensee briefly described the subsurface materials in terms of the geologic units and layer thicknesses. For its site response evaluation, the NRC staff used the base of the reactor building foundation, which corresponds to an elevation of 207.5 m [680.9 ft] above mean sea level (MSL), as the control point elevation for the Beaver Valley site.

The licensee’s SHSR profile is based on in situ geophysical investigations for Unit 1, which consisted of uphole, downhole, and crosshole measurements from five boreholes located in the reactor area as well as seismic refraction profiles across the site. For the deeper rock layers, the licensee used sonic logs recorded in wells within 10 km [7 mi] of the site to determine the compressional wave velocity ( $V_P$ ) and the shear wave velocity ( $V_S$ ). Table 2-4 of the SHSR gives the measured and estimated  $V_S$  determined from the  $V_P$  listed in SHSR, Table 2-3, and assumed Poisson’s ratios.

The licensee’s SHSR basecase profile extends to a depth of 1,336 m [4,381 ft] below the control point elevation. The uppermost layers of the profile consist of Pleistocene age unconsolidated soil (sand and gravel with varying amounts of silt and clay) deposits. The licensee subdivided these soil deposits into two layers with thicknesses of 5 m [16 ft] and 12 m [40 ft] and  $V_S$  of 335 m/sec [1,100 ft/sec] and 366 m/sec [1,200 ft/sec], respectively. For the underlying 23 m [75 ft] of Pennsylvanian age Allegheny Group shales, the licensee measured a  $V_S$  of 1,524 m/sec [5,000 ft/sec]. For the 61 m [200 ft] of Lower Pennsylvanian age Pottsville Group

sandstones, the licensee estimated a  $V_S$  of 1,837 m/sec [6,026 ft/sec]. The remainder of the licensee's profile includes 1,235 m [4,050 ft] of Mississippian and Devonian age shales and sandstones with  $V_S$  ranging from 1,956 m/sec [6,416 ft/sec] to 2,168 m/sec [7,112 ft/sec]. The licensee terminated its profile at the top of the Middle Devonian Tully Limestone Formation, which has a  $V_S$  greater than the reference rock  $V_S$  of 2,831 m/sec [9,285 ft/sec].

Because the soil and rock strata beneath the Beaver Valley site are very well characterized, the NRC staff used the licensee's layer thicknesses and  $V_S$  for its basecase profile.

To capture the uncertainty in its basecase profile, the NRC staff developed lower and upper range (10<sup>th</sup> and 90<sup>th</sup> percentile) profiles by multiplying the basecase  $V_S$  values by scale factors of 0.78 and 1.29, respectively, which corresponds to an epistemic logarithmic standard deviation of 0.20. The weights for the lower, best-estimate, and upper basecase profiles are 0.3, 0.4, and 0.3, respectively. Figure 2.2-3 shows the NRC staff's basecase profiles, which extend to a depth of 1,336 m [4,381 ft] below the control point elevation, at which point the  $V_S$  is assumed to reach the reference rock value of 2,831 m/sec [9,285 ft/sec].

#### 2.2.1.2.2 *Dynamic Material Properties and Site Kappa*

The NRC staff assumed both linear and nonlinear behavior for the soil and rock beneath the Beaver Valley site. To model the nonlinear response within the upper 17 m [56 ft] of soil deposits, the NRC staff used the EPRI soil shear modulus reduction and material damping curves as one alternative and the Peninsular Range curves for the second equally weighted alternative. To model the nonlinear behavior of the uppermost rock strata, the NRC staff used the EPRI rock shear modulus reduction and material damping curves and to model the linear behavior, the NRC staff used a constant damping ratio of 3 percent. The NRC staff assumed two alternative dynamic responses for the 23 m [75 ft] of Allegheny shales (Layer 3) and gave them equal weight. For the remaining 1,296 m [4,250 ft] of its profile, the NRC staff assumed a linear response with material damping ratio values of 0.5 to 1.0 percent to maintain consistency with the site kappa ( $\kappa_0$ ) value for the Beaver Valley site.

To determine the basecase  $\kappa_0$  for the Beaver Valley site, the NRC staff first used the Campbell (2009) Model 1 relationship between  $V_S$  and  $Q_{ef}$  to determine a  $Q_{ef}$  for each layer. Combining these  $Q_{ef}$  values with the thicknesses and  $V_S$  for each of the layers results in a total  $\kappa_0$  value of about 19 msec, which includes the 6 msec assumed for the underlying reference rock. For the lower and upper basecase profiles, the NRC staff calculated  $\kappa_0$  values of 26 and 14 msec, respectively, using the same approach as for the basecase profile. In contrast, the licensee estimated  $\kappa_0$  by using the empirical relationship from the SPID (EPRI, 2012) between  $\kappa_0$  and the average  $V_S$  over the upper 30 m [100 ft] of the profile, which results in  $\kappa_0$  values of 21, 24, and 19 msec for the best-estimate, lower, and upper basecase profiles, respectively. The licensee expanded its range in  $\kappa_0$  values from 15 to 32 msec to capture additional epistemic uncertainty.

Table 2.2-2 provides the layer depths, lithologies,  $V_S$ , unit weights, and dynamic properties for the NRC staff's three basecase profiles. In summary, the site response logic tree developed by the NRC staff for the Beaver Valley site consists of six alternatives: three basecase profiles (each with a different  $\kappa_0$  value) and two alternative dynamic property branches.

### 2.2.1.2.3 Site Response Analysis Results

The NRC staff followed the methodology described in Section 2.1.4 to develop the final site amplification factors. Figure 2.2-4 shows the overall median site amplification factors and their variability for each of the seven spectral frequencies. As shown in Figure 2.2-4, the median site amplification factors range from about 1 to 3 before falling off with higher input spectral accelerations. The lower half of Figure 2.2-4 shows that the logarithmic standard deviations for the site amplification factors range from about 0.05 to 0.20.

### 2.2.1.3 Control Point Hazard Results

The NRC staff implemented Approach 3 from the SPID to develop a weighted control point seismic hazard curve for each of the six unique combinations of the site response logic tree for the Beaver Valley site. After combining these curves to develop the final mean control point hazard curves, the NRC staff determined the  $10^{-4}$  and  $10^{-5}$  UHRS in order to calculate the final GMRS. Figure 2.2-5 shows the final control point mean seismic hazard curves for each of the seven spectral frequencies as well as the NRC staff's UHRS and GMRS, and the licensee's NTTF R2.1 GMRS (Sena, 2014a). As shown in Figure 2.2-5, the NRC staff's GMRS (black curve) is similar to the licensee's GMRS (blue curve) over the entire frequency range.

Layer	Depth (ft)	Description	$V_s$ (ft/sec)			$V_s$ Sigma (ln)	BC Unit Weight (pcf)	Dynamic Properties	
			LR (0.3)	BC (0.4)	UR (0.3)			Alt. 1 (0.5)	Alt. 2 (0.5)
1	16	Soil: sand, silt, clay	851	1,100	1,421	0.25	120	EPRI Soil	Pen.
2	56	Soil: sand, silt, clay	929	1,200	1,551	0.15	120	EPRI Soil	Pen.
3	131	Rock: shale	3,869	5,000	6,461	0.15	140	EPRI Rock	L 3.0%
4	331	Rock: siltstone	4,663	6,026	7,787	0.15	150	L 1.0%	L 1.0%
5	801	Rock: shale, siltstone	5,219	6,744	8,715	0.15	150	L 1.0%	L 1.0%
6	3,675	Rock: shale, sandstone, siltstone	5,504	7,112	9,191	0.15	150	L 0.5%	L 0.5%
7	4,381	Rock: shale	4,965	6,416	8,291	0.15	150	L 0.5%	L 0.5%

LR = lower range; BC = basecase; UR = upper range; ln = natural log; pcf = pounds per cubic foot; L = linear; Alt. = alternative; Pen. = Peninsular.  
 For LR, BC, UR, and Alt.: Values in parentheses refer to weights for site response analysis logic tree branches.

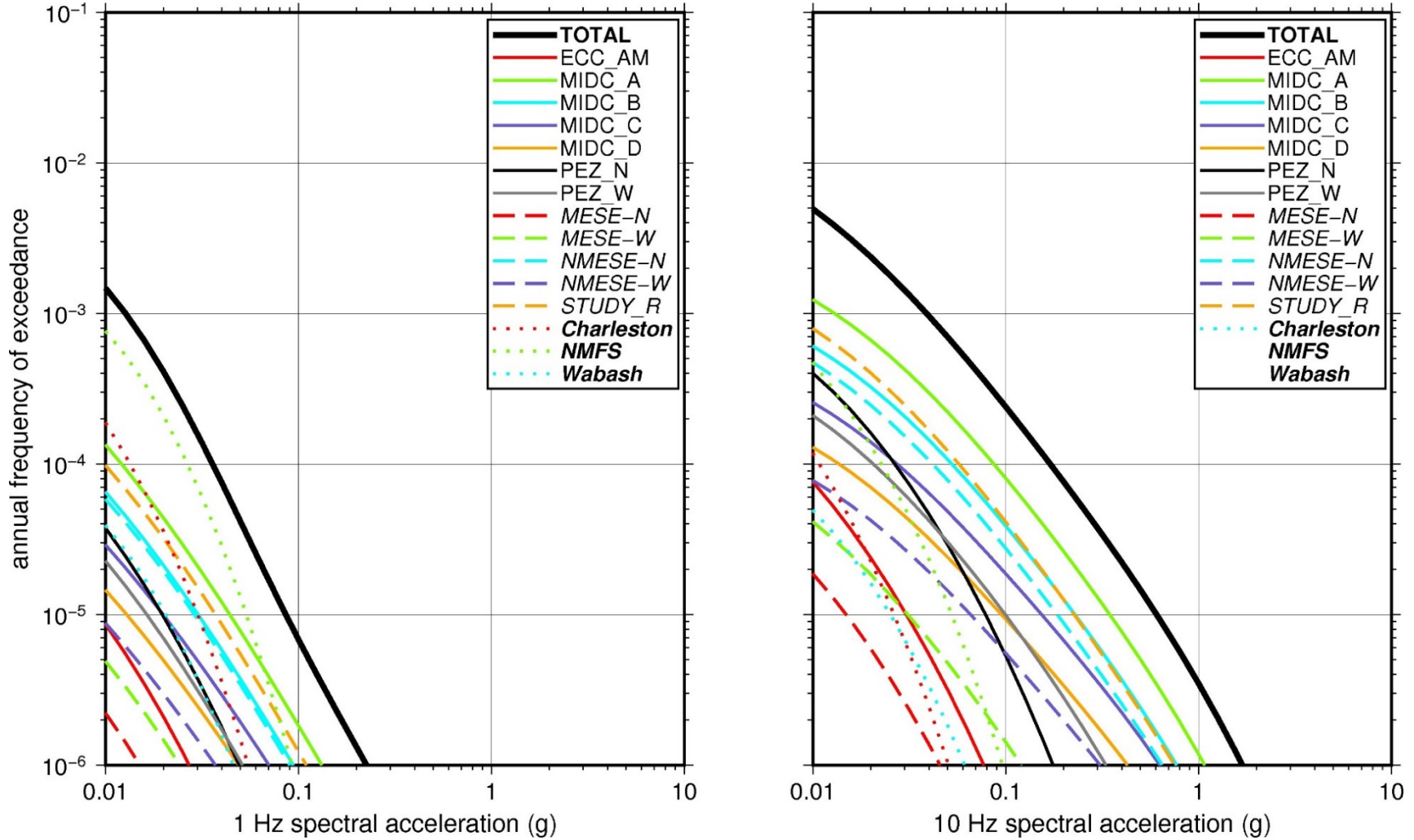


**Figure 2.2-2 Low-Frequency (1 Hz, Left) and High-Frequency (10 Hz, Right) Reference Rock Hazard Curves for Beaver Valley. Total Hazard is Shown as a Bold Black Line; Individual Contributions to the Hazard for Each of the CEUS-SSC Sources are Shown as Colored Lines Defined in the Legend. See Table 2.1-1 for Source Name Definitions**



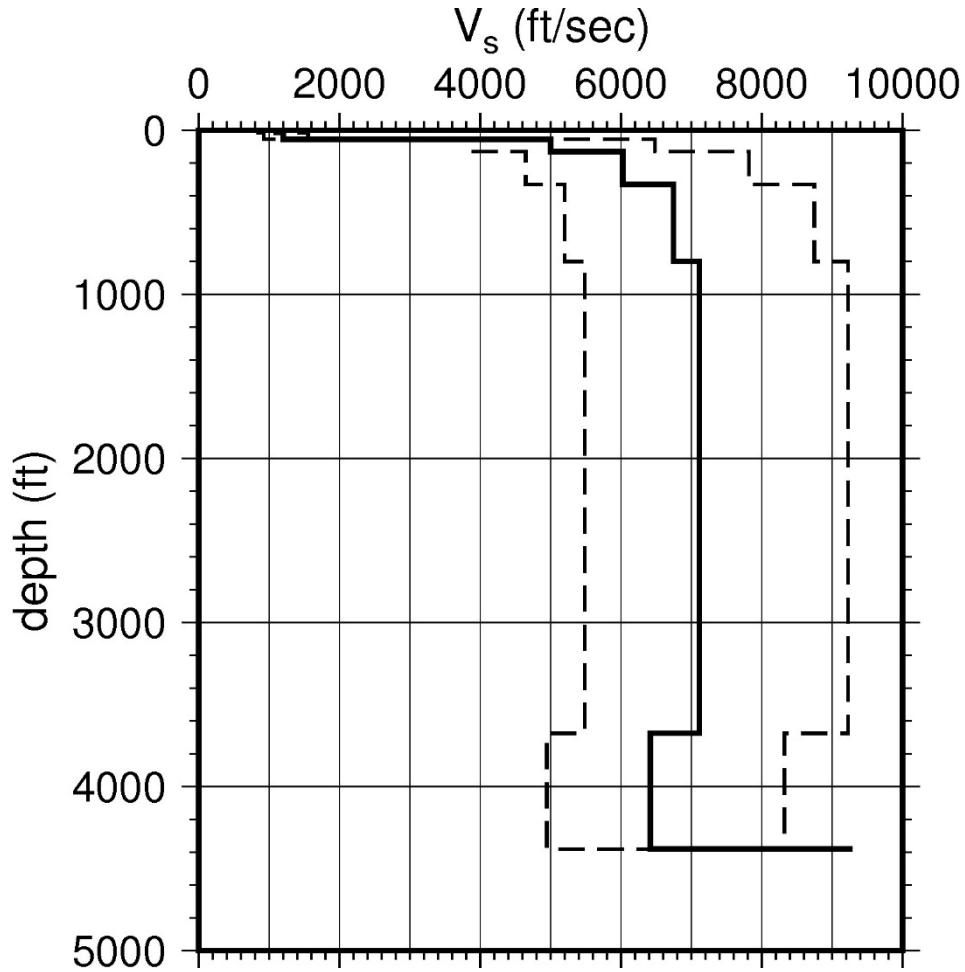


**Figure 2.2-3 Shear Wave Velocity ( $V_s$ ) Profiles for Beaver Valley. Basecase (BC) Profile Shown as Solid Bold Line; Lower and Upper Range (LR and UR) Profiles Shown as Dashed Lines. Profiles Terminate at Reference Rock Velocity of 2,831 m/sec [9,285 ft/sec] per EPRI GMM (2013)**

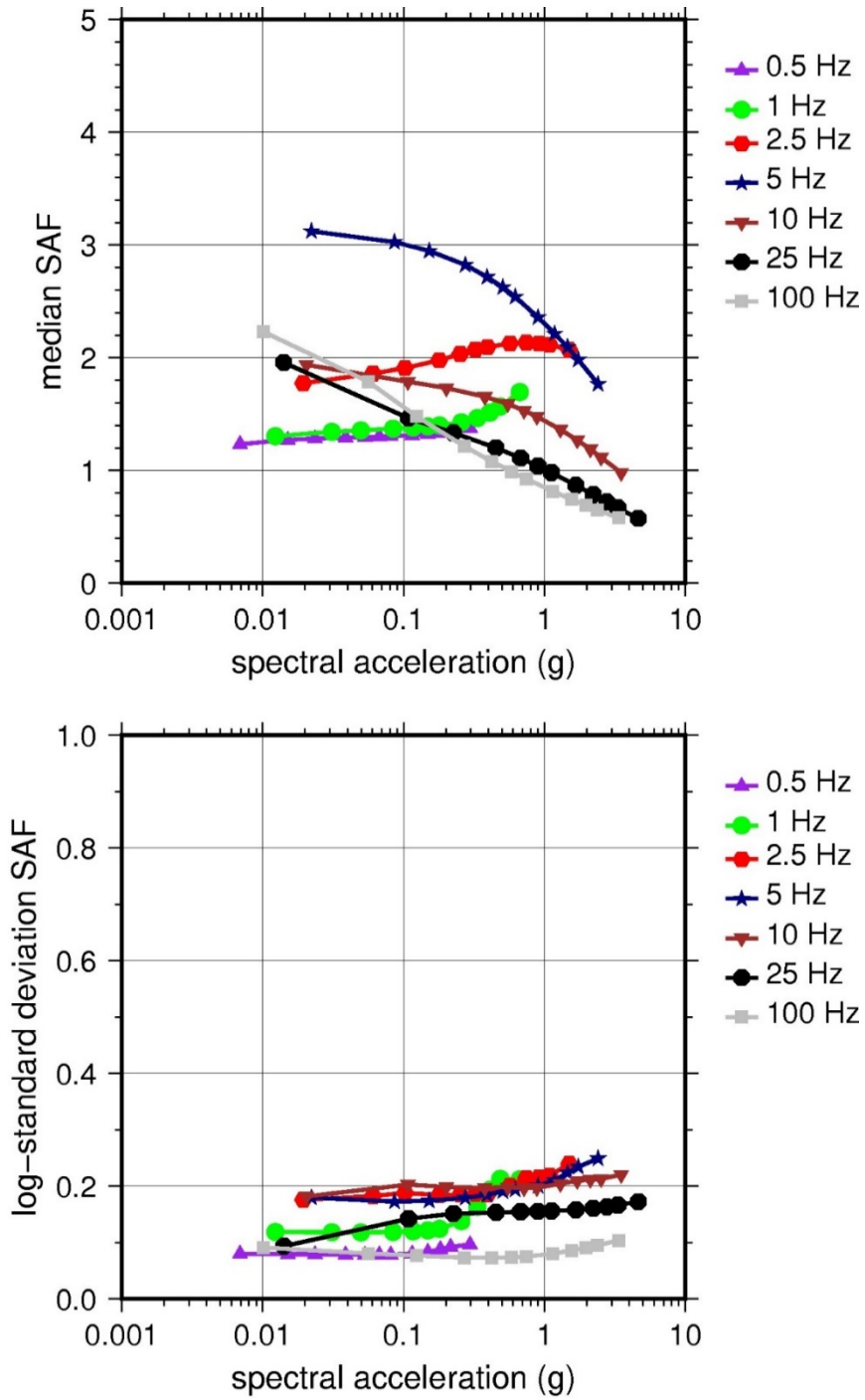


**Figure 2.2-4 Overall Weighted Median Site Amplification Factor (SAF) (Upper) and Log Standard Deviation of the SAF (Lower) as a Function of Input Acceleration for EPRI GMM (2013) Spectral Frequencies**

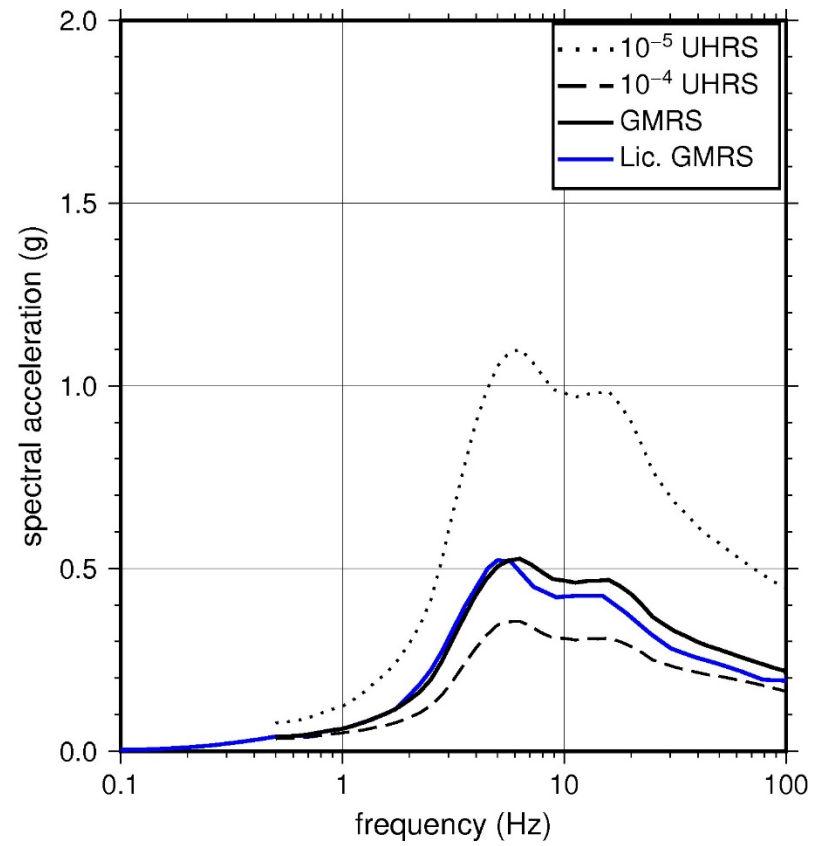
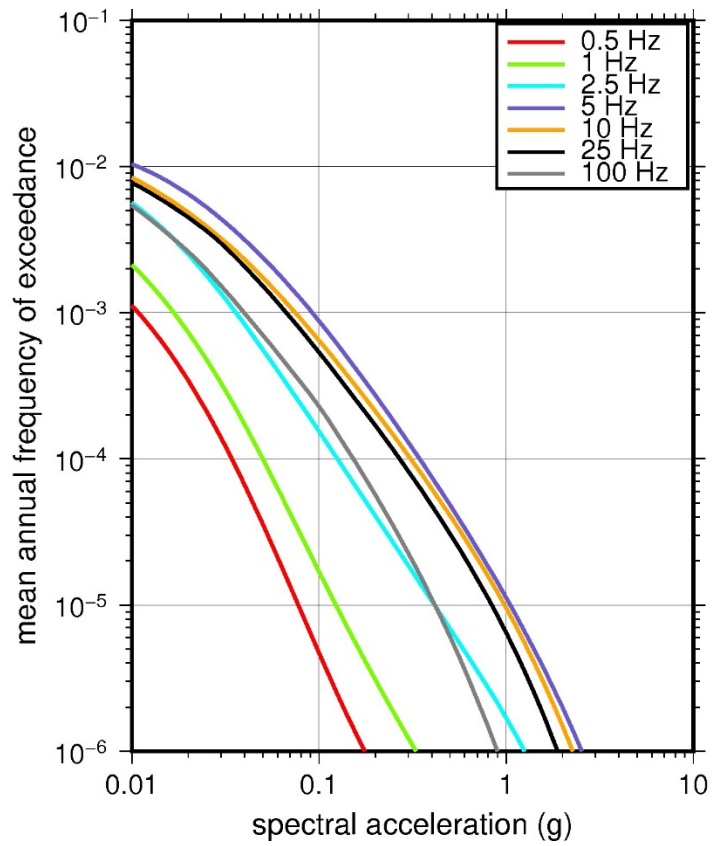


**Figure 2.2-5 Mean Control Point Hazard Curves (Left) for EPRI GMM (2013) Spectral Frequencies, and Ground Motion Response Spectrum/Spectra (GMRS) and UHRS (Right) for Beaver Valley**

## 2.2.2 Calvert Cliffs

The Calvert Cliffs Nuclear Power Plant site is located on the western shore of the Chesapeake Bay within the Coastal Plain physiographic province and is founded on approximately 760 m [2,500 ft] of soil that is underlain by Precambrian crystalline basement rock. The horizontal SSE response spectrum for Calvert Cliffs has a rounded Housner spectral shape and is anchored at a PGA of 0.15g.

### 2.2.2.1 Reference Rock Hazard

For the reference rock PSHA, the NRC staff selected the 10 CEUS-SSC (NRC, 2012b) background seismic source zones that are located within 200 mi [320 km] of the Calvert Cliffs site. In addition, the NRC staff selected the Charleston CEUS-SSC RLME source, which is located about 527 km [325 mi] from the site. To develop the reference rock seismic hazard curves for the site, the NRC staff used the GMPEs in the updated EPRI GMM (2013). As shown in Figure 2.2-6, the Extended Continental Crust—Atlantic Margin (ECC-AM) seismotectonic zone, which is the highest weighted host zone for the Calvert Cliffs site, is the largest contributor to both the 1 Hz and 10 Hz reference rock total mean hazard curves at the  $10^{-4}$  AFE level.

### 2.2.2.2 Site Response Evaluation

#### 2.2.2.2.1 Site Profiles

To develop a basecase profile, the NRC staff used the geologic information in the NTTF R2.1 SHSR (Korsnick, 2014a) submitted by Constellation Energy Nuclear Group (hereafter referred to as “the licensee” within this plant section). As described in the SHSR, the Calvert Cliffs site consists of dense, relatively impervious sandy and clayey silt of Miocene age over dense, relatively pervious sand and silt of Eocene age. The Calvert Cliffs containment buildings are supported on cemented sands within the Chesapeake Formation. In Table 2.3.1-1 of the SHSR, the licensee briefly described the subsurface materials in terms of the geologic units and layer thicknesses. For its site response evaluation, the NRC staff used the plant foundation level, which corresponds to an elevation of  $-1$  ft [ $-0.3$  m] MSL, as the control point elevation for the Calvert Cliffs site.

The licensee’s SHSR profile is based on in situ geophysical investigations for Units 1 and 2 and the COL for Unit 3. These geophysical investigations included multiple seismic refraction surveys and suspension P- and S-wave (P-S) velocity logging performed in multiple site borings, two of which extended to a depth of 122 m [400 ft] below the surface. For the deeper soil layers, the licensee used two sonic logs recorded in wells within 16 km [10 mi] of the site to estimate the  $V_S$  based on the derived  $V_P$  and assumed Poisson’s ratios for the soil and rock strata. Table 2.3.2-1 of the SHSR provides the measured and estimated  $V_S$  determined from the licensee’s site investigations.

The licensee’s SHSR basecase profile extends to a depth of 752 m [2,465 ft] below the control point elevation. The uppermost layers of the profile consist of the Miocene age Chesapeake Formation cemented sand (Stratum IIb) deposit. The licensee subdivided this soil deposit into five layers, each with a thickness of about 1.2 m [4 ft] and a  $V_S$  of 488 m/sec [1,600 ft/sec]. Similarly, the licensee subdivided the underlying 61 m [200 ft] of Chesapeake Formation clays and silts (Stratum IIc) into two layers, with the upper 56 m [185 ft] having a measured median  $V_S$  of 1,250 ft/sec [381 m/sec] and the remaining 6 m [15 ft] a  $V_S$  of 546 m/sec [1,790 ft/sec]. For

the remaining 665 m [2,180 ft] of soil, the  $V_S$  varies from about 579 m/sec [1,900 ft/sec] to 915 m/sec [3,000 ft/sec] at the base of the profile. Finally, the licensee subdivided the 6 m [20 ft] of rock at the base of its profile into two 3 m [10 ft] layers with  $V_S$  of 1,524 m/sec [5,000 ft/sec] and 2,134 m/sec [7,000 ft/sec], respectively.

As the soil strata beneath the Calvert Cliffs site are very well characterized, the NRC staff used the licensee's layer thicknesses and  $V_S$  for the majority of its profile. The minor difference between the NRC staff's and the licensee's profiles are for the uppermost cemented sand deposit. For this soil deposit, the NRC staff used the measured median  $V_S$  from the Unit 3 COL for each of the layers rather than a single fixed value of 488 m/sec [1,600 ft/sec].

To capture the uncertainty in its basecase profile, the NRC staff developed lower and upper range (10<sup>th</sup> and 90<sup>th</sup> percentile) profiles by multiplying the basecase  $V_S$  values by scale factors of 0.83 and 1.21, respectively, which corresponds to an epistemic logarithmic standard deviation of 0.15. The weights for the lower, best-estimate, and upper basecase profiles are 0.3, 0.4, and 0.3, respectively. Figure 2.2-7 shows the NRC staff's profiles, which extend to a depth of 764 m [2,507 ft] below the control point elevation, at which point the  $V_S$  is assumed to reach the reference rock value of 2,831 m/sec [9,285 ft/sec].

#### 2.2.2.2.2 *Dynamic Material Properties and Site Kappa*

The NRC staff assumed both linear and nonlinear behavior for the soil and rock beneath the Calvert Cliffs site. To model the nonlinear response within the upper 110 m [360 ft] of soil deposits, the NRC staff used the EPRI soil shear modulus reduction and damping curves as one alternative and the Peninsular Range curves for the second equally weighted alternative. For the remaining 655 m [2,147 ft] of its profile, the NRC staff assumed a linear response with a damping ratio value of 1 to 2 percent to maintain consistency with the  $\kappa_0$  value for the Calvert Cliffs site.

To determine the basecase  $\kappa_0$  for the Calvert Cliffs site, the NRC staff first used the Campbell (2009) Model 1 relationship between  $V_S$  and  $Q_{ef}$  to determine a  $Q_{ef}$  for each layer. Combining these  $Q_{ef}$  values with the thicknesses and  $V_S$  for each of the layers results in a total  $\kappa_0$  value of about 51 msec, which includes the 6 msec assumed for the underlying reference rock. For the lower and upper basecase profiles, the NRC staff calculated  $\kappa_0$  values of 68 and 38 msec, respectively, using the same approach as for the basecase profile. In contrast, the licensee used a  $\kappa_0$  value of 40 msec for the best-estimate, lower, and upper basecase profiles, which is the maximum value recommended by Appendix B to the SPID (EPRI, 2012) for CEUS deep soil sites.

Table 2.2-3 provides the layer depths, lithologies,  $V_S$ , unit weights, and dynamic properties for the NRC staff's three profiles. In summary, the site response logic tree developed by the NRC staff for the Calvert Cliffs site consists of six alternatives: three basecase profiles (each with a different  $\kappa_0$  value) and two alternative dynamic property branches.

#### 2.2.2.2.3 *Methodology and Results*

The NRC staff followed the methodology described in Section 2.1.4 to develop the final site amplification factors. Figure 2.2-8 shows the overall median site amplification factors and their variability for each of the seven spectral frequencies. As shown in Figure 2.2-8, the median site amplification factors range from about 1 to 3 before falling off with higher input spectral

accelerations. The lower half of Figure 2.2-8 shows that the logarithmic standard deviations for the site amplification factors range from about 0.05 to 0.20.

### 2.2.2.3 Control Point Hazard

The NRC staff implemented Approach 3 from the SPID to develop a weighted control point seismic hazard curve for each of the six unique combinations of the site response logic tree for the Calvert Cliffs site. After combining these curves to develop the final mean control point ground motion response spectra (GMRS) hazard curves, the NRC staff determined the  $10^{-4}$  and  $10^{-5}$  UHRS in order to calculate the final GMRS. Figure 2.2-9 shows the final control point mean seismic hazard curves for each of the seven spectral frequencies as well as the NRC staff's UHRS and GMRS, and the licensee's NTTF R2.1 GMRS (Korsnick, 2014a). As shown in Figure 2.2-9, the NRC staff's GMRS (black curve) is moderately lower than the licensee's GMRS (blue curve) above 10 Hz due to the NRC staff's decision to not cap  $\kappa_0$  at 40 msec.

Layer	Depth (ft)	Description	$V_s$ (ft/sec)			$V_s$ Sigma (ln)	BC Unit Weight (pcf)	Dynamic Properties	
			LR (0.3)	BC (0.4)	UR (0.3)			Alt. 1 (0.5)	Alt. 2 (0.5)
1	15	Soil: sand	1,196	1,450	1,758	0.25	130	EPRI Soil	Pen.
2	30	Soil: sand	1,485	1,800	2,182	0.15	130	EPRI Soil	Pen.
3	45	Soil: sand	932	1,130	1,370	0.15	120	EPRI Soil	Pen.
4	60	Soil: sand	1,436	1,740	2,109	0.15	130	EPRI Soil	Pen.
5	245	Soil: clay, silt	1,031	1,250	1,515	0.15	120	EPRI Soil	Pen.
6	265	Soil: clay, silt	1,477	1,790	2,170	0.15	130	EPRI Soil	Pen.
7	275	Soil: sand	1,898	2,300	2,788	0.15	130	EPRI Soil	Pen.
8	315	Soil: sand	1,675	2,030	2,460	0.15	130	EPRI Soil	Pen.
9	360	Soil: sand	1,592	1,930	2,339	0.15	130	EPRI Soil	Pen.
10	1,045	Soil: clay, silt, sand	1,815	2,200	2,667	0.15	130	L 2.0%	L 2.0%
11	1,545	Soil: sand	1,922	2,330	2,824	0.15	130	L 2.0%	L 2.0%
12	2,045	Soil: sand, clay	2,104	2,550	3,091	0.15	130	L 2.0%	L 2.0%
13	2,482	Soil: clay	2,376	2,880	3,491	0.15	130	L 2.0%	L 2.0%
14	2,507	Rock: granite	5,775	7,000	8,484	0.15	150	L 1.0%	L 1.0%

LR = lower range; BC = basecase; UR = upper range; ln = natural log; pcf = pounds per cubic foot; L = linear; Alt. = alternative; Pen. = Peninsular.  
For LR, BC, UR, and Alt.: Values in parentheses refer to weights for site response analysis logic tree branches.

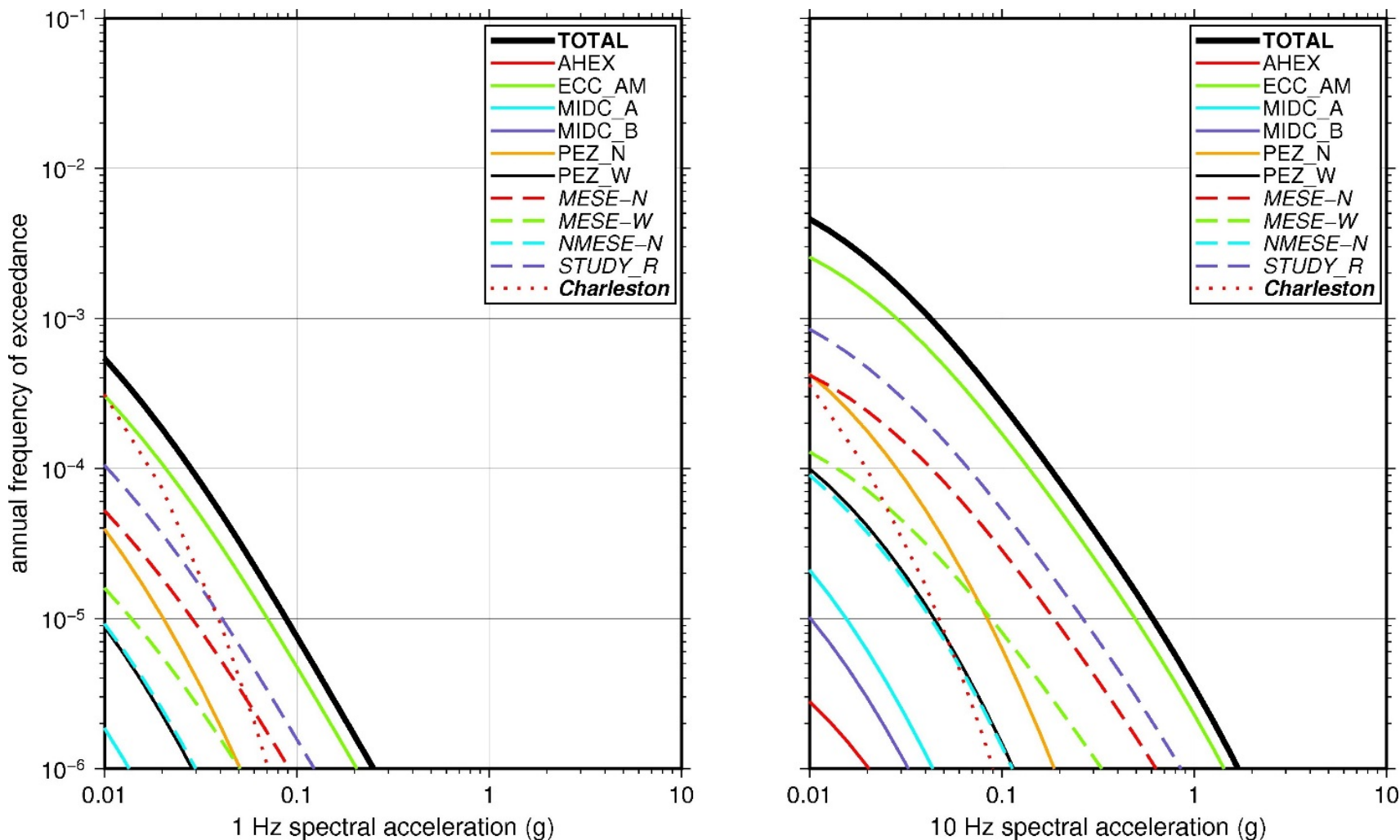


**Figure 2.2-6 Low-Frequency (1 Hz, Left) and High-Frequency (10 Hz, Right) Reference Rock Hazard Curves for Calvert Cliffs. Total Hazard is Shown as a Bold Black Line; Individual Contributions to the Hazard for Each of the CEUS-SSC Sources are Shown as Colored Lines Defined in the Legend. See Table 2.1-1 for Source Name Definitions**

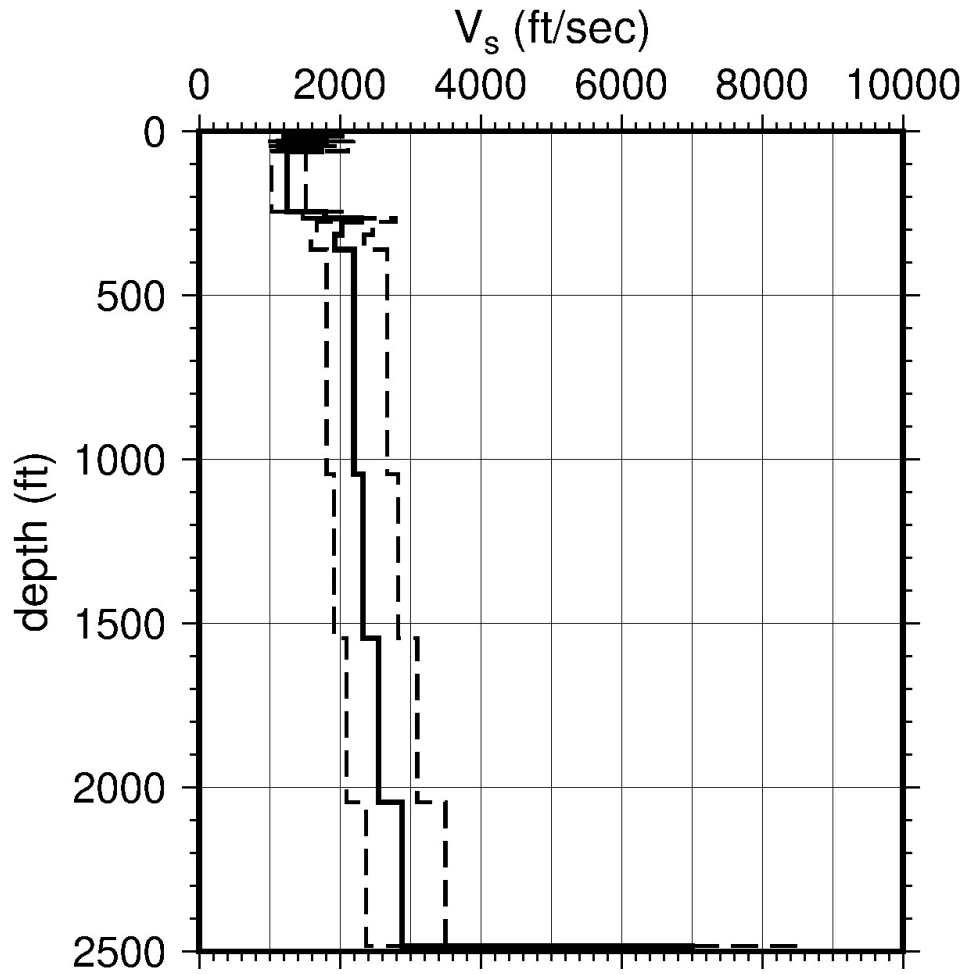


**Figure 2.2-7** Shear Wave Velocity ( $V_s$ ) Profiles for Calvert Cliffs. Basecase (BC) Profile Shown as Solid Bold Line; Lower and Upper Range (LR and UR) Profiles Shown as Dashed Lines. Profiles Terminate at Reference Rock Velocity of 2,831 m/sec [9,285 ft/sec] per EPRI GMM (2013)



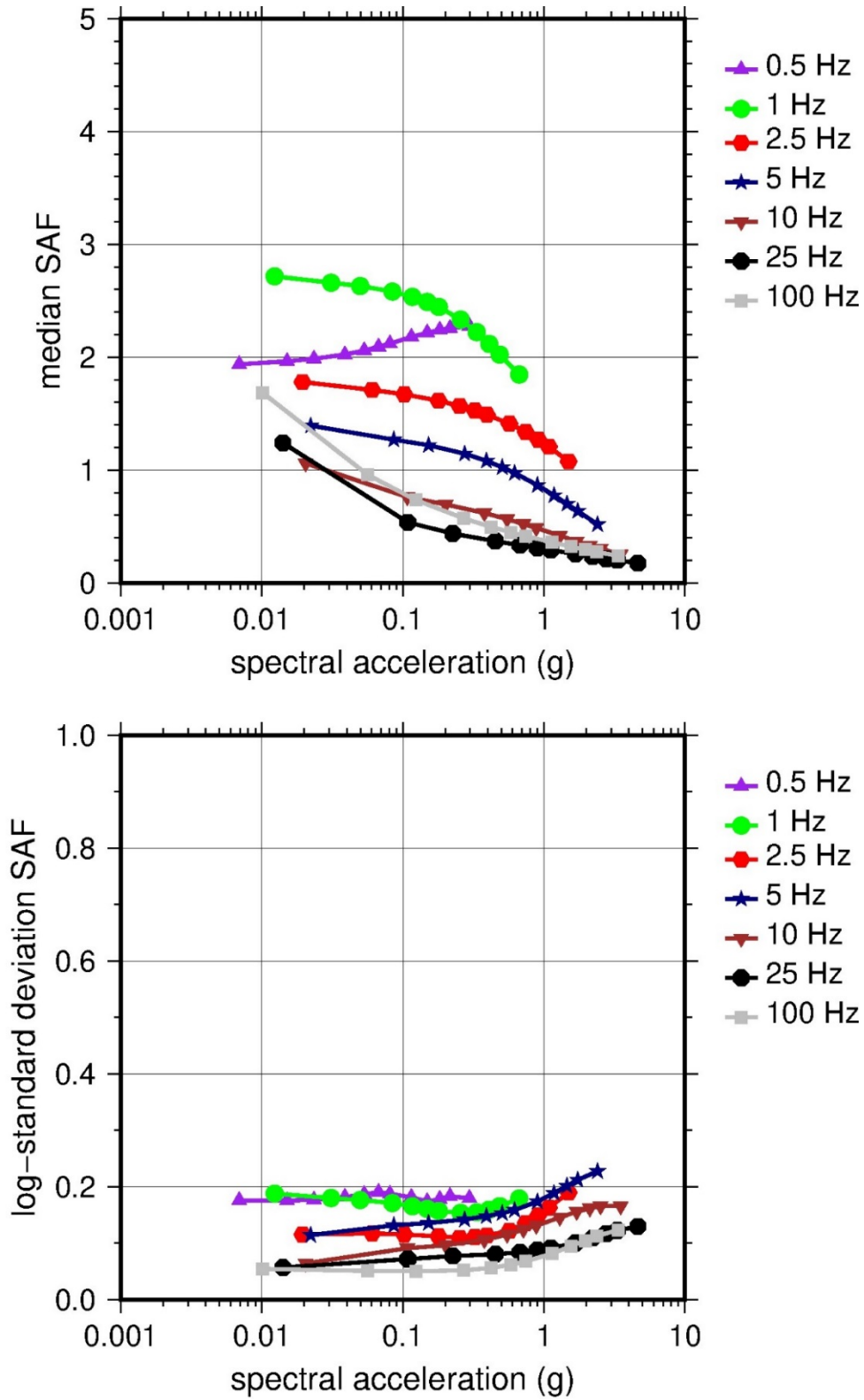


**Figure 2.2-8 Overall Weighted Median Site Amplification Factor (SAF) (Upper) and Log Standard Deviation of the SAF (Lower) as a Function of Input Acceleration for EPRI GMM (2013) Spectral Frequencies**

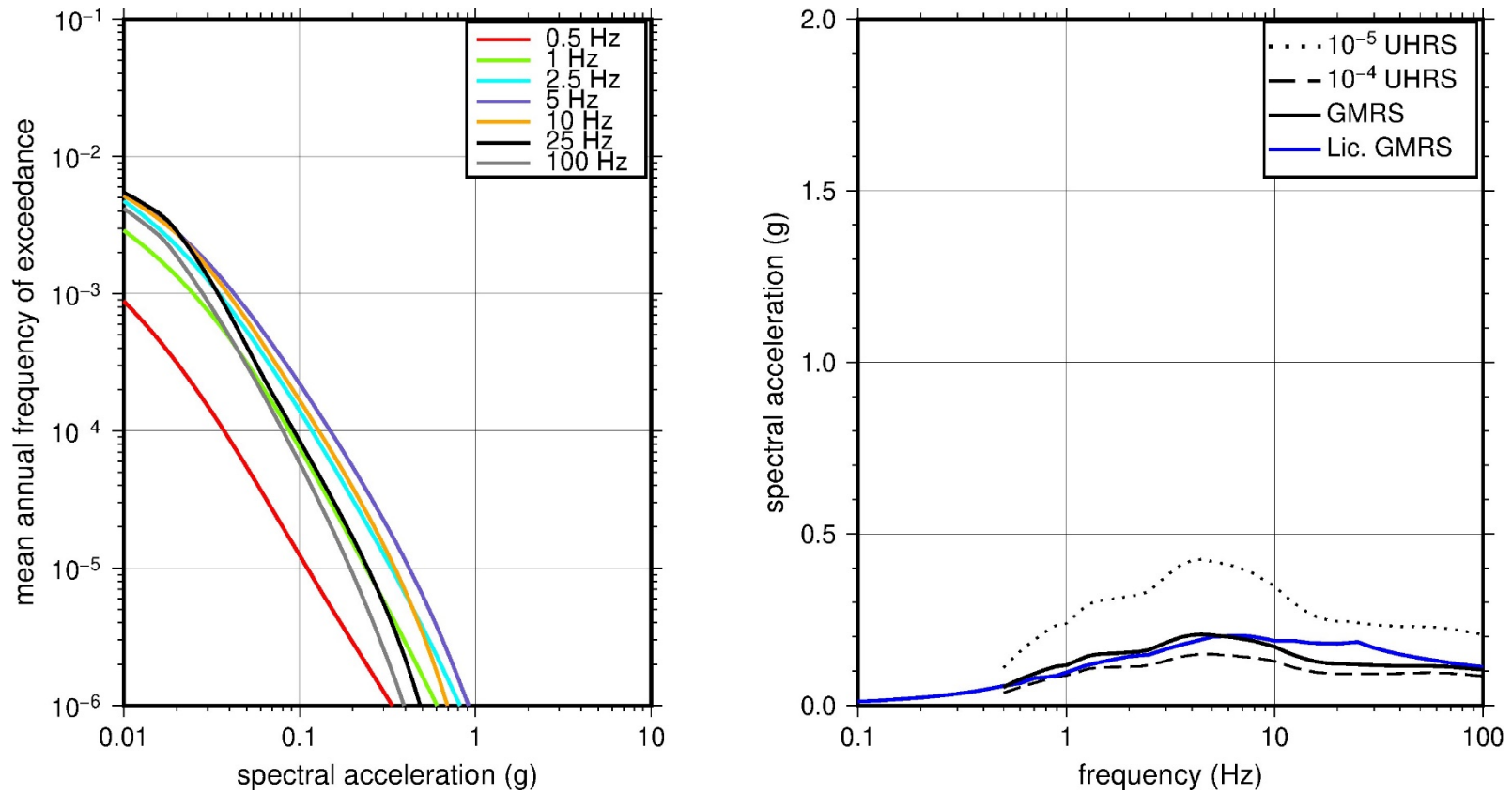


**Figure 2.2-9 Mean Control Point Hazard Curves (Left) for EPRI GMM (2013) Spectral Frequencies, and GMRS and UHRS (Right) for Calvert Cliffs**

### 2.2.3 Ginna

The R.E. Ginna Nuclear Power Plant (Ginna) is located on the shore of Lake Ontario within the Central Lowland physiographic province and is founded on approximately 800 m [2,700 ft] of sedimentary rock (sandstone, shale, and siltstone) that is underlain by Precambrian crystalline rock. The horizontal SSE response spectrum for Ginna has a rounded Housner spectral shape and is anchored at a PGA of 0.20g.

#### 2.2.3.1 Reference Rock Hazard

For the reference rock PSHA, the NRC staff selected the 14 CEUS-SSC (NRC, 2012b) background seismic source zones that are located within 320 km [200 mi] of the Ginna site. In addition, the NRC staff selected the Charlevoix CEUS-SSC RLME source, which is located about 678 km [420 mi] from the site. To develop the reference rock seismic hazard curves for the Ginna site, the NRC staff used the GMPEs in the updated EPRI GMM (2013). As shown in Figure 2.2-10, the St. Lawrence Rift (SLR) seismotectonic zone, which is the highest weighted host zone for the Ginna site, is the largest contributor to both the 1 Hz and 10 Hz reference rock total mean hazard curves at the  $10^{-4}$  AFE level.

#### 2.2.3.2 Site Response Evaluation

##### 2.2.3.2.1 Site Profiles

To develop a basecase profile, the NRC staff used the geologic information in the NTTF R2.1 SHSR (Korsnick, 2014b) submitted by Constellation Energy Nuclear Group (hereafter referred to as “the licensee” within this plant section). As described in the SHSR, the Ginna site consists of a thin layer of glacial deposits overlying dense, fine-grained sandstone, silt, and sandy siltstone, with occasional thin beds of fissile shale. The Ginna structures are supported on the Queenston Formation sandstone, which is of late Paleozoic age. In Table 2.3.1-1 of the SHSR, the licensee briefly described the subsurface materials in terms of the geologic units and layer thicknesses. For its site response evaluation, the NRC staff used the top of rock, which corresponds to an elevation of 71 m [232 ft] MSL, as the control point elevation for the Ginna site.

The field investigation for Ginna, conducted in the 1960s, consisted of a number of borings within the uppermost rock beneath the site. Seismic refraction surveys by the licensee measured  $V_P$  to a depth of about 15 m [50 ft] beneath the site. To determine a  $V_S$  for the upper rock for its R2.1 SHSR profile, the licensee used its measured  $V_P$  and an assumed Poisson’s ratio. For the deeper rock layers, the licensee measured the  $V_P$  at outcrops in the region. Table 2.3.2-1 of the SHSR gives the estimated  $V_S$  determined from the licensee’s site investigations.

The licensee’s SHSR basecase profile extends to a depth of 305 m [1,000 ft] below the control point elevation, which encompasses the Ordovician age sedimentary rock (primarily sandstone with siltstone and shale) from the Queenston Formation. The licensee estimated a  $V_S$  of 2,500 m/sec [8,200 ft/sec] for this rock unit based on a measured  $V_P$  of 3,902 m/sec [12,800 ft/sec] and an assumed Poisson’s ratio of 0.15. The licensee assumed a constant  $V_S$  of 2,500 m/sec [8,200 ft/sec] for the entire 305 m [1,000 ft] of its basecase profile. Below the Queenston Formation are sandstones from the Oswego Formation, for which the licensee estimated a  $V_S$  of 2,743 m/sec [9,000 ft/sec], based on a measured  $V_P$  of 4,268 m/sec [14,000 ft/sec] at a nearby outcrop of this rock unit and an assumed Poisson’s ratio of 0.15. As

this estimated  $V_S$  of 2,743 m/sec [9,000 ft/sec] is close to the reference rock  $V_S$  of 2,831 m/sec [9,285 ft/sec], the licensee terminated its basecase profile at the interface between the Queenston and Oswego Formations.

The NRC staff used the licensee's layer thickness of 305 m [1,000 ft] for the Queenston Formation sandstone but estimated a lower  $V_S$  for this rock layer based on the staff's selection of a higher Poisson's ratio. Based on the range of typical Poisson's ratios for shallow sandstone (0.28 to 0.38), the NRC staff used a value of 0.33, which corresponds to a  $V_P/V_S$  ratio of 2. This results in a  $V_S$  of 1,951 m/sec [6,400 ft/sec], which is much lower than the  $V_S$  of 2,500 m/sec [8,200 ft/sec] estimated by the licensee. Rather than use this same  $V_S$  for the entire 305 m [1,000 ft] of the Queenston Formation, the NRC staff subdivided this layer into increments of 61 m [200 ft] and gradually increased the  $V_S$  for each of the subsequent deeper layers. As the  $V_S$  for the remaining underlying rock strata are either close to or greater than the reference rock  $V_S$  of 2,831 m/sec [9,285 ft/sec], the NRC staff terminated its profile at the base of the Queenston Formation.

To capture the uncertainty in its basecase profile, the NRC staff developed lower and upper range (10<sup>th</sup> and 90<sup>th</sup> percentile) profiles by multiplying the basecase  $V_S$  values by scale factors of 0.83 and 1.21, respectively, which corresponds to an epistemic logarithmic standard deviation of 0.15. The weights for the lower, best-estimate, and upper basecase profiles are 0.3, 0.4, and 0.3, respectively. As shown in Figure 2.2-11, the upper profile terminates at a depth of 183 m [600 ft], and the lower and best-estimate basecase profiles terminate at a depth of 305 m [1,000 ft] below the control point elevation, at which point the  $V_S$  is assumed to reach the reference rock value of 2,831 m/sec [9,285 ft/sec].

#### 2.2.3.2.2 *Dynamic Material Properties and Site Kappa*

The NRC staff assumed both linear and nonlinear dynamic behavior for the rock beneath the Ginna site. To model the nonlinear behavior of the uppermost rock strata, the NRC staff used the EPRI rock shear modulus reduction and material damping curves and to model the linear behavior, the NRC staff used a constant damping ratio of 3 percent. The NRC staff assumed these two alternative dynamic responses for the upper 61 m [200 ft] of the profile. Due to the higher  $V_S$  of this rock layer, the NRC staff assigned weights of 0.7 and 0.3 to the linear and nonlinear alternatives, respectively. For the remaining 229 m [750 ft] of its profile, the NRC staff assumed a linear response with a material damping ratio value of 0.1 percent to maintain consistency with the  $\kappa_0$  value for the Ginna site.

To determine the basecase  $\kappa_0$  for the Ginna site, the NRC staff first used the Campbell (2009) Model 1 relationship between  $V_S$  and  $Q_{ef}$  to determine a  $Q_{ef}$  for each layer. Combining these  $Q_{ef}$  values with the thicknesses and  $V_S$  for each of the layers results in a total  $\kappa_0$  value of about 8 msec, which includes the 6 msec assumed for the underlying reference rock. For the lower and upper basecase profiles, the NRC staff calculated  $\kappa_0$  values of 9 and 7 msec, respectively, using the same approach as for the best-estimate basecase profile. In contrast, the licensee estimated  $\kappa_0$  by combining the lowest low-strain damping values from the EPRI rock material damping curves over the upper 152 m [500 ft] of rock with an assumed damping value of 1.25 percent for the remaining underlying rock layers to estimate best-estimate, lower, and upper basecase  $\kappa_0$  values of 12, 19, and 6 msec, respectively.

Table 2.2-4 provides the layer depths, lithologies,  $V_S$ , unit weights, and dynamic properties for the NRC staff's three profiles. In summary, the site response logic tree developed by the NRC

staff for the Ginna site consists of six alternatives; three basecase profiles (each with a different  $\kappa_0$  value) and two alternative dynamic property branches.

### 2.2.3.2.3 Methodology and Results

The NRC staff followed the methodology described in Section 2.1.4 to develop the final site amplification factors. Figure 2.2-12 shows the overall median site amplification factors and their variability for each of the seven spectral frequencies. As shown in Figure 2.2-12, the median site amplification factors range from about 1.0 to 1.5 before falling off with higher input spectral accelerations. The lower half of Figure 2.2-12 shows that the logarithmic standard deviations for the site amplification factors range from about 0.05 to 0.10.

### 2.2.3.3 Control Point Hazard

The NRC staff implemented Approach 3 from the SPID to develop a weighted control point seismic hazard curve for each of the six unique combinations of the site response logic tree for the Ginna site. After combining these curves to develop the final mean control point hazard curves, the NRC staff determined the  $10^{-4}$  and  $10^{-5}$  UHRS in order to calculate the final GMRS. Figure 2.2-13 shows the final control point mean seismic hazard curves for each of the seven spectral frequencies as well as the NRC staff's UHRS and GMRS, and the licensee's NTTF R2.1 GMRS (Korsnick, 2014b). As shown in Figure 2.2-13, the NRC staff's GMRS (black curve) is slightly higher than the licensee's GMRS (blue curve) above 10 Hz due to differences between the basecase profiles and estimated site  $\kappa_0$  values. For comparison, Figure 2.2-13 also shows the NRC staff's reference rock GMRS (brown dotted curve).

Layer	Depth (ft)	Description	$V_s$ (ft/sec)			$V_s$ Sigma (ln)	BC Unit Weight (pcf)	Dynamic Properties	
			LR (0.3)	BC (0.4)	UR (0.3)			Alt. 1 (0.3)	Alt. 2 (0.7)
1	200	Rock: sandstone	5,280	6,400	7,757	0.25	150	EPRI Rock	L 3.0%
2	400	Rock: sandstone	5,709	6,920	8,387	0.15	150	L 0.1%	L 0.1%
3	600	Rock: sandstone	6,138	7,440	9,018	0.15	160	L 0.1%	L 0.1%
4	800	Rock: sandstone	6,567	7,960	9,285	0.15	160	L 0.1%	L 0.1%
5	1,000	Rock: sandstone	6,997	8,480	9,285	0.15	160	L 0.1%	L 0.1%

LR = lower range; BC = basecase; UR = upper range; ln = natural log; pcf = pounds per cubic foot; L = linear; Alt. = alternative.  
For LR, BC, UR, and Alt.: Values in parentheses refer to weights for site response analysis logic tree branches.

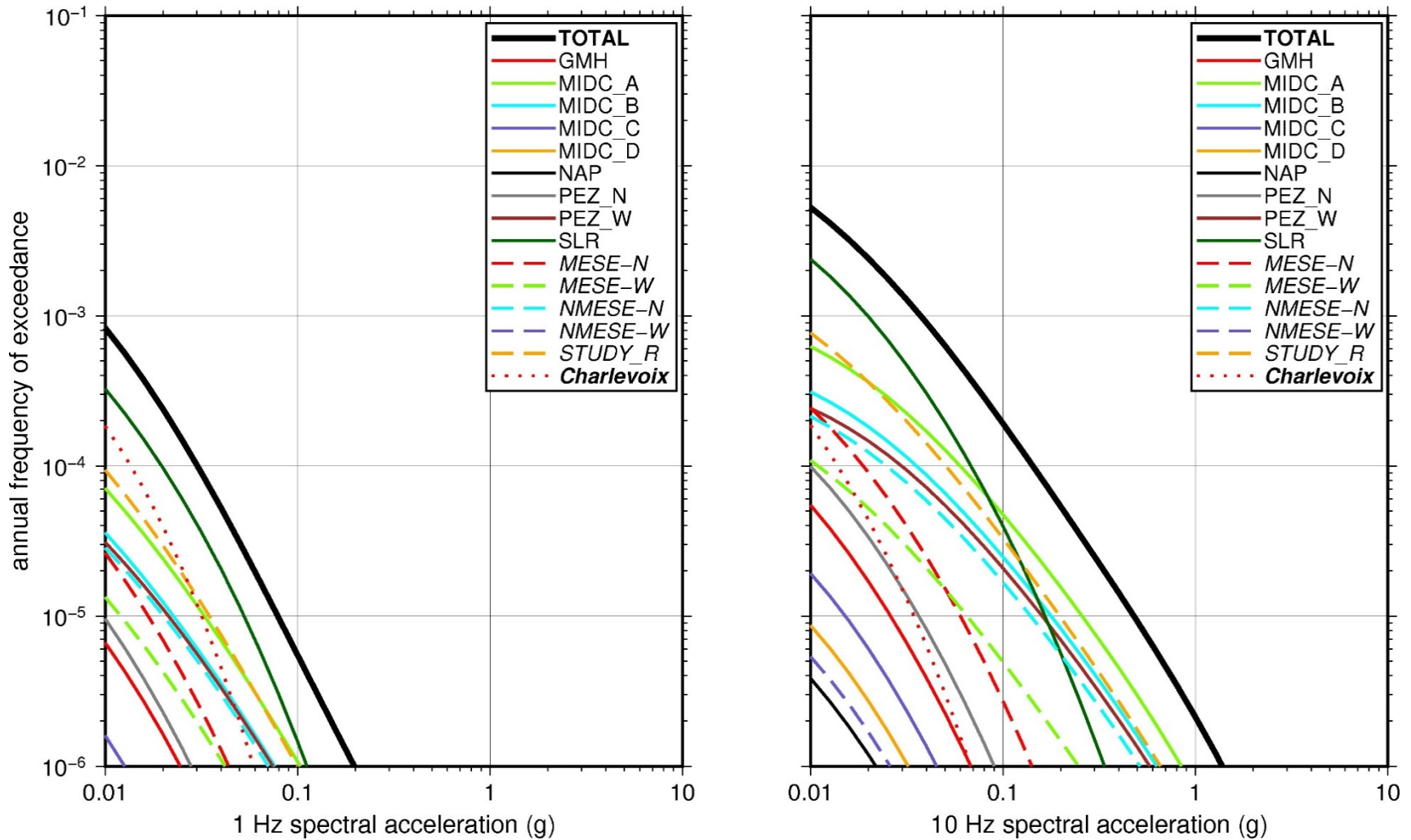


**Figure 2.2-10 Low-Frequency (1 Hz, Left) and High-Frequency (10 Hz, Right) Reference Rock Hazard Curves for Ginna. Total Hazard is Shown as a Bold Black Line; Individual Contributions to the Hazard for Each of the CEUS-SSC Sources are Shown as Colored Lines Defined in the Legend. See Table 2.1-1 for Source Name Definitions**

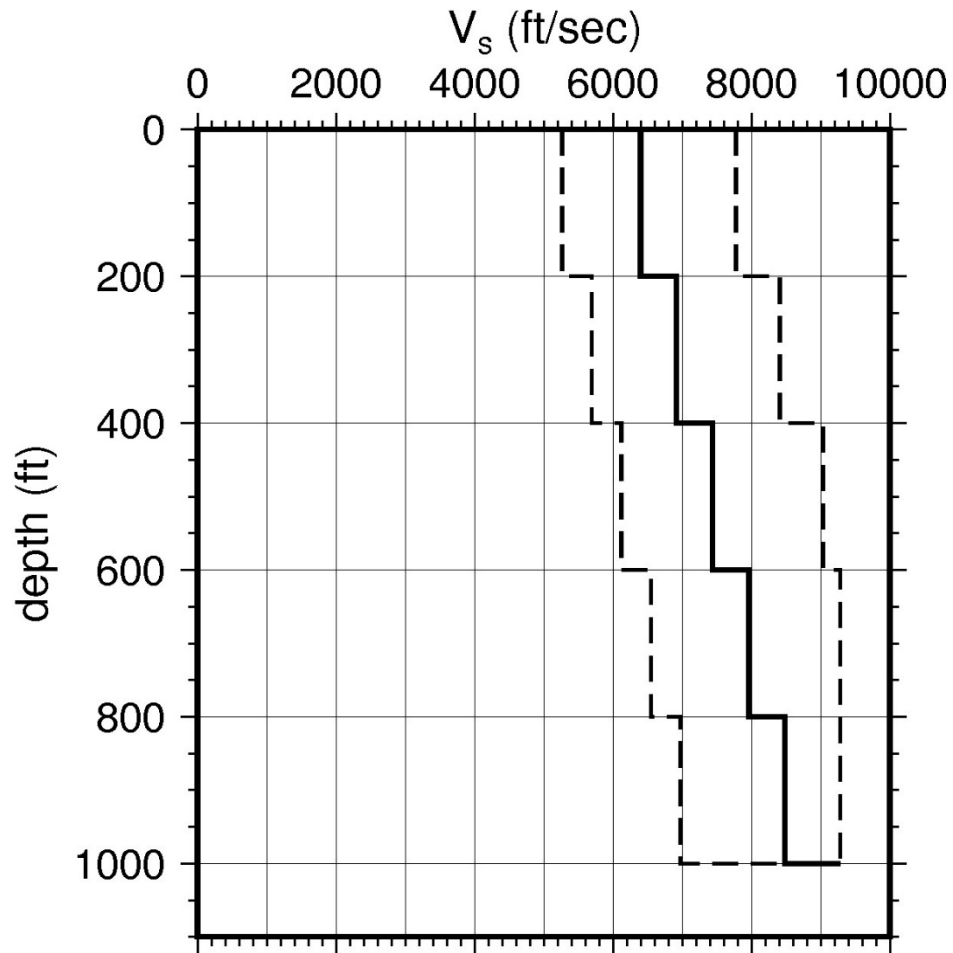


**Figure 2.2-11 Shear Wave Velocity ( $V_s$ ) Profiles for Ginna. Basecase (BC) Profile Shown as Solid Bold Line; Lower and Upper Range (LR and UR) Profiles Shown as Dashed Lines. Profiles Terminate at Reference Rock Velocity of 2,831 m/sec [9,285 ft/sec] per EPRI GMM (2013)**

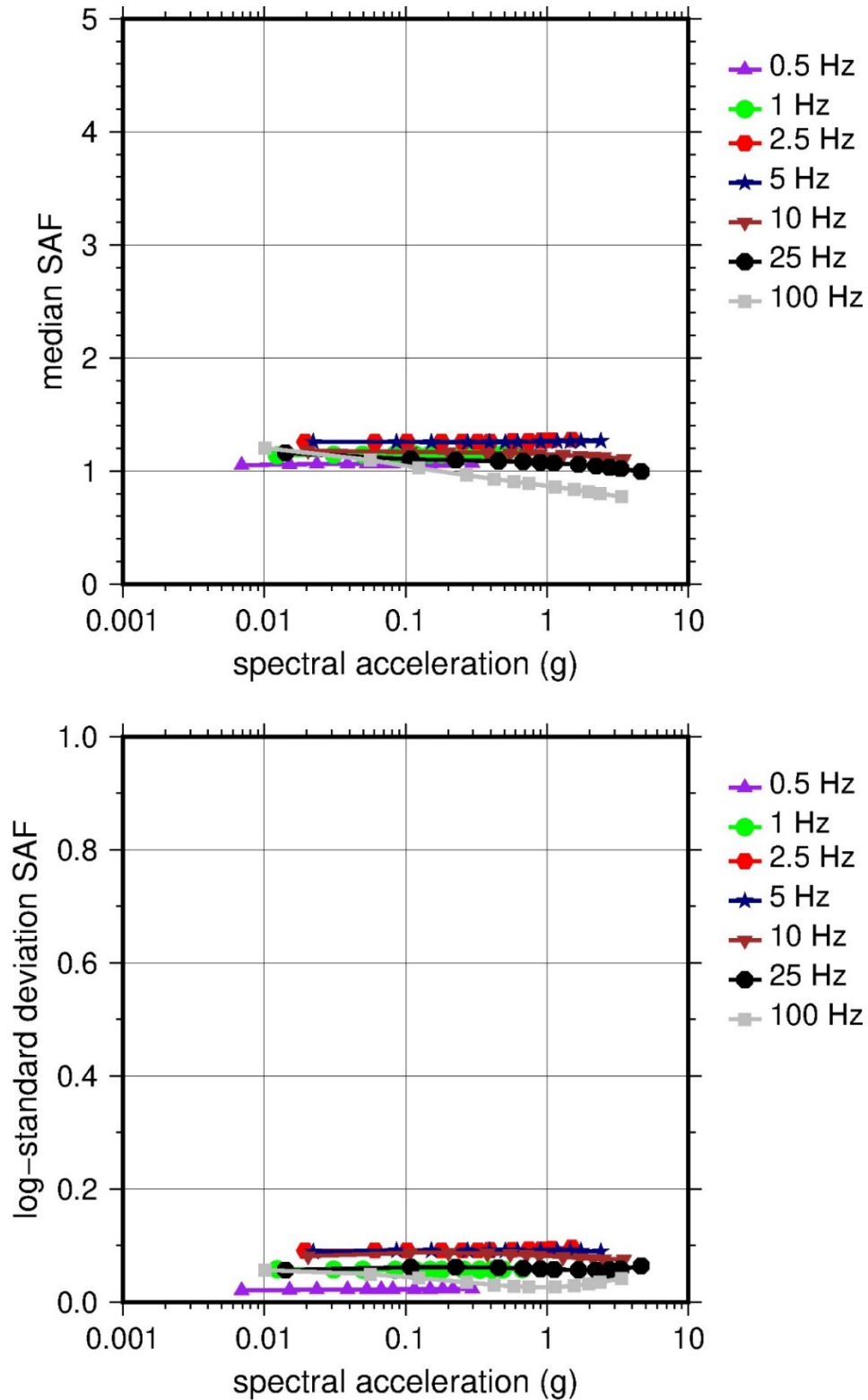


**Figure 2.2-12 Overall Weighted Median Site Amplification Factor (SAF) (Upper) and Log Standard Deviation of the SAF (Lower) as a Function of Input Acceleration for EPRI GMM (2013) Spectral Frequencies**



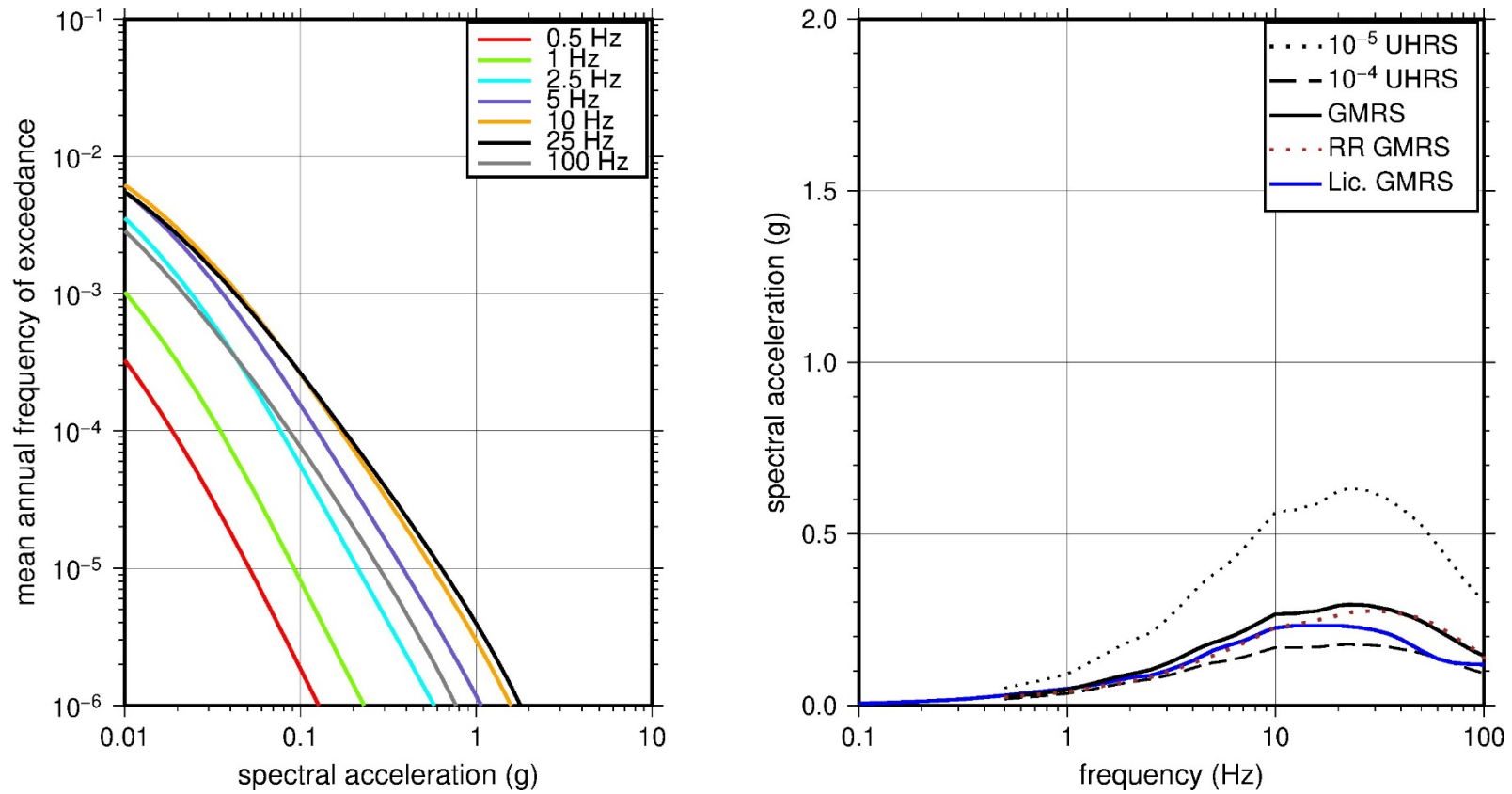


**Figure 2.2-13 Mean Control Point Hazard Curves (Left) for EPRI GMM (2013) Spectral Frequencies, and GMRS and UHRs (Right) for Ginna**

## 2.2.4 Hope Creek and Salem

The site for the Hope Creek Generating Station and Salem Nuclear Generating Station is located on the southern part of Artificial Island on the east bank of the Delaware River within the Atlantic Coastal Plain physiographic province. The Hope Creek-Salem site is founded on about 550 m [1,800 ft] of progressively older dense silty sands that are underlain by basement rock. The horizontal SSE response spectrum for Hope Creek has a spectral shape from Regulatory Guide (RG) 1.60, "Design Response Spectra for Seismic Design of Nuclear Power Plants," Revision 2, issued July 2014 (NRC, 2014), and is anchored at a PGA of 0.2g. The SSE for Salem has a rounded Housner spectral shape and is also anchored at a PGA of 0.2g.

### 2.2.4.1 Reference Rock Hazard

For the reference rock PSHA, the NRC staff selected the 10 CEUS-SSC (NRC, 2012b) background seismic source zones that are located within 320 km [200 mi] of the Hope Creek-Salem site. The NRC staff also selected the Charleston CEUS-SSC RLME source, which is located about 650 km [400 mi] from the site. To develop the reference rock seismic hazard curves for the site, the NRC staff used the GMPEs in the updated EPRI GMM (2013). As shown in Figure 2.2-14, the ECC-AM seismotectonic zone, which is the highest weighted host zone for the site, is the largest contributor to both the 1 Hz and 10 Hz reference rock total mean hazard curves.

### 2.2.4.2 Site Response Evaluation

#### 2.2.4.2.1 Site Profiles

To develop a basecase profile, the NRC staff used the geologic information in the NTTF R2.1 SHSRs for Hope Creek (P.J. Davison, 2014) and Salem (Perry, 2014) developed by Public Service Enterprise Group (PSEG) Nuclear (hereafter referred to as "the licensee" within this plant section). As described in the two SHSRs, the site consists of about 550 m [1,800 ft], of Cretaceous, Tertiary, and Quaternary age unconsolidated to semiconsolidated sediments. The site safety-related structures are founded on the Vincetown Formation, which is a competent, cemented, granular soil. In Tables 2-1 of the SHSRs, the licensee briefly described the subsurface materials in terms of the geologic units and layer thicknesses. For its site response evaluation, the NRC staff used the top of the Vincetown Formation, which corresponds to an elevation of -16 m [-52 ft] MSL, as the control point elevation for the Hope Creek-Salem site.

The licensee based the SHSR profiles for the two sites on in situ geophysical investigations for the two plants and the ESP application (PSEG, 2013). These geophysical investigations included seismic refraction, crosshole, downhole, and suspension P-S velocity logging in multiple site borings extending to a depth of about 192 m [630 ft] below the surface. For the deeper soil layers, the licensee used seismic refraction surveys to estimate the  $V_S$  based on the measured  $V_P$  and assumed Poisson's ratios for the soil. To identify the location of crystalline basement rock, the licensee used a nearby well log located 1 km [0.6 mi] from the site. Table 2-2 of the SHSRs provides the measured and estimated  $V_S$  determined from the licensee's site investigations.

The licensee's SHSR basecase profiles for the two plants differ slightly with respect to the location of the control point. For Hope Creek, the licensee selected its control point to be at a depth of 19 m [62 ft] below grade, which corresponds to the bottom of base mat for that plant. For Salem, the licensee selected its control point to be at a depth of 22 m [71 ft], which

corresponds to the foundation level for that plant. The top layer for the Hope Creek profile is a 3 m [9 ft] layer of compacted backfill with a  $V_S$  of 283 m/sec [927 ft/sec], while the Salem profile starts with the Vincetown Formation soil deposit, which is the second layer for the Hope Creek profile. This additional 3 m [9 ft] top layer of backfill for the Hope Creek profile results in a basecase profile with a total thickness of 518 m [1,699 ft] for that plant, while the Salem basecase profile has a total thickness of 515 m [1,690 ft]. In general, the basecase profiles for both plants begin with the Paleocene to Cretaceous age Vincetown, Hornerstown, and Navesink Formations sand deposits. The licensee subdivided these soil deposits into nine layers, each with a thickness of about 3 m [10 ft] and a  $V_S$  of 686 m/sec [2,250 ft/sec]. Similarly, the licensee subdivided the underlying 127 m [415 ft] of Cretaceous age soil deposits (primarily sand with some clays and silts) into multiple layers, with  $V_S$  ranging from 518 m/sec [1,700 ft/sec] to about 915 m/sec [3,000 ft/sec]. For the remaining 380 m [1,245 ft] of soil, the licensee used the measured  $V_P$  of 1,890 m/sec [6,200 ft/sec] and assumed Poisson's ratios ranging from 0.34 to 0.43 to estimate  $V_S$  of 671 m/sec [2,200 ft/sec], 720 m/sec [2,630 ft/sec], and 933 m/sec [3,060 ft/sec].

As the soil strata beneath the Hope Creek-Salem site are very well characterized, the NRC staff used the licensee's layer thicknesses and  $V_S$  for its profile. Specifically, the NRC staff chose to use the Salem profile for its basecase profile, which begins with the Vincetown Formation soils as the uppermost layer.

To capture the uncertainty in its basecase profile, the NRC staff developed lower and upper range (10<sup>th</sup> and 90<sup>th</sup> percentile) profiles by multiplying the basecase  $V_S$  values by scale factors of 0.83 and 1.21, respectively, which corresponds to an epistemic logarithmic standard deviation of 0.15. The weights for the lower, best-estimate, and upper basecase profiles are 0.3, 0.4, and 0.3, respectively. Figure 2.2-15 shows the NRC staff's profiles, which extend to a depth of 515 m [1,690 ft] below the control point elevation, at which point the  $V_S$  is assumed to reach the reference rock value of 2,831 m/sec [9,285 ft/sec].

#### 2.2.4.2.2 *Dynamic Material Properties and Site Kappa*

The NRC staff assumed both linear and nonlinear behavior for the soil beneath the Hope Creek-Salem site. To model the nonlinear response within the upper 136 m [445 ft] of soil deposits, the NRC staff used the EPRI soil shear modulus reduction and damping curves as one alternative and the Peninsular Range curves for the second equally weighted alternative. For the remaining 380 m [1,245 ft] of its profile, the NRC staff assumed a linear response with a damping ratio value of 1 to 2 percent to maintain consistency with the  $\kappa_0$  value for the Hope Creek-Salem site.

To determine the basecase  $\kappa_0$  for the Hope Creek-Salem site, the NRC staff first used the Campbell (2009) Model 1 relationship between  $V_S$  and  $Q_{ef}$  to determine a  $Q_{ef}$  for each layer. Combining these  $Q_{ef}$  values with the thicknesses and  $V_S$  for each of the layers results in a total  $\kappa_0$  value of about 30 msec, which includes the 6 msec assumed for the underlying reference rock. For the lower and upper basecase profiles, the NRC staff calculated  $\kappa_0$  values of 40 and 23 msec, respectively, using the same approach as for the basecase profile. In contrast, the licensee estimated  $\kappa_0$  by using the empirical relationship from the SPID (EPRI, 2012) between profile thickness and  $\kappa_0$ , which resulted in  $\kappa_0$  values of 37 msec for the best-estimate, lower, and upper basecase profiles, respectively.

Table 2.2-5 provides the layer depths, lithologies,  $V_S$ , unit weights, and dynamic properties for the NRC staff's three profiles. In summary, the site response logic tree developed by the NRC

staff for the site consists of six alternatives; three basecase profiles (each with a different  $\kappa_0$  value) and two alternative dynamic property branches.

#### 2.2.4.2.3 *Methodology and Results*

The NRC staff followed the methodology described in Section 2.1.4 to develop the final site amplification factors. Figure 2.2-16 shows the overall median site amplification factors and their variability for each of the seven spectral frequencies. As shown in Figure 2.2-16, the median site amplification factors range from about 1 to 2 before falling off with higher input spectral accelerations. The lower half of Figure 2.2-16 shows that the logarithmic standard deviations for the site amplification factors range from about 0.05 to 0.20.

#### 2.2.4.3 *Control Point Hazard*

The NRC staff implemented Approach 3 from the SPID to develop a weighted control point seismic hazard curve for each of the six unique combinations of the site response logic tree for the Hope Creek-Salem site. After combining these curves to develop the final mean control point hazard curves, the NRC staff determined the  $10^{-4}$  and  $10^{-5}$  UHRS in order to calculate the final GMRS. Figure 2.2-17 shows the final control point mean seismic hazard curves for each of the seven spectral frequencies as well as the NRC staff's UHRS and GMRS, and the licensee's NTTF R2.1 GMRS for Hope Creek (P.J. Davison, 2014) and Salem (Perry, 2014). As shown in Figure 2.2-17, the NRC staff's GMRS (black curve) is moderately lower than the licensee's GMRS (blue and purple curves) above 10 Hz due to the staff's decision to not implement a lower bound minimum site amplification factor cutoff value of 0.5.

**Table 2.2-5 Layer Depths, Shear Wave Velocities ( $V_s$ ), Unit Weights, and Dynamic Properties for Hope Creek-Salem**

Layer	Depth (ft)	Description	$V_s$ (ft/sec)			$V_s$ Sigma (ln)	BC Unit Weight (pcf)	Dynamic Properties	
			LR (0.3)	BC (0.4)	UR (0.3)			Alt. 1 (0.5)	Alt. 2 (0.5)
1	92	Soil: silty sand	1,856	2,250	2,727	0.25	130	EPRI Soil	Pen.
2	110	Soil: sand	3,234	3,920	4,751	0.15	140	EPRI Soil	Pen.
3	132	Soil: sand	2,054	2,490	3,018	0.15	130	EPRI Soil	Pen.
4	166	Soil: sand	2,492	3,020	3,660	0.15	130	EPRI Soil	Pen.
5	228	Soil: sand, clay	2,054	2,490	3,018	0.15	130	EPRI Soil	Pen.
6	312	Soil: sand, clay	1,411	1,710	2,072	0.15	130	EPRI Soil	Pen.
7	338	Soil: silt, clay)	1,889	2,290	2,776	0.15	130	EPRI Soil	Pen.
8	363	Soil: clay, silt	1,469	1,780	2,157	0.15	130	EPRI Soil	Pen.
9	445	Soil: sand, clay	2,054	2,490	3,018	0.15	130	EPRI Soil	Pen.
10	810	Soil: clay	1,816	2,200	2,667	0.15	130	L 2.0%	L 2.0%
11	1,240	Soil: clay	2,169	2,630	3,188	0.15	130	L 2.0%	L 2.0%
12	1,690	Soil: clay	2,524	3,060	3,709	0.15	130	L 1.0%	L 1.0%

LR = lower range; BC = basecase; UR = upper range; ln = natural log; pcf = pounds per cubic foot; L = linear; Alt. = alternative; Pen. = Peninsular.  
 For LR, BC, UR, and Alt.: Values in parentheses refer to weights for site response analysis logic tree branches.

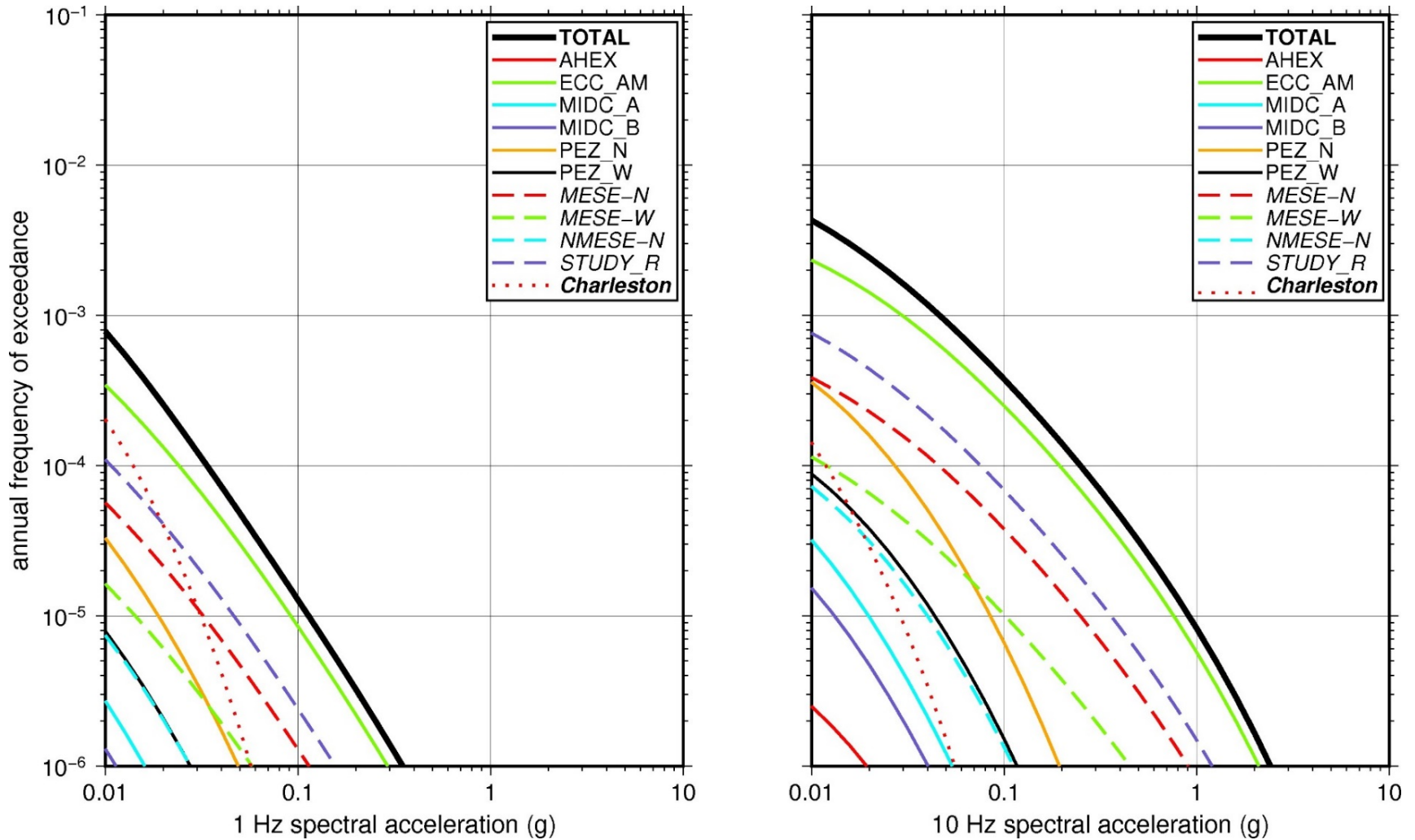


**Figure 2.2-14 Low-Frequency (1 Hz, Left) and High-Frequency (10 Hz, Right) Reference Rock Hazard Curves for Hope Creek-Salem. Total Hazard is Shown as a Bold Black Line; Individual Contributions to the Hazard for Each of the CEUS-SSC Sources are Shown as Colored Lines Defined in the Legend. See Table 2.1-1 for Source Name Definitions**

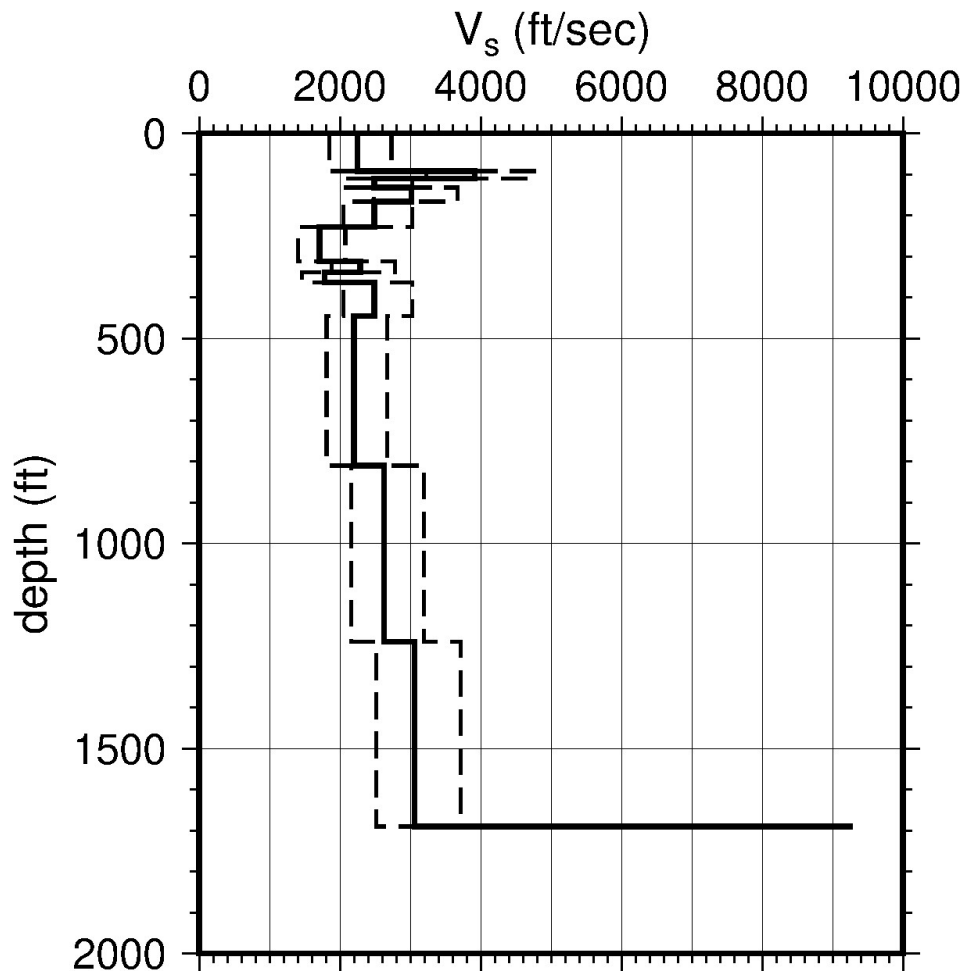


**Figure 2.2-15 Shear Wave Velocity ( $V_s$ ) Profiles for Hope Creek-Salem. Basecase (BC) Profile Shown as Solid Bold Line; Lower and Upper Range (LR and UR) Profiles Shown as Dashed Lines. Profiles Terminate at Reference Rock Velocity of 2,831 m/sec [9,285 ft/sec] per EPRI GMM (2013)**

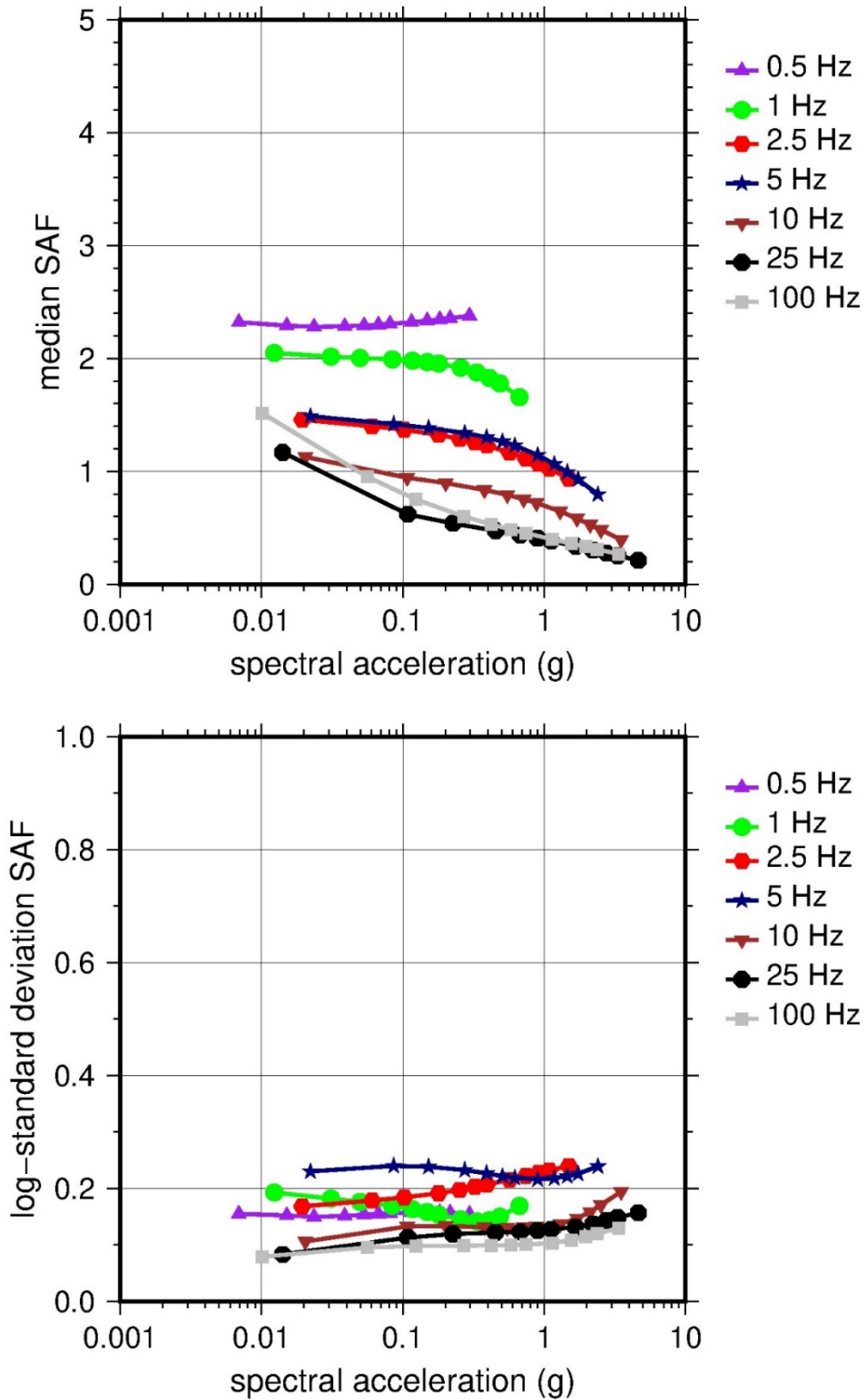


**Figure 2.2-16 Overall Weighted Median Site Amplification Factor (SAF) (Upper) and Log Standard Deviation of the SAF (Lower) as a Function of Input Acceleration for EPRI GMM (2013) Spectral Frequencies**



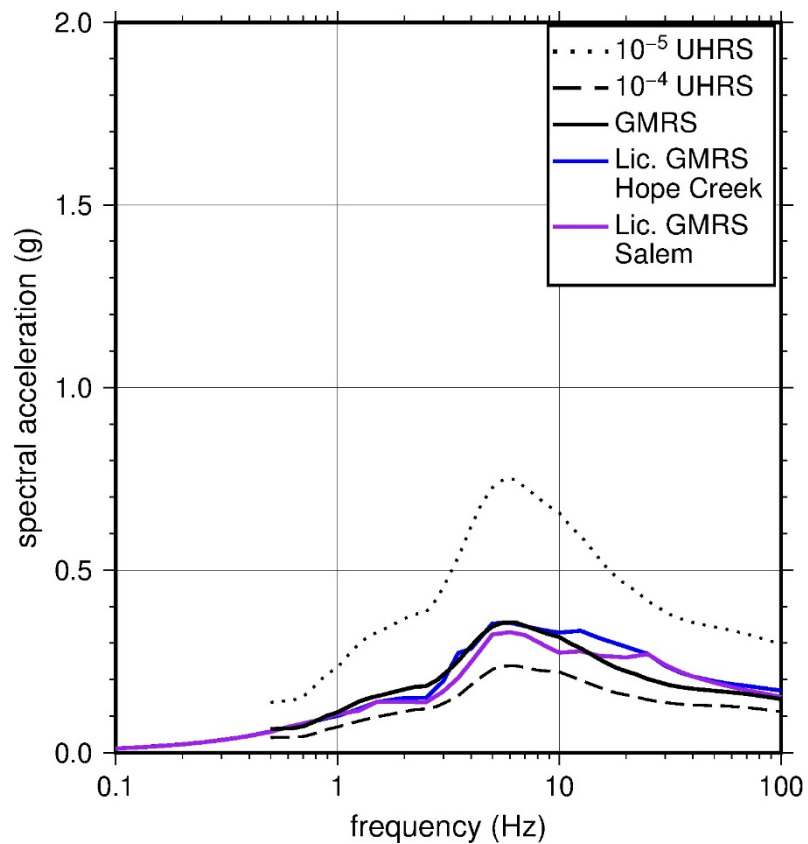
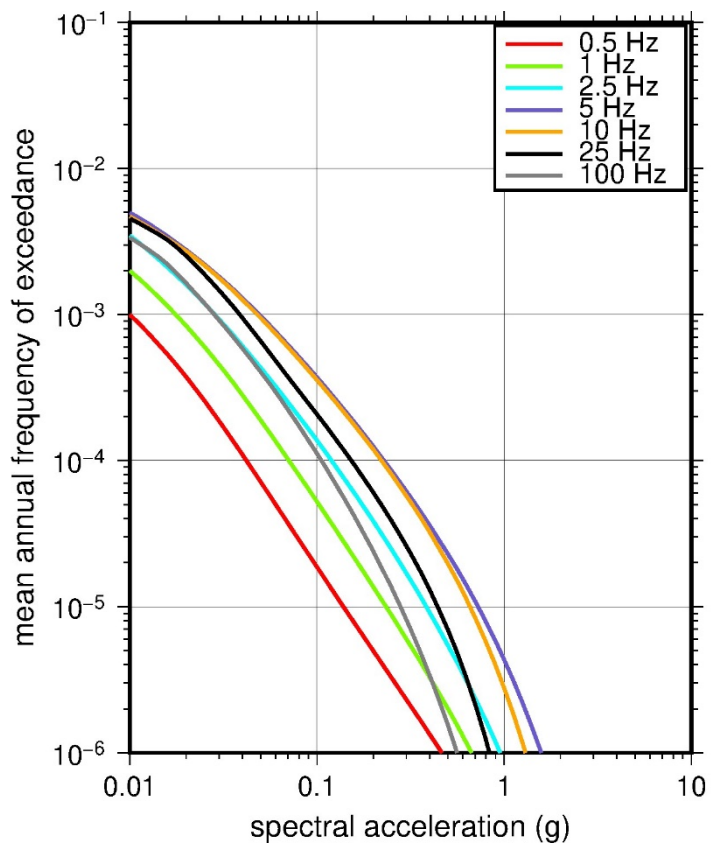


**Figure 2.2-17 Mean Control Point Hazard Curves (Left) for EPRI GMM (2013) Spectral Frequencies, and GMRS and UHRs (Right) for Hope Creek-Salem**

## 2.2.5 Indian Point

The Indian Point Energy Center site is located on the east bank of the Hudson River within the New England physiographic province and is underlain by a complexly deformed sequence of crystalline metamorphic rock. The horizontal SSE response spectrum for Indian Point has a rounded Housner spectral shape and is anchored at a PGA of 0.15g.

### 2.2.5.1 Reference Rock Hazard

For the reference rock PSHA, the NRC staff selected the 12 CEUS-SSC (NRC, 2012b) background seismic source zones that are located within 320 km [200 mi] of the site. The NRC staff also selected the Charlevoix CEUS-SSC RLME source, which is located about 694 km [430 mi] from the site. To develop the reference rock seismic hazard curves for the Indian Point site, the NRC staff used the GMPEs in the updated EPRI GMM (2013). As shown in Figure 2.2-18, the ECC-AM seismotectonic zone, which is the highest weighted host zone for the site, is the largest contributor to both the 1 and 10 Hz reference rock total mean hazard curves at the  $10^{-4}$  AFE level.

### 2.2.5.2 Site Response Evaluation

#### 2.2.5.2.1 Site Profiles

To assess the need to perform a site response evaluation, the NRC staff used the geologic information in the NTTTF R2.1 SHSR (Ventosa, 2014) submitted by Entergy Nuclear Operations, Inc. (hereafter referred to as “the licensee” within this plant section) and the results from other in situ geophysical measurements described below. In its SHSR, the licensee stated that the rocks underlying the Indian Point site are composed primarily of crystalline metamorphic rock with a  $V_S$  greater than the reference rock  $V_S$  of 2,831 m/sec [9,285 ft/sec], which is considered hard rock according to the SPID. Therefore, the licensee did not perform a site response analysis for the Indian Point site. Instead, the licensee used the reference rock hazard curves from the PSHA as its control point hazard curves for determining the GMRS for the Indian Point site. To evaluate the licensee’s conclusion that Indian Point is a hard rock site and, as such, does not need a site response evaluation, the staff performed the following confirmatory analysis.

The Indian Point site is underlain by a complexly deformed sequence of metamorphosed sedimentary or igneous rocks of early Paleozoic to Precambrian age. The uppermost (youngest) of these units is the Manhattan Schist. This unit is underlain by the Inwood Marble, the Lowerre Quartzite, the Yonkers-Pound Ridge granite, and the Fordham gneiss. Indian Point Units 2 and 3 are founded in the Inwood Marble unit. The Inwood Marble consists of a layered sequence of dolomitic and calcitic marbles with occasional lenses of schist. The UFSAR for Indian Point (Entergy Nuclear Operations Inc., 2011) describes the Inwood Marble as exhibiting a distinct layered structure, striking north-south to northeast-southwest, dipping to the east and exhibiting a jointed character. All descriptions of the Inwood Marble state it as being a “firm rock.” As noted above, the licensee estimated that the  $V_S$  of the foundation-bearing Inwood Marble unit is greater than the reference rock  $V_S$  of 2,831 m/sec [9,285 ft/sec]. As no direct  $V_S$  measurements exist within the Inwood Marble near the Unit 2 or Unit 3 reactors (Entergy Nuclear Operations Inc., 2011), the staff examined other nearby geophysical investigations.

Between 2005 and 2007, comprehensive hydrogeologic investigations were performed at the Indian Point site (GZA GeoEnvironmental, Inc., 2008). These investigations were initiated to

understand groundwater flow and contaminant transport at the site. Many borings were advanced to study the site geology, hydrology, and aquifer properties. Some of the test borings provided estimates of the Rock Quality Designation (RQD) for the uppermost rock (inferred to be Inwood Marble) in the vicinity of Units 2 and 3 that, consistent with the description of the Inwood Marble as firm or hard rock, range in value from 60 to 100 for the bedrock. In addition, as part of the hydrogeologic investigation, direct  $V_S$  measurements were obtained in the Inwood Marble at a location about 213 m [700 ft] to the east-southeast of Unit 3 (near the site warehouse). These data consist of 13 profiles that sampled the uppermost portion of the rock. The average rock  $V_S$  of the profiles was approximately 1,494 m/sec [4,900 ft/sec], which is considerably less than the reference rock  $V_S$  of 2,831 m/sec [9,285 ft/sec].

Before the onsite hydrogeologic investigations, the licensee conducted geotechnical investigations in 2003 and 2004 to support modifications to the Unit 2 spent fuel building (Tectonic Engineering, 2004). A shallow P-wave refraction profile was acquired near the Unit 2 spent fuel building as part of those studies, which show  $V_P$  of 12,500 to 3,810 to 4,236 m/sec [13,900 ft/sec]. As part of the geotechnical investigations, the licensee also obtained shallow P-wave velocity measurements near the ISFSI, which is also located some distance away to the north from the Unit 2 and Unit 3 reactor facilities. These measurements show  $V_P$  ranging from 4,260 to 5,180 m/sec [14,000 to 17,000 ft/sec].

Based on the range of velocities from these in situ geophysical measurements of the near-surface Inwood Marble rock unit, the NRC staff estimated a  $V_S$  of 2,073 m/sec [6,800 ft/sec] for its basecase profile. This corresponds to a range of Poisson's ratio values (0.28 to 0.34) appropriate for this type of rock and near-surface conditions. Because the crystalline rock units beneath the site are highly metamorphosed and very firm, the NRC staff developed a fairly shallow {11 m [35 ft]} three-layer basecase profile with  $V_S$  of 2,073 m/sec [6,800 ft/sec], 2,622 m/sec [8,600 ft/sec], and 2,744 m/sec [9,000 ft/sec]. For its site response evaluation, the NRC staff used the top of rock, which corresponds to an elevation of 5 m [15 ft] MSL, as the control point elevation for the Indian Point site.

To capture the uncertainty in its basecase profile, the NRC staff developed lower and upper range (10<sup>th</sup> and 90<sup>th</sup> percentile) profiles by multiplying the basecase  $V_S$  values by scale factors of 0.83 and 1.21, respectively, which corresponds to an epistemic logarithmic standard deviation of 0.15. The weights for the lower, best-estimate, and upper basecase profiles are 0.3, 0.4, and 0.3, respectively. As shown in Figure 2.2-19, the upper profile terminates at a depth of 3 m [10 ft], and the lower and best-estimate basecase profiles terminate at a depth of 11 m [35 ft] below the control point elevation, at which point the  $V_S$  is assumed to reach the reference rock value of 2,831 m/sec [9,285 ft/sec].

#### 2.2.5.2.2 *Dynamic Material Properties and Site Kappa*

The NRC staff assumed both linear and nonlinear dynamic behavior for the rock beneath the Indian Point site. To model the nonlinear behavior of the uppermost rock strata, the NRC staff used the EPRI rock shear modulus reduction and material damping curves. To model the linear behavior, the NRC staff used a constant damping ratio of 3 percent. The NRC staff assumed these two alternative dynamic responses for the upper 3 m [10 ft] of the profile. Due to the higher  $V_S$  of this rock layer, the NRC staff assigned weights of 0.7 and 0.3 to the linear and nonlinear alternatives, respectively. For the remaining 8 m [25 ft] of its profile, the NRC staff assumed a linear response with a material damping ratio value of 0.1 percent to maintain consistency with the  $\kappa_0$  value for the Indian Point site.

To determine the basecase  $\kappa_0$  for the Indian Point site, the NRC staff first used the Campbell (2009) Model 1 relationship between  $V_S$  and  $Q_{ef}$  to determine a  $Q_{ef}$  for each layer. Combining these  $Q_{ef}$  values with the thicknesses and  $V_S$  for each of the layers results in a total  $\kappa_0$  value of about 6.1 msec, which includes the 6 msec assumed for the underlying reference rock. For the lower and upper basecase profiles, the NRC staff calculated  $\kappa_0$  values of 6.2 and 6.0 msec, respectively, using the same approach as for the best-estimate basecase profile. Because the licensee did not perform a site response analysis, it did not determine  $\kappa_0$  for the Indian Point site.

Table 2.2-6 provides the layer depths, lithologies,  $V_S$ , unit weights, and dynamic properties for the NRC staff's three profiles. In summary, the site response logic tree developed by the NRC staff for the Indian Point site consists of six alternatives; three basecase profiles (each with a different  $\kappa_0$  value) and two alternative dynamic property branches.

#### 2.2.5.2.3 Methodology and Results

The NRC staff followed the methodology described in Section 2.1.4 to develop the final site amplification factors. Figure 2.2-20 shows the overall median site amplification factors and their variability for each of the seven spectral frequencies. As shown in Figure 2.2-20, the median site amplification factors are very close to 1 for each of the spectral frequencies. The lower half of Figure 2.2-20 shows that the logarithmic standard deviations for the site amplification factors range from about 0.05 to 0.10.

#### 2.2.5.3 Control Point Hazard

The NRC staff implemented Approach 3 from the SPID to develop a weighted control point seismic hazard curve for each of the six unique combinations of the site response logic tree for the Indian Point site. After combining these curves to develop the final mean control point hazard curves, the NRC staff determined the  $10^{-4}$  and  $10^{-5}$  UHRS in order to calculate the final GMRS. Figure 2.2-21 shows the final control point mean seismic hazard curves for each of the seven spectral frequencies as well as the NRC staff's UHRS and GMRS, and the licensee's NTF R2.1 GMRS (Ventosa, 2014). As shown in Figure 2.2-21, the NRC staff's GMRS (black curve) is slightly lower than the licensee's GMRS (blue curve) above 10 Hz due to the NRC staff's decision to perform a site response analysis. For comparison, Figure 2.2-21 also shows the NRC staff's reference rock GMRS (brown dotted curve).

Layer	Depth (ft)	Description	$V_s$ (ft/sec)			$V_s$ Sigma (ln)	BC Unit Weight (pcf)	Dynamic Properties	
			LR (0.3)	BC (0.4)	UR (0.3)			Alt. 1 (0.3)	Alt. 2 (0.7)
1	10	Rock: Marble	5,610	6,800	8,242	0.25	150	EPRI Rock	L 3.0%
2	22	Rock: Marble	7,096	8,600	9,285	0.15	160	L 0.1%	L 0.1%
3	35	Rock: Marble	7,426	9,000	9,285	0.15	160	L 0.1%	L 0.1%

LR = lower range; BC = basecase; UR = upper range; ln = natural log; pcf = pounds per cubic foot; L = linear; Alt. = alternative.  
 For LR, BC, UR, and Alt.: Values in parentheses refer to weights for site response analysis logic tree branches.

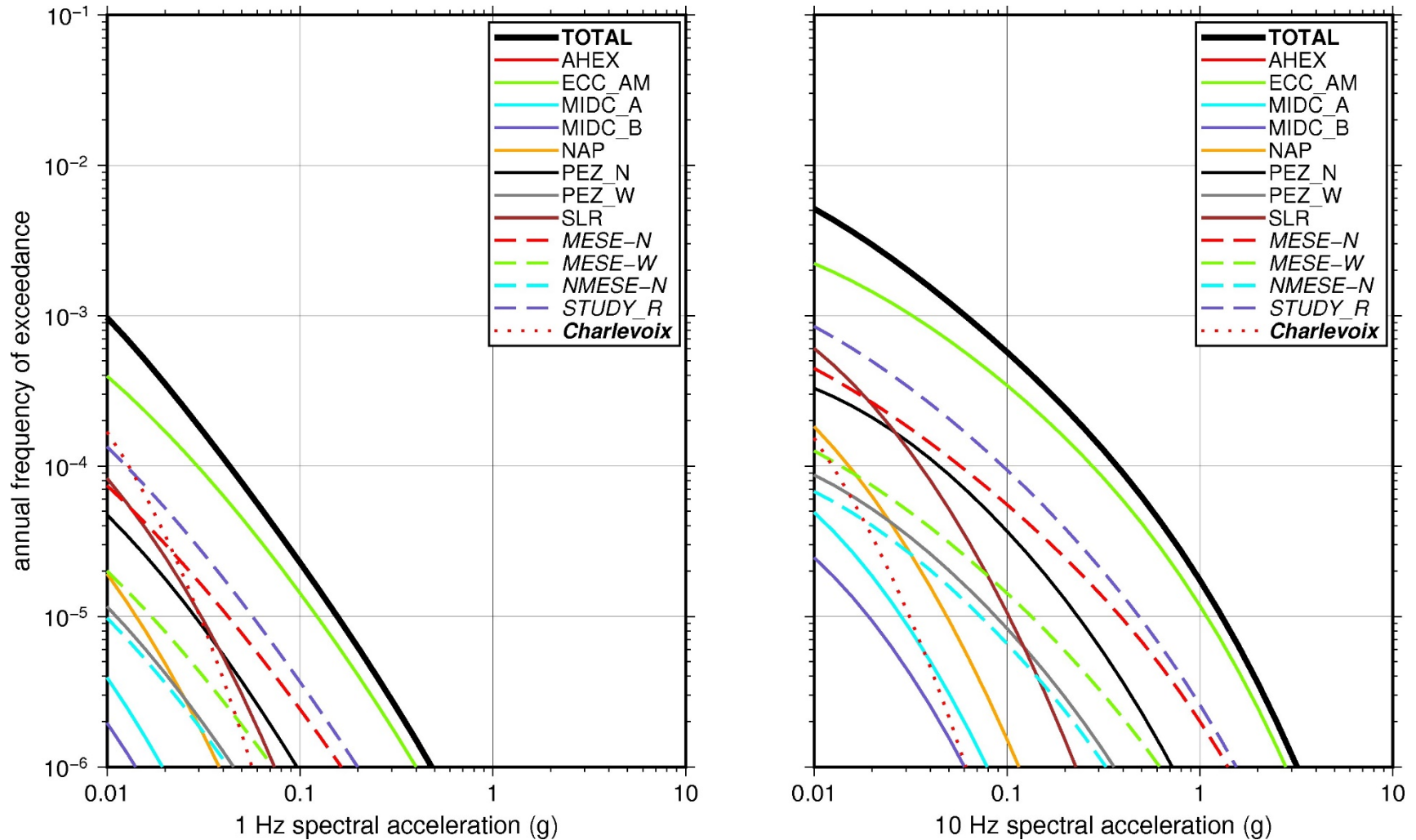


**Figure 2.2-18 Low-Frequency (1 Hz, Left) and High-Frequency (10 Hz, Right) Reference Rock Hazard Curves for Indian Point. Total Hazard is Shown as a Bold Black Line; Individual Contributions to the Hazard for Each of the CEUS-SSC Sources are Shown as Colored Lines Defined in the Legend. See Table 2.1-1 for Source Name Definitions**

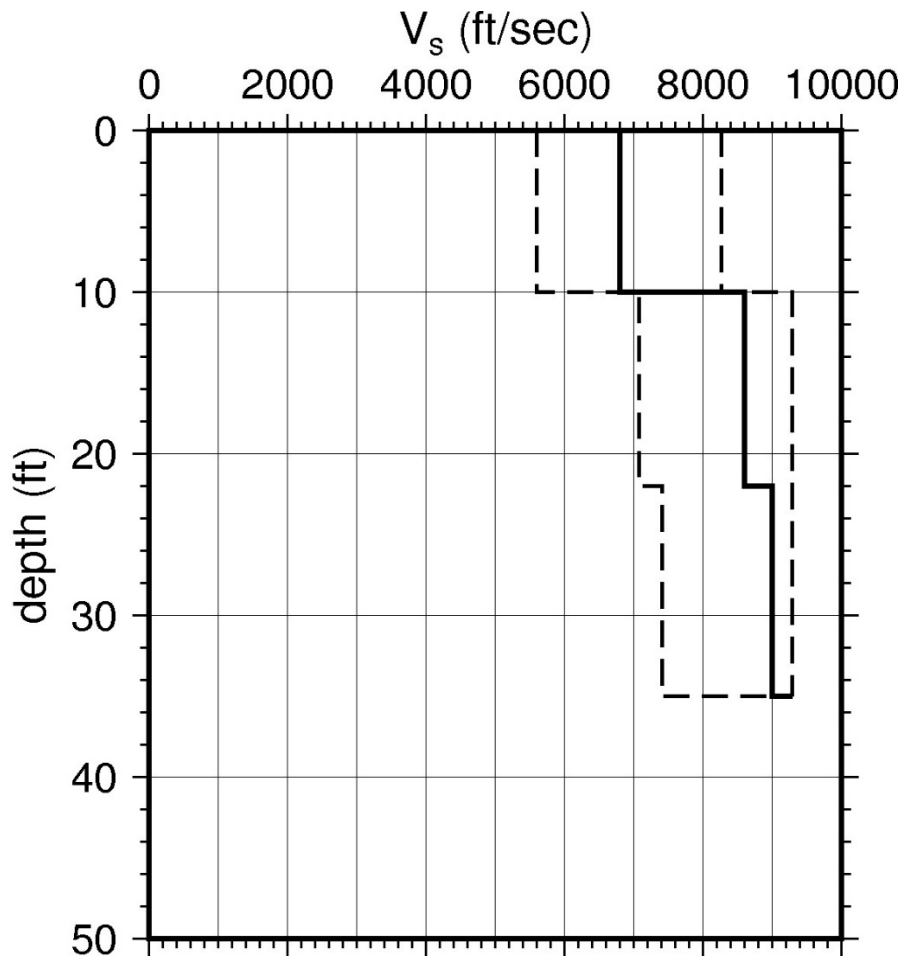


**Figure 2.2-19 Shear Wave Velocity ( $V_s$ ) Profiles for Indian Point. Basecase (BC) Profile Shown as Solid Bold Line; Lower and Upper Range (LR and UR) Profiles Shown as Dashed Lines. Profiles Terminate at Reference Rock Velocity of 2,831 m/sec [9,285 ft/sec] per EPRI GMM (2013)**

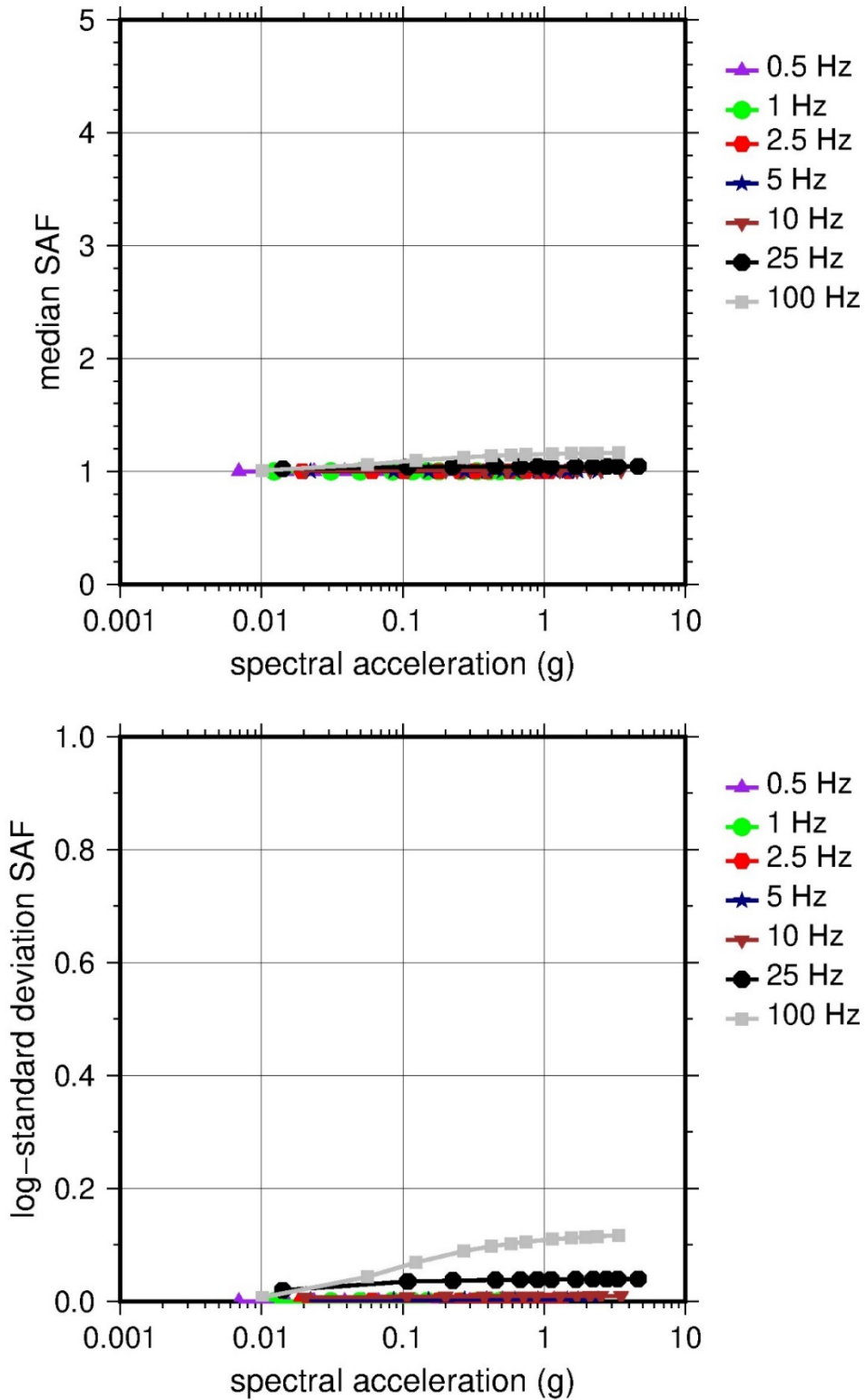


**Figure 2.2-20 Overall Weighted Median Site Amplification Factor (SAF) (Upper) and Log Standard Deviation of the SAF (Lower) as a Function of Input Acceleration for EPRI GMM (2013) Spectral Frequencies**

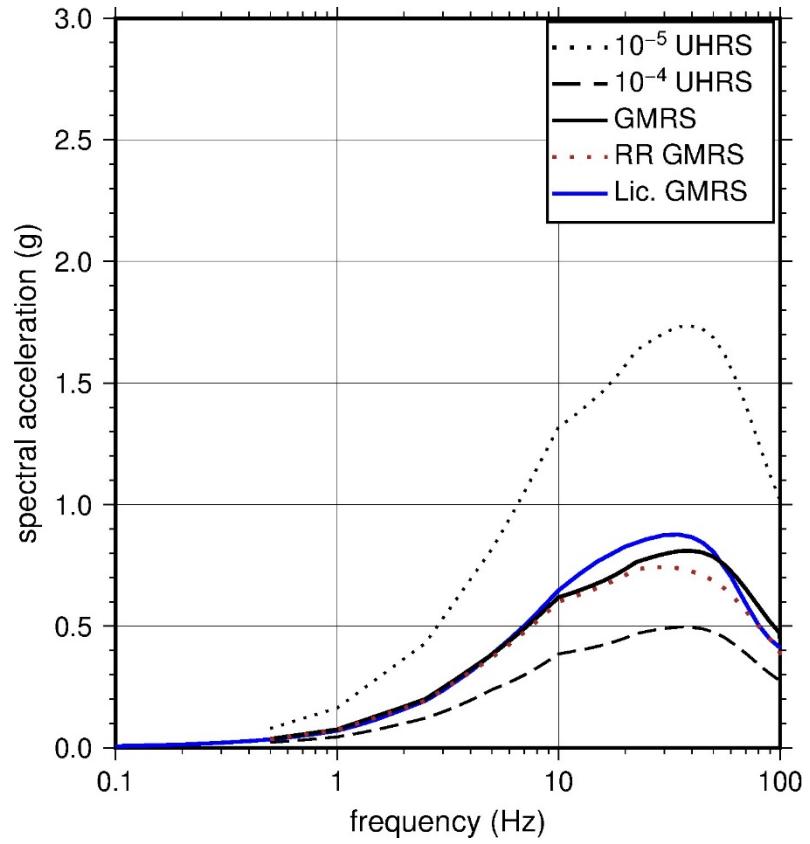
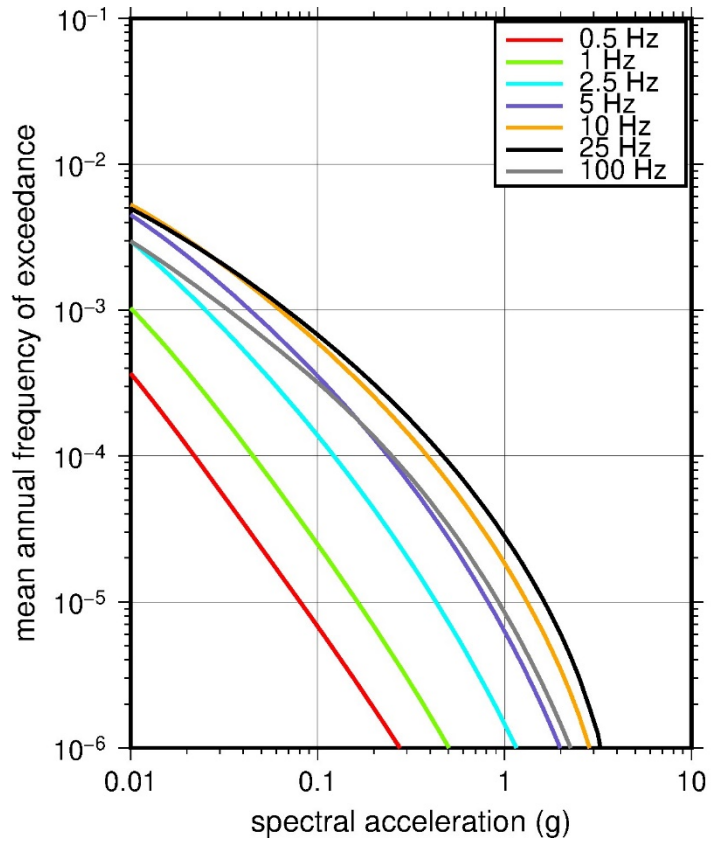


**Figure 2.2-21 Mean Control Point Hazard Curves (Left) for EPRI GMM (2013) Spectral Frequencies, and GMRS and UHRS (Right) for Indian Point**



## 2.2.6 FitzPatrick and Nine Mile Point

The site for the James A. FitzPatrick Nuclear Power Plant and Nine Mile Point Nuclear Station is located on the shore of Lake Ontario within the Central Lowland physiographic province and is founded on approximately 550 m [1,800 ft] of sedimentary (primarily sandstone and shale) rock that is underlain by Precambrian crystalline rock. The horizontal SSE response spectra for FitzPatrick and Nine Mile Point both have rounded Housner spectral shapes and are anchored at PGAs of 0.15g and 0.11g, respectively.

### 2.2.6.1 Reference Rock Hazard

For the reference rock PSHA, the NRC staff selected the 15 CEUS-SSC (NRC, 2012b) background seismic source zones that are located within 320 km [200 mi] of the site. The NRC staff also selected the Charlevoix CEUS-SSC RLME source, which is located about 600 km [375 mi] from the site. To develop the reference rock seismic hazard curves for the site, the NRC staff used the GMPEs in the updated EPRI GMM (2013). As shown in Figure 2.2-22, the SLR seismotectonic zone, which is the highest weighted host zone for the site, is the largest contributor to both the 1 Hz and 10 Hz reference rock total mean hazard curves at the  $10^{-4}$  AFE level.

### 2.2.6.2 Site Response Evaluation

#### 2.2.6.2.1 Site Profiles

To develop a basecase profile, the NRC staff used the geologic information in both the Entergy NTTF R2.1 SHSR for FitzPatrick (Coyle, 2014) and the Constellation Energy Nuclear Group (Constellation) NTTF R2.1 SHSR for Nine Mile Point (Korsnick, 2014c). As described in the two SHSRs, the site consists of a thin veneer of residual soils overlying early Paleozoic medium to fine-grained unfossiliferous sandstone. The site safety-related structures are all founded on sound rock. In Table 2.3.1-1 of the SHSRs, the licensees briefly described the subsurface materials in terms of the geologic units and layer thicknesses. For its basecase profile, the NRC staff used the top of the Oswego Formation sandstone, which corresponds to an elevation of 75 m [245 ft] MSL, as the control point elevation for the site.

The field investigations for FitzPatrick, conducted in the 1960s, consisted of a number of borings through the glacial till and upper portions of the rock beneath the site. Seismic refraction surveys carried out for the siting of FitzPatrick measured  $V_P$  to a depth of about 40 m [130 ft] beneath the site. To develop its SHSR basecase profile for the FitzPatrick site, Entergy used the measured  $V_P$  and an assumed Poisson's ratio to estimate the  $V_S$ . In contrast, to develop its SHSR basecase profile for the Nine Mile Point site, Constellation used the in situ geophysical measurements from the Unit 3 COL site investigation (UniStar Nuclear Services, 2009a). These investigations included many seismic refraction surveys, crosshole surveys, and an offshore geophysical survey in Lake Ontario, which the licensee used to determine the  $V_S$  for the deeper rock layers. Overall, the  $V_S$  for the sedimentary rock strata beneath the site is relatively constant, increasing gradually with depth. As such, the differences between the Entergy and Constellation basecase profiles are minor and their final GMRS are, as a result, very similar. Table 2.3.2-1 of the SHSRs gives the measured and estimated  $V_S$  determined from the licensees' site investigations.

Both Entergy and Constellation selected the top of the Oswego Formation sandstone for their control point elevations. The SHSR basecase profile developed by Constellation for Nine Mile

Point extends to a depth of 532 m [1,745 ft] below the control point elevation. Similarly, the SHSR basecase profile developed by Entergy for FitzPatrick extends to a depth of 518 m [1,700 ft] below the control point elevation. For the Ordovician age Oswego Formation, which is primarily sandstone with siltstone and shale, Entergy estimated a  $V_S$  of 2,287 m/sec [7,500 ft/sec] based on a measured  $V_P$  of about 4,268 m/sec [14,000 ft/sec] and a Poisson's ratio of 0.30. Entergy used this estimated  $V_S$  of 2,287 m/sec [7,500 ft/sec] for its entire basecase profile. In contrast, based on the site investigations for the Unit 3 COL, Constellation developed a more detailed basecase profile that varies from a  $V_S$  of 1,829 m/sec [6,000 ft/sec] for the upper portion of the Oswego Formation to a  $V_S$  of 2,622 m/sec [8,600 ft/sec] for the deepest rock strata. Specifically, for the Oswego Formation, which is about 11 m [35 ft] thick beneath the site, Constellation assigned a median  $V_S$  of 1,829 m/sec [6,000 ft/sec] for the upper portion of this rock unit and 1,982 m/sec [6,500 ft/sec] for the lower portion. Beneath the Oswego Formation sandstone is the Ordovician age Pulaski Formation, which consists of sandstone, siltstone, and shale and is about 31 m [100 ft] thick. Constellation estimated a median  $V_S$  of 2,439 m/sec [8,000 ft/sec] for this rock unit. Underlying the Pulaski Formation are the Ordovician age Whetstone Gulf Formation, which is 231 m [700 ft] thick, and the Trenton Group, which is also about 231 m [700 ft] thick beneath the site. The  $V_S$  for these deeper rock strata varies from 2,134 m/sec [7,000 ft/sec] to 2,622 m/sec [8,600 ft/sec].

For its basecase profile, the NRC staff used the profile developed for the Nine Mile Point Unit 3 COL. Although this profile is slightly more detailed than the basecase profile developed by Constellation for Nine Mile Point and considerably more detailed than the constant profile developed by Entergy for FitzPatrick, the overall differences in the profiles are minor due to the limited range in  $V_S$  for the rock strata beneath the site.

To capture the uncertainty in its basecase profile, the NRC staff developed lower and upper range (10<sup>th</sup> and 90<sup>th</sup> percentile) profiles by multiplying the basecase  $V_S$  values by scale factors of 0.83 and 1.21, respectively, which corresponds to an epistemic logarithmic standard deviation of 0.15. The weights for the lower, best-estimate, and upper basecase profiles are 0.3, 0.4, and 0.3, respectively. Figure 2.2-23 shows the upper 366 m [1,200 ft] of the staff's three basecase profiles. As shown in Figure 2.2-23, the upper profile terminates at a depth of about 218 m [716 ft], at which point the  $V_S$  reaches the reference rock value of 2,831 m/sec [9,285 ft/sec]. In contrast, the lower and best-estimate basecase profiles terminate at a depth of 537 m [1,760 ft] below the control point elevation.

#### 2.2.6.2.2 *Dynamic Material Properties and Site Kappa*

The NRC staff assumed both linear and nonlinear dynamic behavior for the rock beneath the site. To model the nonlinear behavior of the uppermost rock strata, the NRC staff used the EPRI rock shear modulus reduction and material damping curves. To model the linear behavior, the NRC staff used a constant damping ratio of 3 percent. The NRC staff assumed these two alternative dynamic responses for the upper 24 m [79 ft] of the profile. Due to the higher  $V_S$  of this rock layer, the NRC staff assigned weights of 0.7 and 0.3 to the linear and nonlinear alternatives, respectively. For the remaining 513 m [1,681 ft] of its profile, the NRC staff assumed a linear response with a material damping ratio value of 0.1 percent to maintain consistency with the  $\kappa_0$  value for the site.

To determine the basecase  $\kappa_0$  for the site, the NRC staff first used the Campbell (2009) Model 1 relationship between  $V_S$  and  $Q_{ef}$  to determine a  $Q_{ef}$  for each layer. Combining these  $Q_{ef}$  values with the thicknesses and  $V_S$  for each of the layers results in a total  $\kappa_0$  value of about 8 msec, which includes the 9 msec assumed for the underlying reference rock. For the lower and upper

basecase profiles, the NRC staff calculated  $\kappa_0$  values of 10 and 7 msec, respectively, using the same approach as for the best-estimate basecase profile. In contrast, the licensee estimated  $\kappa_0$  by combining the lowest low-strain damping values from the EPRI rock material damping curves over the upper 152 m [500 ft] of rock with an assumed damping value of 1.25 percent for the remaining underlying rock layers to estimate best-estimate, lower, and upper basecase  $\kappa_0$  values of 14, 20, and 6 msec, respectively.

Table 2.2-7 provides the layer depths, lithologies,  $V_s$ , unit weights, and dynamic properties for the NRC staff's three profiles. In summary, the site response logic tree developed by the NRC staff for the FitzPatrick-Nine Mile Point site consists of six alternatives; three basecase profiles (each with a different  $\kappa_0$  value) and two alternative dynamic property branches.

#### 2.2.6.2.3 Methodology and Results

The NRC staff followed the methodology described in Section 2.1.4 to develop the final site amplification factors. As shown in Figure 2.2-24, the median site amplification factors are very close to 1 for each of the spectral frequencies. The lower half of Figure 2.2-24 shows that the logarithmic standard deviations for the site amplification factors range from about 0.05 to 0.10.

#### 2.2.6.3 Control Point Hazard

The NRC staff implemented Approach 3 from the SPID to develop a weighted control point seismic hazard curve for each of the six unique combinations of the site response logic tree for the FitzPatrick-Nine Mile Point site. After combining these curves to develop the final mean control point hazard curves, the NRC staff determined the  $10^{-4}$  and  $10^{-5}$  UHRS in order to calculate the final GMRS. Figure 2.2-25 shows the final control point mean seismic hazard curves for each of the seven spectral frequencies as well as the NRC staff's UHRS and GMRS, and the two NTTF R2.1 GMRS for FitzPatrick (Coyle, 2014) and Nine Mile Point (Korsnick, 2014c), which differ only slightly. As shown in Figure 2.2-25, the NRC staff's GMRS (black curve) is moderately higher than the two licensees' GMRS (blue curve) above 10 Hz due to the lower  $\kappa_0$  values estimated by the NRC staff. For comparison, Figure 2.2-25 also shows the NRC staff's reference rock GMRS (brown dotted curve).

**Table 2.2-7 Layer Depths, Shear Wave Velocities ( $V_s$ ), Unit Weights, and Dynamic Properties for Fitzpatrick and Nine Mile Point**

Layer	Depth (ft)	Description	$V_s$ (ft/sec)			$V_s$ Sigma (ln)	BC Unit Weight (pcf)	Dynamic Properties	
			LR (0.3)	BC (0.4)	UR (0.3)			Alt. 1 (0.3)	Alt. 2 (0.7)
1	17	Rock: sandstone	5,157	6,250	7,575	0.15	150	EPRI Rock	L 3.0%
2	30	Rock: sandstone, shale	5,610	6,800	8,242	0.15	150	EPRI Rock	L 3.0%
3	71	Rock: sandstone	6,147	7,450	9,030	0.15	160	EPRI Rock	L 3.0%
4	79	Rock: sandstone, siltstone	6,188	7,500	9,212	0.15	160	EPRI Rock	L 3.0%
5	131	Rock: siltstone, shale	6,271	7,600	9,090	0.15	160	L 0.1%	L 0.1%
6	326	Rock: shale, sandstone	6,188	7,500	9,212	0.15	160	L 0.1%	L 0.1%
7	521	Rock: shale, sandstone	6,271	7,600	9,285	0.15	160	L 0.1%	L 0.1%
8	716	Rock: shale, sandstone	6,353	7,700	9,285	0.15	160	L 0.1%	L 0.1%
9	911	Rock: shale, sandstone	6,436	7,800	9,285	0.15	160	L 0.1%	L 0.1%
10	1,111	Rock: sandstone, shale	6,580	7,975	9,285	0.15	160	L 0.1%	L 0.1%
11	1,311	Rock: sandstone, shale	6,724	8,150	9,285	0.15	160	L 0.1%	L 0.1%
12	1,511	Rock: sandstone, shale	6,869	8,325	9,285	0.15	160	L 0.1%	L 0.1%
13	1,760	Rock: sandstone, shale	7,013	8,500	9,285	0.15	160	L 0.1%	L 0.1%

LR = lower range; BC = basecase; UR = upper range; ln = natural log; pcf = pounds per cubic foot; L = linear; Alt. = alternative.  
 For LR, BC, UR, and Alt.: Values in parentheses refer to weights for site response analysis logic tree branches.

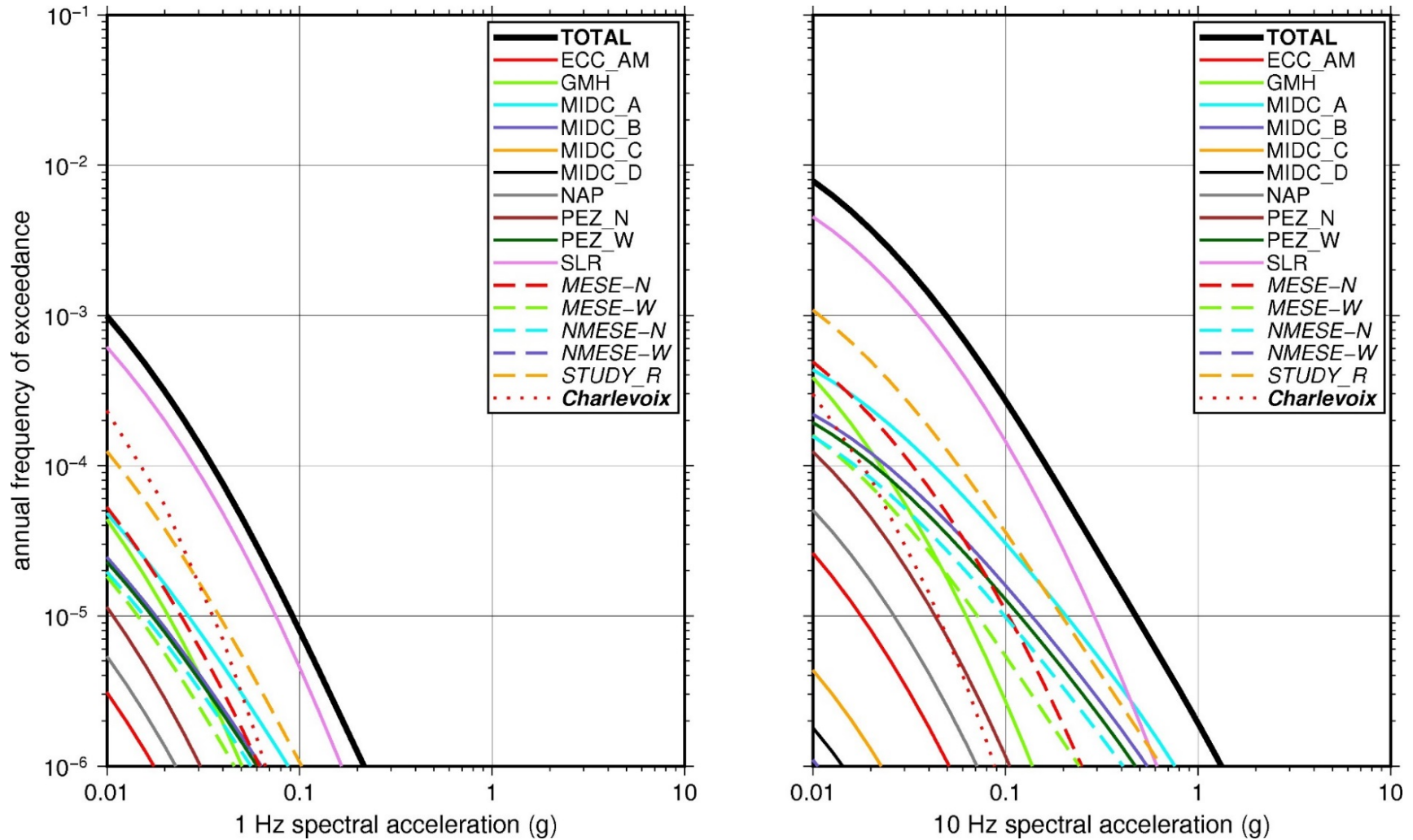


**Figure 2.2-22 Low-Frequency (1 Hz, Left) and High-Frequency (10 Hz, Right) Reference Rock Hazard Curves for Fitzpatrick and Nine Mile Point. Total Hazard is Shown as a Bold Black Line; Individual Contributions to the Hazard for Each of the CEUS-SSC Sources are Shown as Colored Lines Defined in the Legend. See Table 2.1-1 for Source Name Definitions**

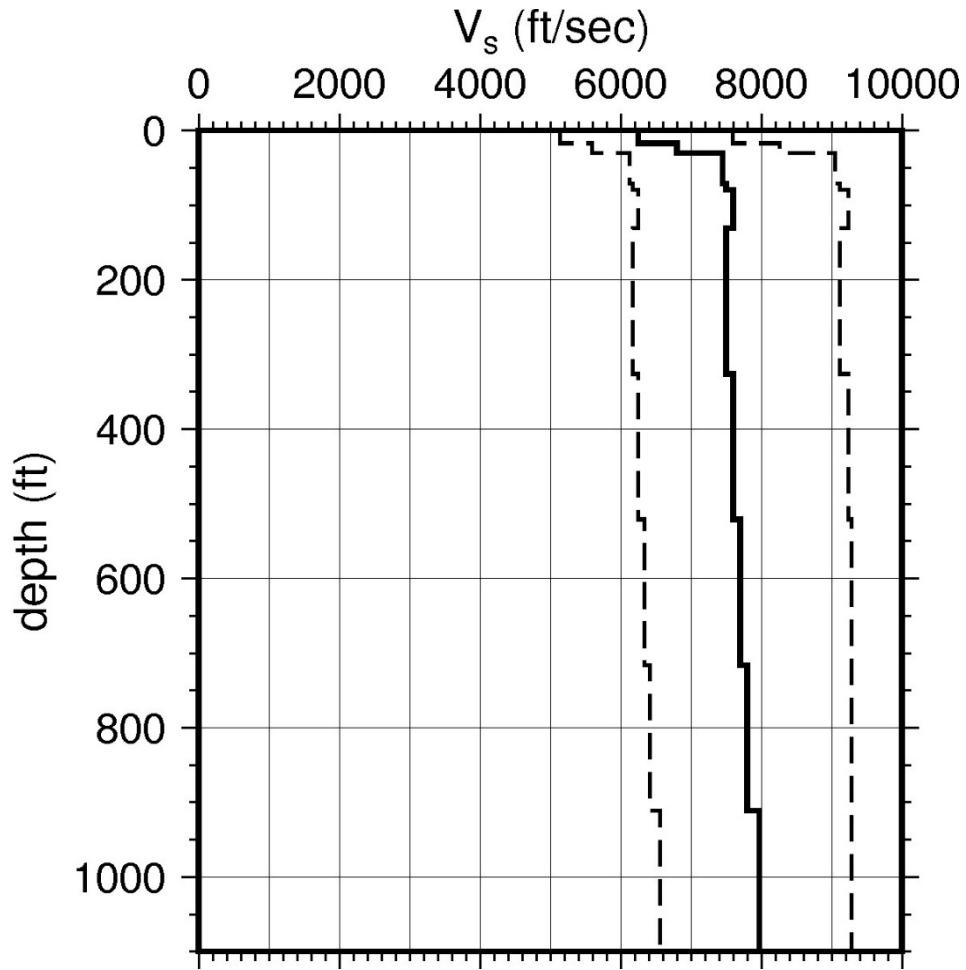


**Figure 2.2-23 Shear Wave Velocity ( $V_s$ ) Profiles for FitzPatrick and Nine Mile Point. Basecase (BC) Profile Shown as Solid Bold Line; Lower and Upper Range (LR and UR) Profiles Shown as Dashed Lines. Profiles Terminate at Reference Rock Velocity of 2,831 m/sec [9,285 ft/sec] per EPRI GMM (2013)**

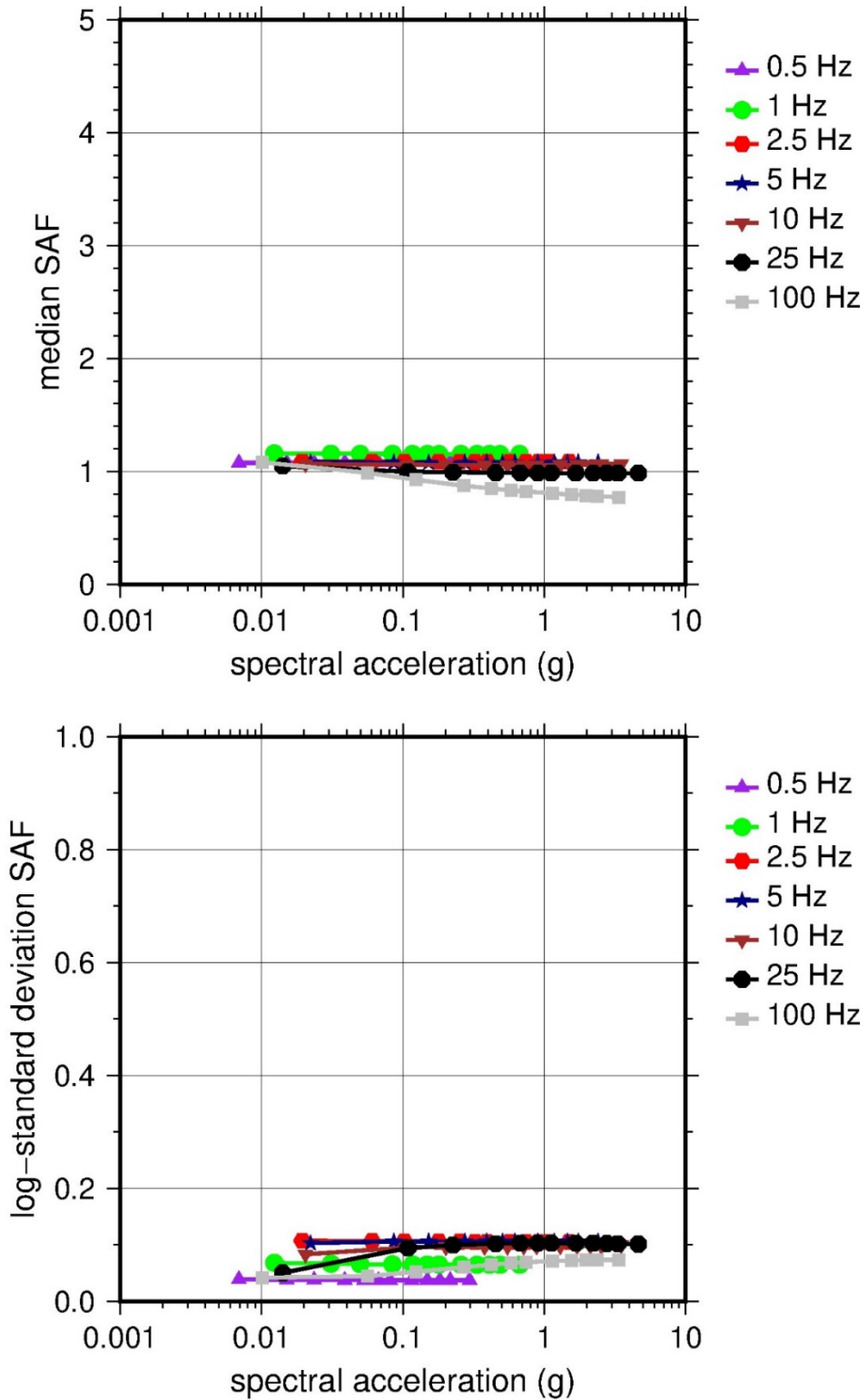


**Figure 2.2-24 Overall Weighted Median Site Amplification Factor (SAF) (Upper) and Log Standard Deviation of the SAF (Lower) as a Function of Input Acceleration for EPRI GMM (2013) Spectral Frequencies**

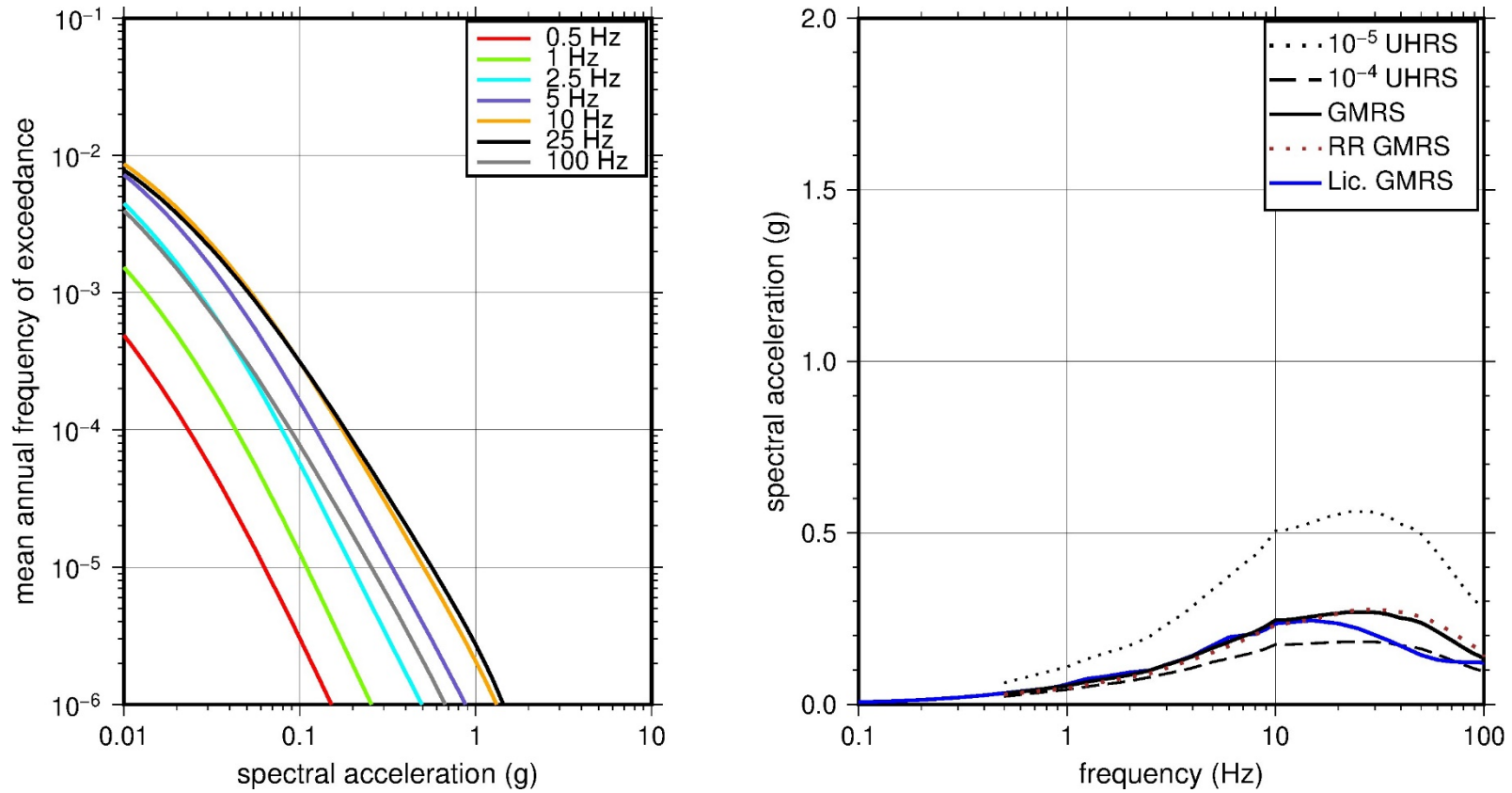


**Figure 2.2-25 Mean Control Point Hazard Curves (Left) for EPRI GMM (2013) Spectral Frequencies, and GMRS and UHS (Right) for FitzPatrick and Nine Mile Point**



## 2.2.7 Limerick

The Limerick Generating Station site is located on the banks of the Schuylkill River in eastern Pennsylvania within the Piedmont physiographic province and is founded on about 2,440 m [8,000 ft] of competent sedimentary rock (shale and sandstone) that is underlain by hard crystalline rock. The horizontal SSE response spectrum for Limerick has a Newmark spectral shape and is anchored at a PGA of 0.15g.

### 2.2.7.1 Reference Rock Hazard

For the reference rock PSHA, the NRC staff selected the 11 CEUS-SSC (NRC, 2012b) background seismic source zones that are located within 320 km [200 mi] of the site. The NRC staff also selected the Charleston CEUS-SSC RLME source, which is located about 849 km [526 mi] from the Limerick site. To develop the reference rock seismic hazard curves for the Limerick site, the NRC staff used the GMPEs in the updated EPRI GMM (2013). As shown in Figure 2.2-26, the ECC-AM seismotectonic zone, which is the highest weighted host zone for the site, is the largest contributor to both the 1 Hz and 10 Hz reference rock total mean hazard curves at the  $10^{-4}$  AFE level.

### 2.2.7.2 Site Response Evaluation

#### 2.2.7.2.1 Site Profiles

To develop a basecase profile, the NRC staff used the geologic information in the NTTF R2.1 SHSR (Barstow, 2014a) submitted by Exelon (hereafter referred to as “the licensee” within this plant section). As described in the licensee’s SHSR, the Limerick site is within the Newark-Gettysburg Basin, which is underlain by red sandstones, shales, and siltstones of the Triassic Newark Group. The site is underlain by a thin veneer of soils overlying about 2,439 m [8,000 ft] of Triassic age sedimentary rock, which is cut by diabase dikes and sills and by minor faulting. The safety-related structures are supported on competent bedrock from the Brunswick Formation. In Table 2.3.1-1 of the SHSR, the licensee briefly described the subsurface materials in terms of the geologic units and layer thicknesses. For its site response evaluation, the NRC staff used the top of rock, which corresponds to an elevation of 62 m [204 ft] MSL, as the control point elevation for the Limerick site.

The field investigations for Limerick, conducted in the 1960s, consisted of a number of borings through the soil and upper portion of rock beneath the site. The licensee’s seismic refraction and uphole surveys measured  $V_P$  and  $V_S$  to a depth of about 46 to 61 m [150 to 200 ft] beneath the site. To determine a  $V_S$  for the upper rock for its SHSR profile, the licensee used the  $V_S$  measured from a more recent ISFSI site investigation, which extended to a depth of about 15 m [50 ft] beneath the site. Table 2.3.2-2 of the SHSR gives the measured and estimated  $V_S$  determined from the licensee’s site investigation.

For its SHSR, the licensee developed a basecase profile that extends to a depth of 2,439 m [8,000 ft] below the control point elevation. The uppermost layers of the profile consist of Triassic age sedimentary rock (primarily siltstone, sandstone, and shale) from the Brunswick (now Passaic) Formation. The Passaic Formation interfingers laterally with the Lockatong Formation and with the Hammer Creek Formation in the narrow neck near the Schuylkill River adjacent to the site. The  $V_S$  determined from the ISFSI investigation for these upper rock units varies from about 580 m/sec [1,900 ft/sec] to 1,500 m/sec [5,000 ft/sec]. Based on this range in  $V_S$ , the licensee selected a  $V_S$  of 1,052 m/sec [3,452 ft/sec] for the top of rock. For the

remainder of its profile, the licensee applied a velocity gradient of 0.5 meters per second per meter (m/sec/m) [0.5 feet per second per foot (ft/sec/ft)], which produces a terminal  $V_S$  of 2,256 m/sec [7,400 ft/sec] at the base of the profile.

Rather than use the  $V_S$  determined from the ISFSI site investigation, which extends only to the uppermost layer of rock beneath the site, the NRC staff used the seismic refraction and uphole seismic surveys. Based on the extensive seismic refraction profiling for the site, Section 2.5.4.2.1 of the UFSAR (Exelon Generation Company, 2012a) states, “neglecting the higher velocities detected from the more deeply buried rock strata, eight refraction velocities yield an average  $V_P$  of 3,622 m/sec [11,880 ft/sec] with an unbiased 1 sigma range of 3,338 m/sec [10,950 ft/sec] to 3,906 m/sec [12,810 ft/sec].” The UFSAR indicates that the higher  $V_P$  measured by the licensee for the deeper rock strata is 6,098 m/sec [20,000 ft/sec]. Using this  $V_P$  and assuming a Poisson’s ratio of 0.33 for firm rock, the  $V_S$  for the deeper rock strata is about 3,049 m/sec [10,000 ft/sec], which exceeds the reference rock  $V_S$  of 2,831 m/sec [9,285 ft/sec]. This measurement implies that the  $V_S$  for the rock strata beneath the Limerick site likely exceeds the reference rock  $V_S$  at a depth of about 46 m [150 ft] to 61 m [200 ft] beneath the control point elevation. This high  $V_P$  at relatively shallow depths beneath the site is likely due to the numerous diabase intrusions into the local sedimentary rock strata.

The licensee’s uphole seismic survey produced a  $V_P$  for the uppermost rock beneath the site that is similar to the  $V_P$  from the seismic refraction profiles. The measurements from the uphole survey also indicate a fairly significant velocity reversal, which would not have been detected by the seismic refraction survey. The measured  $V_P$  from the uphole survey, as described in Section 2.5.4.4.3 of the UFSAR (Exelon Generation Company, 2012a), are 3,841 m/sec [12,600 ft/sec] from the top of rock to a depth of 22 m [73 ft], 2,348 m/sec [7,700 ft/sec] from 22 m [73 ft] to 31 m [103 ft], and 3,841 m/sec [12,600 ft/sec] from 31 m [103 ft] to 46 m [150 ft].

Based on the licensee’s measured  $V_P$  from the seismic refraction and uphole surveys, the NRC staff developed a 61 m [200 ft] thick basecase profile with four layers. The NRC staff used the  $V_P$  from the uphole seismic survey and assumed a Poisson’s ratio of 0.33 to estimate  $V_S$  of 1,921 m/sec [6,300 ft/sec] for Layers 1 and 3 and 1,174 m/sec [3,850 ft/sec] for Layer 2. For the bottom layer (Layer 4) between 46 m [150 ft] to 61 m [200 ft], the NRC staff assumed a  $V_S$  of 2,287 m/sec [7,500 ft/sec]. Consistent with the approximate depth for the larger  $V_P$  measured from the licensee’s seismic refraction survey, the NRC staff terminated its profile at a depth of 61 m [200 ft] beneath the control point elevation. While the staff cannot rule out the deeper profile developed by the licensee, it considers this much shallower basecase profile to be more likely for the firm sedimentary rock with numerous diabase intrusions beneath the Limerick site.

To capture the uncertainty in its basecase profile, the NRC staff developed lower and upper range (10<sup>th</sup> and 90<sup>th</sup> percentile) profiles by multiplying the basecase  $V_S$  values by scale factors of 0.83 and 1.21, respectively, which corresponds to an epistemic logarithmic standard deviation of 0.15. The weights for the lower, best-estimate, and upper basecase profiles are 0.3, 0.4, and 0.3, respectively. Figure 2.2-27 shows the three profiles used by the NRC staff, which extend to a depth of 61 m [200 ft] below the control point elevation, at which point the shear velocity is assumed to reach the reference value of 2,831 m/sec [9,285 ft/sec].

#### 2.2.7.2.2 *Dynamic Material Properties and Site Kappa*

The NRC staff assumed both linear and nonlinear dynamic behavior for the rock beneath the Limerick site. To model the nonlinear behavior of the uppermost rock strata, the NRC staff used the EPRI rock shear modulus reduction and material damping curves. To model the linear

behavior, the NRC staff used a constant damping ratio of 3 percent. The NRC staff assumed these two alternative dynamic responses for the upper 46 m [150 ft] of the profile and gave them equal weight. For the remaining 15 m [50 ft] of its profile, the NRC staff assumed a linear response with a material damping ratio value of 0.1 percent to maintain consistency with the  $\kappa_0$  value for the Limerick site.

To determine the basecase  $\kappa_0$  for the Limerick site, the NRC staff first used the Campbell (2009) Model 1 relationship between  $V_S$  and  $Q_{ef}$  to determine a  $Q_{ef}$  for each layer. Combining these  $Q_{ef}$  values with the thicknesses and  $V_S$  for each of the layers results in a total  $\kappa_0$  value of about 6.6 msec, which includes the 6 msec assumed for the underlying reference rock. For the lower and upper basecase profiles, the NRC staff calculated  $\kappa_0$  values of 6.9 and 6.4 msec, respectively, using the same approach as for the best-estimate basecase profile. In contrast, the licensee estimated  $\kappa_0$  by using the empirical relationship from the SPID (EPRI, 2012) between the average  $V_S$  over the upper 30 m [100 ft] of the profile and  $\kappa_0$ , which results in  $\kappa_0$  values of 23, 36, and 12 msec for the best-estimate, lower, and upper basecase profiles, respectively.

Table 2.2-8 provides the layer depths, lithologies,  $V_S$ , unit weights, and dynamic properties for the NRC staff's three profiles. In summary, the site response logic tree developed by the NRC staff for the Limerick site consists of six alternatives; three basecase profiles (each with a different  $\kappa_0$  value) and two alternative dynamic property branches.

#### 2.2.7.2.3 Methodology and Results

The NRC staff followed the methodology described in Section 2.1.4 to develop the final site amplification factors. Figure 2.2-28 shows the overall median site amplification factors and their variability for each of the seven spectral frequencies. As shown in Figure 2.2-28, the median site amplification factors range from about 1.0 to 1.5 before falling off with higher input spectral accelerations. The lower half of Figure 2.2-28 shows that the logarithmic standard deviations for the site amplification factors range from about 0.05 to 0.20.

#### 2.2.7.3 Control Point Hazard

The NRC staff implemented Approach 3 from the SPID to develop a weighted control point seismic hazard curve for each of the six unique combinations of the site response logic tree for the Limerick site. After combining these curves to develop the final mean control point hazard curves, the NRC staff determined the  $10^{-4}$  and  $10^{-5}$  UHRs in order to calculate the final GMRS. Figure 2.2-29 shows the final control point mean seismic hazard curves for each of the seven spectral frequencies as well as the NRC staff's UHRs and GMRS, and the licensee's NTTFR2.1 GMRS (Barstow, 2014a). As shown in Figure 2.2-29, the NRC staff's GMRS (black curve) is moderately higher than the licensee's GMRS (blue curve) between 1 Hz and 10 Hz and shows higher site amplifications at 8 Hz and 30 Hz. The differences between the two GMRSs are due to the differences between the licensee's and NRC staff's basecase profiles and  $\kappa_0$  values. For comparison, Figure 2.2-29 also shows the NRC staff's reference rock GMRS (brown dotted curve).

**Table 2.2-8 Layer Depths, Shear Wave Velocities ( $V_s$ ), Unit Weights, and Dynamic Properties for Limerick**

Layer	Depth (ft)	Description	$V_s$ (ft/sec)			$V_s$ Sigma (ln)	BC Unit Weight (pcf)	Dynamic Properties	
			LR (0.3)	BC (0.4)	UR (0.3)			Alt. 1 (0.5)	Alt. 2 (0.5)
1	73	Rock: siltstone, shale, sandstone	5,198	6,300	7,636	0.25	150	EPRI Rock	L 3.0%
2	103	Rock: siltstone, shale, sandstone	3,177	3,850	4,666	0.15	140	EPRI Rock	L 3.0%
3	150	Rock: siltstone, shale, sandstone	5,198	6,300	7,636	0.15	150	EPRI Rock	L 3.0%
4	200	Rock: siltstone, shale, sandstone	6,188	7,500	9,090	0.15	160	L 0.1%	L 0.1%

LR = lower range; BC = basecase; UR = upper range; ln = natural log; pcf = pounds per cubic foot; L = linear; Alt. = alternative.  
 For LR, BC, UR, and Alt.: Values in parentheses refer to weights for site response analysis logic tree branches.

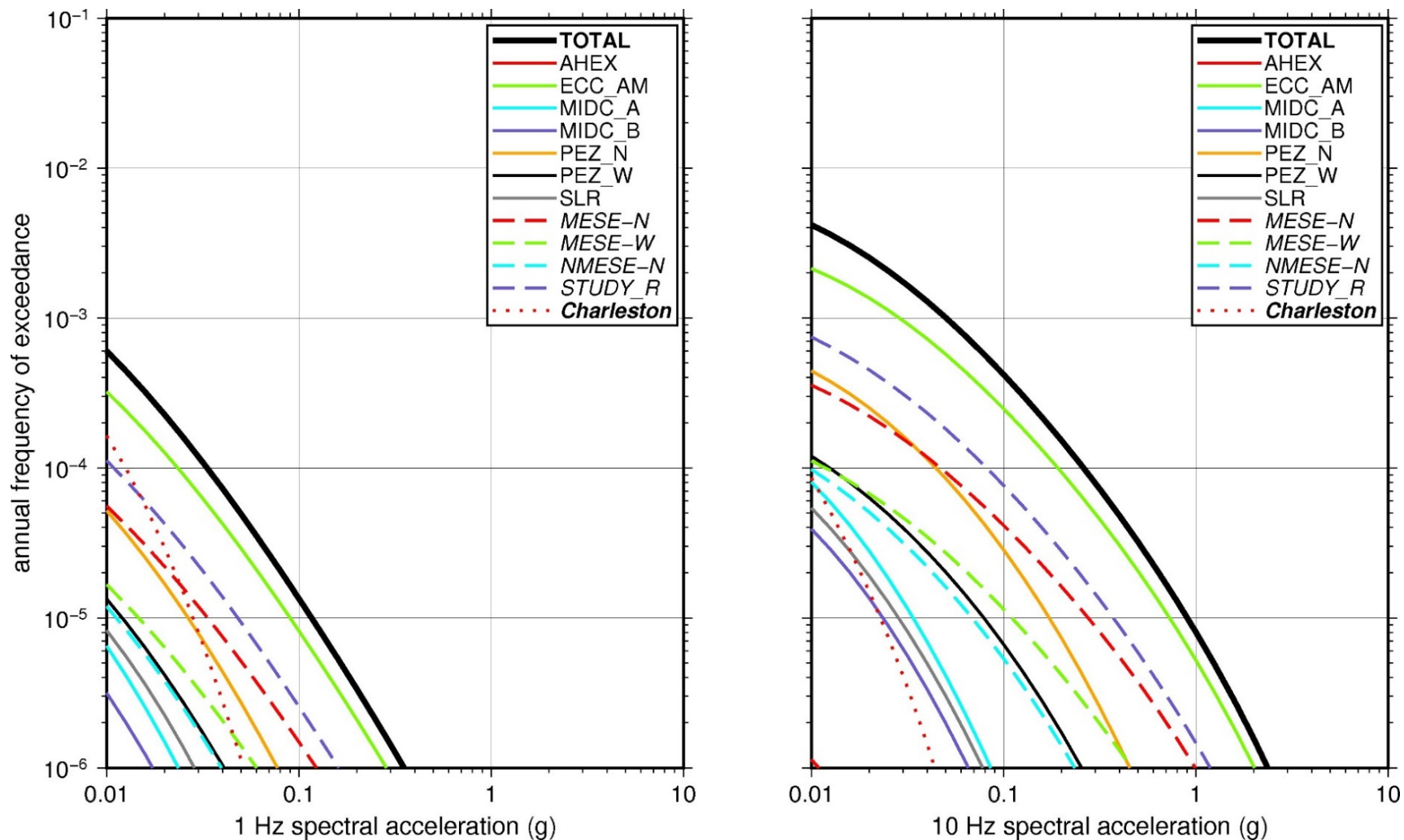


**Figure 2.2-26 Low-Frequency (1 Hz, Left) and High-Frequency (10 Hz, Right) Reference Rock Hazard Curves for Limerick. Total Hazard is Shown as a Bold Black Line; Individual Contributions to the Hazard for Each of the CEUS-SSC Sources are Shown as Colored Lines Defined in the Legend. See Table 2.1-1 for Source Name Definitions**

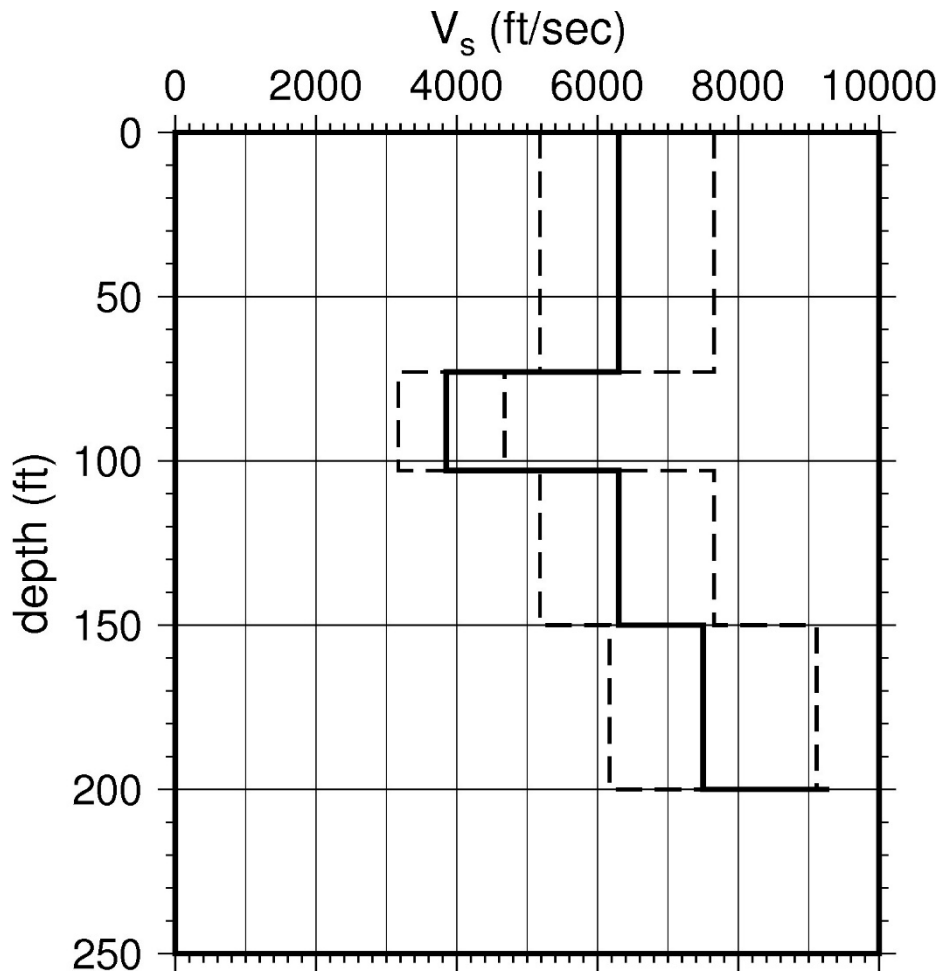


**Figure 2.2-27 Shear Wave Velocity ( $V_s$ ) Profiles for Limerick. Basecase (BC) Profile Shown as Solid Bold Line; Lower and Upper Range (LR and UR) Profiles Shown as Dashed Lines. Profiles Terminate at Reference Rock Velocity of 2,831 m/sec [9,285 ft/sec] per EPRI GMM (2013)**

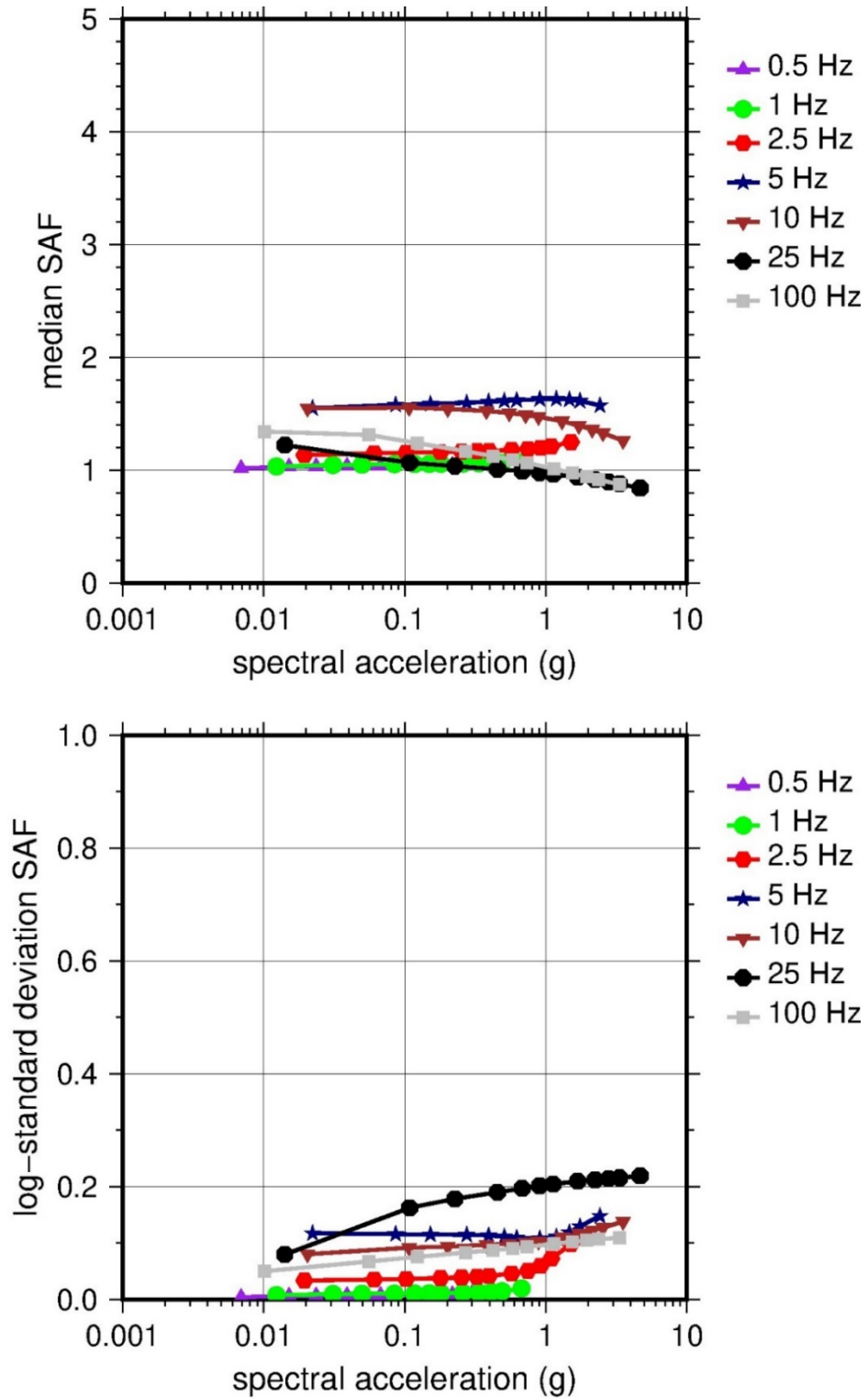


**Figure 2.2-28 Overall Weighted Median Site Amplification Factor (SAF) (Upper) and Log Standard Deviation of the SAF (Lower) as a Function of Input Acceleration for EPRI GMM (2013) Spectral Frequencies**

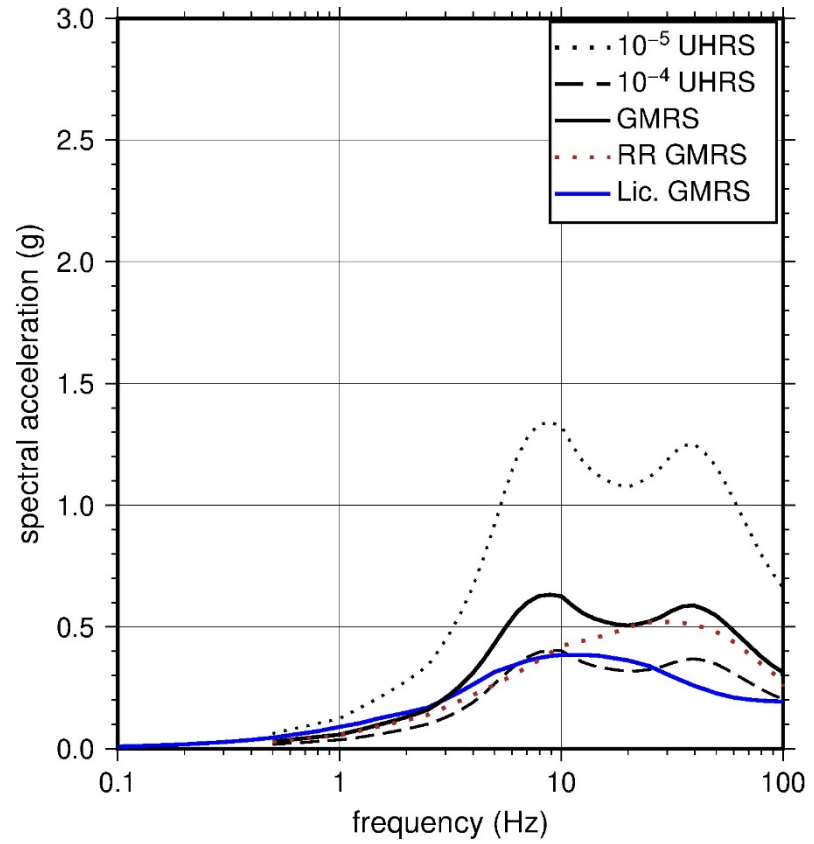
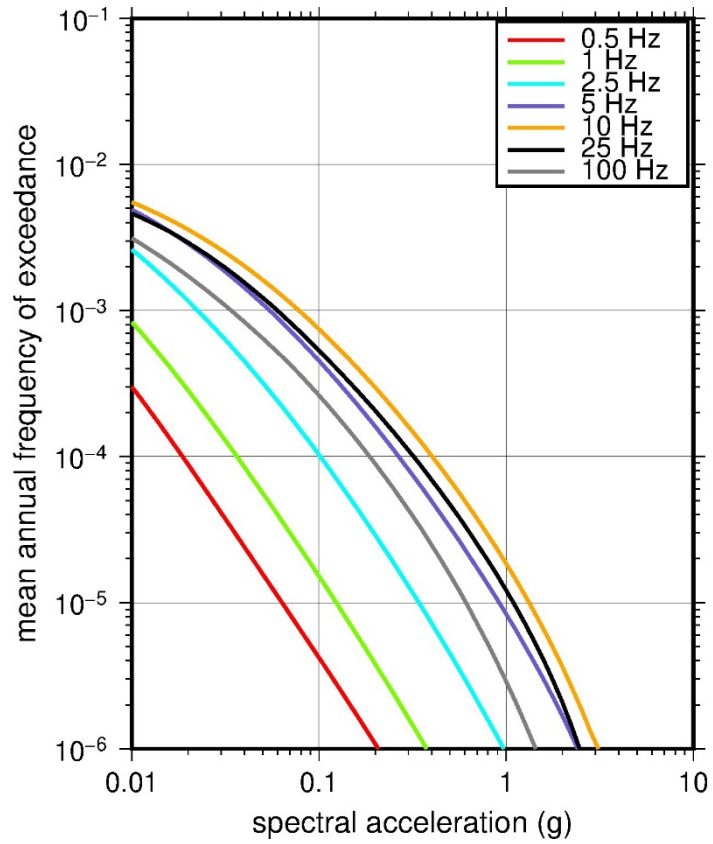


**Figure 2.2-29 Mean Control Point Hazard Curves (Left) for EPRI GMM (2013) Spectral Frequencies, and GMRS and UHS (Right) for Limerick**



## 2.2.8 Millstone

The Millstone Power Station site is located on the southern tip of Millstone Point on Long Island Sound within the New England physiographic province and is underlain by metamorphosed and folded rocks (gneiss and schist) that are over 610 m [2,000 ft] thick. The horizontal SSE response spectrum for Millstone Unit 2 has a rounded Housner spectral shape, and Unit 3 has a Newmark spectral shape. Both spectra are anchored at a PGA of 0.17g.

### 2.2.8.1 Reference Rock Hazard

For the reference rock PSHA, the NRC staff selected the 12 CEUS-SSC (NRC, 2012b) background seismic source zones that are located within 320 km [200 mi] of the Millstone site. The NRC staff also selected the Charlevoix CEUS-SSC RLME source, which is located about 645 km [400 mi] from the site. To develop the reference rock seismic hazard curves for the Millstone site, the NRC staff used the GMPEs in the updated EPRI GMM (2013). As shown in Figure 2.2-30, the ECC-AM seismotectonic zone, which is the highest weighted host zone for the site, is the largest contributor to both the 1 Hz and 10 Hz reference rock total mean hazard curves at the  $10^{-4}$  AFE level.

### 2.2.8.2 Site Response Evaluation

#### 2.2.8.2.1 Site Profiles

To develop a basecase profile, the NRC staff used the geologic information in the NTTF R2.1 SHSR (Heacock, 2014a) submitted by Dominion Nuclear Connecticut, Inc. (hereafter referred to as “the licensee” within this plant section). As described in the licensee’s SHSR, the Millstone site consists of a veneer of glacial till overlying metamorphosed and folded rocks of Ordovician to Silurian age. The Millstone safety-related structures are supported on the Ordovician age Monson Gneiss, which is a part of a series of lower Paleozoic metavolcanic and metasedimentary rocks and granitic gneisses that underlie most of eastern Connecticut. The site is also underlain by the Westerly Granite, which is a molten rock intrusion of Pennsylvanian age or younger. The licensee stated that there are alternative interpretations of the thickness of the Monson Gneiss in the site area and therefore developed two alternative basecase profiles. In Table 2.3.1-1 of the SHSR, the licensee briefly described the subsurface materials in terms of the geologic units and layer thicknesses. For its basecase profile, the NRC staff used the top of rock, which corresponds to an elevation of 5 m [15 ft] MSL, as the control point elevation for the Millstone site.

The field investigations for Millstone, conducted in the 1960s, consisted of a number of borings through the glacial till and upper portion of the rock beneath the site. In addition, crosshole and downhole geophysical surveys by the licensee measured  $V_P$  and  $V_S$  to a depth of about 31 m [100 ft] beneath the site. Table 2.3.1-1 of the SHSR gives the measured and estimated  $V_S$  estimates determined from the licensee’s site investigations.

The licensee’s geophysical measurements of the uppermost portion of the Monson Gneiss produced a  $V_S$  of about 1,982 m/sec [6,500 ft/sec]. The Monson Gneiss is underlain by the Brimfield Schist, a high-grade metamorphic rock. The extent of these geologic units beneath the site is uncertain. A recent USGS quadrangle map of the region indicates that the Monson Gneiss is about 610 m [2,000 ft] thick, while earlier interpretations postulate a thickness of 1,128 m [3,700 ft] for this unit. Based on these alternative interpretations of the regional geology, the licensee developed (1) a shallow R2.1 SHSR basecase profile that extends to a

depth of 610 m [2,000 ft] beneath the control point elevation and (2) a deeper basecase profile that extends to a depth of 1,677 m [5,500 ft]. For both basecase profiles, the licensee used the uppermost measured  $V_S$  of 1,982 m/sec [6,500 ft/sec] and then applied a velocity gradient of 0.5 m/sec/m [0.5 ft/sec/ft] to determine the  $V_S$  for the deeper rock beneath the site. This results in a  $V_S$  of 2,256 m/sec [7,400 ft/sec] at a depth of 610 m [2,000 ft] for the shallow basecase profile and a  $V_S$  of 2,790 m/sec [9,150 ft/sec] at a depth of 1,677 m [5,500 ft] for the deeper basecase profile.

Rather than use the velocity gradient of 0.5 m/sec/m [0.5 ft/sec/ft], which Appendix B to the SPID recommends for sedimentary rock, the NRC staff used a much steeper velocity gradient appropriate for metamorphic and igneous rock. As the measured uppermost  $V_S$  for the Monson Gneiss is 1,982 m/sec [6,500 ft/sec], and typical  $V_S$  for gneiss and granites range from 2,592 m/sec [8,500 ft/sec] to 3,201 m/sec [10,500 ft/sec], the NRC staff used the  $V_{S30}$  6,700 ft/sec [2,032 m/sec] profile template recommended in Appendix B to the SPID. This  $V_{S30}$  profile template reaches the reference rock  $V_S$  of 2,831 m/sec [9,285 ft/sec] at a depth of 31 m [100 ft]. While the staff cannot rule out the deeper profiles developed by the licensee, it considers this much shallower basecase profile to be more likely for the firm metamorphic and igneous rock beneath the Millstone site.

To capture the uncertainty in its basecase profile, the NRC staff developed lower and upper range (10<sup>th</sup> and 90<sup>th</sup> percentile) profiles by multiplying the basecase  $V_S$  values by scale factors of 0.83 and 1.21, respectively, which corresponds to an epistemic logarithmic standard deviation of 0.15. The weights for the lower, best-estimate, and upper basecase profiles are 0.3, 0.4, and 0.3, respectively. As shown in Figure 2.2-31, the upper profile terminates at a depth of 15 m [50 ft], and the lower and best-estimate basecase profiles terminate at a depth of 31 m [100 ft] below the control point elevation, at which point the  $V_S$  is assumed to reach the reference rock value of 2,831 m/sec [9,285 ft/sec].

#### 2.2.8.2.2 *Dynamic Material Properties and Site Kappa*

The NRC staff assumed both linear and nonlinear dynamic behavior for the rock beneath the Millstone site. To model the nonlinear behavior of the uppermost rock strata, the NRC staff used the EPRI rock shear modulus reduction and material damping curves. To model the linear behavior, the NRC staff used a constant damping ratio of 3 percent. The NRC staff assumed these two alternative dynamic responses for the upper 8 m [25 ft] of the profile and, due to the higher  $V_S$  of this rock layer, assigned weights of 0.7 and 0.3 to the linear and nonlinear alternatives, respectively. For the remaining 23 m [75 ft] of its profile, the NRC staff assumed a linear response with a material damping ratio value of 0.1 percent to maintain consistency with the  $\kappa_0$  value for the Millstone site.

To determine the basecase  $\kappa_0$  for the Millstone site, the NRC staff first used the Campbell (2009) Model 1 relationship between  $V_S$  and  $Q_{ef}$  to determine a  $Q_{ef}$  for each layer. Combining these  $Q_{ef}$  values with the thicknesses and  $V_S$  for each of the layers results in a total  $\kappa_0$  value of about 6.2 msec, which includes the 6 msec assumed for the underlying reference rock. For the lower and upper basecase profiles, the NRC staff calculated  $\kappa_0$  values of 6.3 and 6.1 msec, respectively, using the same approach as for the best-estimate basecase profile. In contrast, the licensee estimated  $\kappa_0$  by using two different SPID (EPRI, 2012) approaches that produce  $\kappa_0$  values ranging from 7 to 31 msec for the best-estimate, lower, and upper basecase profiles, respectively.

Table 2.2-9 provides the layer depths, lithologies,  $V_s$ , unit weights, and dynamic properties for the NRC staff's three profiles. In summary, the site response logic tree developed by the NRC staff for the Millstone site consists of six alternatives; three basecase profiles (each with a different  $\kappa_0$  value) and two alternative dynamic property branches.

### 2.2.8.2.3 Methodology and Results

The NRC staff followed the methodology described in Section 2.1.4 to develop the final site amplification factors. Figure 2.2-32 shows the overall median site amplification factors and their variability for each of the seven spectral frequencies. As shown in Figure 2.2-32, the median site amplification factors range from about 1.0 to 1.5 before falling off with higher input spectral accelerations. The lower half of Figure 2.2-32 shows that the logarithmic standard deviations for the site amplification factors range from about 0.05 to 0.15.

### 2.2.8.3 Control Point Hazard

The NRC staff implemented Approach 3 from the SPID to develop a weighted control point seismic hazard curve for each of the six unique combinations of the site response logic tree for the Millstone site. After combining these curves to develop the final mean control point hazard curves, the NRC staff determined the  $10^{-4}$  and  $10^{-5}$  UHRS in order to calculate the final GMRS. Figure 2.2-33 shows the final control point mean seismic hazard curves for each of the seven spectral frequencies as well as the NRC staff's UHRS and GMRS, and the licensee's NTTF R2.1 GMRS (Heacock, 2014a). As shown in Figure 2.2-33, the NRC staff's GMRS (black curve) is moderately higher than the licensee's GMRS (blue curve) due to the NRC staff's shallower basecase profile and lower  $\kappa_0$  values. For comparison, Figure 2.2-33 also shows the NRC staff's reference rock GMRS (brown dotted curve).

Layer	Depth (ft)	Description	$V_s$ (ft/sec)			$V_s$ Sigma (ln)	BC Unit Weight (pcf)	Dynamic Properties	
			LR (0.3)	BC (0.4)	UR (0.3)			Alt. 1 (0.3)	Alt. 2 (0.7)
1	25	Rock: gneiss	5,363	6,500	8,430	0.25	150	EPRI Rock	L 3.0%
2	50	Rock: gneiss	5,937	7,196	8,722	0.15	150	L 0.1%	L 0.1%
3	75	Rock: gneiss	6,511	7,892	9,285	0.15	160	L 0.1%	L 0.1%
4	100	Rock: gneiss	7,086	8,589	9,285	0.15	160	L 0.1%	L 0.1%

LR = lower range; BC = basecase; UR = upper range; ln = natural log; pcf = pounds per cubic foot; L = linear; Alt. = alternative.  
 For LR, BC, UR, and Alt.: Values in parentheses refer to weights for site response analysis logic tree branches.

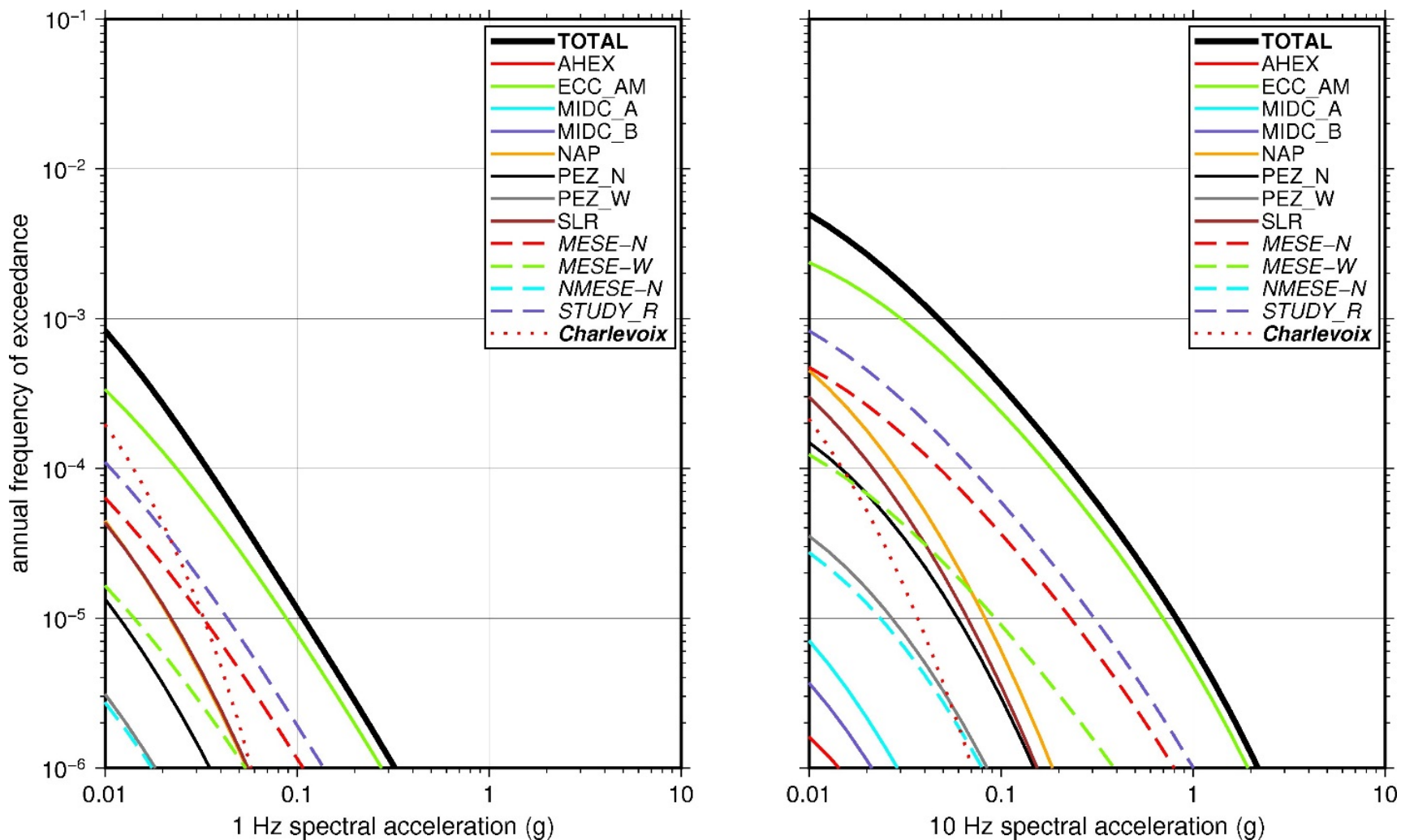


**Figure 2.2-30 Low-Frequency (1 Hz, Left) and High-Frequency (10 Hz, Right) Reference Rock Hazard Curves for Millstone. Total Hazard is Shown as a Bold Black Line; Individual Contributions to the Hazard for Each of the CEUS-SSC Sources are Shown as Colored Lines Defined in the Legend. See Table 2.1-1 for Source Name Definitions**

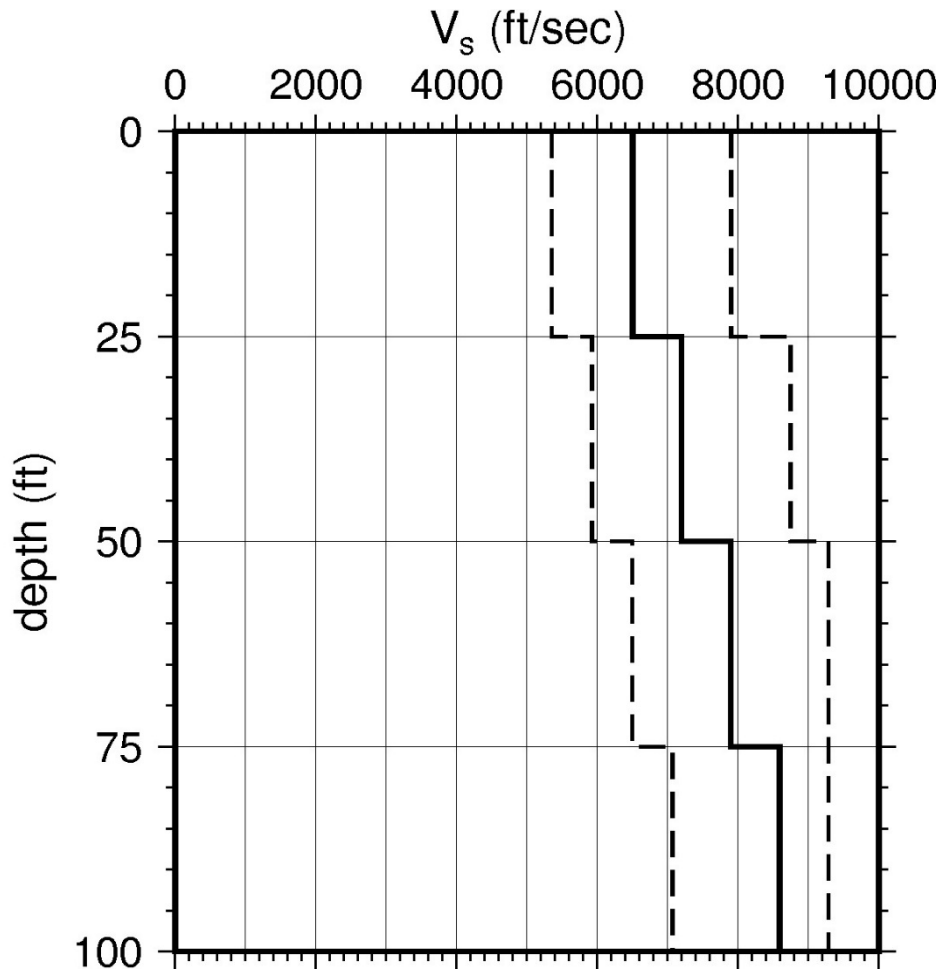


**Figure 2.2-31 Shear Wave Velocity ( $V_s$ ) Profiles for Millstone. Basecase (BC) Profile Shown as Solid Bold Line; Lower and Upper Range (LR and UR) Profiles Shown as Dashed Lines. Profiles Terminate at Reference Rock Velocity of 2,831 m/sec [9,285 ft/sec] per EPRI GMM (2013)**

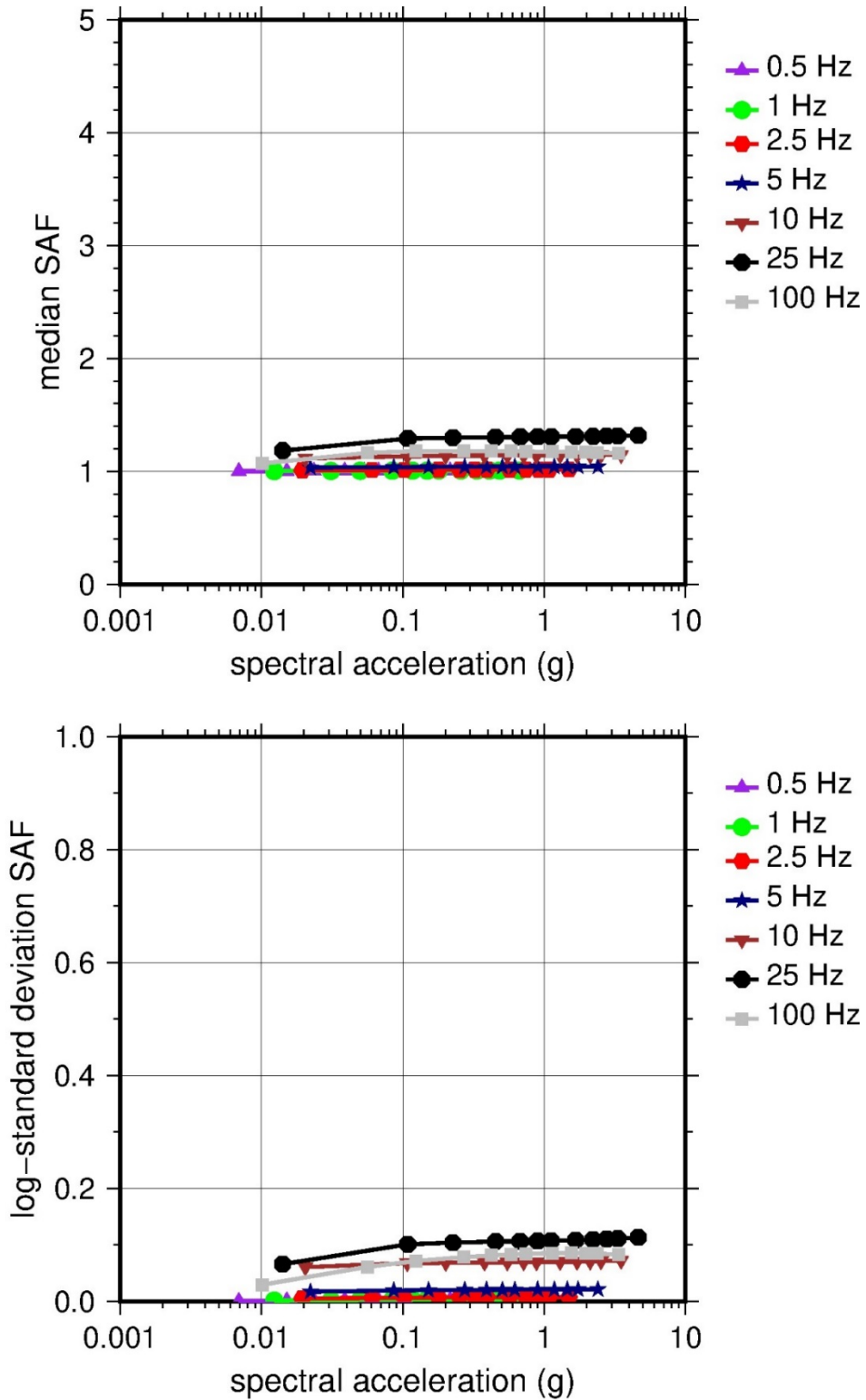


**Figure 2.2-32 Overall Weighted Median Site Amplification Factor (SAF) (Upper) and Log Standard Deviation of the SAF (Lower) as a Function of Input Acceleration for EPRI GMM (2013) Spectral Frequencies**

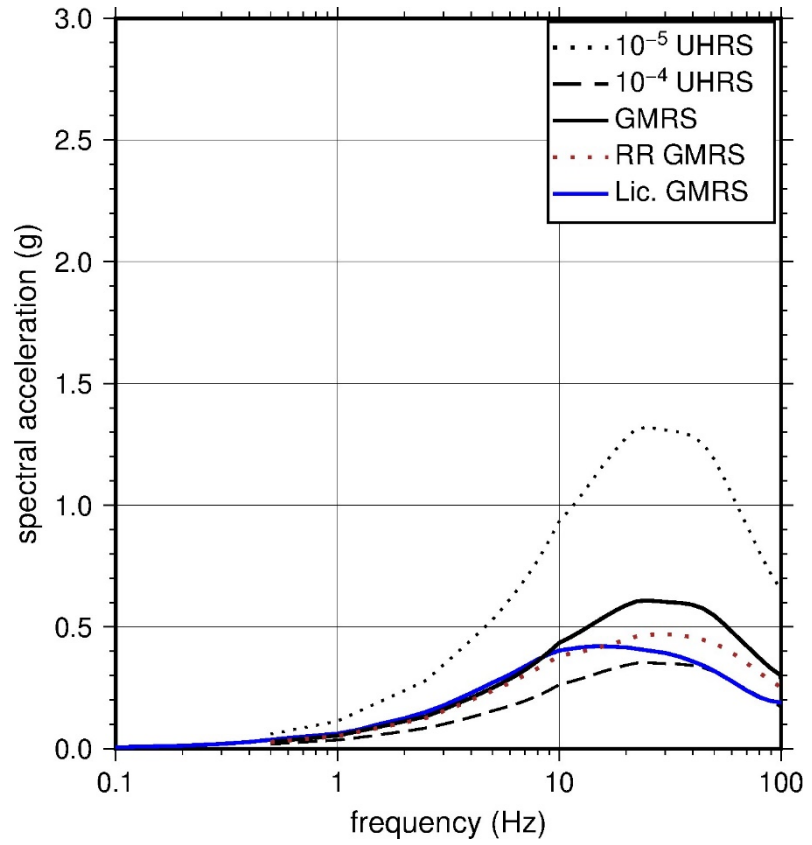
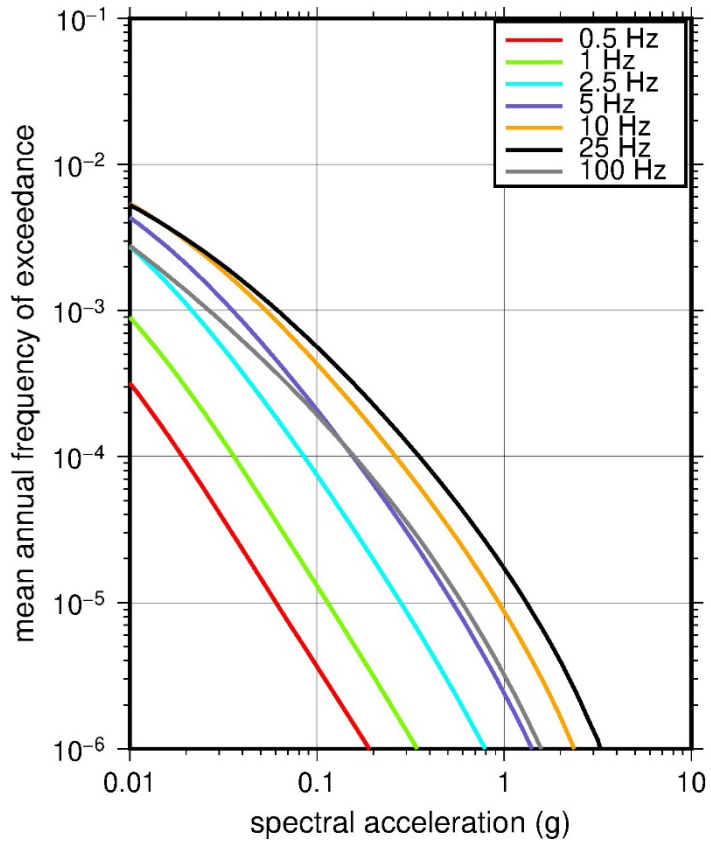


**Figure 2.2-33 Mean Control Point Hazard Curves (Left) for EPRI GMM (2013) Spectral Frequencies, and GMRS and UHS (Right) for Millstone**

## 2.2.9 Oyster Creek

The Oyster Creek Nuclear Generating Station (Oyster Creek) site is located on the south branch of the Forked River in the Atlantic Coastal Plain physiographic province and is founded on about 1,219 m [4,000 ft] of progressively older unconsolidated to semiconsolidated sediments (sand, clay, and silt) that are underlain by basement rock. The original horizontal SSE response spectrum for Oyster Creek has a rounded Housner spectral shape and is anchored at a PGA of 0.22g.

### 2.2.9.1 Reference Rock Hazard

For the reference rock PSHA, the NRC staff selected the 11 CEUS-SSC (NRC, 2012b) background seismic source zones that are located within 320 km [200 mi] of the Oyster Creek site. The NRC staff also selected the Charleston CEUS-SSC RLME source, which is located about 763 km [473 mi] from the site. To develop the reference rock seismic hazard curves for the site, the NRC staff used the GMPEs in the updated EPRI GMM (2013). As shown in Figure 2.2-34, the ECC-AM seismotectonic zone, which is the highest weighted host zone for the site, is the largest contributor to both the 1 Hz and 10 Hz reference rock total mean hazard curves at the  $10^{-4}$  AFE level.

### 2.2.9.2 Site Response Evaluation

#### 2.2.9.2.1 Site Profiles

To develop a basecase profile, the NRC staff used the geologic information in the NTTF R2.1 SHSR (Barstow, 2014b) submitted by Exelon (hereafter referred to as “the licensee” within this plant section). As described in the licensee’s R2.1 SHSR, the Oyster Creek site consists of a sequence of unconsolidated to semiconsolidated deposits of Quaternary, Tertiary, and Cretaceous age. The Oyster Creek structures are founded generally in the fine-to-coarse sand of the Cohansey Formation, which is of late Miocene age. In Table 2.3.1-1 of the SHSR, the licensee briefly described the subsurface materials in terms of the geologic units and layer thicknesses. For its site response evaluation, the NRC staff used the surface, which corresponds to an elevation of 7 m [23 ft] MSL, as the control point elevation for the Oyster Creek site.

The licensee did not obtain any in situ  $V_S$  measurements within the soil strata beneath the site. Therefore, to determine the  $V_S$  for the upper layers of its profile, the licensee used a correlation between seismic wave velocities and Standard Penetration Test (SPT) blow count values. Table 2.3.2-2 of the SHSR gives the  $V_S$  estimates for each of the soil layers determined from the licensee’s site investigations.

For its SHSR, the licensee developed a subsurface profile that extends to a depth of 1,220 m [4,000 ft] below the control point elevation. The uppermost layers of the profile consist of 16 m [52 ft] of fine sands from the Cape May Formation, an upper clay layer, and fine-to-coarse sands from the top of the Cohansey Formation. The age of the uppermost soil strata ranges from Late Pleistocene to Late Miocene, and the licensee’s estimated  $V_S$  ranges from 96 m/sec [315 ft/sec] to 249 m/sec [815 ft/sec]. Below 16 m [52 ft], the licensee used a scaled soil  $V_{S30}$  180 m/sec [590 ft/sec] template profile, which it extended to reach the base of the profile at a depth of 1,220 m [4,000 ft] below the control point elevation.



For its basecase profile, the NRC staff compared the licensee's  $V_S$  values with typical  $V_S$  for dense sands, which predominate within the upper subsurface strata. To guide the development of the deeper portion of its basecase profile, the staff also used the soil  $V_S$  profiles from the two other Atlantic Coastal Plain nuclear power plant sites (Calvert Cliffs and Hope Creek-Salem) that are sited over similar soil strata. Both the Hope Creek-Salem (Section 2.2.4) and Calvert Cliffs (Section 2.2.2) sites are located adjacent to recent ESP and COL siting applications, for which numerous geophysical measurements were made.

Rather than use the in situ residual soil for the upper portion of its basecase profile, the NRC staff used the compacted backfill soils that are located beneath the main structures in the site vicinity. Section 2.5.3.1 of the Oyster Creek UFSAR (Exelon Generation Company, 2014a) states that buildings and structures are founded generally in the third stratum (Cohansey Formation sand) and that after excavation and backfilling, rolling was performed "using loads up to 80,000 pounds on a four-foot square plate." Based on this description of the soil beneath the site, the NRC staff estimated a  $V_S$  of 274 m/sec [900 ft/sec] for the top layer of compacted soil, which is considerably higher than the  $V_S$  range of 96 m/sec [315 ft/sec] to 249 m/sec [815 ft/sec] estimated by the licensee for the top layers of in situ soil.

For the underlying sands of the Cohansey Formation, the licensee stated in the same section of the UFSAR that the "Cohansey sand has a dense to very dense relative density" and that "Results also indicate a marked increase in standard penetration resistance (N-values) at about elevation -30 feet." The SHSR indicates that the  $V_P$  for the Cohansey Formation sand beneath the site ranges from about 1,585 m/sec [5,200 ft/sec] to 1,800 m/sec [5,900 ft/sec]. The  $V_S$  ranges from about 245 m/sec [800 ft/sec] to 520 m/sec [1,700 ft/sec], and the Poisson's ratio value is 0.49. Because these  $V_S$  (1) were not directly measured but are instead based on SPT blow count values that are not provided in either the UFSAR (Exelon Generation Company, 2014a) or the SHSR and (2) are moderately lower than typical  $V_S$  for dense sands at similar depths, the NRC staff used the measured  $V_S$  for similar sand strata from the Calvert Cliffs and Hope Creek-Salem sites to estimate the  $V_S$  for the Cohansey Formation sands. The measured  $V_S$  for the Chesapeake Group sand (Stratum IIb), which is similar in age and located over a similar range of depths beneath the Calvert Cliffs site, is about 500 m/sec [1,600 ft/sec]. For the Hope Creek-Salem site, the measured  $V_S$  for the Vincetown Formation fine-to-medium-grained silty sand is about 685 m/sec [2,250 ft/sec]. However, this sand stratum beneath the Hope Creek-Salem site is older (Paleocene to Eocene [65–34 *mega annum*]) and more deeply buried {22 m [> 71 ft]} than the Cohansey Formation sands beneath Oyster Creek. Based on these two comparisons and the general trend in  $V_S$  in Table 2.3.2-2 of the SHSR, the NRC staff divided the 20 m [66 ft] Cohansey Formation into three sublayers with estimated  $V_S$  of 550 m/sec [1,800 ft/sec], 620 m/sec [2,025 ft/sec], and 695 m/sec [2,275 ft/sec]. For the deeper soil layers beneath Oyster Creek, the NRC staff used the Hope Creek-Salem and Calvert Cliffs profiles for general guidance and varied the  $V_S$  according to soil type and depth within the profile.

To capture the uncertainty in the basecase profile, the NRC staff developed lower range (10<sup>th</sup> percentile) and upper range (90<sup>th</sup> percentile) profiles by multiplying the basecase  $V_S$  by scale factors of 0.73 and 1.38, respectively, which corresponds to a logarithmic sigma value of 0.25. Figure 2.2-35 shows the upper 305 m [1,000 ft] of the three profiles used by the NRC staff, which extend to a depth of 1,220 m [4,000 ft] below the control point elevation, at which point the shear velocity is assumed to reach the reference value of 2,831 m/sec [9,285 ft/sec].

#### 2.2.9.2.2 *Dynamic Material Properties and Site Kappa*

The NRC staff assumed both linear and nonlinear behavior for the soil beneath the Oyster Creek site. To model the nonlinear response within the upper 353 ft [108 m] of soil deposits, the NRC staff used the EPRI soil shear modulus reduction and damping curves as one alternative and the Peninsular Range curves for the second equally-weighted alternative. For the remaining 1,112 m [3,647 ft] of its profile, the NRC staff assumed a linear response with damping ratio values of 1 to 2 percent to maintain consistency with the  $\kappa_0$  value for the Oyster Creek site.

To determine the basecase  $\kappa_0$  for the Oyster Creek site, the NRC staff first used the Campbell (2009) Model 1 relationship between  $V_S$  and  $Q_{ef}$  to determine a  $Q_{ef}$  for each layer. Combining these  $Q_{ef}$  values with the thicknesses and  $V_S$  for each of the layers results in a total  $\kappa_0$  value of about 65 msec, which includes the 6 msec assumed for the underlying reference rock. For the lower and upper basecase profiles, the NRC staff calculated  $\kappa_0$  values of 97 and 43 msec, respectively, using the same approach as for the basecase profile. In contrast, the licensee used a  $\kappa_0$  value of 40 msec for the best-estimate, lower, and upper basecase profiles, which is the maximum value recommended by Appendix B to the SPID (EPRI, 2012) for CEUS deep soil sites.

Table 2.2-10 provides the layer depths, lithologies,  $V_S$ , unit weights, and dynamic properties for the NRC staff's three profiles. In summary, the site response logic tree developed by the NRC staff for the Oyster Creek site consists of six alternatives; three basecase profiles (each with a different  $\kappa_0$  value) and two alternative dynamic property branches.

#### 2.2.9.2.3 *Methodology and Results*

The NRC staff followed the methodology described in Section 2.1.4 to develop the final site amplification factors. Figure 2.2-36 shows the overall median site amplification factors and their variability for each of the seven spectral frequencies. As shown in Figure 2.2-36, the median site amplification factors range from about 1 to 2 before falling off with higher input spectral accelerations. The lower half of Figure 2.2-36 shows that the logarithmic standard deviations for the site amplification factors range from about 0.1 to 0.3.

#### 2.2.9.3 *Control Point Hazard*

The NRC staff implemented Approach 3 from the SPID to develop a weighted control point seismic hazard curve for each of the six unique combinations of the site response logic tree for the Oyster Creek site. After combining these curves to develop the final mean control point hazard curves, the NRC staff determined the  $10^{-4}$  and  $10^{-5}$  UHRS in order to calculate the final GMRS. Figure 2.2-37 shows the final control point mean seismic hazard curves for each of the seven spectral frequencies as well as the NRC staff's UHRS and GMRS, and the licensee's NTTF R2.1 GMRS (Barstow, 2014b). As shown in Figure 2.2-37, the NRC staff's GMRS (black curve) is moderately lower than the licensee's GMRS (blue curve) due to the staff's higher  $V_S$  for the uppermost soil layers and decision to not cap  $\kappa_0$  at 40 msec.

**Table 2.2-10 Layer Depths, Shear Wave Velocities ( $V_s$ ), Unit Weights, and Dynamic Properties for Oyster Creek**

Layer	Depth (ft)	Description	$V_s$ (ft/sec)			$V_s$ Sigma (ln)	BC Unit Weight (pcf)	Dynamic Properties	
			LR (0.3)	BC (0.4)	UR (0.3)			Alt. 1 (0.5)	Alt. 2 (0.5)
1	34	Soil: fill	697	900	1,163	0.25	120	EPRI Soil	Pen.
2	52	Soil: sand	1,393	1,800	2,326	0.15	130	EPRI Soil	Pen.
3	80	Soil: sand	1,567	2,025	2,617	0.15	130	EPRI Soil	Pen.
4	100	Soil: sand	1,760	2,275	2,940	0.15	130	EPRI Soil	Pen.
5	108	Soil: clay, silt, sand	1,567	2,025	2,617	0.15	130	EPRI Soil	Pen.
6	189	Soil: sand	1,702	2,200	2,843	0.15	130	EPRI Soil	Pen.
7	271	Soil: sand	1,780	2,300	2,972	0.15	130	EPRI Soil	Pen.
8	353	Soil: sand	1,857	2,400	3,102	0.15	130	EPRI Soil	Pen.
9	960	Soil: sand	1,780	2,300	2,972	0.15	130	L 2.0%	L 2.0%
10	1,568	Soil: sand, clay, silt	1,857	2,400	3,102	0.15	130	L 2.0%	L 2.0%
11	2,176	Soil: sand, clay, silt	1,934	2,500	3,231	0.15	130	L 2.0%	L 2.0%
12	2,784	Soil: sand, clay, silt	2,011	2,600	3,360	0.15	130	L 1.0%	L 1.0%
13	3,392	Soil: sand, clay, silt	2,089	2,700	3,489	0.15	130	L 1.0%	L 1.0%
14	4,000	Soil: sand, clay, silt	2,167	2,800	3,618	0.15	130	L 1.0%	L 1.0%

LR = lower range; BC = basecase; UR = upper range; ln = natural log; pcf = pounds per cubic foot; L = linear; Alt. = alternative; Pen. = Peninsular.  
 For LR, BC, UR, and Alt.: Values in parentheses refer to weights for site response analysis logic tree branches.

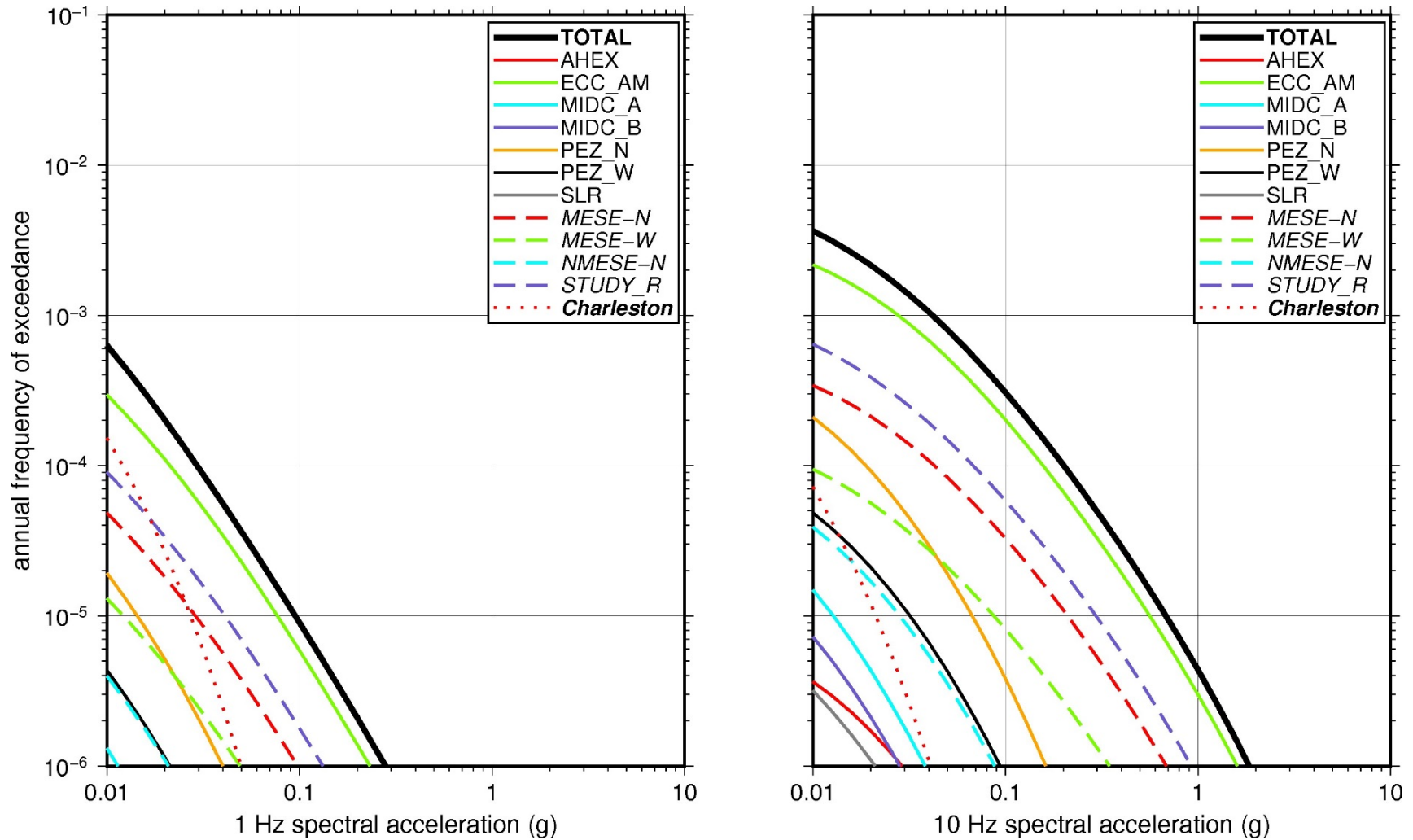


**Figure 2.2-34 Low-Frequency (1 Hz, Left) and High-Frequency (10 Hz, Right) Reference Rock Hazard Curves for Oyster Creek. Total Hazard is Shown as a Bold Black Line; Individual Contributions to the Hazard for Each of the CEUS-SSC Sources are Shown as Colored Lines Defined in the Legend. See Table 2.1-1 for Source Name Definitions**

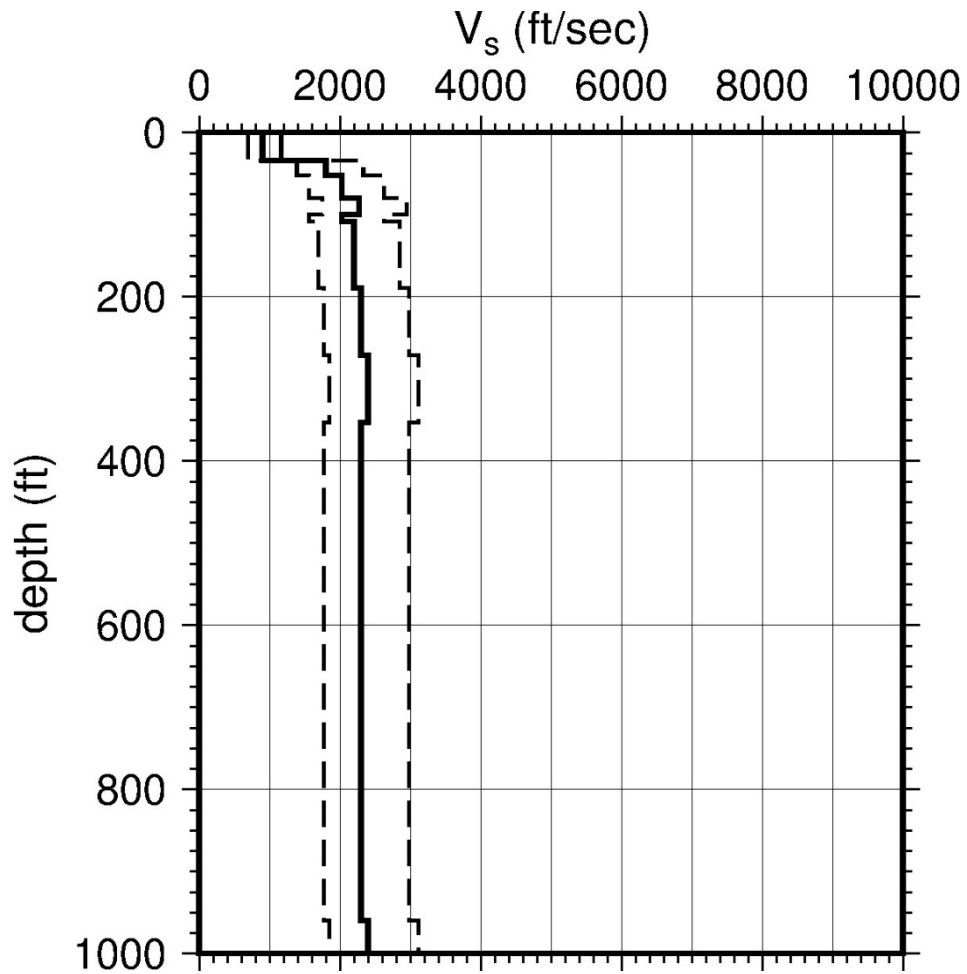


**Figure 2.2-35 Shear Wave Velocity ( $V_s$ ) Profiles for Oyster Creek. Basecase (BC) Profile Shown as Solid Bold Line; Lower and Upper Range (LR and UR) Profiles Shown as Dashed Lines. Profiles Terminate at Reference Rock Velocity of 2,831 m/sec [9,285 ft/sec] per EPRI GMM (2013)**

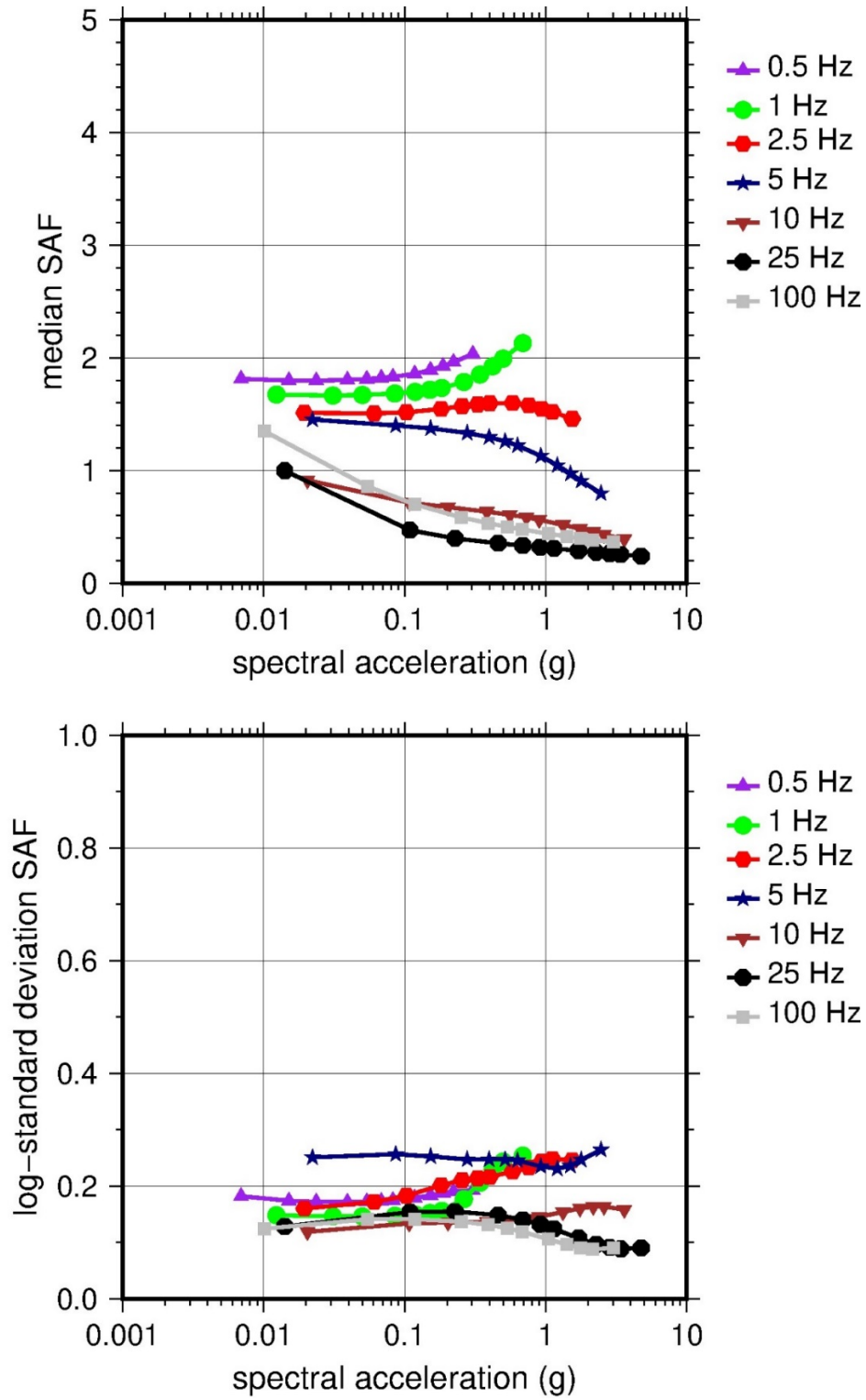


**Figure 2.2-36 Overall Weighted Median Site Amplification Factor (SAF) (Upper) and Log Standard Deviation of the SAF (Lower) as a Function of Input Acceleration for EPRI GMM (2013) Spectral Frequencies**

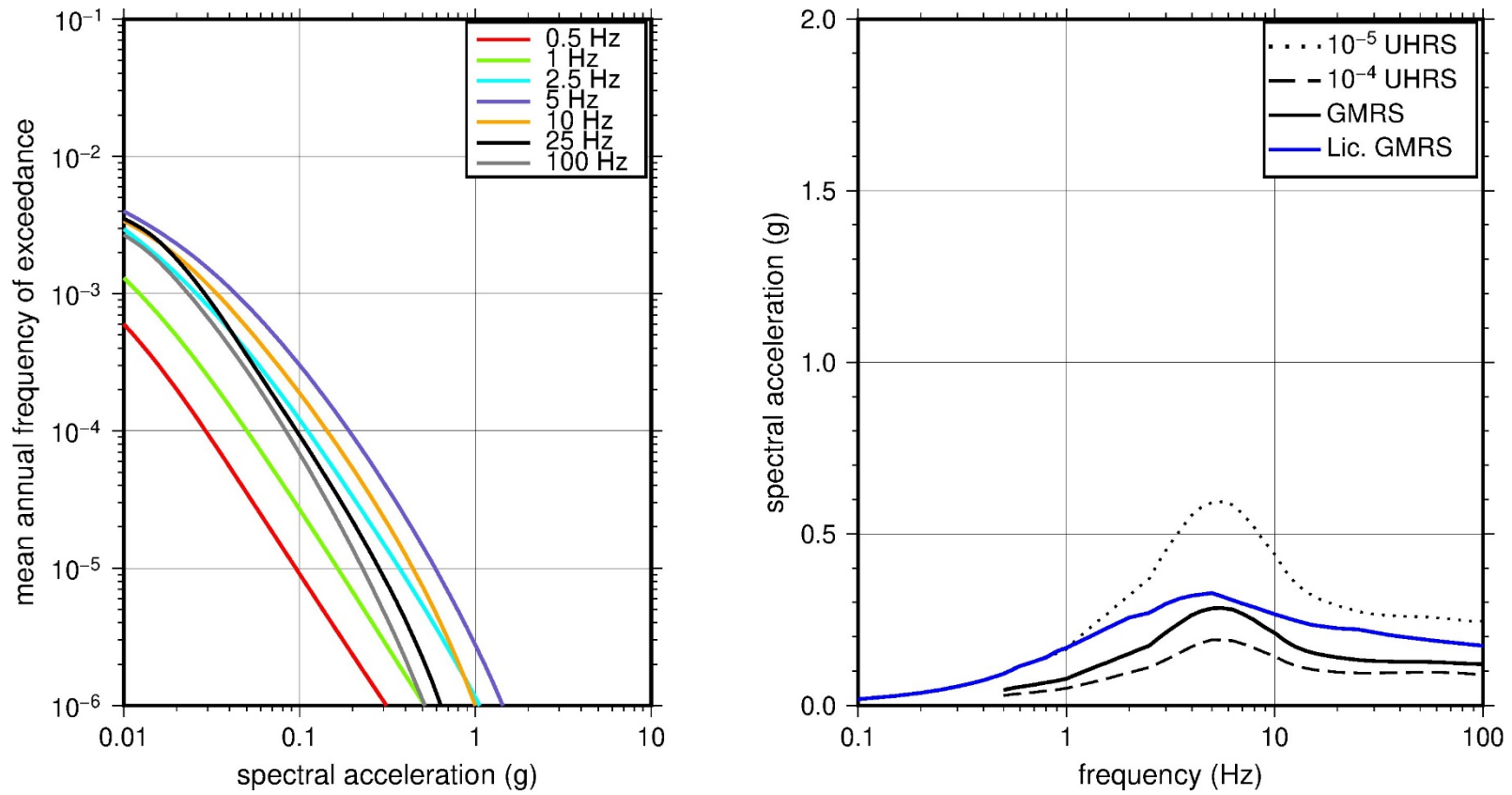


**Figure 2.2-37 Mean Control Point Hazard Curves (Left) for EPRI GMM (2013) Spectral Frequencies, and GMRS and UHRS (Right) for Oyster Creek**

## 2.2.10 Peach Bottom

The Peach Bottom Atomic Power Station site is located on the banks of the Susquehanna River in southern Pennsylvania within the Piedmont physiographic province and is underlain by metamorphosed sedimentary and crystalline rocks. The horizontal SSE response spectrum for Peach Bottom has a rounded Housner spectral shape and is anchored at a PGA of 0.12g.

### 2.2.10.1 Reference Rock Hazard

For the reference rock PSHA, the NRC staff selected the 10 CEUS-SSC (NRC, 2012b) background seismic source zones that are located within 320 km [200 mi] of the site. The NRC staff also selected the Charleston CEUS-SSC RLME source, which is located at a distance of about 776 km [481 mi] from the site. To develop the reference rock seismic hazard curves for the Peach Bottom site, the NRC staff used the GMPEs in the updated EPRI GMM (2013). As shown in Figure 2.2-38, the ECC-AM seismotectonic zone, which is the highest weighted host zone for the site, is the largest contributor to both the 1 Hz and 10 Hz reference rock total mean hazard curves at the  $10^{-4}$  AFE level.

### 2.2.10.2 Site Response Evaluation

#### 2.2.10.2.1 Site Profiles

To develop a basecase profile, the NRC staff used the geologic information in the NTTF R2.1 SHSR (Barstow, 2014c) submitted by Exelon (hereafter referred to as “the licensee” within this plant section). As described in the licensee’s SHSR, the Peach Bottom site consists of a veneer of residual soils overlying partially weathered rock grading into hard unweathered metamorphic rocks. The Peach Bottom reactor buildings are supported on the Peters Creek schist, which is of late Paleozoic or early Precambrian age. In Table 2.3.1-1 of the SHSR, the licensee briefly described the subsurface materials in terms of the geologic units and layer thicknesses. For its site response evaluation, the NRC staff used the top of moderately weathered rock, which corresponds to an elevation of 42 m [136 ft] MSL, as the control point elevation for the Peach Bottom site.

The licensee did not obtain in situ  $V_S$  measurements in the Peters Creek schist at the Peach Bottom site. However, during the original siting investigation, the licensee performed laboratory measurements (shock-scope tests under a range of confining pressures) to obtain  $V_P$  and unit weights from core samples from several boreholes at depths ranging from about 6 m [20 ft] to 40 m [130 ft]. Table 2.3.2-2 of the SHSR gives the licensee’s estimated  $V_S$  determined from the  $V_P$  listed in SHSR, Table 2.3.1-1, and assumed Poisson’s ratios.

For its SHSR, the licensee developed a basecase profile that extends to a depth of 6 m [20 ft] below the control point elevation. The uppermost layers of the profile consist of late Paleozoic metamorphic rock (metagraywackes) from the Wissahickon Formation, which includes the Peters Creek schist member. The licensee estimated a  $V_S$  of 1,140 m/sec [3,741 ft/sec] for the upper 6 m [20 ft] based on an average  $V_P$  of 2,134 m/sec [7,000 ft/sec] and an assumed Poisson’s ratio of 0.30. Below this depth, the laboratory-measured  $V_P$  for the unweathered schist exceeds 4,878 m/sec [16,000 ft/sec], which, combined with an assumed Poisson’s ratio of 0.28, implies a  $V_S$  greater than 2,700 m/sec [8,800 ft/sec]. Because this  $V_S$  is close to the reference value of 2,831 m/sec [9,285 ft/sec], the basecase profile developed by the licensee does not extend below 6 m [20 ft].



To develop its basecase  $V_S$  profile, the NRC staff closely examined Table 2.5.2 of the UFSAR (Exelon Generation Company, 2012b) to evaluate the range in  $V_P$  as a function of depth for each of the rock samples extracted from the multiple borings beneath the site. For the rock samples evaluated at shallower depths {6 m [ $<20$  ft]} from borings H-32 and H-35, the  $V_P$  ranges from about 1,740 m/sec [5,700 ft/sec] to about 3,780 m/sec [12,400 ft/sec], with an average value of about 2,700 m/sec [8,900 ft/sec]. Using this average value and an assumed Poisson's ratio of 0.33 results in a  $V_S$  of about 1,400 m/sec [4,500 ft/sec]. For the rock samples evaluated at greater depths {6 m [20 ft] to 20 m [65 ft]}, the  $V_P$  ranges from about 2,800 ft/sec [9,300 ft/sec] to 5,400 m/sec [17,800 ft/sec], with an average value of about 4,600 m/sec [15,000 ft/sec]. Using this average value and a Poisson's ratio 0.33 results in a  $V_S$  of about 2,300 m/sec [7,600 ft/sec]. Finally, for the deepest rock layer from a depth of 24 m [65 ft] to a depth of 46 m [150 ft], the NRC staff estimated a  $V_S$  of 2,682 m/sec [8,800 ft/sec], which is consistent with the  $V_P$  from the rock sample extracted from Borehole H-32 at a depth of 25 m [79 ft]. In summary, the NRC staff developed a three-layer basecase profile rather than just a single-layer profile using the  $V_P$  data in Table 2.5.2 of the UFSAR (Exelon Generation Company, 2012b) and assuming a slightly higher Poisson's ratio.

To capture the uncertainty in its basecase profile, the NRC staff developed lower and upper range (10<sup>th</sup> and 90<sup>th</sup> percentile) profiles by multiplying the basecase  $V_S$  values by scale factors of 0.83 and 1.21, respectively, which corresponds to an epistemic logarithmic standard deviation of 0.15. The weights for the lower, best-estimate, and upper basecase profiles are 0.3, 0.4, and 0.3, respectively. As shown in Figure 2.2-39, the upper profile terminates at a depth of 15 m [50 ft], and the lower and best-estimate basecase profiles terminate at a depth of 46 m [150 ft] below the control point elevation, at which point the  $V_S$  is assumed to reach the reference rock value of 2,831 m/sec [9,285 ft/sec].

#### 2.2.10.2.2 *Dynamic Material Properties and Site Kappa*

The NRC staff assumed both linear and nonlinear dynamic behavior for the rock beneath the Peach Bottom site. To model the nonlinear behavior of the uppermost rock strata, the NRC staff used the EPRI rock shear modulus reduction and material damping curves. To model the linear behavior, the NRC staff used a constant damping ratio of 3 percent. The NRC staff assumed these two alternative dynamic responses for the upper 6 m [20 ft] of the profile and, due to the higher  $V_S$  of this rock layer, assigned weights of 0.7 and 0.3 to the linear and nonlinear alternatives, respectively. For the remaining 40 m [130 ft] of its profile, the NRC staff assumed a linear response with a material damping ratio value of 0.1 percent to maintain consistency with the  $\kappa_0$  value for the Peach Bottom site.

To determine the basecase  $\kappa_0$  for the Peach Bottom site, the NRC staff first used the Campbell (2009) Model 1 relationship between  $V_S$  and  $Q_{ef}$  to determine a  $Q_{ef}$  for each layer. Combining these  $Q_{ef}$  values with the thicknesses and  $V_S$  for each of the layers results in a total  $\kappa_0$  value of about 6.3 msec, which includes the 6 msec assumed for the underlying reference rock. For the lower and upper basecase profiles, the NRC staff calculated  $\kappa_0$  values of 6.4 and 6.1 msec, respectively, using the same approach as for the best-estimate basecase profile. In contrast, the licensee estimated  $\kappa_0$  using the lowest low-strain damping values from the EPRI rock material damping curves over the upper 6 m [20 ft] of rock to estimate best-estimate, lower, and upper basecase  $\kappa_0$  values of 6.3, 6.6, and 6.2 msec, respectively.

Table 2.2-11 provides the layer depths, lithologies,  $V_S$ , unit weights, and dynamic properties for the NRC staff's three profiles. In summary, the site response logic tree developed by the NRC

staff for the Peach Bottom site consists of six alternatives; three basecase profiles (each with a different  $\kappa_0$  value) and two alternative dynamic property branches.

### 2.2.10.2.3 Methodology and Results

The NRC staff followed the methodology described in Section 2.1.4 to develop the final site amplification factors. Figure 2.2-40 shows the overall median site amplification factors and their variability for each of the seven spectral frequencies. As shown in Figure 2.2-40, the median site amplification factors range from about 1.0 to 1.5 before falling off with higher input spectral accelerations. The lower half of Figure 2.2-40 shows that the logarithmic standard deviations for the site amplification factors range from about 0.05 to 0.20.

### 2.2.10.3 Control Point Hazard

The NRC staff implemented Approach 3 from the SPID to develop a weighted control point seismic hazard curve for each of the six unique combinations of the site response logic tree for the Peach Bottom site. After combining these curves to develop the final mean control point hazard curves, the NRC staff determined the  $10^{-4}$  and  $10^{-5}$  UHRS in order to calculate the final GMRS. Figure 2.2-41 shows the final control point mean seismic hazard curves for each of the seven spectral frequencies as well as the NRC staff's UHRS and GMRS, and the licensee's NTTF R2.1 GMRS (Barstow, 2014c). As shown in Figure 2.2-41, the NRC staff's GMRS (black curve) is moderately higher than the licensee's GMRS (blue curve) due to the differences in the basecase profiles. For comparison, Figure 2.2-41 also shows the NRC staff's reference rock GMRS (brown dotted curve).

Layer	Depth (ft)	Description	$V_s$ (ft/sec)			$V_s$ Sigma (ln)	BC Unit Weight (pcf)	Dynamic Properties	
			LR (0.3)	BC (0.4)	UR (0.3)			Alt. 1 (0.3)	Alt. 2 (0.7)
1	20	Rock: schist	3,713	4,500	5,454	0.25	150	EPRI Rock	L 3.0%
2	65	Rock: schist	6,271	7,600	9,211	0.15	150	L 0.1%	L 0.1%
3	150	Rock: schist	7,261	8,800	9,285	0.15	160	L 0.1%	L 0.1%

LR = lower range; BC = basecase; UR = upper range; ln = natural log; pcf = pounds per cubic foot; L = linear; Alt. = alternative.  
 For LR, BC, UR, and Alt.: Values in parentheses refer to weights for site response analysis logic tree branches.

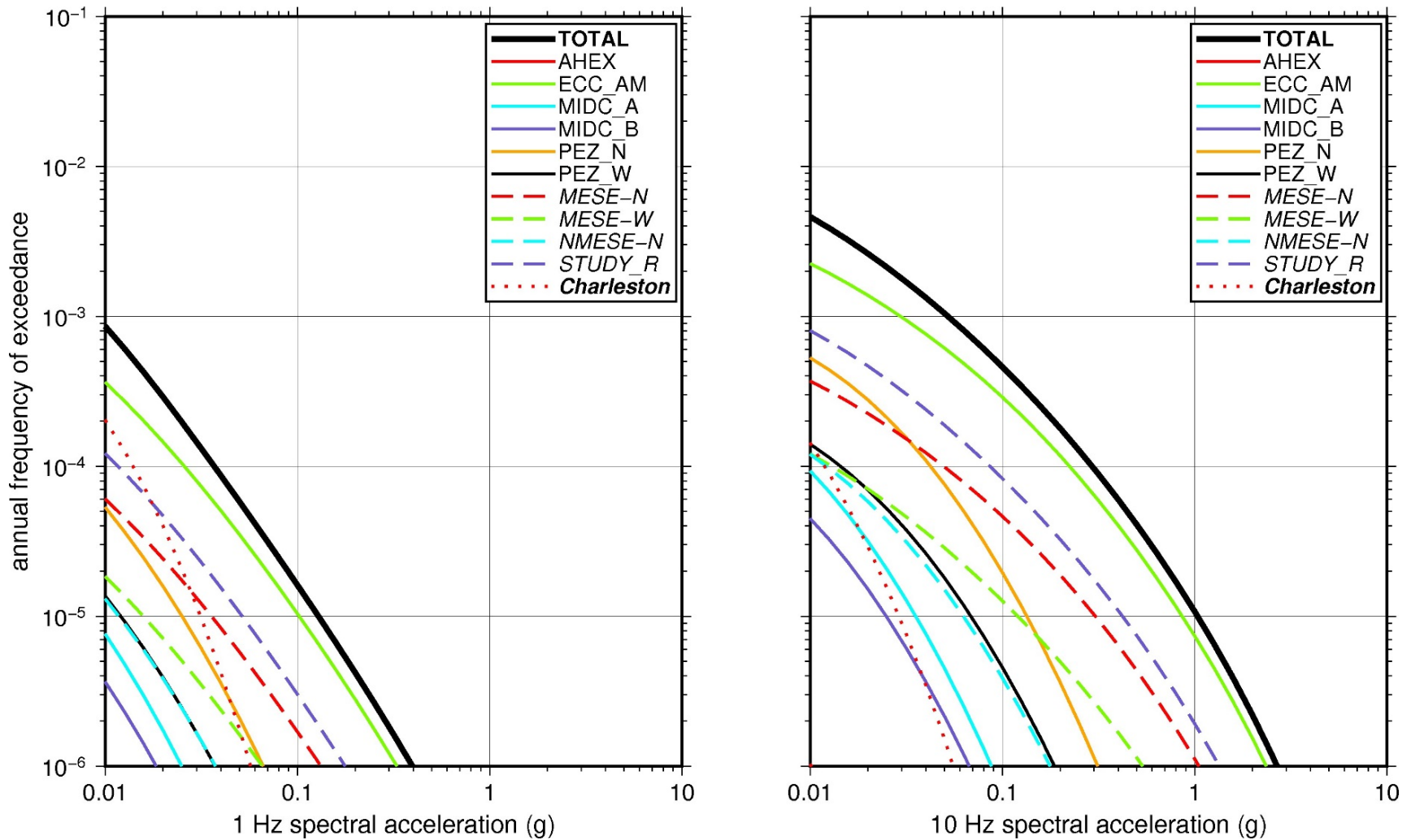


**Figure 2.2-38 Low-Frequency (1 Hz, Left) and High-Frequency (10 Hz, Right) Reference Rock Hazard Curves for Peach Bottom. Total Hazard is Shown as a Bold Black Line; Individual Contributions to the Hazard for Each of the CEUS-SSC Sources are Shown as Colored Lines Defined in the Legend. See Table 2.1-1 for Source Name Definitions**

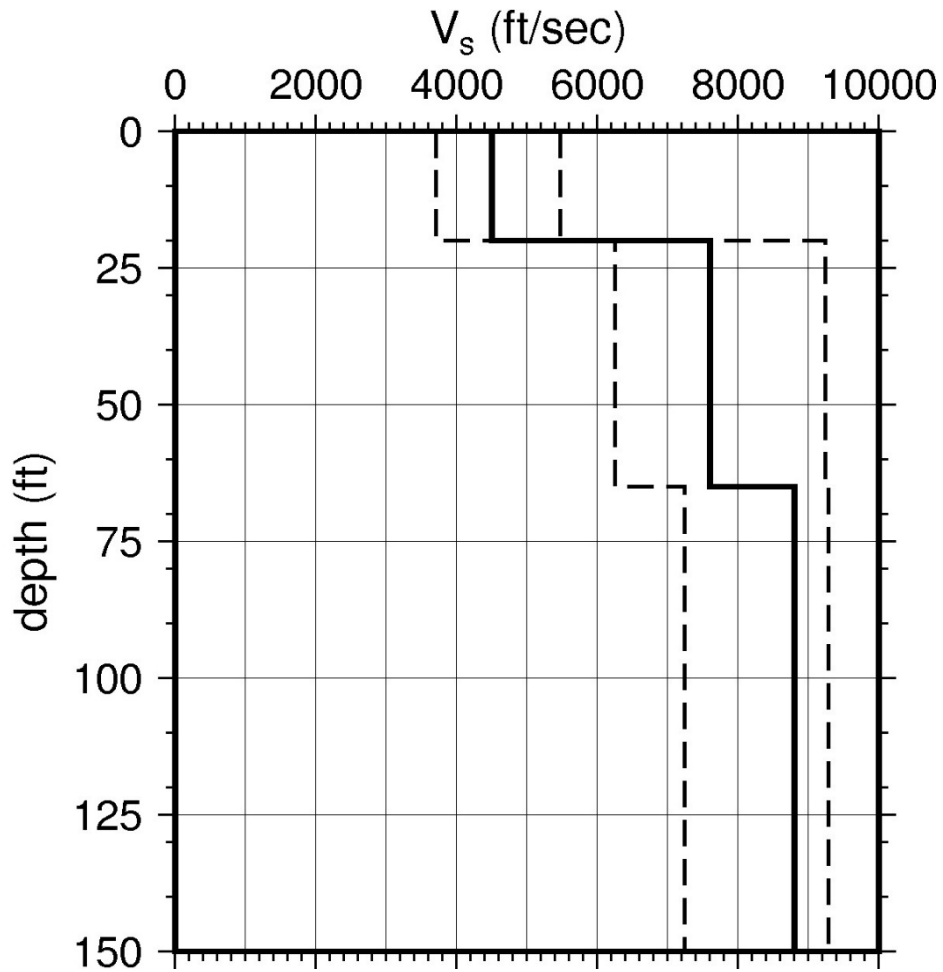


**Figure 2.2-39 Shear Wave Velocity ( $V_s$ ) Profiles for Peach Bottom. Basecase (BC) Profile Shown as Solid Bold Line; Lower and Upper Range (LR and UR) Profiles Shown as Dashed Lines. Profiles Terminate at Reference Rock Velocity of 2,831 m/sec [9,285 ft/sec] per EPRI GMM (2013)**

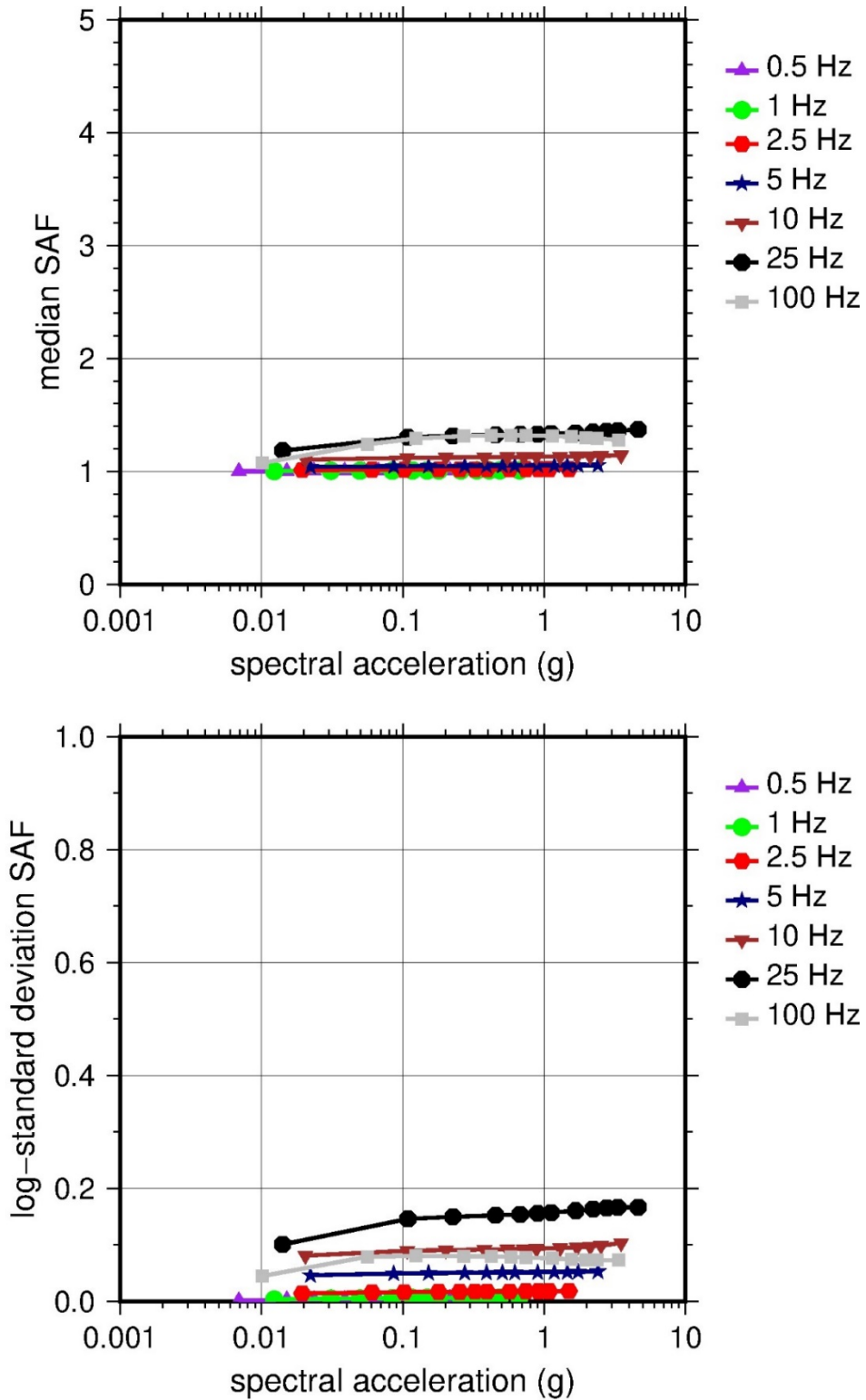


**Figure 2.2-40 Overall Weighted Median Site Amplification Factor (SAF) (Upper) and Log Standard Deviation of the SAF (Lower) as a Function of Input Acceleration for EPRI GMM (2013) Spectral Frequencies**

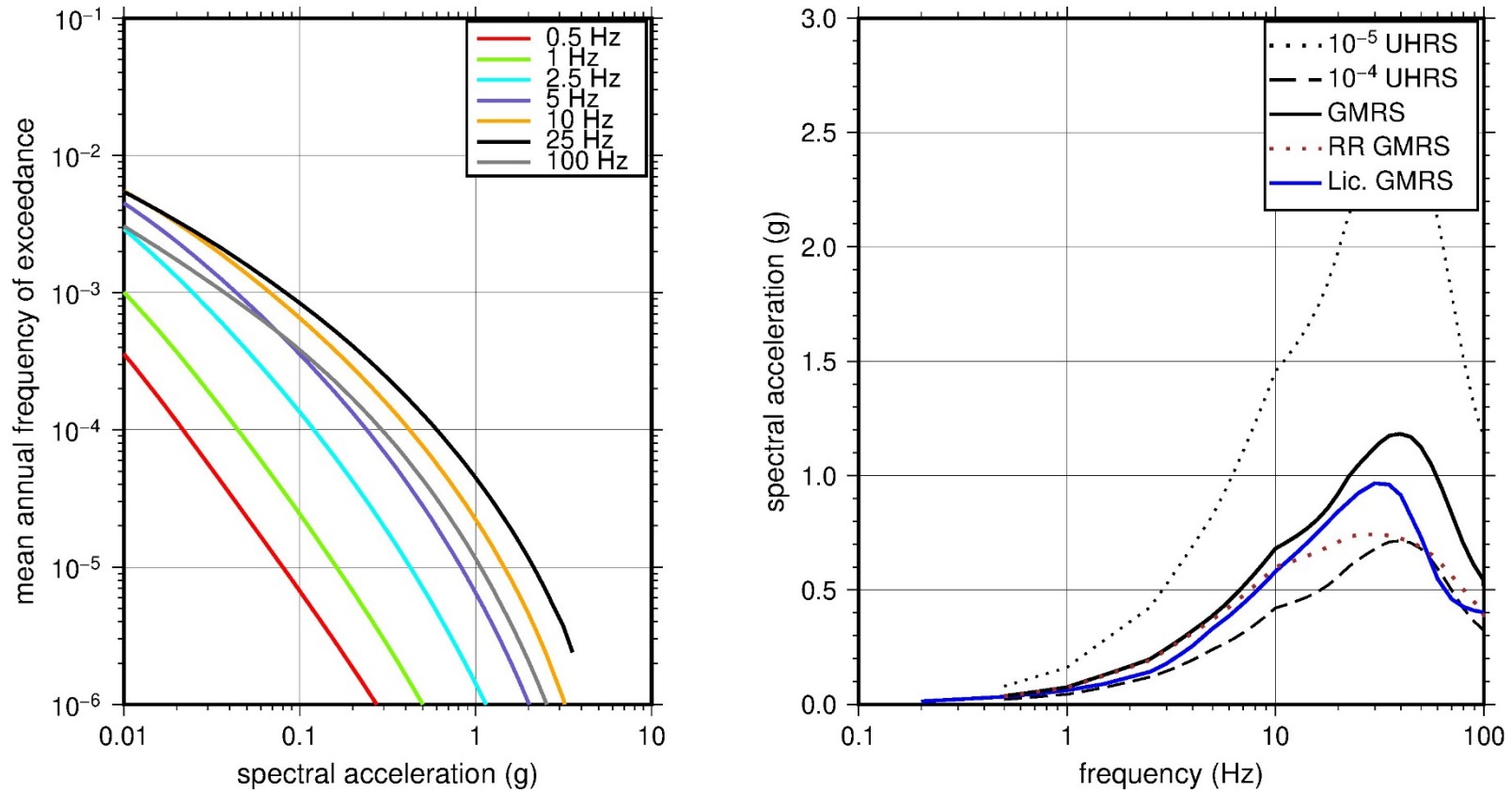


**Figure 2.2-41 Mean Control Point Hazard Curves (Left) for EPRI GMM (2013) Spectral Frequencies, and GMRS and UHRS (Right) for Peach Bottom**

## 2.2.11 Pilgrim

The Pilgrim Nuclear Power Station site is located on the shore of Cape Cod Bay in the New England physiographic province and is founded on about 12 m [40 ft] of glacial outwash, which overlies Precambrian age bedrock of the Dedham granodiorite rock unit. As shown in Figure 2.5-6 of the UFSAR, the horizontal SSE response spectrum for Pilgrim has a semirounded spectral shape and is anchored at a PGA of 0.15g (Entergy Nuclear Operations Inc., 2009).

### 2.2.11.1 Reference Rock Hazard

For the reference rock PSHA, the NRC staff selected the 10 CEUS-SSC (NRC, 2012b) background seismic source zones that are located within 320 km [200 mi] of the site. The NRC staff also selected the Charlevoix CEUS-SSC RLME source, which is located at a distance about 560 km [350 mi] from the Pilgrim site. To develop the reference rock seismic hazard curves for the site, the NRC staff used the GMPEs in the updated EPRI GMM (2013). As shown in Figure 2.2-42, the ECC-AM seismotectonic zone, which is the highest weighted host zone for the Pilgrim site, is the largest contributor to both the 1 Hz and 10 Hz reference rock total mean hazard curves at the  $10^{-4}$  AFE level.

### 2.2.11.2 Site Response Evaluation

#### 2.2.11.2.1 Site Profiles

To develop a basecase profile, the NRC staff used the geologic information in the NTTF R2.1 SHSR (Dent, 2014) submitted by Entergy Nuclear Operations, Inc. (hereafter referred to as “the licensee” within this plant section). As described in the licensee’s SHSR, the Pilgrim site consists of about 27 m [90 ft] of sand, sandy silts, and gravel overlying about 2 m [6 ft] of weathered bedrock with hard metamorphic bedrock below. Table 2.3.2-1 of the SHSR indicates that the reactor building foundation is located at a depth of about 15 m [48 ft] within the glacial outwash and about 12 m [42 ft] above the weathered upper bedrock layer. In Table 2.3.1-1 of the SHSR, the licensee briefly described the subsurface materials in terms of the geologic units and layer thicknesses. For its site response evaluation, the NRC staff used the plant foundation level, which is located within the Pleistocene age glacial deposits {elevation  $-8$  m [ $-26$  ft] MSL}, as the control point elevation for the Pilgrim site.

The field investigations for Pilgrim, conducted in the 1960s, consisted of a number of borings through the soil and upper portion of rock beneath the site. Seismic refraction surveys by the licensee measured  $V_P$  to a depth of about 27 m [90 ft] beneath the site. In addition, the licensee directly measured  $V_S$  from a crosshole seismic survey at a nearby ISFSI. Table 2.3.2-2 of the SHSR gives the measured  $V_S$  determined from the licensee’s site investigations.

For its SHSR, the licensee developed a basecase profile that extends to a depth of 15 m [48 ft] below the control point elevation. The uppermost layers of the profile consist primarily of sand and gravel, for which the licensee measured a  $V_S$  of 550 m/sec [1,800 ft/sec]. For the underlying 2 m [6 ft] of weathered granodiorite, the licensee measured a  $V_S$  of about 1,830 m/sec [6,000 ft/sec]. For the more competent rock below this layer, the licensee measured a  $V_S$  of 3,200 m/sec [10,500 ft/sec]. Because the  $V_S$  for this competent rock exceeds the reference rock  $V_S$ , the licensee terminated its basecase profile at the top of this layer.

As the soil and rock strata beneath the Pilgrim site is fairly well characterized by the licensee's site investigations, the NRC staff used the licensee's layer thicknesses and  $V_S$  for its profile.

To capture the uncertainty in its basecase profile, the NRC staff developed lower and upper range (10<sup>th</sup> and 90<sup>th</sup> percentile) profiles by multiplying the basecase  $V_S$  values by scale factors of 0.78 and 1.29, respectively, which corresponds to an epistemic logarithmic standard deviation of 0.20. The weights for the lower, best-estimate, and upper basecase profiles are 0.3, 0.4, and 0.3, respectively. Figure 2.2-43 shows the three profiles used by the NRC staff, which extend to a depth of 15 m [48 ft] below the control point elevation.

#### 2.2.11.2.2 *Dynamic Material Properties and Site Kappa*

The NRC staff assumed both linear and nonlinear behavior for the soil and rock beneath the Pilgrim site. To model the nonlinear response within the upper 13 m [42 ft] of soil deposits, the NRC staff used the EPRI soil shear modulus reduction and material damping curves as one alternative and the Peninsular Range curves for the second equally weighted alternative. To model the nonlinear behavior of the uppermost weathered rock layer, the NRC staff used the EPRI rock shear modulus reduction and material damping curves. To model the linear behavior, the NRC staff used a constant damping ratio of 3 percent.

To determine the basecase  $\kappa_0$  for the Pilgrim site, the NRC staff first used the Campbell (2009) Model 1 relationship between  $V_S$  and the  $Q_{ef}$  to determine a  $Q_{ef}$  for each layer. Combining these  $Q_{ef}$  values with the thicknesses and  $V_S$  for each of the layers results in a total  $\kappa_0$  value of 7.1 msec, which includes the 6 msec assumed for the underlying reference rock. For the lower and upper basecase profiles, the NRC staff calculated  $\kappa_0$  values of 7.6 and 6.7 msec, respectively, using the same approach as for the basecase profile. In contrast, the licensee estimated  $\kappa_0$  by using the empirical relationship from the SPID (EPRI, 2012) between profile thickness and  $\kappa_0$ , which results in  $\kappa_0$  values of 7 msec for the best-estimate, lower, and upper basecase profiles, respectively.

Table 2.2-12 provides the layer depths, lithologies,  $V_S$ , unit weights, and dynamic properties for the NRC staff's three basecase profiles. In summary, the site response logic tree developed by the NRC staff for the Pilgrim site consists of six alternatives: three basecase profiles (each with a different  $\kappa_0$  value) and two alternative dynamic property branches.

#### 2.2.11.2.3 *Methodology and Results*

The NRC staff followed the methodology described in Section 2.1.4 to develop the final site amplification factors. Figure 2.2-44 shows the overall median site amplification factors and their variability for each of the seven spectral frequencies. As shown in Figure 2.2-44, the median site amplification factors range from about 1.0 to 2.5 before falling off with higher input spectral accelerations. The lower half of Figure 2.2-44 shows that the logarithmic standard deviations for the site amplification factors range from about 0.05 to 0.30.

#### 2.2.11.3 *Control Point Hazard*

The NRC staff implemented Approach 3 from the SPID to develop a weighted control point seismic hazard curve for each of the six unique combinations of the site response logic tree for the Pilgrim site. After combining these curves to develop the final mean control point hazard curves, the NRC staff determined the  $10^{-4}$  and  $10^{-5}$  UHRS in order to calculate the final GMRS. Figure 2.2-45 shows the final control point mean seismic hazard curves for each of the seven



spectral frequencies as well as the NRC staff's UHRS and GMRS, and the licensee's NTTFR2.1 GMRS (Dent, 2014). As shown in Figure 2.2-45, the NRC staff's GMRS (black curve) is similar to the licensee's GMRS (blue curve) over the entire frequency range.

Layer	Depth (ft)	Description	$V_s$ (ft/sec)			$V_s$ Sigma (ln)	BC Unit Weight (pcf)	Dynamic Properties	
			LR (0.3)	BC (0.4)	UR (0.3)			Alt. 1 (0.5)	Alt. 2 (0.5)
1	42	Soil: sand, gravel	1,393	1,800	2,326	0.25	130	EPRI Soil	Pen.
2	6	Rock: granodiorite	4,643	6,000	7,754	0.15	150	EPRI Rock	L 3.0%

LR = lower range; BC = basecase; UR = upper range; ln = natural log; pcf = pounds per cubic foot; L = linear; Alt. = alternative; Pen. = Peninsular.  
 For LR, BC, UR, and Alt.: Values in parentheses refer to weights for site response analysis logic tree branches.

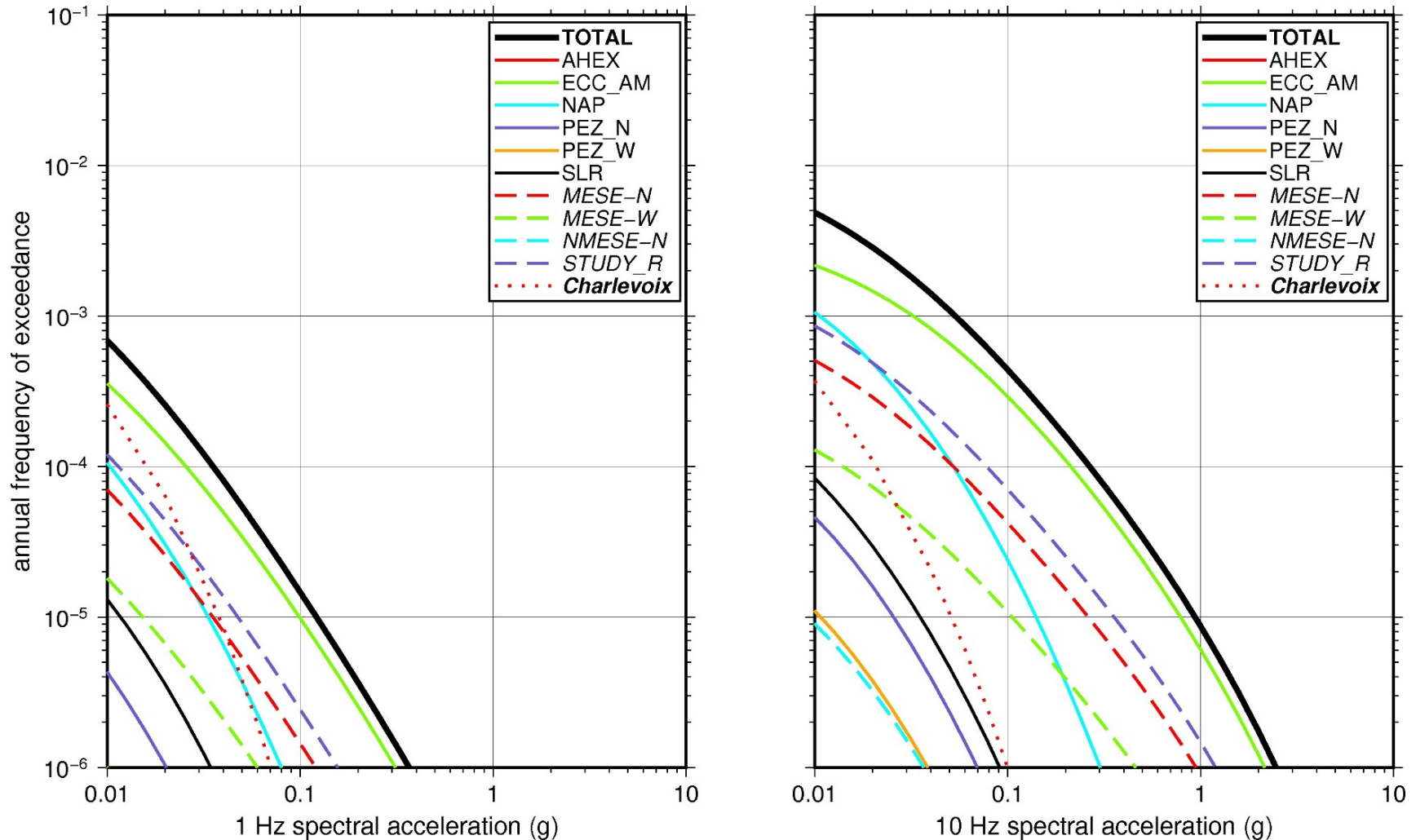


**Figure 2.2-42 Low-Frequency (1 Hz, Left) and High-Frequency (10 Hz, Right) Reference Rock Hazard Curves for Pilgrim. Total Hazard is Shown as a Bold Black Line; Individual Contributions to the Hazard For Each of the CEUS-SSC Sources are Shown as Colored Lines Defined in the Legend. See Table 2.1-1 for Source Name Definitions**

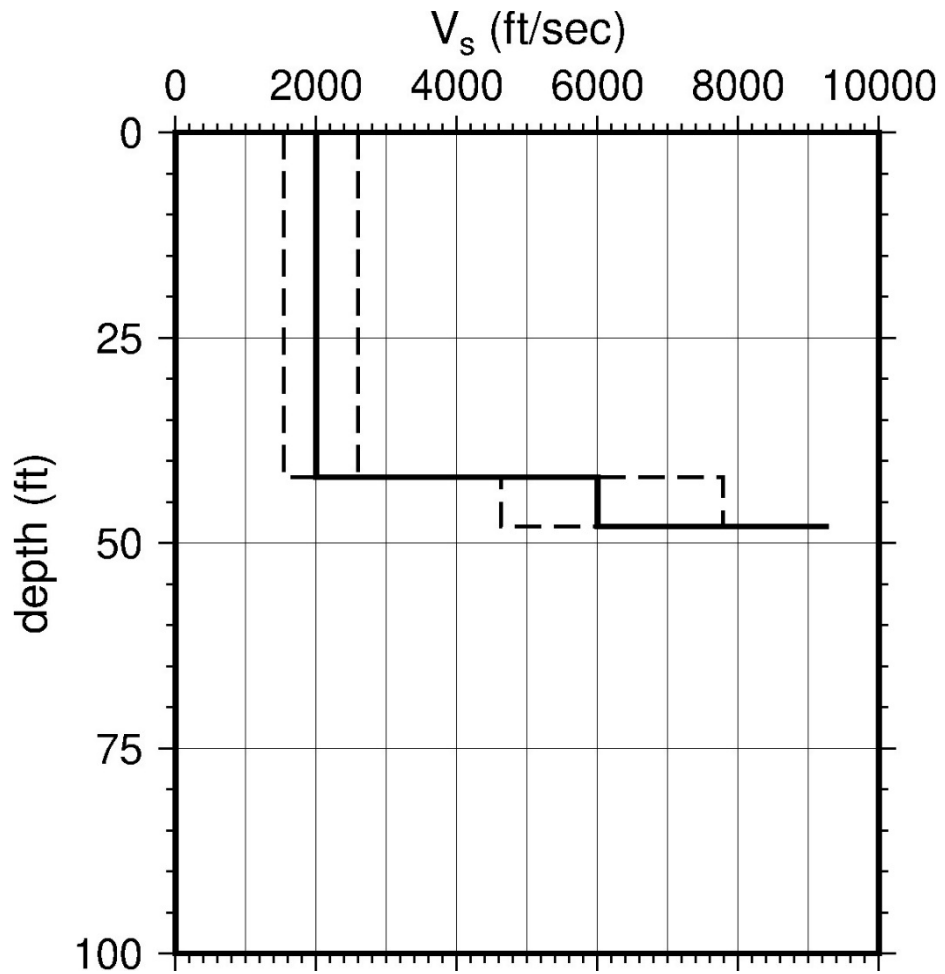


**Figure 2.2-43 Shear Wave Velocity ( $V_s$ ) Profiles for Pilgrim. Basecase (BC) Profile Shown as Solid Bold Line; Lower and Upper Range (LR and UR) Profiles Shown as Dashed Lines. Profiles Terminate at Reference Rock Velocity of 2,831 m/sec [9,285 ft/sec] per EPRI GMM (2013)**

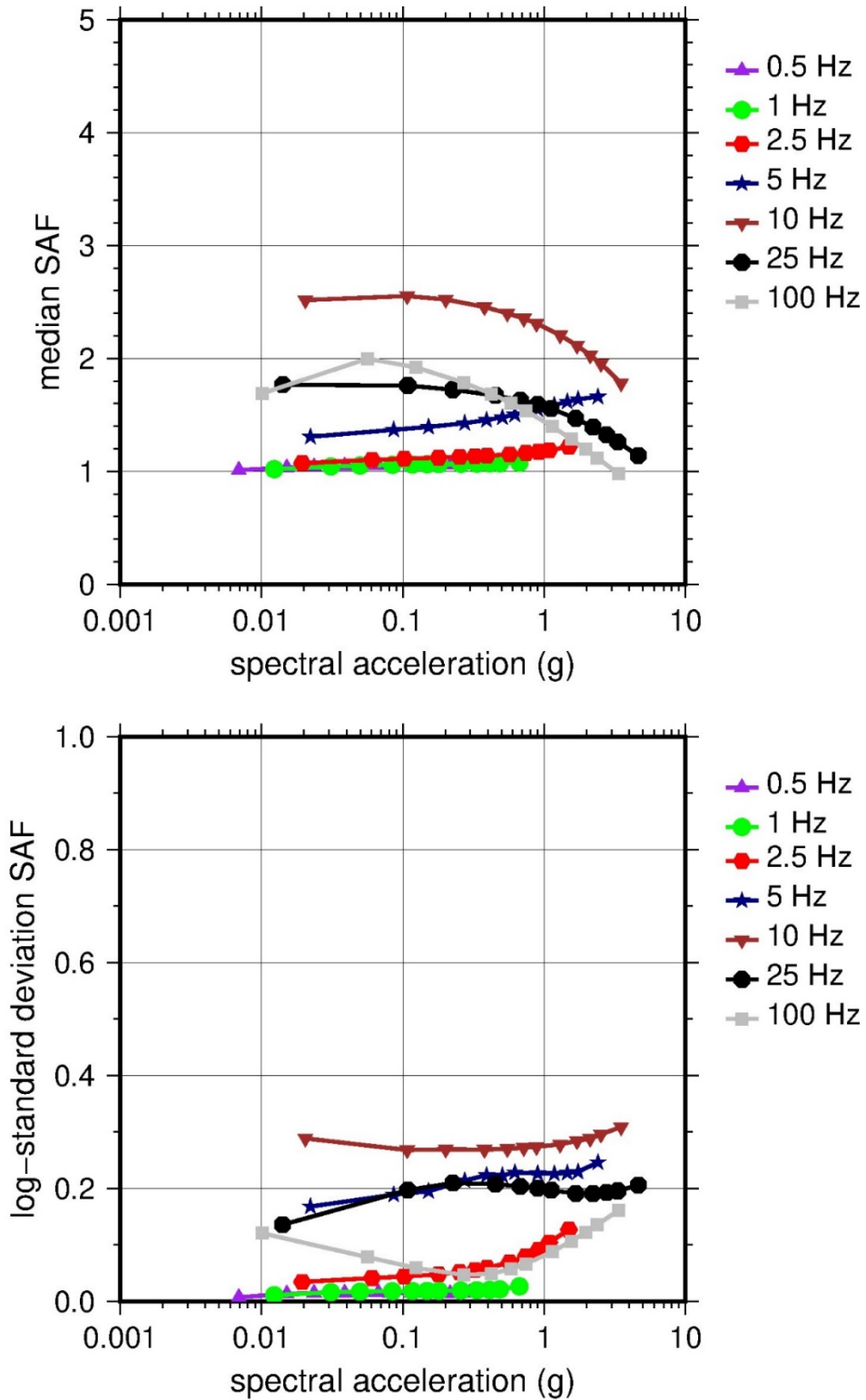


**Figure 2.2-44 Overall Weighted Median Site Amplification Factor (SAF) (Upper) and Log Standard Deviation of the SAF (Lower) as a Function of Input Acceleration for EPRI GMM (2013) Spectral Frequencies**

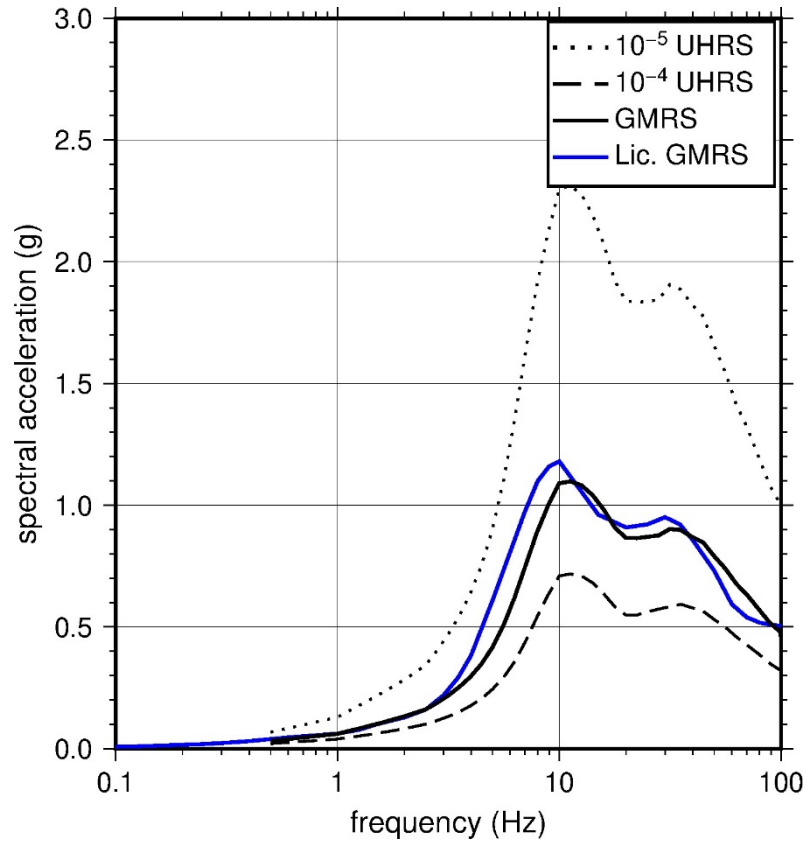
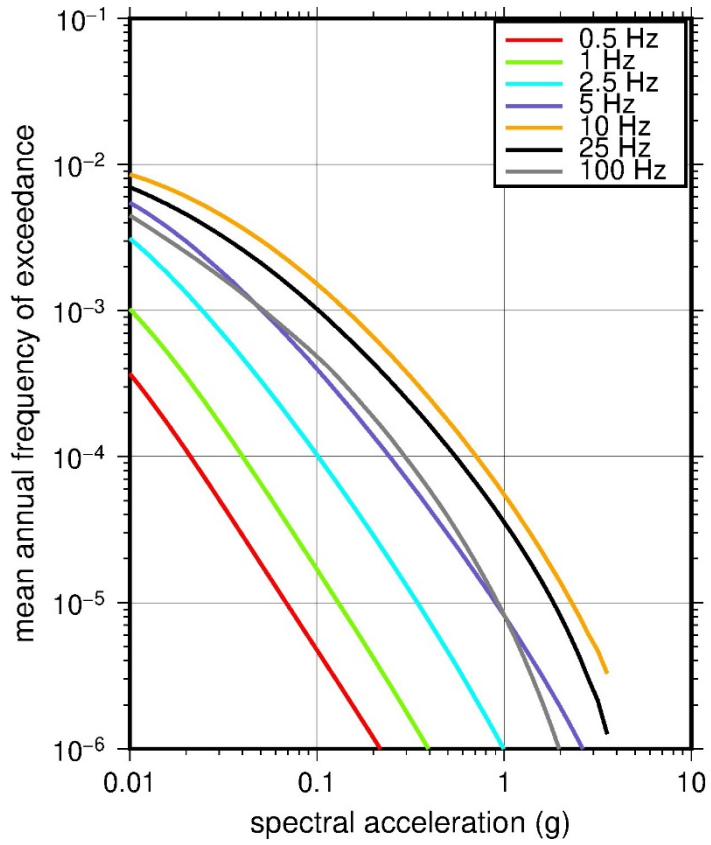


**Figure 2.2-45 Mean Control Point Hazard Curves (Left) for EPRI GMM (2013) Spectral Frequencies, and GMRS and UHS (Right) for Pilgrim**

## 2.2.12 Seabrook

The Seabrook Station site is located on the New Hampshire coast in the New England physiographic province and is founded on late Precambrian to upper Mesozoic age hard crystalline igneous rock (quartz diorite). The horizontal SSE response spectrum for Seabrook has an RG 1.60 spectral shape and is anchored at a PGA of 0.25g.

### 2.2.12.1 Reference Rock Hazard

For the reference rock PSHA, the NRC staff selected the 11 CEUS-SSC (NRC, 2012b) background seismic source zones that are located within 320 km [200 mi] of the Seabrook site. The NRC staff also selected the Charlevoix CEUS-SSC RLME source, which is located about 455 km [282 mi] from the Seabrook site. To develop the reference rock seismic hazard curves for the site, the NRC staff used the GMPEs in the updated EPRI GMM (2013). As shown in Figure 2.2-46, the ECC-AM seismotectonic zone, which is the highest weighted host zone for the Seabrook site, is the largest contributor to both the 1 Hz and 10 Hz reference rock total mean hazard curves at the  $10^{-4}$  AFE level.

### 2.2.12.2 Site Response Evaluation

To assess the need to perform a site response evaluation, the NRC staff used the geologic information in the NTTF R2.1 SHSR (Walsh, 2014) submitted by Next Era Energy (hereafter referred to as “the licensee” within this plant section). As described in the licensee’s SHSR, the Seabrook site consists of a thin veneer of soil overlying hard, crystalline metamorphic and igneous Paleozoic and Precambrian rock. The licensee stated that all of the Seabrook safety-related structures are supported on sound bedrock, on concrete fill extending to sound bedrock, or on controlled backfill extending to sound bedrock. The bedrock beneath the site is either a quartz diorite, which is a crystalline igneous rock, or a metaquartzite and granulite, which occurs as a large relict inclusion welded into the enclosing igneous rock along a broad contact zone. Based on its in situ geophysical investigations of the rock, the licensee stated that the  $V_S$  ranges from 2,400 m/sec [8,000 ft/sec] to 3,050 m/sec [10,000 ft/sec], which encompasses the reference rock  $V_S$  of 2,831 m/sec [9,285 ft/sec] specified by the EPRI GMM (2013). Therefore, the licensee did not perform a site response analysis for the Seabrook site. Instead, the licensee used the reference rock hazard curves from the PSHA as its control point hazard curves for determining the GMRS for the Seabrook site.

Section 2.5.4.3 of the UFSAR (NextEra Energy Seabrook, 2014) describes the licensee’s many subsurface explorations during the 1970s for its site investigations. The licensee performed multiple seismic refraction and reflection surveys as well as uphole and crosshole seismic velocity measurements. Based on its review of the results from these geophysical surveys, the NRC staff concurs with the licensee’s decision to directly use the reference rock hazard curves to develop its GMRS.

### 2.2.12.3 Control Point Hazard

After developing the mean reference rock hazard curves, the NRC staff determined the  $10^{-4}$  and  $10^{-5}$  UHRS in order to calculate the final GMRS. Figure 2.2-47 shows the final mean seismic hazard curves for each of the seven spectral frequencies as well as the NRC staff’s UHRS and GMRS, and the licensee’s NTTF R2.1 GMRS (Walsh, 2014). As shown in Figure 2.2-47, the NRC staff’s GMRS (black curve) is moderately lower than the licensee’s GMRS (blue curve) above 10 Hz. This difference is due to the licensee’s use of a 640 km [400 mi] radius for the

CEUS-SSC background zones as opposed to the 320 km [200 mi] radius used by the NRC staff to develop the reference rock hazard curves.

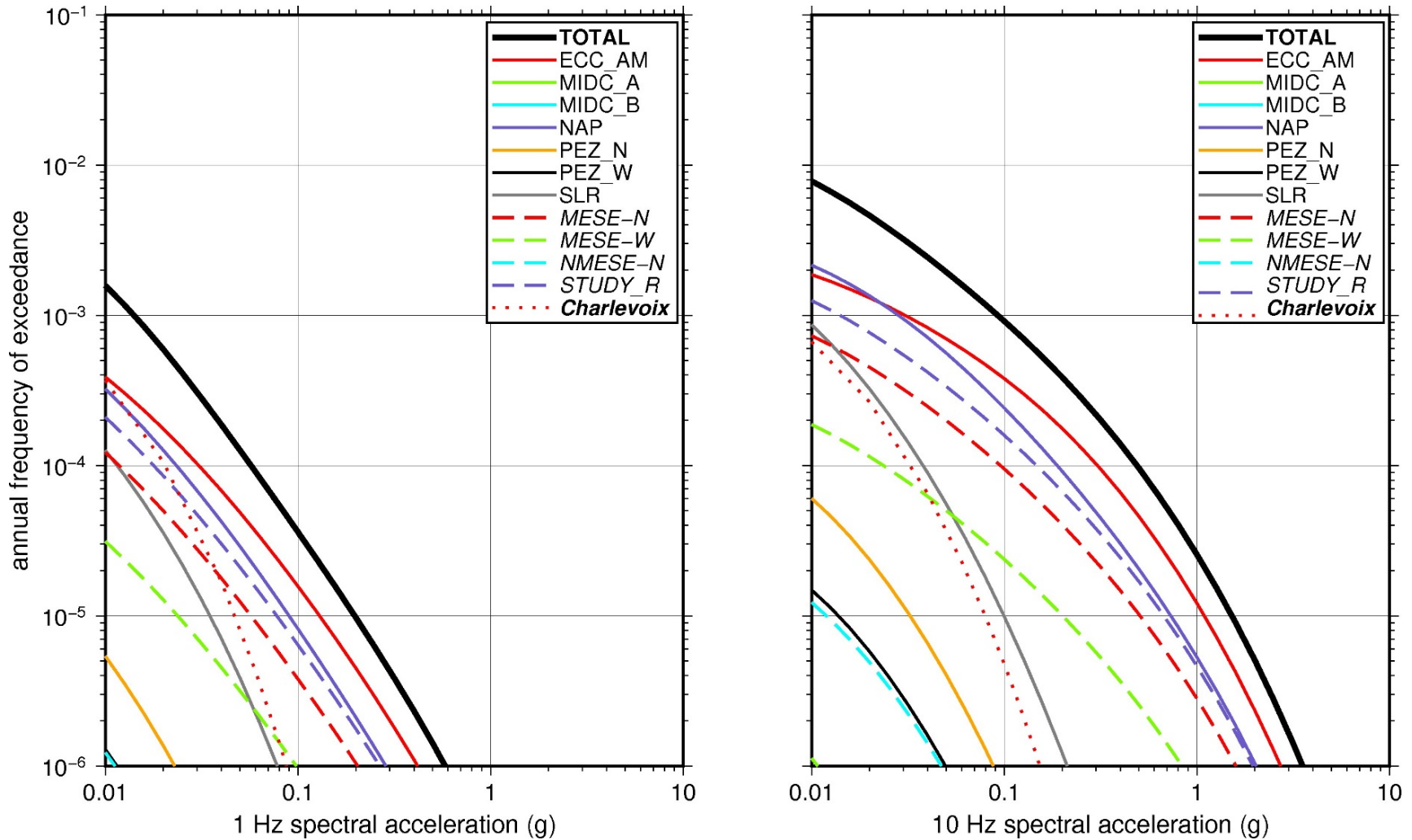


**Figure 2.2-46 Low-Frequency (1 Hz, Left) and High-Frequency (10 Hz, Right) Reference Rock Hazard Curves for Seabrook. Total Hazard is Shown as a Bold Black Line; Individual Contributions to the Hazard for Each of the CEUS-SSC Sources are Shown as Colored Lines Defined in the Legend. See Table 2.1-1 for Source Name Definitions**



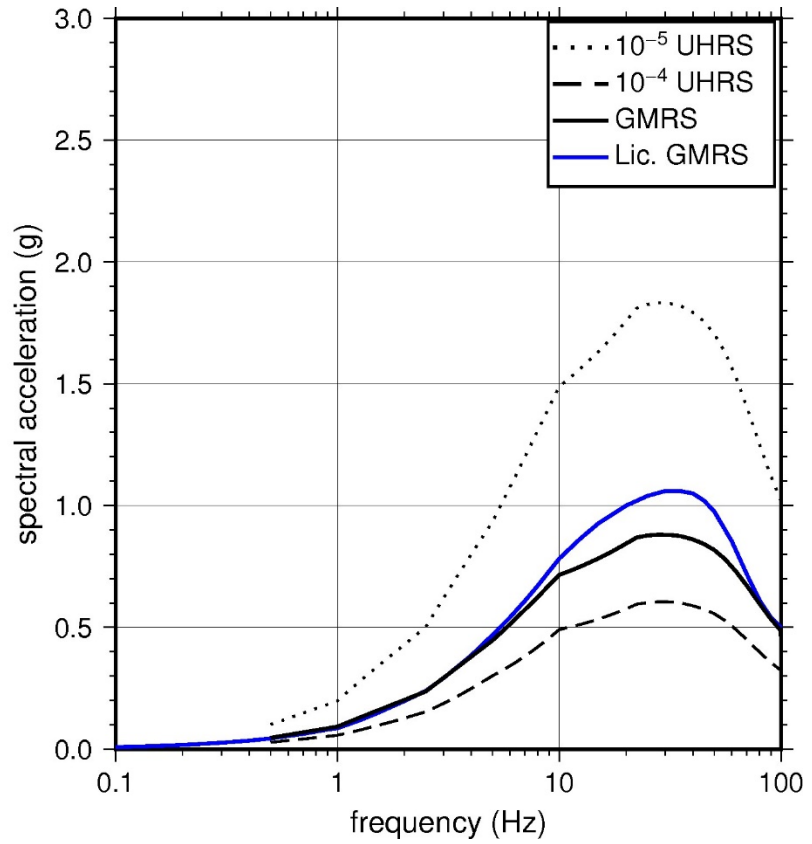
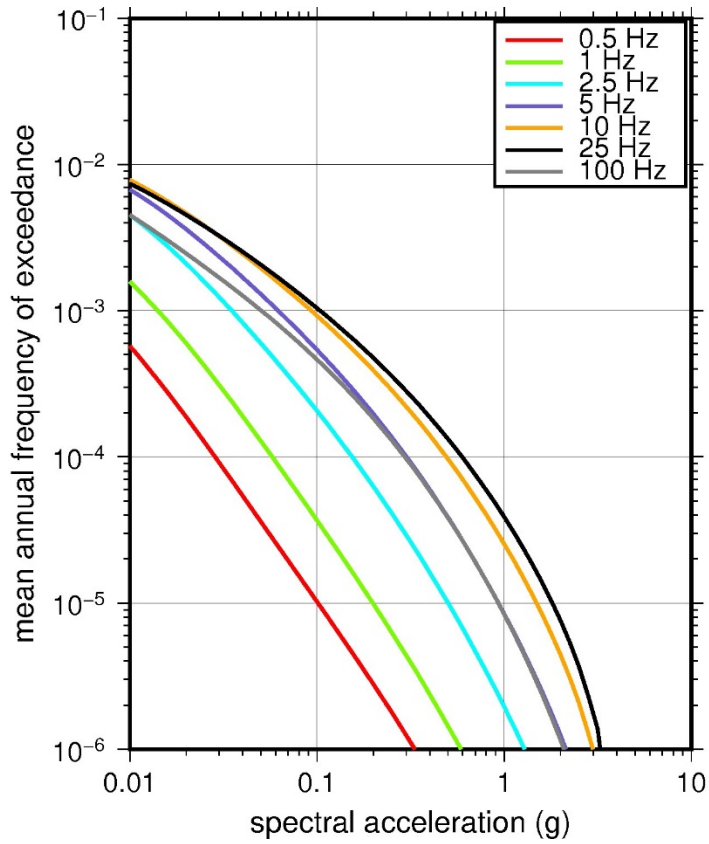


**Figure 2.2-47 Mean Control Point Hazard Curves (Left) for EPRI GMM (2013) Spectral Frequencies, and GMRS and UHRS (Right) for Seabrook**

### 2.2.13 Susquehanna

The Susquehanna Steam Electric Station site is located along the Susquehanna River in the Ridge and Valley physiographic province and is founded on competent Paleozoic sedimentary rock (shale, limestone, and sandstone), which is assumed to be about 10,058 m [33,000 ft] thick. The horizontal SSE response spectrum for Susquehanna has a Newmark spectral shape and is anchored at a PGA of 0.10g.

#### 2.2.13.1 Reference Rock Hazard

For the reference rock PSHA, the NRC staff selected the 10 CEUS-SSC (NRC, 2012b) background seismic source zones that are located within 320 km [200 mi] of the Susquehanna site. The NRC staff also selected the Charleston and Charlevoix CEUS-SSC RLME sources, which are located within 806 km [500 mi] of the site. To develop the reference rock seismic hazard curves for the site, the NRC staff used the GMPEs in the updated EPRI GMM (2013). As shown in Figure 2.2-48, the ECC-AM and Paleozoic Extended Crust (Narrow Geometry) (PEZ-N) seismotectonic zones are the largest contributors to both the 1 Hz and 10 Hz reference rock total mean hazard curves at the  $10^{-4}$  AFE level.

#### 2.2.13.2 Site Response Evaluation

##### 2.2.13.2.1 Site Profiles

To develop a basecase profile, the NRC staff used the geologic information in the NTTF R2.1 SHSR (Rausch, 2014) submitted by PPL Susquehanna, LLC (hereafter referred to as “the licensee” within this plant section). As described in the licensee’s SHSR, the Susquehanna site consists of a thin layer of glacial overburden soils overlying the Devonian age Mahantango Formation shale, which exceeds 460 m [1,500 ft] in thickness. In Table 2.3.1-1 of the SHSR, the licensee briefly described the subsurface materials in terms of the geologic units and layer thicknesses. For its site response evaluation, the NRC staff used the top of the sound bedrock {elevation 195 m [640 ft] MSL} as the control point elevation for the Susquehanna site.

For the siting investigation for the Susquehanna plant, the licensee performed seismic refraction, crosshole, downhole, and uphole surveys to determine the dynamic properties of the bedrock beneath the site. The licensee’s geophysical investigations focused on the upper site soil and rock, extending to a depth of about 40 m [130 ft] below grade. In addition to these site investigations, the licensee also used the numerous geophysical measurements from the now-withdrawn Bell Bend COL, which is located about 1.3 km [0.8 mi] from the Susquehanna site. The geophysical investigations for the Bell Bend site include seismic refraction and P-S suspension logging and downhole surveys in multiple borings across the site. These investigations extend to a depth of about 130 m [420 ft] below the surface. Table 2.3.2-2 of the SHSR gives the measured  $V_S$  from the combined Susquehanna and Bell Bend siting investigations.

For its SHSR, the licensee developed a basecase profile that extends to a depth of 120 m [390 ft] below the control point elevation. The licensee subdivided the Mahantango Formation shale into five sublayers with the  $V_S$  gradually increasing from 2,300 m/sec [7,500 ft/sec] to 2,800 m/sec [9,050 ft/sec] at a depth of 120 m [390 ft].

To develop its basecase  $V_S$  profile, the NRC staff used the best-estimate  $V_S$  profile from the Bell Bend COL, as shown in Figure 2.5-53 of the FSAR (UniStar, 2013). This best-estimate profile

shows that the  $V_S$  increases from about 2,100 m/sec [7,000 ft/sec] over the upper 40 m [130 ft] of the profile to 2,600 m/sec [8,500 ft/sec] for the lower 20 m [60 ft]. Although this range in  $V_S$  is similar to the range used by the licensee for its SHSR profile, the depth at which the  $V_S$  reaches the reference rock value  $V_S$  of 2,831 m/sec [9,285 ft/sec] is much shallower: 60 m [190 ft] versus 120 m [390 ft].

To capture the uncertainty in its basecase profile, the NRC staff developed lower and upper range (10<sup>th</sup> and 90<sup>th</sup> percentile) profiles by multiplying the basecase  $V_S$  values by scale factors of 0.83 and 1.21, respectively, which corresponds to an epistemic logarithmic standard deviation of 0.15. The weights for the lower, best-estimate, and upper basecase profiles are 0.3, 0.4, and 0.3, respectively. As shown in Figure 2.2-49, the upper profile terminates at a depth of 15 m [130 ft], and the lower and best-estimate basecase profiles terminate at a depth of 60 m [190 ft] below the control point elevation, at which point the  $V_S$  is assumed to reach the reference rock value of 2,831 m/sec [9,285 ft/sec].

#### 2.2.13.2.2 *Dynamic Material Properties and Site Kappa*

The NRC staff assumed both linear and nonlinear dynamic behavior for the rock beneath the Susquehanna site. To model the nonlinear behavior of the uppermost rock strata, the NRC staff used the EPRI rock shear modulus reduction and material damping curves. To model the linear behavior, the NRC staff used a constant damping ratio of 3 percent. The staff assumed these two alternative dynamic responses for the upper 20 m [70 ft] of the profile; due to the higher  $V_S$  of this rock layer, the NRC staff assigned weights of 0.7 and 0.3 to the linear and nonlinear alternatives, respectively. For the remaining 35 m [120 ft] of its profile, the NRC staff assumed a linear response with a material damping ratio value of 0.1 percent to maintain consistency with the  $\kappa_0$  value for the Susquehanna site.

To determine the basecase  $\kappa_0$  for the Susquehanna site, the NRC staff first used the Campbell (2009) Model 1 relationship between  $V_S$  and  $Q_{ef}$  to determine a  $Q_{ef}$  for each layer. Combining these  $Q_{ef}$  values with the thicknesses and  $V_S$  for each of the layers results in a total  $\kappa_0$  value of about 6.4 msec, which includes the 6 msec assumed for the underlying reference rock. For the lower and upper basecase profiles, the NRC staff calculated  $\kappa_0$  values of 6.5 and 6.2 msec, respectively, using the same approach as for the best-estimate basecase profile. In contrast, the licensee estimated  $\kappa_0$  by combining the lowest low-strain damping values from the EPRI rock material damping curves over the upper 152 m [500 ft] of rock with an assumed damping value of 1.25 percent for the remaining underlying rock layers to estimate best-estimate, lower, and upper basecase  $\kappa_0$  values of 9, 12, and 6 msec, respectively.

Table 2.2-13 provides the layer depths, lithologies,  $V_S$ , unit weights, and dynamic properties for the NRC staff's three profiles. In summary, the site response logic tree developed by the NRC staff for the Susquehanna site consists of six alternatives: three basecase profiles (each with a different  $\kappa_0$  value) and two alternative dynamic property branches.

#### 2.2.13.2.3 *Methodology and Results*

The NRC staff followed the methodology described in Section 2.1.4 to develop the final site amplification factors. Figure 2.2-50 shows the overall median site amplification factors and their variability for each of the seven spectral frequencies. As shown in Figure 2.2-50, the median site amplification factors range from about 1.0 to 1.5 before falling off with higher input spectral accelerations. The lower half of Figure 2.2-50 shows that the logarithmic standard deviations for the site amplification factors range from about 0.05 to 0.10.

### 2.2.13.3 Control Point Hazard

The NRC staff implemented Approach 3 from the SPID to develop a weighted control point seismic hazard curve for each of the six unique combinations of the site response logic tree for the Susquehanna site. After combining these curves to develop the final mean control point hazard curves, the NRC staff determined the  $10^{-4}$  and  $10^{-5}$  UHRS in order to calculate the final GMRS. Figure 2.2-51 shows the final control point mean seismic hazard curves for each of the seven spectral frequencies as well as the NRC staff's UHRS and GMRS, and the licensee's NTTF R2.1 GMRS (Rausch, 2014). As shown in Figure 2.2-51, the NRC staff's GMRS (black curve) is slightly higher than the licensee's GMRS (blue curve) above 10 Hz due to the licensee's thicker basecase profile and slightly higher  $\kappa_0$  values. For comparison, Figure 2.2-51 also shows the NRC staff's reference rock GMRS (brown dotted curve).

**Table 2.2-13 Layer Depths, Shear Wave Velocities ( $V_s$ ), Unit Weights, and Dynamic Properties for Susquehanna**

Layer	Depth (ft)	Description	$V_s$ (ft/sec)			$V_s$ Sigma (ln)	BC Unit Weight (pcf)	Dynamic Properties	
			LR (0.3)	BC (0.4)	UR (0.3)			Alt. 1 (0.3)	Alt. 2 (0.7)
1	10	Rock: shale	6,064	7,350	8,909	0.25	160	EPRI Rock	L 3.0%
2	30	Rock: shale	5,610	6,800	8,242	0.15	150	EPRI Rock	L 3.0%
3	70	Rock: shale	6,023	7,300	8,848	0.15	150	EPRI Rock	L 3.0%
4	130	Rock: shale	6,188	7,500	9,090	0.15	160	L 0.1%	L 0.1%
5	190	Rock: shale	7,013	8,500	9,285	0.15	160	L 0.1%	L 0.1%

LR = lower range; BC = basecase; UR = upper range; ln = natural log; pcf = pounds per cubic foot; L = linear; Alt. = alternative.  
 For LR, BC, UR, and Alt.: Values in parentheses refer to weights for site response analysis logic tree branches.

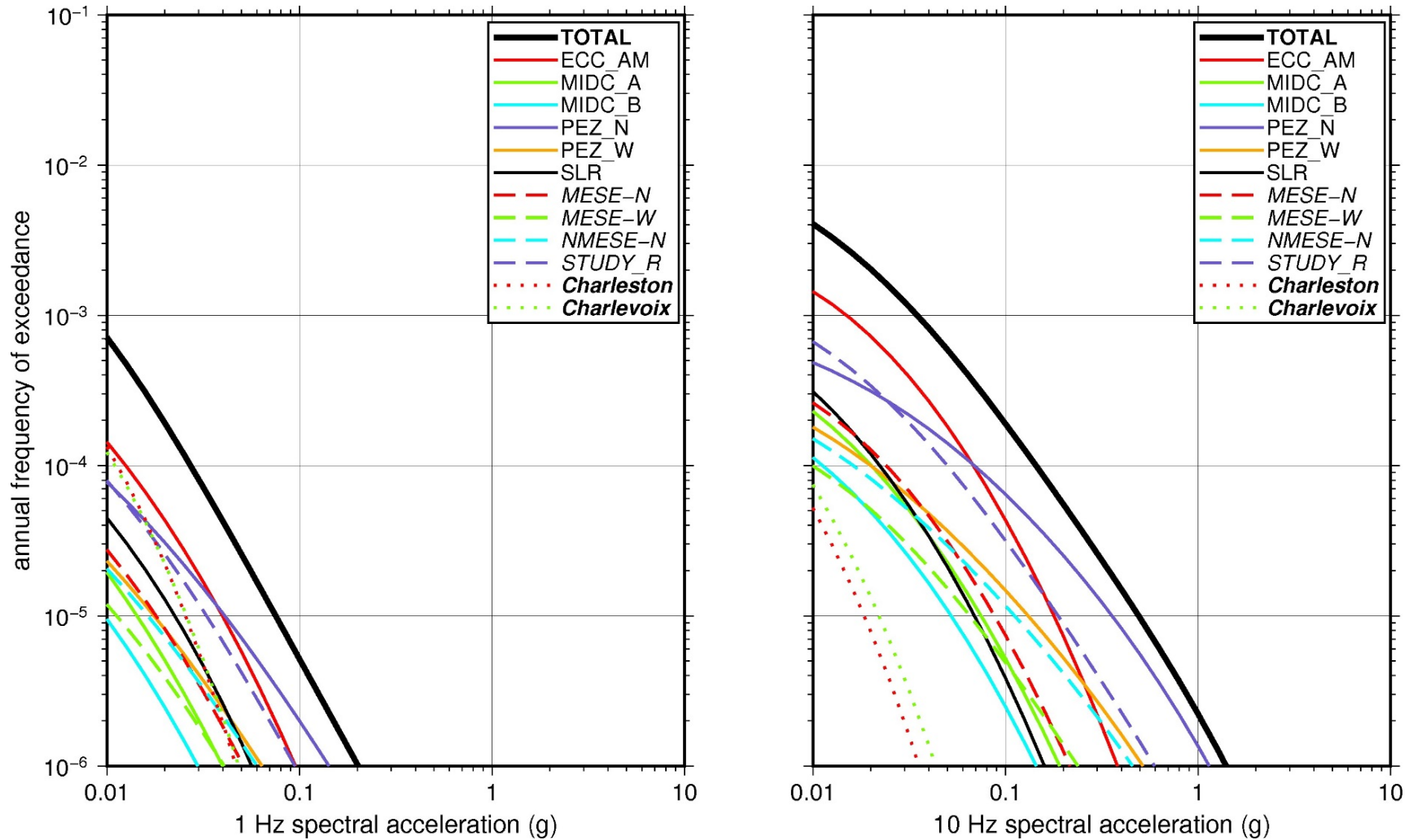


**Figure 2.2-48 Low-Frequency (1 Hz, Left) and High-Frequency (10 Hz, Right) Reference Rock Hazard Curves for Susquehanna. Total Hazard is Shown as a Bold Black Line; Individual Contributions to the Hazard for Each of the CEUS-SSC Sources are Shown as Colored Lines Defined in the Legend. See Table 2.1-1 for Source Name Definitions**

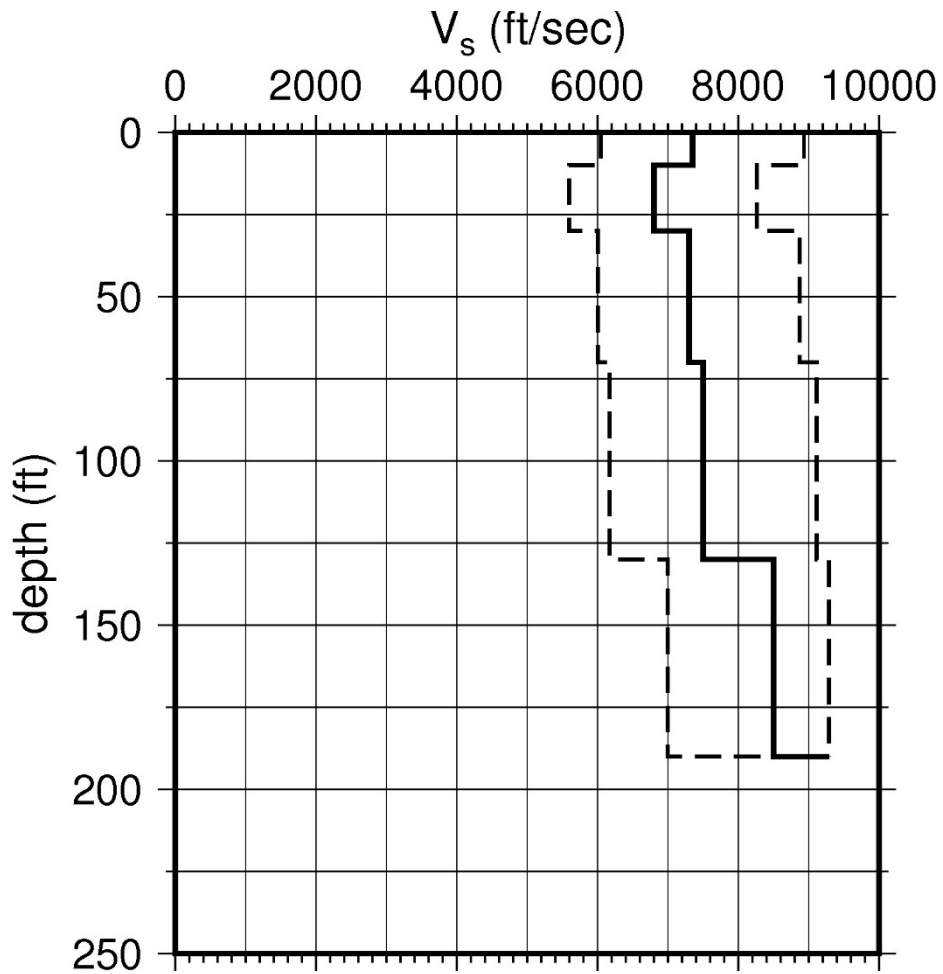


**Figure 2.2-49 Shear Wave Velocity ( $V_s$ ) Profiles for Susquehanna. Basecase (BC) Profile Shown as Solid Bold Line; Lower and Upper Range (LR and UR) Profiles Shown as Dashed Lines. Profiles Terminate at Reference Rock Velocity of 2,831 m/sec [9,285 ft/sec] per EPRI GMM (2013)**

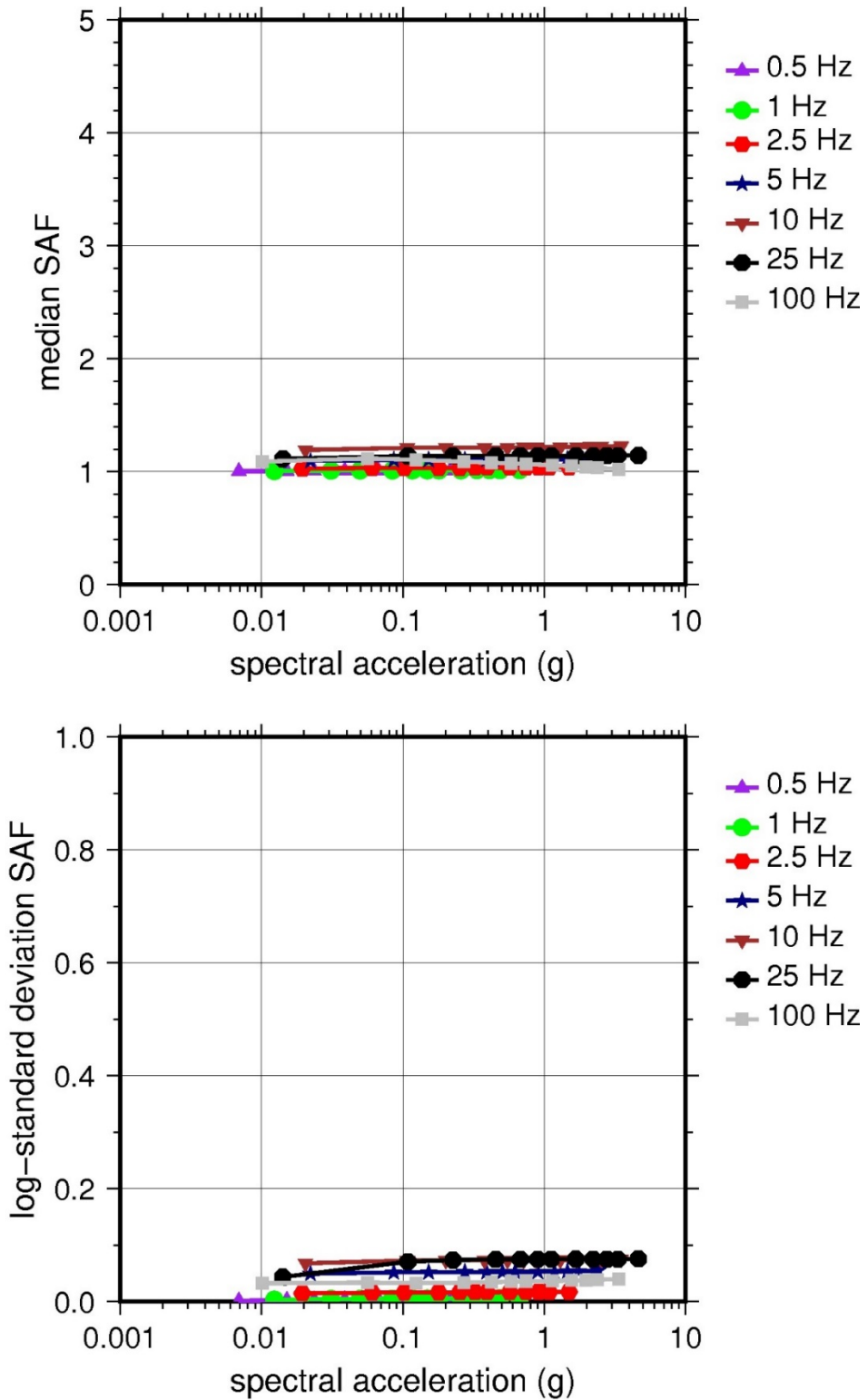


**Figure 2.2-50 Overall Weighted Median Site Amplification Factor (SAF) (Upper) and Log Standard Deviation of the SAF (Lower) as a Function of Input Acceleration for EPRI GMM (2013) Spectral Frequencies**

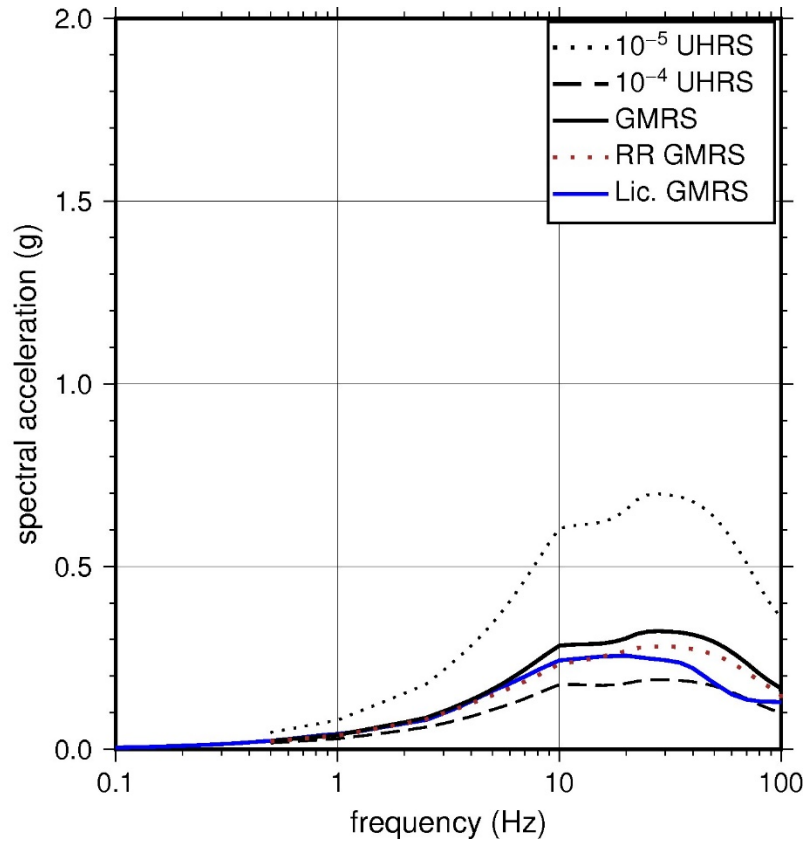
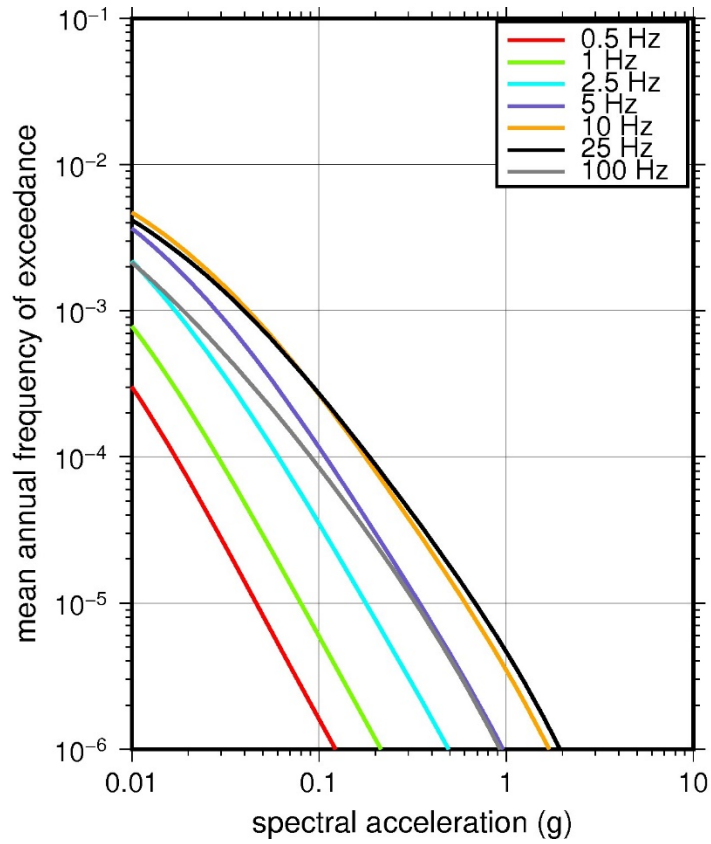


**Figure 2.2-51 Mean Control Point Hazard Curves (Left) for EPRI GMM (2013) Spectral Frequencies, and GMRS and UHRs (Right) for Susquehanna**



## 2.2.14 Three Mile Island

The Three Mile Island Nuclear Station site is located on an island in the Susquehanna River within the Piedmont physiographic province and is founded on Paleozoic sedimentary rock (sandstone and shale), which is assumed to be about 4,878 m [16,000 ft] thick. The horizontal SSE response spectrum for Three Mile Island has a rounded spectral shape that was developed from the Golden Gate Park recording of the 1957 earthquake in San Francisco, CA. The Three Mile Island SSE is anchored at a PGA of 0.10g.

### 2.2.14.1 Reference Rock Hazard

For the reference rock PSHA, the NRC staff selected the 13 CEUS-SSC (NRC, 2012b) background seismic source zones that are located within 320 km [200 mi] of the site. The NRC staff also selected the Charleston CEUS-SSC RLME source, which is located about 691 km [428 mi] from the Three Mile Island site. To develop the reference rock seismic hazard curves for the site, the NRC staff used the GMPEs in the updated EPRI GMM (2013). As shown in Figure 2.2-52, the ECC-AM seismotectonic zone, which is the highest weighted host zone for the site, is the largest contributor to both the 1 Hz and 10 Hz reference rock total mean hazard curves at the  $10^{-4}$  AFE level.

### 2.2.14.2 Site Response Evaluation

#### 2.2.14.2.1 Site Profiles

To develop a basecase profile, the NRC staff used the geologic information in the NTTF R2.1 SHSR (Barstow, 2014d) submitted by Exelon Generation Company, LLC (hereafter referred to as “the licensee” within this plant section). As described in the licensee’s SHSR, the Three Mile Island site consists of a thin layer (2 m [6 ft]) of silty sand, gravel, and clayey silt overlying medium-hard to hard sandstone, conglomerates, and shales. The primary safety-related Three Mile Island structures are founded on this sound rock, which is from the Gettysburg Formation and is of Triassic age. In Table 2.3.1-1 of the SHSR, the licensee briefly describes the subsurface materials in terms of the geologic units and layer thicknesses. For its site response evaluation, the NRC staff used the top of the Gettysburg Formation {elevation 85 m [280 ft] MSL} as the control point elevation for the Three Mile Island site.

The field investigations for Three Mile Island, conducted in the 1960s, consisted of a number of borings through the soil and upper portion of rock beneath the site. Because the licensee did not obtain in situ  $V_S$  measurements within the Gettysburg Formation at the Three Mile Island site, it used the measured  $V_P$  from its seismic refraction profiles and an assumed Poisson’s ratio to estimate the  $V_S$  for the uppermost rock stratum. Table 2.3.2-2 of the SHSR gives the estimated  $V_S$  determined from the  $V_P$  listed in Table 2.3.1-1 of the SHSR.

For its SHSR, the licensee developed a basecase profile that extends to a depth of 2,000 m [6,500 ft] below the control point elevation. The uppermost layers of the profile consist of sandstones, conglomerates, and shales, for which the licensee estimated a  $V_S$  of 1,500 m/sec [5,000 ft/sec], based on  $V_P$  ranging from 2,400 m/sec [8,000 ft/sec] to 3,050 m/sec [10,000 ft/sec] and a Poisson’s ratio 0.35. For the remainder of its profile, the licensee assumed a velocity gradient of 0.5 ft/sec/ft [m/sec/m], which results in a  $V_S$  of 2,500 m/sec [8,235 ft/sec] at a depth of 2,000 m [6,500 ft].

Rather than use the velocity gradient of 0.5 m/sec/m [0.5 ft/sec/ft], which Appendix B to the SPID recommends for sedimentary rock, the NRC staff used a much steeper velocity gradient appropriate for sedimentary rock that has been heavily metamorphosed and intruded by diabase sheets. The NRC staff's decision to use a much steeper velocity gradient is based on its review of the Hawk (2004) report that discusses exploratory borings to investigate the engineering properties of the bedrock for construction of the new Susquehanna River Bridge, located just upstream from the Three Mile Island site. As described in the report, during the early Jurassic, the Triassic strata (i.e., Gettysburg Formation) were intruded by extensive diabase sheets, which baked and thermally altered the host rock. In particular, the report points out that a large diabase sheet borders the western shoreline of the Susquehanna River downstream of the existing Pennsylvania Turnpike Bridge in the general vicinity of the Three Mile Island site. Based on the likelihood that the Paleozoic sedimentary rock beneath the Three Mile Island site has been heavily metamorphosed, the NRC staff developed a 152 m [500 ft] basecase profile with three layers that increase in  $V_S$  from 1,500 m/sec [5,000 ft/sec] to 2,100 m/sec [7,000 ft/sec] at its base.

To capture the uncertainty in its basecase profile, the NRC staff developed lower and upper range (10<sup>th</sup> and 90<sup>th</sup> percentile) profiles by multiplying the basecase  $V_S$  values by scale factors of 0.78 and 1.29, respectively, which corresponds to an epistemic logarithmic standard deviation of 0.20. The weights for the lower, best-estimate, and upper basecase profiles are 0.3, 0.4, and 0.3, respectively. Figure 2.2-53 shows the three profiles used by the NRC staff, which extend to a depth of 152 m [500 ft] below the control point elevation.

#### 2.2.14.2.2 *Dynamic Material Properties and Site Kappa*

The NRC staff assumed both linear and nonlinear dynamic behavior for the rock beneath the Three Mile Island site. To model the nonlinear behavior of the uppermost rock strata, the NRC staff used the EPRI rock shear modulus reduction and material damping curves. To model the linear behavior, the NRC staff used a constant damping ratio of 3 percent. The NRC staff assumed these two alternative dynamic responses for the upper 30 m [100 ft] of the profile and weighted each alternative equally. For the remaining 120 m [400 ft] of its profile, the NRC staff assumed a linear response with a material damping ratio value of 0.1 percent to maintain consistency with the  $\kappa_0$  value for the Three Mile Island site.

To determine the basecase  $\kappa_0$  for the Three Mile Island site, the NRC staff first used the Campbell (2009) Model 1 relationship between  $V_S$  and  $Q_{ef}$  to determine a  $Q_{ef}$  for each layer. Combining these  $Q_{ef}$  values with the thicknesses and  $V_S$  for each of the layers results in a total  $\kappa_0$  value of about 7.4 msec, which includes the 6 msec assumed for the underlying reference rock. For the lower and upper basecase profiles, the NRC staff calculated  $\kappa_0$  values of 8.3 and 6.9 msec, respectively, using the same approach as for the best-estimate basecase profile. In contrast, the licensee estimated  $\kappa_0$  by using the empirical relationship from the SPID (EPRI, 2012) between the average  $V_S$  over the upper 30 m [100 ft] of the profile and  $\kappa_0$ , which results in  $\kappa_0$  values of 15, 24, and 9 msec for the best-estimate, lower, and upper basecase profiles, respectively.

Table 2.2-14 provides the layer depths, lithologies,  $V_S$ , unit weights, and dynamic properties for the NRC staff's three profiles. In summary, the site response logic tree developed by the NRC staff for the Three Mile Island site consists of six alternatives; three basecase profiles (each with a different  $\kappa_0$  value) and two alternative dynamic property branches.

### 2.2.14.2.3 Methodology and Results

The NRC staff followed the methodology described in Section 2.1.4 to develop the final site amplification factors. Figure 2.2-54 shows the overall median site amplification factors and their variability for each of the seven spectral frequencies. As shown in Figure 2.2-54, the median site amplification factors range from about 1.0 to 1.5 before falling off with higher input spectral accelerations. The lower half of Figure 2.2-54 shows that the logarithmic standard deviations for the site amplification factors range from about 0.05 to 0.18.

### 2.2.14.3 Control Point Hazard

The NRC staff implemented Approach 3 from the SPID to develop a weighted control point seismic hazard curve for each of the six unique combinations of the site response logic tree for the Three Mile Island site. After combining these curves to develop the final mean control point hazard curves, the NRC staff determined the  $10^{-4}$  and  $10^{-5}$  UHRS in order to calculate the final GMRS. Figure 2.2-55 shows the final control point mean seismic hazard curves for each of the seven spectral frequencies as well as the NRC staff's UHRS and GMRS, and the licensee's NTTF R2.1 GMRS (Barstow, 2014d). As shown in Figure 2.2-55, the NRC staff's GMRS (black curve) is moderately higher than the licensee's GMRS (blue curve) due to the differences between the licensee's and staff's basecase profiles and  $\kappa_0$  values. For comparison, Figure 2.2-55 also shows the NRC staff's reference rock GMRS (brown dotted curve).

**Table 2.2-14 Layer Depths, Shear Wave Velocities ( $V_s$ ), Unit Weights, and Dynamic Properties for Three Mile Island**

Layer	Depth (ft)	Description	$V_s$ (ft/sec)			$V_s$ Sigma (ln)	BC Unit Weight (pcf)	Dynamic Properties	
			LR (0.3)	BC (0.4)	UR (0.3)			Alt. 1 (0.5)	Alt. 2 (0.5)
1	100	Rock: sandstone	3,869	5,000	6,461	0.25	140	EPRI Rock	L 3.0%
2	300	Rock: sandstone	4,643	6,000	7,754	0.15	150	L 0.1%	L 0.1%
3	500	Rock: sandstone	5,417	7,000	9,046	0.15	150	L 0.1%	L 0.1%

LR = lower range; BC = basecase; UR = upper range; ln = natural log; pcf = pounds per cubic foot; L = linear; Alt. = alternative.  
For LR, BC, UR, and Alt.: Values in parentheses refer to weights for site response analysis logic tree branches.

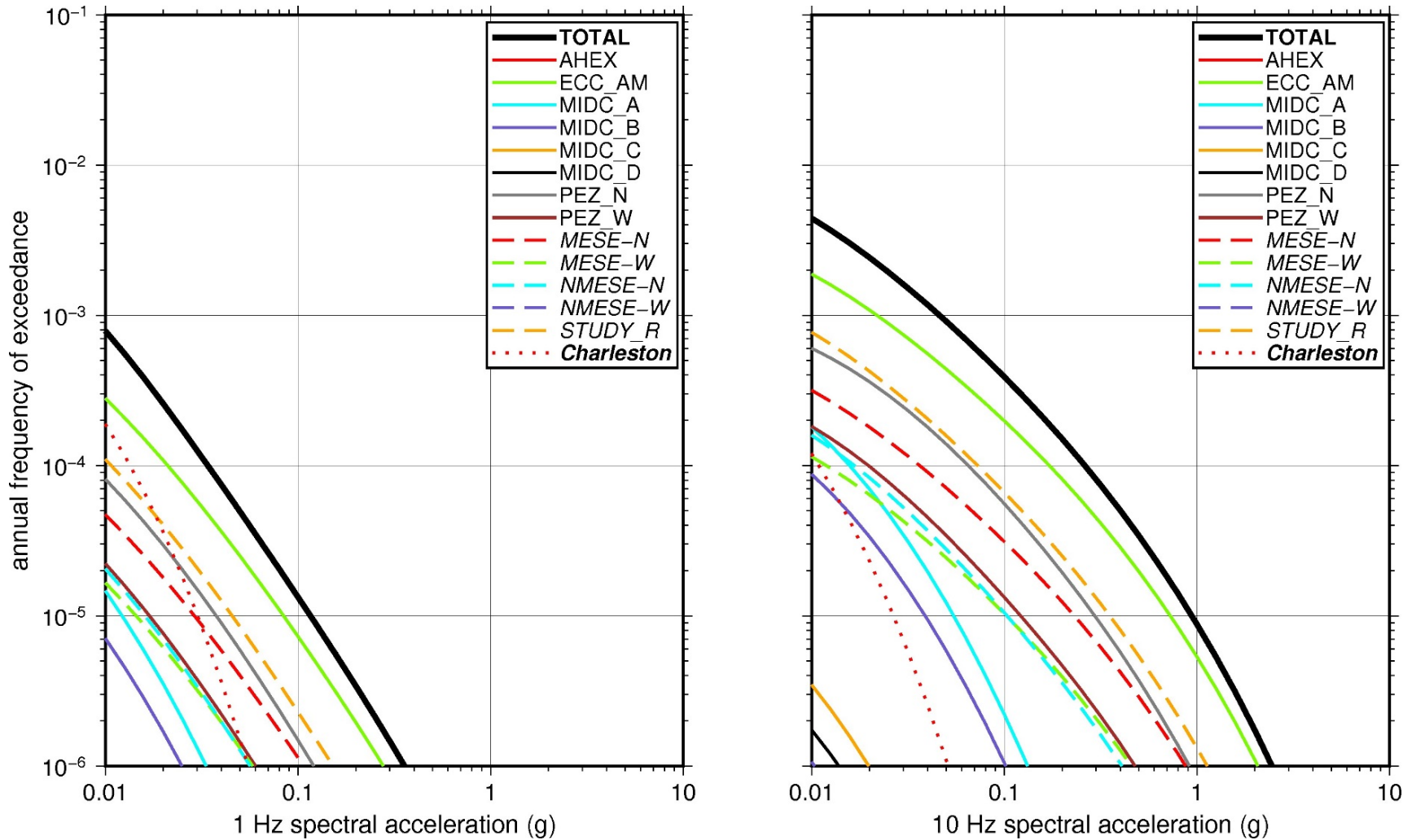


**Figure 2.2-52 Low-Frequency (1 Hz, Left) and High-Frequency (10 Hz, Right) Reference Rock Hazard Curves for Three Mile Island. Total Hazard is Shown as a Bold Black Line; Individual Contributions to the Hazard for Each of the CEUS-SSC Sources are Shown as Colored Lines Defined in the Legend. See Table 2.1-1 for Source Name Definitions**

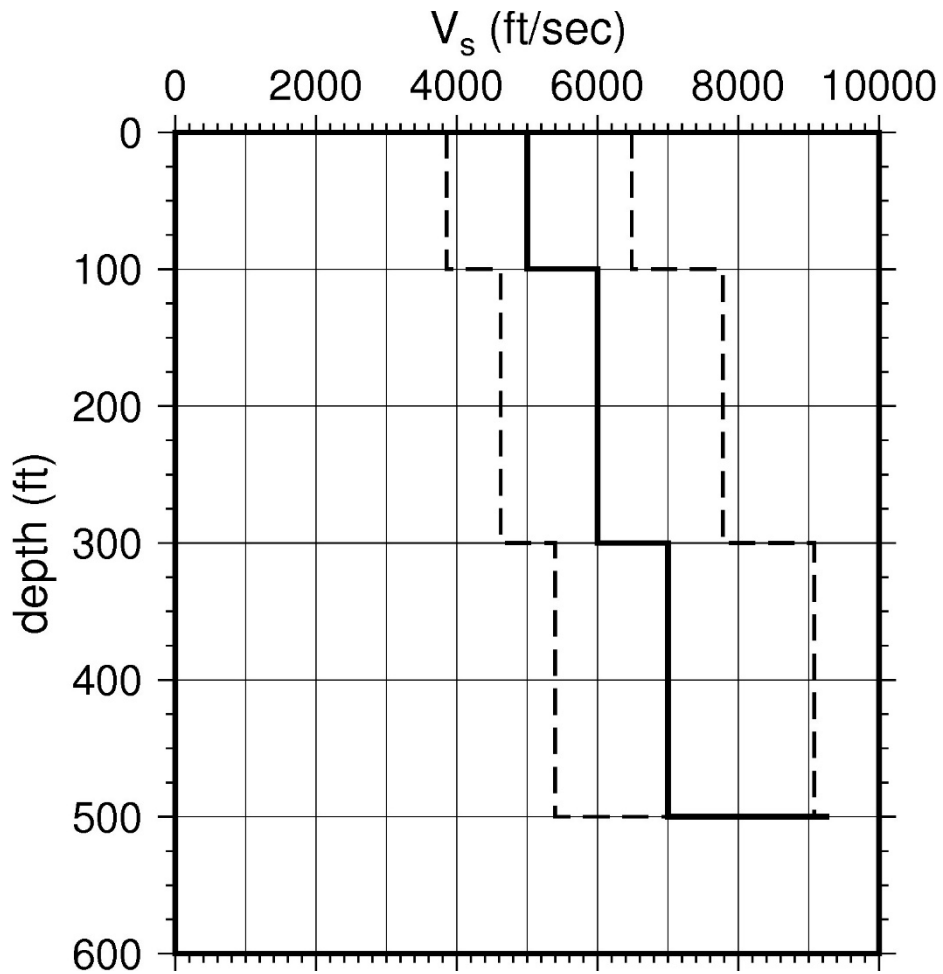


**Figure 2.2-53 Shear Wave Velocity ( $V_s$ ) Profiles for Three Mile Island. Basecase (BC) Profile Shown as Solid Bold Line; Lower and Upper Range (LR and UR) Profiles Shown as Dashed Lines. Profiles Terminate at Reference Rock Velocity of 2,831 m/sec [9,285 ft/sec] per EPRI GMM (2013)**

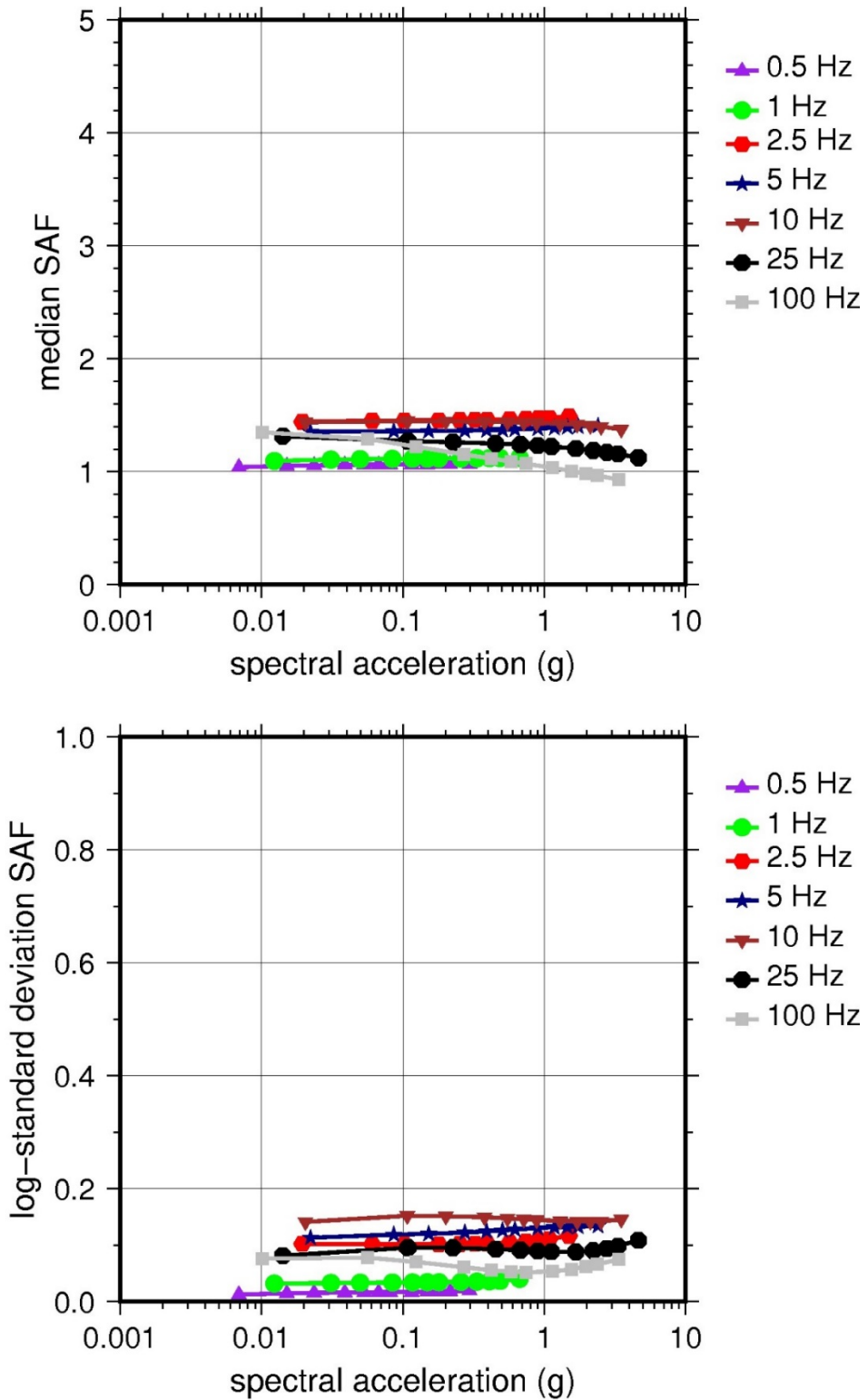


**Figure 2.2-54 Overall Weighted Median Site Amplification Factor (SAF) (Upper) and Log Standard Deviation of the SAF (Lower) as a Function of Input Acceleration for EPRI GMM (2013) Spectral Frequencies**

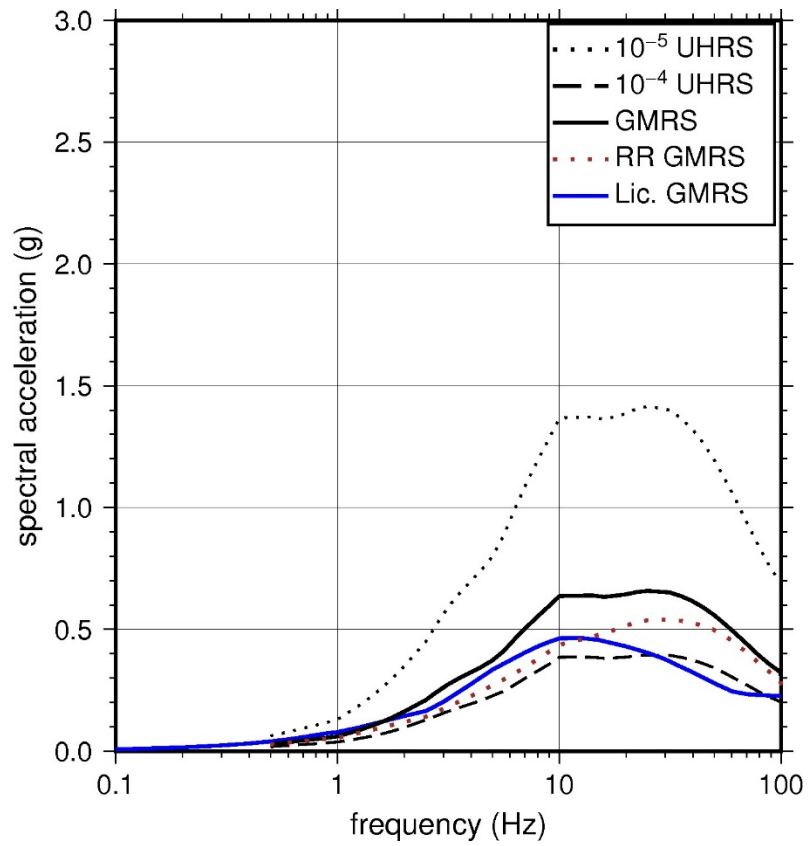
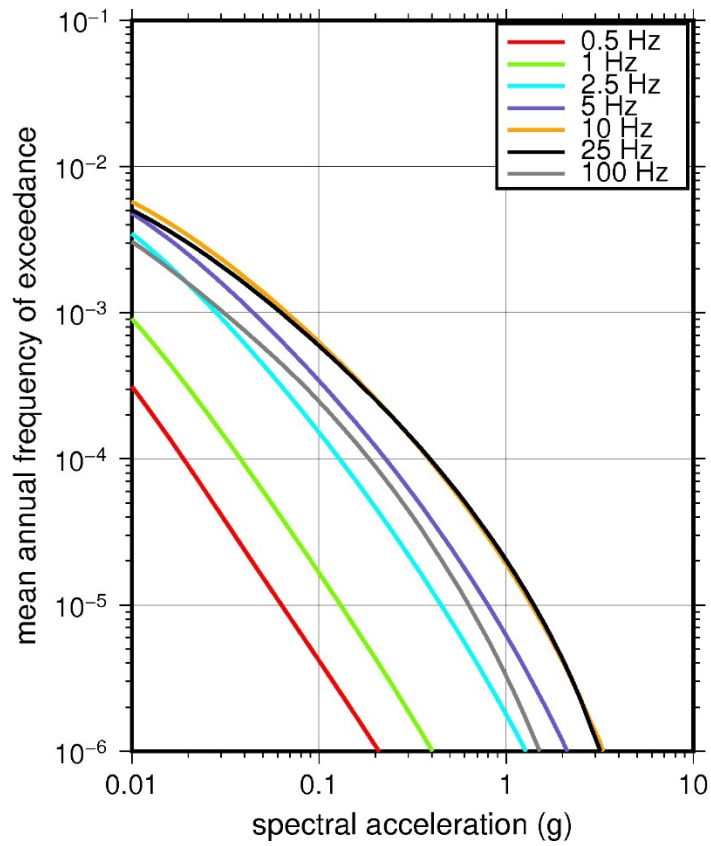


**Figure 2.2-55 Mean Control Point Hazard Curves (Left) for EPRI GMM (2013) Spectral Frequencies, and GMRS and UHRs (Right) for Three Mile Island**

### **2.3 Region II Sites**

The NRC staff characterized the seismic hazard for the 18 Region II nuclear plant sites shown in Table 2.3-1 and Figure 2.3-1. As shown in Table 2.3-1, 10 of the 18 Region II NPPs are founded on rock, 4 on soil over sedimentary rock, 3 on alternating rock and soil substrates, and 1 on soil. Table 2.3-1 also shows the State, the physiographic province, and whether there is a co-located ESP or COL for each site. Figure 2.3-1 shows each Region II site overlain on the physiographic provinces, the highest weighted CEUS-SSC (NRC, 2012b) seismotectonic source zone configuration, the CEUS-SSC earthquake epicenters, and the CEUS-SSC RLME sources that are used to develop the reference rock hazard curves for at least one Region II site.

The following subsections describe the NRC staff's development of reference rock hazard curves, site response analyses, and use of Approach 3 to develop control point seismic hazard curves and a GMRS for each Region II site.



**Table 2.3-1 Region II CEUS Plant Names, Site Names, States, Geology, Physiographic Provinces, and Co-Located ESPs/COLs**

<b>Plant Name</b>	<b>Site Name</b>	<b>State</b>	<b>Geology</b>	<b>Physiographic Province</b>	<b>ESP/COL (Y/N)</b>
Bellefonte Nuclear Plant*	Bellefonte	AL	Rock	Appalachian Plateaus	Y
Browns Ferry Nuclear Plant	Browns Ferry	AL	Rock	Interior Low Plateaus	N
Brunswick Steam Electric Plant	Brunswick	NC	Soil over rock	Coastal Plain	N
Catawba Nuclear Station	Catawba	SC	Rock	Piedmont	N
Joseph M. Farley Nuclear Plant	Farley	AL	Rock and soil	Coastal Plain	N
Shearon Harris Nuclear Power Plant	Harris	NC	Rock	Piedmont	Y
Edwin I. Hatch Nuclear Plant	Hatch	GA	Rock and soil	Coastal Plain	N
McGuire Nuclear Station	McGuire	NC	Rock	Piedmont	N
North Anna Power Station	North Anna	VA	Rock	Piedmont	Y
Oconee Nuclear Station	Oconee	SC	Rock	Piedmont	N
H. B. Robinson Steam Electric Plant	Robinson	SC	Soil over rock	Coastal Plain	N
Sequoyah Nuclear Plant	Sequoyah	TN	Rock	Ridge and Valley	N
St. Lucie Plant	St. Lucie	FL	Soil over rock	Coastal Plain	N
Virgil C. Summer Nuclear Station	Summer	SC	Rock	Piedmont	Y
Surry Power Station	Surry	VA	Soil	Coastal Plain	N
Turkey Point Nuclear Generating Station	Turkey Point	FL	Rock and soil	Coastal Plain	Y
Vogtle Electric Generating Plant	Vogtle	GA	Soil over rock	Coastal Plain	Y
Watts Bar Nuclear Plant	Watts Bar	TN	Rock	Ridge and Valley	N

\*Plant is not operating.

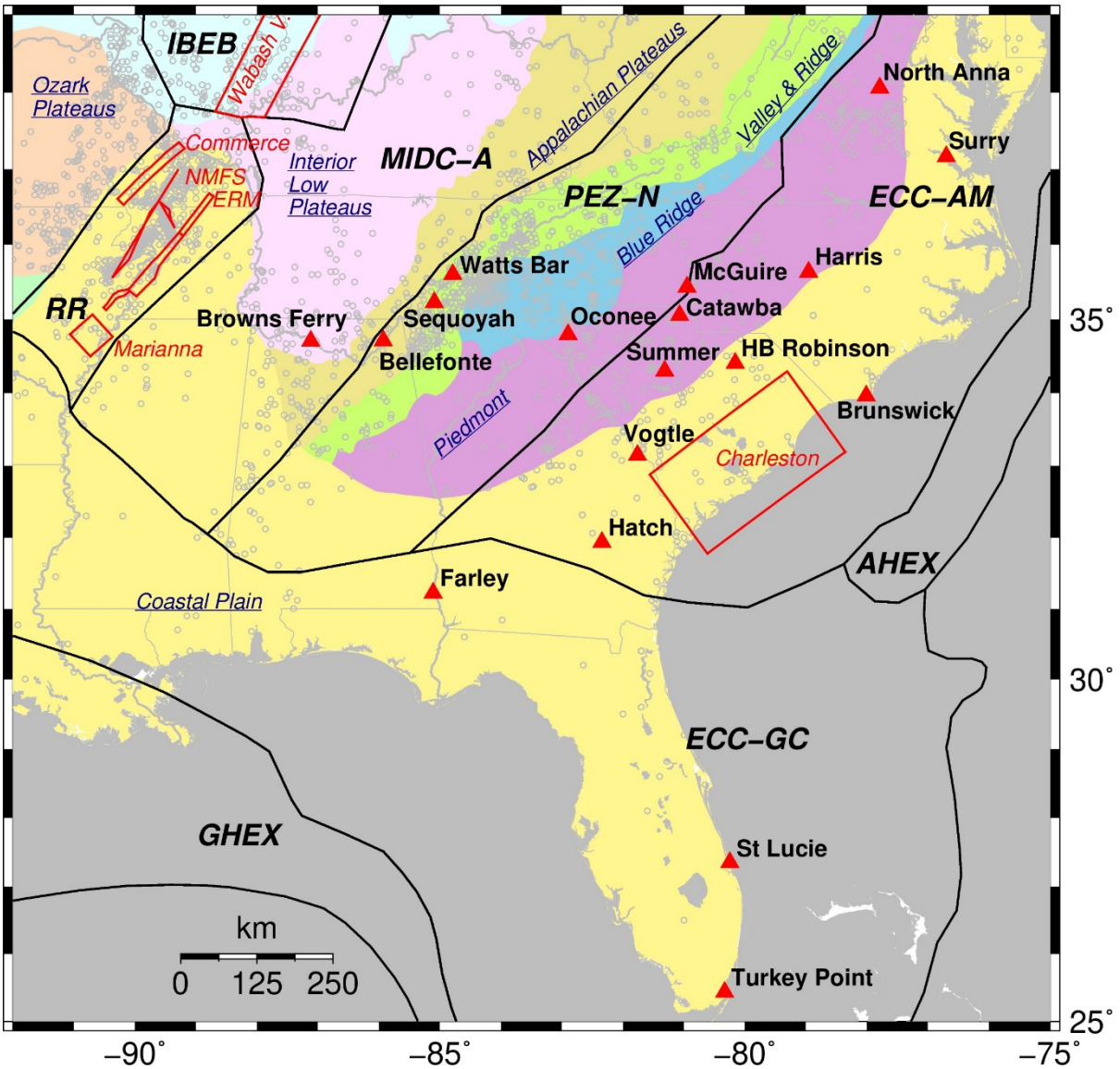


**Figure 2.3-1** Location Map Showing NPPs (Red Triangles) in Region II; RLMEs, Indicated by Solid Red Lines, and Seismotectonic Source Zones, Indicated by Solid Black Lines (from NUREG-2115), with Acronyms Defined in Table 2.1-1 of this Report; and Physiographic Provinces, Identified by Underlined Italicized Labels, with Water Bodies Represented in Gray. Earthquake Epicenters (from NUREG-2115) are Shown with Open Gray Circles

### 2.3.1 Bellefonte

The Bellefonte Nuclear Plant site is located on Guntersville Reservoir along the Tennessee River in the Appalachian Plateaus physiographic province and is founded on Middle Ordovician age limestone and interbedded shale. The horizontal SSE response spectrum for Bellefonte has an RG 1.60 spectral shape and is anchored at a PGA of 0.18g.

#### 2.3.1.1 Reference Rock Hazard

For the reference rock PSHA, the NRC staff selected the 14 CEUS-SSC (NRC, 2012b) background seismic source zones that are located within 320 km [200 mi] of the Bellefonte site. The NRC staff also selected the seven CEUS-SSC RLME sources that are located within 806 km [500 mi] of the site. To develop the reference rock seismic hazard curves for the Bellefonte site, the NRC staff used the GMPEs in the updated EPRI GMM (2013). As shown in Figure 2.3-2, the NMFS RLME, which is located about 557 km [345 mi] to the west of Bellefonte, is the largest contributor to the 1 Hz reference rock total mean hazard curve at the  $10^{-4}$  AFE level. For the 10 Hz reference rock total mean hazard curve, the PEZ-N seismotectonic source zone is the largest contributor at the  $10^{-4}$  AFE level.

#### 2.3.1.2 Site Response Evaluation

##### 2.3.1.2.1 Site Profiles

To assess the need to perform a site response evaluation, the NRC staff used the geologic information in the NTTF R2.1 SHSR (Shea, 2014) submitted by Tennessee Valley Authority (TVA) (hereafter referred to as “the licensee” within this plant section) and the FSAR for the now-withdrawn COL application for Units 3 and 4 (TVA, 2010). As described in the licensee’s SHSR and COL application, the Bellefonte site consists of a thin layer {2 to 12 m [5 to 40 ft]} of residual silts and clays overlying weathered rock to hard, unweathered bedrock. The Bellefonte safety-related structures are primarily founded on the limestones of the Ordovician age Stones River Group. Based on the field investigations for Units 1 and 2 and the COL for Units 3 and 4, the licensee concluded that the  $V_s$  for the bedrock beneath the plant exceeds the reference rock condition { $V_s$  of 2,831 m/sec [9,285 ft/sec]} specified by the EPRI GMM (2013). Therefore, the licensee did not perform a site response analysis for the Bellefonte site. Instead, the licensee used the reference rock hazard curves from the PSHA as its control point hazard curves for determining the GMRS for the Bellefonte site.

As described in the licensee’s SHSR, the bedrock beneath the Bellefonte site consists of alternating layers of gently dipping Ordovician limestone (originally mapped as the Chickamauga Limestone) of the Stones River Group, the Nashville Group, and Sequatchie Formation. The Stones River Group is composed of three subunits (Upper Stones River, Middle Stones River, and Lower Stones River) that differ slightly from one another in composition and texture, containing alternative beds of limestone to dolomitic limestone and argillaceous and silty limestone, with some cherty limestone. The Middle Stones River subunit is further divided into six distinct lithologic units, designated Units A through F. These six units of the Middle Stones River subunit comprise a total thickness of about 138 m [453 ft] within the 320 m [1,050 ft] thick Stones River Group.

The bedrock directly beneath the plant is composed of the Middle Stones River subunit, which is further subdivided into Units A through F. Geophysical surveys for the Bellefonte site, which include seismic refraction surveys and suspension and downhole logging tests, show a  $V_s$  of

about 2,300 m/sec [7,500 ft/sec] for the thin {3 m [10 ft]} layer of weathered rock, a  $V_S$  of about 3,050 m/sec [10,000 ft/sec] for Units B, D, E, and F, and a  $V_S$  of about 2,100 m/sec [7,000 ft/sec] for Unit C. Unit C, which is laterally continuous across the site with a thickness of about 21 m [70 ft], is a dark gray argillaceous and silty dolomitic limestone.

Because the  $V_S$  for the thin weathered rock layer and the thicker argillaceous and silty limestone layer (Unit C) are both well below the reference rock  $V_S$  of 2,831 m/sec [9,285 ft/sec], the NRC staff developed a simple three-layer profile. This profile consists of a 3 m [10 ft] thick weathered rock layer underlain by a 21 m [70 ft] argillaceous and silty limestone layer and a 30 m [100 ft] thick dolomitic limestone layer (Unit B).

To capture the uncertainty in the basecase profile, the NRC staff developed lower and upper range (10<sup>th</sup> and 90<sup>th</sup> percentile) profiles by multiplying the basecase  $V_S$  values by scale factors of 0.83 and 1.21, respectively, which corresponds to an epistemic logarithmic standard deviation of 0.15. The weights for the lower, best-estimate, and upper basecase profiles are 0.3, 0.4, and 0.3, respectively. Figure 2.3-3 shows the three profiles used by the NRC staff, which extend to a depth of 55 m [180 ft] below the control point elevation.

#### 2.3.1.2.2 *Dynamic Material Properties and Site Kappa*

The NRC staff assumed both linear and nonlinear dynamic behavior for the rock beneath the Bellefonte site. To model the nonlinear behavior of the uppermost rock strata, the NRC staff used the EPRI rock shear modulus reduction and material damping curves. To model the linear behavior, the NRC staff used a constant damping ratio of 3 percent. The NRC staff assumed these two alternative dynamic responses for the entire 55 m [180 ft] of the profile. Due to the higher  $V_S$  of this rock strata, the NRC staff assigned weights of 0.7 and 0.3 to the linear and nonlinear alternatives, respectively.

To determine the basecase  $\kappa_\theta$  for the Bellefonte site, the NRC staff first used the Campbell (2009) Model 1 relationship between  $V_S$  and  $Q_{ef}$  to determine a  $Q_{ef}$  for each layer. Combining these  $Q_{ef}$  values with the thicknesses and  $V_S$  for each of the layers results in a total  $\kappa_\theta$  value of about 6.3 msec, which includes the 6 msec assumed for the underlying reference rock. For the lower and upper basecase profiles, the NRC staff calculated  $\kappa_\theta$  values of 6.4 and 6.2 msec, respectively, using the same approach as for the best-estimate basecase profile. Because the licensee did not perform a site response analysis, it did not determine  $\kappa_\theta$  for the Bellefonte site.

Table 2.3-2 provides the layer depths, lithologies,  $V_S$ , unit weights, and dynamic properties for the NRC staff's three profiles. In summary, the site response logic tree developed by the NRC staff for the Bellefonte site consists of six alternatives; three basecase profiles (each with a different  $\kappa_\theta$  value) and two alternative dynamic property branches.

#### 2.3.1.2.3 *Methodology and Results*

The NRC staff followed the methodology described in Section 2.1.4 to develop the final site amplification factors. Figure 2.3-4 shows the overall median site amplification factors and their variability for each of the seven spectral frequencies. As shown in Figure 2.3-4, the median site amplification factors are very close to 1 for each of the spectral frequencies. The lower half of Figure 2.3-4 shows that the logarithmic standard deviations for the site amplification factors range from about 0.05 to 0.10.

### 2.3.1.3 Control Point Hazard

The NRC staff implemented Approach 3 from the SPID to develop a weighted control point seismic hazard curve for each of the six unique combinations of the site response logic tree for the Bellefonte site. After combining these curves to develop the final mean control point hazard curves, the NRC staff determined the  $10^{-4}$  and  $10^{-5}$  UHRS in order to calculate the final GMRS. Figure 2.3-5 shows the final control point mean seismic hazard curves for each of the seven spectral frequencies as well as the NRC staff's UHRS and GMRS, and the licensee's NTTF R2.1 GMRS (Shea, 2014). As shown in Figure 2.3-5, the NRC staff's GMRS (black curve) is similar in amplitude to the licensee's GMRS (blue curve) but shows two prominent peaks at about 10 Hz and 40 Hz due to the NRC staff's development of the basecase profiles shown in Table 2.3-2. For comparison, Figure 2.3-5 also shows the NRC staff's reference rock GMRS (brown dotted curve).

Layer	Depth (ft)	Description	$V_s$ (ft/sec)			$V_s$ Sigma (ln)	BC Unit Weight (pcf)	Dynamic Properties	
			LR (0.3)	BC (0.4)	UR (0.3)			Alt. 1 (0.3)	Alt. 2 (0.7)
1	10	Rock: limestone	6,188	7,500	9,090	0.25	160	EPRI Rock	L 3.0%
2	80	Rock: limestone	7,661	9,285	9,285	0.15	160	EPRI Rock	L 3.0%
3	180	Rock: limestone	5,775	7,000	8,484	0.15	150	EPRI Rock	L 3.0%

LR = lower range; BC = basecase; UR = upper range; ln = natural log; pcf = pounds per cubic foot; L = linear; Alt. = alternative.  
 For LR, BC, UR, and Alt.: Values in parentheses refer to weights for site response analysis logic tree branches.

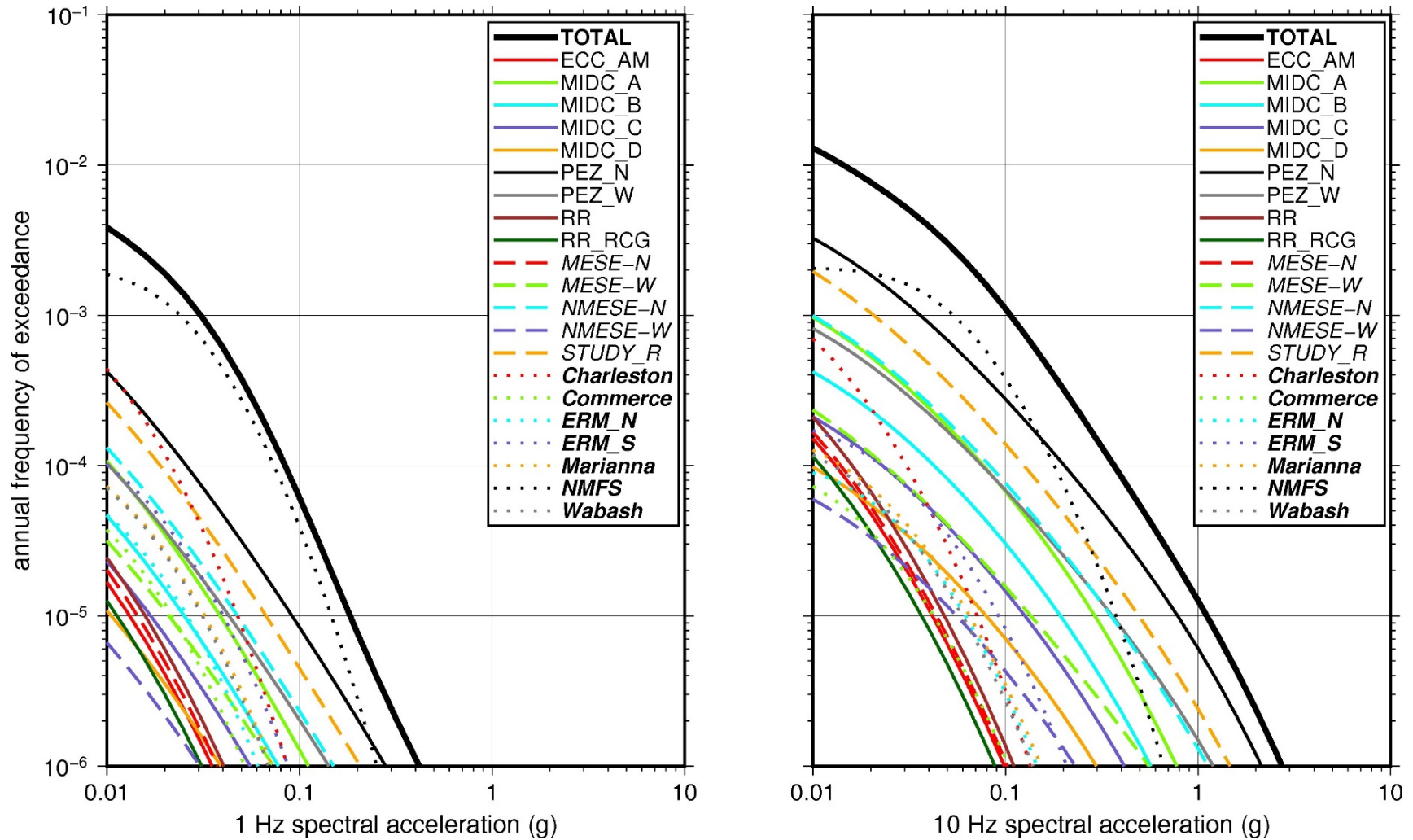


**Figure 2.3-2 Low-Frequency (1 Hz, Left) and High-Frequency (10 Hz, Right) Reference Rock Hazard Curves for Bellefonte. Total Hazard Is Shown as a Bold Black Line; Individual Contributions to the Hazard for Each of the CEUS-SSC Sources are Shown as Colored Lines Defined in the Legend. See Table 2.1-1 for Source Name Definitions**

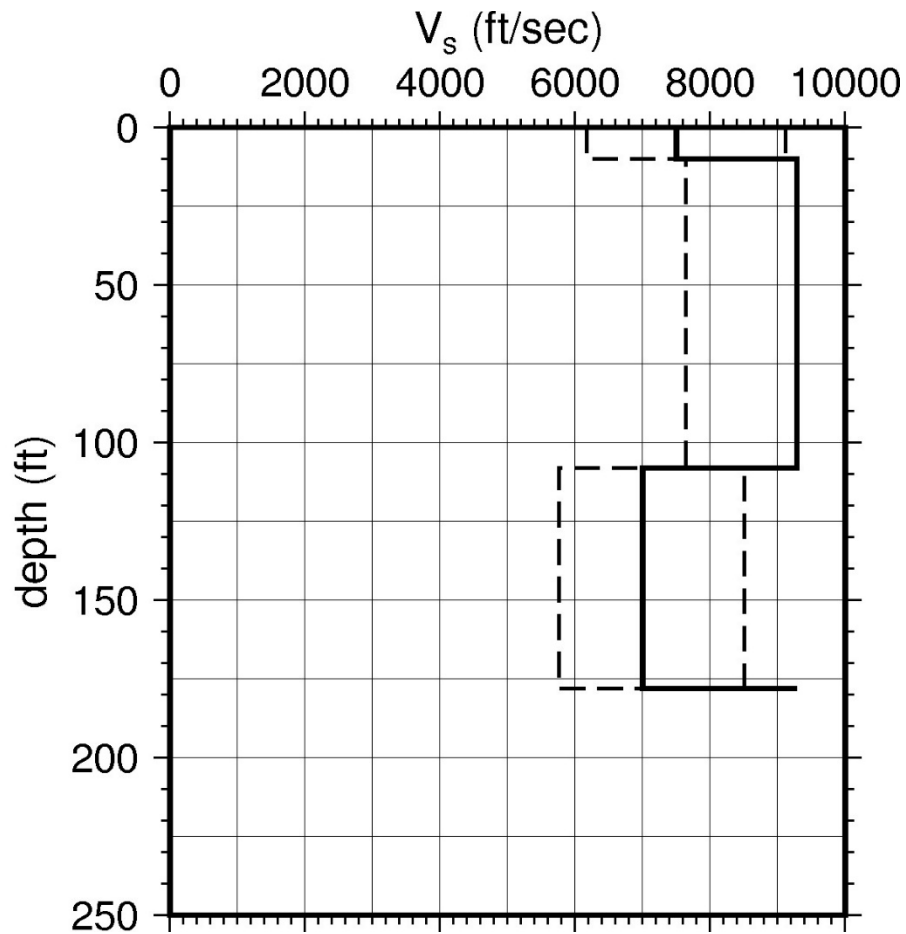


**Figure 2.3-3** Shear Wave Velocity ( $V_s$ ) Profiles for Bellefonte. Basecase (BC) Profile Shown as Solid Bold Line; Lower and Upper Range (LR and UR) Profiles Shown as Dashed Lines. Profiles Terminate at Reference Rock Velocity of 2,831 m/sec [9,285 ft/sec] per EPRI GMM (2013)

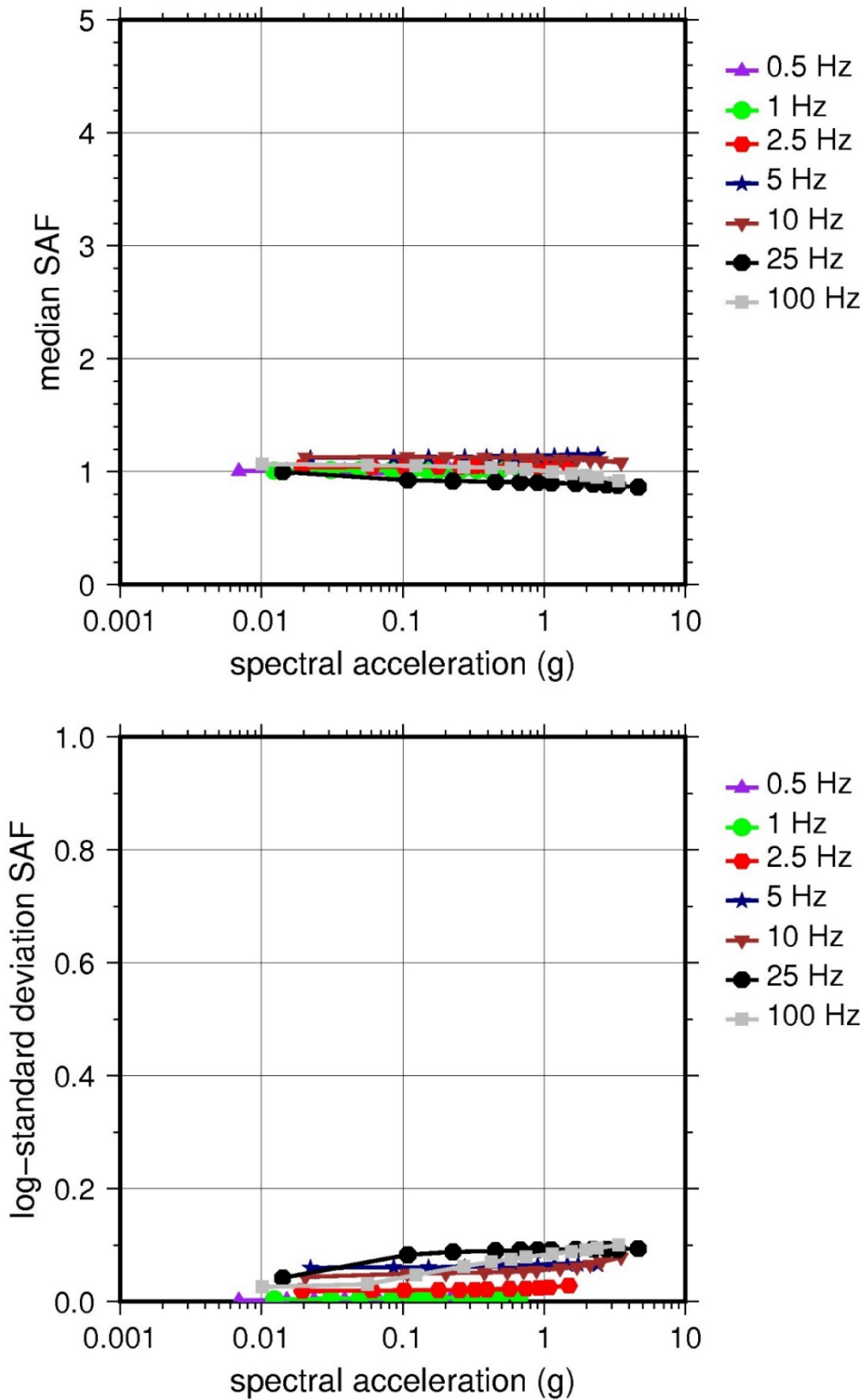


**Figure 2.3-4 Overall Weighted Median Site Amplification Factor (SAF) (Upper) and Log Standard Deviation of the SAF (Lower) as a Function of Input Acceleration for EPRI GMM (2013) Spectral Frequencies**



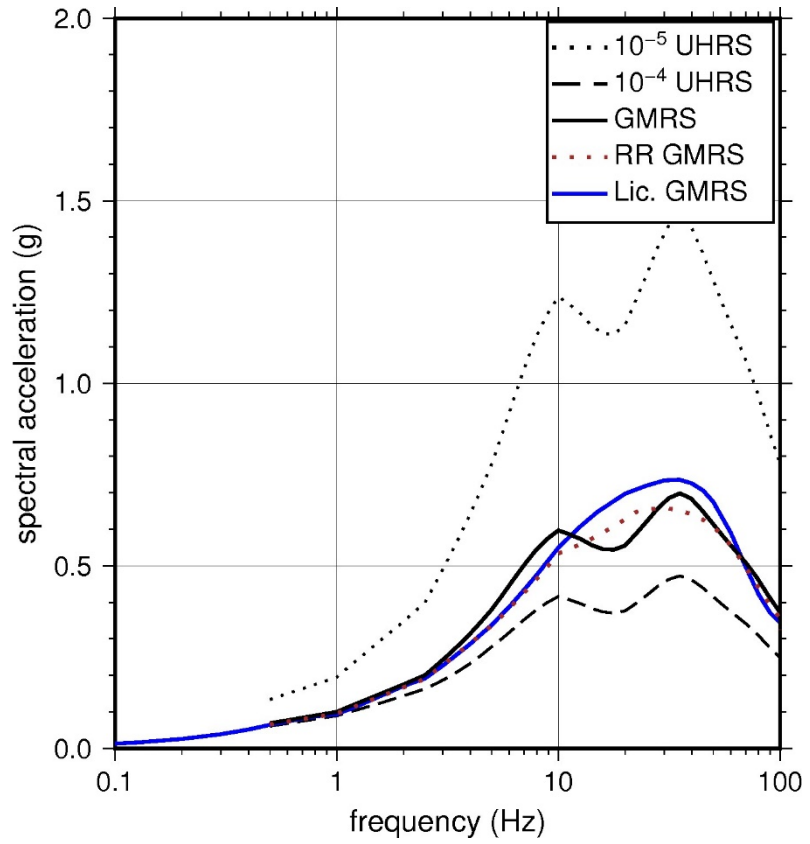
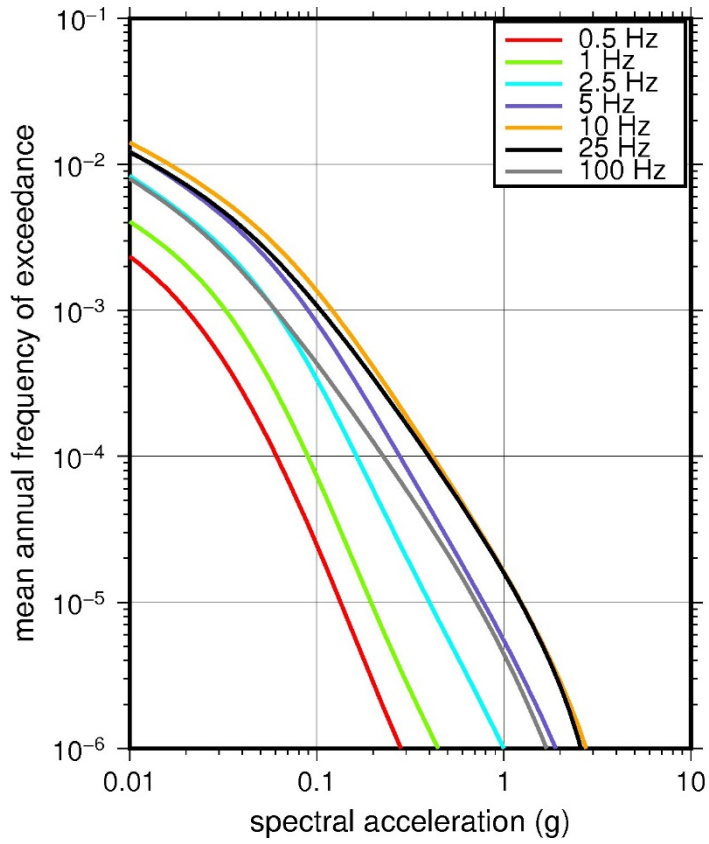


**Figure 2.3-5 Mean Control Point Hazard Curves (Left) for EPRI GMM (2013) Spectral Frequencies, and GMRS and UHRs (Right) for Bellefonte**

## 2.3.2 Browns Ferry

The Browns Ferry Nuclear Plant (Browns Ferry) site is located on the northern shore of Wheeler Reservoir along the Tennessee River within the Interior Low Plateaus physiographic province and is founded on competent sedimentary rock (limestone, shale, and dolomite) of Paleozoic age, which is assumed to be about 1,220 m [4,000 ft] thick. The horizontal SSE response spectrum for Browns Ferry has a rounded Housner spectral shape and is anchored at a PGA of 0.20g.

### 2.3.2.1 Reference Rock Hazard

For the reference rock PSHA, the NRC staff selected the 14 CEUS-SSC (NRC, 2012b) background seismic source zones that are located within 320 km [200 mi] of the site. The NRC staff also selected the eight CEUS-SSC RLME sources that are located within 806 km [500 mi] of the Browns Ferry site. To develop the reference rock seismic hazard curves for the site, the NRC staff used the GMPEs in the updated EPRI GMM (2013). As shown in Figure 2.3-6, the NMFS RLME, which is located about 250 km [155 mi] to the west of the site, is the largest contributor to both the 1 Hz and 10 Hz reference rock total mean hazard curves at the  $10^{-4}$  AFE level.

### 2.3.2.2 Site Response Evaluation

#### 2.3.2.2.1 Site Profiles

To develop a basecase profile, the NRC staff used the geologic information in the NTTF R2.1 SHSR (Shea, 2014) submitted by the TVA (hereafter referred to as “the licensee” within this plant section). As described in the licensee’s SHSR, the Browns Ferry site consists of a thin layer {about 15 m [48 ft]} of clay, clayey gravel, and gravel overlying about 15 m [50 ft] of fossiliferous limestone that grades into the Fort Payne Formation, which contains chert, cherty limestone, and shale. The major structures of the Browns Ferry plant are founded in the Fort Payne Formation. In Table 2.3.1-1 of the SHSR, the licensee briefly described the subsurface materials in terms of the geologic units and layer thicknesses. For its site response evaluation, the NRC staff used the top of the Fort Payne Formation, which corresponds to an elevation of 158 m [519 ft] MSL, as the control point elevation for the Browns Ferry site.

The licensee did not obtain in situ  $V_S$  measurements in the Fort Payne Formation at the Browns Ferry site. However, the rock formations that underlie the Browns Ferry site are similar to those that underlie the Watts Bar plant, for which the licensee performed Spectral Analysis of Surface Waves (SASW) testing. Therefore, the licensee used the  $V_S$  from the SASW testing at Watts Bar to develop its  $V_S$  profile for the Browns Ferry site. Table 2.3.2-1 of the SHSR gives these estimated  $V_S$  for Browns Ferry.

For its SHSR, the licensee developed a basecase profile that extends to a depth of 1,211 m [3,973 ft] below the control point elevation. The uppermost layers {60 m [198 ft]} of the profile consist of the Mississippian age Fort Payne Formation, for which the licensee assumed the reference  $V_S$  of 2,831 m/sec [9,285 ft/sec]. For the underlying 236 m [775 ft] of shale from the Chattanooga Shale Formation and Silurian age shale and siltstone from the Red Mountain Formation, the licensee assumed a  $V_S$  of 2,134 m/sec [7,000 ft/sec]. Beneath this predominantly shale layer are limestones from the Ordovician age Sequatchie Formation and Chickamauga Group, for which the licensee assumed the reference  $V_S$  of 2,831 m/sec [9,285 ft/sec]. Finally, for the dolomites and limestones that comprise the Ordovician to

Cambrian age Knox Group and the shales from the Cambrian age Conasauga Group, the licensee assumed a  $V_S$  of 2,134 m/sec [7,000 ft/sec]. The licensee terminated its basecase profile at the top of the underlying Cambrian age Rome Formation sandstone, for which the licensee estimated a  $V_S$  of 3,050 m/sec [10,000 ft/sec].

For its basecase profile, the NRC staff used the licensee's layer thicknesses and estimated  $V_S$ . However, for the shale layers, the NRC staff applied the velocity gradient of 0.5 m/sec/m [0.5 ft/sec/ft] recommended by the SPID for sedimentary rock.

To capture the uncertainty in its basecase profile, the NRC staff developed lower and upper range (10<sup>th</sup> and 90<sup>th</sup> percentile) profiles by multiplying the basecase  $V_S$  values by scale factors of 0.83 and 1.21, respectively, which corresponds to an epistemic logarithmic standard deviation of 0.15. The weights for the lower, best-estimate, and upper basecase profiles are 0.3, 0.4, and 0.3, respectively. As shown in Figure 2.3-7, the upper profile terminates at a depth of 450 m [1,473 ft], and the lower and best-estimate basecase profiles terminate at a depth of 1,211 m [3,973 ft] below the control point elevation, at which point the  $V_S$  is assumed to exceed the reference rock value of 2,831 m/sec [9,285 ft/sec].

#### 2.3.2.2.2 *Dynamic Material Properties and Site Kappa*

The NRC staff assumed both linear and nonlinear dynamic behavior for the rock beneath the Browns Ferry site. To model the nonlinear behavior of the uppermost rock strata, the NRC staff used the EPRI rock shear modulus reduction and material damping curves. To model the linear behavior, the NRC staff used a constant damping ratio of 3 percent. The NRC staff assumed these two alternative dynamic responses for the upper 144 m [473 ft] of the profile. Because of the higher  $V_S$  of these rock strata, the NRC staff assigned weights of 0.7 and 0.3 to the linear and nonlinear alternatives, respectively. For the remaining 1,067 m [3,500 ft] of its profile, the NRC staff assumed a linear response with a material damping ratio value of 0.1 percent to maintain consistency with the  $\kappa_0$  value for the Browns Ferry site.

To determine the basecase  $\kappa_0$  for the Browns Ferry site, the NRC staff first used the Campbell (2009) Model 1 relationship between  $V_S$  and  $Q_{ef}$  to determine a  $Q_{ef}$  for each layer. Combining these  $Q_{ef}$  values with the thicknesses and  $V_S$  for each of the layers results in a total  $\kappa_0$  value of about 13 msec, which includes the 6 msec assumed for the underlying reference rock. For the lower and upper basecase profiles, the NRC staff calculated  $\kappa_0$  values of 16 and 8 msec, respectively, using the same approach as for the best-estimate basecase profile. In contrast, the licensee estimated  $\kappa_0$  by using the empirical relationship from the SPID (EPRI, 2012) between the average  $V_S$  over the upper 30 m [100 ft] of the profile and  $\kappa_0$ , which results in  $\kappa_0$  values of 6, 12, and 6 msec for the best-estimate, lower, and upper basecase profiles, respectively.

Table 2.3-3 provides the layer depths, lithologies,  $V_S$ , unit weights, and dynamic properties for the NRC staff's three profiles. In summary, the site response logic tree developed by the NRC staff for the Browns Ferry site consists of six alternatives; three basecase profiles (each with a different  $\kappa_0$  value) and two alternative dynamic property branches.

#### 2.3.2.2.3 *Methodology and Results*

The NRC staff followed the methodology described in Section 2.1.4 to develop the final site amplification factors. Figure 2.3-8 shows the overall median site amplification factors and their variability for each of the seven spectral frequencies. As shown in Figure 2.3-8, the median site

amplification factors are close to 1 before falling off with higher input spectral accelerations. The lower half of Figure 3.3-8 shows that the logarithmic standard deviations for the site amplification factors range from about 0.05 to 0.15.

### 2.3.2.3 Control Point Hazard

The NRC staff implemented Approach 3 from the SPID to develop a weighted control point seismic hazard curve for each of the six unique combinations of the site response logic tree for the Browns Ferry site. After combining these curves to develop the final mean control point hazard curves, the NRC staff determined the  $10^{-4}$  and  $10^{-5}$  UHRS in order to calculate the final GMRS. Figure 2.3-9 shows the final control point mean seismic hazard curves for each of the seven spectral frequencies as well as the NRC staff's UHRS and GMRS, and the licensee's NTTF R2.1 GMRS (Shea, 2014). As shown in Figure 2.3-9, the NRC staff's GMRS (black curve) is moderately lower than the licensee's GMRS (blue curve) due to the licensee's higher  $\kappa_0$  values and larger epistemic uncertainty for its three basecase profiles. For comparison, Figure 2.3-9 also shows the NRC staff's reference rock GMRS (brown dotted curve).

**Table 2.3-3 Layer Depths, Shear Wave Velocities ( $V_s$ ), Unit Weights, and Dynamic Properties for Browns Ferry**

Layer	Depth (ft)	Description	$V_s$ (ft/sec)			$V_s$ Sigma (ln)	BC Unit Weight (pcf)	Dynamic Properties	
			LR (0.3)	BC (0.4)	UR (0.3)			Alt. 1 (0.3)	Alt. 2 (0.7)
1	198	Rock: limestone	7,661	9,285	9,285	0.25	160	EPRI Rock	L 3.0%
2	298	Rock: shale	5,775	7,000	8,484	0.15	150	EPRI Rock	L 3.0%
3	473	Rock: shale	5,848	7,088	8,591	0.15	150	EPRI Rock	L 3.0%
4	723	Rock: shale	5,951	7,213	8,742	0.15	150	L 0.1%	L 0.1%
5	973	Rock: shale	6,054	7,338	8,894	0.15	150	L 0.1%	L 0.1%
6	1,117	Rock: limestone	7,661	9,285	9,285	0.15	160	L 0.1%	L 0.1%
7	1,473	Rock: shale	6,188	7,500	9,090	0.15	160	L 0.1%	L 0.1%
8	1,973	Rock: shale	6,394	7,750	9,285	0.15	160	L 0.1%	L 0.1%
9	2,473	Rock: shale	6,600	8,000	9,285	0.15	160	L 0.1%	L 0.1%
10	2,973	Rock: shale	6,807	8,250	9,285	0.15	160	L 0.1%	L 0.1%
11	3,473	Rock: shale	7,013	8,500	9,285	0.15	160	L 0.1%	L 0.1%
12	3,973	Rock: shale	7,219	8,750	9,285	0.15	160	L 0.1%	L 0.1%

LR = lower range; BC = basecase; UR = upper range; ln = natural log; pcf = pounds per cubic foot; L = linear; Alt. = alternative.

For LR, BC, UR, and Alt.: Values in parentheses refer to weights for site response analysis logic tree branches.

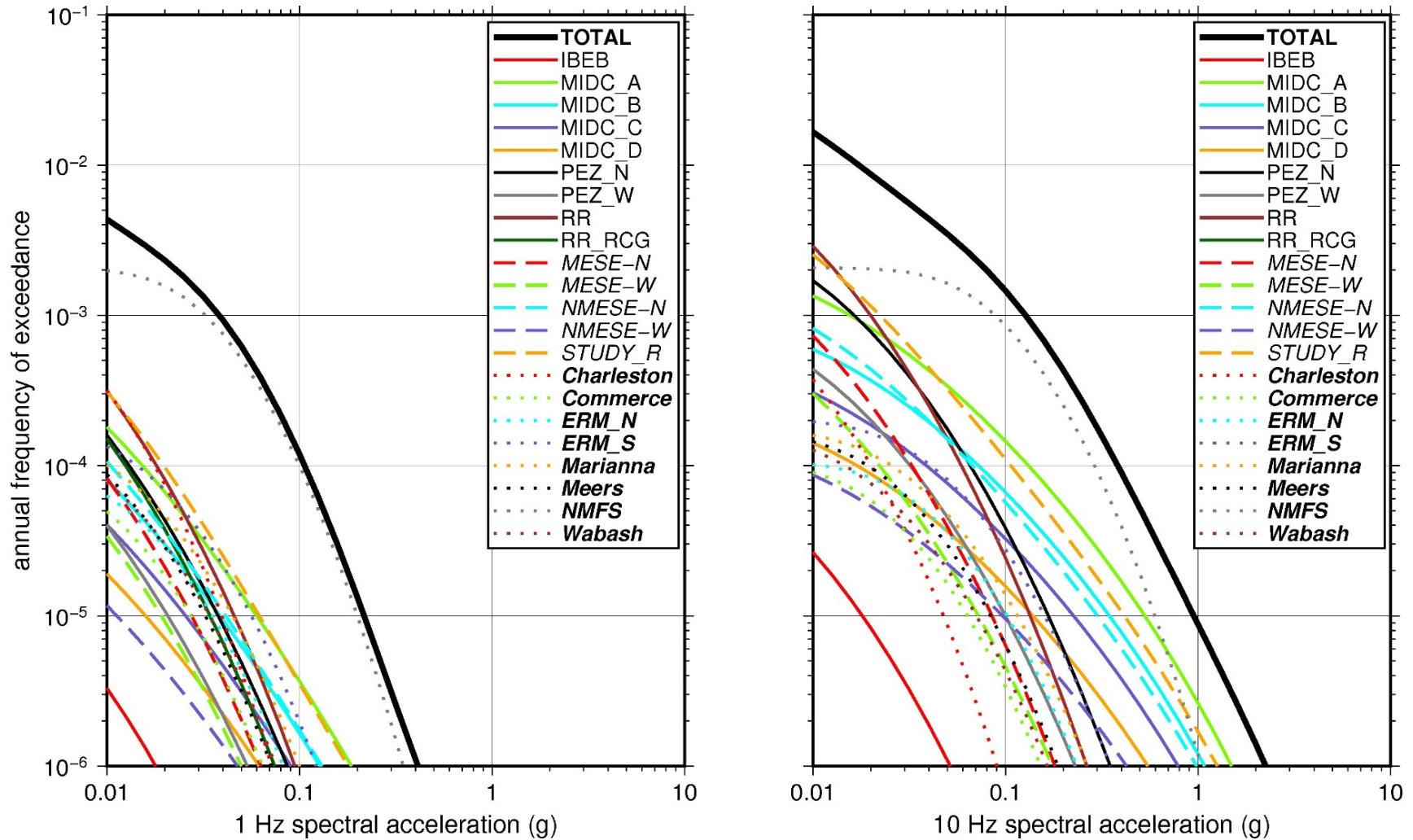


**Figure 2.3-6 Low-Frequency (1 Hz, Left) and High-Frequency (10 Hz, Right) Reference Rock Hazard Curves for Browns Ferry. Total Hazard is Shown as a Bold Black Line; Individual Contributions to the Hazard for each of the CEUS-SSC Sources are Shown as Colored Lines Defined in the Legend. See Table 2.1-1 for Source Name Definitions**

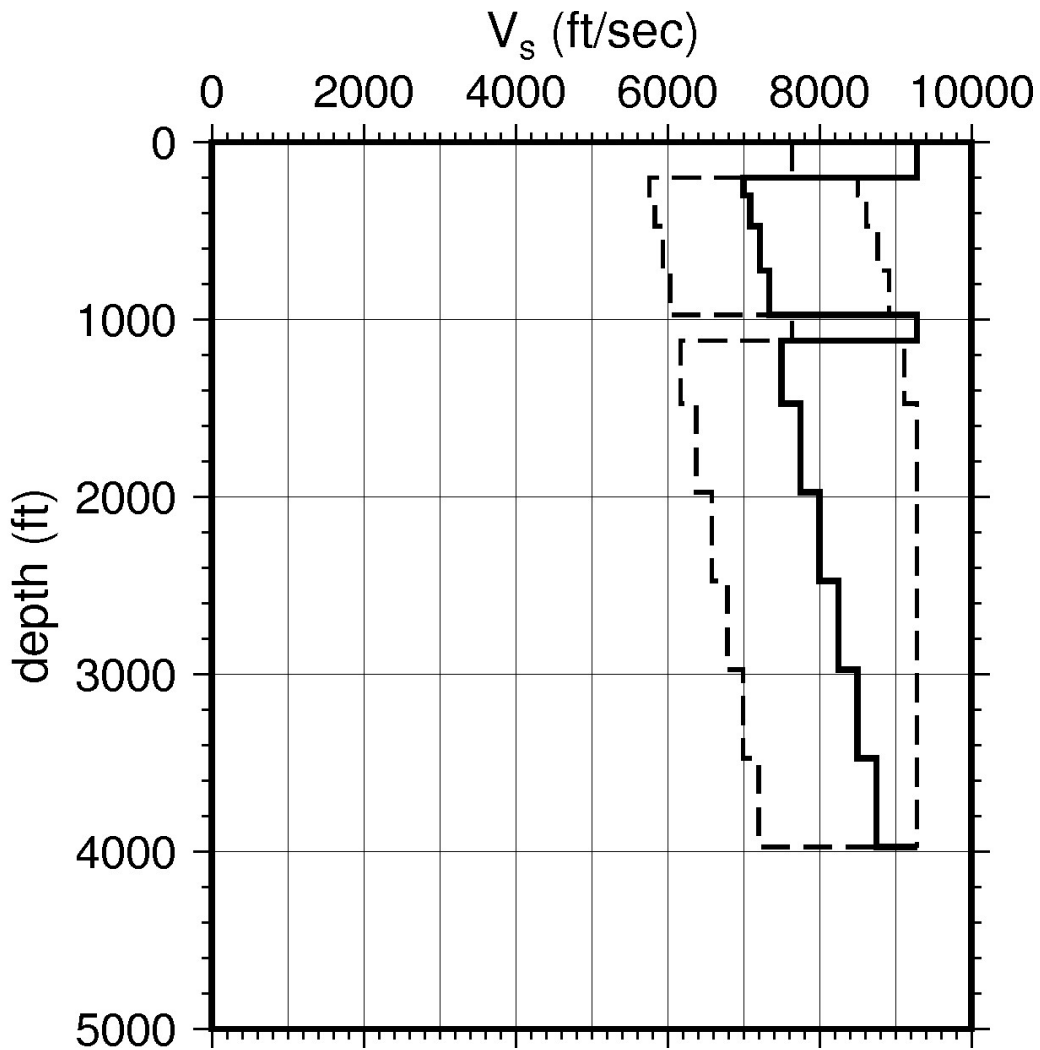


**Figure 2.3-7** Shear Wave Velocity ( $V_s$ ) Profiles for Browns Ferry. Basecase (BC) Profile Shown as Solid Bold Line; Lower and Upper Range (LR and UR) Profiles Shown as Dashed Lines. Profiles Terminate at Reference Rock Velocity of 2,831 m/sec [9,285 ft/sec] per EPRI GMM (2013)

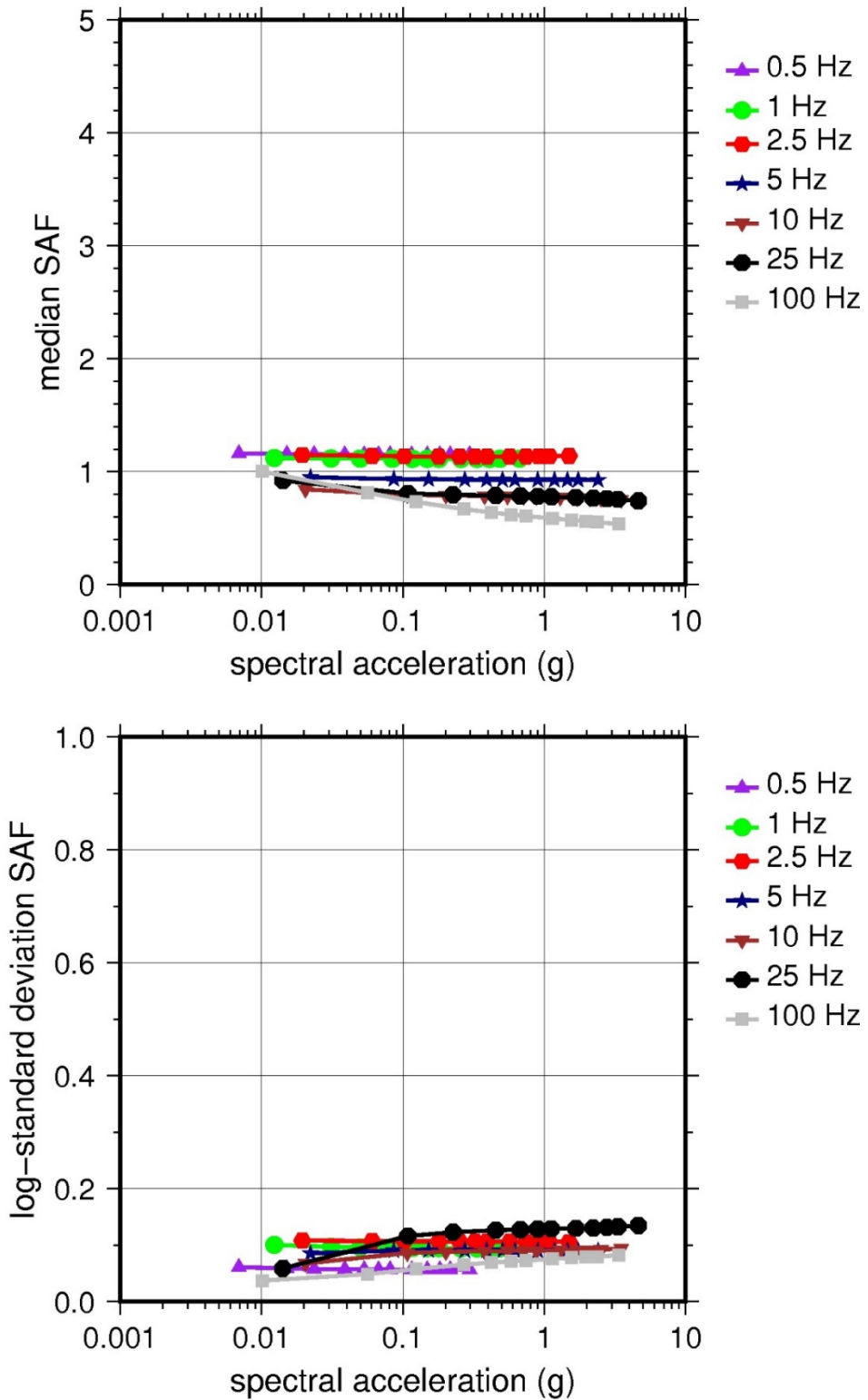


**Figure 2.3-8 Overall Weighted Median Site Amplification Factor (SAF) (Upper) and Log Standard Deviation of the SAF (Lower) as a Function of Input Acceleration for EPRI GMM (2013) Spectral Frequencies**



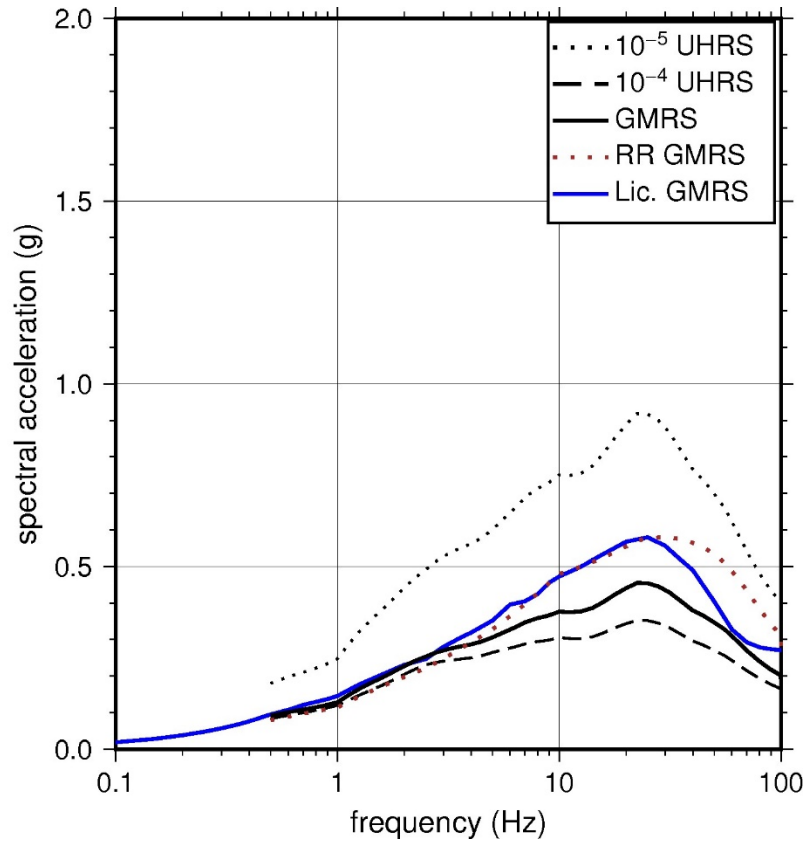
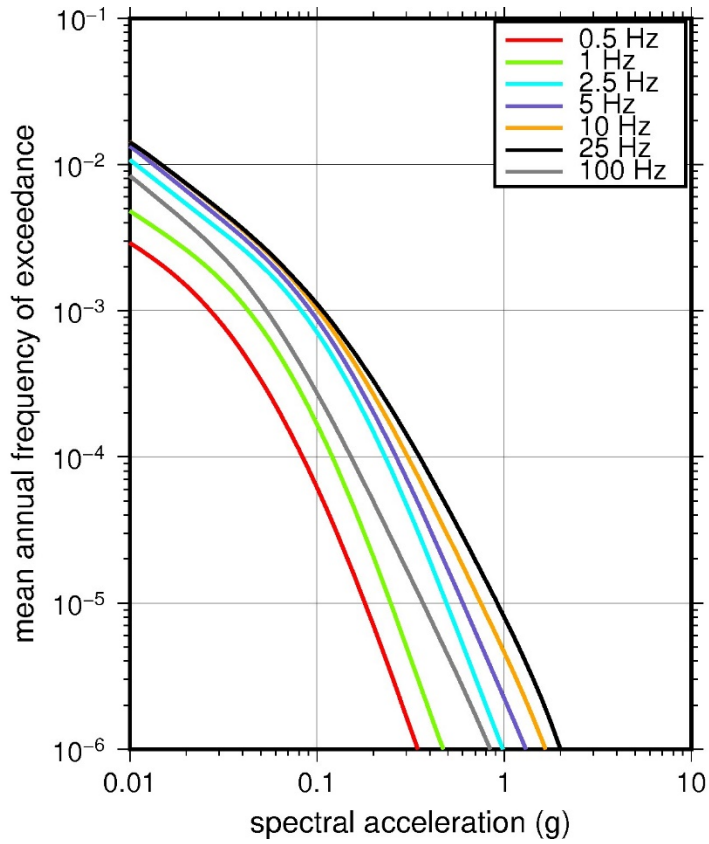


**Figure 2.3-9 Mean Control Point Hazard Curves (Left) for EPRI GMM (2013) Spectral Frequencies, and GMRS and UHRS (Right) for Browns Ferry**

### 2.3.3 Brunswick

The Brunswick Steam Electric Plant (Brunswick) site is located in North Carolina adjacent to the Cape Fear River and the Atlantic Ocean, within the Coastal Plain physiographic province and is founded on about 460 m [1,500 ft] of sedimentary strata (sand, clay, and limestone). The horizontal SSE response spectrum for Brunswick has a spectral shape that envelopes the 1940 North-South El Centro, CA, strong motion record and is anchored at a PGA of 0.16g.

#### 2.3.3.1 Reference Rock Hazard

For the reference rock PSHA, the NRC staff selected the nine CEUS-SSC (NRC, 2012b) background seismic source zones that are located within 320 km [200 mi] of the site. The NRC staff also selected the Charleston CEUS-SSC RLME source, whose regional configuration extends to about 92 km [57 mi] to the southwest of the Brunswick site. To develop the reference rock seismic hazard curves for the site, the NRC staff used the GMPEs in the updated EPRI GMM (2013). As shown in Figure 2.3-10, the Charleston RLME is the largest contributor to both the 1 Hz and 10 Hz reference rock total mean hazard curves at the  $10^{-4}$  AFE level.

#### 2.3.3.2 Site Response Evaluation

##### 2.3.3.2.1 Site Profiles

To develop a basecase profile, the NRC staff used the geologic information in the NTF R2.1 SHSR (Hamrick, 2014) submitted by Duke Energy (hereafter referred to as “the licensee” within this plant section). As described in the licensee’s SHSR, the Brunswick site consists of 7 m [22 ft] of dense sands overlying 13 m [43 ft] of stiff clays and sands, below which lies 427 m [1,400 ft] of clayey limestone. The major structures of the Brunswick plant are either founded within dense sands or on structural fill overlying the dense sands. In Table 2.3.1-1 of the SHSR, the licensee briefly described the subsurface materials in terms of the geologic units and layer thicknesses. For its site response evaluation, the NRC staff used the top of the Lower Yorktown Formation, which corresponds to an elevation of 8.5 m [28 ft] below MSL, as the control point elevation for the Brunswick site.

The field explorations for Brunswick consisted of a number of borings through the soil and upper portion of rock beneath the site. Seismic refraction, crosshole, and uphole surveys by the licensee measured  $V_P$  and  $V_S$  to a depth of about 67 m [220 ft] beneath the site. Table 2.3.2-2 of the SHSR gives the measured and estimated  $V_S$  determined from the licensee’s site investigations.

For its SHSR, the licensee developed a basecase profile that extends to a depth of 452 m [1,482 ft] below the control point elevation. The uppermost layers {7 m [22 ft]} of the profile consist of the Pliocene age Yorktown Formation sands, for which the licensee measured an average  $V_S$  of 342 m/sec [1,122 ft/sec]. Beneath this layer of sand is a 13 m [43 ft] thick layer of Oligocene age clay with a  $V_S$  of about 1,677 m/sec [5,500 ft/sec]. Underlying these two units is a 39 m [127 ft] thick layer of limestone from the Eocene age Castle Hayne Formation, which has a  $V_S$  of about 1,372 m/sec [4,500 ft/sec]. The remaining 393 m [1,290 ft] of the licensee’s profile consists of limestone from the Cretaceous age Peedee Formation, for which the licensee measured a  $V_S$  of 914 m/sec [3,000 ft/sec].

As the soil and rock strata beneath the Brunswick site has been characterized by multiple geophysical field investigations, the NRC staff used the licensee’s layer thicknesses and  $V_S$  for

its basecase profile. However, the soil and rock identifications in Table 2.3.1-1 of the SHSR do not coincide with the descriptions of the strata in Section 2.3.1 of the SHSR, which has been extracted from Section 2.5.1.2 of the FSAR (Progress Energy, 2012). Based on the subsurface description in Section 2.3.1 of the SHSR and the geological cross sections shown in Figure 2-33 of the UFSAR for boreholes 1, 2, 8, and 9, the NRC staff concludes that the uppermost 7 m [22 ft] of the licensee's basecase profile consists of sand from the Castle Hayne Formation rather than the Yorktown Formation. The underlying 13 m [43 ft] thick layer is the Peedee Confining Unit, which consists of clay, silty clay, and sandy clay, with short lenses of limestone. Beneath this layer is a 39 m [127 ft] thick layer of limestone from the Peedee Formation rather than from the Castle Hayne Formation. Finally, the bottom 393 m [1,290 ft] thick layer consists of Cretaceous age strata from the Peedee Formation, Black Creek Group, and Middendorf and Cape Fear Formations. These units are primarily composed of clay and sand and not limestone as identified in Table 2.3.1-1 of the SHSR. As described in the following section, this distinction is important for the modeling of potential nonlinear behavior under dynamic loading for the uppermost soil and rock strata beneath the site.

To capture the uncertainty in its basecase profile, the NRC staff developed lower and upper range (10<sup>th</sup> and 90<sup>th</sup> percentile) profiles by multiplying the basecase  $V_S$  values by scale factors of 0.78 and 1.29, respectively, which corresponds to an epistemic logarithmic standard deviation of 0.20. The weights for the lower, best-estimate, and upper basecase profiles are 0.3, 0.4, and 0.3, respectively. Figure 2.3-11 shows the NRC staff's basecase profiles.

#### 2.3.3.2.2 *Dynamic Material Properties and Site Kappa*

The NRC staff assumed both linear and nonlinear behavior for the soil and rock beneath the Brunswick site. To model the nonlinear response within the upper 152 m [500 ft] of soil deposits (Layers 1, 2 and 4), the NRC staff used the EPRI soil shear modulus reduction and material damping curves as one alternative and the Peninsular Range curves for the second equally weighted alternative. To model the nonlinear behavior of the rock strata, the NRC staff used the EPRI rock shear modulus reduction and material damping curves. To model the linear behavior, the NRC staff used a constant damping ratio of 3 percent. The NRC staff assumed these two alternative dynamic responses for the 39 m [127 ft] of the Peedee limestone (Layer 3) and gave them equal weight. For the remaining 1,296 m [1,290 ft] of its profile, the NRC staff assumed a linear response with a material damping ratio value of 1.0 percent to maintain consistency with the  $\kappa_0$  value for the Brunswick site. In contrast, the licensee applied the EPRI rock shear modulus reduction and material damping curves along with a linear 3 percent damping alternative for 152 m [500 ft] of its profile. For the remaining 280 m [917 ft] of its profile, the licensee assumed a constant damping ratio value of 1.25 percent.

To determine the basecase  $\kappa_0$  for the Brunswick site, the NRC staff first used the Campbell (2009) Model 1 relationship between  $V_S$  and the  $Q_{ef}$  to determine the  $Q_{ef}$  for each layer. Combining these  $Q_{ef}$  values with the thicknesses and  $V_S$  for each of the layers results in a total  $\kappa_0$  value of 21 msec, which includes the 6 msec assumed for the underlying reference rock. For the lower and upper profiles, the NRC staff calculated  $\kappa_0$  values of 30 and 16 msec, respectively, using the same approach as for the basecase profile. In contrast to the approach used by the NRC staff to determine  $\kappa_0$ , the licensee used the lowest low-strain damping values from the material damping curves over the top 152 m [500 ft] of the profile and assumed a constant damping value of 1.25 percent for the remainder to estimate  $\kappa_0$  values of 24, 33, and 17 msec for the basecase, lower, and upper profiles, respectively.

Table 2.3-4 provides the layer depths, lithologies,  $V_s$ , unit weights, and dynamic properties for the NRC staff's three profiles. In summary, the site response logic tree developed by the NRC staff for the Brunswick site consists of six alternatives; three basecase profiles (each with a different  $\kappa_0$  value) and two alternative dynamic property branches.

#### 2.3.3.2.3 *Methodology and Results*

The NRC staff followed the methodology described in Section 2.1.4 to develop the final site amplification factors. Figure 2.3-12 shows the overall median site amplification factors and their variability for each of the seven spectral frequencies. As shown in Figure 2.3-12, the median site amplification factors range from 1.5 to 2.5 before falling off with higher input spectral accelerations. The lower half of Figure 2.3-12 shows that the logarithmic standard deviations for the site amplification factors range from about 0.1 to 0.3.

#### 2.3.3.3 *Control Point Hazard*

The NRC staff implemented Approach 3 from the SPID to develop a weighted control point seismic hazard curve for each of the six unique combinations of the site response logic tree for the Brunswick site. After combining these curves to develop the final mean control point hazard curves, the NRC staff determined the  $10^{-4}$  and  $10^{-5}$  UHRS in order to calculate the final GMRS. Figure 2.3-13 shows the final control point mean seismic hazard curves for each of the seven spectral frequencies as well as the NRC staff's UHRS and GMRS, and the licensee's NTTF R2.1 GMRS (Hamrick, 2014). As shown in Figure 2.3-13, the NRC staff's GMRS (black curve) is moderately higher than the licensee's GMRS (blue curve) due to the differences in the modeling of potential nonlinear behavior, which are described in Section 2.3.3.2.2.

**Table 2.3-4 Layer Depths, Shear Wave Velocities ( $V_s$ ), Unit Weights, and Dynamic Properties for Brunswick**

Layer	Depth (ft)	Description	$V_s$ (ft/sec)			$V_s$ Sigma (ln)	BC Unit Weight (pcf)	Dynamic Properties	
			LR (0.3)	BC (0.4)	UR (0.3)			Alt. 1 (0.5)	Alt. 2 (0.5)
1	22	Soil: sand	868	1,122	1,450	0.25	120	EPRI Soil	Pen.
2	65	Soil: clay	4,256	5,500	7,108	0.15	150	EPRI Soil	Pen.
3	192	Rock: limestone	3,482	4,500	5,815	0.15	140	EPRI Rock	L 3.0%
4	500	Soil: sand, clay	2,322	3,000	3,877	0.15	130	EPRI Soil	Pen.
5	1,482	Soil: sand, clay	2,322	3,000	3,877	0.15	130	L 1%	L 1.0%

LR = lower range; BC = basecase; UR = upper range; ln = natural log; pcf = pounds per cubic foot; L = linear; Alt. = alternative; Pen. = Peninsular.  
 For LR, BC, UR, and Alt.: Values in parentheses refer to weights for site response analysis logic tree branches.

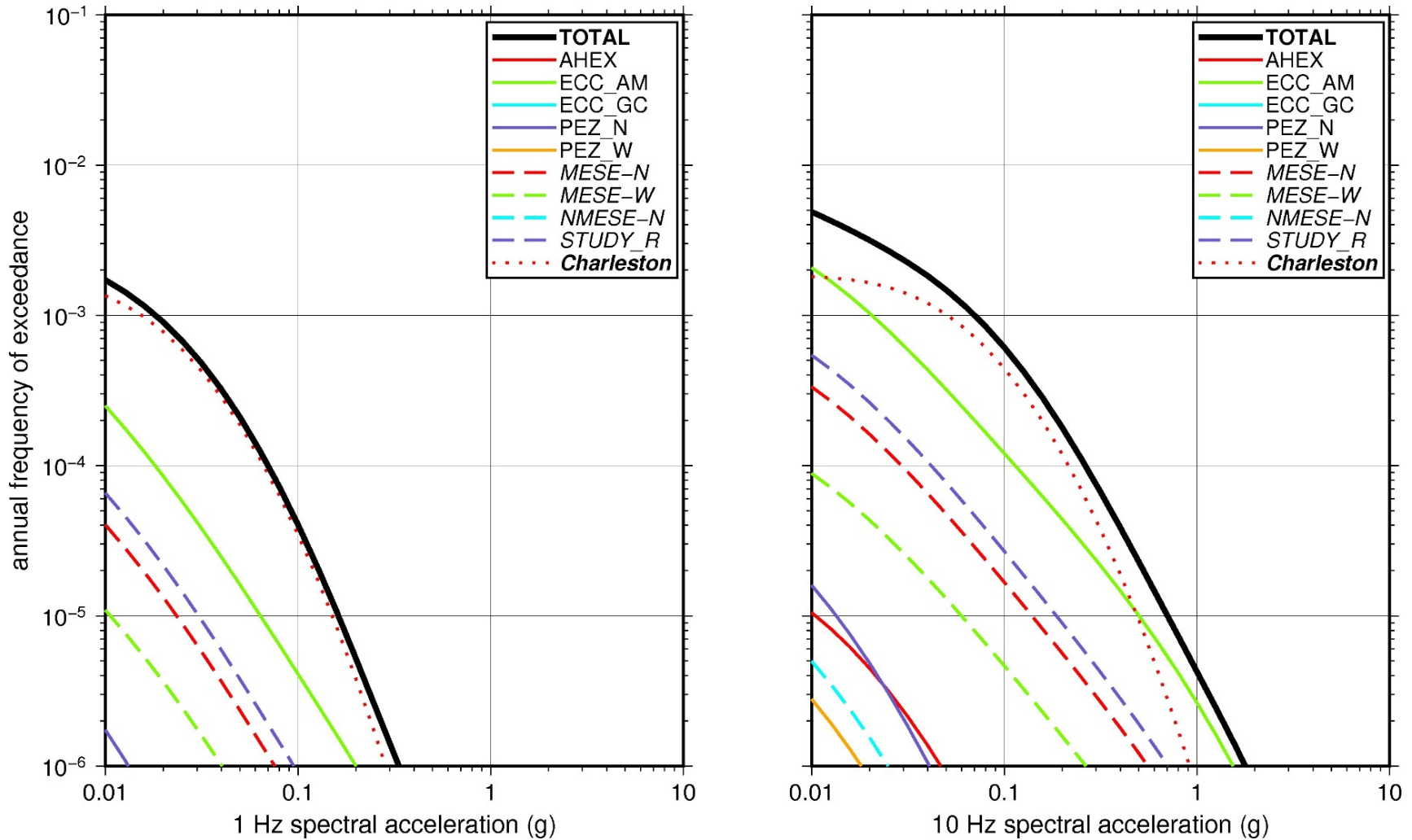


**Figure 2.3-10 Low-Frequency (1 Hz, Left) and High-Frequency (10 Hz, Right) Reference Rock Hazard Curves for Brunswick. Total Hazard is Shown as a Bold Black Line; Individual Contributions to the Hazard for Each of the CEUS-SSC Sources are Shown as Colored Lines Defined in the Legend. See Table 2.1-1 for Source Name Definitions**

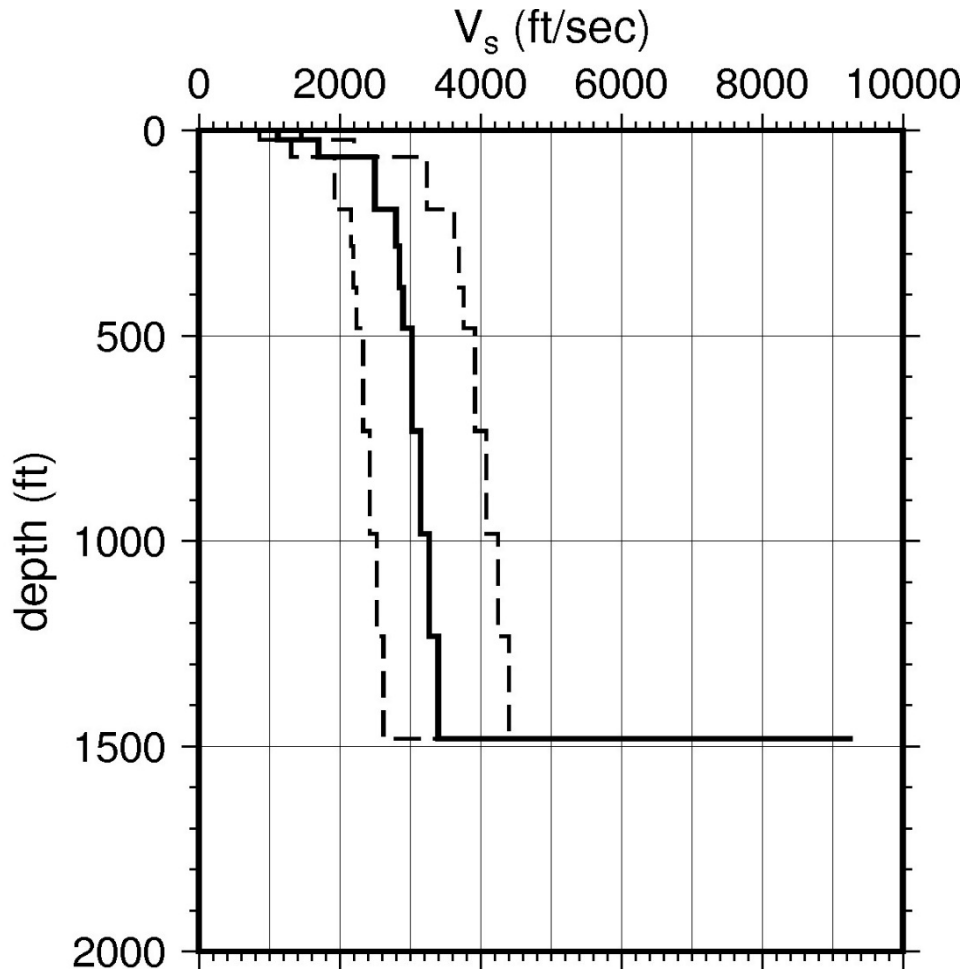


**Figure 2.3-11 Shear Wave Velocity ( $V_s$ ) Profiles for Brunswick. Basecase (BC) Profile Shown as Solid Bold Line; Lower and Upper Range (LR and UR) Profiles Shown as Dashed Lines. Profiles Terminate at Reference Rock Velocity of 2,831 m/sec [9,285 ft/sec] per EPRI GMM (2013)**

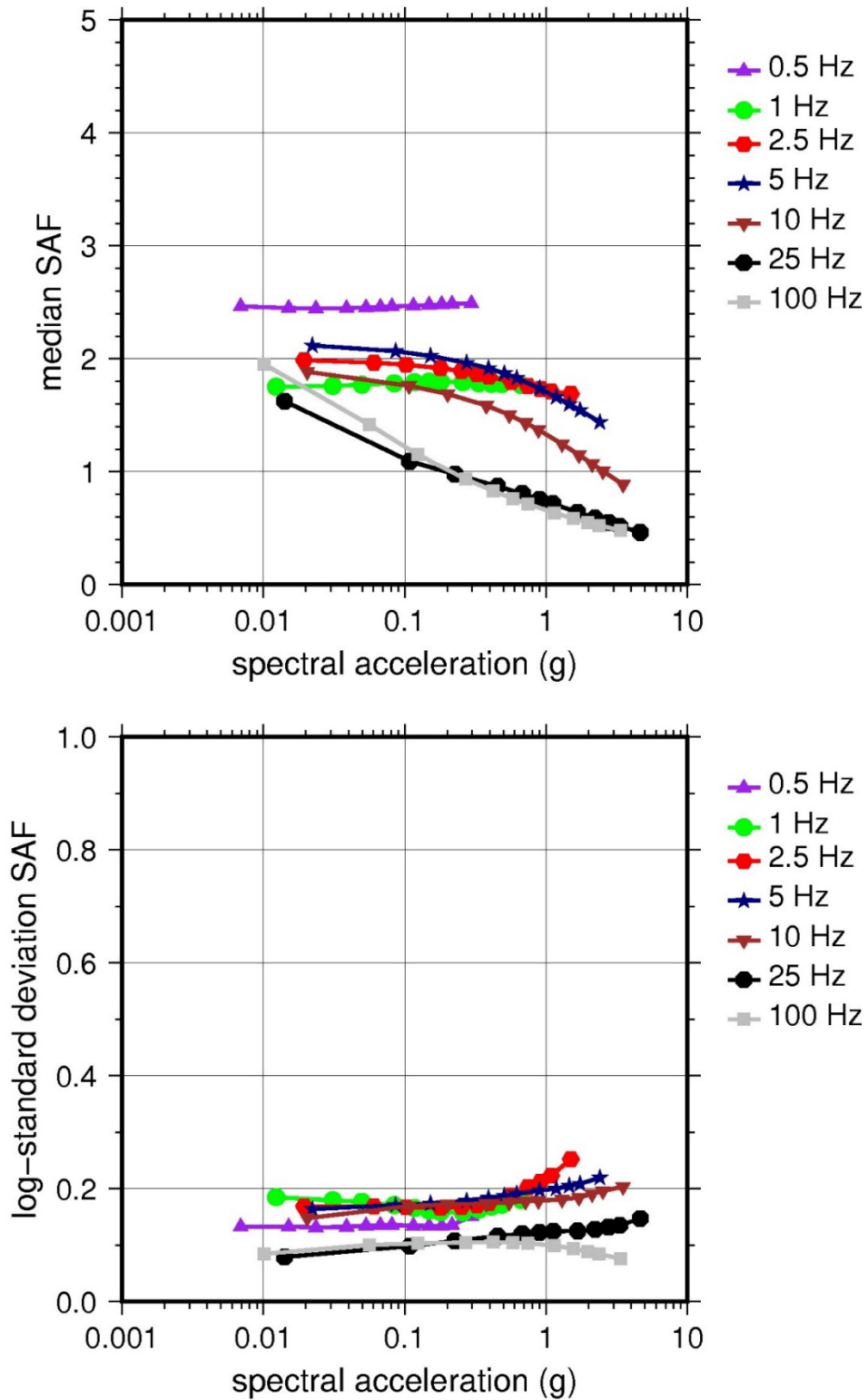


**Figure 2.3-12 Overall Weighted Median Site Amplification Factor (SAF) (Upper) and Log Standard Deviation of the SAF (Lower) as a Function of Input Acceleration for EPRI GMM (2013) Spectral Frequencies**



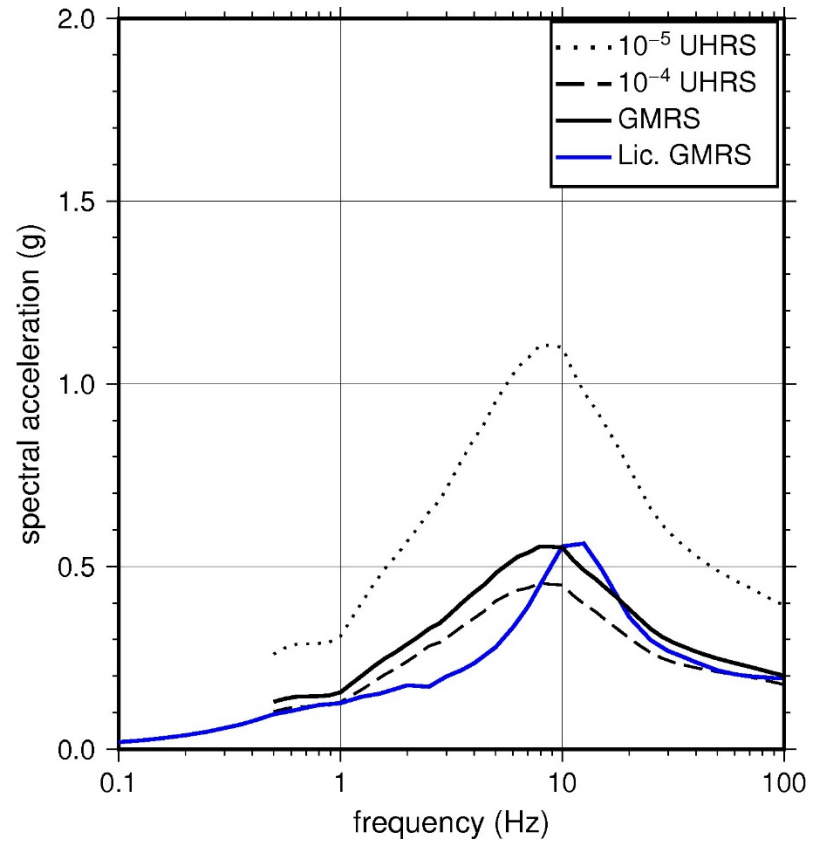
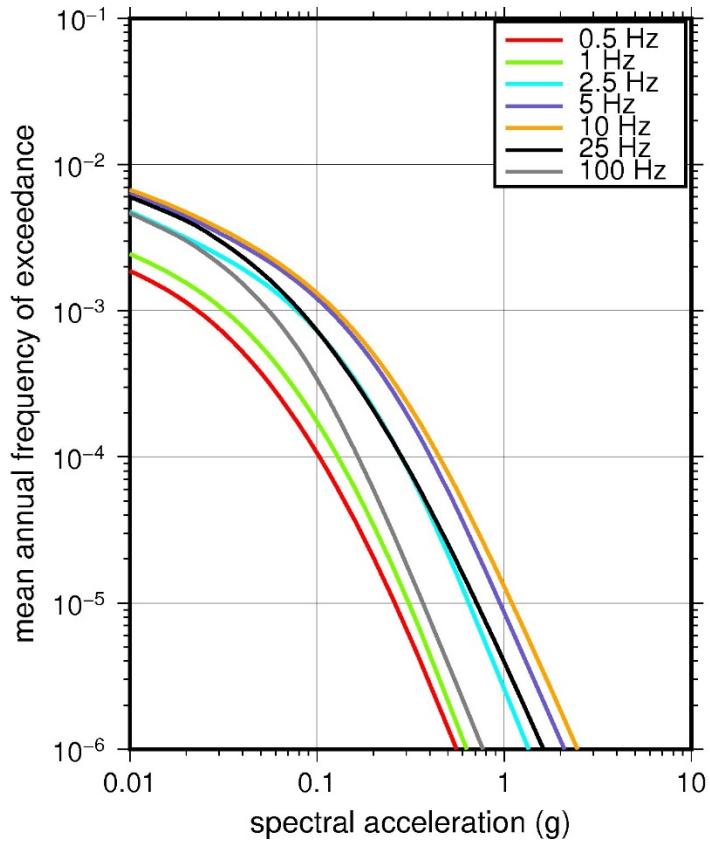


**Figure 2.3-13 Mean Control Point Hazard Curves (Left) for EPRI GMM (2013) Spectral Frequencies, and GMRS and UHRS (Right) for Brunswick**

## 2.3.4 Catawba

The Catawba Nuclear Station site is located in South Carolina adjacent to Lake Wylie in the Piedmont physiographic province and is founded on competent metamorphic igneous rock (adamellite) of Paleozoic age, which is partially weathered near the surface. The horizontal SSE response spectrum for Catawba has a Newmark spectral shape and is anchored at a PGA of 0.15g.

### 2.3.4.1 Reference Rock Hazard

For the reference rock PSHA, the NRC staff selected the nine CEUS-SSC (NRC, 2012b) background seismic source zones that are located within 320 km [200 mi] of the site. The NRC staff also selected the five CEUS-SSC RLME sources that are located within 806 km [500 mi] of the Catawba site. To develop the reference rock seismic hazard curves for the Catawba site, the NRC staff used the GMPEs in the updated EPRI GMM (2013). As shown in Figure 2.3-14, the Charleston RLME, which is located about 181 km [112 mi] to the west of Catawba, is the largest contributor to the 1 Hz reference rock total mean hazard curve at the  $10^{-4}$  AFE level. For the 10 Hz reference rock total mean hazard curve, the ECC-AM provides the highest overall contribution at the  $10^{-4}$  AFE level.

### 2.3.4.2 Site Response Evaluation

#### 2.3.4.2.1 Site Profiles

To develop a basecase profile, the NRC staff used the geologic information in the NTTF R2.1 SHSR (Henderson, 2014) submitted by Duke Energy (hereafter referred to as “the licensee” within this plant section). As described in the licensee’s SHSR, the Catawba site consists primarily of adamellite, which is a metamorphosed igneous rock of the Charlotte Belt. The site is underlain by a thin veneer of soils {about 8 m [25 ft]} overlying partially weathered rock grading into hard metamorphic igneous rock. The safety-related structures are supported on fill concrete, which overlies hard adamellite rock. In Table 2.3.1-1 of the SHSR, the licensee briefly described the subsurface materials in terms of the geologic units and layer thicknesses. For its site response evaluation, the NRC staff used a depth of 19 m [63 ft] from the surface, which is within the hard adamellite rock just beneath the concrete fill, as the control point elevation {elevation 162 m [531 ft] MSL} for the Catawba site.

The field investigations for Catawba consisted of a number of borings through the soil and upper portion of rock beneath the site. Seismic refraction, uphole, and crosshole surveys by the licensee measured  $V_P$  and  $V_S$  to a depth of about 31 m [100 ft] beneath the site. To determine a  $V_S$  for the concrete fill, the licensee used the unit weight, the unconfined compressive strength, and an assumed Poisson’s ratio. Table 2.3.2-2 of the SHSR gives the measured and estimated  $V_S$  determined from the licensee’s site investigations.

For its SHSR, the licensee developed a basecase profile that extends to a depth of 18 m [60 ft] below the control point elevation. The entire profile consists of fill concrete overlying hard adamellite rock (primarily siltstone, sandstone, and shale) from the Charlotte Belt. The  $V_S$  determined from the licensee’s geophysical investigations varies from about 1,738 m/sec [5,700 ft/sec] for the uppermost rock to 2,700 m/sec [8,850 ft/sec] at the base of the profile. Based on the material properties of the fill concrete, the licensee estimated a  $V_S$  of 2,073 m/sec [6,800 ft/sec] for the uppermost layer of the profile.

As multiple geophysical field investigations have characterized the rock strata beneath the Catawba site, the NRC staff used the licensee's layer thicknesses and  $V_S$  for its basecase profile.

To capture the uncertainty in its basecase profile, the NRC staff developed lower and upper range (10<sup>th</sup> and 90<sup>th</sup> percentile) profiles by multiplying the basecase  $V_S$  values by scale factors of 0.83 and 1.21, respectively, which corresponds to an epistemic logarithmic standard deviation of 0.15. The weights for the lower, best-estimate, and upper basecase profiles are 0.3, 0.4, and 0.3, respectively. As shown in Figure 2.3-15, the upper profile terminates at a depth of 9 m [29 ft], and the lower and best-estimate basecase profiles terminate at a depth of 19 m [61 ft] below the control point elevation.

#### 2.3.4.2.2 *Dynamic Material Properties and Site Kappa*

The NRC staff assumed both linear and nonlinear dynamic behavior for the rock beneath the Catawba site. To model the nonlinear behavior of the uppermost rock strata, the NRC staff used the EPRI rock shear modulus reduction and material damping curves. To model the linear behavior, the NRC staff used a constant damping ratio of 3 percent. The staff assumed these two alternative dynamic responses for the upper 8 m [26 ft] of the profile. Because of the higher  $V_S$  of these rock layers, the NRC staff assigned weights of 0.7 and 0.3 to the linear and nonlinear alternatives, respectively. For the remaining 11 m [35 ft] of its profile, the NRC staff assumed a linear response with a material damping ratio value of 0.1 percent to maintain consistency with the  $\kappa_0$  value for the Catawba site.

To determine the basecase  $\kappa_0$  for the Catawba site, the NRC staff first used the Campbell (2009) Model 1 relationship between  $V_S$  and  $Q_{ef}$  to determine a  $Q_{ef}$  for each layer. Combining these  $Q_{ef}$  values with the thicknesses and  $V_S$  for each of the layers results in a total  $\kappa_0$  value of about 6.1 msec, which includes the 6 msec assumed for the underlying reference rock. For the lower and upper basecase profiles, the NRC staff calculated  $\kappa_0$  values of 6.2 and 6.0 msec, respectively, using the same approach as for the best-estimate basecase profile. In contrast, the licensee estimated  $\kappa_0$  by combining the lowest low-strain damping values from the EPRI rock material damping curves over the entire profile to estimate best-estimate, lower, and upper basecase  $\kappa_0$  values of 6.5, 6.6, and 6.4 msec, respectively.

Table 2.3-5 provides the layer depths, lithologies,  $V_S$ , unit weights, and dynamic properties for the NRC staff's three profiles. In summary, the site response logic tree developed by the NRC staff for the Catawba site consists of six alternatives; three basecase profiles (each with a different  $\kappa_0$  value) and two alternative dynamic property branches.

#### 2.3.4.2.3 *Methodology and Results*

The NRC staff followed the methodology described in Section 2.1.4 to develop the final site amplification factors. Figure 2.3-16 shows the overall median site amplification factors and their variability for each of the seven spectral frequencies. As shown in Figure 2.3-16, the median site amplification factors are all close to 1. The lower half of Figure 2.3-16 shows that the logarithmic standard deviations for the site amplification factors are less than 0.1.

#### 2.3.4.3 *Control Point Hazard*

The NRC staff implemented Approach 3 from the SPID to develop a weighted control point seismic hazard curve for each of the six unique combinations of the site response logic tree for

the Catawba site. After combining these curves to develop the final mean control point hazard curves, the NRC staff determined the  $10^{-4}$  and  $10^{-5}$  UHRS in order to calculate the final GMRS. Figure 2.3-17 shows the final control point mean seismic hazard curves for each of the seven spectral frequencies as well as the NRC staff's UHRS and GMRS, and the licensee's NTTF R2.1 GMRS (Henderson, 2014). As shown in Figure 2.3-17, the NRC staff's GMRS (black curve) is similar to the licensee's GMRS (blue curve) over the entire frequency range. For comparison, Figure 2.3-17 also shows the NRC staff's reference rock GMRS (brown dotted curve).

Layer	Depth (ft)	Description	$V_s$ (ft/sec)			$V_s$ Sigma (ln)	BC Unit Weight (pcf)	Dynamic Properties	
			LR (0.3)	BC (0.4)	UR (0.3)			Alt. 1 (0.3)	Alt. 2 (0.7)
1	12	Rock: adamellite	5,610	6,800	8,242	0.25	150	EPRI Rock	L 3.0%
2	14	Rock: adamellite	4,722	5,723	6,937	0.15	150	EPRI Rock	L 3.0%
3	26	Rock: adamellite	5,738	6,955	8,430	0.15	150	EPRI Rock	L 3.0%
4	37	Rock: adamellite	6,421	7,783	9,285	0.15	160	L 0.1%	L 0.1%
5	44	Rock: adamellite	7,056	8,552	9,285	0.15	160	L 0.1%	L 0.1%
6	61	Rock: adamellite	7,305	8,854	9,285	0.15	160	L 0.1%	L 0.1%

LR = lower range; BC = basecase; UR = upper range; ln = natural log; pcf = pounds per cubic foot; L = linear; Alt. = alternative.  
 For LR, BC, UR, and Alt.: Values in parentheses refer to weights for site response analysis logic tree branches.

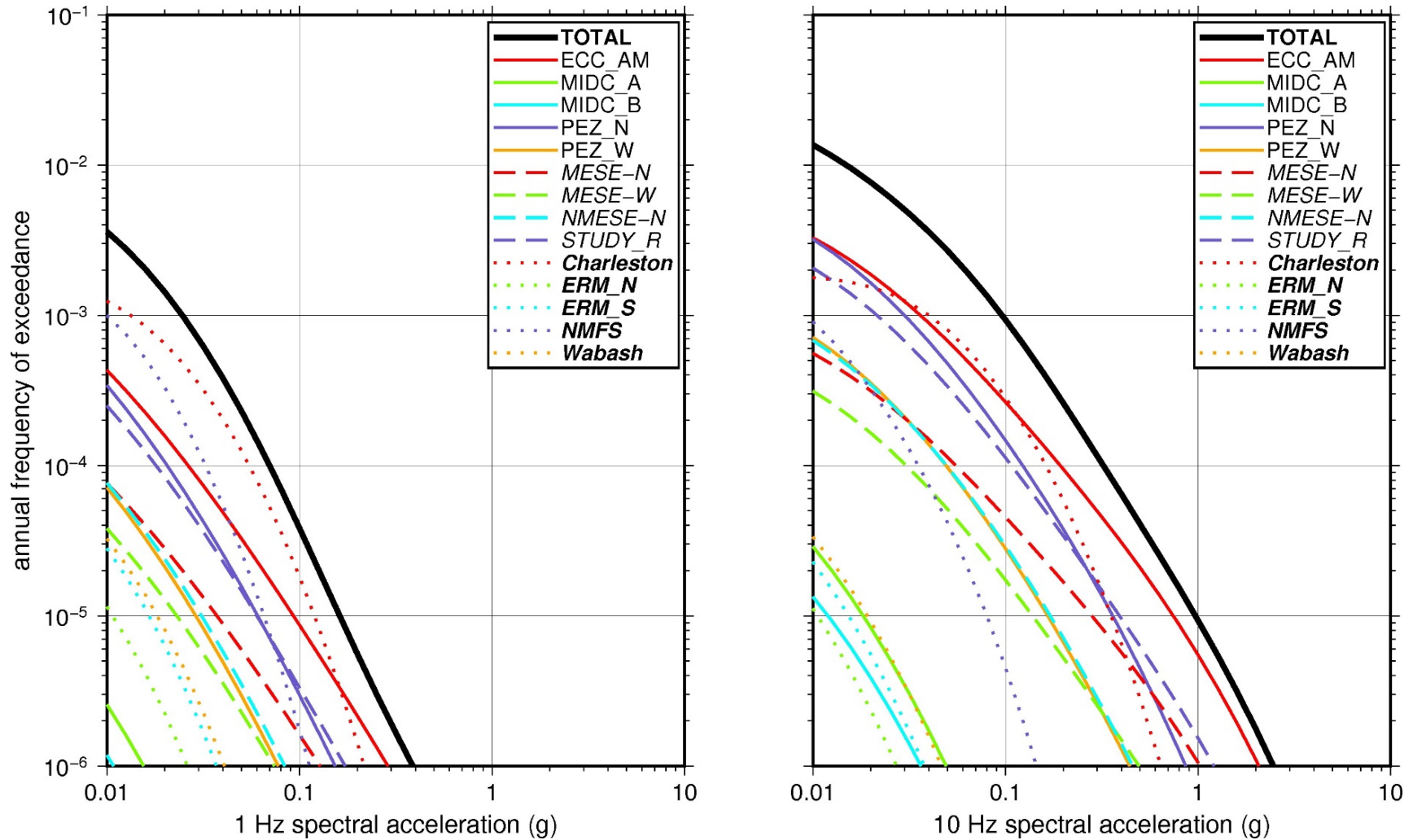


**Figure 2.3-14 Low-Frequency (1 Hz, Left) and High-Frequency (10 Hz, Right) Reference Rock Hazard Curves for Catawba. Total Hazard is Shown as a Bold Black Line; Individual Contributions to the Hazard for Each of the CEUS-SSC Sources are Shown as Colored Lines Defined in the Legend. See Table 2.1-1 for Source Name Definitions**

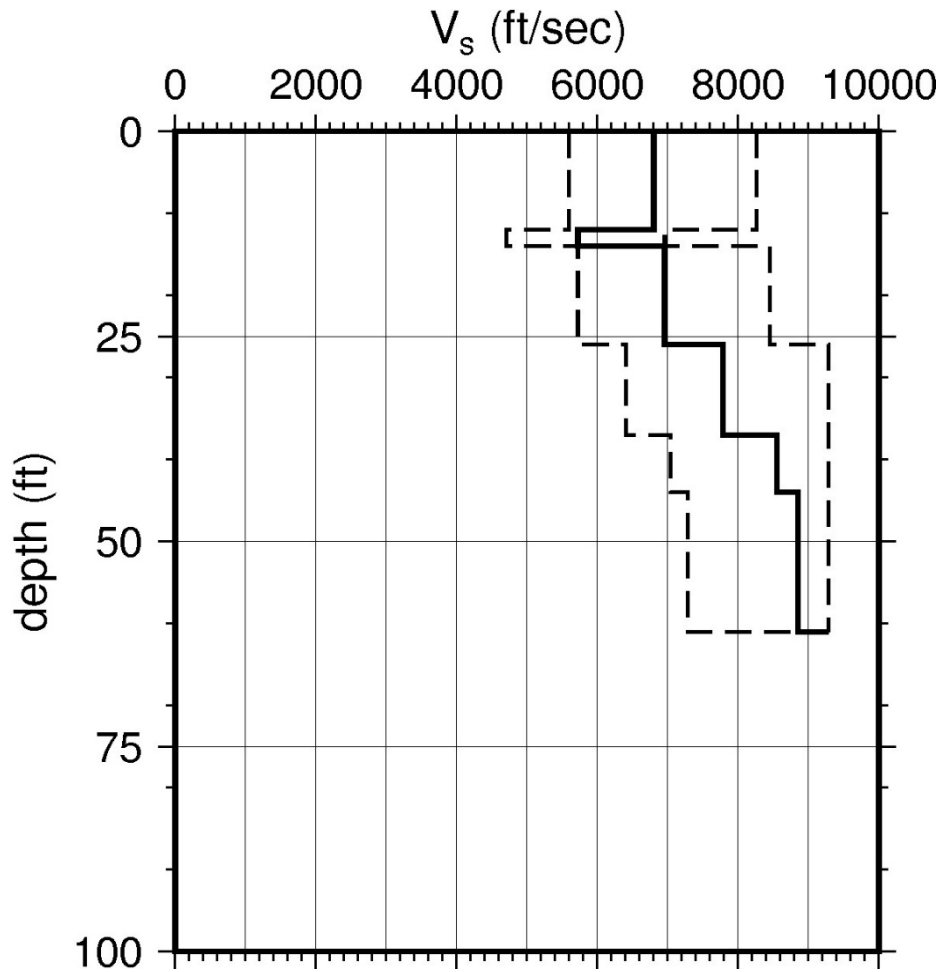


**Figure 2.3-15 Shear Wave Velocity ( $V_s$ ) Profiles for Catawba. Basecase (BC) Profile Shown as Solid Bold Line; Lower and Upper Range (LR and UR) Profiles Shown as Dashed Lines. Profiles Terminate at Reference Rock Velocity of 2,831 m/sec [9,285 ft/sec] per EPRI GMM (2013)**

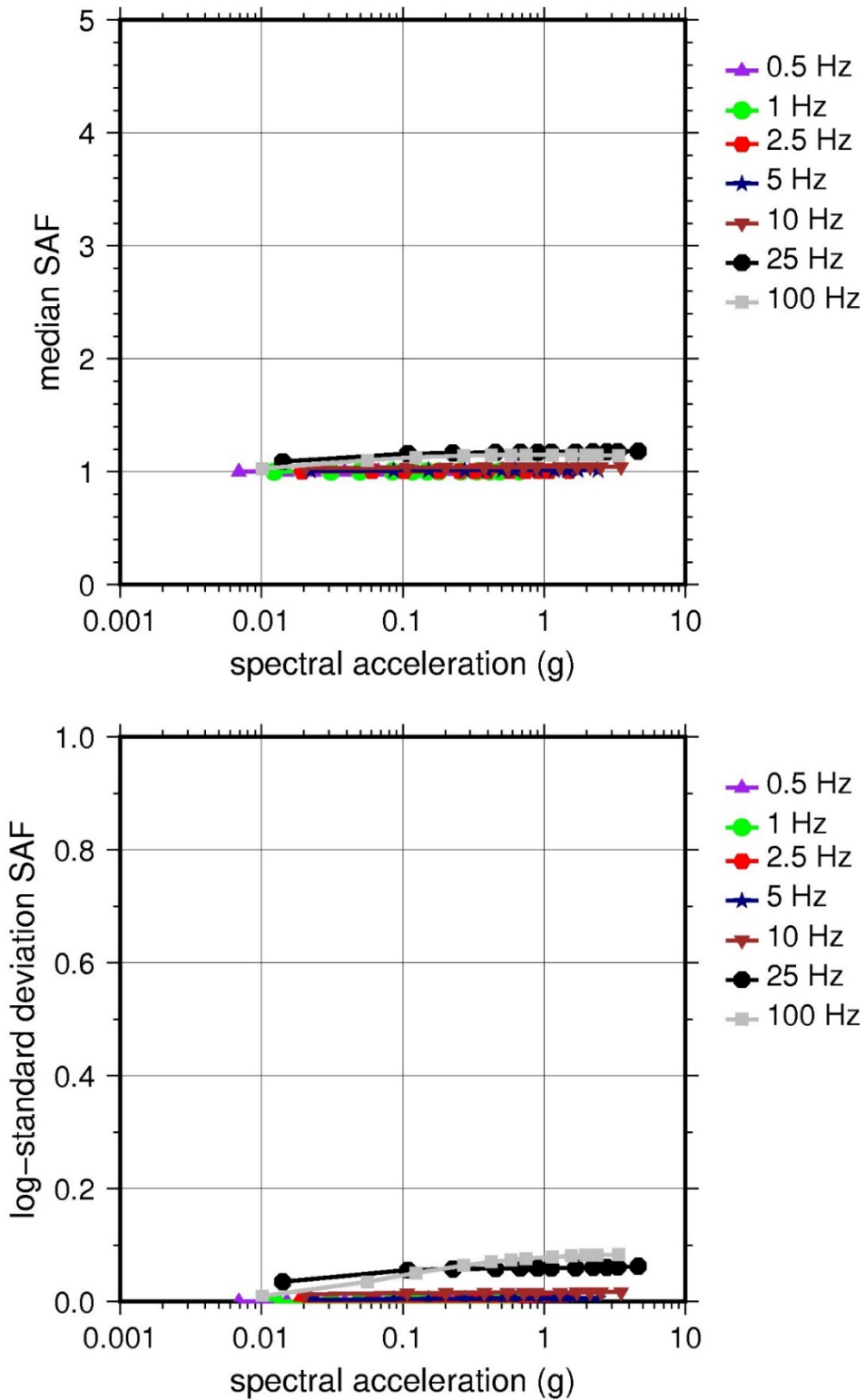


**Figure 2.3-16 Overall Weighted Median Site Amplification Factor (SAF) (Upper) and Log Standard Deviation of the SAF (Lower) as a Function of Input Acceleration for EPRI GMM (2013) Spectral Frequencies**

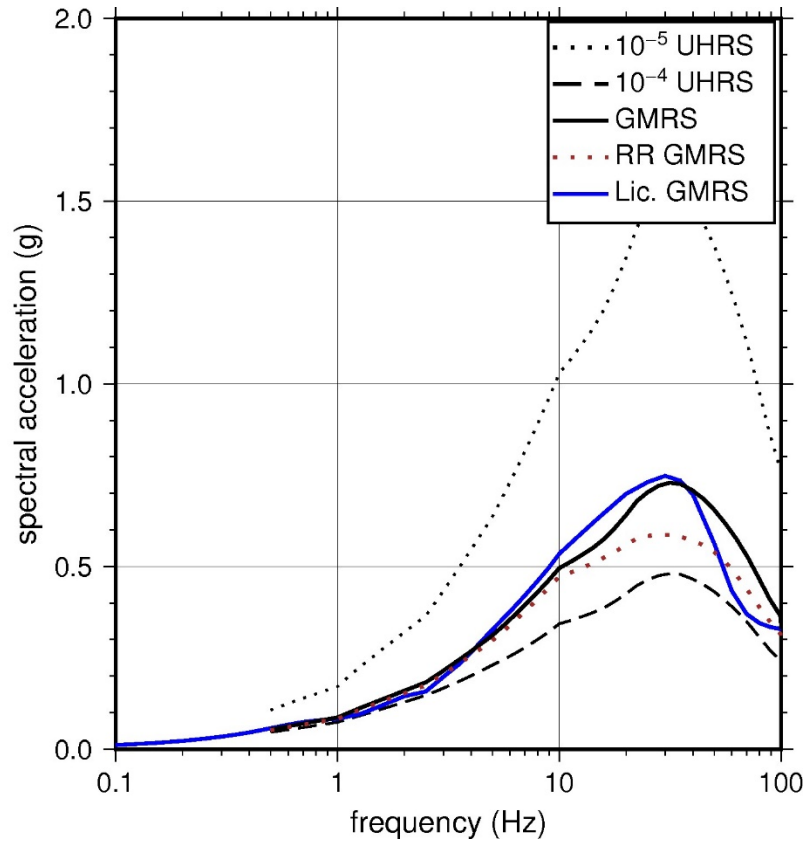
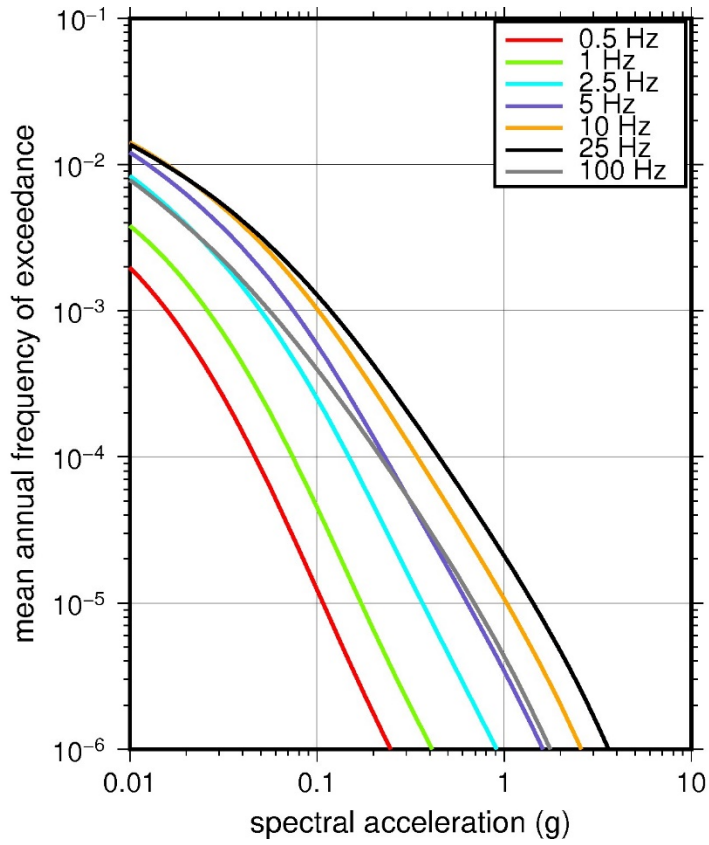


**Figure 2.3-17 Mean Control Point Hazard Curves (Left) for EPRI GMM (2013) Spectral Frequencies, and GMRS and UHRs (Right) for Catawba**



### 2.3.5 Farley

The Joseph M. Farley Nuclear Plant site is located in Alabama on the west side of the Chattahoochee River within the Coastal Plain physiographic province and is founded on about 2,134 m [7,000 ft] of sedimentary strata over basement rock of Paleozoic age. The horizontal SSE response spectrum for Catawba has a Newmark spectral shape and is anchored at a PGA of 0.10g.

#### 2.3.5.1 Reference Rock Hazard

For the reference rock PSHA, the NRC staff selected the 13 CEUS-SSC (NRC, 2012b) background seismic source zones that are located within 320 km [200 mi] of the site. In addition to the Charleston CEUS-SSC RLME, the NRC staff also selected additional RLME sources that are within 806 km [500 mi]. To develop the reference rock seismic hazard curves for the site, the NRC staff used the GMPEs in the updated EPRI GMM (2013). As shown in Figure 2.3-18, the NMFS RLME is the largest contributor to both the 1 Hz and 10 Hz reference rock total mean hazard curves at the  $10^{-4}$  AFE level.

#### 2.3.5.2 Site Response Evaluation

##### 2.3.5.2.1 Site Profiles

To develop a basecase profile, the NRC staff used the geologic information in the NTTF R2.1 SHSR (Pierce, 2014a) submitted by Southern Nuclear Operating Company (hereafter referred to as “the licensee” within this plant section). As described in the licensee’s SHSR, the Farley site consists of alternating layers of uncemented sands, clays, and indurated sediments, including claystone, siltstone, limestone, and shale. The safety-related structures are supported on siltstone, sandstone, limestone, and sands from the Lisbon Formation. In Table 2.3.1-2 of the SHSR, the licensee briefly described the subsurface materials in terms of the geologic units and layer thicknesses. For its site response evaluation, the NRC staff used the top of the ground surface, which corresponds to an elevation of 56 m [185 ft] above MSL, as the control point elevation for the Farley site.

The siting explorations for Farley consisted of a number of borings through the uppermost soil and rock beneath the site. Seismic refraction, uphole, and crosshole surveys by the licensee for both the original plant siting investigation and a more recent ISFSI measured  $V_P$  and  $V_S$  to a depth of about 55 m [180 ft] beneath the site. To determine the  $V_S$  for the strata below the exploration depth at the plant, the licensee used the sonic velocities from nearby boreholes along with assumed Poisson’s ratio values appropriate for the sediment type. Table 2.3.2-2 of the SHSR gives the measured and estimated  $V_S$  determined from the licensee’s site investigations.

For its SHSR, the licensee developed a basecase profile that extends to a depth of 2,400 m [7,850 ft] below the control point elevation. The uppermost layers {7 m [90 ft]} of the profile consist of overburden material (sand and clay), for which the licensee measured an average  $V_S$  of 248 m/sec [812 ft/sec]. Beneath this layer of sand and clay is a 37 m [120 ft] thick layer of claystone, limestone, and sand from the Eocene age Lisbon Formation of the Clairborne Group, which has an average  $V_S$  of about 915 m/sec [3,000 ft/sec]. Underlying the Lisbon Formation is the Tallahatta Formation, which is also from the Clairborne Group and consists of sand, clay, sandstone, and limestone. This unit has a thickness of 41 m [135 ft] and an average  $V_S$  of 496 m/sec [1,628 ft/sec]. Below the Lisbon and Clairborne Formations are over 610 m [2,000 ft]

of sedimentary strata from the Wilcox, Midway, and Selma Groups, which range in age from Eocene to Late Cretaceous and in  $V_S$  from about 610 m/sec [2,000 ft/sec] to 1,200 m/sec [4,000 ft/sec]. Underlying the Selma Group are sandstones from the Cretaceous age Eutaw Formation and shale, sandstone, sand, and gravel from the Tuscaloosa Formation. These two formations have an average  $V_S$  of about 1,220 m/sec [4,000 ft/sec] and a thickness of about 201 m [660 ft]. For the remaining 1,250 m [4,100 ft] of Cretaceous age sediments, the licensee assumed that the  $V_S$  gradually increases from about 1,220 m/sec [4,000 ft/sec] to 1,830 m/sec [6,000 ft/sec]. Finally, the licensee included 168 m [550 ft] of Paleozoic age sedimentary strata, for which it estimated a  $V_S$  of 1,921 m/sec [6,300 ft/sec].

As the soil and rock strata beneath the Farley site has been characterized by multiple geophysical field investigations along with sonic velocities from regional boreholes, the NRC staff used the licensee's layer thicknesses and  $V_S$  for its basecase profile. However, rather than extend the basecase profile to a depth of 2,400 m [7,850 ft], the NRC staff terminated its profile at a depth of 1,220 m [4,000 ft] below the control point elevation. The NRC staff concluded that a profile thickness of 1,220 m [4,000 ft] is sufficient to capture the site amplification of the lowest spectral frequency of interest at 0.5 Hz.

To capture the uncertainty in its basecase profile, the NRC staff developed lower and upper range (10<sup>th</sup> and 90<sup>th</sup> percentile) profiles by multiplying the basecase  $V_S$  values by scale factors of 0.78 and 1.29, respectively, which corresponds to an epistemic logarithmic standard deviation of 0.20. The weights for the lower, best-estimate, and upper basecase profiles are 0.3, 0.4, and 0.3, respectively. Figure 2.3-19 shows the NRC staff's basecase profiles.

#### 2.3.5.2.2 *Dynamic Material Properties and Site Kappa*

The NRC staff assumed both linear and nonlinear behavior for the soil and rock beneath the Farley site. To model the nonlinear response within the upper 27 m [90 ft] of soil deposits (Layer 1), the NRC staff used the EPRI soil shear modulus reduction and material damping curves as one alternative and the Peninsular Range curves for the second equally weighted alternative. To model the nonlinear behavior of the rock strata, the NRC staff used the EPRI rock shear modulus reduction and material damping curves. To model the linear behavior, the NRC staff used a constant damping ratio of 3 percent. The NRC staff assumed these two alternative dynamic responses for the Lisbon and Tallahatta Formations (Layers 2 to 6) and gave them equal weight. For the remaining 1,123 m [3,683 ft] of the profile, the NRC staff assumed a linear response with a material damping ratio value of 1 percent to maintain consistency with the  $\kappa_0$  value for the Farley site.

To determine the basecase  $\kappa_0$  for the Farley site, the NRC staff first used the Campbell (2009) Model 1 relationship between  $V_S$  and  $Q_{ef}$  to determine the  $Q_{ef}$  for each layer. Combining these  $Q_{ef}$  values with the thicknesses and  $V_S$  for each of the layers results in a total  $\kappa_0$  value of 37 msec, which includes the 6 msec assumed for the underlying reference rock. For the lower and upper profiles, the NRC staff calculated values of 55 and 26 msec, respectively, using the same approach as for the basecase profile. In contrast, the licensee used a  $\kappa_0$  value of 40 msec for the basecase, lower, and upper profiles, which is the maximum value recommended by Appendix B to the SPID (EPRI, 2012) for CEUS deep soil sites. For comparison, using the Chapman and Conn (2016) Gulf Coast  $\kappa_0$  relationship with a sedimentary thickness of 2,000 m [6,560 ft] for the Farley site results in a  $\kappa_0$  value of 62 msec.

Table 2.3-6 provides the layer depths, lithologies,  $V_S$ , unit weights, and dynamic properties for the NRC staff's three profiles. In summary, the site response logic tree developed by the NRC

staff for the Farley site consists of six alternatives; three basecase profiles (each with a different  $\kappa_0$  value) and two alternative dynamic property branches.

#### 2.3.5.2.3 *Methodology and Results*

The NRC staff followed the methodology described in Section 2.1.4 to develop the final site amplification factors. Figure 2.3-20 shows the overall median site amplification factors and their variability for each of the seven spectral frequencies. As shown in Figure 2.3-20, the median site amplification factors vary from 2 to 3 before falling off with higher input spectral accelerations. The lower half of Figure 2.3-20 shows that the logarithmic standard deviations for the site amplification factors vary from 0.05 to 0.3.

#### 2.3.5.3 *Control Point Hazard*

The NRC staff implemented Approach 3 from the SPID to develop a weighted control point seismic hazard curve for each of the six unique combinations of the site response logic tree for the Farley site. After combining these curves to develop the final mean control point hazard curves, the NRC staff determined the  $10^{-4}$  and  $10^{-5}$  UHRS in order to calculate the final GMRS. Figure 2.3-21 shows the final control point mean seismic hazard curves for each of the seven spectral frequencies as well as the NRC staff's UHRS and GMRS, and the licensee's NTTF R2.1 GMRS (Pierce, 2014a). As shown in Figure 2.3-21, the NRC staff's GMRS (black curve) is similar to the licensee's GMRS (blue curve) over the entire frequency range.

**Table 2.3-6 Layer Depths, Shear Wave Velocities ( $V_s$ ), Unit Weights, and Dynamic Properties for Farley**

Layer	Depth (ft)	Description	$V_s$ (ft/sec)			$V_s$ Sigma (ln)	BC Unit Weight (pcf)	Dynamic Properties	
			LR (0.3)	BC (0.4)	UR (0.3)			Alt. 1 (0.5)	Alt. 2 (0.5)
1	90	Soil: sand, clay	628	812	1,049	0.25	120	EPRI Soil	Pen.
2	120	Rock & Soil: siltstone, sand	2,335	3,018	3,900	0.15	130	EPRI Rock	L 3.0%
3	135	Rock & Soil: siltstone, sand	1,260	1,628	2,104	0.15	130	EPRI Rock	L 3.0%
4	185	Rock & Soil: siltstone, sand	1,432	1,850	2,391	0.15	130	EPRI Rock	L 3.0%
5	251	Rock & Soil: limestone, sand, clay	2,817	3,640	4,704	0.15	140	EPRI Rock	L 3.0%
6	317	Rock & Soil: limestone, sand, clay	2,468	3,189	4,121	0.15	130	EPRI Rock	L 3.0%
7	1,011	Rock & Soil: sand, sandstone	3,107	4,015	5,188	0.15	140	L 1.0%	L 1.0%
8	1,901	Rock & Soil: sand, shale, sandstone	3,132	4,048	5,231	0.15	140	L 1.0%	L 1.0%
9	2,501	Rock & Soil: sand, shale, sandstone	3,019	3,901	5,041	0.15	140	L 1.0%	L 1.0%
10	3,501	Rock & Soil: sand, shale, sandstone	3,518	4,546	5,875	0.15	140	L 1.0%	L 1.0%
11	4,000	Rock & Soil: sand, shale, sandstone	3,869	5,000	6,461	0.15	140	L 1.0%	L 1.0%

LR = lower range; BC = basecase; UR = upper range; ln = natural log; pcf = pounds per cubic foot; L = linear; Alt. = alternative; Pen. = Peninsular.  
 For LR, BC, UR, and Alt.: Values in parentheses refer to weights for site response analysis logic tree branches.

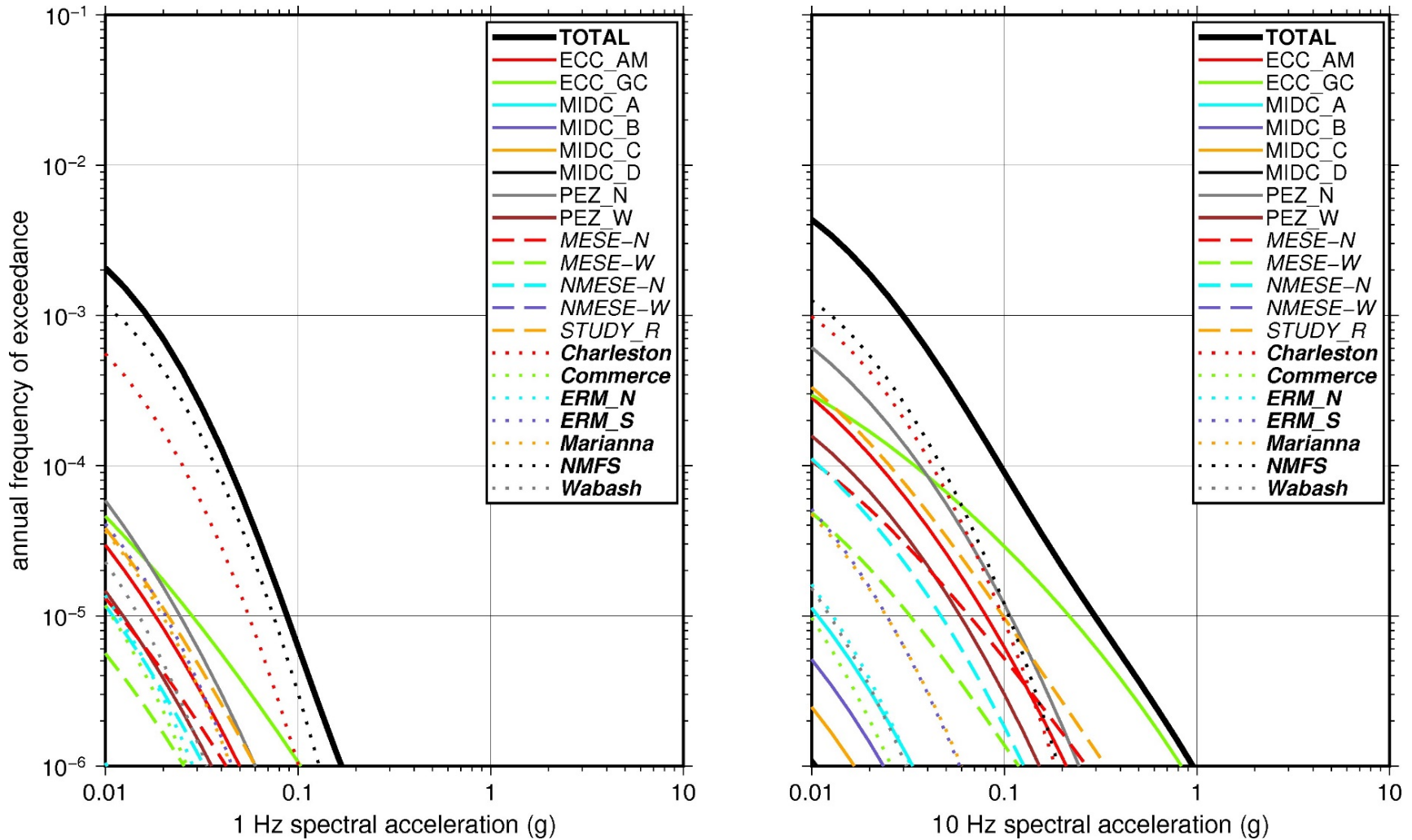


**Figure 2.3-18 Low-Frequency (1 Hz, Left) and High-Frequency (10 Hz, Right) Reference Rock Hazard Curves for Farley. Total Hazard is Shown as a Bold Black Line; Individual Contributions to the Hazard for Each of the CEUS-SSC Sources are Shown as Colored Lines Defined in the Legend. See Table 2.1-1 for Source Name Definitions**

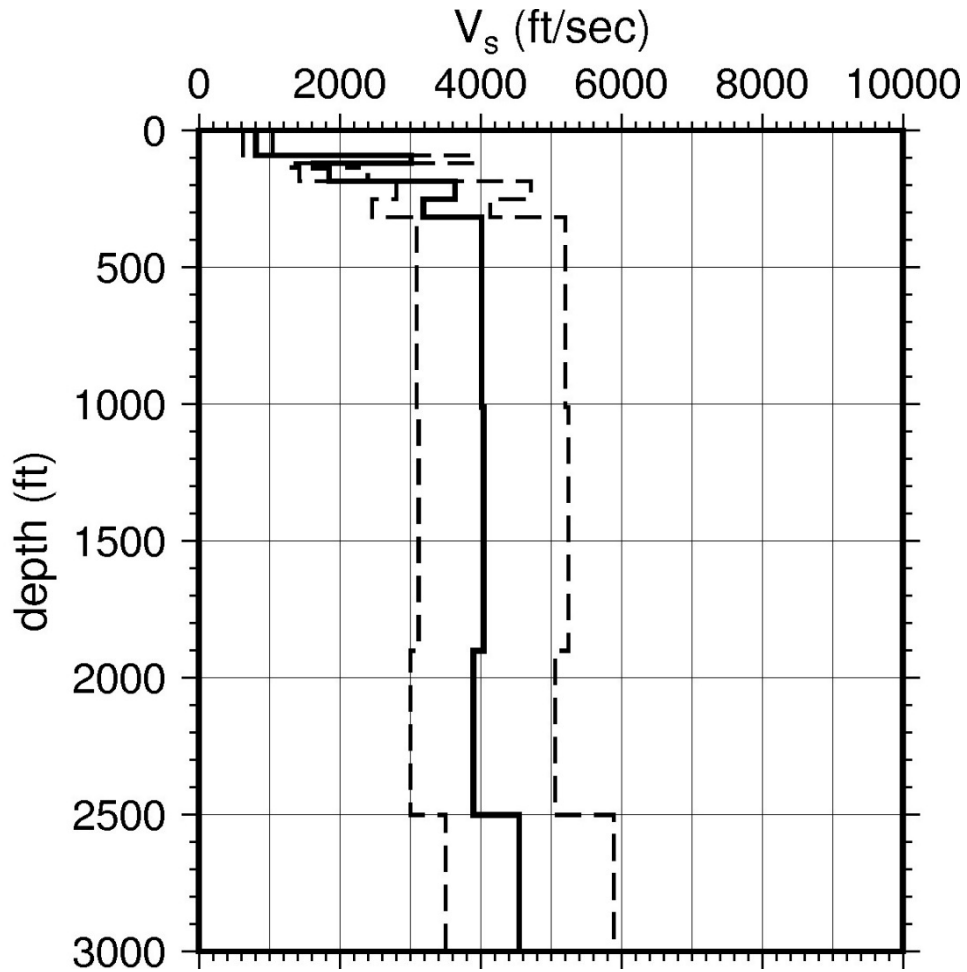


**Figure 2.3-19 Shear Wave Velocity ( $V_s$ ) Profiles for Farley. Basecase (BC) Profile Shown as Solid Bold Line; Lower and Upper Range (LR and UR) Profiles Shown as Dashed Lines. Profiles Terminate at Reference Rock Velocity of 2,831 m/sec [9,285 ft/sec] per EPRI GMM (2013)**

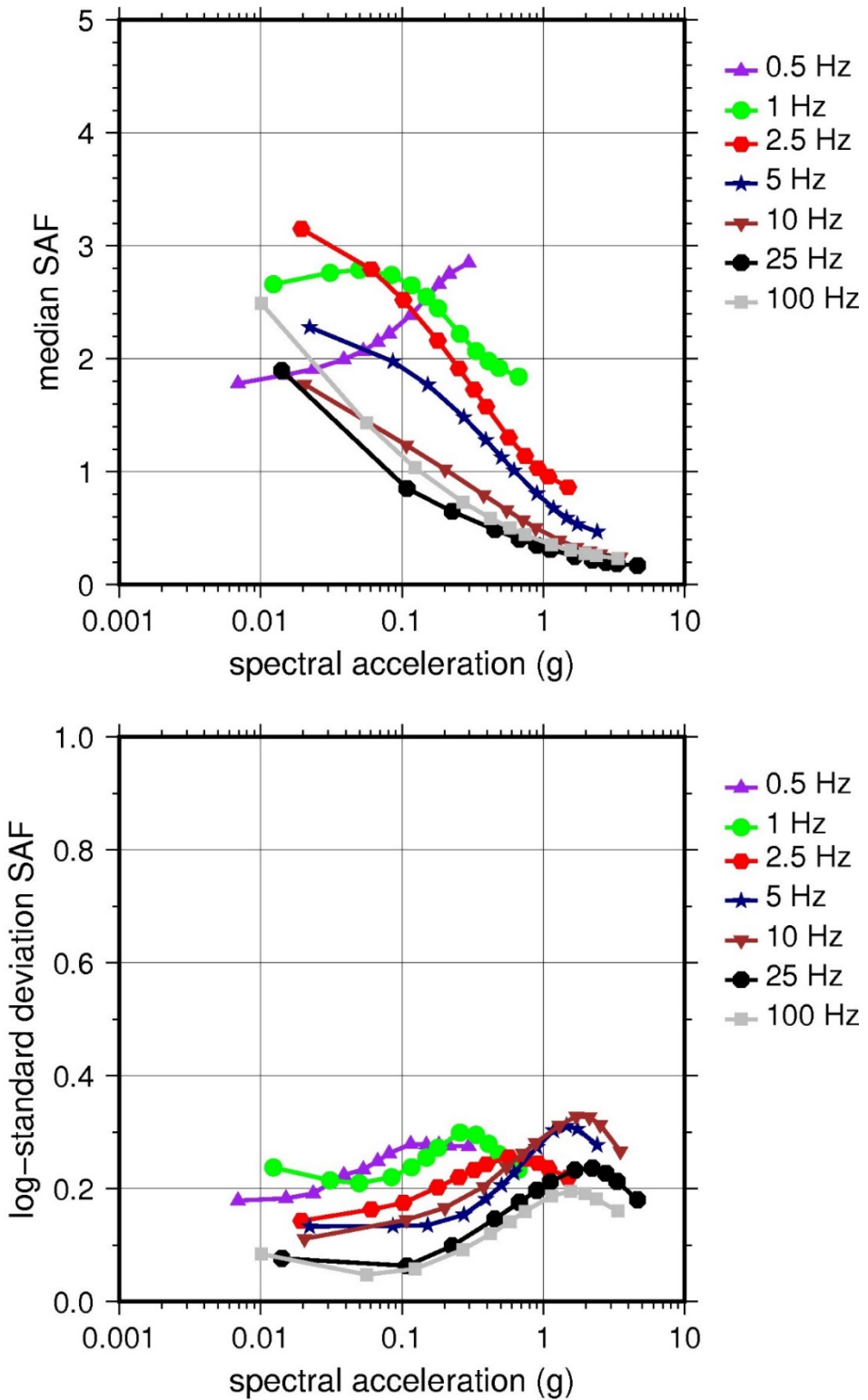


**Figure 2.3-20 Overall Weighted Median Site Amplification Factor (SAF) (Upper) and Log Standard Deviation of the SAF (Lower) as a Function of Input Acceleration for EPRI GMM (2013) Spectral Frequencies**

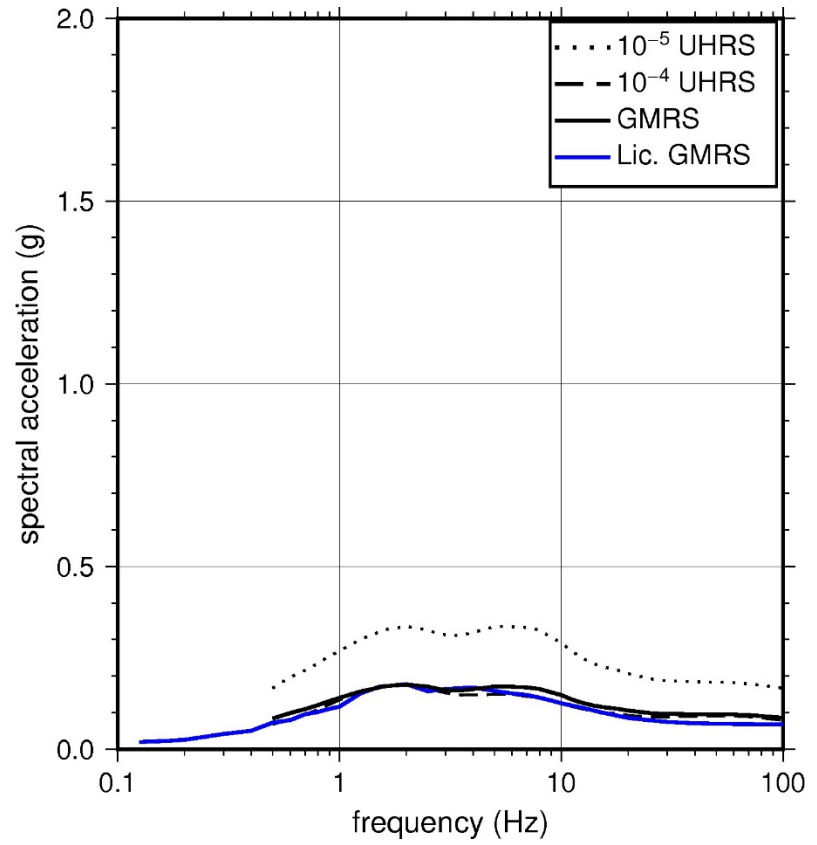
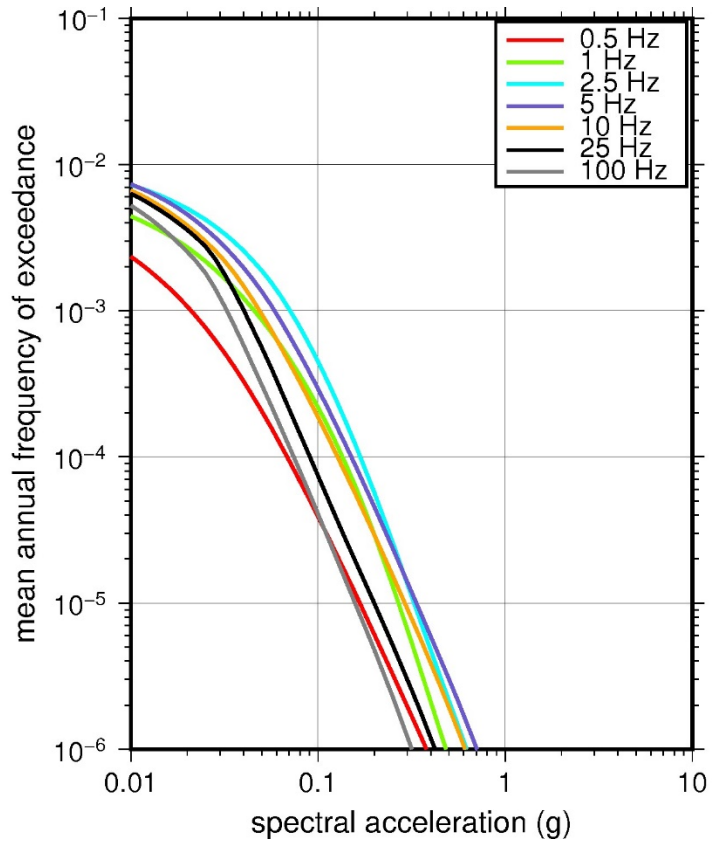


**Figure 2.3-21 Mean Control Point Hazard Curves (Left) for EPRI GMM (2013) Spectral Frequencies, and GMRS and UHRS (Right) for Farley**



## 2.3.6 Harris

The Shearon Harris Nuclear Power Plant site is located in North Carolina adjacent to Harris Lake within the Piedmont physiographic province and is founded on competent sedimentary rock (siltstone and sandstone) of Mesozoic age, which is assumed to be about 1,524 m [5,000 ft] thick. The horizontal SSE response spectrum for Harris has an RG 1.60 spectral shape and is anchored at a PGA of 0.15g.

### 2.3.6.1 Reference Rock Hazard

For the reference rock PSHA, the NRC staff selected the eight CEUS-SSC (NRC, 2012b) background seismic source zones that are located within 320 km [200 mi] of the site. The NRC staff also selected the Charleston and NMFS CEUS-SSC RLME sources, which are located about 152 km [95 mi] and 933 km [579 mi], respectively, from the Harris site. To develop the reference rock seismic hazard curves for the site, the NRC staff used the GMPEs in the updated EPRI GMM (2013). As shown in Figure 2.3-22, the Charleston RLME is the largest contributor to both the 1 Hz and 10 Hz reference rock total mean hazard curves at the  $10^{-4}$  AFE level.

### 2.3.6.2 Site Response Evaluation

#### 2.3.6.2.1 Site Profiles

To develop a basecase profile, the NRC staff used the geologic information in the NTTF R2.1 SHSR (Kapapoulos, 2014) submitted by Duke Energy (hereafter referred to as “the licensee” within this plant section). As described in the licensee’s SHSR, the Harris site consists of a veneer of residual soils overlying partially weathered rock grading into sound bedrock. The site structures are founded on fluvial clastic rocks (siltstone and sandstone) of the Deep River Triassic Basin, which is a trough-like topographic lowland located mostly within the Piedmont physiographic province. In Table 2.3.1-1 of the SHSR, the licensee briefly described the subsurface materials in terms of the geologic units and layer thicknesses. For its site response evaluation, the NRC staff used the top of the sound rock at a depth of 5 m [16 ft], which corresponds to an elevation of 78 m [255 ft] MSL, as the control point elevation for the Harris site.

The licensee’s SHSR profile is based on in situ geophysical investigations for Unit 1, which included multiple seismic refraction surveys and ambient vibration measurements. Although numerous geophysical measurements, including seismic suspension logging, downhole velocity surveys, and SASW, were performed for the now-withdrawn COL for Units 2 and 3, the licensee only used these measured  $V_S$  to confirm the uppermost  $V_S$  for the sound bedrock beneath the plant obtained from the original siting investigations. Therefore, for the bedrock beneath the plant, Table 2.3.1-1 of the SHSR gives only the  $V_S$  for uppermost layer of sound bedrock at a depth of 5 m [16 ft] below the surface.

For its SHSR, the licensee developed a basecase profile that extends to a depth of 1,524 m [5,000 ft] below the control point elevation. The uppermost layers of the profile consist of Triassic age sedimentary rock (primarily siltstone and sandstone) from the Sanford Formation. The  $V_S$  determined from the Unit 1 investigation for this upper rock unit is 1,707 m/sec [5,600 ft/sec]. For the remainder of its profile, the licensee applied a velocity gradient of 0.5 m/sec/m [0.5 ft/sec/ft], which produces a terminal  $V_S$  of 2,455 m/sec [8,053 ft/sec] at the base of the profile.

Rather than use the  $V_S$  solely determined from the Unit 1 site investigations, which extends only to the uppermost layer of rock beneath the site, the NRC staff used the  $V_S$  profile developed from the geophysical surveys for the COL for Units 2 and 3. The numerous COL geophysical investigations measured the  $V_S$  to a depth of about 61 m [200 ft] below the surface. For the deeper  $V_S$ , sonic data from a nearby well {3 mi [5 km] north of the site} were used to estimate a velocity profile. The sonic data provided  $V_P$  from a depth of 152 m [500 ft] to 1,128 m [3,700 ft], which is mostly within the Sanford Formation but also likely captures the upper rock units from the underlying Cumnock Formation. Assuming a Poisson's ratio of 0.32, the NRC staff converted the  $V_P$  from the sonic well log to develop a  $V_S$  profile. Figures 2.5.2-261 and 2.5.2-262 in the COL UFSAR (Progress Energy, 2014) show that the  $V_S$  gradually increases from a value of 1,250 m/sec [4,100 ft/sec] at the control point elevation to 2,287 m/sec [7,500 ft/sec] at a depth of 1,128 m [3,700 ft]. The NRC staff concluded that a profile thickness of 1,128 m [3,700 ft] is sufficient to capture the site amplification of the lowest spectral frequency of interest at 0.5 Hz.

To capture the uncertainty in its basecase profile, the NRC staff developed lower and upper range (10<sup>th</sup> and 90<sup>th</sup> percentile) profiles by multiplying the basecase  $V_S$  values by scale factors of 0.78 and 1.27, respectively, which corresponds to an epistemic logarithmic standard deviation of 0.20. The weights for the lower, best-estimate, and upper basecase profiles are 0.3, 0.4, and 0.3, respectively. Figure 2.3-23 shows the upper 152 m [500 ft] of the NRC staff's profiles. The upper profile terminates at a depth of 488 m [1,600 ft], and the lower and best-estimate basecase profiles terminate at a depth of 1,128 m [3,700 ft] below the control point elevation.

#### 2.3.6.2.2 *Dynamic Material Properties and Site Kappa*

The NRC staff assumed both linear and nonlinear dynamic behavior for the rock beneath the Harris site. To model the nonlinear behavior of the uppermost rock strata, the NRC staff used the EPRI rock shear modulus reduction and material damping curves. To model the linear behavior, the NRC staff used a constant damping ratio of 3 percent. The NRC staff assumed these two alternative dynamic responses for the upper 31 m [103 ft] of the profile and gave them equal weight. For the remaining 1,097 m [3,597 ft] of its profile, the NRC staff assumed a linear response with a material damping ratio value of 0.1 percent to maintain consistency with the  $\kappa_0$  value for the Harris site.

To determine the basecase  $\kappa_0$  for the Harris site, the NRC staff first used the Campbell (2009) Model 1 relationship between  $V_S$  and  $Q_{ef}$  to determine a  $Q_{ef}$  for each layer. Combining these  $Q_{ef}$  values with the thicknesses and  $V_S$  for each of the layers results in a total  $\kappa_0$  value of about 14 msec, which includes the 6 msec assumed for the underlying reference rock. For the lower and upper basecase profiles, the NRC staff calculated  $\kappa_0$  values of 19 and 8 msec, respectively, using the same approach as for the best-estimate basecase profile. In contrast, the licensee estimated  $\kappa_0$  by using the empirical relationship from the SPID (EPRI, 2012) between the average  $V_S$  over the upper 30 m [100 ft] of the profile and  $\kappa_0$ , which resulted in  $\kappa_0$  values of 13, 22, and 8 msec for the best-estimate, lower, and upper basecase profiles, respectively.

Table 2.3-7 provides the layer depths, lithologies,  $V_S$ , unit weights, and dynamic properties for the NRC staff's three profiles. In summary, the site response logic tree developed by the NRC staff for the Harris site consists of six alternatives; three basecase profiles (each with a different  $\kappa_0$  value) and two alternative dynamic property branches.

#### 2.3.6.2.3 *Methodology and Results*

The NRC staff followed the methodology described in Section 2.1.4 to develop the final site amplification factors. Figure 2.3-24 shows the overall median site amplification factors and their variability for each of the seven spectral frequencies. As shown in Figure 2.3-24, the median site amplification factors for the seven spectral frequencies are close to 1, with the higher spectral frequencies (25 Hz and 100 Hz) decreasing with increasing input spectral acceleration levels. The median site amplification factors range from about 1.0 to 1.5 before falling off with higher input spectral accelerations. The lower half of Figure 2.3-24 shows that the logarithmic standard deviations for the site amplification factors range from about 0.05 to 0.10.

#### 2.3.6.3 *Control Point Hazard*

The NRC staff implemented Approach 3 from the SPID to develop a weighted control point seismic hazard curve for each of the six unique combinations of the site response logic tree for the Harris site. After combining these curves to develop the final mean control point hazard curves, the NRC staff determined the  $10^{-4}$  and  $10^{-5}$  UHRS in order to calculate the final GMRS. Figure 2.3-25 shows the final control point mean seismic hazard curves for each of the seven spectral frequencies as well as the NRC staff's UHRS and GMRS, and the licensee's NTTF R2.1 GMRS (Kapapoulos, 2014). As shown in Figure 2.3-25, the NRC staff's GMRS (black curve) is similar to the licensee's GMRS (blue curve) over the entire frequency range. For comparison, Figure 2.3-25 also shows the NRC staff's reference rock GMRS (brown dotted curve).

**Table 2.3-7 Layer Depths, Shear Wave Velocities ( $V_s$ ), Unit Weights, and Dynamic Properties for Harris**

Layer	Depth (ft)	Description	$V_s$ (ft/sec)			$V_s$ Sigma (ln)	BC Unit Weight (pcf)	Dynamic Properties	
			LR (0.3)	BC (0.4)	UR (0.3)			Alt. 1 (0.5)	Alt. 2 (0.5)
1	11	Rock: siltstone, sandstone	3,173	4,100	5,298	0.25	140	EPRI Rock	L 3.0%
2	22	Rock: siltstone, sandstone	3,947	5,100	6,591	0.15	140	EPRI Rock	L 3.0%
3	48	Rock: siltstone, sandstone	4,256	5,500	7,108	0.15	150	EPRI Rock	L 3.0%
4	98	Rock: siltstone, sandstone	4,720	6,100	7,883	0.15	150	EPRI Rock	L 3.0%
5	103	Rock: siltstone, sandstone	3,211	4,150	5,363	0.15	140	EPRI Rock	L 3.0%
6	1,600	Rock: siltstone, sandstone	5,223	6,750	8,723	0.15	150	L 0.1%	L 0.1%
7	3,700	Rock: claystone, shale	5,804	7,500	9,285	0.15	160	L 0.1%	L 0.1%

LR = lower range; BC = basecase; UR = upper range; ln = natural log; pcf = pounds per cubic foot; L = linear; Alt. = alternative.  
 For LR, BC, UR, and Alt.: Values in parentheses refer to weights for site response analysis logic tree branches.

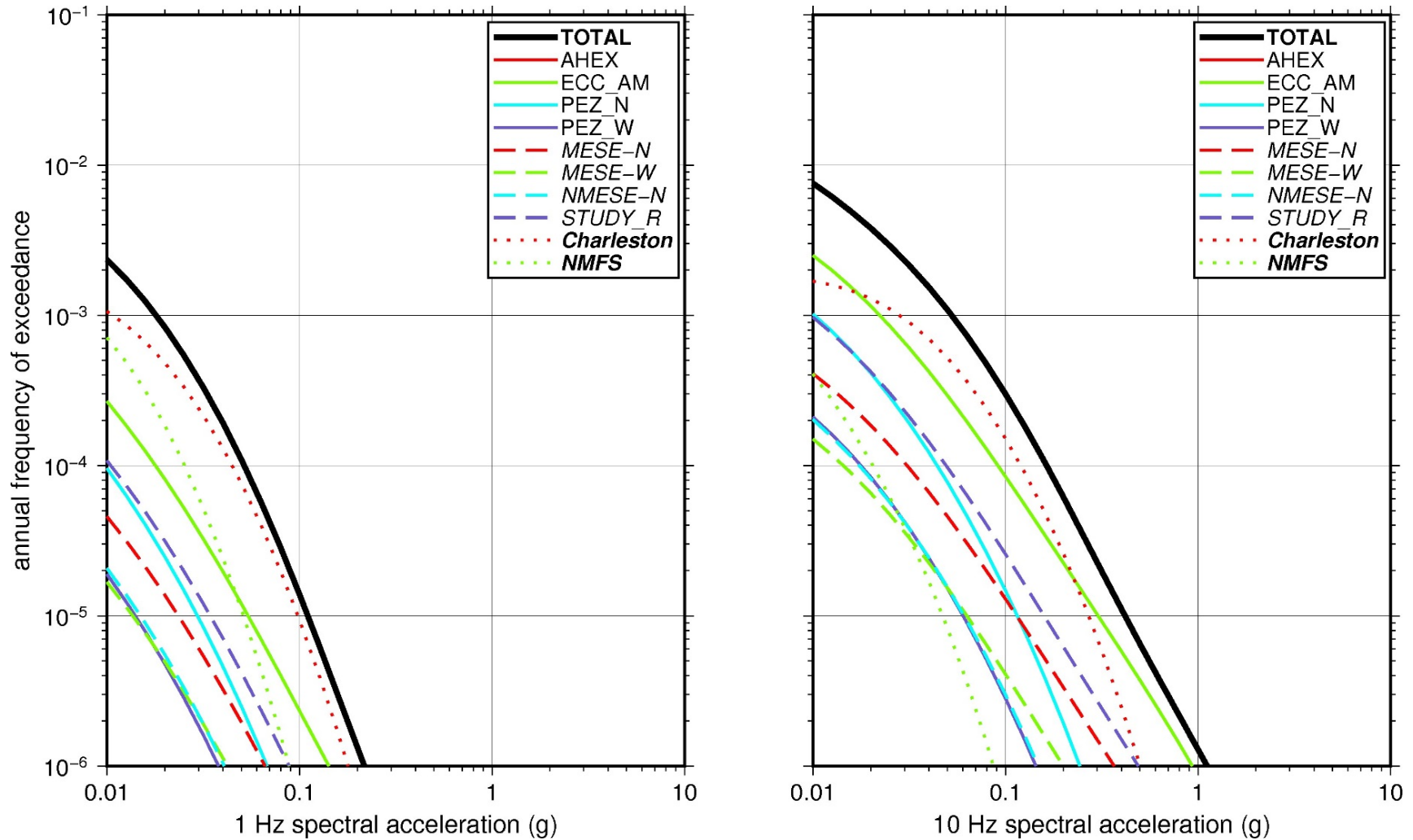


**Figure 2.3-22 Low-Frequency (1 Hz, Left) and High-Frequency (10 Hz, Right) Reference Rock Hazard Curves for Harris. Total Hazard is Shown as a Bold Black Line; Individual Contributions to the Hazard for Each of the CEUS-SSC Sources are Shown as Colored Lines Defined in the Legend. See Table 2.1-1 for Source Name Definitions**

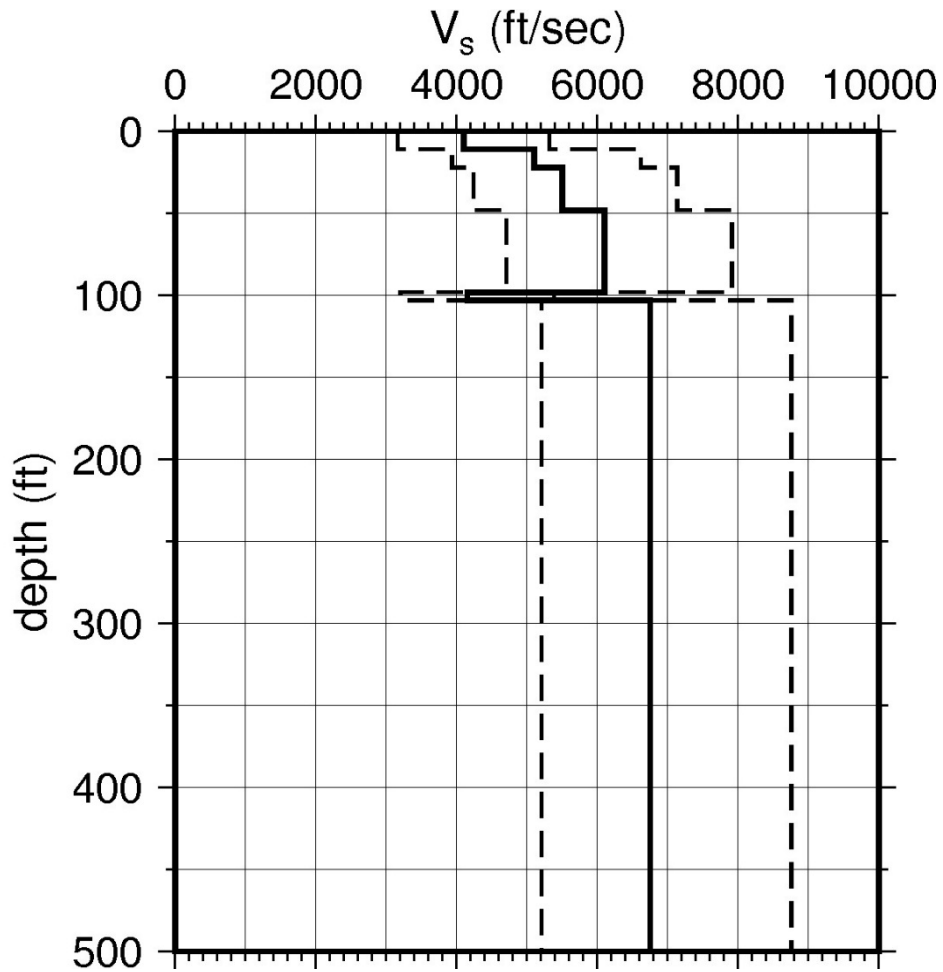


**Figure 2.3-23 Shear Wave Velocity ( $V_s$ ) Profiles for Harris. Basecase (BC) Profile Shown as Solid Bold Line; Lower and Upper Range (LR and UR) Profiles Shown as Dashed Lines. Profiles Terminate at Reference Rock Velocity of 2,831 m/sec [9,285 ft/sec] per EPRI GMM (2013)**

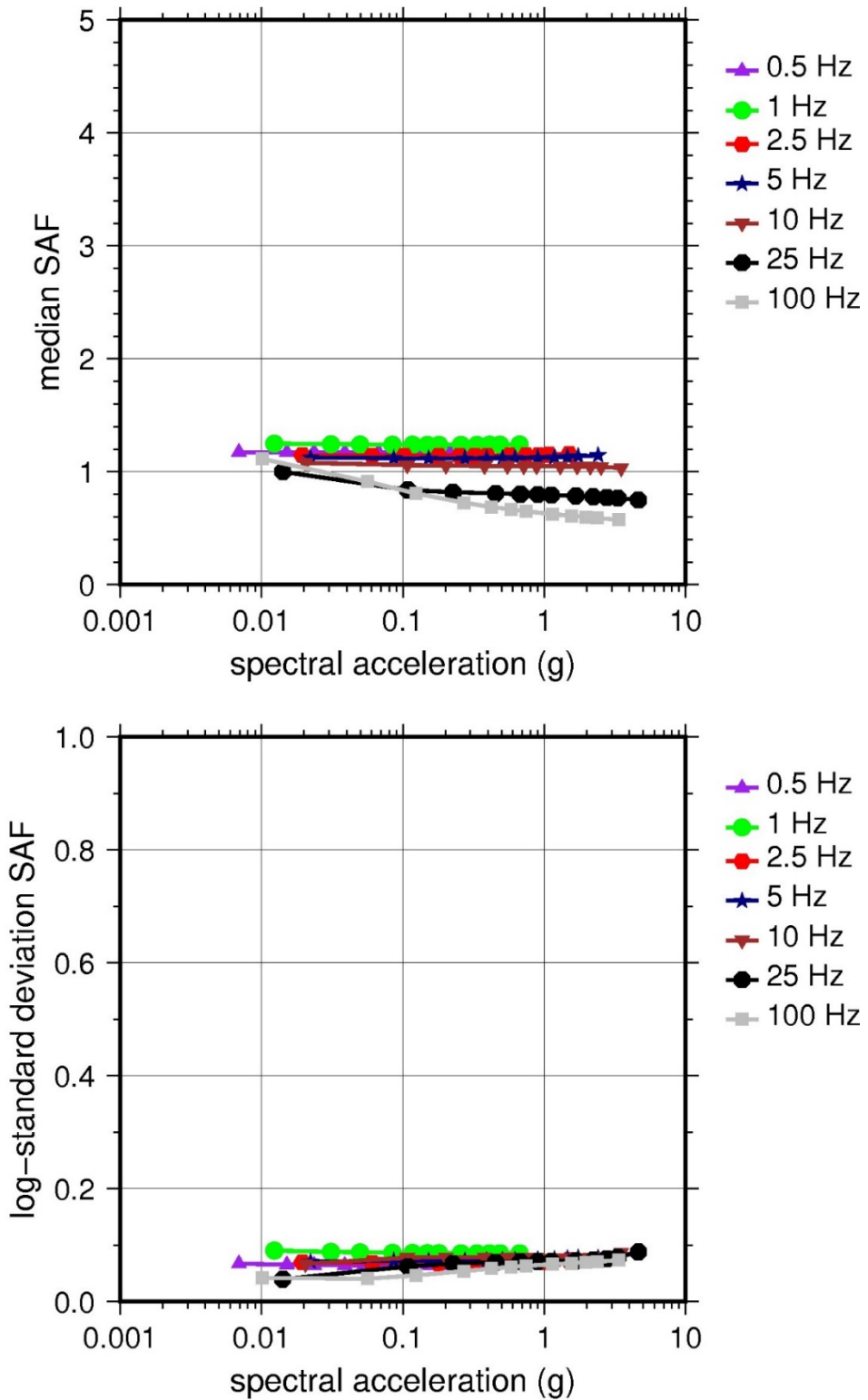


**Figure 2.3-24 Overall Weighted Median Site Amplification Factor (SAF) (Upper) and Log Standard Deviation of the SAF (Lower) as a Function of Input Acceleration for EPRI GMM (2013) Spectral Frequencies**

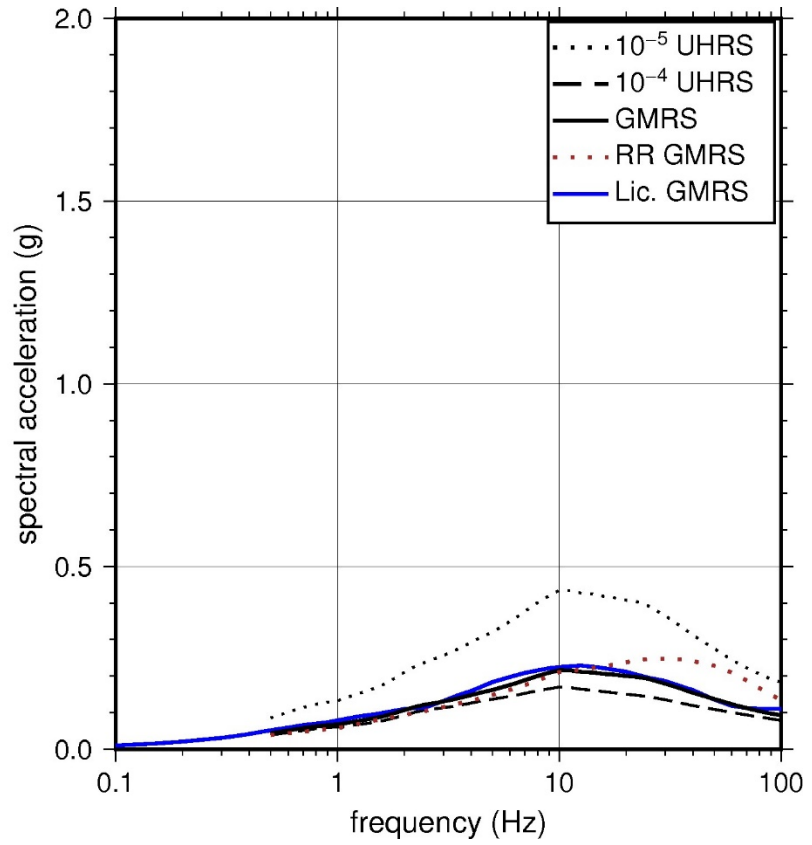
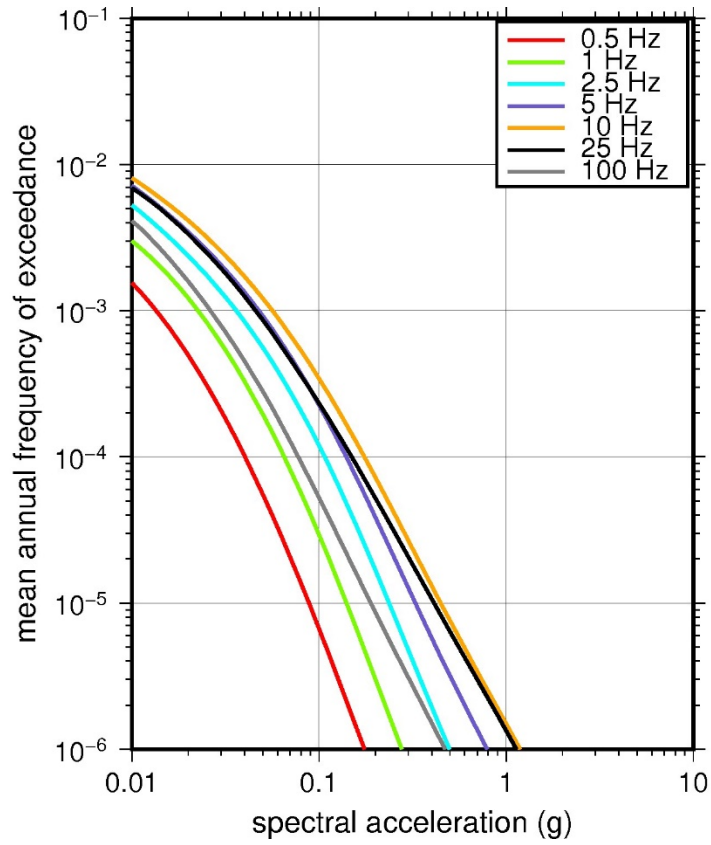


**Figure 2.3-25 Mean Control Point Hazard Curves (Left) for EPRI GMM (2013) Spectral Frequencies, and GMRS and UHRs (Right) for Harris**



### 2.3.7 Hatch

The Edwin I. Hatch Nuclear Plant site is located in Georgia along the south bank of the Altamaha River within the Coastal Plain physiographic province and is founded on about 1,220 m [4,000 ft] of sedimentary strata over basaltic basement rock of Mesozoic age. The horizontal SSE response spectrum for Unit 1 has a rounded Housner spectral shape and Unit 2 has a Newmark spectral shape. Both spectra are anchored at a PGA of 0.15g.

#### 2.3.7.1 Reference Rock Hazard

For the reference rock PSHA, the NRC staff selected the eight CEUS-SSC (NRC, 2012b) background seismic source zones that are located within 320 km [200 mi] of the site. In addition to the nearby Charleston CEUS-SSC RLME, the NRC staff also selected additional RLME sources that are within 806 km [500 mi]. To develop the reference rock seismic hazard curves for the site, the NRC staff used the GMPEs in the updated EPRI GMM (2013). As shown in Figure 2.3-26, the Charleston RLME is the largest contributor to both the 1 Hz and 10 Hz reference rock total mean hazard curves at the  $10^{-4}$  AFE level.

#### 2.3.7.2 Site Response Evaluation

##### 2.3.7.2.1 Site Profiles

To develop a basecase profile, the NRC staff used the geologic information in the NTTF R2.1 SHSR (Pierce, 2014b) submitted by Southern Nuclear Operating Company, Inc. (hereafter referred to as “the licensee” within this plant section). As described in the licensee’s SHSR, the Hatch site consists of about 1,220 m [4,000 ft] of relatively unconsolidated Mesozoic and Cenozoic age sands, gravels, clays, marls, claystones, sandstones, and limestones. The major plant structures for the Hatch plant are founded in the Pliocene to Miocene age Hawthorn Formation, which consists of sand, clay, and cemented sand and clay layers. In Table 2.3.1-2 of the SHSR, the licensee briefly described the subsurface materials in terms of the geologic units and layer thicknesses. For its site response evaluation, the NRC staff used the top of the ground surface, which corresponds to an elevation of 39 m [129 ft] above MSL, as the control point elevation for the Hatch site.

The field investigations for Hatch, conducted in the late 1960s, consisted of a number of borings through the uppermost soils beneath the site. In addition, seismic refraction surveys by the licensee measured  $V_P$  and  $V_S$  to a depth of about 31 m [100 ft] beneath the site. Subsequent investigations for an ISFSI measured  $V_S$  to a depth of about 70 m [230 ft] in the plant area. To augment its  $V_S$  profile, the licensee used the sonic well log data from a deep borehole located 43 km [27 mi] southwest of the plant. The well log data provided measurements of  $V_P$  to a depth of about 3,354 m [11,000 ft] in the region, and the borehole lithology (alternating layers of sand, clayey sand, sandy clay, and marl) closely matches the lithology beneath the plant site. Table 2.3.2-2 of the SHSR gives the estimated  $V_S$  determined from the licensee’s  $V_P$  and assumed Poisson’s ratios listed in Table 2.3.2-1 of the SHSR.

For its SHSR, the licensee developed a basecase profile that extends to a depth of 1,246 m [4,087 ft] below the control point elevation. The uppermost layer {16 m [54 ft]} of the profile consist of backfill material (sand and clay), for which the licensee measured an average  $V_S$  of 305 m/sec [1,000 ft/sec]. Beneath this layer of backfill are the sands and clays from the Hawthorn Formation, which has an average  $V_S$  that gradually increases from about 305 m/sec [1,000 ft/sec] to 610 m/sec [2,000 ft/sec] over a thickness of 79 m [260 ft]. Underlying the

Hawthorn Formation is about 357 m [1,170 ft] of calcitized fossiliferous limestones and dolomitic limestones from the Tampa, Ocala, and Lisbon Formations, which range in age from Miocene to Eocene. The  $V_S$  for these limestones increases from 670 m/sec [2,200 ft/sec] for the upper Tampa Formation (sandy to clayey fossiliferous limestone) to about 1,829 m/sec [6,000 ft/sec] for the lower portion of the Lisbon Formation (dolomitic limestone). The remainder of the licensee's profile {804 m [2,637 ft]} consists of a mixture of soil (primarily sand) and rock (marl and limestone), for which the  $V_S$  varies from about 1,524 m/sec [5,000 ft/sec] to 1,646 m/sec [5,400 ft/sec].

As multiple geophysical field investigations have characterized the soil and rock strata beneath the Hatch site, along with sonic velocities from a regional borehole, the NRC staff used the licensee's layer thicknesses and  $V_S$  for its basecase profile.

To capture the uncertainty in its basecase profile, the NRC staff developed lower and upper range (10<sup>th</sup> and 90<sup>th</sup> percentile) profiles by multiplying the basecase  $V_S$  values by scale factors of 0.78 and 1.29, respectively, which corresponds to an epistemic logarithmic standard deviation of 0.20. The weights for the lower, best-estimate, and upper basecase profiles are 0.3, 0.4, and 0.3, respectively. Figure 2.3-27 shows the upper 762 m [2,500 ft] of the NRC staff's basecase profiles.

#### 2.3.7.2.2 *Dynamic Material Properties and Site Kappa*

The NRC staff assumed both linear and nonlinear behavior for the soil and rock beneath the Hatch site. To model the nonlinear response within the upper 79 m [260 ft] of soil strata (Layers 1 to 4), the NRC staff used the EPRI soil shear modulus reduction and material damping curves as one alternative and the Peninsular Range curves for the second equally weighted alternative. To model the nonlinear behavior of the rock strata, the NRC staff used the EPRI rock shear modulus reduction and material damping curves. To model the linear behavior, the NRC staff used a constant damping ratio of 3 percent. The NRC staff assumed these two alternative dynamic responses for the fossiliferous limestone layers (Layers 5 to 7) and gave them equal weight. For the remaining 1,075 m [3,527 ft] of its profile, the NRC staff assumed a linear response with a material damping ratio value of 1 percent to maintain consistency with the  $\kappa_0$  value for the Hatch site.

To determine the basecase  $\kappa_0$  for the Hatch site, the NRC staff first used the Campbell (2009) Model 1 relationship between  $V_S$  and  $Q_{ef}$  to determine the  $Q_{ef}$  for each layer. Combining these  $Q_{ef}$  values with the thicknesses and  $V_S$  for each of the layers results in a total  $\kappa_0$  value of 35 msec, which includes the 6 msec assumed for the underlying reference rock. For the lower and upper profiles, the NRC staff calculated values of 51 and 24 msec, respectively, using the same approach as for the basecase profile. In contrast, the licensee used a  $\kappa_0$  value of 40 msec for the basecase profile, which is the maximum value recommended by Appendix B to the SPID (EPRI, 2012) for CEUS deep soil sites. For its lower and upper profiles, the licensee assumed an epistemic standard deviation of 0.40 to develop  $\kappa_0$  values of 67 and 24 msec, respectively.

Table 2.3-8 provides the layer depths, lithologies,  $V_S$ , unit weights, and dynamic properties for the NRC staff's three profiles. In summary, the site response logic tree developed by the NRC staff for the Hatch site consists of six alternatives; three basecase profiles (each with a different  $\kappa_0$  value) and two alternative dynamic property branches.

### 2.3.7.2.3 Methodology and Results

The NRC staff followed the methodology described in Section 2.1.4 to develop the final site amplification factors. Figure 2.3-28 shows the overall median site amplification factors and their variability for each of the seven spectral frequencies. As shown in Figure 2.3-28, the median site amplification factors vary from 2.0 to 3.5 before falling off with higher input spectral accelerations. The lower half of Figure 2.3-28 shows that the logarithmic standard deviations for the site amplification factors vary from 0.05 to 0.3.

### 2.3.7.3 Control Point Hazard

The NRC staff implemented Approach 3 from the SPID to develop a weighted control point seismic hazard curve for each of the six unique combinations of the site response logic tree for the Hatch site. After combining these curves to develop the final mean control point hazard curves, the NRC staff determined the  $10^{-4}$  and  $10^{-5}$  UHRs in order to calculate the final GMRS. Figure 2.3-29 shows the final control point mean seismic hazard curves for each of the seven spectral frequencies as well as the NRC staff's UHRs and GMRS, and the licensee's NTTF R2.1 GMRS (Pierce, 2014b). As shown in Figure 2.3-29, the NRC staff's GMRS (black curve) is slightly higher than the licensee's GMRS (blue curve) over the entire frequency range.

**Table 2.3-8 Layer Depths, Shear Wave Velocities ( $V_s$ ), Unit Weights, and Dynamic Properties for Hatch**

Layer	Depth (ft)	Description	$V_s$ (ft/sec)			$V_s$ Sigma (In)	BC Unit Weight (pcf)	Dynamic Properties	
			LR (0.3)	BC (0.4)	UR (0.3)			Alt. 1 (0.5)	Alt. 2 (0.5)
1	54	Soil: fill	774	1,000	1,292	0.25	120	EPRI Soil	Pen.
2	121	Soil: sand, clay	851	1,100	1,422	0.15	120	EPRI Soil	Pen.
3	188	Soil: sand, clay	1,161	1,500	1,938	0.15	130	EPRI Soil	Pen.
4	260	Soil: sand, clay	1,548	2,000	2,585	0.15	130	EPRI Soil	Pen.
5	350	Rock: limestone	1,702	2,200	2,843	0.15	130	EPRI Rock	L 3.0%
6	440	Rock: limestone	2,012	2,600	3,360	0.15	130	EPRI Rock	L 3.0%
7	500	Rock: limestone	2,708	3,500	4,523	0.15	140	EPRI Rock	L 3.0%
8	560	Rock: limestone	3,095	4,000	5,169	0.15	140	L 1.0%	L 1.0%
9	700	Rock: limestone	3,328	4,300	5,557	0.15	140	L 1.0%	L 1.0%
10	840	Rock: limestone	3,405	4,400	5,686	0.15	140	L 1.0%	L 1.0%
11	1,145	Rock: limestone	3,947	5,100	6,591	0.15	140	L 1.0%	L 1.0%
12	1,450	Rock: limestone	4,643	6,000	7,754	0.15	150	L 1.0%	L 1.0%

**Table 2.3-8 Layer Depths, Shear Wave Velocities ( $V_s$ ), Unit Weights, and Dynamic Properties for Hatch (cont.)**

Layer	Depth (ft)	Description	$V_s$ (ft/sec)			$V_s$ Sigma (ln)	BC Unit Weight (pcf)	Dynamic Properties	
			LR (0.3)	BC (0.4)	UR (0.3)			Alt. 1 (0.5)	Alt. 2 (0.5)
13	1,700	Rock and Soil: sand, marls	3,869	5,000	6,461	0.15	140	L 1.0%	L 1.0%
14	2,015	Rock and Soil: limestone, sand	4,179	5,400	6,978	0.15	150	L 1.0%	L 1.0%
15	4,087	Rock and Soil: sand, marls	3,869	5,000	6,461	0.15	140	L 1.0%	L 1.0%

LR = lower range; BC = basecase; UR = upper range; ln = natural log; pcf = pounds per cubic foot; L = linear; Alt. = alternative; Pen. = Peninsular.

For LR, BC, UR, and Alt.: Values in parentheses refer to weights for site response analysis logic tree branches.

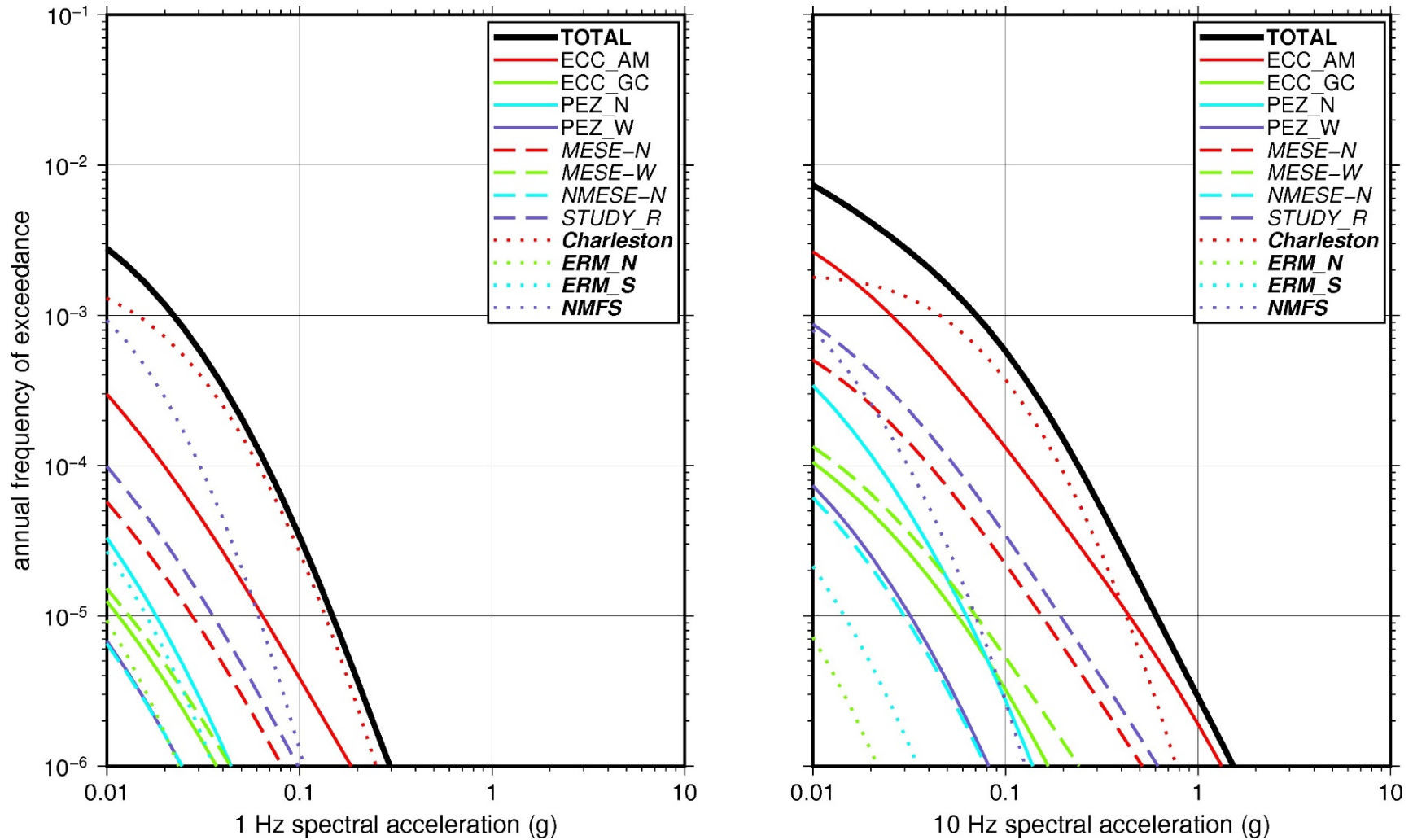


**Figure 2.3-26 Low-Frequency (1 Hz, Left) and High-Frequency (10 Hz, Right) Reference Rock Hazard Curves for Hatch. Total Hazard is Shown as a Bold Black Line; Individual Contributions to the Hazard for Each of the CEUS-SSC Sources are Shown as Colored Lines Defined in the Legend. See Table 2.1-1 for Source Name Definitions**

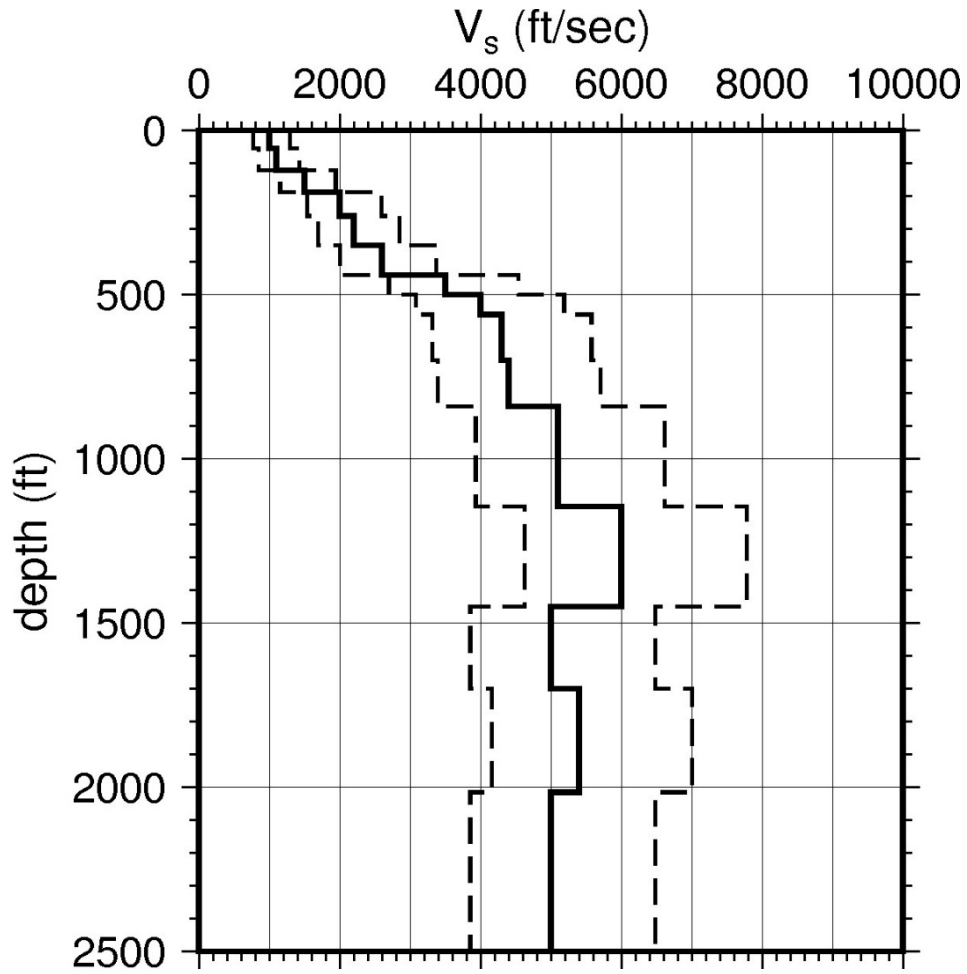


**Figure 2.3-27 Shear Wave Velocity ( $V_s$ ) Profiles for Hatch. Basecase (BC) Profile Shown as Solid Bold Line; Lower and Upper Range (LR and UR) Profiles Shown as Dashed Lines. Profiles Terminate at Reference Rock Velocity of 2,831 m/sec [9,285 ft/sec] per EPRI GMM (2013)**

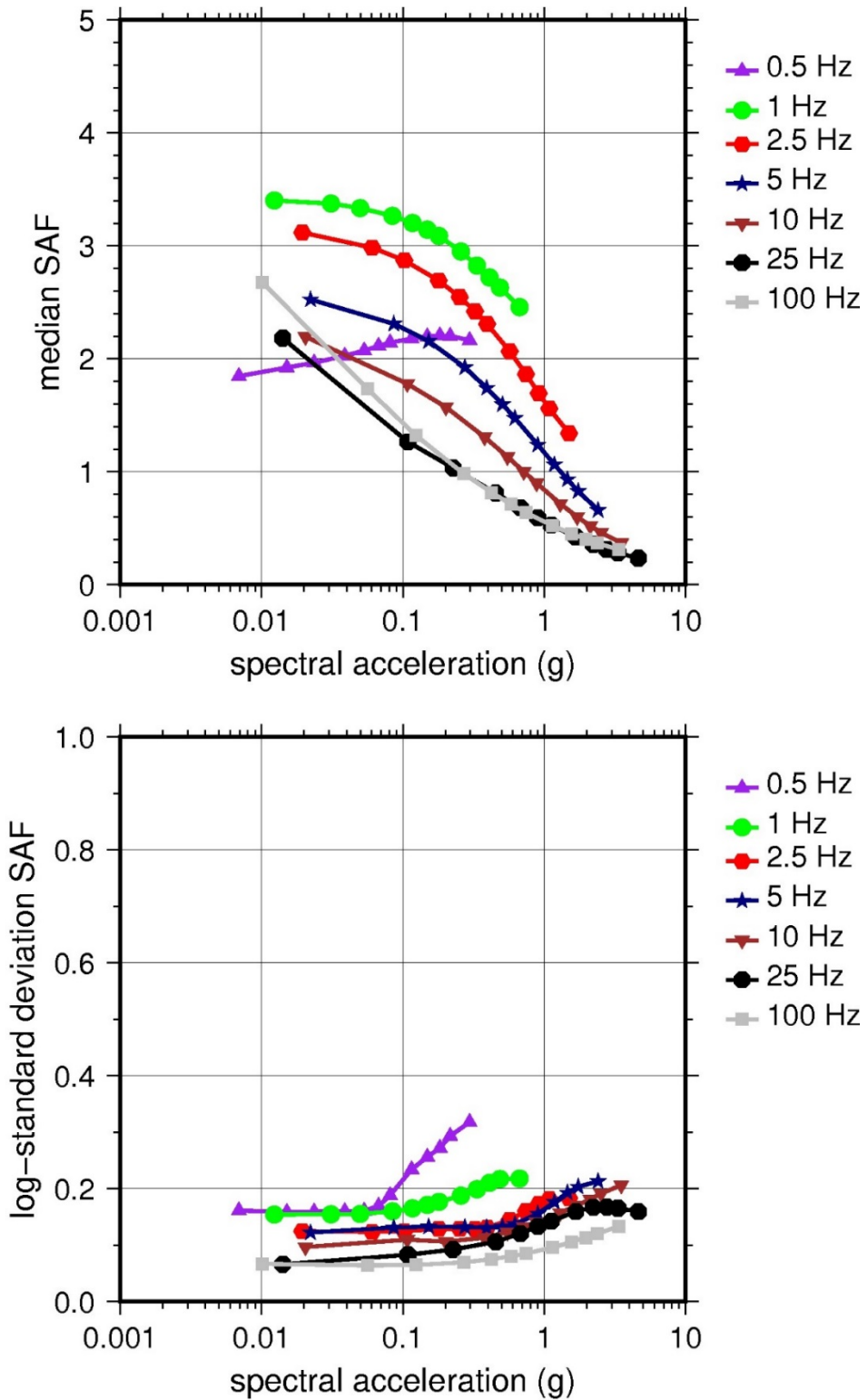


**Figure 2.3-28 Overall Weighted Median Site Amplification Factor (SAF) (Upper) and Log Standard Deviation of the SAF (Lower) as a Function of Input Acceleration for EPRI GMM (2013) Spectral Frequencies**

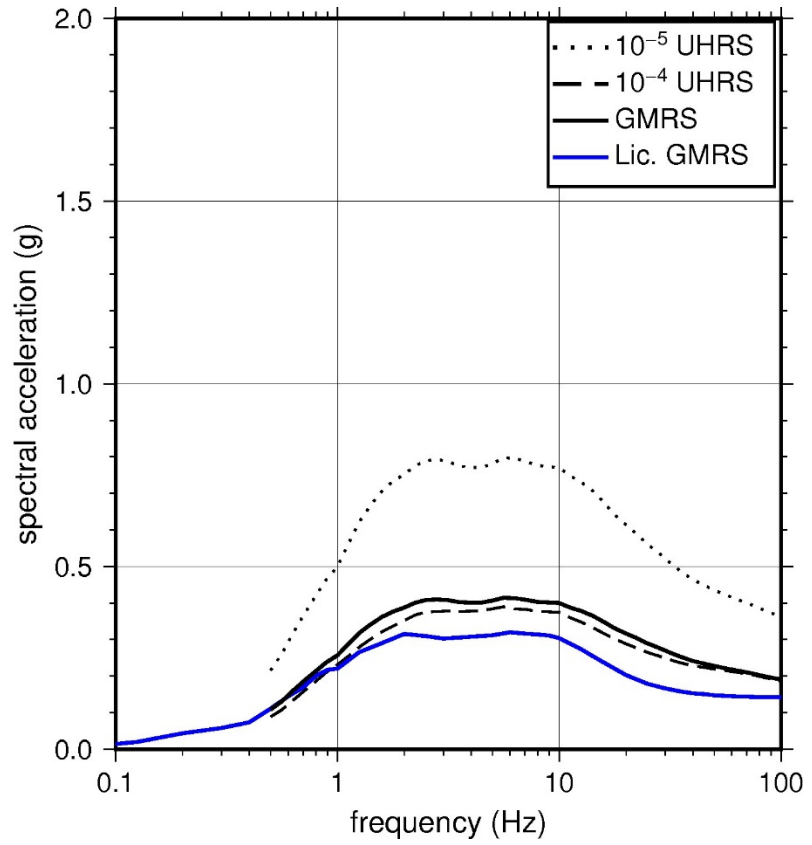
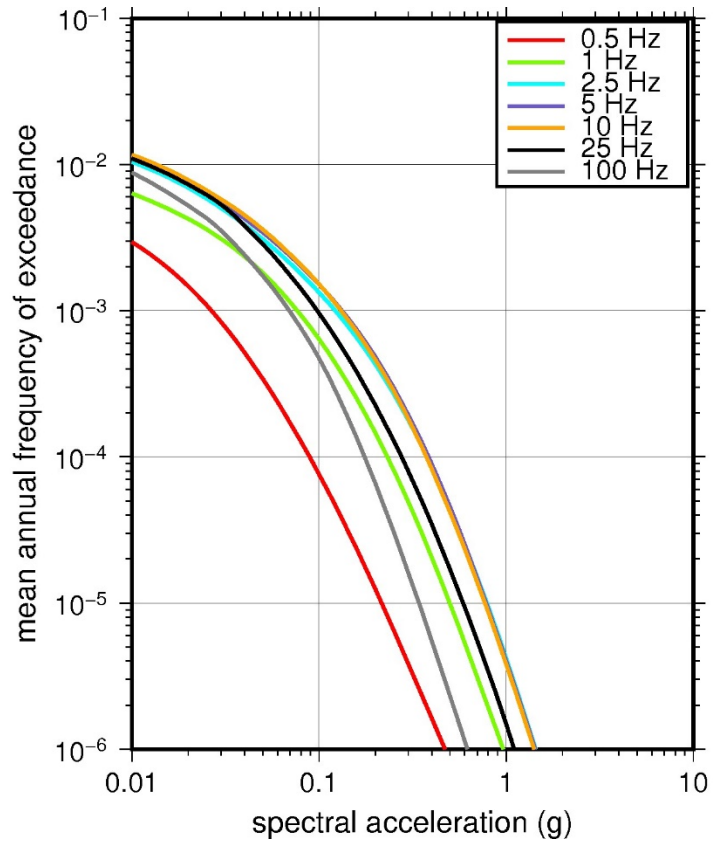


**Figure 2.3-29 Mean Control Point Hazard Curves (Left) for EPRI GMM (2013) Spectral Frequencies, and GMRS and UHRS (Right) for Hatch**



## 2.3.8 McGuire

The McGuire Nuclear Station site is located in North Carolina adjacent to Lake Norman in the Piedmont physiographic province and is founded on competent metamorphic igneous rock of Paleozoic age, which is partially weathered near the surface. The horizontal SSE response spectrum for McGuire has a Newmark spectral shape and is anchored at a PGA of 0.15g.

### 2.3.8.1 Reference Rock Hazard

For the reference rock PSHA, the NRC staff selected the nine CEUS-SSC (NRC, 2012b) background seismic source zones that are located within 320 km [200 mi] of the site. The NRC staff also selected the five CEUS-SSC RLME sources that are located within 806 km [500 mi] of the McGuire site. To develop the reference rock seismic hazard curves for the site, the NRC staff used the GMPEs in the updated EPRI GMM (2013). As shown in Figure 2.3-30, the Charleston RLME, which is located about 195 km [121 mi] to the west of the site, is the largest contributor to the 1 Hz reference rock total mean hazard curve at the  $10^{-4}$  AFE level. For the 10 Hz reference rock total mean hazard curve, the Charleston RLME, ECC-AM, and PEZ-N seismotectonic zones provide the highest overall contribution at the  $10^{-4}$  AFE level.

### 2.3.8.2 Site Response Evaluation

#### 2.3.8.2.1 Site Profiles

To develop a basecase profile, the NRC staff used the geologic information in the NTTF R2.1 SHSR (Capps, 2014) submitted by Duke Energy Carolinas, LLC (hereafter referred to as “the licensee” within this plant section). As described in the licensee’s SHSR, the McGuire site consists of metamorphosed sedimentary and igneous rock from the Paleozoic age Charlotte Belt. The site is underlain by a thin veneer of soils overlying partially weathered rock grading into hard metamorphic igneous rock (diorite). The safety-related structures are supported on sound rock, with an RQD of 75 percent or higher. In Table 2.3.1-1 of the SHSR, the licensee briefly described the subsurface materials in terms of the geologic units and layer thicknesses. For its site response evaluation, the NRC staff used a depth of 13 m [44 ft] from the surface, which is within the weathered rock, as the control point elevation {elevation 218 m [716 ft] MSL} for the McGuire site.

The field explorations for McGuire consisted of a number of borings through the upper rock beneath the site. Seismic refraction, uphole, and downhole surveys by the licensee measured  $V_P$  and  $V_S$  to a depth of about 17 m [55 ft] beneath the site. Table 2.3.2-2 of the SHSR gives the measured and estimated  $V_S$  determined from the licensee’s site investigations.

For its SHSR, the licensee developed a basecase profile that extends to a depth of 6.3 m [20.5 ft] below the control point elevation. The entire profile consists of 2 m [6.5 ft] of weathered rock over 4 m [14 ft] of sound rock with  $V_S$  of 1,372 m/sec [4,500 ft/sec] and 2,195 m/sec [7,200 ft/sec], respectively. Based on the rock type (hard metamorphic igneous rock), the licensee estimated that the profile  $V_S$  reaches the reference rock  $V_S$  of 2,831 m/sec [9,285 ft/sec] at a fairly shallow depth beneath the plant.

As multiple geophysical field investigations have characterized the rock strata beneath the McGuire site, the NRC staff used the licensee’s layer thicknesses and  $V_S$  its basecase profile.

To capture the uncertainty in its basecase profile, the NRC staff developed lower and upper range (10<sup>th</sup> and 90<sup>th</sup> percentile) profiles by multiplying the basecase  $V_S$  values by scale factors of 0.83 and 1.21, respectively, which corresponds to an epistemic logarithmic standard deviation of 0.15. The weights for the lower, best-estimate, and upper basecase profiles are 0.3, 0.4, and 0.3, respectively. Figure 2.3-31 shows the basecase, lower, and upper profiles used by the NRC staff.

#### 2.3.8.2.2 *Dynamic Material Properties and Site Kappa*

The NRC staff assumed both linear and nonlinear dynamic behavior for the rock beneath the McGuire site. To model the nonlinear behavior of the rock, the NRC staff used the EPRI rock shear modulus reduction and material damping curves. To model the linear behavior, the NRC staff used a constant damping ratio of 3 percent. The NRC staff assumed these two alternative dynamic responses for the entire profile. Due to the higher  $V_S$  of this rock layer, the NRC staff assigned weights of 0.7 and 0.3 to the linear and nonlinear alternatives, respectively.

To determine the basecase  $\kappa_\theta$  for the McGuire site, the NRC staff first used the Campbell (2009) Model 1 relationship between  $V_S$  and  $Q_{ef}$  to determine a  $Q_{ef}$  for each layer. Combining these  $Q_{ef}$  values with the thicknesses and  $V_S$  for each of the layers results in a total  $\kappa_\theta$  value of about 6.1 msec, which includes the 6 msec assumed for the underlying reference rock. For the lower and upper basecase profiles, the NRC staff calculated  $\kappa_\theta$  values of 6.2 and 6.0 msec, respectively, using the same approach as for the best-estimate basecase profile. In contrast, the licensee estimated  $\kappa_\theta$  by combining the lowest low-strain damping values from the EPRI rock material damping curves over the entire profile to estimate best-estimate, lower, and upper basecase  $\kappa_\theta$  values of 6.2, 6.3, and 6.2 msec, respectively.

Table 2.3-9 provides the layer depths, lithologies,  $V_S$ , unit weights, and dynamic properties for the NRC staff's three profiles. In summary, the site response logic tree developed by the NRC staff for the McGuire site consists of six alternatives; three basecase profiles (each with a different  $\kappa_\theta$  value) and two alternative dynamic property branches.

#### 2.3.8.2.3 *Methodology and Results*

The NRC staff followed the methodology described in Section 2.1.4 to develop the final site amplification factors. Figure 2.3-32 shows the overall median site amplification factors and their variability for each of the seven spectral frequencies. As shown in Figure 2.3-32, the median site amplification factors are all close to 1. The lower half of Figure 2.3-32 shows that the logarithmic standard deviations for the site amplification factors are generally less than 0.1.

#### 2.3.8.3 *Control Point Hazard*

The NRC staff implemented Approach 3 from the SPID to develop a weighted control point seismic hazard curve for each of the six unique combinations of the site response logic tree for the McGuire site. After combining these curves to develop the final mean control point hazard curves, the NRC staff determined the  $10^{-4}$  and  $10^{-5}$  UHRS in order to calculate the final GMRS. Figure 2.3-33 shows the final control point mean seismic hazard curves for each of the seven spectral frequencies as well as the NRC staff's UHRS and GMRS, and the licensee's NTTFR2.1 GMRS (Capps, 2014). As shown in Figure 2.3-33, the NRC staff's GMRS (black curve) is similar to the licensee's GMRS (blue curve) over the entire frequency range. For comparison, Figure 2.3-33 also shows the NRC staff's reference rock GMRS (brown dotted curve).

**Table 2.3-9 Layer Depths, Shear Wave Velocities ( $V_s$ ), Unit Weights, and Dynamic Properties for McGuire**

Layer	Depth (ft)	Description	$V_s$ (ft/sec)			$V_s$ Sigma (ln)	BC Unit Weight (pcf)	Dynamic Properties	
			LR (0.3)	BC (0.4)	UR (0.3)			Alt. 1 (0.3)	Alt. 2 (0.7)
1	6.5	Rock: gabbro, granite	3,919	4,750	5,757	0.25	140	EPRI Rock	L 3.0%
2	20	Rock: gabbro, granite	5,940	7,200	8,727	0.15	150	EPRI Rock	L 3.0%

LR = lower range; BC = basecase; UR = upper Range; ln = natural log; pcf = pounds per cubic foot; L = linear; Alt. = alternative.  
 For LR, BC, UR, and Alt.: Values in parentheses refer to weights for site response analysis logic tree branches.

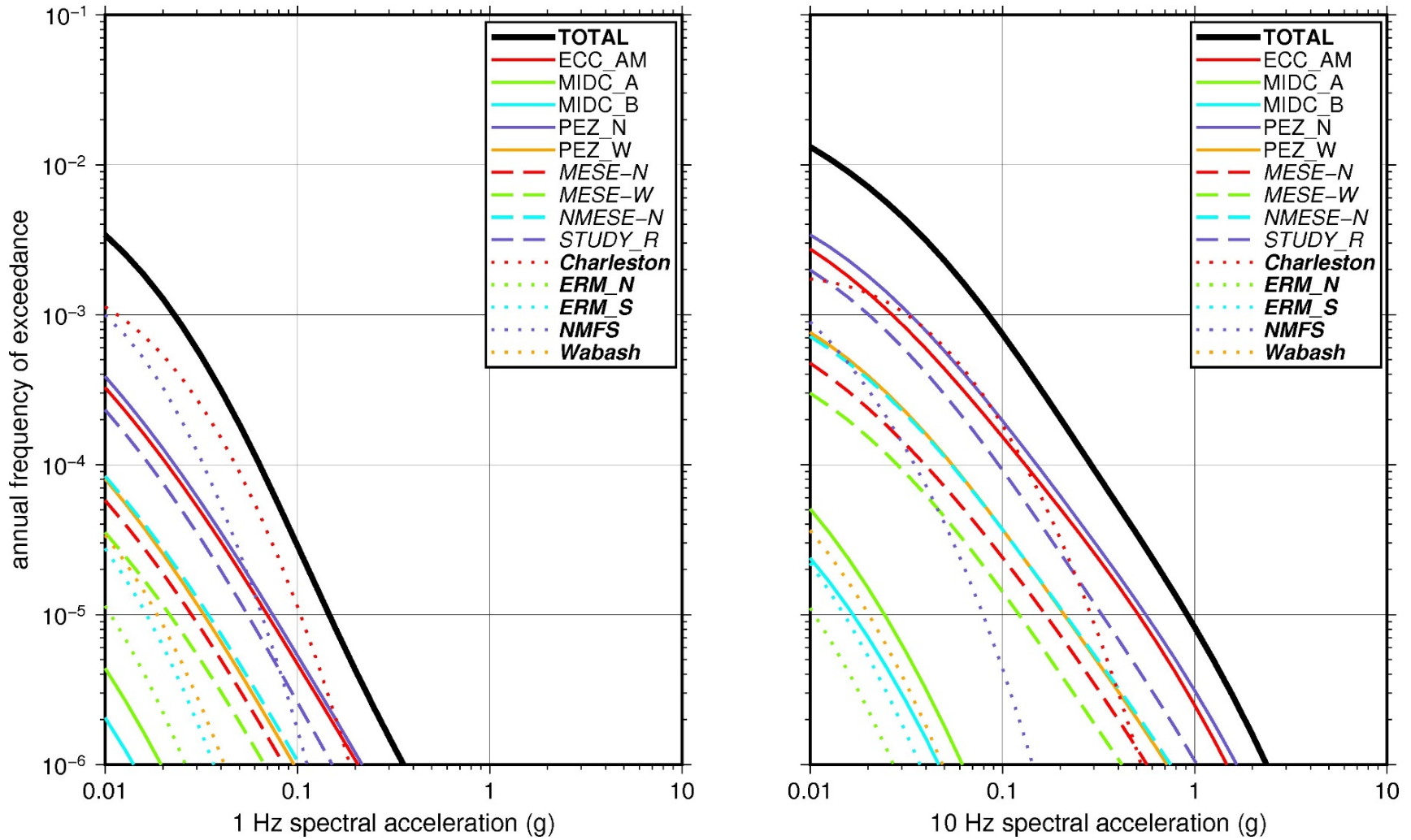


**Figure 2.3-30 Low-Frequency (1 Hz, Left) and High-Frequency (10 Hz, Right) Reference Rock Hazard Curves for McGuire. Total Hazard is Shown as a Bold Black Line; Individual Contributions to the Hazard for Each of the CEUS-SSC Sources are Shown as Colored Lines Defined in the Legend. See Table 2.1-1 for Source Name Definitions**

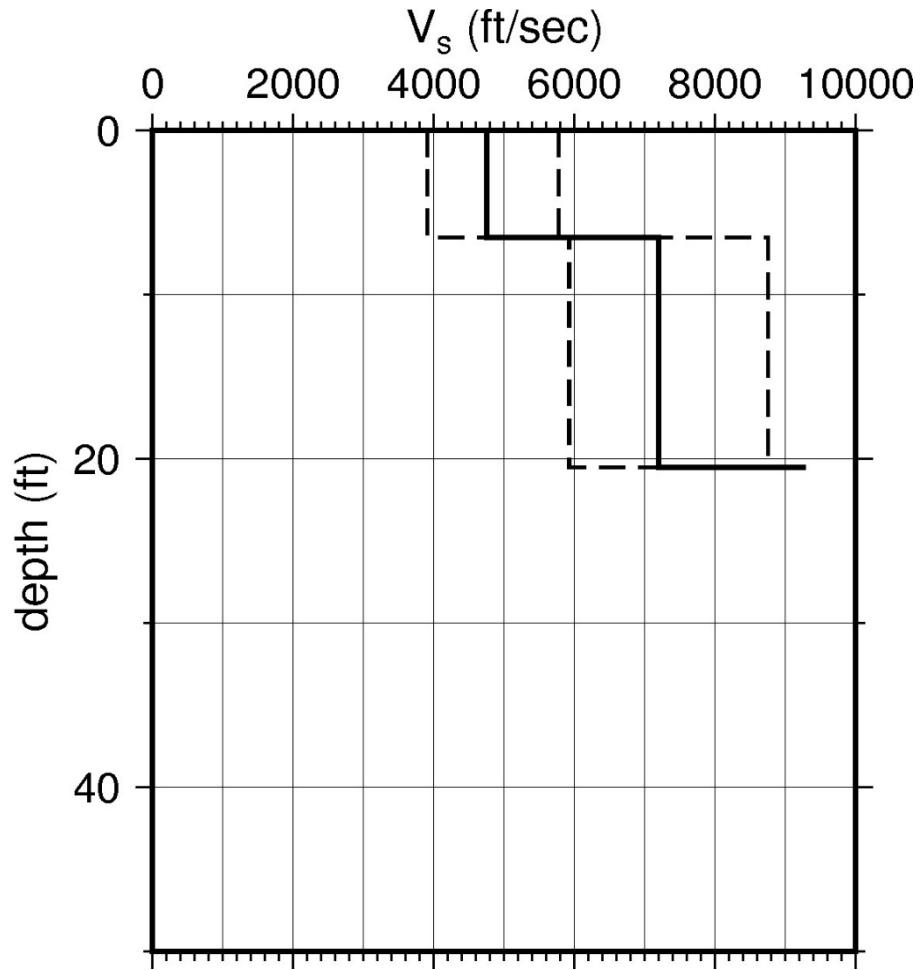


**Figure 2.3-31 Shear Wave Velocity ( $V_s$ ) Profiles for McGuire. Basecase (BC) Profile Shown as Solid Bold Line; Lower and Upper Range (LR and UR) Profiles Shown as Dashed Lines. Profiles Terminate at Reference Rock Velocity of 2,831 m/sec [9,285 ft/sec] per EPRI GMM (2013)**

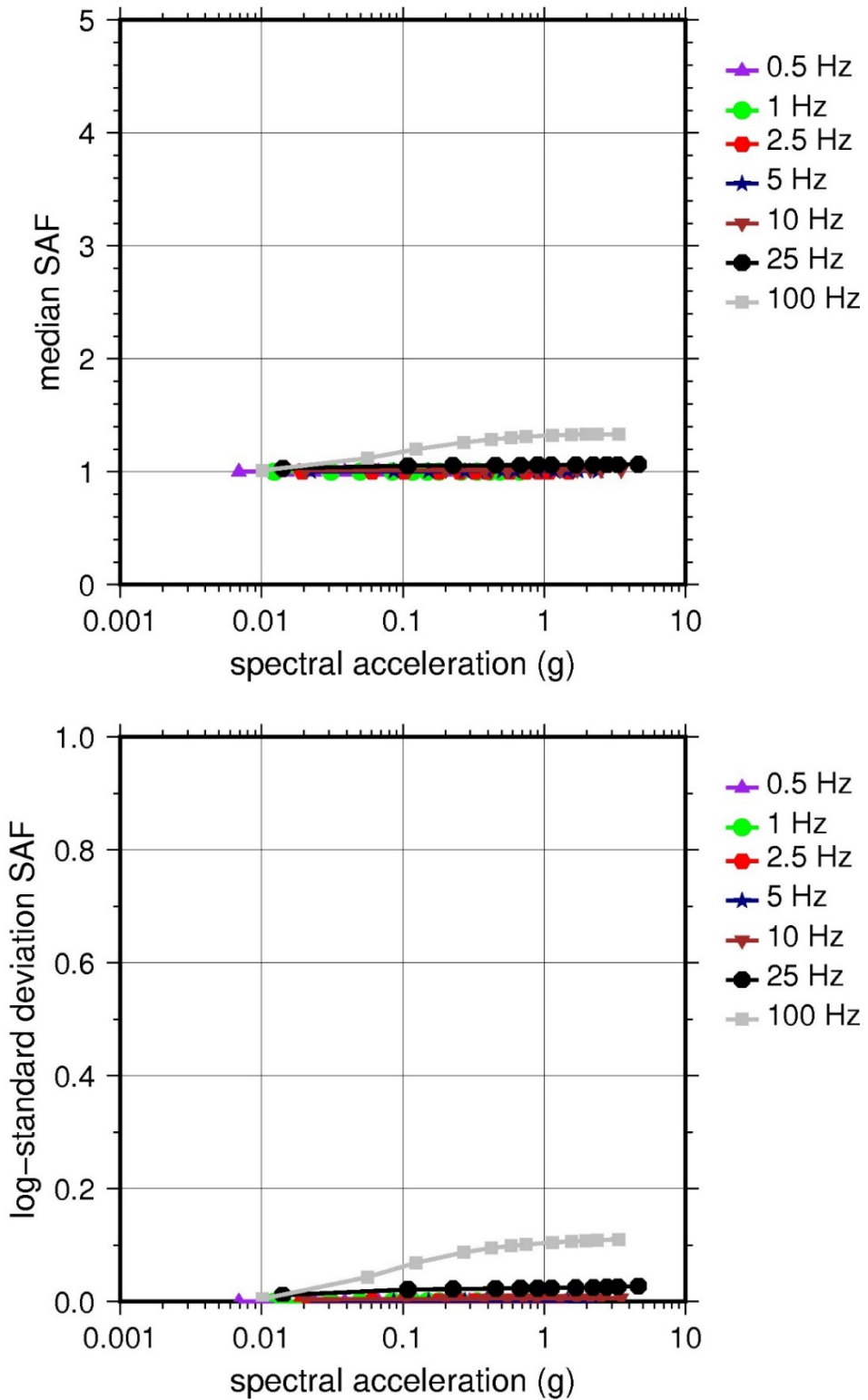


**Figure 2.3-32 Overall Weighted Median Site Amplification Factor (SAF) (Upper) and Log Standard Deviation of the SAF (Lower) as a Function of Input Acceleration for EPRI GMM (2013) Spectral Frequencies**

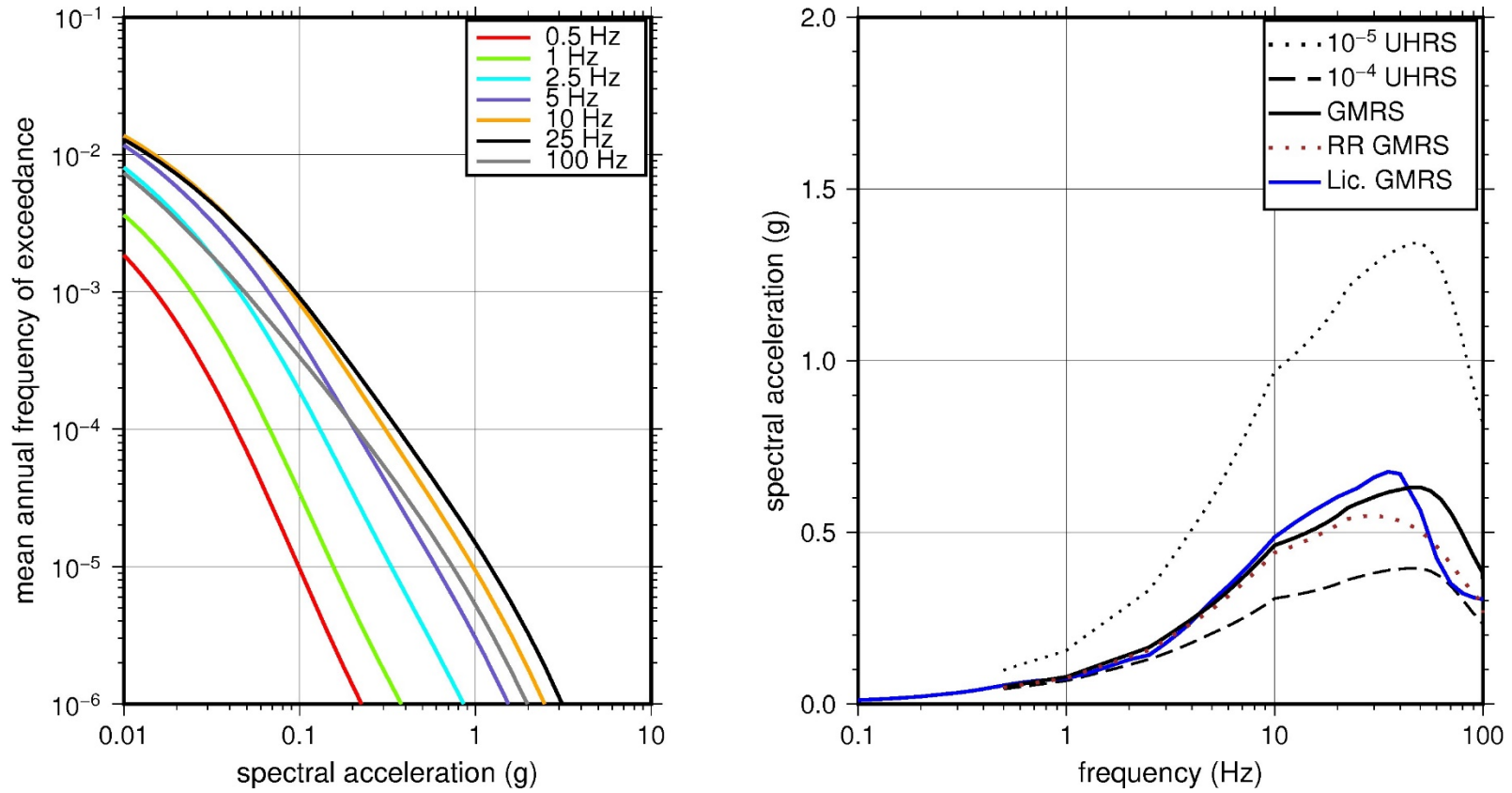


**Figure 2.3-33 Mean Control Point Hazard Curves (Left) for EPRI GMM (2013) Spectral Frequencies, and GMRS and UHRS (Right) for McGuire**

### 2.3.9 North Anna

The North Anna Power Station site is located in Virginia adjacent to Lake Anna within the Piedmont physiographic province and is founded on competent metamorphic rock (gneiss and schist) of Paleozoic age. The rock horizontal SSE response spectrum for North Anna has a Newmark spectral shape and is anchored at a PGA of 0.12g.

#### 2.3.9.1 Reference Rock Hazard

For the reference rock PSHA, the NRC staff selected the 10 CEUS-SSC (NRC, 2012b) background seismic source zones that are located within 320 km [200 mi] of the site. The NRC staff also selected the Charleston CEUS-SSC RLME source, which is located about 444 km [275 mi] from the North Anna site. To develop the reference rock seismic hazard curves for the site, the NRC staff used the GMPEs in the updated EPRI GMM (2013). As shown in Figure 2.3-34, the ECC-AM seismotectonic zone is the largest contributor to both the 1 Hz and 10 Hz reference rock total mean hazard curves at the  $10^{-4}$  AFE level.

#### 2.3.9.2 Site Response Evaluation

##### 2.3.9.2.1 Site Profiles

To develop a basecase profile, the NRC staff used the geologic information in the NTTF R2.1 SHSR (Heacock, 2014b) submitted by Virginia Electric and Power Company (hereafter referred to as “the licensee” within this plant section). As described in the licensee’s SHSR, the North Anna site consists of a thin veneer of saprolitic soil (clays, clayey silts, and sands) overlying weathered rock grading into hard metamorphic igneous rock (gneiss and schist) from the Cambrian age Chopawamsic Belt. The North Anna reactor buildings are founded on sound rock, which the licensee described as Zone III-IV moderately to slightly weathered rock. In Table 2.3.1-1 of the SHSR, the licensee briefly described the subsurface materials in terms of the geologic units and layer thicknesses. For its site response evaluation, the NRC staff used the top of the weathered rock at a depth of 1 m [3 ft], which corresponds to an elevation of 82 m [268 ft] MSL, as the control point elevation for the North Anna site.

The field explorations for North Anna consist of a number of borings through the upper rock beneath the site. Geophysical investigations for the proposed Unit 3 COL (Dominion Energy, Inc., 2013) include borehole geophysical measurements (P-S suspension logging) in five boreholes, with the deepest measurement at a depth of about 75 m [246 ft] beneath the site. Table 2.3.2-2 of the SHSR gives the measured  $V_S$  determined from the licensee’s site investigations.

For its SHSR, the licensee developed a basecase profile that extends to a depth of 41 m [133 ft] below the control point elevation. The entire profile consists of 13 m [44 ft] of weathered rock, 17 m [54 ft] of moderately weathered rock, and 11 m [35 ft] of slightly weathered rock with a  $V_S$  of 1,295 m/sec [4,250 ft/sec], about 1,615 m/sec [5,300 ft/sec], and 2,682 m/sec [8,800 ft/sec], respectively. Based on the rock type (hard metamorphic igneous rock), the profile  $V_S$  reaches the reference rock  $V_S$  of 2,831 m/sec [9,285 ft/sec] at a fairly shallow depth beneath the plant.

As multiple geophysical field investigations have characterized the rock strata beneath the North Anna site, the NRC staff used the licensee’s layer thicknesses and  $V_S$  for its basecase profile.



To capture the uncertainty in its basecase profile, the NRC staff developed lower and upper range (10<sup>th</sup> and 90<sup>th</sup> percentile) profiles by multiplying the basecase  $V_S$  values by scale factors of 0.83 and 1.21, respectively, which corresponds to an epistemic logarithmic standard deviation of 0.15. The weights for the lower, best-estimate, and upper basecase profiles are 0.3, 0.4, and 0.3, respectively. Figure 2.3-35 shows the basecase, lower, and upper profiles used by the NRC staff.

#### 2.3.9.2.2 *Dynamic Material Properties and Site Kappa*

The NRC staff assumed both linear and nonlinear dynamic behavior for the rock beneath the North Anna site. To model the nonlinear behavior of the uppermost rock strata, the NRC staff used the EPRI rock shear modulus reduction and material damping curves. To model the linear behavior, the NRC staff used a constant damping ratio of 3 percent. The NRC staff assumed these two alternative dynamic responses for the upper 30 m [97 ft] of the profile and gave them equal weight. For the remaining 11 m [35 ft] of its profile, the NRC staff assumed a linear response with a material damping ratio value of 0.1 percent to maintain consistency with the  $\kappa_0$  value for the North Anna site.

To determine the basecase  $\kappa_0$  for the North Anna site, the NRC staff first used the Campbell (2009) Model 1 relationship between  $V_S$  and  $Q_{ef}$  to determine a  $Q_{ef}$  for each layer. Combining these  $Q_{ef}$  values with the thicknesses and  $V_S$  for each of the layers results in a total  $\kappa_0$  value of about 6.5 msec, which includes the 6 msec assumed for the underlying reference rock. For the lower and upper basecase profiles, the NRC staff calculated  $\kappa_0$  values of 6.7 and 6.3 msec, respectively, using the same approach as for the best-estimate basecase profile. In contrast, the licensee included only the 6 msec assumed for the underlying reference rock for its site response analysis.

Table 2.3-10 provides the layer depths, lithologies,  $V_S$ , unit weights, and dynamic properties for the NRC staff's three profiles. In summary, the site response logic tree developed by the NRC staff for the North Anna site consists of six alternatives; three basecase profiles (each with a different  $\kappa_0$  value) and two alternative dynamic property branches.

#### 2.3.9.2.3 *Methodology and Results*

The NRC staff followed the methodology described in Section 2.1.4 to develop the final site amplification factors. Figure 2.3-36 shows the overall median site amplification factors and their variability for each of the seven spectral frequencies. As shown in Figure 2.3-36, the median site amplification factors for the seven spectral frequencies range from about 1 to 2. The lower half of Figure 2.3-36 shows that the logarithmic standard deviations for the site amplification factors range from about 0.05 to 0.20.

#### 2.3.9.3 *Control Point Hazard*

The NRC staff implemented Approach 3 from the SPID to develop a weighted control point seismic hazard curve for each of the six unique combinations of the site response logic tree for the North Anna site. After combining these curves to develop the final mean control point hazard curves, the NRC staff determined the 10<sup>-4</sup> and 10<sup>-5</sup> UHRS in order to calculate the final GMRS. Figure 2.3-37 shows the final control point mean seismic hazard curves for each of the seven spectral frequencies as well as the NRC staff's UHRS and GMRS, and the licensee's NTTF R2.1 GMRS (Heacock, 2014b). As shown in Figure 2.3-37, the NRC staff's GMRS (black curve) is similar to the licensee's GMRS (blue curve) up to 10 Hz and then is moderately lower

for the higher frequencies. This difference is most likely due to the NRC staff's use of multiple basecase profiles and alternative modeling of nonlinear dynamic behavior for the weathered rock. For comparison, Figure 2.3-37 also shows the NRC staff's reference rock GMRS (brown dotted curve).

Layer	Depth (ft)	Description	$V_s$ (ft/sec)			$V_s$ Sigma (ln)	BC Unit Weight (pcf)	Dynamic Properties	
			LR (0.3)	BC (0.4)	UR (0.3)			Alt. 1 (0.5)	Alt. 2 (0.5)
1	44	Rock: gneiss, schist	3,507	4,250	5,151	0.25	140	EPRI Rock	L 3.0%
2	63	Rock: gneiss, schist	4,497	5,450	6,606	0.15	150	EPRI Rock	L 3.0%
3	98	Rock: gneiss, schist	4,274	5,180	6,278	0.15	140	EPRI Rock	L 3.0%
4	133	Rock: gneiss, schist	7,261	8,800	9,285	0.15	160	L 0.1%	L 0.1%

LR = lower range; BC = basecase; UR = upper range; ln = natural log; pcf = pounds per cubic foot; L = linear; Alt. = alternative.  
 For LR, BC, UR, and Alt.: Values in parentheses refer to weights for site response analysis logic tree branches.

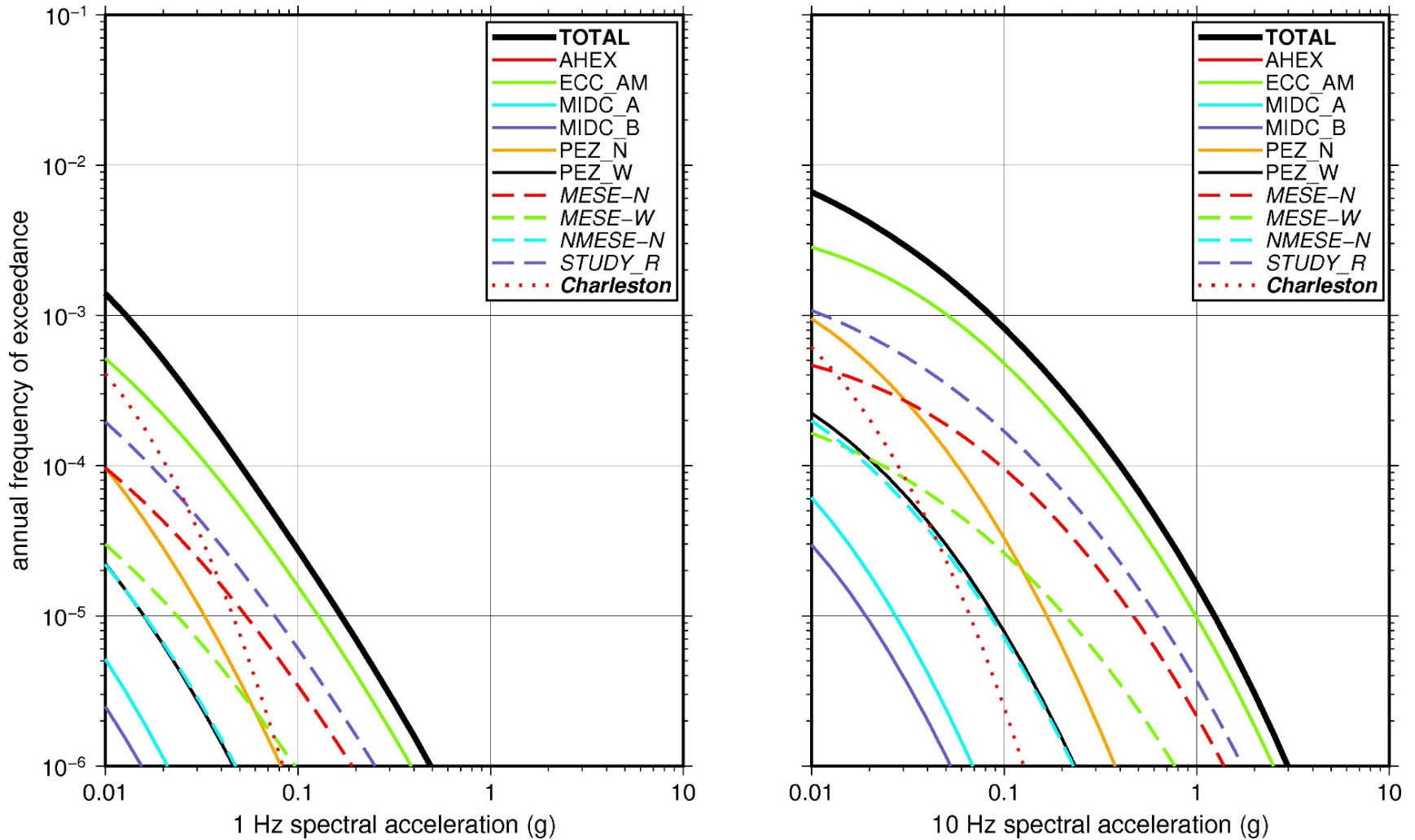


**Figure 2.3-34 Low-Frequency (1 Hz, Left) and High-Frequency (10 Hz, Right) Reference Rock Hazard Curves for North Anna. Total Hazard is Shown as a Bold Black Line; Individual Contributions to the Hazard for Each of the CEUS-SSC Sources are Shown as Colored Lines Defined in the Legend. See Table 2.1-1 for Source Name Definitions.**

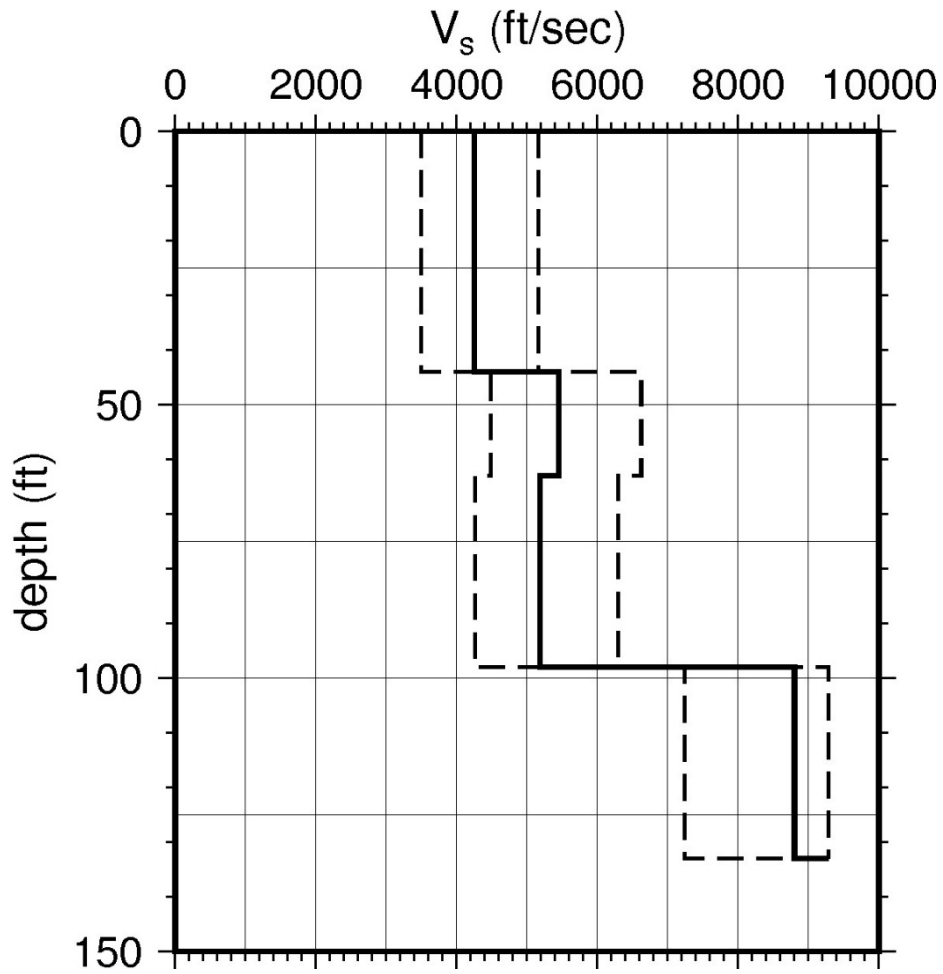
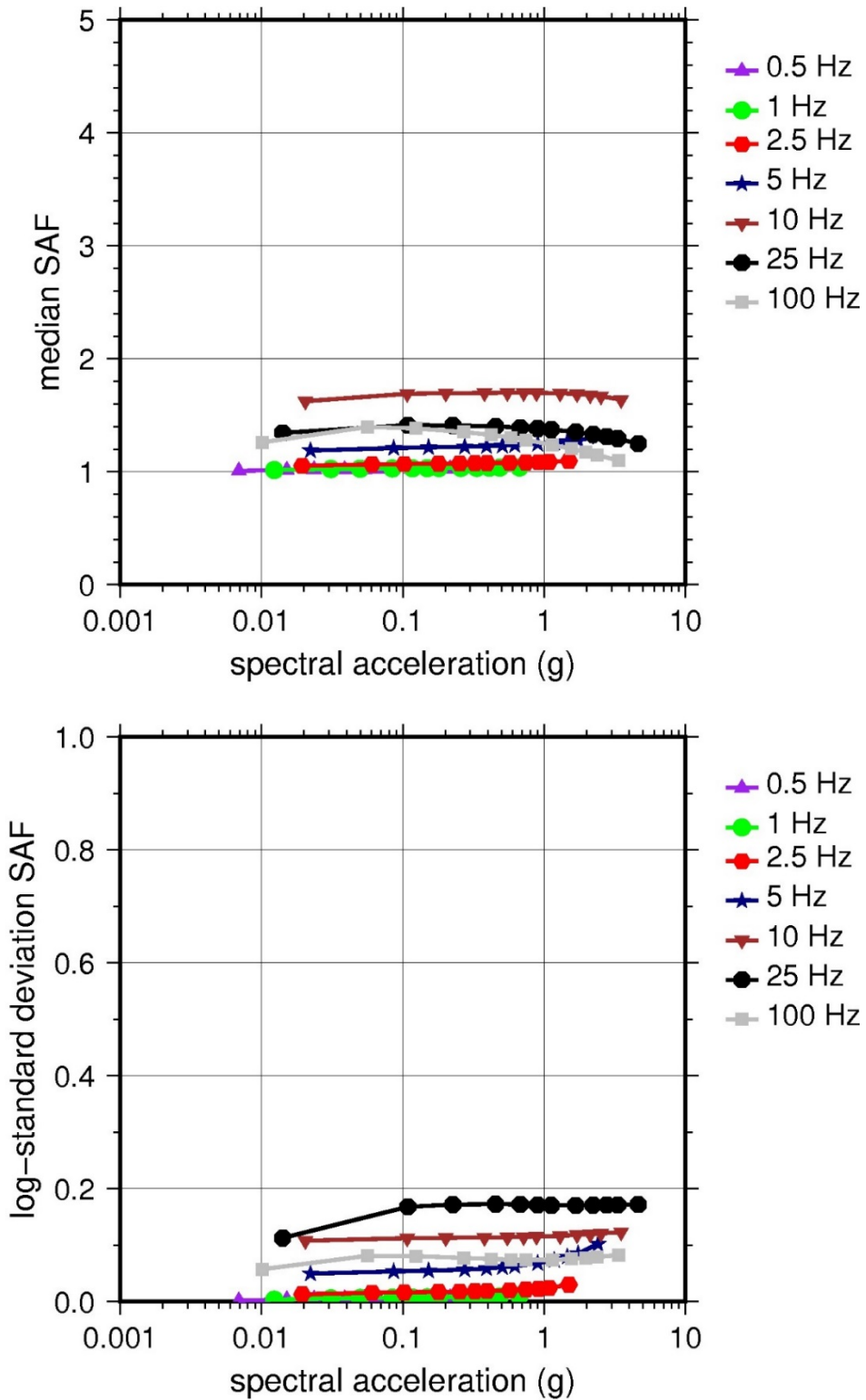
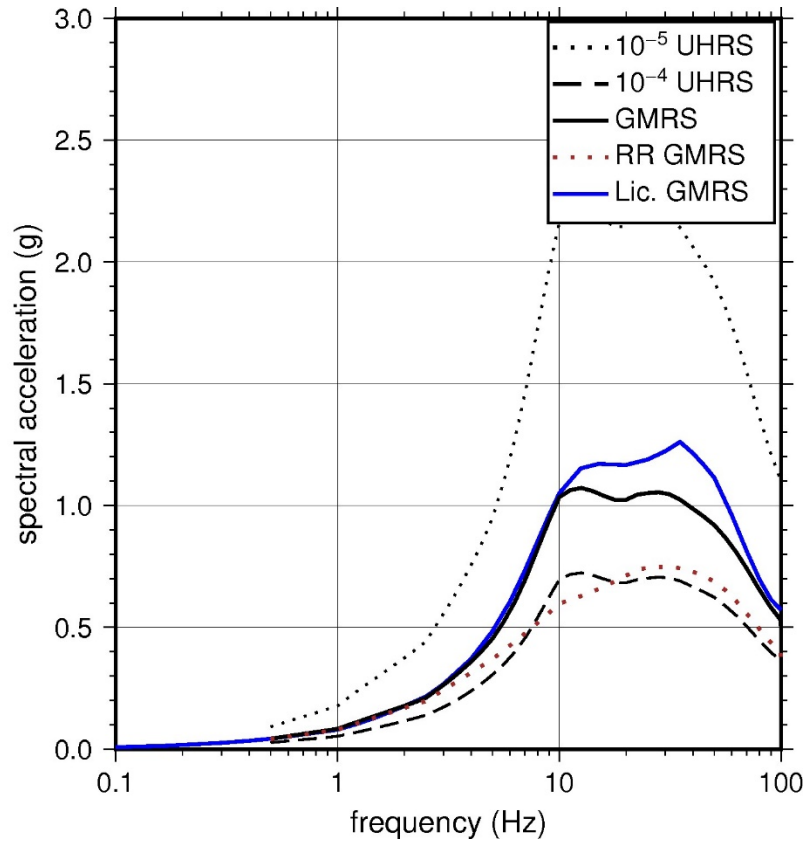
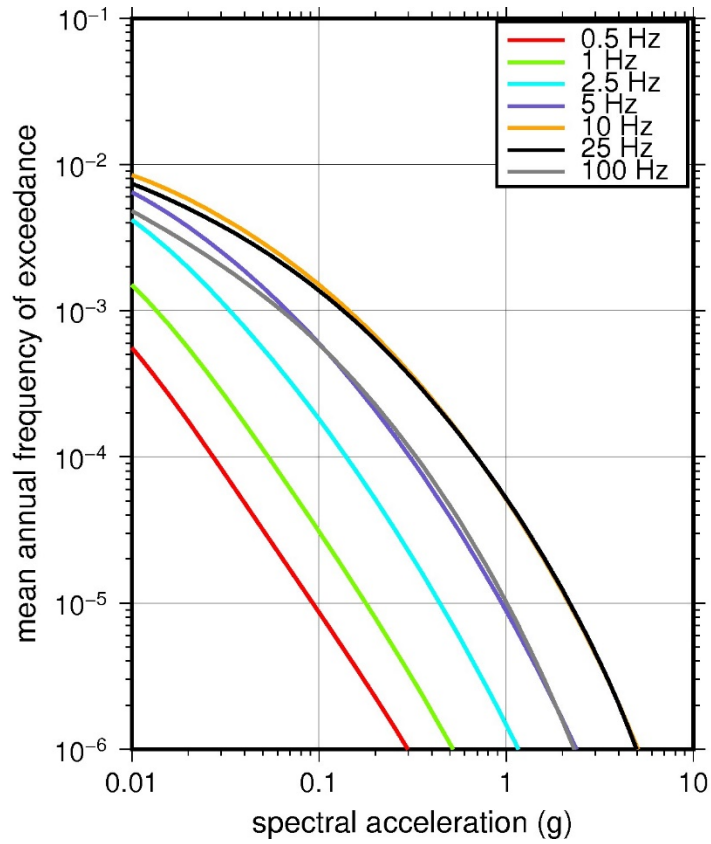


Figure 2.3-35 Shear Wave Velocity ( $V_s$ ) Profiles for North Anna. Basecase (BC) Profile Shown as Solid Bold Line; Lower and Upper Range (LR and UR) Profiles Shown as Dashed Lines. Profiles Terminate at Reference Rock Velocity of 2,831 m/sec [9,285 ft/sec] per EPRI GMM (2013)



**Figure 2.3-36 Overall Weighted Median Site Amplification Factor (SAF) (Upper) and Log Standard Deviation of the SAF (Lower) as a Function of Input Acceleration for EPRI GMM (2013) Spectral Frequencies**



**Figure 2.3-37 Mean Control Point Hazard Curves (Left) for EPRI GMM (2013) Spectral Frequencies, and GMRS and UHRs (Right) for North Anna**

### 2.3.10 Oconee

The Oconee Nuclear Station site is located on Lake Keowee in the Piedmont physiographic province and is founded on Paleozoic age metamorphic rock. The horizontal SSE response spectrum for Oconee has a Housner type spectral shape and is anchored at a PGA of 0.10g.

#### 2.3.10.1 Reference Rock Hazard

For the reference rock PSHA, the NRC staff selected the 12 CEUS-SSC (NRC, 2012b) background seismic source zones that are located within 320 km [200 mi] of the Oconee site. The NRC staff also selected the seven CEUS-SSC RLME sources that are located within 806 km [500 mi] of the site. To develop the reference rock seismic hazard curves for the Oconee site, the NRC staff used the GMPEs in the updated EPRI GMM (2013). As shown in Figure 2.3-38, the NMFS and Charleston RLMEs and the PEZ-N seismotectonic source zone are the largest contributors to the 1 Hz reference rock total mean hazard curve at the  $10^{-4}$  AFE level. For the 10 Hz reference rock total mean hazard curve, the PEZ-N source zone is the largest contributor at the  $10^{-4}$  AFE level.

#### 2.3.10.2 Site Response Evaluation

##### 2.3.10.2.1 Site Profiles

To develop a basecase profile, the NRC staff used the geologic information in the NTTF R2.1 SHSR (Batson, 2014) submitted by Duke Energy (hereafter referred to as “the licensee” within this plant section). As described in the licensee’s SHSR, the Oconee site consists of a thin layer of residual soils (clay, sandy silt, and sand) overlying about 3 ft [1 m] of weathered bedrock with hard metamorphic igneous bedrock below. The Oconee structures are founded on granitoid gneiss, which is a typical rock for the southeastern Inner Piedmont Belt. In Tables 2.3.1-1, 2.3.1-2, and 2.3.2-3 of the SHSR, the licensee briefly described the subsurface materials in terms of the geologic units and layer thicknesses. For its site response evaluation, the NRC staff used the bottom of the reactor building’s mat foundation, which corresponds to an elevation of 230 m [753 ft] MSL, as the control point elevation for the Oconee site.

The geophysical field investigations for Oconee, conducted in the 1960s, consist of two seismic refraction lines, an uphole velocity survey, and velocity measurements of core rock samples. Recently, as part of its main steam isolation valve project, the licensee performed borehole geophysical measurements (P-S suspension logging) in multiple boreholes, with the deepest measurement reaching about 34 m [110 ft] beneath the site. Tables 2.3.1-1, 2.3.1-2, and 2.3.1-3 of the SHSR give the  $V_S$  measurements from three of the main steam isolation valve project boreholes. Table 2.3.2-2 of the SHSR gives the average measured  $V_S$  determined from the licensee’s site investigations.

For its SHSR, the licensee developed a basecase profile that extends to a depth of 20 m [67 ft] below the control point elevation. The entire profile consists of the metamorphic igneous rock (granitoid gneisses), for which the licensee measured an average  $V_S$  of 2,520 m/sec [8,265 ft/sec]. Based on the lithology of the bedrock beneath the site, the licensee assumed that the  $V_S$  attained the reference rock  $V_S$  of 2,831 m/sec [9,285 ft/sec] at a depth of 20 m [67 ft] beneath the site, which is the deepest borehole geophysical measurement.

As multiple geophysical field investigations have characterized the rock strata beneath the Oconee site, the NRC staff used the licensee’s layer thicknesses and  $V_S$  for its basecase profile.

To capture the uncertainty in its basecase profile, the NRC staff developed lower and upper range (10<sup>th</sup> and 90<sup>th</sup> percentile) profiles by multiplying the basecase  $V_S$  values by scale factors of 0.83 and 1.21, respectively, which corresponds to an epistemic logarithmic standard deviation of 0.15. The weights for the lower, best-estimate, and upper basecase profiles are 0.3, 0.4, and 0.3, respectively. Figure 2.3-39 shows the basecase, lower, and upper profiles used by the NRC staff.

#### 2.3.10.2.2 *Dynamic Material Properties and Site Kappa*

The NRC staff assumed both linear and nonlinear dynamic behavior for the rock beneath the Oconee site. To model the nonlinear behavior of the rock, the NRC staff used the EPRI rock shear modulus reduction and material damping curves. To model the linear behavior, the NRC staff used a constant damping ratio of 3 percent. The NRC staff assumed these two alternative dynamic responses for the entire profile and, because of the higher  $V_S$  of this rock layer, assigned weights of 0.7 and 0.3 to the linear and nonlinear alternatives, respectively.

To determine the basecase  $\kappa_0$  for the Oconee site, the NRC staff first used the Campbell (2009) Model 1 relationship between  $V_S$  and  $Q_{ef}$  to determine a  $Q_{ef}$  for each layer. Combining these  $Q_{ef}$  values with the thicknesses and  $V_S$  for each of the layers results in a total  $\kappa_0$  value of about 6.1 msec, which includes the 6 msec assumed for the underlying reference rock. For the lower and upper basecase profiles, the NRC staff also calculated a  $\kappa_0$  value of 6.1 msec, respectively, using the same approach as for the best-estimate basecase profile. In contrast, the licensee estimated  $\kappa_0$  by combining the lowest low-strain damping values from the EPRI rock material damping curves over the entire profile to estimate best-estimate, lower, and upper basecase  $\kappa_0$  values of 6.5, 6.7, and 6.0 msec, respectively.

Table 2.3-11 provides the layer depths, lithologies,  $V_S$ , unit weights, and dynamic properties for the NRC staff's three profiles. In summary, the site response logic tree developed by the NRC staff for the Oconee site consists of six alternatives; three basecase profiles (each with a different  $\kappa_0$  value) and two alternative dynamic property branches.

#### 2.3.10.2.3 *Methodology and Results*

The NRC staff followed the methodology described in Section 2.1.4 to develop the final site amplification factors. Figure 2.3-40 shows the overall median site amplification factors and their variability for each of the seven spectral frequencies. As shown in Figure 2.3-40, the median site amplification factor for the seven spectral frequencies are all close to 1. The lower half of Figure 2.3-40 shows that the logarithmic standard deviations for the site amplification factors range from about 0.05 to 0.10.

#### 2.3.10.3 *Control Point Hazard*

The NRC staff implemented Approach 3 from the SPID to develop a weighted control point seismic hazard curve for each of the six unique combinations of the site response logic tree for the Oconee site. After combining these curves to develop the final mean control point hazard curves, the NRC staff determined the  $10^{-4}$  and  $10^{-5}$  UHRS in order to calculate the final GMRS. Figure 2.3-41 shows the final control point mean seismic hazard curves for each of the seven spectral frequencies as well as the NRC staff's UHRS and GMRS, and the licensee's NTTF R2.1 GMRS (Batson, 2014). As shown in Figure 2.3-41, the NRC staff's GMRS (black curve) is similar to the licensee's GMRS (blue curve) up to 10 Hz and then is slightly higher for the higher



frequencies. For comparison, Figure 2.3-41 also shows the NRC staff's reference rock GMRS (brown dotted curve).

Layer	Depth (ft)	Description	$V_s$ (ft/sec)			$V_s$ Sigma (ln)	BC Unit Weight (pcf)	Dynamic Properties	
			LR (0.3)	BC (0.4)	UR (0.3)			Alt. 1 (0.3)	Alt. 2 (0.7)
1	67	Rock: gneiss	6,819	8,265	9,285	0.25	160	EPRI Rock	L 3.0%

LR = lower range; BC = basecase; UR = upper range; ln = natural log; pcf = pounds per cubic foot; L = linear; Alt. = alternative.  
 For LR, BC, UR, and Alt.: Values in parentheses refer to weights for site response analysis logic tree branches.

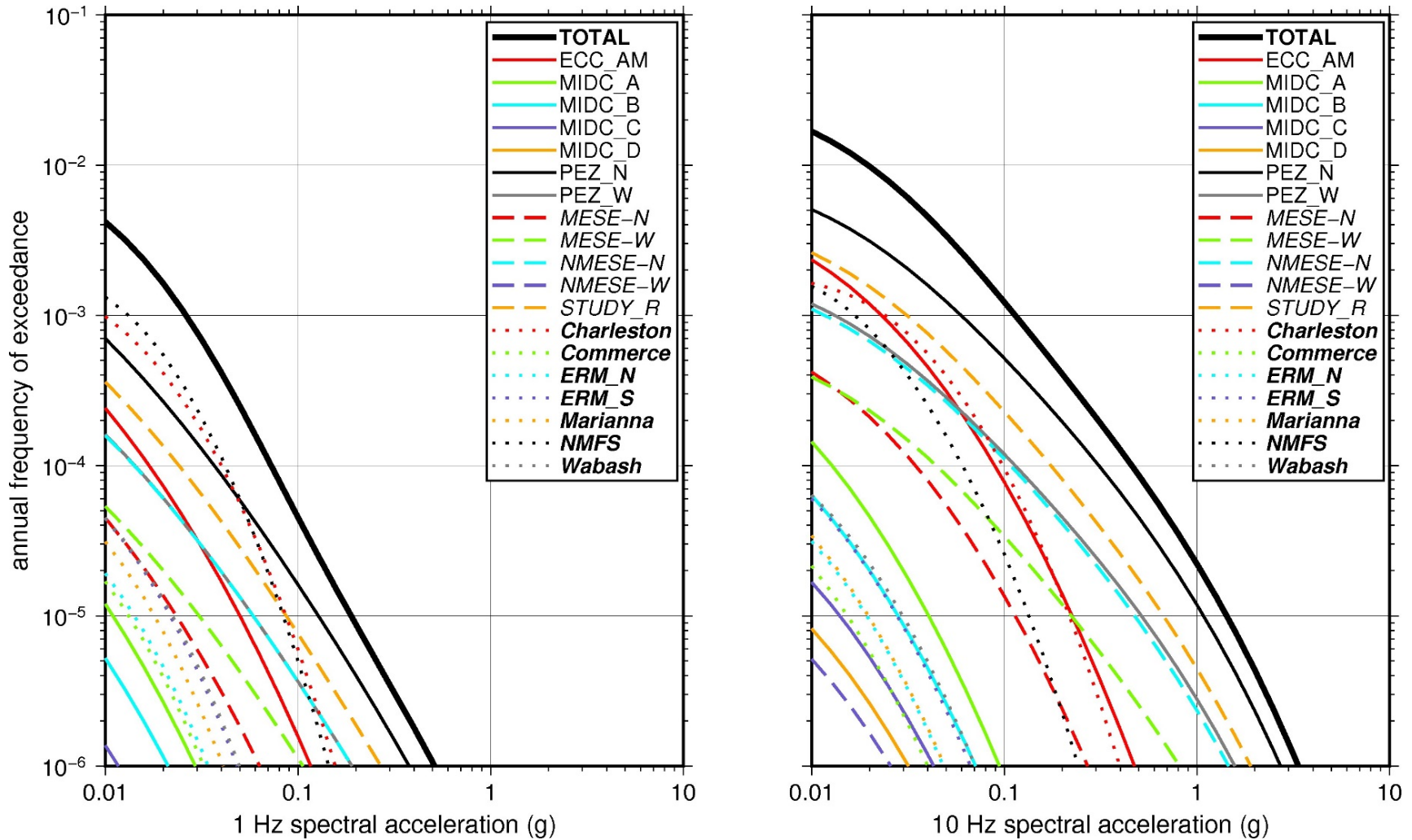


**Figure 2.3-38 Low-Frequency (1 Hz, Left) and High-Frequency (10 Hz, Right) Reference Rock Hazard Curves for Oconee. Total Hazard is Shown as a Bold Black Line; Individual Contributions to the Hazard for Each of the CEUS-SSC Sources are Shown as Colored Lines Defined in the Legend. See Table 2.1-1 for Source Name Definitions**

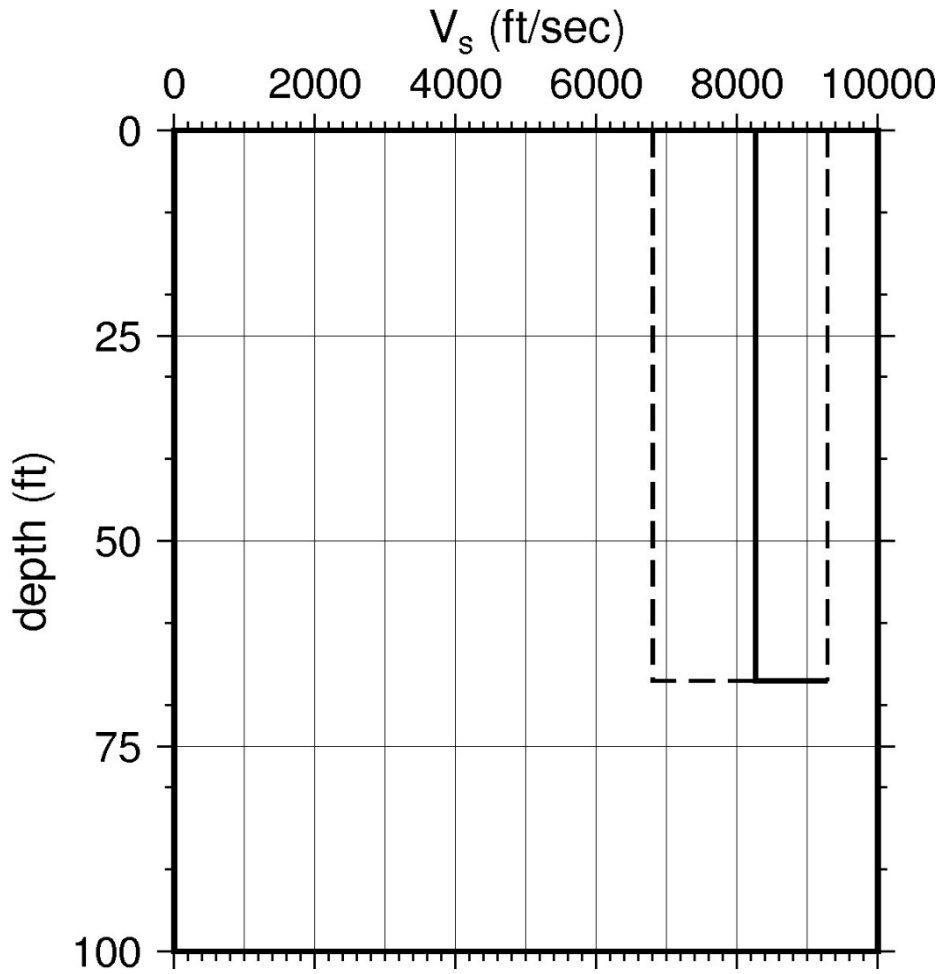


**Figure 2.3-39 Shear Wave Velocity ( $V_s$ ) Profiles for Oconee. Basecase (BC) Profile Shown as Solid Bold Line; Lower and Upper Range (LR and UR) Profiles Shown as Dashed Lines. Profiles Terminate at Reference Rock Velocity of 2,831 m/sec [9,285 ft/sec] per EPRI GMM (2013)**

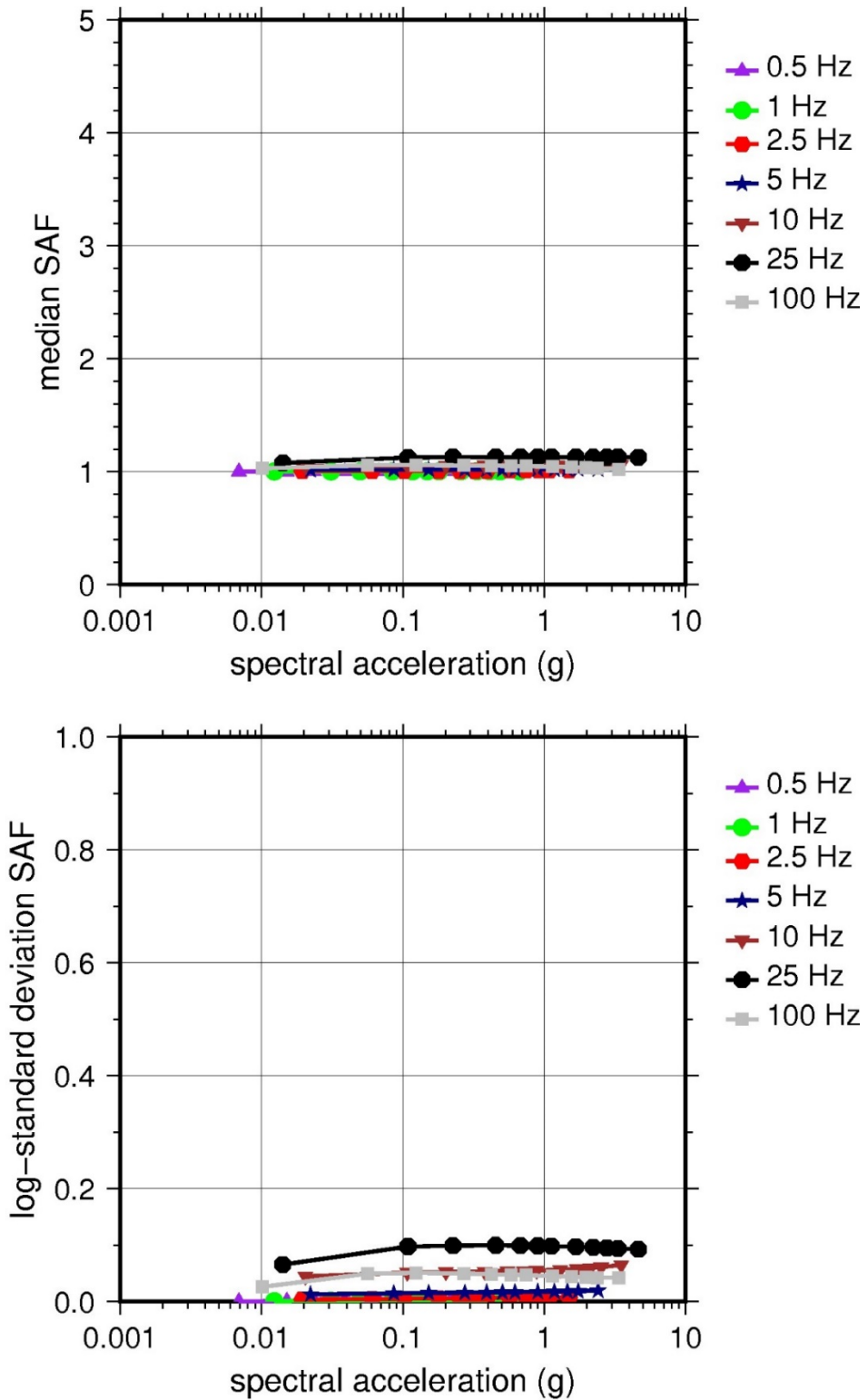


**Figure 2.3-40 Overall Weighted Median Site Amplification Factor (SAF) (Upper) and Log Standard Deviation of the SAF (Lower) as a Function of Input Acceleration for EPRI GMM (2013) Spectral Frequencies**

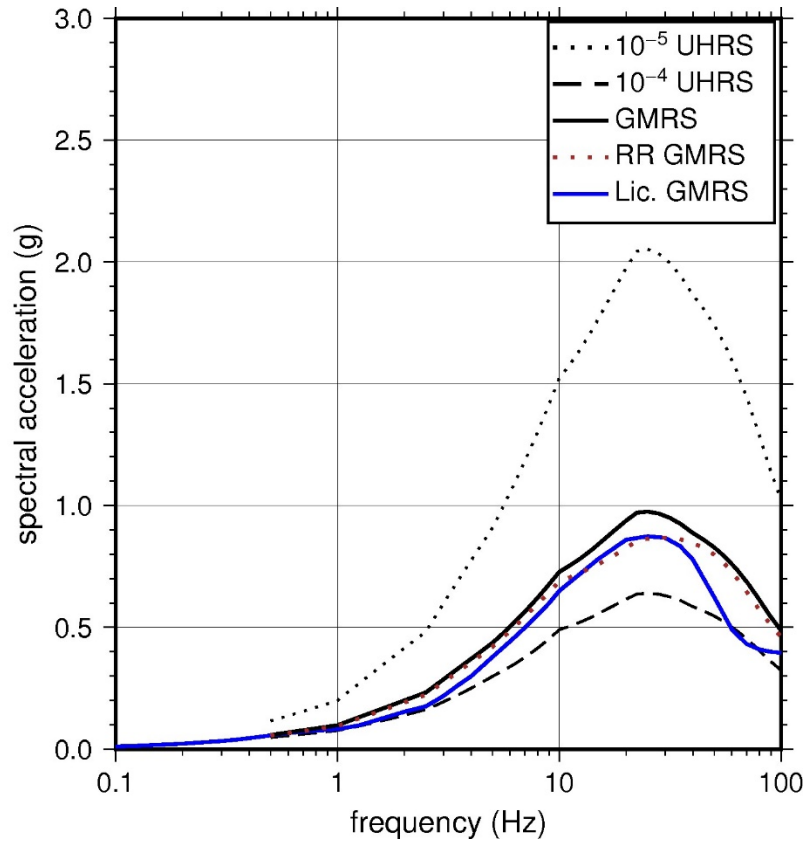
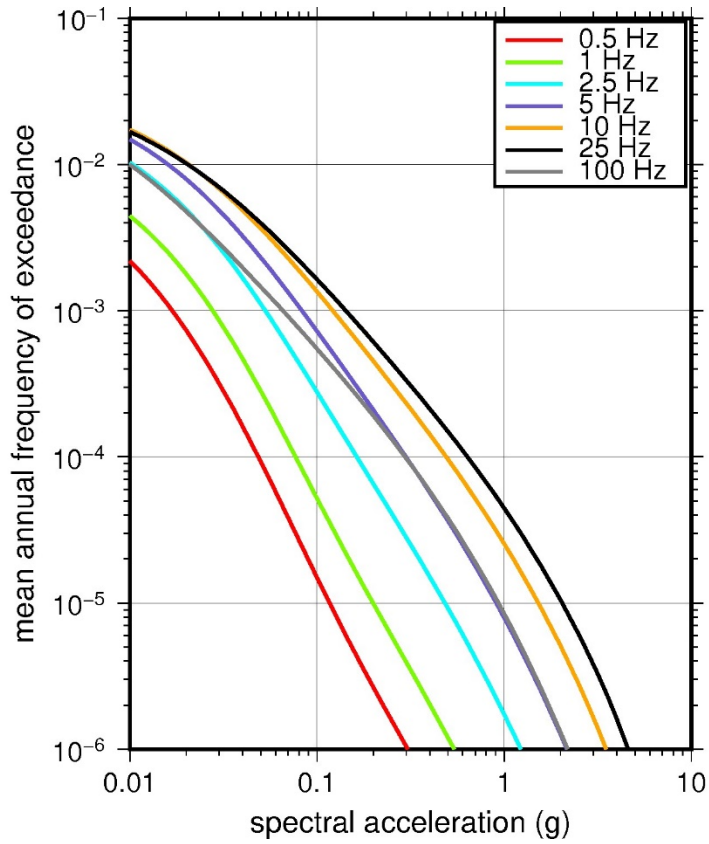


**Figure 2.3-41 Mean Control Point Hazard Curves (Left) for EPRI GMM (2013) Spectral Frequencies, and GMRS and UHRS (Right) for Oconee**

### 2.3.11 H.B. Robinson

The H.B. Robinson Steam Electric Plant site is located in South Carolina adjacent to Lake Robinson within the Coastal Plain physiographic province and is founded on about 122 m [400 ft] of sedimentary strata over metamorphic rock of Paleozoic age. The horizontal SSE response spectrum for Robinson has a Housner type spectral shape and is anchored at a PGA of 0.20g.

#### 2.3.11.1 Reference Rock Hazard

For the reference rock PSHA, the NRC staff selected the seven CEUS-SSC (NRC, 2012b) background seismic source zones that are located within 320 km [200 mi] of the site. The NRC staff also selected the Charleston and NMFS CEUS-SSC RLME sources. To develop the reference rock seismic hazard curves for the Robinson site, the NRC staff used the GMPEs in the updated EPRI GMM (2013). As shown in Figure 2.3-42, the Charleston RLME is the largest contributor to both the 1 Hz and 10 Hz reference rock total mean hazard curves at the  $10^{-4}$  AFE level.

#### 2.3.11.2 Site Response Evaluation

##### 2.3.11.2.1 Site Profiles

To develop a basecase profile, the NRC staff used the geologic information in the NTTF R2.1 SHSR (Gideon, 2014) and revised SHSR (Glover, 2015) submitted by Duke Energy (hereafter referred to as “the licensee” within this plant section). As described in the licensee’s SHSR, the Robinson site consists of about 116 m [380 ft] of sedimentary strata (sand, clay, gravel) overlying a thin layer of weathered rock (claystone) grading into hard metamorphic rock. The Robinson structures are supported on the Middendorf Formation, which is of Late Cretaceous age. In Table 2.3.1-1 of the revised SHSR, the licensee briefly described the subsurface materials in terms of the geologic units and layer thicknesses. For its site response evaluation, the NRC staff used the top of the ground surface, which corresponds to an elevation of 69 m [226 ft] above MSL, as the control point elevation for the Robinson site.

The licensee’s basecase  $V_S$  profile is based on recent borehole geophysical measurements (P-S suspension logging) from a single deep borehole that extended through the soil to the hard metamorphic rock beneath the plant and two SASW profiles to the north and south of the major plant structures. Combining these three geophysical measurements, the licensee developed three weighted alternative basecase profiles, shown in Table 3.2.2-1 of the revised SHSR.

For its SHSR, the licensee developed a basecase profile that extends to a depth of 125 m [410 ft] below the control point elevation. The majority of the profile consists of sedimentary strata from the Cretaceous age Middendorf Formation, for which the licensee measured a  $V_S$  of about 274 m/sec [900 ft/sec] for the upper soil layers to 762 m/sec [2,500 ft/sec] for the deeper soil layers. The licensee encountered weathered rock (claystone), which has an estimated  $V_S$  of about 1,433 m/sec [4,700 ft/sec], at a depth of 115 m [379 ft] and sound rock (tuffaceous phyllite), which has an estimated  $V_S$  of about 2,287 m/sec [7,500 ft/sec], at a depth of 121 m [398 ft].

As multiple geophysical field investigations have characterized the rock strata beneath the Robinson site, the NRC staff used the licensee’s layer thicknesses and  $V_S$  for its basecase profile.

To capture the uncertainty in its basecase profile, the NRC staff developed lower and upper range (10<sup>th</sup> and 90<sup>th</sup> percentile) profiles by multiplying the basecase  $V_S$  values by scale factors of 0.78 and 1.27, respectively, which corresponds to an epistemic logarithmic standard deviation of 0.20. The weights for the lower, best-estimate, and upper basecase profiles are 0.3, 0.4, and 0.3, respectively. Figure 2.3-43 shows the basecase, lower and upper profiles used by the NRC staff, which extend to a depth of 125 m [410 ft] below the control point elevation.

#### 2.3.11.2.2 *Dynamic Material Properties and Site Kappa*

The NRC staff assumed both linear and nonlinear behavior for the soil and rock beneath the Robinson site. To model the nonlinear response within the upper 116 m [379 ft] of soil deposits (Layers 1 to 4), the NRC staff used the EPRI soil shear modulus reduction and material damping curves as one alternative and the Peninsular Range curves for the second equally weighted alternative. To model the nonlinear behavior of the rock strata, the NRC staff used the EPRI rock shear modulus reduction and material damping curves. To model the linear behavior, the NRC staff used a constant damping ratio of 3 percent. The NRC staff assumed these two alternative dynamic responses for the thin layer of weathered rock (Layer 5) and gave them equal weight. For the remaining 4 m [12 ft] of the profile, the NRC staff assumed a linear response with a material damping ratio value of 0.1 percent to maintain consistency with the  $\kappa_0$  value for the Robinson site.

To determine the basecase  $\kappa_0$  for the Robinson site, the NRC staff first used the Campbell (2009) Model 1 relationship between  $V_S$  and the  $Q_{ef}$  to determine the  $Q_{ef}$  for each layer. Combining these  $Q_{ef}$  values with the thicknesses and  $V_S$  for each of the layers results in a total  $\kappa_0$  value of 16 msec, which includes the 6 msec assumed for the underlying reference rock. For the lower and upper profiles, the NRC staff calculated values of 21 and 13 msec, respectively, using the same approach as for the basecase profile. In contrast, the licensee used a  $\kappa_0$  value of 14 msec for the basecase, lower, and upper profiles based on using the empirical relationship from the SPID (EPRI, 2012) between profile thickness and  $\kappa_0$ .

Table 2.3-12 provides the layer depths, lithologies,  $V_S$ , unit weights, and dynamic properties for the NRC staff's three profiles. In summary, the site response logic tree developed by the NRC staff for the Robinson site consists of six alternatives; three basecase profiles (each with a different  $\kappa_0$  value) and two alternative dynamic property branches.

#### 2.3.11.2.3 *Methodology and Results*

The NRC staff followed the methodology described in Section 2.14 to develop the final site amplification factors. Figure 2.3-44 shows the overall median site amplification factors and their variability for each of the seven spectral frequencies. As shown in Figure 2.3-44, the median site amplification factors vary from around 1.5 to 3.0 before falling off with higher input spectral accelerations. The lower half of Figure 2.3-44 shows that the logarithmic standard deviations for the site amplification factors vary from 0.05 to 0.3.

#### 2.3.11.3 *Control Point Hazard*

The NRC staff implemented Approach 3 from the SPID to develop a weighted control point seismic hazard curve for each of the six unique combinations of the site response logic tree for the Robinson site. After combining these curves to develop the final mean control point hazard curves, the NRC staff determined the  $10^{-4}$  and  $10^{-5}$  UHRS in order to calculate the final GMRS. Figure 2.3-45 shows the final control point mean seismic hazard curves for each of the seven

spectral frequencies as well as the NRC staff's UHRS and GMRS, and the licensee's NTTF R2.1 GMRS (Glover, 2015). As shown in Figure 2.3-45, the NRC staff's GMRS (black curve) is moderately higher than the licensee's GMRS (blue curve) due to the licensee's changes to the magnitude recurrence parameters of the CEUS-SSC model for the region surrounding the site (Glover, 2015). These changes to the recurrence parameters are based on a reevaluation of the CEUS-SSC earthquake catalog to remove (1) events likely to be reservoir induced and (2) mislocated or duplicative events following the 1886 Charleston, SC earthquake sequence. The net effect of these changes is to moderately reduce the control point hazard results for the Robinson site.

**Table 2.3-12 Layer Depths, Shear Wave Velocities ( $V_s$ ), Unit Weights, and Dynamic Properties for Robinson**

Layer	Depth (ft)	Description	$V_s$ (ft/sec)			$V_s$ Sigma (ln)	BC Unit Weight (pcf)	Dynamic Properties	
			LR (0.3)	BC (0.4)	UR (0.3)			Alt. 1 (0.5)	Alt. 2 (0.5)
1	62	Soil: sand	684	884	1,142	0.25	120	EPRI Soil	Pen.
2	177	Soil: clay	1,687	2,180	2,818	0.15	130	EPRI Soil	Pen.
3	237	Soil: clay, sand, gravel	1,471	1,900	2,456	0.15	130	EPRI Soil	Pen.
4	379	Soil: clay, sand, gravel	2,174	2,809	3,630	0.15	130	EPRI Soil	Pen.
5	398	Rock: claystone, clay	3,626	4,686	6,056	0.15	140	EPRI Rock	L 3.0%
6	410	Rock: tuffaceous, phyllite)	5,814	7,513	9,285	0.15	160	L 0.1%	L 0.1%

LR = lower range; BC = basecase; UR = upper range; ln = natural log; pcf = pounds per cubic foot; L = linear; Alt. = alternative; Pen. = Peninsular.  
 For LR, BC, UR, and Alt.: Values in parentheses refer to weights for site response analysis logic tree branches.



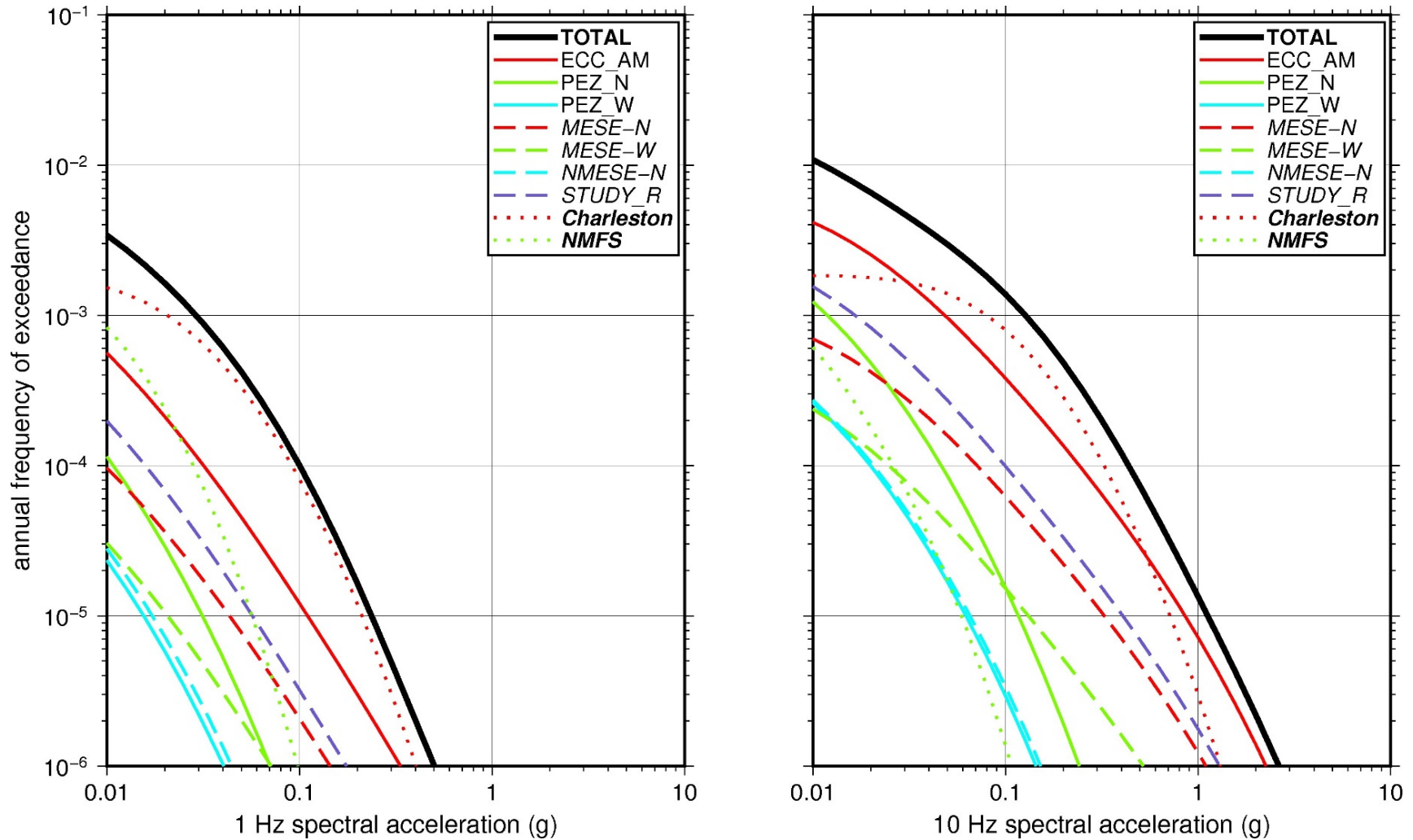


**Figure 2.3-42 Low-Frequency (1 Hz, Left) and High-Frequency (10 Hz, Right) Reference Rock Hazard Curves For Robinson. Total Hazard is Shown as a Bold Black Line; Individual Contributions to the Hazard for Each of the CEUS-SSC Sources are Shown as Colored Lines Defined in the Legend. See Table 2.1-1 for Source Name Definitions**

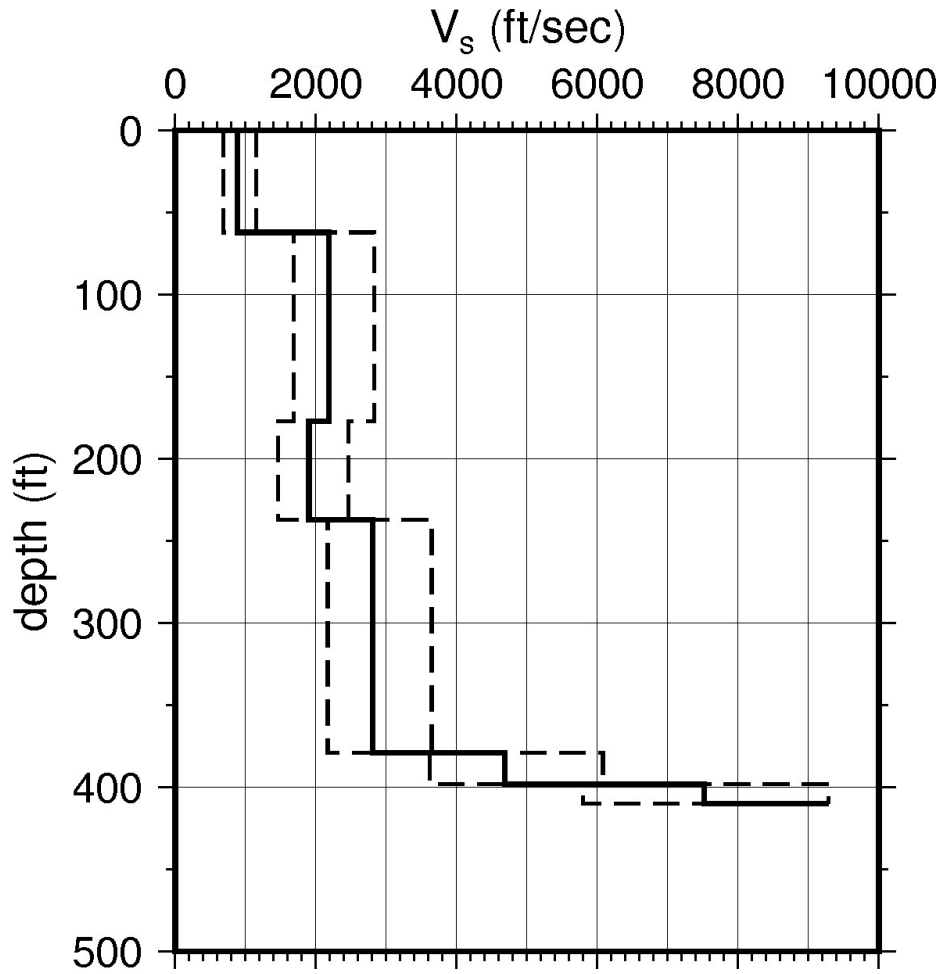


**Figure 2.3-43 Shear Wave Velocity ( $V_s$ ) Profiles for Robinson. Basecase (BC) Profile Shown as Solid Bold Line; Lower and Upper Range (LR and UR) Profiles Shown as Dashed Lines. Profiles Terminate at Reference Rock Velocity of 2,831 m/sec [9,285 ft/sec] per EPRI GMM (2013)**

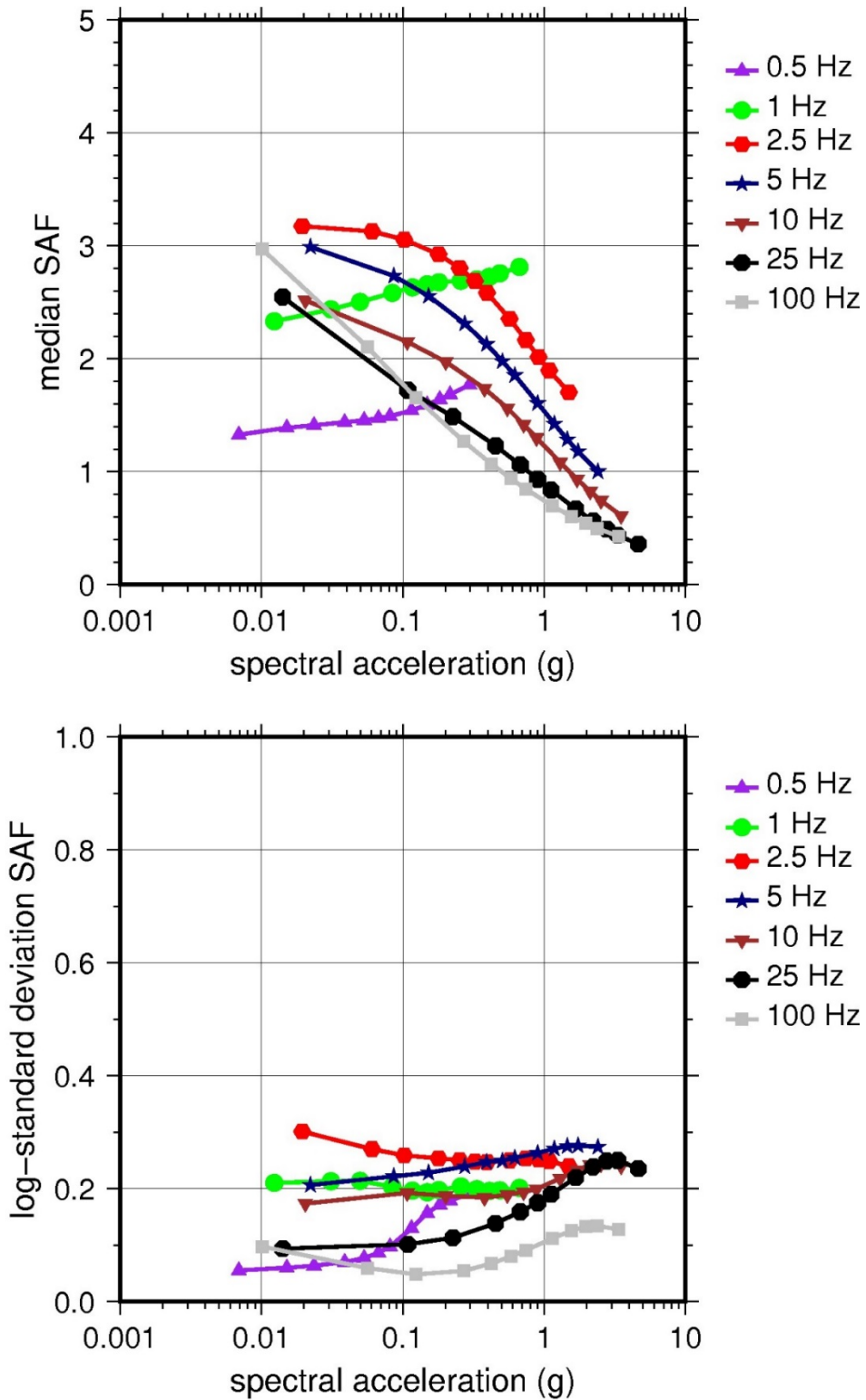


**Figure 2.3-44 Overall Weighted Median Site Amplification Factor (SAF) (Upper) and Log Standard Deviation of the SAF (Lower) as a Function of Input Acceleration for EPRI GMM (2013) Spectral Frequencies**

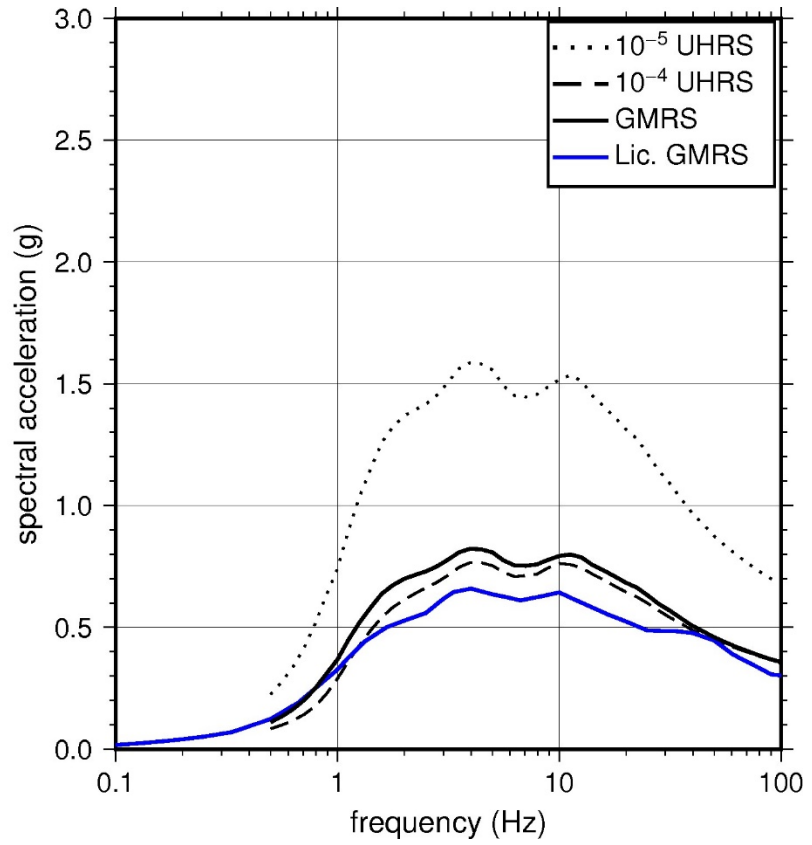
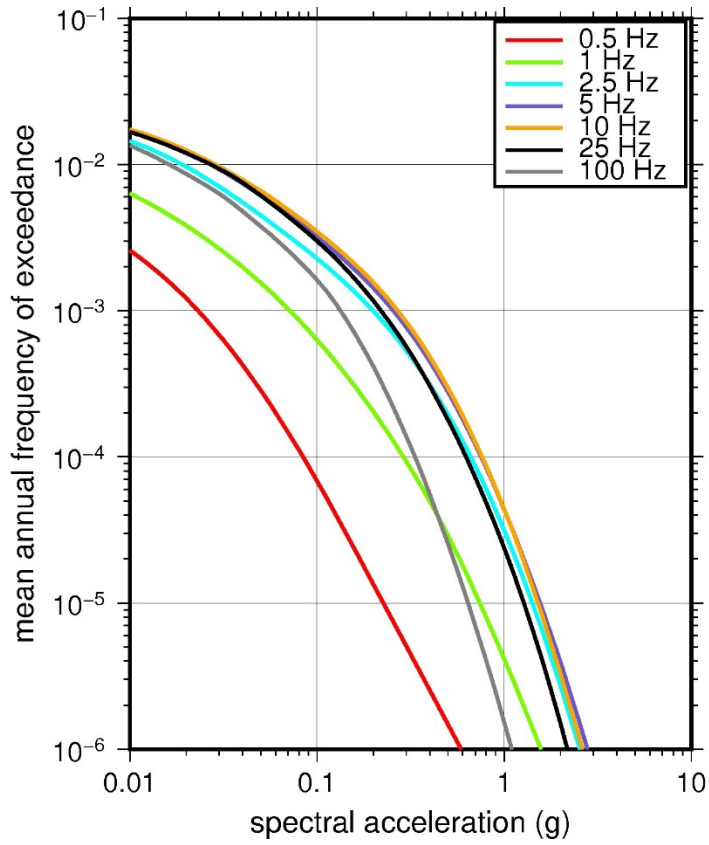


**Figure 2.3-45 Mean Control Point Hazard Curves (Left) for EPRI GMM (2013) Spectral Frequencies, and GMRS and UHRs (Right) for Robinson**

### 2.3.12 Sequoyah

The Sequoyah Nuclear Plant site is located on the western shore of Chickamauga Reservoir along the Tennessee River within the Ridge and Valley physiographic province and is founded on over 3,659 m [12,000 ft] of competent sedimentary rock (limestone, shale, and dolomite) of Paleozoic age. The horizontal SSE response spectrum for Sequoyah has a Housner type spectral shape and is anchored at a PGA of 0.18g.

#### 2.3.12.1 Reference Rock Hazard

For the reference rock PSHA, the NRC staff selected the 15 CEUS-SSC (NRC, 2012b) background seismic source zones that are located within 320 km [200 mi] of the site. The NRC staff also selected the seven CEUS-SSC RLME sources that are located within 806 km [500 mi] of the Sequoyah site. To develop the reference rock seismic hazard curves for the Sequoyah site, the NRC staff used the GMPEs in the updated EPRI GMM (2013). As shown in Figure 2.3-46, the NMFS RLME, which is located about 250 km [155 mi] to the west of Sequoyah, is the largest contributor to the 1 Hz reference rock total mean hazard curve at the  $10^{-4}$  AFE level. For the 10 Hz reference rock total mean hazard curve, the PEZ-N seismotectonic source zone is the largest contributor at the  $10^{-4}$  AFE level.

#### 2.3.12.2 Site Response Evaluation

##### 2.3.12.2.1 Site Profiles

To develop a basecase profile, the NRC staff used the geologic information in the NTTF R2.1 SHSR (Shea, 2014) submitted by the TVA (hereafter referred to as “the licensee” within this plant section). As described in the licensee’s SHSR, the Sequoyah site consists of about 12 m [38 ft] of residual clays and silts overlying interbedded limestone and shale bedrock of the Conasauga Group. The primary Sequoyah structures are founded on the Conasauga Group, which is of Middle Cambrian age. In Tables 2.3.1-1 and 2.3.1-2 of the SHSR, the licensee briefly described the subsurface materials in terms of the geologic units and layer thicknesses. For its site response evaluation, the NRC staff used the top of the Conasauga Group, which corresponds to an elevation of 195 m [641 ft] MSL, as the control point elevation for the Sequoyah site.

The licensee’s basecase  $V_s$  profile is based on downhole and crosshole geophysical measurements of the uppermost soil and rock strata to a depth of 31 m [103 ft] along with more recent SASW measurements at the Watts Bar nuclear power plant site, which is situated over the same rock formations as Sequoyah. Combining these geophysical measurements, the licensee developed three weighted alternative basecase profiles, shown in Table 2.3.2-1 of the SHSR.

For its SHSR, the licensee developed a basecase profile that extends to a depth of 1,628 m [6,186 ft] below the control point elevation. The major controlling geologic feature of the Sequoyah site is the Kingston Thrust fault. Movement along this fault resulted in the Conasauga Group at the plant site resting upon the younger Ordovician age Knox Group dolomite, which normally overlies the Conasauga. The majority of the licensee’s basecase profile consists of sedimentary strata from the Conasauga and the Knox Groups, for which the licensee estimated a  $V_s$  of about 1,829 m/sec [6,000 ft/sec] to 2,134 m/sec [7,000 ft/sec]. In between the Conasauga and Knox Group strata is 46 m [150 ft] of limestone from the Pond Springs Formation, which has an estimated  $V_s$  of 2,896 m/sec [9,500 ft/sec]. In summary, the

sequence of sedimentary strata and thrust faults underlying the site is as follows:

(1) Conasauga Group (Cambrian), (2) Kingston Fault, (3) Pond Springs Formation (Ordovician), (4) Knox Group (Ordovician-Cambrian), (5) Conasauga Group (Cambrian), (6) Rome Formation (Cambrian), (7) Chattanooga Fault, (8) Knox Group (Ordovician-Cambrian), (9) Conasauga Group (Cambrian), (10) Rome Formation (Cambrian), (11) Sequatchie Valley Fault, (12) Rome Formation (Cambrian), and (13) basement rock. The licensee terminated its basecase profile at the top of the first instance of the Rome Formation above the Chattanooga Fault. This decision is based on the estimated  $V_S$  of 3,049 m/sec [10,000 ft/sec] for the Rome Formation, which consists of sandstone, siltstone, and shale.

For its basecase profile, the NRC staff used the licensee's layer thicknesses and estimated  $V_S$ . However, the NRC staff applied the velocity gradient of 0.5 m/sec/m [ft/sec/ft] recommended by the SPID for sedimentary rock to the uppermost Conasauga Group stratum.

To capture the uncertainty in the basecase profile, the NRC staff developed lower and upper range (10<sup>th</sup> and 90<sup>th</sup> percentile) profiles by multiplying the basecase  $V_S$  values by scale factors of 0.83 and 1.21, respectively, which corresponds to an epistemic logarithmic standard deviation of 0.15. The weights for the lower, best-estimate, and upper basecase profiles are 0.3, 0.4, and 0.3, respectively. Figure 2.3-47 shows the three profiles used by the NRC staff, which extend to a depth of 1,921 m [6,300 ft] below the control point elevation.

#### 2.3.12.2.2 *Dynamic Material Properties and Site Kappa*

The NRC staff assumed both linear and nonlinear dynamic behavior for the rock beneath the Sequoyah site. To model the nonlinear behavior of the uppermost rock stratum, the NRC staff used the EPRI rock shear modulus reduction and material damping curves. To model the linear behavior, the NRC staff used a constant damping ratio of 3 percent. The NRC staff assumed these two alternative dynamic responses for the upper 152 m [500 ft] of the profile; due to the higher  $V_S$  of this rock stratum, the NRC staff assigned weights of 0.7 and 0.3 to the linear and nonlinear alternatives, respectively. For the remaining 1,768 m [5,800 ft] of its profile, the NRC staff assumed a linear response with material damping ratio values of 1, 0.25, and 0.1 percent to maintain consistency with the  $\kappa_0$  value for the Sequoyah site.

To determine the basecase  $\kappa_0$  for the Sequoyah site, the NRC staff first used the Campbell (2009) Model 1 relationship between  $V_S$  and  $Q_{ef}$  to determine a  $Q_{ef}$  for each layer. Combining these  $Q_{ef}$  values with the thicknesses and  $V_S$  for each of the layers results in a total  $\kappa_0$  value of about 20 msec, which includes the 6 msec assumed for the underlying reference rock. For the lower and upper basecase profiles, the NRC staff calculated  $\kappa_0$  values of 27 and 16 msec, respectively, using the same approach as for the best-estimate basecase profile. In contrast, the licensee estimated  $\kappa_0$  by using the empirical relationship from the SPID (EPRI, 2012) between the average  $V_S$  over the upper 100 ft [30 m] of the profile and  $\kappa_0$ , which results in  $\kappa_0$  values of 12, 20, and 6 msec for the best-estimate, lower, and upper basecase profiles, respectively.

Table 2.3-13 provides the layer depths, lithologies,  $V_S$ , unit weights, and dynamic properties for the NRC staff's three profiles. In summary, the site response logic tree developed by the NRC staff for the Sequoyah site consists of six alternatives; three basecase profiles (each with a different  $\kappa_0$  value) and two alternative dynamic property branches.

### 2.3.12.2.3 Methodology and Results

The NRC staff followed the methodology described in Section 2.1.4 to develop the final site amplification factors. Figure 2.3-48 shows the overall median site amplification factors and their variability for each of the seven spectral frequencies. As shown in Figure 2.3-48, the median site amplification factors are all close to 1 for low-input spectral accelerations and decrease to about 0.6 for higher input accelerations. The lower half of Figure 2.3-32 shows that the logarithmic standard deviations for the site amplification factors are between 0.1 and 0.2.

### 2.3.12.3 Control Point Hazard

The NRC staff implemented Approach 3 from the SPID to develop a weighted control point seismic hazard curve for each of the six unique combinations of the site response logic tree for the Sequoyah site. After combining these curves to develop the final mean control point hazard curves, the NRC staff determined the  $10^{-4}$  and  $10^{-5}$  UHRs in order to calculate the final GMRS. Figure 2.3-49 shows the final control point mean seismic hazard curves for each of the seven spectral frequencies as well as the NRC staff's UHRs and GMRS, and the licensee's NTTF R2.1 GMRS (Shea, 2014). As shown in Figure 2.3-49, the NRC staff's GMRS (black curve) is similar to the licensee's GMRS (blue curve) up to 10 Hz and then falls off more rapidly for the higher frequencies. This difference between GMRS for the higher frequencies is due to the higher  $\kappa_0$  values estimated by the NRC staff for the Sequoyah site. For comparison, Figure 2.3-49 also shows the NRC staff's reference rock GMRS (brown dotted curve).

**Table 2.3-13 Layer Depths, Shear Wave Velocities ( $V_s$ ), Unit Weights, and Dynamic Properties for Sequoyah**

Layer	Depth (ft)	Description	$V_s$ (ft/sec)			$V_s$ Sigma (ln)	BC Unit Weight (pcf)	Dynamic Properties	
			LR (0.3)	BC (0.4)	UR (0.3)			Alt. 1 (0.3)	Alt. 2 (0.7)
1	500	Rock: shale, limestone	4,950	6,000	7,273	0.25	150	EPRI Rock	L 3.0%
2	1,000	Rock: shale, limestone	5,157	6,250	7,576	0.15	150	L 1.0%	L 1.0%
3	1,500	Rock: shale, limestone	5,363	6,500	7,879	0.15	150	L 1.0%	L 1.0%
4	1,650	Rock: limestone	7,661	9,285	9,285	0.15	160	L 0.1%	L 0.1%
5	4,850	Rock: dolomite	5,775	7,000	8,485	0.15	150	L 0.25%	L 0.25%
6	6,300	Rock: shale, limestone	5,775	7,000	8,485	0.15	150	L 0.25%	L 0.25%

LR = lower range; BC = basecase; UR = upper range; ln = natural log; pcf = pounds per cubic foot; L = linear; Alt. = alternative.  
For LR, BC, UR, and Alt.: Values in parentheses refer to weights for site response analysis logic tree branches.

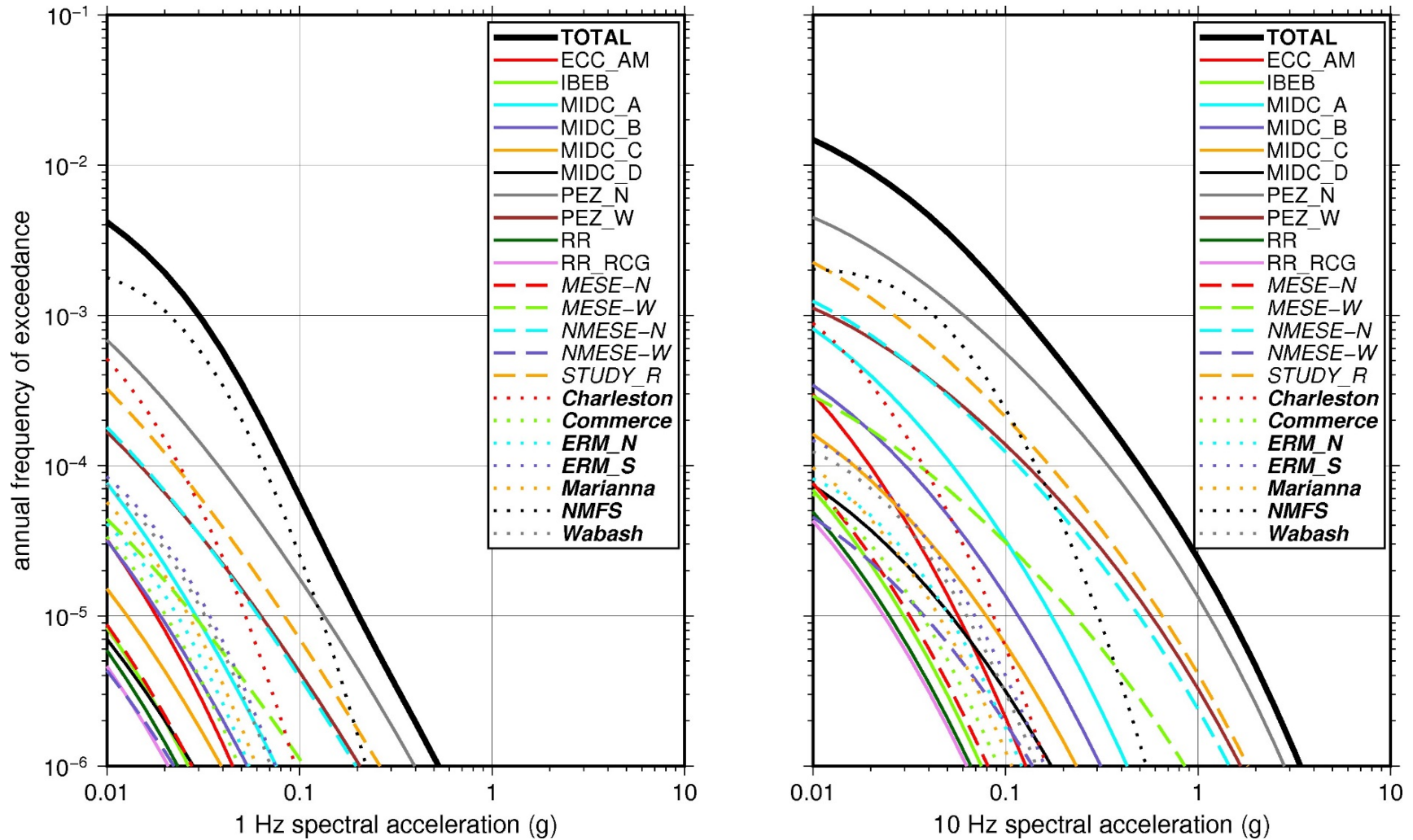


**Figure 2.3-46 Low-Frequency (1 Hz, Left) and High-Frequency (10 Hz, Right) Reference Rock Hazard Curves for Sequoyah. Total Hazard is Shown as a Bold Black Line; Individual Contributions to the Hazard for Each of the CEUS-SSC Sources are Shown as Colored Lines Defined in the Legend. See Table 2.1-1 for Source Name Definitions**



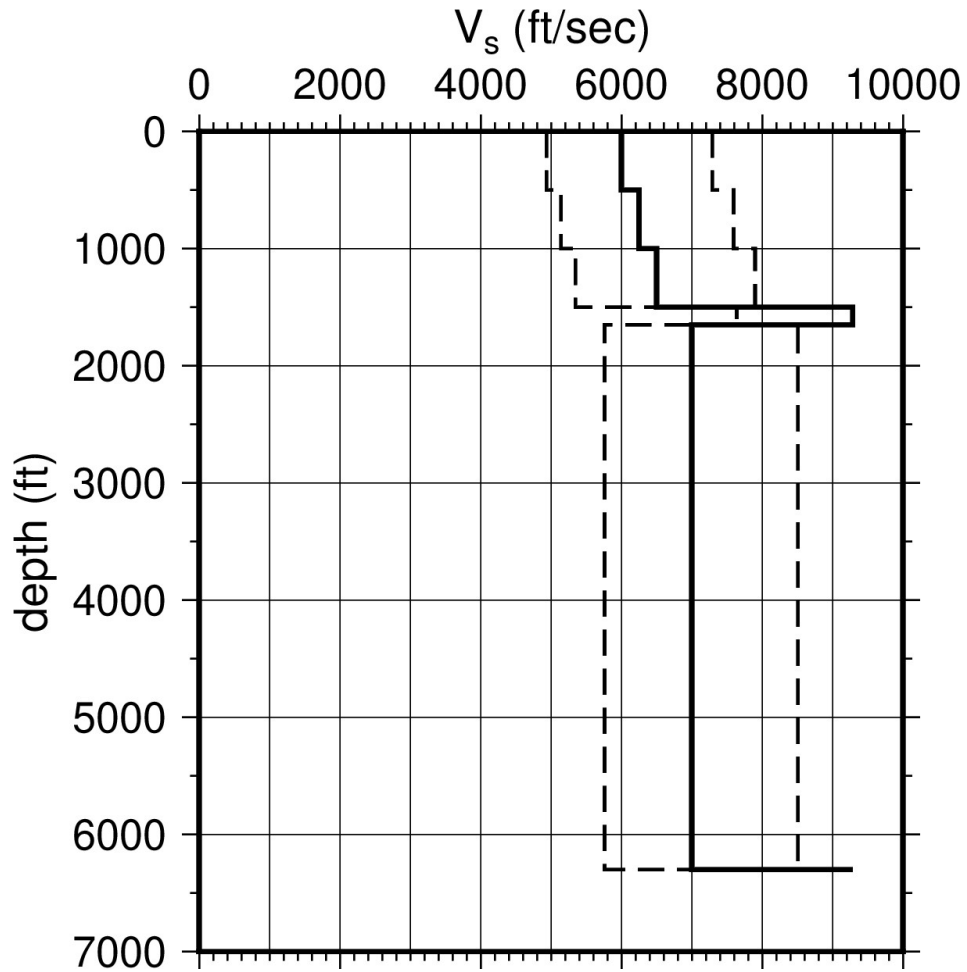


**Figure 2.3-47 Shear Wave Velocity ( $V_s$ ) Profiles for Sequoyah. Basecase (BC) Profile Shown as Solid Bold Line; Lower and Upper Range (LR and UR) Profiles Shown as Dashed Lines. Profiles Terminate at Reference Rock Velocity of 2,831 m/sec [9,285 ft/sec] per EPRI GMM (2013)**

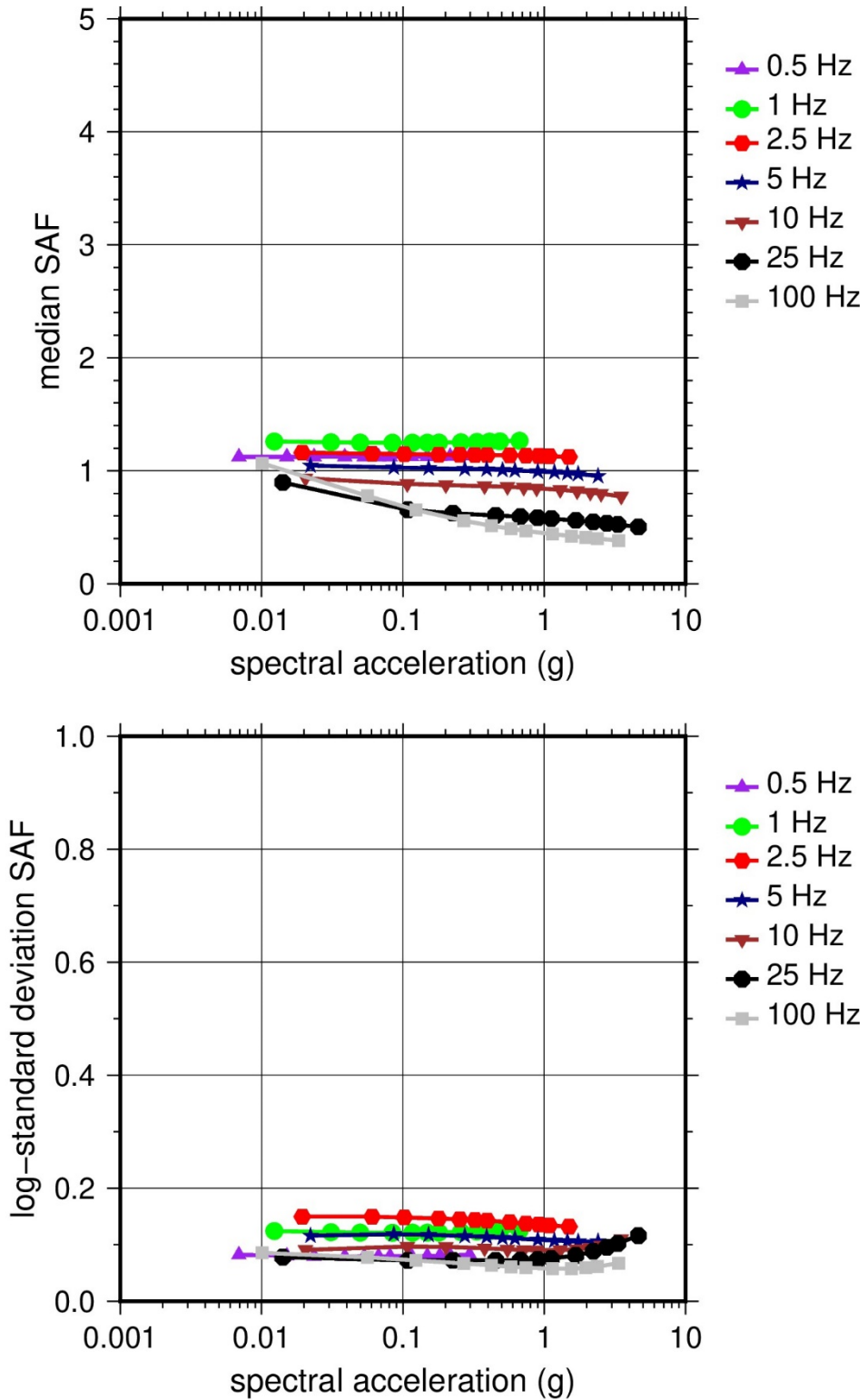


**Figure 2.3-48 Overall Weighted Median Site Amplification Factor (SAF) (Upper) and Log Standard Deviation of the SAF (Lower) as a Function of Input Acceleration for EPRI GMM (2013) Spectral Frequencies**

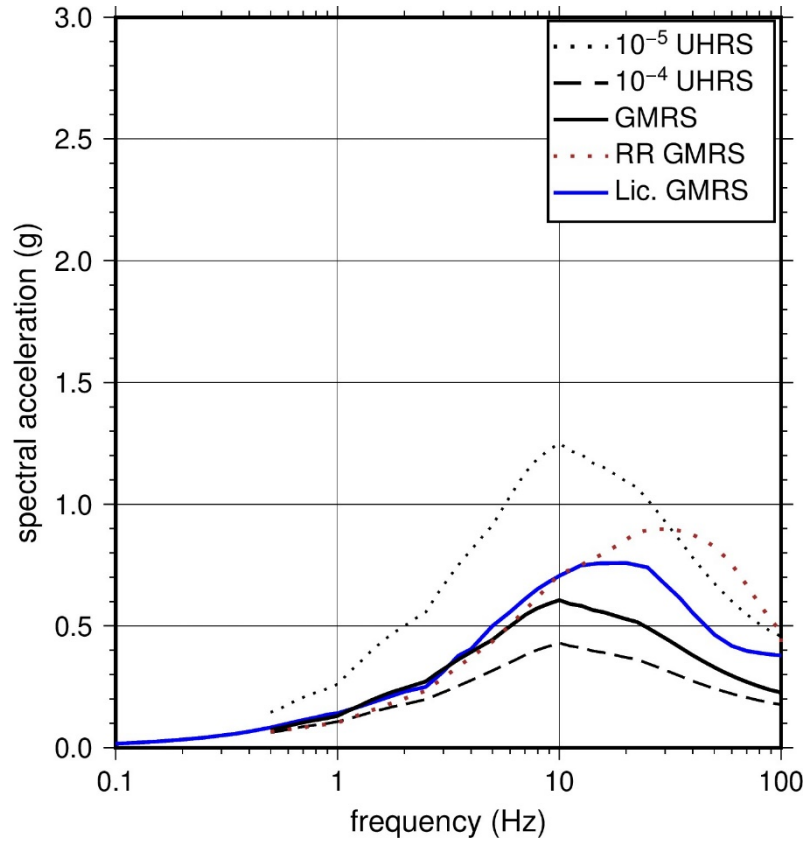
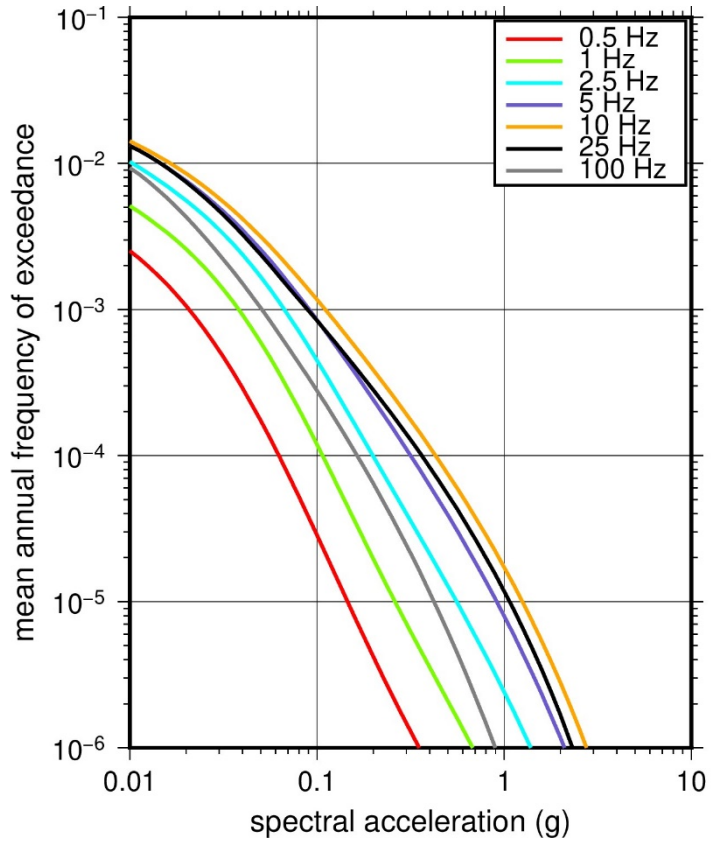


**Figure 2.3-49 Mean Control Point Hazard Curves (Left) for EPRI GMM (2013) Spectral Frequencies, and GMRS and UHRS (Right) for Sequoyah**

### 2.3.13 St. Lucie

The St. Lucie Plant site is located in Florida on Hutchinson Island adjacent to the Atlantic coast within the Coastal Plain physiographic province and is founded on about 213 m [700 ft] of soil over 3,963 m [13,000 ft] of carbonate rock of Mesozoic age. The horizontal SSE response spectrum for St. Lucie has a smooth Housner spectral shape and is anchored at a PGA of 0.10g.

#### 2.3.13.1 Reference Rock Hazard

For the reference rock PSHA, the NRC staff selected the four CEUS-SSC (NRC, 2012b) background seismic source zones that are located within 320 km [200 mi] of the site. In addition, the NRC staff selected the Charleston RLME source, which is about 500 km [306 mi] to the north of the site. To develop the reference rock seismic hazard curves for the St. Lucie site, the NRC staff used the GMPEs in the updated EPRI GMM (2013). As shown in Figure 2.3-50, the Charleston RLME is the largest contributor to the 1 Hz reference rock total mean hazard curves at the  $10^{-4}$  AFE level. For the 10 Hz reference rock total mean hazard curve, the Extended Continental Crust—Gulf Coast (ECC-GC) seismotectonic source zone is the largest contributor at the  $10^{-4}$  AFE level.

#### 2.3.13.2 Site Response Evaluation

##### 2.3.13.2.1 Site Profiles

To develop the basecase profile, the NRC staff used the geologic information in the NTTF R2.1 SHSR (Jensen, 2014), submitted by Florida Power & Light Company (hereafter referred to as “the licensee” within this plant section). As described in the licensee’s SHSR, the St. Lucie site consists of fill overlying sedimentary strata (predominantly sand with limestone fragments), which lies above a sequence of several thousand feet of carbonate rock. The primary St. Lucie structures are founded on engineered fill. In Table 2.3.1-1 of the SHSR, the licensee briefly described the subsurface materials in terms of the geologic units and layer thicknesses. For its site response evaluation, the NRC staff used the ground surface, which corresponds to an elevation of 5.6 m [18.5 ft] above MSL, as the control point elevation for the St. Lucie site.

The field investigations for St. Lucie consisted of a number of borings through the uppermost soils beneath the site. In addition, seismic refraction profiling and a crosshole survey by the licensee measured  $V_P$  and  $V_S$  to a depth of about 49 m [160 ft] beneath the site. Table 2.3.1-1 of the SHSR gives the measured  $V_S$  values from the licensee’s site investigations.

For its SHSR, the licensee developed a basecase profile that extends to a depth of 1,549 m [5,079 ft] below the control point elevation. The upper 24 m [80 ft] consists of a very dense sand fill material, for which the licensee measured a  $V_S$  that gradually increases from 244 m/sec [800 ft/sec] to 305 m [1,000 ft/sec]. Beneath the fill material is 27 m [90 ft] of a very firm and dense fine silty sand from the Pleistocene age Anastasia Formation. The licensee measured a  $V_S$  for this sand formation that ranges from 305 m [1,000 ft/sec] to 396 m/sec [1,300 ft/sec]. For the underlying Pliocene and Miocene age Tamiami and Peace River formations, which consist of a mix of fine-grained limestone and sands, the licensee used one of the velocity templates from the SPID. The licensee’s application of the SPID velocity template results in a  $V_S$  that increases from 396 m/sec [1,300 ft/sec] to about 640 m/sec [2,100 ft/sec] at a depth of about 229 m/sec [750 ft]. For the underlying limestone formations, the licensee estimated an

uppermost  $V_S$  of 1,524 m/sec [5,000 ft/sec] and then applied a gradient of 0.5 m/sec/m [0.5 ft/sec/ft], which results in a  $V_S$  of 2,256 m/sec [7,400 ft/sec] at the base of the profile.

For its basecase profile, the NRC staff used the licensee's layer thicknesses and measured  $V_S$  for the upper sand strata to a depth of 52 m [170 ft]. However, for the underlying sedimentary strata, the NRC staff used the measured  $V_S$  from the Turkey Point (Section 2.3.16) COL application, which is underlain by the same formations as St. Lucie. This results in a higher  $V_S$  of 1,098 m/sec [3,600 ft/sec] for the Hawthorne Group (Peace River and Arcadia Formations) sedimentary strata, which are a mix of sands, clays, and fossiliferous carbonate rock. For the underlying carbonate rock units (primarily limestone), the  $V_S$  gradually increases from 1,128 m/sec [3,700 ft/sec] to 2,561 m/sec [8,400 ft/sec] at a depth of about 1,290 m [4,230 ft].

To capture the uncertainty in its basecase profile, the NRC staff developed lower and upper range (10<sup>th</sup>- and 90<sup>th</sup>- percentile) profiles by multiplying the basecase  $V_S$  values by scale factors of 0.78 and 1.29, respectively, which corresponds to an epistemic logarithmic standard deviation of 0.20. The weights for the lower, best-estimate, and upper basecase profiles are 0.3, 0.4, and 0.3, respectively. Figure 2.3-51 shows the upper 915 m [3,000 ft] of the NRC staff's basecase profiles.

#### 2.3.13.2.2 *Dynamic Material Properties and Site Kappa*

The NRC staff assumed both linear and nonlinear behavior for the soil and rock beneath the St. Lucie site. To model the nonlinear response within the upper 122 m [400 ft] of soil (Layers 1 to 6), the NRC staff used the EPRI soil shear modulus reduction and material damping curves as one alternative and the Peninsular Range curves for the second equally weighted alternative. To model the nonlinear behavior of the rock strata, the NRC staff used the EPRI rock shear modulus reduction and material damping curves. To model the linear behavior, the NRC staff used a constant damping ratio of 3 percent. The NRC staff assumed these two alternative dynamic responses for the Arcadia Formations (Layer 7) and gave them equal weight. For the remaining 1,030 m [3,380 ft] of the profile, the NRC staff assumed a linear response with a material damping ratio values of 0.5 and 1 percent to maintain consistency with the  $\kappa_0$  value for the St. Lucie site.

To determine the basecase  $\kappa_0$  for the St. Lucie site, the NRC staff first used the Campbell (2009) Model 1 relationship between  $V_S$  and  $Q_{ef}$  to determine the  $Q_{ef}$  for each layer. Combining these  $Q_{ef}$  values with the thicknesses and  $V_S$  for each of the layers results in a total  $\kappa_0$  value of 37 msec, which includes the 6 msec assumed for the underlying reference rock. For the lower and upper profiles, the NRC staff calculated values of 54 and 26 msec, respectively, using the same approach as for the basecase profile. In contrast, the licensee used the lowest low-strain damping value from the material damping curves over the top 152 m [500 ft] of the profile and assumed a constant damping value of 1.25 percent for the remainder to estimate  $\kappa_0$  values of 33, 40, and 17 msec for the basecase, lower, and upper profiles, respectively.

Table 2.3-14 provides the layer depths, lithologies,  $V_S$ , unit weights, and dynamic properties for the NRC staff's three profiles. In summary, the site response logic tree developed by the NRC staff for the St. Lucie site consists of six alternatives; three basecase profiles (each with a different  $\kappa_0$  value) and two alternative dynamic property branches.

### 2.3.13.2.3 Methodology and Results

The NRC staff followed the methodology described in Section 2.1.4 to develop the final site amplification factors. Figure 2.3-52 shows the overall median site amplification factors and their variability for each of the seven spectral frequencies. As shown in Figure 2.3-52, the median site amplification factors range from about 2 to 4 before falling off with higher input spectral accelerations. The lower half of Figure 2.3-52 shows that the logarithmic standard deviations for the site amplification factors range from about 0.1 to 0.2.

### 2.3.13.3 Control Point Hazard

The NRC staff implemented Approach 3 from the SPID to develop a weighted control point seismic hazard curve for each of the six unique combinations of the site response logic tree for the St. Lucie site. After combining these curves to develop the final mean control point hazard curves, the NRC staff determined the  $10^{-4}$  and  $10^{-5}$  UHRs in order to calculate the final GMRS. Figure 2.3-53 shows the final control point mean seismic hazard curves for each of the seven spectral frequencies as well as the NRC staff's UHRs and GMRS, and the licensee's NTTF R2.1 GMRS (Jensen, 2014). As shown in Figure 2.3-53, the NRC staff's GMRS (black curve) is similar to the licensee's GMRS (blue curve).

**Table 2.3-14 Layer Depths, Shear Wave Velocities ( $V_s$ ), Unit Weights, and Dynamic Properties for St. Lucie**

Layer	Depth (ft)	Description	$V_s$ (ft/sec)			$V_s$ Sigma (ln)	BC Unit Weight (pcf)	Dynamic Properties	
			LR (0.3)	BC (0.4)	UR (0.3)			Alt. 1 (0.5)	Alt. 2 (0.5)
1	40	Soil: fill	619	800	1,034	0.25	120	EPRI Soil	Pen.
2	80	Soil: fill	774	1,000	1,292	0.15	120	EPRI Soil	Pen.
3	125	Soil: sand	851	1,100	1,422	0.15	120	EPRI Soil	Pen.
4	170	Soil: sand	1,006	1,300	1,680	0.15	120	EPRI Soil	Pen.
5	200	Soil: sand	1,161	1,500	1,938	0.15	130	EPRI Soil	Pen.
6	400	Soil: sand	1,277	1,650	2,132	0.15	130	EPRI Soil	Pen.
7	850	Rock: limestone	2,863	3,700	4,781	0.15	140	EPRI Rock	L 3.0%
8	1,030	Rock: limestone	3,095	4,000	5,169	0.15	140	L 1.0%	L 1.0%
9	1,230	Rock: limestone	3,405	4,400	5,686	0.15	140	L 1.0%	L 1.0%
10	1,430	Rock: limestone	3,637	4,700	6,074	0.15	140	L 1.0%	L 1.0%
11	1,830	Rock: limestone	3,985	5,150	6,655	0.15	140	L 1.0%	L 1.0%
12	2,230	Rock: limestone	4,333	5,600	7,237	0.15	150	L 1.0%	L 1.0%

**Table 2.3-14 Layer Depths, Shear Wave Velocities ( $V_s$ ), Unit Weights, and Dynamic Properties for St. Lucie (cont.)**

Layer	Depth (ft)	Description	$V_s$ (ft/sec)			$V_s$ Sigma (ln)	BC Unit Weight (pcf)	Dynamic Properties	
			LR (0.3)	BC (0.4)	UR (0.3)			Alt. 1 (0.5)	Alt. 2 (0.5)
13	3,930	Rock: limestone	5,107	6,600	8,529	0.15	150	L 0.5%	L 0.5%
14	4,230	Rock: limestone	6,500	8,400	9,285	0.15	160	L 0.5%	L 0.5%

LR = lower range; BC = basecase; UR = upper range; ln = natural log; pcf = pounds per cubic foot; L = linear; Alt. = alternative.  
 For LR, BC, UR, and Alt.: Values in parentheses refer to weights for site response analysis logic tree branches.

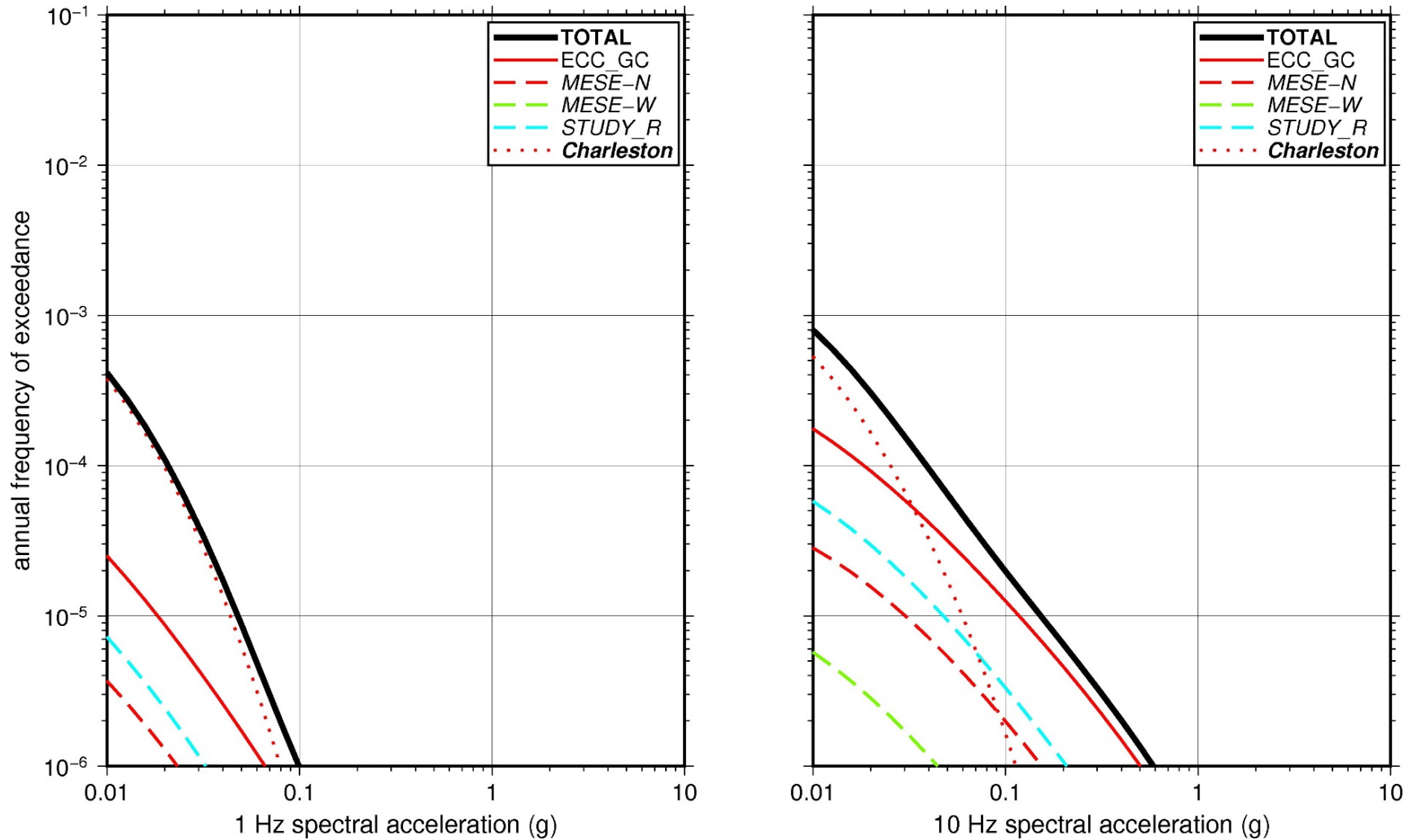


**Figure 2.3-50 Low-Frequency (1 Hz, Left) and High-Frequency (10 Hz, Right) Reference Rock Hazard Curves for St. Lucie. Total Hazard is Shown as a Bold Black Line; Individual Contributions to the Hazard for Each of the CEUS-SSC Sources are Shown as Colored Lines Defined in the legend. See Table 2.1-1 for Source Name Definitions**



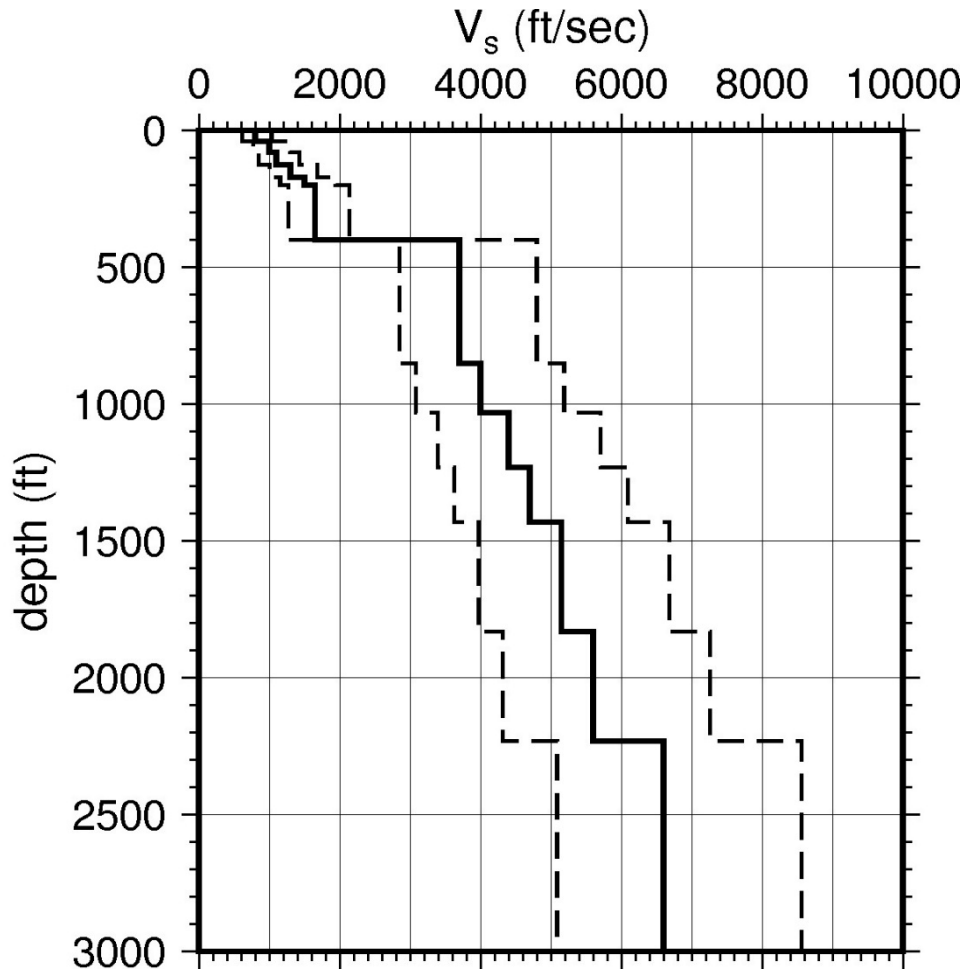


**Figure 2.3-51 Shear Wave Velocity ( $V_s$ ) Profiles for St. Lucie. Basecase (BC) Profile Shown as Solid Bold Line; Lower and Upper Range (LR and UR) Profiles Shown as Dashed Lines. Profiles Terminate at Reference Rock Velocity of 2,831 m/sec [9,285 ft/sec] per EPRI GMM (2013)**

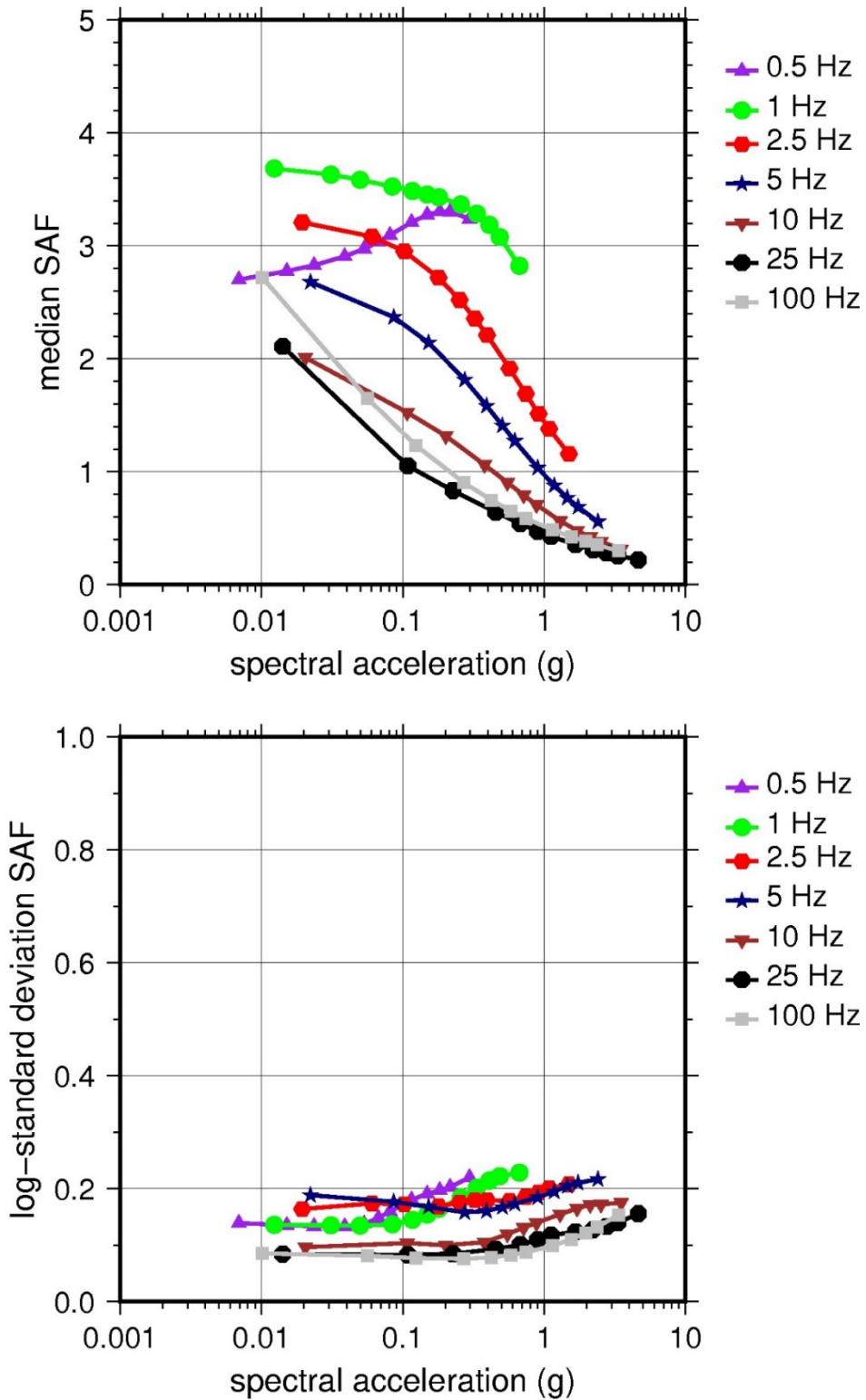


**Figure 2.3-52 Overall Weighted Median Site Amplification Factor (SAF) (Upper) and Log Standard Deviation of the SAF (Lower) as a Function of Input Acceleration for EPRI GMM (2013) Spectral Frequencies**

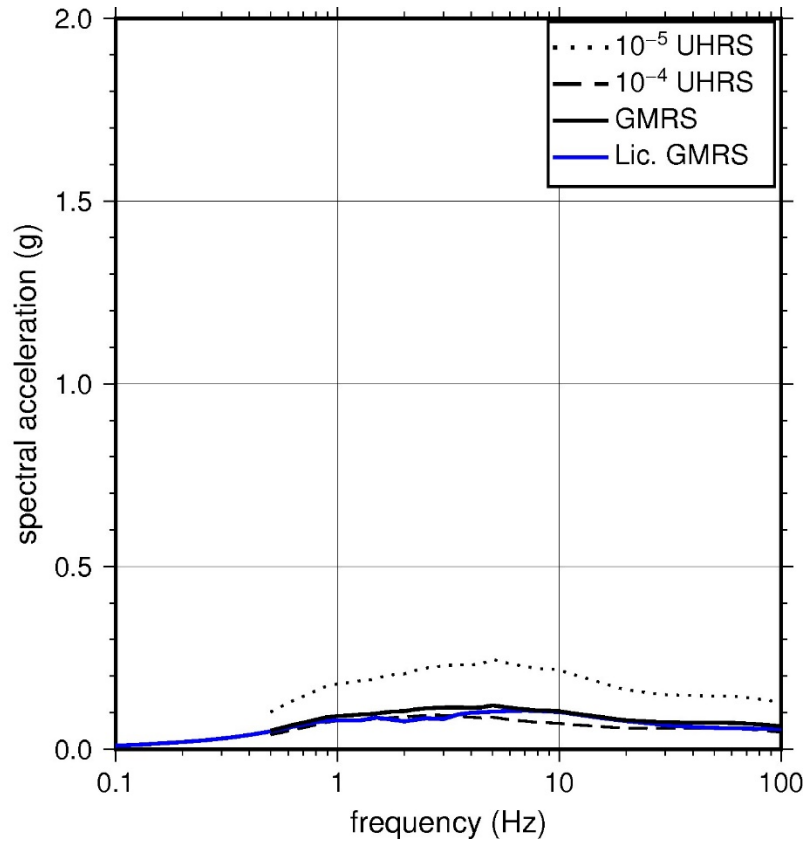
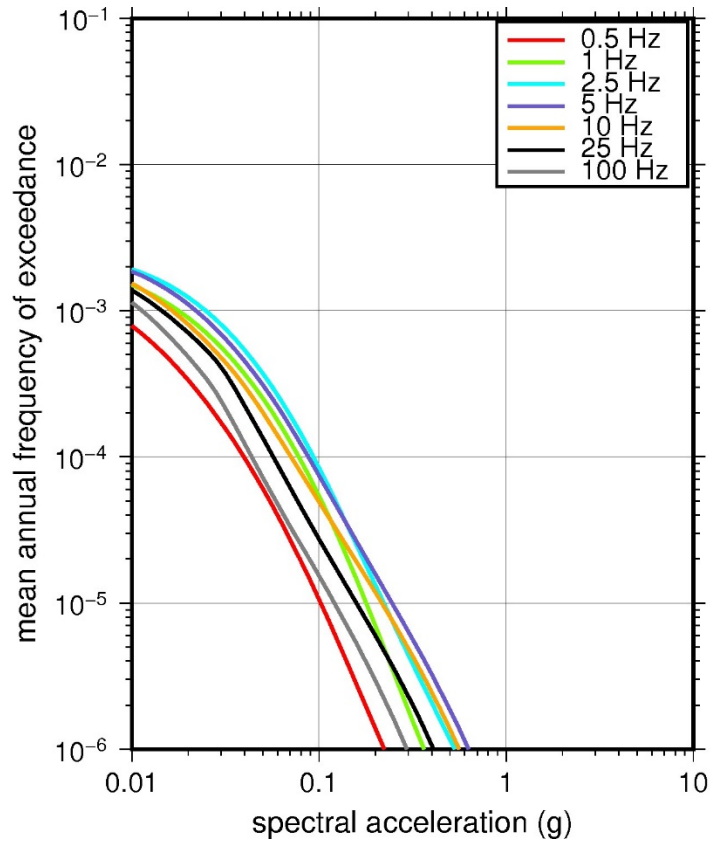


**Figure 2.3-53 Mean Control Point Hazard Curves (Left) for EPRI GMM (2013) Spectral Frequencies, and GMRS and UHRS (Right) for St. Lucie**

### 2.3.14 Summer

The Virgil C. Summer Nuclear Station site is located adjacent to the Monticello Reservoir in the Piedmont physiographic province and is founded on early Paleozoic age metamorphic and igneous rock. The rock horizontal SSE response spectrum for Summer has a Newmark spectral shape and is anchored at a PGA of 0.15g.

#### 2.3.14.1 Reference Rock Hazard

For the reference rock PSHA, the NRC staff selected the seven CEUS-SSC (NRC, 2012b) background seismic source zones that are located within 320 km [200 mi] of the Summer site, and the five CEUS-SSC RLME sources that are located within 500 mi [806 km] of the site. To develop the reference rock seismic hazard curves for the Summer site, the NRC staff used the GMPEs in the updated EPRI GMM (2013). As shown in Figure 2.3-54, the Charleston RLME, located about 160 km [100 mi] from the site, is the largest contributor to the 1 Hz reference rock total mean hazard curve at the  $10^{-4}$  AFE level. For the 10 Hz reference rock total mean hazard curve, the ECC-AM seismotectonic zone is the largest contributor at the  $10^{-4}$  AFE level.

#### 2.3.14.2 Site Response Evaluation

##### 2.3.14.2.1 Site Profiles

To assess the need for a site response evaluation, the NRC staff used the geologic information in the NTTF R2.1 SHSR (Gatlin, 2014) submitted by South Carolina Electric & Gas (SCE&G) (hereafter referred to as “the licensee” within this plant section) and the information in the FSAR for the Summer Unit 2 and 3 COL (SCE&G, 2010). In its SHSR, the licensee stated that the rocks underlying the Summer site are composed of crystalline igneous rock (granodiorite and quartz diorite) with a  $V_S$  greater than the reference rock  $V_S$  of 2,831 m/sec [9,285 ft/sec], which is considered hard rock according to guidance in the SPID. Therefore, the licensee did not perform a site response analysis for the site. Instead, the licensee used the reference rock hazard curves from the PSHA as its control point hazard curves for determining the GMRS for the Summer site.

The bedrock directly beneath the plant is primarily composed of granodiorite and quartz diorite from the Winnsboro plutonic complex. Borehole geophysical surveys (P-S suspension logging) for the Summer site (SCE&G, 2010) show a  $V_S$  of about 1,982 m/sec [6,500 ft/sec] for the uppermost portion, 6 m [15 ft] of sound rock, and a  $V_S$  of about 2,439 m/sec [8,000 ft/sec] for the underlying 3 m [10 ft] of rock. Below these two upper layers, the  $V_S$  of the rock reaches 3,048 m/sec [10,000 ft/sec]. Because the  $V_S$  for the uppermost portion of sound rock is below the reference rock  $V_S$  of 2,831 m/sec [9,285 ft/sec], the NRC staff developed a simple two-layer profile with the control point elevation at 108 m [355 ft] MSL.

To capture the uncertainty in its basecase profile, the NRC staff developed lower and upper range (10<sup>th</sup> and 90<sup>th</sup> percentile) profiles by multiplying the basecase  $V_S$  values by scale factors of 0.83 and 1.21, respectively, which corresponds to an epistemic logarithmic standard deviation of 0.15. The weights for the lower, best-estimate, and upper basecase profiles are 0.3, 0.4, and 0.3, respectively. As shown in Figure 2.3-55, the upper profile terminates at a depth of 6 m [15 ft], and the lower and best-estimate basecase profiles terminate at a depth of 8 m [25 ft] below the control point elevation.

#### 2.3.14.2.2 *Dynamic Material Properties and Site Kappa*

The NRC staff assumed both linear and nonlinear dynamic behavior for the rock beneath the Summer site. To model the nonlinear behavior of the uppermost rock strata, the NRC staff used the EPRI rock shear modulus reduction and material damping curves. To model the linear behavior, the NRC staff used a constant damping ratio of 3 percent. The NRC staff assumed these two alternative dynamic responses for the upper 6 m [15 ft] of the profile; due to the higher  $V_S$  of this rock layer, the NRC staff assigned weights of 0.7 and 0.3 to the linear and nonlinear alternatives, respectively. For the remaining 3 m [10 ft] of its profile, the NRC staff assumed a linear response with a material damping ratio value of 0.1 percent to maintain consistency with the  $\kappa_0$  value for the Summer site.

To determine the basecase  $\kappa_0$  for the Summer site, the NRC staff first used the Campbell (2009) Model 1 relationship between  $V_S$  and  $Q_{ef}$  to determine a  $Q_{ef}$  for each layer. Combining these  $Q_{ef}$  values with the thicknesses and  $V_S$  for each of the layers results in a total  $\kappa_0$  value of about 6.1 msec, which includes the 6 msec assumed for the underlying reference rock. For the lower and upper basecase profiles, the NRC staff calculated  $\kappa_0$  values of 6.1 and 6.0 msec, respectively, using the same approach as for the best-estimate basecase profile.

Table 2.3-15 provides the layer depths, lithologies,  $V_S$ , unit weights, and dynamic properties for the NRC staff's three profiles. In summary, the site response logic tree developed by the NRC staff for the Summer site consists of six alternatives; three basecase profiles (each with a different  $\kappa_0$  value) and two alternative dynamic property branches.

#### 2.3.14.2.3 *Methodology and Results*

The NRC staff followed the methodology described in Section 2.14 to develop the final site amplification factors. Figure 2.3-56 shows the overall median site amplification factors and their variability for each of the seven spectral frequencies. As shown in Figure 2.3-56, the median site amplification factors for the seven spectral frequencies are close to 1. The lower half of Figure 2.3-56 shows that the logarithmic standard deviations for the site amplification factors range from about 0.01 to 0.10.

#### 2.3.14.3 *Control Point Hazard*

The NRC staff implemented Approach 3 from the SPID to develop a weighted control point seismic hazard curve for each of the six unique combinations of the site response logic tree for the Summer site. After combining these curves to develop the final mean control point hazard curves, the NRC staff determined the  $10^{-4}$  and  $10^{-5}$  UHRS in order to calculate the final GMRS. Figure 2.3-57 shows the final control point mean seismic hazard curves for each of the seven spectral frequencies as well as the NRC staff's UHRS and GMRS, and the licensee's NTTF R2.1 GMRS (Gatlin, 2014). As shown in Figure 2.3-57, the NRC staff's GMRS (black curve) is moderately higher than the licensee's GMRS (blue curve) due to the licensee's changes to the magnitude recurrence parameters of the CEUS-SSC model for the region surrounding the site (Gatlin, 2014). These changes to the recurrence parameters are based on a reevaluation of the CEUS-SSC earthquake catalog to remove (1) events likely to be reservoir induced and (2) mislocated or duplicative events following the 1886 Charleston, SC earthquake sequence. The net effect of these changes is to moderately reduce the control point hazard results for the Summer site.

**Table 2.3-15 Layer Depths, Shear Wave Velocities ( $V_s$ ), Unit Weights, and Dynamic Properties for Summer**

Layer	Depth (ft)	Description	$V_s$ (ft/sec)			$V_s$ Sigma (ln)	BC Unit Weight (pcf)	Dynamic Properties	
			LR (0.3)	BC (0.4)	UR (0.3)			Alt. 1 (0.3)	Alt. 2 (0.7)
1	15	Rock: granodiorite	5,363	6,500	7,878	0.25	150	EPRI Rock	L 3.0%
2	25	Rock: granodiorite	6,600	8,000	9,285	0.15	160	L 0.1%	L 0.1%

LR = lower range; BC = basecase; UR = upper range; ln = natural log; pcf = pounds per cubic foot; L = linear; Alt. = alternative.  
 For LR, BC, UR, and Alt.: Values in parentheses refer to weights for site response analysis logic tree branches.

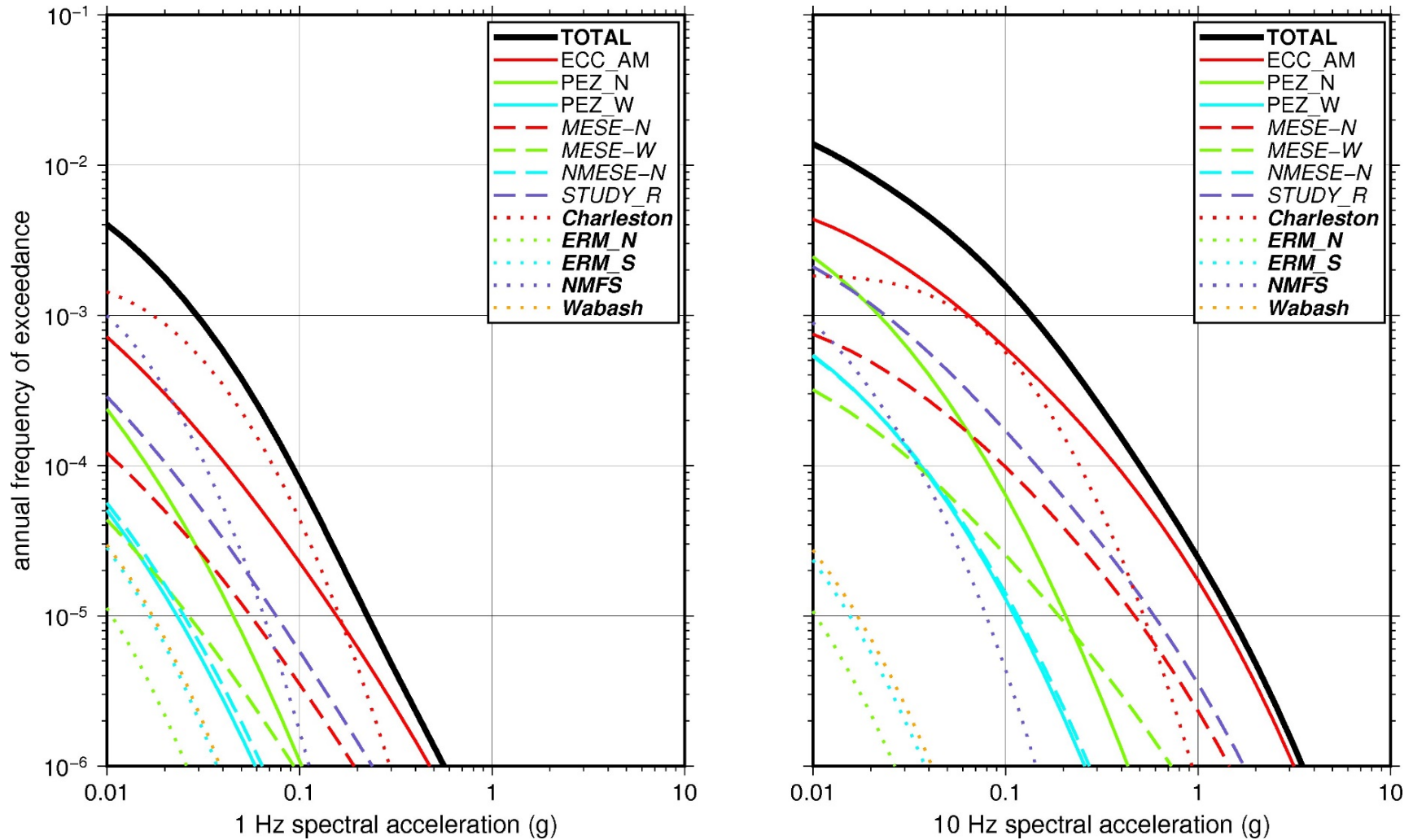


**Figure 2.3-54 Low-Frequency (1 Hz, Left) and High-Frequency (10 Hz, Right) Reference Rock Hazard Curves for Summer. Total Hazard is Shown as a Bold Black Line; Individual Contributions to the Hazard for Each of the CEUS-SSC Sources are Shown as Colored Lines Defined in the Legend. See Table 2.1-1 for Source Name Definitions**

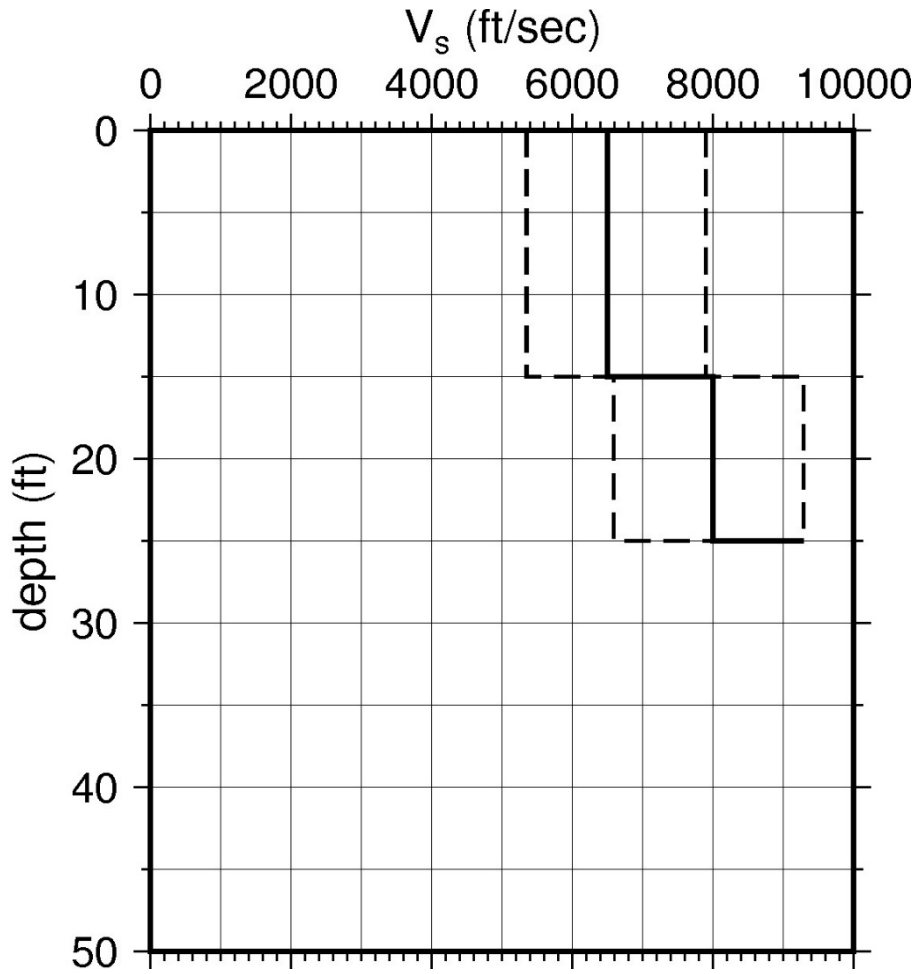


**Figure 2.3-55 Shear Wave Velocity ( $V_s$ ) Profiles for Summer. Basecase (BC) Profile Shown as Solid Bold Line; Lower and Upper Range (LR and UR) Profiles Shown as Dashed Lines. Profiles Terminate at Reference Rock Velocity of 2,831 m/sec [9,285 ft/sec] per EPRI GMM (2013)**



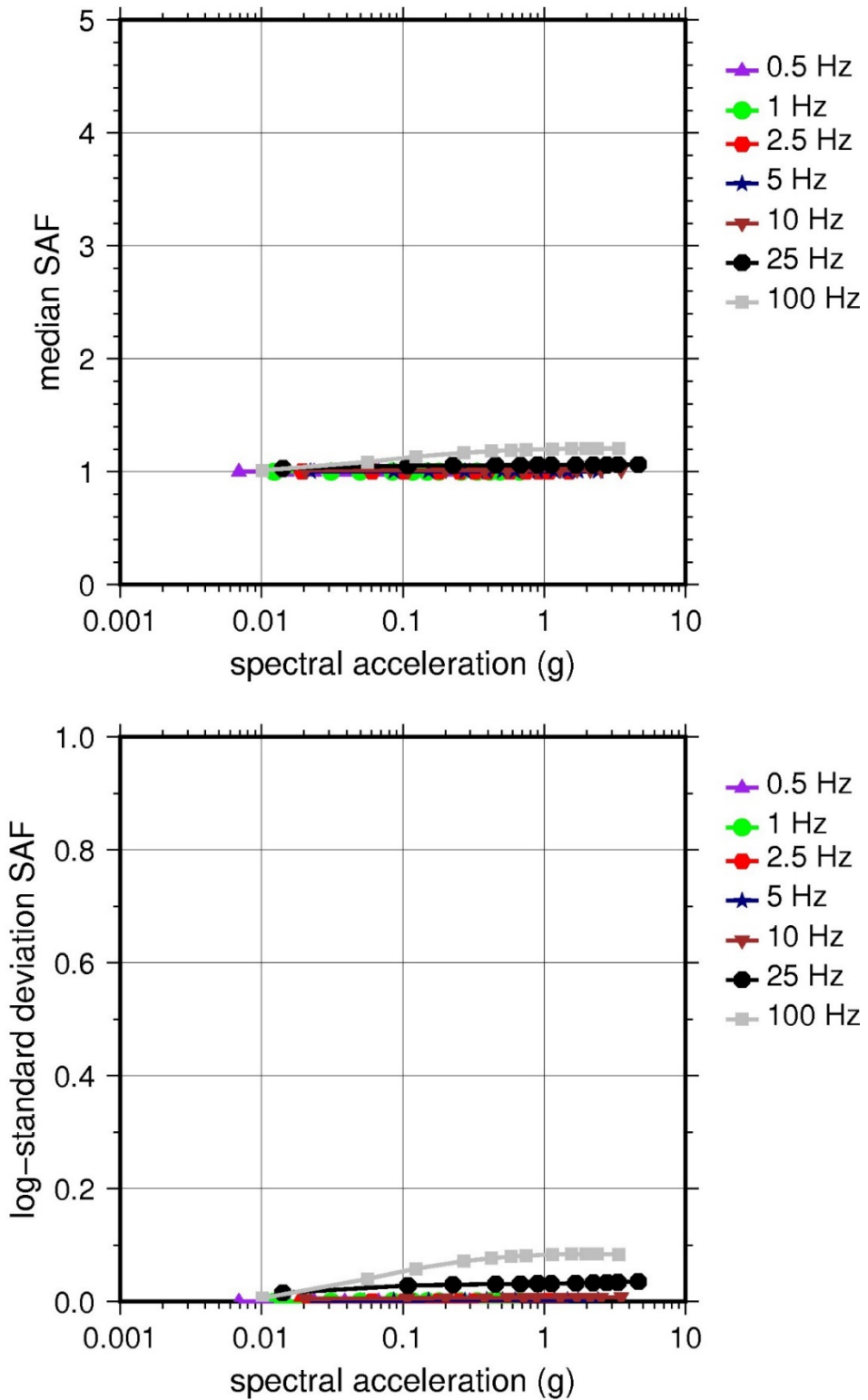


**Figure 2.3-56 Overall Weighted Median Site Amplification Factor (SAF) (Upper) and Log Standard Deviation of the SAF (Lower) as a Function of Input Acceleration for EPRI GMM (2013) Spectral Frequencies**

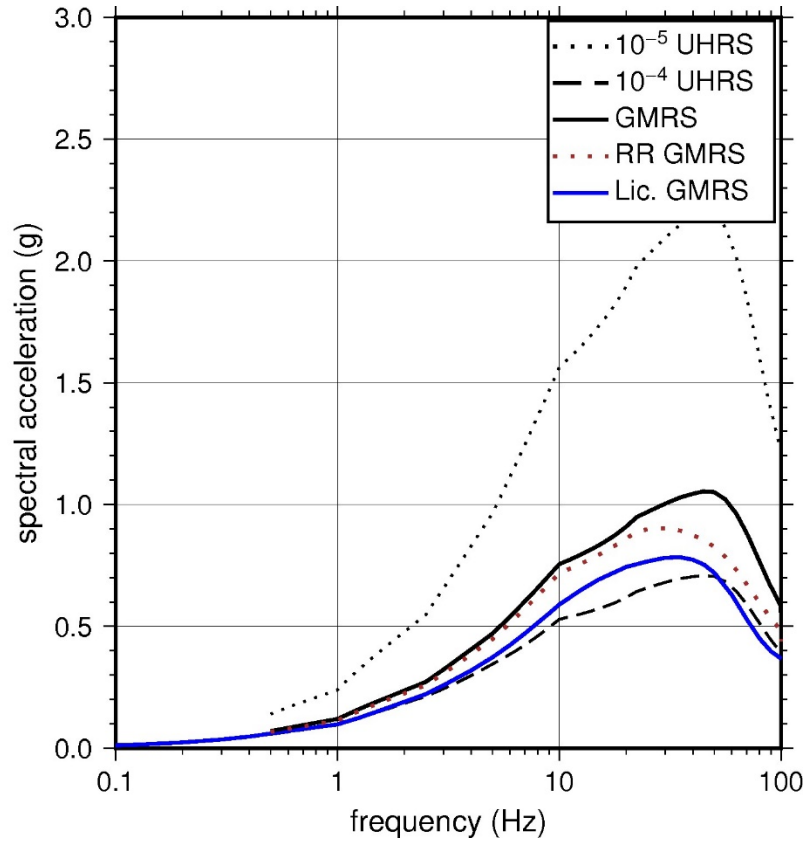
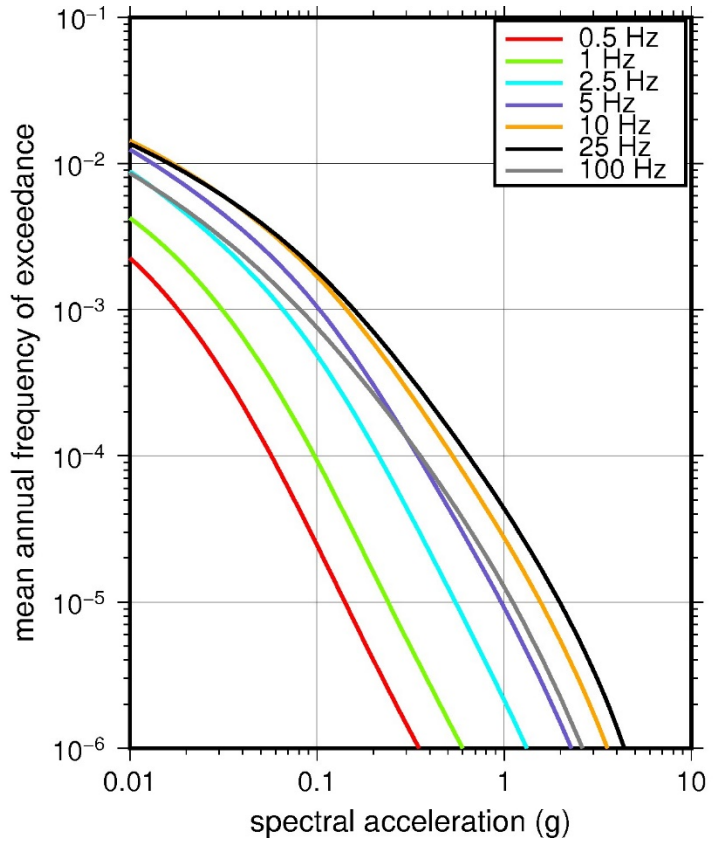


**Figure 2.3-57 Mean Control Point Hazard Curves (Left) for EPRI GMM (2013) Spectral Frequencies, and GMRS and UHRS (Right) for Summer**

### 2.3.15 Surry

The site for the Surry Power Station in Virginia is located adjacent to the James River in the Atlantic Coastal Plain physiographic province. The Surry site is founded on about 400 m [1,300 ft] of sedimentary strata (clays, sands, and marl) that are underlain by crystalline basement rock. The horizontal SSE response spectrum for Surry has a rounded Housner spectral shape and is anchored at a PGA of 0.18g.

#### 2.3.15.1 Reference Rock Hazard

For the reference rock PSHA, the NRC staff selected the eight CEUS-SSC (NRC, 2012b) background seismic source zones that are located within 320 km [200 mi] of the site. The NRC staff also selected the Charleston CEUS-SSC RLME source, which is located about 400 km [245 mi] from the site. To develop the reference rock seismic hazard curves for the Surry site, the NRC staff used the GMPEs in the updated EPRI GMM (2013). As shown in Figure 2.3-58, the Charleston RLME is the largest contributor to the 1 Hz reference rock total mean hazard curve, while the ECC-AM seismotectonic zone is the largest contributor to the 10 Hz reference rock total mean hazard curve.

#### 2.3.15.2 Site Response Evaluation

##### 2.3.15.2.1 Site Profiles

To develop a basecase profile, the NRC staff used the geologic information in the NTTF R2.1 SHSR (Heacock, 2014c) submitted by Virginia Electric and Power Company (hereafter referred to as “the licensee” within this plant section). As described in the licensee’s SHSR, the Surry site consists of alternating layers of unconsolidated to semiconsolidated sediments. The containment foundation is supported on about 73 m [240 ft] of stiff clays with occasional sand and silt layers from the Chesapeake Group. In Table 2.3.1-1 of the SHSR, the licensee briefly described the subsurface materials in terms of the geologic units and layer thicknesses. For its site response evaluation, the NRC staff used the top of the ground surface, which corresponds to an elevation of 8 m [27 ft] above MSL, as the control point elevation for the Surry site.

The licensee’s SHSR profile is based on in situ investigations for Units 1 and 2. These investigations included multiple laboratory tests of soil samples from borings, which extended to a depth of 61 m [200 ft] beneath the site. To determine the  $V_S$  of the uppermost soils beneath the site, the licensee performed seismic refraction surveys. For the deeper strata to a depth of 43 m [140 ft], the licensee used blow count values from Standard Penetration Testing (SPT). For the deeper soil layers to a depth of 488 m [1,600 ft], the licensee estimated the  $V_S$  based on the soil type and its depth beneath the site. Table 2.3.2-1 of the SHSR gives the measured and estimated  $V_S$  determined from the licensee’s site investigations.

The licensee’s SHSR basecase profile extends to a depth of 518 m [1,700 ft] below the control point elevation. The uppermost layers of the profile consist of the Pleistocene age Norfolk Estuarine Formation sands and clays, which extend to a depth of 20 m [67 ft] beneath the site. The  $V_S$  for these uppermost sands and clays varies from about 243 m/sec [800 ft/sec] to 290 m/sec [950 ft/sec]. Beneath the sands and clays is a 73 m [240 ft] thick layer of stiff clay and marl from the Miocene age Chesapeake Group, for which the licensee measured a  $V_S$  of 287 m/sec [940 ft/sec]. For the deeper Paleogene and Cretaceous age sediments, the licensee estimated  $V_S$  ranging from about 305 m/sec [1,000 ft/sec] to 610 m/sec [2,000 ft/sec]. Based on

a nearby deep borehole, the licensee estimated the depth to crystalline basement rock to be about 488 m [1,600 ft].

As the soil strata beneath the Surry site has been well characterized, the NRC staff used the licensee's layer thicknesses and  $V_S$  for the majority of its profile. The minor differences between the NRC staff's and licensee's profiles are for the deeper soil strata, for which the NRC staff estimated somewhat higher  $V_S$  based on the profiles developed for similar Atlantic Coastal Plain sites. In addition, the NRC staff developed a profile that is 396 m [1,300 ft] thick based on the statement in Section 2.3.1 of the SHSR that metamorphic and igneous rock is "estimated to be roughly 1,300 ft deep at the site based upon seismic investigations conducted about 2 miles southeast of the site."

To capture the uncertainty in its basecase profile, the NRC staff developed lower and upper range (10<sup>th</sup> and 90<sup>th</sup> percentile) profiles by multiplying the basecase  $V_S$  values by scale factors of 0.77 and 1.29, respectively, which corresponds to an epistemic logarithmic standard deviation of 0.20. The weights for the lower, best-estimate, and upper basecase profiles are 0.3, 0.4, and 0.3, respectively. Figure 2.3-59 shows the NRC staff's profiles, which extend to a depth of 396 m [1,300 ft] below the control point elevation, at which point the  $V_S$  is assumed to reach the reference rock value of 2,831 m/sec [9,285 ft/sec].

#### 2.3.15.2.2 *Dynamic Material Properties and Site Kappa*

The NRC staff assumed both linear and nonlinear behavior for the soil beneath the Surry site. To model the nonlinear response within the upper 124 m [407 ft] of soil deposits, the NRC staff used the EPRI soil shear modulus reduction and damping curves as one alternative and the Peninsular Range curves for the second equally weighted alternative. For the remaining 272 m [893 ft] of its profile, the NRC staff assumed a linear response with a damping ratio value of 1 percent to maintain consistency with the  $\kappa_0$  value for the Surry site.

To determine the basecase  $\kappa_0$  for the Surry site, the NRC staff first used the Campbell (2009) Model 1 relationship between  $V_S$  and  $Q_{ef}$  to determine a  $Q_{ef}$  for each layer. Combining these  $Q_{ef}$  values with the thicknesses and  $V_S$  for each of the layers results in a total  $\kappa_0$  value of about 48 msec, which includes the 6 msec assumed for the underlying reference rock. For the lower and upper basecase profiles, the NRC staff calculated  $\kappa_0$  values of 69 and 34 msec, respectively, using the same approach as for the basecase profile. In contrast, the licensee used a  $\kappa_0$  value of 34 msec for the best-estimate, lower, and upper basecase profiles, based on the guidance in Appendix B to the SPID (EPRI, 2012) for CEUS deep soil sites.

Table 2.3-16 provides the layer depths, lithologies,  $V_S$ , unit weights, and dynamic properties for the NRC staff's three profiles. In summary, the site response logic tree developed by the NRC staff for the Surry site consists of six alternatives; three basecase profiles (each with a different  $\kappa_0$  value) and two alternative dynamic property branches.

#### 2.3.15.2.3 *Methodology and Results*

The NRC staff followed the methodology described in Section 2.1.4 to develop the final site amplification factors. Figure 2.3-60 shows the overall median site amplification factors and their variability for each of the seven spectral frequencies. As shown in Figure 2.3-60, the median site amplification factors range from about 1.5 to 3.5 before falling off with higher input spectral accelerations. The lower half of Figure 2.3-60 shows that the logarithmic standard deviations for the site amplification factors range from about 0.1 to 0.3.

### 2.3.15.3 Control Point Hazard

The NRC staff implemented Approach 3 from the SPID to develop a weighted control point seismic hazard curve for each of the six unique combinations of the site response logic tree for the Surry site. After combining these curves to develop the final mean control point hazard curves, the NRC staff determined the  $10^{-4}$  and  $10^{-5}$  UHRS in order to calculate the final GMRS. Figure 2.3-61 shows the final control point mean seismic hazard curves for each of the seven spectral frequencies as well as the NRC staff's UHRS and GMRS, and the licensee's NTTF R2.1 GMRS (Heacock, 2014c). As shown in Figure 2.3-60, the licensee's GMRS (blue curve) is moderately higher than the NRC staff's GMRS (black curve) for the higher frequencies due to the licensee's lower  $\kappa_0$  value (34 msec) compared to the NRC staff's  $\kappa_0$  value (48 msec).

**Table 2.3-16 Layer Depths, Shear Wave Velocities ( $V_s$ ), Unit Weights, and Dynamic Properties for Surry**

Layer	Depth (ft)	Description	$V_s$ (ft/sec)			$V_s$ Sigma (ln)	BC Unit Weight (pcf)	Dynamic Properties	
			LR (0.3)	BC (0.4)	UR (0.3)			Alt. 1 (0.5)	Alt. 2 (0.5)
1	16	Soil: fill	774	1,000	1,292	0.25	120	EPRI Soil	Pen.
2	27	Soil: clay	611	790	1,020	0.15	120	EPRI Soil	Pen.
3	40	Soil: sand	735	950	1,228	0.15	120	EPRI Soil	Pen.
4	52	Soil: clay	549	710	917	0.15	120	EPRI Soil	Pen.
5	67	Soil: sand	642	830	1,072	0.15	120	EPRI Soil	Pen.
6	307	Soil: clay, marl	727	940	1,214	0.15	120	EPRI Soil	Pen.
7	362	Soil: marl, sand	1,393	1,800	2,326	0.15	130	EPRI Soil	Pen.
8	407	Soil: clay, sand	1,161	1,500	1,938	0.15	130	EPRI Soil	Pen.
9	700	Soil: sand, clay	1,548	2,000	2,584	0.15	130	L 1.0%	L 1.0%
10	1,000	Soil: sand, clay	1,664	2,150	2,778	0.15	130	L 1.0%	L 1.0%
11	1,300	Soil: sand, clay	1,780	2,300	2,972	0.15	130	L 1.0%	L 1.0%

LR = lower range; BC = basecase; UR = upper range; ln = natural log; pcf = pounds per cubic foot; L = linear; Alt. = alternative; Pen. = Peninsular.  
 For LR, BC, UR, and Alt.: Values in parentheses refer to weights for site response analysis logic tree branches.

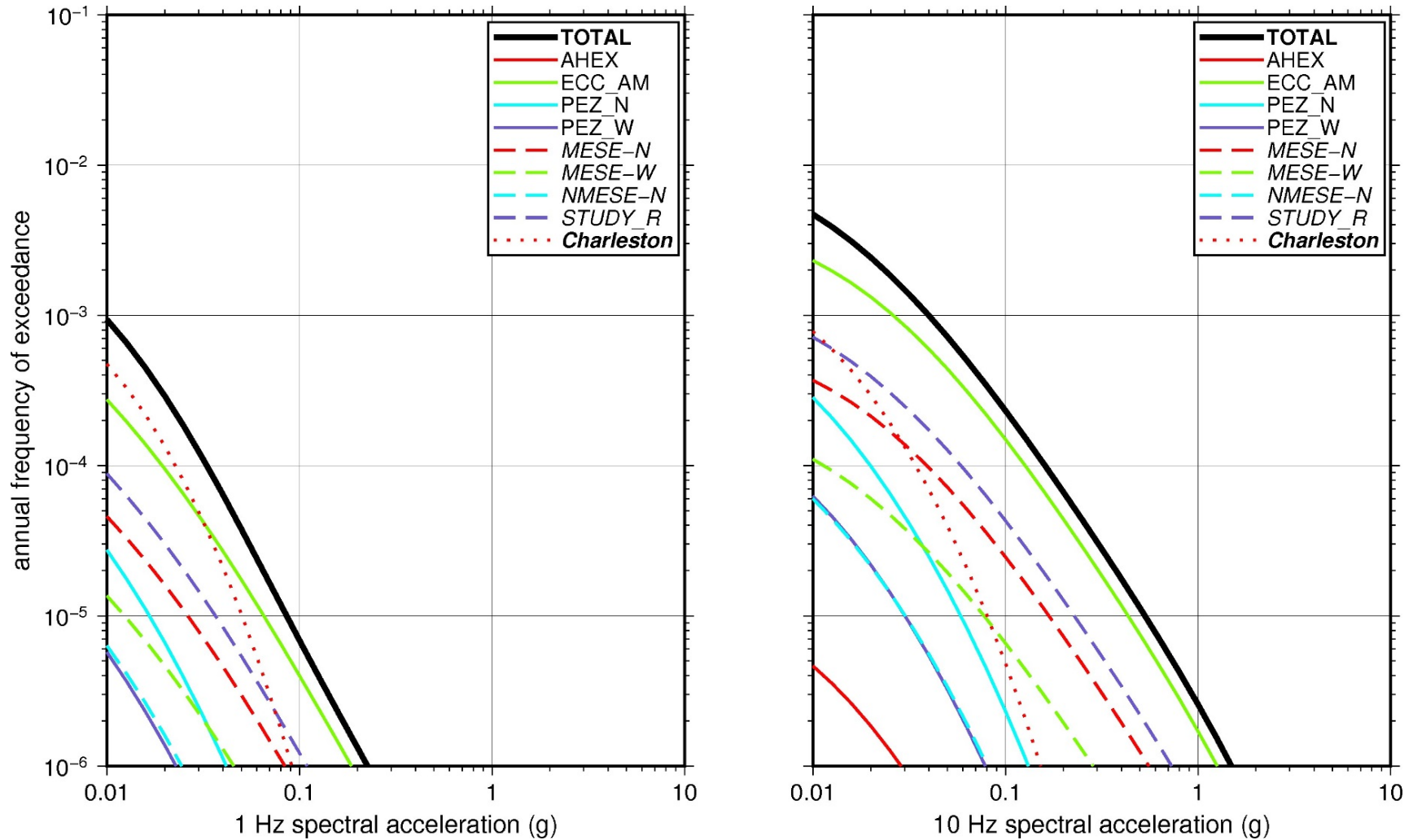


**Figure 2.3-58 Low-Frequency (1 Hz, Left) and High-Frequency (10 Hz, Right) Reference Rock Hazard Curves for Surry. Total Hazard is Shown as a Bold Black Line; Individual Contributions to the Hazard for Each of the CEUS-SSC Sources are Shown as Colored Lines Defined in the Legend. See Table 2.1-1 for Source Name Definitions**

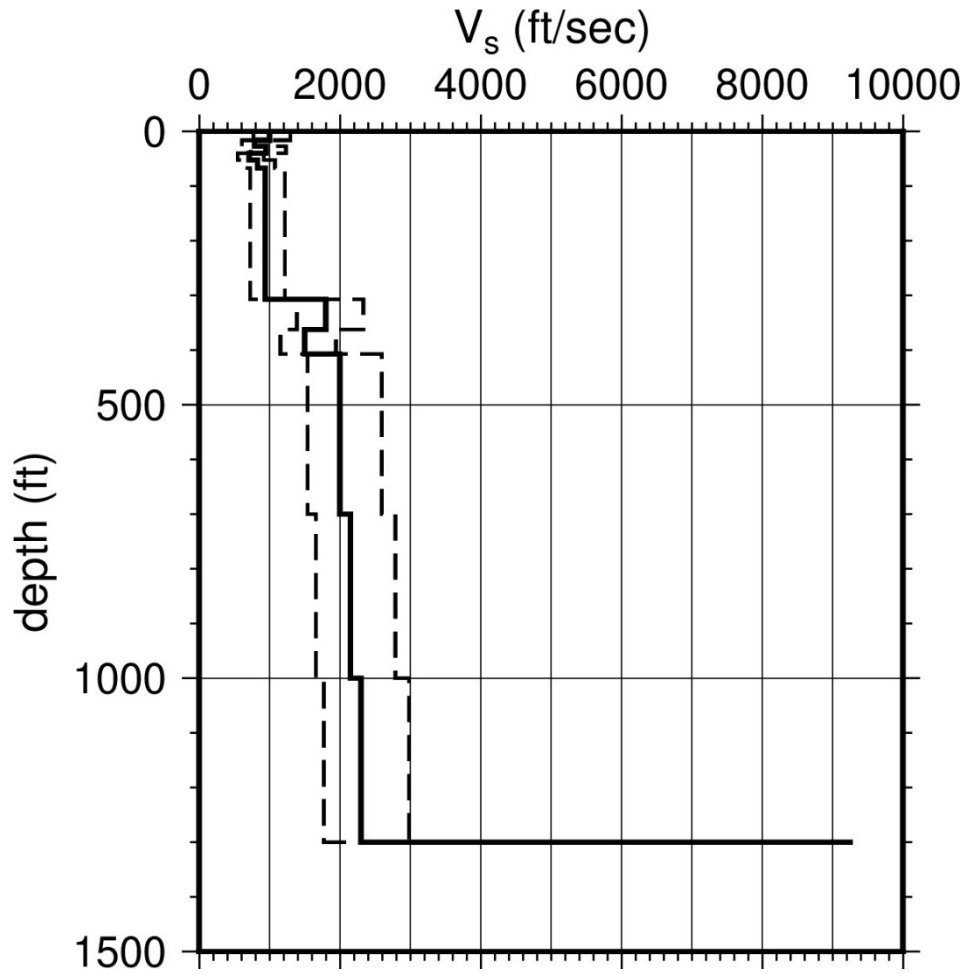


**Figure 2.3-59** Shear Wave Velocity ( $V_s$ ) Profiles for Surry. Basecase (BC) Profile Shown as Solid Bold Line; Lower and Upper Range (LR and UR) Profiles Shown as Dashed Lines. Profiles Terminate at Reference Rock Velocity of 2,831 m/sec [9,285 ft/sec] per EPRI GMM (2013)

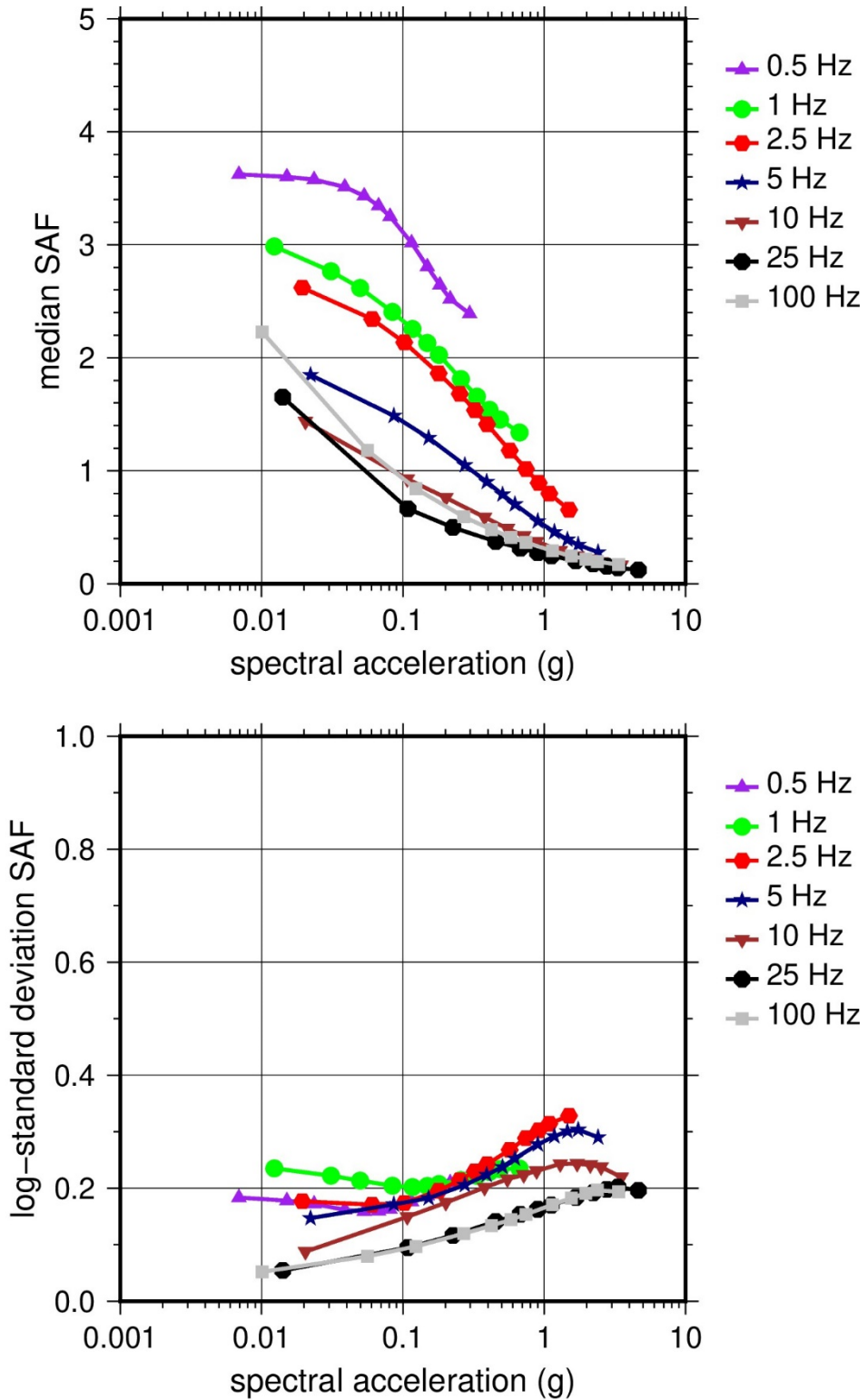


**Figure 2.3-60 Overall Weighted Median Site Amplification Factor (SAF) (Upper) and Log Standard Deviation of the SAF (Lower) as a Function of Input Acceleration for EPRI GMM (2013) Spectral Frequencies**



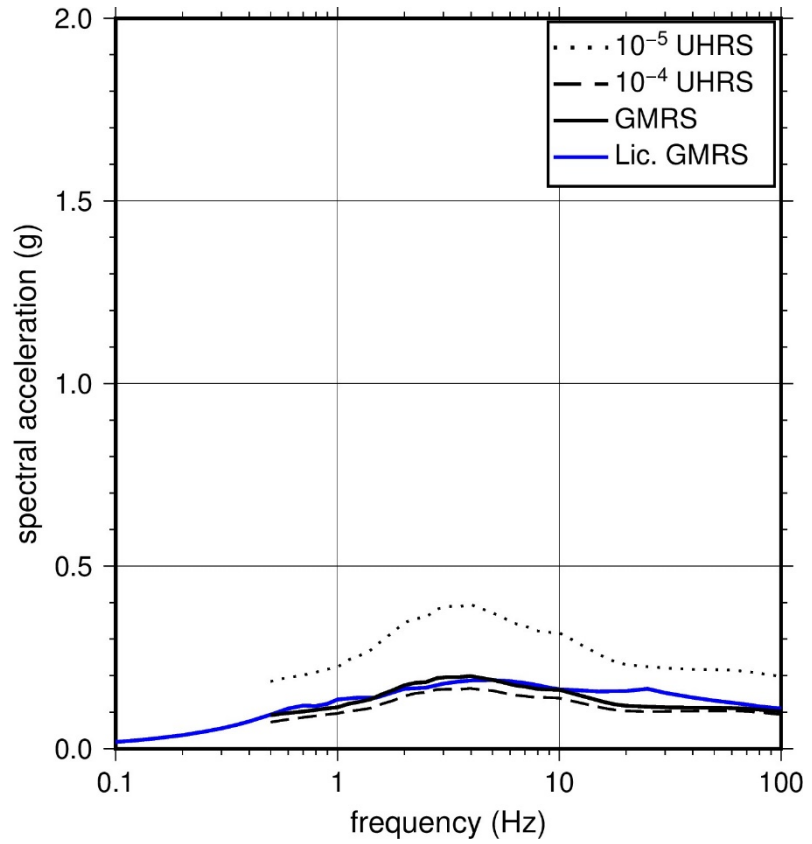
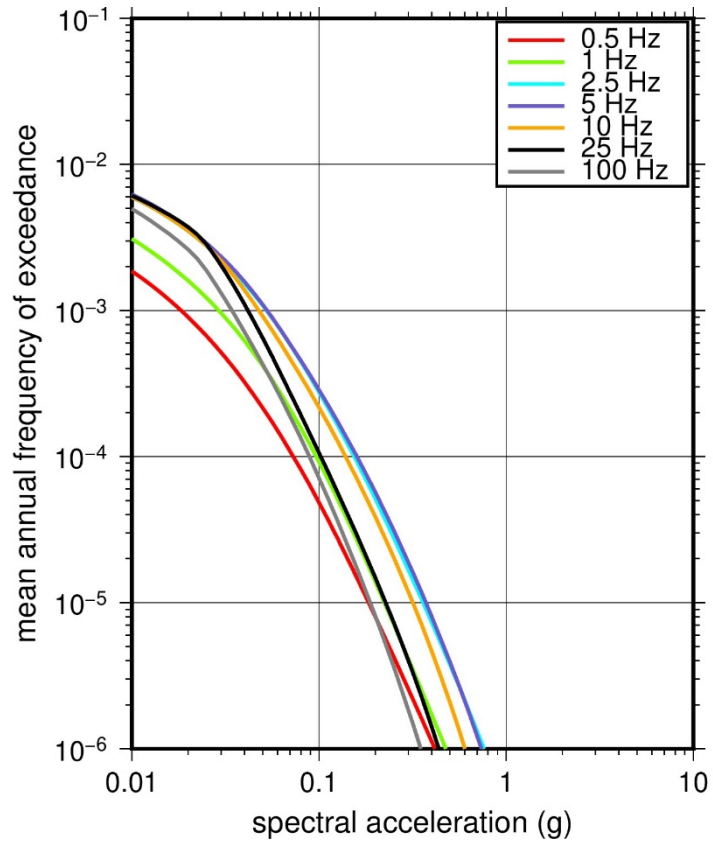


**Figure 2.3-61 Mean Control Point Hazard Curves (Left) for EPRI GMM (2013) Spectral Frequencies, and GMRS and UHRS (Right) for Surry**

### 2.3.16 Turkey Point

The Turkey Point Nuclear Generating Station site is located in southern Florida on the Atlantic coast within the Coastal Plain physiographic province and consists of carbonate rock, which unconformably overlies soil (primarily marl, clay, and sand) of Miocene age. Underlying the Miocene soils is about 4,575 m [15,000 ft] of sedimentary rock (limestone) above Paleozoic crystalline basement. The horizontal SSE response spectrum for Turkey Point has a smooth Housner spectral shape and is anchored at a PGA of 0.15g.

#### 2.3.16.1 Reference Rock Hazard

For the reference rock PSHA, the NRC staff selected the four CEUS-SSC (NRC, 2012b) background seismic source zones that are located within 320 km [200 mi] of the site. In addition, the NRC staff selected the Charleston RLME source, which is about 700 km [440 mi] to the north of the site. To develop the reference rock seismic hazard curves for the Turkey Point site, the NRC staff used the GMPEs in the updated EPRI GMM (EPRI, 2013). As shown in Figure 2.3-62, the Charleston RLME is the largest contributor to the 1 Hz reference rock total mean hazard curves at the  $10^{-4}$  AFE level. For the 10 Hz reference rock total mean hazard curve, the ECC-GC seismotectonic source zone is the largest contributor at the  $10^{-4}$  AFE level.

#### 2.3.16.2 Site Response Evaluation

##### 2.3.16.2.1 Site Profiles

To develop the basecase profile, the NRC staff used the geologic information in the NTTF R2.1 SHSR (Kiley, 2014), submitted by Florida Power & Light Company (hereafter referred to as “the licensee” within this plant section). As described in the licensee’s SHSR, the Turkey Point site consists of fill overlying sedimentary rock (predominantly limestone), which lies above a sequence of soil and several thousand feet of carbonate rock. The primary Turkey Point structures are founded on carbonate rock. In Table 2.3.1-1 of the SHSR, the licensee briefly described the subsurface materials in terms of the geologic units and layer thicknesses. For its site response evaluation, the NRC staff used the top of plant grade, which corresponds to an elevation of 5.5 m [18 ft] above mean low water, as the control point elevation for the Turkey Point site.

The geophysical field investigation for Turkey Point Units 3 and 4 consisted of a single seismic downhole survey used to measure the  $V_P$  and  $V_S$  for the foundation-bearing material to a depth of about 12 m [40 ft]. For the COL application for Units 6 and 7, the applicant measured  $V_P$  and  $V_S$  to a depth of about 183 m [600 ft] from six P-S suspension borings for each unit and two downhole velocity tests (one for each unit). To extend its basecase profile to a depth of 1,220 m [4,000 ft], the licensee used sonic log data from nearby oil and gas exploration boreholes to estimate  $V_S$  from measured  $V_P$  and an assumed Poisson’s ratio. Table 2.3.2-1 of the SHSR gives the measured and estimated  $V_S$  values from the licensee’s site investigations.

For its SHSR, the licensee developed a basecase profile that extends to a depth of 1,220 m [4,000 ft] below the control point elevation. The upper 9 m [28 ft] consists of a very dense limerock, sand, and silt fill material, for which the licensee measured a  $V_S$  of about 262 m/sec [860 ft/sec]. Beneath the fill material is 8 m [25 ft] of a porous, fossiliferous limestone referred to as the Miami Oolite with a  $V_S$  of about 1,098 m/sec [3,600 ft/sec]. For the underlying 24 m [80 ft] of limestone strata from the Key Largo Limestone and Fort Thompson formations, the licensee measured  $V_S$  of 1,768 m/sec [5,800 ft/sec] and 1,296 m/sec [4,250 ft/sec], respectively.

Beneath these two layers of limestone are soils (silty sands and sandy silt) from the Upper and Lower Tamiami Formations and the Peace River Formation, for which the licensee measured  $V_S$  ranging from 427 m/sec [1,400 ft/sec] to 503 m/sec [1,650 ft/sec]. Finally, at a depth of about 189 m [620 ft] are Miocene to Paleocene age limestone strata from the Arcadia, Avon Park, Oldsmar, and Cedar Keys formations, with  $V_S$  increasing from 1,098 m/sec [3,600 ft/sec] to about 2,561 m/sec [8,400 ft/sec] at a depth of 1,200 m [4,000 ft]. Although there are several thousands of feet of additional sedimentary rock before reaching Precambrian age crystalline rock, the licensee terminated its profile at a depth of 1,220 m [4,000 ft], which it deemed sufficient to capture the site amplification of the lowest spectral frequency of interest at 0.5 Hz.

As multiple geophysical field investigations have characterized the sedimentary strata beneath the Turkey Point site, the NRC staff used the licensee's layer thicknesses and  $V_S$  for its basecase profile.

To capture the uncertainty in its basecase profile, the NRC staff developed lower and upper range (10<sup>th</sup> and 90<sup>th</sup> percentile) profiles by multiplying the basecase  $V_S$  values by scale factors of 0.78 and 1.29, respectively, which corresponds to an epistemic logarithmic standard deviation of 0.20. The weights for the lower, best-estimate, and upper basecase profiles are 0.3, 0.4, and 0.3, respectively. Figure 2.3-63 shows the upper 915 m [3,000 ft] of the NRC staff's basecase profiles.

#### 2.3.16.2.2 *Dynamic Material Properties and Site Kappa*

The NRC staff assumed both linear and nonlinear behavior for the soil and rock beneath the Turkey Point site. To model the nonlinear response within the upper 9 m [28 ft] of fill material (Layer 1), the NRC staff used the EPRI soil shear modulus reduction and material damping curves as one alternative and the Peninsular Range curves for the second equally weighted alternative. To model the nonlinear behavior of the rock strata, the NRC staff used the EPRI rock shear modulus reduction and material damping curves; to model the linear behavior, the NRC staff used a constant damping ratio of 3 percent. The NRC staff assumed these two alternative dynamic responses for the Miami Oolite, Key Largo Limestone, and Fort Thompson formations (Layers 2 to 4) and gave them equal weight. For the remaining 1,166 m [3,823 ft] of the profile, the NRC staff assumed a linear response with a material damping ratio value of 1 percent to maintain consistency with the  $\kappa_0$  value for the Turkey Point site.

To determine the basecase  $\kappa_0$  for the Turkey Point site, the NRC staff first used the Campbell (2009) Model 1 relationship between  $V_S$  and  $Q_{ef}$  to determine the  $Q_{ef}$  for each layer. Combining these  $Q_{ef}$  values with the thicknesses and  $V_S$  for each of the layers results in a total  $\kappa_0$  value of 31 msec, which includes the 6 msec assumed for the underlying reference rock. For the lower and upper profiles, the NRC staff calculated values of 44 and 21 msec, respectively, using the same approach as for the basecase profile. In contrast, the licensee used the lowest low-strain damping value from the material damping curves over the top 152 m [500 ft] of the profile and assumed a constant damping value of 1.25 percent for the remainder to estimate  $\kappa_0$  values of 27, 39, and 20 msec for the basecase, lower, and upper profiles, respectively.

Table 2.3-17 provides the layer depths, lithologies,  $V_S$ , unit weights, and dynamic properties for the NRC staff's three profiles. In summary, the site response logic tree developed by the NRC staff for the Turkey Point site consists of six alternatives; three basecase profiles (each with a different  $\kappa_0$  value) and two alternative dynamic property branches.

### 2.3.16.2.3 Methodology and Results

The NRC staff followed the methodology described in Section 2.1.4 to develop the final site amplification factors. Figure 2.3-64 shows the overall median site amplification factors and their variability for each of the seven spectral frequencies. As shown in Figure 2.3-64, the median site amplification factors range from about 2 to 3 before falling off with higher input spectral accelerations. The lower half of Figure 2.3-64 shows that the logarithmic standard deviations for the site amplification factors range from about 0.1 to 0.4.

### 2.3.16.3 Control Point Hazard

The NRC staff implemented Approach 3 from the SPID to develop a weighted control point seismic hazard curve for each of the six unique combinations of the site response logic tree for the Turkey Point site. After combining these curves to develop the final mean control point hazard curves, the NRC staff determined the  $10^{-4}$  and  $10^{-5}$  UHRS in order to calculate the final GMRS. Figure 2.3-65 shows the final control point mean seismic hazard curves for each of the seven spectral frequencies as well as the NRC staff's UHRS and GMRS, and the licensee's NTTF R2.1 GMRS (Kiley, 2014). As shown in Figure 2.3-65, the NRC staff's GMRS (black curve) is similar to the licensee's GMRS (blue curve) over the entire frequency range.

**Table 2.3-17 Layer Depths, Shear Wave Velocities ( $V_s$ ), Unit Weights, and Dynamic Properties for Turkey Point**

Layer	Depth (ft)	Description	$V_s$ (ft/sec)			$V_s$ Sigma (ln)	BC Unit Weight (pcf)	Dynamic Properties	
			LR (0.3)	BC (0.4)	UR (0.3)			Alt. 1 (0.5)	Alt. 2 (0.5)
1	28	Soil: fill	666	860	1,111	0.25	120	EPRI Soil	Pen.
2	53	Rock: limestone	2,786	3,600	4,652	0.15	140	EPRI Rock	L 3.0%
3	67	Rock: limestone	4,488	5,800	7,495	0.15	150	EPRI Rock	L 3.0%
4	133	Rock: limestone	3,289	4,250	5,492	0.15	140	EPRI Rock	L 3.0%
5	177	Soil: sand	1,083	1,400	1,809	0.15	130	L 1.0%	L 1.0%
6	233	Soil: silt	1,238	1,600	2,068	0.15	130	L 1.0%	L 1.0%
7	470	Soil: sand	1,277	1,650	2,132	0.15	130	L 1.0%	L 1.0%
8	620	Rock: limestone	2,786	3,600	4,652	0.15	140	L 1.0%	L 1.0%
9	800	Rock: limestone	3,095	4,000	5,169	0.15	140	L 1.0%	L 1.0%
10	1,000	Rock: limestone	3,405	4,400	5,686	0.15	140	L 1.0%	L 1.0%
11	1,200	Rock: limestone	3,637	4,700	6,074	0.15	140	L 1.0%	L 1.0%
12	1,300	Rock: limestone	3,869	5,000	6,461	0.15	140	L 1.0%	L 1.0%
13	1,600	Rock: limestone	4,101	5,300	6,849	0.15	140	L 1.0%	L 1.0%

**Table 2.3-17 Layer Depths, Shear Wave Velocities ( $V_s$ ), Unit Weights, and Dynamic Properties for Turkey Point (cont.)**

Layer	Depth (ft)	Description	$V_s$ (ft/sec)			$V_s$ Sigma (ln)	BC Unit Weight (pcf)	Dynamic Properties	
			LR (0.3)	BC (0.4)	UR (0.3)			Alt. 1 (0.5)	Alt. 2 (0.5)
14	2,000	Rock: limestone	4,333	5,600	7,237	0.15	150	L 1.0%	L 1.0%
15	3,700	Rock: limestone	5,107	6,600	8,529	0.15	150	L 1.0%	L 1.0%
16	4,000	Rock: limestone	6,500	8,400	9,285	0.15	160	L 1.0%	L 1.0%

LR = lower range; BC = basecase; UR = upper range; ln = natural log; pcf = pounds per cubic foot; L = linear; Alt. = alternative; Pen. = Peninsular.  
 For LR, BC, UR, and Alt.: Values in parentheses refer to weights for site response analysis logic tree branches.

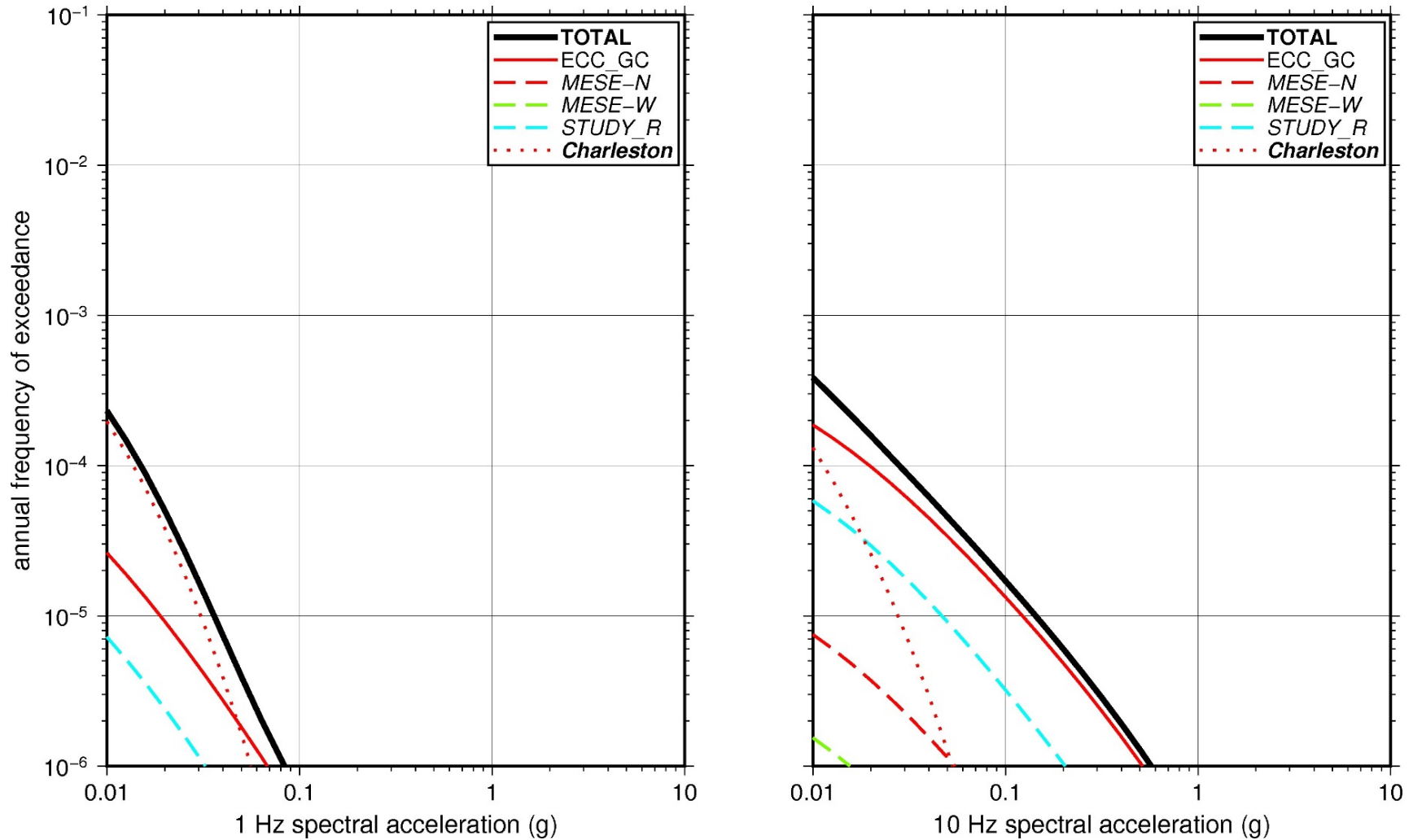


**Figure 2.3-62 Low-Frequency (1 Hz, Left) and High-Frequency (10 Hz, Right) Reference Rock Hazard Curves for Turkey Point. Total Hazard is Shown as a Bold Black Line; Individual Contributions to the Hazard for Each of the CEUS-SSC Sources are Shown as Colored Lines Defined in the Legend. See Table 2.1-1 for Source Name Definitions**

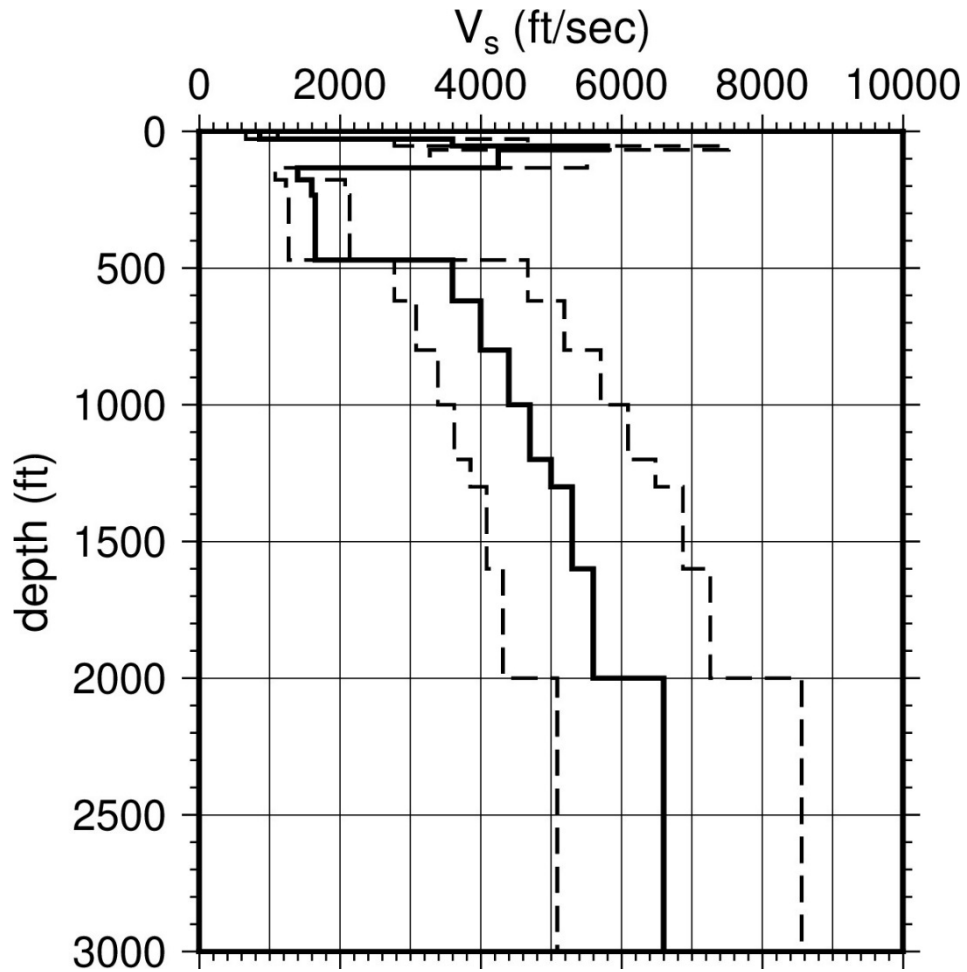


**Figure 2.3-63** Shear Wave Velocity ( $V_s$ ) Profiles for Turkey Point. Basecase (BC) Profile Shown as Solid Bold Line; Lower and Upper Range (LR and UR) Profiles Shown as Dashed Lines. Profiles Terminate at Reference Rock Velocity of 2,831 m/sec [9,285 ft/sec] per EPRI GMM (2013)

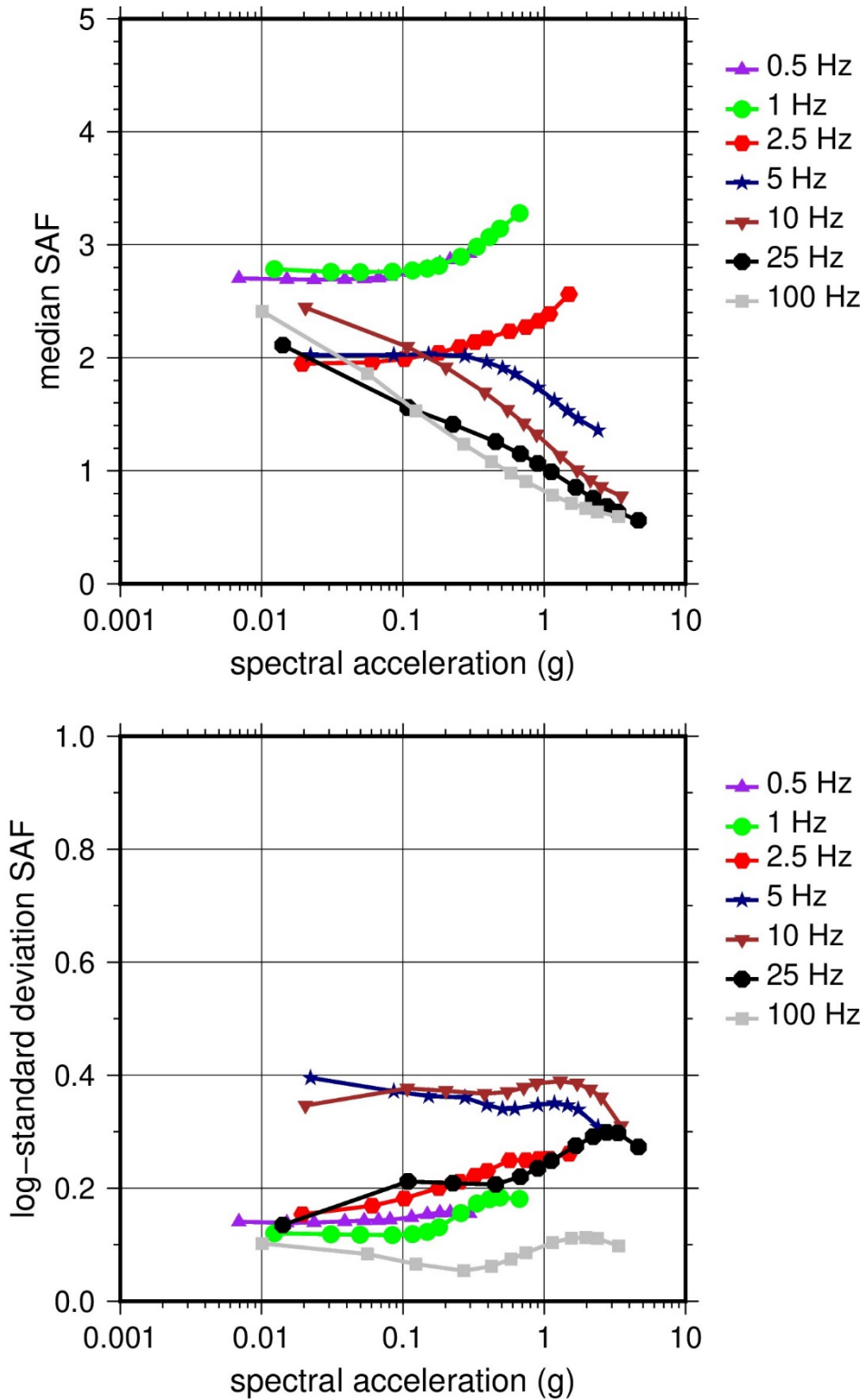


**Figure 2.3-64 Overall Weighted Median Site Amplification Factor (SAF) (Upper) and Log Standard Deviation of the SAF (Lower) as a Function of Input Acceleration for EPRI GMM (2013) Spectral Frequencies**



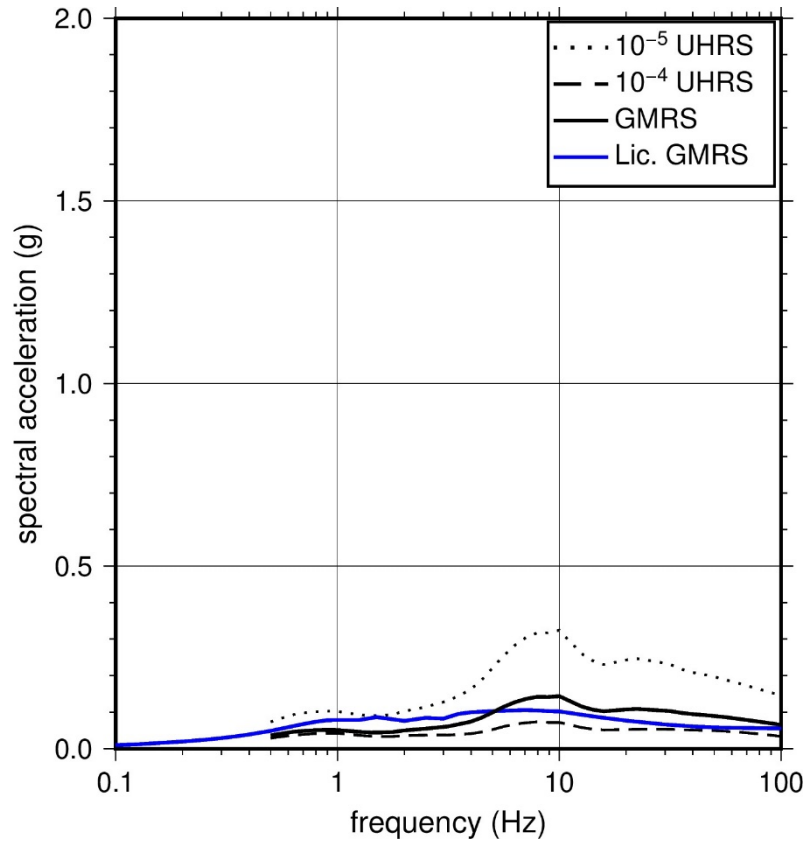
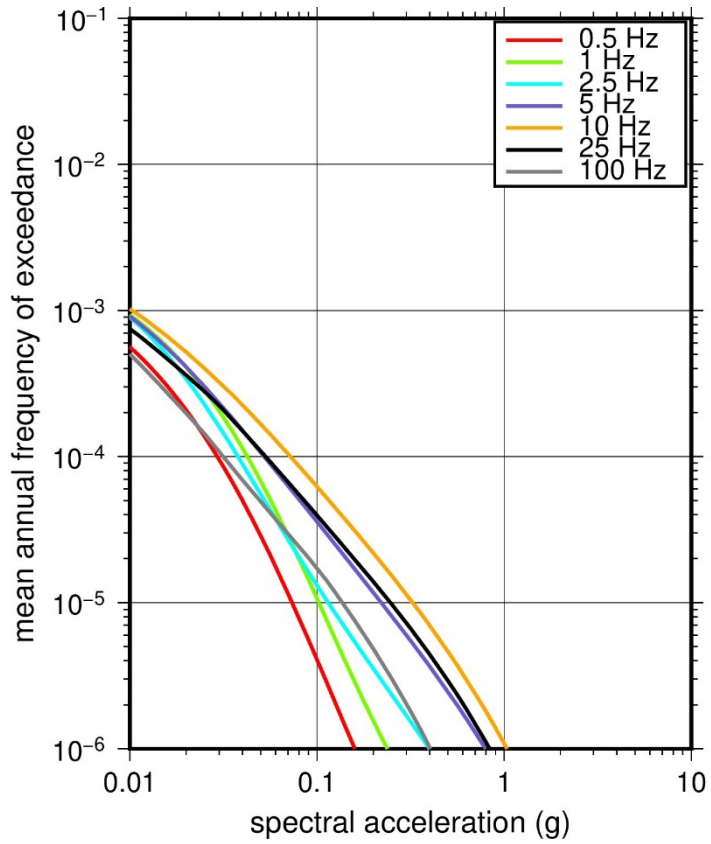


**Figure 2.3-65 Mean Control Point Hazard Curves (Left) for EPRI GMM (2013) Spectral Frequencies, and GMRS and UHRS (Right) for Turkey Point**

### 2.3.17 Vogtle

The Vogtle Electric Generating Plant site is located in Georgia along the Savannah River within the Coastal Plain physiographic province and is founded on about 305 m [1,000 ft] of soil (sand and clay) over sedimentary rock of Mesozoic age. The horizontal SSE response spectrum for the Vogtle site has an RG 1.60 spectral shape and is anchored at a PGA of 0.20g.

#### 2.3.17.1 Reference Rock Hazard

For the reference rock PSHA, the NRC staff selected the eight CEUS-SSC (NRC, 2012b) background seismic source zones that are located within 320 km [200 mi] of the site. In addition to the nearby Charleston CEUS-SSC RLME, the NRC staff selected additional RLME sources that are within 806 km [500 mi] of the site. To develop the reference rock seismic hazard curves for the site, the NRC staff used the GMPEs in the updated EPRI GMM (2013). As shown in Figure 2.3-66, the Charleston RLME is the largest contributor to both the 1 Hz and 10 Hz reference rock total mean hazard curves at the  $10^{-4}$  AFE level. For the 10 Hz reference rock total mean hazard curve, the ECC-AM seismotectonic zone also makes a significant contribution at the  $10^{-4}$  AFE level.

#### 2.3.17.2 Site Response Evaluation

##### 2.3.17.2.1 Site Profiles

To develop a basecase profile, the NRC staff used the geologic information in the NTTF R2.1 revised SHSR (Pierce, 2014c) submitted by Southern Nuclear Operating Company (hereafter referred to as “the licensee” within this plant section). As described in the licensee’s SHSR, the Vogtle site consists of about 305 m [1,000 ft] of sedimentary deposits (primarily sands, silty sands, clayey sands, limestone, marl, and silt) overlying the Triassic-Jurassic sedimentary rock of the Dunbarton Basin, which is part of the South Georgia Rift Basin. The licensee stated that the upper sand stratum and the Utley Limestone were removed and replaced with 27 m [88 ft] of compacted backfill within the powerblock areas. In Tables 2.3.1-1 and 2.3.1-2 of the SHSR, the licensee briefly described the subsurface materials in terms of the geologic units and layer thicknesses. For its site response evaluation, the NRC staff used the top of ground surface, which corresponds to an elevation of 67 m [220 ft] above MSL, as the control point elevation for the Vogtle site.

The field investigations for Vogtle include the initial siting investigations for Vogtle Units 1 and 2 (Southern Nuclear Operating Company, 2014), the investigation carried out for the ISFSI (Bechtel Power Corporation, 2011), and the investigations for the ESP and COL for Vogtle Units 3 and 4 (Southern Nuclear Operating Company, 2013). These investigations consist of numerous geophysical profiles, including crosshole methods and P-S velocity logging to a depth of 408 m [1,338 ft] in the deepest borehole for Units 3 and 4. The licensee also relied on geophysical investigations from the nearby Savannah River site to determine the  $V_S$  for the deeper strata within the Dunbarton Basin. SHSR Tables 2.3.1-1, 2.3.1-2, and 2.3.2-2 give the measured  $V_S$  from the licensee’s reported data for Vogtle Units 1 and 2, Vogtle Units 3 and 4, the ISFSI investigation, and recent  $V_S$  measurements for the backfill collected during the construction phase at Units 3 and 4.

For its SHSR, the licensee developed a basecase profile that extends to a depth of about 671 m [2,200 ft] below the control point elevation. The uppermost layers of the profile consist of approximately 27 m [88 ft] of compacted fill, for which the licensee measured a  $V_S$  that

increases from 178 m/sec [583 ft/sec] near the surface to about 347 m/sec [1,138 ft/sec] at its base.

Below the compacted fill is about 21 m [68 ft] of hard calcareous clay marl, referred to as the Blue Bluff Marl. The  $V_S$  of the Blue Bluff Marl increases from 486 m/sec [1,594 ft/sec] to 672 m/sec [2,206 ft/sec]. Beneath the Blue Bluff Marl is 274 m [900 ft] of dense, coarse-to-fine sand with interbedded silty clay and clayey silt referred to as the Lower Sand Stratum. The  $V_S$  for the Lower Sand Stratum ranges from about 483 m/sec [1,586 ft/sec] to 842 m/sec [2,764 ft/sec]. The  $V_S$  for the underlying Triassic age Dunbarton Basin increases from about 1,341 m/sec [4,400 ft/sec] to about 2,624 m/sec [8,610 ft/sec] with the reference rock  $V_S$  of 2,831 m/sec [9,285 ft/sec] at a depth of 671 m [2,200 ft].

As multiple geophysical field investigations have characterized the sedimentary strata beneath the Vogtle site, the NRC staff used the licensee's layer thicknesses and  $V_S$  for its basecase profile.

To capture the uncertainty in its basecase profile, the NRC staff developed lower and upper range (10<sup>th</sup> and 90<sup>th</sup> percentile) profiles by multiplying the basecase  $V_S$  values by scale factors of 0.83 and 1.21, respectively, which corresponds to an epistemic logarithmic standard deviation of 0.15. The weights for the lower, best-estimate, and upper basecase profiles are 0.3, 0.4, and 0.3, respectively. Figure 2.3-67 shows the basecase, lower, and upper profiles used by the NRC staff.

#### 2.3.17.2.2 *Dynamic Material Properties and Site Kappa*

The NRC staff assumed both linear and nonlinear behavior for the soil and rock beneath the Vogtle site. To model the nonlinear response within the upper 148 m [486 ft] of soil deposits, the NRC staff used the EPRI soil shear modulus reduction and damping curves as one alternative and the Peninsular Range curves for the second equally weighted alternative. For the remaining 550 m [1,802 ft] of its profile, the NRC staff assumed a linear response with a damping ratio value of 1 percent to maintain consistency with the  $\kappa_0$  value for the Vogtle site.

To determine the basecase  $\kappa_0$  for the Vogtle site, the NRC staff first used the Campbell (2009) Model 1 relationship between  $V_S$  and  $Q_{ef}$  to determine a  $Q_{ef}$  for each layer. Combining these  $Q_{ef}$  values with the thicknesses and  $V_S$  for each of the layers results in a total  $\kappa_0$  value of about 29 msec, which includes the 6 msec assumed for the underlying reference rock. For the lower and upper basecase profiles, the NRC staff calculated  $\kappa_0$  values of 38 and 22 msec, respectively, using the same approach as for the basecase profile. In contrast, the licensee used a  $\kappa_0$  value of 10 msec for its single basecase profile, based on the damping ratio values that it measured or estimated for each of the sedimentary layers beneath the site.

Table 2.3-18 provides the layer depths, lithologies,  $V_S$ , unit weights, and dynamic properties for the NRC staff's three profiles. In summary, the site response logic tree developed by the NRC staff for the Vogtle site consists of six alternatives; three basecase profiles (each with a different  $\kappa_0$  value) and two alternative dynamic property branches.

#### 2.3.17.2.3 *Methodology and Results*

The NRC staff followed the methodology described in Section 2.1.4 to develop the final site amplification factors. Figure 2.3-68 shows the overall median site amplification factors and their variability for each of the seven spectral frequencies. As shown in Figure 2.3-68, the median

site amplification factors range from about 2 to 3 before falling off with higher input spectral accelerations. The lower half of Figure 2.3-68 shows that the logarithmic standard deviations for the site amplification factors range from about 0.1 to 0.2.

### 2.3.17.3 Control Point Hazard

The NRC staff implemented Approach 3 from the SPID to develop a weighted control point seismic hazard curve for each of the six unique combinations of the site response logic tree for the Vogtle site. After combining these curves to develop the final mean control point hazard curves, the NRC staff determined the  $10^{-4}$  and  $10^{-5}$  UHRS in order to calculate the final GMRS. Figure 2.3-69 shows the final control point mean seismic hazard curves for each of the seven spectral frequencies as well as the NRC staff's UHRS and GMRS, and the licensee's NTTF R2.1 GMRS (Pierce, 2014c). As shown in Figure 2.3-69, the NRC staff's GMRS (black curve) is moderately lower than the licensee's GMRS (blue curve) due to the staff's higher estimate of  $\kappa_0$  for the Vogtle site.

**Table 2.3-18 Layer Depths, Shear Wave Velocities ( $V_s$ ), Unit Weights, and Dynamic Properties for Vogtle**

Layer	Depth (ft)	Description	$V_s$ (ft/sec)			$V_s$ Sigma (ln)	Unit Weight (pcf)	Dynamic Properties	
			LR (0.3)	BC (0.4)	UR (0.3)			Alt. 1 (0.5)	Alt. 2 (0.5)
1	6	Soil: fill	481	583	707	0.15	120	EPRI Soil	Pen.
2	18	Soil: fill	696	844	1,023	0.15	120	EPRI Soil	Pen.
3	88	Soil: fill	939	1,138	1,379	0.15	120	EPRI Soil	Pen.
4	106	Soil: clay marl	1,315	1,594	1,932	0.15	130	EPRI Soil	Pen.
5	156	Soil: clay marl	1,820	2,206	2,674	0.15	130	EPRI Soil	Pen.
6	220	Soil: sand	1,309	1,586	1,922	0.15	130	EPRI Soil	Pen.
7	486	Soil: sand	1,662	2,014	2,441	0.15	130	EPRI Soil	Pen.
8	1,058	Soil: sand	2,281	2,764	3,350	0.15	130	L 1.0%	L 1.0%
9	1,100	Rock: siltstone	3,630	4,400	5,333	0.15	140	L 1.0%	L 1.0%
10	1,150	Rock: siltstone	4,662	5,650	6,848	0.15	150	L 1.0%	L 1.0%
11	1,225	Rock: siltstone	5,487	6,650	8,060	0.15	150	L 1.0%	L 1.0%
12	1,575	Rock: siltstone	6,907	8,372	9,285	0.15	160	L 1.0%	L 1.0%
13	1,950	Rock: siltstone	7,104	8,610	9,285	0.15	160	L 1.0%	L 1.0%

LR = lower range; BC = basecase; UR = upper range; ln = natural log; pcf = pounds per cubic foot; L = linear; Alt. = alternative; Pen. = Peninsular.  
For LR, BC, UR, and Alt.: Values in parentheses refer to weights for site response analysis logic tree branches.

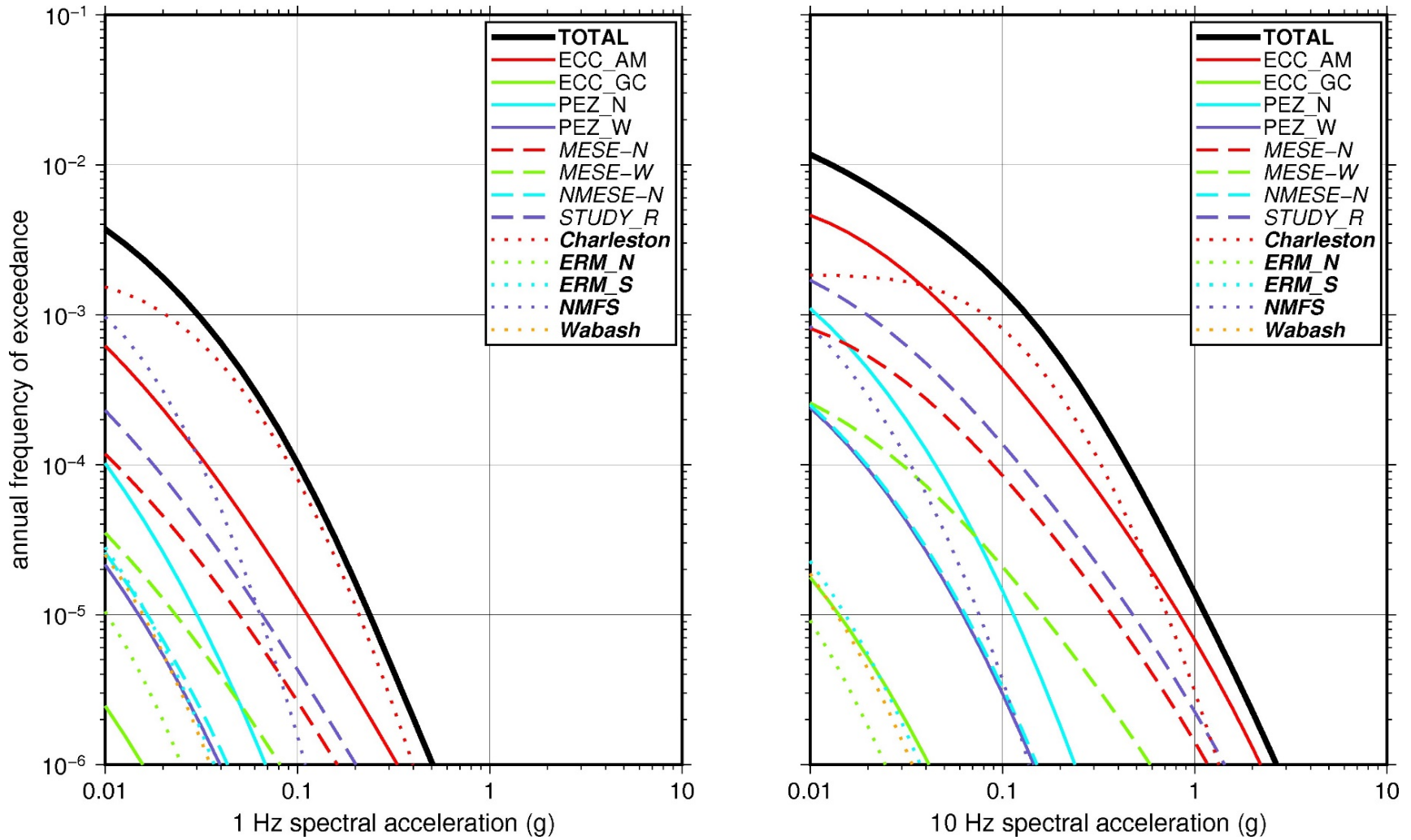


**Figure 2.3-66 Low-Frequency (1 Hz, Left) and High-Frequency (10 Hz, Right) Reference Rock Hazard Curves for Vogtle. Total Hazard is Shown as a Bold Black Line; Individual Contributions to the Hazard for Each of the CEUS-SSC Sources are Shown as Colored Lines Defined in the Legend. See Table 2.1-1 for Source Name Definitions**

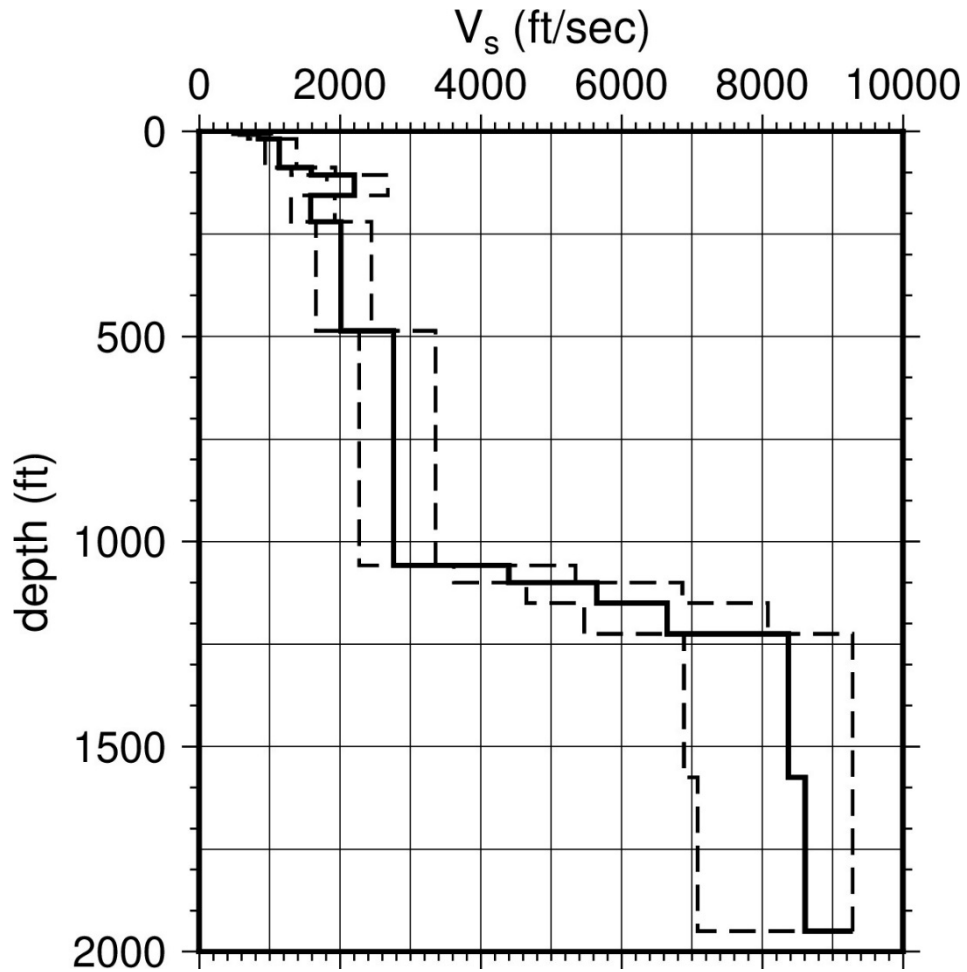


**Figure 2.3-67 Shear Wave Velocity ( $V_s$ ) Profiles for Vogtle. Basecase (BC) Profile Shown as Solid Bold Line; Lower and Upper Range (LR and UR) Profiles Shown as Dashed Lines. Profiles Terminate at Reference Rock Velocity of 2,831 m/sec [9,285 ft/sec] per EPRI GMM (2013)**

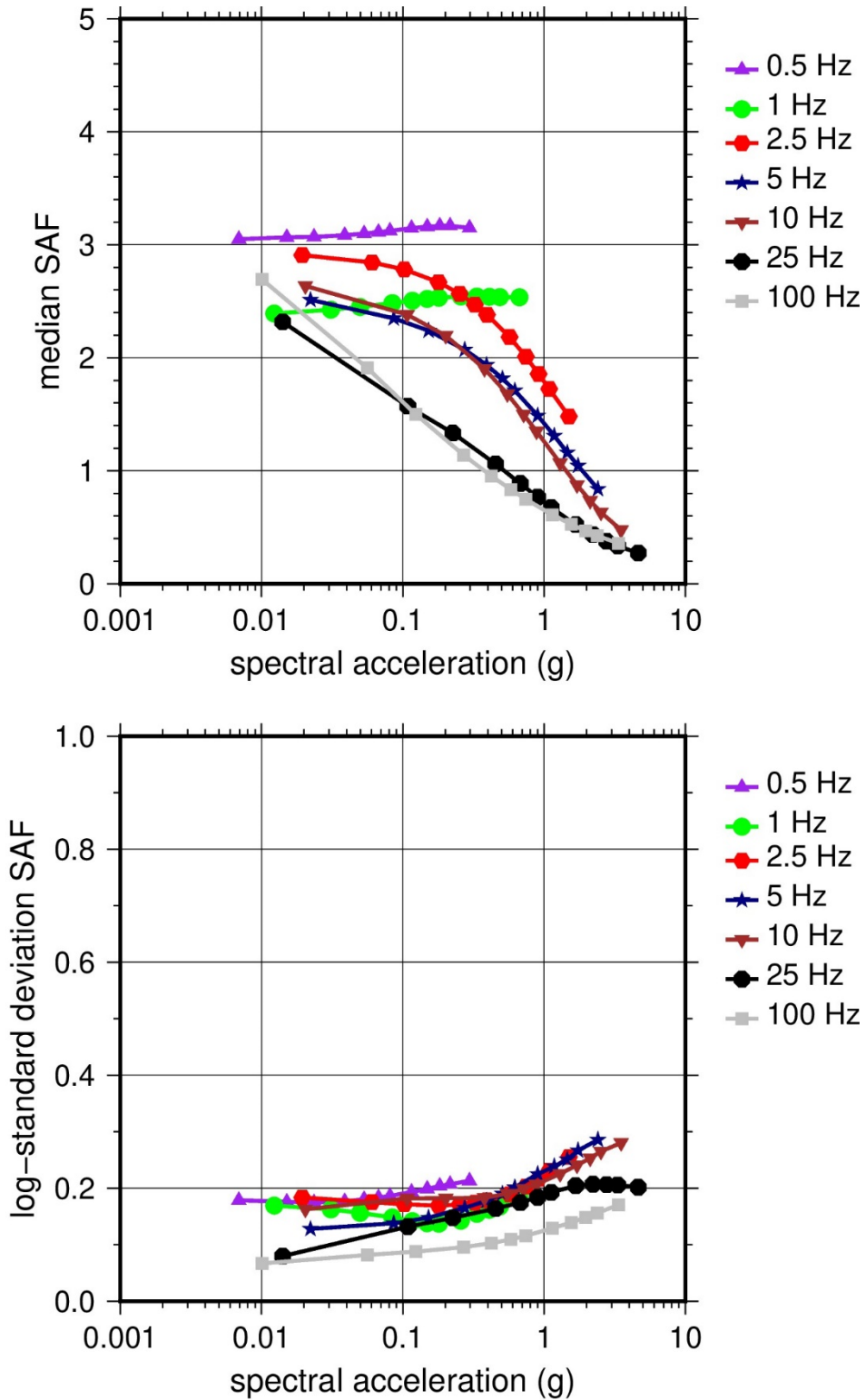


**Figure 2.3-68 Overall Weighted Median Site Amplification Factor (SAF) (Upper) and Log Standard Deviation of the SAF (Lower) as a Function of Input Acceleration for EPRI GMM (2013) Spectral Frequencies**

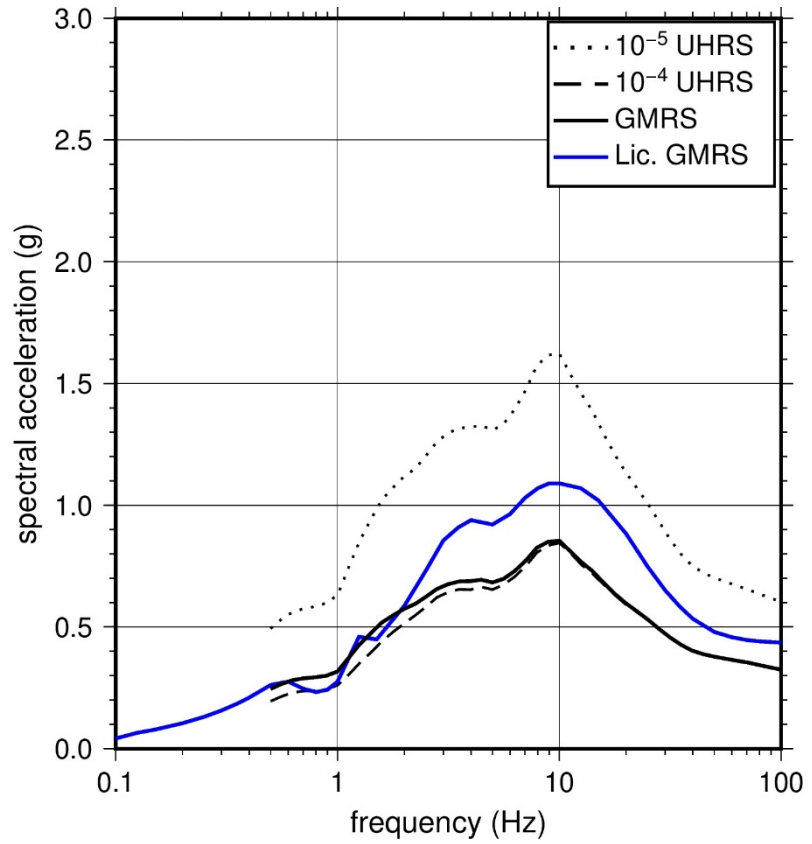
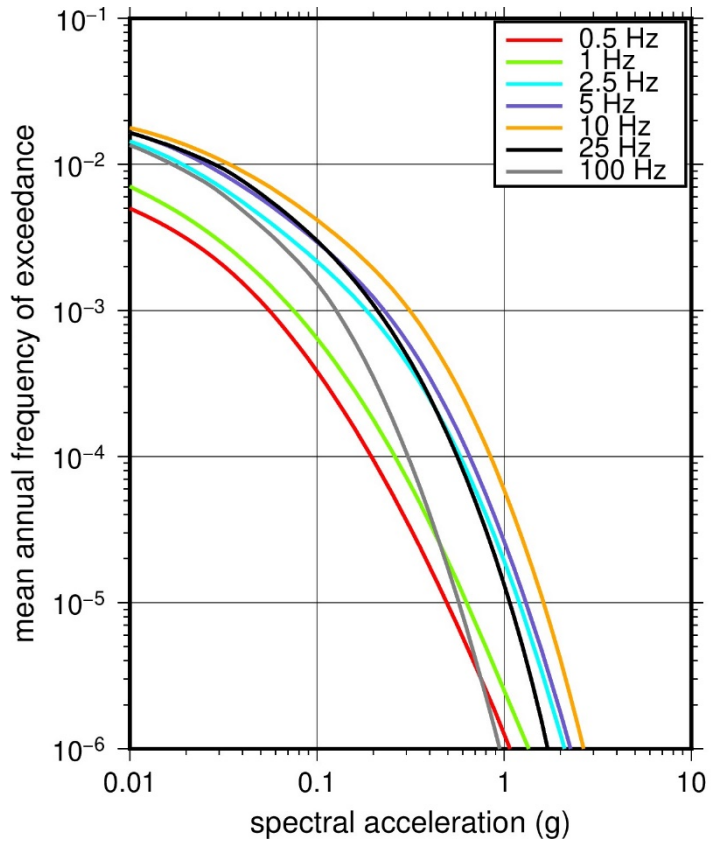


**Figure 2.3-69 Mean Control Point Hazard Curves (Left) for EPRI GMM (2013) Spectral Frequencies, and GMRS and UHRS (Right) for Vogtle**



### 2.3.18 Watts Bar

The Watts Bar Nuclear Plant site is located 80 km [50 mi] northeast of Chattanooga, TN, on the west side of the Tennessee River in the Valley and Ridge physiographic province and consists of about 3,354 m [11,000 ft] of competent sedimentary rock (shale, limestone, dolomite, and sandstone) of Paleozoic age. The horizontal SSE response spectrum for Watts Bar has a Newmark spectral shape and is anchored at a PGA of 0.18 g.

#### 2.3.18.1 Reference Rock Hazard

For the reference rock PSHA, the NRC staff selected the 15 CEUS-SSC (NRC, 2012b) background seismic source zones that are located within 320 km [200 mi] of the site. The NRC staff also selected the 7 CEUS-SSC RLME sources that are located within 806 km [500 mi] of the site. To develop the reference rock seismic hazard curves for the Watts Bar site, the NRC staff used the GMPEs in the updated EPRI GMM (2013). As shown in Figure 2.3-70, the NMFS RLME, which is located about 250 km [155 mi] to the west of Watts Bar, is the largest contributor to the 1 Hz reference rock total mean hazard curve at the  $10^{-4}$  AFE level. For the 10 Hz reference rock total mean hazard curve, the PEZ-N seismotectonic zone provides the highest contribution at the  $10^{-4}$  AFE level.

#### 2.3.18.2 Site Response Evaluation

##### 2.3.18.2.1 Site Profiles

To develop a basecase profile, the NRC staff used the geologic information in the NTTF R2.1 SHSR (Shea, 2014) submitted by the TVA (hereafter referred to as “the licensee” within this plant section). As described in the licensee’s SHSR, the Watts Bar site consists of about 10 m [32 ft] of clay, silt, sand and gravel, overlying shale and limestone units from the Conasauga Group. The primary Watts Bar structures are founded at a depth of 19 m [64 ft], which lies below the uppermost weathered portions of the interbedded shales and limestones. In Tables 2.3.1-1 and 2.3.1-2 of the SHSR, the licensee briefly described the subsurface materials in terms of the geologic units and layer thicknesses. For its site response evaluation, the NRC staff used a depth of 19 m [64 ft] from the surface, which is within the Conasauga shales and limestones, as the control point elevation for the Watts Bar site.

The field investigation for Watts Bar, conducted as part of the original siting investigations, included continuous  $V_P$  collected by the licensee in seven boreholes at the site. In addition, the licensee also used SASW testing to estimate the  $V_S$  for the near-surface bedrock and deeper rock layers beneath the site. Table 2.3.1-2 of the SHSR gives the measured and estimated  $V_S$  determined from the licensee’s site investigations.

For its SHSR, the licensee developed two basecase profiles. The first basecase profile extends to a depth of 181 m [592 ft] below the control point elevation, and the second basecase profile extends to a depth of 285 m [936 ft] below the control point elevation. The major controlling geologic feature of the Watts Bar site is the Kingston Thrust fault. Movement along this fault resulted in the Cambrian age Conasauga Group and underlying Rome Formation at the plant site resting upon the younger Ordovician age Knox Group dolomites, which would normally overlie the Conasauga and Rome sedimentary strata. The majority of the licensee’s basecase profile consists of sedimentary strata from the Conasauga (shale and limestone) and the Rome Formation (sandstone), for which the licensee estimated  $V_S$  of about 1,829 m/sec [6,000 ft/sec] and 2,362 m/sec [7,750 ft/sec], respectively. At a depth of 305 m [1,000 ft] within the Rome

Formation, the licensee estimated a  $V_S$  of 3,049 m/sec [10,000 ft/sec]. The licensee developed two basecase profiles to capture the possibility that the  $V_S$  of the sandstones of the Rome Formation attain or exceed the reference rock condition { $V_S$  of 2,831 m/sec [9,285 ft/sec]} specified by the EPRI GMM (2013) at a depth of either 181 m [592 ft] or 285 m [936 ft] below the control point elevation.

For its basecase profile, the NRC staff used the licensee's layer thicknesses and estimated  $V_S$  for the deeper profile; however, the NRC staff applied the velocity gradient of 0.5 m/sec/m [0.5 ft/sec/ft] recommended by the SPID for sedimentary rock to the uppermost Conasauga Group stratum.

To capture the uncertainty in the basecase profile, the NRC staff developed lower and upper range (10<sup>th</sup> and 90<sup>th</sup> percentile) profiles by multiplying the basecase  $V_S$  values by scale factors of 0.83 and 1.21, respectively, which corresponds to an epistemic logarithmic standard deviation of 0.15. The weights for the lower, best-estimate, and upper basecase profiles are 0.3, 0.4, and 0.3, respectively. Figure 2.3-71 shows that the NRC staff's basecase, lower, and upper profiles extend to depths of 198 m [650 ft] (upper profile) and 320 m [1,050 ft] (basecase and lower profiles) below the control point elevation.

#### 2.3.18.2.2 *Dynamic Material Properties and Site Kappa*

The NRC staff assumed both linear and nonlinear dynamic behavior for the rock beneath the Watts Bar site. To model the nonlinear behavior of the uppermost rock strata, the NRC staff used the EPRI rock shear modulus reduction and material damping curves. To model the linear behavior, the NRC staff used a constant damping ratio of 3 percent. The NRC staff assumed these two alternative dynamic responses for the upper 20 m [65 ft] of the profile and gave them equal weight. For the remaining 300 m [985 ft] of its profile, the NRC staff assumed a linear response with a material damping ratio value of 0.1 percent to maintain consistency with the  $\kappa_0$  value for the Watts Bar site.

To determine the basecase  $\kappa_0$  for the Watts Bar site, the NRC staff first used the Campbell (2009) Model 1 relationship between  $V_S$  and  $Q_{ef}$  to determine a  $Q_{ef}$  for each layer. Combining these  $Q_{ef}$  values with the thicknesses and  $V_S$  for each of the layers results in a total  $\kappa_0$  value of about 9 msec, which includes the 6 msec assumed for the underlying reference rock. For the lower and upper basecase profiles, the NRC staff calculated  $\kappa_0$  values of 10 and 7 msec, respectively, using the same approach as for the best-estimate basecase profile. In contrast, the licensee estimated  $\kappa_0$  by combining the lowest low-strain damping values from the EPRI rock material damping curves over the upper 152 m [500 ft] of its six profiles to estimate  $\kappa_0$  values of 8 to 20 msec.

Table 2.3-19 provides the layer depths, lithologies,  $V_S$ , unit weights, and dynamic properties for the NRC staff's three profiles. In summary, the site response logic tree developed by the NRC staff for the Watts Bar site consists of six alternatives; three basecase profiles (each with a different  $\kappa_0$  value) and two alternative dynamic property branches.

#### 2.3.18.2.3 *Methodology and Results*

The NRC staff followed the methodology described in Section 2.1.4 to develop the final site amplification factors. Figure 2.3-72 shows the overall median site amplification factors and their variability for each of the seven spectral frequencies. As shown in Figure 2.3-72, the median site amplification factors are all close to 1 for low-input spectral accelerations and decrease to

about 0.8 for higher input accelerations. The lower half of Figure 2.3-72 shows that the logarithmic standard deviations for the site amplification factors are between 0.05 and 0.20.

### 2.3.18.3 Control Point Hazard

The NRC staff implemented Approach 3 from the SPID to develop a weighted control point seismic hazard curve for each of the six unique combinations of the site response logic tree for the Watts Bar site. After combining these curves to develop the final mean control point hazard curves, the NRC staff determined the  $10^{-4}$  and  $10^{-5}$  UHRS in order to calculate the final GMRS. Figure 2.3-73 shows the final control point mean seismic hazard curves for each of the seven spectral frequencies as well as the NRC staff's UHRS and GMRS, and the licensee's NTTF R2.1 GMRS (Shea, 2014). As shown in Figure 2.3-73, the licensee's GMRS (blue curve) is moderately lower than the NRC staff's GMRS (black curve) up to 10 Hz and then falls off more rapidly for the higher frequencies. This difference between GMRS for the higher frequencies is due to the licensee's application of the EPRI rock shear modulus reduction and material damping curves for 152 m [500 ft] of its profiles compared to only 20 m [65 ft] used by the NRC staff. The NRC staff applied the EPRI rock shear modulus reduction and material damping curves for only 20 m [65 ft] to maintain consistency with the relatively low  $\kappa_0$  values estimated by the NRC staff for the Watts Bar site. For comparison, Figure 2.3-73 also shows the NRC staff's reference rock GMRS (brown dotted curve).

**Table 2.3-19 Layer Depths, Shear Wave Velocities ( $V_s$ ), Unit Weights, and Dynamic Properties for Watts Bar**

Layer	Depth (ft)	Description	$V_s$ (ft/sec)			$V_s$ Sigma (ln)	BC Unit Weight (pcf)	Dynamic Properties	
			LR (0.3)	BC (0.4)	UR (0.3)			Alt. 1 (0.5)	Alt. 2 (0.5)
1	31	Rock: shale, limestone	4,785	5,800	7,030	0.25	150	EPRI Rock	L 3.0%
2	65	Rock: shale, limestone	4,960	6,000	7,272	0.15	150	EPRI Rock	L 3.0%
3	100	Rock: shale, limestone	4,964	6,017	7,293	0.15	150	L 0.1%	L 0.1%
4	150	Rock: shale, limestone	4,985	6,042	7,323	0.15	150	L 0.1%	L 0.1%
5	200	Rock: shale, limestone	5,005	6,067	7,353	0.15	150	L 0.1%	L 0.1%
6	300	Rock: shale, limestone	5,046	6,117	7,414	0.15	150	L 0.1%	L 0.1%
7	450	Rock: shale, limestone	5,109	6,192	7,505	0.15	150	L 0.1%	L 0.1%
8	650	Rock: shale, limestone	5,191	6,292	7,626	0.15	150	L 0.1%	L 0.1%
9	850	Rock: sandstone	6,394	7,750	9,285	0.15	160	L 0.1%	L 0.1%
10	1,050	Rock: sandstone	6,477	7,850	9,285	0.15	160	L 0.1%	L 0.1%

LR = lower range; BC = basecase; UR = upper range; ln = natural log; pcf = pounds per cubic foot; L = linear; Alt. = alternative.  
 For LR, BC, UR, and Alt.: Values in parentheses refer to weights for site response analysis logic tree branches.

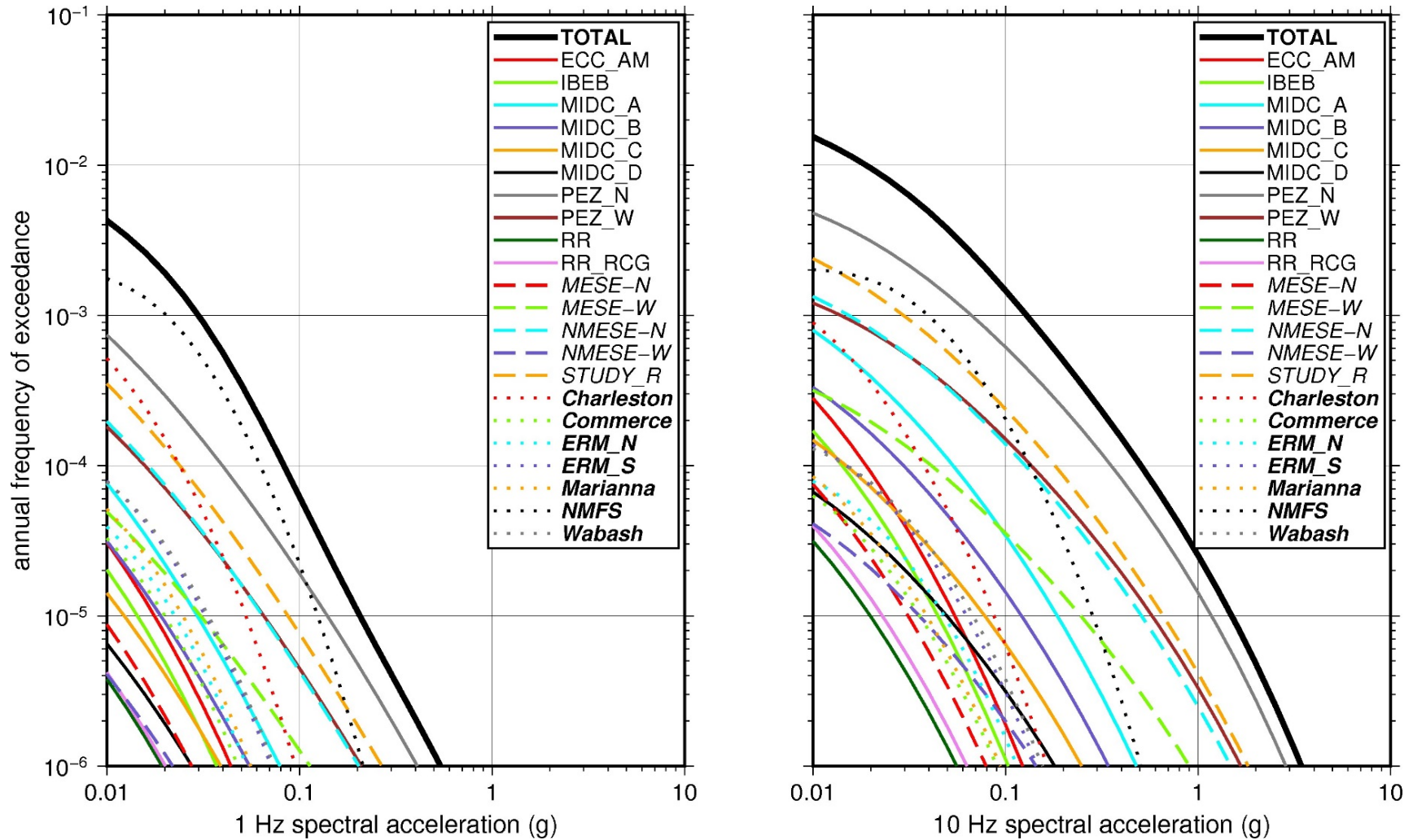


**Figure 2.3-70 Low-Frequency (1 Hz, Left) and High-Frequency (10 Hz, Right) Reference Rock Hazard Curves for Watts Bar. Total Hazard as Shown as a Bold Black Line; Individual Contributions to the Hazard for Each of the CEUS-SSC Sources are Shown as Colored Lines Defined in the Legend. See Table 2.1-1 for Source Name Definitions**

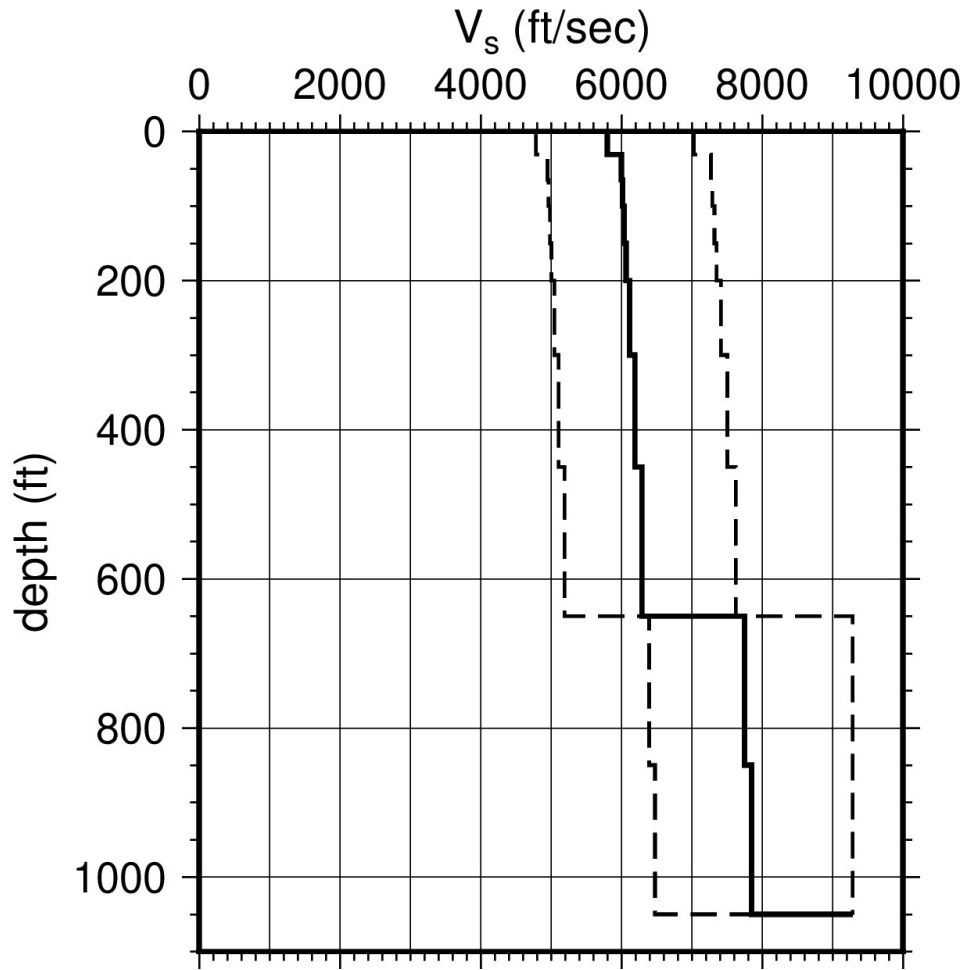


**Figure 2.3-71 Shear Wave Velocity ( $V_s$ ) Profiles for Watts Bar. Basecase (BC) Profile Shown as Solid Bold Line; Lower and Upper Range (LR and UR) Profiles Shown as Dashed Lines. Profiles Terminate at Reference Rock Velocity of 2,831 m/sec [9,285 ft/sec] per EPRI GMM (2013)**

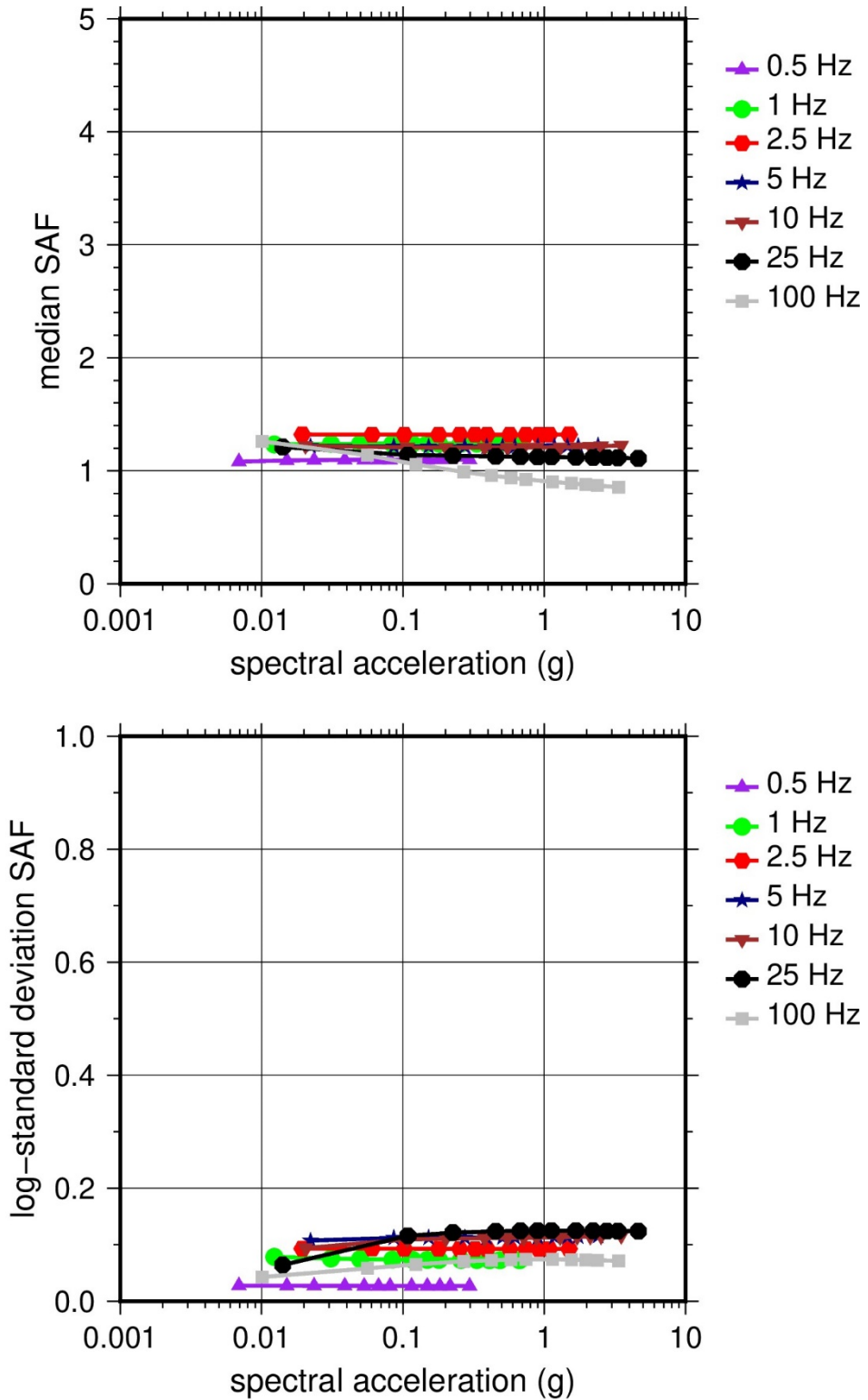


**Figure 2.3-72 Overall Weighted Median Site Amplification Factor (SAF) (Upper) and Log Standard Deviation of the SAF (Lower) as a Function of Input Acceleration for EPRI GMM (2013) Spectral Frequencies**

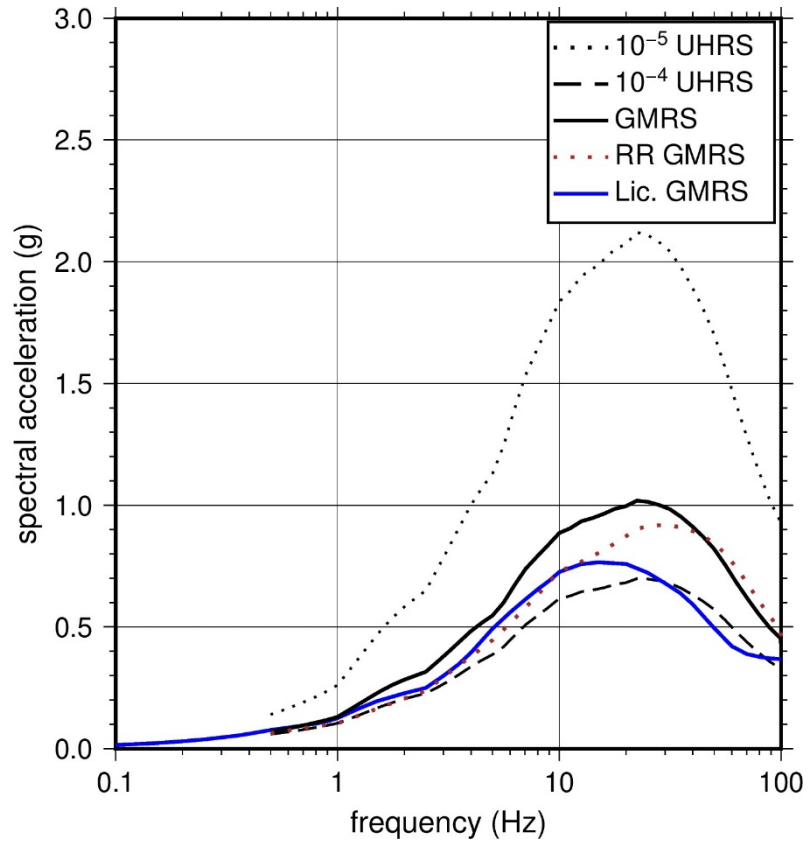
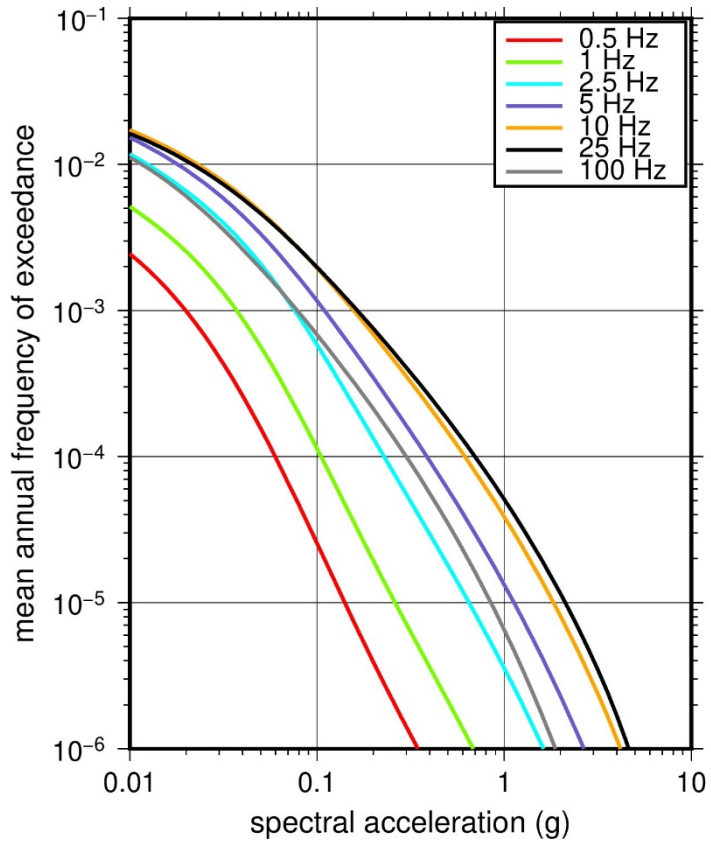


**Figure 2.3-73 Mean Control Point Hazard Curves (Left) for EPRI GMM (2013) Spectral Frequencies, and GMRS and UHRS (Right) for Watts Bar**

## 2.4 Region III Sites

The NRC staff characterized the seismic hazard for the 15 Region III CEUS nuclear plant sites shown below in Table 2.4-1 and Figure 2.4-1. As shown in Table 2.4-1, 8 of the 15 Region III NPPs are founded on rock and 7 on soil over sedimentary rock. Table 2.4-1 also shows the State, the physiographic province, and whether there is a co-located ESP or COL for each site. Figure 2.4-1 shows the Region III sites overlain on the physiographic provinces, the highest weighted CEUS-SSC (NRC, 2012b) seismotectonic source zone configuration, and the CEUS-SSC earthquake epicenters. Figure 2.4-1 also shows the CEUS-SSC RLME sources used to develop the reference rock hazard curves for at least one Region III site.

<b>Plant Name</b>	<b>Site Name</b>	<b>State</b>	<b>Geology</b>	<b>Physiographic Province</b>	<b>ESP/COL (Y/N)</b>
Braidwood Nuclear Generating Station	Braidwood	IL	Rock	Central Lowland	N
Byron Generating Station	Byron	IL	Rock	Central Lowland	N
Clinton Power Station	Clinton	IL	Soil over rock	Central Lowland	Y
Davis Besse Nuclear Power Station	Davis Besse	OH	Rock	Central Lowland	N
Donald C. Cook Nuclear Plant	D.C. Cook	MI	Soil over rock	Central Lowland	N
Dresden Nuclear Power Station	Dresden	IL	Rock	Central Lowland	N
Duane Arnold Energy Center*	Duane Arnold	IA	Rock	Central Lowland	N
Fermi Nuclear Power Plant	Fermi	MI	Rock	Central Lowland	Y
LaSalle County Generating Station	LaSalle	IL	Soil over rock	Central Lowland	N
Monticello Nuclear Generating Plant	Monticello	MN	Soil over rock	Central Lowland	N
Palisades Nuclear Plant	Palisades	MI	Soil over rock	Central Lowland	N
Perry Nuclear Power Plant	Perry	OH	Rock	Central Lowland	N
Prairie Island Nuclear Generating Plant	Prairie Island	MN	Soil over rock	Central Lowland	N
Point Beach Nuclear Plant	Point Beach	WI	Soil over rock	Central Lowland	N



<b>Table 2.4-1 Region III CEUS Plant Names, Site Names, States, Geology, Physiographic Provinces, and Co-Located ESPs/COLs (cont.)</b>					
<b>Plant Name</b>	<b>Site Name</b>	<b>State</b>	<b>Geology</b>	<b>Physiographic Province</b>	<b>ESP/COL (Y/N)</b>
Quad Cities Nuclear Power Station	Quad Cities	IL	Rock	Central Lowland	N
*Plant was shut down or has subsequently been shut down.					

The following subsections describe the NRC staff's development of reference rock hazard curves, site response analyses, and use of Approach 3 to develop control point seismic hazard curves and a GMRS for each Region III site.

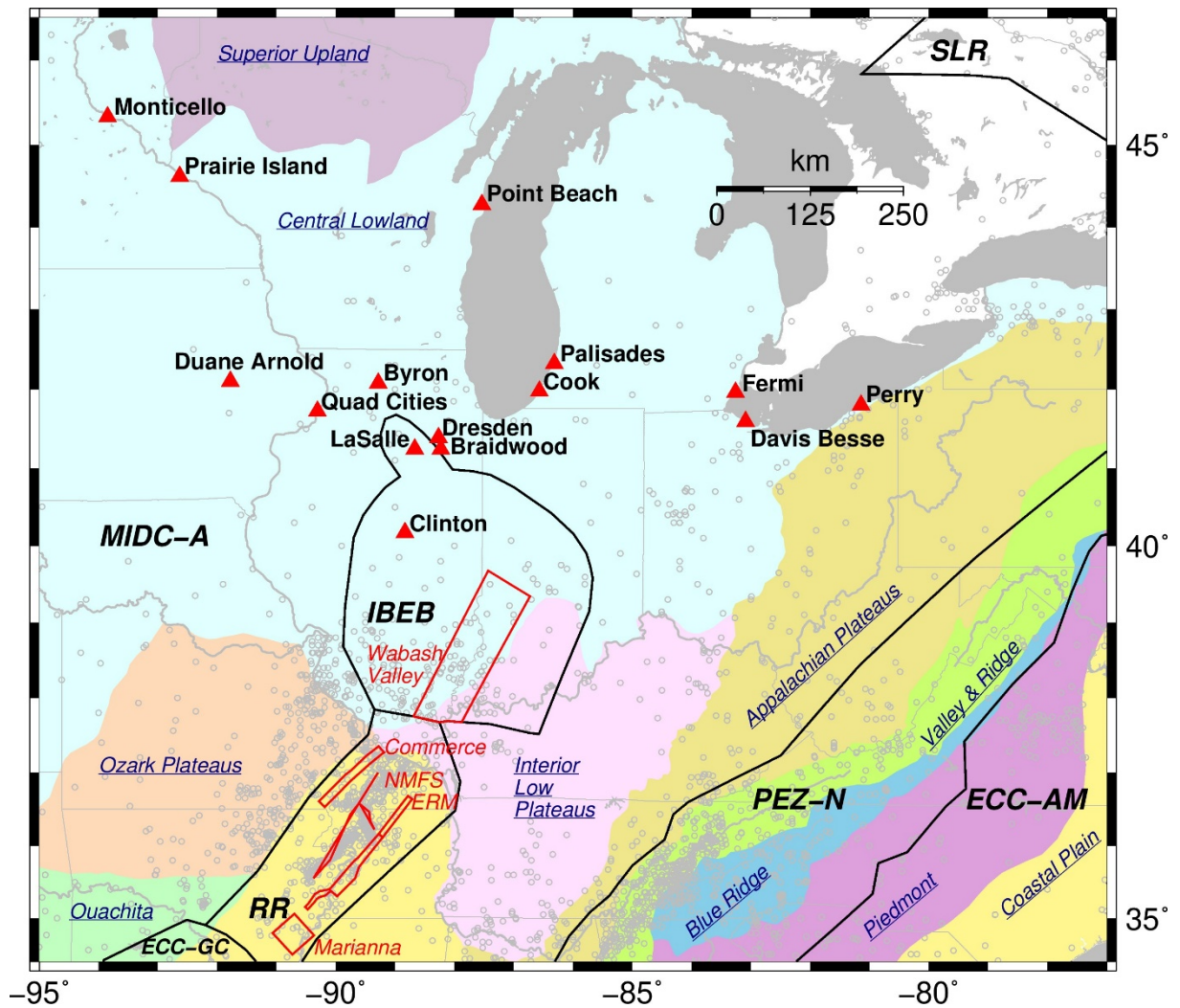


**Figure 2.4-1** Location Map Showing NPPs (Red Triangles) in Region III; RLMEs, Indicated by Solid Red Lines, and Seismotectonic Source Zones, Indicated by Solid Black Lines (from NUREG-2115), with Acronyms Defined in Table 2.1-1 of this Report; and Physiographic Provinces, Identified by Underlined Italicized Labels, with Water Bodies Represented in Gray. Earthquake Epicenters (from NUREG-2115) are Shown by Open Gray Circles

## 2.4.1 Braidwood

The Braidwood Nuclear Generating Station site is located in northeastern Illinois within the Central Lowland physiographic province and consists of 13 m [42 ft] of soil overlying about 1,524 m [5,000 ft] of firm sedimentary rock (limestone, dolomite, shale, and sandstone). The horizontal SSE response spectrum for Braidwood has an RG 1.60 spectral shape and is anchored at a PGA of 0.20g.

### 2.4.1.1 Reference Rock Hazard

For the reference rock PSHA, the NRC staff selected the nine CEUS-SSC (NRC, 2012b) background seismic source zones that are located within 320 km [200 mi] of the site. In addition, the NRC staff also selected the six CEUS-SSC (NRC, 2012b) RLME sources that are located within 807 km [500 mi] of the site. To develop the reference rock seismic hazard curves for the Braidwood site, the NRC staff used the GMPEs developed by the updated EPRI GMM (2013). As shown in Figure 2.4-2, the NMFS RLME is the largest contributor to the 1 Hz reference rock total mean hazard curve at the  $10^{-4}$  AFE level. For the 10 Hz reference rock total mean hazard curve, the Illinois Basin Extended Basement (IBEB) seismotectonic source zone is the largest contributor at the  $10^{-4}$  AFE level.

### 2.4.1.2 Site Response Evaluation

#### 2.4.1.2.1 Site Profiles

To develop a basecase profile, the NRC staff used the geologic information in the NTTF R2.1 SHSR (Kaegi, 2014a) submitted by Exelon Generation Company (hereafter referred to as “the licensee” within this plant section). As described in the licensee’s SHSR, the Braidwood site consists of about 13 m [42 ft] of soil deposits (silty sand and clay, gravel, cobbles, and boulders) overlying Paleozoic-age sedimentary rock, which lies above Precambrian basement rock. The reactor building foundation is founded on the Pennsylvanian-age sedimentary rock of the Carbondale Formation. In Table 2.3.1-1 of the SHSR, the licensee briefly described the subsurface materials in terms of the geologic units and layer thicknesses. For its site response evaluation, the NRC staff used the top of bedrock, which corresponds to an elevation of 171 m [562 ft] above MSL, as the control point elevation for the Braidwood site.

The field investigations for Braidwood, conducted in the early 1970s, consisted of a number of test pits and borings, with the deepest boring (L-2) reaching a depth of 95 m [312 ft] within the upper portion of the bedrock beneath the site. The licensee’s geophysical field investigations for Units 1 and 2 primarily measured  $V_P$  to a depth of about 61 m [200 ft] and consisted of seismic refraction and downhole and uphole surveys. To determine the  $V_S$  for each rock layer, the licensee used its measured  $V_P$  with an assumed Poisson’s ratio appropriate for the rock type. In addition to the field investigations for Units 1 and 2, the licensee also used the geophysical measurements conducted for the siting of an ISFSI on the Braidwood site. Table 2.3.2-1 of the SHSR gives the estimated  $V_S$  determined from the licensee’s site investigations.

For its SHSR, the licensee developed a basecase profile that extends to a depth of 1,543 m [5,062 ft] below the control point elevation. The uppermost layers of the profile consist of 31 m [100 ft] of Pennsylvanian-age sedimentary rock (primarily siltstone, coal, and shale, with some sandstone) from the Carbondale and Spoon Formations, which comprise the Kewanee Group. The licensee estimated a  $V_S$  of 976 m/sec [3,200 ft/sec] for these rock units. Below the

Pennsylvanian bedrock is Ordovician-age sedimentary rock (limestone and shale) from the Maquoketa Group (Fort Atkinson and Scales Formations). For the Fort Atkinson Formation limestone, which is about 11 m [37 ft] thick, the licensee measured an average  $V_P$  of 4,573 m/sec [15,000 ft/sec] and used a Poisson's ratio of 0.37 to estimate a  $V_S$  of 2,073 m/sec [6,800 ft/sec]. For the underlying Scales Formation shale, which is about 26.5 m [87 ft] thick, the licensee measured an average  $V_P$  of 3,201 m/sec [10,500 ft/sec] and assumed a Poisson's ratio of 0.44 to estimate a  $V_S$  of 1,037 m/sec [3,400 ft/sec]. Beneath the Maquoketa Group at a depth of 68 m [224 ft] below the control point elevation is the Ordovician-age Galena Group sedimentary rock from the Wise Lake, Dunleith, and Guttenberg Formations. For these three formations, which are primarily dolomites, the licensee measured a  $V_P$  of 5,000 m/sec [16,400 ft/sec] and assumed a Poisson's ratio of 0.30 to estimate a  $V_S$  of 2,658 m/sec [8,700 ft/sec]. To reach Precambrian crystalline rock, the licensee extended its basecase profile by several thousand feet to a depth of 1,528 m [5,000 ft], assuming the  $V_S$  of 2,658 m/sec [8,700 ft/sec] that it estimated for the Galena-Trenton and Platteville Group rock units.

To corroborate the licensee's reported  $V_S$  and Poisson's ratios, the NRC staff used the data from the extensive field and laboratory geotechnical investigations for the proposed Superconducting Super Collider in northeastern Illinois (Bauer et al., 1991), which directly measured the  $V_S$  for many of the same rock units that underlie the Braidwood site. In addition, to estimate the  $V_S$  for the deeper sedimentary rock layers, the NRC staff used the velocity model developed by Kaven et al. (2015) for the Decatur, IL, carbon capture and storage site.

For the upper 68 m [224 ft] of its basecase profile, the NRC staff used the licensee's layer thicknesses but estimated higher  $V_S$  based on its selection of lower Poisson's ratio values. For the top layer of Pennsylvanian sedimentary rock, the licensee measured an average  $V_P$  of 2,439 m/sec [8,000 ft/sec]. Using this average  $V_P$  value along with a Poisson's ratio of 0.41, the licensee determined a  $V_S$  of 976 m/sec [3,200 ft/sec]. However, based on an average RQD value of 71 percent and the licensee's description of this rock as slightly to moderately weathered in the UFSAR (Exelon Generation Company, 2014b), the NRC staff selected a lower Poisson's ratio of 0.33, which results in a  $V_S$  of 1,229 m/sec [4,030 ft/sec]. Similarly, the NRC staff used a Poisson's ratio of 0.33 for both the Fort Atkinson Formation limestone and the Scales Formation shale to estimate  $V_S$  values of 2,640 m/sec [7,500 ft/sec] and 1,848 m/sec [5,300 ft/sec], respectively. The NRC staff's  $V_S$  for these two rock formations, which comprise the Maquoketa Group, are similar to the values reported in Bauer et al. (1991) for the Superconducting Super Collider site. For the underlying Galena-Trenton and Platteville Group rock layers, the NRC staff used the  $V_S$  of 2,652 m/sec [8,700 ft/sec] estimated by the licensee, as this value is consistent with the  $V_S$  measurements reported in Bauer et al. (1991) for the same rock units. Finally, for the lower Ordovician-age St. Peter Formation sandstone layer, the NRC staff estimated a  $V_S$  of 2,134 m/sec [7,000 ft/sec] and a thickness of 92 m [300 ft]. These estimates are based on the stratigraphy developed by the Illinois State Geological Survey for the northeastern portion of the Illinois Basin and the  $V_P$  values from Kaven et al. (2015), together with an assumed Poisson's ratio of 0.30. For the remaining Ordovician- and Cambrian-age strata, the NRC staff assumed that the  $V_S$  exceeds the reference rock  $V_S$  of 2,831 m/sec [9,285 ft/sec]. Therefore, the basecase profile developed by the NRC staff extends to a depth of 270 m [900 ft] below the control point elevation, rather than the total thickness of 1,543 m [5,062 ft] assumed by the licensee.

To capture the uncertainty in its basecase profile, the NRC staff developed lower and upper range (10<sup>th</sup> and 90<sup>th</sup> percentile) profiles by multiplying the basecase  $V_S$  values by scale factors of 0.83 and 1.21, respectively, which corresponds to an epistemic logarithmic standard deviation of 0.15. The weights for the lower, basecase, and upper profiles are 0.3, 0.4, and 0.3,

respectively. Figure 2.4-3 shows the NRC staff's profiles, which extend to a depth of 274 m [900 ft] below the control point elevation.

#### 2.4.1.2.2 *Dynamic Material Properties and Site Kappa*

The NRC staff assumed both linear and nonlinear dynamic behavior for the rock beneath the Braidwood site. To model the nonlinear behavior of the uppermost rock strata, the NRC staff used the EPRI rock shear modulus reduction and material damping ratio curves. To model the linear behavior, the NRC staff used a constant damping ratio of 3 percent. The staff assumed these two alternative dynamic responses for the upper 68 m [224 ft] of the profile, giving them equal weight. For the remaining 206 m [676 ft] of the profile, the NRC staff assumed a linear response with a material damping ratio of 0.1 percent to maintain consistency with the  $\kappa_0$  value for the Braidwood site.

To determine the basecase  $\kappa_0$  for the Braidwood site, the NRC staff first used the Campbell (2009) Model 1 relationship between  $V_S$  and  $Q_{ef}$  to determine a  $Q_{ef}$  for each layer. Combining these  $Q_{ef}$  values with the thickness and  $V_S$  for each layer results in a total  $\kappa_0$  value of about 8 msec, which includes the 6 msec assumed for the underlying reference rock. For the lower and upper profiles, the NRC staff calculated  $\kappa_0$  values of 9 and 7 msec, respectively, using the same approach as for the basecase profile. In contrast, the licensee used the empirical relationship from the SPID (EPRI, 2012) between  $\kappa_0$  and the average  $V_S$  over the upper 30 m [100 ft] of the profile to estimate basecase, lower, and upper  $\kappa_0$  values of 24, 31, and 19 msec, respectively. The licensee expanded its range in  $\kappa_0$  values from 11 to 40 msec to capture additional epistemic uncertainty.

Table 2.4-2 provides the layer depths, lithologies,  $V_S$ , unit weights, and dynamic properties for the NRC staff's three profiles. In summary, the site response logic tree developed by the NRC staff for the Braidwood site consists of six alternatives; three velocity profiles (each with a different  $\kappa_0$  value) and two alternative dynamic property branches.

#### 2.4.1.2.3 *Methodology and Results*

The NRC staff followed the methodology described in Section 2.1.4 to develop the final site amplification factors. Figure 2.4-4 shows the overall median site amplification factors and their variability for each of the seven spectral frequencies. As shown in Figure 2.4-4, the median site amplification factors range from about 1 to 2 before falling off with higher input spectral accelerations. The lower half of Figure 2.4-4 shows that the logarithmic standard deviations for the site amplification factors range from about 0.05 to 0.20.

#### 2.4.1.3 *Control Point Hazard*

The NRC staff implemented Approach 3 from the SPID to develop a weighted control point seismic hazard curve for each of the six unique combinations of the site response logic tree for the Braidwood site. After combining these curves to develop the final mean control point hazard curves, the NRC staff determined the  $10^{-4}$  and  $10^{-5}$  UHRS in order to calculate the GMRS. Figure 2.4-5 shows the final control point mean seismic hazard curves for the seven spectral frequencies, as well as the NRC staff's UHRS and GMRS and the licensee's NTF R2.1 GMRS (Kaegi, 2014a). As shown in Figure 2.4-5, the NRC staff's GMRS (black curve) is moderately higher than the licensee's GMRS (blue curve) for frequencies above 5 Hz due to differences between the basecase profiles and estimated  $\kappa_0$  values. For comparison, Figure 2.4-5 also shows the NRC staff's reference rock GMRS (brown dotted curve).

**Table 2.4-2 Layer Depths, Shear Wave Velocities ( $V_s$ ), Unit Weights, and Dynamic Properties for Braidwood**

Layer	Depth (ft)	Description	$V_s$ (ft/sec)			$V_s$ Sigma (ln)	BC Unit Weight (pcf)	Dynamic Properties	
			LR (0.3)	BC (0.4)	UR (0.3)			Alt. 1 (0.5)	Alt. 2 (0.5)
1	100	Rock: siltstone, shale, coal	3,325	4,030	4,885	0.25	140	EPRI Rock	L 3.0%
2	137	Rock: limestone	6,188	7,500	9,285	0.15	160	EPRI Rock	L 3.0%
3	224	Rock: shale	4,373	5,300	6,424	0.15	150	EPRI Rock	L 3.0%
4	600	Rock: dolomite	7,178	8,700	9,285	0.15	160	L 0.1%	L 0.1%
5	900	Rock: sandstone	5,775	7,000	8,484	0.15	150	L 0.1%	L 0.1%

LR = lower range; BC = basecase; UR = upper range; ln = natural log; pcf = pounds per cubic foot; L = linear; Alt. = alternative.

For LR, BC, UR, and Alt.: Values in parentheses refer to weights for site response analysis logic tree branches.

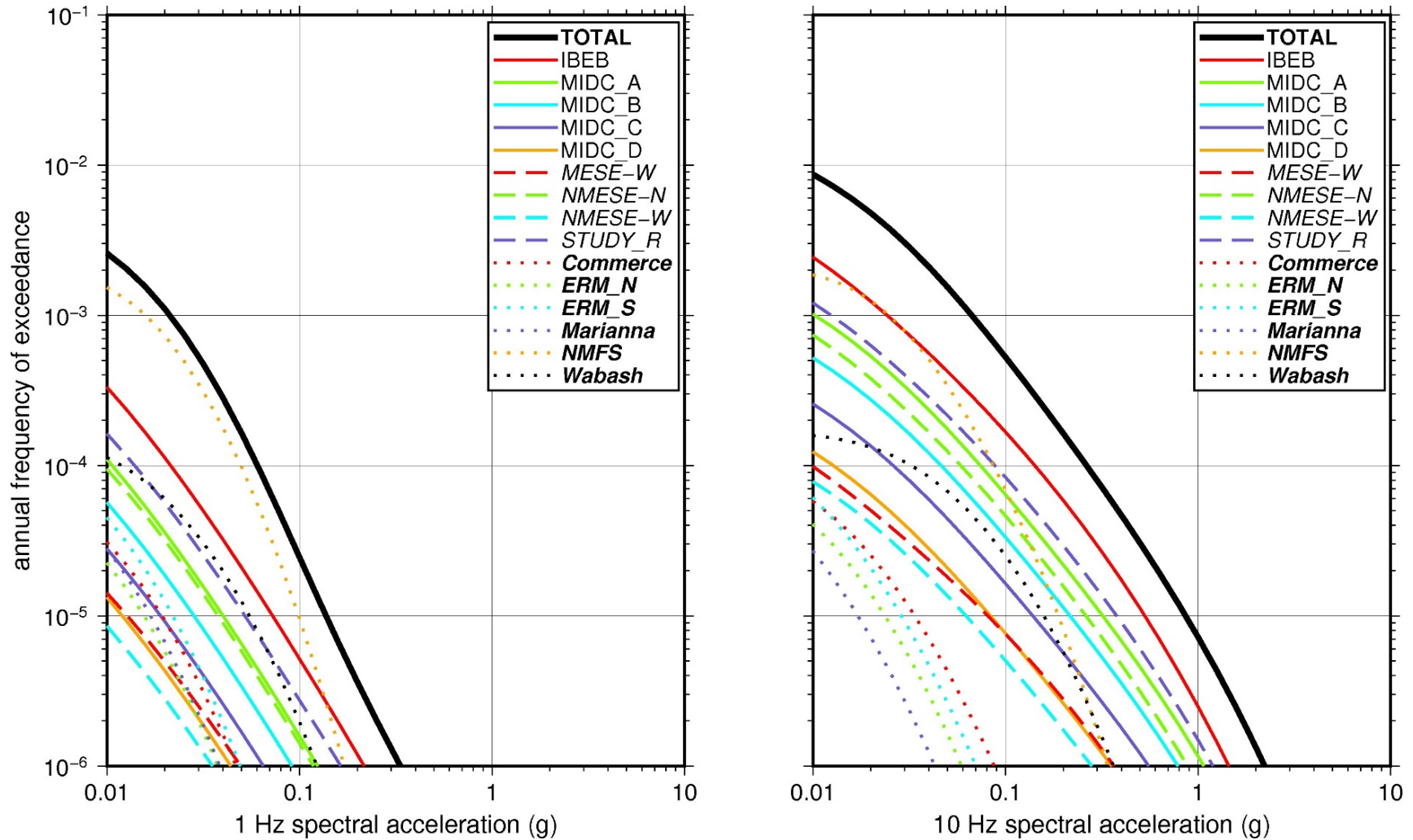


**Figure 2.4-2 Low-Frequency (1 Hz, Left), and High-Frequency (10 Hz, Right) Reference Rock Hazard Curves for Braidwood. Total Hazard is Shown as a Bold Black Line; Individual Contributions to the Hazard for Each of the CEUS-SSC Sources are Shown as Colored Lines Defined in the Legend. See Table 2.1-1 for Source Name Definitions**

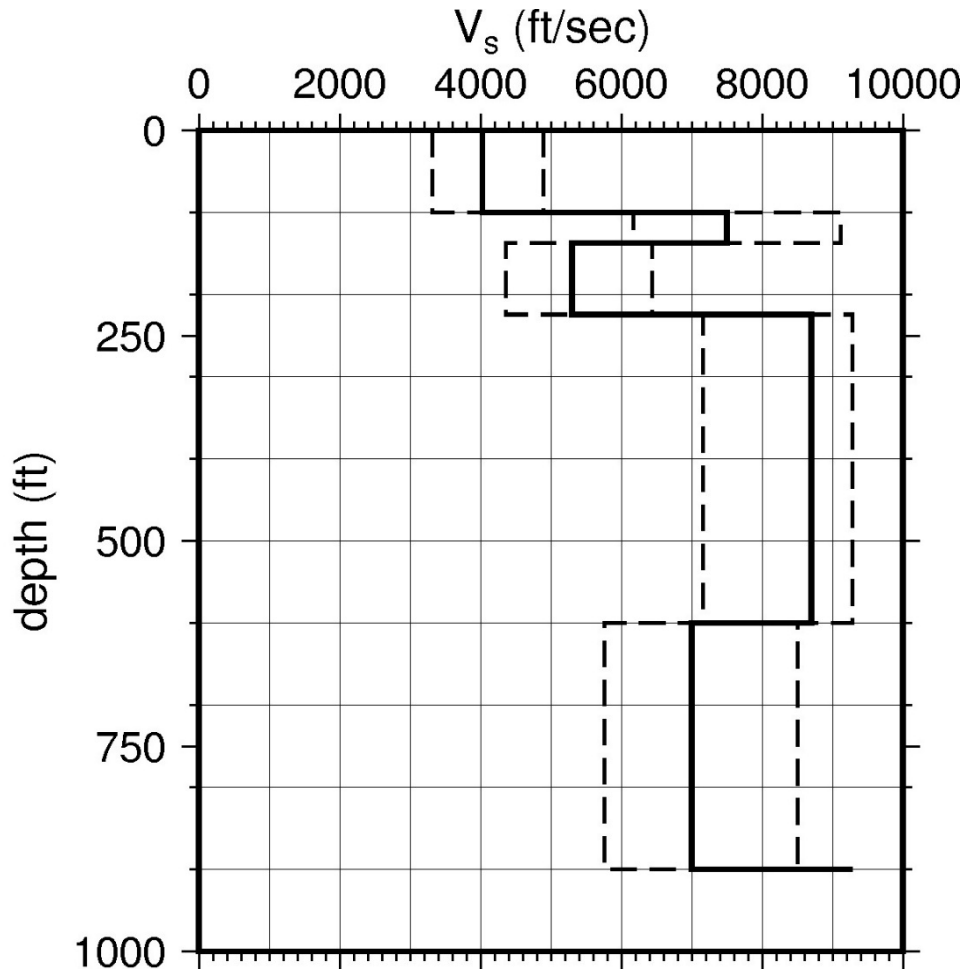


**Figure 2.4-3 Shear Wave Velocity ( $V_s$ ) Profiles for Braidwood. Basecase (BC) Profile Shown as Solid Bold Line; Lower and Upper Range (LR and UR) Profiles Shown as Dashed Lines. Profiles Terminate at Reference Rock Velocity of 2,831 m/sec [9,285 ft/sec] per EPRI GMM (2013)**



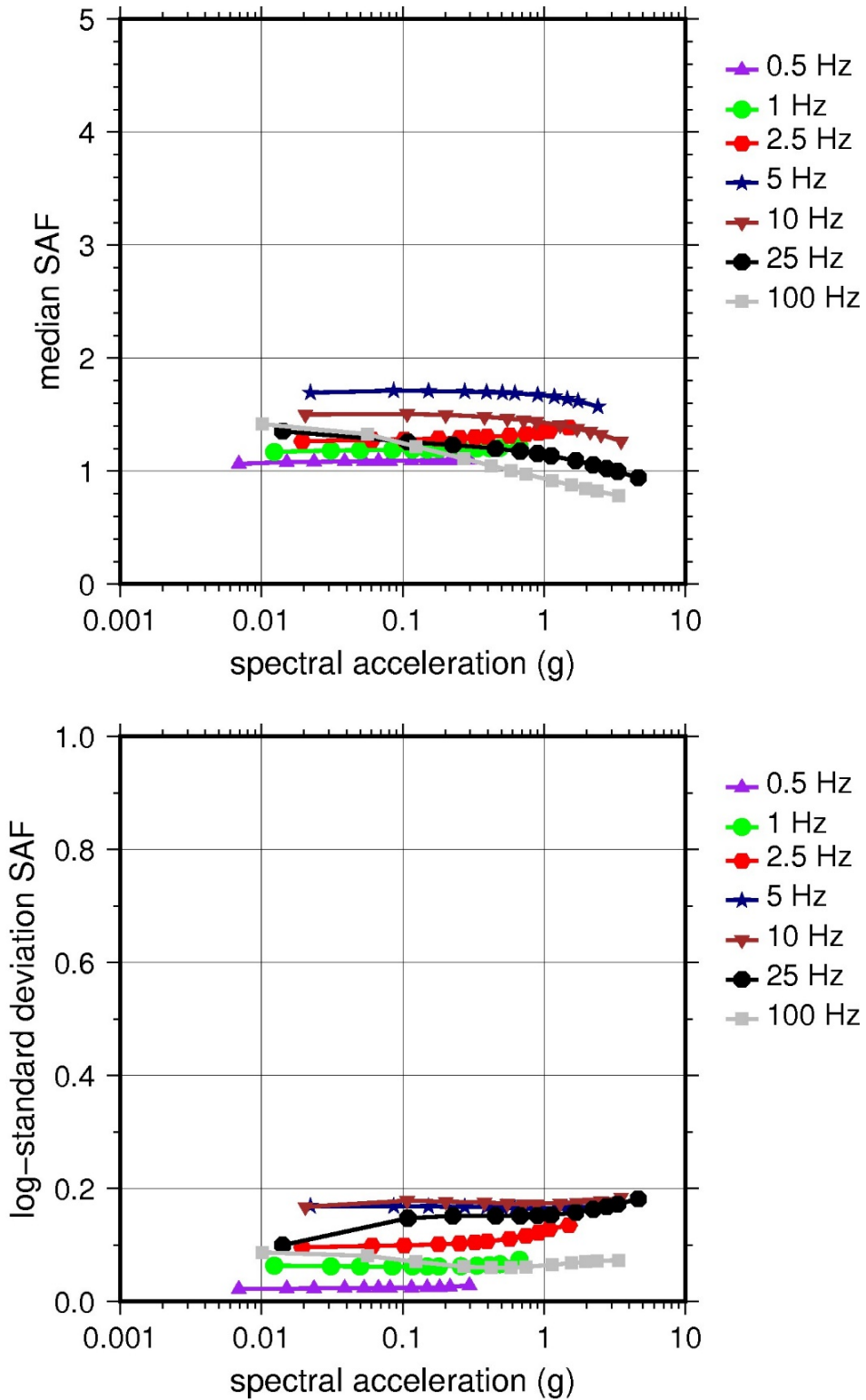


**Figure 2.4-4 Overall Weighted Median Site Amplification Factor (SAF) (Upper) and Log Standard Deviation of the SAF (Lower) as a Function of Input Acceleration for EPRI GMM (2013) Spectral Frequencies**

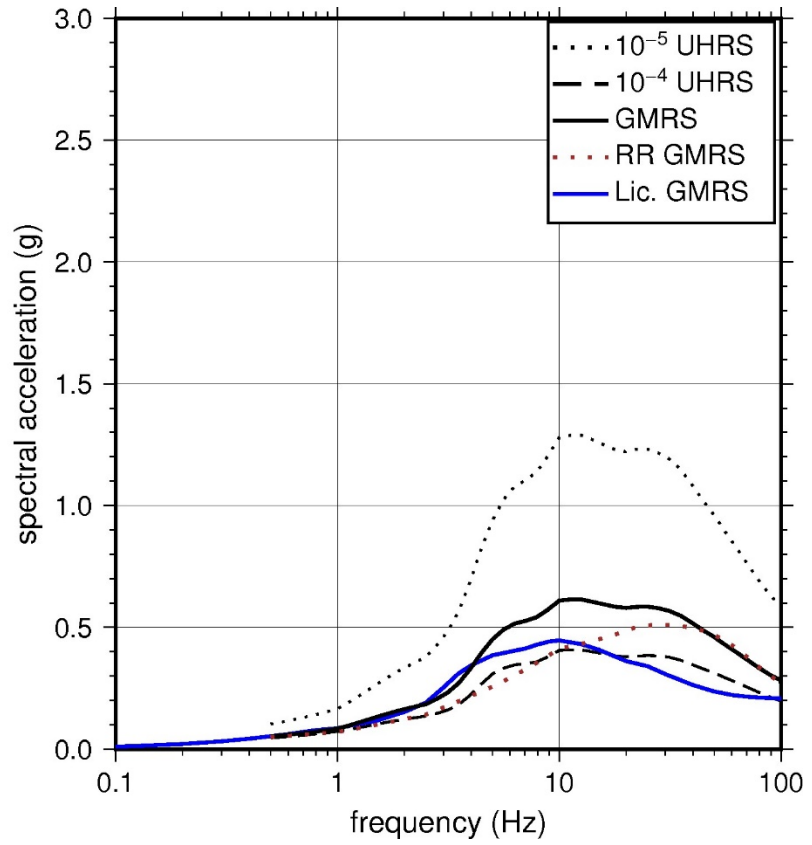
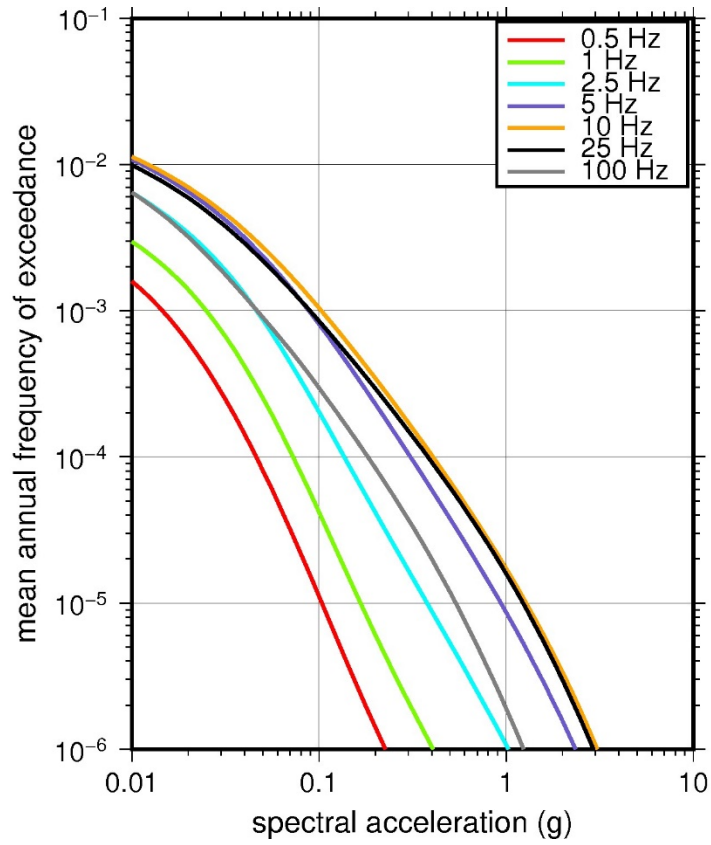


**Figure 2.4-5 Mean Control Point Hazard Curves (Left) for EPRI GMM (2013) Spectral Frequencies, and GMRS and UHRs (Right) for Braidwood**

## 2.4.2 Byron

The Byron Generating Station site is located in north-central Illinois within the Central Lowland physiographic province and consists of 2 m [5 ft] of till overlying about 762 m [2,500 ft] of firm sedimentary rock (dolomite, shale, and sandstone). The horizontal SSE response spectrum for Byron has an RG 1.60 spectral shape and is anchored at a PGA of 0.20g.

### 2.4.2.1 Reference Rock Hazard

For the reference rock PSHA, the NRC staff selected the nine CEUS-SSC (NRC, 2012b) background seismic source zones that are located within 320 km [200 mi] of the site. In addition, the NRC staff selected the six CEUS-SSC (NRC, 2012b) RLME sources that are located within 807 km [500 mi] of the site. To develop the reference rock seismic hazard curves for the Byron site, the NRC staff used the GMPEs developed by the updated EPRI GMM (2013). As shown in Figure 2.4-6, the NMFS RLME is the largest contributor to the 1 Hz reference rock total mean hazard curve at the  $10^{-4}$  AFE level. For the 10 Hz reference rock total mean hazard curve, the MIDC-A seismotectonic source zone and the Study Region  $M_{\max}$  zone are the largest contributors at the  $10^{-4}$  AFE level.

### 2.4.2.2 Site Response Evaluation

#### 2.4.2.2.1 Site Profiles

To develop a basecase profile, the NRC staff used the geologic information in the NTTF R2.1 SHSR (Kaegi, 2014b) submitted by Exelon Generation Company (hereafter referred to as “the licensee” within this plant section). As described in the licensee’s SHSR, the Byron site consists of about 2 m [5 ft] of glacial deposits (loess and till soils) overlying Paleozoic-age sedimentary rock, which lies above Precambrian basement rock. The major plant structures are founded on Ordovician-age sedimentary rock (slightly to moderately weathered dolomite). In Table 2.3.1-1 of the SHSR, the licensee briefly described the subsurface materials in terms of the geologic units and layer thicknesses. For its site response evaluation, the NRC staff used the top of bedrock, which corresponds to an elevation of 265 m [869 ft] above MSL, as the control point elevation for the Byron site.

The licensee’s profile is based on the investigations carried out for Units 1 and 2 as well as a nearby ISFSI. These subsurface investigations included a number of test pits and borings, with the deepest boring extending into the upper portion of the Ordovician-age St. Peter Formation sandstone. The licensee’s geophysical field investigations for Units 1 and 2 primarily measured  $V_P$  to a depth of about 52 m [170 ft] and consisted of seismic refraction and downhole and uphole surveys. To determine the  $V_S$  for each rock layer, the licensee used its measured  $V_P$  with an assumed Poisson’s ratio. Table 2.3.2-1 of the SHSR gives the estimated  $V_S$  determined from the licensee’s site investigations.

The licensee’s profile, which is 915 m [3,000 ft] in total thickness, begins at the top of bedrock, which consists of about 31 m [100 ft] of Ordovician sedimentary rock (primarily dolomite) from the Dunleith and Guttenberg Formations of the Galena Group. The licensee measured average  $V_P$  values of 2,820 m/sec [9,250 ft/sec] for the Dunleith Formation and 3,773 m/sec [12,375 ft/sec] for the Guttenberg Formation. Using these values along with an assumed Poisson’s ratio of 0.41, the licensee estimated  $V_S$  values of 976 m/sec [3,200 ft/sec] and 1,293 m/sec [4,242 ft/sec], respectively, for these two rock layers. Below the Galena Group is the Platteville Group dolomite, which is made up of the Quimbys Mill, Nachusa, Grand Detour,

Mifflin, and Pecatonica Formations. For the Quimbys Mill Formation, the licensee measured an average  $V_P$  of 4,153 m/sec [13,625 ft/sec] and assumed a Poisson's ratio of 0.35 in order to estimate a  $V_S$  of 1,993 m/sec [6,536 ft/sec]. The licensee measured a  $V_P$  value of about 4,726 m/sec [15,500 ft/sec] for the underlying formations (Nachusa and Grand Detour) and assumed a Poisson's ratio of 0.25 for these deeper dolomite layers, which results in a  $V_S$  of about 2,744 m/sec [9,000 ft/sec]. As this  $V_S$  is close to the reference rock  $V_S$  of 2,831 m/sec [9,285 ft/sec], the licensee terminated its basecase and upper profiles at the base of the Quimbys Mill Formation, which is 35 m [114 ft] below the control point elevation. The licensee extended its lower basecase profile to a depth of 915 m [3,000 ft], which it assumed to be the top of Precambrian-age basement rock beneath the Byron site.

To corroborate the licensee's reported  $V_S$  and Poisson's ratios, the NRC staff used data from the extensive field and laboratory geotechnical investigations for the proposed Superconducting Super Collider in northeastern Illinois (Bauer et al., 1991), which directly measured the  $V_S$  for many of the same rock units that underlie the Byron site.

The NRC staff used the licensee's layer thicknesses for its basecase profile but estimated higher  $V_S$  for the upper rock layers based on its selection of lower Poisson's ratio values. For the Dunleith and Guttenberg Formations, the NRC staff assumed a Poisson's ratio of 0.35, which results in estimated  $V_S$  values of 1,421 m/sec [4,660 ft/sec] and 1,900 m/sec [6,233 ft/sec], respectively, for these two rock units. The NRC staff used this lower Poisson's ratio, which is typical for this rock type (e.g., Burger, 1992), based on the licensee's description of the rock as slightly to moderately weathered in the UFSAR (Exelon Generation Company, 2014c). The NRC staff also assumed this lower Poisson's ratio for the underlying Quimbys Mill Formation, which has an RQD value of 70 percent (Exelon Generation Company, 2014c). Based on this Poisson's ratio, the estimated  $V_S$  for the Quimbys Mill Formation is 2,092 m/sec [6,863 ft/sec]. For the deeper Ordovician-age rock layers, the NRC staff used a Poisson's ratio of 0.25, which is consistent with the value assumed by the licensee and results in a  $V_S$  of about 2,744 m/sec [9,000 ft/sec]. For the remaining Ordovician- and Cambrian-age strata, the NRC staff assumed that the  $V_S$  values exceed the reference rock  $V_S$  of 2,831 m/sec [9,285 ft/sec].

To capture the uncertainty in its basecase profile, the NRC staff developed lower and upper range (10<sup>th</sup> and 90<sup>th</sup> percentile) profiles by multiplying the basecase  $V_S$  values by scale factors of 0.83 and 1.21, respectively, which corresponds to an epistemic logarithmic standard deviation of 0.15. The weights for the lower, basecase, and upper profiles are 0.3, 0.4, and 0.3, respectively. Figure 2.4-7 shows the NRC staff's profiles. As shown in Figure 2.4-7, the upper profile terminates at a depth of 31 m [101 ft], and the lower and best-estimate basecase profiles terminate at a depth of 239 m [784 ft].

#### 2.4.2.2.2 *Dynamic Material Properties and Site Kappa*

The NRC staff assumed both linear and nonlinear dynamic behavior for the rock beneath the Byron site. To model the nonlinear behavior of the uppermost rock strata, the NRC staff used the EPRI rock shear modulus reduction and material damping curves. To model the linear behavior, the NRC staff used a constant damping ratio of 3 percent. The staff assumed these two alternative dynamic responses for the upper 30 m [97 ft] of the profile, giving them equal weight. For the underlying 210 m [687 ft] of sedimentary rock, the NRC staff assumed a linear response with a material damping ratio of 0.1 percent to maintain consistency with the  $\kappa_0$  value for the Byron site.

To determine the basecase  $\kappa_0$  for the Byron site, the NRC staff first used the Campbell (2009) Model 1 relationship between  $V_S$  and  $Q_{ef}$  to determine a  $Q_{ef}$  for each layer. Combining these  $Q_{ef}$  values with the thickness and  $V_S$  for each layer results in a total  $\kappa_0$  value of about 7 msec, which includes the 6 msec assumed for the underlying reference rock. For the lower and upper profiles, the NRC staff calculated  $\kappa_0$  values of 8 and 6 msec, respectively, using the same approach as for the basecase profile. In contrast, the licensee used an empirical relationship (EPRI, 2012) between  $\kappa_0$  and the average  $V_S$  over the top 30 m [100 ft] of the profile to estimate basecase, lower, and upper  $\kappa_0$  values of 8, 23, and 8 msec, respectively.

Table 2.4-3 provides the layer depths, lithologies,  $V_S$ , unit weights, and dynamic properties for the NRC staff's three profiles. In summary, the site response logic tree developed by the NRC staff for the Byron site consists of six alternatives; three velocity profiles (each with a different  $\kappa_0$  value) and two alternative dynamic property branches.

#### 2.4.2.2.3 Methodology and Results

The NRC staff followed the methodology described in Section 2.1.4 to develop the final site amplification factors. Figure 2.4-8 shows the overall median site amplification factors and their variability for each of the seven spectral frequencies. As shown in Figure 2.4-8, the median site amplification factors range from about 1 to 2 before falling off with higher input spectral accelerations. The lower half of Figure 2.4-8 shows that the logarithmic standard deviations for the site amplification factors range from about 0.05 to 0.20.

#### 2.4.2.3 Control Point Hazard

The NRC staff implemented Approach 3 from the SPID to develop a weighted control point seismic hazard curve for each of the six unique combinations of the site response logic tree for the Byron site. After combining these curves to develop the final mean control point hazard curves, the NRC staff determined the  $10^{-4}$  and  $10^{-5}$  UHRS in order to calculate the GMRS. Figure 2.4-9 shows the final control point mean seismic hazard curves for the seven spectral frequencies, as well as the NRC staff's UHRS and GMRS and the licensee's NTTF R2.1 GMRS (Kaegi, 2014b). As shown in Figure 2.4-9, the NRC staff's GMRS (black curve) is moderately higher than the licensee's (blue curve) for frequencies above 8 Hz. This is because the licensee used a higher  $\kappa_0$  value for its lower basecase profile and assumed a nonlinear dynamic response for the upper 152 m [500 ft] of the profile, whereas the NRC staff assumed a nonlinear dynamic response only for the upper 30 m [97 ft] of the profile. For comparison, Figure 2.4-9 also shows the NRC staff's reference rock GMRS (brown dotted curve).

**Table 2.4-3 Layer Depths, Shear Wave Velocities ( $V_s$ ), Unit Weights, and Dynamic Properties for Byron**

Layer	Depth (ft)	Description	$V_s$ (ft/sec)			$V_s$ Sigma (ln)	BC Unit Weight (pcf)	Dynamic Properties	
			LR (0.3)	BC (0.4)	UR (0.3)			Alt. 1 (0.5)	Alt. 2 (0.5)
1	97	Rock: dolomite	3,845	4,600	5,648	0.25	140	EPRI Rock	L 3.0%
2	101	Rock: dolomite	5,143	6,233	7,555	0.15	150	L 0.1%	L 0.1%
3	114	Rock: dolomite	5,662	6,863	8,318	0.15	150	L 0.1%	L 0.1%
4	314	Rock: dolomite	7,384	8,950	9,285	0.15	160	L 0.1%	L 0.1%
5	514	Rock: dolomite	7,466	9,050	9,285	0.15	160	L 0.1%	L 0.1%
6	784	Rock: dolomite	7,578	9,185	9,285	0.15	160	L 0.1%	L 0.1%

LR = lower range; BC = basecase; UR = upper range; ln = natural log; pcf = pounds per cubic foot; L = linear; Alt. = alternative.  
 For LR, BC, UR, and Alt.: Values in parentheses refer to weights for site response analysis logic tree branches.

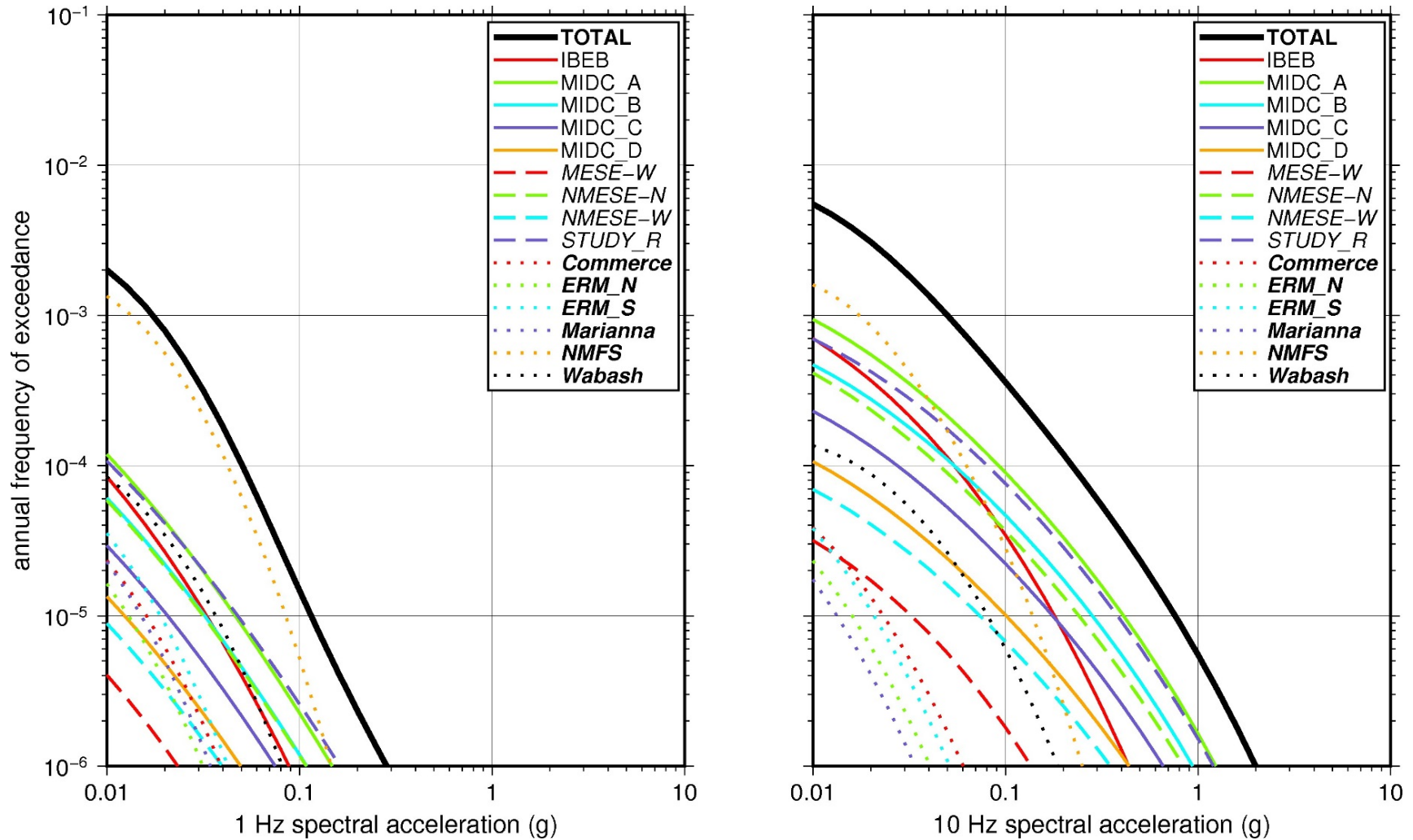


**Figure 2.4-6 Low-Frequency (1 Hz, Left), and High-Frequency (10 Hz, Right) Reference Rock Hazard Curves for Byron. Total Hazard is Shown as a Bold Black Line; Individual Contributions to the Hazard for Each of the CEUS-SSC Sources are Shown as Colored Lines Defined in the Legend. See Table 2.1-1 for Source Name Definitions**

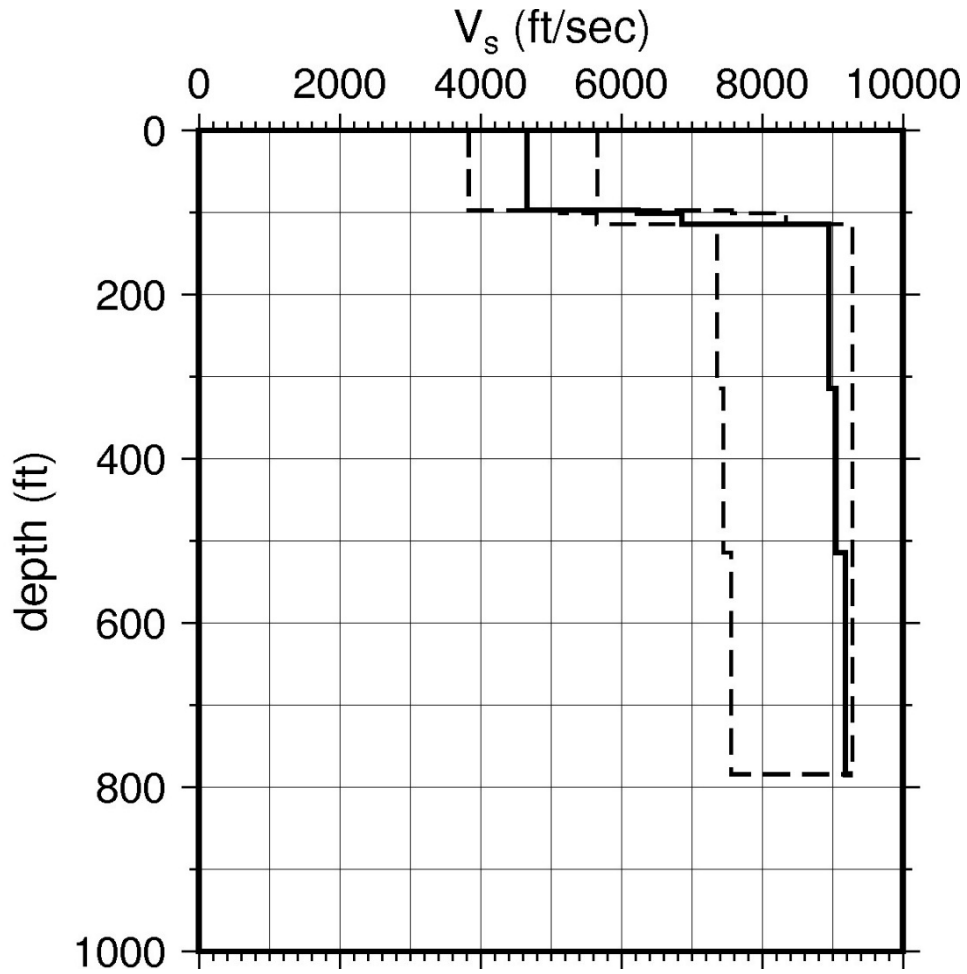


**Figure 2.4-7 Shear Wave Velocity ( $V_s$ ) Profiles for Byron. Basecase (BC) Profile Shown as Solid Bold Line; Lower and Upper Range (LR and UR) Profiles Shown as Dashed Lines. Profiles Terminate at Reference Rock Velocity of 2,831 m/sec [9,285 ft/sec] per EPRI GMM (2013)**



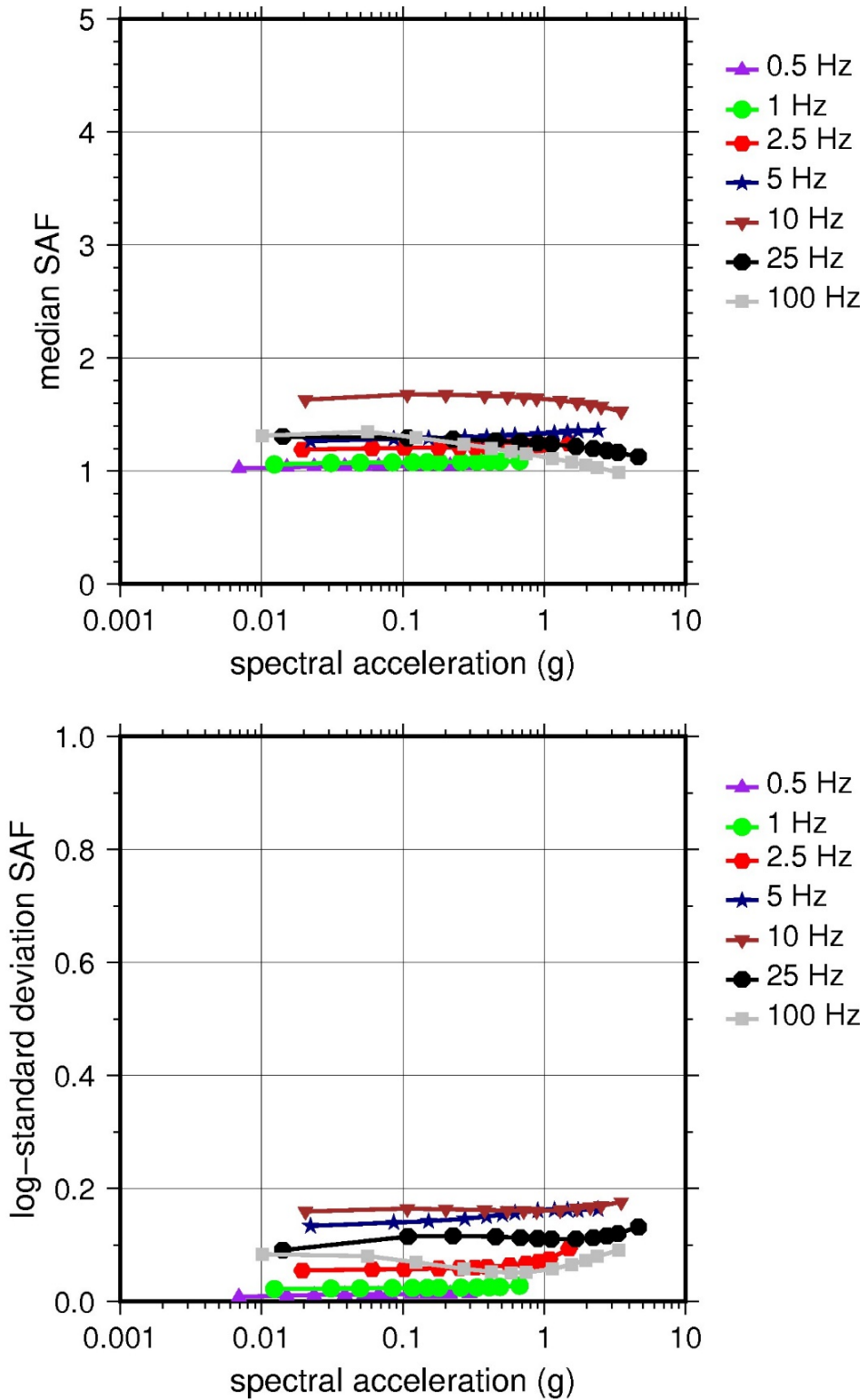


**Figure 2.4-8 Overall Weighted Median Site Amplification Factor (SAF) (Upper) and Log Standard Deviation of the SAF (Lower) as a Function of Input Acceleration for EPRI GMM (2013) Spectral Frequencies**

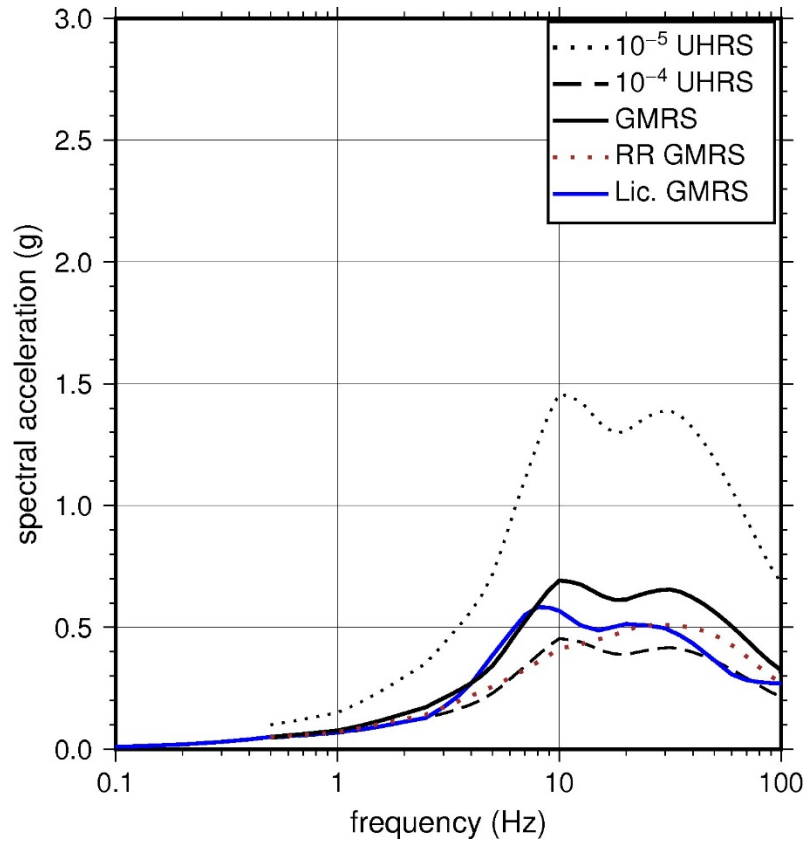
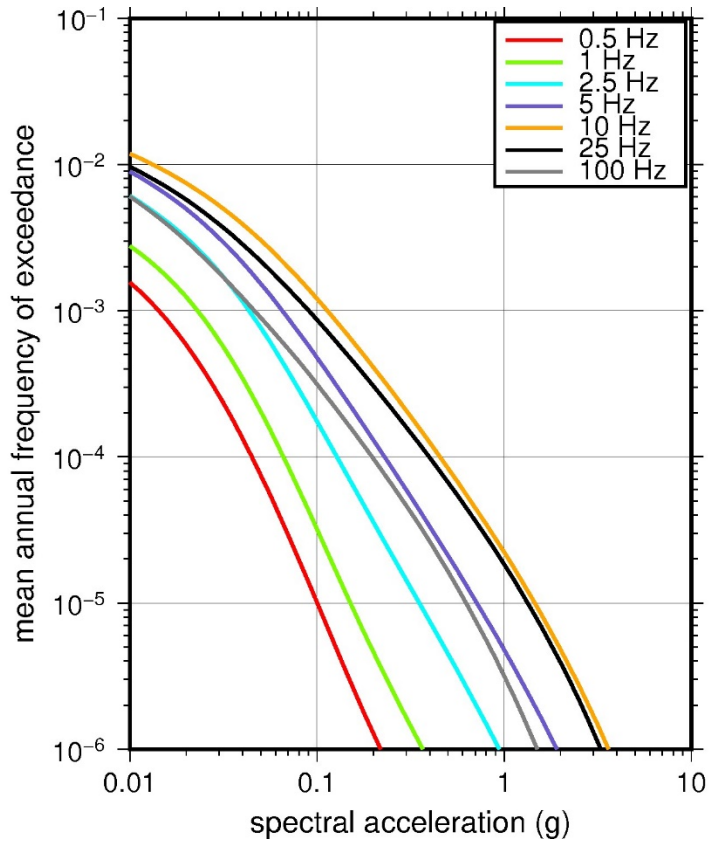


**Figure 2.4-9 Mean Control Point Hazard Curves (Left) for EPRI GMM (2013) Spectral Frequencies, and GMRS and UHRS (Right) for Byron**

### 2.4.3 Clinton

The Clinton Power Station site is located in central Illinois within the Central Lowland physiographic province and consists of 91 m [300 ft] of till overlying about 1,707 m [5,600 ft] of firm sedimentary rock (shale, dolomite, sandstone, and limestone). The horizontal SSE response spectrum for Clinton has an RG 1.60 spectral shape and is anchored at a PGA of 0.26g.

#### 2.4.3.1 Reference Rock Hazard

For the reference rock PSHA, the NRC staff selected the 12 CEUS-SSC (NRC, 2012b) background seismic source zones that are located within 320 km [200 miles] of the site. In addition, the NRC staff selected the six six CEUS-SSC (NRC, 2012b) RLME sources that are located within 807 km [500 mi] of the site. To develop the reference rock seismic hazard curves for the Clinton site, the NRC staff used the GMPEs developed by the updated EPRI GMM (2013). As shown in Figure 2.4-10, the NMFS RLME is the largest contributor to the 1 Hz reference rock total mean hazard curve at the  $10^{-4}$  AFE level. For the 10 Hz reference rock total mean hazard curve, the IBEB seismotectonic zone is the largest contributor at the  $10^{-4}$  AFE level.

#### 2.4.3.2 Site Response Evaluation

##### 2.4.3.2.1 Site Profiles

To develop a basecase profile, the NRC staff used the geologic information in the NTTF R2.1 SHSR (Kaegi, 2014c) submitted by Exelon Generation Company (hereafter referred to as “the licensee” within this plant section). As described in the licensee’s SHSR, the Clinton site consists of about 91 m [300 ft] of Quaternary-age overburden (Wisconsinan, Illinoian, and Pre-Illinoian glacial deposits) overlying Pennsylvanian-age bedrock. The deepest foundations within the powerblock are situated on soils (clayey silt with sand and gravel) from the Illinoian-age Glasford Formation. In Table 2.3.1-1 of the SHSR, the licensee briefly described the subsurface materials in terms of the geologic units and layer thicknesses. For its site response evaluation, the NRC staff used the ground surface, which corresponds to an elevation of 224 m [736 ft] above MSL, as the control point elevation for the Clinton site. Table 2.3.2-1 of the SHSR gives the measured and estimated  $V_S$  determined from the licensee’s site investigations.

The licensee’s profile is based on investigations carried out for Unit 1 (Clinton Power Station, 2013), as well as nearby investigations for an ESP application (Exelon Generation Company, 2006). The licensee’s field investigations for Unit 1, conducted in the early 1970s, consisted of a number of test pits and borings, with the deepest boring of 494 m [1,621 ft] extending into the Silurian-age dolomite. The licensee’s geophysical field investigations for Unit 1 primarily measured  $V_P$  through the till to the top of bedrock at a depth of about 91 m [300 ft] using seismic refraction surveys. To determine the  $V_S$  for each soil layer down to the top of rock, the licensee used the results of the refraction, uphole, and downhole geophysical surveys conducted for Unit 1 and for the ESP. For the  $V_S$  for the rock layers, the ESP applicant used the  $V_P$  profiles from deep borings drilled within about 16,093 m [10 mi] of the site. It assumed Poisson’s ratios of 0.33 for the shallower rock layers {above 579 m [1,900 ft]} and 0.25 for the deeper rock layers. Table 2.3.2-1 of the SHSR gives the estimated  $V_S$  determined from the licensee’s site investigations.

The licensee's profile, which is 1,840 m [6,036 ft] in total thickness, begins within the Wisconsin-age glacial tills of the Wedron Formation, which consist of about 11 m [36 ft] of very stiff clayey sandy silt with lenses of stratified sand, gravel, or silt with a  $V_S$  of about 305 m/sec [1,000 ft/sec]. For the underlying Illinoian-age glacial tills of the weathered Glasford Formation, which are about 6 m [20 ft] thick and consist of clayey silt with discontinuous lenses of silts, sands, or sandy silts, the licensee measured a  $V_S$  of about 427 m/sec [1,400 ft/sec]. Beneath the weathered Glasford Formation is the unaltered Glasford Formation of hard sandy silt overlying a Pre-Illinoian-age lacustrine deposit of clayey silt and finally a layer of silty clay. The total thickness of these soil deposits is about 61 m [200 ft], for which the licensee's measured  $V_S$  is about 640 m/sec [2,100 ft/sec]. The top of bedrock consists of about 104 m [340 ft] of Pennsylvanian-age weathered sedimentary rock (limestone, shale, sandstone, coal, and siltstone) from the Bond and Modesto Formations, with measured  $V_S$  ranging from about 1,220 m/sec [4,000 ft/sec] to 1,433 m/sec [4,700 ft/sec]. Beneath this weathered rock layer is a layer of Mississippian-age limestone that is 168 m [550 ft] thick and contains some siltstone and shale. This layer has a  $V_S$  of about 1,676 m/sec [5,500 ft/sec]. It overlies a layer of Devonian- and Silurian-age shale and limestone 213 m [700 ft] thick with a  $V_S$  of 1,982 m/sec [6,500 ft/sec]. The rest of the profile consists of Ordovician- and Cambrian-age shales, limestones, sandstones, and dolomites, for which the licensee estimated a  $V_S$  of 2,591 m/sec [8,500 ft/sec].

For its basecase profile, the NRC staff used the licensee's layer thicknesses and  $V_S$  values as reported in the NTTF R2.1 report (Kaegi, 2014c) for the upper soil layers. However, for the lower soil layers and the underlying sedimentary rock layers, the NRC staff used the ESP applicant's  $V_S$  profile (Exelon Generation Company, 2006). Based on an evaluation of the  $V_P$  from the regional well logs used for the ESP, the NRC staff terminated its basecase profile at a depth of 686 m [2,250 ft], within the Ordovician-age sedimentary strata. The well log data indicates that the deepest strata within the Cambrian rock may have a slightly lower velocity than the reference  $V_S$  of 2,831 m/sec [9,285 ft/sec]; however, the NRC staff concluded that most of the Ordovician- and Cambrian-age rock is likely to have  $V_S$  values higher than the reference  $V_S$ .

To capture the uncertainty in its basecase profile, the NRC staff developed lower and upper range (10<sup>th</sup> and 90<sup>th</sup> percentile) profiles by multiplying the basecase  $V_S$  values by scale factors of 0.83 and 1.21, respectively, which corresponds to an epistemic logarithmic standard deviation of 0.15. The weights for the lower, basecase, and upper profiles are 0.3, 0.4, and 0.3, respectively. Figure 2.4-11 shows the NRC staff's profiles. As shown in Figure 2.4-11, the upper profile terminates at a depth of about 550 m [1,800 ft] below the control point elevation, and the lower and best-estimate basecase profiles terminate at a depth of 686 m [2,250 ft].

#### 2.4.3.2.2 *Dynamic Material Properties and Site Kappa*

The NRC staff assumed both linear and nonlinear dynamic behavior for the soil and rock beneath the Clinton site. To model the nonlinear behavior of the soil (Layers 1–4), the NRC staff used the EPRI soil and Peninsular Range shear modulus reduction and material damping curves as two equally weighted alternatives. For the 104 m [340 ft] of weathered sedimentary rock (Layers 5–7), the NRC staff used the EPRI rock shear modulus reduction and material damping curves to model the nonlinear dynamic behavior, and it used a constant damping ratio of 3 percent to model the linear dynamic behavior. Again, the staff weighted these two alternatives equally. For the underlying sedimentary rock, the NRC staff assumed a linear dynamic response with a material damping ratio of 0.1 percent to maintain consistency with the  $\kappa_0$  value for the Clinton site.

To determine the basecase  $\kappa_0$  for the Clinton site, the NRC staff first used the Campbell (2009) Model 1 relationship between  $V_S$  and  $Q_{ef}$  to determine a  $Q_{ef}$  for each layer. Combining these  $Q_{ef}$  values with the thickness and  $V_S$  for each layer results in a total  $\kappa_0$  value of about 19 msec, which includes the 6 msec assumed for the underlying reference rock. For the lower and upper profiles, the NRC staff calculated  $\kappa_0$  values of 24 and 15 msec, respectively, using the same approach as for the basecase profile. In contrast, the licensee estimated  $\kappa_0$  by using the lowest low-strain damping value from the material damping curves over the top 152 m [500 ft] of the profile and assumed a constant damping value of 1.25 percent for the remainder to estimate basecase, lower, and upper  $\kappa_0$  values of 31, 40, and 26 msec, respectively.

Table 2.4-4 provides the layer depths, lithologies,  $V_S$ , unit weights, and dynamic properties for the three profiles. In summary, the site response logic tree developed by the NRC staff for the Clinton site consists of six alternatives; three velocity profiles (each with a different  $\kappa_0$  value) and two alternative dynamic property branches.

#### 2.4.3.2.3 Methodology and Results

The NRC staff followed the methodology described in Section 2.1.4 to develop the final site amplification factors. Figure 2.4-12 shows the overall median site amplification factors and their variability for each of the seven spectral frequencies. As shown in Figure 2.4-12, the median site amplification factors for the seven spectral frequencies range from about 1.5 to 3.0 before falling off with higher input spectral accelerations. The lower half of Figure 2.4-12 shows that the logarithmic standard deviations for the site amplification factors range from about 0.05 to 0.20.

#### 2.4.3.3 Control Point Hazard

The NRC staff implemented Approach 3 from the SPID to develop a weighted control point seismic hazard curve for each of the six unique combinations of the site response logic tree for the Clinton site. After combining these curves to develop the final mean control point hazard curves, the NRC staff determined the  $10^{-4}$  and  $10^{-5}$  UHRS in order to calculate the GMRS. Figure 2.4-13 shows the final control point mean seismic hazard curves for the seven spectral frequencies, as well as the NRC staff's UHRS and GMRS and the licensee's NTTF R2.1 GMRS (Kaegi, 2014c). As shown in Figure 2.4-13, the NRC staff's GMRS (black curve) is similar in shape to the licensee's GMRS (blue curve) but is slightly higher over the entire frequency range.

**Table 2.4-4 Layer Depths, Shear Wave Velocities ( $V_s$ ), Unit Weights, and Dynamic Properties for Clinton**

Layer	Depth (ft)	Description	$V_s$ (ft/sec)			$V_s$ Sigm a (ln)	BC Unit Weight (pcf)	Dynamic Properties	
			LR (0.3)	BC (0.4)	UR (0.3)			Alt. 1 (0.5)	Alt. 2 (0.5)
1	36	Soil: clay, sandy silt	825	1,000	1,212	0.25	120	EPRI Soil	Pen.
2	57	Soil: clay silt	1,320	1,600	1,939	0.15	130	EPRI Soil	Pen.
3	290	Soil: sandy silt	1,732	2,100	2,545	0.15	130	EPRI Soil	Pen.
4	308	Soil: clay silt	2,640	3,200	3,879	0.15	130	EPRI Soil	Pen.
5	398	Rock: limestone, shale, sandstone	3,300	4,000	4,848	0.15	140	EPRI Rock	L 3.0%
6	448	Rock: limestone, shale, sandstone	3,548	4,300	5,212	0.15	140	EPRI Rock	L 3.0%
7	648	Rock: limestone, shale, sandstone	3,878	4,700	5,697	0.15	140	EPRI Rock	L 3.0%
8	898	Rock: limestone, shale	4,538	5,500	6,666	0.15	150	L 0.1%	L 0.1%
9	1,198	Rock: limestone, shale	5,115	6,200	7,514	0.15	150	L 0.1%	L 0.1%
10	1,498	Rock: limestone, shale	5,610	6,800	8,242	0.15	150	L 0.1%	L 0.1%
11	1,798	Rock: limestone, shale	5,940	7,200	8,726	0.15	150	L 0.1%	L 0.1%
12	2,250	Rock: dolomite, sandstone, limestone	6,600	8,000	9,285	0.15	160	L 0.1%	L 0.1%

LR = lower range; BC = basecase; UR = upper range; ln = natural log; pcf = pounds per cubic foot; L = linear; Alt. = alternative; Pen. = Peninsular.  
 For LR, BC, UR, and Alt.: Values in parentheses refer to weights for site response analysis logic tree branches.

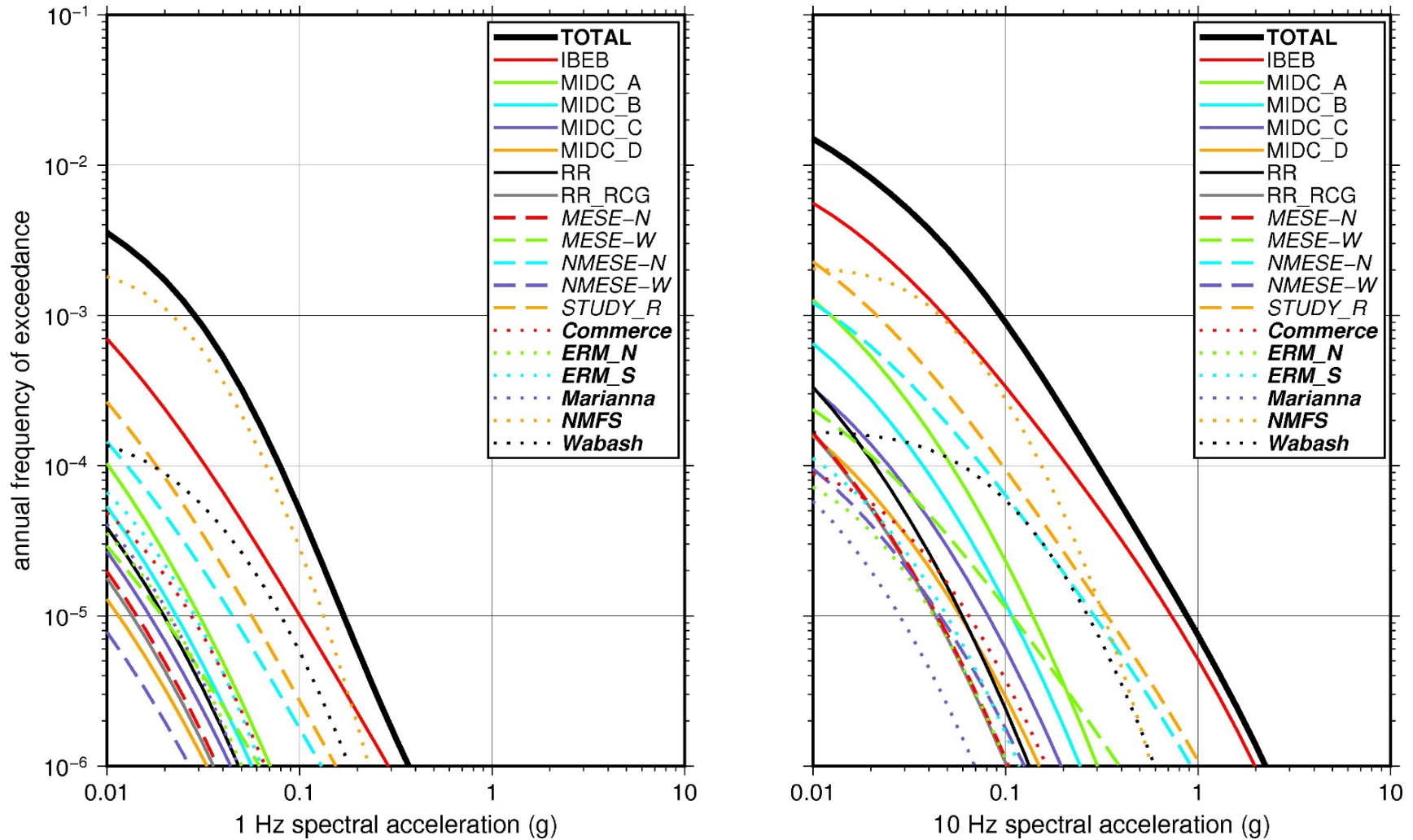


**Figure 2.4-10 Low-Frequency (1 Hz, Left), and High-Frequency (10 Hz, Right) Reference Rock Hazard Curves for Clinton. Total Hazard is Shown as a Bold Black Line; Individual Contributions to the Hazard for Each of the CEUS-SSC Sources are Shown as Colored Lines Defined in the Legend. See Table 2.1-1 for Source Name Definitions**

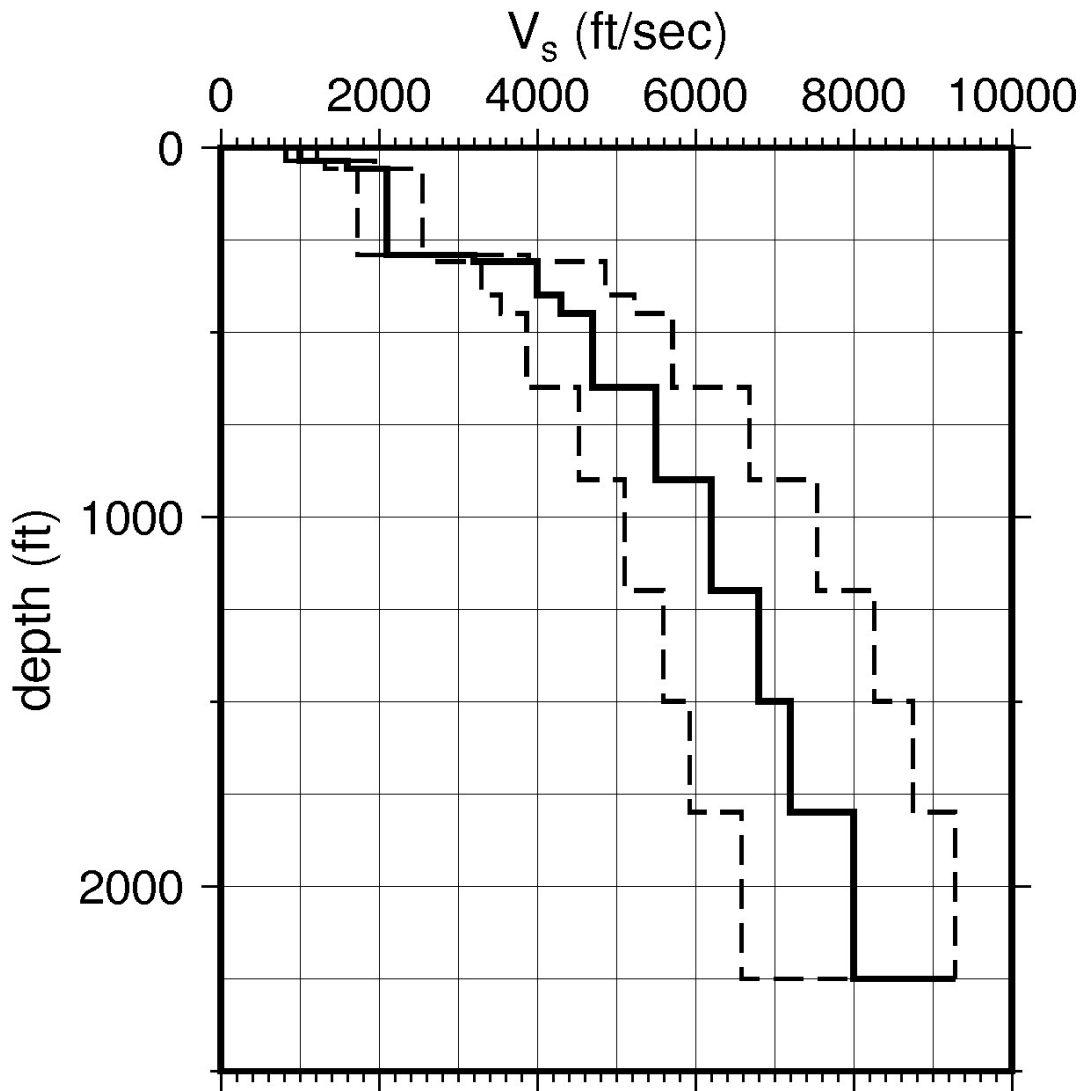


**Figure 2.4-11 Shear Wave Velocity ( $V_s$ ) Profiles for Clinton. Basecase (BC) Profile Shown as Solid Bold Line; Lower and Upper Range (LR and UR) Profiles Shown as Dashed Lines. Profiles Terminate at Reference Rock Velocity of 2,831 m/sec [9,285 ft/sec] per EPRI GMM (2013)**



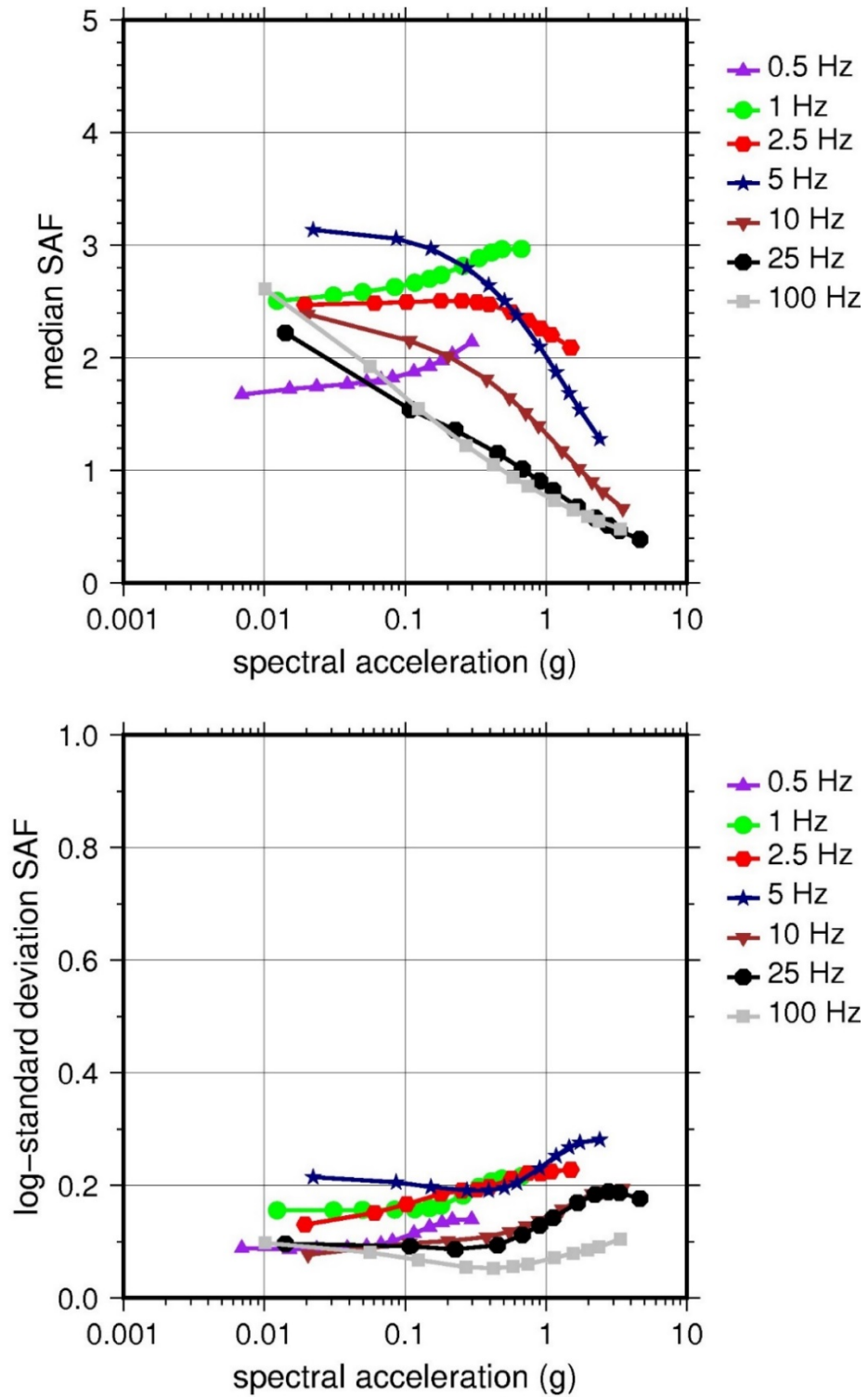


**Figure 2.4-12 Overall Weighted Median Site Amplification Factor (SAF) (Upper) and Log Standard Deviation of the SAF (Lower) as a Function of Input Acceleration for EPRI GMM (2013) Spectral Frequencies**

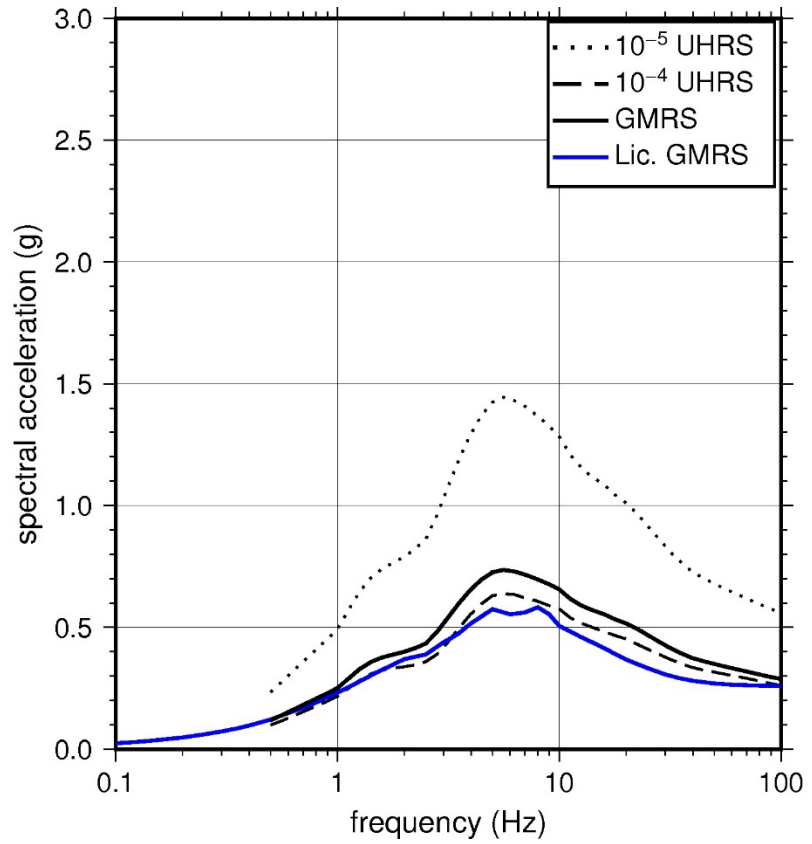
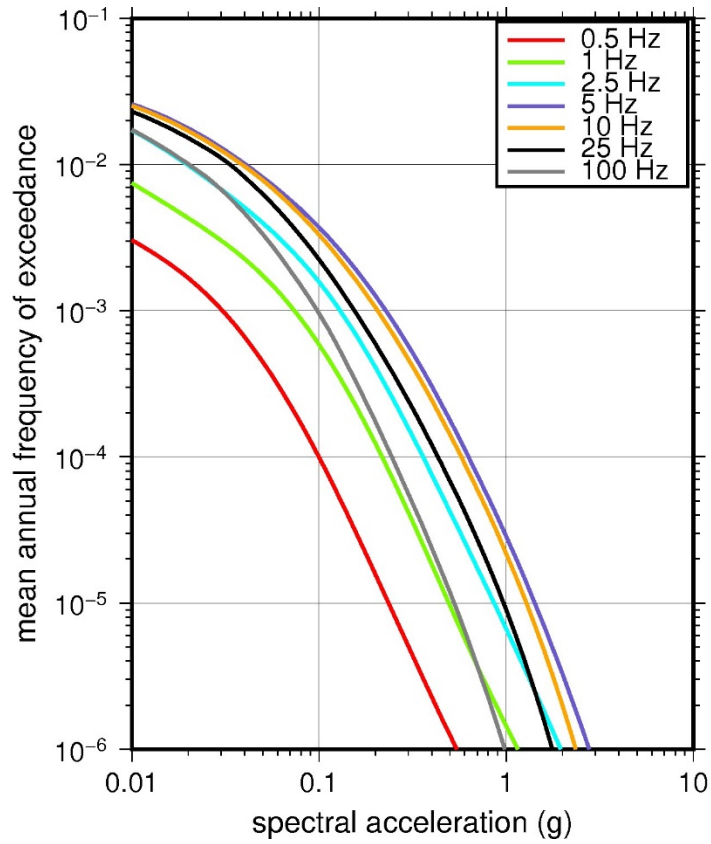


**Figure 2.4-13 Mean Control Point Hazard Curves (Left) for EPRI GMM (2013) Spectral Frequencies, and GMRS and UHRS (Right) for Clinton**

## 2.4.4 Davis Besse

The Davis Besse Nuclear Power Station site is located in northern Ohio along Lake Erie within the Central Lowland physiographic province and consists of 5 m [15 ft] of soil (silty to sandy clay with gravel) overlying about 854 m [2,800 ft] of sedimentary rock (dolomite, shale, limestone, and sandstone). The horizontal SSE response spectrum for Davis Besse has a Newmark spectral shape and is anchored at a PGA of 0.15g.

### 2.4.4.1 Reference Rock Hazard

For the reference rock PSHA, the NRC staff selected the 10 CEUS-SSC (NRC, 2012b) background seismic source zones that are located within 320 km [200 mi] of the site. In addition, the NRC staff selected the five CEUS-SSC (NRC, 2012b) RLME sources that are located within 807 km [500 mi] of the site. To develop the reference rock seismic hazard curves for the Davis Besse site, the NRC staff used the GMPEs developed by the updated EPRI GMM (2013). As shown in Figure 2.4-14, the NMFS RLME is the largest contributor to the 1 Hz reference rock total mean hazard curve at the  $10^{-4}$  AFE level. For the 10 Hz reference rock total mean hazard curve, the MIDC-A seismotectonic source zone is the largest contributor at the  $10^{-4}$  AFE level.

### 2.4.4.2 Site Response Evaluation

#### 2.4.4.2.1 Site Profiles

To develop a basecase profile, the NRC staff used the geologic information in the NTTF R2.1 SHSR (Sena, 2014b) submitted by the First Energy Nuclear Operating Company (hereafter referred to as “the licensee” within this plant section). As described in the licensee’s SHSR, the Davis Besse site consists of about 5 m [15 ft] of glacial tills and glaciolacustrine deposits overlying Silurian-age sedimentary rock (argillaceous dolomite) from the Tymochtee Formation. The major plant structures are founded in the dolomite bedrock. In Table 2-2 of the SHSR, the licensee briefly described the subsurface materials in terms of the geologic units and layer thicknesses. For its site response evaluation, the NRC staff used the reactor building foundation as the control point elevation for the Davis Besse site. This control point is located at the top of rock at an elevation of 165 m [540 ft] above MSL.

The licensee’s profile is based on site investigations carried out for Davis Besse and on geophysical data from nearby deep well logs, which the licensee obtained from the Ohio Geological Survey. The site investigations included numerous borings, crosshole geophysical testing, and a seismic refraction survey that measured the  $V_P$  of the site bedrock. For the deeper rock stratigraphy and velocities, the licensee used the sonic logs from local and regional boreholes. The licensee converted the  $V_P$  profiles from the sonic logs to  $V_S$  using Poisson’s ratios appropriate for the rock type. Table 2-3 of the SHSR gives the measured and estimated  $V_S$  determined from the licensee’s site investigations.

The licensee’s basecase profile, which is 424 m [1,390 ft] in total thickness, consists of several layers of Silurian- to Ordovician-age sedimentary rocks (primarily dolomite, shale, sandstone, and limestone) from the Salina and Lockport Groups; it ends with the Queenston and Kope (formerly Eden) Formations. The  $V_S$  values are about 1,524 m/sec [5,000 ft/sec] for the upper Silurian-age dolomites and increase to about 2,652 m/sec [8,700 ft/sec] for the middle to lower Silurian-age dolomite, shale, and limestone. For the Ordovician-age sedimentary rocks from the Queenston and Kope Formations, the licensee estimated a  $V_S$  of about 1,829 m/sec

[6,000 ft/sec]. Because the  $V_S$  values for the underlying Ordovician-age Trenton Formation limestone are higher than the reference rock  $V_S$  of 2,831 m/sec [9,285 ft/sec] assumed for the EPRI GMM (2013), the licensee terminated its profile at the top of this layer.

Because the licensee's basecase profile is based on numerous onsite and regional geophysical measurements, the NRC staff used the licensee's profile without any alterations.

To capture the uncertainty in its basecase profile, the NRC staff developed lower and upper range (10<sup>th</sup> and 90<sup>th</sup> percentile) profiles by multiplying the basecase  $V_S$  values by scale factors of 0.83 and 1.21, respectively, which corresponds to an epistemic logarithmic standard deviation of 0.15. The weights for the lower, basecase, and upper profiles are 0.3, 0.4, and 0.3, respectively. Figure 2.4-15 shows the NRC staff's profiles, which terminate at a depth of 424 m [1,390 ft] below the control point elevation.

#### 2.4.4.2.2 *Dynamic Material Properties and Site Kappa*

The NRC staff assumed both linear and nonlinear dynamic behavior for the rock beneath the Davis Besse site. To model the nonlinear behavior of the uppermost weathered rock layers (Layers 1–4), the NRC staff used the EPRI rock shear modulus reduction and material damping curves. To model the linear behavior of these rock layers, the NRC staff assumed a constant damping ratio of 3 percent. The staff weighted these two alternatives equally. For the underlying more intact sedimentary rock layers, the NRC staff assumed a linear dynamic response with a damping ratio of 0.1 percent to maintain consistency with the  $\kappa_0$  value for the Davis Besse site.

To determine the basecase  $\kappa_0$  for the Davis Besse site, the NRC staff first used the Campbell (2009) Model 1 relationship between  $V_S$  and  $Q_{ef}$  to determine a  $Q_{ef}$  for each layer. Combining these  $Q_{ef}$  values with the thickness and  $V_S$  for each layer results in a total  $\kappa_0$  value of 9 msec, which includes the 6 msec assumed for the underlying reference rock. For the lower and upper profiles, the NRC staff calculated  $\kappa_0$  values of 11 and 8 msec, respectively, using the same approach as for the basecase profile. In contrast, the licensee estimated  $\kappa_0$  by combining the lowest low-strain damping values from the EPRI rock material damping curves over the upper 152 m [500 ft] of rock and assumed a damping value of 1.25 percent for the remaining underlying rock layers to estimate basecase, lower, and upper  $\kappa_0$  values of 14, 15, and 13 msec, respectively.

Table 2.4-5 provides the layer depths, lithologies,  $V_S$ , unit weights, and dynamic properties for the NRC staff's three profiles. In summary, the site response logic tree developed by the NRC staff for the Davis Besse site consists of six alternatives; three velocity profiles (each with a different  $\kappa_0$  value) and two alternative dynamic property branches.

#### 2.4.4.2.3 *Methodology and Results*

The NRC staff followed the methodology described in Section 2.1.4 to develop the final site amplification factors. Figure 2.4-16 shows the overall median site amplification factors and their variability for each of the seven spectral frequencies. As shown in Figure 2.4-16, the median site amplification factors range from about 1 to 1.5 before falling off with higher input spectral accelerations. The lower half of Figure 2.4-16 shows that the logarithmic standard deviations for the site amplification factors range from about 0.05 to 0.15.

### 2.4.4.3 Control Point Hazard

The NRC staff implemented Approach 3 from the SPID to develop a weighted control point seismic hazard curve for each of the six unique combinations of the site response logic tree for the Davis Besse site. After combining these curves to develop the final mean control point hazard curves, the NRC staff determined the  $10^{-4}$  and  $10^{-5}$  UHRS in order to calculate the GMRS. Figure 2.4-17 shows the final control point mean seismic hazard curves for the seven spectral frequencies, as well as the NRC staff's UHRS and GMRS and the licensee's NTTF R2.1 GMRS (Sena, 2014b). As shown in Figure 2.4-17, the NRC staff's GMRS (black curve) is moderately higher than the licensee's (blue curve) over the higher frequencies ( $>10$  Hz), because of the licensee's higher  $\kappa_0$  values. For comparison, Figure 2.4-17 also shows the NRC staff's reference rock GMRS (brown dotted curve).

**Table 2.4-5 Layer Depths, Shear Wave Velocities ( $V_s$ ), Unit Weights, and Dynamic Properties for Davis Besse**

Layer	Depth (ft)	Description	$V_s$ (ft/sec)			$V_s$ Sigm a (ln)	BC Unit Weight (pcf)	Dynamic Properties	
			LR (0.3)	BC (0.4)	UR (0.3)			Alt. 1 (0.5)	Alt. 2 (0.5)
1	12	Rock: dolomite	4,082	4,948	5,997	0.25	140	EPRI Rock	L 3.0%
2	22	Rock: shale	3,275	3,970	4,812	0.15	140	EPRI Rock	L 3.0%
3	32	Rock: dolomite	4,777	5,790	7,018	0.15	150	EPRI Rock	L 3.0%
4	80	Rock: dolomite	3,359	4,071	4,934	0.15	140	EPRI Rock	L 3.0%
5	170	Rock: dolomite	4,680	5,672	6,875	0.15	150	EPRI Rock	L 3.0%
6	510	Rock: dolomite	7,245	8,782	9,285	0.15	160	L 0.1%	L 0.1%
7	560	Rock: shale	7,312	8,862	9,285	0.15	160	L 0.1%	L 0.1%
8	645	Rock: dolomite, limestone, shale	7,108	8,615	9,285	0.15	160	L 0.1%	L 0.1%
9	1,225	Rock: shale, siltstone	5,374	6,514	7,895	0.15	150	L 0.1%	L 0.1%
10	1,390	Rock: shale, limestone	4,947	5,996	7,267	0.15	150	L 0.1%	L 0.1%

LR = lower range; BC = basecase; UR = upper range; ln = natural log; pcf = pounds per cubic foot; L = linear; Alt. = alternative.  
 For LR, BC, UR, and Alt.: Values in parentheses refer to weights for site response analysis logic tree branches.

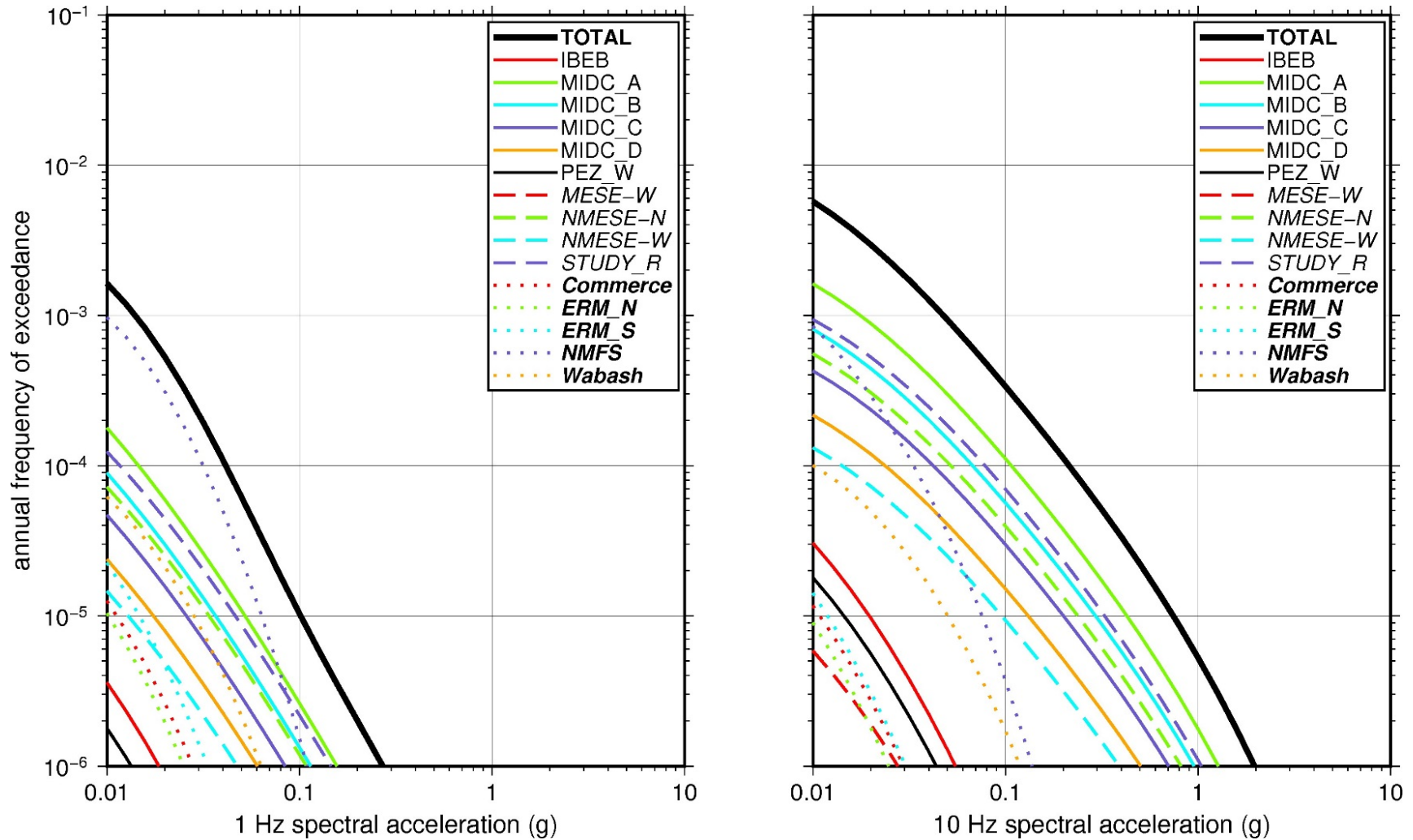


**Figure 2.4-14 Low-Frequency (1 Hz, Left), and High-Frequency (10 Hz, Right) Reference Rock Hazard Curves for Davis Besse. Total Hazard is Shown as a Bold Black Line; Individual Contributions to the Hazard for Each of the CEUS-SSC Sources are Shown as Colored Lines Defined in the Legend. See Table 2.1-1 for Source Name Definitions**

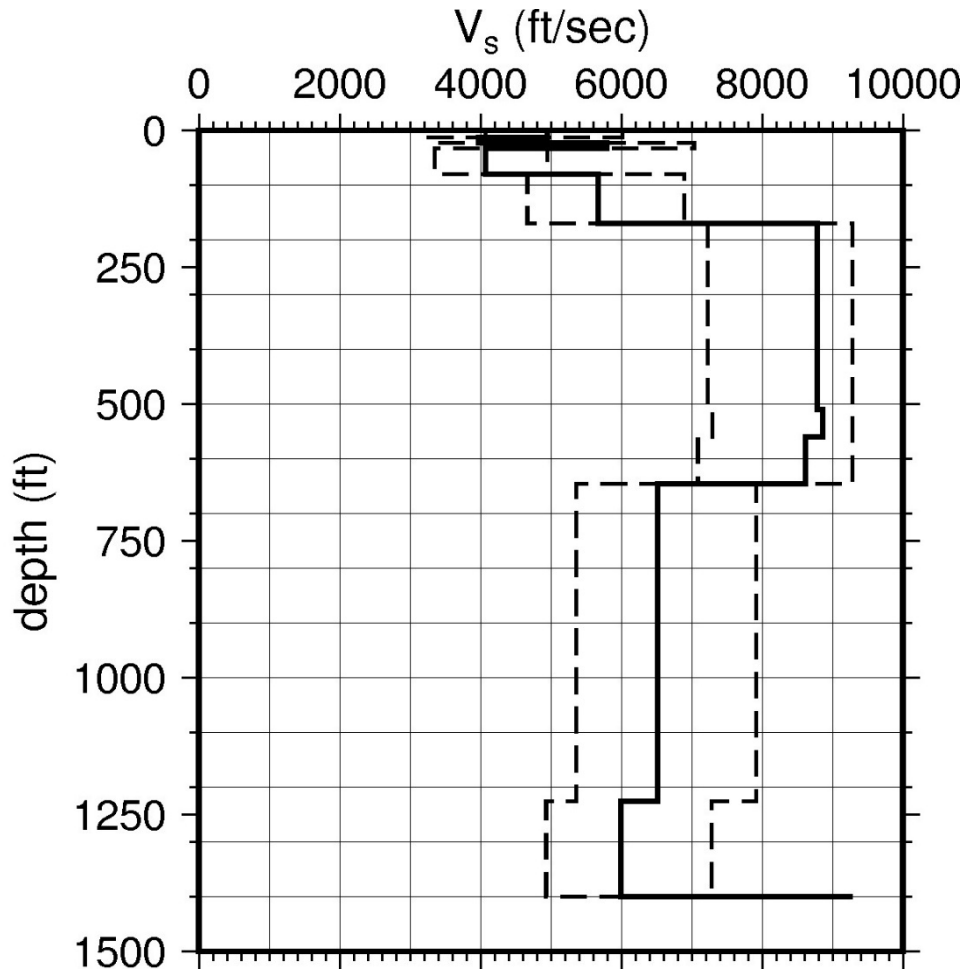


**Figure 2.4-15** Shear Wave Velocity ( $V_s$ ) Profiles for Davis Besse. Basecase (BC) Profile Shown as Solid Bold Line; Lower and Upper Range (LR and UR) Profiles Shown as Dashed Lines. Profiles Terminate at Reference Rock Velocity of 2,831 m/sec [9,285 ft/sec] per EPRI GMM (2013)

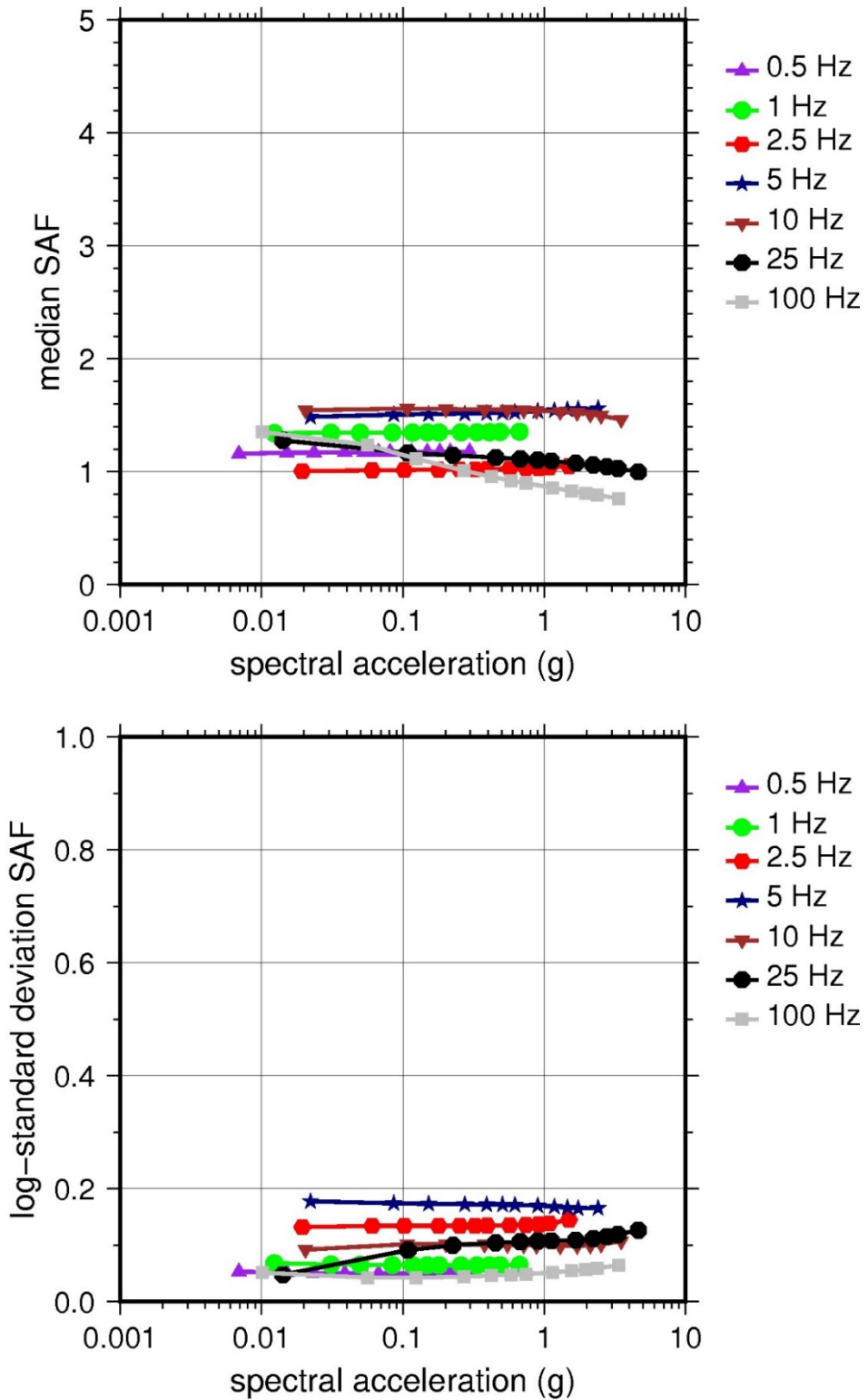


**Figure 2.4-16 Overall Weighted Median Site Amplification Factor (SAF) (Upper) and Log Standard Deviation of the SAF (Lower) as a Function of Input Acceleration for EPRI GMM (2013) Spectral Frequencies**



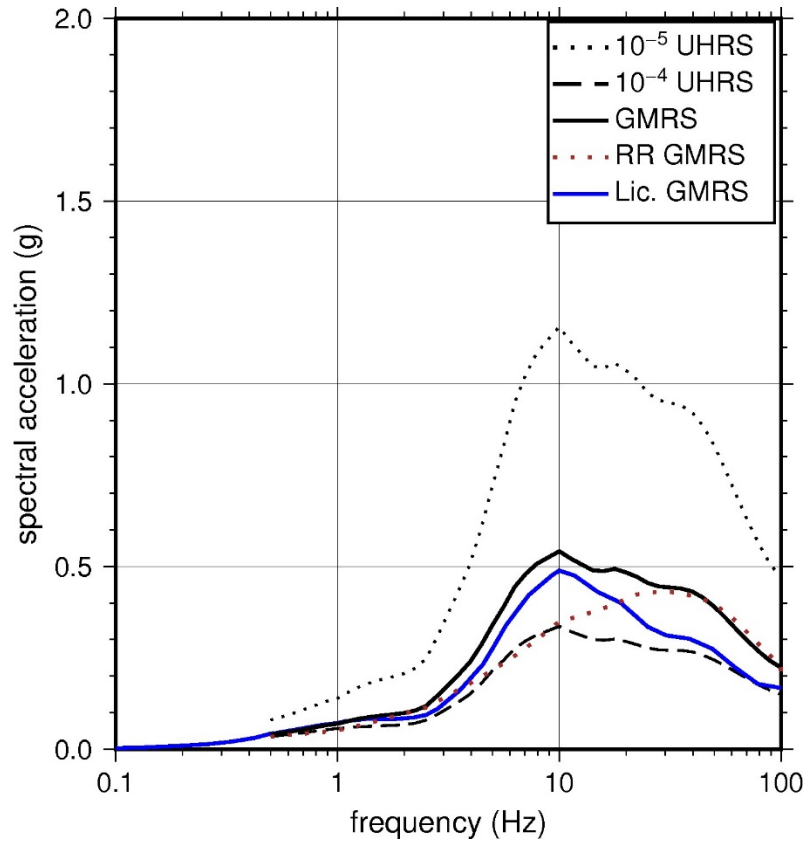
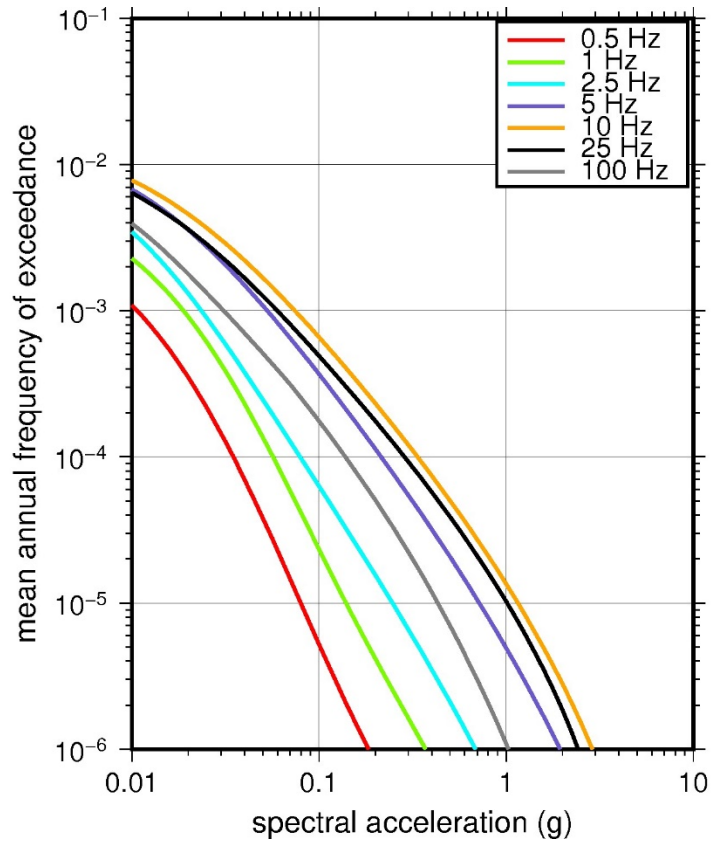


**Figure 2.4-17 Mean Control Point Hazard Curves (Left) for EPRI GMM (2013) Spectral Frequencies, and GMRS and UHRs (Right) for Davis Besse**

## 2.4.5 Donald C. Cook

The Donald C. Cook Nuclear Plant (Cook) site is located in southwestern Michigan on the eastern shore of Lake Michigan within the Central Lowland physiographic province and consists of 52 m [171 ft] of soil (sand and glacial till) overlying about 976 m [3,200 ft] of firm sedimentary rock (shale, dolomite, sandstone, and limestone). The horizontal SSE response spectrum for Cook has a spectral shape that is a smoothed representation of the El Centro north-south recording of the 1940 *M*7.1 earthquake in Imperial Valley, CA. The SSE is anchored at a PGA of 0.20g.

### 2.4.5.1 Reference Rock Hazard

For the reference rock PSHA, the NRC staff selected the nine CEUS-SSC (NRC, 2012b) background seismic source zones that are located within 320 km [200 mi] of the site. In addition, the NRC staff selected the five RLME sources that are located within 807 km [500 mi] of the site. To develop the reference rock seismic hazard curves for the Cook site, the NRC staff used the GMPEs developed by the updated EPRI GMM (2013). As shown in Figure 2.4-18, the NMFS RLME is the largest contributor to the 1 Hz reference rock total mean hazard curve at the  $10^{-4}$  AFE level. For the 10 Hz reference rock total mean hazard curve, the MIDC-A seismotectonic source zone is the largest contributor at the  $10^{-4}$  AFE level.

### 2.4.5.2 Site Response Evaluation

#### 2.4.5.2.1 Site Profiles

To develop a basecase profile, the NRC staff used the geologic information in the NTTF R2.1 SHSR (Lies, 2014) submitted by the Indiana Michigan Power Company (hereafter referred to as “the licensee” within this plant section). As described in the licensee’s SHSR, the Cook site consists of about 52 m [171 ft] of sand and glacial till overlying Devonian-age shale. The plant structures are founded within the dune sands that overlie the lake deposit clays and silts. In Table 2.3.1-1 of the SHSR, the licensee briefly described the subsurface materials in terms of the geologic units and layer thicknesses. For its site response evaluation, the NRC staff used a horizon within the dense dune sand, which corresponds to an elevation of 179 m [587 ft] above MSL, as the control point elevation for the Cook site.

The licensee’s profile is based on site investigations carried out in the mid-1960s, which included numerous borings and a seismic refraction survey that measured  $V_P$  to the top of bedrock, at a depth of about 39 m [127 ft] below the control point elevation. To determine the  $V_S$  for each soil and rock layer, the licensee used its measured  $V_P$  with an estimated Poisson’s ratio appropriate for the soil or rock type. Table 2.3.2-2 of the SHSR gives the estimated  $V_S$  determined from the licensee’s site investigations.

The licensee developed two sets of basecase profiles that differ considerably in total thickness. For the first set, the licensee terminated each profile at a depth of 39 m [127 ft], which corresponds to the top of bedrock. For the second set, the total thickness of each profile is 984 m [3,227 ft]. Both sets of basecase profiles start at the top of the 29-m-thick [94-ft-thick] layer of glacial lake deposits (clays and silts), for which the licensee estimated a  $V_S$  of 488 m/sec [1,600 ft/sec]. However, after interactions with the NRC staff, the licensee updated its profile to include the upper 10 m [33 ft] of dune and beach sand, which it had inadvertently omitted from its first NTTF R2.1 submittal. The licensee estimated a  $V_S$  of 244 m [800 ft/sec] for this uppermost layer of sand. Underlying the sand layer and the glacial lake deposits is a

Devonian-age shale layer with thin interbeds of shaly limestone, for which the licensee estimated a  $V_S$  of 3,049 m/sec [10,000 ft/sec]. This value is based on an estimated  $V_P$  of 5,183 m/sec [17,000 ft/sec] and an assumed Poisson's ratio of 0.23. Rather than use this estimated  $V_S$  to develop a single set of basecase profiles, the licensee developed two equally weighted alternative profile sets as described above. For its first set of profiles, the licensee assumed that the  $V_S$  for the uppermost shale layer and the underlying sedimentary rock layers exceeds the reference rock  $V_S$  of 2,831 m/sec [9,285 ft/sec]. For its second set of profiles, the licensee assumed a constant basecase  $V_S$  of 1,524 m/sec [5,000 ft/sec] for the uppermost shale layer and for the entire sedimentary rock column, which the licensee assumed to have a total thickness of 984 m [3,227 ft].

The NRC staff used the licensee's  $V_S$  values and layer thicknesses for the upper 39 m [127 ft] of soil but developed a different profile for the underlying sedimentary rock layers. To extend the upper portion of its basecase profile to the deeper sedimentary rock layers, the NRC staff used several publications containing detailed stratigraphy (e.g., Lilienthal, 1978; Eils, 1979; Millstein, 1989) and  $V_P$  or  $V_S$  values for specific rock formations (e.g., Liu et al., 2000; Grammer, 2007) within the Michigan Basin. Based on this information, and consistent with the licensee's identification of the bedrock as a Devonian shale, the NRC staff concluded that this rock layer is likely the Ellsworth Formation, with a thickness of about 76 m [250 ft] beneath the site. Underlying the Ellsworth Formation is the Antrim Formation shale layer, with an estimated thickness of about 37 m [120 ft]. The NRC staff estimated a  $V_S$  of 1,829 m/sec [6,000 ft/sec] for the upper 31 m [100 ft] of the Ellsworth Formation, which is likely to be weathered and moderately fractured, and a  $V_S$  of 2,134 m/sec [7,000 ft/sec] for the remaining 46 m [150 ft] of this rock layer. For the underlying Antrim Formation shale, the NRC staff estimated a  $V_S$  of 2,439 m/sec [8,000 ft/sec], based on the laboratory measurements of Liu et al. (2000). For the remaining Devonian-, Silurian-, and Ordovician-age sedimentary rock layers (primarily shale, limestone, and dolomite), the NRC staff assumed that the  $V_S$  exceeds the reference rock  $V_S$  of 2,831 m/sec [9,285 ft/sec]. This assumption is based on  $V_P$  measurements of Silurian and Ordovician limestone specimens within the Michigan Basin (Grammer, 2007), which exceed 6,100 m/sec [20,000 ft/sec].

To capture the uncertainty in its basecase profile, the NRC staff developed lower and upper range (10<sup>th</sup> and 90<sup>th</sup> percentile) profiles by multiplying the basecase  $V_S$  values by scale factors of 0.78 and 1.29, respectively, which corresponds to an epistemic logarithmic standard deviation of 0.20. The weights for the lower, basecase, and upper profiles are 0.3, 0.4, and 0.3, respectively. Figure 2.4-19 shows the NRC staff's profiles. The upper profile terminates at a depth of 115 m [377 ft], while the best-estimate basecase and lower profiles extend to a depth of 152 m [500 ft] below the control point elevation.

#### 2.4.5.2.2 *Dynamic Material Properties and Site Kappa*

The NRC staff assumed both linear and nonlinear dynamic behavior for the soil and rock beneath the Cook site. To model the nonlinear behavior of the soil layers (Layers 1–3), the NRC staff used the EPRI soil and Peninsular Range shear modulus reduction and material damping curves as two equally weighted alternatives. For the uppermost weathered sedimentary rock (Layer 4), the NRC staff used the EPRI rock shear modulus reduction and material damping curves to model the nonlinear dynamic behavior and a constant damping ratio of 3 percent to model the linear dynamic behavior. The staff also weighted these two alternatives equally. For the underlying sedimentary rock, the NRC staff assumed a linear dynamic response with a material damping ratio of 0.1 percent to maintain consistency with the  $\kappa_0$  value for the Cook site.

To determine the basecase  $\kappa_0$  for the Cook site, the NRC staff first used the Campbell (2009) Model 1 relationship between  $V_S$  and  $Q_{ef}$  to determine a  $Q_{ef}$  for each layer. Combining these  $Q_{ef}$  values with the thickness and  $V_S$  for each layer results in a total  $\kappa_0$  value of 13 msec, which includes the 6 msec assumed for the underlying reference rock. For the lower and upper profiles, the NRC staff calculated  $\kappa_0$  values of 16 and 10 msec, respectively, using the same approach as for the basecase profile. In contrast, the licensee estimated  $\kappa_0$  by combining the lowest low-strain damping values from the material damping curves over the top 49 m [160 ft] of soil (Profiles 1, 2, and 3) and 152 m [500 ft] of soil and rock (Profiles 4, 5, and 6). For both profile sets, the licensee assumed a material damping ratio of 1.25 percent for the deeper rock layers. This resulted in two sets of  $\kappa_0$  values ranging from 7 to 34 msec.

Table 2.4-6 provides the layer depths, lithologies,  $V_S$ , unit weights, and dynamic properties for the NRC staff's three profiles. In summary, the site response logic tree developed by the NRC staff for the Cook site consists of six alternatives; three velocity profiles (each with a different  $\kappa_0$  value) and two alternative dynamic property branches.

#### 2.4.5.2.3 Methodology and Results

The NRC staff followed the methodology described in Section 2.1.4 to develop the final site amplification factors. Figure 2.4-20 shows the overall median site amplification factors and their variability for each of the seven spectral frequencies. As shown in Figure 2.4-20, the median site amplification factors range from about 1 to 4 before falling off with higher input spectral accelerations. The lower half of Figure 2.4-20 shows that the logarithmic standard deviations for the site amplification factors range from about 0.05 to 0.30.

#### 2.4.5.3 Control Point Hazard

The NRC staff implemented Approach 3 from the SPID to develop a weighted control point seismic hazard curve for each of the six unique combinations of the site response logic tree for the Cook site. After combining these curves to develop the final mean control point hazard curves, the NRC staff determined the  $10^{-4}$  and  $10^{-5}$  UHRS in order to calculate the GMRS. Figure 2.4-21 shows the final control point mean seismic hazard curves for the seven spectral frequencies, as well as the NRC staff's UHRS and GMRS and the licensee's NTTF R2.1 GMRS<sup>1</sup>. As shown in Figure 2.4-21, the NRC staff's GMRS (black curve) is moderately (about 20 percent) higher than the licensee's (blue curve) over the intermediate frequency range due to differences between the basecase profiles and estimated  $\kappa_0$  values.

---

<sup>1</sup> The licensee provided this revised GMRS to the NRC staff on February 14, 2018.

**Table 2.4-6 Layer Depths, Shear Wave Velocities ( $V_s$ ), Unit Weights, and Dynamic Properties for Cook**

Layer	Depth (ft)	Description	$V_s$ (ft/sec)			$V_s$ Sigma (ln)	BC Unit Weight (pcf)	Dynamic Properties	
			LR (0.3)	BC (0.4)	UR (0.3)			Alt. 1 (0.5)	Alt. 2 (0.5)
1	33	Soil: sand	619	800	1,034	0.25	120	EPRI Soil	Pen.
2	127	Soil: clay, silt	1,238	1,600	2,068	0.15	130	EPRI Soil	Pen.
3	277	Rock: shale	4,643	6,000	7,754	0.15	150	EPRI Rock	L 3.0%
4	377	Rock: shale	5,417	7,000	9,046	0.15	150	L 0.1%	L 0.1%
5	500	Rock: shale	6,191	8,000	9,285	0.15	160	L 0.1%	L 0.1%

LR = lower range; BC = basecase; UR = upper range; ln = natural log; pcf = pounds per cubic foot; L = linear; Alt. = alternative; Pen. = Peninsular  
 For LR, BC, UR, and Alt.: Values in parentheses refer to weights for site response analysis logic tree branches

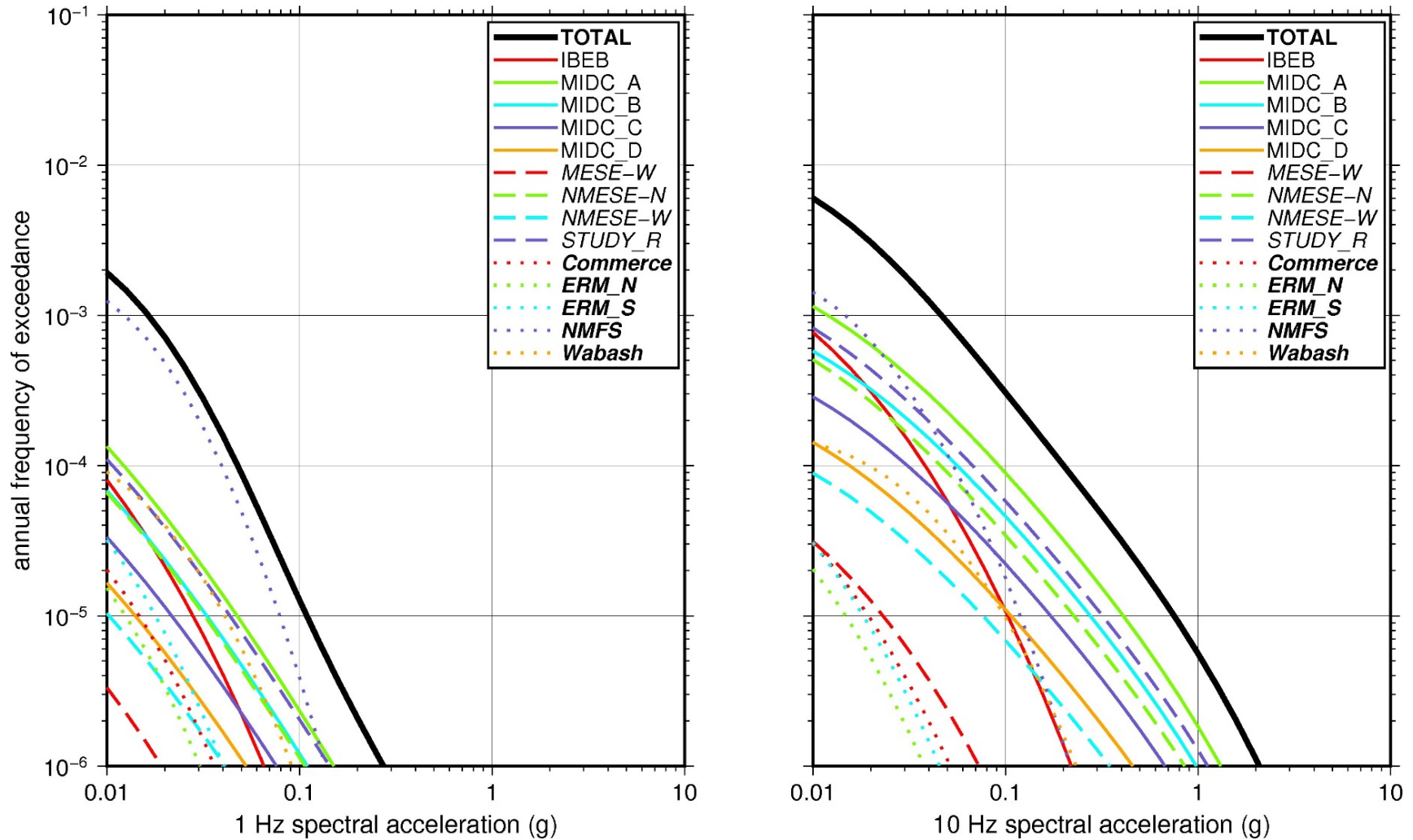


**Figure 2.4-18 Low-Frequency (1 Hz, Left), and High-Frequency (10 Hz, Right) Reference Rock Hazard Curves for Cook. Total Hazard is Shown as a Bold Black Line; Individual Contributions to the Hazard for Each of the CEUS-SSC Sources are Shown as Colored Lines Defined in the Legend. See Table 2.1-1 for Source Name Definitions**

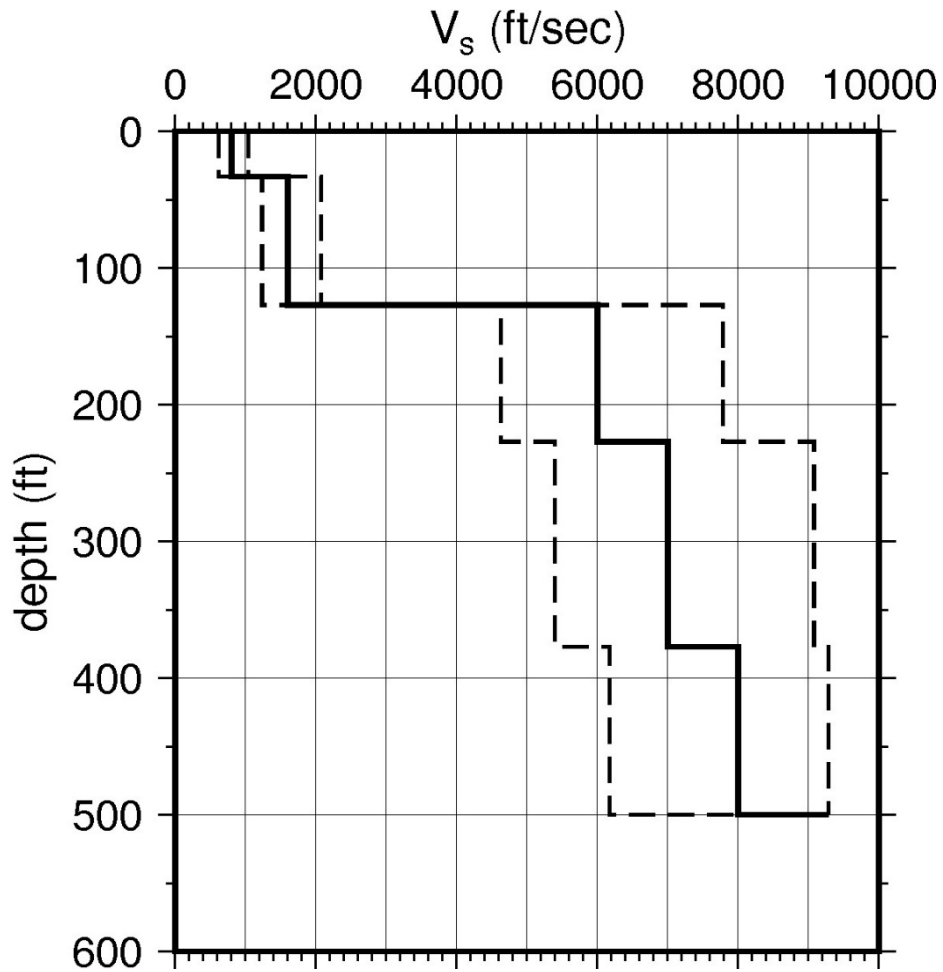


**Figure 2.4-19 Shear Wave Velocity ( $V_s$ ) Profiles for Cook. Basecase (BC) Profile Shown as Solid Bold Line; Lower and Upper Range (LR and UR) Profiles Shown as Dashed Lines. Profiles Terminate at Reference Rock Velocity of 2,831 m/sec [9,285 ft/sec] per EPRI GMM (2013)**

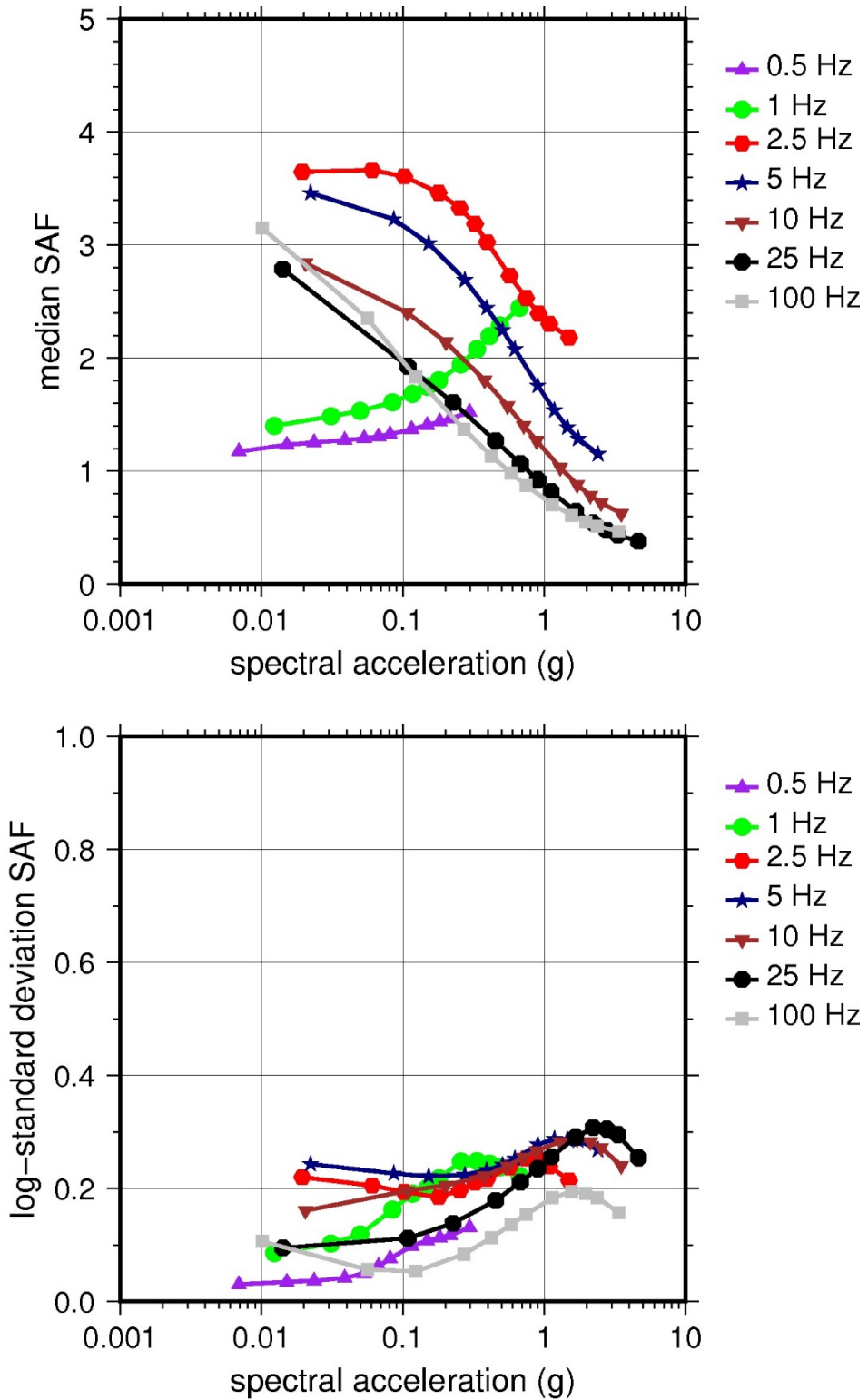


**Figure 2.4-20 Overall Weighted Median Site Amplification Factor (SAF) (Upper) and Log Standard Deviation of the SAF (Lower) as a Function of Input Acceleration for EPRI GMM (2013) Spectral Frequencies**



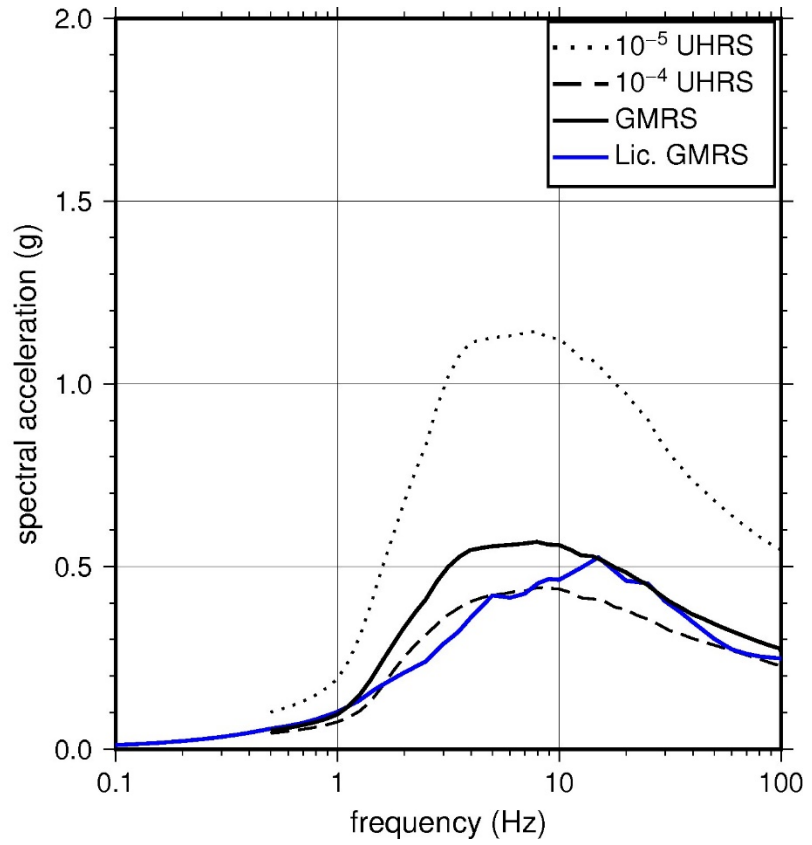
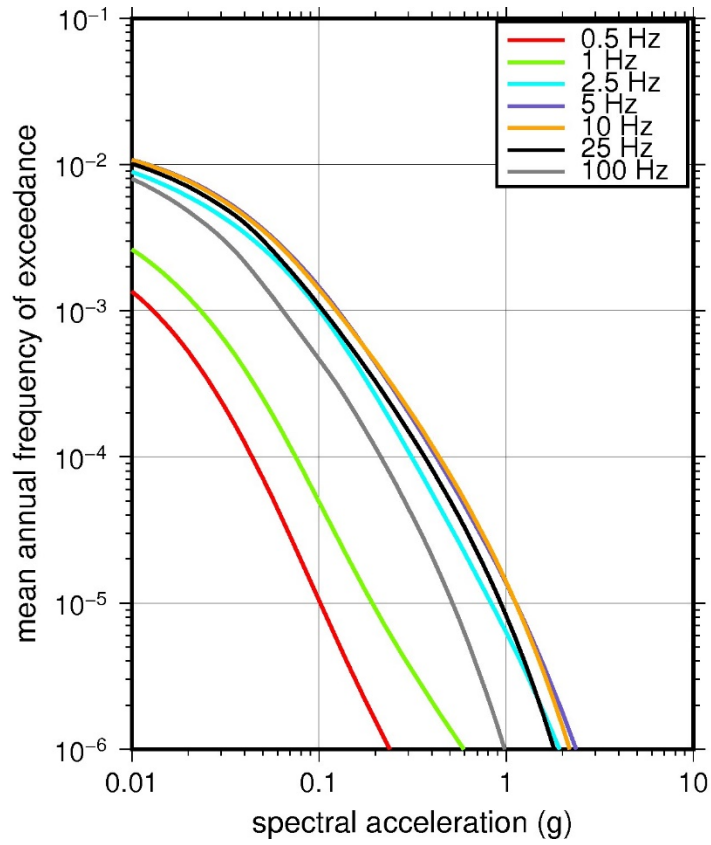


**Figure 2.4-21 Mean Control Point Hazard Curves (Left) for EPRI GMM (2013) Spectral Frequencies, and GMRS and UHRS (Right) for Cook**

## 2.4.6 Dresden

The Dresden Nuclear Power Station site is located in north-central Illinois within the Central Lowland physiographic province and consists of 3 m [10 ft] of soil overlying about 1,524 m [5,000 ft] of firm sedimentary rock (shale, dolomite, sandstone, and limestone). The horizontal SSE response spectrum for Dresden has a rounded Housner spectral shape and is anchored at a PGA of 0.20g.

### 2.4.6.1 Reference Rock Hazard

For the reference rock PSHA, the NRC staff selected the nine CEUS-SSC (NRC, 2012b) background seismic source zones that are located within 320 km [200 mi] of the site. In addition, the NRC staff selected the six CEUS-SSC (NRC, 2012b) RLME sources that are located within 807 km [500 mi] of the site. To develop the reference rock seismic hazard curves for the Dresden site, the NRC staff used the GMPEs developed by the updated EPRI GMM (2013). As shown in Figure 2.4-22, the NMFS RLME is the largest contributor to the 1 Hz reference rock total mean hazard curve at the  $10^{-4}$  AFE level. For the 10 Hz reference rock total mean hazard curve, the IBEB seismotectonic source zone is the largest contributor at the  $10^{-4}$  AFE level.

### 2.4.6.2 Site Response Evaluation

#### 2.4.6.2.1 Site Profiles

To develop a basecase profile, the NRC staff used the geologic information in the NTTF R2.1 SHSR (Kaegi, 2014d) submitted by the Exelon Generation Company (hereafter referred to as “the licensee” within this plant section). As described in the licensee’s SHSR, the Dresden site consists of less than 3 m [10 ft] of glacial drift overlying Pennsylvanian-age sandstone from the Spoon Formation. The deepest foundations within the powerblock are situated on Ordovician-age limestone from the Maquoketa Formation, which generally underlies the Spoon Formation sandstone. In Table 2.3.1-1 of the SHSR, the licensee briefly described the subsurface materials in terms of the geologic units and layer thicknesses. For its site response evaluation, the NRC staff used the top of bedrock, which corresponds to an elevation of 157 m [515 ft] above MSL, as the control point elevation for the Dresden site.

The licensee’s profile is based on investigations carried out for Units 1, 2, and 3 (Exelon Generation Company, 2011), including site borings and laboratory measurements conducted in the mid-1950s of the  $V_P$  for the upper rock layers. More recently, the licensee measured the  $V_P$  of the upper rock layers in order to site an ISFSI in the southwest corner of the site, near the now demolished training building for Unit 1. The licensee’s shallow excavation for the ISFSI pad encountered numerous abandoned underground pipes and cables, which may have affected its measured  $V_P$  values. To determine the  $V_S$  for each rock layer, the licensee used its measured  $V_P$  with an assumed Poisson’s ratio appropriate for the rock type. Table 2.3.2-1 of the SHSR gives the estimated  $V_S$  determined from the licensee’s site investigations.

The licensee developed two sets of basecase profiles that differ considerably in total thickness. For the first set, the licensee terminated each profile at a depth of 305 m [1,000 ft]; for the second set, the total thickness of each profile is 1,528 m [5,000 ft]. Both sets of profiles begin with a layer of about 12 m [40 ft] of Pennsylvanian-age weathered sedimentary rock (primarily sandstone) from the Spoon Formation, which is part of the Kewanee Group. Based on the ISFSI geophysical survey, the  $V_P$  of this rock layer ranges from 823 m/sec [2,700 ft/sec] to

1,524 m/sec [5,000 ft/sec]. The licensee assumed a  $V_P$  of 1,372 m/sec [4,500 ft/sec] and a Poisson's ratio of 0.25 to estimate a  $V_S$  of 793 m/sec [2,600 ft/sec] for this layer. Below the Pennsylvanian bedrock is upper Ordovician-age sedimentary rock (limestone and shale) from the Maquoketa Group (Fort Atkinson and Scales Formations). For the Fort Atkinson limestone, which is about 20 ft [6 m] thick, the licensee measured an average  $V_P$  of 4,268 m/sec [14,000 ft/sec] and used a Poisson's ratio of 0.20 to estimate a  $V_S$  of 2,622 m/sec [8,600 ft/sec]. For the underlying Scales Formation shale, which is about 26.5 m [70 ft] thick, the licensee measured an average  $V_P$  of 2,378 m/sec [7,800 ft/sec] and assumed a Poisson's ratio of 0.28 to estimate a  $V_S$  of 1,311 m/sec [4,300 ft/sec]. Beneath the Maquoketa Group, at a depth of 40 m [130 ft] below the control point elevation, is Ordovician-age Galena-Trenton Group sedimentary rock from the Wise Lake, Dunleith, and Guttenberg Formations. These rock units are primarily dolomites for which the licensee estimated a  $V_S$  of 1,311 m/sec [4,700 ft/sec] based on a  $V_P$  of 2,591 m/s [8,500 ft/sec] and an assumed Poisson's ratio of 0.28. Starting at a depth of 110 m [360 ft] below the control point elevation, the licensee used a velocity gradient of 0.5 m/sec/m [0.5 ft/sec/ft] for the rest of its two basecase profiles.

To corroborate the licensee's reported  $V_S$  and Poisson's ratios, the NRC staff used data from the nearby Braidwood NPP, located 16 km [10 mi] south of Dresden, and from the extensive field and laboratory geotechnical investigations for the proposed Superconducting Super Collider in northeastern Illinois (Bauer et al., 1991). For the deeper sedimentary rock layers within the Illinois Basin, the NRC staff used the velocity model developed by Kaven et al. (2015) for the Decatur, IL, carbon capture and storage site.

The NRC staff used the licensee's layer thicknesses and  $V_S$  for the upper 39.6 m [130 ft] of its basecase profile but used a higher  $V_S$  of 2,652 m/sec [8,700 ft/sec] for the 70.1-m-thick [230-ft-thick] layer of dolomite from the Ordovician Galena-Trenton Group (Layer 4). This decision was based on a comparison of the Dresden profile with the profiles of the nearby Braidwood site and other Region III sites (e.g., LaSalle and Byron). For further confirmation, the NRC staff compared the  $V_S$  value for this rock formation with the values reported in Bauer et al. (1991) for the Superconducting Super Collider site and in Kaven et al. (2015) for the Decatur, IL, carbon capture and storage site. Finally, for the lower Ordovician-age St. Peter Formation sandstone layer, the NRC staff estimated a  $V_S$  of about 2,134 m/sec [7,000 ft/sec] and a thickness of about 92 m [300 ft]. These estimates were based on the stratigraphy developed by the Illinois State Geological Survey for the northeastern portion of the Illinois Basin and the  $V_P$  values from Kaven et al. (2015), together with an assumed Poisson's ratio of 0.30. For the remaining Ordovician- and Cambrian-age strata, the NRC staff assumed that the  $V_S$  values exceed the reference rock  $V_S$  of 2,831 m/sec [9,285 ft/sec].

To capture the uncertainty in its basecase profile, the NRC staff developed lower and upper range (10<sup>th</sup> and 90<sup>th</sup> percentile) profiles by multiplying the basecase  $V_S$  values by scale factors of 0.83 and 1.21, respectively, which corresponds to an epistemic logarithmic standard deviation of 0.15. The weights for the lower, basecase, and upper profiles are 0.3, 0.4, and 0.3, respectively. Figure 2.4-23 shows the NRC staff's profiles, which extend to a depth of 253 m [830 ft] below the control point elevation.

#### 2.4.6.2.2 *Dynamic Material Properties and Site Kappa*

The NRC staff assumed both linear and nonlinear dynamic behavior for the rock beneath the Dresden site. To model the nonlinear behavior of the uppermost rock strata, the NRC staff used the EPRI rock shear modulus reduction and material damping curves. To model the linear behavior, the NRC staff used a constant damping ratio of 3 percent. The staff assumed these

two alternative dynamic responses for the upper 40 m [130 ft] of the profile (Layers 1–3), giving them equal weight. For the underlying 213 m [700 ft] of sedimentary rock, the NRC staff assumed a linear response with a material damping ratio of 0.1 percent to maintain consistency with the  $\kappa_0$  value for the Dresden site.

To determine the basecase  $\kappa_0$  for the Dresden site, the NRC staff first used the Campbell (2009) Model 1 relationship between  $V_S$  and  $Q_{ef}$  to determine a  $Q_{ef}$  for each layer. Combining these  $Q_{ef}$  values with the thickness and  $V_S$  for each layer results in a total  $\kappa_0$  value of 8 msec, which includes the 6 msec assumed for the underlying reference rock. For the lower and upper profiles, the NRC staff calculated  $\kappa_0$  values of 9 and 7 msec, respectively, using the same approach as for the basecase profile. In contrast, the licensee estimated  $\kappa_0$  by combining the lowest low-strain damping value from the material damping curves over the top 500 ft of the profile with an assumed constant damping ratio of 1.25 percent for the rest of the profile to estimate  $\kappa_0$  values of 16, 27, and 9 msec for the basecase, lower, and upper profiles (P1–P3), respectively. For its second set of profiles, the licensee used the relationship between  $\kappa_0$  and  $V_{S100}$  {average shear wave velocity over the upper 30 m [100 ft]} from the SPID (EPRI, 2012) to determine  $\kappa_0$  values of 21, 35, and 12 msec for the basecase, lower, and upper profiles (P4–P6), respectively.

Table 2.4-7 provides the layer depths, lithologies,  $V_S$ , unit weights, and dynamic properties for the NRC staff's three profiles. In summary, the site response logic tree developed by the NRC staff for the Dresden site consists of six alternatives; three velocity profiles (each with a different  $\kappa_0$ ) and two alternative dynamic property branches.

#### 2.4.6.2.3 Methodology and Results

The NRC staff followed the methodology described in Section 2.1.4 to develop the final site amplification factors. Figure 2.4-24 shows the median site amplification factors and their variability for each of the seven spectral frequencies. As shown in Figure 2.4-24, the median site amplification factors range from about 1 to 2 before falling off with higher input spectral accelerations. The lower half of Figure 2.4-24 shows that the logarithmic standard deviations for the site amplification factors range from about 0.05 to 0.20.

#### 2.4.6.3 Control Point Hazard

The NRC staff implemented Approach 3 from the SPID to develop a weighted control point seismic hazard curve for each of the six unique combinations of the site response logic tree for the Dresden site. After combining these curves to develop the final mean control point hazard curves, the NRC staff determined the  $10^{-4}$  and  $10^{-5}$  UHRS in order to calculate the GMRS. Figure 2.4-25 shows the final control point mean seismic hazard curves for the seven spectral frequencies, as well as the NRC staff's UHRS and GMRS and the licensee's NTTF R2.1 GMRS (Kaegi, 2014d). As shown in Figure 2.4-25, the NRC staff's GMRS (black curve) is moderately higher than the licensee's GMRS (blue curve) for frequencies above 3 Hz due to the differences in profiles, treatment of dynamic properties, and  $\kappa_0$  values. For comparison, Figure 2.4-25 also shows the NRC staff's reference rock GMRS (brown dotted curve).

**Table 2.4-7 Layer Depths, Shear Wave Velocities ( $V_s$ ), Unit Weights, and Dynamic Properties for Dresden**

Layer	Depth (ft)	Description	$V_s$ (ft/sec)			$V_s$ Sigma (ln)	BC Unit Weight (pcf)	Dynamic Properties	
			LR (0.3)	BC (0.4)	UR (0.3)			Alt. 1 (0.5)	Alt. 2 (0.5)
1	40	Rock: sandstone	2,145	2,600	3,151	0.25	130	EPRI Rock	L 3.0%
2	60	Rock: limestone, shale	7,145	8,600	9,285	0.15	160	EPRI Rock	L 3.0%
3	130	Rock: shale	3,547	4,300	5,212	0.15	140	EPRI Rock	L 3.0%
4	530	Rock: dolomite	7,178	8,700	9,285	0.15	160	L 0.1%	L 0.1%
5	830	Rock: sandstone	5,775	7,000	8,484	0.15	150	L 0.1%	L 0.1%

LR = lower range; BC = basecase; UR = upper range; ln = natural log; pcf = pounds per cubic foot; L = linear; Alt. = alternative  
 For LR, BC, UR, and Alt.: Values in parentheses refer to weights for site response analysis logic tree branches

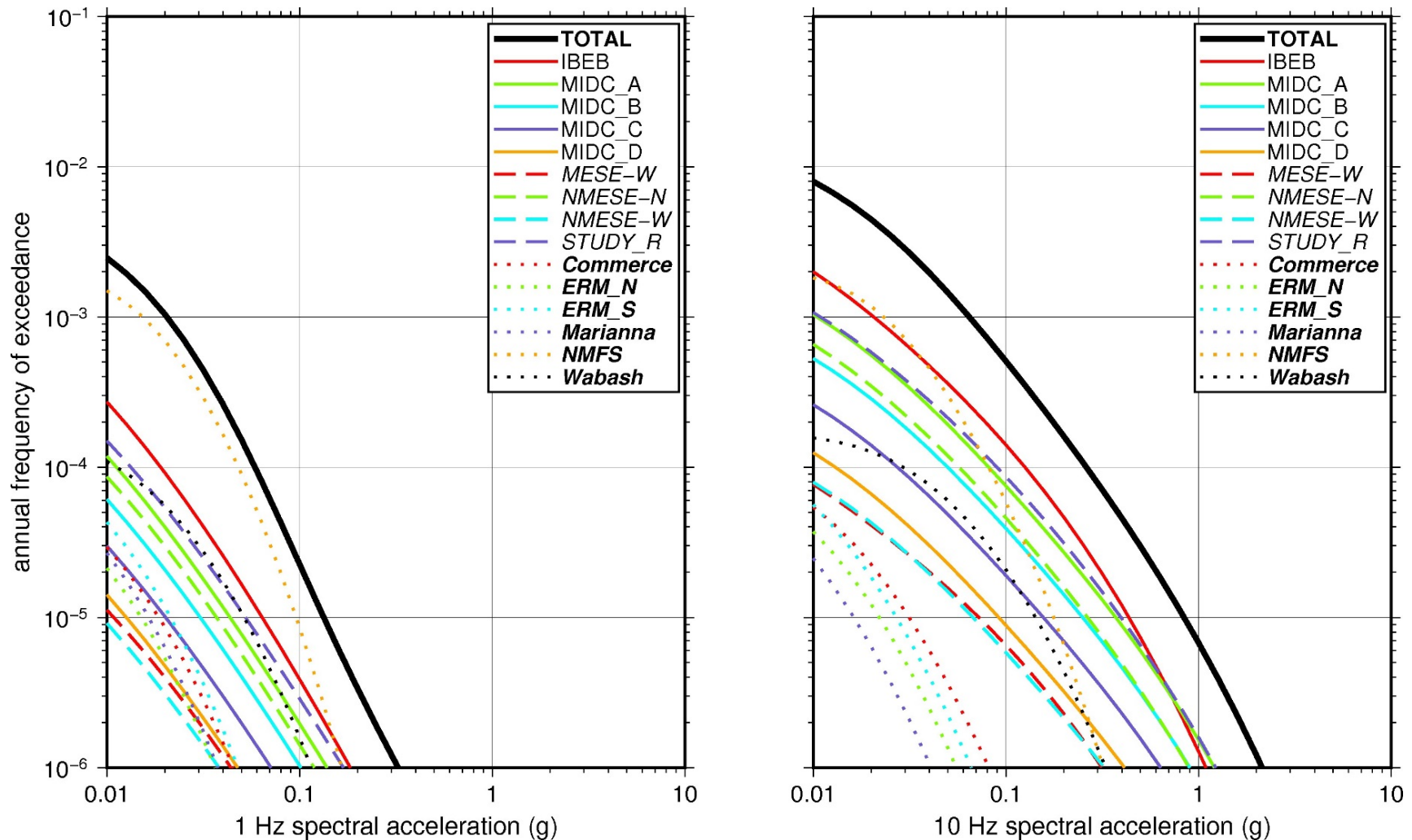


**Figure 2.4-22 Low-Frequency (1 Hz, Left), and High-Frequency (10 Hz, Right) Reference Rock Hazard Curves for Dresden. Total Hazard is Shown as a Bold Black Line; Individual Contributions to the Hazard for Each of the CEUS-SSC Sources are Shown as Colored Lines Defined in the Legend. See Table 2.1-1 for Source Name Definitions**

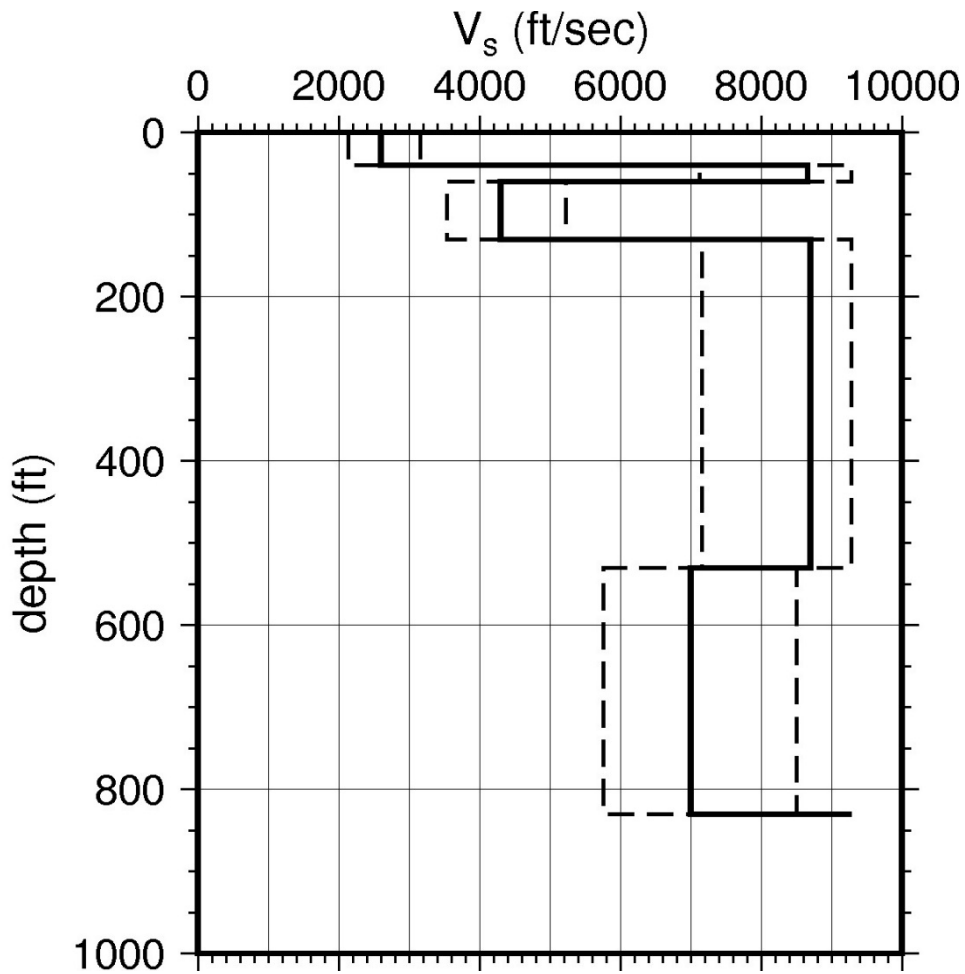


**Figure 2.4-23 Shear Wave Velocity ( $V_s$ ) Profiles for Dresden. Basecase (BC) Profile Shown as Solid Bold Line; Lower and Upper Range (LR and UR) Profiles Shown as Dashed Lines. Profiles Terminate at Reference Rock Velocity of 2,831 m/sec [9,285 ft/sec] per EPRI GMM (2013)**

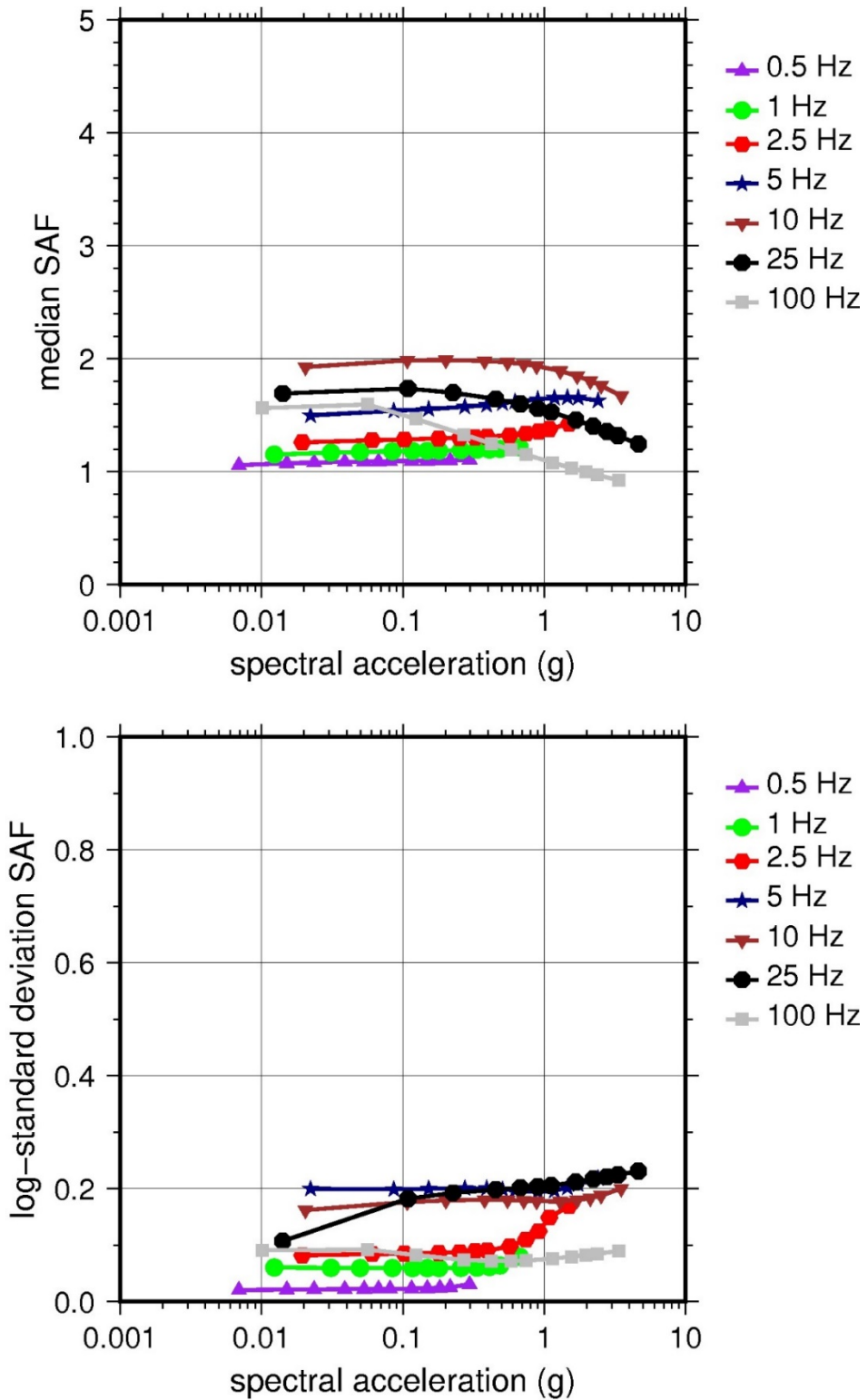


**Figure 2.4-24 Overall Weighted Median Site Amplification Factor (SAF) (Upper) and Log Standard Deviation of the SAF (Lower) as a Function of Input Acceleration for EPRI GMM (2013) Spectral Frequencies**



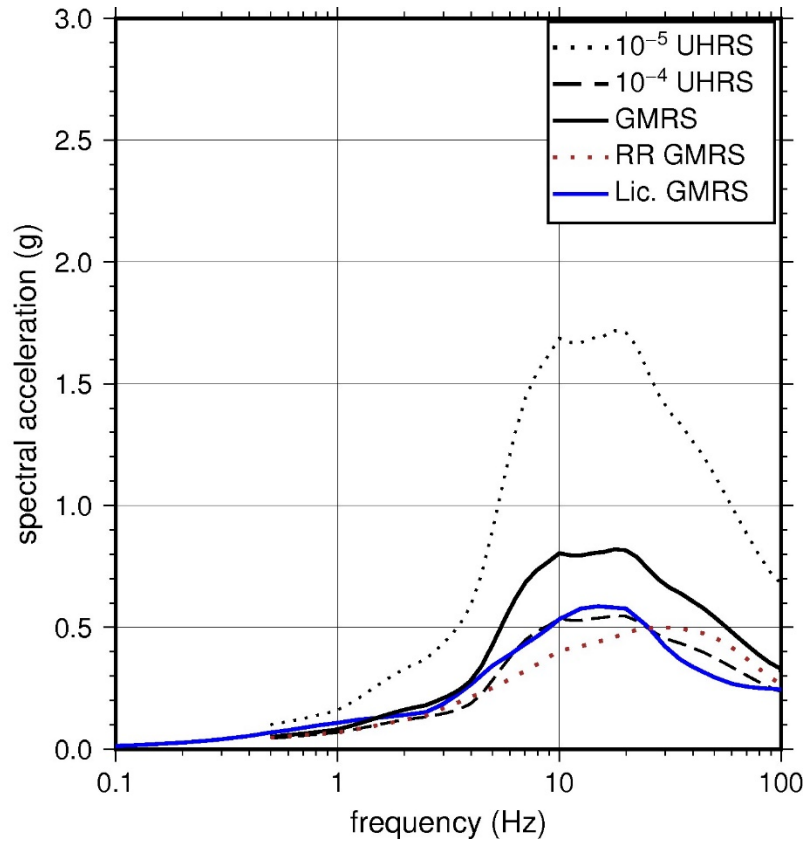
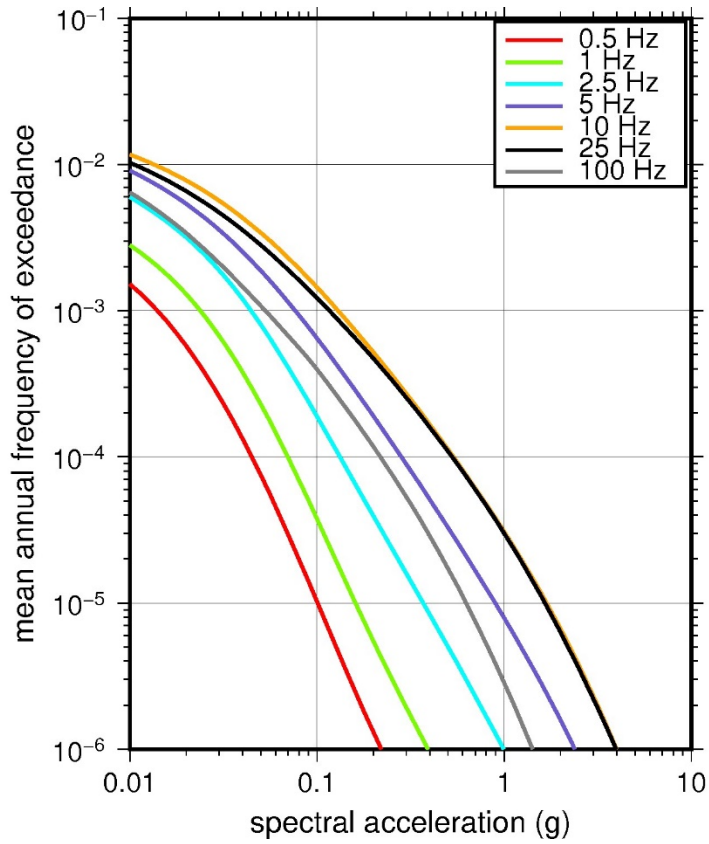


**Figure 2.4-25 Mean Control Point Hazard Curves (Left) for EPRI GMM (2013) Spectral Frequencies, and GMRS and UHRS (Right) for Dresden**

## 2.4.7 Duane Arnold

The Duane Arnold Energy Center site is located in eastern Iowa within the northern portion of the Central Lowland physiographic province and consists of 6 m [20 ft] of soil overlying about 762 m [2,500 ft] of firm sedimentary rock (shale, dolomite, sandstone, and limestone). The horizontal SSE response spectrum for Duane Arnold has a rounded Housner spectral shape and is anchored at a PGA of 0.12g.

### 2.4.7.1 Reference Rock Hazard

For the reference rock PSHA, the NRC staff selected the nine CEUS-SSC (NRC, 2012b) background seismic source zones that are located within 320 km [200 mi] of the site. In addition, the NRC staff selected the six CEUS-SSC (NRC, 2012b) RLME sources that are located within 807 km [500 mi] of the site. To develop the reference rock seismic hazard curves for the Duane Arnold site, the NRC staff used the GMPEs developed by the updated EPRI GMM (2013). As shown in Figure 2.4-26, the NMFS RLME is the largest contributor to the 1 Hz reference rock total mean hazard curve at the  $10^{-4}$  AFE level. For the 10 Hz reference rock total mean hazard curve, the MIDC-A seismotectonic source zone and the NMFS RLME are the largest contributors at the  $10^{-4}$  AFE level.

### 2.4.7.2 Site Response Evaluation

#### 2.4.7.2.1 Site Profiles

To develop a basecase profile, the NRC staff used the geologic information in the NTTF R2.1 SHSR (Anderson, 2014) submitted by NextEra Energy (hereafter referred to as “the licensee” within this plant section). As described in the licensee’s SHSR, the Duane Arnold site consists of 6 m [20 ft] of clay till with some sand and gravel overlying partially weathered dolomitic limestone. The reactor building foundation is founded 15 m [50 ft] below plant grade in these Devonian-age dolomitic limestones. In Table 2.3.1-1 of the SHSR, the licensee briefly described the subsurface materials in terms of the geologic units and layer thicknesses. For its site response evaluation, the NRC staff used the top of bedrock, which corresponds to an elevation of 216 m [707 ft] above MSL, as the control point elevation for the Duane Arnold site.

The licensee’s field investigations, conducted in the late 1960s, consisted of a number of test pits and borings, with the deepest borings extending into the Silurian-age limestone. The licensee’s geophysical field investigations measured  $V_P$  to a depth of about 61 m [200 ft] using seismic refraction surveys. To determine the  $V_S$  for each rock layer, the licensee used its measured  $V_P$  with an assumed Poisson’s ratio. Table 2.3.2-1 of the SHSR gives the estimated  $V_S$  determined from the licensee’s site investigations.

The licensee’s basecase profile, which is 116 m [380 ft] in total thickness, begins within the Wapsipinicon Formation, which consists of about 20 m [67 ft] of Devonian-age dolomitic limestone. Underlying the Wapsipinicon Formation are 95 m [313 ft] of Silurian limestones and dolomites. For both the Devonian- and the Silurian-age rocks, the licensee measured an average  $V_P$  of 4,268 m/sec [14,000 ft/sec] and assumed a Poisson’s ratio of 0.20 to estimate a  $V_S$  of 2,262 m/sec [8,600 ft/sec]. Below the Silurian-age limestones and dolomites are 646 m [2,120 ft] of Ordovician- and Cambrian-age sedimentary rocks (dolomite, limestone, shale, and sandstone), for which the licensee assumed the reference rock  $V_S$  of 2,831 m/sec [9,285 ft/sec].

The NRC staff used the licensee's layer thicknesses for its basecase profile but estimated lower  $V_S$  for the uppermost rock layers, having selected higher Poisson's ratio values. For the top layer of dolomitic limestone, the NRC staff assumed a Poisson's ratio of 0.33, which is more appropriate for moderately weathered limestone. This yields a  $V_S$  of 2,134 m/sec [7,000 ft/sec], which is lower than the licensee's estimated  $V_S$  of 2,262 m/sec [8,600 ft/sec]. For the deeper 95 m [313 ft] of Silurian-age limestones and dolomites, the NRC staff assumed a Poisson's ratio of 0.25, which is a typical value for less weathered, more intact carbonate rock. This yields a  $V_S$  of 2,470 m/sec [8,100 ft/sec]. Assuming that the  $V_S$  of the remaining 646 m [2,120 ft] of sedimentary rock exceeds the reference rock  $V_S$  of 2,831 m/sec [9,285 ft/sec], the NRC staff terminated its basecase profile at a depth of 116 m [380 ft].

To capture the uncertainty in its basecase profile, the NRC staff developed lower and upper range (10<sup>th</sup> and 90<sup>th</sup> percentile) profiles by multiplying the basecase  $V_S$  values by scale factors of 0.83 and 1.21, respectively, which corresponds to an epistemic logarithmic standard deviation of 0.15. The weights for the lower, basecase, and upper profiles are 0.3, 0.4, and 0.3, respectively. Figure 2.4-27 shows the NRC staff's profiles. As shown in Figure 2.4-27, the upper profile terminates at a depth of 20 m [67 ft], and the lower and best-estimate basecase profiles terminate at a depth of 116 m [380 ft]. In contrast, the licensee extended its lower basecase profile to a depth of 762 m [2,500 ft] below the control point elevation, using a velocity gradient of 0.5 m/sec/m [0.5 ft/sec/ft].

#### 2.4.7.2.2 *Dynamic Material Properties and Site Kappa*

The NRC staff assumed both linear and nonlinear dynamic behavior for the rock beneath the Duane Arnold site. To model the nonlinear behavior of the uppermost rock strata, the NRC staff used the EPRI rock shear modulus reduction and material damping curves. To model the linear behavior, the NRC staff used a constant damping ratio of 3 percent. The staff assumed these two alternative dynamic responses for the upper 20 m [67 ft] of the profile. Because these rock layers have high velocities {1,524 m/sec [>5,000 ft/sec]}, the NRC staff assigned weights of 0.7 and 0.3 to the linear and nonlinear alternatives, respectively. For the underlying 95 m [313 ft] of Silurian limestones and dolomites, the NRC staff assumed a linear response with a material damping ratio of 0.1 percent to maintain consistency with the  $\kappa_0$  value for the Duane Arnold site.

To determine the basecase  $\kappa_0$  for the Duane Arnold site, the NRC staff first used the Campbell (2009) Model 1 relationship between  $V_S$  and  $Q_{ef}$  to determine a  $Q_{ef}$  for each layer. Combining these  $Q_{ef}$  values with the thickness and  $V_S$  for each layer results in a total  $\kappa_0$  value of 6.7 msec, which includes the 6 msec assumed for the underlying reference rock. For the lower and upper profiles, the NRC staff calculated  $\kappa_0$  values of 7.0 and 6.1 msec, respectively, using the same approach as for the basecase profile. In contrast, the licensee estimated  $\kappa_0$  by using the lowest low-strain damping value of 3 percent from the EPRI rock material damping curves for the upper rock layers and a constant damping ratio of 1.25 percent for the deeper layers to estimate basecase, lower, and upper  $\kappa_0$  values of 8, 20, and 6 msec, respectively.

Table 2.4-8 provides the layer depths, lithologies,  $V_S$ , unit weights, and dynamic properties for the three profiles. In summary, the site response logic tree developed by the NRC staff for the Duane Arnold site consists of six alternatives; three velocity profiles (each with a different  $\kappa_0$  value) and two alternative dynamic property branches.

### 2.4.7.2.3 Methodology and Results

The NRC staff followed the methodology described in Section 2.1.4 to develop the final site amplification factors. Figure 2.4-28 shows the overall median site amplification factors and their variability for each of the seven spectral frequencies. As shown in Figure 2.4-28, the median site amplification factors are all very close to 1. The lower half of Figure 2.4-28 shows that the logarithmic standard deviations for the site amplification factors range from about 0.05 to 0.15.

### 2.4.7.3 Control Point Hazard

The NRC staff implemented Approach 3 from the SPID to develop a weighted control point seismic hazard curve for each of the three unique combinations of the site response logic tree for the Duane Arnold site. After combining these curves to develop the final mean control point hazard curves, the NRC staff determined the  $10^{-4}$  and  $10^{-5}$  UHRS in order to calculate the GMRS. Figure 2.4-29 shows the final control point mean seismic hazard curves for the seven spectral frequencies, as well as the NRC staff's UHRS and GMRS and the licensee's NTTF R2.1 GMRS (Anderson, 2014). As shown in Figure 2.4-29, the NRC staff's GMRS (black curve) is similar to the licensee's (blue curve) below 10 Hz but is moderately higher than the licensee's GMRS for higher spectral frequencies. This is due to the licensee's higher  $\kappa_0$  value for the lower basecase profile. For comparison, Figure 2.4-29 also shows the NRC staff's reference rock GMRS (brown dotted curve).

**Table 2.4-8 Layer Depths, Shear Wave Velocities ( $V_s$ ), Unit Weights, and Dynamic Properties for Duane Arnold**

Layer	Depth (ft)	Description	$V_s$ (ft/sec)			$V_s$ Sigma (ln)	BC Unit Weight (pcf)	Dynamic Properties	
			LR (0.3)	BC (0.4)	UR (0.3)			Alt. 1 (0.3)	Alt. 2 (0.7)
1	67	Rock: dolomite, limestone	5,417	7,000	9,046	0.25	150	EPRI Rock	L 3.0%
2	380	Rock: dolomite, limestone	6,268	8,100	9,285	0.15	160	L 0.1%	L 0.1%
3	880	Rock: shale, limestone, sandstone	7,200	9,285	9,285	0.15	160	L 0.1%	L 0.1%
4	1,380	Rock: shale, limestone, sandstone	7,450	9,285	9,285	0.15	160	L 0.1%	L 0.1%
5	1,880	Rock: shale, limestone, sandstone	7,700	9,285	9,285	0.15	160	L 0.1%	L 0.1%
6	2,500	Rock: shale, limestone, sandstone	8,010	9,285	9,285	0.15	160	L 0.1%	L 0.1%

LR = lower range; BC = basecase; UR = upper range; ln = natural log; pcf = pounds per cubic foot; L = linear; Alt. = alternative  
 For LR, BC, UR, and Alt.: Values in parentheses refer to weights for site response analysis logic tree branches

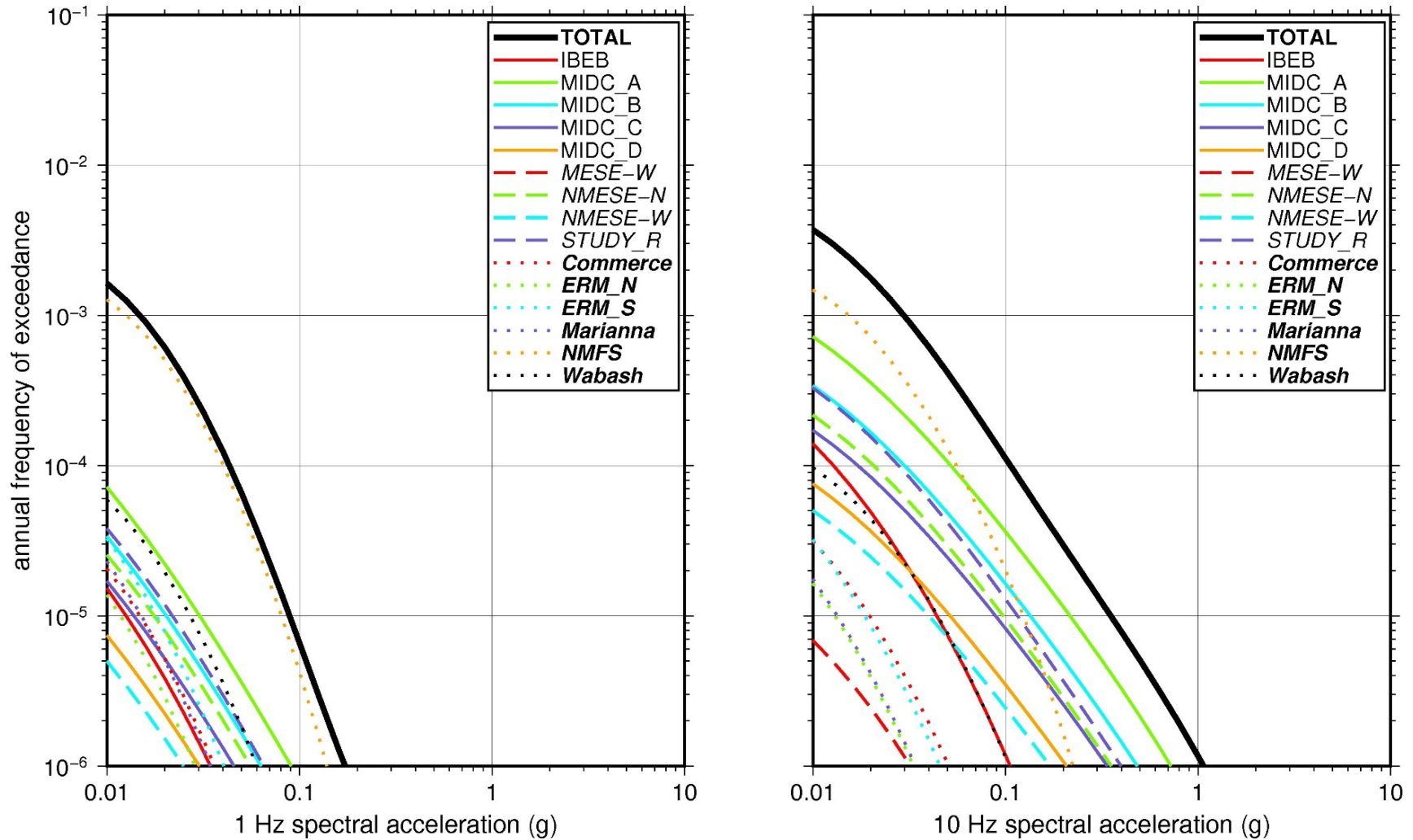


**Figure 2.4-26 Low-Frequency (1 Hz, Left), and High-Frequency (10 Hz, Right) Reference Rock Hazard Curves for Duane Arnold. Total Hazard is Shown as a Bold Black Line; Individual Contributions to the Hazard for Each of the CEUS-SSC Sources are Shown as Colored Lines Defined in the Legend. See Table 2.1-1 for Source Name Definitions**

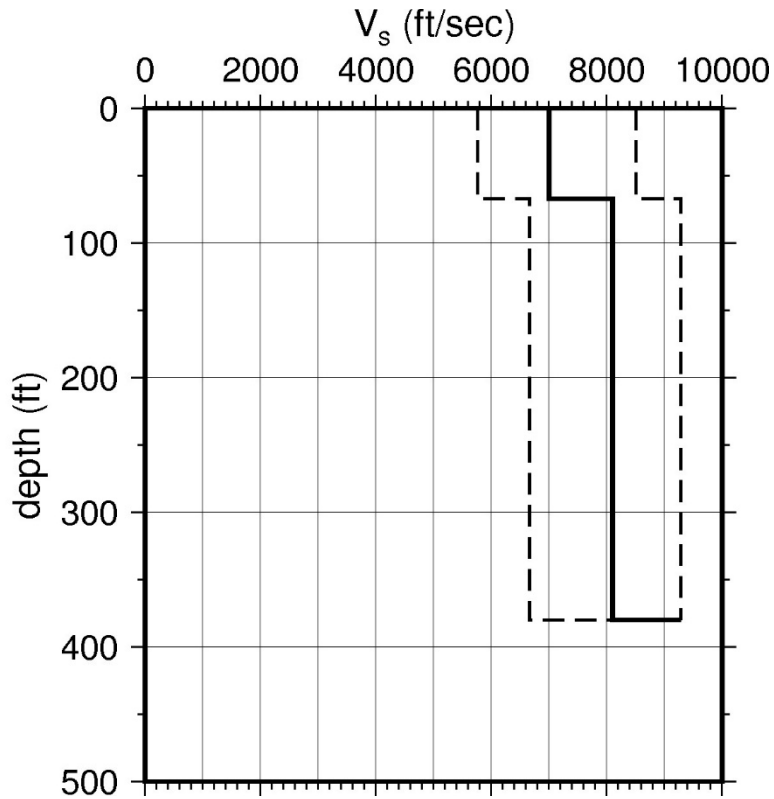


**Figure 2.4-27 Shear Wave Velocity ( $V_s$ ) Profiles for Duane Arnold. Basecase (BC) Profile Shown as Solid Bold Line; Lower and Upper Range (LR and UR) Profiles Shown as Dashed Lines. Profiles Terminate at Reference Rock Velocity of 2,831 m/sec [9,285 ft/sec] per EPRI GMM (2013)**

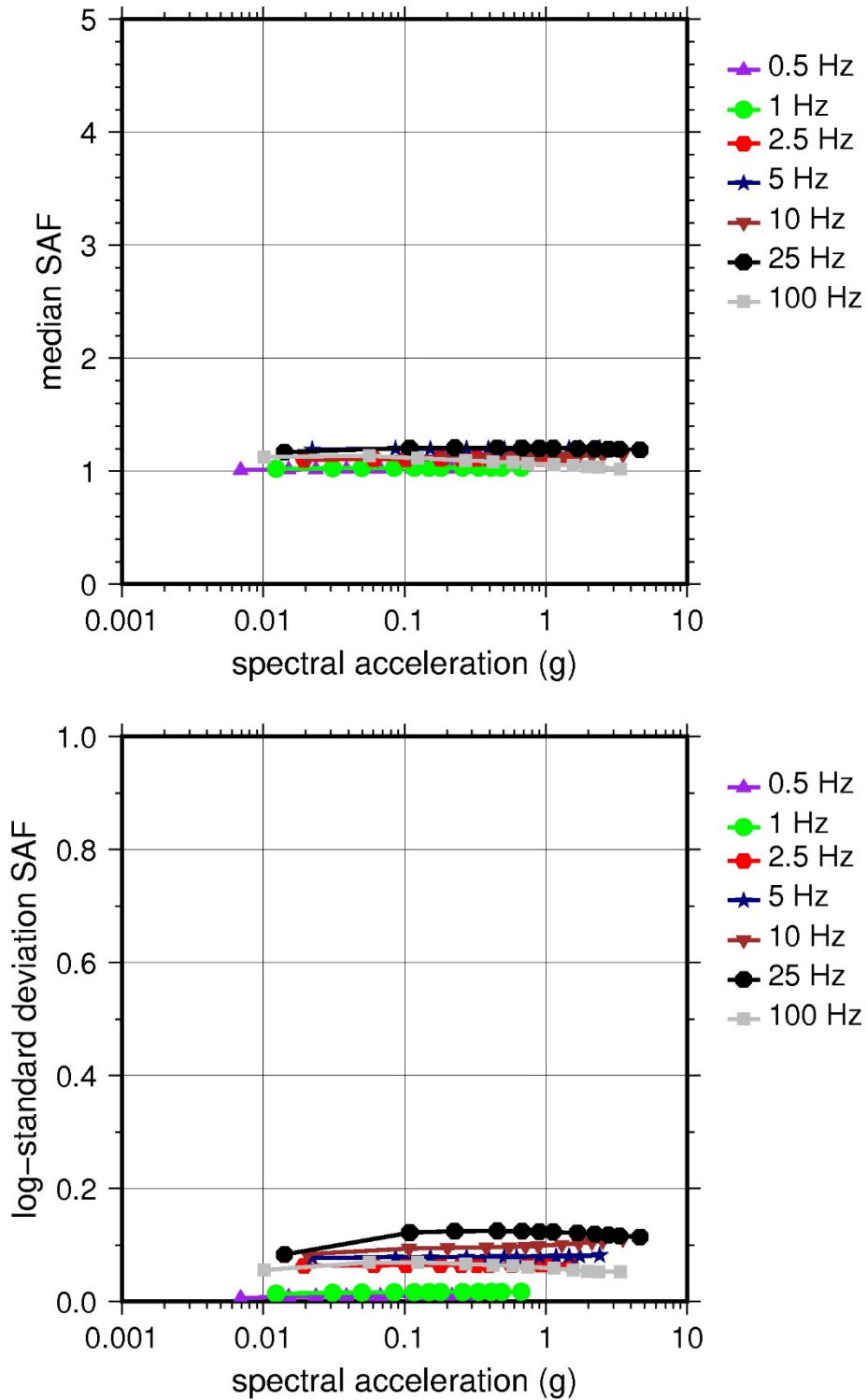


**Figure 2.4-28 Overall Weighted Median Site Amplification Factor (SAF) (Upper) and Log Standard Deviation of the SAF (Lower) as a Function of Input Acceleration for EPRI GMM (2013) Spectral Frequencies**

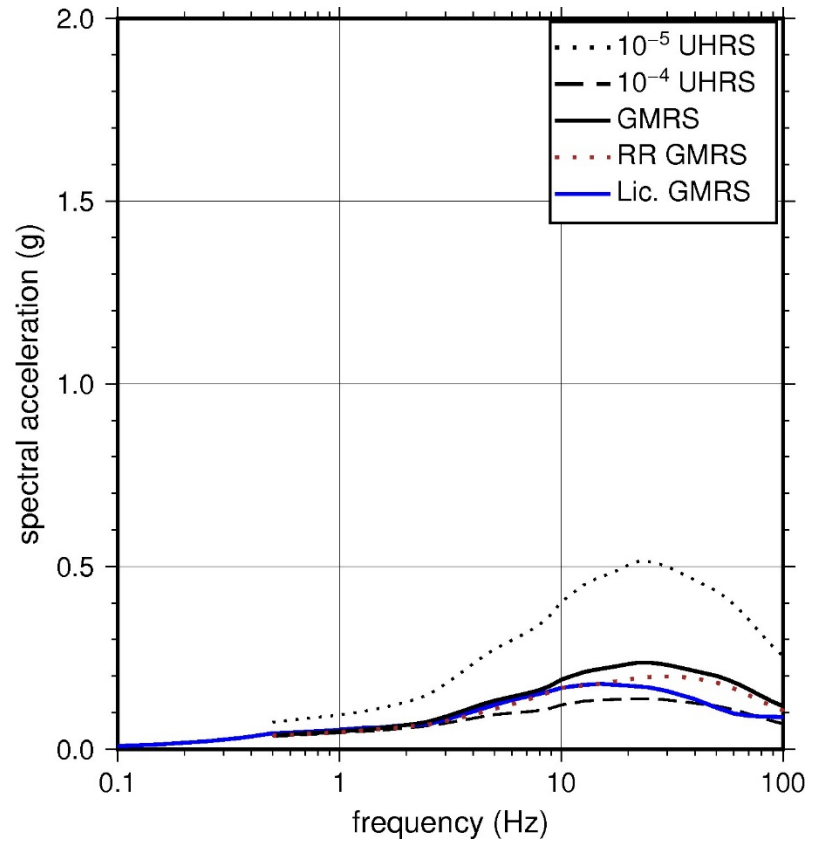
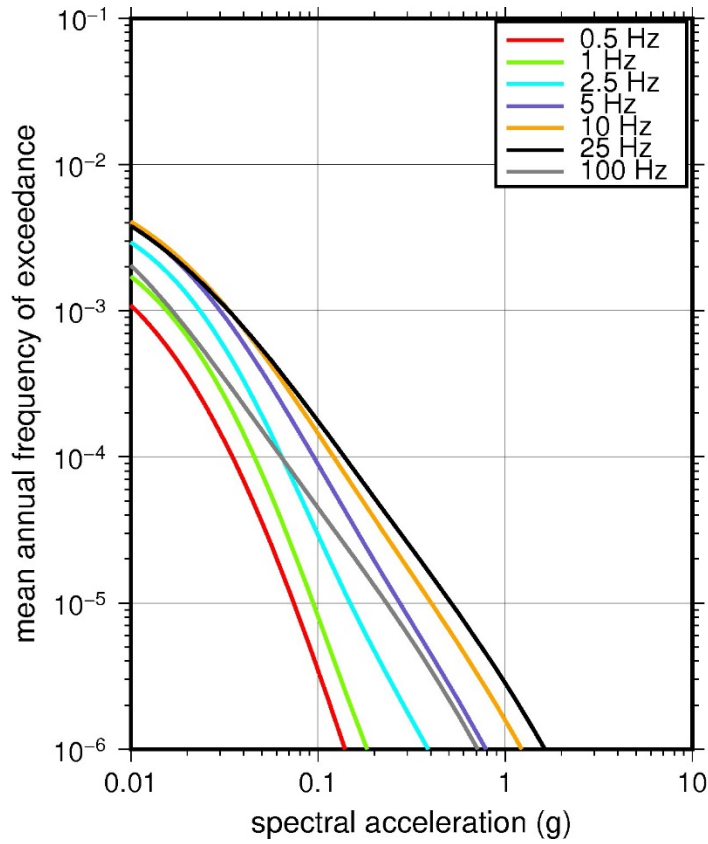


**Figure 2.4-29 Mean Control Point Hazard Curves (Left) for EPRI GMM (2013) Spectral Frequencies, and GMRS and UHRs (Right) for Duane Arnold**



## 2.4.8 Fermi

The Fermi Nuclear Power Plant site is located in southeastern Michigan on the western end of Lake Erie within the Central Lowland physiographic province and consists of 6 m [20 ft] of soil (silty to sandy clay with gravel) overlying about 945 m [3,100 ft] of sedimentary rock (dolomite, shale, and sandstone). The horizontal SSE response spectrum for Fermi has a spectral shape that is a smoothed representation of the El Centro spectrum of the 1940 *M*7.1 earthquake in Imperial Valley, CA, with minor adjustments to account for spectra from the 1935 *M*6.2 earthquake in Helena, MT, and the 1949 *M*6.7 earthquake in Olympia, WA. The SSE is anchored at a PGA of 0.15g.

### 2.4.8.1 Reference Rock Hazard

For the reference rock PSHA, the NRC staff selected the 10 CEUS-SSC (NRC, 2012b) background seismic source zones that are located within 320 km [200 mi] of the site. In addition, the NRC staff selected four of the CEUS-SSC (NRC, 2012b) RLME sources that are located within 807 km [500 mi] of the site. To develop the reference rock seismic hazard curves for the Fermi site, the NRC staff used the GMPEs developed by the updated EPRI GMM (2013). As shown in Figure 2.4-30, the NMFS RLME is the largest contributor to the 1 Hz reference rock total mean hazard curve at the  $10^{-4}$  AFE level. For the 10 Hz reference rock total mean hazard curve, the MIDC-A seismotectonic zone is the largest contributor at the  $10^{-4}$  AFE level.

### 2.4.8.2 Site Response Evaluation

#### 2.4.8.2.1 Site Profiles

To develop a basecase profile, the NRC staff used the geologic information in the NTTF R2.1 SHSR (Conner, 2014) submitted by the DTE Electric Company (hereafter referred to as “the licensee” within this plant section). As described in the licensee’s SHSR, the Fermi site consists of 6 m [20 ft] of glaciolacustrine deposits and glacial till overlying Silurian-age dolomites. The major plant structures are founded on the dolomite bedrock. In Figure 2-1 of the SHSR, the licensee briefly described the subsurface materials in terms of the geologic units and layer thicknesses. For its site response evaluation, the NRC staff used the bottom of the reactor building foundation as the control point elevation for the Fermi site. This control point is located 5 m [16 ft] below the top of rock at an elevation of 163 m [536 ft] above MSL.

The licensee’s profile is based on site investigations carried out for Unit 2 and for the COL application for Unit 3. These investigations included numerous borings, borehole geophysical measurements, and a seismic refraction profile that measured the  $V_P$  of the site bedrock. Table 2-1 of the SHSR gives the measured  $V_S$  determined from the licensee’s site investigations.

The licensee’s basecase profile, which is 88 m [290 ft] in total thickness, consists of several layers of Silurian-age sedimentary rocks (dolomite, shale, and limestone) from the Bass Island and Salina Groups. Based on extensive geophysical profiling for Unit 2 and the proposed Unit 3, the licensee used an average measured  $V_S$  or  $V_P$  with an assumed Poisson’s ratio for each layer and terminated its profile at a depth of 32 m [106 ft] within the Salina Group Unit C formation. At this depth, the licensee reported a  $V_S$  value of 2,744 m [9,000 ft/sec], which is just below the reference rock  $V_S$  of 2,831 m/sec [9,285 ft/sec] assumed for the EPRI GMM (2013).

Because the geophysical investigations carried out for the Fermi site were extensive, reaching to a depth of 135 m [443 ft] below the surface, the NRC staff used the licensee's layer thicknesses and  $V_S$  as reported in the NTTF R2.1 report (Conner, 2014).

To capture the uncertainty in its basecase profile, the NRC staff developed lower and upper range (10<sup>th</sup> and 90<sup>th</sup> percentile) profiles by multiplying the basecase  $V_S$  values by scale factors of 0.83 and 1.21, respectively, which corresponds to an epistemic logarithmic standard deviation of 0.15. The weights for the lower, basecase, and upper profiles are 0.3, 0.4, and 0.3, respectively. Figure 2.4-31 shows the NRC staff's profiles, which extend to a depth of 88 m [290 ft] below the control point elevation.

#### 2.4.8.2.2 *Dynamic Material Properties and Site Kappa*

The NRC staff assumed both linear and nonlinear dynamic behavior for the rock beneath the Fermi site. To model the nonlinear behavior of the uppermost weathered rock layers (Layers 1–3), the NRC staff used the EPRI rock shear modulus reduction and material damping curves. To model the linear behavior of these rock layers, the NRC staff assumed a constant damping ratio of 3 percent. The staff weighted these two alternatives equally. For the underlying more intact sedimentary rock layers, the NRC staff assumed a linear dynamic response with a material damping ratio of 0.1 percent to maintain consistency with the  $\kappa_0$  value for the Fermi site.

To determine the basecase  $\kappa_0$  for the Fermi site, the NRC staff first used the Campbell (2009) Model 1 relationship between  $V_S$  and  $Q_{ef}$  to determine a  $Q_{ef}$  for each layer. Combining these  $Q_{ef}$  values with the thickness and  $V_S$  for each layer results in a total  $\kappa_0$  value of 7.3 msec, which includes the 6 msec assumed for the underlying reference rock. For the lower and upper profiles, the NRC staff calculated  $\kappa_0$  values of 7.8 and 6.9 msec, respectively, using the same approach as for the basecase profile. In contrast, the licensee estimated  $\kappa_0$  by combining the low-strain damping values from the EPRI rock material damping curves over the 88 m [290 ft] of rock to estimate basecase, lower, and upper  $\kappa_0$  values of 10, 11, and 9 msec, respectively.

Table 2.4-9 provides the layer depths, lithologies,  $V_S$ , unit weights, and dynamic properties for the NRC staff's three profiles. In summary, the site response logic tree developed by the NRC staff for the Fermi site consists of six alternatives; three velocity profiles (each with a different  $\kappa_0$  value) and two alternative dynamic property branches.

#### 2.4.8.2.3 *Methodology and Results*

The NRC staff followed the methodology described in Section 2.1.4 to develop the final site amplification factors. Figure 2.4-32 shows the overall median site amplification factors and their variability for each of the seven spectral frequencies. As shown in Figure 2.4-32, the median site amplification factors range from about 1 to 2 before falling off with higher input spectral accelerations. The lower half of Figure 2.4-32 shows that the logarithmic standard deviations for the site amplification factors range from about 0.05 to 0.20.

#### 2.4.8.3 *Control Point Hazard*

The NRC staff implemented Approach 3 from the SPID to develop a weighted control point seismic hazard curve for each of the six unique combinations of the site response logic tree for the Fermi site. After combining these curves to develop the final mean control point hazard curves, the NRC staff determined the  $10^{-4}$  and  $10^{-5}$  UHRS in order to calculate the GMRS.

Figure 2.4-33 shows the final control point mean seismic hazard curves for the seven spectral frequencies, as well as the NRC staff's UHRS and GMRS and the licensee's NTTF R2.1 GMRS (Conner, 2014). As shown in Figure 2.4-33, the NRC staff's GMRS (black curve) is very similar to the licensee's (blue curve) over the entire frequency range. For comparison, Figure 2.4-33 also shows the NRC staff's reference rock GMRS (brown dotted curve).

Layer	Depth (ft)	Description	$V_s$ (ft/sec)			$V_s$ Sigma (ln)	BC Unit Weight (pcf)	Dynamic Properties	
			LR (0.3)	BC (0.4)	UR (0.3)			Alt. 1 (0.5)	Alt. 2 (0.5)
1	64	Rock: dolomite	5,404	6,550	7,939	0.25	150	EPRI Rock	L 3.0%
2	124	Rock: shale	2,805	3,400	4,121	0.15	140	EPRI Rock	L 3.0%
3	184	Rock: dolomite	3,135	3,800	4,606	0.15	140	EPRI Rock	L 3.0%
4	290	Rock: dolomite	6,105	7,400	8,969	0.15	160	L 0.1%	L 0.1%

LR = lower range; BC = basecase; UR = upper range; ln = natural log; pcf = pounds per cubic foot; L = linear; Alt. = alternative  
 For LR, BC, UR, and Alt.: Values in parentheses refer to weights for site response analysis logic tree branches

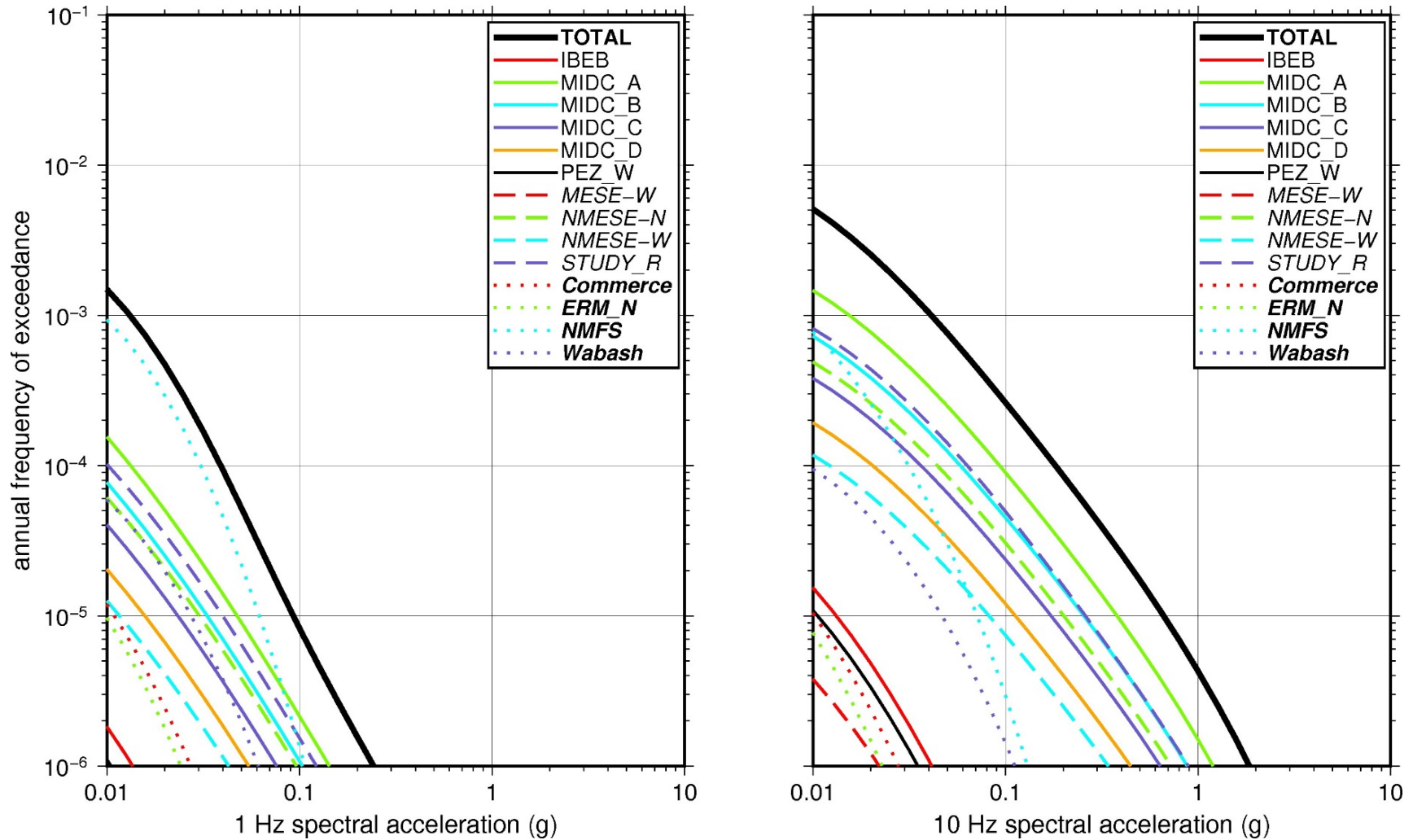


**Figure 2.4-30 Low-Frequency (1 Hz, Left), and High-Frequency (10 Hz, Right) Reference Rock Hazard Curves for Fermi. Total Hazard is Shown as a Bold Black Line; Individual Contributions to the Hazard for Each of the CEUS-SSC Sources are Shown as Colored Lines Defined in the Legend. See Table 2.1-1 for Source Name Definitions**

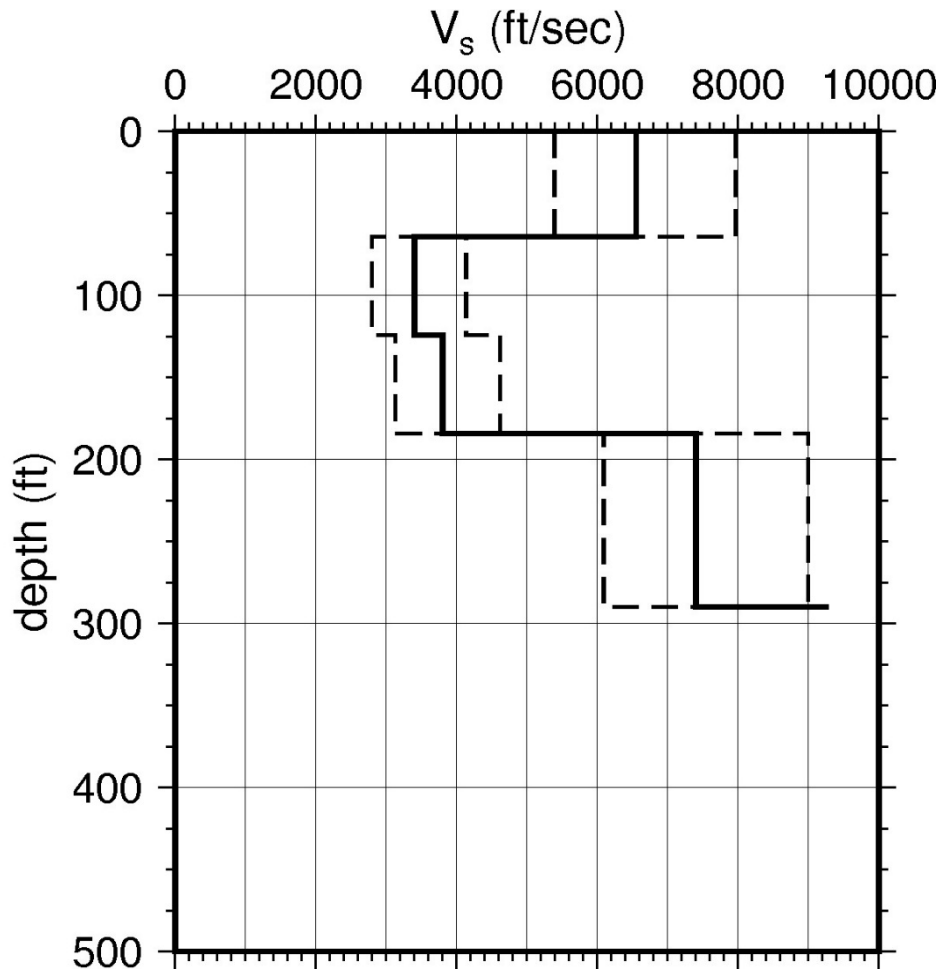


**Figure 2.4-31 Shear Wave Velocity ( $V_s$ ) Profiles for Fermi. Basecase (BC) Profile Shown as Solid Bold Line; Lower and Upper Range (LR and UR) Profiles Shown as Dashed Lines. Profiles Terminate at Reference Rock Velocity of 2,831 m/sec [9,285 ft/sec] per EPRI GMM (2013)**

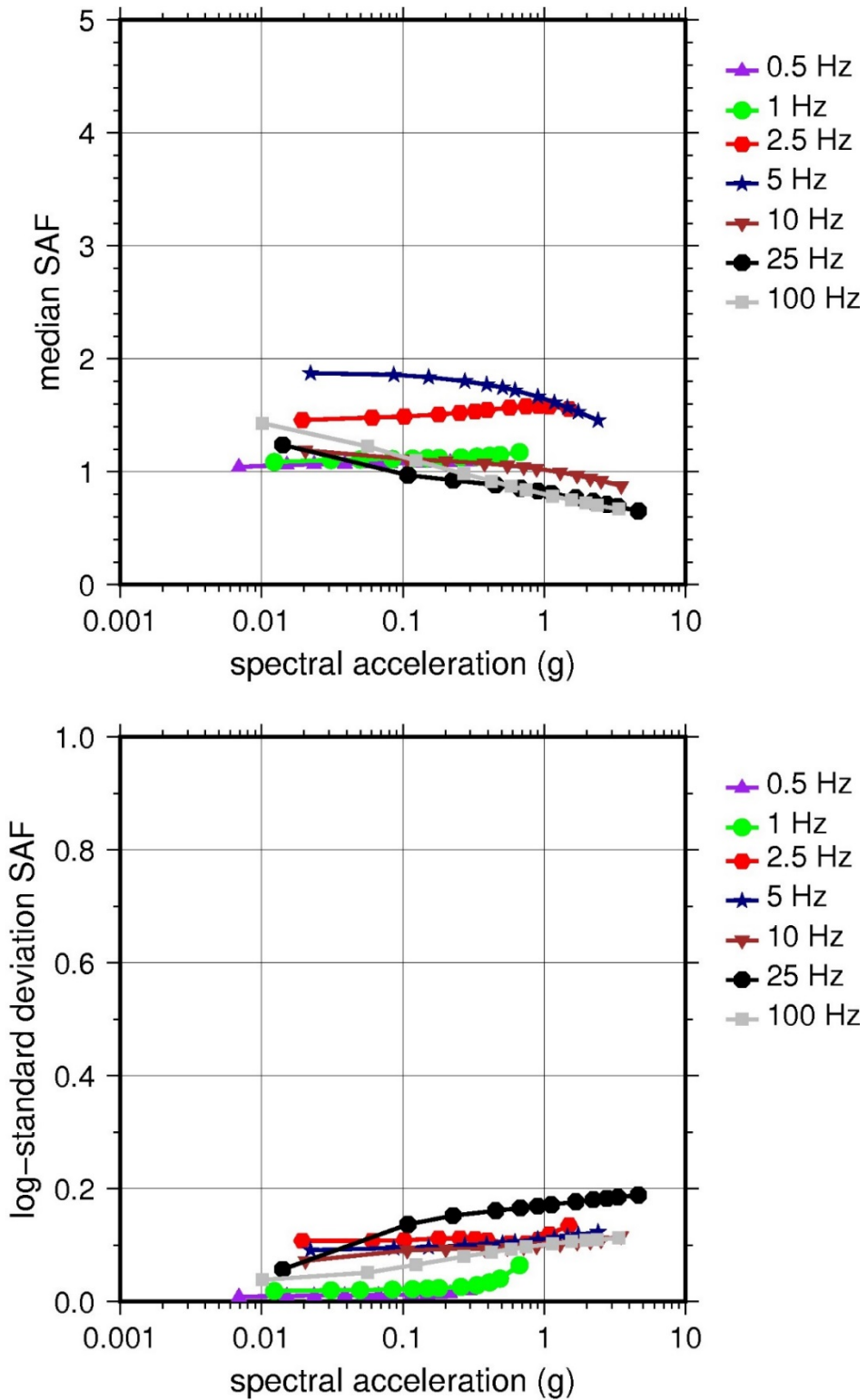


**Figure 2.4-32 Overall Weighted Median Site Amplification Factor (SAF) (Upper) and Log Standard Deviation of the SAF (Lower) as a Function of Input Acceleration for EPRI GMM (2013) Spectral Frequencies**

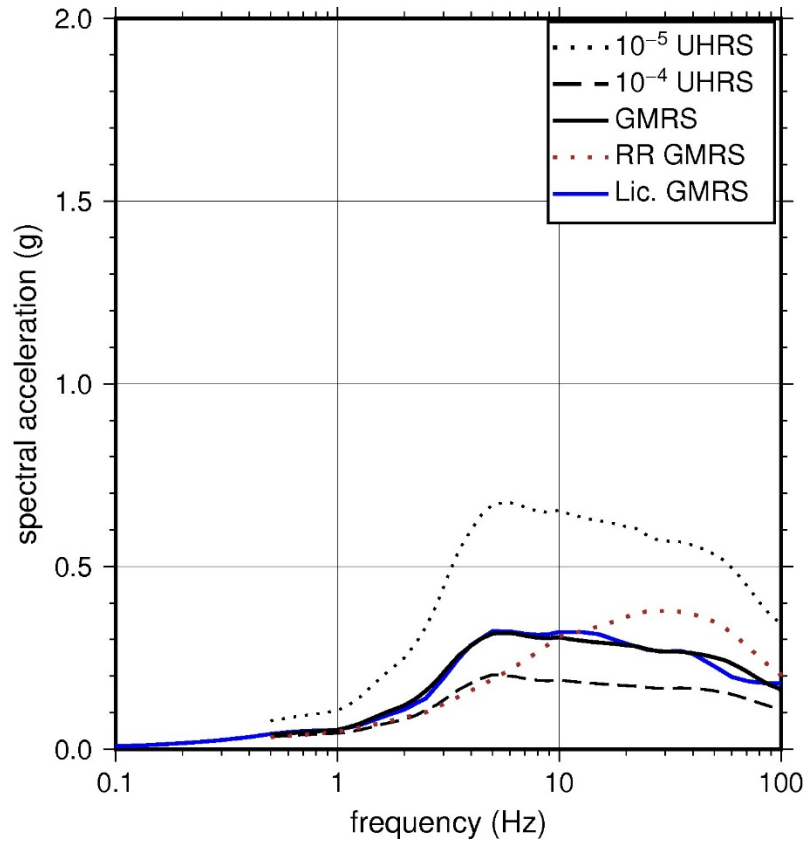
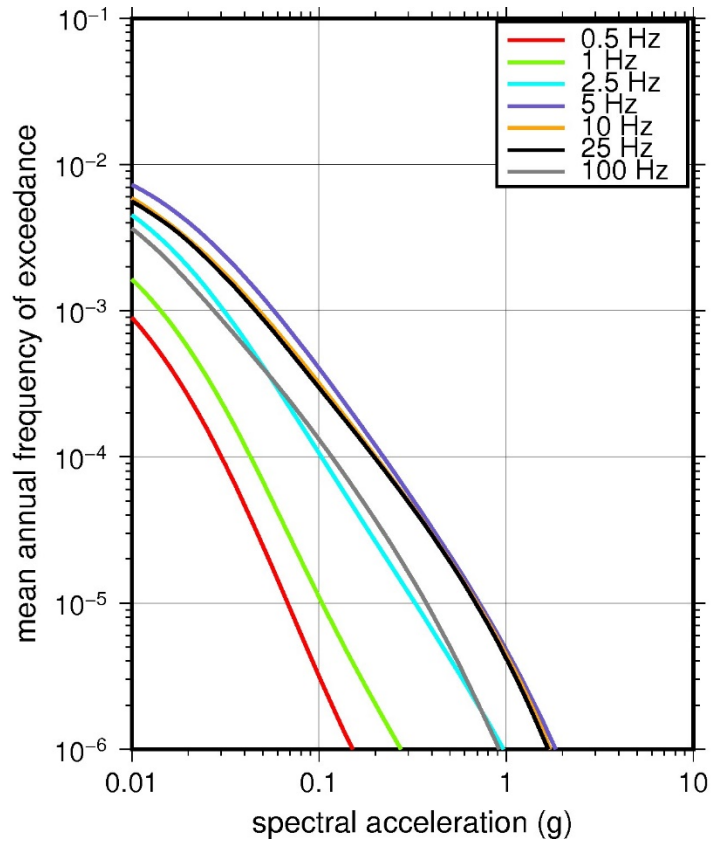


**Figure 2.4-33 Mean Control Point Hazard Curves (Left) for EPRI GMM (2013) Spectral Frequencies, and GMRS and UHRS (Right) for Fermi**

## 2.4.9 LaSalle

The LaSalle County Generating Station site is located in north-central Illinois within the Till Plains Section of the Central Lowland physiographic province and consists of about 40 m [130 ft] of soil overlying about 1,311 m [4,300 ft] of firm sedimentary rock (shale, dolomite, sandstone, and limestone). The horizontal SSE response spectrum for LaSalle has a Newmark spectral shape and is anchored at a PGA of 0.20g.

### 2.4.9.1 Reference Rock Hazard

For the reference rock PSHA, the NRC staff selected the nine CEUS-SSC (NRC, 2012b) background seismic source zones that are located within 320 km [200 mi] of the site. In addition, the NRC staff selected the six CEUS-SSC (NRC, 2012b) RLME sources that are located within 807 km [500 mi] of the site. To develop the reference rock seismic hazard curves for the LaSalle site, the NRC staff used the GMPEs developed by the updated EPRI GMM (2013). As shown in Figure 2.4-34, the NMFS RLME is the largest contributor to the 1 Hz reference rock total mean hazard curve at the  $10^{-4}$  AFE level. For the 10 Hz reference rock total mean hazard curve, the IBEB seismotectonic zone is the largest contributor at the  $10^{-4}$  AFE level.

### 2.4.9.2 Site Response Evaluation

#### 2.4.9.2.1 Site Profiles

To develop a basecase profile, the NRC staff used the geologic information in the NTTF R2.1 SHSR (Kaegi, 2014e) submitted by the Exelon Generation Company (hereafter referred to as “the licensee” within this plant section). As described in the licensee’s SHSR, the LaSalle site consists of 37–43 m [120–140 ft] of Pleistocene-age glacial till overlying Pennsylvanian-age bedrock. The major plant structures are founded on dense soils (clayey silt). In Table 2.3.1-1 of the SHSR, the licensee briefly described the subsurface materials in terms of the geologic units and layer thicknesses. For its site response evaluation, the NRC staff used the bottom of the reactor building basement, which corresponds to an elevation of 265 m [666 ft] above MSL, as the control point elevation for the LaSalle site.

The licensee’s profile is based on investigations conducted in the early 1970s for Units 1 and 2. These consisted of a number of test pits and borings, with the deepest boring of 110 m [360 ft] extending into the Ordovician-age dolomite. The licensee’s geophysical field investigations for Units 1 and 2 primarily measured  $V_P$  to a depth of about 52 m [170 ft] using seismic refraction surveys. To determine the  $V_S$  for each rock layer, the licensee used its measured  $V_P$  with an assumed Poisson’s ratio. Table 2.3.2-1 of the SHSR gives the estimated  $V_S$  determined from the licensee’s site investigations.

The licensee’s basecase profile, which is 1,328 m [4,356 ft] in total thickness, begins within the Wedron Group, which consists of about 37 m [120 ft] of Pleistocene-age till (silty clay over clayey silt). The upper portion of this soil layer has an average  $V_P$  of 335 m/sec [1,100 ft/sec], and at the control point elevation {13.4 m [44 ft] below finished grade level} the licensee estimated a  $V_S$  of 208 m/sec [683 ft/sec] based on an assumed Poisson’s ratio of 0.22. For the underlying more compact, very dense clayey silt layer, the licensee measured a  $V_P$  of about 1,677 m/sec [5,600 ft/sec] and used a Poisson’s ratio of 0.45 to compute a  $V_S$  of 517 m/sec [1,694 ft/sec]. For the Pennsylvanian-age shales and siltstones of the Carbondale and Spoon Formations, the licensee measured a  $V_P$  of 2,988 m/sec [9,800 ft/sec] and assumed a



Poisson's ratio of 0.32 to compute a  $V_S$  of 1,471 m/sec [4,825 ft/sec]. The licensee assumed this same  $V_S$  value for the rest of the profile, down to the top of Precambrian basement rock at a depth of 1,328 m [4,356 ft].

The NRC staff used the licensee's layer thicknesses for its basecase profile but estimated higher  $V_S$ , in general, for most of the soil and rock layers. For the uppermost soil layers within the Wedron Group, the NRC staff noted that the licensee excavated these less dense and lower velocity layers to a depth of 18 m [60 ft] below plant surface grade, which corresponds to a depth of 5 m [16 ft] below the control point elevation. As these soils were excavated and replaced with compacted fill, the NRC staff assumed a  $V_S$  of 305 m/sec [1,000 ft/sec] for the upper soil layer, which is higher than the  $V_S$  of 208 m/sec [683 ft/sec] assumed by the licensee for the in situ soils. For the underlying very dense clayey silt layer, the NRC staff used the licensee's  $V_S$  of 517 m/sec [1,694 ft/sec], as this value is based on both a measured  $V_P$  and Poisson's ratio. Similarly, for the Pennsylvanian-age shales and siltstones of the Carbondale and Spoon Formations, the NRC staff used the licensee's  $V_S$  of 1,471 m/sec [4,825 ft/sec]. However, rather than assuming that this  $V_S$  stays constant for the remaining 1,381 m [4,529 ft] of the basecase profile, the NRC staff developed its profile using other regional measured velocities within the Illinois Basin. Specifically, underlying the Carbondale and Spoon Formations are the Ordovician-age Platteville and Ancell Group dolomites and sandstones. Borehole measurements of these rock formations at similar depths {below 30.5 m [100 ft]} for other nearby plant sites [Braidwood (Section 3.3.1) and Byron (Section 3.3.2)] and for the Superconducting Super Collider in northeastern Illinois (Bauer et al., 1991) indicate  $V_S$  values of about 2,683 m/sec [8,800 ft/sec] for the Platteville Group dolomites and about 2,439 m/sec [8,000 ft/sec] for the Ancell Group (primarily St. Peter Formation) sandstones. For the underlying Cambrian-age strata, the NRC staff assumed that the  $V_S$  exceeds the reference rock  $V_S$  of 2,831 m/sec [9,285 ft/sec].

To capture the uncertainty in its basecase profile, the NRC staff developed lower and upper range (10<sup>th</sup> and 90<sup>th</sup> percentile) profiles by multiplying the basecase  $V_S$  values by scale factors of 0.78 and 1.29, respectively, which corresponds to an epistemic logarithmic standard deviation of 0.20. The weights for the lower, basecase, and upper profiles are 0.3, 0.4, and 0.3, respectively. Figure 2.4-35 shows the NRC staff's profiles. As shown in Figure 2.4-35, the lower and best-estimate basecase profiles extend to a depth of 188 m [616 ft] below the control point elevation, and the upper profile terminates at a depth of about 92 m [300 ft].

#### 2.4.9.2.2 *Dynamic Material Properties and Site Kappa*

The NRC staff assumed both linear and nonlinear dynamic behavior for the soil and rock beneath the LaSalle site. To model the nonlinear behavior of the soil (Layers 1–2), the NRC staff used the EPRI soil and Peninsular Range shear modulus reduction and material damping curves as two equally weighted alternatives. For the Carbondale and Spoon Formation shales (Layer 3), the NRC staff used the EPRI rock shear modulus reduction and material damping curves to model the nonlinear dynamic behavior and a constant damping ratio of 3 percent to model the linear dynamic behavior. The staff weighted these two alternatives equally. For the underlying sedimentary strata, the NRC staff assumed a linear dynamic response with a material damping ratio of 0.1 percent to maintain consistency with the  $\kappa_0$  value for the LaSalle site.

To determine the basecase  $\kappa_0$  for the LaSalle site, the NRC staff first used the Campbell (2009) Model 1 relationship between  $V_S$  and  $Q_{ef}$  to determine a  $Q_{ef}$  for each layer. Combining these  $Q_{ef}$  values with the thickness and  $V_S$  for each layer results in a total  $\kappa_0$  value of 13 msec, which

includes the 6 msec assumed for the underlying reference rock. For the lower and upper profiles, the NRC staff calculated  $\kappa_0$  values of 17 and 10 msec, respectively, using the same approach as for the basecase profile. In contrast, the licensee estimated  $\kappa_0$  by combining the low-strain damping values from the material damping curves over the top 152 m [500 ft] of the profile and assumed a constant damping ratio of 1.25 percent for the remainder to estimate basecase, lower, and upper  $\kappa_0$  values of 34, 40, and 12 msec, respectively.

Table 2.4-10 provides the layer depths, lithologies,  $V_s$ , unit weights, and dynamic properties for the three profiles. In summary, the site response logic tree developed by the NRC staff for the LaSalle site consists of six alternatives; three velocity profiles (each with a different  $\kappa_0$  value) and two alternative dynamic property branches.

#### 2.4.9.2.3 Methodology and Results

The NRC staff followed the methodology described in Section 2.1.4 to develop the final site amplification factors. Figure 2.4-36 shows the overall median site amplification factors and their variability for each of the seven spectral frequencies. As shown in Figure 2.4-36, the median site amplification factors range from about 1 to 4 before falling off with higher input spectral accelerations. The lower half of Figure 2.4-36 shows that the logarithmic standard deviations for the site amplification factors range from about 0.05 to 0.30.

#### 2.4.9.3 Control Point Hazard

The NRC staff implemented Approach 3 from the SPID to develop a weighted control point seismic hazard curve for each of the six unique combinations of the site response logic tree for the LaSalle site. After combining these curves to develop the final mean control point hazard curves, the NRC staff determined the  $10^{-4}$  and  $10^{-5}$  UHRS in order to calculate the GMRS. Figure 2.4-37 shows the final control point mean seismic hazard curves for the seven spectral frequencies, as well as the NRC staff's UHRS and GMRS and the licensee's NTF R2.1 GMRS (Kaegi, 2014e). As shown in Figure 2.4-37, the NRC staff's GMRS (black curve) is moderately higher than the licensee's (blue curve), because of differences in the basecase profiles and  $\kappa_0$  values.

Layer	Depth (ft)	Description	$V_s$ (ft/sec)			$V_s$ Sigma (ln)	Unit Weight (pcf)	Dynamic Properties	
			LR (0.3)	BC (0.4)	UR (0.3)			Alt. 1 (0.5)	Alt. 2 (0.5)
1	66	Soil: fill	774	1,000	1,292	0.25	120	EPRI Soil	Pen.
2	126	Soil: silt	1,311	1,694	2,189	0.15	130	EPRI Soil	Pen.
3	296	Rock: shale, limestone, sandstone	3,734	4,825	6,235	0.15	140	EPRI Rock	L 3.0%
4	366	Rock: dolomite	6,785	8,800	9,285	0.15	160	L 0.1%	L 0.1%
5	616	Rock: sandstone	6,168	8,000	9,285	0.15	160	L 0.1%	L 0.1%

LR = lower range; BC = basecase; UR = upper range; ln = natural log; pcf = pounds per cubic foot; L = linear; Alt. = alternative; Pen. = Peninsular  
 For LR, BC, UR, and Alt.: Values in parentheses refer to weights for site response analysis logic tree branches

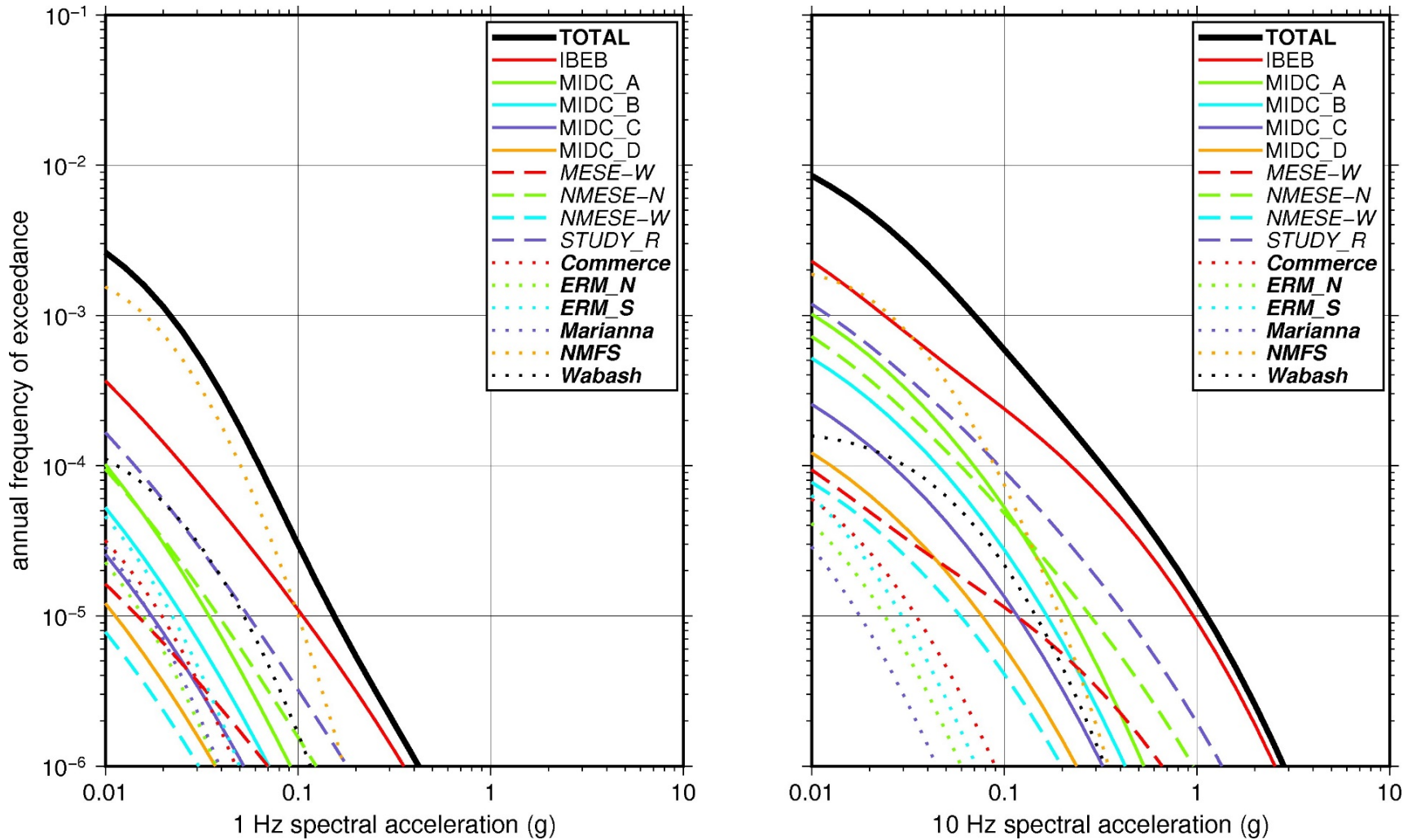


**Figure 2.4-34 Low-Frequency (1 Hz, Left), and High-Frequency (10 Hz, Right) Reference Rock Hazard Curves for LaSalle. Total Hazard is Shown as a Bold Black Line; Individual Contributions to the Hazard for Each of the CEUS-SSC Sources are Shown as Colored Lines Defined in the Legend. See Table 2.1-1 for Source Name Definitions**

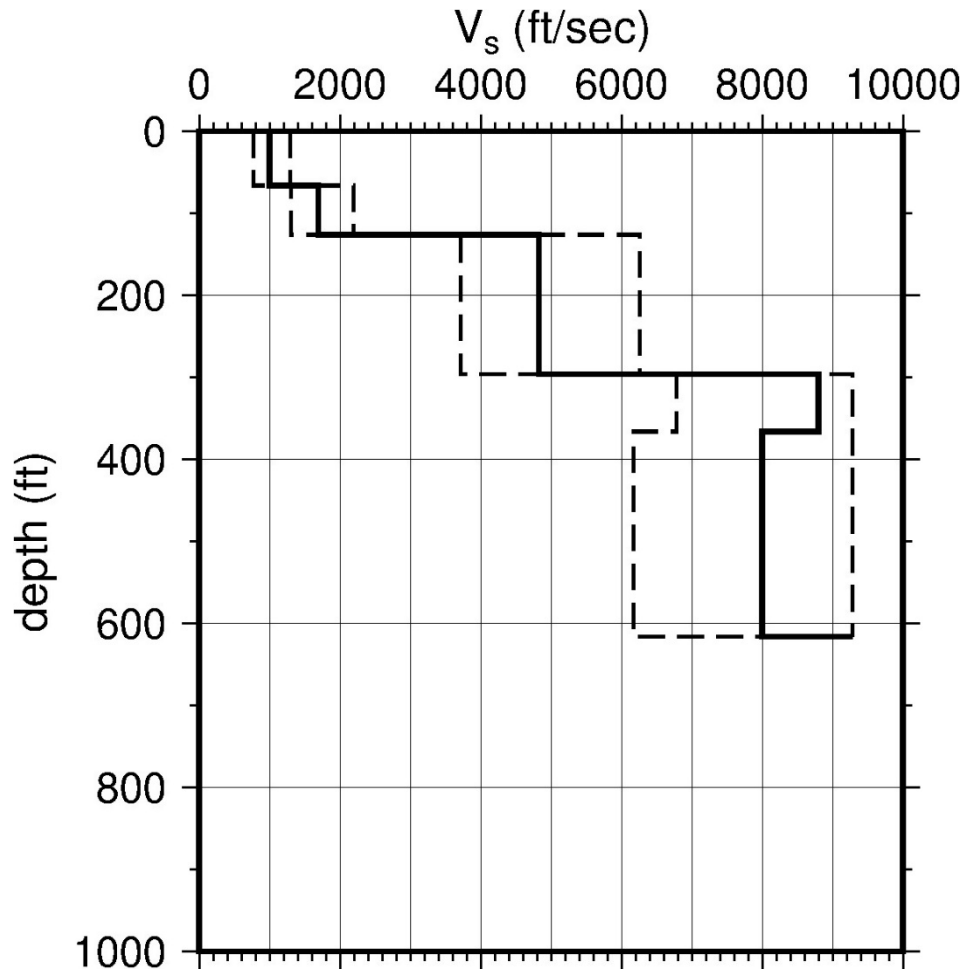


**Figure 2.4-35 Shear Wave Velocity ( $V_s$ ) Profiles for LaSalle. Basecase (BC) Profile Shown as Solid Bold Line; Lower and Upper Range (LR and UR) Profiles Shown as Dashed Lines. Profiles Terminate at Reference Rock Velocity of 2,831 m/sec [9,285 ft/sec] per EPRI GMM (2013)**

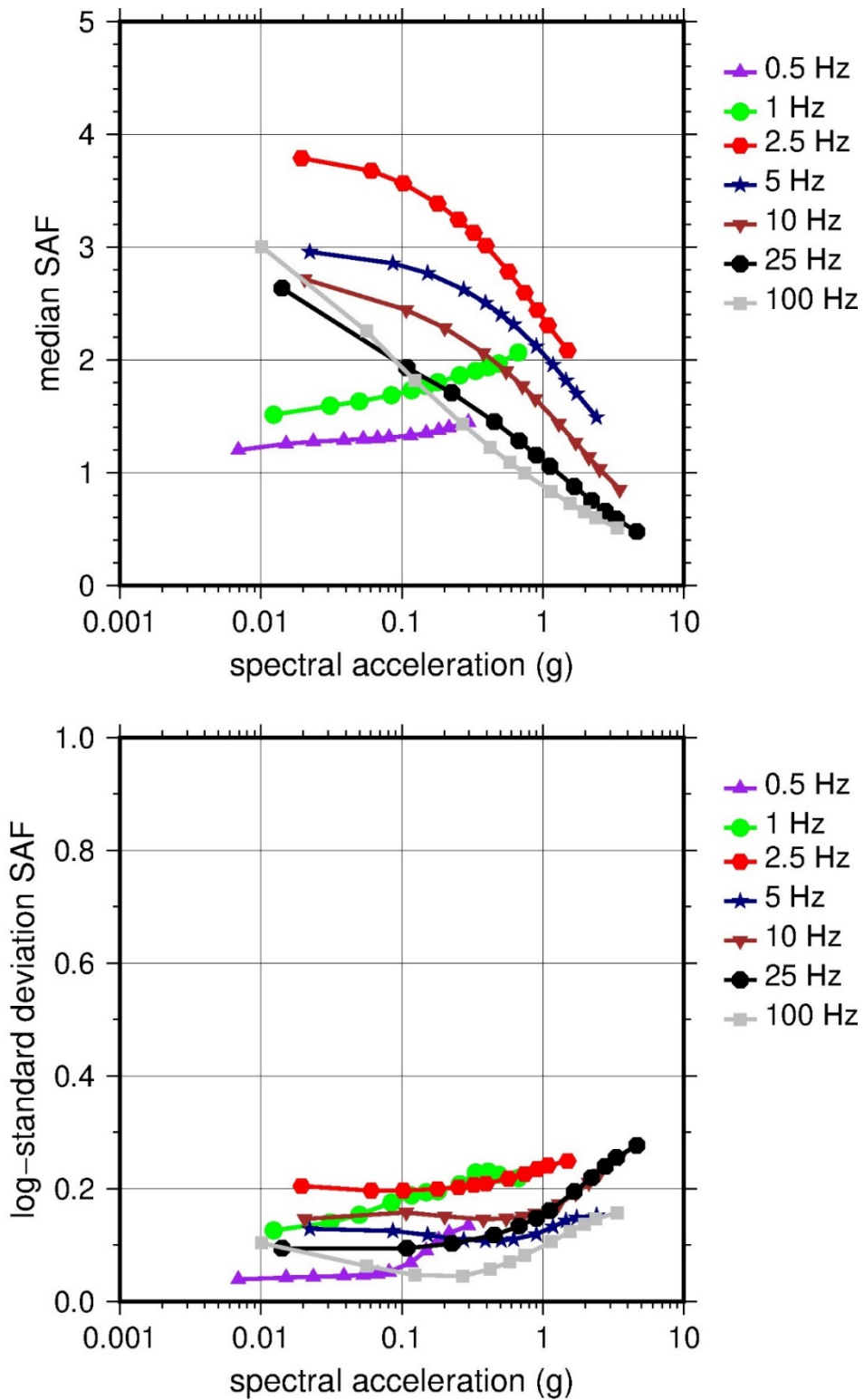


**Figure 2.4-36 Overall Weighted Median Site Amplification Factor (SAF) (Upper) and Log Standard Deviation of the SAF (Lower) as a Function of Input Acceleration for EPRI GMM (2013) Spectral Frequencies**

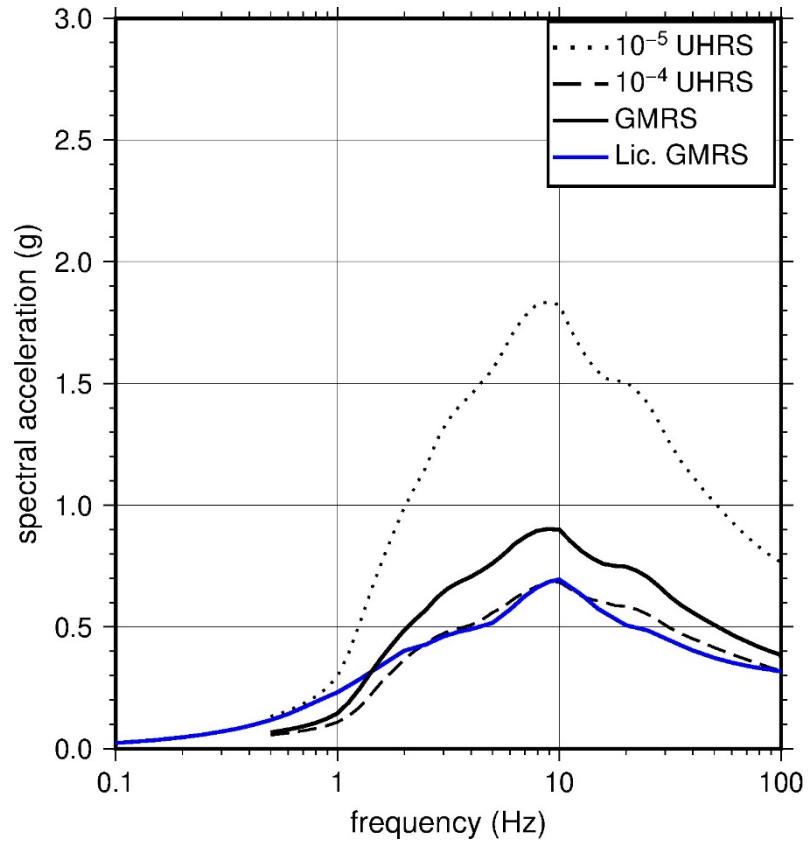
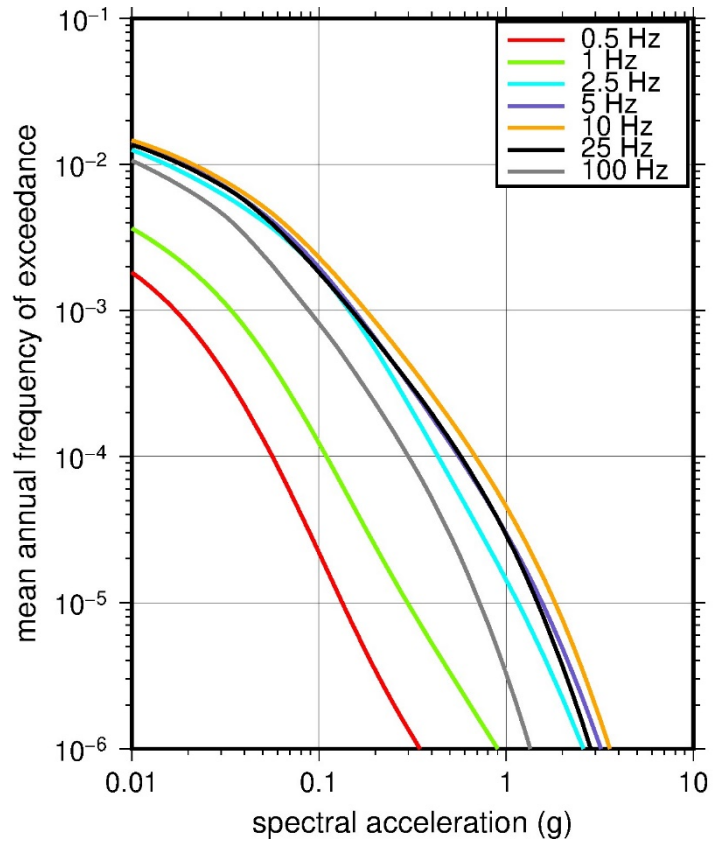


**Figure 2.4-37 Mean Control Point Hazard Curves (Left) for EPRI GMM (2013) Spectral Frequencies, and GMRS and UHRS (Right) for LaSalle**

## 2.4.10 Monticello

The Monticello Nuclear Generating Plant site is located in eastern Minnesota along the Mississippi River within the Central Lowland physiographic province and consists of 18 m [60 ft] of soil (sand with gravels) overlying about 15 m [50 ft] of weathered sedimentary (sandstone) and igneous (granite) rock. The horizontal SSE response spectrum for Monticello is a smoothed interpolation of the spectrum from the N69°W component of the Taft recording of the 1952 earthquake in Kern County, CA. The SSE is anchored at a PGA of 0.12g.

### 2.4.10.1 Reference Rock Hazard

For the reference rock PSHA, the NRC staff selected the seven CEUS-SSC (NRC, 2012b) background seismic source zones that are located within 320 km [200 mi] of the site. In addition, the NRC staff selected the NMFS RLME source, which is located within 1,046 km [650 mi] of the site. To develop the reference rock seismic hazard curves for the Monticello site, the NRC staff used the GMPEs developed by the updated EPRI GMM (2013). As shown in Figure 2.4-38, the NMFS RLME is the largest contributor to the 1 Hz reference rock total mean hazard curve at the  $10^{-4}$  AFE level. For the 10 Hz reference rock total mean hazard curve, the MIDC-A seismotectonic zone is the largest contributor at the  $10^{-4}$  AFE level.

### 2.4.10.2 Site Response Evaluation

#### 2.4.10.2.1 Site Profiles

To develop a basecase profile, the NRC staff used the geologic information in the NTTF R2.1 SHSR (Fili, 2014) submitted by the Northern States Power Company (hereafter referred to as “the licensee” within this plant section). As described in the licensee’s SHSR, the Monticello site consists of about 18 m [60 ft] of alluvial strata (clean sands with gravel) overlying 3–5 m [10–15 ft] of medium-grained quartz sandstone. Section 2.5.3 of the UFSAR (Northern States Power Company, 2005) states that the upper surface of the underlying rock can support unit foundation loads “up to 15,000 pounds per square foot.” In Table 2.3.1-1 of the SHSR, the licensee briefly described the subsurface materials in terms of the geologic units and layer thicknesses. For its site response evaluation, the NRC staff used the surface at an elevation of 284 m [930 ft] above MSL as the control point elevation for the Monticello site.

The licensee’s profile is based on site investigations carried out in the 1960s, which included numerous test pits and borings. To determine the  $V_S$  for the upper 34 m [110 ft] of the profile, the licensee used the geophysical measurements conducted for an ISFSI on the site. Table 2.3.2-1 of the SHSR gives the estimated  $V_S$  determined from the licensee’s site investigations.

The licensee’s basecase profile, which is 34 m [110 ft] in total thickness, begins with a soil layer 18 m [60 ft] thick, composed of fine to coarse sand with gravel. Based on geophysical measurements for the nearby ISFSI, the licensee estimated a  $V_S$  of 213 m/sec [700 ft/sec] for the top 3 m [10 ft] and a  $V_S$  of 427 m/sec [1,400 ft/sec] for the remaining 15 m [50 ft]. For the underlying 15 m [50 ft] of Precambrian-age sandstone, decomposed medium-soft granitic rock, and hard weathered granite, the licensee estimated a  $V_S$  of 762 m/sec [2,500 ft/sec] based on the results of the ISFSI downhole survey. The licensee terminated its profile at a depth of 34 m [110 ft], based on the assumption that the  $V_S$  of the Precambrian-age crystalline rock exceeds the reference rock  $V_S$  of 2,831 m/sec [9,285 ft/sec] assumed for the EPRI GMM (2013).

To augment the licensee's subsurface profile, the NRC staff used several publications containing detailed stratigraphy for eastern Minnesota (e.g., Morey, 1977; Mossler, 2008) and  $V_P$  values for specific rock formations from seismic refraction profiling in Minnesota and northwestern Wisconsin (e.g., Mooney et al., 1970).

The NRC staff used the licensee's layer thicknesses and  $V_S$  values for its basecase profile, except for the sandstone layer 5 m [15 ft] thick that underlies the 18 m [60 ft] of glacial deposits. Because of the reported limitations of the geophysical measurements developed from the site ISFSI (Fili, 2014) and the availability of nearby seismic refraction data from Mooney et al. (1970), the NRC staff estimated a  $V_S$  of 2,058 m/sec [6,750 ft/sec] for this weathered sandstone layer from the Hinckley Formation of the Keweenawan Supergroup. This estimate is based on a measured  $V_P$  of 4,115 m/sec [13,500 ft/sec] from the nearby Line 71 of Mooney et al. (1970) and an assumed Poisson's ratio of 0.33. This  $V_S$  is higher than the licensee's estimated value from the ISFSI survey {762 m/sec [2,500 ft/sec]} but is typical for what the Monticello UFSAR (Northern States Power Company, 2005) describes as a "medium-grain quartz sandstone which, in general, is moderately well cemented" that "can support unit foundation loads up to 15,000 pounds per square foot." For the underlying 9 m [30 ft] of heavily decomposed medium-soft granite and diabase, the NRC staff used the same  $V_S$  as the licensee, 762 m/sec [2,500 ft/sec], as this is a typical value for this type of decomposed rock. Finally, for the remaining 1.5 m [5 ft] of hard weathered granite, the NRC staff assumed a  $V_S$  of 2,439 m/sec [8,000 ft/sec], which is a typical value for partially weathered crystalline rock (e.g., Moos and Zoback, 1983). The NRC staff terminated its basecase profile at a depth of 34 m [110 ft], on the assumption that the partially weathered granite graded to intact Precambrian-age crystalline basement rock. Mooney et al. (1970) measured a  $V_P$  of 6,037 m/sec [19,800 ft/sec] at a depth of 61 m [200 ft] on Line 71 for what it considered to be igneous basement rock resulting from dense igneous flows of middle Keweenawan age (see also Morey, 1977).

To capture the uncertainty in its basecase profile, the NRC staff developed lower and upper range (10<sup>th</sup> and 90<sup>th</sup> percentile) profiles by multiplying the basecase  $V_S$  values by scale factors of 0.78 and 1.29, respectively, which corresponds to an epistemic logarithmic standard deviation of 0.20. The weights for the lower, basecase, and upper profiles are 0.3, 0.4, and 0.3, respectively. Figure 2.4-39 shows the NRC staff's profiles. As shown in Figure 2.4-39, the lower and best-estimate basecase profiles extend to a depth of 34 m [110 ft] below the control point elevation, while the upper profile extends to a depth of 32 m [105 ft].

#### 2.4.10.2.2 *Dynamic Material Properties and Site Kappa*

The NRC staff assumed both linear and nonlinear dynamic behavior for the soil and rock beneath the Monticello site. To model the nonlinear behavior of the soil layers (Layers 1–2), the NRC staff used the EPRI soil and Peninsular Range shear modulus reduction and material damping curves as two equally weighted alternatives. For the weathered rock layers (Layers 3–4), the NRC staff used the EPRI rock shear modulus reduction and material damping curves (EPRI, 2012). To model the linear behavior of these rock layers, the NRC staff assumed a constant damping ratio of 3 percent. The staff weighted these two alternatives equally. For the underlying harder weathered granite layer (Layer 5), the NRC staff assumed a linear dynamic response with a material damping ratio of 1 percent to maintain consistency with the  $\kappa_0$  value for the Monticello site.

To determine the basecase  $\kappa_0$  for the Monticello site, the NRC staff first used the Campbell (2009) Model 1 relationship between  $V_S$  and  $Q_{ef}$  to determine a  $Q_{ef}$  for each layer. Combining these  $Q_{ef}$  values with the thickness and  $V_S$  for each layer results in a total  $\kappa_0$  value of 9.5 msec,



which includes the 6 msec assumed for the underlying reference rock. For the lower and upper profiles, the NRC staff calculated  $\kappa_0$  values of 11.1 and 8.3 msec, respectively, using the same approach as for the basecase profile. In contrast, the licensee estimated  $\kappa_0$  by combining the low-strain damping values from the soil and rock material damping curves over the 34 m [110 ft] of its profile to estimate basecase, lower, and upper  $\kappa_0$  values of 9, 10, and 8 msec, respectively.

Table 2.4-11 provides the layer depths, lithologies,  $V_s$ , unit weights, and dynamic properties for the NRC staff's three profiles. In summary, the site response logic tree developed by the NRC staff for the Monticello site consists of six alternatives; three velocity profiles (each with a different  $\kappa_0$  value) and two alternative dynamic property branches.

#### 2.4.10.2.3 Methodology and Results

The NRC staff followed the methodology described in Section 2.1.4 to develop the final site amplification factors. Figure 2.4-40 shows the overall median site amplification factors and their variability for each of the seven spectral frequencies. As shown in Figure 2.4-40, the median site amplification factors range from about 1 to 2.5 before falling off with higher input spectral accelerations. The lower half of Figure 2.4-40 shows that the logarithmic standard deviations for the site amplification factors range from about 0.02 to 0.40.

#### 2.4.10.3 Control Point Hazard

The NRC staff implemented Approach 3 from the SPID to develop a weighted control point seismic hazard curve for each of the six unique combinations of the site response logic tree for the Monticello site. After combining these curves to develop the final mean control point hazard curves, the NRC staff determined the  $10^{-4}$  and  $10^{-5}$  UHRS in order to calculate the GMRS. Figure 2.4-41 shows the final control point mean seismic hazard curves for the seven spectral frequencies, as well as the NRC staff's UHRS and GMRS and the licensee's NTTF R2.1 GMRS (Fili, 2014). As shown in Figure 2.4-41, the NRC staff's GMRS (black curve) is similar to the licensee's (blue curve) over the entire frequency range.

**Table 2.4-11 Layer Depths, Shear Wave Velocities ( $V_s$ ), Unit Weights, and Dynamic Properties for Monticello**

Layer	Depth (ft)	Description	$V_s$ (ft/sec)			$V_s$ Sigma (ln)	BC Unit Weight (pcf)	Dynamic Properties	
			LR (0.3)	BC (0.4)	UR (0.3)			Alt. 1 (0.5)	Alt. 2 (0.5)
1	10	Soil: sand with gravel	542	700	905	0.25	120	EPRI Soil	Pen.
2	60	Soil: sand with gravel	1,083	1,400	1,809	0.15	130	EPRI Soil	Pen.
3	75	Rock: sandstone	5,223	6,750	8,772	0.15	150	EPRI Rock	L 3.0%
4	105	Rock: granite	1,935	2,500	3,231	0.15	130	EPRI Rock	L 3.0%
5	115	Rock: granite	6,191	8,000	9,285	0.15	160	L 1.0%	L1.0%

LR = lower range; BC = basecase; UR = upper range; ln = natural log; pcf = pounds per cubic foot; L = linear; Alt. = alternative; Pen. = Peninsular  
 For LR, BC, UR, and Alt.: Values in parentheses refer to weights for site response analysis logic tree branches

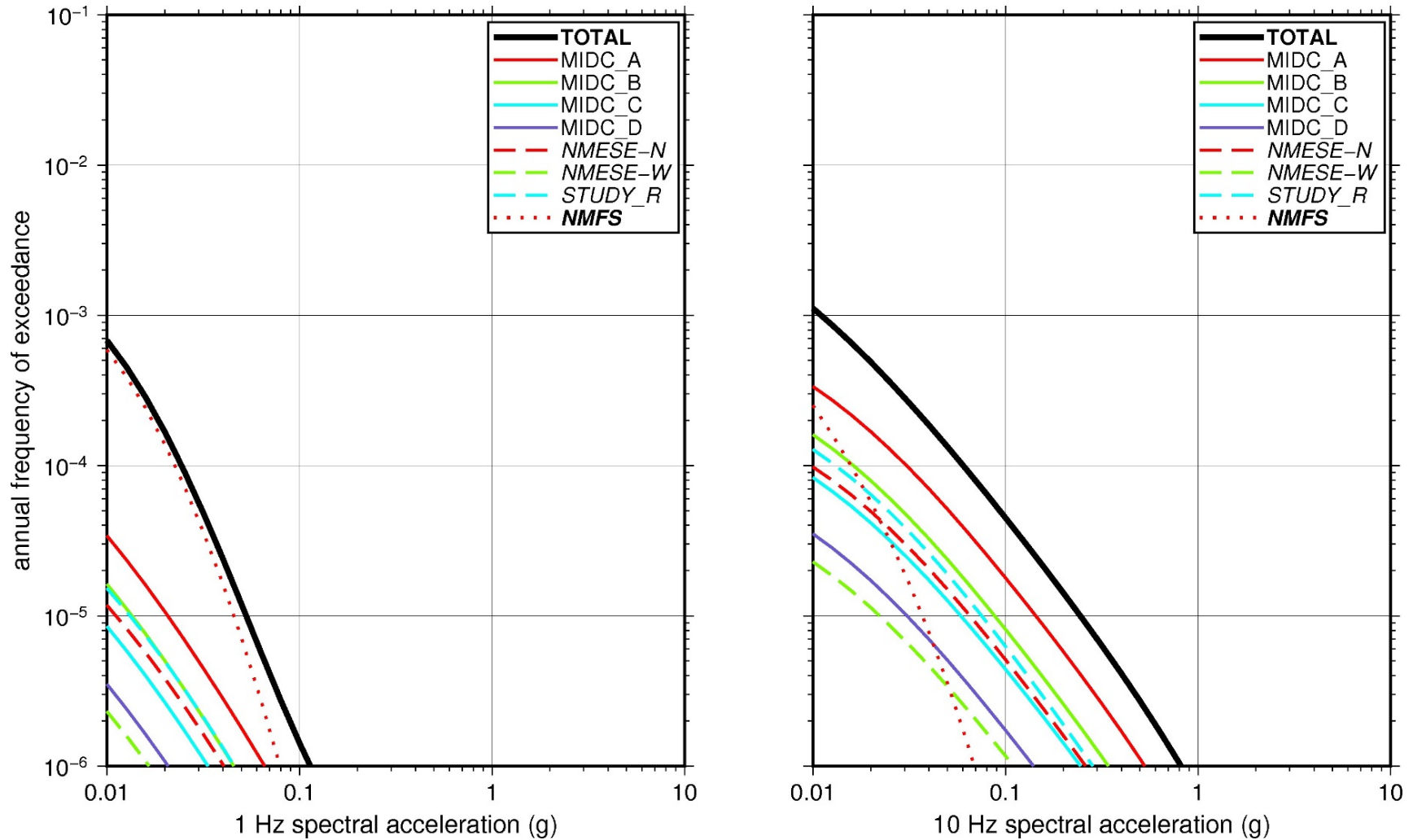


**Figure 2.4-38 Low-Frequency (1 Hz, Left), and High-Frequency (10 Hz, Right) Reference Rock Hazard Curves for Monticello. Total Hazard is Shown as a Bold Black Line; Individual Contributions to the Hazard for Each of the CEUS-SSC Sources are Shown as Colored Lines Defined in the Legend. See Table 2.1-1 for Source Name Definitions**

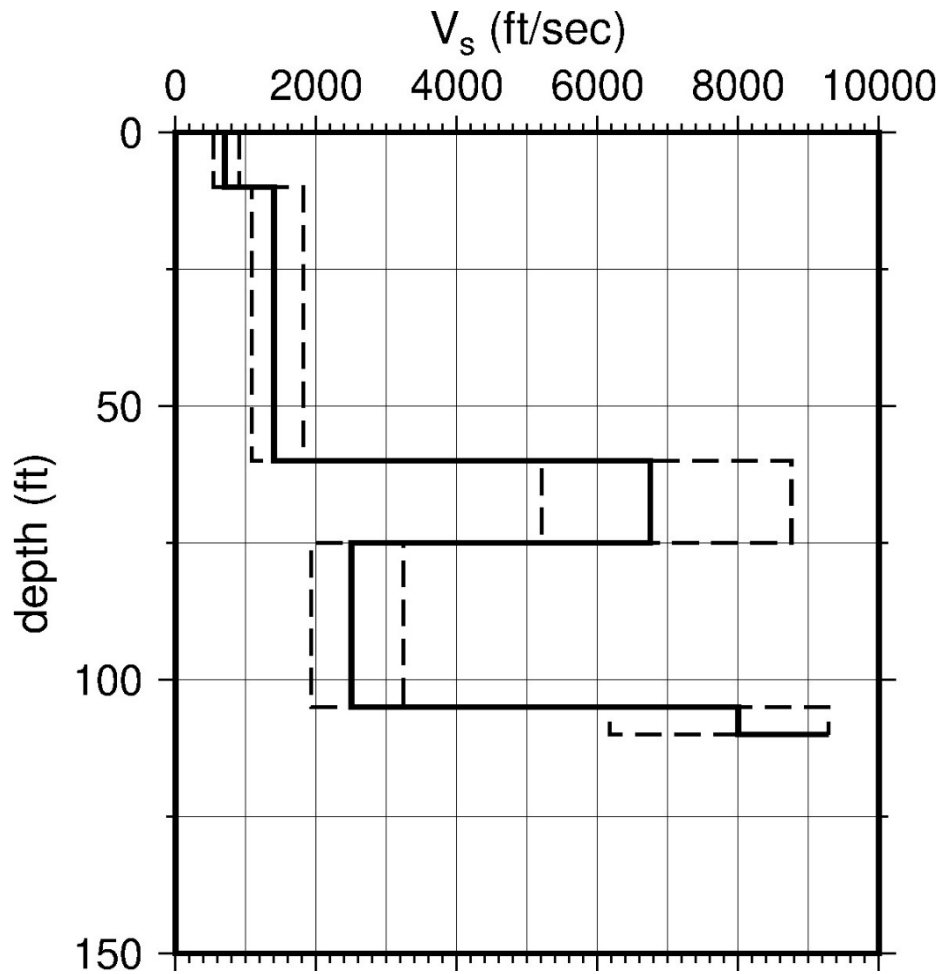


**Figure 2.4-39** Shear Wave Velocity ( $V_s$ ) Profiles for Monticello. Basecase (BC) Profile Shown as Solid Bold Line; Lower and Upper Range (LR and UR) Profiles Shown as Dashed Lines. Profiles Terminate at Reference Rock Velocity of 2,831 m/sec [9,285 ft/sec] per EPRI GMM (2013)

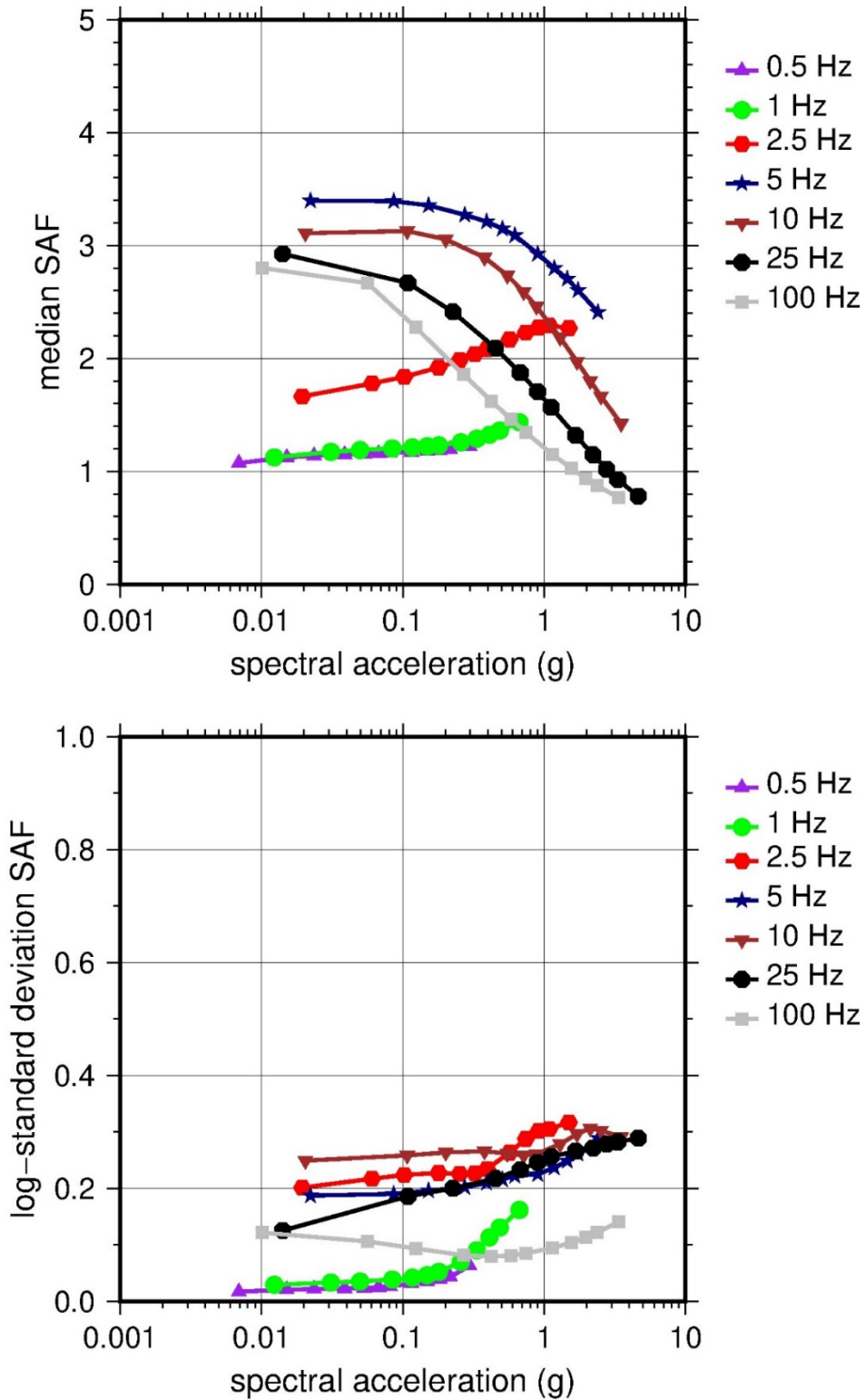


**Figure 2.4-40 Overall Weighted Median Site Amplification Factor (SAF) (Upper) and Log Standard Deviation of the SAF (Lower) as a Function of Input Acceleration for EPRI GMM (2013) Spectral Frequencies**

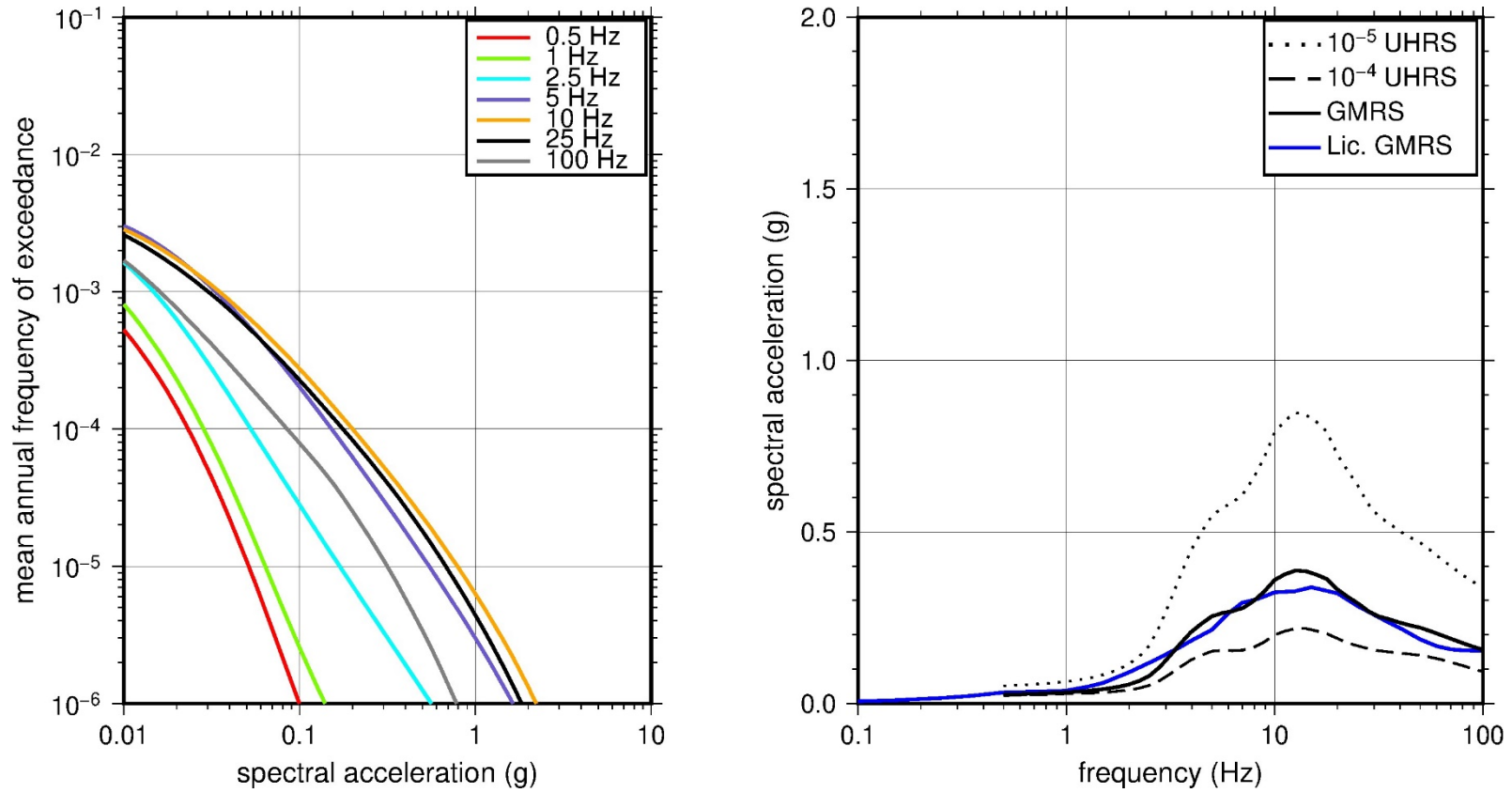


**Figure 2.4-41 Mean Control Point Hazard Curves (Left) for EPRI GMM (2013) Spectral Frequencies, and GMRS and UHS (Right) for Monticello**

## 2.4.11 Palisades

The Palisades Nuclear Plant site is located in southwestern Michigan on the eastern shore of Lake Michigan within the Central Lowland physiographic province and consists of 43 m [140 ft] of soil (sand and glacial till) overlying about 1,024 m [3,360 ft] of firm sedimentary rock (shale, dolomite, sandstone, and limestone). The horizontal SSE response spectrum for Palisades has a rounded Housner spectral shape and is anchored at a PGA of 0.20g.

### 2.4.11.1 Reference Rock Hazard

For the reference rock PSHA, the NRC staff selected the nine CEUS-SSC (NRC, 2012b) background seismic source zones that are located within 320 km [200 mi] of the site. In addition, the NRC staff selected the five CEUS-SSC RLME sources that are located within 807 km [500 mi] of the site. To develop the reference rock seismic hazard curves for the Palisades site, the NRC staff used the GMPEs developed by the updated EPRI GMM (2013). As shown in Figure 2.4-42, the NMFS RLME is the largest contributor to the 1 Hz reference rock total mean hazard curve at the  $10^{-4}$  AFE level. For the 10 Hz reference rock total mean hazard curve, the MIDC-A seismotectonic zone is the largest contributor at the  $10^{-4}$  AFE level.

### 2.4.11.2 Site Response Evaluation

#### 2.4.11.2.1 Site Profiles

To develop a basecase profile, the NRC staff used the geologic information in the NTTF R2.1 SHSR (Vitale, 2014) submitted by Entergy Nuclear Operations Inc. (hereafter referred to as “the licensee” within this plant section). As described in the licensee’s SHSR, the Palisades site consists of about 43 m [140 ft] of sand and glacial till overlying Mississippian-age shale. The plant structures are founded within the dune sands that overlie the lake deposit clays and silts. In Table 2.3.1-1 of the SHSR, the licensee briefly described the subsurface materials in terms of the geologic units and layer thicknesses. For its site response evaluation, the NRC staff used the top of the dense dune sand, which corresponds to an elevation of 180 m [589 ft] above MSL, as the control point elevation for the Palisades site.

The licensee’s profile is based on site investigations carried out in the mid-1960s, which included numerous borings and a seismic refraction survey that measured  $V_P$  to the top of bedrock, at a depth of about 61 m [200 ft]. To determine the  $V_S$  for each soil and rock layer, the licensee used its measured  $V_P$  with an estimated Poisson’s ratio appropriate for the soil or rock type. Table 2.3.2-2 of the SHSR gives the estimated  $V_S$  determined from the licensee’s site investigations.

The licensee’s basecase profile begins at the top of the 8-m-thick [25-ft-thick] dense dune sand layer, for which the licensee estimated a  $V_S$  of 229 m/sec [750 ft/sec]. The dune sand layer overlies 38 m [123 ft] of glacial lake deposits (sand, clay, and gravelly sandy clay), which the licensee divided into three layers with estimated  $V_S$  values of 274 m/sec [900 ft/sec], 305 m/sec [1,000 ft/sec], and 488 m/sec [1,600 ft/sec], respectively. The licensee identified the bedrock underlying the 45 m [148 ft] of soil as the Mississippian-age Coldwater Shale Formation, for which it measured a  $V_P$  of 3,049 m/sec [10,000 ft/sec]. To capture the epistemic uncertainty in the  $V_S$  for this layer and the rest of the sedimentary rock column beneath the site, the licensee assumed two alternative, equally weighted basecase profiles. For the first, the licensee assumed that the  $V_S$  for the uppermost rock layer and the underlying sedimentary rock layers attains the reference rock  $V_S$  of 2,831 m/sec [9,285 ft/sec] used by the EPRI GMM (2013). For

the second, the licensee assumed a  $V_P/V_S$  ratio of 2, which corresponds to a Poisson's ratio of 0.33, resulting in an estimated  $V_S$  of 1,524 m/sec [5,000 ft/sec] for the uppermost rock layer. In this second profile, the licensee kept the  $V_S$  for the entire sedimentary rock column {which it assumed to have a total thickness of 924 m [3,091 ft]} fixed at 1,524 m/sec [5,000 ft/sec].

The NRC staff used the licensee's basecase profile for the upper 148 ft [45 m] of soil but developed a different profile for the underlying sedimentary rock layers. To extend the upper portion of its basecase profile to the deeper sedimentary rock layers, the NRC staff used several publications containing detailed stratigraphy (e.g., Lilienthal, 1978; Ells, 1979; Millstein, 1989) and  $V_P$  or  $V_S$  values for specific rock formations (e.g., Liu et al., 2000; Grammer, 2007) within the Michigan Basin. For the upper 16 m [52 ft] of sedimentary rock (the Coldwater Shale Formation), the NRC staff used the same  $V_P/V_S$  ratio of 2 assumed by the licensee, which is typical for weathered sedimentary rock (Burger, 1992), to estimate a  $V_S$  of 1,524 m/sec [5,000 ft/sec]. Based on descriptions of the stratigraphy for the southwestern side of the Michigan Basin (Lilienthal, 1978; Ells, 1979; Millstein, 1989), the NRC staff assumed a thickness of 152 m [500 ft] for the Coldwater Shale Formation, with the lower 137 m [450 ft] likely being less weathered (more intact) and having a  $V_S$  of 1,982 m/sec [6,500 ft/sec]. Underlying the Coldwater Shale Formation in western Michigan are the Devonian-age Ellsworth Formation and Antrim Formation shale layers, with estimated thicknesses of 76 m [250 ft] and 37 m [120 ft], respectively. The NRC staff assigned  $V_S$  values of 2,134 m/sec [7,000 ft/sec] to the Ellsworth Formation shale layer and 2,439 m/sec [8,000 ft/sec] to the underlying Antrim Formation shale layer, based on laboratory measurements of Liu et al. (2000) for these shale specimens. For the rest of the Devonian-age layers and the underlying older sedimentary rock layers (primarily shale, limestone, and dolomite), the NRC staff assumed that the  $V_S$  exceeds the reference rock  $V_S$  of 2,831 m/sec [9,285 ft/sec]. This assumption is based on  $V_P$  measurements of Silurian- and Ordovician-age limestone specimens within the Michigan Basin (Grammer, 2007), which exceed 6,100 m/sec [20,000 ft/sec].

To capture the uncertainty in its basecase profile, the NRC staff developed lower and upper range (10<sup>th</sup> and 90<sup>th</sup> percentile) profiles by multiplying the basecase  $V_S$  values by scale factors of 0.78 and 1.29, respectively, which corresponds to an epistemic logarithmic standard deviation of 0.20. The weights for the lower, basecase, and upper profiles are 0.3, 0.4, and 0.3, respectively. Figure 2.4-43 shows the NRC staff's profiles. As shown in Figure 2.4-43, the lower and best-estimate basecase profiles extend to a depth of 366 m [1,200 ft], while the upper profile extends to a depth of 274 m [900 ft] below the control point elevation.

#### 2.4.11.2.2 *Dynamic Material Properties and Site Kappa*

The NRC staff assumed both linear and nonlinear dynamic behavior for the soil and rock beneath the Palisades site. To model the nonlinear behavior of the soil layers (Layers 1–4), the NRC staff used the EPRI soil and Peninsular Range shear modulus reduction and material damping curves as two equally weighted alternatives. For the weathered rock layer (Layer 5), the NRC staff used the EPRI rock shear modulus reduction and material damping curves. To model the linear behavior of this rock layer, the NRC staff assumed a constant damping ratio of 3 percent. The staff weighted these two alternatives equally. For the underlying sedimentary rock, the NRC staff assumed a linear dynamic response with a material damping ratio of 0.1 percent to maintain consistency with the  $\kappa_0$  value for the Palisades site.

To determine the basecase  $\kappa_0$  for the Palisades site, the NRC staff first used the Campbell (2009) Model 1 relationship between  $V_S$  and  $Q_{ef}$  to determine a  $Q_{ef}$  for each layer. Combining these  $Q_{ef}$  values with the thickness and  $V_S$  for each layer results in a total  $\kappa_0$  value of 16 msec,

which includes the 6 msec assumed for the underlying reference rock. For the lower and upper profiles, the NRC staff calculated  $\kappa_0$  values of 21 and 13 msec, respectively, using the same approach as for the basecase profile. In contrast, the licensee estimated  $\kappa_0$  by combining the low-strain damping values from the material damping curves over the top 45 m [148 ft] of soil (Profiles 1, 2, and 3) and 152 m [500 ft] of soil and rock (Profiles 4, 5, and 6) and assumed a damping ratio of 1.25 percent for the remaining deeper rock layers to estimate six  $\kappa_0$  values ranging from 9 to 38 msec.

Table 2.4-12 provides the layer depths, lithologies,  $V_s$ , unit weights, and dynamic properties for the NRC staff's three profiles. In summary, the site response logic tree developed by the NRC staff for the Palisades site consists of six alternatives; three velocity profiles (each with a different  $\kappa_0$  value) and two alternative dynamic property branches.

#### *2.4.11.2.3 Methodology and Results*

The NRC staff followed the methodology described in Section 2.1.4 to develop the final site amplification factors. Figure 2.4-44 shows the overall median site amplification factors and their variability for each of the seven spectral frequencies. As shown in Figure 2.4-44, the median site amplification factors range from about 1 to 4 before falling off with higher input spectral accelerations. The lower half of Figure 2.4-44 shows that the logarithmic standard deviations for the site amplification factors range from about 0.05 to 0.20.

#### *2.4.11.3 Control Point Hazard*

The NRC staff implemented Approach 3 from the SPID to develop a weighted control point seismic hazard curve for each of the six unique combinations of the site response logic tree for the Palisades site. After combining these curves to develop the final mean control point hazard curves, the NRC staff determined the  $10^{-4}$  and  $10^{-5}$  UHRS in order to calculate the GMRS. Figure 2.4-45 shows the final control point mean seismic hazard curves for the seven spectral frequencies, as well as the NRC staff's UHRS and GMRS and the licensee's NTTF R2.1 GMRS (Vitale, 2014). As shown in Figure 2.4-45, the NRC staff's GMRS (black curve) is similar to the licensee's (blue curve) up to about 7 Hz, above which the licensee's GMRS is moderately higher than the NRC staff's GMRS. The difference is likely due to the licensee's use of higher epistemic uncertainty (six profiles versus three profiles) in the basecase  $V_s$  profile.



**Table 2.4-12 Layer Depths, Shear Wave Velocities ( $V_s$ ), Unit Weights, and Dynamic Properties for Palisades**

Layer	Depth (ft)	Description	$V_s$ (ft/sec)			$V_s$ Sigma (ln)	BC Unit Weight (pcf)	Dynamic Properties	
			LR (0.3)	BC (0.4)	UR (0.3)			Alt. 1 (0.5)	Alt. 2 (0.5)
1	25	Soil: sand	580	750	969	0.25	120	EPRI Soil	Pen.
2	48	Soil: sand, silt	697	900	1,163	0.15	120	EPRI Soil	Pen.
3	70	Soil: clay	774	1,100	1,292	0.15	120	EPRI Soil	Pen.
4	148	Soil: sandy clay	1,238	1,600	2,068	0.15	130	EPRI Soil	Pen.
5	200	Rock: shale	3,869	5,000	6,461	0.15	140	EPRI Rock	L 3.0%
6	650	Rock: shale	5,030	6,500	8,400	0.15	150	L 0.1%	L 0.1%
7	900	Rock: shale	5,416	7,000	9,046	0.15	150	L 0.1%	L 0.1%
8	1,020	Rock: shale	6,190	8,000	9,285	0.15	160	L 0.1%	L 0.1%

LR = lower range; BC = basecase; UR = upper range; ln = natural log; pcf = pounds per cubic foot; L = linear;

Alt. = alternative; Pen. = Peninsular

For LR, BC, UR, and Alt.: Values in parentheses refer to weights for site response analysis logic tree branches

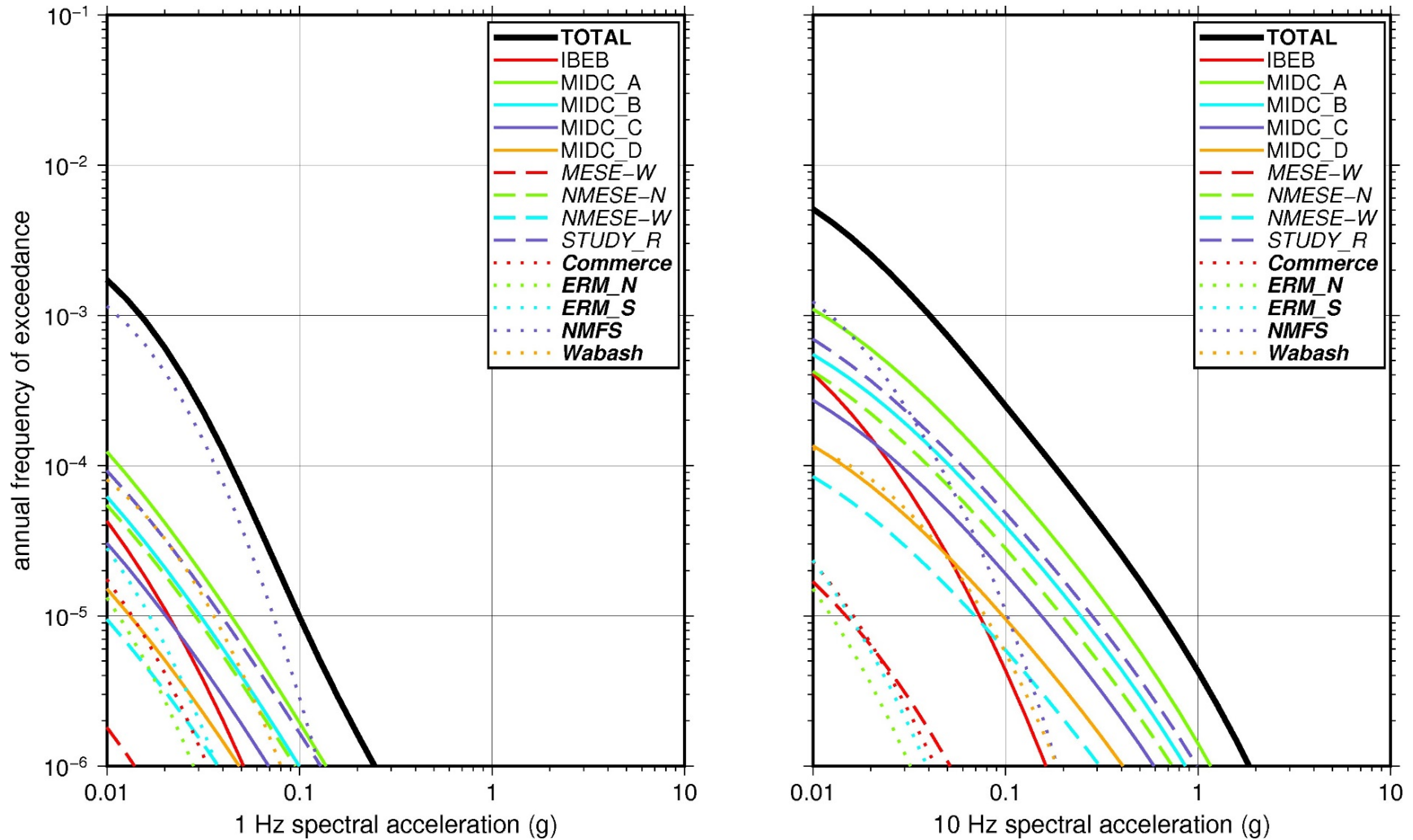


**Figure 2.4-42 Low-Frequency (1 Hz, Left), and High-Frequency (10 Hz, Right) Reference Rock Hazard Curves for Palisades. Total Hazard is Shown as a Bold Black Line; Individual Contributions to the Hazard for Each of the CEUS-SSC Sources are Shown as Colored Lines Defined in the Legend. See Table 2.1-1 for Source Name Definitions**

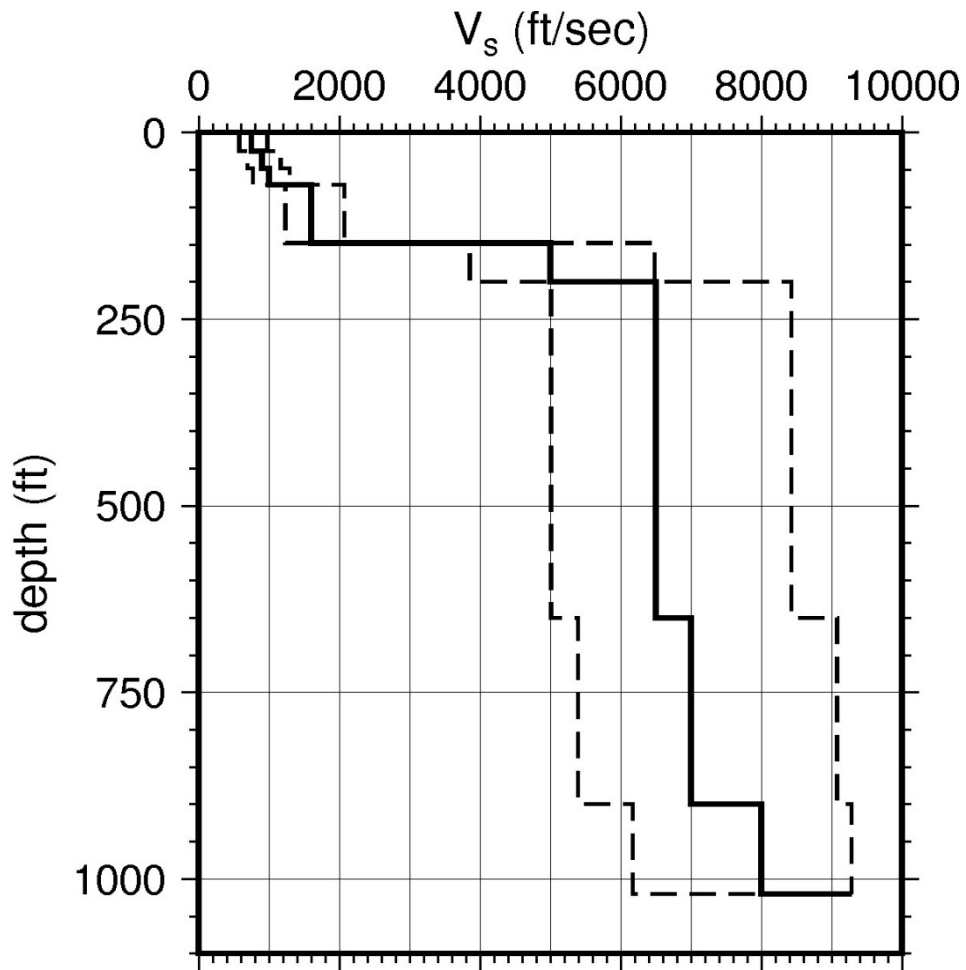


**Figure 2.4-43 Shear Wave Velocity ( $V_s$ ) Profiles for Palisades. Basecase (BC) Profile Shown as Solid Bold Line; Lower and Upper Range (LR and UR) Profiles Shown as Dashed Lines. Profiles Terminate at Reference Rock Velocity of 2,831 m/sec [9,285 ft/sec] per EPRI GMM (2013)**

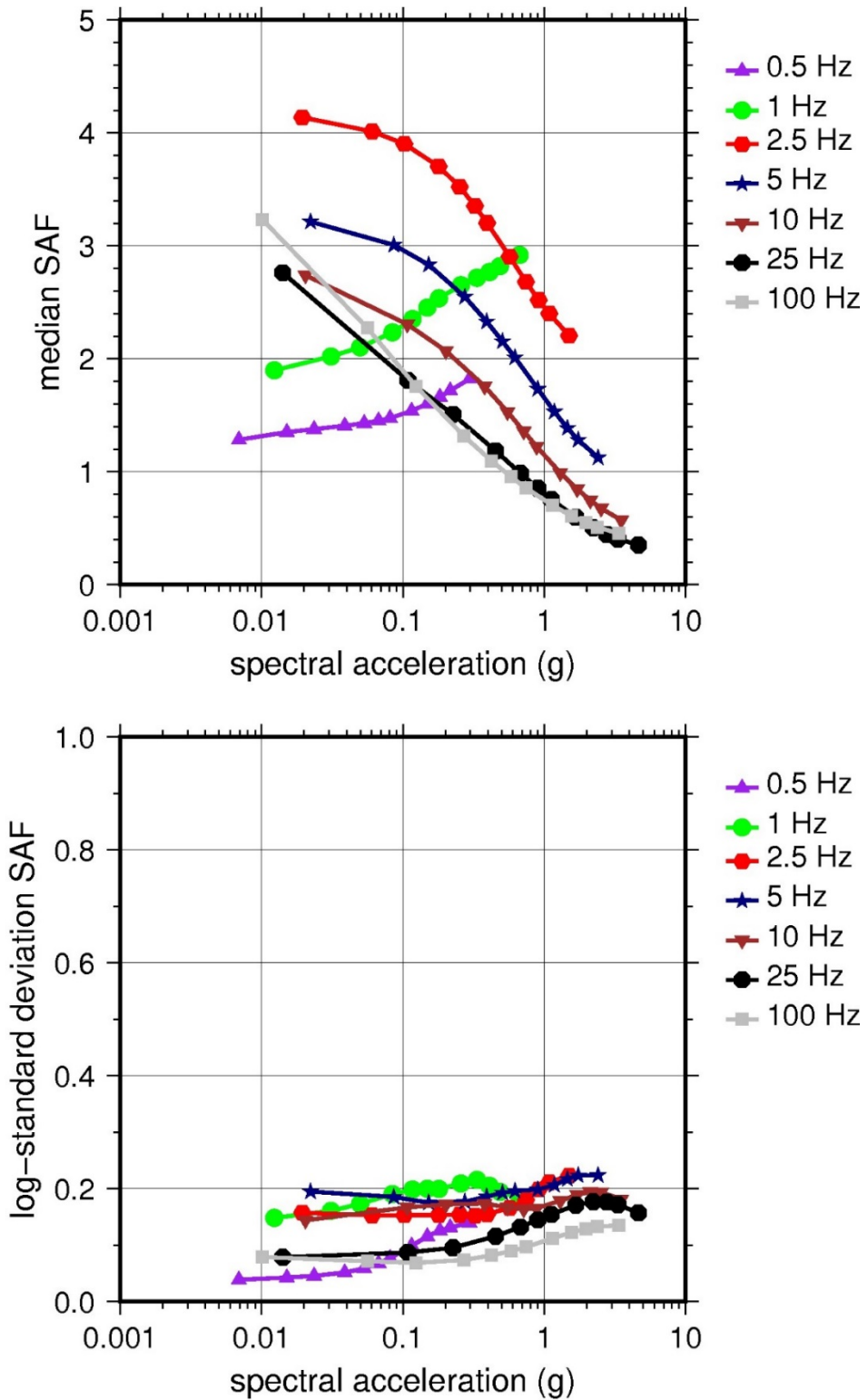


**Figure 2.4-44 Overall Weighted Median Site Amplification Factor (SAF) (Upper) and Log Standard Deviation of the SAF (Lower) as a Function of Input Acceleration for EPRI GMM (2013) Spectral Frequencies**

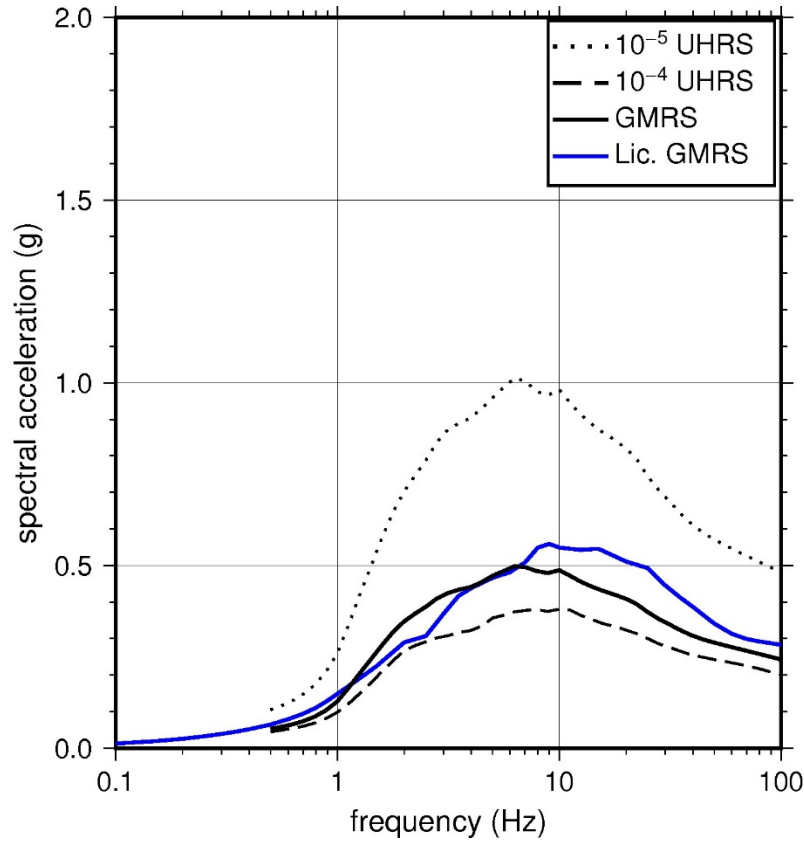
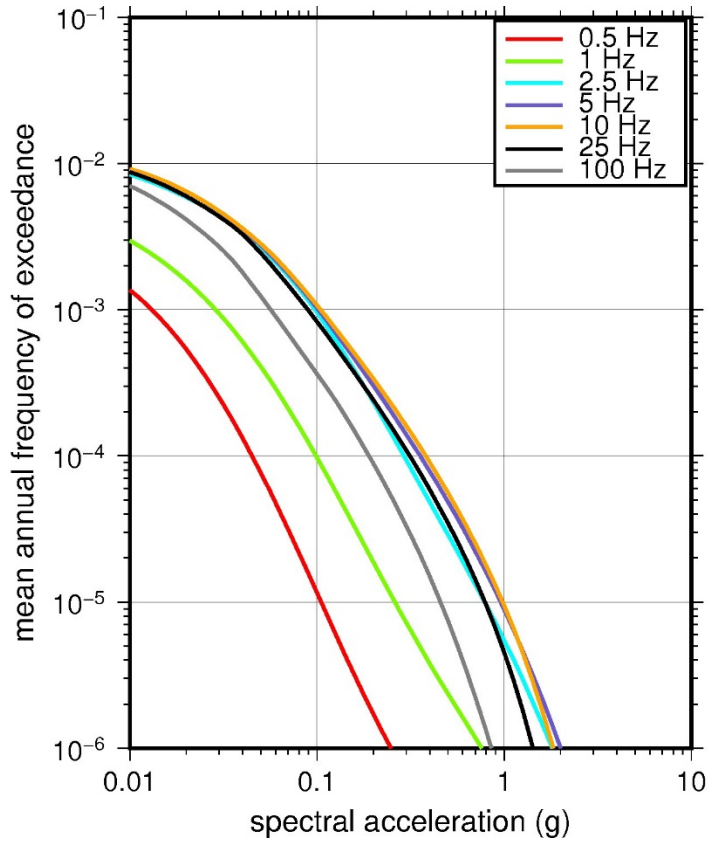


Figure 2.4-45 Mean Control Point Hazard Curves (Left) for EPRI GMM (2013) Spectral Frequencies, and GMRS and UHRS (Right) for Palisades

## 2.4.12 Perry

The Perry Nuclear Power Plant site is located in northeastern Ohio along Lake Erie within the Central Lowland physiographic province and consists of 18 m [60 ft] of soil (sandy silt and clay) overlying about 1,829 m [6,000 ft] of sedimentary rock (dolomite, shale, limestone, and sandstone). The horizontal SSE response spectrum for Perry has an RG 1.60 spectral shape and is anchored at a PGA of 0.15g.

### 2.4.12.1 Reference Rock Hazard

For the reference rock PSHA, the NRC staff selected the 10 CEUS-SSC (NRC, 2012b) background seismic source zones that are located within 323 km [200 mi] of the site. In addition, the NRC staff selected the Wabash Valley CEUS-SSC (NRC, 2012b) RLME source, which is located within 807 km [500 mi] of the site, and the NMFS RLME, which is located within 1,048 km [650 mi] of the site. To develop the reference rock seismic hazard curves for the Perry site, the NRC staff used the GMPEs developed by the updated EPRI GMM (2013). As shown in Figure 2.4-46, the NMFS RLME is the largest contributor to the 1 Hz reference rock total mean hazard curve at the  $10^{-4}$  AFE level. For the 10 Hz reference rock total mean hazard curves, the MIDC-A seismotectonic zone is the largest contributor at the  $10^{-4}$  AFE level.

### 2.4.12.2 Site Response Evaluation

#### 2.4.12.2.1 Site Profiles

To develop a basecase profile, the NRC staff used the geologic information in the NTTF R2.1 SHSR (Sena, 2014c) submitted by the FirstEnergy Nuclear Operating Company (hereafter referred to as “the licensee” within this plant section). As described in the licensee’s SHSR, the Perry site consists of 8 m [25 ft] of lacustrine deposits (sandy silt) and 9 m [30 ft] of glacial till (dense clay interspersed with rock fragments) overlying Devonian-age shales. The primary plant structures are founded in the shale bedrock. In Table 2-3 of the SHSR, the licensee briefly described the subsurface materials in terms of the geologic units and layer thicknesses. For its site response evaluation, the NRC staff used the reactor building foundation as the control point elevation for the Perry site. This control point is located at the top of rock at an elevation of 171 m [561 ft] above MSL.

The licensee’s profile is based on site investigations carried out for Perry and on geophysical data from nearby deep well logs that the licensee obtained from the Ohio Geological Survey. The site investigations included numerous borings, crosshole geophysical testing, and a seismic refraction survey that measured the  $V_P$  of the site bedrock. For the deeper rock stratigraphy and velocities, the licensee used the sonic logs from boreholes located within 6 km [4 mi] of the site. The licensee converted the  $V_P$  profiles from the sonic logs to  $V_S$  profiles using Poisson’s ratios appropriate for the rock type. Table 2-4 of the SHSR gives the estimated  $V_S$  determined from the licensee’s site investigations and related data.

The licensee’s basecase profile, which is 388 m [1,274 ft] in total thickness, begins with several layers of Devonian-age shale from the Ohio Formation (Chagrin and Huron Members) and ends at the upper Ordovician-age Queenston Formation, which is also primarily shale. Between these two shale formations are several layers of Devonian- and Silurian-age sedimentary rocks (shale, limestone, sandstone, and dolomite), with  $V_S$  values for the uppermost shale layers ranging from about 1,524 m/sec [5,000 ft/sec] to 1,890 m/sec [6,200 ft/sec]. Although the  $V_S$  values for some of the underlying limestone and dolomite layers are higher than the reference

rock velocity of 2,831 m/sec [9,285 ft/sec] assumed for the EPRI GMM (2013), the licensee extended its lower basecase profile to encompass the even deeper Silurian- and upper Ordovician-age shale and sandstone layers, which have relatively lower velocities {i.e.,  $V_S$  values of about 2,439 m/sec [8,000 ft/sec]}.

The NRC staff used the licensee's basecase profile but terminated all three of its profiles (best-estimate, lower, and upper) at a depth of 387 m [1,270 ft] below the control point elevation, which corresponds to the bottom of the Devonian-age Ohio Formation. Beneath these shale layers are several Devonian- and Silurian-age sedimentary rocks for which the licensee estimated a  $V_S$  of 2,213 m/sec [10,540 ft/sec], which exceeds the reference rock velocity. Beneath these higher velocity layers are a few hundred feet of somewhat lower velocity sedimentary rock layers with  $V_S$  values of about 2,439 m/sec [8,000 ft/sec]. Because these deeper rock layers exhibit only a minor velocity reversal relative to the upper layers, with  $V_S$  close to the reference rock velocity, the NRC staff did not extend its basecase profiles to encompass these layers.

To capture the uncertainty in its basecase profile, the NRC staff developed lower and upper range (10<sup>th</sup> and 90<sup>th</sup> percentile) profiles by multiplying the basecase  $V_S$  values by scale factors of 0.83 and 1.21, respectively, which corresponds to an epistemic logarithmic standard deviation of 0.15. The weights for the lower, basecase, and upper profiles are 0.3, 0.4, and 0.3, respectively. Figure 2.4-47 shows the NRC staff's profiles, which extend to a depth of 387 m [1,270 ft] below the control point elevation.

#### 2.4.12.2.2 Dynamic Material Properties and Site Kappa

The NRC staff assumed both linear and nonlinear dynamic behavior for the rock beneath the Perry site. To model the nonlinear behavior of the uppermost weathered rock layer (Layer 1), the NRC staff used the EPRI rock shear modulus reduction and material damping curves. To model the linear behavior of this rock layer, the NRC staff assumed a constant damping ratio of 3 percent. The staff weighted these two alternatives equally. For the underlying more intact sedimentary rock layers, the NRC staff assumed a linear dynamic response with a damping ratio of 0.5 percent to maintain consistency with the  $\kappa_0$  value for the Perry site.

To determine the basecase  $\kappa_0$  for the Perry site, the NRC staff first used the Campbell (2009) Model 1 relationship between  $V_S$  and  $Q_{ef}$  to determine a  $Q_{ef}$  for each layer. Combining these  $Q_{ef}$  values with the thickness and  $V_S$  for each layer results in a total  $\kappa_0$  value of 11 msec, which includes the 6 msec assumed for the underlying reference rock. For the lower and upper profiles, the NRC staff calculated  $\kappa_0$  values of 13 and 9 msec, respectively, using the same approach as for the basecase profile. In contrast, the licensee estimated  $\kappa_0$  by combining the low-strain damping values from the EPRI rock material damping curves over the upper 152 m [500 ft] of the profile and assumed a damping ratio of 1.25 percent for the remaining underlying rock layers to estimate basecase, lower, and upper  $\kappa_0$  values ranging from 10 to 31 msec.

Table 2.4-13 provides the layer depths, lithologies,  $V_S$ , unit weights, and dynamic properties for the NRC staff's three profiles. In summary, the site response logic tree developed by the NRC staff for the Perry site consists of six alternatives; three velocity profiles (each with a different  $\kappa_0$  value) and two alternative dynamic property branches.

### 2.4.12.2.3 Methodology and Results

The NRC staff followed the methodology described in Section 2.1.4 to develop the final site amplification factors. Figure 2.4-48 shows the overall median site amplification factors and their variability for each of the seven spectral frequencies. As shown in Figure 2.4-48, the median site amplification factors range from about 1 to 2 before falling off with higher input spectral accelerations. The lower half of Figure 2.4-48 shows that the logarithmic standard deviations for the site amplification factors range from about 0.05 to 0.15.

### 2.4.12.3 Control Point Hazard

The NRC staff implemented Approach 3 from the SPID (EPRI, 2012) to develop a weighted control point seismic hazard curve for each of the six unique combinations of the site response logic tree for the Perry site. After combining these curves to develop the final mean control point hazard curves, the NRC staff determined the  $10^{-4}$  and  $10^{-5}$  UHRS in order to calculate the GMRS. Figure 2.4-49 shows the final control point mean seismic hazard curves for the seven spectral frequencies, as well as the NRC staff's UHRS and GMRS and the licensee's NTTF R2.1 GMRS (Sena, 2014c). As shown in Figure 2.4-49, the NRC staff's GMRS (black curve) is moderately higher than the licensee's GMRS (blue curve) over the middle to upper frequency range. This is probably because the licensee used a deeper lower basecase profile, producing a higher  $\kappa_0$  value, and because the licensee used the EPRI rock curves for the upper 152 m [500 ft] of the profile. For comparison, Figure 2.4-49 also shows the NRC staff's reference rock GMRS (brown dotted curve).

**Table 2.4-13 Layer Depths, Shear Wave Velocities ( $V_s$ ), Unit Weights, and Dynamic Properties for Perry**

Layer	Depth (ft)	Description	$V_s$ (ft/sec)			$V_s$ Sigma (ln)	BC Unit Weight (pcf)	Dynamic Properties	
			LR (0.3)	BC (0.4)	UR (0.3)			Alt. 1 (0.3)	Alt. 2 (0.7)
1	51	Rock: shale	3,937	4,772	5,784	0.25	140	EPRI Rock	L 3.0%
2	169	Rock: shale	4,351	5,273	6,391	0.15	140	L 0.5%	L 0.5%
3	1031	Rock: shale	4,293	5,203	6,306	0.15	140	L 0.5%	L 0.5%
4	1270	Rock: shale	5,105	6,187	7,499	0.15	150	L 0.5%	L 0.5%

LR = lower range; BC = basecase; UR = upper range; ln = natural log; pcf = pounds per cubic foot; L = linear; Alt. = alternative.

For LR, BC, UR, and Alt.: Values in parentheses refer to weights for site response analysis logic tree branches.



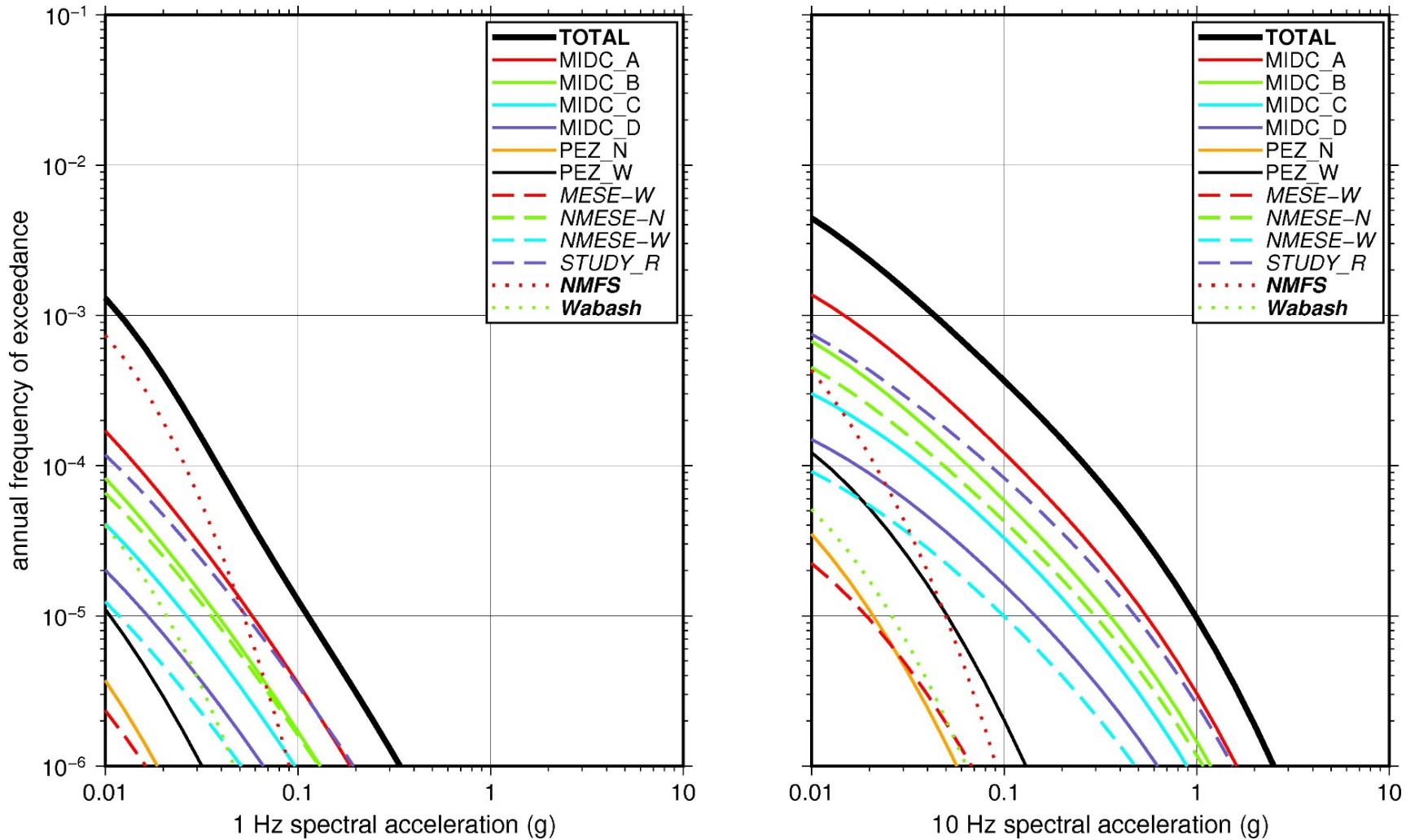


**Figure 2.4-46 Low-Frequency (1 Hz, Left), and High-Frequency (10 Hz, Right) Reference Rock Hazard Curves for Perry. Total Hazard is Shown as a Bold Black Line; Individual Contributions to the Hazard for Each of the CEUS-SSC Sources are Shown as Colored Lines Defined in the Legend. See Table 2.1-1 for Source Name Definitions**

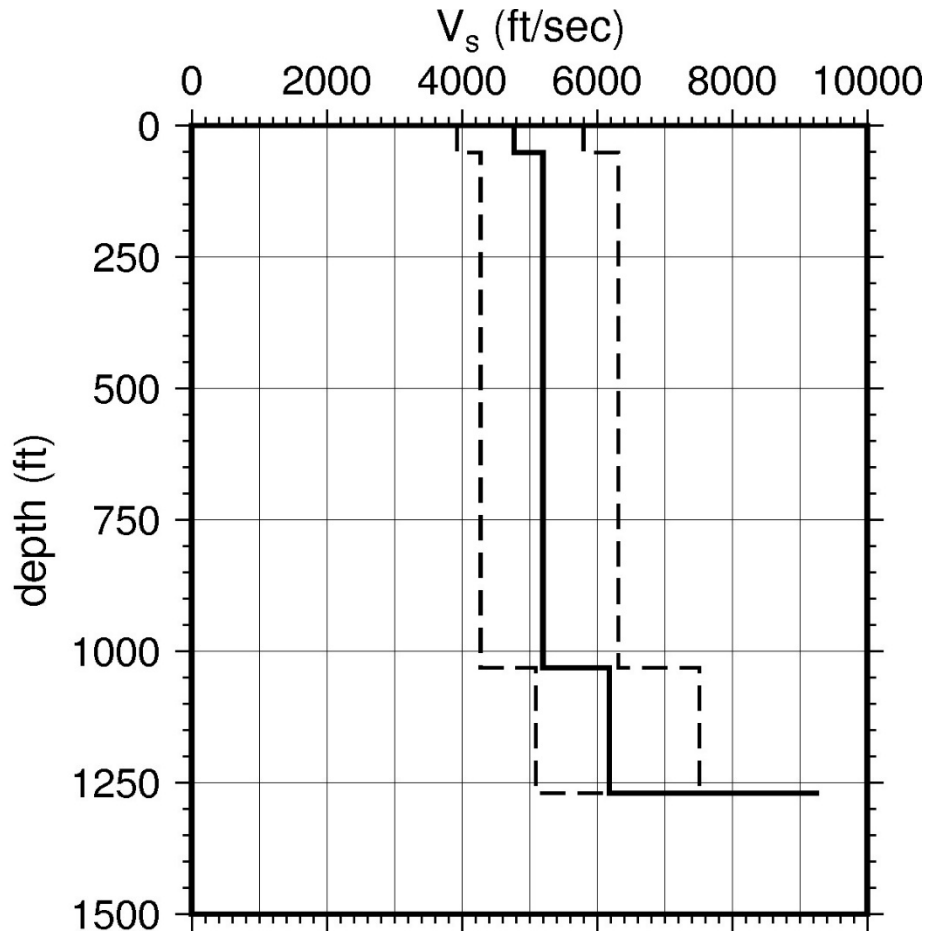


**Figure 2.4-47 Shear Wave Velocity ( $V_s$ ) Profiles for Perry. Basecase (BC) Profile Shown as Solid Bold Line; Lower and Upper Range (LR and UR) Profiles Shown as Dashed Lines. Profiles Terminate at Reference Rock Velocity of 2,831 m/sec [9,285 ft/sec] per EPRI GMM (2013)**

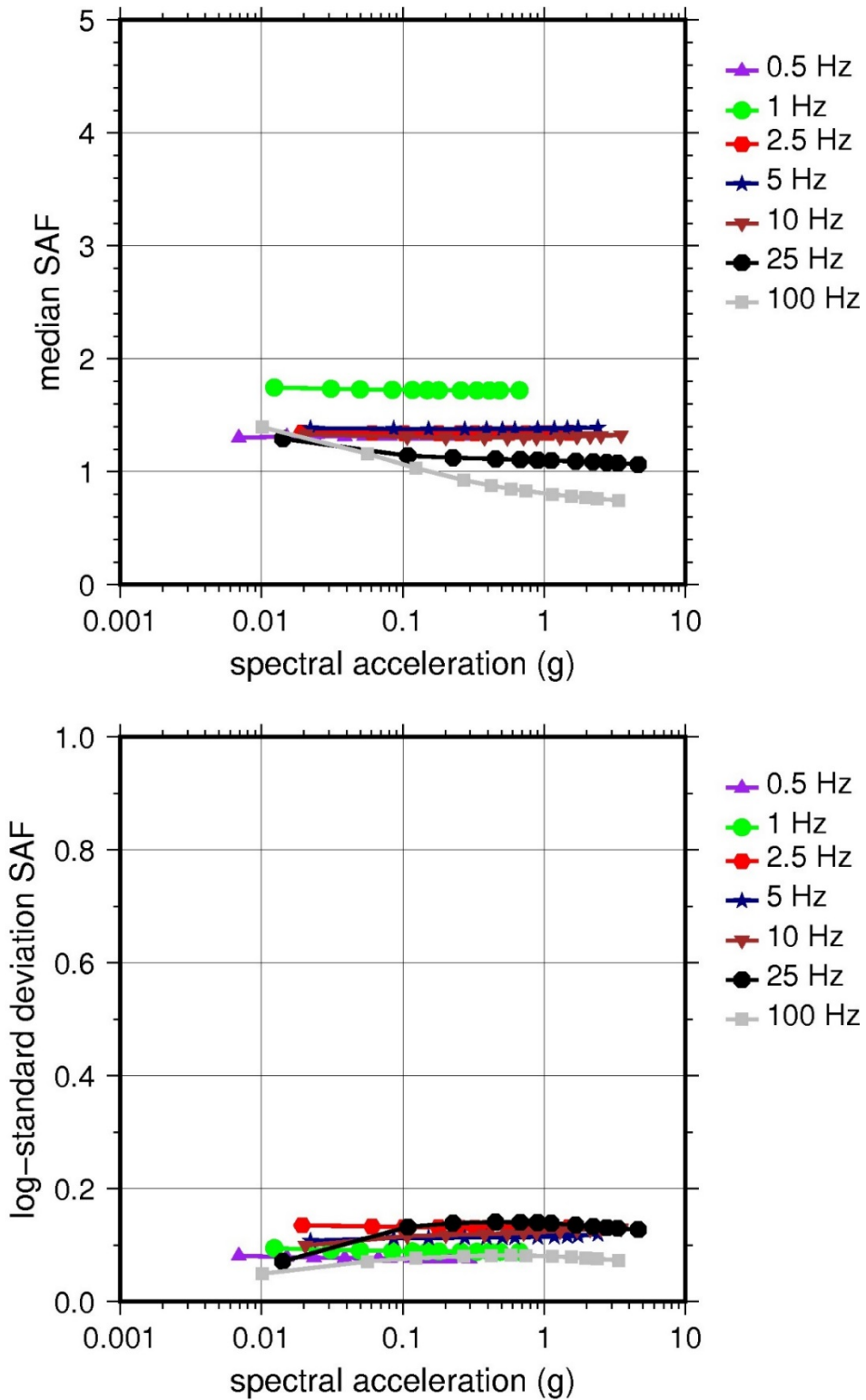


**Figure 2.4-48 Overall Weighted Median Site Amplification Factor (SAF) (Upper) and Log Standard Deviation of the SAF (Lower) as a Function of Input Acceleration for EPRI GMM (2013) Spectral Frequencies**

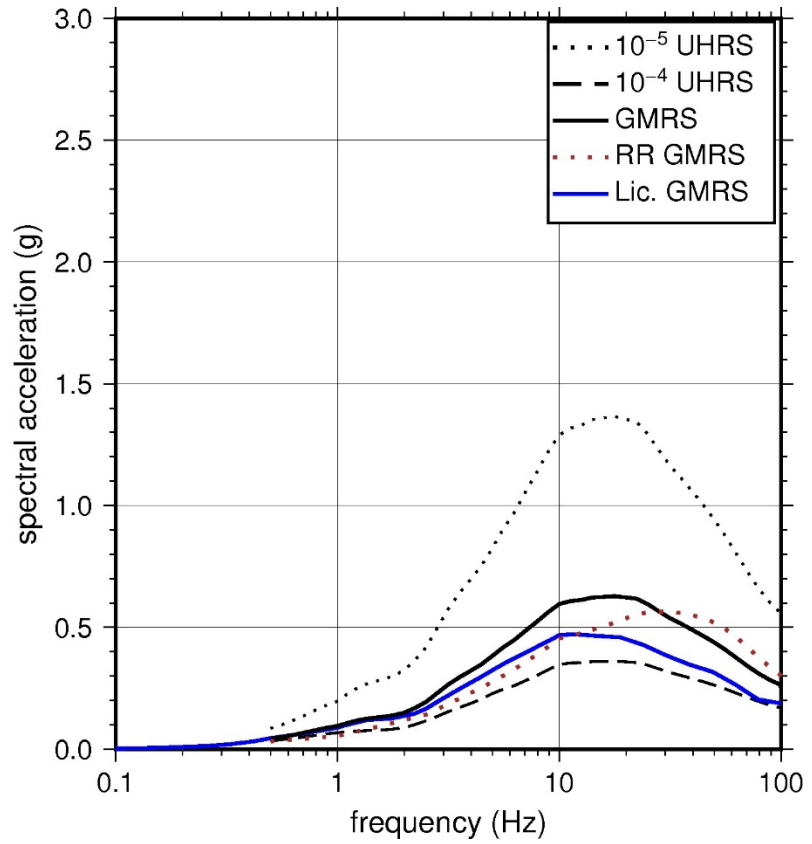
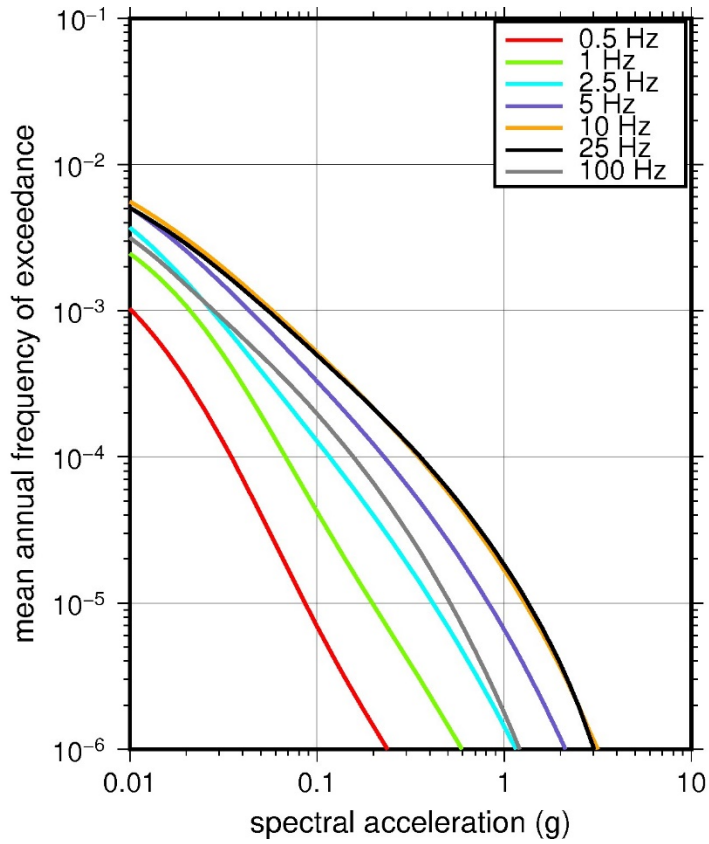


**Figure 2.4-49 Mean Control Point Hazard Curves (Left) for EPRI GMM (2013) Spectral Frequencies, and GMRS and UHRS (Right) for Perry**

### 2.4.13 Prairie Island

The Prairie Island Nuclear Generating Plant site is located in southeastern Minnesota along the Mississippi River within the Central Lowland physiographic province and consists of 43 m [180 ft] of soil (sand with gravel) overlying about 1,830 m [6,000 ft] of firm sedimentary rock (primarily sandstone). The horizontal SSE response spectrum for Prairie Island has a rounded Housner spectral shape and is anchored at a PGA of 0.12g.

#### 2.4.13.1 Reference Rock Hazard

For the reference rock PSHA, the NRC staff selected the seven CEUS-SSC (NRC, 2012b) background seismic source zones that are located within 320 km [200 mi] of the site. In addition, the NRC staff also selected the Wabash Valley and NMFS CEUS-SSC (NRC, 2012b) RLME sources, which are located within 807 km [500 mi] and 1,046 km [650 mi], respectively, of the site. To develop the reference rock seismic hazard curves for the Prairie Island site, the NRC staff used the GMPEs developed by the updated EPRI GMM (2013). As shown in Figure 2.4-50, the NMFS RLME is the largest contributor to the 1 Hz reference rock total mean hazard curves at the  $10^{-4}$  AFE level. For the 10 Hz reference rock total mean hazard curve, the MIDC-A seismotectonic zone is the largest contributor at the  $10^{-4}$  AFE level.

#### 2.4.13.2 Site Response Evaluation

##### 2.4.13.2.1 Site Profiles

To develop a basecase profile, the NRC staff used the geologic information in the NTTF R2.1 SHSR (K. Davison, 2014) submitted by the Northern States Power Company (hereafter referred to as “the licensee” within this plant section). As described in the licensee’s SHSR, the Prairie Island site consists of about 43 m [180 ft] of permeable sandy alluvium overlying Paleozoic-age sandstones. The plant structures are founded within a layer of compacted site fill, which overlies a layer of glacial till. In Table 2.3.1-1 of the SHSR, the licensee briefly described the subsurface materials in terms of the geologic units and layer thicknesses. For its site response evaluation, the NRC staff used the surface at an elevation of 211 m [692 ft] above MSL as the control point elevation for the Prairie Island site.

The licensee’s profile is based on site investigations carried out in the mid-1960s, which included numerous borings and a seismic refraction survey that measured the  $V_P$  to the top of bedrock, at a depth of about 55 m [180 ft]. To determine the  $V_S$  for each soil and rock layer, the licensee used its measured  $V_P$  with an assumed Poisson’s ratio. Table 2.3.2-1 of the SHSR gives the estimated  $V_S$  determined from the licensee’s site investigations.

The licensee’s basecase profile, which is 1,250 m [4,100 ft] in total thickness, begins with a layer of compacted fill 15 m [50 ft] thick, which is composed of fine to medium sand with gravel. Based on a measured  $V_P$  of 1,448 m/sec [4,750 ft/sec] and an assumed Poisson’s ratio of 0.37, the licensee estimated a  $V_S$  of 656 m/sec [2,150 ft/sec]. The compacted fill layer overlies 40 m [130 ft] of glacial outwash deposits (sand and gravelly sand), for which the licensee estimated a  $V_S$  of 872 m/sec [2,860 ft/sec] based on a measured  $V_P$  of 1,921 m/sec [6,300 ft/sec] and an assumed Poisson’s ratio of 0.37. The licensee identified the bedrock underlying the 55 m [180 ft] of soil as simply “Cambrian and Precambrian sandstone with minor shale horizons,” for which it estimated a  $V_S$  of 1,530 m/sec [5,020 ft/sec] based on a measured  $V_P$  of 2,805 m/sec [9,200 ft/sec] and an assumed Poisson’s ratio of 0.28. The licensee assumed a constant  $V_S$

and extended this rock layer from 55 m [180 ft] to 1,250 m [4,100 ft], at which depth it assumed the location of the reference rock horizon, with a  $V_S$  of 2,831 m/sec [9,285 ft/sec].

The NRC staff used the licensee's basecase profile for the upper 45 m [180 ft] of soil but developed a different profile for the underlying sedimentary rock layers. To augment the licensee's sedimentary rock profile, the NRC staff used several publications containing detailed stratigraphy for southeastern Minnesota (e.g., Morey, 1977; Mossler, 2008) and  $V_P$  values for specific rock formations from seismic refraction profiling in Minnesota and northwestern Wisconsin (e.g., Mooney et al., 1970). Based on the stratigraphy developed by Mossler (2008) for nearby Goodhue County, the NRC staff identified the sandstone underlying the 55 m [180 ft] of soil as the lower Cambrian-age Lone Rock, Wonewoc, Eau Clair, and Mt. Simon Formations (formerly known as the Franconia and Dresbach Formations). The NRC staff used the licensee's estimated  $V_S$  of about 1,524 m/sec [5,000 ft/sec] for this Cambrian-age sandstone layer, as it matches the  $V_S$  that the NRC staff estimated from the  $V_P$  of 2,896 m/sec [9,500 ft/sec] measured by Mooney et al. (1970) from nearby seismic profiles (Lines 81 and 90), with an assumed Poisson's ratio of 0.30. The NRC staff used a velocity gradient of 0.5 m/sec/m [0.5 ft/sec/ft] for this sandstone layer and assumed a total thickness of 95 m [310 ft] based on Mossler (2008). Underlying this Cambrian-age sandstone are the Precambrian-age sedimentary rock formations of the Keweenaw Supergroup, which consist of the Hinckley (sandstone), Fond du Lac (shale and sandstone), and Solor Church (sandstone, siltstone, and shale) Formations (Morey, 1977). Mooney et al. (1970) measured a  $V_P$  of about 3,963 m/sec [13,000 ft/sec] for what it referred to as "Keweenaw Sandstones" from numerous seismic refraction profiles in the region surrounding the site. On seismic refraction Lines 81 and 90, which are closest to the site, Mooney et al. (1970) measured a  $V_P$  of 5,183 m [17,000 ft/sec] at a depth of 1,860 m [6,100 ft], which they assumed to be igneous basement rock. Based on these seismic refraction measurements, the NRC staff subdivided the Precambrian sedimentary rock strata into six layers that extend from a depth of 189 m [620 ft] to a depth of 1,860 m [5,317 ft]. Assuming a Poisson's ratio of 0.25 and a velocity gradient of 0.5 m/sec/m [0.5 ft/sec/ft], the  $V_S$  values for these six layers gradually increase from 2,287 m/sec [7,500 ft/sec] for the top layer to 2,788 m/sec [9,144 ft/sec] for the bottom layer.

To capture the uncertainty in its basecase profile, the NRC staff developed lower and upper range (10<sup>th</sup> and 90<sup>th</sup> percentile) profiles by multiplying the basecase  $V_S$  values by scale factors of 0.78 and 1.29, respectively, which corresponds to an epistemic logarithmic standard deviation of 0.20. The weights for the lower, basecase, and upper profiles are 0.3, 0.4, and 0.3, respectively. Figure 2.4-51 shows the NRC staff's profiles. As shown in Figure 2.4-51, the lower and best-estimate basecase profiles extend to a depth of 1,860 m [5,317 ft] below the control point elevation, while the upper basecase profile terminates at a depth of 189 m [620 ft].

#### 2.4.13.2.2 *Dynamic Material Properties and Site Kappa*

The NRC staff assumed both linear and nonlinear dynamic behavior for the soil and rock beneath the Prairie Island site. To model the nonlinear behavior of the soil layers (Layers 1–2), the NRC staff used the EPRI soil and Peninsular Range shear modulus reduction and material damping curves as two equally weighted alternatives. For the weathered rock layers (Layers 3–4), the NRC staff used the EPRI rock shear modulus reduction and material damping curves. To model the linear behavior of these rock layers, the NRC staff assumed a constant damping ratio of 3 percent. The staff weighted these two alternatives equally. For the underlying more intact sedimentary rock, the NRC staff assumed a linear dynamic response with a material damping ratio of 0.1 percent to maintain consistency with the  $\kappa_0$  value for the Prairie Island site.

To determine the basecase  $\kappa_0$  for the Prairie Island site, the NRC staff first used the Campbell (2009) Model 1 relationship between  $V_S$  and  $Q_{ef}$  to determine a  $Q_{ef}$  for each layer. Combining these  $Q_{ef}$  values with the thickness and  $V_S$  for each layer results in a total  $\kappa_0$  value of 18 msec, which includes the 6 msec assumed for the underlying reference rock. For the lower and upper profiles, the NRC staff calculated  $\kappa_0$  values of 25 and 9 msec, respectively, using the same approach as for the basecase profile. In contrast, the licensee estimated  $\kappa_0$  by combining the low-strain damping values from the material damping curves over the top 55 m [180 ft] of soil and 152 m [500 ft] of rock and assumed a damping ratio of 1.25 percent for the deeper rock layers to estimate basecase, lower, and upper  $\kappa_0$  values of 30, 40, and 21 msec, respectively.

Table 2.4-14 provides the layer depths, lithologies,  $V_S$ , unit weights, and dynamic properties for the NRC staff's three profiles. In summary, the site response logic tree developed by the NRC staff for the Prairie Island site consists of six alternatives; three velocity profiles (each with a different  $\kappa_0$  value) and two alternative dynamic property branches.

#### *2.4.13.2.3 Methodology and Results*

The NRC staff followed the methodology described in Section 2.1.4 to develop the final site amplification factors. Figure 2.4-52 shows the overall median site amplification factors and their variability for each of the seven spectral frequencies. As shown in Figure 2.4-52, the median site amplification factors range from about 1 to 2 before falling off with higher input spectral accelerations. The lower half of Figure 2.4-52 shows that the logarithmic standard deviations for the site amplification factors range from about 0.05 to 0.20.

#### *2.4.13.3 Control Point Hazard*

The NRC staff implemented Approach 3 from the SPID to develop a weighted control point seismic hazard curve for each of the six unique combinations of the site response logic tree for the Prairie Island site. After combining these curves to develop the final mean control point hazard curves, the NRC staff determined the  $10^{-4}$  and  $10^{-5}$  UHRS in order to calculate the GMRS. Figure 2.4-53 shows the final control point mean seismic hazard curves for the seven spectral frequencies, as well as the NRC staff's UHRS and GMRS and the licensee's NTTF R2.1 GMRS (K. Davison, 2014). As shown in Figure 2.4-53, the NRC staff's GMRS (black curve) is moderately higher than licensee's GMRS (blue curve), because the licensee estimated higher  $\kappa_0$  values.

**Table 2.4-14 Layer Depths, Shear Wave Velocities ( $V_s$ ), Unit Weights, and Dynamic Properties for Prairie Island**

Layer	Depth (ft)	Description	$V_s$ (ft/sec)			$V_s$ Sigma (ln)	BC Unit Weight (pcf)	Dynamic Properties	
			LR (0.3)	BC (0.4)	UR (0.3)			Alt. 1 (0.5)	Alt. 2 (0.5)
1	50	Soil: sand with gravel	1,664	2,150	2,778	0.25	130	EPRI Soil	Pen.
2	180	Soil: sand with gravel	2,213	2,860	3,696	0.15	130	EPRI Soil	Pen.
3	310	Rock: sandstone	3,869	5,000	6,461	0.15	140	EPRI Rock	L 3.0%
4	360	Rock: sandstone	3,889	5,025	6,494	0.15	140	EPRI Rock	L 3.0%
5	420	Rock: sandstone	3,912	5,055	6,532	0.15	140	L 0.1%	L 0.1%
6	620	Rock: sandstone	3,989	5,155	6,662	0.15	140	L 0.1%	L 0.1%
7	1,402	Rock: sandstone, shale, siltstone	5,804	7,500	9,285	0.15	160	L 0.1%	L 0.1%
8	2,185	Rock: sandstone, shale, siltstone	6,058	7,828	9,285	0.15	160	L 0.1%	L 0.1%
9	2,968	Rock: sandstone, shale, siltstone	6,312	8,157	9,285	0.15	160	L 0.1%	L 0.1%
10	3,751	Rock: sandstone, shale, siltstone	6,567	8,486	9,285	0.15	160	L 0.1%	L 0.1%
11	4,534	Rock: sandstone, shale, siltstone	6,821	8,815	9,285	0.15	160	L 0.1%	L 0.1%
12	5,317	Rock: sandstone, shale, siltstone	7,075	9,144	9,285	0.15	160	L 0.1%	L 0.1%

LR = lower range; BC = basecase; UR = upper range; ln = natural log; pcf = pounds per cubic foot; L = linear; Alt. = alternative; Pen. = Peninsular.

For LR, BC, UR, and Alt.: Values in parentheses refer to weights for site response analysis logic tree branches.



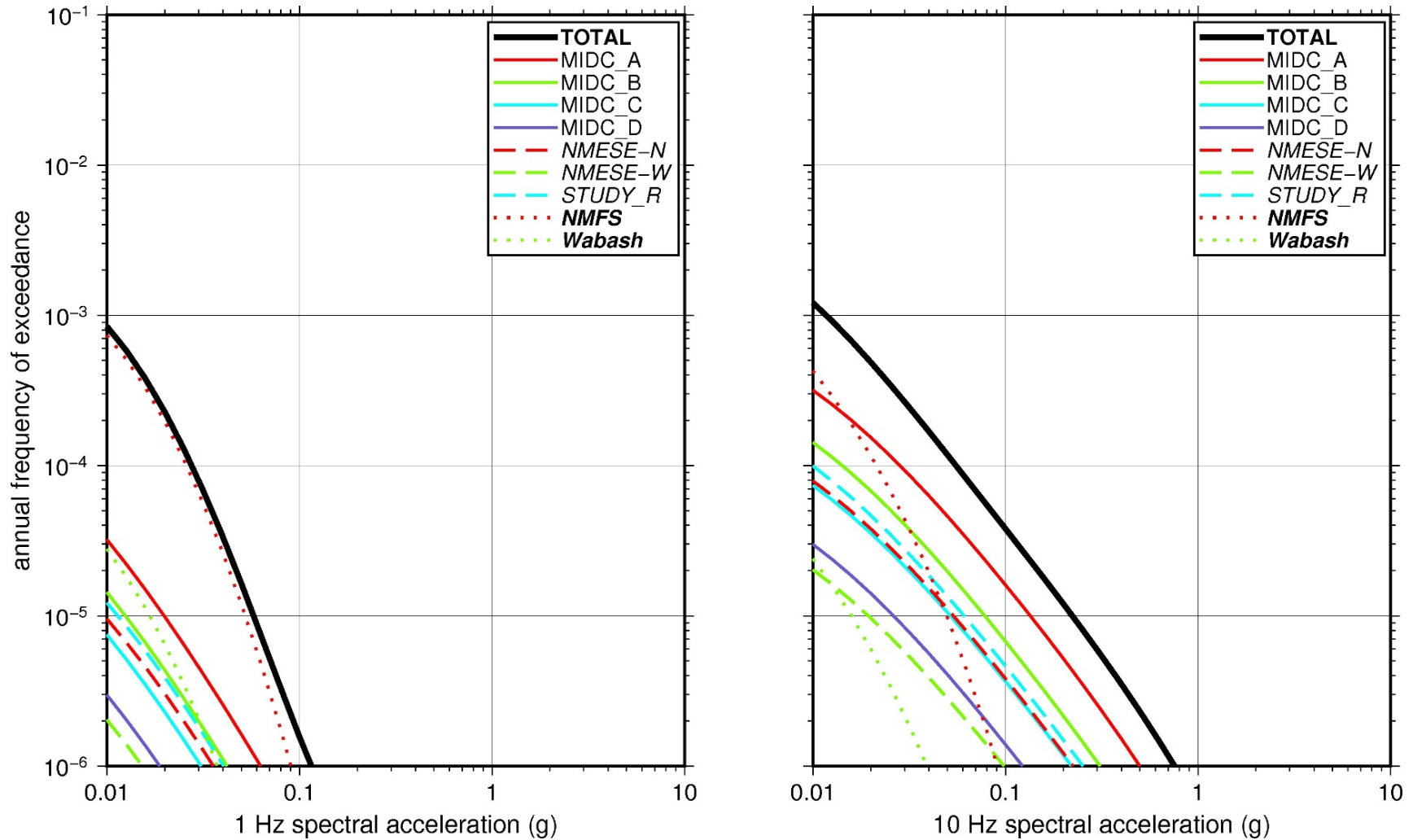


**Figure 2.4-50 Low-Frequency (1 Hz, Left), and High-Frequency (10 Hz, Right) Reference Rock Hazard Curves for Prairie Island. Total Hazard is Shown as a Bold Black Line; Individual Contributions to the Hazard for Each of the CEUS-SSC Sources are Shown as Colored Lines Defined in the Legend. See Table 2.1-1 for Source Name Definitions**

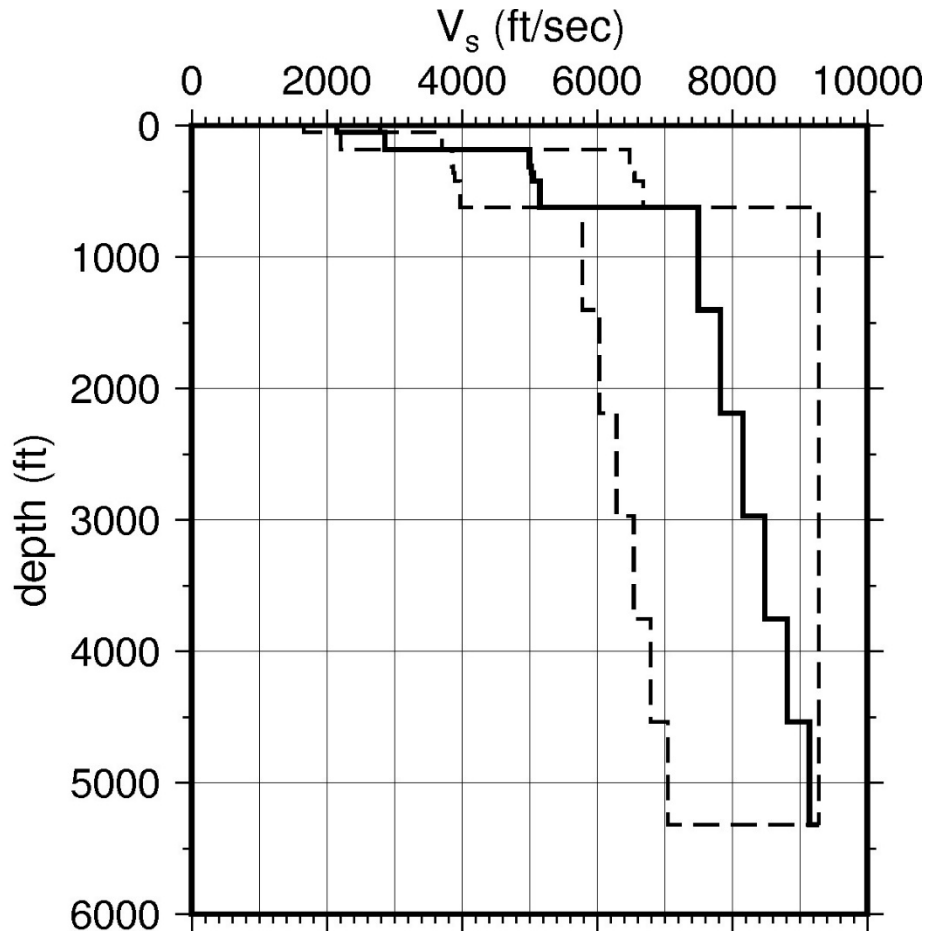


**Figure 2.4-51 Shear Wave Velocity ( $V_s$ ) Profiles for Prairie Island. Basecase (BC) Profile Shown as Solid Bold Line; Lower and Upper Range (LR and UR) Profiles Shown as Dashed Lines. Profiles Terminate at Reference Rock Velocity of 2,831 m/sec [9,285 ft/sec] per EPRI GMM (2013)**

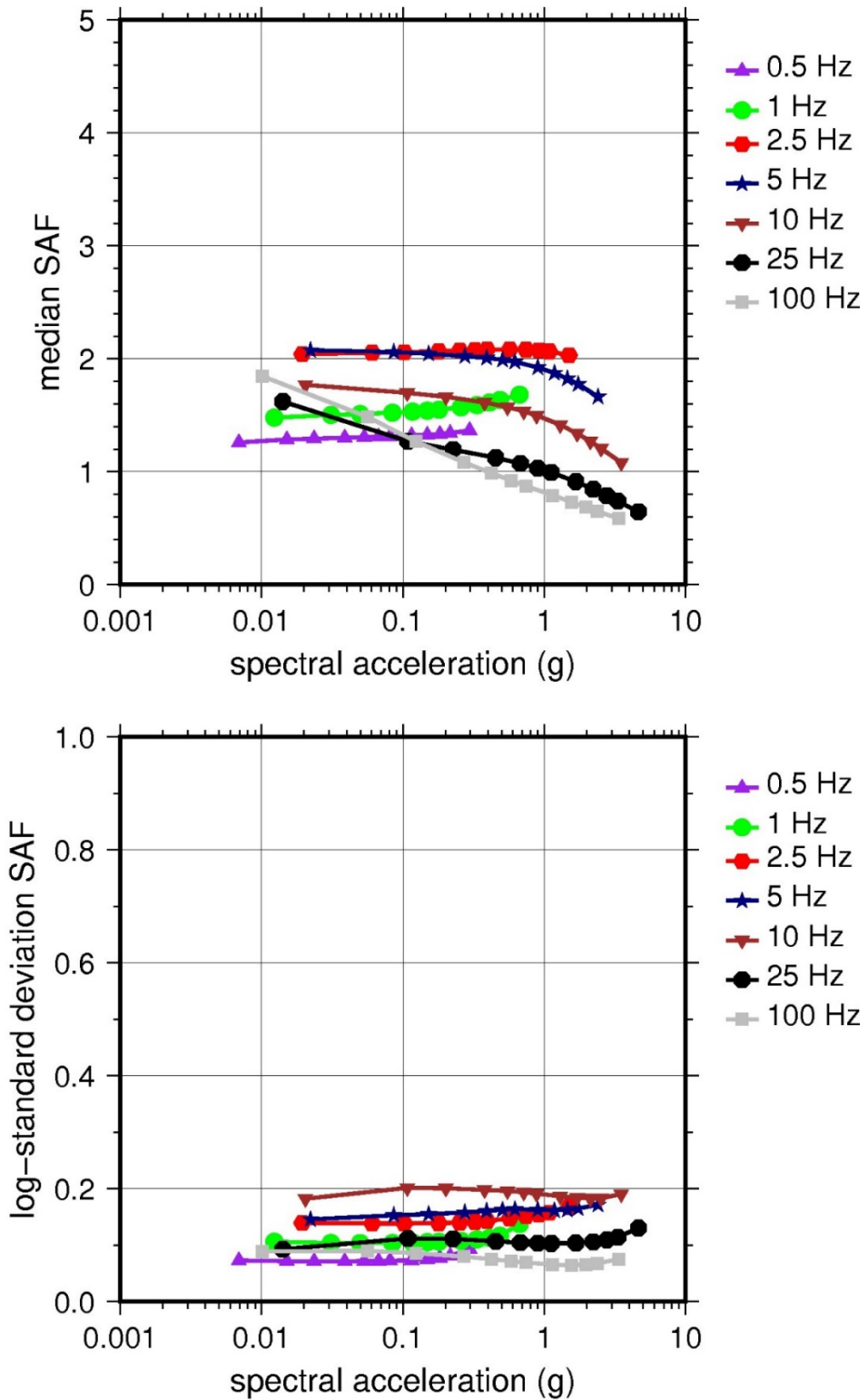


**Figure 2.4-52 Overall Weighted Median Site Amplification Factor (SAF) (Upper) and Log Standard Deviation of the SAF (Lower) as a Function of Input Acceleration for EPRI GMM (2013) Spectral Frequencies**

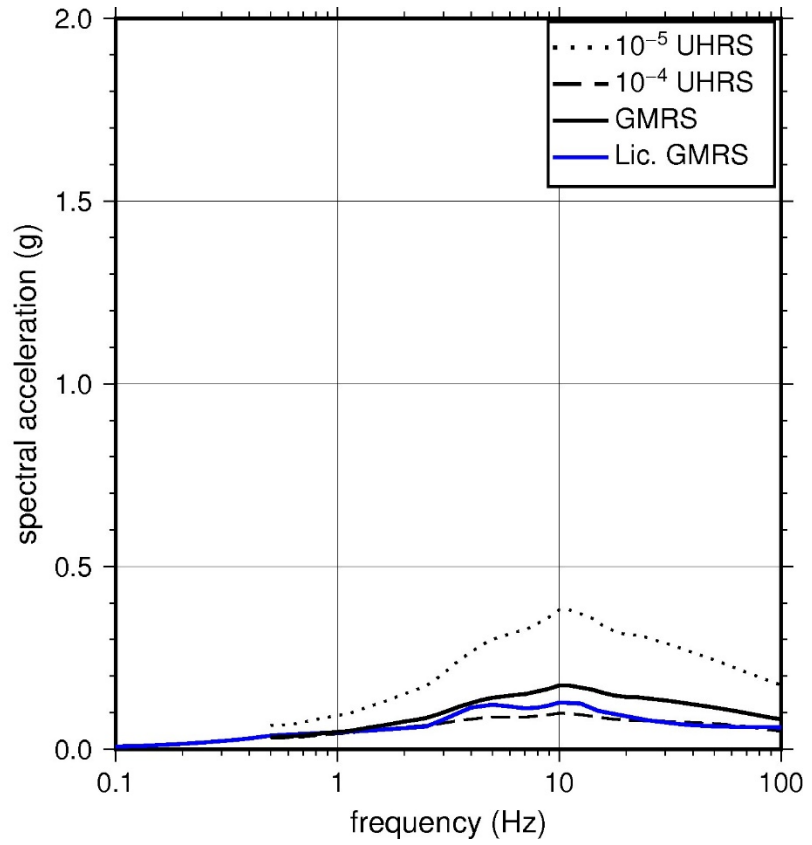
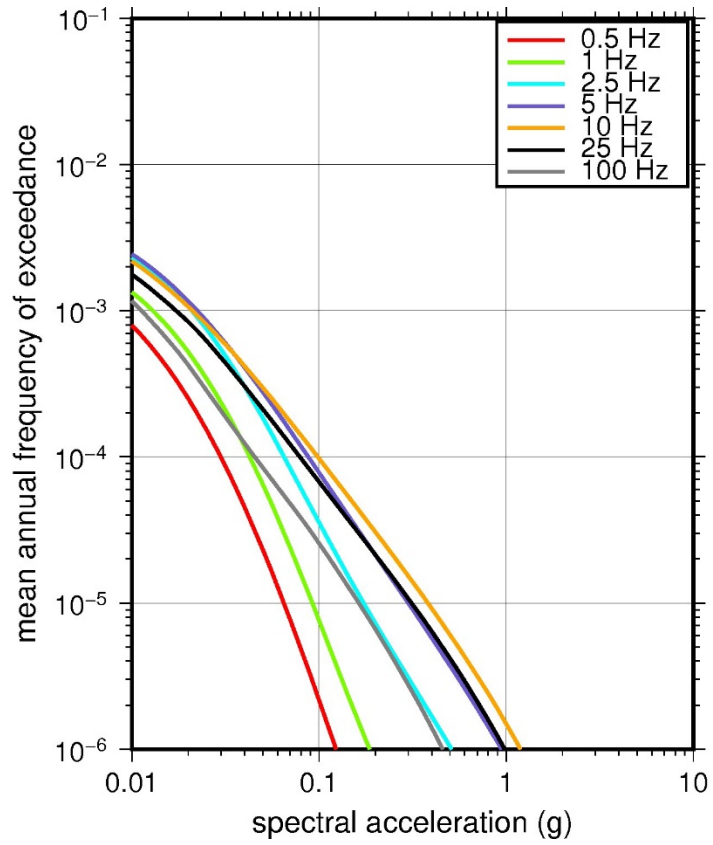


**Figure 2.4-53 Mean Control Point Hazard Curves (Left) for EPRI GMM (2013) Spectral Frequencies, and GMRS and UHRS (Right) for Prairie Island**

## 2.4.14 Point Beach

The Point Beach Nuclear Plant site is located in eastern Wisconsin along Lake Michigan within the Central Lowland physiographic province and consists of 26 m [85 ft] of soil (silty clay with sand) overlying about 457 m [1,500 ft] of sedimentary rock (dolomite, shale, and sandstone). The horizontal SSE response spectrum for Point Beach is a smoothed interpolation of the response spectrum from the N86°E Olympia Highway Test Office recording of the 1949 *M*6.7 earthquake in Olympia, WA. The SSE is anchored at a PGA of 0.06g.

### 2.4.14.1 Reference Rock Hazard

For the reference rock PSHA, the NRC staff selected the nine CEUS-SSC (NRC, 2012b) background seismic source zones that are located within 320 km [200 mi] of the site. In addition, the NRC staff selected the CEUS-SSC (NRC, 2012b) Commerce fault zone and Wabash Valley RLME sources, which are located within 807 km [500 mi] of the site; and the NMFS RLME source, which is located within 1,048 km [650 mi] of the site. To develop the reference rock seismic hazard curves for the Point Beach site, the NRC staff used the GMPEs developed by the updated EPRI GMM (2013). As shown in Figure 2.4-54, the NMFS RLME is the largest contributor to the 1 Hz reference rock total mean hazard curve at the  $10^{-4}$  AFE level. For the 10 Hz reference rock total mean hazard curve, the MIDC-A seismotectonic zone is the largest contributor at the  $10^{-4}$  AFE level.

### 2.4.14.2 Site Response Evaluation

#### 2.4.14.2.1 Site Profiles

To develop a basecase profile, the NRC staff used the geologic information in the NTTF R2.1 SHSR (McCartney, 2014) submitted by NextEra Energy Point Beach (hereafter referred to as “the licensee” within this plant section). As described in the licensee’s SHSR, the Point Beach site consists of 26 m [85 ft] of glacial till, outwash, and lacustrine deposits overlying Paleozoic-age sedimentary rock. The primary plant structures are founded on these soil deposits, which overlie dolomite bedrock. In Table 2.3.1-1 of the SHSR, the licensee briefly described the subsurface materials in terms of the geologic units and layer thicknesses. For its site response evaluation, the NRC staff used the highest foundation of key safety-related structures as the control point elevation for the Point Beach site. This control point is located at a depth of 6 m [18 ft] below the plant surface at an elevation of 178 m [585 ft] above MSL and is within the glacial till.

The licensee’s profile is based on site investigations carried out in the 1960s, which included numerous borings. To determine the  $V_S$  for the upper 25 m [83 ft] of the profile, the licensee used estimates that it developed for the Point Beach Individual Plant Examination of External Events (Point Beach Nuclear Plant, 1995). Table 2.3.2-1 of the SHSR gives the estimated  $V_S$  determined from the licensee’s site investigations.

The licensee’s basecase profile, which is 25 m [83 ft] in total thickness, consists of several soil layers of silty clay with sand. The licensee estimated a  $V_S$  of 274 m/sec [900 ft/sec] for the top 10 m [33 ft] of its profile and 305 m/sec [1,000 ft/sec] for the remaining 15 m [50 ft] of the profile. For the underlying Silurian-age dolomites of the Niagara Escarpment, the licensee assumed the reference rock  $V_S$  of 2,831 m/sec [9,285 ft/sec].

To augment the licensee's soil and rock subsurface profile, the NRC staff used several publications containing detailed stratigraphy for eastern Wisconsin (e.g., Harris et al., 1998; Luczaj, 2013) and  $V_P$  values for nearby near-surface glacial till and rock (Hart, 2011). Based on typical  $V_S$  values for fairly stiff glacial tills at other Region III sites, the NRC staff assumed a  $V_S$  of 305 m [1,000 ft/sec] for the upper 10 m [33 ft] of soil. For the underlying 15 m [50 ft] of stiffer glacial till, the NRC staff estimated a  $V_S$  of 762 m/sec [2,500 ft/sec], based on the measured  $V_P$  of about 1,524 m/sec [5,000 ft/sec] from Hart (2011) for stiff tills in nearby Calumet County, WI, and an assumed Poisson's ratio of 0.33. Hart (2011) measured  $V_P$  values of about 3,659 m/sec [12,000 ft/sec] for the weathered Silurian-age dolomites beneath the glacial till and about 4,572 m/sec [15,000 ft/sec] for the deeper, more intact dolomites. Assuming a Poisson's ratio of 0.27, the NRC staff estimated  $V_S$  values of 2,043 m/sec [6,700 ft/sec] and 2,561 m/sec [8,400 ft/sec], respectively, for these two rock layers. Based on the stratigraphy described in Luczaj (2013), the NRC staff assumed a thickness of 78 m [257 ft] for the Niagara Escarpment in eastern Wisconsin (i.e., the eastern end of the cross section shown in Figure 6 in Luczaj, 2013). Similarly, based on Luczaj (2013), the NRC staff assumed thicknesses of 128 m [420 ft] for the underlying Ordovician-age Maquoketa Formation shale layer and 79 m [260 ft] for the underlying Ordovician-age Sinipee Group (Galena and Platteville Formations) dolomite. The rest of the NRC staff's basecase profile consists of 37 m [120 ft] of sandstone from the Ordovician St. Peter Formation. To estimate  $V_S$  for these deeper sedimentary layers, the NRC staff used geotechnical data in Bauer et al. (1991) on the parts of these rock formations located in northeastern Illinois. Specifically, the NRC staff assumed  $V_S$  values of 1,677 m/sec [5,500 ft/sec] for the Maquoketa Formation shale layer and 1,988 m/sec [6,520 ft/sec] for the St. Peter Formation sandstone. Based on the profiles for other Region III sites (e.g., Clinton), the NRC staff assumed that the middle and lower Ordovician-age dolomites (Sinipee and Prairie du Chien Groups) and the deeper Cambrian-age strata have  $V_S$  values that exceed the reference rock  $V_S$  of 2,831 m/sec [9,285 ft/sec].

To capture the uncertainty in its basecase profile, the NRC staff developed lower and upper range (10<sup>th</sup> and 90<sup>th</sup> percentile) profiles by multiplying the basecase  $V_S$  values by scale factors of 0.78 and 1.29, respectively, which corresponds to an epistemic logarithmic standard deviation of 0.20. The weights for the lower, basecase, and upper profiles are 0.3, 0.4, and 0.3, respectively. Figure 2.4-55 shows the NRC staff's profiles, which extend to a depth of 348 m [1,140 ft] below the control point elevation.

#### 2.4.14.2.2 *Dynamic Material Properties and Site Kappa*

The NRC staff assumed both linear and nonlinear dynamic behavior for the soil and rock beneath the Point Beach site. To model the nonlinear behavior of the soil layers (Layers 1–2), the NRC staff used the EPRI soil and Peninsular Range shear modulus reduction and material damping curves as two equally weighted alternatives. For the weathered rock layer (Layer 3), the NRC staff used the EPRI rock shear modulus reduction and material damping curves. To model the linear behavior of this rock layer, the NRC staff assumed a constant damping ratio of 3 percent. The staff weighted these two alternatives equally. For the underlying more intact sedimentary rock layers, the NRC staff assumed a linear dynamic response with a material damping ratio of 0.1 percent to maintain consistency with the  $\kappa_0$  value for the Point Beach site.

To determine the basecase  $\kappa_0$  for the Point Beach site, the NRC staff first used the Campbell (2009) Model 1 relationship between  $V_S$  and  $Q_{ef}$  to determine a  $Q_{ef}$  for each layer. Combining these  $Q_{ef}$  values with the thickness and  $V_S$  for each layer results in a total  $\kappa_0$  value of 11 msec, which includes the 6 msec assumed for the underlying reference rock. For the lower and upper profiles, the NRC staff calculated  $\kappa_0$  values of 14 and 10 msec, respectively, using the same

approach as for the basecase profile. In contrast, the licensee estimated  $\kappa_0$  by combining the low-strain damping values from the material damping curves over the 34 m [83 ft] of soil to estimate basecase, lower, and upper  $\kappa_0$  values of 8, 9, and 7 msec, respectively.

Table 2.4-15 provides the layer depths, lithologies,  $V_S$ , unit weights, and dynamic properties for the NRC staff's three profiles. In summary, the site response logic tree developed by the NRC staff for the Point Beach site consists of six alternatives; three velocity profiles (each with a different  $\kappa_0$  value) and two alternative dynamic property branches.

#### *2.4.14.2.3 Methodology and Results*

The NRC staff followed the methodology described in Section 2.1.4 to develop the final site amplification factors. Figure 2.4-56 shows the overall median site amplification factors and their variability for each of the seven spectral frequencies. As shown in Figure 2.4-56, the median site amplification factors range from about 1 to 3 before falling off with higher input spectral accelerations. The lower half of Figure 2.4-56 shows that the logarithmic standard deviations for the site amplification factors range from about 0.05 to 0.40.

#### *2.4.14.3 Control Point Hazard*

The NRC staff implemented Approach 3 from the SPID to develop a weighted control point seismic hazard curve for each of the six unique combinations of the site response logic tree for the Point Beach site. After combining these curves to develop the final mean control point hazard curves, the NRC staff determined the  $10^{-4}$  and  $10^{-5}$  UHRS in order to calculate the GMRS. Figure 2.4-57 shows the final control point mean seismic hazard curves for the seven spectral frequencies, as well as the NRC staff's UHRS and GMRS and the licensee's NTTF R2.1 GMRS (McCartney, 2014). As shown in Figure 2.4-57, the NRC staff's GMRS (black curve) is moderately lower than the licensee's (blue curve) over the frequency range from 1 to 4 Hz and slightly higher than the licensee's for the remaining frequencies (4 to 100 Hz).

**Table 2.4-15 Layer Depths, Shear Wave Velocities ( $V_s$ ), Unit Weights, and Dynamic Properties for Point Beach**

Layer	Depth (ft)	Description	$V_s$ (ft/sec)			$V_s$ Sigma (ln)	BC Unit Weight (pcf)	Dynamic Properties	
			LR (0.3)	BC (0.4)	UR (0.3)			Alt. 1 (0.5)	Alt. 2 (0.5)
1	33	Soil: silty clay with sand	774	1,000	1,292	0.25	120	EPRI Soil	Pen.
2	83	Soil: silty clay with sand	1,935	2,500	3,231	0.15	130	EPRI Soil	Pen.
3	133	Rock: dolomite	5,185	6,700	8,658	0.15	150	EPRI Rock	L 3.0%
4	340	Rock: dolomite	6,500	8,400	9,285	0.15	160	L 0.1%	L 0.1%
5	760	Rock: shale	4,256	5,500	7,108	0.15	150	L 0.1%	L 0.1%
6	1,020	Rock: dolomite	7,185	9,285	9,285	0.15	160	L 0.1%	L 0.1%
7	1,140	Rock: sandstone	5,045	6,520	8,426	0.15	150	L 0.1%	L 0.1%

LR = lower range; BC = basecase; UR = upper range; ln = natural log; pcf = pounds per cubic foot; L = linear; Alt. = alternative; Pen. = Peninsular.  
 For LR, BC, UR, and Alt.: Values in parentheses refer to weights for site response analysis logic tree branches.



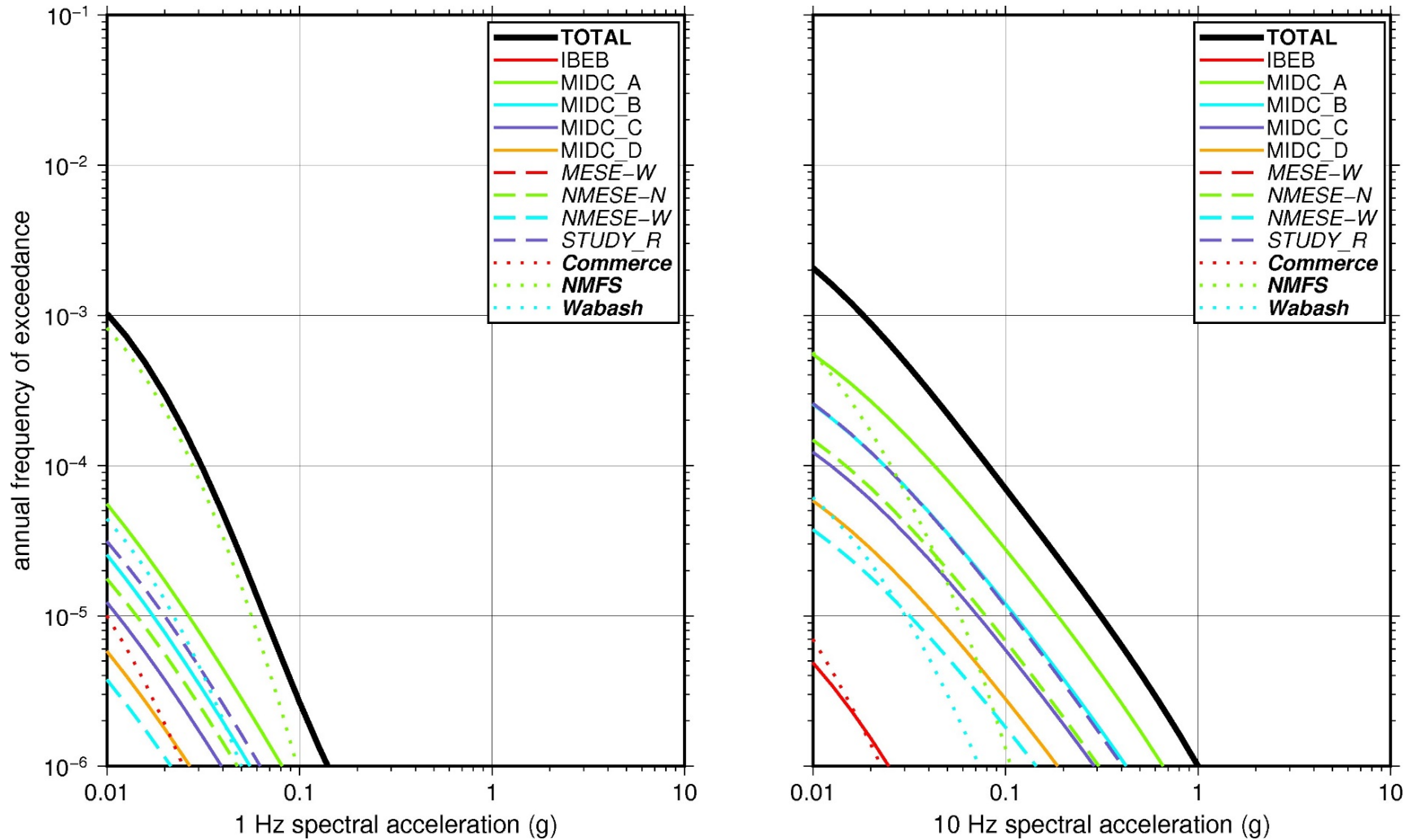


**Figure 2.4-54** Low-Frequency (1 Hz, Left), and High-Frequency (10 Hz, Right) Reference Rock Hazard Curves for Point Beach. Total Hazard is Shown as a Bold Black Line; Individual Contributions to the Hazard for Each of the CEUS-SSC Sources are Shown as Colored Lines Defined in the Legend. See Table 2.1-1 for Source Name Definitions

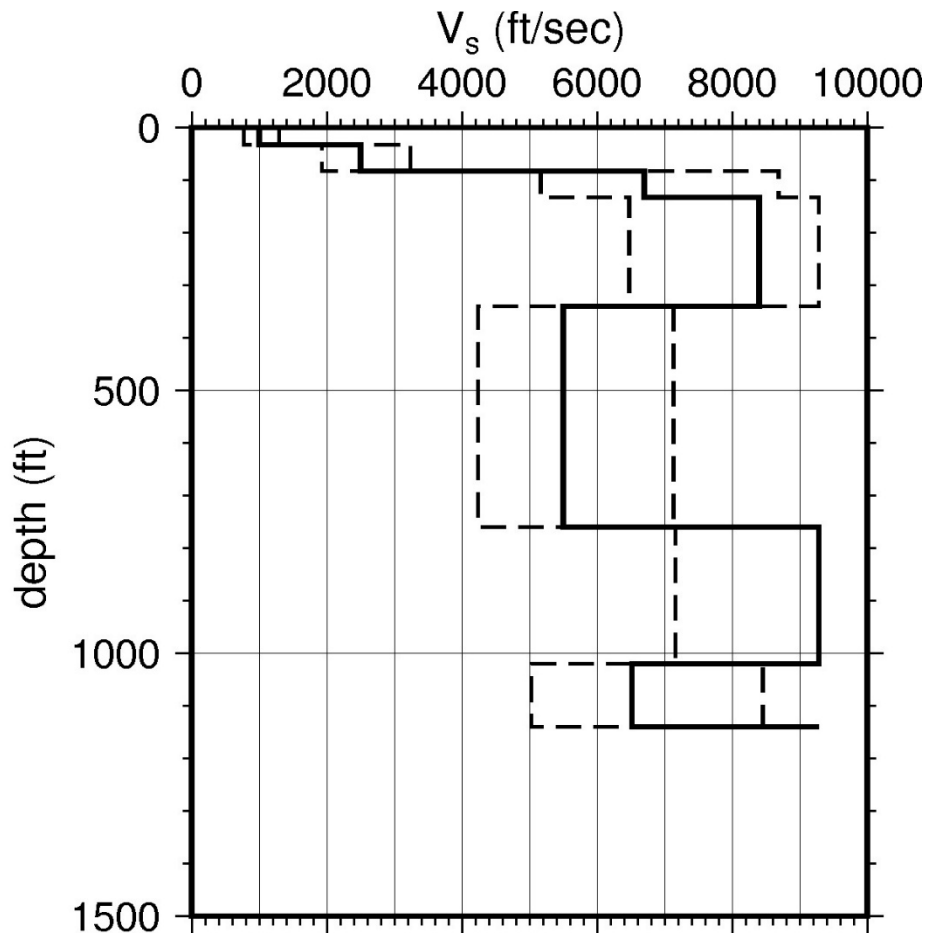


**Figure 2.4-55 Shear Wave Velocity ( $V_s$ ) Profiles for Point Beach. Basecase (BC) Profile Shown as Solid Bold Line; Lower and Upper Range (LR and UR) Profiles Shown as Dashed Lines. Profiles Terminate at Reference Rock Velocity of 2,831 m/sec [9,285 ft/sec] per EPRI GMM (2013)**

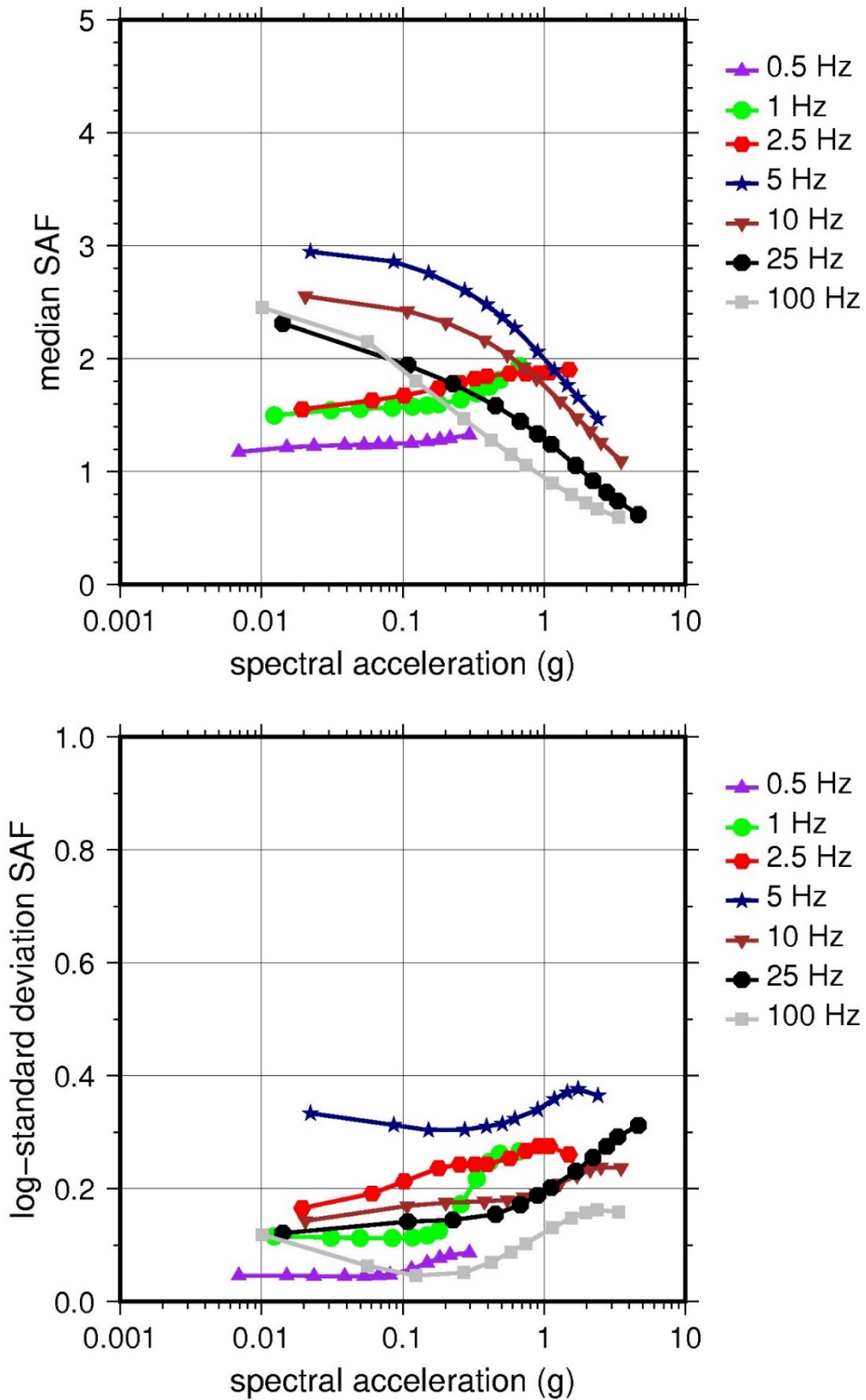


**Figure 2.4-56 Overall Weighted Median Site Amplification Factor (SAF) (Upper) and Log Standard Deviation of the SAF (Lower) as a Function of Input Acceleration for EPRI GMM (2013) Spectral Frequencies**

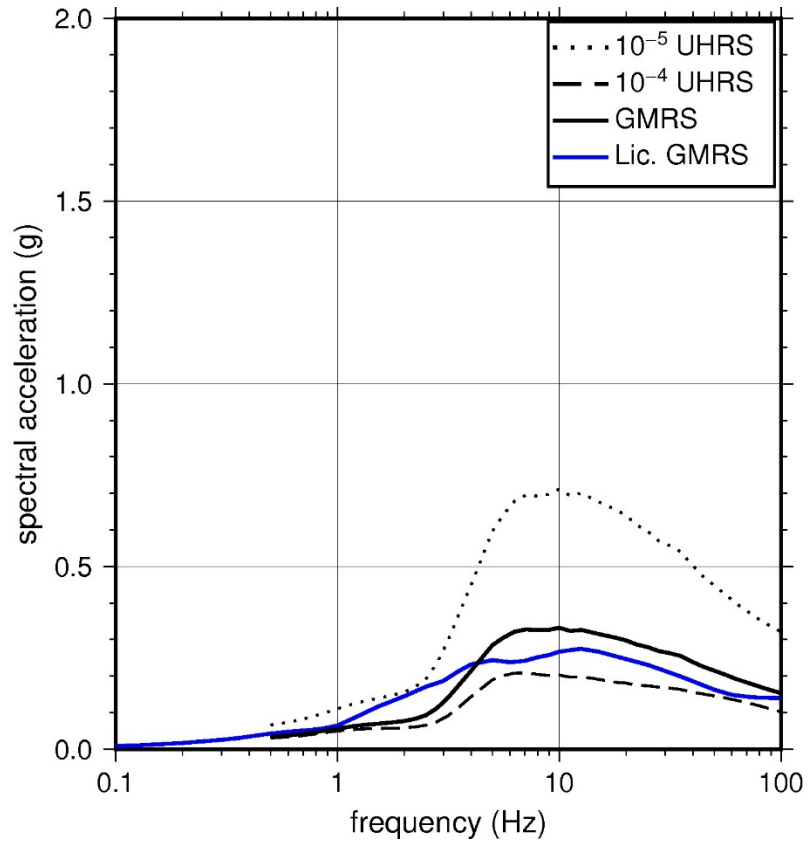
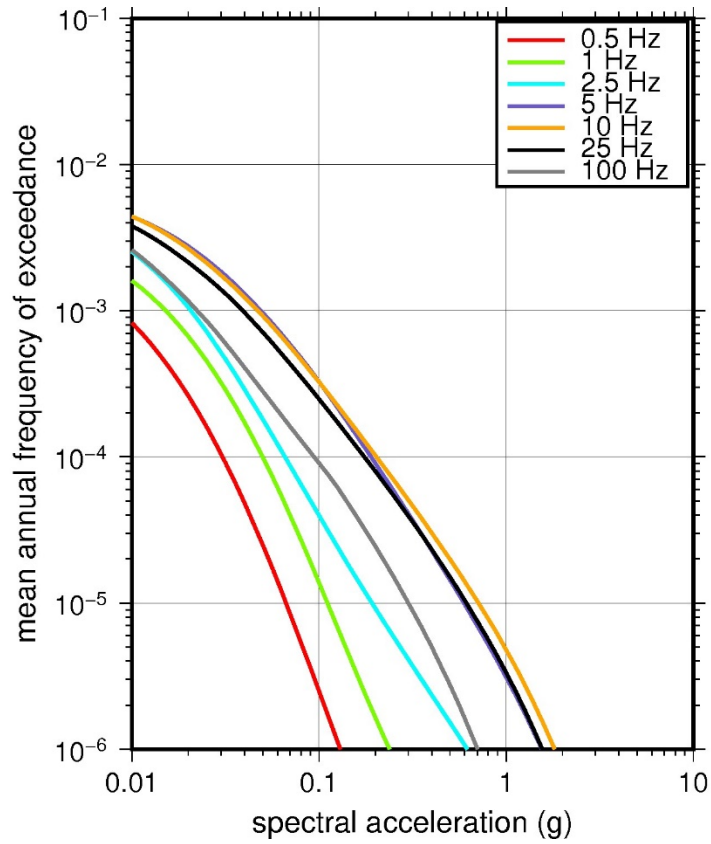


**Figure 2.4-57 Mean Control Point Hazard Curves (Left) for EPRI GMM (2013) Spectral Frequencies, and GMRS and UHRS (Right) for Point Beach**

## 2.4.15 Quad Cities

The Quad Cities Nuclear Power Station site is located in northwestern Illinois within the Till Plains Section of the Central Lowland physiographic province and consists of about 30 m [100 ft] of soil overlying about 991 m [3,250 ft] of firm sedimentary rock (shale, dolomite, sandstone, and limestone). The horizontal SSE response spectrum for Quad Cities comprises three different response spectra (the Golden Gate Park [S80°E] spectrum from the 1957 earthquake in San Francisco, CA; the El Centro [north-south] spectrum from the 1940 earthquake in Imperial Valley, CA; and a rounded Housner design response spectrum), each anchored at a PGA of 0.24g.

### 2.4.15.1 Reference Rock Hazard

For the reference rock PSHA, the NRC staff selected the nine CEUS-SSC (NRC, 2012b) background seismic source zones that are located within 320 km [200 mi] of the site. In addition, the NRC staff selected the six CEUS-SSC (NRC, 2012b) RLME sources that are located within 807 km [500 mi] of the site. To develop the reference rock seismic hazard curves for the Quad Cities site, the NRC staff used the GMPEs developed by the updated EPRI GMM (2013). As shown in Figure 2.4-58, the NMFS RLME is the largest contributor to the 1 Hz reference rock total mean hazard curve at the  $10^{-4}$  AFE level. For the 10 Hz reference rock total mean hazard curve, the MIDC-A seismotectonic zone is the largest contributor at the  $10^{-4}$  AFE level.

### 2.4.15.2 Site Response Evaluation

#### 2.4.15.2.1 Site Profiles

To develop a basecase profile, the NRC staff used the geologic information in the NTTF R2.1 SHSR (Kaegi, 2014f) submitted by Exelon Generation Company (hereafter referred to as “the licensee” within this plant section). As described in the licensee’s SHSR, the Quad Cities site consists of about 30 m [100 ft] of unconsolidated deposits of glacial till, outwash, and lacustrine sediments overlying Paleozoic bedrock. The plant structures are founded on dolomite bedrock. In Table 2.3.1-1 of the SHSR, the licensee briefly described the subsurface materials in terms of the geologic units and layer thicknesses. For its site response evaluation, the NRC staff used the top of the sedimentary rock, which corresponds to an elevation of 168 m [550 ft] above MSL, as the control point elevation for the Quad Cities site.

The licensee’s field investigation for Units 1 and 2, conducted in the late 1960s, consisted of a number of test pits and borings. In addition, the licensee’s geophysical field investigations for Units 1 and 2 measured  $V_P$  to a depth of about 61 m [200 ft] using seismic refraction surveys. To determine the  $V_S$  for each rock layer, the licensee used its measured  $V_P$  with an assumed Poisson’s ratio. Table 2.3.2-1 of the SHSR gives the estimated  $V_S$  determined from the licensee’s site investigations.

The licensee’s basecase profile, which is 991 m [3,250 ft] in total thickness, begins at the top of the Silurian-age sedimentary rock beneath the site. The licensee divided this rock strata, which primarily consists of about 76 m [250 ft] of weathered dolomites from the Niagarian and Alexandrian Formations, into four main layers. Refraction surveys performed by the licensee for Units 1 and 2 measured  $V_P$  ranging from about 2,439 m/sec [8,000 ft/sec] to about 4,268 m/sec [14,000 ft/sec]. For these four main layers, the licensee estimated  $V_S$  values of 1,181 m/sec [3,873 ft/sec], 2,045 m/sec [6,708 ft/sec], 1,074 m/sec [3,521 ft/sec], and 2,045 m/sec

[6,708 ft/sec], respectively. For the underlying Ordovician-age dolomites of the Galena Formation and the remaining Ordovician- and Cambrian-age rock, the licensee did not measure  $V_P$ . Instead, the licensee assumed that the  $V_S$  value of 2,045 m/sec [6,708 ft/sec] for the bottom layer of the overlying Silurian-age dolomites (Layer 4) gradually increases through the rest of the profile at a gradient of 0.5 m/sec/m [0.5 ft/sec/ft], reaching a  $V_S$  of 2,495 m/sec [8,183 ft/sec] at a depth of 991 m [3,250 ft].

For its basecase profile, the NRC staff used the licensee's layer thickness of 76 m [250 ft] for the weathered dolomites from the Niagaran and Alexandrian Formations but assumed a different  $V_S$ . Because the licensee's  $V_S$  values for the upper 76 m [250 ft] of its profile are based on a seismic refraction survey, the  $V_S$  reversal from Layer 2 to Layer 3, as described above, could not have been detected. In addition, EPRI (1989) reports that "results from geophysical explorations that include uphole velocity measurement and inhole measurements (Birdwell 3D logs)" performed at Quad Cities showed "a shear wave velocity for the dolomite of 1,920 m/sec [6,300 ft/sec] for the top of the dolomite." Therefore, the NRC staff used this measured  $V_S$  of 1,920 m/sec [6,300 ft/sec] for the upper 76 m [250 ft] of its profile. For the underlying Ordovician-age dolomites of the Galena and Platteville Groups and the sandstones of the Ancell Group, the NRC staff used the estimated  $V_S$  and layer thicknesses for the same formations from several other Region III sites (e.g., Dresden, Braidwood, LaSalle). Thus, the NRC staff assumed a thickness of 107 m [350 ft] and  $V_S$  of 2,652 m/sec [8,700 ft/sec] for the dolomites and a thickness of 92 m [300 ft] and  $V_S$  of 2,134 m/sec [7,000 ft/sec] for the sandstones. For the underlying Cambrian-age strata, the NRC staff assumed that the  $V_S$  exceeds the reference rock  $V_S$  of 2,831 m/sec [9,285 ft/sec].

To capture the uncertainty in its basecase profile, the NRC staff developed lower and upper range (10<sup>th</sup> and 90<sup>th</sup> percentile) profiles by multiplying the basecase  $V_S$  values by scale factors of 0.78 and 1.29, respectively, which corresponds to an epistemic logarithmic standard deviation of 0.20. The weights for the lower, basecase, and upper profiles are 0.3, 0.4, and 0.3, respectively. Figure 2.4-59 shows the NRC staff's profiles, which extend to a depth of 274 m [900 ft] below the control point elevation.

#### 2.4.15.2.2 *Dynamic Material Properties and Site Kappa*

The NRC staff assumed both linear and nonlinear dynamic behavior for the rock beneath the Quad Cities site. To model the nonlinear behavior of the uppermost layer of weathered rock, the NRC staff used the EPRI rock shear modulus reduction and material damping curves. To model the linear behavior of this rock layer, the NRC staff assumed a constant damping ratio of 3 percent. Because this rock layer has a higher velocity, the NRC staff assigned weights of 0.7 and 0.3 to the linear and nonlinear alternatives, respectively. For the underlying more intact sedimentary rock layers, the NRC staff assumed a linear dynamic response with a material damping ratio of 0.1 percent to maintain consistency with the  $\kappa_0$  value for the Quad Cities site.

To determine the basecase  $\kappa_0$  for the Quad Cities site, the NRC staff first used the Campbell (2009) Model 1 relationship between  $V_S$  and  $Q_{ef}$  to determine a  $Q_{ef}$  for each layer. Combining these  $Q_{ef}$  values with the thickness and  $V_S$  for each layer results in a total  $\kappa_0$  value of 8 msec, which includes the 6 msec assumed for the underlying reference rock. For the lower and upper profiles, the NRC staff calculated  $\kappa_0$  values of 9 and 7 msec, respectively, using the same approach as for the basecase profile. In contrast, the licensee used an empirical relationship between  $V_{S100}$  and  $\kappa_0$  found in the SPID to estimate basecase, lower, and upper  $\kappa_0$  values of 17, 28, and 7 msec, respectively.

Table 2.4-16 provides the layer depths, lithologies,  $V_s$ , unit weights, and dynamic properties for the NRC staff's three profiles. In summary, the site response logic tree developed by the NRC staff for the Quad Cities site consists of six alternatives; three velocity profiles (each with a different  $\kappa_0$  value) and two alternative dynamic property branches.

#### 2.4.15.2.3 Methodology and Results

The NRC staff followed the methodology described in Section 2.1.4 to develop the final site amplification factors. Figure 2.4-60 shows the median site amplification factors and their variability for the basecase velocity profile and the EPRI rock curves. As shown in Figure 2.4-60, the median site amplification factors range from about 1 to 1.5 before falling off with higher input spectral accelerations. The lower half of Figure 2.4-60 shows that the logarithmic standard deviations for the site amplification factors range from about 0.02 to 0.20.

#### 2.4.15.3 Control Point Hazard

The NRC staff implemented Approach 3 from the SPID to develop a weighted control point seismic hazard curve for each of the six unique combinations of the site response logic tree for the Quad Cities site. After combining these curves to develop the final mean control point hazard curves, the NRC staff determined the  $10^{-4}$  and  $10^{-5}$  UHRS in order to calculate the GMRS. Figure 2.4-61 shows the final control point mean seismic hazard curves for the seven spectral frequencies, as well as the NRC staff's UHRS and GMRS and the licensee's NTTF R2.1 GMRS (Kaegi, 2014f). As shown in Figure 2.4-61, the NRC staff's GMRS (black curve) is similar to the licensee's (blue curve) below 10 Hz but is moderately higher than the licensee's for higher spectral frequencies. This is due to the licensee's higher  $\kappa_0$  values for the lower and best-estimate basecase profiles. For comparison, Figure 2.4-61 also shows the NRC staff's reference rock GMRS (brown dotted curve).

Layer	Depth (ft)	Description	$V_s$ (ft/sec)			$V_s$ Sigma (ln)	Unit Weight (pcf)	Dynamic Properties	
			LR (0.3)	BC (0.4)	UR (0.3)			Alt. 1 (0.3)	Alt. 2 (0.7)
1	20	Rock: dolomite	4,275	5,525	7,140	0.25	150	EPRI Rock	L 3.0%
2	40	Rock: dolomite	4,508	5,825	7,528	0.15	150	EPRI Rock	L 3.0%
3	80	Rock: dolomite	3,772	4,875	6,300	0.15	150	EPRI Rock	L 3.0%
4	250	Rock: dolomite	4,508	5,825	7,528	0.15	150	EPRI Rock	L 3.0%
5	3,250	Rock: dolomite, shale, sandstone	7,185	9,285	9,285	0.15	160	L 0.1%	L 0.1%

LR = lower range; BC = basecase; UR = upper range; ln = natural log; pcf = pounds per cubic foot; L = linear; Alt. = alternative.  
 For LR, BC, UR, and Alt.: Values in parentheses refer to weights for site response analysis logic tree branches.

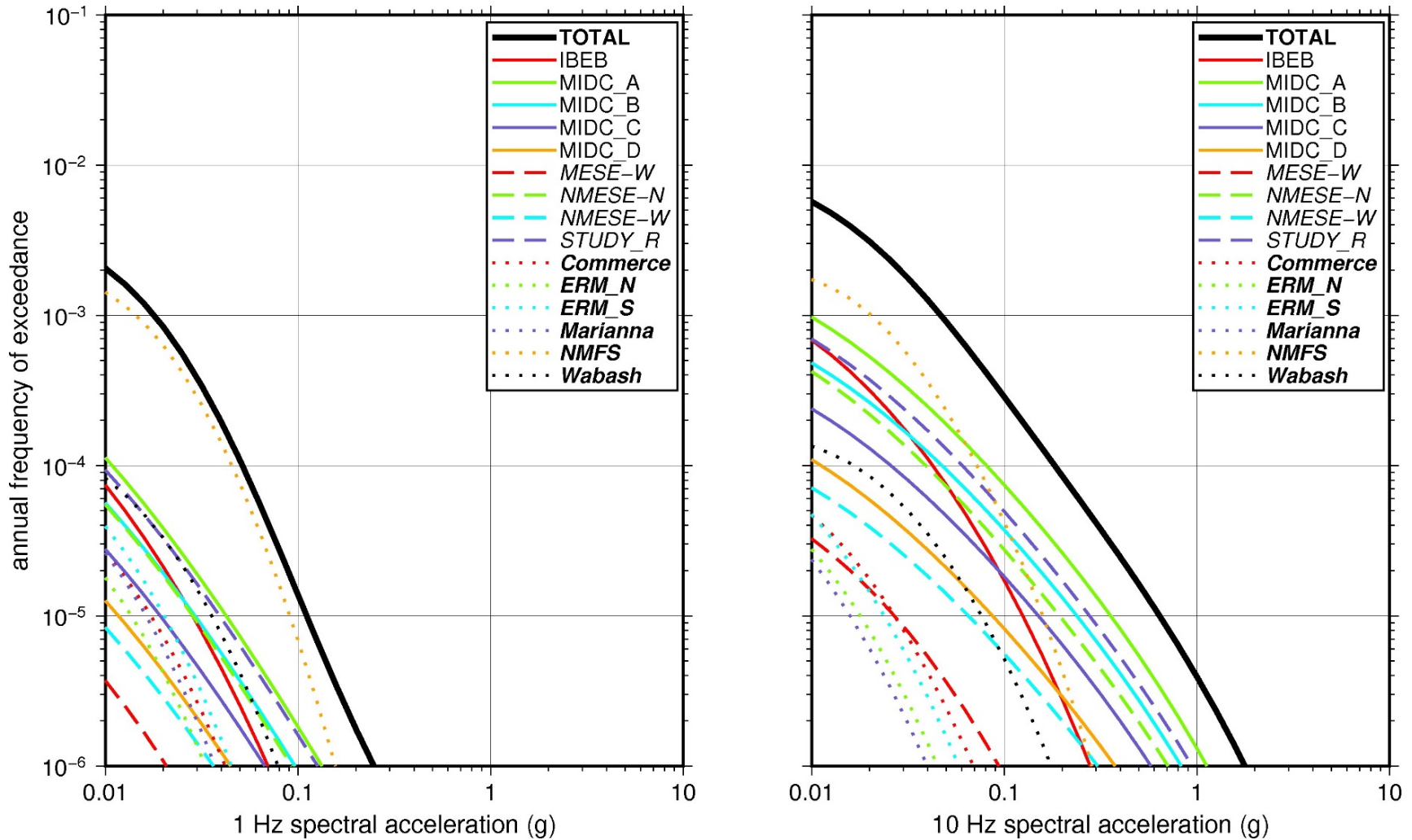


**Figure 2.4-58 Low-Frequency (1 Hz, Left), and High-Frequency (10 Hz, Right) Reference Rock Hazard Curves for Quad Cities. Total Hazard is Shown as a Bold Black Line; Individual Contributions to the Hazard for Each of the CEUS-SSC Sources are Shown as Colored Lines Defined in the Legend. See Table 2.1-1 for Source Name Definitions**



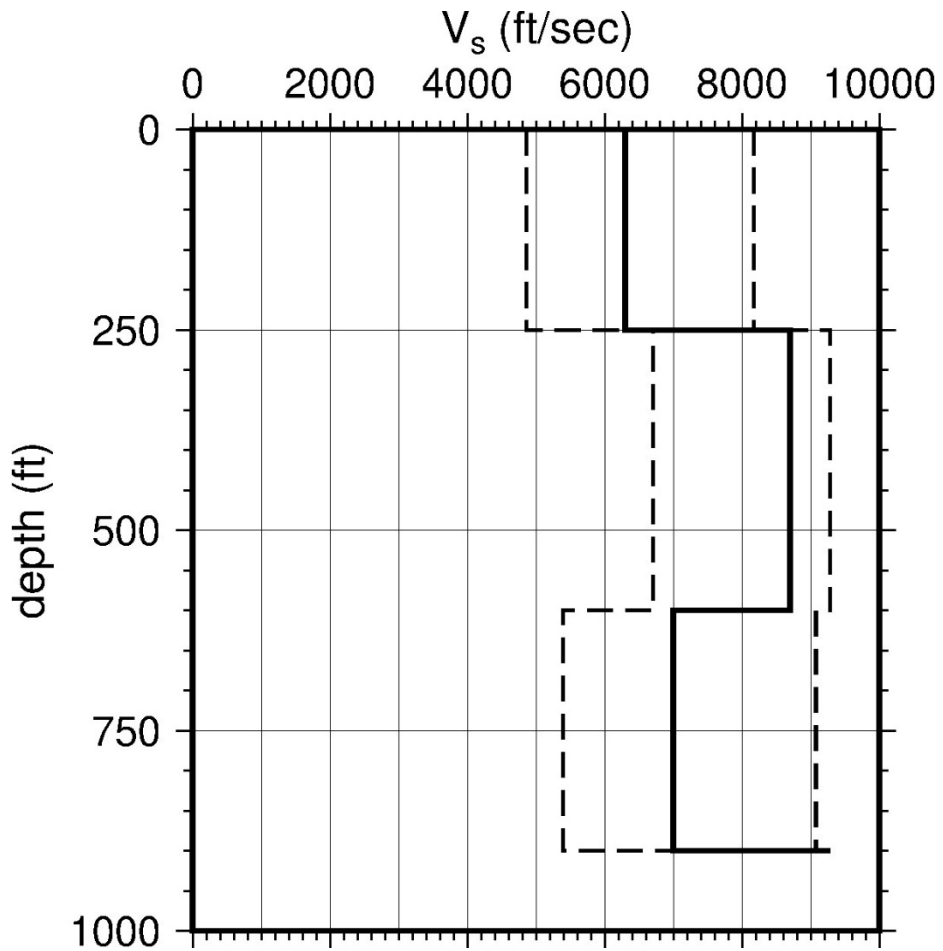


**Figure 2.4-59 Shear Wave Velocity ( $V_s$ ) Profiles for Quad Cities. Basecase (BC) Profile Shown as Solid Bold Line; Lower and Upper Range (LR and UR) Profiles Shown as Dashed Lines. Profiles Terminate at Reference Rock Velocity of 2,831 m/sec [9,285 ft/sec] per EPRI GMM (2013)**

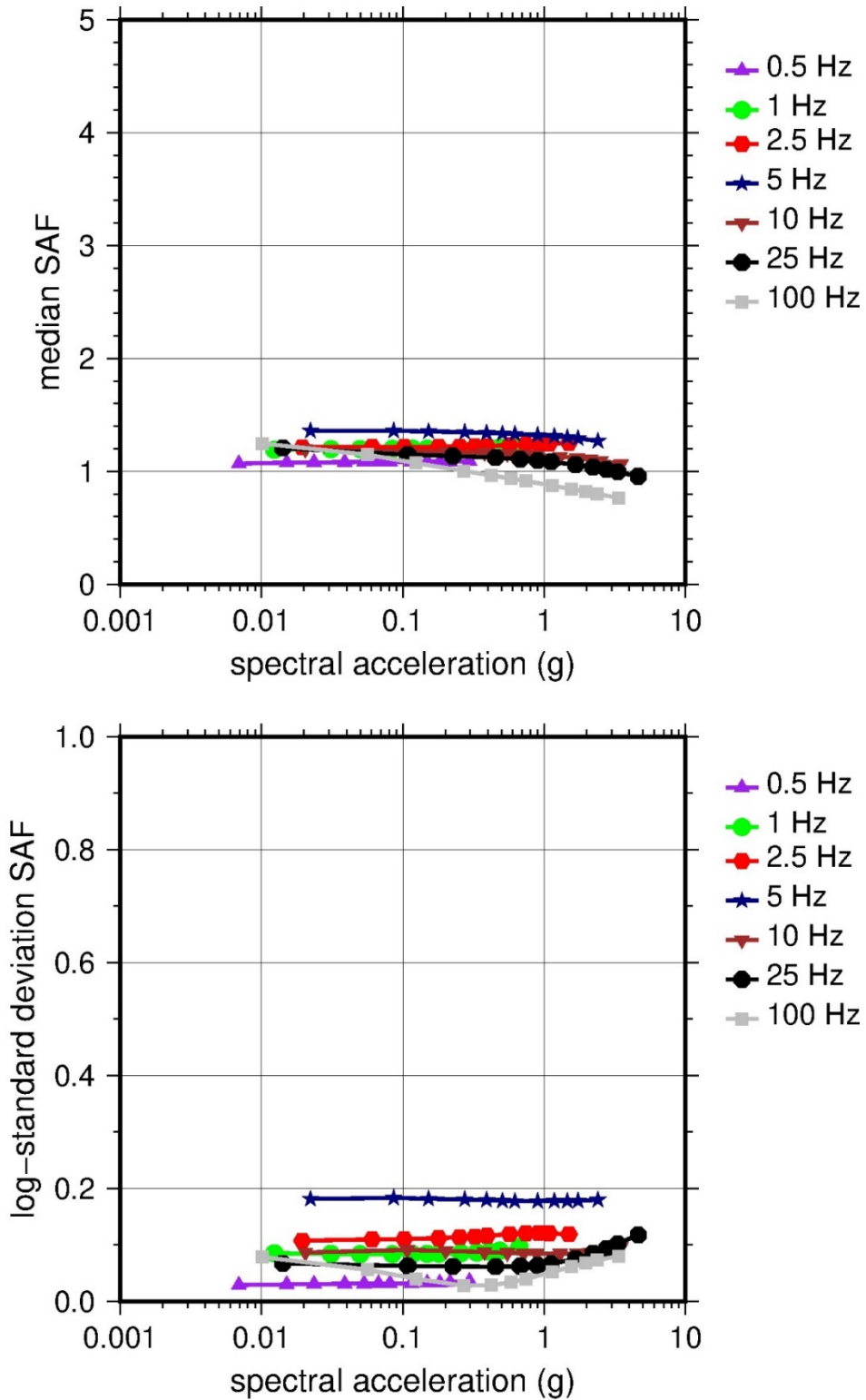


**Figure 2.4-60 Overall Weighted Median Site Amplification Factor (SAF) (Upper) and Log Standard Deviation of the SAF (Lower) as a Function of Input Acceleration for EPRI GMM (2013) Spectral Frequencies**

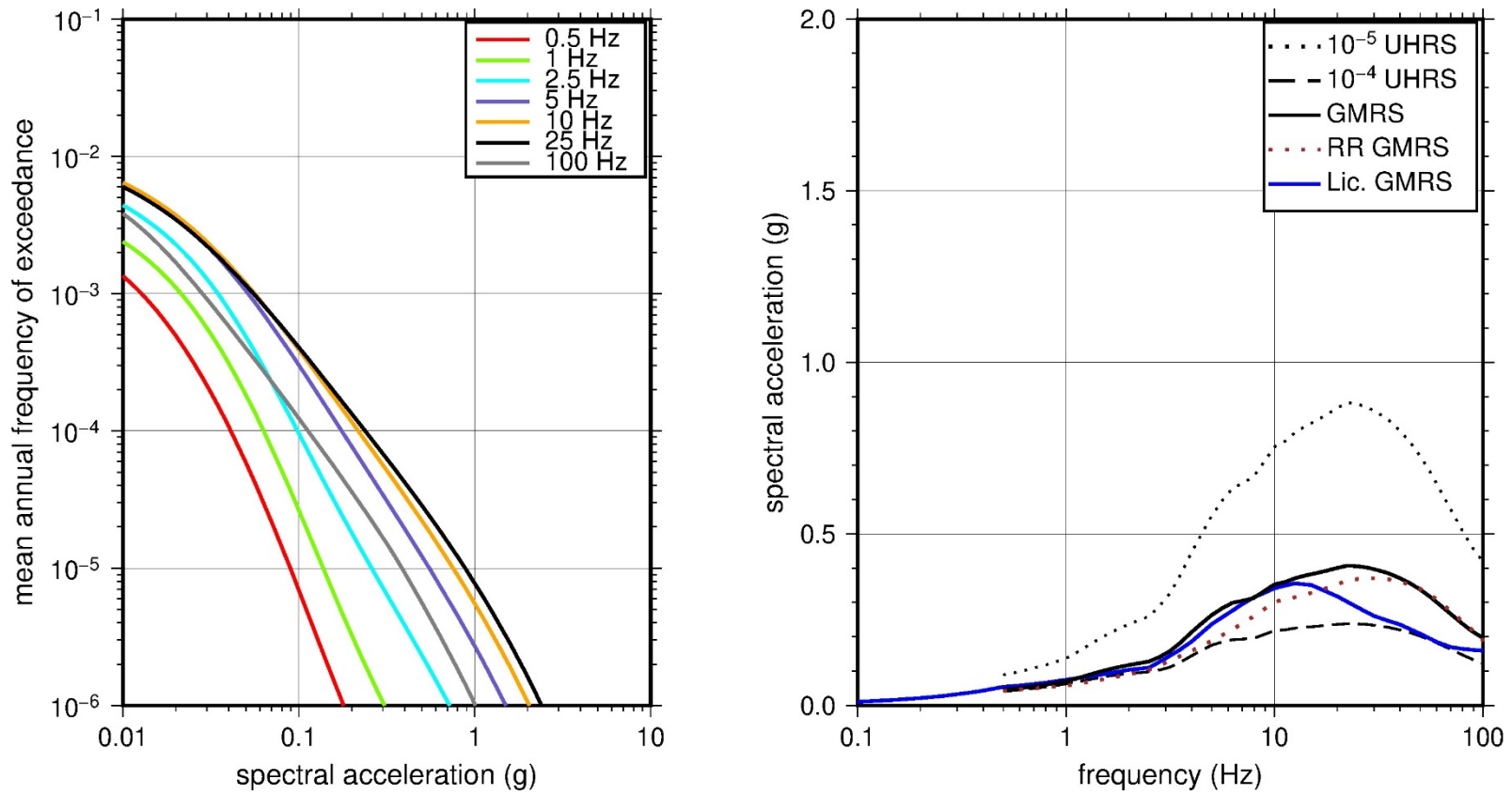


**Figure 2.4-61 Mean Control Point Hazard Curves (Left) for EPRI GMM (2013) Spectral Frequencies, and GMRS and UHRS (Right) for Quad Cities**

## 2.5 Region IV Sites

The NRC staff characterized the seismic hazard for the 10 Region IV CEUS nuclear plant sites shown below in Table 2.5-1 and Figure 2.5-1. As shown in Table 2.5-1, 2 of the 10 Region IV NPPs are founded on rock, 4 on soil over sedimentary rock, and 4 on deep soil. Table 2.5-1 also shows the State, physiographic province, and whether there is a co-located ESP or COL for each site. Figure 2.5-1 shows the Region IV CEUS sites overlain on the physiographic provinces, the highest weighted CEUS-SSC (NRC, 2012b) seismotectonic source zone configuration, and the CEUS-SSC earthquake epicenters. Figure 2.5-1 also shows the CEUS-SSC RLME sources used to develop the reference rock hazard curves for at least one Region IV site.

<b>Plant Name</b>	<b>Site Name</b>	<b>State</b>	<b>Geology</b>	<b>Physiographic Province</b>	<b>ESP/COL (Y/N)</b>
Arkansas Nuclear One	Arkansas	AK	Rock	Ouachita	N
Callaway Plant	Callaway	MO	Soil over rock	Central Lowland	Y
Comanche Peak Nuclear Power Plant	Comanche Peak	TX	Rock	Great Plains	Y
Cooper Nuclear Station	Cooper	NE	Soil over rock	Central Lowland	N
Fort Calhoun Nuclear Station*	Ft. Calhoun	NE	Soil over rock	Central Lowland	N
Grand Gulf Nuclear Station	Grand Gulf	MS	Soil	Coastal Plain	Y
River Bend Station	River Bend	LA	Soil	Coastal Plain	Y
South Texas Project	South Texas	TX	Soil	Coastal Plain	Y
Waterford Steam Electric Station	Waterford	LA	Soil	Coastal Plain	N
Wolf Creek Generating Station	Wolf Creek	KS	Soil over rock	Central Lowland	N

\*Plant was shut down or has subsequently been shut down.

The following subsections describe the NRC staff's development of reference rock hazard curves, site response analyses, and use of Approach 3 to develop control point seismic hazard curves and a GMRS for each Region IV site.

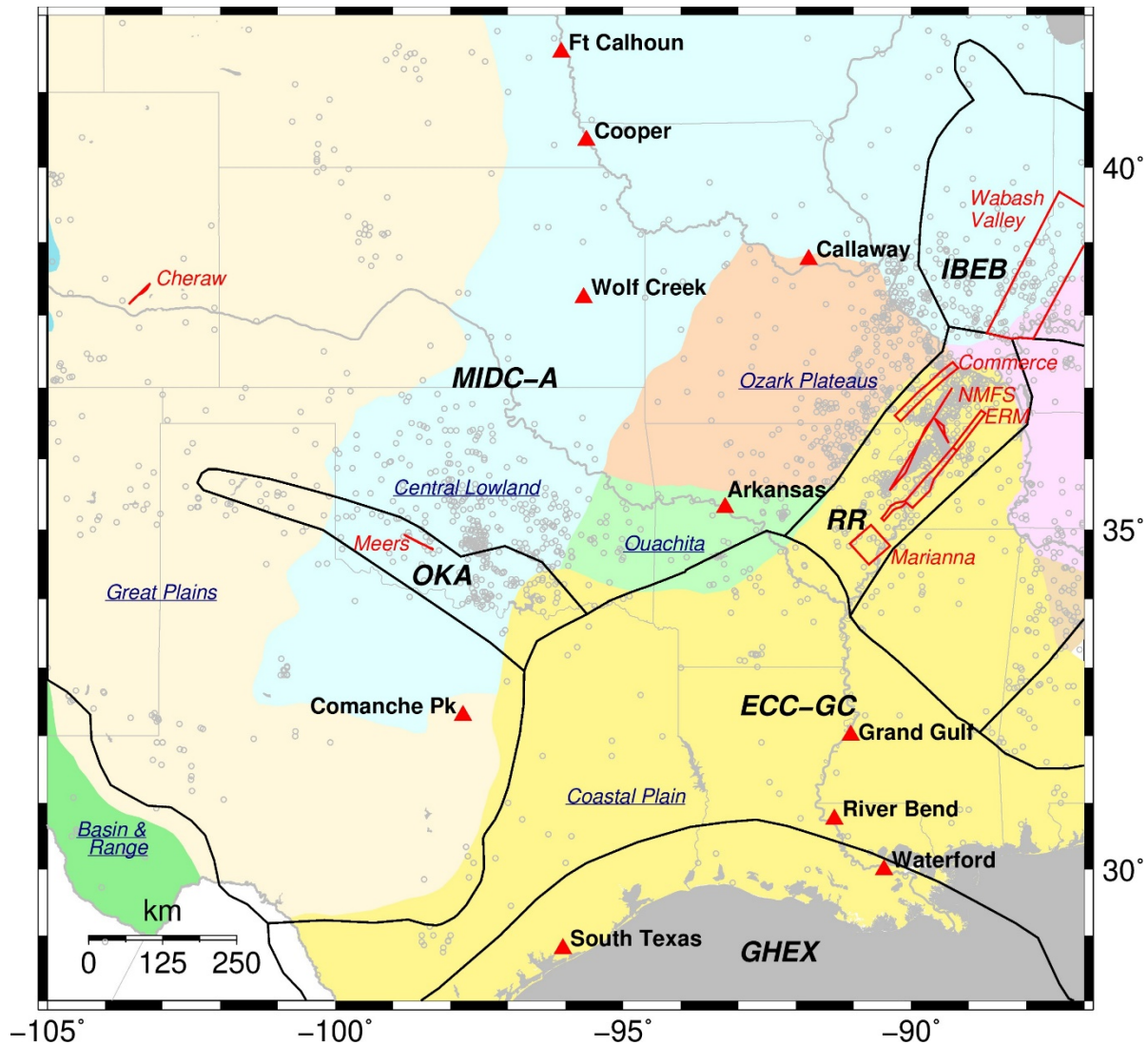


**Figure 2.5-1** Location Map Showing NPPs (Red Triangles) in Region IV; RLMEs, Indicated by Solid Red Lines, and Seismotectonic Source Zones, Indicated by Solid Black Lines (from NUREG-2115), with Acronyms Defined in Table 2.1-1 of this Report; and Physiographic Provinces, Identified by Underlined Italicized Labels, with Water Bodies Represented in Gray. Earthquake Epicenters (from NUREG-2115) are Shown with Open Gray Circles

## 2.5.1 Arkansas

The Arkansas Nuclear One site is located in central Arkansas along a peninsula formed by the Dardanelle Reservoir within the Ouachita physiographic province and consists of 2 to 9 m [8 to 30 ft] of soil (clay) overlying about 3,659 m [12,000 ft] of sedimentary rock (shale, sandstone, limestone, and dolomite). The horizontal SSE response spectrum for Unit 1 has a rounded Housner spectral shape and is anchored at a PGA of 0.20g. The SSE for Unit 2 has a Newmark spectral shape and is also anchored at a PGA of 0.20g.

### 2.5.1.1 Reference Rock Hazard

For the reference rock PSHA, the NRC staff selected the 13 CEUS-SSC (NRC, 2012b) background seismic source zones that are located within 323 km [200 mi] of the site. In addition, the NRC staff selected the 7 CEUS-SSC (NRC, 2012b) RLME sources that are located within 807 km [500 mi] of the site. To develop the reference rock seismic hazard curves for the Arkansas site, the NRC staff used the GMPEs developed by the updated EPRI GMM (2013). As shown in Figure 2.5-2, the NMFS RLME is the largest contributor to both the 1 Hz and the 10 Hz reference rock total mean hazard curves at the  $10^{-4}$  AFE level.

### 2.5.1.2 Site Response Evaluation

#### 2.5.1.2.1 Site Profiles

To develop a basecase profile, the NRC staff used the geologic information in the NTTF R2.1 SHSR (Browning, 2014) submitted by Entergy Nuclear Operations Inc. (hereafter referred to as “the licensee” within this plant section). As described in the licensee’s SHSR, the Arkansas site is located within the Arkoma Basin and consists of about 9 m [30 ft] of clay overlying approximately 1,524 m [5,000 ft] of shale and sandstone. The Arkansas site is founded on the McAlester Formation, which is composed of hard, dense, Pennsylvanian-age shale. The foundations for all of the principal plant structures are within this shale bedrock layer. For its site response evaluation, the NRC staff used the top of bedrock, which corresponds to an elevation of 99 m [326 ft] above MSL, as the control point elevation for the Arkansas site.

The field investigations for Arkansas consisted of a seismic refraction survey carried out in the mid-1960s and numerous boreholes at the site. The licensee based the  $V_S$  for the upper shale bedrock layer on an assumed Poisson’s ratio and the  $V_P$  that it measured during the seismic refraction survey. Table 2.3.2-1 of the SHSR gives the estimated  $V_S$  determined from the licensee’s site investigations.

For its SHSR, the licensee developed a basecase profile that extends to a depth of 1,524 m [5,000 ft] below the control point elevation. The licensee’s profile begins within the shale bedrock of the McAlester Formation. To determine the  $V_S$  for this shale layer, the licensee used the lowest  $V_P$  measured from its seismic refraction profile, which was 3,049 m/sec [10,000 ft/sec], and an assumed Poisson’s ratio of 0.30, which yielded a  $V_S$  of 1,616 m/sec [5,300 ft/sec]. For the rest of its profile, down to a depth of 1,524 m [5,000 ft], the licensee assumed a velocity gradient of 0.5 m/sec/m [0.5 ft/sec/ft], which resulted in a maximum  $V_S$  of 2,370 m/sec [7,772 ft/sec] at the bottom of the profile.

To augment the licensee’s profile, the NRC staff examined several geological resources, including reports from the Arkansas Geological Survey. Based on a well-exposed outcrop just south of Russellville, AK, the McAlester Formation is about 14 m [47 ft] thick; the underlying

Hartshorne Formation, which is predominantly sandstone, is approximately 45 m [146 ft] thick. These thicknesses are similar to those beneath the plant, based on site borehole data (Entergy Operations Inc., 2014). The Pennsylvanian-age Atoka Formation, which consists of shale, siltstone, and sandstone, underlies the McAlester and Hartshorne Formations and becomes thicker southward across the Arkoma Basin, increasing from about 350 m [1,150 ft] to about 6,400 m [21,000 ft]. The remaining Pennsylvanian-age rock units that underlie the Atoka Formation are from the Morrow Group, which consists of the Hale Formation (sandstone) and the Bloyd Formation (shale). The total thickness of the Pennsylvanian-age sedimentary rock units beneath the Arkansas site is about 2,260 m [7,413 ft]. For the underlying Mississippian- to Cambrian-age sedimentary rocks, stratigraphic profiles from the Arkansas Geological Survey show a thickness of about 1,463 m [4,800 ft]. Therefore, the total sedimentary rock thickness for the middle of the Arkoma Basin in the vicinity of Russellville, AK, is about 3,720 m [12,200 ft].

Rather than assuming the simple velocity gradient used by the licensee for its  $V_S$  profile, the NRC staff used the  $V_P$  model developed by Yezerki and Cemen (2014) and an assumed Poisson's ratio of 0.30 to estimate  $V_S$  values for the Hartshorne Formation and the upper, middle, and lower Atoka Formations. The resulting  $V_S$  values for these formations are 1,875 m/sec [6,150 ft/sec], 1,860 m/sec [6,100 ft/sec], 2,152 m/sec [7,060 ft/sec], and 2,250 m/sec [7,380 ft/sec], respectively. Using the same method and assumed Poisson's ratio, the NRC staff estimated a  $V_S$  of 2,400 m/sec [7,900 ft/sec] for the underlying Morrow Group. Based on numerous geologic profiles in the vicinity of the site, the approximate thicknesses of the upper, middle, and lower Atoka Formations and the Morrow Group are approximately 701 m [2,300 ft], 1,159 m [3,800 ft], 305 m [1,000 ft], and 37 m [120 ft], respectively. To evaluate the  $V_S$  of the rock units beneath the Pennsylvanian-age strata, the NRC staff used the one-dimensional seismic velocity model developed by Ogwari et al. (2016) for their study of the 2010 Guy-Greenbrier, AK, earthquake sequence. In this model, for the deeper sedimentary rock layers in the eastern portion of the Arkoma Basin,  $V_S$  increases from 2,400 m/sec [7,800 ft/sec] to 3,100 m/sec [10,160 ft/sec] at a depth of about 1,500 m [5,000 ft]. It then remains fairly constant down to a depth of about 4,000 m [13,120 ft], which Ogwari et al. (2016) consider to be the bottom of the Arkoma Basin in the vicinity of the Guy-Greenbrier earthquake sequence. Because this  $V_S$  {3,100 m/sec [10,160 ft/sec]} exceeds the reference rock value of 2,830 m/sec [9,285 ft/sec], the NRC staff terminated its basecase profile at the base of the Pennsylvanian-age strata.

To capture the uncertainty in its basecase profile, the NRC staff developed lower and upper range (10<sup>th</sup> and 90<sup>th</sup> percentile) profiles by multiplying the basecase  $V_S$  values by scale factors of 0.78 and 1.29, respectively, which corresponds to an epistemic logarithmic standard deviation of 0.20. The weights for the lower, basecase, and upper profiles are 0.3, 0.4, and 0.3, respectively. Figure 2.5-3 shows the upper 1,219 m [4,000 ft] of the NRC staff's profiles, which terminate at a depth of 2,260 m [7,413 ft] below the control point elevation. In contrast to the NRC staff's profiles, the licensee's profiles extend to a depth of 1,524 m [5,000 ft].

#### 2.5.1.2.2 *Dynamic Material Properties and Site Kappa*

The NRC staff assumed both linear and nonlinear dynamic behavior for the rock beneath the Arkansas site. To model the nonlinear behavior of the uppermost weathered rock layers (Layers 1–2), the NRC staff used the EPRI rock shear modulus reduction and material damping curves. To model the alternative linear behavior of these rock layers, the NRC staff assumed a constant damping ratio of 3 percent. Because these upper rock layers have high velocities {1,524 m/sec [ $>5,000$  ft/sec]}, the NRC staff assigned weights of 0.7 and 0.3 to the linear and

nonlinear alternatives, respectively. For the underlying more intact sedimentary rock layers, the NRC staff assumed a linear response with damping ratios of either 0.25 or 0.50 percent to maintain consistency with the  $\kappa_0$  value for the Arkansas site.

To determine the basecase  $\kappa_0$  for the Arkansas site, the NRC staff first used the Campbell (2009) Model 1 relationship between  $V_S$  and  $Q_{ef}$  to determine a  $Q_{ef}$  for each layer. Combining these  $Q_{ef}$  values with the thickness and  $V_S$  for each layer results in a total  $\kappa_0$  value of 23 msec, which includes the 6 msec assumed for the underlying reference rock. For the lower and upper profiles, the NRC staff calculated  $\kappa_0$  values of 34 and 15 msec, respectively, using the same approach as for the basecase profile. In contrast, the licensee estimated  $\kappa_0$  by using the average  $V_S$  over the upper 30 m [100 ft] of rock. This relationship between  $V_{S100}$  and  $\kappa_0$  produces basecase, lower, and upper  $\kappa_0$  estimates of 14, 23, and 9 msec, respectively, which are lower than the NRC staff's estimates.

Table 2.5-2 provides the layer depths, lithologies,  $V_S$ , unit weights, and dynamic properties for the NRC staff's three profiles. In summary, the site response logic tree developed by the NRC staff for the Arkansas site consists of six alternatives; three velocity profiles (each with a different  $\kappa_0$  value) and two alternative dynamic property branches.

#### 2.5.1.2.3 Methodology and Results

The NRC staff followed the methodology described in Section 2.1.4 to develop the final site amplification factors. Figure 2.5-4 shows the overall median site amplification factors and their variability for each of the seven spectral frequencies. As shown in Figure 2.5-4, the median site amplification factors range from about 1.0 to 1.5 before falling off with higher input spectral accelerations. The lower half of Figure 2.5-4 shows that the logarithmic standard deviations for the site amplification factors range from about 0.05 to 0.15.

#### 2.5.1.3 Control Point Hazard

The NRC staff implemented Approach 3 from the SPID (EPRI, 2012) to develop a weighted control point seismic hazard curve for each of the six unique combinations of the site response logic tree for the Arkansas site. After combining these curves to develop the final mean control point hazard curves, the NRC staff determined the  $10^{-4}$  and  $10^{-5}$  UHRS in order to calculate the GMRS. Figure 2.5-5 shows the final control point mean seismic hazard curves for the seven spectral frequencies, as well as the NRC staff's UHRS and GMRS and the licensee's NTTF R2.1 GMRS (Browning, 2014). As shown in Figure 2.5-5, the NRC staff's GMRS (black curve) is moderately lower than the licensee's GMRS (blue curve). This is because the NRC staff estimated a higher  $\kappa_0$  value and used the actual  $V_S$  for the rock strata within the Arkoma Basin, rather than a simple velocity gradient based on the  $V_S$  for the uppermost rock layer.



**Table 2.5-2 Layer Depths, Shear Wave Velocities ( $V_s$ ), Unit Weights, and Dynamic Properties for Arkansas**

Layer	Depth (ft)	Description	$V_s$ (ft/sec)			$V_s$ Sigma (ln)	BC Unit Weight (pcf)	Dynamic Properties	
			LR (0.3)	BC (0.4)	UR (0.3)			Alt. 1 (0.3)	Alt. 2 (0.7)
1	47	Rock: shale	4,101	5,300	6,849	0.25	140	EPRI Rock	L 3.0%
2	193	Rock: sandstone	4,756	6,147	7,944	0.15	150	EPRI Rock	L 3.0%
3	2,493	Rock: shale, siltstone, sandstone	4,715	6,094	7,875	0.15	150	L 0.5%	L 0.5%
4	6,293	Rock: shale, siltstone, sandstone	5,459	7,056	9,118	0.15	150	L 0.25%	L 0.25%
5	7,293	Rock: shale, siltstone, sandstone	5,707	7,376	9,285	0.15	160	L 0.25%	L 0.25%
6	7,413	Rock: sandstone, shale	6,094	7,877	9,285	0.15	160	L 0.25%	L 0.25%

LR = lower range; BC = basecase; UR = upper range; ln = natural log; pcf = pounds per cubic foot; L = linear; Alt. = alternative.  
 For LR, BC, UR, and Alt.: Values in parentheses refer to weights for site response analysis logic tree branches.

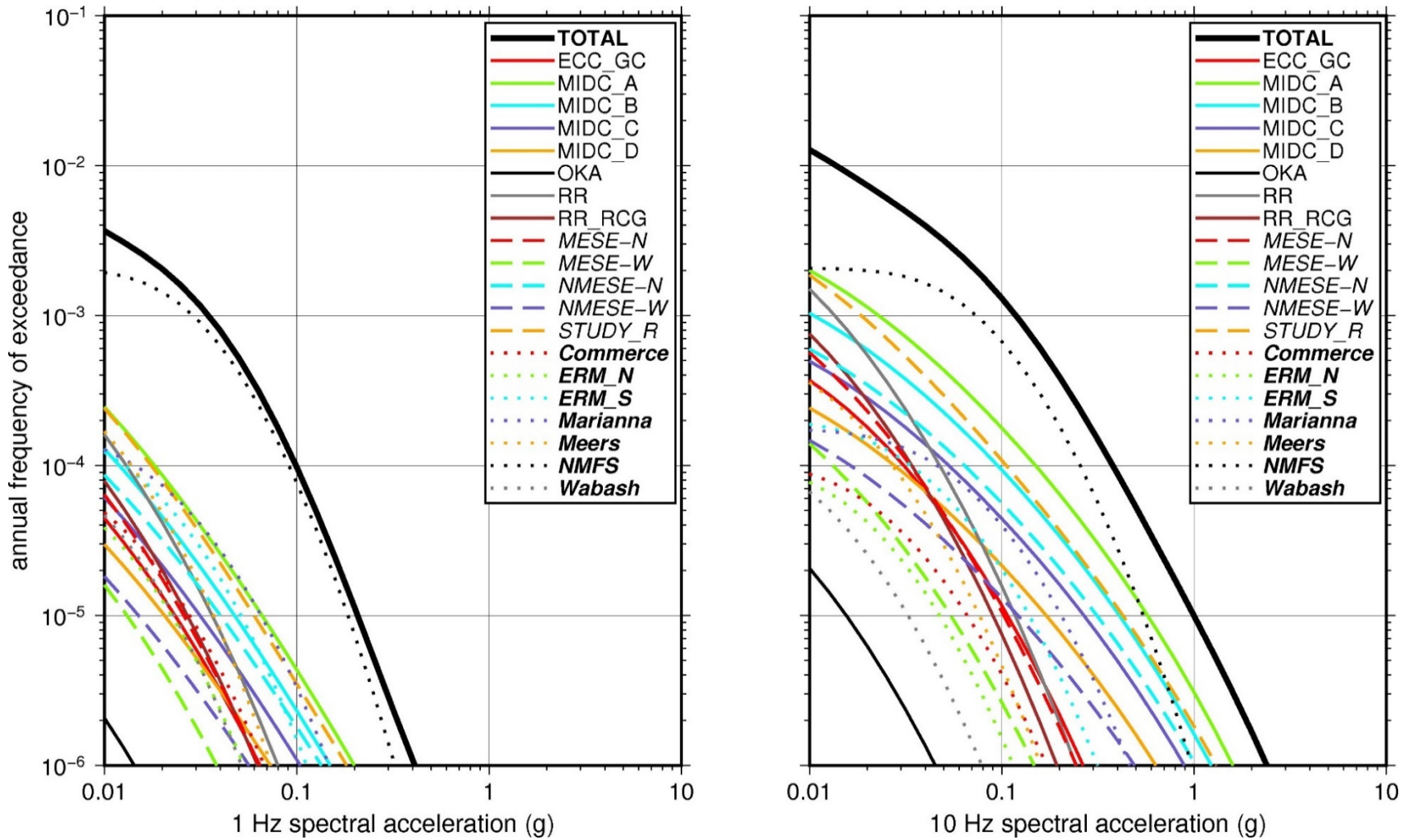


**Figure 2.5-2 Low-Frequency (1 Hz, Left), and High-Frequency (10 Hz, Right) Reference Rock Hazard Curves for Arkansas. Total Hazard is Shown as a Bold Black Line; Individual Contributions to the Hazard for Each of the CEUS-SSC Sources are Shown as Colored Lines Defined in the Legend. See Table 2.1-1 for Source Name Definitions**

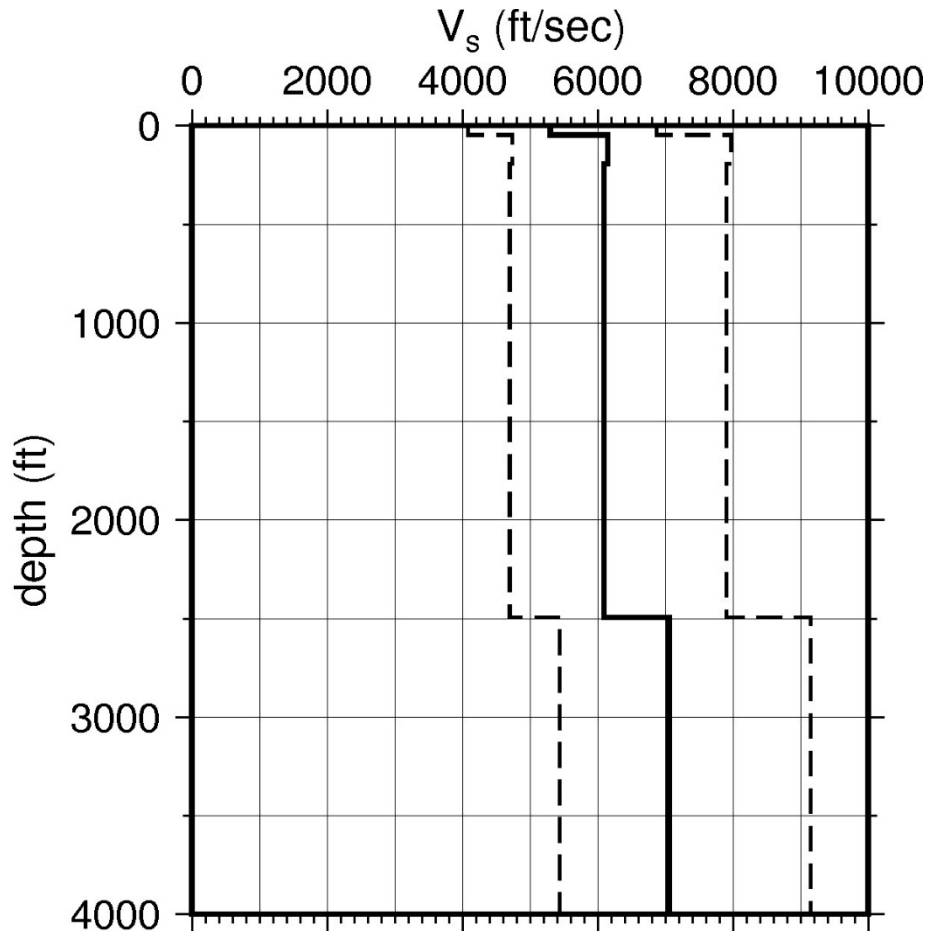


**Figure 2.5-3** Shear Wave Velocity ( $V_s$ ) Profiles for Arkansas. Basecase (BC) Profile Shown as Solid Bold Line; Lower and Upper Range (LR and UR) Profiles Shown as Dashed Lines. Profiles Terminate at Reference Rock Velocity of 2,831 m/sec [9,285 ft/sec] per EPRI GMM (2013)

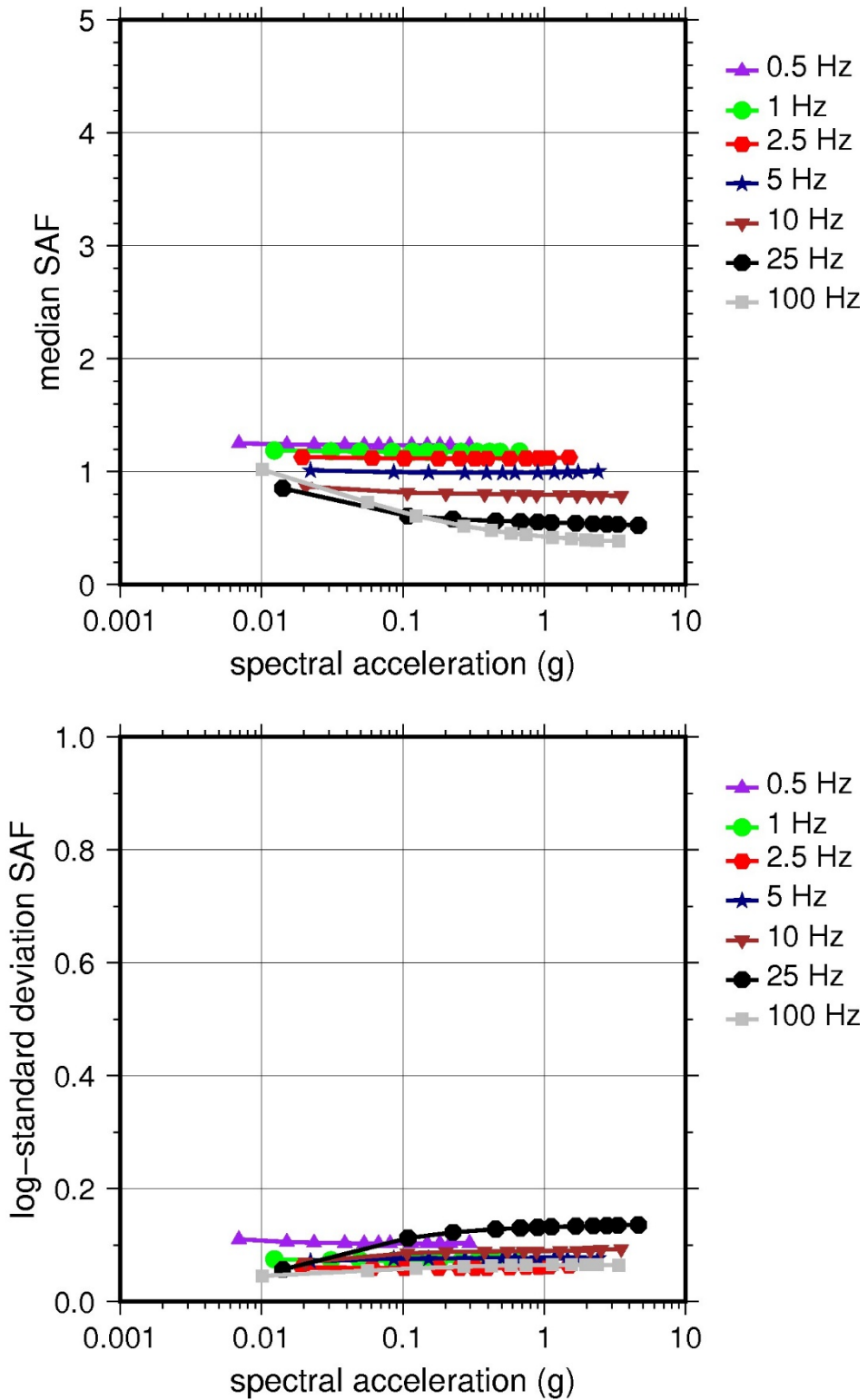


**Figure 2.5-4 Overall Weighted Median Site Amplification Factor (SAF) (Upper) and Log Standard Deviation of the SAF (Lower) as a Function of Input Acceleration for EPRI GMM (2013) Spectral Frequencies**

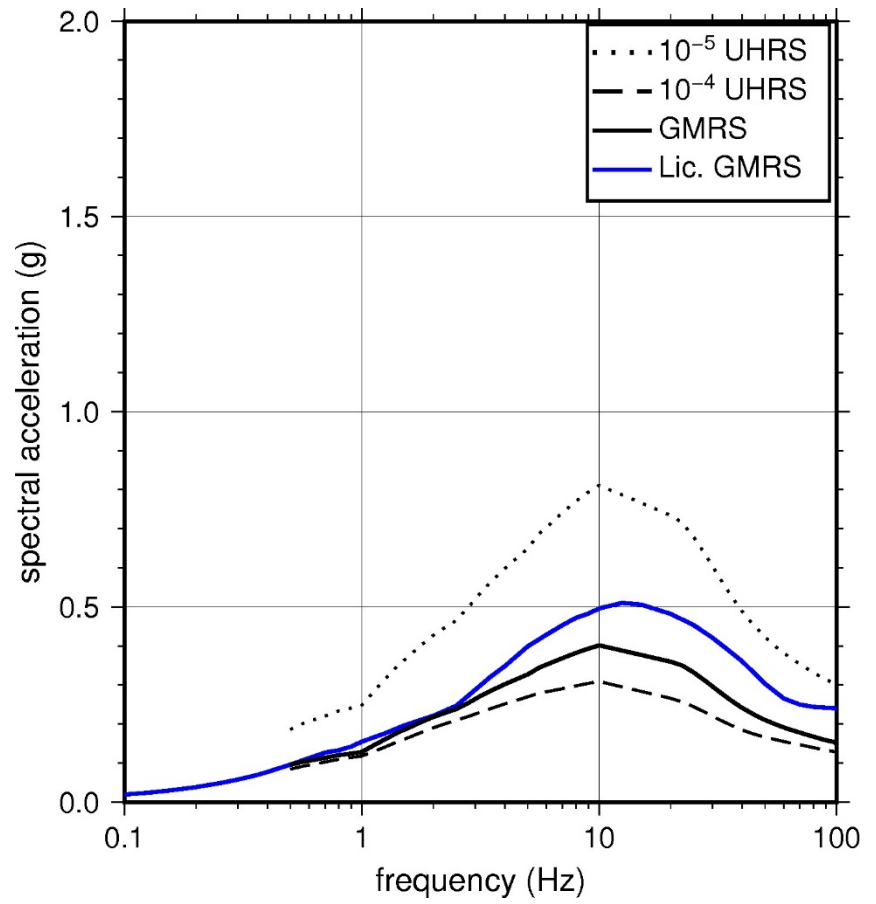
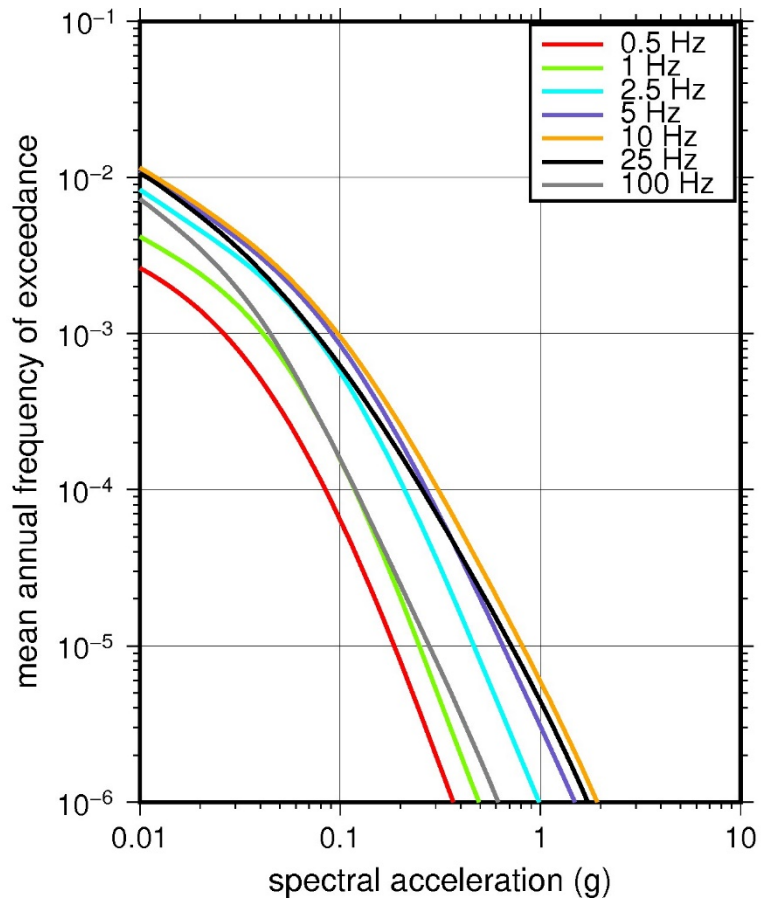


**Figure 2.5-5 Mean Control Point Hazard Curves (Left) for EPRI GMM (2013) Spectral Frequencies, and GMRS and UHRS (Right) for Arkansas**

## 2.5.2 Callaway

The Callaway Plant site is located in central Missouri near the city of Fulton within the Central Lowland physiographic province and consists of 9 m [26 ft] of backfill material overlying about 662 m [2,174 ft] of sedimentary rock (limestone, sandstone, shale, and dolomite). The horizontal SSE response spectrum for Callaway has an RG 1.60 spectral shape and is anchored at PGA of 0.20g.

### 2.5.2.1 Reference Rock Hazard

For the reference rock PSHA, the NRC staff selected the 12 CEUS-SSC (NRC, 2012b) background seismic source zones that are located within 323 km [200 mi] of the site. In addition, the NRC staff also selected the 7 CEUS-SSC (NRC, 2012b) RLME sources that are located within 807 km [500 mi] of the site. To develop the reference rock seismic hazard curves for the Callaway site, the NRC staff used the GMPEs developed by the updated EPRI GMM (2013). As shown in Figure 2.5-6, the NMFS RLME is the largest contributor to both the 1 Hz and the 10 Hz reference rock total mean hazard curves at the  $10^{-4}$  AFE level.

### 2.5.2.2 Site Response Evaluation

#### 2.5.2.2.1 Site Profiles

To develop a basecase profile, the NRC staff used the geologic information in the NTTF R2.1 SHSR (Neterer, 2014) submitted by Ameren Missouri (hereafter referred to as “the licensee” within this plant section). As described in the licensee’s SHSR, the Callaway site consists of about 9 m [31 ft] of soils overlying about 662 m [2,174 ft] of sedimentary rock. The licensee stated that all major plant structures are supported on competent rock. In Table 2.3.1-1 of the SHSR, the licensee briefly described the subsurface materials in terms of the geologic units and layer thicknesses. For its site response evaluation, the NRC staff used the finished grade as the control point elevation for the Callaway site, which corresponds to an elevation of 256 m [840 ft] above MSL.

The licensee’s profile is based on site investigations carried out for Unit 1 and the now withdrawn COL for the proposed Unit 2 (UniStar Nuclear Services, 2009b). The licensee’s geophysical field investigations measured  $V_P$  to a depth of about 43 m [140 ft] using seismic refraction surveys. To determine the  $V_S$  for each rock layer, the licensee used its measured  $V_P$  with an assumed Poisson’s ratio. In the SHSR, the licensee stated that similar  $V_S$  values had been obtained from the downhole, cross hole, suspension logging, and refraction surveys carried out for the Unit 2 COL. Table 2.3.2-1 of the SHSR gives the estimated  $V_S$  determined from the licensee’s site investigations.

For its SHSR, the licensee developed a basecase profile that extends to a depth of 672 m [2,204 ft] below the control point elevation. The uppermost layers of the profile consist of 1 m [4 ft] of silty clay overlying 8 m [26 ft] of glacial till, which consists of silty clay with sand and gravel. For the uppermost silty clay layer, the licensee estimated a  $V_S$  of about 152 m/sec [500 ft/sec] based on a measured  $V_P$  of 610 m/sec [2,000 ft/sec] and an assumed Poisson’s ratio of 0.47. Similarly, for the glacial till layer, the licensee estimated a  $V_S$  of 319 m/sec [1,045 ft/sec] based on a measured  $V_P$  of 1,341 m/sec [4,400 ft/sec] and an assumed Poisson’s ratio of 0.47. Underlying these two soil layers is a mixed soil and rock Pennsylvanian-age layer known as the Graydon Chert Conglomerate, which consists of cherty clay, sandstone, and sandy chert conglomerate. For this layer, which is 9 m [30 ft] thick, the licensee estimated a  $V_S$

of 762 m/sec [2,500 ft/sec] based on a measured  $V_P$  of 1,829 m/sec [6,000 ft/sec] and an assumed Poisson's ratio of 0.39. Beneath the conglomerate layer are the Mississippian- to Devonian-age Burlington, Bushberg, Snyder Creek, and Callaway Formations, which are primarily limestone, sandstone, and shale. The licensee combined these rock units into a single layer, for which it estimated a  $V_S$  of 1,116 m/sec [3,661 ft/sec] based on a measured  $V_P$  of 3,049 m/sec [10,000 ft/sec] and a Poisson's ratio of 0.42. For the underlying Ordovician-age Cotter-Jefferson City Formation, which is primarily dolomite, the licensee estimated a  $V_S$  of 2,287 m/sec [7,500 ft/sec] based on a measured  $V_P$  of 4,207 m/sec [13,800 ft/sec] and an assumed Poisson's ratio of 0.29. For the remaining 620 m [2,032 ft] of Ordovician- and Cambrian-age sedimentary rock, the licensee assumed a constant  $V_S$  of 2,541 m/sec [8,333 ft/sec].

Rather than using the licensee's basecase profile, the NRC staff developed its profile based on the  $V_S$  as directly measured for the COL for nearby Unit 2 (Callaway Energy, 2013). These measurements are based on numerous test borings and modern geophysical methods; they extend to a depth of about 107 m [350 ft]. For the uppermost layer of its profile, the NRC staff used the backfill material, which underlies the containment building down to a depth of 8 m [25 ft] below grade, rather than the removed in situ soils. The NRC staff divided the backfill layer into three sublayers, to which it assigned  $V_S$  values of 274 m/sec [900 ft/sec], 305 m/sec [1,000 ft/sec], and 320 m/sec [1,050 ft/sec] to capture the increase in velocity with increasing effective pressure. In addition, rather than combining the Mississippian- to Devonian-age rock formations into a single layer, the NRC staff used the layer groupings developed for the Unit 2 subsurface profile. Consequently, the NRC staff's profile included a reversal in seismic velocity between the two Snyder Creek Formation sublayers. The downhole geophysical measurements for Unit 2 extend to the bottom of the Cotter-Jefferson City Formation, which is subdivided into two layers. The measured median  $V_S$  is 2,119 m/sec [6,950 ft/sec] for the upper 10 m [33 ft] and 2,530 m/sec [8,300 ft/sec] for the remaining 54 m [178 ft]. Beneath the Cotter-Jefferson City Formation are the Roubidoux Formation, which consists primarily of sandstone and dolomite, and the Gasconade Formation, which is primarily dolomite. For the Roubidoux Formation, the NRC staff assumed a  $V_S$  of 2,591 m/sec [8,500 ft/sec]. For the Gasconade Formation and the underlying Cambrian-age strata, the NRC staff assumed that the  $V_S$  exceeds the reference rock  $V_S$  of 2,831 m/sec [9,285 ft/sec]. As a result, the NRC staff's basecase profile has a total thickness of 143 m [470 ft], as opposed to the thickness of 672 m [2,204 ft] modeled by the licensee. The NRC staff's decision to terminate its profile at this depth is based on an examination of (1) the lithology for these deeper formations (Eminence, Potosi, Derby-Doe Run, Davis, Bonneterre, and Lamotte), which are primarily dolomite with some sandstone and shale, and (2) the  $V_S$  values for similar deep Paleozoic sedimentary rock strata at other Region III and Region IV sites.

To capture the uncertainty in its basecase profile, the NRC staff developed lower and upper range (10<sup>th</sup> and 90<sup>th</sup> percentile) profiles by multiplying the basecase  $V_S$  values by scale factors of 0.78 and 1.29, respectively, which corresponds to an epistemic logarithmic standard deviation of 0.15. The weights for the lower, basecase, and upper profiles are 0.3, 0.4, and 0.3, respectively. As shown in Figure 2.5-7, the upper profile terminates at a depth of 52 m [172 ft], while the best-estimate basecase and lower profiles extend to a depth of 143 m [470 ft] below the control point elevation.

#### 2.5.2.2.2 *Dynamic Material Properties and Site Kappa*

The NRC staff assumed both linear and nonlinear dynamic behavior for the soil and rock beneath the Callaway site. To model the nonlinear behavior of the soil layers (Layers 1–3), the

NRC staff used the EPRI soil and Peninsular Range shear modulus reduction and material damping curves as two equally weighted alternatives. For the weathered rock layers (Layers 4–7), the NRC staff used the EPRI rock shear modulus reduction and material damping curves. To model the linear behavior of these rock layers, the NRC staff assumed a constant damping ratio of 3 percent. The staff weighted these two alternatives equally. For the higher velocity rock layers, the NRC staff assumed a linear dynamic response with damping values of 0.25 percent to maintain consistency with the  $\kappa_0$  value for the Callaway site.

To determine the basecase  $\kappa_0$  for the Callaway site, the NRC staff first used the Campbell (2009) Model 1 relationship between  $V_S$  and  $Q_{ef}$  to determine a  $Q_{ef}$  for each layer. Combining these  $Q_{ef}$  values with the thickness and  $V_S$  for each layer results in a total  $\kappa_0$  value of 9 msec, which includes the 6 msec assumed for the underlying reference rock. For the lower and upper profiles, the NRC staff calculated  $\kappa_0$  values of 10 and 8 msec, respectively, using the same approach as for the basecase profile. In contrast, the licensee estimated  $\kappa_0$  by combining the low-strain damping values from the material damping curves over the top 152 m [500 ft] of soil and rock and assumed a damping value of 1.25 percent for the remaining deeper rock layers to estimate basecase, lower, and upper  $\kappa_0$  values of 16, 20, and 9 msec, respectively.

Table 2.5-3 provides the layer depths, lithologies,  $V_S$ , unit weights, and dynamic properties for the NRC staff's three profiles. In summary, the site response logic tree developed by the NRC staff for the Callaway site consists of six alternatives; three velocity profiles (each with a different  $\kappa_0$  value) and two alternative dynamic property branches.

#### 2.5.2.2.3 Methodology and Results

The NRC staff followed the methodology described in Section 2.1.4 to develop the final site amplification factors. Figure 2.5-8 shows the overall median site amplification factors and their variability for each of the seven spectral frequencies. As shown in Figure 2.5-8, the median site amplification factors range from about 1.0 to 3.5 before falling off with higher input spectral accelerations. The lower half of Figure 2.5-8 shows that the logarithmic standard deviations for the site amplification factors range from about 0.1 to 0.3.

#### 2.5.2.3 Control Point Hazard

The NRC staff implemented Approach 3 from the SPID (EPRI, 2012) to develop a weighted control point seismic hazard curve for each of the six unique combinations of the site response logic tree for the Callaway site. After combining these curves to develop the final mean control point hazard curves, the NRC staff determined the  $10^{-4}$  and  $10^{-5}$  UHRS in order to calculate the GMRS. Figure 2.5-9 shows the final control point mean seismic hazard curves for the seven spectral frequencies, as well as the NRC staff's UHRS and GMRS and the licensee's NTTF R2.1 GMRS (Neterer, 2014). As shown in Figure 2.5-9, the NRC staff's GMRS (black curve) is similar to the licensee's GMRS (blue curve) over the entire frequency range.



**Table 2.5-3 Layer Depths, Shear Wave Velocities ( $V_s$ ), Unit Weights, and Dynamic Properties for Callaway**

Layer	Depth (ft)	Description	$V_s$ (ft/sec)			$V_s$ Sigma (In)	BC Unit Weight (pcf)	Dynamic Properties	
			LR (0.3)	BC (0.4)	UR (0.3)			Alt. 1 (0.5)	Alt. 2 (0.5)
1	8	Soil Fill	743	900	1,091	0.25	120	EPRI Soil	Pen.
2	17	Soil Fill	825	1,000	1,212	0.15	120	EPRI Soil	Pen.
3	26	Soil Fill	866	1,050	1,273	0.15	120	EPRI Soil	Pen.
4	57	Soil & Rock conglomerate	1,928	2,337	2,833	0.15	130	EPRI Rock	L 3.0%
5	71	Rock: limestone, sandstone	3,343	4,052	4,911	0.15	140	EPRI Rock	L 3.0%
6	81	Rock: limestone	4,990	6,048	7,330	0.15	150	EPRI Rock	L 3.0%
7	101	Rock: shale, limestone	3,064	3,714	4,502	0.15	140	EPRI Rock	L 3.0%
8	139	Rock: limestone	6,896	8,358	9,285	0.15	160	L 0.25%	L 0.25%
9	172	Rock: dolomite	5,734	6,950	8,424	0.15	150	L 0.25%	L 0.25%
10	350	Rock: dolomite	6,847	8,300	9,285	0.15	160	L 0.25%	L 0.25%
11	470	Rock: sandstone, dolomite	7,013	8,500	9,285	0.15	160	L 0.25%	L 0.25%

LR = lower range; BC = basecase; UR = upper range; ln = natural log; pcf = pounds per cubic foot; L = linear; Alt. = alternative; Pen. = Peninsular.  
 For LR, BC, UR, and Alt.: Values in parentheses refer to weights for site response analysis logic tree branches.

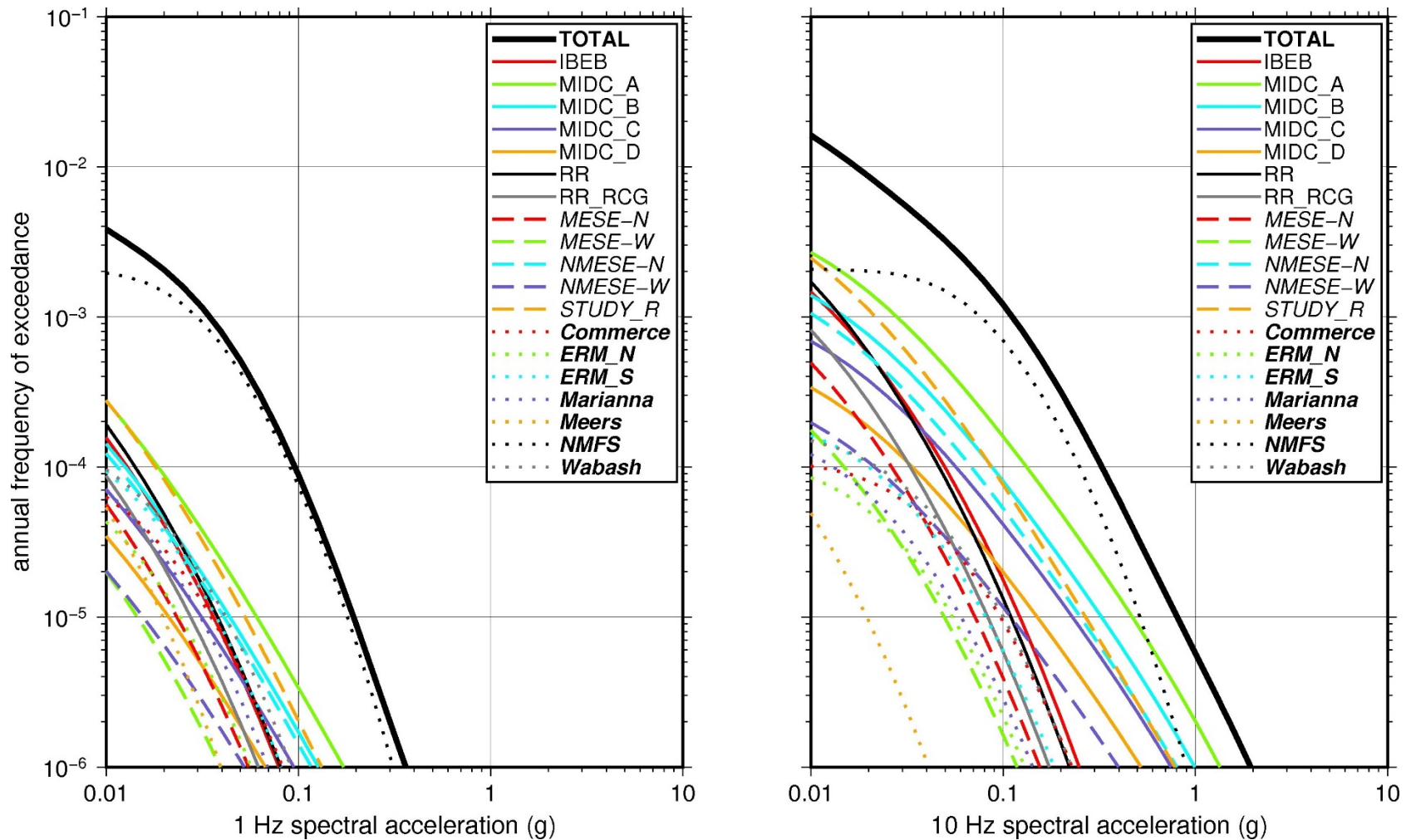


**Figure 2.5-6 Low-Frequency (1 Hz, Left), and High-Frequency (10 Hz, Right) Reference Rock Hazard Curves for Callaway. Total Hazard is Shown as a Bold Black Line; Individual Contributions to the Hazard for Each of the CEUS-SSC Sources are Shown as Colored Lines Defined in the Legend. See Table 2.1-1 for Source Name Definitions**

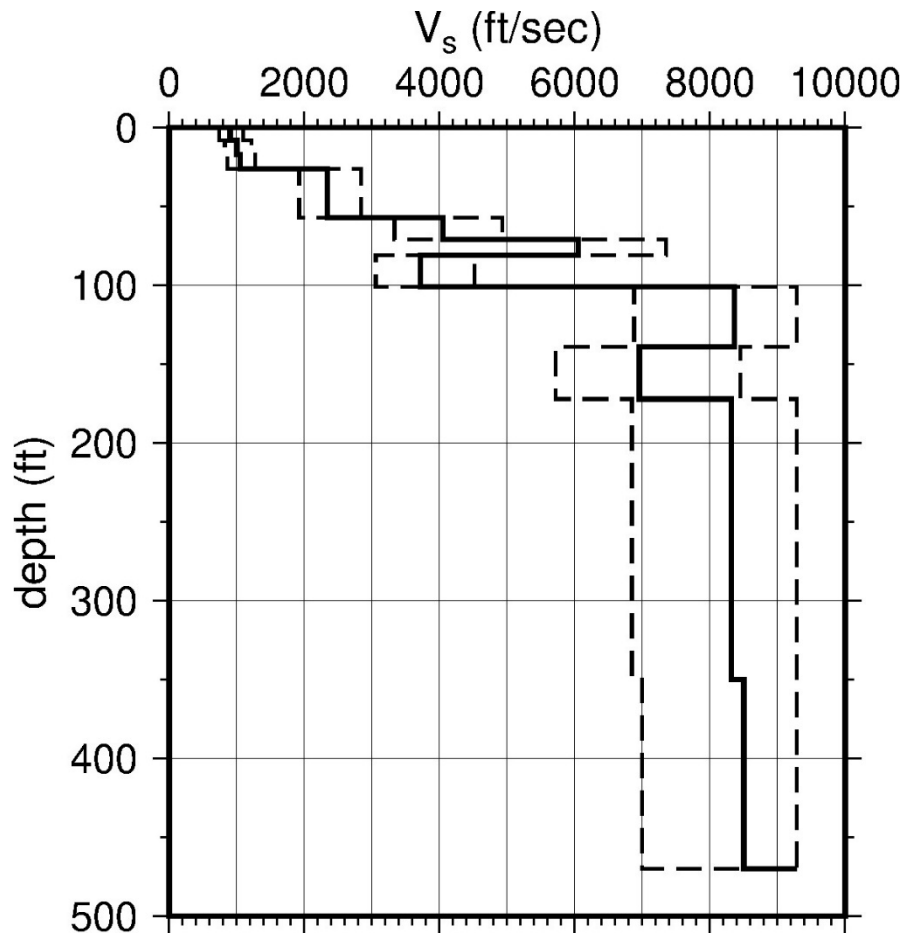


**Figure 2.5-7** Shear Wave Velocity ( $V_s$ ) Profiles for Callaway. Basecase (BC) Profile Shown as Solid Bold Line; Lower and Upper Range (LR and UR) Profiles Shown as Dashed Lines. Profiles Terminate at Reference Rock Velocity of 2,831 m/sec [9,285 ft/sec] per EPRI GMM (2013)

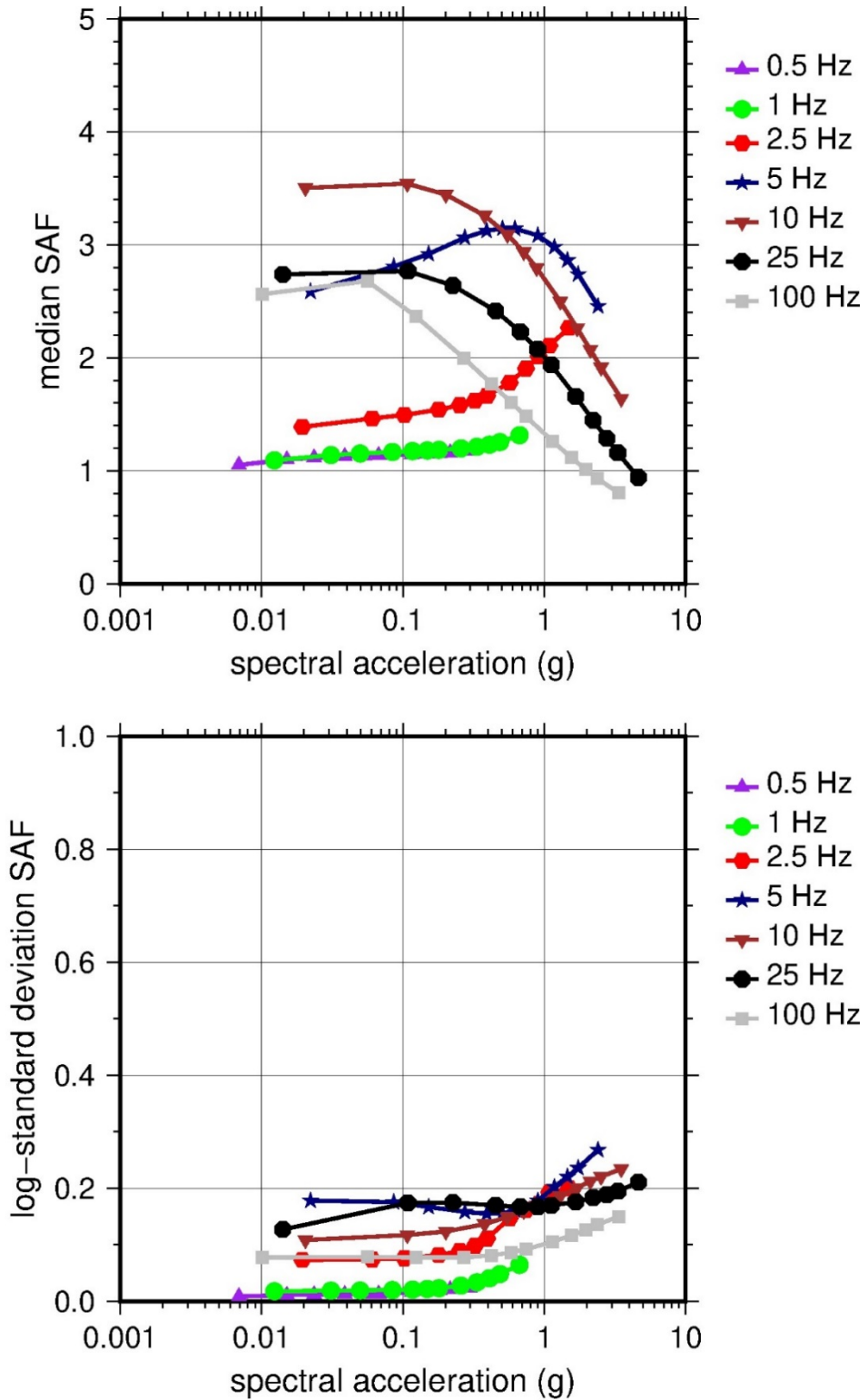


**Figure 2.5-8 Overall Weighted Median Site Amplification Factor (SAF) (Upper) and Log Standard Deviation of the SAF (Lower) as a Function of Input Acceleration for EPRI GMM (2013) Spectral Frequencies**

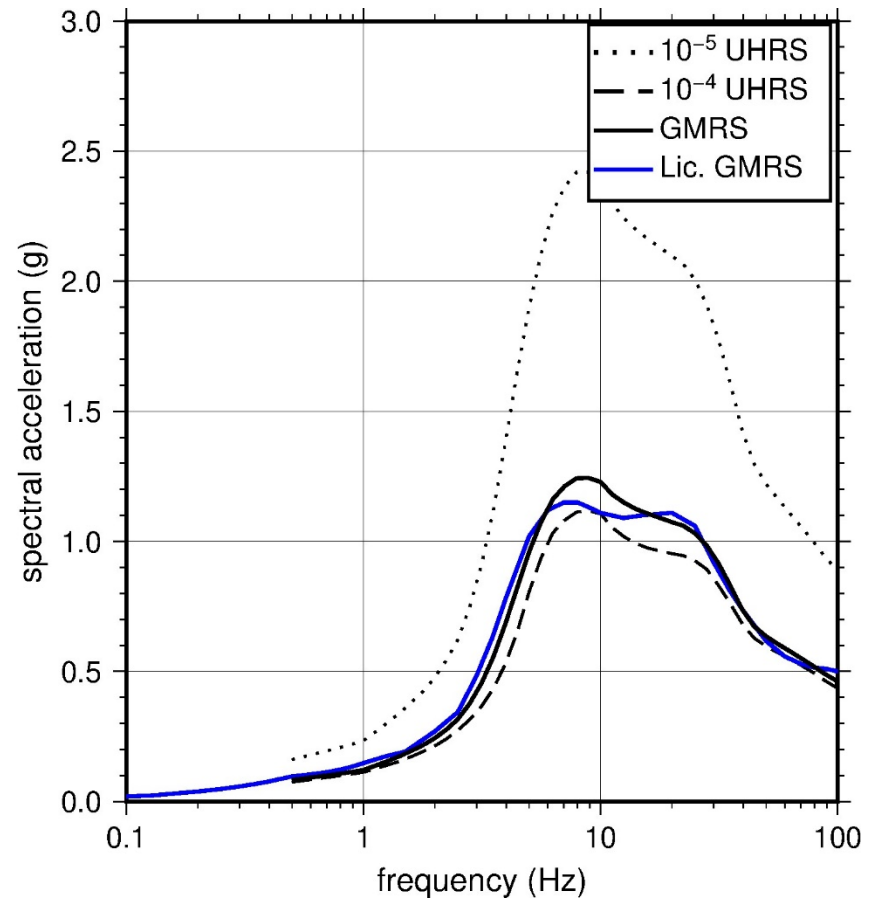
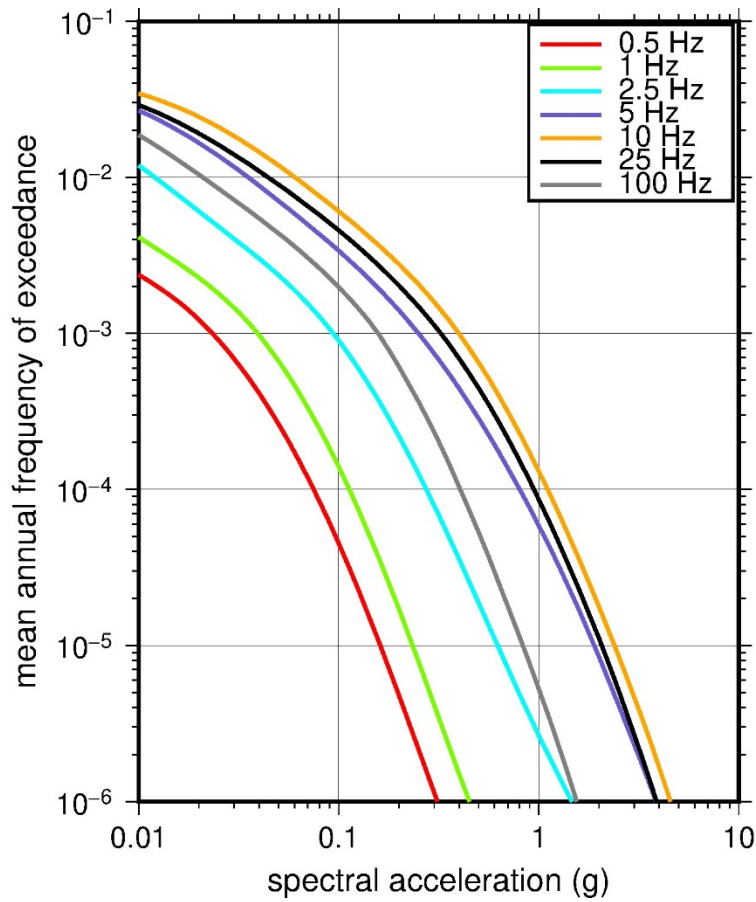


**Figure 2.5-9 Mean Control Point Hazard Curves (Left) for EPRI GMM (2013) Spectral Frequencies, and GMRS and UHRS (Right) for Callaway**

### 2.5.3 Comanche Peak

The Comanche Peak Nuclear Power Plant site is located in north-central Somervell County, TX, within the Great Plains physiographic province and is underlain by over 2,134 m [7,000 ft] of sedimentary rock. The horizontal SSE response spectrum for Comanche Peak has an RG 1.60 spectral shape and is anchored at a PGA of 0.12g.

#### 2.5.3.1 Reference Rock Hazard

For the reference rock PSHA, the NRC staff selected the 12 CEUS-SSC (NRC, 2012b) background seismic source zones that are located within 323 km [200 miles] of the site. In addition, the NRC staff also selected the 4 CEUS-SSC (NRC, 2012b) RLME sources that are located within 807 km [500 miles] of the site. To develop the reference rock seismic hazard curves for the Comanche Peak site, the NRC staff used the GMPEs developed by the updated EPRI GMM (2013). As shown in Figure 2.5-10, the NMFS RLME is the largest contributor to the 1 Hz reference rock total mean hazard curve at the  $10^{-4}$  AFE level. For the 10 Hz reference rock total mean hazard curve, the Meers Fault RLME is the largest contributor at the  $10^{-4}$  AFE level.

#### 2.5.3.2 Site Response Evaluation

##### 2.5.3.2.1 Site Profiles

To develop a basecase profile, the NRC staff used the geologic information in the NTTF R2.1 SHSR (Flores, 2014) submitted by Luminant Power (hereafter referred to as “the licensee” within this plant section). As described in the licensee’s SHSR, the Comanche Peak site is located on the southern flank of the Fort Worth Basin and consists of about 122 m [400 ft] of early Cretaceous sedimentary rocks overlying Paleozoic-age sedimentary rocks (predominantly shale, limestone, and sandstone). The plant is founded on firm sedimentary rock (limestone) of the early Cretaceous Glen Rose Formation. In Table 2.3.1-1 of the SHSR, the licensee briefly described the subsurface materials in terms of the geologic units and layer thicknesses. For its site response evaluation, the NRC staff used the ground surface, which corresponds to an elevation of 248 m [814 ft] above MSL, as the control point elevation for the Comanche Peak site.

Comanche Peak Units 1 and 2 are co-located on the same plateau with the proposed Units 3 and 4, with a separation of about 915 m [3,000 ft]. Consequently, the licensee used the more modern and extensive field investigations from the COL for Units 3 and 4, which consisted of boreholes, seismic suspension logging, and other studies of the subsurface (Luminant Power, 2009). For the deeper rock layers, below a depth of 120 m [393 ft], the COL applicant used the  $V_s$  measured from a single nearby well log {10 km [6 mi] away} over a limited depth interval to estimate the velocity gradient for the rest of its basecase profile. Table 2.3.2-2 of the SHSR gives the measured and estimated  $V_s$  determined from the licensee’s site investigations.

For its SHSR, the licensee developed a basecase profile that extends to a depth of about 1,600 m [5,300 ft] below the control point elevation. The uppermost layers of the profile consist of the early Cretaceous Glen Rose Formation, which is primarily limestone and shale and is about 49 m [160 ft] thick. The licensee divided the Glen Rose Formation into five sublayers, with  $V_s$  ranging from about 915 m/sec to 2,134 m/sec [3,000 ft/sec to 7,000 ft/sec]. Beneath the Glen Rose Formation is the Twin Mountains Formation, which consists of limestone, shale, and sandstone, with measured  $V_s$  of about 1,006 m/sec [3,300 ft/sec]. Underlying the Twin

Mountains Formation are several formations comprising the Pennsylvanian-age Strawn Group. The uppermost of these is the Mineral Wells Formation, for which the licensee measured a  $V_S$  of 1,691 m/sec [5,546 ft/sec]. For the underlying Atoka Group, which consists of sandstone, limestone, and shale, the licensee inferred a  $V_S$  of 2,330 m/sec [7,642 ft/sec] based on the general rock type, age, and depth. As described above, the licensee used the  $V_S$  measured from a nearby well for the Mississippian-age Marble Falls limestone ( $V_S = 3,207$  m/sec [10,520 ft/sec]) and Barnett Formation shale ( $V_S = 2,373$  m/sec [7,783 ft/sec]).

To corroborate the licensee's reported  $V_S$  and Poisson's ratios, the NRC staff used data from the field and laboratory investigations for the proposed Units 3 and 4. The NRC staff's basecase profile is the same as the licensee's profile, with two minor exceptions. Rather than use the  $V_S$  of 1,691 m/sec [5,546 ft/sec] measured for the Mineral Wells Formation for the entire 671-m-thick [2,202-ft-thick] Strawn Group, the NRC staff divided this layer into four sublayers and used a  $V_S$  gradient of 0.5 m/sec/m [0.5 ft/sec/ft] to estimate the velocities for the lower three layers. Similarly, the NRC staff divided the 581-m-thick [1,905-ft-thick] Atoka Group into two sublayers, for which it used the same  $V_S$  gradient.

To capture the uncertainty in its basecase profile, the NRC staff developed lower and upper range (10<sup>th</sup> and 90<sup>th</sup> percentile) profiles by multiplying the basecase  $V_S$  values by scale factors of 0.78 and 1.29, respectively, which corresponds to an epistemic logarithmic standard deviation of 0.20. The weights for the lower, basecase, and upper profiles are 0.3, 0.4, and 0.3, respectively. Figure 2.5-11 shows the upper 1,220 m [4,000 ft] of the NRC staff's profiles. As shown in Figure 2.5-11, the upper profile terminates at a depth of 791 m [2,595 ft], while the basecase and lower profiles extend to a depth of 1,616 m [5,300 ft] below the control point elevation.

#### 2.5.3.2.2 *Dynamic Material Properties and Site Kappa*

The NRC staff assumed both linear and nonlinear dynamic behavior for the rock beneath the Comanche Peak site. To model the nonlinear behavior of the uppermost weathered rock layers (Layers 1–6), the NRC staff used the EPRI rock shear modulus reduction and material damping curves. To model the alternative linear behavior of these rock layers, the NRC staff assumed a constant damping ratio of 3 percent. Because these rock layers have high velocities {1,524 m/sec [ $>5,000$  ft/sec]}, the NRC staff assigned weights of 0.7 and 0.3 to the linear and nonlinear alternatives, respectively. For the underlying more intact sedimentary rock layers, the NRC staff assumed a linear response with a material damping ratio of 0.10 to maintain consistency with the  $\kappa_0$  value for the Comanche Peak site.

To determine the basecase  $\kappa_0$  for the Comanche Peak site, the NRC staff first used the Campbell (2009) Model 1 relationship between  $V_S$  and  $Q_{ef}$  to determine a  $Q_{ef}$  for each layer. Combining these  $Q_{ef}$  values with the thickness and  $V_S$  for each layer results in a total  $\kappa_0$  value of 19 msec, which includes the 6 msec assumed for the underlying reference rock. For the lower and upper profiles, the NRC staff calculated  $\kappa_0$  values of 28 and 12 msec, respectively, using the same approach as for the basecase profile. In contrast, the licensee estimated  $\kappa_0$  using the average  $V_S$  over the upper 30 m [100 ft] of rock. The relationship between  $V_{S100}$  and  $\kappa_0$  produces basecase, lower, and upper  $\kappa_0$  estimates of 19, 25, and 15 msec, respectively, which are similar to the NRC staff's estimates.

Table 2.5-4 provides the layer depths, lithologies,  $V_S$ , unit weights, and dynamic properties for the NRC staff's three profiles. In summary, the site response logic tree developed by the NRC

staff for the Comanche Peak site consists of six alternatives; three velocity profiles (each with a different  $\kappa_0$  value) and two alternative dynamic property branches.

#### 2.5.3.2.3 *Methodology and Results*

The NRC staff followed the methodology described in Section 2.1.4 to develop the final site amplification factors. Figure 2.5-12 shows the overall median site amplification factors and their variability for each of the seven spectral frequencies. As shown in Figure 2.5-12, the median site amplification factors range from about 1.0 to 1.5 before falling off with higher input spectral accelerations. The lower half of Figure 2.5-12 shows that the logarithmic standard deviations for the site amplification factors range from about 0.05 to 0.15.

#### 2.5.3.3 *Control Point Hazard*

The NRC staff implemented Approach 3 from the SPID (EPRI, 2012) to develop a weighted control point seismic hazard curve for each of the six unique combinations of the site response logic tree for the Comanche Peak site. After combining these curves to develop the final mean control point hazard curves, the NRC staff determined the  $10^{-4}$  and  $10^{-5}$  UHRS in order to calculate the GMRS. Figure 2.5-13 shows the final control point mean seismic hazard curves for the seven spectral frequencies, as well as the NRC staff's UHRS and GMRS and the licensee's NTTF R2.1 GMRS (Flores, 2014). As shown in Figure 2.5-13, the NRC staff's GMRS (black curve) is similar to the licensee's GMRS (blue curve) over the entire frequency range.



**Table 2.5-4 Layer Depths, Shear Wave Velocities ( $V_s$ ), Unit Weights, and Dynamic Properties for Comanche Peak**

Layer	Depth (ft)	Description	$V_s$ (ft/sec)			$V_s$ Sigma (ln)	BC Unit Weight (pcf)	Dynamic Properties	
			LR (0.3)	BC (0.4)	UR (0.3)			Alt. 1 (0.3)	Alt. 2 (0.7)
1	65	Rock: limestone	4,399	5,685	7,347	0.25	150	EPRI Rock	L 3.0%
2	68	Rock: shale	2,336	3,019	3,901	0.15	130	EPRI Rock	L 3.0%
3	92	Rock: limestone	3,825	4,943	6,388	0.15	140	EPRI Rock	L 3.0%
4	126	Rock: limestone	5,324	6,880	8,891	0.15	150	EPRI Rock	L 3.0%
5	160	Rock: limestone	3,128	4,042	5,223	0.15	140	EPRI Rock	L 3.0%
6	393	Rock: limestone, shale, sandstone	2,538	3,280	4,239	0.15	130	EPRI Rock	L 3.0%
7	893	Rock: shale, sandstone, limestone	4,292	5,546	7,167	0.15	150	L 0.1%	L 0.1%
8	1,393	Rock: shale, sandstone, limestone	4,485	5,796	7,490	0.15	150	L 0.1%	L 0.1%
9	1,893	Rock: shale, sandstone, limestone	4,679	6,046	7,813	0.15	150	L 0.1%	L 0.1%
10	2,595	Rock: shale, sandstone, limestone	4,950	6,397	8,267	0.15	150	L 0.1%	L 0.1%
11	3,547	Rock: sandstone	5,914	7,642	9,285	0.15	160	L 0.1%	L 0.1%
12	4,500	Rock: sandstone	6,283	8,112	9,285	0.15	160	L 0.1%	L 0.1%
13	5,000	Rock: limestone	7,185	9,285	9,285	0.15	160	L 0.1%	L 0.1%
14	5,300	Rock: shale	6,023	7,783	9,285	0.15	160	L 0.1%	L 0.1%

LR = lower range; BC = basecase; UR = upper range; ln = natural log; pcf = pounds per cubic foot; L = linear; Alt. = alternative.  
 For LR, BC, UR, and Alt.: Values in parentheses refer to weights for site response analysis logic tree branches.

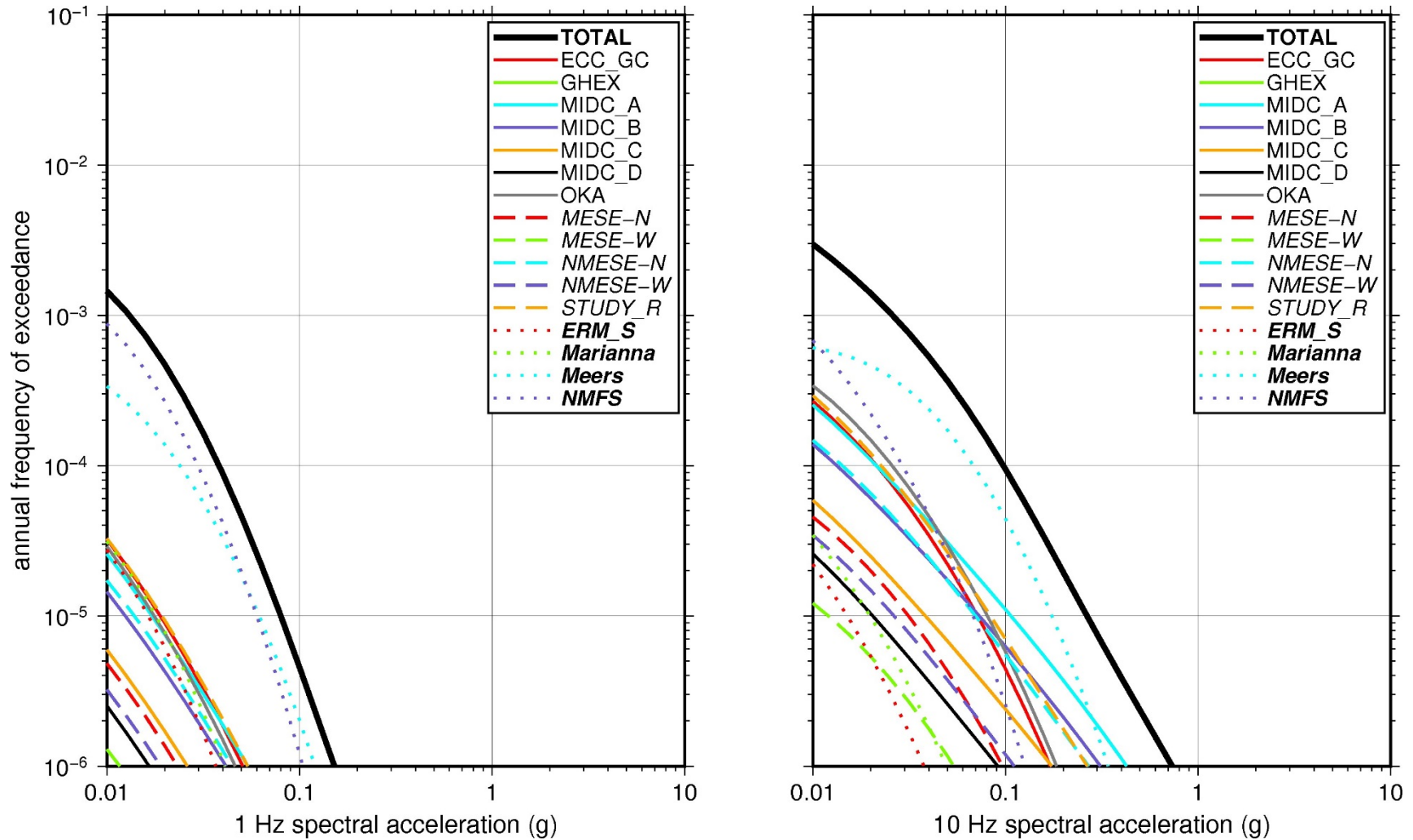


**Figure 2.5-10** Low-Frequency (1 Hz, Left), and High-Frequency (10 Hz, Right) Reference Rock Hazard Curves for Comanche Peak. Total Hazard is Shown as a Bold Black Line; Individual Contributions to the Hazard for Each of the CEUS-SSC Sources are Shown as Colored Lines Defined in the Legend. See Table 2.1-1 for Source Name Definitions

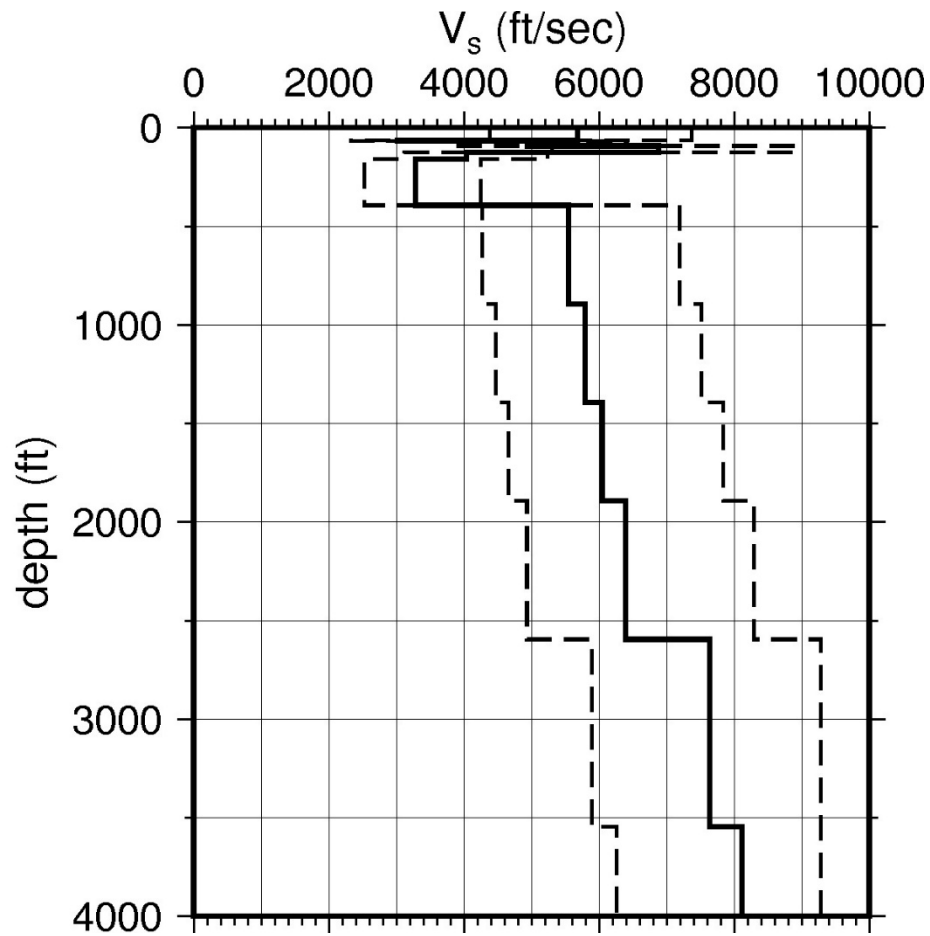


**Figure 2.5-11 Shear Wave Velocity ( $V_s$ ) Profiles for Comanche Peak. Basecase (BC) Profile Shown as Solid Bold Line; Lower and Upper Range (LR and UR) Profiles Shown as Dashed Lines. Profiles Terminate at Reference Rock Velocity of 2,831 m/sec [9,285 ft/sec] per EPRI GMM (2013)**

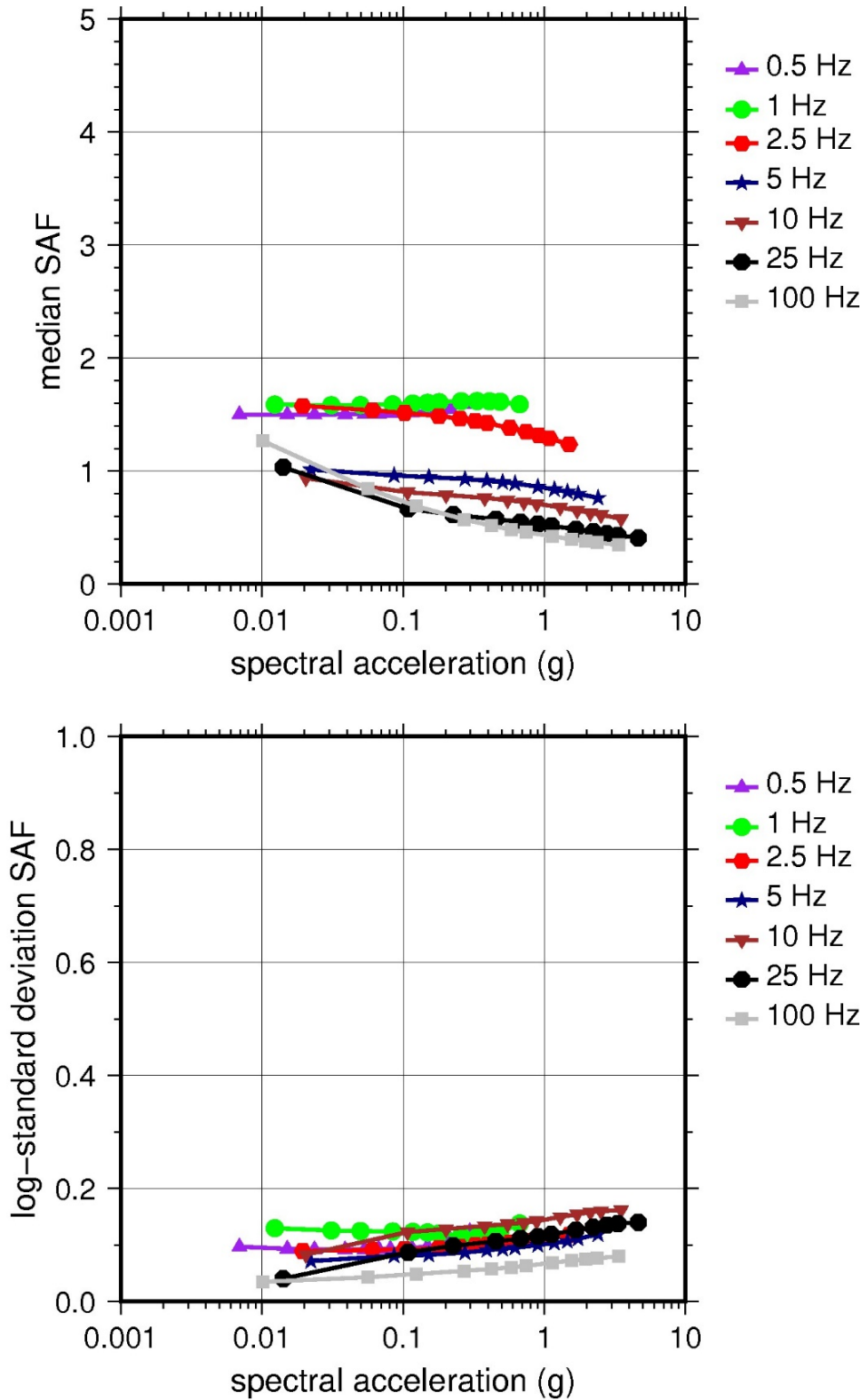


**Figure 2.5-12 Overall Weighted Median Site Amplification Factor (SAF) (Upper) and Log Standard Deviation of the SAF (Lower) as a Function of Input Acceleration for EPRI GMM (2013) Spectral Frequencies**

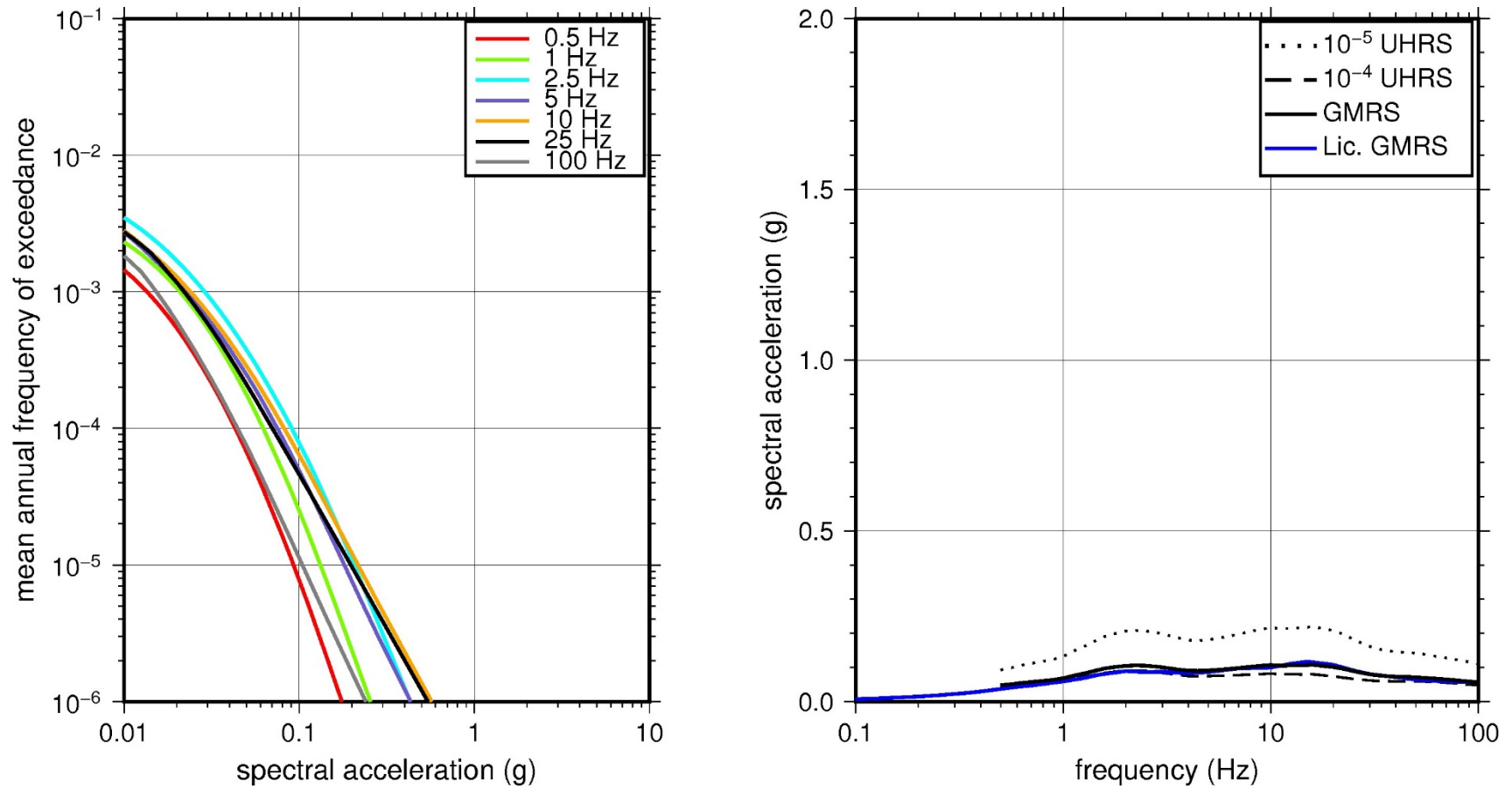


**Figure 2.5-13 Mean Control Point Hazard Curves (Left) for EPRI GMM (2013) Spectral Frequencies, and GMRS and UHRs (Right) for Comanche Peak**

## 2.5.4 Cooper

The Cooper Nuclear Station site is located in southeastern Nebraska along the Missouri River within the Central Lowland physiographic province and consists of 15 m [50 ft] of soil (silt and till) overlying about 1,067 m [3,500 ft] of sedimentary rock (shale, sandstone, and limestone). The horizontal SSE response spectrum for Cooper is a smoothed interpolation of the response spectrum from the N69°W Taft, CA, recording of the 1952 *M*7.5 earthquake in Kern County, CA. The SSE is anchored at a PGA of 0.20g.

### 2.5.4.1 Reference Rock Hazard

For the reference rock PSHA, the NRC staff selected the seven CEUS-SSC (NRC, 2012b) background seismic source zones that are located within 200 miles [323 km] of the site. In addition, the NRC staff selected the eight CEUS-SSC (NRC, 2012b) RLME sources that are located within 807 km [500 miles] of the site. To develop the reference rock seismic hazard curves for the Cooper site, the NRC staff used the GMPEs developed by the updated EPRI GMM (2013). As shown in Figure 2.5-14, the NMFS RLME is the largest contributor to the 1 Hz reference rock total mean hazard curve at the  $10^{-4}$  AFE level. For the 10 Hz reference rock total mean hazard curve at the  $10^{-4}$  AFE level, the MIDC-A seismotectonic source zone is the largest contributor.

### 2.5.4.2 Site Response Evaluation

#### 2.5.4.2.1 Site Profiles

To develop a basecase profile, the NRC staff used the geologic information in the NTTF R2.1 SHSR (Limpas, 2015) submitted by Nebraska Public Power District (hereafter referred to as “the licensee” within this plant section). As described in the licensee’s SHSR, the Cooper site is underlain by the Forest City Basin and consists of 15 m [50 ft] of fill and compacted alluvium overlying gently dipping sedimentary rock strata. The Cooper plant structures are founded on dense structural fill. In Tables 2.3.1-1a and 2.3.1-1b of the SHSR, the licensee briefly described the subsurface materials in terms of the geologic units and layer thicknesses. For its site response evaluation, the NRC staff used the top of the compacted fill layer, which corresponds to an elevation of 265 m [870 ft] above MSL, as the control point elevation for the Cooper site.

The field investigations for Cooper consisted of suspension logging and downhole seismic testing to determine the  $V_S$  for the upper 30 m [97 ft] of fill material and uppermost layers of rock. Table 2.3.2-1 of the SHSR gives the measured and estimated  $V_S$  determined from the licensee’s site investigations.

For its SHSR, the licensee developed a basecase profile with a total thickness of 1,081 m [3,547 ft]. The licensee’s profile begins with 15 m [50 ft] of fill overlying 14 m [45 ft] of soft and weathered Permian-age rock from the Admire Group, which is predominantly shale and limestone. The licensee measured  $V_S$  values of about 305 m/sec [1,000 ft/sec] for the uppermost fill layer and about 518 m/sec [1,700 ft/sec] for the soft rock within the Admire Group. For the underlying Pennsylvanian-age sedimentary rock of the Wabaunsee Group, which consists of shale, sandstone, and interbedded limestone, the licensee measured a  $V_S$  of about 2,223 m/sec [7,292 ft/sec]. Starting with this  $V_S$ , the licensee assumed a velocity gradient of 0.5 m/sec/m [0.5 ft/sec/ft] for the remaining 1,053 m [3,455 ft] of Paleozoic sedimentary rock. As a result, the terminal  $V_S$  for the licensee’s basecase profile is 2,744 m/sec [9,000 ft/sec] at the base of the profile.

For its basecase profile, the NRC staff used the licensee's layer thicknesses and  $V_S$  down through the Permian-age soft rock from the Admire Group. Like the licensee, the NRC staff assumed a velocity gradient of 0.5 m/sec/m [0.5 ft/sec/ft] beginning with the Pennsylvanian-age sedimentary rock of the Wabaunsee Group. However, the NRC staff terminated its profile at the base of the Cherokee Group, which is at the base of the Pennsylvanian-age strata, rather than extending it through the entire Paleozoic sedimentary column. The NRC staff based its decision to terminate its profile here on an examination of the lithology for the deeper sedimentary rock, which is predominantly limestone and dolomite. The NRC staff concluded that the  $V_S$  for these deeper carbonate rock layers likely exceeds the reference rock  $V_S$  of 2,831 m/sec [9,285 ft/sec]. Therefore, the NRC staff's basecase profile extends to approximately 585 m [1,920 ft] below the control point elevation, as opposed to the 1,081 m [3,547 ft] of the licensee's profile.

To capture the uncertainty in its basecase profile, the NRC staff developed lower and upper range (10<sup>th</sup> and 90<sup>th</sup> percentile) profiles by multiplying the basecase  $V_S$  values by scale factors of 0.78 and 1.29, respectively, which corresponds to an epistemic logarithmic standard deviation of 0.20. The weights for the lower, basecase, and upper profiles are 0.3, 0.4, and 0.3, respectively. Figure 2.5-15 shows the upper 305 m [1,000 ft] of the NRC staff's profiles. As shown in Figure 2.5-15, the upper profile terminates at a depth of 29 m [95 ft], while the basecase and lower profiles extend to a depth of 585 m [1,920 ft] below the control point elevation.

#### 2.5.4.2.2 *Dynamic Material Properties and Site Kappa*

The NRC staff assumed both linear and nonlinear dynamic behavior for the soil and rock beneath the Cooper site. To model the nonlinear behavior of the top fill layers (Layers 1–2), the NRC staff used the EPRI soil and Peninsular Range shear modulus reduction and material damping curves as two equally weighted alternatives. For the weathered rock layers (Layers 3–5), the NRC staff used the EPRI rock shear modulus reduction and material damping curves. To model the alternative linear behavior of these rock layers, the NRC staff assumed a constant damping ratio of 3 percent. The staff weighted these two alternatives equally. For the higher velocity rock layers, the NRC staff assumed a linear dynamic response with a material damping ratio of 0.1 percent to maintain consistency with the  $\kappa_0$  value for the Cooper site.

To determine the basecase  $\kappa_0$  for the Cooper site, the NRC staff first used the Campbell (2009) Model 1 relationship between  $V_S$  and  $Q_{ef}$  to determine a  $Q_{ef}$  for each layer. Combining these  $Q_{ef}$  values with the thickness and  $V_S$  for each layer results in a total  $\kappa_0$  value of 13 msec, which includes the 6 msec assumed for the underlying reference rock. For the lower and upper profiles, the NRC staff calculated  $\kappa_0$  values of 18 and 9 msec, respectively, using the same approach as for the basecase profile. In contrast, the licensee estimated  $\kappa_0$  by combining the low-strain damping values from the material damping curves over the top 152 m [500 ft] of soil and rock and assumed a damping value of 1.25 percent for the remaining deeper rock layers to estimate basecase, lower, and upper  $\kappa_0$  values of 21, 30, and 8 msec, respectively.

Table 2.5-5 provides the layer depths, lithologies,  $V_S$ , unit weights, and dynamic properties for the NRC staff's three profiles. In summary, the site response logic tree developed by the NRC staff for the Cooper site consists of six alternatives; three velocity profiles (each with a different  $\kappa_0$  value) and two alternative dynamic property branches.

#### 2.5.4.2.3 *Methodology and Results*

The NRC staff followed the methodology described in Section 2.1.4 to develop the final site amplification factors. Figure 2.5-16 shows the overall median site amplification factors and their variability for each of the seven spectral frequencies. As shown in Figure 2.5-16, the median site amplification factors range from about 1 to 3 before falling off with higher input spectral accelerations. The lower half of Figure 2.5-16 shows that the logarithmic standard deviations for the site amplification factors range from about 0.05 to 0.30.

#### 2.5.4.3 *Control Point Hazard*

The NRC staff implemented Approach 3 from the SPID (EPRI, 2012) to develop a weighted control point seismic hazard curve for each of the six unique combinations of the site response logic tree for the Cooper site. After combining these curves to develop the final mean control point hazard curves, the NRC staff determined the  $10^{-4}$  and  $10^{-5}$  UHRS in order to calculate the GMRS. Figure 2.5-17 shows the final control point mean seismic hazard curves for the seven spectral frequencies, as well as the NRC staff's UHRS and GMRS and the licensee's NTTF R2.1 GMRS (Limpias, 2015). As shown in Figure 2.5-17, the NRC staff's GMRS (black curve) is similar to the licensee's GMRS (blue curve) over the entire frequency range.



**Table 2.5-5 Layer Depths, Shear Wave Velocities ( $V_s$ ), Unit Weights, and Dynamic Properties for Cooper**

Layer	Depth (ft)	Description	$V_s$ (ft/sec)			$V_s$ Sigma (ln)	BC Unit Weight (pcf)	Dynamic Properties	
			LR (0.3)	BC (0.4)	UR (0.3)			Alt. 1 (0.5)	Alt. 2 (0.5)
1	41	Soil: fill	797	1,030	1,331	0.25	120	EPRI Soil	Pen.
2	50	Soil: fill	867	1,120	1,447	0.15	120	EPRI Soil	Pen.
3	60	Rock: limestone, shale	1,254	1,620	2,094	0.15	130	EPRI Rock	L 3.0%
4	85	Rock: limestone, shale	1,362	1,760	2,274	0.15	130	EPRI Rock	L 3.0%
5	95	Rock: limestone, shale, sandstone	2,128	2,750	3,554	0.15	130	EPRI Rock	L 3.0%
6	460	Rock: shale, limestone, sandstone	5,642	7,292	9,285	0.15	150	L 0.1%	L 0.1%
7	825	Rock: sandstone, limestone, dolomite	5,784	7,475	9,285	0.15	160	L 0.1%	L 0.1%
8	1,190	Rock: sandstone, limestone, dolomite	5,926	7,658	9,285	0.15	160	L 0.1%	L 0.1%
9	1,555	Rock: sandstone, limestone, dolomite	6,067	7,841	9,285	0.15	160	L 0.1%	L 0.1%
10	1,920	Rock: sandstone, limestone, dolomite	6,209	8,024	9,285	0.15	160	L 0.1%	L 0.1%

LR = lower range; BC = basecase; UR = upper range; ln = natural log; pcf = pounds per cubic foot; L = linear; Alt. = alternative; Pen. = Peninsular.  
 For LR, BC, UR, and Alt.: Values in parentheses refer to weights for site response analysis logic tree branches.

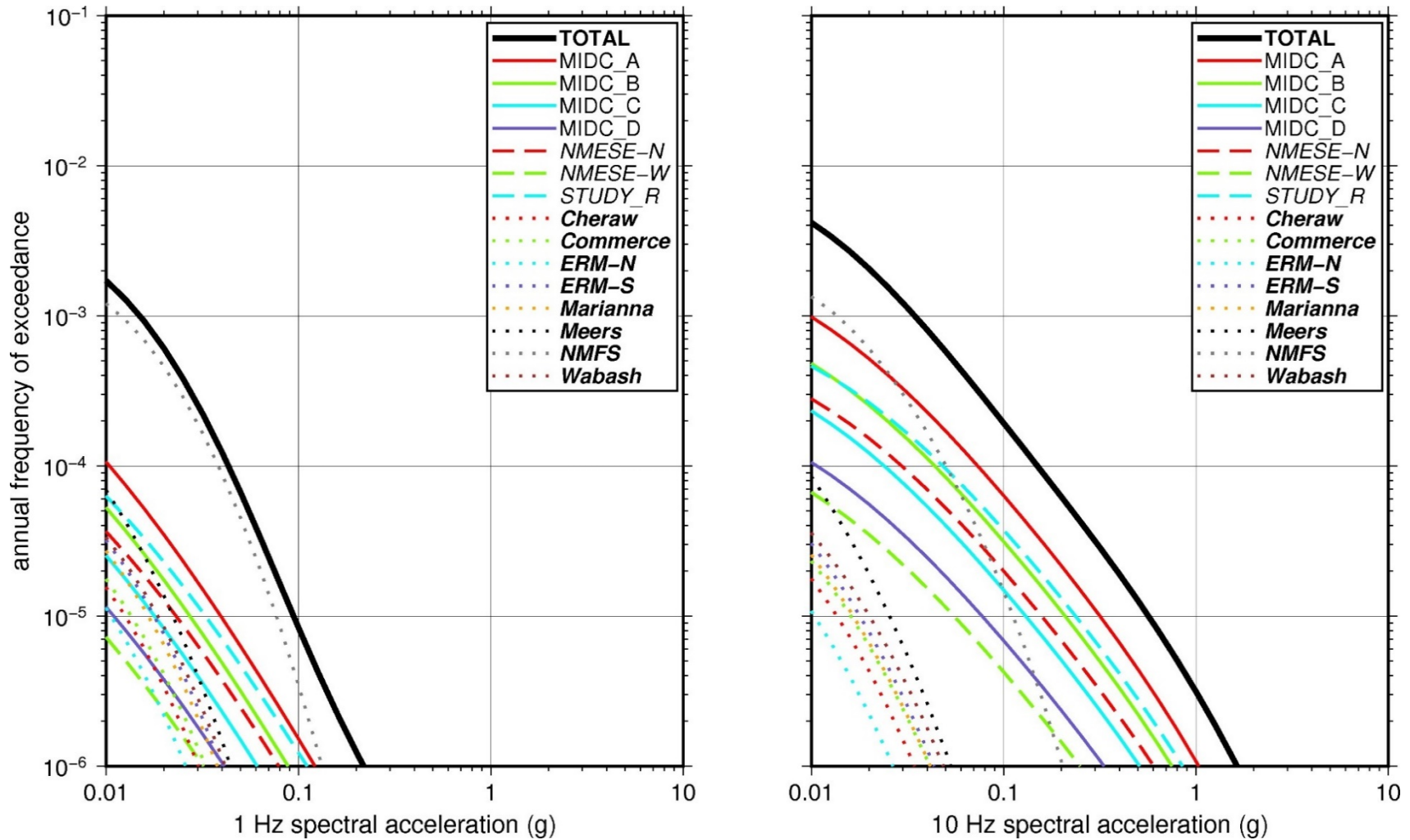


**Figure 2.5-14 Low-Frequency (1 Hz, Left), and High-Frequency (10 Hz, Right) Reference Rock Hazard Curves For Cooper. Total Hazard is Shown as a Bold Black Line; Individual Contributions to the Hazard for Each of the CEUS-SSC Sources are Shown as Colored Lines Defined in the Legend. See Table 2.1-1 for Source Name Definitions**

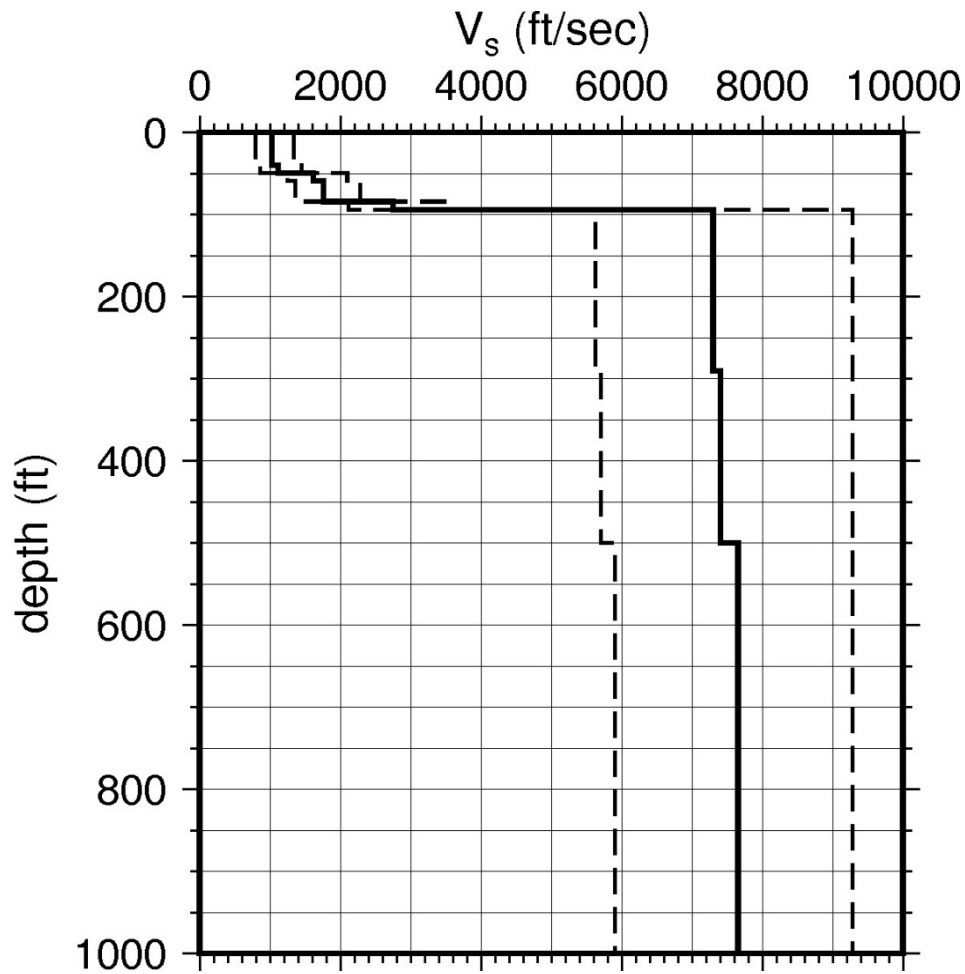


**Figure 2.5-15 Shear Wave Velocity ( $V_s$ ) Profiles for Cooper. Basecase (BC) Profile Shown as Solid Bold Line; Lower and Upper Range (LR and UR) Profiles Shown as Dashed Lines. Profiles Terminate at Reference Rock Velocity of 2,831 m/sec [9,285 ft/sec] per EPRI GMM (2013)**

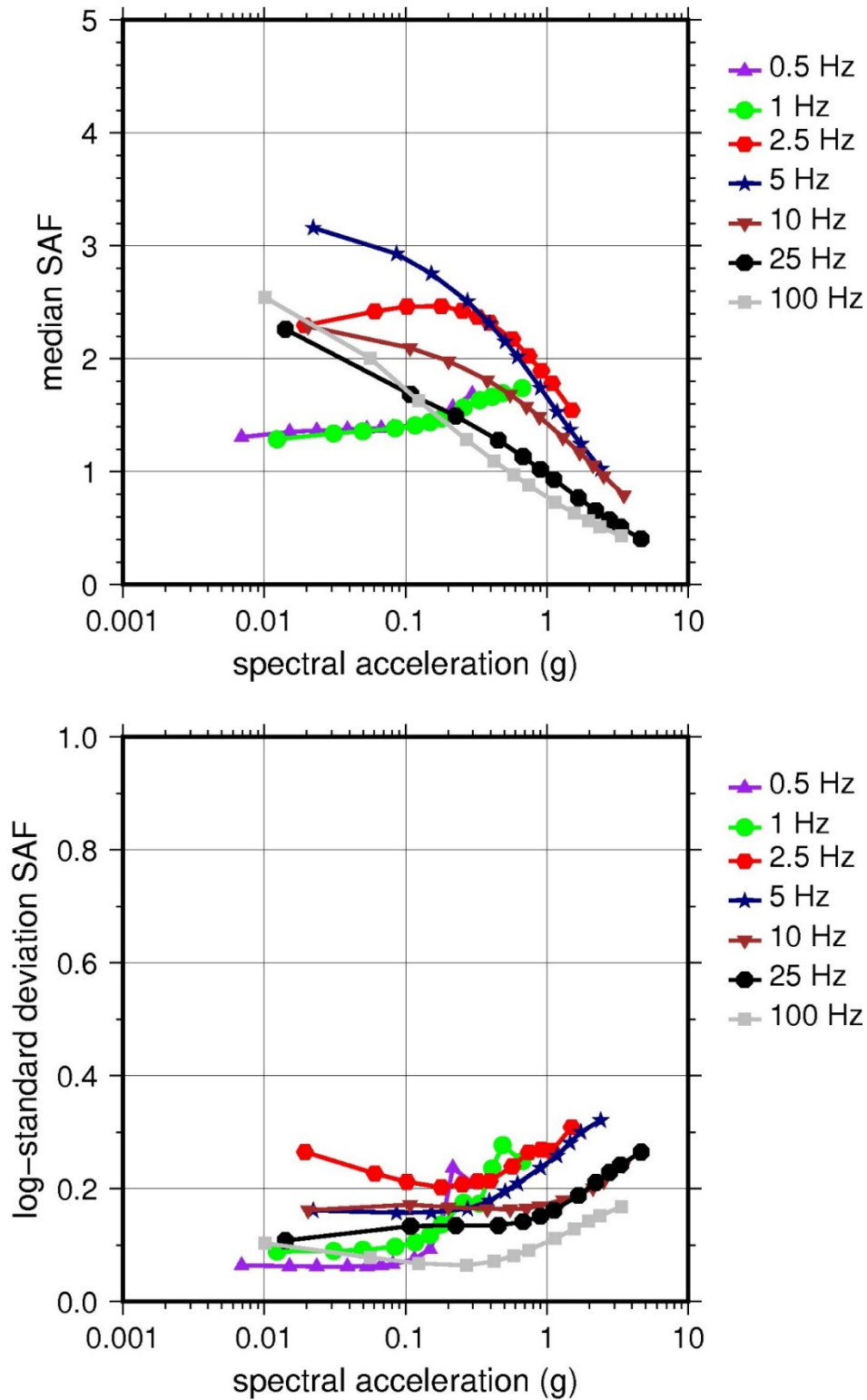


**Figure 2.5-16 Overall Weighted Median Site Amplification Factor (SAF) (Upper) and Log Standard Deviation of the SAF (Lower) as a Function of Input Acceleration for EPRI GMM (2013) Spectral Frequencies**

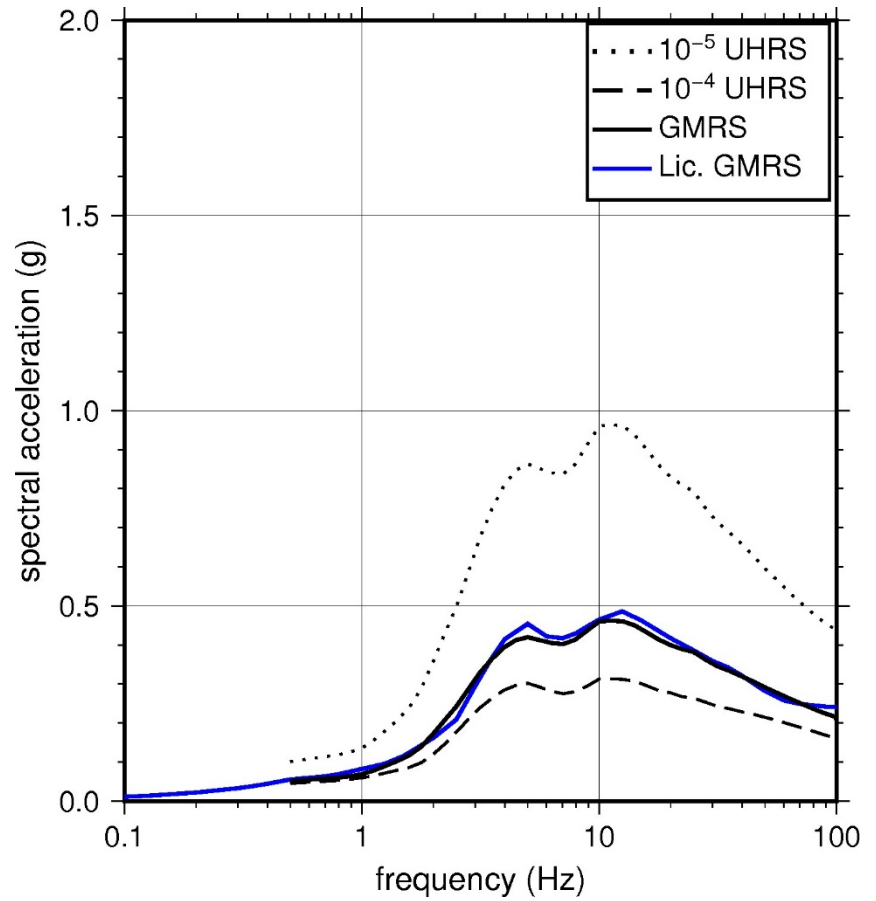
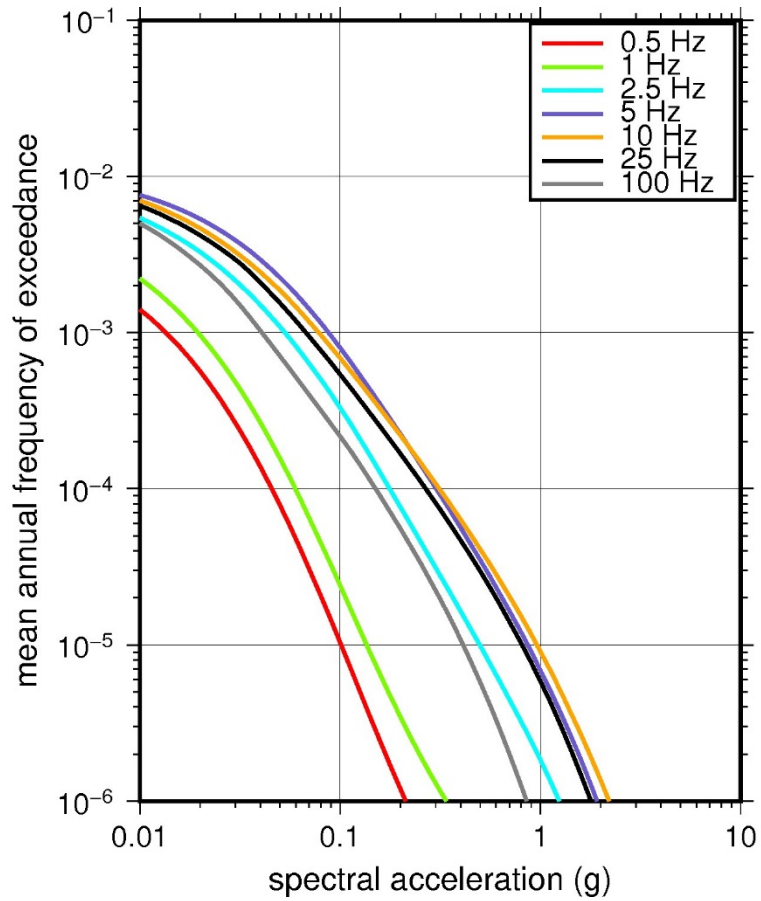


**Figure 2.5-17 Mean Control Point Hazard Curves (Left) for EPRI GMM (2013) Spectral Frequencies, and GMRS and UHRS (Right) for Cooper**

## 2.5.5 Fort Calhoun

The Fort Calhoun Nuclear Station site is located in eastern Nebraska along the Missouri River within the Central Lowland physiographic province and consists of 23 m [75 ft] of soil (silt, clay, and sand) overlying about 648 m [2,125 ft] of sedimentary rock (limestone, shale, sandstone, and dolomite). The horizontal SSE response spectrum for Ft. Calhoun has a rounded Housner spectral shape and is anchored at a PGA of 0.17g.

### 2.5.5.1 Reference Rock Hazard

For the reference rock PSHA, the NRC staff selected the seven CEUS-SSC (NRC, 2012b) background seismic source zones that are located within 323 km [200 miles] of the site. In addition, the NRC staff also selected the five CEUS-SSC (NRC, 2012b) RLME sources that are located within 807 km [500 mi] of the site. To develop the reference rock seismic hazard curves for the Ft. Calhoun site, the NRC staff used the GMPEs developed by the updated EPRI GMM (2013). As shown in Figure 2.5-18, the NMFS RLME is the largest contributor to the 1 Hz reference rock total mean hazard curve at the  $10^{-4}$  AFE level. For the 10 Hz reference rock total mean hazard curve at the  $10^{-4}$  AFE level, the MIDC-A seismotectonic source zone is the largest contributor.

### 2.5.5.2 Site Response Evaluation

#### 2.5.5.2.1 Site Profiles

To develop a basecase profile, the NRC staff used the geologic information in the NTTF R2.1 SHSR (Cortopassi, 2014) submitted by Omaha Public Power District (hereafter referred to as “the licensee” within this plant section). As described in the licensee’s SHSR, the Ft. Calhoun site lies on an old river terrace called the Ft. Calhoun Terrace, which formed from several overbank events along the right (east) bank of the Missouri River. The site consists of 1.5–3 m [5–10 ft] of compacted earth fill, 1.5–6 m [5–20 ft] of fine alluvium, and 15–18 m [50–60 ft] of coarse granular alluvium overlying limestone/shale bedrock at a depth of about 23 m [75 ft]. The Category I structures at Ft. Calhoun are founded on a common basement supported by steel piles driven into bedrock. In Table 2.3.1-1 of the SHSR, the licensee briefly described the subsurface materials in terms of the geologic units and layer thicknesses. For its site response evaluation, the NRC staff used the surface, which corresponds to an elevation of 306 m [1,005 ft] above MSL, as the control point elevation for the Ft. Calhoun site.

The field investigations for Ft. Calhoun, consisting of the original siting investigation in the mid-1960s and more recent investigations in 2011, included standard penetration test data, cone penetration test soundings, seismic refraction profiling, and the refraction microtremor method. Table 2.3.2-2 of the SHSR gives the measured and estimated  $V_S$  determined from the licensee’s site investigations.

For its SHSR, the licensee developed a basecase profile whose total thickness is 1,081 m [2,200 ft]. The licensee’s profile begins with 3 m [10 ft] of fill overlying 3 m [30 ft] of alluvial clay, silt, and sand, which the licensee divided into two layers. The licensee measured  $V_S$  values of 305 m/sec [1,000 ft/sec] for the fill layer; 152 m/sec [500 ft/sec] and 305 m/sec [1,000 ft/sec], respectively, for the two underlying alluvial layers; and 457 m/sec [1,500 ft/sec] for the deepest soil layer, which the licensee identified as “older” sand. The licensee estimated a  $V_S$  of 1,524 m/sec [5,000 ft/sec] for the uppermost rock layer using direct measurements from the refraction microtremor method and from measurements of  $V_P$  from a seismic refraction profile.

To convert from  $V_P$  to  $V_S$  for the uppermost rock layer, the licensee used an assumed Poisson's ratio of 0.28. The licensee identified this rock layer as interbedded limestone and shale of Pennsylvanian age. For the remaining 617 m [2,025 ft] of sedimentary rock strata, the licensee estimated the  $V_S$  based on the percentage of rock type (e.g., limestone versus shale) within each geologic unit, its age, and its depth. These estimates are based on data from regional oil and gas wells.

To corroborate the licensee's reported  $V_S$  and Poisson's ratios, the NRC staff used data from the Nebraska Geological Survey and the U.S. Geological Survey (e.g., Miller, 1964). For the upper 31 m [100 ft] of its basecase profile, the NRC staff used the licensee's direct measurements of the  $V_S$  for the soil and upper rock. For the lower layers, rather than assuming a constant  $V_S$  of 1,524 m/sec [5,000 ft/sec] for the entire 191 m [625 ft] of the Pennsylvanian-age strata, the NRC staff divided this layer into several sublayers and assumed a velocity gradient of 0.5 m/sec/m [0.5 ft/sec/ft], as specified in the SPID, Appendix B (EPRI, 2012) for sedimentary rock sites in the CEUS. For the deeper rock strata, the NRC staff used the licensee's  $V_S$  estimates, as there are no nearby data, and the range of values assumed by the licensee are typical for the rock type, depth of burial, and geologic age.

To capture the uncertainty in its basecase profile, the NRC staff developed lower and upper range (10<sup>th</sup> and 90<sup>th</sup> percentile) profiles by multiplying the basecase  $V_S$  values by scale factors of 0.78 and 1.29, respectively, which corresponds to an epistemic logarithmic standard deviation of 0.20. The weights for the lower, basecase, and upper profiles are 0.3, 0.4, and 0.3, respectively. Figure 2.5-19 shows the upper 305 m [1,000 ft] of the NRC staff's profiles. The upper profile terminates at a depth of 400 m [1,310 ft], while the basecase and lower profiles extend to a depth of 670 m [2,200 ft] below the control point elevation.

#### 2.5.5.2.2 *Dynamic Material Properties and Site Kappa*

The NRC staff assumed both linear and nonlinear dynamic behavior for the soil and rock beneath the Ft. Calhoun site. To model the nonlinear behavior of the top soil layers (Layers 1–4), the NRC staff used the EPRI soil and Peninsular Range shear modulus reduction and material damping curves as two equally weighted alternatives. For the uppermost weathered rock layers (Layers 5–6), the NRC staff used the EPRI rock shear modulus reduction and material damping curves. To model the linear behavior of these rock layers, the NRC staff assumed a constant damping ratio of 3 percent. The staff weighted these two alternatives equally. For the underlying higher velocity rock layers, the NRC staff assumed a linear dynamic response with a material damping ratio of 0.1 percent to maintain consistency with the  $\kappa_0$  value for the Ft. Calhoun site.

To determine the basecase  $\kappa_0$  for the Ft. Calhoun site, the NRC staff first used the Campbell (2009) Model 1 relationship between  $V_S$  and  $Q_{ef}$  to determine a  $Q_{ef}$  for each layer. Combining these  $Q_{ef}$  values with the thickness and  $V_S$  for each layer results in a total  $\kappa_0$  value of 16 msec, which includes the 6 msec assumed for the underlying reference rock. For the lower and upper profiles, the NRC staff calculated  $\kappa_0$  values of 22 and 12 msec, respectively, using the same approach as for the basecase profile. In contrast, the licensee estimated  $\kappa_0$  by combining the lowest low-strain damping values from the material damping curves over the top 152 m [500 ft] of soil and rock and assumed a damping value of 1.25 percent for the remaining deeper rock layers to estimate basecase, lower, and upper  $\kappa_0$  values of 20, 25, and 13 msec, respectively.

Table 2.5-6 provides the layer depths, lithologies,  $V_S$ , unit weights, and dynamic properties for the NRC staff's three profiles. In summary, the site response logic tree developed by the NRC

staff for the Ft. Calhoun site consists of six alternatives; three velocity profiles (each with a different  $\kappa_0$  value) and two alternative dynamic property branches.

#### 2.5.5.2.3 *Methodology and Results*

The NRC staff followed the methodology described in Section 2.1.4 to develop the final site amplification factors. Figure 2.5-20 shows the overall median site amplification factors and their variability for each of the seven spectral frequencies. As shown in Figure 2.5-20, the median site amplification factors range from about 1 to 4 before falling off with higher input spectral accelerations. The lower half of Figure 2.5-20 shows that the logarithmic standard deviations for the site amplification factors range from about 0.05 to 0.20.

#### 2.5.5.3 *Control Point Hazard*

The NRC staff implemented Approach 3 from the SPID (EPRI, 2012) to develop a weighted control point seismic hazard curve for each of the six unique combinations of the site response logic tree for the Ft. Calhoun site. After combining these profiles to develop the final mean control point hazard curves, the NRC staff determined the  $10^{-4}$  and  $10^{-5}$  UHRS in order to calculate the GMRS. Figure 2.5-21 shows the final control point mean seismic hazard curves for the seven spectral frequencies, as well as the NRC staff's UHRS and GMRS and the licensee's NTTF R2.1 GMRS (Cortopassi, 2014). As shown in Figure 2.5-21, the NRC staff's GMRS (black curve) is similar to the licensee's GMRS (blue curve) over the entire frequency range.



**Table 2.5-6 Layer Depths, Shear Wave Velocities ( $V_s$ ), Unit Weights, and Dynamic Properties for Ft. Calhoun**

Layer	Depth (ft)	Description	$V_s$ (ft/sec)			$V_s$ Sigma (ln)	BC Unit Weight (pcf)	Dynamic Properties	
			LR (0.3)	BC (0.4)	UR (0.3)			Alt. 1 (0.5)	Alt. 2 (0.5)
1	10	Soil: fill	774	1,000	1,292	0.25	120	EPRI Soil	Pen.
2	20	Soil: clay, silt	387	500	646	0.15	120	EPRI Soil	Pen.
3	40	Soil: sand, silt	774	1,000	1,292	0.15	120	EPRI Soil	Pen.
4	75	Soil: sand	1,161	1,500	1,938	0.15	130	EPRI Soil	Pen.
5	175	Rock: limestone, shale	3,869	5,000	6,461	0.15	140	EPRI Rock	L 3.0%
6	425	Rock: limestone, shale	3,966	5,125	6,623	0.15	140	EPRI Rock	L 3.0%
7	700	Rock: limestone, shale	4,073	5,263	6,801	0.15	140	L 0.1%	L 0.1%
8	970	Rock: limestone, shale, dolomite	6,965	9,000	9,285	0.15	160	L 0.1%	L 0.1%
9	1,310	Rock: shale, dolomite	4,643	6,000	7,754	0.15	150	L 0.1%	L 0.1%
10	1,720	Rock: dolomite, shale, sandstone	5,417	7,000	9,046	0.15	150	L 0.1%	L 0.1%
11	2,130	Rock: dolomite, shale, sandstone	5,576	7,205	9,285	0.15	150	L 0.1%	L 0.1%
12	2,200	Rock: sandstone, dolomite	6,576	8,500	9,285	0.15	160	L 0.1%	L 0.1%

LR = lower range; BC = basecase; UR = upper range; ln = natural log; pcf = pounds per cubic foot; L = linear; Alt. = alternative; Pen. = Peninsular.  
 For LR, BC, UR, and Alt.: Values in parentheses refer to weights for site response analysis logic tree branches.

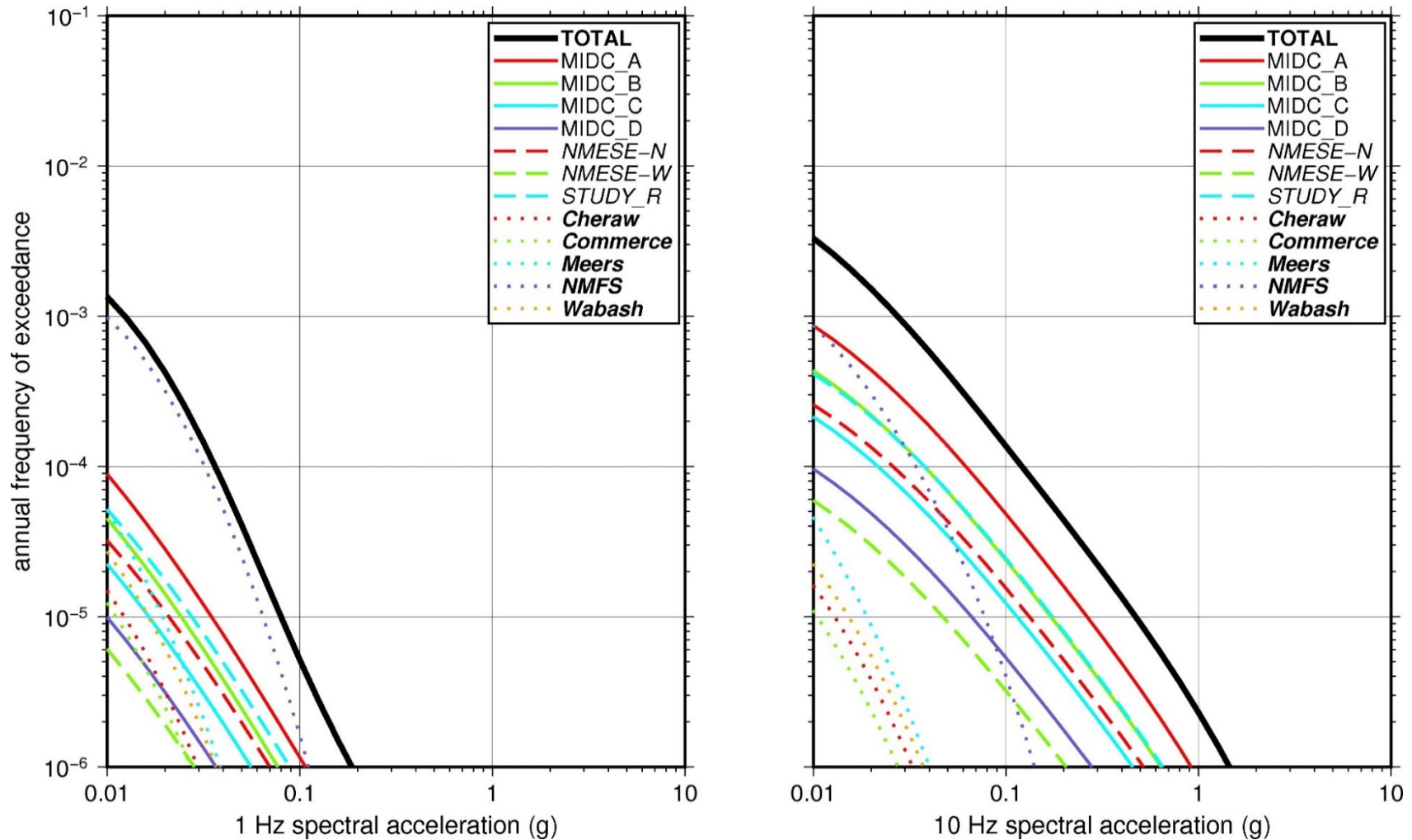


**Figure 2.5-18** Low-Frequency (1 Hz, Left), and High-Frequency (10 Hz, Right) Reference Rock Hazard Curves for Ft. Calhoun. Total Hazard is Shown as a Bold Black Line; Individual Contributions to the Hazard for Each of the CEUS-SSC Sources are Shown as Colored Lines Defined in the Legend. See Table 2.1-1 for Source Name Definitions

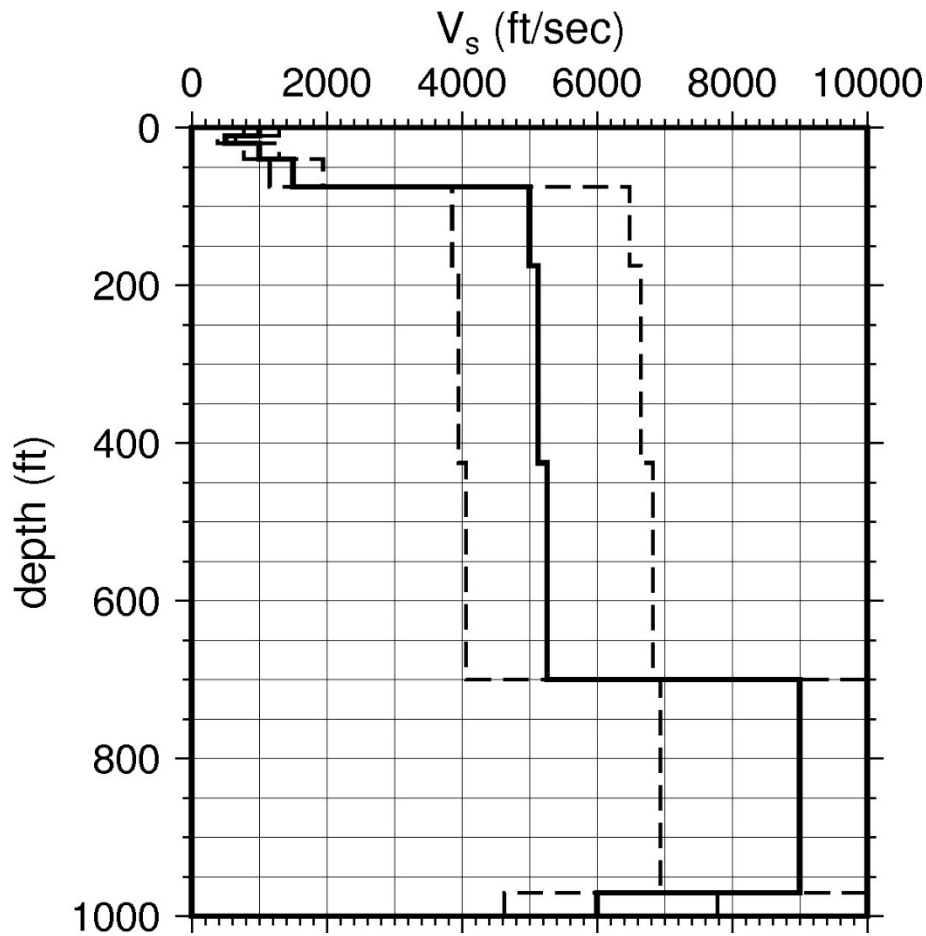


**Figure 2.5-19 Shear Wave Velocity ( $V_s$ ) Profiles for Ft. Calhoun. Basecase (BC) Profile Shown as Solid Bold Line; Lower and Upper Range (LR and UR) Profiles Shown as Dashed Lines. Profiles Terminate at Reference Rock Velocity of 2,831 m/sec [9,285 ft/sec] per EPRI GMM (2013)**

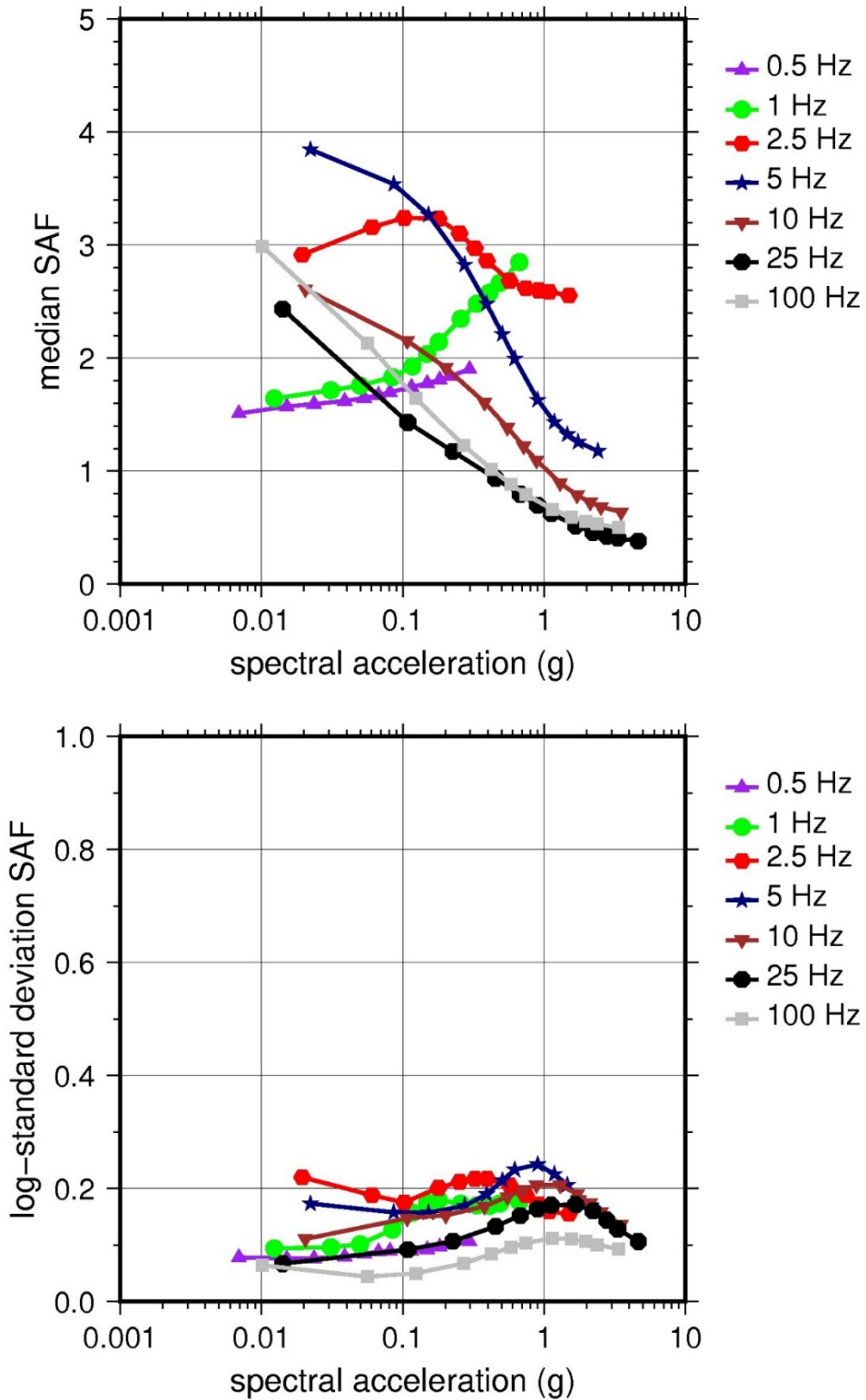


**Figure 2.5-20 Overall Weighted Median Site Amplification Factor (SAF) (Upper) and Log Standard Deviation of the SAF (Lower) as a Function of Input Acceleration for EPRI GMM (2013) Spectral Frequencies**

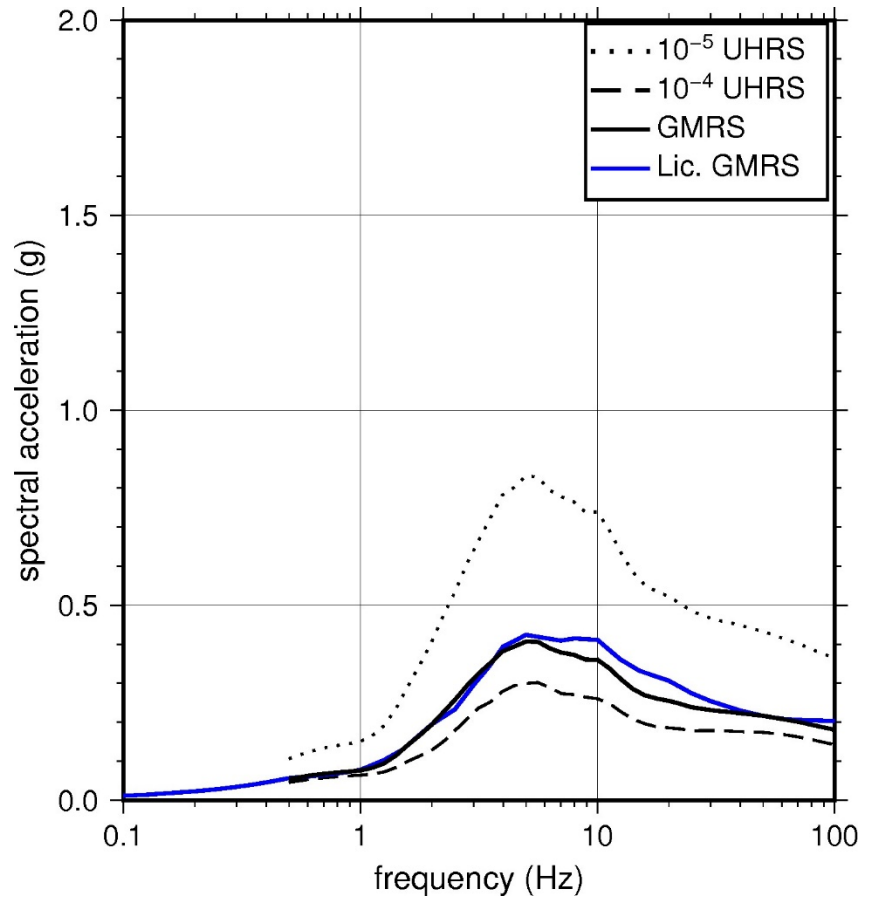
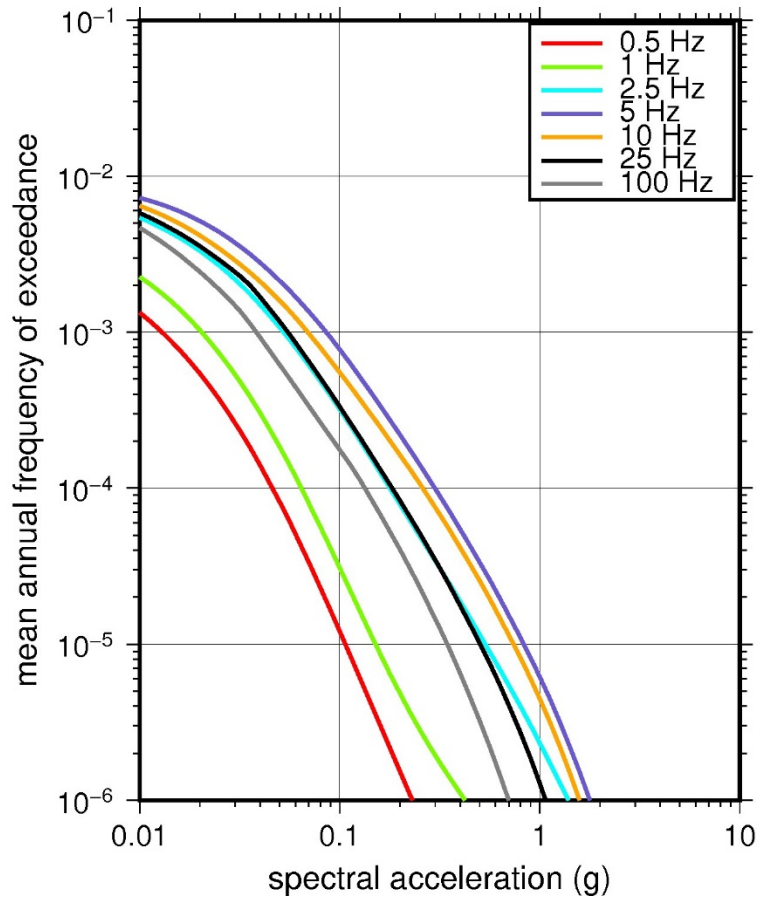


**Figure 2.5-21 Mean Control Point Hazard Curves (Left) for EPRI GMM (2013) Spectral Frequencies, and GMRS and UHRS (Right) for Ft. Calhoun**

## 2.5.6 Grand Gulf

The Grand Gulf Nuclear Station site is located in western Mississippi along the Mississippi River within the Coastal Plain physiographic province and is underlain by over 7,000 m [23,000 ft] of sediment and sedimentary rock. The horizontal SSE response spectrum for Grand Gulf has a Newmark spectral shape and is anchored at a PGA of 0.15g.

### 2.5.6.1 Reference Rock Hazard

For the reference rock PSHA, the NRC staff selected the 15 CEUS-SSC (NRC, 2012b) background seismic source zones that are located within 323 km [200 mi] of the site. In addition, the NRC staff also selected the seven CEUS-SSC (NRC, 2012b) RLME sources that are located within 807 km [500 miles] of the site. To develop the reference rock seismic hazard curves for the Grand Gulf site, the NRC staff used the GMPEs developed by the updated EPRI GMM (2013). As shown in Figure 2.5-22, the NMFS RLME is the largest contributor to both the 1 Hz and the 10 Hz reference rock total mean hazard curves at the  $10^{-4}$  AFE level.

### 2.5.6.2 Site Response Evaluation

#### 2.5.6.2.1 Site Profiles

To develop a basecase profile, the NRC staff used the geologic information in the NTF R2.1 SHSR (Mulligan, 2014) submitted by Entergy Nuclear Operations Inc. (hereafter referred to as “the licensee” within this plant section), as well as the geologic information and geophysical measurements in the ESP site safety analysis report (Entergy Nuclear Operations Inc., 2005) for the Grand Gulf site. As described in the licensee’s SHSR and the now-withdrawn application for the Grand Gulf ESP, the Grand Gulf site is located within the structural and depositional Gulf Coast Basin, and the subsurface consists of Cretaceous and Cenozoic sands, gravels, clays, marls, claystones, sandstones, and limestones. The licensee stated that the Catahoula Formation, of Miocene age, is the foundation-bearing stratum for the major plant structures. In Table 2.3.1-1 of the SHSR, the licensee briefly described the subsurface materials in terms of the geologic units and layer thicknesses. For its site response evaluation, the NRC staff used the top of the Catahoula Formation, which corresponds to an elevation of 27 m [87 ft] above MSL, as the control point elevation for the Grand Gulf site.

The field investigations for Grand Gulf, conducted in support of the ESP application, consisted of boreholes, seismic refraction, suspension logging, resonant column and torsional shear analyses, and other studies of the subsurface. The ESP applicant (Entergy) correlated these relatively new data with data collected during initial licensing of the operating plant, demonstrating consistency in the subsurface properties between the two sites. Table 2.3.2-2 of the SHSR gives the measured and estimated  $V_S$  determined from the licensee’s site investigations.

For its SHSR, the licensee developed a basecase profile that extends to a depth of 1,220 m [4,000 ft] in total thickness below the control point elevation. The uppermost layers of the profile consist of 120 m [392 ft] of the Miocene-age Catahoula Formation, which consists of silty to sandy clay. The licensee divided this layer into several sublayers, with measured  $V_S$  increasing from 488 m/sec [1,600 ft/sec] to 571 m/sec [1,873 ft/sec]. Beneath the Catahoula Formation are the deposits of the Oligocene-age Vicksburg Group, which consist of clay, sand, fossiliferous limestone, marl, and silt. The measured  $V_S$  for these deposits is 640 m/sec [2,100 ft/sec].

Underlying the Vicksburg Group are the Eocene-age Jackson, Claiborne, and Wilcox Groups, which consist of marl, clay, sand, and silt. The  $V_S$  for these sedimentary layers gradually increases from 747 m/sec [2,450 ft/sec] to 931 m/sec [3,054 ft/sec] at a depth of 1,220 m [4,000 ft] below the control point elevation. Although there are several thousand feet of additional sediment and sedimentary rock before reaching Precambrian-age crystalline rock, the licensee terminated its profile at a depth of 1,220 m [4,000 ft], which it deemed sufficient to capture the site amplification of the lowest spectral frequency of interest at 0.5 Hz.

As multiple geophysical field investigations have characterized the sedimentary strata beneath the Grand Gulf site, the NRC staff used the licensee's layer thicknesses and  $V_S$  for its basecase profile.

To capture the uncertainty in its basecase profile, the NRC staff developed lower and upper range (10<sup>th</sup> and 90<sup>th</sup> percentile) profile by multiplying the basecase  $V_S$  values by scale factors of 0.78 and 1.29, respectively, which corresponds to an epistemic logarithmic standard deviation of 0.20. The weights for the lower, basecase, and upper profiles are 0.3, 0.4, and 0.3, respectively. Figure 2.5-23 shows the NRC staff's profiles, which extend to a depth of 1,220 m [4,000 ft] below the control point elevation.

#### 2.5.6.2.2 *Dynamic Material Properties and Site Kappa*

The NRC staff assumed both linear and nonlinear dynamic behavior for the soil beneath the Grand Gulf site. To model the nonlinear behavior of the top soil layers (Layers 1–3), the NRC staff used the EPRI soil and Peninsular Range shear modulus reduction and material damping curves as two equally weighted alternatives. For the underlying higher velocity soil layers, the NRC staff assumed a linear dynamic response with a material damping ratio of 1 percent to maintain consistency with the  $\kappa_0$  value for the Grand Gulf site.

To determine the basecase  $\kappa_0$  for the Grand Gulf site, the NRC staff first used the Campbell (2009) Model 1 relationship between  $V_S$  and  $Q_{ef}$  to determine a  $Q_{ef}$  for each layer. Combining these  $Q_{ef}$  values with the thickness and  $V_S$  for each layer results in a total  $\kappa_0$  value of 64 msec, which includes the 6 msec assumed for the underlying reference rock. For the lower and upper profiles, the NRC staff calculated  $\kappa_0$  values of 95 and 43 msec, respectively, using the same approach as for the basecase profile. In contrast, the licensee used a  $\kappa_0$  value of 40 msec for the basecase, lower, and upper profiles, which is the maximum value recommended by Appendix B of the SPID (EPRI, 2012) for CEUS deep soil sites. For comparison, using the Chapman and Conn (2016) Gulf Coast  $\kappa_0$  relationship with a sedimentary thickness of 7,000 m [22,960 ft] for the Grand Gulf site yields a  $\kappa_0$  value of 111 msec.

Table 2.5-7 provides the layer depths, lithologies,  $V_S$ , unit weights, and dynamic properties for the NRC staff's three profiles. In summary, the site response logic tree developed by the NRC staff for the Grand Gulf site consists of six alternatives; three velocity profiles (each with a different  $\kappa_0$  value) and two alternative dynamic property branches.

#### 2.5.6.2.3 *Methodology and Results*

The NRC staff followed the methodology described in Section 2.1.4 to develop the final site amplification factors. Figure 23.5-24 shows the overall median site amplification factors and their variability for each of the seven spectral frequencies. As shown in Figure 2.5-24, the median site amplification factors range from about 1.0 to 2.5 before falling off with higher input

spectral accelerations. The lower half of Figure 2.5-24 shows that the logarithmic standard deviations for the site amplification factors range from about 0.10 to 0.25.

### 2.5.6.3 Control Point Hazard

The NRC staff implemented Approach 3 from the SPID (EPRI, 2012) to develop a weighted control point seismic hazard curve for each of the six unique combinations of the site response logic tree for the Grand Gulf site. After combining these curves to develop the final mean control point hazard curves, the NRC staff determined the  $10^{-4}$  and  $10^{-5}$  UHRS in order to calculate the GMRS. Figure 2.5-25 shows the final control point mean seismic hazard curves for the seven spectral frequencies, as well as the NRC staff's UHRS and GMRS and the licensee's NTTF R2.1 GMRS (Mulligan, 2014). As shown in Figure 2.5-25, the NRC staff's GMRS (black curve) is similar to the licensee's GMRS (blue curve) over the entire frequency range.

Layer	Depth (ft)	Description	$V_s$ (ft/sec)			$V_s$ Sigma (ln)	BC Unit Weight (pcf)	Dynamic Properties	
			LR (0.3)	BC (0.4)	UR (0.3)			Alt. 1 (0.5)	Alt. 2 (0.5)
1	70	Soil: clay	1,254	1,620	2,094	0.25	130	EPRI Soil	Pen.
2	191	Soil: clay	1,331	1,720	2,223	0.15	130	EPRI Soil	Pen.
3	392	Soil: clay	1,432	1,850	2,391	0.15	130	EPRI Soil	Pen.
4	1,049	Soil: clay, marls, sand, silt	1,625	2,100	2,714	0.15	130	L 1.0%	L 1.0%
5	2,033	Soil: clay, marls, sand, silt	1,896	2,450	3,166	0.15	130	L 1.0%	L 1.0%
6	2,689	Soil: clay, marls, sand, silt	2,222	2,871	3,710	0.15	130	L 1.0%	L 1.0%
7	4,000	Soil: clay, marls, sand, silt	2,363	3,054	3,947	0.15	130	L 1.0%	L 1.0%

LR = lower range; BC = basecase; UR = upper range; ln = natural log; pcf = pounds per cubic foot; L = linear; Alt. = alternative; Pen. = Peninsular.  
For LR, BC, UR, and Alt.: Values in parentheses refer to weights for site response analysis logic tree branches.



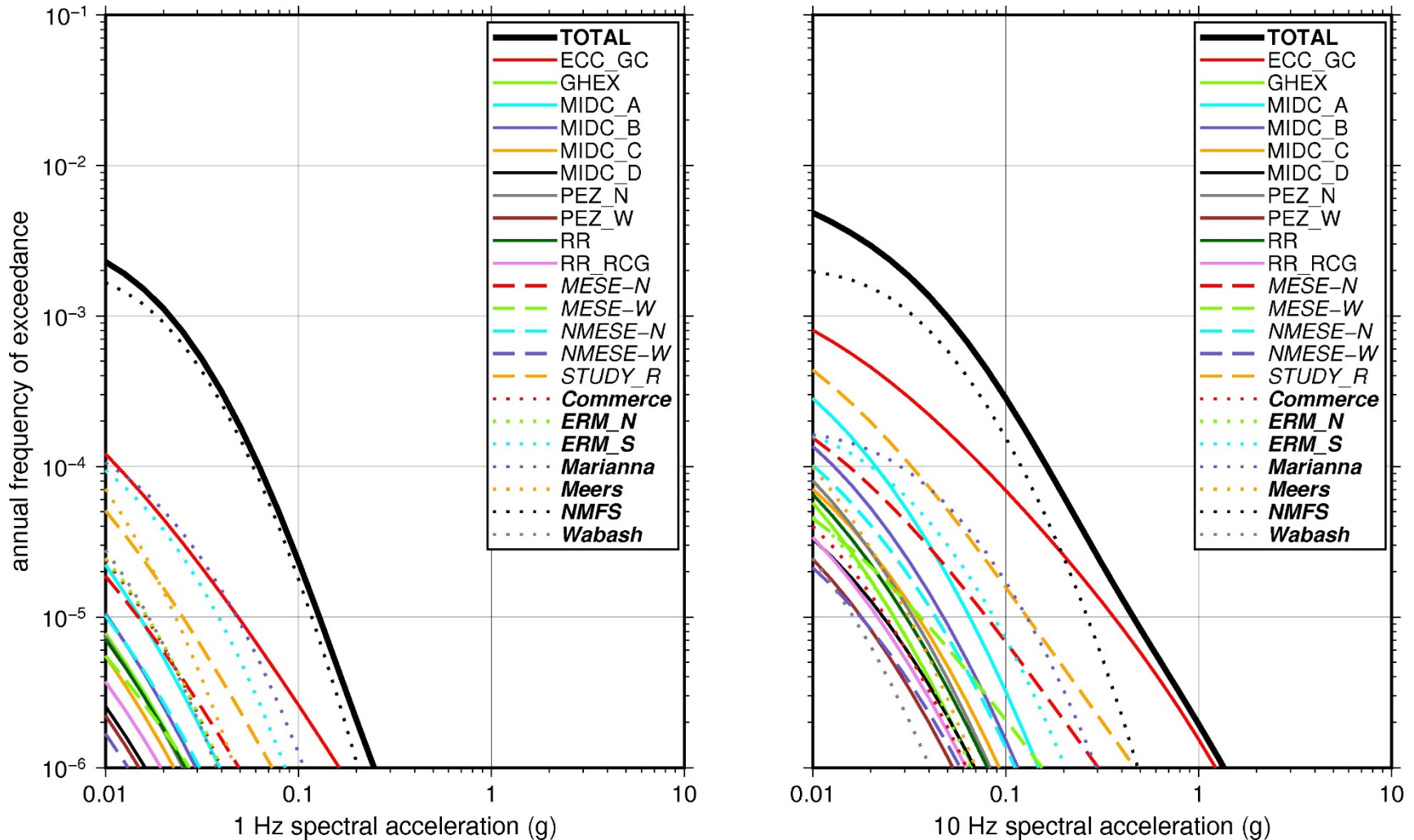


**Figure 2.5-22 Low-Frequency (1 Hz, Left), and High-Frequency (10 Hz, Right) Reference Rock Hazard Curves for Grand Gulf. Total Hazard is Shown as a Bold Black Line; Individual Contributions to the Hazard for Each of the CEUS-SSC Sources are Shown as Colored Lines Defined in the Legend. See Table 2.1-1 for Source Name Definitions**

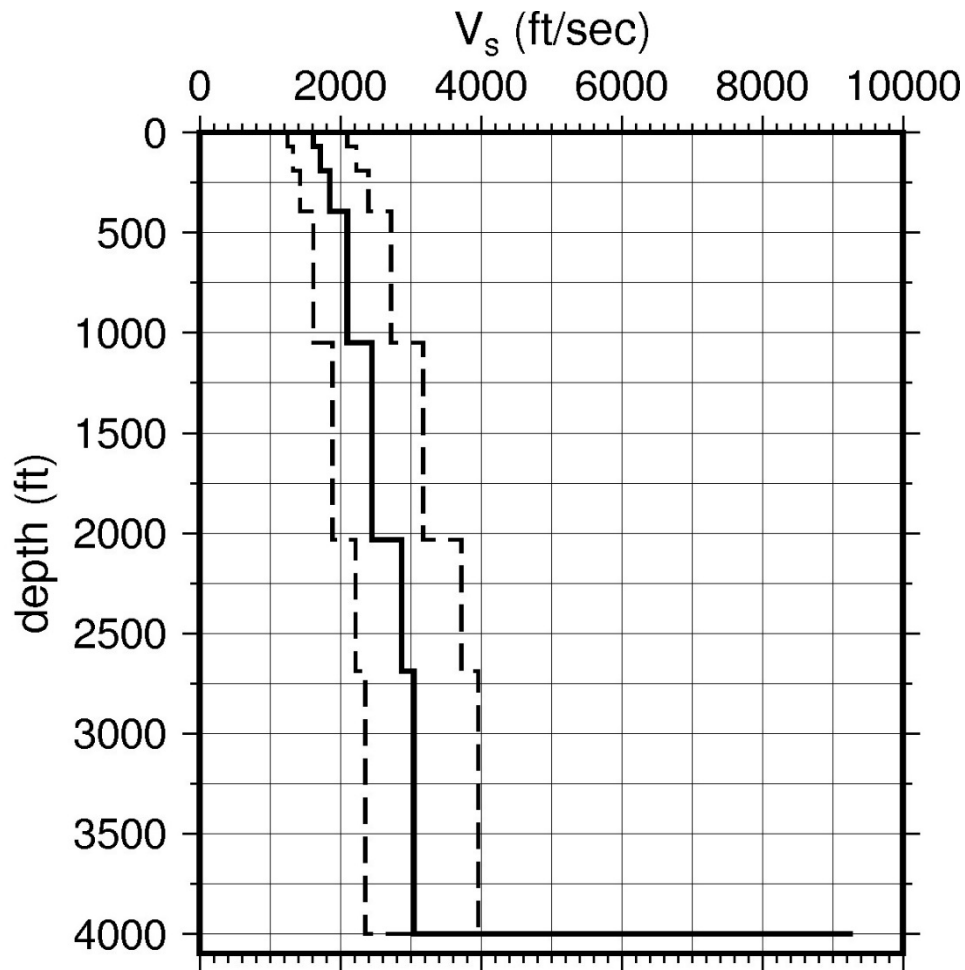


**Figure 2.5-23 Shear Wave Velocity ( $V_s$ ) Profiles for Grand Gulf. Basecase (BC) Profile Shown as Solid Bold Line; Lower and Upper Range (LR and UR) Profiles Shown as Dashed Lines. Profiles Terminate at Reference Rock Velocity of 2,831 m/sec [9,285 ft/sec] per EPRI GMM (2013)**

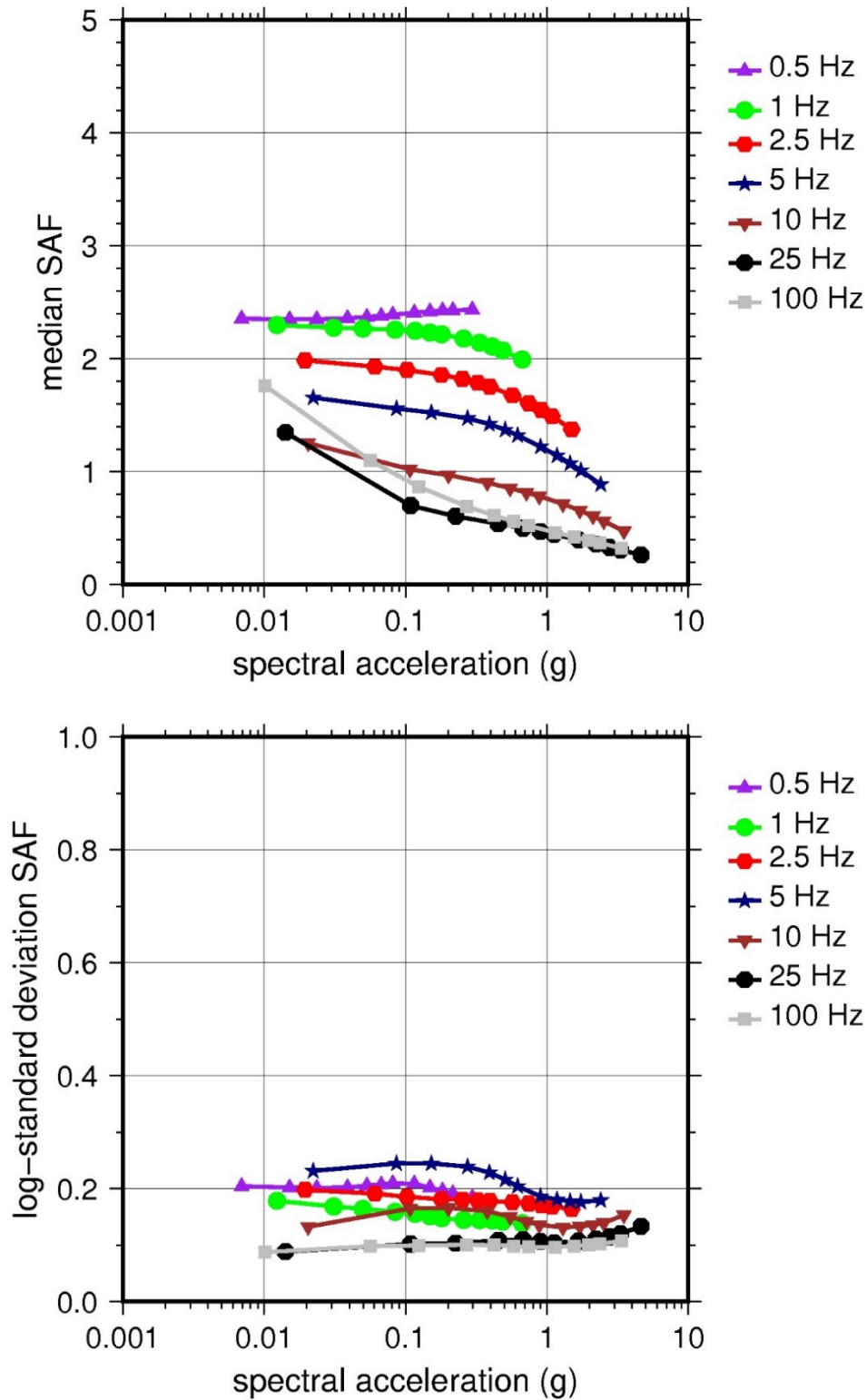


**Figure 2.5-24 Overall Weighted Median Site Amplification Factor (SAF) (Upper) and Log Standard Deviation of the SAF (Lower) as a Function of Input Acceleration for EPRI GMM (2013) Spectral Frequencies**

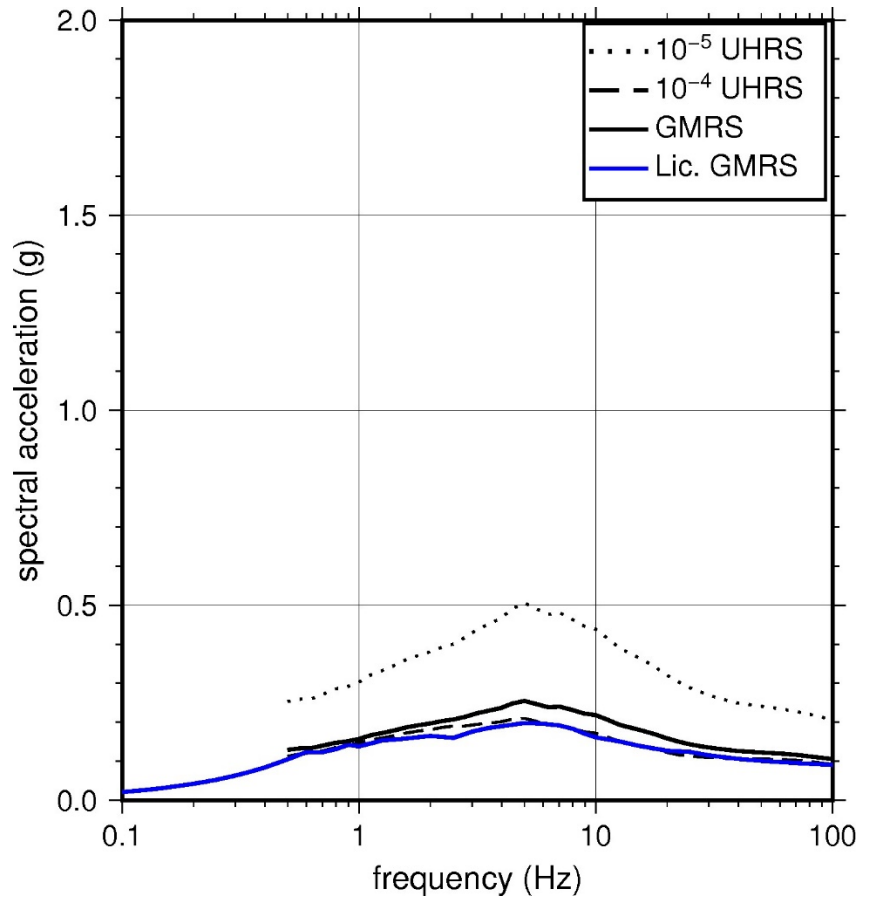
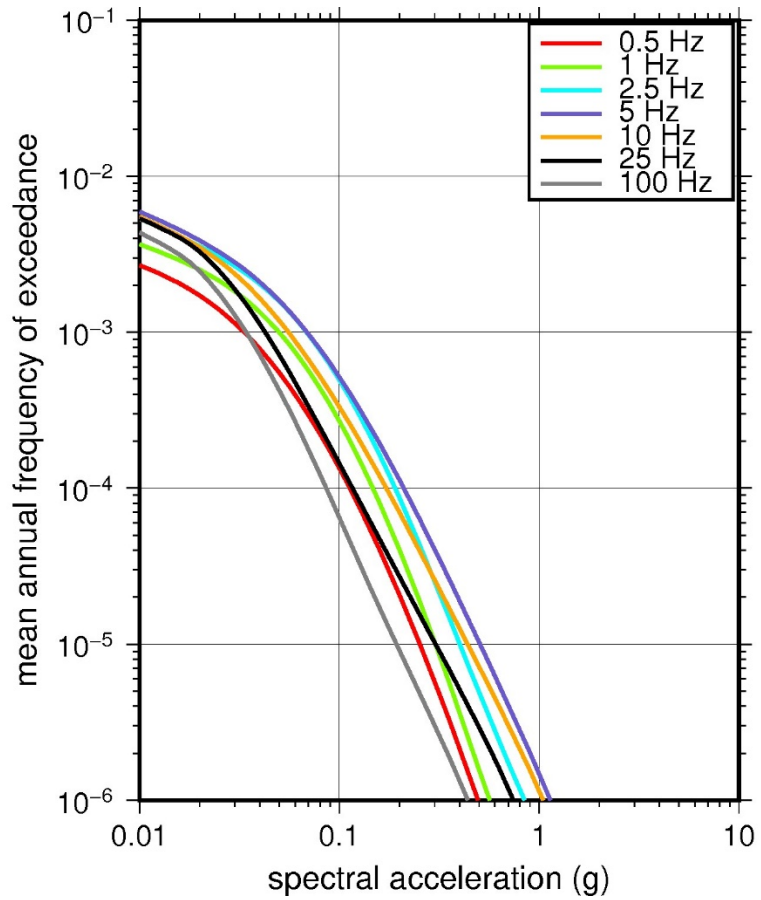


**Figure 2.5-25 Mean Control Point Hazard Curves (Left) for EPRI GMM (2013) Spectral Frequencies, and GMRS and UHRS (Right) for Grand Gulf**

## 2.5.7 River Bend

The River Bend Station site is located in southern Louisiana along the Mississippi River within the Coastal Plain physiographic province and is underlain by over 12,000 m [39,000 ft] of sediment and sedimentary rock. The horizontal SSE response spectrum for River Bend has an RG 1.60 spectral shape and is anchored at a PGA of 0.10g.

### 2.5.7.1 Reference Rock Hazard

For the reference rock PSHA, the NRC staff selected the 13 CEUS-SSC (NRC, 2012b) background seismic source zones that are located within 323 km [200 miles] of the site. In addition, the NRC staff also selected the six CEUS-SSC (NRC, 2012b) RLME sources that are located within 807 km [500 miles] of the site. To develop the reference rock seismic hazard curves for the River Bend site, the NRC staff used the GMPEs developed by the updated EPRI GMM (2013). As shown in Figure 2.5-26, the NMFS RLME is the largest contributor to the 1 Hz reference rock total mean hazard curve at the  $10^{-4}$  AFE level. For the 10 Hz reference rock total mean hazard curve, the ECC-GC seismotectonic zone is the largest contributor at the  $10^{-4}$  AFE level.

### 2.5.7.2 Site Response Evaluation

#### 2.5.7.2.1 Site Profiles

To develop a basecase profile, the NRC staff used the geologic information in the NTTF R2.1 SHSR (Mashburn, 2014) submitted by Entergy Nuclear Operations Inc. (hereafter referred to as “the licensee” within this plant section), as well as the geologic information and geophysical measurements in the COL application (Entergy Nuclear Operations Inc., 2008) for the River Bend site. The licensee stated that the strata underlying the River Bend site consist of a thick and stratigraphically complex sequence of relatively flat-lying sediments that are part of the Gulf Coast geosyncline. As described in the licensee’s SHSR and the COL application, the River Bend site consists of about 21 m [70 ft] of loess, silts, clays, sands, Citronelle Formation buried channel deposits, and Pascagoula Formation clays overlying a Mesozoic-age sequence of limestone. The auxiliary, control, and diesel-generating buildings are founded at an elevation of 65 ft [920 m] above MSL, which corresponds to sands and clayey sands. In Table 2.3.1-1 of the SHSR, the licensee briefly described the subsurface materials in terms of the geologic units and layer thicknesses. For its site response evaluation, the NRC staff used the foundations of the auxiliary, control, and diesel-generating buildings, which correspond to an elevation of 20 m [65 ft] above MSL, as the control point elevation for the River Bend site.

The field investigations for the River Bend site, conducted as part of the COL application, included the drilling of boreholes, seismic refraction, downhole and crosshole surveys, resonant column and torsional shear analyses, and other studies of the subsurface. The COL applicant correlated these relatively new data with data collected during initial licensing of the operating plant, demonstrating consistency in the subsurface properties between the two sites. For the deeper soil layers, below a depth of 152 m [500 ft], the COL applicant used  $V_P$  measured in deep wells in the region with an assumed Poisson’s ratio to estimate the  $V_S$ . Table 2.3.2-2 of the SHSR gives the measured and estimated  $V_S$  determined from the licensee’s site investigations.

For its SHSR, the licensee developed a basecase profile that extends to a depth of 1,220 m [4,000 ft] below the control point elevation. The uppermost layers of the profile comprise 33 m

[108 ft] of the Pleistocene- to Pliocene-age Port Hickey and Citronelle Formations, which consist of sand, clay, and gravel. The licensee divided these soil formations into three layers, with measured  $V_S$  increasing from 305 m/sec [1,000 ft/sec] to 357 m/sec [1,170 ft/sec]. Beneath the Port Hickey and Citronelle Formations is the Miocene-age Pascagoula Formation, which consists primarily of clay and sand. The measured  $V_S$  for these deposits ranges from 318 m/sec [1,042 ft/sec] to 1,189 m/sec [3,900 ft/sec] at a depth of 1,220 m [4,000 ft] below the control point elevation. Although there are several thousand feet of additional sediment and sedimentary rock before reaching Precambrian-age crystalline rock, the licensee terminated its profile at a depth of 1,220 m [4,000 ft], which it deemed sufficient to capture the site amplification of the lowest spectral frequency of interest at 0.5 Hz.

As multiple geophysical field investigations have characterized the sedimentary strata beneath the River Bend site, the NRC staff used the licensee's layer thicknesses and  $V_S$  for its basecase profile.

To capture the uncertainty in its basecase profile, the NRC staff developed lower and upper range (10<sup>th</sup> and 90<sup>th</sup> percentile) profiles by multiplying the basecase  $V_S$  values by scale factors of 0.78 and 1.29, respectively, which corresponds to an epistemic logarithmic standard deviation of 0.20. The weights for the lower, basecase, and upper profiles are 0.3, 0.4, and 0.3, respectively. Figure 2.5-27 shows the NRC staff's profiles, which extend to a depth of 1,220 m [4,000 ft] below the control point elevation.

#### 2.5.7.2.2 *Dynamic Material Properties and Site Kappa*

The NRC staff assumed both linear and nonlinear dynamic behavior for the soil beneath the River Bend site. To model the nonlinear behavior of the top soil layers (Layers 1–8), the NRC staff used the EPRI soil and Peninsular Range shear modulus reduction and material damping curves as two equally weighted alternatives. As another alternative, the NRC staff also performed its site response analysis using the Vucetic and Dobry (1991) curves for clayey soils, which made no appreciable difference to the final results. For the underlying higher velocity soil layers, the NRC staff assumed a linear dynamic response with a material damping ratio of 1 percent to maintain consistency with the  $\kappa_0$  value for the River Bend site.

To determine the basecase  $\kappa_0$  for the River Bend site, the NRC staff first used the Campbell (2009) Model 1 relationship between  $V_S$  and  $Q_{ef}$  to determine a  $Q_{ef}$  for each layer. Combining these  $Q_{ef}$  values with the thickness and  $V_S$  for each layer results in a total  $\kappa_0$  value of 63 msec, which includes the 6 msec assumed for the underlying reference rock. For the lower and upper profiles, the NRC staff calculated  $\kappa_0$  values of 94 and 43 msec, respectively, using the same approach as for the basecase profile. In contrast, the licensee used a  $\kappa_0$  value of 40 msec for the basecase, lower, and upper profiles, which is the maximum value recommended by Appendix B to the SPID (EPRI, 2012) for CEUS deep soil sites. For comparison, using the Chapman and Conn (2016) Gulf Coast  $\kappa_0$  relationship with a sedimentary thickness of 12,000 m [39,360 ft] for the River Bend site yields a  $\kappa_0$  value of 159 msec.

Table 2.5-8 provides the layer depths, lithologies,  $V_S$ , unit weights, and dynamic properties for the NRC staff's three profiles. In summary, the site response logic tree developed by the NRC staff for the River Bend site consists of six alternatives; three velocity profiles (each with a different  $\kappa_0$  value) and two alternative dynamic property branches.

### 2.5.7.2.3 Methodology and Results

The NRC staff followed the methodology described in Section 2.1.4 to develop the final site amplification factors. Figure 2.5-28 shows the overall median site amplification factors and their variability for each of the seven spectral frequencies. As shown in Figure 2.5-28, the median site amplification factors range from about 1.5 to 3.0 before falling off with higher input spectral accelerations. The lower half of Figure 2.5-28 shows that the logarithmic standard deviations for the site amplification factors range from about 0.10 to 0.20.

### 2.5.7.3 Control Point Hazard

The NRC staff implemented Approach 3 from the SPID (EPRI, 2012) to develop a weighted control point seismic hazard curve for each of the six unique combinations of the site response logic tree for the River Bend site. After combining these curves to develop the final mean control point hazard curves, the NRC staff determined the  $10^{-4}$  and  $10^{-5}$  UHRS in order to calculate the GMRS. Figure 2.5-29 shows the final control point mean seismic hazard curves for the seven spectral frequencies, as well as the NRC staff's UHRS and GMRS and the licensee's NTTF R2.1 GMRS (Mashburn, 2014). As shown in Figure 2.5-29, the NRC staff's GMRS (black curve) is similar to the licensee's GMRS (blue curve) over the entire frequency range.

**Table 2.5-8 Layer Depths, Shear Wave Velocities ( $V_s$ ), Unit Weights, and Dynamic Properties for River Bend**

Layer	Depth (ft)	Description	$V_s$ (ft/sec)			$V_s$ Sigma (ln)	BC Unit Weight (pcf)	Dynamic Properties	
			LR (0.3)	BC (0.4)	UR (0.3)			Alt. 1 (0.5)	Alt. 2 (0.5)
1	25	Soil: sand	774	1,000	1,292	0.25	120	EPRI Soil	Pen.
2	45	Soil: clay, sand	813	1,050	1,357	0.15	120	EPRI Soil	Pen.
3	108	Soil: clay, sand	905	1,170	1,512	0.15	120	EPRI Soil	Pen.
4	138	Soil: clay	963	1,245	1,609	0.15	120	EPRI Soil	Pen.
5	212	Soil: clay	806	1,042	1,347	0.15	120	EPRI Soil	Pen.
6	344	Soil: clay	1,243	1,606	2,075	0.15	130	EPRI Soil	Pen.
7	489	Soil: sand	1,083	1,400	1,809	0.15	130	EPRI Soil	Pen.
8	942	Soil: clay	1,337	1,728	2,233	0.15	130	EPRI Soil	Pen.
9	1,318	Soil: clay	1,898	2,453	3,170	0.15	130	L 1.0%	L 1.0%
10	1,693	Soil: clay	2,451	3,167	4,092	0.15	130	L 1.0%	L 1.0%
11	4,000	Soil: clay	3,018	3,900	5,040	0.15	140	L 1.0%	L 1.0%

LR = lower range; BC = basecase; UR = upper range; ln = natural log; pcf = pounds per cubic foot; L = linear; Alt. = alternative; Pen. = Peninsular.  
For LR, BC, UR, and Alt.: Values in parentheses refer to weights for site response analysis logic tree branches.

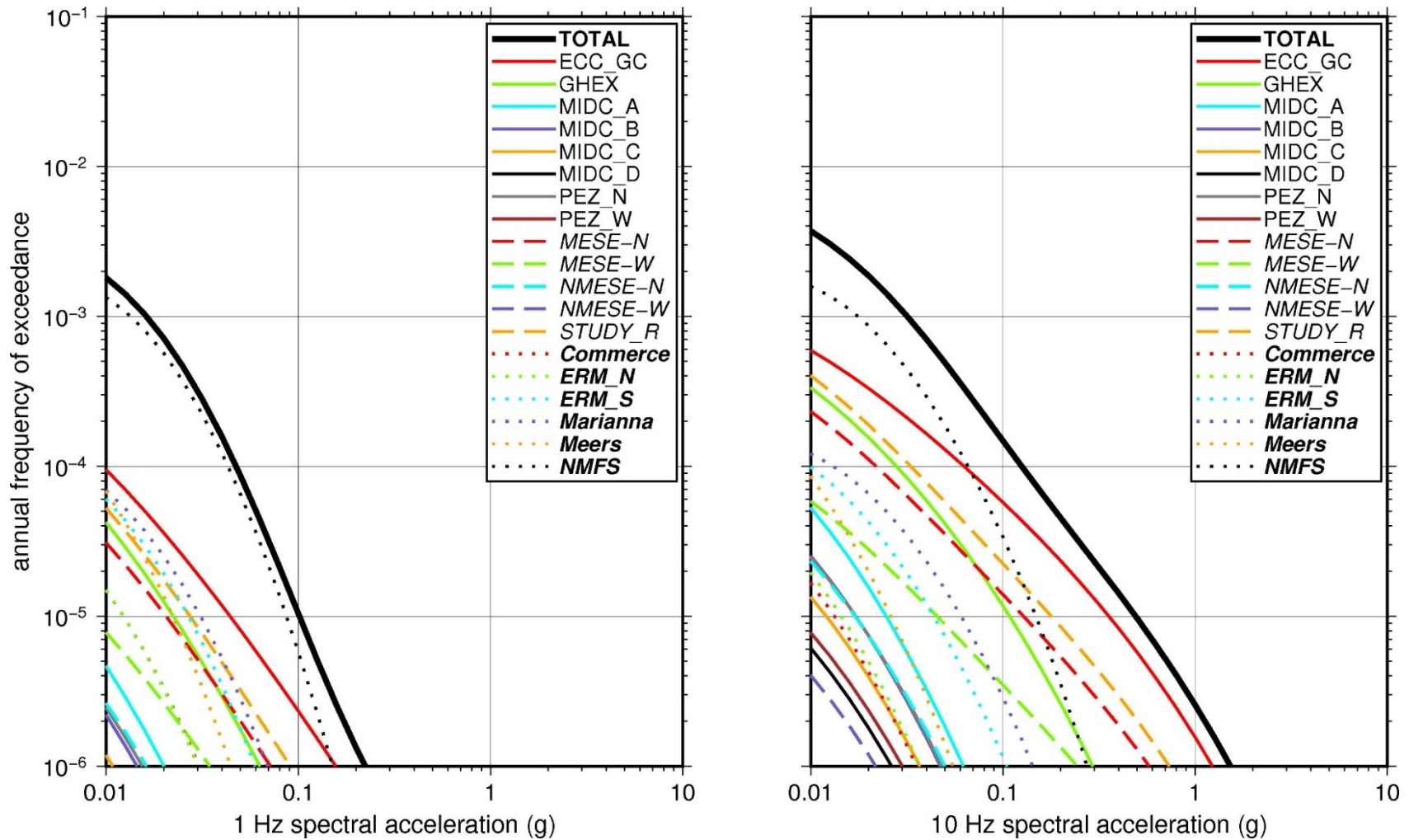


**Figure 2.5-26 Low-Frequency (1 Hz, Left), and High-Frequency (10 Hz, Right) Reference Rock Hazard Curves for River Bend. Total Hazard is Shown as a Bold Black Line; Individual Contributions to the Hazard for Each of the CEUS-SSC Sources are Shown as Colored Lines Defined in the Legend. See Table 2.1-1 for Source Name Definitions**



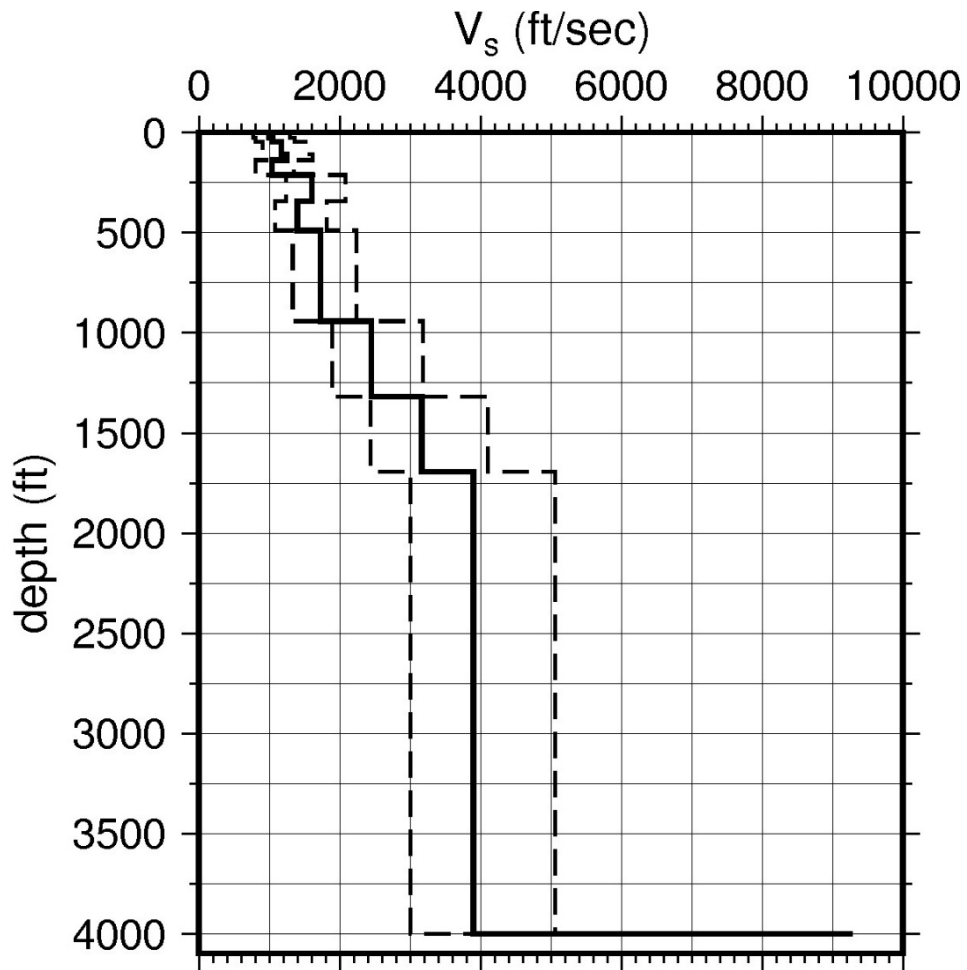
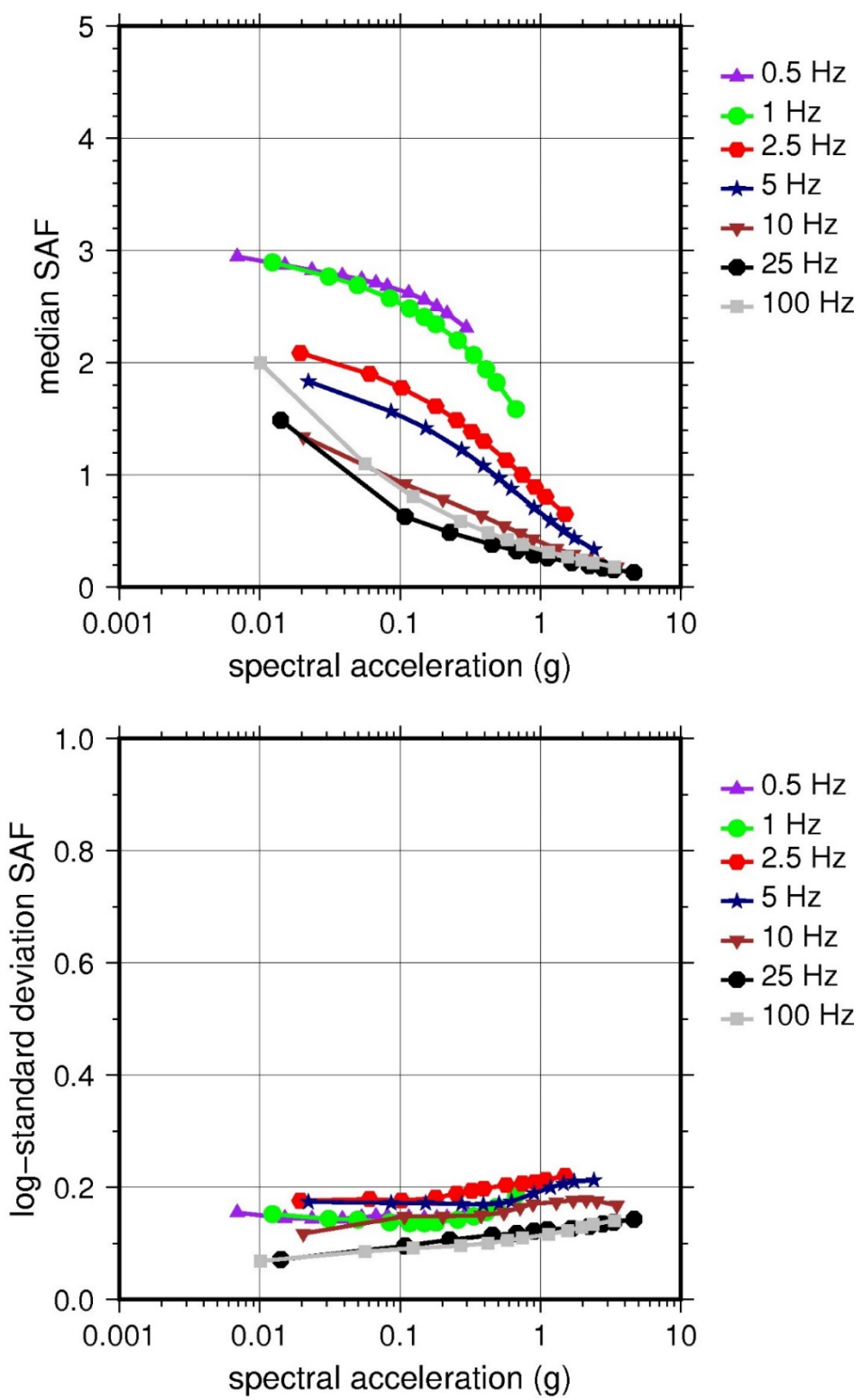
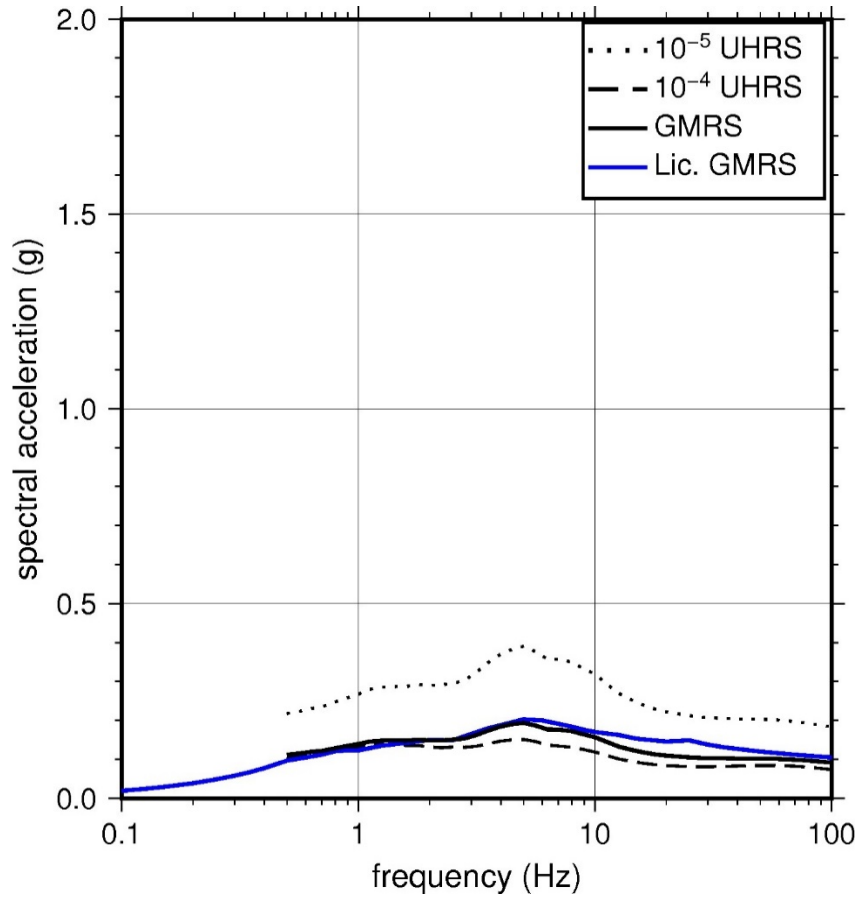
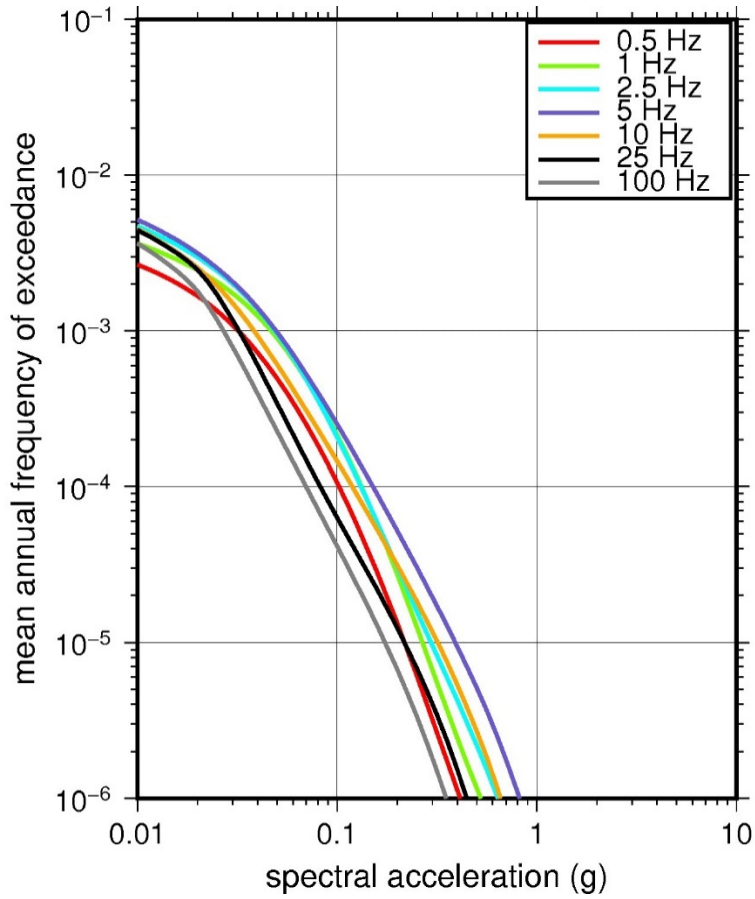


Figure 2.5-27 Shear Wave Velocity ( $V_s$ ) Profiles for River Bend. Basecase (BC) Profile Shown as Solid Bold Line; Lower and Upper Range (LR and UR) Profiles Shown as Dashed Lines. Profiles Terminate at Reference Rock Velocity of 2,831 m/sec [9,285 ft/sec] per EPRI GMM (2013)



**Figure 2.5-28 Overall Weighted Median Site Amplification Factor (SAF) (Upper) and Log Standard Deviation of the SAF (Lower) as a Function of Input Acceleration for EPRI GMM (2013) Spectral Frequencies**



**Figure 2.5-29 Mean Control Point Hazard Curves (Left) for EPRI GMM (2013) Spectral Frequencies, and GMRS and UHRS (Right) for River Bend**

## 2.5.8 South Texas

The South Texas Project Electric Generating Station site is located in south-central Matagorda County, TX, within the Coastal Plain physiographic province and is underlain by over 10,518 m [34,500 ft] of sediment and sedimentary rock. The horizontal SSE response spectrum for South Texas has an RG 1.60 spectral shape and is anchored at a PGA of 0.10g.

### 2.5.8.1 Reference Rock Hazard

For the reference rock PSHA, the NRC staff selected the 11 CEUS-SSC (NRC, 2012b) background seismic source zones that are located within 323 km [200 mi] of the site. In addition, the NRC staff also selected the Meers fault CEUS-SSC (NRC, 2012b) RLME source, which is located within 807 km [500 miles] of the site; and the NMFS RLME, which is located within 1,048 km [650 miles] of the site. To develop the reference rock seismic hazard curves for the South Texas site, the NRC staff used the GMPEs developed by the updated EPRI GMM (2013). As shown in Figure 2.5-30, the NMFS RLME is the largest contributor to the 1 Hz reference rock total mean hazard curve at the  $10^{-4}$  AFE level. For the 10 Hz reference rock total mean hazard curve, the Gulf Coast Highly Extended Crust (GHEX) seismotectonic zone is the largest contributor at the  $10^{-4}$  AFE level.

### 2.5.8.2 Site Response Evaluation

#### 2.5.8.2.1 Site Profiles

To develop a basecase profile, the NRC staff used the geologic information in the NTTF R2.1 SHSR (Powell, 2014) submitted by the South Texas Project Nuclear Operating Company (hereafter referred to as “the licensee” within this plant section), as well as the geologic information and geophysical measurements in the COL FSAR (South Texas Project Nuclear Operating Company, 2014) for the South Texas site. As described in the licensee’s SHSR and the COL FSAR, the South Texas site consists of about 18 m [60 ft] of dense, fine sand, underlain by 230 m [750 ft] of Pleistocene sediments; over 914 m [3,000 ft] of soil and soft rock deposits of Pleistocene, Pliocene, and Miocene ages; and significant sequences of Cretaceous bedrock before encountering Mesozoic basement rock. The licensee stated that the reactor containment buildings at the South Texas site are founded on dense to very dense fine sand at 60 ft [18 m] below plant grade. In Table 2.3.1-2 of the SHSR, the licensee briefly described the subsurface materials in terms of the geologic units and layer thicknesses. For its site response evaluation, the NRC staff used the ground surface, which corresponds to an elevation of 9 m [28 ft] above MSL, as the control point elevation for the South Texas site.

The field investigations for South Texas, conducted to support initial licensing and the COL application, consisted of boreholes, seismic crosshole surveys, suspension logging, and other studies of the subsurface; the deepest boring penetrated to a depth of 798 m [2,620 ft]. For the deeper soil layers, below a depth of 183 m [600 ft], the licensee used  $V_P$  measured in deep oil wells in the region with an assumed Poisson’s ratio to estimate the  $V_S$ . Table 2.3.2-2 of the SHSR gives the measured and estimated  $V_S$  determined from the licensee’s site investigations.

For its SHSR, the licensee developed a basecase profile that extends to a depth of 6,065 m [19,894 ft] below the control point elevation. The uppermost layers of the profile consist of multiple layers of clay and silty sand within the Beaumont Formation, which is Pleistocene in age and extends to a depth of 229 m [750 ft] beneath the site. The Beaumont Formation is underlain by the Pleistocene-age Lissie and Willis Formations, which combined are 183–213 m

[600–700 ft] thick and consist of soil deposits similar to those of the Beaumont Formation. These formations overlie another 4,572–6,096 m [15,000–20,000 ft] of Tertiary soils and sedimentary rock, for which the  $V_S$  values gradually increase from 600 ft/sec [183 m/sec] at the surface to about 1,524–1,828 m/sec [5,000–6,000 ft/sec] at the bottom of the profile. Over the upper 101 m [331 ft], the licensee used the mean Unit 1 and 2  $V_S$  measurements for one of its basecase profiles and the mean Unit 3 and 4  $V_S$  values for the other. For both profiles, below 101 m [331 ft], the licensee used the Unit 3 and 4 measured  $V_S$  values to a depth of 183 m [600 ft] and the velocities from the regional oil well logs for the rest.

As multiple geophysical field investigations have characterized the sedimentary strata beneath the South Texas site, the NRC staff generally used the licensee's layer thicknesses and  $V_S$  for its basecase profile. Based on the licensee's site description in Section 2.5.4 of the FSAR (South Texas Project Nuclear Operating Company, 2014), the NRC staff included a layer of engineered backfill for the top 18 m [60 ft] of its profile, rather than the in situ uppermost soil strata (Soil Strata A–E). Below this layer of backfill the NRC staff used the average of the licensee's Unit 1 and 2  $V_S$  measurements and its Unit 3 and 4  $V_S$  measurements, which are very similar, down to a depth of 101 m [331 ft]. Below this depth, the NRC staff used the licensee's  $V_S$  values down to a depth of 1,220 m [4,000 ft]. Although there are several thousand feet of additional soil and sedimentary rock before reaching Precambrian-age crystalline rock, the NRC staff terminated its profile at a depth of 1,220 m [4,000 ft], which it deemed sufficient to capture the site amplification of the lowest spectral frequency of interest at 0.5 Hz.

To capture the uncertainty in its basecase profile, the NRC staff developed lower and upper range (10<sup>th</sup> and 90<sup>th</sup> percentile) profiles by multiplying the basecase  $V_S$  values by scale factors of 0.78 and 1.29, respectively, which corresponds to an epistemic logarithmic standard deviation of 0.20. The weights for the lower, basecase, and upper profiles are 0.3, 0.4, and 0.3, respectively. Figure 2.5-31 shows the NRC staff's profiles, which extend to a depth of 1,220 m [4,000 ft] below the control point elevation.

#### 2.5.8.2.2 *Dynamic Material Properties and Site Kappa*

The NRC staff assumed both linear and nonlinear dynamic behavior for the soil beneath the South Texas site. To model the nonlinear behavior of the top soil layers (Layers 1–3), the NRC staff used the EPRI soil and Peninsular Range shear modulus reduction and material damping curves as two equally weighted alternatives. As an alternative, the NRC staff also performed its site response analysis using the Vucetic and Dobry (1991) curves for clayey soils, which made no appreciable difference to the final results. For the underlying higher velocity soil layers, the NRC staff assumed a linear dynamic response with a material damping ratio of 1 percent to maintain consistency with the  $\kappa_0$  value for the South Texas site.

To determine the basecase  $\kappa_0$  for the South Texas site, the NRC staff first used the Campbell (2009) Model 1 relationship between  $V_S$  and  $Q_{ef}$  to determine a  $Q_{ef}$  for each layer. Combining these  $Q_{ef}$  values with the thickness and  $V_S$  for each layer results in a total  $\kappa_0$  value of 80 msec, which includes the 6 msec assumed for the underlying reference rock. For the lower and upper profiles, the NRC staff calculated  $\kappa_0$  values of 118 and 53 msec, respectively, using the same approach as for the basecase profile. In contrast, the licensee used  $\kappa_0$  values of 24, 40, and 67 msec for its two basecase profiles. For comparison, using the Chapman and Conn (2016) Gulf Coast  $\kappa_0$  relationship with a thickness of 10,000 m [32,800 ft] for the South Texas site yields a  $\kappa_0$  value of 140 msec.

Table 2.5-9 provides the layer depths, lithologies,  $V_s$ , unit weights, and dynamic properties for the NRC staff's three profiles. In summary, the site response logic tree developed by the NRC staff for the South Texas site consists of six alternatives; three velocity profiles (each with a different  $\kappa_0$  value) and two alternative dynamic property branches.

#### 2.5.8.2.3 Methodology and Results

The NRC staff followed the methodology described in Section 2.1.4 to develop the final site amplification factors. Figure 2.5-32 shows the overall median site amplification factors and their variability for each of the seven spectral frequencies. As shown in Figure 2.5-32, the median site amplification factors range from about 1.5 to 3.0 before falling off with higher input spectral accelerations. The lower half of Figure 2.5-32 shows that the logarithmic standard deviations for the site amplification factors range from about 0.10 to 0.20.

#### 2.5.8.3 Control Point Hazard

The NRC staff implemented Approach 3 from the SPID (EPRI, 2012) to develop a weighted control point seismic hazard curve for each of the six unique combinations of the site response logic tree for the South Texas site. After combining these curves to develop the final mean control point hazard curves, the NRC staff determined the  $10^{-4}$  and  $10^{-5}$  UHRS in order to calculate the GMRS. Figure 2.5-33 shows the final control point mean seismic hazard curves for the seven spectral frequencies, as well as the NRC staff's UHRS and GMRS and the licensee's NTTF R2.1 GMRS (Powell, 2014). As shown in Figure 2.5-33, the NRC staff's GMRS (black curve) is similar to the licensee's GMRS (blue curve) over the entire frequency range.

**Table 2.5-9 Layer Depths, Shear Wave Velocities ( $V_s$ ), Unit Weights, and Dynamic Properties for South Texas**

Layer	Depth (ft)	Description	$V_s$ (ft/sec)			$V_s$ Sigma (ln)	BC Unit Weight (pcf)	Dynamic Properties	
			LR (0.3)	BC (0.4)	UR (0.3)			Alt. 1 (0.5)	Alt. 2 (0.5)
1	60	Soil: fill	774	1,000	1,292	0.25	120	EPRI Soil	Pen.
2	82	Soil: clay, sand	863	1,115	1,441	0.15	120	EPRI Soil	Pen.
3	341	Soil: clay, sand	942	1,217	1,573	0.15	120	EPRI Soil	Pen.
4	694	Soil: clay, sand	1,145	1,479	1,911	0.15	130	L 1.0%	L 1.0%
5	1,094	Soil: clay, sand	1,370	1,770	2,287	0.15	130	L 1.0%	L 1.0%
6	1,494	Soil: sand	1,607	2,077	2,684	0.15	130	L 1.0%	L 1.0%
7	1,894	Soil: sand	1,798	2,324	3,003	0.15	130	L 1.0%	L 1.0%
8	2,294	Soil: sand	2,016	2,605	3,366	0.15	130	L 1.0%	L 1.0%
9	3,094	Rock: sandstone	2,335	3,018	3,900	0.15	130	L 1.0%	L 1.0%
10	4,000	Rock: sandstone	2,951	3,813	4,927	0.15	140	L 1.0%	L 1.0%

LR = lower range; BC = basecase; UR = upper range; ln = natural log; pcf = pounds per cubic foot; L = linear; Alt. = alternative; Pen. = Peninsular.

For LR, BC, UR, and Alt.: Values in parentheses refer to weights for site response analysis logic tree branches.

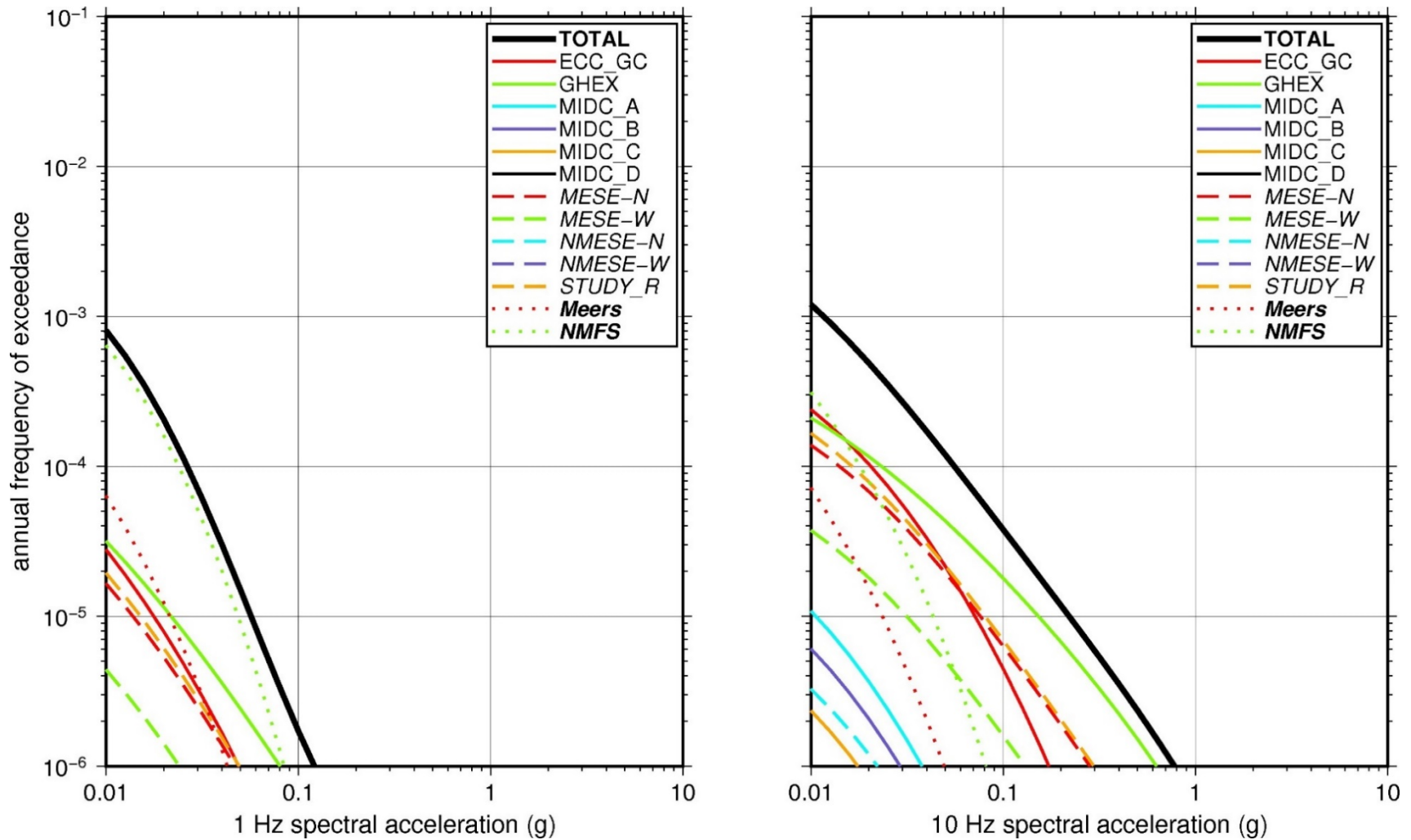


**Figure 2.5-30 Low-Frequency (1 Hz, Left), and High-Frequency (10 Hz, Right) Reference Rock Hazard Curves for South Texas. Total Hazard is Shown as a Bold Black Line; Individual Contributions to the Hazard for Each of the CEUS-SSC Sources are Shown as Colored Lines Defined in the Legend. See Table 2.1-1 for Source Name Definitions**



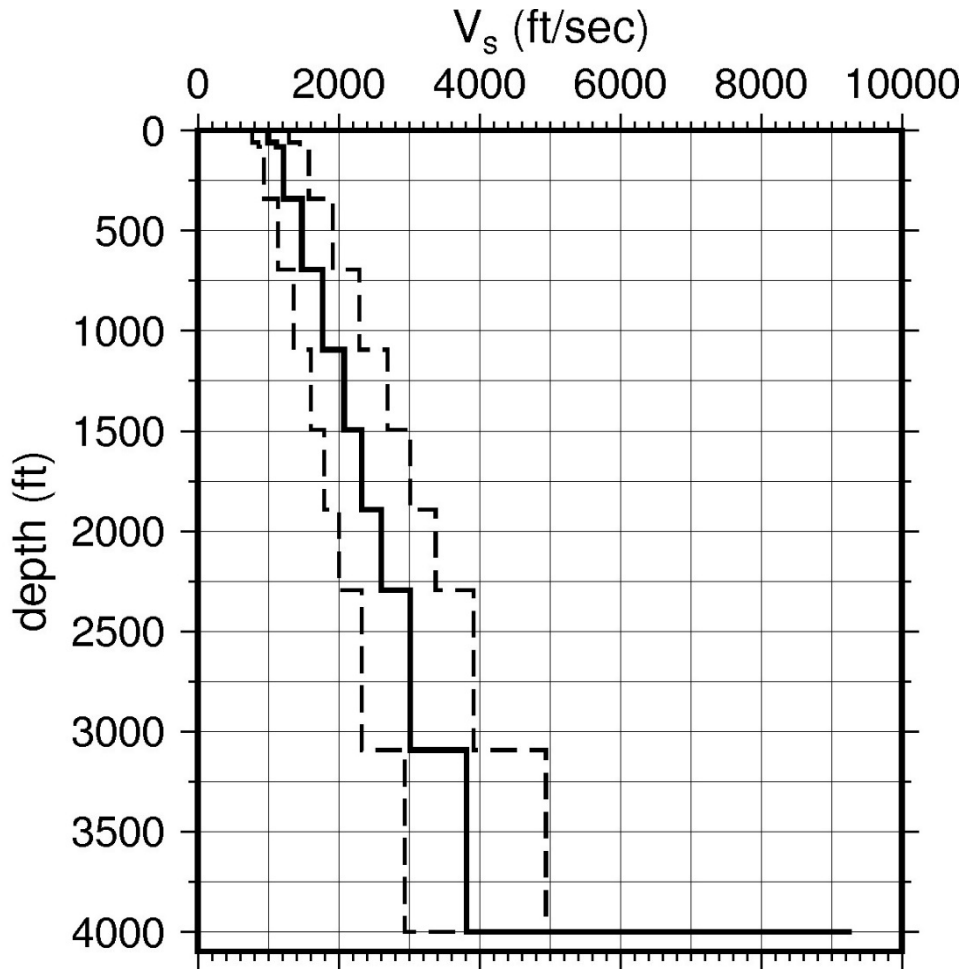


**Figure 2.5-31 Shear Wave Velocity ( $V_s$ ) Profiles for South Texas. Basecase (BC) Profile Shown as Solid Bold Line; Lower and Upper Range (LR and UR) Profiles Shown as Dashed Lines. Profiles Terminate at Reference Rock Velocity of 2,831 m/sec [9,285 ft/sec] per EPRI GMM (2013)**

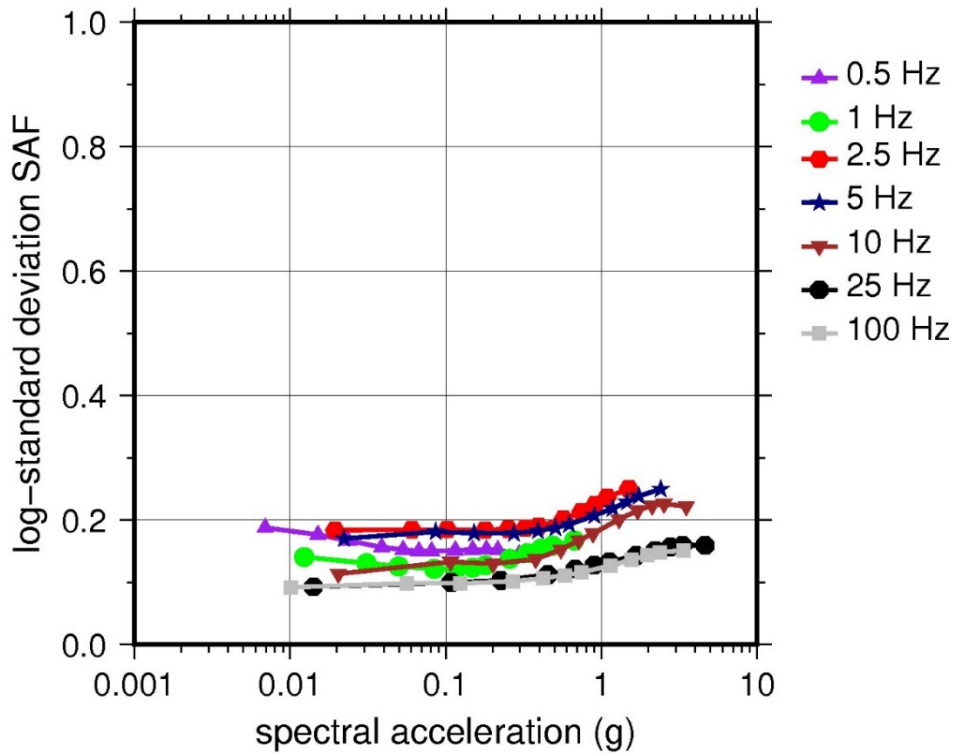
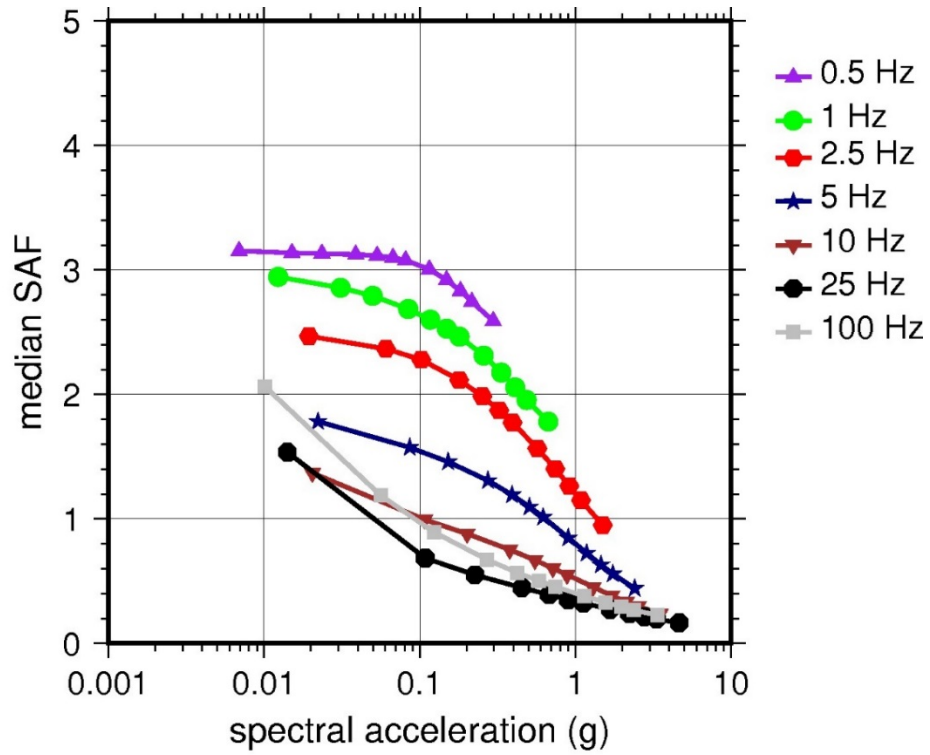


**Figure 2.5-32 Overall Weighted Median Site Amplification Factor (SAF) (Upper) and Log Standard Deviation of the SAF (Lower) as a Function of Input Acceleration for EPRI GMM (2013) Spectral Frequencies**

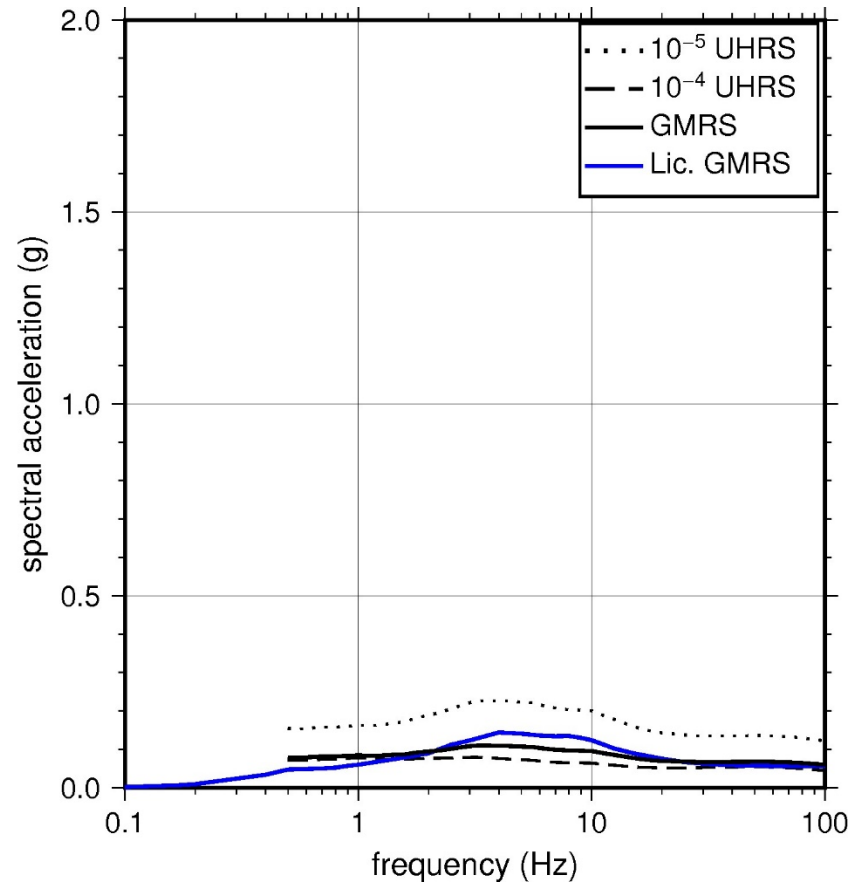
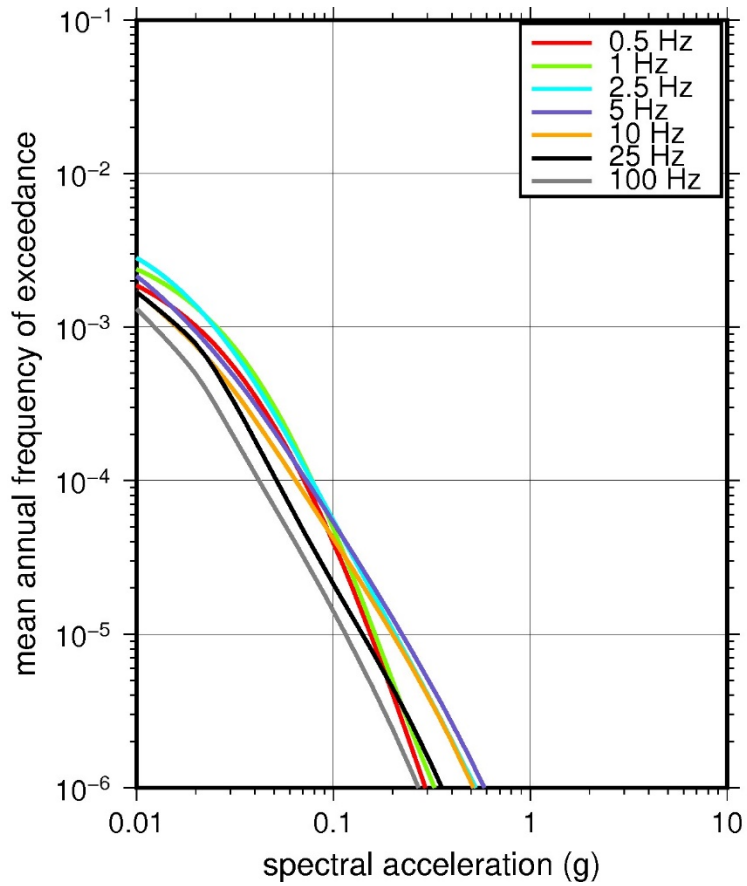


**Figure 2.5-33 Mean Control Point Hazard Curves (Left) for EPRI GMM (2013) Spectral Frequencies, and GMRS and UHRS (Right) for South Texas**

## 2.5.9 Waterford

The Waterford Steam Electric Station site is located in southern Louisiana along the Mississippi River within the Coastal Plain physiographic province and is underlain by over 11,000 m [36,000 ft] of sediment and sedimentary rock. The horizontal SSE response spectrum for Waterford has a Newmark spectral shape and is anchored at a PGA of 0.10g.

### 2.5.9.1 Reference Rock Hazard

For the reference rock PSHA, the NRC staff selected the 13 CEUS-SSC (NRC, 2012b) background seismic source zones that are located within 323 km [200 mi] of the site. In addition, the NRC staff selected the six CEUS-SSC (NRC, 2012b) RLME sources that are located within 807 km [500 mi] of the site. To develop the reference rock seismic hazard curves for the Waterford site, the NRC staff used the GMPEs developed by the updated EPRI GMM (2013). As shown in Figure 2.5-34, the NMFS RLME is the largest contributor to the 1 Hz reference rock total mean hazard curve at the  $10^{-4}$  AFE level. For the 10 Hz reference rock total mean hazard curve, the GHEX seismotectonic source zone is the largest contributor at the  $10^{-4}$  AFE level.

### 2.5.9.2 Site Response Evaluation

#### 2.5.9.2.1 Site Profiles

To develop a basecase profile, the NRC staff used the geologic information in the NTTF R2.1 SHSR (Chisum, 2014) submitted by Entergy Nuclear Operations Inc. (hereafter referred to as “the licensee” within this plant section). As described in the SHSR, the Waterford site consists of 152 m [500 ft] of interbedded sands and clays with varying amounts of silt, overlying 1,500 m [4,900 ft] of soil atop 12,200 m [35,100 ft] of firm sedimentary rock. The licensee stated that all seismic Category I structures are founded at an elevation of 14 m [47 ft] below MSL on a 0.3-m-thick [1-ft-thick] compacted shell filter blanket on top of the Pleistocene clay. In Table 2.3.1-1 of the SHSR, the licensee briefly described the subsurface materials in terms of the geologic composition and layer thicknesses for the uppermost 167 m [550 ft] of the subsurface. For its site response evaluation, the NRC staff used the top of the Pleistocene-age Prairie Formation clay, which corresponds to an elevation of 14 m [47 ft] below MSL, as the control point elevation for the Waterford site.

The field investigations for Waterford, conducted during initial licensing, included seismic refraction surveys, uphole and crosshole surveys, and cyclic triaxial testing of the shallow subsurface. The licensee’s geophysical field investigations primarily measured  $V_p$  to a depth of about 52 m [173 ft] from uphole velocity surveys. Table 2.3.2-2 of the SHSR gives the measured and estimated  $V_s$  determined from the licensee’s site investigations.

For its SHSR, the licensee developed a basecase profile that extends to a depth of 1,220 m [4,000 ft] below the control point elevation. The uppermost layers of the profile comprise 579 m [1,900 ft] of the Pleistocene- to Pliocene-age Prairie and Citronelle Formations, which consist of sand, clay, and silt. Beneath these two formations is the Pascagoula Formation, which is predominantly clay and extends for another several hundred feet. The licensee divided these soil formations into multiple layers, with measured  $V_s$  increasing from 259 m/sec [850 ft/sec] to 495 m/sec [1,625 ft/sec] at a depth of 140 m [460 ft]. Below 140 m [460 ft], the licensee used one of the soil  $V_s$  templates recommended in Appendix B to the SPID (EPRI, 2012) to extend its profile to a depth of 1,220 m [4,000 ft]. Although there are tens of thousands of feet of

additional sediment and sedimentary rock before reaching Precambrian-age crystalline rock, the licensee terminated its profile at a depth of 1,220 m [4,000 ft], which it deemed sufficient to capture the site amplification of the lowest spectral frequency of interest at 0.5 Hz.

As multiple geophysical field investigations have characterized the upper sedimentary strata beneath the Waterford site, the NRC staff used the licensee's layer thicknesses and  $V_S$  for its basecase profile. To estimate the  $V_S$  for the deeper sedimentary layers, the NRC staff used an approximation of the deeper portion of the River Bend site basecase profile, which also consists of the Citronelle and Pascagoula Formations (Entergy Nuclear Operations Inc., 2008). The basecase profile below 152 m [500 ft] for the River Bend site, located along the Mississippi River to the northwest of Waterford, was developed from  $V_P$  measured in deep wells in the region with an assumed Poisson's ratio to estimate the  $V_S$  (Entergy Nuclear Operations Inc., 2008). The measured  $V_S$  for these deeper deposits ranges from 610 m/sec [2,000 ft/sec] to 10,679 m/sec [3,500 ft/sec] at a depth of 1,220 m [4,000 ft] below the control point elevation.

To capture the uncertainty in its basecase profile, the NRC staff developed lower and upper range (10<sup>th</sup> and 90<sup>th</sup> percentile) profiles by multiplying the basecase  $V_S$  values by scale factors of 0.78 and 1.29, respectively, which corresponds to an epistemic logarithmic standard deviation of 0.20. The weights for the lower, basecase, and upper profiles are 0.3, 0.4, and 0.3, respectively. Figure 2.5-35 shows the NRC staff's profiles, which extend to a depth of 1,220 m [4,000 ft] below the control point elevation.

#### 2.5.9.2.2 *Dynamic Material Properties and Site Kappa*

The NRC staff assumed both linear and nonlinear dynamic behavior for the soil beneath the Waterford site. To model the nonlinear behavior of the top soil layers (Layers 1–8), the NRC staff used the EPRI soil and Peninsular Range shear modulus reduction and material damping curves as two equally weighted alternatives. As an alternative, the NRC staff also performed its site response analysis using the Vucetic and Dobry (1991) curves for clayey soils, which made no appreciable difference to the final results. For the underlying higher velocity soil layers, the NRC staff assumed a linear dynamic response with a material damping ratio of 0.5 to 1.0 percent to maintain consistency with the  $\kappa_0$  value for the Waterford site.

To determine the basecase  $\kappa_0$  for the Waterford site, the NRC staff first used the Campbell (2009) Model 1 relationship between  $V_S$  and  $Q_{ef}$  to determine a  $Q_{ef}$  for each layer. Combining these  $Q_{ef}$  values with the thickness and  $V_S$  for each layer results in a total  $\kappa_0$  value of 65 msec, which includes the 6 msec assumed for the underlying reference rock. For the lower and upper profiles, the NRC staff calculated  $\kappa_0$  values of 96 and 30 msec, respectively, using the same approach as for the basecase profile. In contrast, the licensee used a  $\kappa_0$  value of 40 msec for the basecase, lower, and upper profiles, which is the maximum value recommended by Appendix B of the SPID (EPRI, 2012) for CEUS deep soil sites. For comparison, using the Chapman and Conn (2016) Gulf Coast  $\kappa_0$  relationship with a sedimentary thickness of 11,000 m [36,080 ft] for the Waterford site yields a  $\kappa_0$  value of 150 msec.

Table 2.5-10 provides the layer depths, lithologies,  $V_S$ , unit weights, and dynamic properties for the NRC staff's three profiles. In summary, the site response logic tree developed by the NRC staff for the Waterford site consists of six alternatives; three velocity profiles (each with a different  $\kappa_0$  value) and two alternative dynamic property branches.

### 2.5.9.2.3 Methodology and Results

The NRC staff followed the methodology described in Section 2.1.4 to develop the final site amplification factors. Figure 2.5-36 shows the overall median site amplification factors and their variability for each of the seven spectral frequencies. As shown in Figure 2.5-36, the median site amplification factors range from about 1.5 to 3.0 before falling off with higher input spectral accelerations. The lower half of Figure 2.5-36 shows that the logarithmic standard deviations for the site amplification factors range from about 0.10 to 0.20.

### 2.5.9.3 Control Point Hazard

The NRC staff implemented Approach 3 from the SPID (EPRI, 2012) to develop a weighted control point seismic hazard curve for each of the six unique combinations of the site response logic tree for the Waterford site. After combining these curves to develop the final mean control point hazard curves, the NRC staff determined the  $10^{-4}$  and  $10^{-5}$  UHRS in order to calculate the GMRS. Figure 2.5-37 shows the final control point mean seismic hazard curves for the seven spectral frequencies, as well as the NRC staff's UHRS and GMRS and the licensee's NTTF R2.1 GMRS (Chisum, 2014). As shown in Figure 2.5-37, the NRC staff's GMRS (black curve) is similar to the licensee's GMRS (blue curve) over the entire frequency range.

**Table 2.5-10 Layer Depths, Shear Wave Velocities ( $V_s$ ), Unit Weights, and Dynamic Properties for Waterford**

Layer	Depth (ft)	Description	$V_s$ (ft/sec)			$V_s$ Sigma (ln)	BC Unit Weight (pcf)	Dynamic Properties	
			LR (0.3)	BC (0.4)	UR (0.3)			Alt. 1 (0.5)	Alt. 2 (0.5)
1	37	Soil: clay	658	850	1,098	0.25	120	EPRI Soil	Pen.
2	68	Soil: sand, clay, silt	716	925	1,195	0.15	120	EPRI Soil	Pen.
3	87	Soil: clay	774	1,000	1,292	0.15	120	EPRI Soil	Pen.
4	272	Soil: clay, silt, sand	871	1,125	1,454	0.15	120	EPRI Soil	Pen.
5	460	Soil: sand	1,258	1,625	2,100	0.15	130	EPRI Soil	Pen.
6	913	Soil: clay	1,548	2,000	2,585	0.15	130	L 1.0%	L 1.0%
7	1,289	Soil: clay	1,935	2,500	3,231	0.15	130	L 1.0%	L 1.0%
8	1,664	Soil: clay	2,322	3,000	3,877	0.15	130	L 1.0%	L 1.0%
9	4,000	Soil: clay	2,708	3,500	4,523	0.15	140	L 0.5%	L 0.5%

LR = lower range; BC = basecase; UR = upper range; ln = natural log; pcf = pounds per cubic foot; L = linear; Alt. = alternative; Pen. = Peninsular.

For LR, BC, UR, and Alt.: Values in parentheses refer to weights for site response analysis logic tree branches.

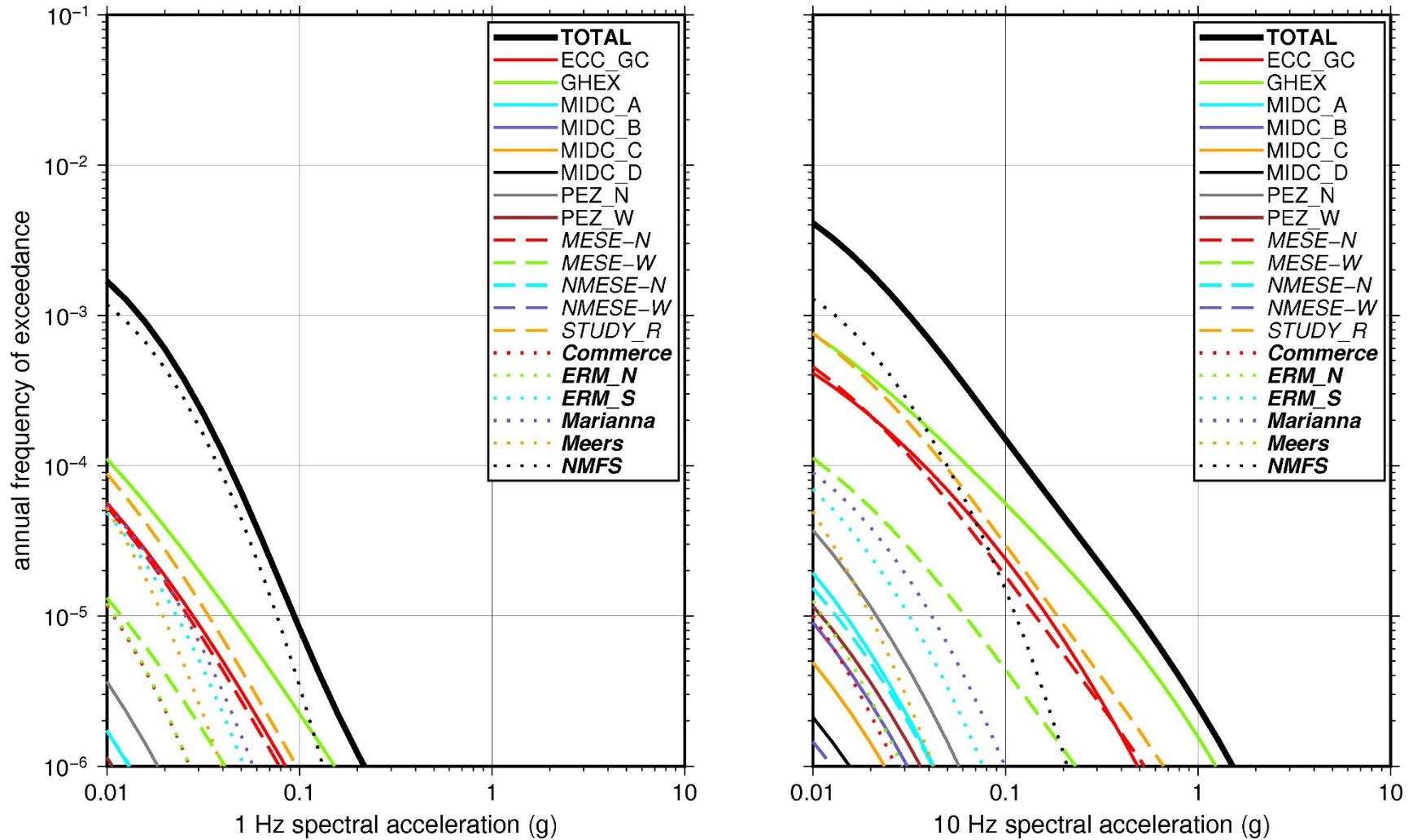


**Figure 2.5-34 Low-Frequency (1 Hz, Left), and High-Frequency (10 Hz, Right) Reference Rock Hazard Curves for Waterford. Total Hazard is Shown as a Bold Black Line; Individual Contributions to the Hazard for Each of the CEUS-SSC Sources are Shown as Colored Lines Defined in the Legend. See Table 2.1-1 for Source Name Definitions**

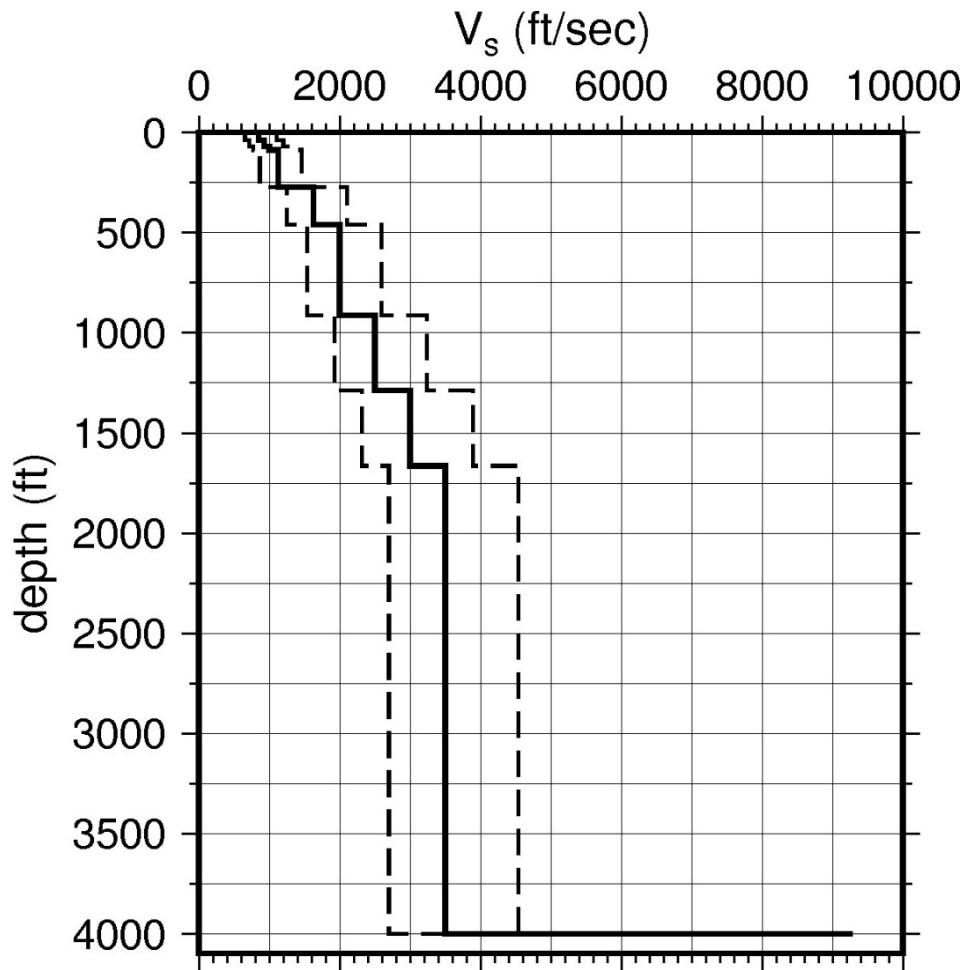


**Figure 2.5-35 Shear Wave Velocity ( $V_s$ ) Profiles for Waterford. Basecase (BC) Profile Shown as Solid Bold Line; Lower and Upper Range (LR and UR) Profiles Shown as Dashed Lines. Profiles Terminate at Reference Rock Velocity of 2,831 m/sec [9,285 ft/sec] per EPRI GMM (2013)**



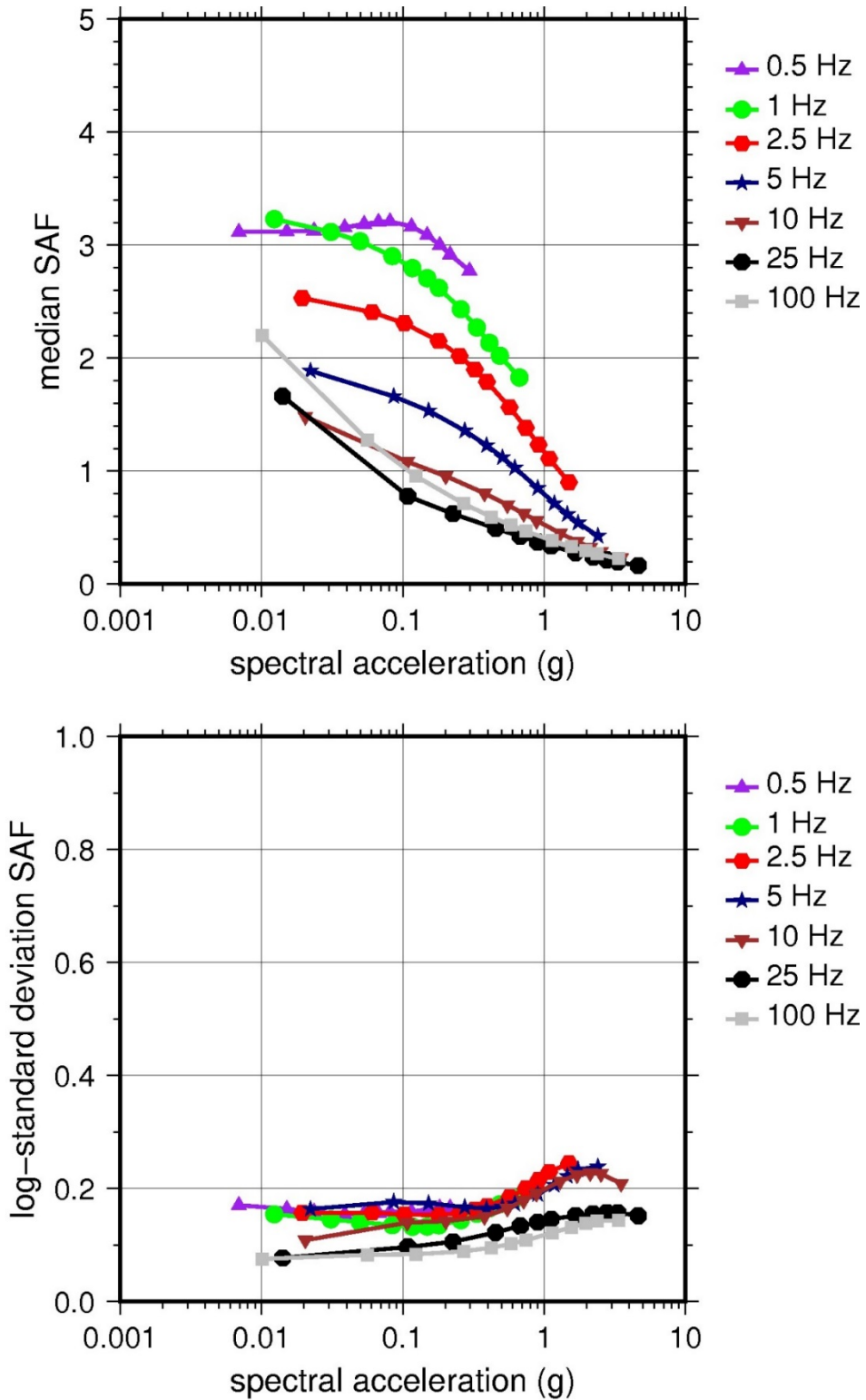


**Figure 2.5-36 Overall Weighted Median Site Amplification Factor (SAF) (Upper) and Log Standard Deviation of the SAF (Lower) as a Function of Input Acceleration for EPRI GMM (2013) Spectral Frequencies**

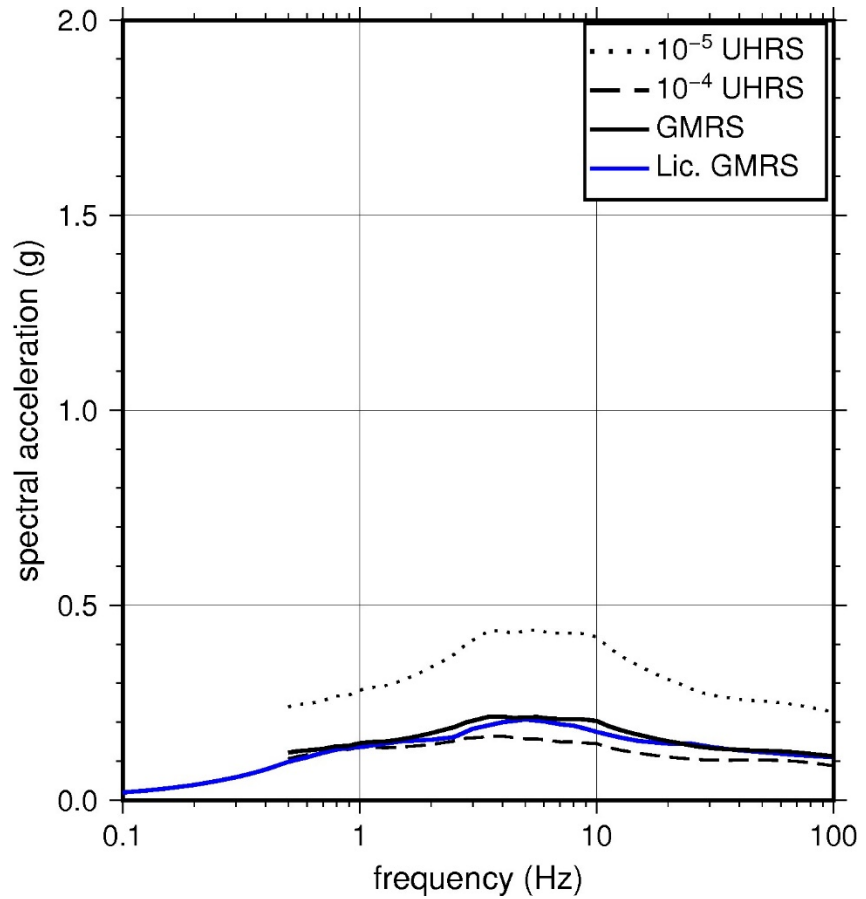
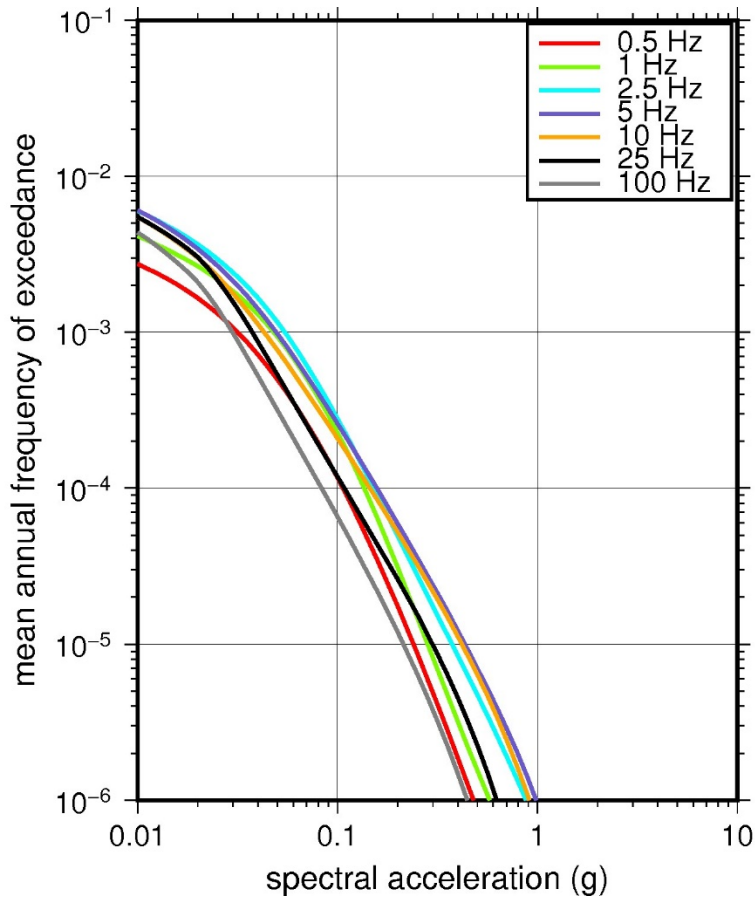


**Figure 2.5-37 Mean Control Point Hazard Curves (Left) for EPRI GMM (2013) Spectral Frequencies, and GMRS and UHRS (Right) for Waterford**

## 2.5.10 Wolf Creek

The Wolf Creek Generating Station site is located in eastern Kansas along Coffey County Lake within the Central Lowland physiographic province and consists of 3 m [10 ft] of soil (clay) overlying about 823 m [2,700 ft] of sedimentary rock (shale, sandstone, limestone, and dolomite). The horizontal SSE response spectrum for Wolf Creek has an RG 1.60 spectral shape and is anchored at PGAs of 0.15g for nonpowerblock structures and 0.20g for the powerblock.

### 2.5.10.1 Reference Rock Hazard

For the reference rock PSHA, the NRC staff selected the seven CEUS-SSC (NRC, 2012b) background seismic source zones that are located within 323 km [200 mi] of the site. In addition, the NRC staff selected the eight CEUS-SSC (NRC, 2012b) RLME sources that are located within 807 km [500 mi] of the site. To develop the reference rock seismic hazard curves for the Wolf Creek site, the NRC staff used the GMPEs developed by the updated EPRI GMM (2013). As shown in Figure 2.4-38, the NMFS RLME is the largest contributor to the 1 Hz reference rock total mean hazard curve at the  $10^{-4}$  AFE level. For the 10 Hz reference rock total mean hazard curve, the NMFS RLME and the MIDC-A seismotectonic source zone are the two largest contributors at the  $10^{-4}$  AFE level.

### 2.5.10.2 Site Response Evaluation

#### 2.5.10.2.1 Site Profiles

To develop a basecase profile, the NRC staff used the geologic information in the NTTF R2.1 SHSR (Smith, 2014) submitted by Wolf Creek Nuclear Operating Corporation (hereafter referred to as “the licensee” within this plant section). As described in the licensee’s SHSR, the Wolf Creek site is underlain by approximately 3 m [10 ft] of soil (silty clay and weathered shale) overlying bedrock (somewhat clayey calcareous shale). The major plant structures are supported on bedrock. In Table 2.3.1-1 of the SHSR, the licensee briefly described the subsurface materials in terms of the geologic units and layer thicknesses. For its site response evaluation, the NRC staff used the finished grade, which corresponds to an elevation of 335 m [1,100 ft] above MSL, as the control point elevation for the Wolf Creek site.

The field investigations for Wolf Creek, conducted in support of initial licensing, include seismic refraction surveys and geophysical logging in the upper 122 m [400 ft] from three boreholes on site. Table 2.3.2-2 of the SHSR gives the measured and estimated  $V_S$  determined from the licensee’s site investigations.

The licensee developed a basecase profile that extends to a depth of 823 m [2,700 ft] below the control point elevation. The uppermost layers of the profile consist of 3 m [10 ft] of clay overlying the 22-m-thick [72-ft-thick] Pennsylvanian-age Oread Limestone Formation within the Shawnee Group. The licensee divided the Oread Limestone Formation into four layers based on differences in the lithology and the measured velocities. For the uppermost 8 m [26 ft] of clayey calcareous shale, the median  $V_S$  is 442 m/sec [1,450 ft/sec]. This layer overlies a harder 4-m [12-ft] layer of limestone with shale, which has a  $V_S$  of 1,890 m/sec [6,200 ft/sec]. The next layer, which is 5 m [16 ft] thick, is a mixture of carbonaceous shale, limestone, and calcareous shale with a  $V_S$  of 1,067 m/sec [3,500 ft/sec]. The bottom layer within the Oread Limestone Formation is the Toronto Limestone Member, which is 6 m [18 ft] thick with a  $V_S$  of 1,890 m/sec [6,200 ft/sec]. Beneath the Oread Limestone Formation are the Lawrence and

Stranger Formations, within the Douglas Group. The licensee divided the Lawrence Formation into two layers with thicknesses of 53 m [173 ft] and 2 m [7 ft], respectively. The  $V_S$  for the thicker layer, composed of shale and sandstone with some limestone, is 1,220 m/sec [4,000 ft/sec], while the  $V_S$  for the thinner layer, composed of limestone, is 2,439 m/sec [8,000 ft/sec]. For the Stranger Formation, which is 40 m [131 ft] thick, the licensee measured a  $V_S$  of 1,296 m/sec [4,250 ft/sec]. Underlying the Douglas Group is the Lansing Group, which consists primarily of limestone and shale layers. For the Stanton Limestone Formation, which is uppermost within the Lansing Group, the licensee measured a  $V_S$  of 2,439 m/sec [8,000 ft/sec]. Below this, at a depth of 123 m [403 ft] below the control point elevation, the licensee applied a velocity gradient of 0.5 m/sec/m [0.5 ft/sec/ft], so that the  $V_S$  increased from 2,439 m/sec [8,000 ft/sec] to 2,767 m/sec [9,075 ft/sec] at a depth of 823 m [2,700 ft].

As multiple geophysical field investigations have characterized the sedimentary strata beneath the Wolf Creek site, the NRC staff used the licensee's layer thicknesses and  $V_S$  for the upper 123 m [403 ft] of its basecase profile. However, rather than include the in-situ soils for the uppermost 3 m [10 ft] layer, the NRC staff's top layer is the backfill material that the licensee placed to support Category I structures (Wolf Creek Nuclear Operating Corporation, 2013). For the backfill layer, the NRC staff estimated a  $V_S$  of 305 m/sec [1,000 ft/sec]. In addition, for the 700 m [2,300 ft] of sedimentary strata below the Stanton Limestone Formation, rather than using the velocity gradient of 0.5 m/sec/m [0.5 ft/sec/ft], the NRC staff used the stratigraphic column developed by the Kansas Geological Survey from a profile through Coffey County, as well as the one-dimensional velocity model developed by Nolte (2017) for the Wellington oil field in south-central Kansas. In the Nolte (2017) model,  $V_S$  increases from 2,200 m/sec [7,216 ft/sec] to 2,850 m/sec [9,348 ft/sec] at a depth of 500 m [1,640 ft], which roughly corresponds to the boundary between Pennsylvanian and Pre-Pennsylvanian strata. Therefore, the NRC staff terminated its profile at a depth of 437 m [1,432 ft] to match the Kansas Geological Survey's stratigraphic profile for Coffey County. The NRC staff assumed a velocity gradient of 0.5 m/sec/m [0.5 ft/sec/ft] for the 314 m [1,029 ft] of Pennsylvanian-age strata (Lansing, Kansas City, Pleasanton, Marmaton, and Cherokee Groups), for which the licensee has no measured  $V_S$ . This gradient yielded a terminal  $V_S$  of 2,591 m/sec [8,500 ft/sec] at a depth of 437 m [1,432 ft] below the control point elevation.

To capture the uncertainty in its basecase profile, the NRC staff developed lower and upper range (10<sup>th</sup> and 90<sup>th</sup> percentile) profiles by multiplying the basecase  $V_S$  values by scale factors of 0.78 and 1.29, respectively, which corresponds to an epistemic logarithmic standard deviation of 0.20. The weights for the lower, basecase, and upper profiles are 0.3, 0.4, and 0.3, respectively. Figure 2.5-39 shows the upper 305 m [1,000 ft] of the NRC staff's profiles. As shown in Figure 2.5-39, the upper profile terminates at a depth of 122 m [399 ft], while the basecase and lower profiles extend to a depth of 437 m [1,432 ft] below the control point elevation.

#### 2.5.10.2.2 *Dynamic Material Properties and Site Kappa*

The NRC staff assumed both linear and nonlinear dynamic behavior for the soil and rock beneath the Wolf Creek site. To model the nonlinear behavior of the top soil layer (Layer 1), the NRC staff used the EPRI soil and Peninsular Range shear modulus reduction and material damping curves as two equally weighted alternatives. For the upper rock layers (Layers 2–6), the NRC staff used the EPRI rock shear modulus reduction and material damping curves. To model the linear behavior of these rock layers, the NRC staff assumed a constant damping ratio of 3 percent. The staff weighted these two alternatives equally. For the higher velocity rock

layers, the NRC staff assumed a linear dynamic response with a material damping ratio of 0.1 percent to maintain consistency with the  $\kappa_0$  value for the Wolf Creek site.

To determine the basecase  $\kappa_0$  for the Wolf Creek site, the NRC staff first used the Campbell (2009) Model 1 relationship between  $V_S$  and  $Q_{ef}$  to determine a  $Q_{ef}$  for each layer. Combining these  $Q_{ef}$  values with the thickness and  $V_S$  for each layer results in a total  $\kappa_0$  value of 11 msec, which includes the 6 msec assumed for the underlying reference rock. For the lower and upper profiles, the NRC staff calculated  $\kappa_0$  values of 14 and 8 msec, respectively, using the same approach as for the basecase profile. In contrast, the licensee estimated  $\kappa_0$  by combining the lowest low-strain damping values from the material damping curves over the top 152 m [500 ft] of soil and rock and assumed a damping value of 1.25 percent for the remaining deeper rock layers to estimate basecase, lower, and upper  $\kappa_0$  values of 20, 29, and 11 msec, respectively.

Table 2.5-11 provides the layer depths, lithologies,  $V_S$ , unit weights, and dynamic properties for the NRC staff's three profiles. In summary, the site response logic tree developed by the NRC staff for the Wolf Creek site consists of six alternatives; three velocity profiles (each with a different  $\kappa_0$  value) and two alternative dynamic property branches.

### 2.5.10.2.3 Methodology and Results

The NRC staff followed the methodology described in Section 2.1.4 to develop the final site amplification factors. Figure 2.5-40 shows the overall median site amplification factors and their variability for each of the seven spectral frequencies. As shown in Figure 2.5-40, the median site amplification factors range from about 1 to 3 before falling off with higher input spectral accelerations. The lower half of Figure 2.5-40 shows that the logarithmic standard deviations for the site amplification factors range from about 0.05 to 0.30.

### 2.5.10.3 Control Point Hazard

The NRC staff implemented Approach 3 from the SPID (EPRI, 2012) to develop a weighted control point seismic hazard curve for each of the six unique combinations of the site response logic tree for the Wolf Creek site. After combining these curves to develop the final mean control point hazard curves, the NRC staff determined the  $10^{-4}$  and  $10^{-5}$  UHRS in order to calculate the GMRS. Figure 2.5-41 shows the final control point mean seismic hazard curves for the seven spectral frequencies, as well as the NRC staff's UHRS and GMRS and the licensee's NTTF R2.1 GMRS (Smith, 2014). As shown in Figure 2.5-41, the NRC staff's GMRS (black curve) is similar to the licensee's GMRS (blue curve) over the entire frequency range.

Layer	Depth (ft)	Description	$V_S$ (ft/sec)			$V_S$ Sigma (ln)	BC Unit Weight (pcf)	Dynamic Properties	
			LR (0.3)	BC (0.4)	UR (0.3)			Alt. 1 (0.5)	Alt. 2 (0.5)
1	10	Soil: fill	774	1,000	1,293	0.25	120	EPRI Soil	Pen.
2	36	Rock: shale	1,122	1,450	1,874	0.15	130	EPRI Rock	L 3.0%
3	48	Rock: limestone	4,798	6,200	8,012	0.15	150	EPRI Rock	L 3.0%

**Table 2.5-11 Layer Depths, Shear Wave Velocities ( $V_s$ ), Unit Weights, and Dynamic Properties for Wolf Creek (cont.)**

Layer	Depth (ft)	Description	$V_s$ (ft/sec)			$V_s$ Sigma (ln)	BC Unit Weight (pcf)	Dynamic Properties	
			LR (0.3)	BC (0.4)	UR (0.3)			Alt. 1 (0.5)	Alt. 2 (0.5)
4	64	Rock: shale	2,708	3,500	4,523	0.15	140	EPRI Rock	L 3.0%
5	82	Rock: limestone	4,798	6,200	8,012	0.15	150	EPRI Rock	L 3.0%
6	255	Rock: shale, siltstone, sandstone	3,095	4,000	5,169	0.15	140	EPRI Rock	L 3.0%
7	262	Rock: limestone	6,190	8,000	9,285	0.15	160	L 0.1%	L 0.1%
8	399	Rock: shale, siltstone, sandstone	3,289	4,250	5,492	0.15	140	L 0.1%	L 0.1%
9	408	Rock: limestone, shale, sandstone	5,804	8,000	9,285	0.15	160	L 0.1%	L 0.1%
10	474	Rock: sandstone, limestone, dolomite, shale	6,216	8,033	9,285	0.15	160	L 0.1%	L 0.1%
11	832	Rock: sandstone, limestone, dolomite, shale	6,355	8,212	9,285	0.15	160	L 0.1%	L 0.1%
12	982	Rock: sandstone, limestone, dolomite, shale	6,413	8,287	9,285	0.15	160	L 0.1%	L 0.1%
13	1,132	Rock: sandstone, limestone, dolomite, shale	6,471	8,362	9,285	0.15	160	L 0.1%	L 0.1%
14	1,432	Rock: sandstone, limestone, dolomite, shale	6,578	8,500	9,285	0.15	160	L 0.1%	L 0.1%

LR = lower range; BC = basecase; UR = upper range; ln = natural log; pcf = pounds per cubic foot; L = linear; Alt. = alternative; Pen. = Peninsular.  
 For LR, BC, UR, and Alt.: Values in parentheses refer to weights for site response analysis logic tree branches.

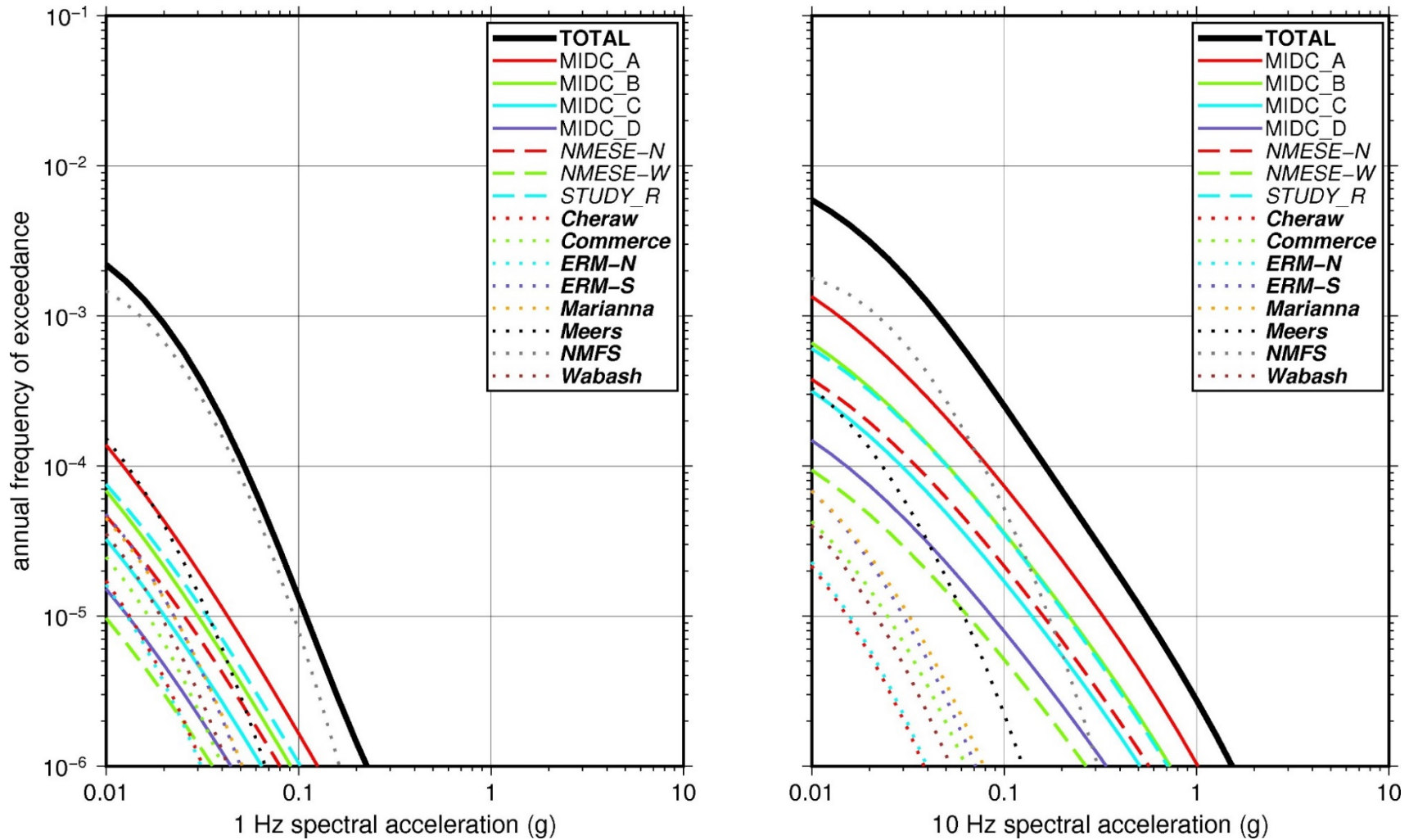


**Figure 2.5-38** Low-Frequency (1 Hz, Left), and High-Frequency (10 Hz, Right) Reference Rock Hazard Curves for Wolf Creek. Total Hazard is Shown as a Bold Black Line; Individual Contributions to the Hazard for Each of the CEUS-SSC Sources are Shown as Colored Lines Defined in the Legend. See Table 2.1-1 for Source Name Definitions

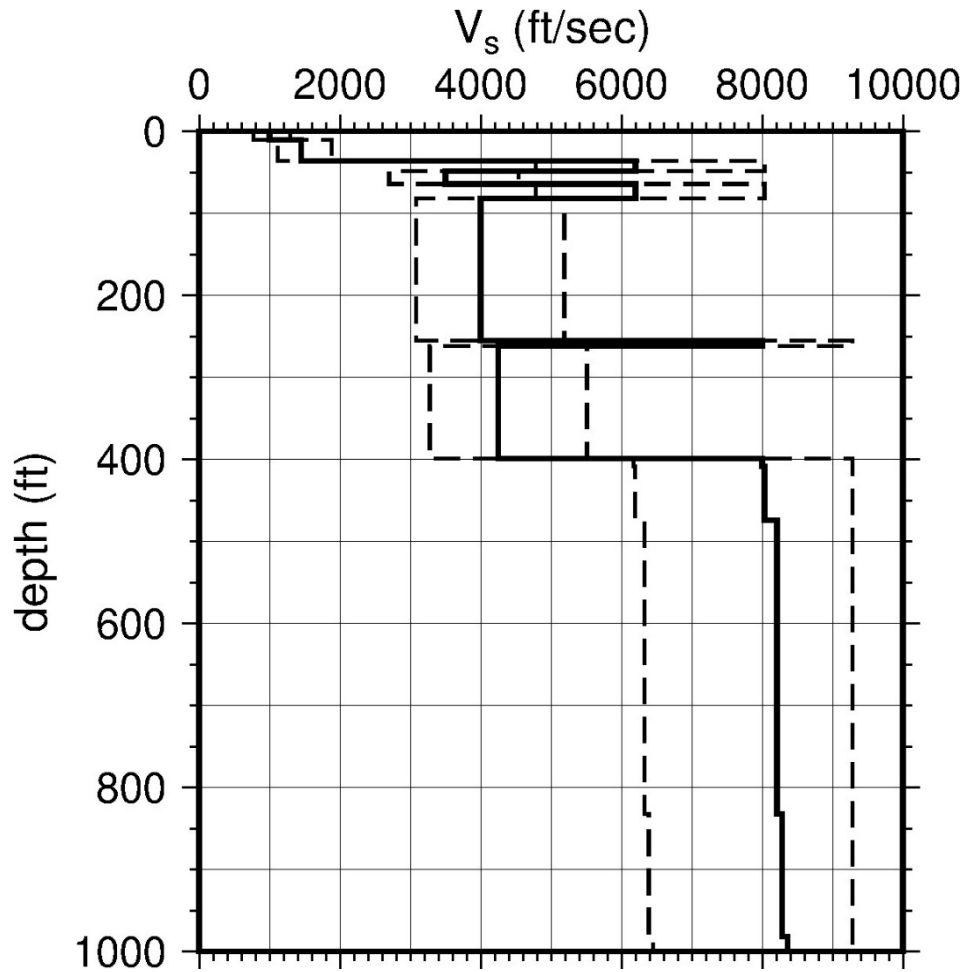


**Figure 2.5-39 Shear Wave Velocity ( $V_s$ ) Profiles for Wolf Creek. Basecase (BC) Profile Shown as Solid Bold Line; Lower and Upper Range (LR and UR) Profiles Shown as Dashed Lines. Profiles Terminate at Reference Rock Velocity of 2,831 m/sec [9,285 ft/sec] per EPRI GMM (2013)**



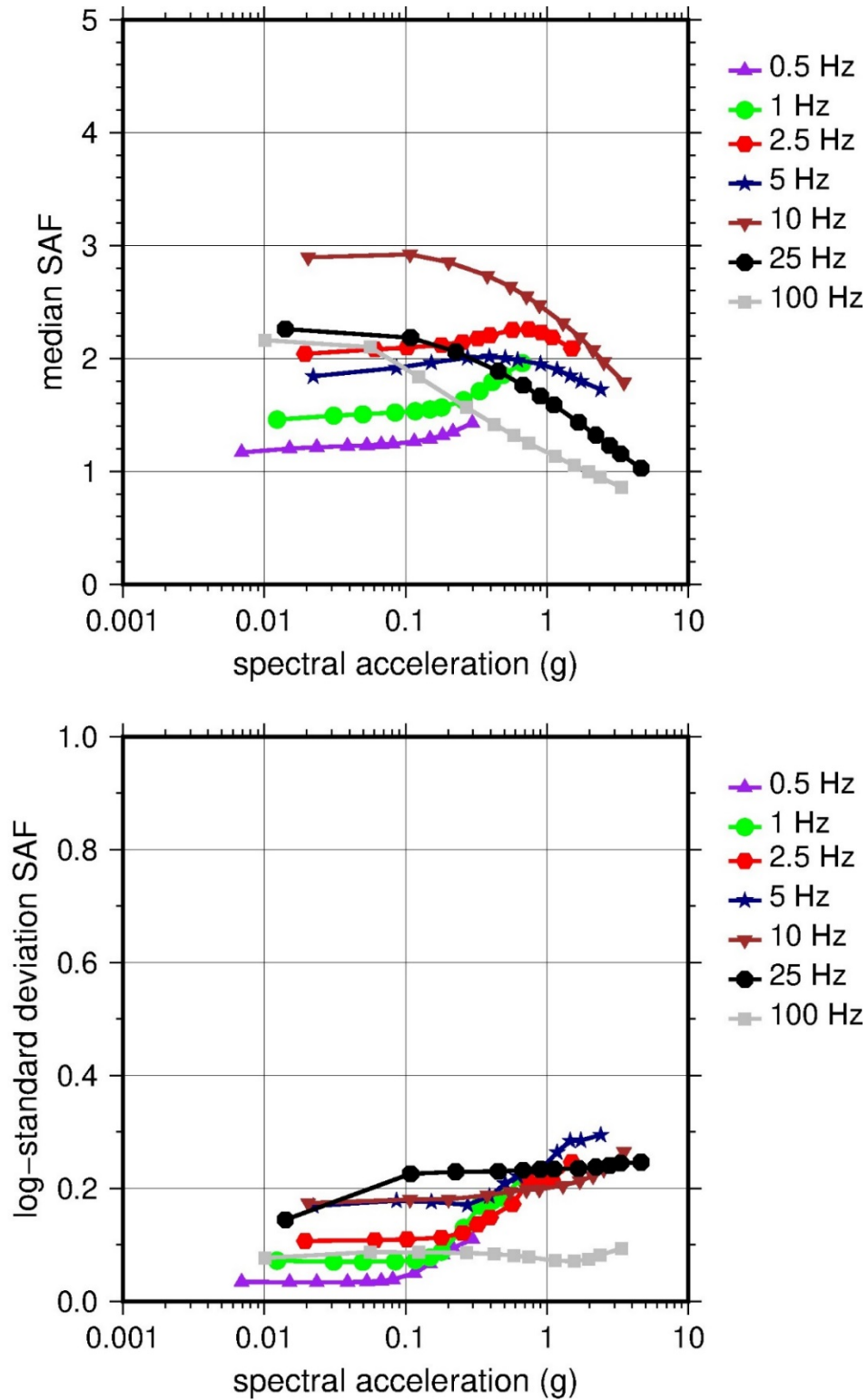


**Figure 2.5-40 Overall Weighted Median Site Amplification Factor (SAF) (Upper) and Log Standard Deviation of the SAF (Lower) as a Function of Input Acceleration for EPRI GMM (2013) Spectral Frequencies**

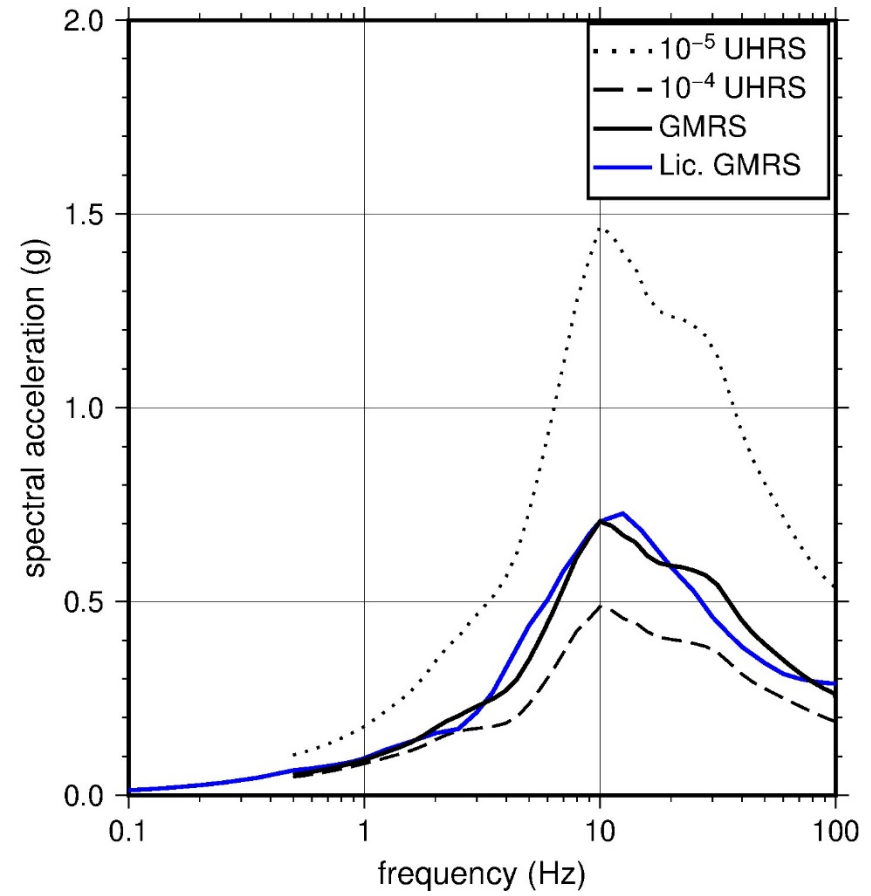
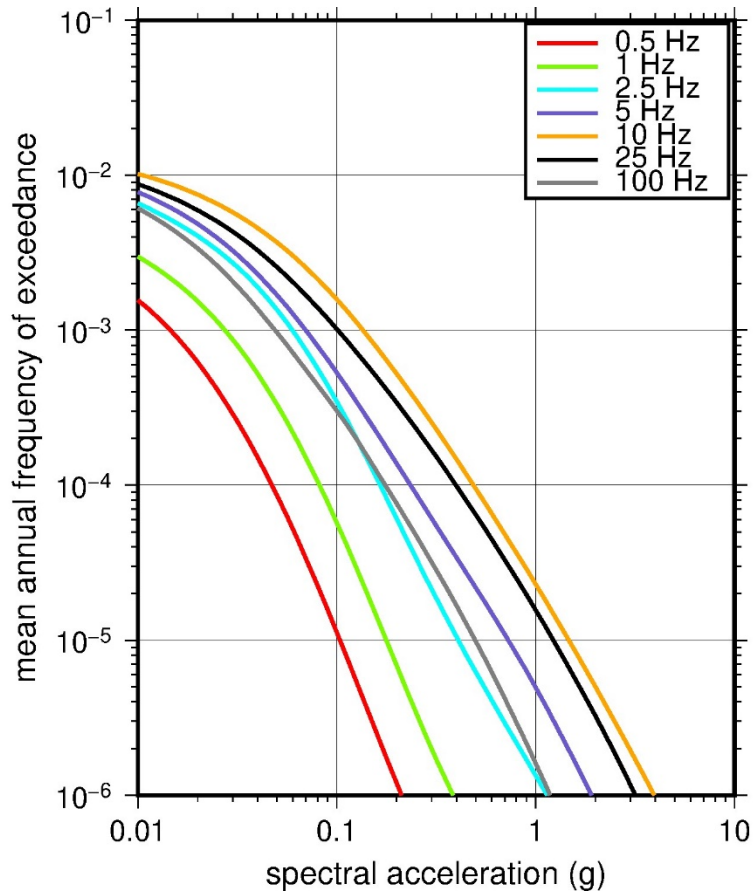


**Figure 2.5-41 Mean Control Point Hazard Curves (Left) for EPRI GMM (2013) Spectral Frequencies, and GMRS and UHRS (Right) for Wolf Creek**

## 2.6 References

Anderson, R. Letter from NextEra Energy to the U.S. Nuclear Regulatory Commission (NRC), Response to NRC Request for Information Pursuant to 10 CFR 50.54(f) Regarding Recommendation 2.1 of the Near-Term Task Force Review of Insights from the Fukushima Dai-ichi Accident. March 28, 2014. Agencywide Documents Access and Management System (ADAMS) Accession No. ML14092A331.

Barstow, J. Letter from Exelon Generation Company, LLC, to the NRC, Exelon Generation Company, LLC, Seismic Hazard and Screening Report (Central and Eastern United States (CEUS) Sites), Response to NRC Request for Information Pursuant to 10 CFR 50.54(f) Regarding Recommendation 2.1 of the Near-Term Task Force Review of Insights from the Fukushima Dai-ichi Accident. Limerick Generating Station, Units 1 and 2. March 31, 2014a. ADAMS Accession No. ML14090A236.

Barstow, J. Letter from Exelon Generation Company, LLC, to the NRC, Exelon Generation Company, LLC, Seismic Hazard and Screening Report (Central and Eastern United States (CEUS) Sites), Response to NRC Request for Information Pursuant to 10 CFR 50.54(f) Regarding Recommendation 2.1 of the Near-Term Task Force Review of Insights from the Fukushima Dai-ichi Accident. Oyster Creek Nuclear Generating Station. March 31, 2014b. ADAMS Accession No. ML14090A241.

Barstow, J. Letter from Exelon Generation Company, LLC, to the NRC, Exelon Generation Company, LLC, Seismic Hazard and Screening Report (Central and Eastern United States (CEUS) Sites), Response to NRC Request for Information Pursuant to 10 CFR 50.54(f) Regarding Recommendation 2.1 of the Near-Term Task Force Review of Insights from the Fukushima Dai-ichi Accident. Peach Bottom Atomic Power Station, Units 2 and 3. March 31, 2014c. ADAMS Accession No. ML14090A247.

Barstow, J. Letter from Exelon Generation Company, LLC, to the NRC, Exelon Generation Company, LLC, Seismic Hazard and Screening Report (Central and Eastern United States (CEUS) Sites), Response to NRC Request for Information Pursuant to 10 CFR 50.54(f) Regarding Recommendation 2.1 of the Near-Term Task Force Review of Insights from the Fukushima Dai-ichi Accident. Three Mile Island Nuclear Station, Unit 1. March 31, 2014d. ADAMS Accession No. ML14090A271.

Batson, S.L. Letter from Duke Energy Carolinas, LLC, to the NRC, Seismic Hazard and Screening Report (CEUS Sites), Response to NRC Request for Information Pursuant to 10 CFR 50.54(f) Regarding Recommendations 2.1, 2.3, and 9.3 of the Near-Term Task Force Review of Insights from the Fukushima Dai-ichi Accident. March 31, 2014. ADAMS Accession No. ML14092A024.

Bauer, R.A., B.B. Curry, A.M. Graese, R.C. Vaiden, W.J. Su, and M.J. Hasek. "Geotechnical Properties of Selected Pleistocene, Silurian, and Ordovician Deposits of Northeastern Illinois." Illinois State Geological Survey, *Environmental Geology*. Vol. 139. 1991.

Bazzurro, P., and C.A. Cornell. "Nonlinear Soil-Site Effects in Probabilistic Seismic-Hazard Analysis." *Bulletin of the Seismological Society of America*. Vol. 94, Issue 6. pp. 2,110–2,123. 2004.

Bechtel Power Corporation. "Preliminary Engineering Report for Foundation Alternatives for the Large Pad Independent Fuel Storage Installation." Revision 00A. Prepared for Vogtle Electric Generating Plant, Units 1 and 2. Frederick, MD. 2011.

Browning, J. Letter from Entergy Operations, Inc., to the NRC, Seismic Hazard and Screening Report (CEUS Sites), Response to NRC Request for Information Pursuant to 10 CFR 50.54(f) Regarding Recommendation 2.1 of the Near-Term Task Force Review of Insights from the Fukushima Dai-ichi Accident. Arkansas Nuclear One, Units 1 and 2. March 2014. ADAMS Accession No. ML14092A021.

Burger, H. *Exploration Geophysics of the Shallow Subsurface*. Prentice Hall. Englewood Cliffs, NJ. 1992.

Cabas, A., and A. Rodriguez-Marek. " $V_S$ - $\kappa_0$  Correction Factors for Input Ground Motions Used in Seismic Site Response Analyses." *Earthquake Spectra*. Vol. 33, No. 3. pp. 917–941. August 2017.

Callaway Energy. "Callaway Energy Center Final Safety Analysis Report (FSAR)." Revision OL-20. December 2013.

Campbell, K.W. "Estimates of Shear-Wave Q and  $\kappa_0$  for Unconsolidated and Semiconsolidated Sediments in Eastern North America." *Bulletin of the Seismological Society of America*. Vol. 99, No. 4. pp. 2,365–2,392. August 2009.

Capps, S.D. Letter from Duke Energy Carolinas, LLC, to the NRC, Seismic Hazard and Screening Report (CEUS Sites), Response to NRC 10 CFR 50.54(f) Request for Information Pursuant to Title 10 of the Code of Federal Regulations 50.54(f) Regarding Recommendations 2.1, 2.3, and 9.3 of the Near-Term Task Force Review of Insights from the Fukushima Dai-ichi Accident. March 20, 2014. ADAMS Accession No. ML14098A421.

Chapman, M., and A. Conn. "A Model for  $L_g$  Propagation in the Gulf Coastal Plain of the Southern United States." *Bulletin of the Seismological Society of America*. Vol. 106, No. 2. pp. 349–363. 2016.

Chisum, M. Letter from Entergy Nuclear Operations Inc., to the NRC, Entergy Seismic Hazard and Screening Report (CEUS Sites), Response to NRC Request for Information Pursuant to 10 CFR 50.54(f) Regarding Recommendation 2.1 of the Near-Term Task Force Review of Insights from the Fukushima Dai-ichi Accident. Waterford Steam Electric Station, Unit 3. March 27, 2014. ADAMS Accession No. ML14086A427.

Clinton Power Station. "Updated Final Safety Analysis Report (UFSAR)." Revision 15. 2013. ADAMS Accession No. ML16306A066.

*Code of Federal Regulations* (CFR), "Domestic licensing of production and utilization facilities." Part 50, Chapter 1, Title 10, "Energy." Washington, DC. September 2019.

Conner, J.T. Letter from DTE Energy to NRC, Seismic Hazard and Screening Report, Response to NRC Request for Information Pursuant to 10 CFR 50.54(f) Regarding Recommendation 2.1 of the Near-Term Task Force Review of Insights from the Fukushima Dai-ichi Accident. March 31, 2014. ADAMS Accession No. ML14090A326.

Cortopassi, L. Letter from Omaha Public Power District to the NRC, Seismic Hazard and Screening Report (CEUS Sites), Response to NRC Request for Information Pursuant to 10 CFR 50.54(f) Regarding Recommendation 2.1 of the Near-Term Task Force Review of Insights from the Fukushima Dai-ichi Accident. March 31, 2014. ADAMS Accession No. ML14097A087.

Coyle, L.M. Letter from Entergy Nuclear Operations Inc., to the NRC, Entergy Seismic Hazard and Screening Report (CEUS Sites), Response to NRC Request for Information Pursuant to 10 CFR 50.54(f) Regarding Recommendation 2.1 of the Near-Term Task Force Review of Insights from the Fukushima Dai-ichi Accident. March 31, 2014. ADAMS Accession No. ML14090A243.

Davison, P.J. Letter from PSEG Nuclear LLC to the NRC, Seismic Hazard and Screening Report (CEUS Sites), Response to NRC Request for Information Pursuant to 10 CFR 50.54(f) Regarding Recommendation 2.1 of the Near-Term Task Force Review of Insights from the Fukushima Dai-ichi Accident. Hope Creek Generating Station. March 28, 2014. ADAMS Accession No. ML14087A436.

Davison, K. Letter from Northern States Power Company/Xcel Energy to the NRC, Seismic Hazard and Screening Report (CEUS Sites), Response to NRC Request for Information Pursuant to 10 CFR 50.54(f) Regarding Recommendation 2.1 of the Near-Term Task Force Review of Insights from the Fukushima Dai-ichi Accident. Prairie Island Nuclear Generating Plant, Units 1 and 2. March 27, 2014. ADAMS Accession No. ML14086A628.

Dent, J.A. Letter from Entergy Nuclear Operations, Inc., to the NRC, Entergy's Seismic Hazard and Screening Report (CEUS Sites), Response to NRC Request for Information Pursuant to 10 CFR 50.54(f) Regarding the Seismic Aspects of Recommendation 2.1 of the Near-Term Task Force Review of Insights from the Fukushima Dai-ichi Accident. Pilgrim Nuclear Power Station. March 31, 2014. ADAMS Accession No. ML14092A023.

Dominion Energy, Inc. "North Anna Unit 3 Combined License Application Final Safety Analysis Report, Rev. 7." December, 2013. ADAMS Accession No. ML14007A640.

Ells, G.D. "Stratigraphic Cross Sections Extending from Devonian Antrim Shale to Mississippian Sunbury Shale in the Michigan Basin: Topical Report." Geological Survey Report of Investigation 22. Michigan Department of Natural Resources, Geological Survey Division. 1979.

Entergy Operations Inc. "Arkansas Nuclear One—Unit 1, SAR Amendment 26." Docket No. 50-313. Russellville, AK. February 2014.

Entergy Nuclear Operations Inc. "Indian Point Energy Center (IPEC) Unit 3 Updated Final Safety Analysis Report (UFSAR)." Revision 4. 2011. ADAMS Accession No. ML16106A095.

Entergy Nuclear Operations Inc. "Pilgrim Nuclear Power Station Final Safety Analysis Report (Updated) (UFSAR)." Revision 27. 2009. ADAMS Accession No. ML16083A494.

Entergy Nuclear Operations Inc. "River Bend Station, Unit 3, Combined License Application, Part 2: Final Safety Analysis Report." September 2008. ADAMS Accession No. ML082830247.

Entergy Nuclear Operations Inc. "Grand Gulf Early Site Permit Application." Docket No. 52-009. Revision 2. October 2005. ADAMS Accession No. ML052780449 (package).

Electric Power Research Institute (EPRI). "EPRI Ground Motion Model Review Final Report." Palo Alto, CA. June 3, 2013. ADAMS Accession No. ML13155A553.

EPRI. "Seismic Evaluation Guidance, Screening, Prioritization and Implementation Details (SPID) for the Resolution of Fukushima Near-Term Task Force Recommendation 2.1: Seismic." EPRI Report 1025287. Palo Alto, CA. November 27, 2012. ADAMS Accession No. ML12333A170.

EPRI. "Program on Technology Innovation: Truncation of the Lognormal Distribution and Value of the Standard Deviation for Ground Motion Models in the Central and Eastern United States." EPRI Report 1013105, Technical Update. Palo Alto, CA. February 2006. ADAMS Accession No. ML061670087.

EPRI. "CEUS Ground Motion Project Final Report." EPRI Report 1009684. Palo Alto, CA. December 2004. ADAMS Accession No. ML050450305.

EPRI. "Guidelines for Determining Design Basis Ground Motions." EPRI TR-102293, Vols. 1-5. Palo Alto, CA. 1993.

EPRI. "Probabilistic Seismic Hazard Evaluations at Nuclear Plant Sites in the Central and Eastern United States: Resolution of the Charleston Earthquake Issue." Product ID NP-6395-D. Palo Alto, CA. 1989.

Exelon Generation Company. "Oyster Creek Nuclear Generating Station, Updated Final Safety Analysis Report (UFSAR), Revision 19, Fire Hazards Analysis Report (FHAR), Revision 18, and UFSAR and FHAR Reference Drawings." 2014a. ADAMS Accession No. ML15307A558 (package).

Exelon Generation Company. "Braidwood Station, Units 1 and 2, Updated Final Safety Analysis Report (UFSAR)." Revision 15. 2014b. ADAMS Accession No. ML14363A393 (package).

Exelon Generation Company. "Byron Station, Units 1 and 2, Updated Final Safety Analysis Report (UFSAR)." Revision 14. 2014c. ADAMS Accession No. ML13043A158.

Exelon Generation Company. "Limerick Generating Station, Units 1 and 2, Updated Final Safety Analysis Report (UFSAR), Revision 16 and UFSAR Reference Drawings." 2012a. ADAMS Accession No. ML16357A167.

Exelon Generation Company. "Peach Bottom Atomic Power Station, Units 2 and 3, Updated Final Safety Analysis Report (UFSAR)." Revision 24. April 30, 2012b. ADAMS Accession No. ML18193A773.

Exelon Generation Company. "Dresden Station, Units 2 and 3, Updated Final Safety Analysis Report (UFSAR)." Revision 10. 2011. ADAMS Accession No. ML11202A179.

Exelon Generation Company. "Early Site Permit Application for the Clinton ESP Site Safety Analysis Report." Revision 4. 2006. ADAMS Accession No. ML061100260 (package).

Fili, L. Letter from Xcel Energy to the NRC, Response to NRC Request for Information Pursuant to 10 CFR 50.54(f) Regarding Recommendation 2.1 of the Near-Term Task Force Review of Insights from the Fukushima Dai-ichi Accident. May 14, 2014. ADAMS Accession No. ML14136A288.

Flores, R. Letter from Luminant Power Company to the NRC, Comanche Peak Nuclear Power Plant, Docket Nos. 50-445 and 50-446, Seismic Hazard and Screening Report (CEUS Sites), Response to NRC Request for Information Pursuant to 10 CFR 50.54(f) Regarding Recommendation 2.1 of the Near-Term Task Force Review of Insights from the Fukushima Dai-ichi Accident. March 27, 2014. ADAMS Accession No. ML14099A197.

Gatlin, T.D. Letter from South Carolina Electric & Gas (SCE&G) to the NRC, Seismic Hazard and Screening Report (CEUS Sites), Response to NRC Request for Information Pursuant to 10 CFR 50.54(f) Regarding Recommendation 2.1 of the Near-Term Task Force Review of Insights from the Fukushima Dai-ichi Accident. March 26, 2014. ADAMS Accession No. ML14092A250.

Gideon, W.R. Letter from Duke Energy to the NRC, Seismic Hazard Evaluation, Response to the NRC Request for Information Pursuant to 10 CFR 50.54(f) Regarding Recommendations 2.1, 2.3, and 9.3 of the Near-Term Task Force Review of Insights from the Fukushima Dai-ichi Accident. H.B. Robinson Steam Electric Plant, Unit 2. March 31, 2014. ADAMS Accession No. ML14099A204.

Glover, R.M. Letter from Duke Energy to the NRC, Submittal of Revision to Seismic Hazard Evaluation to Include New Ground Motion Response Spectra (GMRS) Using New Geotechnical Data and Shear-Wave Testing for H.B. Robinson Steam Electric Plant, Unit 2. July 17, 2015. ADAMS Accession No. ML15201A006.

Grammer, G.M. "Summary of Research through Phase II/Year 2 of Initially Approved 3 Phase/3 Year Project—Establishing the Relationship between Fracture-Related Dolomite and Primary Rock Fabric on the Distribution of Reservoirs in the Michigan Basin." Department of Energy Technical Report DE-FC26-04NT15513. Western Michigan University, Department of Geosciences. Kalamazoo, MI. 2007.

GZA GeoEnvironmental, Inc. "Hydrogeologic Site Investigation Report." Indian Point Energy Center. Norwood, MA. 2008. ADAMS Accession No. ML12335A626.

Hamrick, G. Letter from Duke Energy to the NRC, Seismic Hazard and Screening Report (CEUS Sites), Response to NRC Request for Information Pursuant to 10 CFR 50.54(f) Regarding the Seismic Aspects of Recommendation 2.1 of the Near-Term Task Force Review of Insights from the Fukushima Dai-ichi Accident. March 31, 2014. ADAMS Accession No. ML14106A461.

Harris, M.T., J.J. Kuglitsch, R. Watkins, D.P. Hegrenes, and K.R. Waldhuetter. "Early Silurian Stratigraphic Sequences of Eastern Wisconsin." In: E. Landing and M.E. Johnson, eds., *Silurian Cycles: Linkages of Dynamic Stratigraphy with Atmospheric, Oceanic, and Tectonic Changes*. New York State Museum Bulletin 491. pp. 39–49. 1998.

Hart, D. "Mapping Bedrock: Verifying Depth to Bedrock in Calumet County Using Seismic Refraction." University of Wisconsin—Extension, Discovery Farms. 2011.

Hawk, J. "The Role of Geology and Engineering Properties of the Gettysburg Formation in the Geomorphic Form of the Susquehanna River at Highspire, Pennsylvania." Master's thesis. Eberly College of Arts and Science. West Virginia University. 2004.

Heacock, D.A. Letter from Dominion Nuclear Connecticut, Inc., to the NRC, Millstone Power Station, Units 2 and 3, Response to March 12 2012 Information Request, Seismic Hazard and Screening Report (CEUS Sites) for Recommendation 2.1. March 31, 2014a. ADAMS Accession No. ML14092A417.

Heacock, D.A. Letter from Virginia Electric and Power Company to the NRC, North Anna Power Station Units 1 and 2, Response to March 12, 2012 Information Request, Seismic Hazard and Screening Report (CEUS Sites) for Recommendation 2.1. March 31, 2014b. ADAMS Accession No. ML14092A416.

Heacock, D.A. Letter from Virginia Electric and Power Company to the NRC, Surry Power Station Units 1 and 2, Response to March 12, 2012, Information Request Seismic Hazard and Screening Report (CEUS Sites) for Recommendation 2.1. March 31, 2014c. ADAMS Accession No. ML14092A414.

Henderson, K. Letter from Duke Energy Carolina, LLC, to the NRC, Catawba Nuclear Station, Units 1 and 2, Seismic Hazard and Screening Report (CEUS Sites), Response to NRC Request for Additional Information Pursuant to 10 CFR 50.54(f) Regarding Recommendations 2.1, 2.3, and 9.3 of the Near-Term Task Force Review of Insights from the Fukushima Dai-ichi Accident. March 31, 2014. ADAMS Accession No. ML14093A052.

Jensen, J. Letter from Florida Power & Light Company to the NRC, Seismic Hazard and Screening Report (CEUS Sites), Response NRC Request for Information Pursuant to 10 CFR 50.54(f) Regarding Recommendation 2.1 of the Near-Term Task Force Review of Insights from the Fukushima Dai-ichi Accident. St. Lucie Nuclear Station, Units 1 and 2. March 31, 2014. ADAMS Accession No. ML14099A106.

Kaegi, G.T. Letter from Exelon Generation Company, LLC, to the NRC, Response to NRC Request for Information Pursuant to 10 CFR 50.54(f) Regarding Recommendation 2.1 of the Near-Term Task Force Review of Insights from the Fukushima Dai-ichi Accident. Braidwood Plant. March 31, 2014a. ADAMS Accession No. ML14091A243.

Kaegi, G. Letter from Exelon Generation Company, LLC, to the NRC, Seismic Hazard and Screening Report (CEUS Sites), Response to NRC Request for Information Pursuant to 10 CFR 50.54(f) Regarding Recommendation 2.1 of the Near-Term Task Force Review of Insights from the Fukushima Dai-ichi Accident. Byron Generating Station, Units 1 and 2. March 31, 2014b. ADAMS Accession No. ML14091A010.

Kaegi, G. Letter from Exelon Generation Company, LLC, to the NRC, Seismic Hazard and Screening Report (CEUS Sites), Response to NRC Request for Information Pursuant to 10 CFR 50.54(f) Regarding Recommendation 2.1 of the Near-Term Task Force Review of Insights from the Fukushima Dai-ichi Accident. Clinton Power Station. March 31, 2014c. ADAMS Accession No. ML14091A011.



Kaegi, G. Letter from Exelon Generation Company, LLC, to the NRC, Seismic Hazard and Screening Report (CEUS Sites), Response to NRC Request for Information Pursuant to 10 CFR 50.54(f) Regarding Recommendation 2.1 of the Near-Term Task Force Review of Insights from the Fukushima Dai-ichi Accident. Dresden Nuclear Power Station. March 31, 2014d. ADAMS Accession No. ML14091A012.

Kaegi, G. Letter from Exelon Generation Company, LLC, to the NRC, Response to NRC Request for Information Pursuant to 10 CFR 50.54(f) Regarding the Seismic Aspects of Recommendation 2.1 of the Near-Term Task Force Review of Insights from the Fukushima Dai-ichi Accident. LaSalle Plant. March 31, 2014e. ADAMS Accession No. ML14091A013.

Kaegi, G. Letter from Exelon Generation Company, LLC, to the NRC, Response to NRC Request for Information Pursuant to 10 CFR 50.54(f) Regarding Recommendation 2.1 of the Near-Term Task Force Review of Insights from the Fukushima Dai-ichi Accident. Quad Cities, Units 1 and 2. March 31, 2014f. ADAMS Accession No. ML14090A526.

Kapapoulos, E.J., Jr. Letter from Duke Energy Progress, Inc., Harris Nuclear Plant, to the NRC, Seismic Hazard and Screening Report (CEUS Sites), Response to NRC 10 CFR 50.54(f) Request for Information Pursuant to Title 10 of the Code of Federal Regulations 50.54(f) regarding Recommendations 2.1, 2.3, and 9.3 of the Near-Term Task Force Review of Insights from the Fukushima Dai-ichi Accident. March 27, 2014. ADAMS Accession No. ML14090A441.

Kaven, J.O., S.H. Hickman, A.F. McGarr, and W.L. Ellsworth. "Surface Monitoring of Microseismicity at Decatur, Illinois, CO<sub>2</sub> Sequestration Demonstration Site." *Seismological Research Letters*. Vol. 86, No. 4. pp. 1–6. 2015.

Kiley, M. Letter from Florida Power & Light Company to the NRC, Turkey Point Units 3 and 4, Seismic Hazard and Screening Report (CEUS Sites) Response to NRC Request for Information Pursuant to 10 CFR 50.54(f) Regarding the Seismic Aspects of Recommendation 2.1 of the Near-Term Task Force Review of Insights from the Fukushima Dai-ichi Accident. March 27, 2014. ADAMS Accession No. ML14106A032.

Korsnick, M. Letter from Constellation Energy Nuclear Group to the NRC, Seismic Hazard and Screening Report (CEUS Sites), Response to NRC Request for Information Pursuant to 10 CFR 50.54(f) Regarding Recommendation 2.1 of the Near-Term Task Force Review of Insights from the Fukushima Dai-ichi Accident. Attachment 1, Calvert Cliffs Nuclear Power Plant, Units 1 and 2. March 31, 2014a. ADAMS Accession No. ML14099A196.

Korsnick, M. Letter from Constellation Energy Nuclear Group to the NRC, Seismic Hazard and Screening Report (CEUS Sites), Response to NRC Request for Information Pursuant to 10 CFR 50.54(f) Regarding Recommendation 2.1 of the Near-Term Task Force Review of Insights from the Fukushima Dai-ichi Accident. Attachment 2. R.E. Ginna Nuclear Power Plant. March 31, 2014b. ADAMS Accession No. ML14099A196.

Korsnick, M. Letter from Constellation Energy Nuclear Group to the NRC, Seismic Hazard and Screening Report (CEUS Sites), Response to NRC Request for Information Pursuant to 10 CFR 50.54(f) Regarding Recommendation 2.1 of the Near-Term Task Force Review of Insights from the Fukushima Dai-ichi Accident. Attachment 3. Nine Mile Point Nuclear Station, Units 1 and 2. March 31, 2014c. ADAMS Accession No. ML14099A196.

Ktenidou, O.-J., N.A. Abrahamson, S. Drouet, and F. Cotton. "Understanding the Physics of Kappa ( $\kappa$ ): Insights from a Downhole Array." *Geophysical Journal International*. Vol. 203, Issue 1. pp. 678–691. 2015.

Laurendeau, A., F. Cotton, O.-J. Ktenidou, L.-F. Bonilla, and F. Hollender. "Rock and Stiff-Soil Site Amplification: Dependency on  $V_{S30}$  and Kappa ( $\kappa$ )." *Bulletin of the Seismological Society of America*. Vol. 103, Issue 6. pp. 3,131–3,148. 2013.

Lies, Q.S. Letter from Indiana Michigan Power to the NRC, Seismic Hazard and Screening Report (CEUS Sites), Response to NRC Request for Information Pursuant to 10 CFR 50.54(f) Regarding Recommendation 2.1 of the Near-Term Task Force Review of Insights from the Fukushima Dai-ichi Accident. March 27, 2014. ADAMS Accession No. ML14092A329.

Lilienthal, R.T. "Stratigraphic Cross-Sections of the Michigan Basin." Michigan Geological Survey Report of Investigations 19. Michigan Department of Environmental Quality, Geological and Land Management Division. 1978.

Limpas, O. Letter from Nebraska Public Power District to the NRC, Revision to Nebraska Public Power District's Response to NRC Request for Information Pursuant to 10 CFR 50.54(f) Regarding Recommendation 2.1 of the Near-Term Task Force Review of Insights from the Fukushima Dai-ichi Accident. February 11, 2015. ADAMS Accession No. ML15050A165.

Liu, E., J.H. Queen, and V.D. Cox. "Anisotropy and Attenuation of Crosshole Channel Waves from the Antrim Shale Gas Play, Michigan Basin." *Journal of Applied Geophysics*. Vol. 44, Issue 1. pp. 47–61. 2000.

Luczaj, J.A. "Geology of the Niagara Escarpment in Wisconsin." *Geoscience Wisconsin*. Vol. 22, Part 1. pp. 1–34. 2013.

Luminant Power. "Comanche Peak Nuclear Power Plant, Units 3 and 4." Docket Nos. 52-034 and 52-036. Final Safety Analysis Report (FSAR-3/4). Revision 7. October 2009.

Mashburn, W.F. Letter from Entergy Nuclear Operations Inc. to the NRC, Response to NRC Request for Information Pursuant to 10 CFR 50.54(f) Regarding Recommendation 2.1 of the Near-Term Task Force Review of Insights from the Fukushima Dai-ichi Accident. March 26, 2014. ADAMS Accession No. ML14091A426.

McCartney, E. Letter from NextEra Energy to the NRC, Response to NRC Request for Information Pursuant to 10 CFR 50.54(f) Regarding Recommendation 2.1 of the Near-Term Task Force Review of Insights from the Fukushima Dai-ichi Accident. March 31, 2014. ADAMS Accession No. ML14090A275.

Miller, R.D. "Geology of the Omaha–Council Bluffs Area, Nebraska–Iowa." U.S. Geological Survey Professional Paper 472. Government Printing Office. Washington, DC. 1964.

Millstein, R.L. "Subsurface Stratigraphy of Cambrian Rocks in the Southern Peninsula of Michigan: Michigan Basin." Bulletin #7. Michigan Department of Natural Resources. 1989.

Mooney, H.W., P.R. Farnham, S.H. Johnson, G. Volz, and C. Craddock. "Seismic Studies over the Midcontinent Gravity High in Minnesota and Northwestern Wisconsin." Report of Investigations 11. Minnesota Geological Survey. 1970.

Moos, D., and M.D. Zoback. "In Situ Studies of Velocity in Fractured Crystalline Rocks." *Journal of Geophysical Research*. Vol. 88, No. B3. pp. 2,345–2,358. 1983.

Morey, G.B. "Revised Keweenawan Subsurface Stratigraphy, Southeastern Minnesota." Report of Investigations 16. Minnesota Geological Survey. 1977.

Mossler, J.H. "Paleozoic Stratigraphic Nomenclature for Minnesota." Report of Investigations 65. Minnesota Geological Survey. 2008.

Mulligan, K. Letter from Entergy Nuclear Operations Inc. to the NRC, Response to NRC Request for Information Pursuant to 10 CFR 50.54(f) Regarding Recommendation 2.1 of the Near-Term Task Force Review of Insights from the Fukushima Dai-ichi Accident. March 31, 2014. ADAMS Accession Nos. ML14090A098.

Neterer, D. Letter from Ameren Missouri to Marc Dapas, NRC, Transmittal of Seismic Hazard and Screening Report (CEUS Sites). March 28, 2014. ADAMS Accession No. ML14090A448.

NextEra Energy Seabrook, LLC. "Seabrook Station Updated Final Safety Analysis Report, Rev. 16. 2014. ADAMS Accession No. ML14317A481.

Nolte, K.A. "Monitoring Induced Seismicity near the Wellington Oil Field, South Central Kansas." Unpublished master's thesis. University of Kansas. Lawrence, KS. 2017.

Northern States Power Company. "Monticello Nuclear Generating Plant Updated Safety Analysis Report (USAR)." Revision 22. 2005.

U.S. Nuclear Regulatory Commission (NRC). "Design Response Spectra for Seismic Design of Nuclear Power Plants." Regulatory Guide 1.60. Revision 2. Washington, DC. July 2014. ADAMS Accession No. ML13210A432.

NRC. Letter from Eric J. Leeds, Director, Office of Nuclear Reactor Regulation, and Michael R. Johnson, Director, Office of New Reactors, to All Power Reactor Licensees and Holders of Construction Permits in Active or Deferred Status, Request for Information Pursuant to Title 10 of the *Code of Federal Regulations* 50.54(f) Regarding Recommendations 2.1, 2.3, and 9.3, of the Near-Term Task Force Review of Insights from the Fukushima Dai-ichi Accident. Washington, DC. March 12, 2012a. ADAMS Accession No. ML12053A340.

NRC. "Central and Eastern United States Seismic Source Characterization for Nuclear Facilities." NUREG-2115. Washington, DC. January 2012b.

NRC. "Technical Basis for Revision of Regulatory Guidance on Design Ground Motions: Hazard- and Risk-Consistent Ground Motion Spectra Guidelines." NUREG/CR-6728. McGuire, R.K., W.J. Silva, and C. Costantino. Washington, DC. October 2001. ADAMS Accession No. ML013100232.

Ogwari, P.O., S.P. Horton, and S. Ausbrooks. "Characteristics of Induced/Triggered Earthquakes During the Startup Phase of the Guy-Greenbrier Earthquake Sequence in North-Central Arkansas." *Seismological Research Letters*. Vol. 87, No. 3. pp. 620–630. 2016.

Perry, J. Letter from PSEG Nuclear LLC to the NRC, PSEG Nuclear LLC's Seismic Hazard and Screening Report (CEUS Sites), Response to NRC Request for Information Pursuant to 10 CFR 50.54(f) Regarding Recommendation 2.1 of the Near-Term Task Force Review of Insights from the Fukushima Dai-ichi Accident—Salem Generating Station. March 28, 2014. ADAMS Accession No. ML14090A043.

Pierce, C. Letter from Southern Nuclear Operating Company, Inc., to the NRC, Seismic Hazard and Screening Report for CEUS Sites. Joseph M. Farley Nuclear Plant, Units 1 and 2. March 31, 2014a. ADAMS Accession No. ML14092A020.

Pierce, C. Letter from Southern Nuclear Operating Company, Inc., to the NRC, Edwin I. Hatch Nuclear Plant, Units 1 and 2, Seismic Hazard and Screening Report for CEUS Sites. March 31, 2014b. ADAMS Accession No. ML14092A017.

Pierce, C. Letter from Southern Nuclear Operating Company, Inc., to the NRC, Vogtle Electric Generating Plant, Units 1 and 2, Seismic Hazard and Screening Report for CEUS Sites. March 31, 2014c. ADAMS Accession No. ML14092A019.

PNNL. "Hanford Sitewide Probabilistic Seismic Hazard Analysis." PNNL-23361. Richland, WA. 2014.

Point Beach Nuclear Plant. Point Beach Letter VPNPD-95-056, "Generic Letter 88-20, Supplement 4 Summary Report on Individual Plant Examination of External Events for Severe Accident Vulnerabilities," June 30, 1995.

Powell, G.T. Letter from South Texas Project Nuclear Operating Company to the NRC, Response to NRC Request for Information Pursuant to 10 CFR 50.54(f) Regarding Recommendation 2.1 of the Near-Term Task Force Review of Insights from the Fukushima Dai-ichi Accident. March 31, 2014. ADAMS Accession No. ML14099A235.

Progress Energy. "Shearon Harris Nuclear Power Plant Updated Final Safety Analysis Report." Amendment No. 59. 2014.

Progress Energy. "Shearon Harris Nuclear Power Plant Units 2 and 3 COL Application Part 2, Final Safety Analysis Report." Revision 4. 2012. ADAMS Accession No. ML12122A656.

PSEG Power, LLC. "Site Safety Analysis Report." PSEG Site Early Site Permit Application. Revision 2. March 27, 2013. ADAMS Accession No. ML13098A775 (package).

Rausch, T.S. Letter from PPL Susquehanna, LLC, to the NRC, Susquehanna Steam Electric Station Seismic Hazard and Screening Report (CEUS Sites), Response to NRC Request for Information Pursuant to 10 CFR 50.54(f) Regarding Recommendation 2.1 of the Near-Term Task Force Review of Insights from the Fukushima Dai-ichi Accident. March 31, 2014. ADAMS Accession No. ML14086A163.

Rodriguez-Marek, A., E.M. Rathje, J.J. Bommer, F. Scherbaum, and P.J. Stafford. "Application of Single-Station Sigma and Site-Response Characterization in a Probabilistic Seismic-Hazard Analysis for a New Nuclear Site." *Bulletin of the Seismological Society of America*. Vol. 104, Issue 4. pp. 1,601–1,619. 2014.

South Carolina Electric & Gas (SCE&G). "Virgil C. Summer Nuclear Station Units 2 & 3 Final Safety Analysis Report (Updated)." Revision 2. 2010. ADAMS Accession No. ML100360598 (Package).

Sena, P. Letter from FirstEnergy Nuclear Operating Company to the NRC, Beaver Valley Power Station, Units 1 and 2, Seismic Hazard and Screening Report (CEUS Sites), Response to NRC Request for Information Pursuant to 10 CFR 50.54(f) Regarding Recommendation 2.1 of the Near-Term Task Force Review of Insights from the Fukushima Dai-ichi Accident. March 31, 2014a. ADAMS Accession Nos. ML14092A203, ML14090A144, and ML14090A146.

Sena, P. Letter from FirstEnergy Nuclear Operating Company to the NRC, Seismic Hazard and Screening Report (CEUS Sites), Response to NRC Request for Information Pursuant to 10 CFR 50.54(f) Regarding Recommendation 2.1 of the Near-Term Task Force Review of Insights from the Fukushima Dai-ichi Accident. Davis Besse Nuclear Power Station. March 31, 2014b. ADAMS Accession Nos. ML14092A203 and ML14090A148.

Sena, P. Letter from FirstEnergy Nuclear Operating Company to the NRC, Seismic Hazard and Screening Report (CEUS Sites), Response to NRC Request for Information Pursuant to 10 CFR 50.54(f) Regarding Recommendation 2.1 of the Near-Term Task Force Review of Insights from the Fukushima Dai-ichi Accident. Perry Nuclear Power Plant. March 31, 2014c. ADAMS Accession Nos. ML14092A203 and ML14090A145.

Shea, J.W. Letter from Tennessee Valley Authority to the NRC, Tennessee Valley Authority's Seismic Hazard and Screening Report (CEUS Sites), Response to NRC Request for Information Pursuant to 10 CFR 50.54(f) Regarding Recommendation 2.1 of the Near-Term Task Force Review of Insights from the Fukushima Dai-ichi Accident." March 31, 2014. ADAMS Accession No. ML14098A478.

Silva, W.J., N. Abrahamson, G. Toro, and C. Costantino. "Description and Validation of the Stochastic Ground Motion Model." Report by Pacific Engineering and Analysis submitted to Brookhaven National Laboratory, Associated Universities, Inc. Contract No. 770573. Upton, NY. 1996.

Smith, R. Letter from Wolf Creek Nuclear Operating Corporation to the NRC, Seismic Hazard and Screening Report (CEUS Sites), Response to NRC Request for Information Pursuant to 10 CFR 50.54(f) Regarding Recommendation 2.1 of the Near-Term Task Force Review of Insights from the Fukushima Dai-ichi Accident. March 31, 2014. ADAMS Accession No. ML14097A020.

Southern Nuclear Operating Company. "Updated Final Safety Analysis Report, Units 1 and 2 (UFSAR)." Revision 19. Vogtle Electric Generating Plant. Birmingham, AL. 2014.

Southern Nuclear Operating Company. "Vogtle Electric Generating Plant Units 3 and 4 Updated Final Safety Analysis Report." Revision 2. Birmingham, AL. 2013.

South Texas Project Nuclear Operating Company (STP). "South Texas Project, Units 3 and 4 Final Safety Analysis Report (FSAR)." Revision 11. 2014. ADAMS Accession No. ML14307B516 (package).

Stewart, J.P., K. Afshari, and C.A. Goulet. "Non-ergodic Site Response in Seismic Hazard Analysis." *Earthquake Spectra*. Vol. 33, Issue 4. pp. 1,385–1,414. 2017.

Tectonic Engineering Consultants. "Geotechnical Investigation Report for Modification to Fuel Storage Building, Indian Point Unit 2." Report to Entergy Nuclear Northeast. 2004.

Tennessee Valley Authority (TVA). "Bellefonte Nuclear Plant Units 3 & 4, COL Application, Part 2, Final Safety Analysis Report." Revision 3. December 22, 2010. ADAMS Accession No. ML110040897 (package).

Toro, G. "Probabilistic Models of the Site Velocity Profiles for Generic and Site-Specific Ground-Motion Amplification Studies." Technical Report No. 779574. Brookhaven National Laboratory. Upton, NY. 1995.

UniStar Nuclear Services. "Bell Bend Nuclear Power Project Final Safety Analysis Report." Baltimore, MD. 2013.

UniStar Nuclear Services. "Final Safety Analysis Report (FSAR) of the Nine Mile Point Unit 3 Combined License Application." Revision 1. Section 2.5, "Geology, Seismology, and Geotechnical Engineering." Baltimore, MD. 2009a.

UniStar Nuclear Services. "FSAR: Section 2.5.2, Callaway Plant Unit 2." Revision 2. Baltimore, MD. 2009b. ADAMS Accession No. ML090710349.

Ventosa, J.A. Letter from Entergy Nuclear Northeast to the NRC, Entergy Seismic Hazard and Screening Report (CEUS Sites), Response to NRC Request for Information Pursuant to 10 CFR 50.54(f) Regarding Recommendation 2.1 of the Near-Term Task Force Review of Insights from the Fukushima Dai-ichi Accident. Indian Point Nuclear Generating Unit 2. March 31, 2014. ADAMS Accession Nos. ML14099A110 and ML14099A111.

Vitale, A.J. Letter from Entergy Nuclear Operations Inc. to the NRC, Response to NRC Request for Information Pursuant to 10 CFR 50.54(f) Regarding the Seismic Aspects of Recommendation 2.1 of the Near-Term Task Force Review of Insights from the Fukushima Dai-ichi Accident. March 31, 2014. ADAMS Accession No. ML14090A069.

Vucetic, M., and R. Dobry. "Effects of Soils Plasticity on Cyclic Response." *Journal of Geotechnical Engineering*. American Society of Civil Engineers. Vol. 117, No. 1. pp. 1–19. 1991.

Walsh, K. Letter from NextEra Energy Seabrook, LLC, to the NRC, NextEra Energy Seabrook, LLC, Seismic Hazard and Screening Report (CEUS Sites), Response to NRC Request for Information Pursuant to 10 CFR 50.54(f) Regarding Recommendation 2.1 of the Near-Term Task Force Review of Insights from the Fukushima Dai-ichi Accident. March 31, 2014. ADAMS Accession No. ML14092A413.

Wheeler, R.L. "Methods of  $M_{max}$  Estimation East of the Rocky Mountains." USGS Open-File Report 2009–1018. U.S. Geological Survey. Reston, VA. 2009.

Wolf Creek Nuclear Operating Corporation. "Wolf Creek Updated Safety Analysis Report (USAR), Revision 26." March 2013.

Yezerki, D.J., and I. Cemen. "Structural Geology of the Frontal Ouachita-Arkoma Basin Transition Zone in Western Arkansas." *Search and Discovery*. Article No. 51022. 2014.

## 3 WESTERN UNITED STATES SITES

### 3.1. Background

As described more fully in Section 1 of this report, on March 12, 2012, the U.S. Nuclear Regulatory Commission (NRC) issued a request for information to all power reactor licensees and holders of construction permits (NRC, 2012a) to provide updated seismic hazard assessments. This letter issued under Title 10 of the *Code of Federal Regulations* (10 CFR) 50.54(f) [50.54(f) letter] specified that licensees in the western United States (WUS) use the Senior Seismic Hazard Analysis Committee (SSHAC) Level 3 process to develop the seismic source characterization (SSC) and ground motion characterization (GMC) models as inputs to updates to site-specific probabilistic seismic hazard analysis (PSHAs). These site-specific SSHAC Level 3 studies were necessary for the WUS sites because these sites could not use the updated regional GMC models in the Electric Power Research Institute's (EPRI's) "Ground Motion Model Review Final Report," dated June 3, 2013 (EPRI, 2013), or the SSC models in NUREG-2115, "Central and Eastern United States Seismic Source Characterization for Nuclear Facilities," issued January 2012 (NRC, 2012b), which licensees in the central and eastern United States (CEUS) use.

#### 3.1.1. Overview of Senior Seismic Hazard Analysis Committee Level 3 Studies

The NRC's 50.54(f) letter specified that each of the four nuclear power stations in the WUS (Figure 3.1-1) develop updated SSHAC Level 3 studies. These nuclear power plants (NPPs) are the following:

- (1) Palo Verde Nuclear Generating Station (PVNGS) located outside Phoenix, AZ, and operated by Arizona Public Service (APS)
- (2) Diablo Canyon Power Plant (DCPP) located in San Luis County, CA, and operated by Pacific Gas & Electric Company (PG&E)
- (3) Columbia Generating Station (CGS) located on the U.S. Department of Energy (DOE) Hanford Site outside Richland, WA, and operated by Energy Northwest
- (4) San Onofre Nuclear Generating Station located south of San Clemente, CA, and operated by Southern California Edison

However, in June 2013, Southern California Edison notified the NRC that it had permanently ceased operation of Units 2 and 3 at San Onofre. The NRC staff subsequently verified San Onofre's intent to decommission and determined that it was therefore exempt from the 50.54(f) letter. Thus, while San Onofre initiated a SSHAC Level 3 study and held several SSHAC workshops, the SSHAC Level 3 study was terminated in 2013, before its completion.

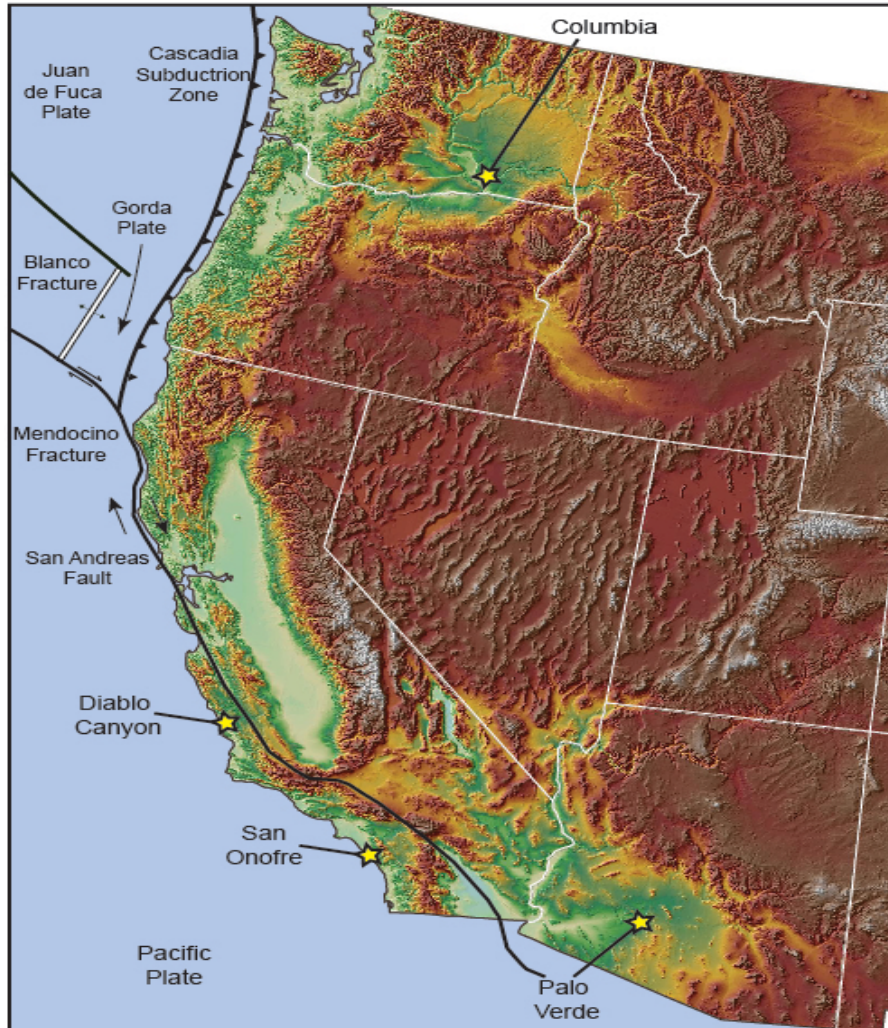


**Figure 3.1-1 Digital Elevation Model of the Western United States Showing the Location of the Plant Sites Relative to the Major Tectonic Features of Western North America. The Base Digital Elevation Model is Derived from the USGS National Elevation Dataset**

The three sites conducted SSHAC Level 3 studies using the guidelines in NUREG/CR-6372, "Recommendations for Probabilistic Seismic Hazard Analysis: Guidance on Uncertainty and Use of Experts," issued April 1997 (NRC, 1997), and NUREG-2117, "Practical Implementation Guidelines for SSHAC Level 3 and 4 Hazard Studies (Revision 2)," issued April 2012 (NRC, 2012c). Although the SSHAC Level 3 studies were completed as site-specific studies, it is important to note that two aspects of the studies incorporated characteristics of regional SSHAC studies. For the CGS PSHA, the SSC and GMC models were developed for the entire Hanford Site as part of a SSHAC study cosponsored by the DOE and Energy Northwest. Results from the Hanford SSC and GMC models were then used to develop site-specific reference-rock hazard results for various Hanford facility sites, including CGS. Energy Northwest then developed its own site response analyses to compute hazard results at the control point elevation of the site. DCP and PVNGS used a single GMC model developed from a SSHAC study cosponsored by PG&E and APS called the southwestern United States (SWUS) GMC



model. The SWUS GMC model was then adjusted using site-specific ground motion parameters to develop reference hazard curves at the specified reference horizons for both PVNGS and DCP. APS and PG&E subsequently conducted their own site response analysis to compute the control point hazard curves for their respective power plant sites.

Each of the WUS SSHAC studies followed the same general process. The Technical Integration Team (TI Team) developed a project plan, organized a project database, and held a series of three workshops to discuss applicable data, models, and methods. The TI Teams, led by a project technical integrator, developed the SSC and GMC models and were responsible for complete documentation of the results. The TI Team members served as both evaluator and integrator experts during the SSHAC process. An important part of a SSHAC Level 3 process is the Participatory Peer Review Panel (PPRP), which provides active review and feedback to the TI Teams throughout the study. The PPRP attended workshops and working meetings, reviewed work products, and provided input to the TI Teams throughout SSC and GMC model development.

The first workshop focused on the compilation and development of the data needed to support the SSC and GMC models, including presentations by resource experts from the larger technical community. The second workshop focused on evaluation of data, models, and methods, and consideration of alternative models. The alternative models were derived from work of the larger technical community and were described by (and advocated for) at Workshop 2 by proponent experts. The TI Team then developed preliminary models and performed initial hazard calculations and sensitivity analyses for presentation and discussion at the third workshop. Following Workshop 3, the TI Teams adjusted the preliminary models based on feedback from the PPRP, computed the final hazard calculations and sensitivity analyses, and documented the results in the final project report. The PPRP also provided a formal review of the resulting final report and issued a closure letter confirming its review. The NRC staff attended and observed all workshops.

### **3.1.2. Conduct of the NRC Staff Review**

The NRC staff, with contract support from the Center for Nuclear Waste Regulatory Analyses (CNWRA®) at Southwest Research Institute® (SwRI®) (hereafter referred to collectively as “the NRC staff”) reviewed the WUS submittals. For each of the three WUS sites, the review teams included geologists, seismologists, geotechnical engineers, and project managers.

As noted in Section 1.3 of this report, the overall purpose of this NUREG/KM is to capture the information used for and knowledge gained by the NRC staff in its reviews of the PSHA results for all U.S. NPPs following the accident at the Fukushima Dai-ichi NPP in Japan. However, the NRC staff’s review of the three Seismic Hazard and Screening Reports (SHSRs) for the WUS plants and associated SSHAC studies differed from the approach taken by the staff reviewing the CEUS seismic reevaluations. For the CEUS, the licensees and the NRC staff relied on the existing regional SSHAC studies for SSC (NRC, 2012b) and GMC models (EPRI, 2013). Because these regional models were already developed and endorsed, the NRC staff’s efforts focused on the site-specific site response analyses. Moreover, for the CEUS sites, the NRC staff was tasked to complete its reviews within a compressed timeline. As a result, the NRC staff developed a review strategy in which, before the licensee submittals, the staff gathered and evaluated as much publicly available site data as possible and then used that site data to construct preliminary site response analyses. The NRC staff then refined these preliminary site response analyses as new and more comprehensive site information was developed or as the licensees provided new information in the SHSRs. This strategy greatly accelerated the NRC

staff's reviews because preliminary hazard results were available to the NRC staff as the SHSRs were submitted. Thus, and as described in Section 2 of this report, the knowledge capture of the NRC staff's CEUS reviews is mostly in reference to the geological, geophysical, and geotechnical information gathered by the NRC staff to support its site response analyses reviews and on the NRC staff's accomplishments in developing and refining its independent site response analyses for the CEUS plants.

In contrast to the CEUS, each of the WUS plants conducted new PSHA studies that included new site-specific SSC and GMC models and new site-specific site response analyses. For the WUS sites, the NRC staff reviewed the SSHAC Level 3 studies used to develop the SSC and GMC models, the resulting reference point hazards, the site-specific site response analyses, and the final control point hazards. Because of these differences, the information and knowledge captured in this section of this report differ from that in Section 2 and instead documents the overall NRC staff's review of the WUS SHSRs, emphasizing how the NRC staff identified and evaluated the most significant contributors to the resulting seismic hazards. Because these reviews entailed a comprehensive evaluation of each WUS site-specific PSHA, this section of this report contains a more thorough summary of the NRC staff's work. For reference, the staff assessments for PVNGS (NRC, 2016a), CGS (NRC, 2016b), and DCCP (NRC, 2016c) document a complete description of the NRC staff reviews.

The NRC staff conducted the WUS reviews in a hierarchical fashion. First, the NRC staff observed and assessed the appropriateness of the licensees' respective SSHAC processes by attending the workshop series and evaluating whether the licensees properly followed the SSHAC process as described in NUREG/CR-6372 (NRC, 1997), NUREG-2117 (NRC, 2012c), and NUREG-2213, "Updated Implementation Guidelines for SSHAC Hazard Studies," issued October 2018 (NRC, 2018). The NRC staff also reviewed the correspondence between the PPRP and the various SSHAC project teams, focusing on how the SSHAC teams and licensees responded to PPRP comments and recommendations. The NRC staff's review ensured that (1) the SSHAC documentation was sufficiently complete and transparent to accurately document the study, (2) all technical decisions used to evaluate the data, models, and methods included an adequate technical basis, (3) a reasonable range of resource and proponent experts were engaged in the SSHAC workshops to provide a broad range of alternative data, models, and methods, and (4) the resulting SSC and GMC models captured the center, body, and range of the technically defensible interpretations.

Second, the staff evaluated the data, models, and methods various SSHAC TI Teams used for the SSC and GMC models. This aspect of the evaluation followed a standard technical review based on (1) review procedures and acceptance criteria in industry and NRC guidance (e.g., American National Standards Institute (ANSI)/American Nuclear Society (ANS) Standard ANSI/ANS-2.29-2008, "Probabilistic Seismic Hazard Analysis"; NUREG/CR-6728, "Technical Basis for Revision of Regulatory Guidance on Design Ground Motions: Hazard- and Risk-consistent Ground Motion Spectra Guidelines," issued October 2001 (NRC, 2001); and Regulatory Guide (RG) 1.208, "A Performance-Based Approach to Define the Site-Specific Earthquake Ground Motion" (NRC, 2007), (2) scientific and engineering judgment, (3) previously reviewed seismic studies, and (4) peer-reviewed scientific and engineering literature. Through this review, the NRC staff determined that the data, models, and methods used to develop the SSHAC studies were reasonable and consistent with state of scientific and engineering practice.

Third, as needed, the NRC staff developed confirmatory analyses to corroborate select aspects of the SSC and GMC models and the site response analyses. Examples of these confirmatory analyses include verification of fault slip rates, sensitivity of alternative fault geometries,

evaluation of uncertainty in near-surface attenuation, and comparison of alternative regional attenuation models. As part of these confirmatory analyses, the NRC staff performed PSHA calculations to evaluate and verify the PSHA results and to identify which aspects of the SSC and GMC models were the dominant contributors to the final hazard results, including their associated uncertainties.

Fourth, the NRC staff performed independent analyses to critically assess the most hazard-sensitive parameters or alternative interpretations of geological, geophysical, or seismic information, including those technical aspects of the seismic hazard analyses that had been the focus of additional scrutiny by external stakeholders. Results from these independent analyses provide additional regulatory assurance that the licensees' results accounted for all viable interpretations of the existing data, models, and methods and thus are reasonably representative of the site seismic hazard conditions necessary to develop robust and reliable PSHA results.

### **3.2. Palo Verde Nuclear Generating Station**

The PVNGS site is located on a 1,600-hectare [4,000-acre] site in western Arizona, approximately 72 kilometers (km) [45 miles (mi)] west of Phoenix, AZ (Figure 3.2-1). It consists of three pressurized-water reactors, each with an original capacity to produce 1.27 gigawatts of electric power. APS (hereafter referred to as "the licensee" in this subsection) operates the plant, which is owned by a collection of utilities, including APS, the Salt River Project, El Paso Electric Company, Southern California Edison, Public Service Company of New Mexico, the Southern California Public Power Authority, and the Los Angeles Department of Water and Power.

The PVNGS site resides within a relatively flat intermountain valley, called the Tonopah Desert Valley, within the southern Basin and Range (SBR) physiographic province of the Sonoran Desert (Figure 3.2-2). This valley is cut by surface drainages that flow southward toward the Gila River. During the last several million years, surrounding drainages transported clastic sediments (i.e., clay, sand, and gravel) into the Tonopah Desert Valley to form an alluvial deposit that is about 130 meters (m) [425 feet (ft)] thick beneath the PVNGS site.

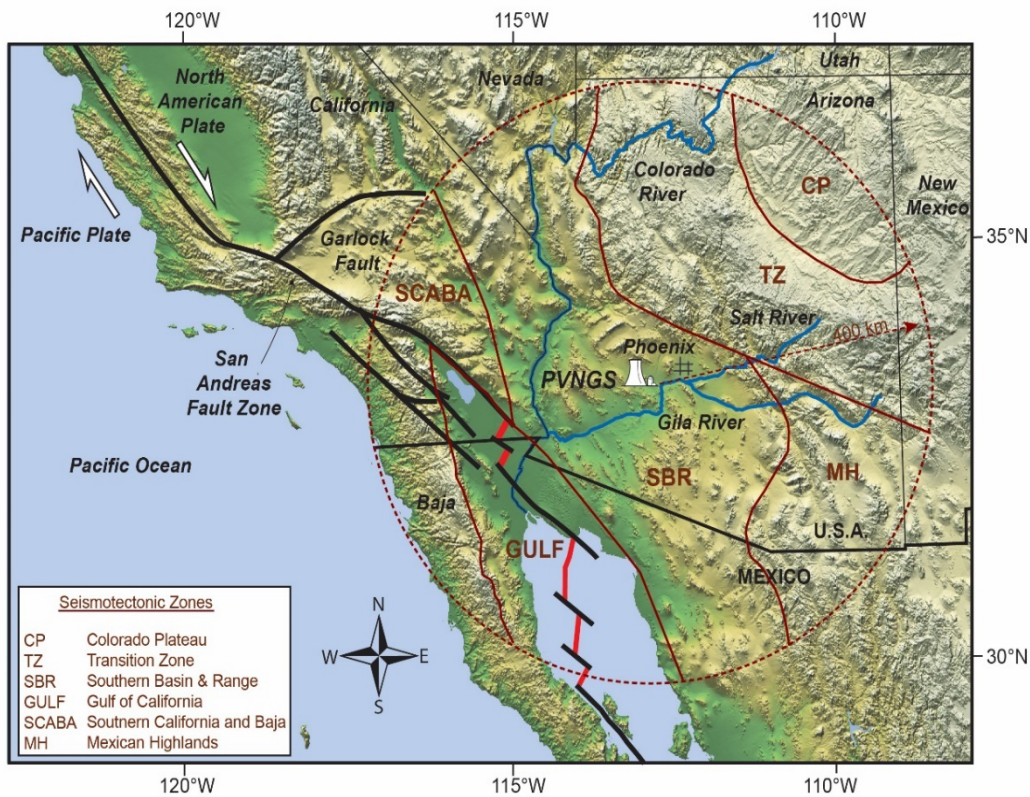


**Figure 3.2-1 Digital Topographic Map of Northern Mexico (Including the Northern Baja Peninsula and the Northern Gulf of California), Western Arizona, and Southern California Showing the Location of the PVNGS Relative to Geographic and Tectonic Features. The Base Digital Elevation Model is Derived from the USGS National Elevation Dataset**

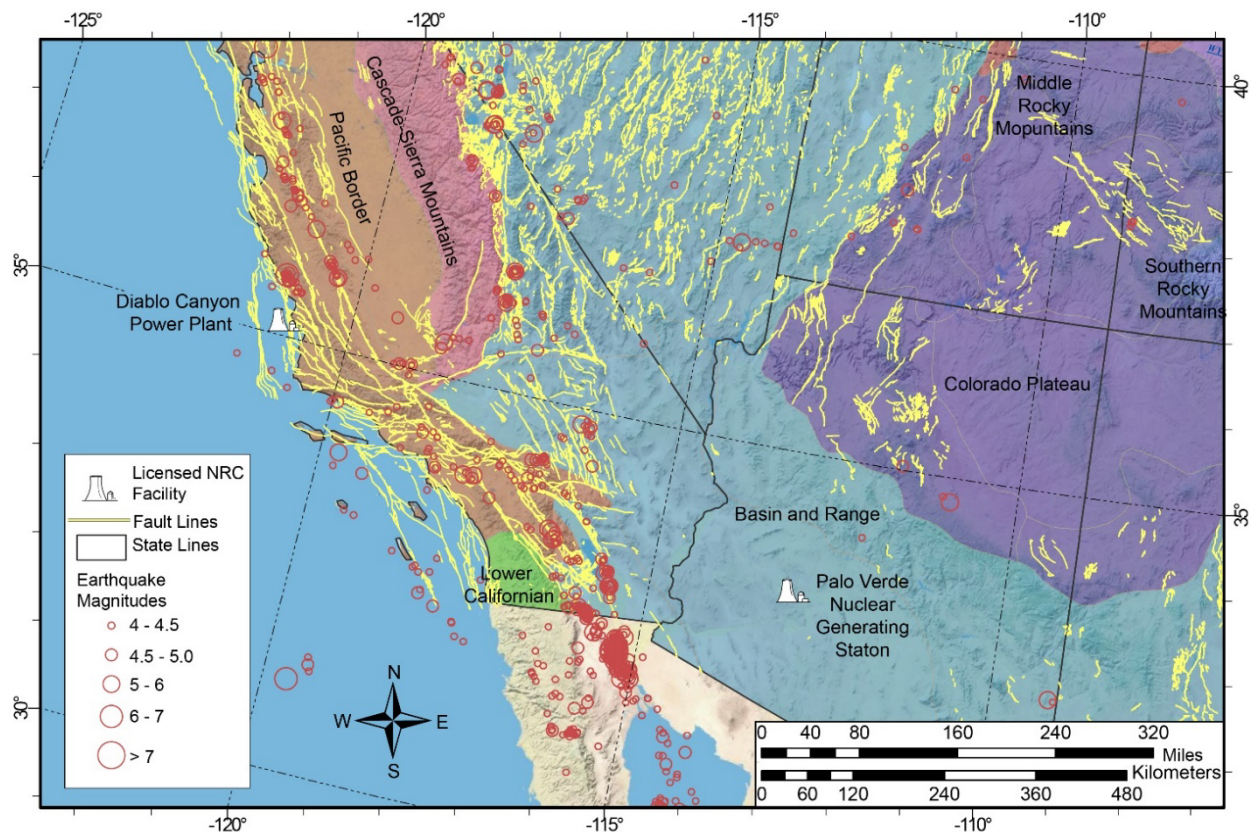


**Figure 3.2-2 Map of the United States Southwest Showing the Distribution of Earthquakes Relative to Physiographic Provinces, Quaternary Faults, and Other Tectonic Features. The Earthquake Epicenters are from the U.S. Geological Survey (USGS) Advanced National Seismic System Catalog, Spanning the Period 1900–2018**

This alluvial section rests above a thicker 235-m [770-ft] thick section of older volcanic rocks and interbedded sediments deposited about 15–20 million years ago (Ma)<sup>1</sup>. Crystalline basement (i.e., Precambrian<sup>2</sup> granitic and metamorphic rocks) is located about 365 m [1,200 ft] beneath the PVNGS site (APS, 2013).

For operating reactors licensed before 1997, the Safe Shutdown Earthquake (SSE) is the plant licensing-basis earthquake and is characterized by a peak ground acceleration (PGA) value that anchors a standardized response spectrum at high frequencies (i.e., typically at 20 to 33 Hertz (Hz) for the existing fleet of NPPs); response spectra shapes that depict the amplified response at all frequencies below the PGA; and a control point location where the SSE is defined. For the PVNGS, the SSE is defined as an RG 1.60, “Design Response Spectra for Seismic Design of Nuclear Power Plants,” issued October 1973 (U.S. Atomic Energy Agency, 1973), design spectral response curve anchored to a PGA of 0.20g. The control point for the SSE is located at the plant grade foundation level for all units, which is 290 m [950 ft] above mean sea level.

<sup>1</sup> Ma stands for *mega annum* and is a million years. It is used to designate a point in time from the present.  
<sup>2</sup> The Precambrian period is all geologic time before 570 Ma.

### 3.2.1. Seismotectonic and Geologic Setting

The PVNGS region can be subdivided into four physiographic provinces. From east to west, these provinces are the Colorado Plateau, Basin and Range, Pacific Border, and Lower California. These physiographic provinces are further subdivided into five seismotectonic regions based on the unique geologic and geophysical characteristics that control the origin, magnitude, ground motion attenuation, and fault rupture style of the seismic hazard. These five seismotectonic provinces, shown in Figure 3.2-1, are the (1) Colorado Plateau, (2) Transition Zone between the Colorado Plateau and the Basin and Range, (3) SBR, (4) Southern California and Northern Baja Transform, and (5) Gulf of California.

The PVNGS is situated within the SBR. Historic earthquakes within the SBR are small to moderate in magnitude and relatively infrequent. They mainly occur as extensional events on normal faults within a higher heat flow and attenuated crust. There are few faults exposed in the SBR that are Quaternary<sup>3</sup> or younger. Only a few geologic slip-rates are published for faults in the SBR. These rates indicate that normal faults are characterized by very slow slip rates and long recurrence intervals (Pearthree et al., 1983). The SBR faults typically show normal displacements, but some faults with reverse and strike-slip fault displacements also occur in the SBR. The adjacent tectonic provinces experienced moderately greater faulting activity during the Quaternary and typically have higher slip rates, shorter recurrence intervals, and larger magnitude historic earthquakes. Earthquakes originating in the Colorado Plateau or Transition Zone (TZ) also consist of relatively infrequent and small-magnitude events within an over-thickened and relatively cold crystalline crust. Seismicity within the SBR, Colorado Plateau, and TZ is generally not associated with known faults.

The nearest fault to the PVNGS site that shows any evidence of movement in the last 2.6 million years is the Sand Tank fault, which is located about 60 km [37 mi] south-southwest of the site. Based on the fault characterization framework of dePolo and Anderson (2000), the slip-rate estimated for the Sand Tank fault is on the order of 0.001 millimeter/year (mm/yr) [0.0004 inches/year (in/yr)] or less. There are other mapped faults closer to the site; however, there is no geologic evidence for Quaternary activity on these faults.

In contrast to the low-to-moderate seismic activity in the SBR, Colorado Plateau, and TZ, the physiographic provinces of Southern California and Northern Baja Transform and Gulf of California are characterized by quite frequent moderate-to-large-magnitude strike-slip earthquakes on the San Andreas plate boundary system, including the San Andreas, Elsinore, and San Jacinto fault zones. Frequent earthquakes of moderate to larger magnitude also occur on normal and transform faults within the incipient spreading ridge and within the transform fault system of the Gulf of California. Major seismogenic structures within the transform fault system include the Cerro Prieto, Laguna Salada, and Imperial faults (Figure 3.2-3). Large strike-slip faults that are part of the Pacific-North America plate boundary are located approximately 240–300 km [150–185 mi] west of the PVNGS. Compared to SBR faults, these faults (such as the San Andreas fault) have high slip rates with repeated moderate- and large-magnitude earthquakes during the last 10,000 yr. The closest large strike-slip fault to PVNGS is the San Andreas fault, which is approximately 240 km [150 mi] west of the PVNGS.

---

<sup>3</sup> The Quaternary is the most recent of the three geologic periods in the Cenozoic Era and includes the Pleistocene and Holocene epochs. It encompasses the last 2.58 million years of geologic time.

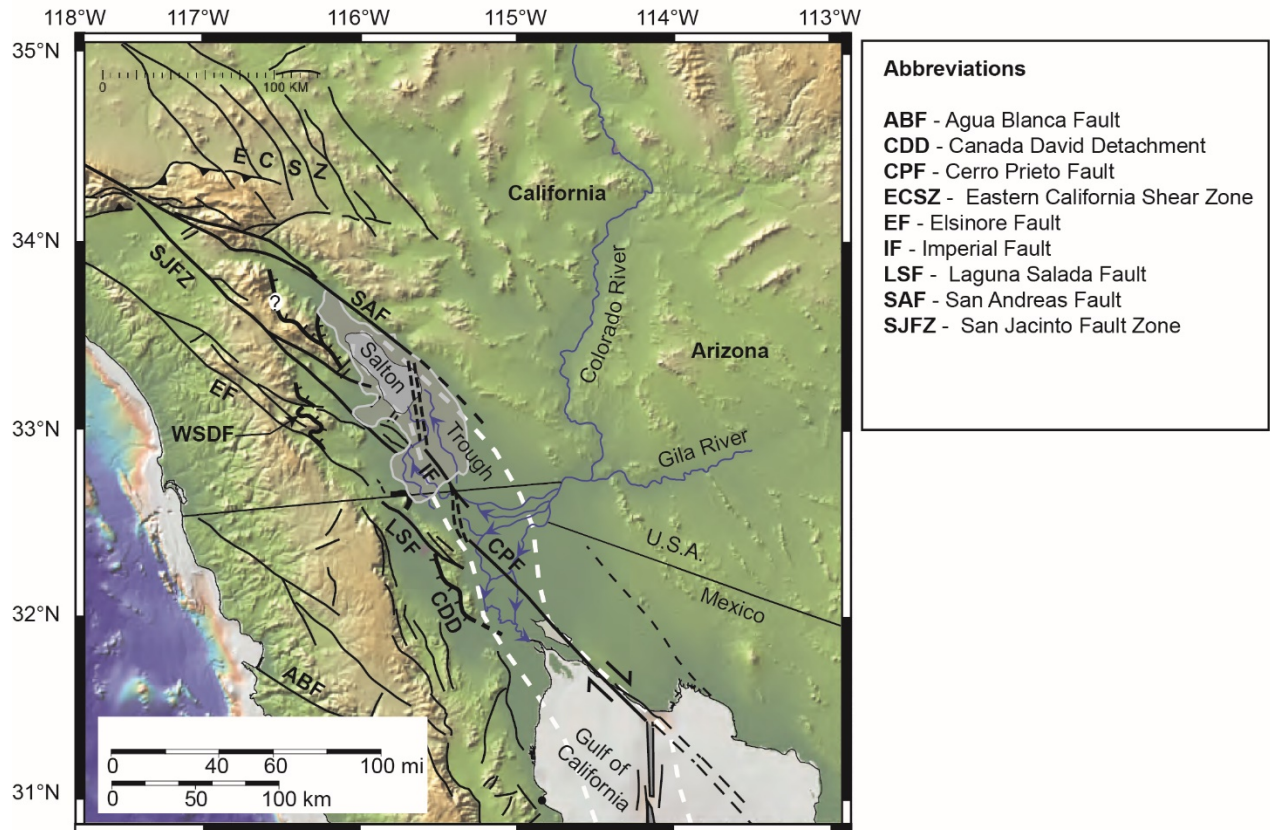


**Figure 3.2-3 Map of Faults in the California Strike-Slip Boundary, Redrafted from Dorsey and Umhoefer (2012). The PVNGS Site is Just Off the Right Edge of the Map**

This bimodal distribution of seismicity rates and magnitudes between the seismic-tectonic provinces surrounding the PVNGS site and the distant California strike-slip boundary results in a bimodal distribution of ground motion hazards at the PVNGS site. The moderate to high oscillator frequency ground motions (above approximately 5 Hz) are controlled by the proximal small- to moderate-magnitude, but relatively infrequent, earthquakes in the SBR and surrounding seismic-tectonic provinces. The low oscillator frequency ground motions (less than 5 Hz) are controlled by equal contributions from earthquakes in the SBR and surrounding provinces and the much more frequent, but distant, large-magnitude earthquakes on the plate boundary faults.

### 3.2.2. Senior Seismic Hazard Analysis Committee Process

The licensee performed the PSHA based on two SSHAC studies. In one study, the licensee developed an SSC model for the region surrounding the site. In a second jointly sponsored study, the licensee developed the SWUS GMC<sup>4</sup> model.

<sup>4</sup> At the time the SWUS SSHAC was developed, ground-motion studies referred to the resulting models as GMC models. Since then, the seismological community has adopted the simpler terminology of GMM. In the context of this report, GMC models and GMM mean the same.

The PVNGS SSC and SWUS GMC SSHAC studies followed the established SSHAC Level 3 process<sup>5</sup> (NRC, 2012c), including three structured workshops and several formal and informal working meetings of the SSC and GMC TI Teams (hereafter referred to as the SSC TI Team and the GMC TI Team). Details of the PVNGS SSC and SWUS GMC SSHAC studies, including the workshops, NRC observations at the workshops, and the review conducted by the SSHAC PPRP are provided in the licensee submittal (Cadogan, 2015a, 2015b; APS, 2015; GeoPentech, 2015) and the NRC's SA (NRC, 2016a).

### **3.2.3. Seismic Source Characterization**

The goal of the SSC TI Team was to develop an SSC model for the PSHA based on its evaluation of available geological, geophysical, and seismological information. The SSC TI Team considered two types of seismic sources: faults and areal source zones. Input parameters to the SSC model for these seismic sources were derived by the SSC TI Team from (1) earthquake records, based on the instrumented and historical seismicity catalogued for the region, (2) geologic evidence of the magnitude, age, and frequency of past seismic events, and (3) geophysical evidence for crustal strain based on Global Positioning System (GPS) measurements.

To develop the SSC for the PVNGS site, the SSC TI Team compiled existing information from plant licensing documents, USGS reports, and published technical information. Based on the discussions during Workshop 1, the SSC TI Team performed additional field review and data collection in the PVNGS site area and site vicinity. These studies included Quaternary geologic mapping of the site area {8-km [5-mi] radius} and site vicinity {40-km [25-mi] radius} in collaboration with the Arizona Geological Survey. The Quaternary geologic mapping was released as a separate report (APS, 2014). Members of the SSC TI Team also performed field reconnaissance along the Sand Tank fault and an unnamed fault mapped by Gilbert (1991) in the Eastern Gila Bend Mountains to independently evaluate several geologic exposures.

The PVNGS SSC model included (1) a catalog of historical seismicity used to define and characterize areal source zones and (2) attributes of local and regional faults used to characterize the seismic potential of geologic faults that could affect the site. The important seismic source parameters in the SSC TI Team model are the magnitudes and locations of future earthquakes that could affect the PVNGS site, including magnitude recurrence rates, seismogenic thickness, and the geometries of the fault sources.

---

<sup>5</sup> NUREG-2117 was the most current SSHAC guidance available at the time.



### 3.2.3.1. Earthquake Catalog

The SSC TI Team developed a composite catalog of historical seismicity based on information from available published and unpublished earthquake catalogs. Magnitudes in the catalog were converted to moment magnitudes ( $M$ ), the catalog was declustered, and the spatial and temporal completeness of the declustered catalog was evaluated using standard methods to identify independent events and remove foreshocks or aftershocks. The composite catalog included 1,941 entries with  $M2.7$  or greater, spanning the interval from 1852–2012. Declustering removed 1,048 duplicates, foreshocks, and aftershocks events, leaving a final catalog with 893 earthquakes.

### 3.2.3.2. Areal Source Zones

The SSC TI Team used areal source zones to model the temporal and spatial distribution of seismicity in regions with limited or nonexistent geologic or geophysical evidence that allows past earthquakes to be associated with known faults. The SSC TI Team developed two alternative conceptual models for areal source zones: the Two-Zone Model and the Seismotectonic Model (Figure 3.2-4). The Two-Zone Model separates the region into a western zone that is dominated by shear-tectonic features from interactions of the Pacific-North American plates and an eastern zone that is dominated by continental extensional tectonic features. The Seismotectonic Model further subdivides the Two-Zone Model into six smaller subzones, with each subzone roughly corresponding to major physiographic provinces in the southwestern United States. Within each areal source zone, the SSC TI Team assigned a range of possible virtual fault orientations, fault dips, fault width (based on depth to the base of the seismogenic crust), and fault rupture mechanisms. The distribution of rupture mechanisms and orientations assigned to these virtual faults within each areal source is based on the characteristics of mapped Quaternary faults and earthquake focal mechanisms.

The SSC TI Team determined distributions of seismogenic thickness for each zone by analyzing depths of historical earthquakes, or other geophysical information, and expert judgment. To develop distributions for the maximum earthquake magnitude ( $M_{\max}$ ) in each zone, the SSC TI Team considered the range of historical seismicity, crustal thickness, and the prevalence or absence of Quaternary-age faults in the source zone. For each areal source zone, the SSC TI Team developed an  $M_{\max}$  distribution that ranges from  $M6.8$  to  $M7.9$ , except for the Colorado Plateau source zone in the Seismotectonic Model, which uses a range of  $M6.5$  to  $M7.9$ . These  $M_{\max}$  distributions encompass the largest known earthquakes in the source zones, including the uncertainty in these magnitudes.

The SSC TI Team then used the methodology adopted in NUREG-2115 (NRC, 2012b) to develop recurrence parameters to model the seismicity in each areal source. This methodology uses a spatially variable approach based on patterns of historical seismicity to develop the final areal source zone inputs to the SSC logic tree. The SSC TI Team noted that the underlying technical basis for the methodology in NUREG-2115 (NRC, 2012b) is that the past pattern of low-to-moderate levels of historical seismicity provides a defensible basis to predict the location, rate, and magnitude distribution of future earthquakes. The SSC TI Team concluded that this assumption is reasonable because seismicity patterns are driven by large-scale forces due to plate tectonics. Plate tectonic forces change slowly, over millions of years, which greatly exceed the time periods that are considered when developing the PSHA. The SSC TI Team developed 24 alternative sets of recurrence parameters to capture the epistemic and statistical uncertainty in the recurrence rate for each of the areal sources.

For each of the areal sources, the SSC TI Team developed logic trees to define the potential locations, sizes, and rates of future earthquakes. Specific parameter values captured by each of the source logic trees included (1) maximum magnitude, (2) earthquake rupture mechanism, (3) seismogenic thickness, and (4) recurrence model and rates. Each of these parameters is represented as a node in the logic tree with multiple weighted branches at each node providing alternative parameter values for that element. In addition, the SSC TI Team developed separate logic tree branches for the Two-Zone and the Six-Zone areal source alternatives (Figure 3.2-4). The logic tree branches for each of the areal sources define a unique set of parameters for future potential earthquakes, primarily based on the characteristics of the known Quaternary faults and historical seismicity within each of the source zones. Tables 3.2-1 and 3.2-2 give detailed source information for each of two alternative areal source zone branches.

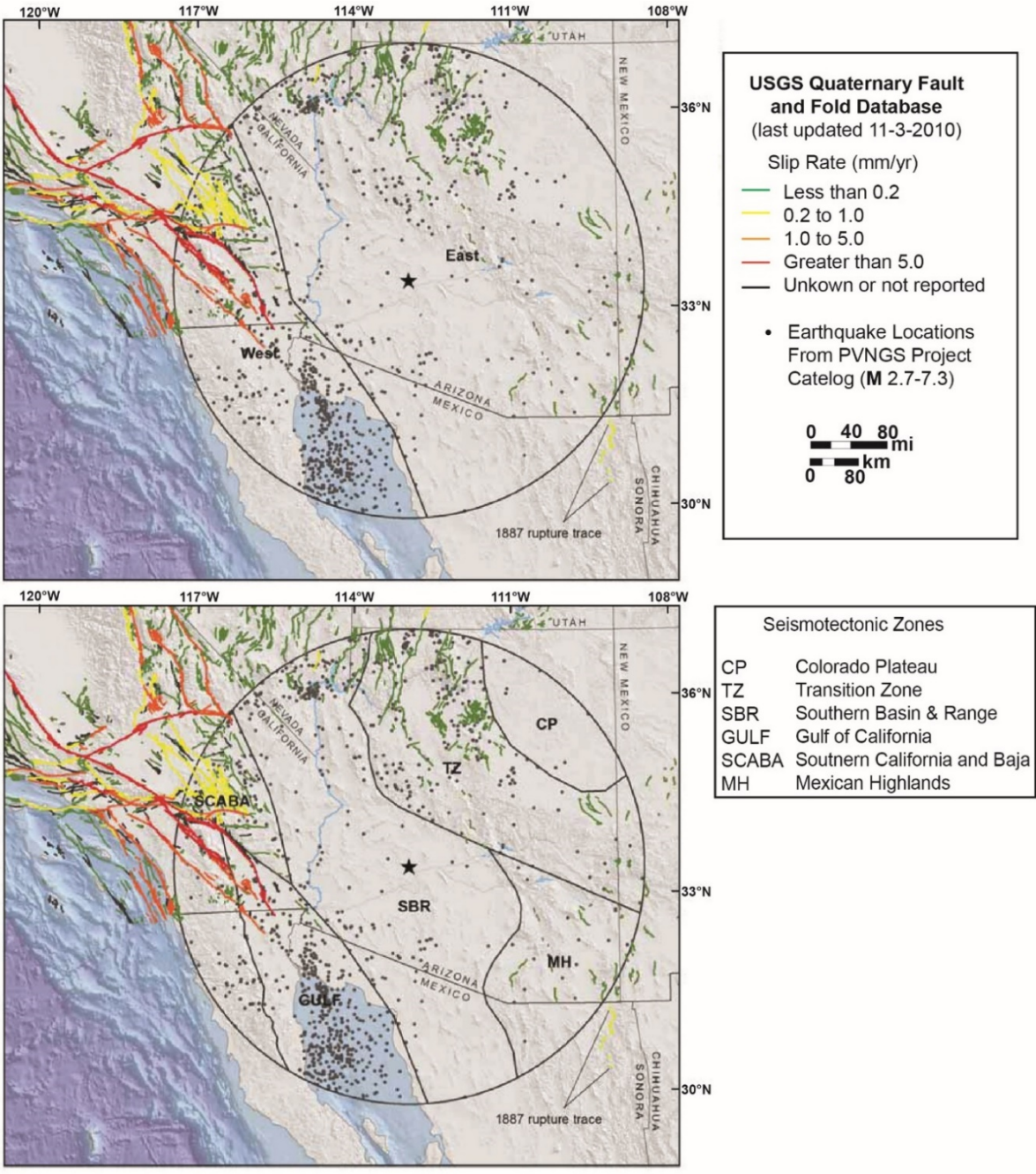


**Figure 3.2-4** Map Showing the Two-Zone (Top Panel) and Six-Zone (Bottom Panel) Areal Source Alternatives. The Large Circle is the Area Within a Radius of 400 km [250 mi] of the PVNGS (Star). Redrafted from Figures 9-2 and 9-7 in APS (2015)

**Table 3.2-1 Source Characterization Parameters for the Two-Zone Areal Source Alternative**

AREAL SOURCE ZONE	SEISMO-GENIC THICKNESS (km)	FAULT STYLE <sup>2</sup>	ORIENTATION OF RUPTURES		M <sub>MAX</sub>	MAGNITUDE RECURRENCE MODEL	SPATIAL VARIATION OF RATE FUNCTION
			STRIKE (DEGREE)	DIP (°)			
West	12 [0.20] <sup>1</sup>	R [0.10]	325 [0.20]	R: 30 [0.20]	6.8 [0.10]	G-R <sup>3</sup>	Penalized Maximum Likely <sup>4</sup>
	15 [0.60]	N [0.10]	315 [0.60]	45 [0.60]	7.0 [0.25]		
	18 [0.30]	SS [0.80]	305 [0.20]	60 [0.20]	7.2 [0.40]		
				N: 35 [0.20]	7.5 [0.20]		
				50 [0.60]	7.9 [0.05]		
				65 [0.20]			
				SS:70 [0.20]			
				80 [0.20]			
				90 [0.60]			
East	12 [0.20]	N [0.80]	20 [0.10]	N: 35 [0.20]	6.5 [0.30]	G-R	Penalized Maximum Likely
	15 [0.60]	SS [0.20]	0 [0.10]	50 [0.60]	6.75 [0.40]		
	18 [0.30]		340 [0.40]	65 [0.20]	7.0 [0.30]		
			320 [0.20]	SS: 70 [0.20]	7.25 [0.09]		
			Random [0.20]	80 [0.20]	7.5 [0.01]		
				90 [0.60]			

Notes: <sup>1</sup> Numbers inside the brackets are the assigned weights.  
<sup>2</sup> For fault style, normal (N), reverse (R), and strike-slip (SS).  
<sup>3</sup> Gutenberg and Richter (1956).  
<sup>4</sup> See Section 5.3.2 of NUREG-2215 (NRC, 2012b).

**Table 3.2-2 Source Characterization Parameters for the Six-Zone Areal Source Alternative**

AREAL SOURCE ZONE	SEISMO-GENIC THICKNESS (km)	FAULT STYLE <sup>2</sup>	ORIENTATION OF RUPTURES		M <sub>MAX</sub>	MAGNITUDE RECURRENCE MODEL	SPATIAL VARIATION OF RATE FUNCTION
			STRIKE (°)	DIP (°)			
SCABA	12 [0.20] <sup>1</sup>	R [0.10]	325	R: 30 [0.20]	6.8 [0.15]	G-R <sup>3</sup>	Penalized Maximum Likely <sup>4</sup>
	15 [0.60]	SS [0.90]	[0.20]	45 [0.60]	7.0 [0.25]		
	18 [0.30]		315	60 [0.20]	7.2 [0.40]		
			[0.60]	SS:70	7.5 [0.15]		
			305	[0.20]	7.9 [0.05]		
			[0.20]	80 [0.20]			
				90 [0.60]			
GULF	12 [0.30]	12 [0.30]	325	N: 35 [0.20]	6.8 [0.05]	G-R	Penalized Maximum Likely
	14 [0.60]	14 [0.60]	[0.20]	50 [0.60]	7.0 [0.30]		
	16 [0.10]	16 [0.10]	315	65 [0.20]	7.2 [0.30]		
			[0.60]	SS:70[0.20]	7.5 [0.30]		
			305	80 [0.20]	7.9 [0.05]		
			[0.20]	90 [0.60]			
SBR	12 [0.20]	N [0.80]	0 [0.20]	N: 35 [0.20]	6.8 [0.10]	G-R	Penalized Maximum Likely
	15 [0.60]	SS [0.20]	340	50 [0.60]	7.0 [0.25]		
	18 [0.30]		[0.40]	65 [0.20]	7.2 [0.40]		
			325	SS:70[0.20]	7.5 [0.20]		
			[0.20]	80 [0.20]	7.9 [0.05]		
			RANDO	90 [0.60]			
			M [0.20]				
MH	12 [0.10]	N [0.80]	0 [0.20]	N: 35 [0.20]	6.8 [0.05]	G-R	Penalized Maximum Likely
	15 [0.60]	SS [0.20]	340	50 [0.60]	7.0 [0.25]		
	18 [0.30]		[0.40]	65 [0.20]	7.2 [0.40]		

AREAL SOURCE ZONE	SEISMO-GENIC THICKNESS (km)	FAULT STYLE <sup>2</sup>	ORIENTATION OF RUPTURES		M <sub>MAX</sub>	MAGNITUDE RECURRENCE MODEL	SPATIAL VARIATION OF RATE FUNCTION
			STRIKE (°)	DIP (°)			
			325 [0.20] RANDO M [0.20]	SS:70[0.20] 80 [0.20] 90 [0.60]	7.5 [0.20] 7.9 [0.05]		
TZ	14 [0.20] 17 [0.60] 20 [0.20]	N [0.70] SS [0.30]	20 [0.25] 340 [0.25] RANDO M [0.50]	N: 35 [0.20] 50 [0.60] 65 [0.20] SS:70[0.20] 80 [0.20] 90 [0.60]	6.8 [0.20] 7.0 [0.25] 7.2 [0.30] 7.5 [0.20] 7.9 [0.05]	G-R	Penalized Maximum Likely
CP	15 [0.20] 20 [0.60] 25 [0.20]	N [0.80] SS [0.20]	RANDO M [1.00]	N: 35 [0.20] 50 [0.60] 65 [0.20] SS:70[0.20] 80 [0.20] 90 [0.60]	6.5 [0.20] 7.0 [0.35] 7.2 [0.25] 7.5 [0.20] 7.9 [0.05]	G-R	Penalized Maximum Likely
Notes:	<sup>1</sup> Numbers inside the brackets are the assigned weights. <sup>2</sup> For fault style, normal (N), reverse (R), and strike-slip (SS). <sup>3</sup> Gutenberg and Richter (1956). <sup>4</sup> See Section 5.3.2 of NUREG-2215 (NRC, 2012b). CP – Colorado Plateau source; GULF – Gulf of California source; MH – Mexican Highlands source; SBR – southern Basin and Range source; SCABA – Southern California and Baja Areal source; TZ – Transition Zone source.						

### 3.2.3.3. Fault Sources

The SSC TI Team developed a database of all possible fault sources within 400 km [250 mi] of the PVNGS site from a variety of published fault databases, including the 2008 National Seismic Hazard Mapping Project (Petersen et al., 2008a) and faults in the Uniform California Earthquake Rupture Forecast model (UCERF3) (Field et al., 2013), as well as published geologic maps for Arizona and Mexico (e.g., Pearthree et al., 1983). In addition, the SSC TI Team conducted additional mapping investigations to identify potential Quaternary-age features. These investigations focused on three principal areas: (1) evaluation of geomorphic features and existing map information around the U.S.-Mexico border region, including six previously unmapped Quaternary-age faults that were then added to the SSC fault database, (2) additional geologic mapping within 40 km [25 mi] of the PVNGS site, which included evaluation of a potential 5-km [3 mi]-long, Quaternary-age fault from Gilbert (1991), and (3) investigations of the Quaternary Sand Tank fault, which is located about 60 km [37 mi] south-southwest of the PVNGS site.

Based on this information, the SSC TI Team catalogued 168 Quaternary-age faults within approximately 400 km [250 mi] of the PVNGS site. Most of these faults are located more than 100 km [62 mi] from the site and are concentrated in three areas: (1) the active plate-boundary faults in Southern California and Baja California, (2) faults in northern Arizona within the Colorado Plateau transition zone, and (3) faults to the southeast of PVNGS in the Mexican Highlands. Based on published information (e.g., Field et al., 2013), comparison of geomorphic features to analogous faults with well-constrained slip rates (e.g., dePolo and Anderson, 2000), and a range of published magnitude-scaling relationships (e.g., Wells and Coppersmith, 1994), the SSC TI Team characterized each of the 168 faults by their faulting type (normal, reverse, strike-slip, or thrust), location, geometry, depth, slip direction, slip rate, magnitude, and

magnitude-frequency distribution function. Sensitivity analyses showed that only 18 of the 168 Quaternary faults provide at least a moderate contribution to the overall total hazard at the site (Figure 3.2-5). Table 3.2-3 provides the detailed source information for each of these 18 Quaternary faults.

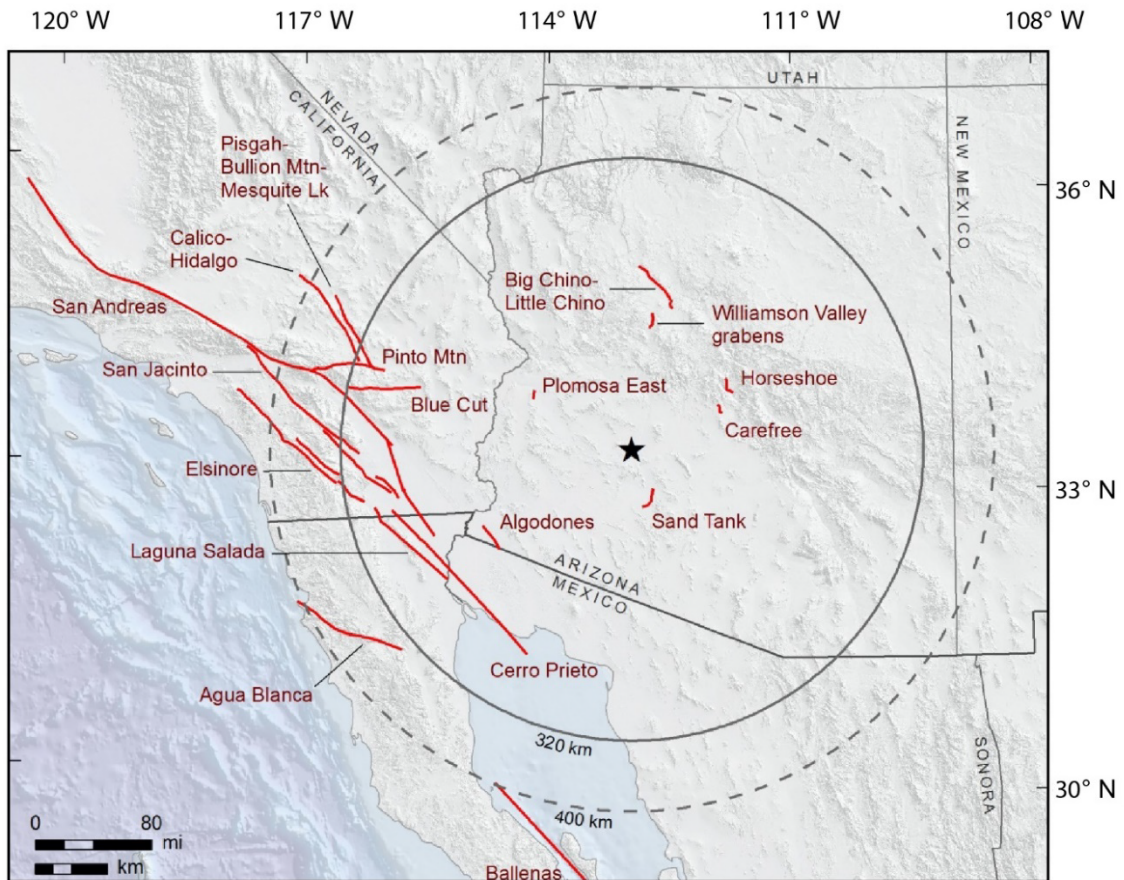


**Figure 3.2-5 Final 18 Fault Sources Included in PVNGS Hazard Calculations. The Black Star Shows the Location of the PVNGS Site. Redrafted from Figure 11-1 in APS (2015)**

**Table 3.2-3 Summary of Seismic Hazard Characteristics for the 18 Fault Sources in the PVNGS SSC Model**

FAULT NAME	FAULT STYLE <sup>1</sup>	LAYER <sup>2</sup>	LENGTH <sup>3</sup> (km)	DIP (°)	DEPTH (km)	WIDTH (km)	RUPTURE AREA (km <sup>2</sup> )	M <sub>CHAR</sub> (±0.2)	SLIP RATE (mm/yr) <sup>4</sup>			DIST. <sup>5</sup> (km)
Agua Blanca	SS		130	90	15	15	1,950	7.4	4.0 [0.2]	5.0 [0.6]	6.0 [0.2]	401
Algodones	N		32	50 NE	14	18	576	7.1	0.20 [0.8]	0.14 [0.1]	0.24 [0.1]	219
Ballenas Transform	SS	1	160	90	14	14	2,240	7.5	15.0 [0.2]	20.0 [0.6]	25.0 [0.2]	424
		2	80	90	14	14	1,120	7.1		20.0 [1.0]		400
		3	80	90	14	14	1,120	7.1	35.0 [0.2]	40.0 [0.6]	45.0 [0.2]	400
Big Chino-Little Chino	N		63	50 SW	17	22	1,386	7.2	0.10 [0.8]	0.10 [0.1]	0.14 [0.1]	203
Blue Cut	SS		79	90	15	15	1,185	7.2	0.39 [0.5]	0.59 [0.5]		285
Calico-Hidalgo	SS		118	90	15	15	1,770	7.4	1.8 [1.0]			380
Carefree	N		11	50 W	15	20	220	6.5	0.005 [0.2]	0.01 [0.6]	0.02 [0.2]	125
Cerro Prieto	SS	1	50	90	14	14	700	6.9	8.3 [0.2]	10.0 [0.6]	11.7 [0.2]	283
		2	168	90	14	14	2,352	7.6	29.3 [0.2]	34.0 [0.6]	38.7 [0.2]	283
		3	218	90	14	14	3,052	7.7	0.7 [0.2]	1.0 [0.6]	1.3 [0.2]	283
Elsinore	SS	1	38	90	15	15	570	6.7	2.1 [0.2]	3.5 [0.6]	4.9 [0.2]	310
		2	40	90	15	15	600	6.8	0.6 [0.2]	1.0 [0.6]	1.4 [0.2]	310
		3	39	90	15	15	585	6.8	0.3 [0.2]	0.5 [0.6]	0.7 [0.2]	370
		4	78	90	15	15	1,170	7.2	0.6 [0.2]	1.0 [0.6]	1.4 [0.2]	370
		5	154	90	15	15	2,310	7.6	1.5 [0.2]	2.5 [0.6]	3.5 [0.2]	310
		6	192	90	15	15	2,880	7.7	0.3 [0.2]	0.5 [0.6]	0.7 [0.2]	310
		7	63	90	15	15	954	7.0	1.0 [0.2]	2.5 [0.6]	3.0 [0.2]	320
Horseshoe	N		21	50 NE	17	22	462	6.8	0.02 [0.2]	0.03 [0.6]	0.06 [0.2]	147
Laguna Salada	SS		114	90	14	14	1,596	7.3	1.0 [0.2]	3.0 [0.6]	5.0 [0.2]	297
Pinto Mountain	SS		83	90	15	15	1,245	7.2	2.5 [0.5]	2.1 [0.5]		345
Pisgah-Bullion Mountain- Mesquite Lake	SS		91	90	15	15	1,365	7.3	1.0 [1.0]			348
Plomosa East	N		10	50 NW	15	20	200	6.4	0.005 [0.2]	0.01 [0.6]	0.02 [0.2]	150

FAULT NAME	FAULT STYLE <sup>1</sup>	LAYER <sup>2</sup>	LENGTH <sup>3</sup> (km)	DIP (°)	DEPTH (km)	WIDTH (km)	RUPTURE AREA (km <sup>2</sup> )	M <sub>CHAR</sub> (±0.2)	SLIP RATE (mm/yr) <sup>4</sup>			DIST. <sup>5</sup> (km)
San Andreas	SS	1	306	90	15	15	4,590	8.0	29.0 [.2]	31.0 [.6]	33.0 [.2]	420
		2	204	90	15	15	3,060	7.7	13.0 [.2]	17.0 [.6]	26.0 [.2]	305
		3	504	90	15	15	7,560	8.2	2.0 [.2]	3.0 [.6]	4.0 [.2]	305
		4	62	90	15	15	930	7.0	20.0 [.2]	25.0 [.6]	30.0 [.2]	275
San Jacinto	SS	1	80	90	15	15	1,203	7.2	9.0 [.2]	10.0 [.6]	11.0 [.2]	376
		2	93	90	15	15	1,395	7.3	3.0 [.2]	4.5 [.6]	7.0 [.2]	296
		3	173	90	15	15	2,598	7.6	3.0 [.2]	3.5 [.6]	4.0 [.2]	296
		4	46	90	15	15	693	6.9	5.0 [.2]	6.0 [.6]	7.0 [.2]	339
		5	77	90	15	15	1,158	7.2	1.0 [.2]	5.0 [.6]	10.0 [.2]	268
		6	26	90	15	15	395	6.6	2.0 [.2]	7.0 [.6]	9.0 [.2]	265
		7	36	90	15	15	543	6.7	2.0 [.2]	4.0 [.6]	6.0 [.2]	258
Sand Tank <sup>6</sup>	N		UNCERT.	50 W	15	17	UNCERT.	6.9 [.84] 7.2 [.16]	0.001 [.2]	0.010 [.6]	0.036 [.2]	73
Williamson Valley	N		19	50 E	17	22	418		0.040 [.2]	0.08 [.6]	0.16 [.2]	162
Notes:	<sup>1</sup> For fault style, reverse (R), oblique (O), and strike-slip (SS), with the weights assigned by the SSC TI Team. <sup>2</sup> The SSC TI Team used a layered-fault model approach to accommodate alternative slip-rate models along the strike of a fault source. This approach was used for faults in which there was paleoseismic or other evidence for segmented rupture behavior. The slip rate of each fault layer in this approach represents some portion of the total (or "target") fault-slip rate for the source. When the contributions from all layers (rupture scenarios) for a given fault source are summed, the total slip rate equals the target slip-rate budget for that particular fault. <sup>3</sup> Fault length, dip, depth, thickness, rupture area, M <sub>char</sub> , and slip-rate data are from Appendix F to APS (2015). Divide the lengths by 1.61 to convert from km to miles. <sup>4</sup> The SSC TI Team slip-rate distributions (logic tree inputs) are for each fault source. The assigned weights for each branch are in brackets. To convert from mm/yr to in./yr, divide by 25.4. <sup>5</sup> Distance (dst.) is the closest approach of the fault measured as the horizontal distance from the closest point on the fault trace to the PVNGS. These measures of the fault's closest approach to the PVNGS were obtained by using the proximity toolset in ArcGIS® and based on the map fault traces in Figure 11.1 of APS (2015). <sup>6</sup> Due to complex geologic conditions, the SSC TI Team was unable to develop a reliable geometric characterization of the fault trace, especially fault length, which is listed as uncertain (uncert.). The SSC TI Team assigned fault dip, seismogenic thickness, and earthquake recurrence according to the same logic as all other normal faults in the SSC TI Team database. The SSC TI Team derived the seismic parameters from measured fault displacement using the average displacement-per-event or maximum displacement-per-event regressions for all slip types of faults in Wells and Coppersmith (1994).											



For the large faults on the San Andreas boundary, the SSC TI Team characterized each of the individual fault sources as a series of straight-line fault segments, allowing future earthquake ruptures possibly to occur on one or more of the segments. Of these faults along the San Andreas boundary, the SSC TI Team determined that only the San Andreas, Cerro Prieto, and San Jacinto faults contributed to the 1 Hz hazard at the PVNGS site. None of the normal faults nearer to the site in Arizona, Nevada, and New Mexico, such as the Sand Tank fault, contributed to the hazard because they all have very low slip rates.

Because the fault-slip rates for these 18 Quaternary faults and activity rates for earthquakes in the areal source zones are such important parameters for the PSHA results, the SSC TI Team considered both the deformation rates from geologic field investigations and those derived from geodetic observations obtained principally from GPS measurements (e.g., Stein, 2007). The SSC TI Team found that consistent with many continental regions with relatively low tectonic strain rates, deformation rates estimated from the fault-slip data are substantially less than deformation rates from the geodetic observations. As noted by several proponent experts at Workshop 2 of the SSC SSHAC, the higher extension rates indicated by the GPS results typically would be expected to manifest as significant surface faulting and relatively high seismic activity rates. In contrast, much of the SBR exhibits little, if any, geologic evidence of recent surface faulting activity and has very low rates of historical seismicity. Thus, to incorporate the uncertainty with this interpretation of seismic activity based on the GPS data into the SSC model, and consistent with the principles of the SSHAC approach, the SSC TI Team included alternative branches in its logic tree with fault activity rates based on the GPS data, albeit with lower weight than branches with slip rates based only on the geologic and earthquake data.

Similar to the areal sources, the SSC TI Team developed logic tree branches for each of the fault sources that define the potential locations, sizes, and rates of future earthquakes. Specific parameter values captured by each of the source logic trees included (1) maximum magnitude, (2) earthquake rupture mechanism, (3) rupture dip angle, (4) depth to the top of rupture, (5) seismogenic thickness, and (6) recurrence model and rates. Each of these parameters is represented as a node in the logic tree with multiple weighted branches at each node providing alternative parameter values for that element.

#### **3.2.4. Ground Motion Characterization**

The GMC is the second element required to perform a PSHA for the PVNGS site. The goal of the SWUS GMC TI Team was to characterize median ground motions and their associated aleatory variability ( $\sigma$ ) for both nearby shallow crustal events and distant large-magnitude earthquakes associated with the San Andreas plate boundary (Figure 3.2-1). The GMC model consists of two suites of ground motion prediction equations (GMPEs) for 5-percent damped horizontal spectral accelerations for 20 oscillator frequencies including PGA. The GMC TI Team developed one suite of GMPEs for use with the nearby shallow crustal earthquakes and another for the distant large-magnitude earthquakes associated with the plate boundary.

##### *3.2.4.1. Ground Motion Databases and Seed Model Selection*

To develop the SWUS database of empirical ground motions, the GMC TI Team compiled data from four existing databases: the Pacific Earthquake Engineering Research (PEER) Next Generation Attenuation (NGA)-West2 database (Ancheta et al., 2014), a database of earthquakes from Taiwan (Lin et al., 2011), a database of earthquakes from Arizona (Kishida et al., 2014), and the Reference Database of Seismic Ground Motion in Europe (Akkar et al., 2014). The SWUS GMC TI Team focused its data selection on earthquakes with

$M \geq 5$  that were recorded at multiple stations (more than three recordings) within 70 km [43 mi] of the epicenter, and where the recording sites had a  $V_{S30}$  (i.e., travel-time-averaged shear wave velocity ( $V_s$ ) in the top 30 m [100 ft]) greater than 250 meters per second (m/sec) [820 feet per second (ft/sec)].

The GMC TI Team used the resulting SWUS database to evaluate existing GMPE models, inform the selection of models for use in the final GMC model, and to evaluate the weighting of the final GMC suite of models. Further, the GMC TI Team used the earthquake dataset from Arizona to constrain the travel-path effects from the distant California and Mexico sources and to estimate the local-site attenuation. In addition, the GMC TI Team used the database from Taiwan in its development of the aleatory variability component of the GMC model. Based on an evaluation of multiple GMPEs, the GMC TI Team ultimately selected five models for development of the GMC model for use in the distant active tectonic regions (Abrahamson et al., 2014; Boore et al., 2014; Campbell and Bozorgnia, 2014; Chiou and Youngs, 2014; Idriss, 2014). For the local sources surrounding the site, the GMC TI Team included three additional GMPEs (Akkar et al., 2014; Zhao et al., 2006; Zhao and Lu, 2011) as candidate models. These eight existing GMPEs are referred to as “seed” models for the development of the final GMC model, which is described below.

#### *3.2.4.2. Median Ground Motion Models*

The final GMC model consists of two sets of median GMPEs: one for local (both fault and distributed) sources and one for distant fault sources. For the local fault sources, the GMC TI Team developed a set of GMPEs by implementing a two-dimensional (2D) visualization process, referred to as Sammon’s maps (Sammon, 1969). The purpose of the Sammon’s map approach is to develop a continuous distribution of median GMPEs that also captures alternative magnitude- and distance-scaling approaches. For the distant, active tectonic regions, the GMC TI Team relied on the four existing NGA-West2 models described above with Arizona-specific corrections to the median predictions.

#### Local Sources

The GMC TI Team recognized that the characterization and quantification of uncertainties, especially epistemic uncertainty, is a fundamentally important element of GMC. The traditional approach to characterizing uncertainty in ground motions from future earthquakes is to select and assign weights to existing GMPEs. One disadvantage to this approach is that the existing suite of GMPEs may not represent a set of mutually exclusive and collectively exhaustive models (Abrahamson and Bommer, 2005). Further, this approach will not provide extrapolation beyond, and may not appropriately interpolate between, existing models. Based on the eight seed models noted above, the GMC TI Team produced a large suite of new GMPEs that both interpolate between, and extrapolate beyond, the seed models.

After its analysis of the eight seed models, the GMC TI Team identified a common functional GMPE form (parameterized in terms of magnitude, distance, and style of faulting). The common form model was then fit to the spectral acceleration results from each of the seed GMPEs, resulting in eight common-form model versions that represent the original seed models. Based on the mean and variance for each of the common-form model coefficients, as well as the covariance among the coefficients, the team developed a suite of 2,000 new candidate GMPEs that span a broad range of ground motion space.

The GMC TI Team used visualization techniques to map the suite of new models into a 2D plane (Scherbaum et al., 2010) and used the Sammon's maps technique (Figure 3.2-6) to visualize a 2D representation of the median model space. The model space was then discretized into a small number of cells with a representative model selected for each cell. Weights were then assigned to each cell based on the comparisons with hazard-relevant datasets (empirical and/or simulated) and with the density of the suite of representative models within each cell to represent the center, body, and range of median predictions. This technique was applied independently to each spectral frequency. The resulting GMC model has up to 31 weighted GMPEs for each spectral period (although some periods have fewer than 31 models).

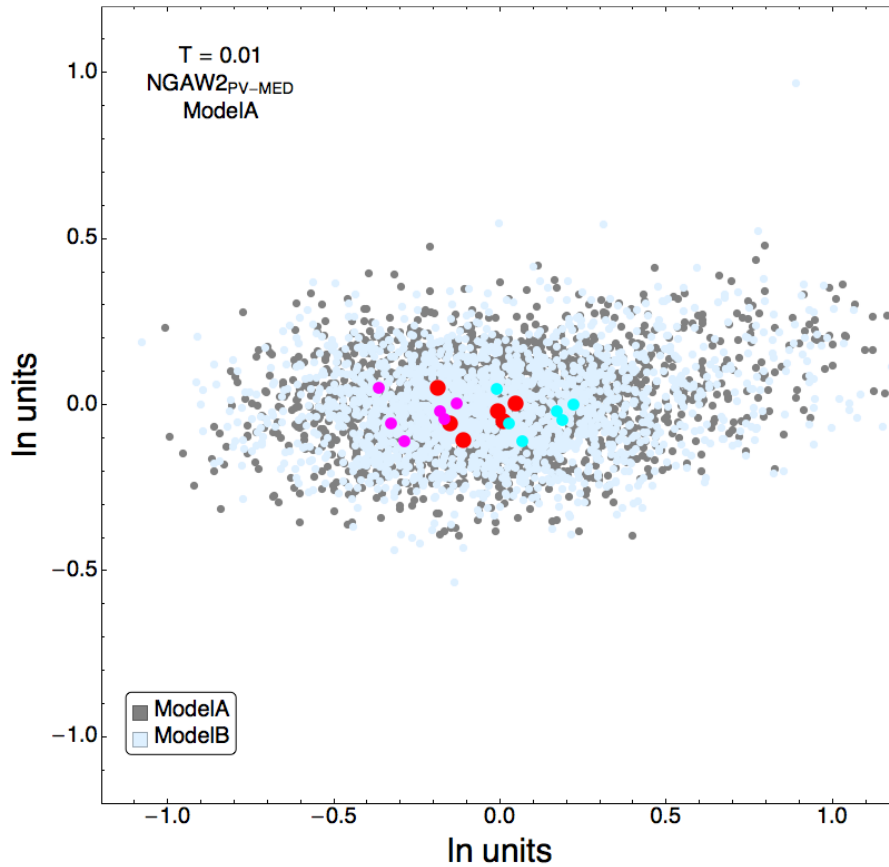


**Figure 3.2-6 Example Map of 2,000 Sampled Models in Sammon's Space, for 100 Hz (0.01 Second Period). Model A and Model B Represent Two Alternative Distance Measures Used in the Common Functional Form. The Red Dots Show the Location of the Candidate or Seed GMPEs Used to Develop the Ground Motion Distributions. The Magenta and Cyan Dots Show Plus and Minus Two Standard Deviations in Epistemic Uncertainty, Respectively, about the Seed GMPEs. Modified from Figure 6.4.3-3 in the SWUS GMC Report (GeoPentech, 2015)**

### California and Mexico Sources

The GMC TI Team determined that it did not need the Sammon's map technique for the distant earthquake sources, which only impact the hazard at lower oscillator frequencies. To develop the GMC model for the California and Mexico regions, the GMC TI Team selected the five NGA-West2 GMPEs and then added path-specific adjustment factors to take advantage of the available ground motion data in Arizona from these distant sources. The SWUS GMC TI Team also evaluated potential differences in attenuation arising from path effects and added two alternative branches to the logic tree (one that accounts for path effects and one that does not). In addition to adding these two alternative branches, the GMC TI Team added epistemic uncertainty to the median ground motion estimates to account for the limited range of predicted spectral accelerations for earthquakes with greater than *M*7. In the resultant logic tree for the median ground motions, each of the five NGA-West 2 GMPEs is augmented by 12 alternative branches that account for path effects and magnitude scaling, resulting in a final set of 60 GMPEs for the California and Mexico sources.

#### *3.2.4.3. Ground Motion Variability*

In addition to developing GMPEs that predict median ground motions, the GMC TI Team developed models to characterize the random (i.e., aleatory) variability about the median ground motion. Because Enclosure 1 to the 50.54(f) letter (NRC, 2012a) requests that licensees perform a detailed site response analysis, the GMC TI Team first separated the residuals between the predicted and observed ground motions into its component pieces to remove the repeatable effects of site response (and avoid double counting that effect in the control point hazard calculations). The partitioning of the total aleatory variability into its component parts is important because the site-to-site portion of the total aleatory variability is a property of the site. This site term is the systematic difference between the ground motions at a site and the median prediction of the GMPE for that site; this is potentially a knowable quantity and is most appropriately treated as an epistemic uncertainty. The GMC TI Team then combined the standard deviations for each of the remaining components of the total residuals to produce the partially nonergodic aleatory standard deviation, which is referred to as "single-station sigma."

To develop a model for single-station sigma for the crustal earthquake GMPEs, the GMC TI Team first constructed models for the between-event standard deviation and the single-site within-event standard deviation and assumed that both models depend on earthquake magnitude. For the distant larger sources, the GMC TI Team used recordings from California and Mexico earthquakes from a group of sites around PVNGS to estimate the repeatable similar path-to-region component of sigma. In addition to developing models for each of the individual components of sigma, the GMC TI Team developed epistemic uncertainty distributions for each of these components. The GMC TI Team then combined these epistemic uncertainty distributions to develop a final continuous distribution for single-station sigma, which it represented in the logic tree by the low, central, and high values (5<sup>th</sup>, 50<sup>th</sup>, and 95<sup>th</sup> percentiles) of the cumulative distribution of single-station sigmas.

#### *3.2.4.4. Implementation of Ground Motion Characterization Model*

The GMC TI Team developed logic trees for the local areal and distant fault sources, with branches that captured the (1) alternative datasets used in evaluating existing GMPEs, (2) alternative published GMPEs used to construct the Sammon's map, (3) additional epistemic uncertainty, and (4) path effects. The GMC logic tree for the regional Arizona sources includes nodes and branches for each of the different median models, two alternative distance

parameters, and multiple hanging-wall effects. For the distant California and Mexico sources, the GMC logic tree includes nodes and branches for each of the five NGA-West2 GMPEs, path term effects, and epistemic uncertainty for large-magnitude scaling. The sigma logic trees include nodes and branches for magnitude dependence, the distribution of epistemic uncertainty in single-station sigma, and the use of either a normal distribution or a mixture model for the final distribution of ground motion residuals.

### 3.2.5. Probabilistic Seismic Hazard Analysis

The licensee used the results of the SSC and GMC SSHAC studies to develop PSHA results for the baserock horizon beneath the site. The licensee then used the baserock horizon hazard curves as inputs to the site response analysis. Additional uses of the PSHA are to identify the fault and areal seismic sources that have the largest impact on the hazard and to identify the specific magnitude and distance combinations that control the hazard at  $10^{-4}$ ,  $10^{-5}$ , and  $10^{-6}$  annual frequencies of exceedance (AFE).

Figure 3.2-7 shows total mean site-specific rock hazard curves for seven spectral frequencies. For both the 1 Hz and 10 Hz spectral frequencies, the areal sources are the dominant contributors to hazard. Except for the 1 Hz spectral frequency, the areal source hazard and total hazard are nearly identical (Figure 3.2-8). These results show that the 18 fault sources, which capture the hazard from the largest faults in the region, are relatively minor contributors to hazard at PVNGS, largely because they are so distant from the PVNGS site. Deaggregation of the resulting rock hazard curves at  $10^{-4}$ ,  $10^{-5}$ , and  $10^{-6}$  mean AFE confirmed the bimodal distribution, with contributions to low (1 Hz and 2.5 Hz) and high (5 Hz and 10 Hz) frequency spectral accelerations. For the 5 Hz and 10 Hz frequencies, the proximal earthquakes with moderate magnitudes (in the range of **M6.1–M6.3** at distances from 7 to 21 km [4 to 13 mi]) dominate the hazard, while for the 1 Hz and 2.5 Hz frequencies, large distant earthquakes (in range of **M7.4–M7.6** at distances of around 200 km [125 mi]) dominate the hazard. Because the six-zone Seismotectonic Model is weighted more heavily than the Two-Zone areal source alternative and the site is located within the SBR, the hazard contribution from earthquakes originating in the SBR dominates the 10 Hz hazard. The SBR is also a significant contributor to the 1 Hz hazard.

### 3.2.6. Staff Confirmatory Evaluation of the Probabilistic Seismic Hazard Analysis

The NRC staff performed multiple confirmatory evaluations to support its review of the PVNGS SSC and GMC models. This report summarizes the results of the NRC staff's confirmatory PSHA for the baserock hazard beneath the site. The NRC SA (NRC, 2016a) provides a complete description of all the confirmatory analyses staff relied on for its review.

The NRC staff performed a confirmatory evaluation for the seismic sources that contribute the most to the hazard in order to test the reasonableness of the 1 Hz and 10 Hz mean hazard results for a few selected seismic sources, and to evaluate the sensitivity of the key source and ground motion parameters on the final hazard results. For this confirmatory analysis, the NRC staff selected a subset of the branches that focus on the highest weighted components of the logic trees. Specifically, the NRC staff evaluated the hazard from the SBR, which is the host areal source zone, and the TZ source zone. These areal zones are two of the six-zone seismotectonic sources that are significant contributors to both the 1 Hz and 10 Hz total mean hazard for PVNGS. Because the locations of the causative faults within the SBR and TZ are not known, the NRC staff developed a set of virtual faults to simulate earthquake sources in the two areal source zones. For each of the virtual faults, the NRC staff determined the fault geometry,

faulting mechanism, dip angle, and seismogenic thickness of the crust, based on the highest weighted branches in the logic tree for each of the sources. For each of the virtual faults in the SBR and TZ, the NRC staff calculated the hazard using a range of earthquake magnitudes from *M*5 to the highest weighted maximum magnitude earthquake, which is *M*7.2 for both the SBR and TZ. In addition, the NRC staff used each of the 1 and 10 Hz SWUS GMC median models and the highest weighted standard deviation. The staff developed a seismic hazard curve for each of the virtual faults and then summed the results to obtain mean 1 Hz and 10 Hz hazard curves for the SBR and TZ.

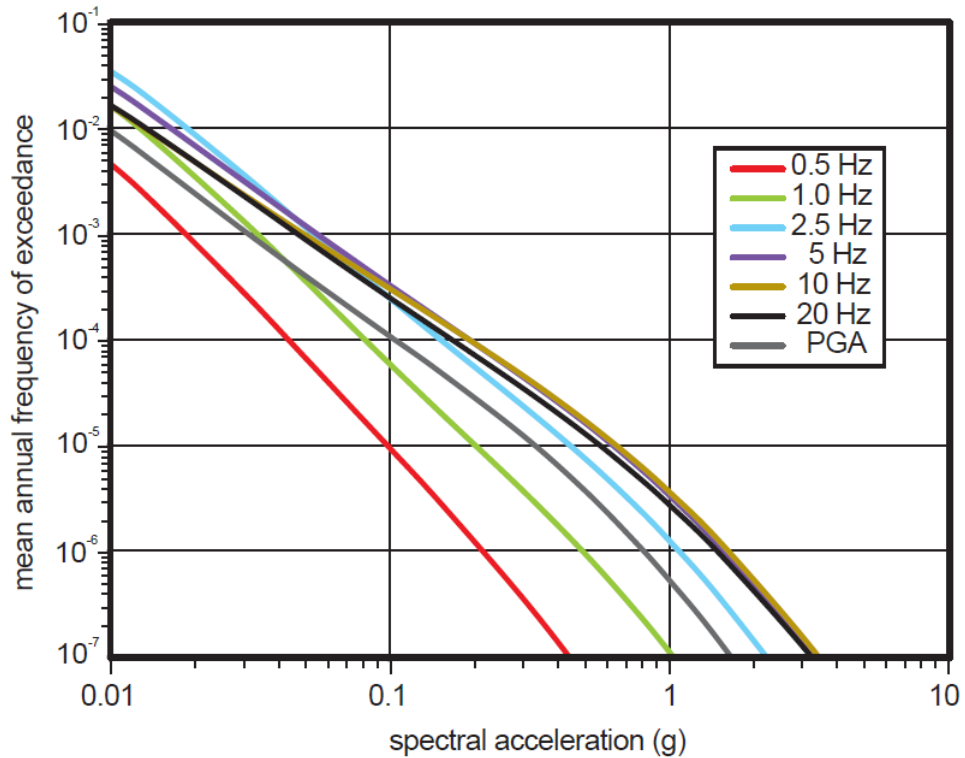


**Figure 3.2-7 Total Mean Site-Specific Rock Hazard Curves Showing Seven Spectral Frequencies, Based on the Data in Table 2 in Cadogan (2015a)**

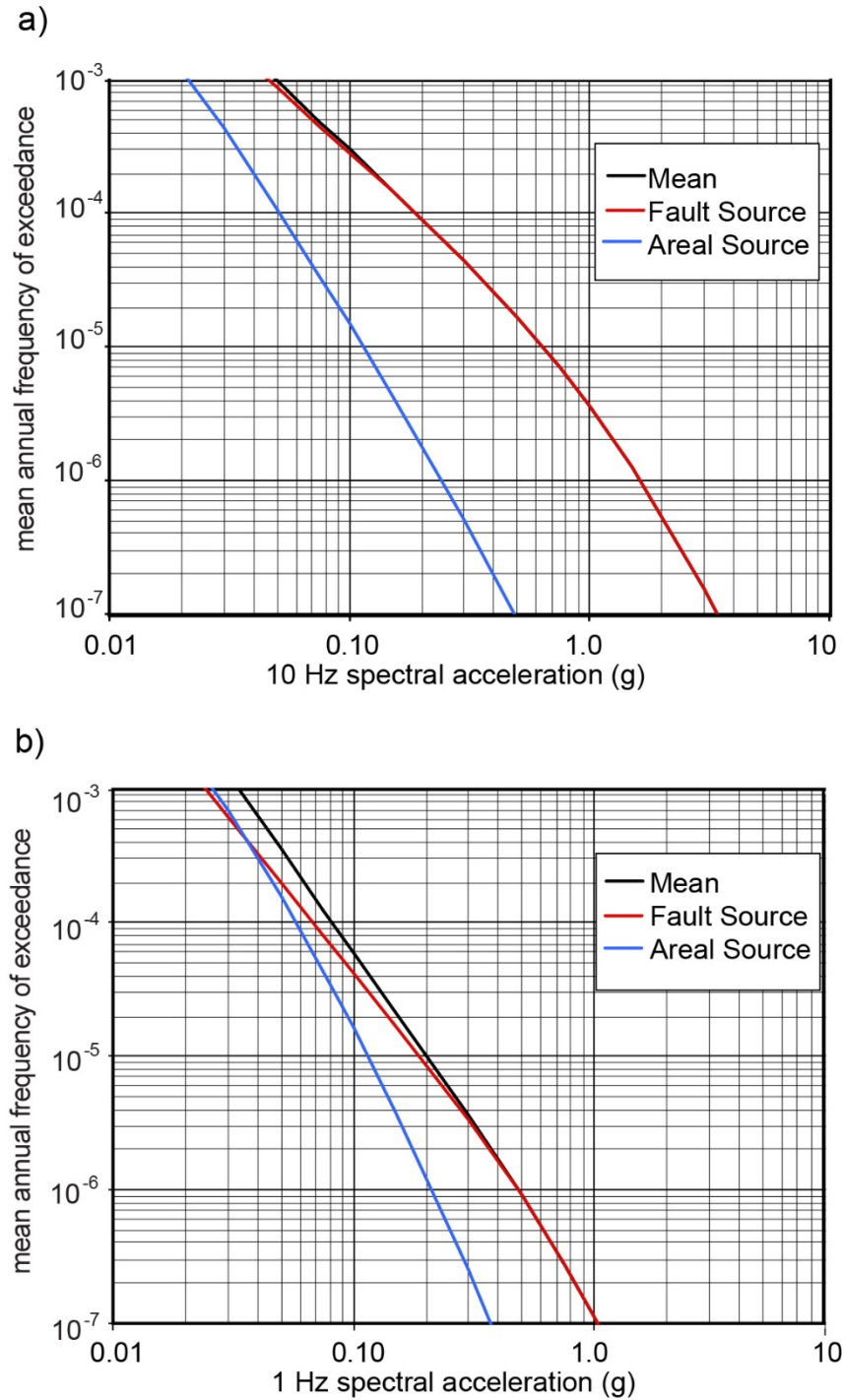


**Figure 3.2-8 (a) Site-Specific Rock Hazard Curves Showing Total Mean Hazard and Contributions from Area Sources and Faults for 10 Hz Spectral Acceleration (from Figure 10 in Cadogan, 2015a) and (b) Site-Specific Rock Hazard Curves Showing Total Mean Hazard and Contributions from Area Sources and Faults for 1 Hz Spectral Acceleration (Redrafted from Figure 11 in Cadogan, 2015a)**

Figure 3.2-9 shows the location of the virtual faults for the SBR (blue) and TZ (brown) areal source zones. For the analysis, the density of the virtual faults was greater near the PVNGS site (red triangle) and more widely spaced out to 250 km [155 mi] to ensure that the local and distant sources were evenly sampled. The NRC staff developed this distribution of virtual faults to capture the entire range of possible source-to-site distances. The virtual faults shown in Figure 3.2-9 are all *M*7.2 normal faults, each fault having a strike length of about 65 km [40 mi] and a down-dip width of about 20 km [12.5 mi]. To represent the structural characteristics of the source zones, each fault was oriented randomly between N40°W and N–S for the SBR, and randomly between N20°W to N20°E for the TZ. To obtain the final confirmatory results, the NRC staff added up the hazard curves for each of the virtual faults (377 for SBR and 83 for TZ). Figure 3.2-10 shows the 1 Hz (left) and 10 Hz (right) mean hazard curves for the SBR (blue) and TZ (brown) areal sources. The solid, heavy line indicates the NRC staff's PSHA confirmatory results. The dashed, heavy line indicates the licensee's results. As shown in Figure 3.2-10, the staff's confirmatory results closely match the licensee's results for both the 1 Hz and 10 Hz mean hazard curves.

### 3.2.7. Site Response Analysis

In order to develop control point hazard curves and the ground motion response spectra (GMRS) at the control point elevation, the licensee conducted a site response analysis to determine the site amplification resulting from the bedrock ground motions propagating upward through the soil/rock column to the surface. The licensee developed its site response model to a depth sufficient to reach the generic or baserock conditions, referred to as the reference horizon.

The critical parameters that determine what frequencies of ground motion are affected by the upward propagation of bedrock motions are the layering of soil and/or soft rock, the thicknesses of these layers, the shear wave velocities ( $V_s$ ) and low-strain damping of the layers, and the degree to which the shear modulus and damping change with increasing input bedrock amplitude. Appendix B to EPRI Report 1025287, "Seismic Evaluation Guidance: Screening, Prioritization, and Implementation Details (SPID) for the Resolution of Fukushima NTF Recommendation 2.1: Seismic," dated November 27, 2012 (EPRI, 2012) (hereafter called the SPID), provides detailed guidance on the development of site-specific amplification factors (including the treatment of uncertainty) for sites that do not have detailed, measured soil and rock parameters to extensive depths. In addition, the 50.54(f) letter specifies that the subsurface site response model, for both soil and rock sites, should extend to sufficient depths to reach the generic or baserock conditions as defined in the GMC models used in the PSHA. In order to transfer the median ground motions predicted by the GMC models for generic rock conditions (referred to as the "host" conditions) to the site-specific baserock (referred to as the "target" conditions), the licensee developed a distribution of adjustment factors.

#### 3.2.7.1. Site Basecase Profiles

To perform a site response analysis, the licensee developed both shallow and deep stratigraphic models for the PVNGS site. For each of the profiles, the licensee used site data to determine the physical properties, such as  $V_s$ , and the thickness of each of the layers. The licensee used the shallow profile to calculate the site amplification factors for development of the control point hazard curves and GMRS and used the deeper profile to develop the host-to-target adjustment factors for the SWUS GMC model.



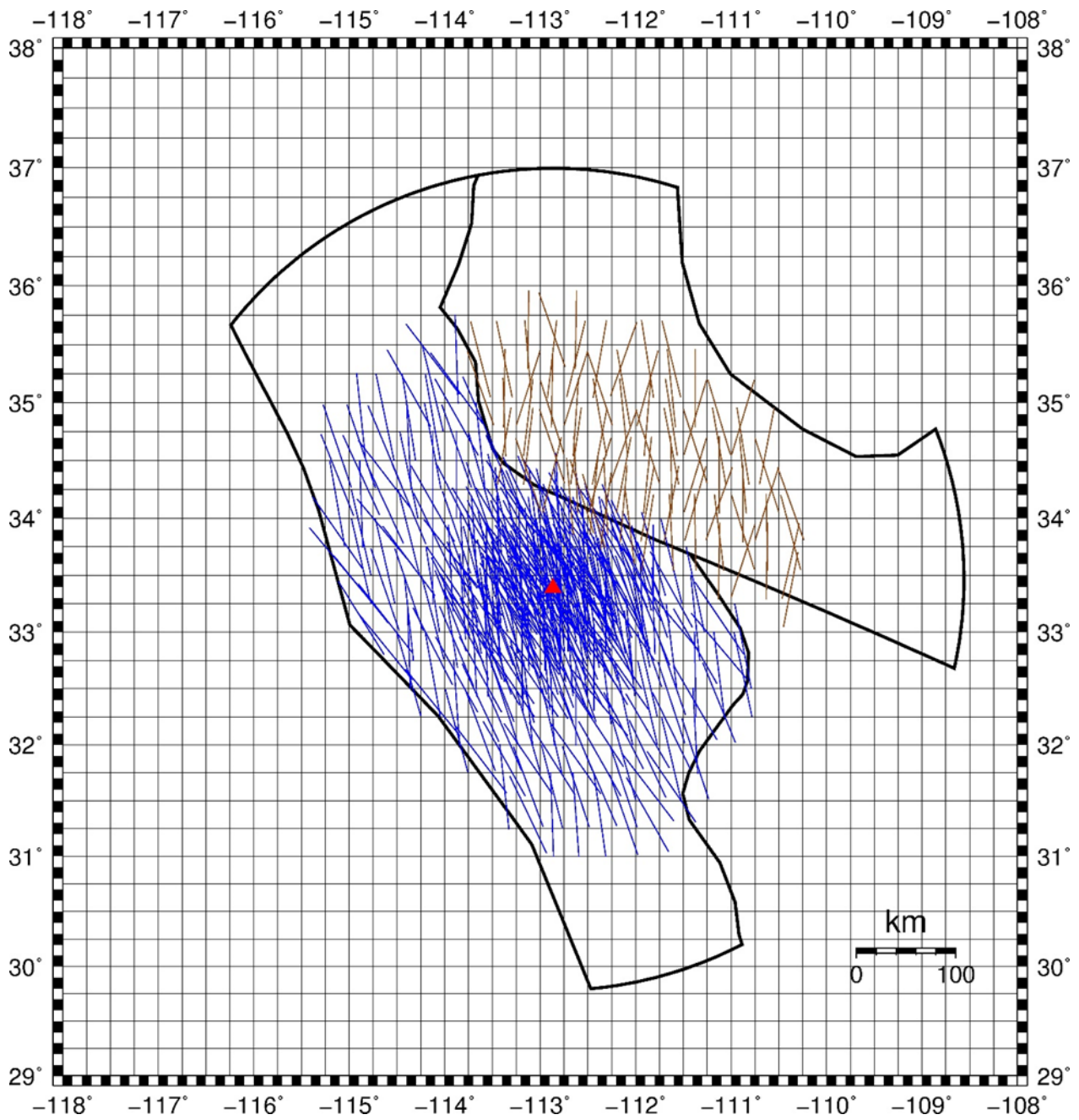


**Figure 3.2-9** Location of the Virtual Faults for the SBR (Blue) and TZ (brown) Areal Source Zones (Outlined in Black) Relative to the PVNGS Site (Red Triangle)

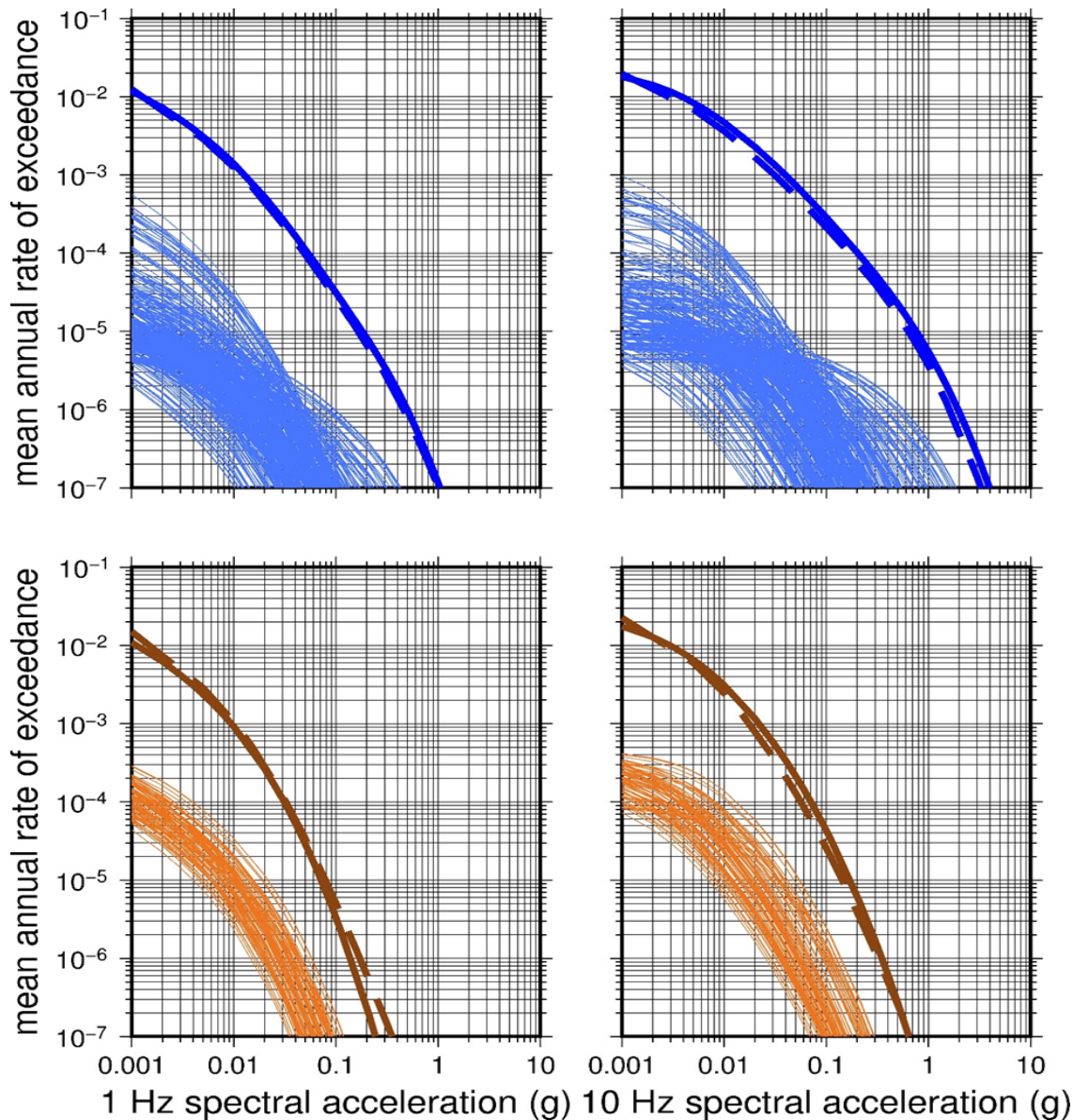


**Figure 3.2-10 Mean Hazard Curves for the SBR (Blue Lines) and TZ (Brown Lines) Areal Sources Showing the Staff's PSHA Confirmatory Analysis Results (Solid Heavy Lines) and the Licensee's Results (Dashed Heavy Lines)**

The shallow subsurface at the PVNGS site is composed of approximately 105 m [344 ft] of interbedded sands and clays and 26 m [85 ft] of fanglomerate overlying the volcanic rocks that characterize the top of the deep profile. The licensee developed its basecase profile using data from the original site investigation and more recently collected downhole and Spectral Analysis of Surface Waves (SASW) data. To capture the epistemic uncertainty in the basecase model, the licensee developed upper and lower basecase profiles using a natural log standard deviation that ranged from 0.15 to 0.23 and depended on the variation of the observed seismic velocities with depth.

The deeper profile extends from an average depth of 120–1,968 m [394–6,460 ft] and is composed mainly of volcanic rocks that rest atop the Precambrian granitic and metamorphic crystalline basement. The licensee developed the basecase profile for the deeper rock layers from data presented in the Updated Final Safety Analysis Report (UFSAR) (APS, 2013), as well as a regional seismic refraction profile for central Arizona (Warren, 1969). To capture the epistemic uncertainty in the basecase profile, the licensee developed upper and lower basecase profiles using a natural log standard deviation value of 0.35, as recommended in Appendix B to the SPID (EPRI, 2012).

#### *3.2.7.2. Dynamic Material Properties*

Equivalent-linear seismic site response modeling requires two inputs to characterize the dynamic material properties of the strata in the column of material above the reference bedrock. These are shear modulus reduction (changes in the ratio of stress to strain in the material under vibratory loading) and material damping ratios (changes in the percent damping of the material under increasing strain). Consistent with the guidance in the SPID (EPRI, 2012), APS derived the dynamic material properties of the soils from the EPRI soil shear modulus and damping curves (EPRI, 1993) and the Peninsular Range curves (Silva et al., 1996, 1998). For the clay layers in the basecase profiles, the licensee used the Vucetic and Dobry (1991) curves.

Site kappa ( $\kappa_0$ ) is defined as the damping contributed by both intrinsic hysteretic damping and the scattering of seismic energy due to wave propagation in heterogeneous materials near the surface. The licensee estimated the site-specific or target kappa value and the site kappa value assumed for the SWUS GMC model. The licensee estimated a target site kappa value of 33 milliseconds (msec) based on earthquake ground motion recordings at sites near PVNGS that were developed as part of the SWUS GMC model (GeoPentech, 2015). To capture the epistemic uncertainty in the target site kappa value for the PVNGS site, the licensee used a natural log standard deviation of 0.5 to develop the upper and lower estimates of kappa. For the host site kappa value associated with the SWUS GMC model, the licensee estimated an average value of 41 msec.

#### *3.2.7.3. Input Spectra*

To develop input ground motions for the site response analysis, the licensee used the results from its deaggregation of the PSHA (see Section 3.2.5). Specifically, the licensee used the magnitude and distance pairs from the deaggregation to develop high-frequency and low-frequency input spectra at hazard levels ranging from  $10^{-4}$  to  $10^{-6}$  AFE. The licensee then scaled these input spectra to 11 different PGA amplitudes between 0.01g and 1.5g, resulting in a suite of 22 input GMRS. Next, these WUS input spectra were adjusted to the site-specific subsurface conditions using the set of  $V_S$ -kappa conversion factors described above. The licensee then used these  $V_S$ -kappa-adjusted input spectra to drive the shallow site basecase profiles to determine the final site amplification factor distributions.

#### *3.2.7.4. Site Response Methods and Results*

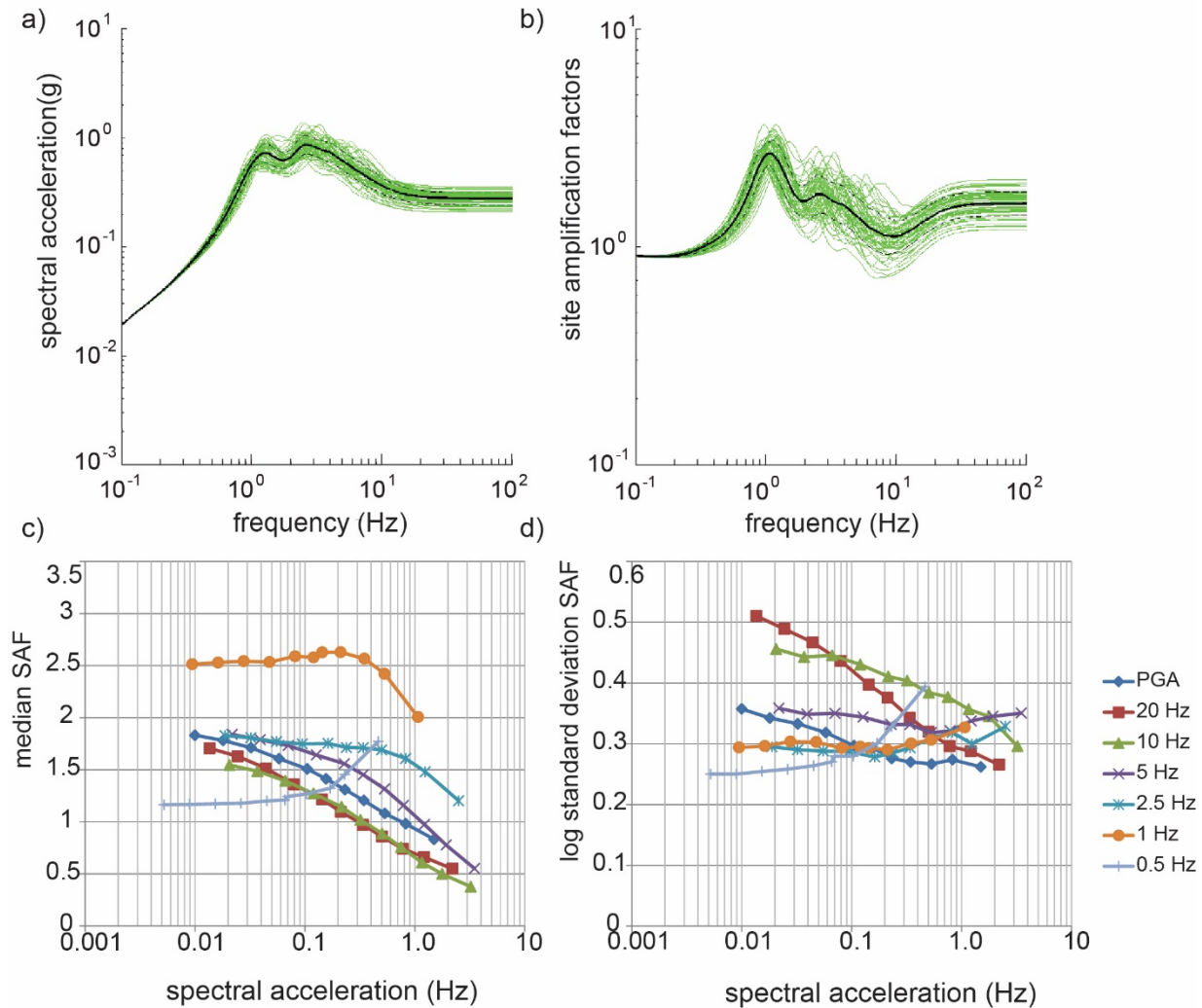
The licensee used the random vibration theory (RVT) approach to perform its site response calculations. Specifically, for each combination of  $V_S$ -kappa-adjusted input spectra, three basecase  $V_S$  profiles, and shear modulus and damping curves, the licensee developed 60 random profiles to calculate a median amplification factor and associated log standard deviation. Following guidance in the SPID (EPRI, 2012), the licensee used a minimum median amplification value of 0.5 in its determination of the control point hazard curves and GMRS.

Figure 3.2-11 shows the final amplification factors developed with all combinations of the varied parameters for each of the three profiles (basecase, lower range, and upper range).

The licensee used Approach 3, as described in NUREG/CR-6728 (NRC, 2001) and Appendix B to the SPID (EPRI, 2012) to develop probabilistic site-specific control point hazard curves. The licensee's implementation of Approach 3 involved computing the site-specific control point elevation hazard curves for a broad range of spectral accelerations by combining the site-specific reference rock hazard curves, as described in Section 3.2.5 of this report, and the amplification functions and associated uncertainties that were determined from its site response analysis.

### **3.2.8. Control Point Hazard Results**

In summary, the licensee conducted SSHAC Level 3 studies to develop both SSC and GMC models in response to the NRC staff's 50.54(f) letter request. The licensee's PSHA shows that the primary contributor to the hazard at the  $10^{-4}$  annual frequency of exceedance is the host areal source zone (SBR). Distant fault sources in California and Mexico (associated with the San Andreas plate boundary) only contribute to the hazard at low spectral frequencies (1–2.5 Hz) and AFE greater than  $10^{-5}$ . To develop probabilistic site-specific control point hazard curves, the licensee followed Approach 3 of NUREG/CR-6728 (NRC, 2001). The licensee calculated the GMRS for the PVNGS using the site-specific rock hazard curves and soil amplification functions to calculate control point hazard curves (Figure 3.2-12a). Uniform hazard response spectra at the  $10^{-4}$ ,  $10^{-5}$ , and  $10^{-6}$  AFE were then derived from these control point hazard curves. The GMRS, shown in Figure 3.2-12b, was developed using the criteria in RG 1.208 (NRC, 2007).



**Figure 3.2-11 Basecase Profile for (a) Surface Response Spectra and (b) Site Amplification Factors for  $10^{-5}$  High Frequency Input Motion (Reference Rock Spectral Amplitudes of 0.01–1.50g) Using The EPRI Soil Material Model, and a Single Reference Rock to Local Rock Adjustment Function, Showing Spectra for 60 Individual Randomized Profiles (Green Lines), Median (Black Solid Line), and  $\pm 1\sigma_{in}$  (Black Dashed Lines). Redrafted from Figure 41 in Cadogan (2015a). Basecase Profile for (c) Median Amplification Factors and (d) Log Standard Deviation as a Function of Spectral Acceleration. Redrafted from Figure 42 in Cadogan (2015a)**

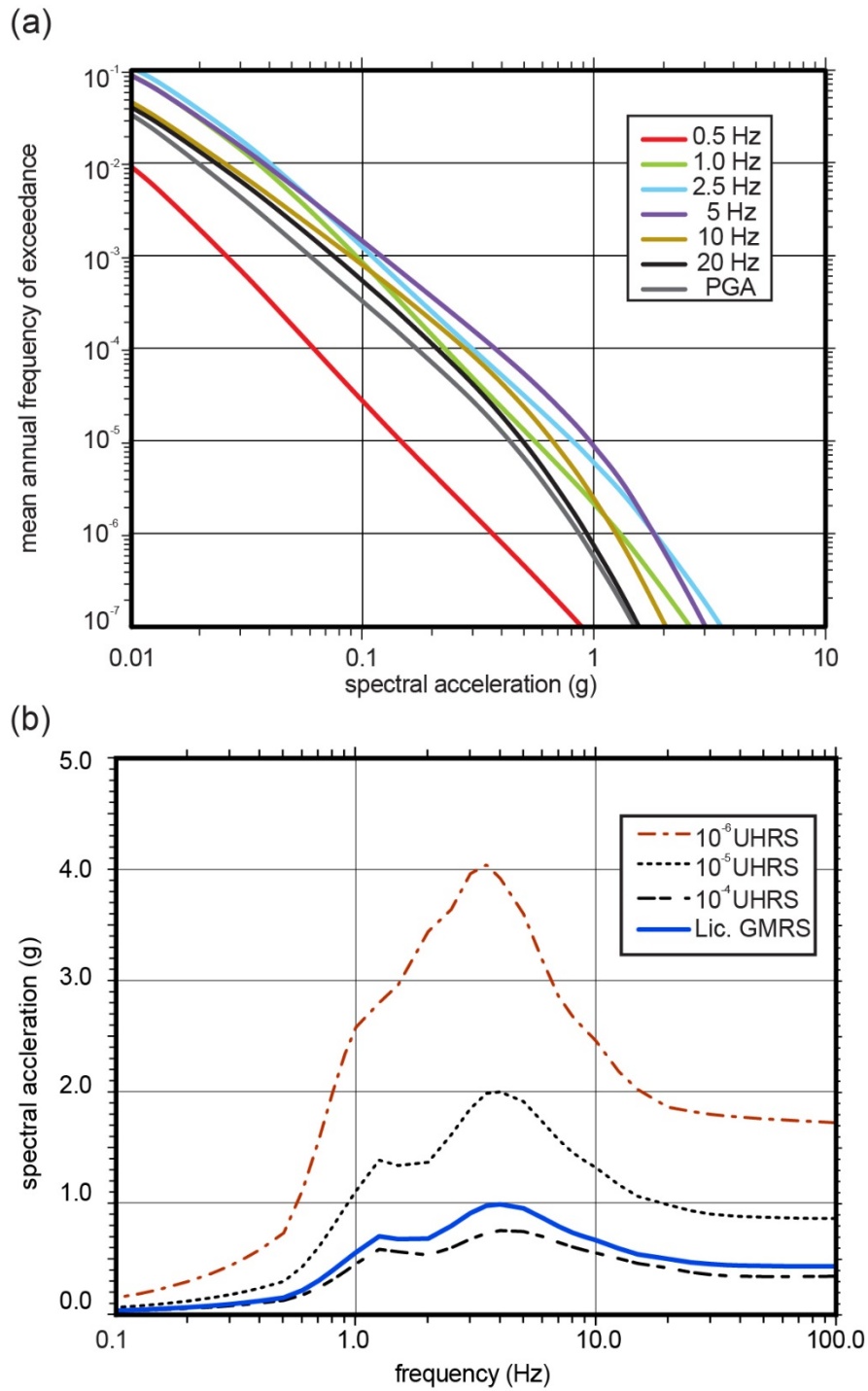


**Figure 3.2-12 (a) Total Mean Site-Specific Control Point Hazard Curves Plotted for Seven Spectral Frequencies, Based on the Data in Table 10 in Cadogan (2015a), (b) Uniform Hazard Response Spectra and the GMRS are Plotted Based on the Data from Table 11 in Cadogan (2015a)**

### 3.3. Diablo Canyon Power Plant

DCPP is located on an approximately 360-hectare [9,000-acre] site along the Pacific Coast just north of Avila Beach in San Luis Obispo County, California (Figure 3.3-1). It consists of two Westinghouse-designed, four-loop pressurized-water nuclear reactors and is operated by PG&E, hereafter referred to as “the licensee” in this subsection. The DCPP rests atop a relatively broad Quaternary<sup>1</sup> terrace on the southwestern margin of the Irish Hills, an area of moderate relief bordered by Point Buchon to the northwest, Point San Luis and San Luis Obispo Bay to the south, San Luis Obispo Creek to the east, Los Osos Valley to the northeast, and Morro Bay to the north (Figure 3.3-1). The Irish Hills are the northwestern part of the San Luis Range, which trends approximately west-northwest to east-southeast and separates the coastal town of Pismo Beach and the Santa Maria River Valley to the south from the Edna Valley to the north. The structure of the Irish Hills is a syncline<sup>2</sup>, with older Tertiary<sup>3</sup> or pre-Tertiary rocks of the late Mesozoic<sup>4</sup> age Franciscan Complex and Cretaceous sedimentary rocks forming the exposed limbs of the syncline and younger late Tertiary rocks of the Obispo, Monterey, and Pismo formation forming the syncline’s core (e.g., Lettis et al., 2004). The Franciscan Formation is a chaotic mélange of basaltic volcanic rocks (many of which have been altered to greenstone), radiolarian chert, sandstone, limestone, serpentinite, shale, and high-pressure metamorphic rocks. Bedrock directly beneath the DCPP site consists of the Miocene<sup>5</sup> Obispo Formation, which is a 400-m [1,300-ft]-thick strata of thin to moderately thick-bedded marine volcanic and volcanoclastic deposits. This bedrock is overlain by a thin veneer {1–2 m [3–6 ft] thick} of marine sands and gravels overtopping a relatively thick sequence {1 to several tens of meters [1 to 100 ft] thick} of nonmarine fluvial sands, gravel, and colluvium. The basal contact between the overlying marine sands and gravels and the underlying Obispo Formation is a gently southwestwardly sloping marine terrace platform that eroded during the last interglacial marine high-stand about 120 thousand years ago (ka)<sup>6</sup> (e.g., Hanson et al., 1994).

In Section 3.1 of the SHSR (PG&E, 2015a), the licensee described its seismic design bases for the DCPP site and specified that the SSE control point is at the finished grade level for the major structures at DCPP. This control point corresponds to an elevation of 26 m [85 ft] mean sea level, which the licensee used in its site response evaluations. DCPP has a unique and complex seismic design and licensing bases compared to other commercial NPPs, in that it is composed of four seismic design response spectra used in the seismic design of Units 1 and 2 (Figure 3.3-2). These are the (1) design earthquake, (2) double design earthquake, (3) Hosgri earthquake, and (4) Long-Term Seismic Program (LTSP) ground motions. Each spectrum is based on a different set of analysis assumptions (e.g., damping values) and different performance criteria. NUREG-0675, “Safety Evaluation Report Related to the Operation of Diablo Canyon Nuclear Power Plant, Units 1 and 2,” Supplement No. 7, issued May 26, 1978 (NRC, 1978), provides a more complete discussion of these spectra.

---

<sup>1</sup> The Quaternary is the most recent of the three geologic periods in the Cenozoic Era and includes the Pleistocene and Holocene epochs. It encompasses the last 2.58 million years of geologic time.

<sup>2</sup> A syncline is a concave-upward fold of rock layers in which the younger strata form the center of the fold, along the fold axis.

<sup>3</sup> Tertiary is the geologic period from approximately 65 Ma to 2.58 Ma.

<sup>4</sup> Mesozoic is the era of geologic time from approximately 250 to 65 Ma

<sup>5</sup> Miocene is the geologic epoch from approximately 23 to 5.3 Ma.

<sup>6</sup> ka stands for *kilo annum*, or thousands of years before present.

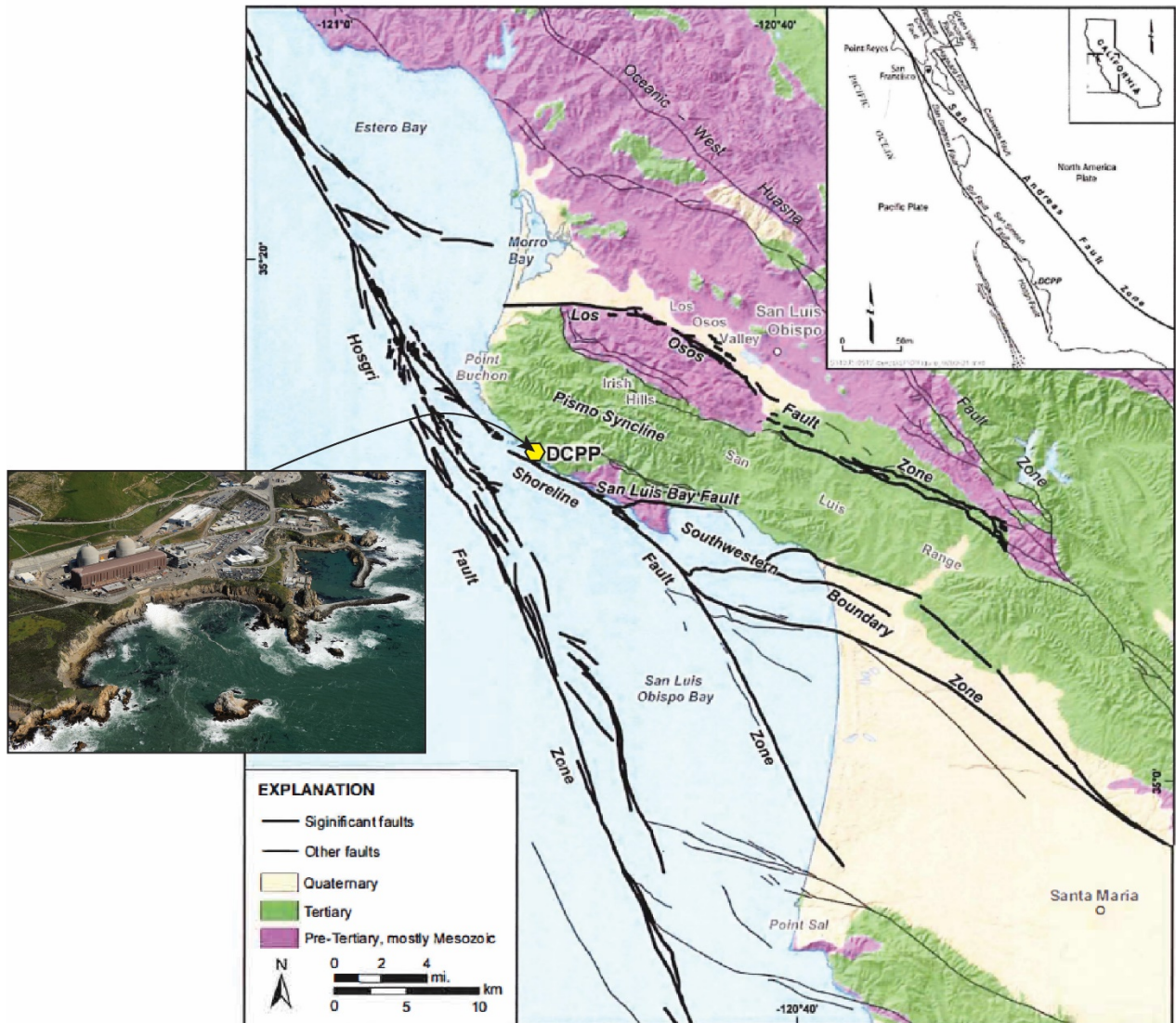


**Figure 3.3-1 Simplified Geologic Map of the Central California Coast Showing the Location of the DCPD, Reprinted from Figure 2.01 in PG&E (2015a). The Inset Image on the Left is an Aerial Photograph Showing the Power Plant on Top of the Late Quaternary Marine Terrace**

### 3.3.1. Seismotectonic Setting

The Irish Hills and the San Luis Range are located within a region of distributed transpressional dextral shear, situated between the eastern margin of the Pacific Plate and the western margin of the North American Plate and several bounding microplates, including the Sierra Nevada–Great Valley microplate. The San Andreas Fault Zone is located approximately 85 km [53 mi] northeast of DCPD (Figure 3.3-3), and it accommodates most of this tectonic motion. However, west of the San Andreas, an additional component of Pacific–Sierra Nevada plate motion is accommodated by fault slip on various Quaternary faults bounding crustal blocks and, to a lesser extent, by deformation within the blocks themselves.



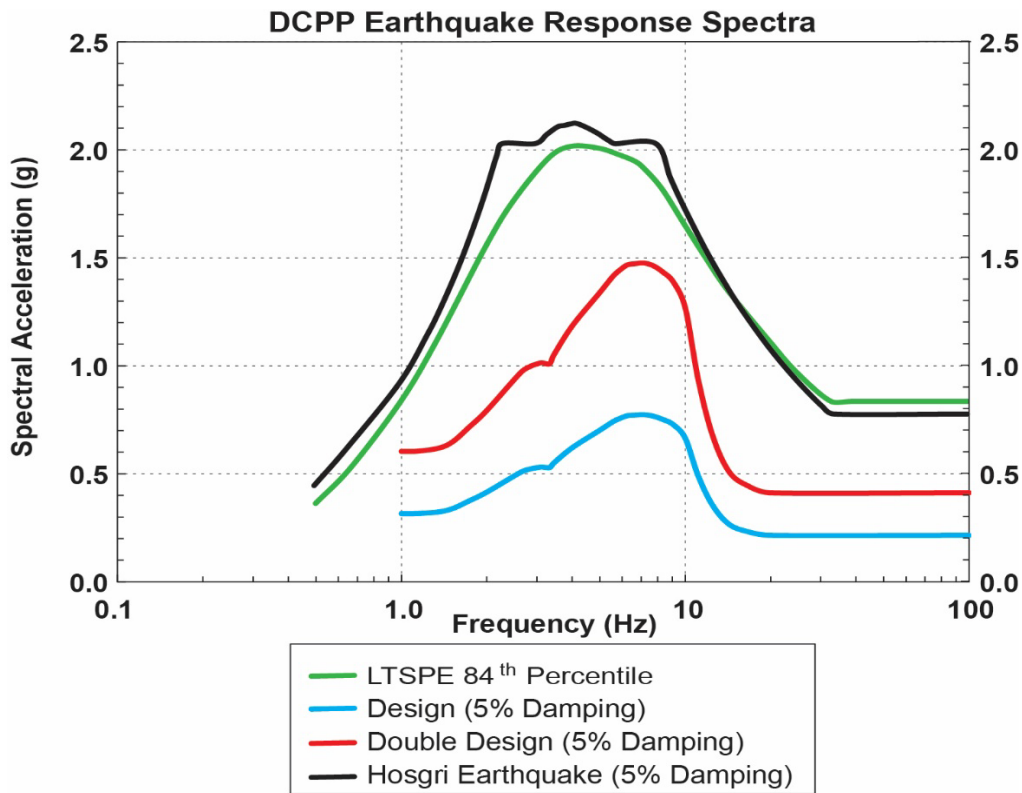


**Figure 3.3-2 Control Point Design Spectra for the DCP, Replotted from the Data Provided in PG&E (2015a)**

The San Luis Range and adjacent valleys and ranges are underlain by crustal blocks that together make up a larger tectonic element called the Los Osos domain (see Figure 1-1 in Lettis et al., 2004). Individual blocks within the Los Osos domain are bounded by northwest-striking reverse, oblique, and strike-slip fault zones. Of these, the most significant to the DCP seismic hazard assessment are the Los Osos, either because of the close proximity to the DCP or because of their seismic activity; faults of the “southwest boundary zone” (including the San Luis Bay, Wilmar Avenue, Los Berros, and Oceano fault zones); the Shoreline fault; and the Hosgri Fault Zone (HFZ) (Figures 3.3-3 and 3.3-4).

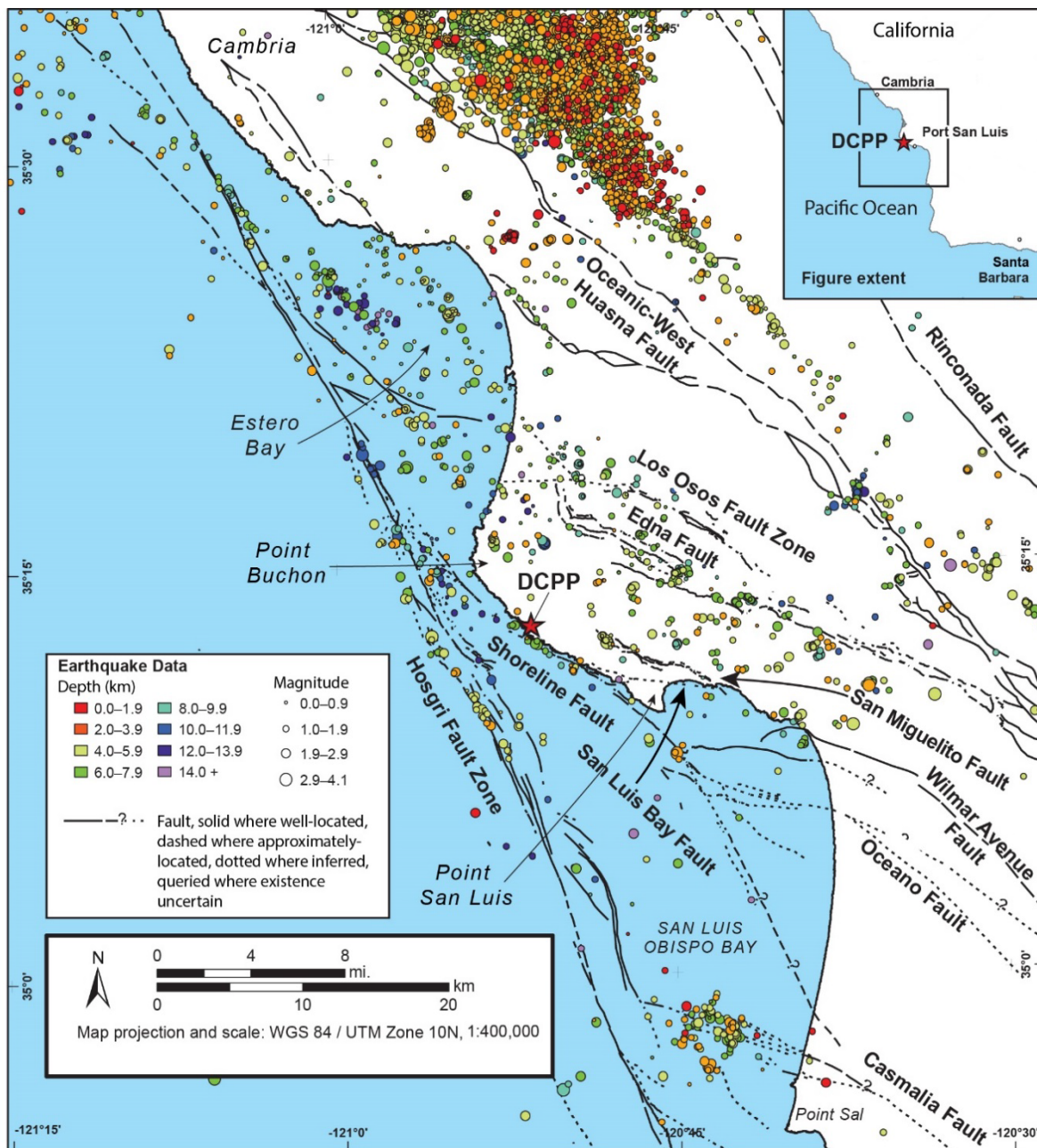


**Figure 3.3-3 Regional Seismicity Patterns from Recorded Earthquakes Between 1987 and 2013 Relative to the Mapped Traces of Known Faults, Redrafted from Figure 5-16 in PG&E (2015b)**

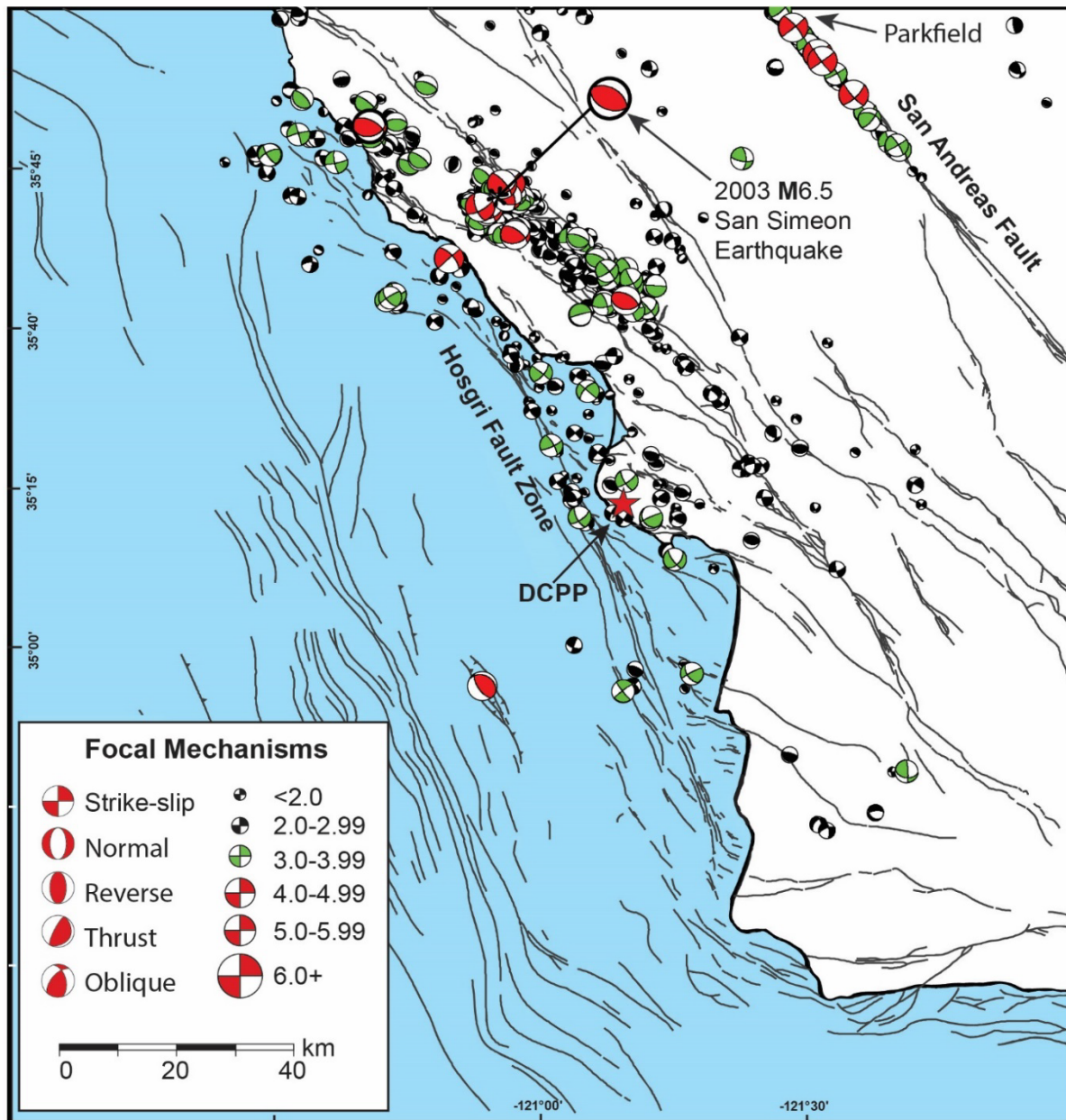


**Figure 3.3-4 Seismicity Patterns and Focal Mechanisms for the Central California Coastal Region Based on Hardebeck (2010) for Events Between 1987 and 2008. Redrafted from Figure 5-24 in PG&E (2015b)**

An important geological dataset used to interpret the recent tectonic and seismic history of the DCPP site is the marine terraces and their associated wave-cut platforms and paleoshorelines. These marine terraces develop at the shoreline impact zone, as waves cut into and erode rocks along the beach line. The identification and dating of these marine terraces in the DCPP region, coupled with the known chronology of sea-level elevations during different sea-level “stands” (i.e., periods of time when the sea level was stable long enough for a platform to be developed), allow geologists to estimate the uplift rates of the fault-bounded blocks of the California Coastal

Ranges, including the San Luis Range and the Irish Hills. The location, elevation, geomorphic characteristics, and ages of these features were mapped in detail by Hanson et al. (1994) and by the licensee as part of the LTSP (PG&E, 1988, 1991a). These studies showed that the uplift rate for the Irish Hills is approximately 0.2 mm/yr [0.008 in./yr], compared to a lower uplift rate of less than 0.1 mm/yr [0.003 in./yr] for areas south of the DCP, including San Luis Bay.

Earthquake focal mechanisms in south-central California (Figure 3.3-3) are mainly reverse and strike-slip, consistent with right-lateral transpression (e.g., McLaren and Savage, 2001; Hardebeck, 2010). In particular, focal mechanisms and the spatial distribution of seismic events along the Hosgri fault in the subsurface are predominantly right-lateral strike-slip on a fault zone that is nearly vertical to steeply east-dipping, with active seismicity to a depth of about 12 km [7.5 mi] (McLaren and Savage, 2001; Hardebeck, 2010; McLaren et al., 2008). A similar distribution of hypocenters illuminates the Shoreline fault. There is also relatively abundant seismicity recorded beneath the DCP and to the east of the Hosgri fault, with both reverse and strike-slip focal mechanisms. However, the rates of seismicity diminish considerably west of the Hosgri fault within the Santa Maria Basin. The 2003 *M*6.5 San Simeon earthquake, one of the largest recorded earthquakes in the central California Coastal Ranges (Figure 3.3-4), was primarily a reverse-faulting event that resulted from right-lateral transpression. McLaren et al. (2008) concluded that the fault patterns illuminated by the main shock, which was approximately 40 km [25 mi] north-northwest from the DCP, and aftershocks showed well-defined reverse slip on the Oceanic fault with antithetic back-thrusting, resulting in uplift of the Santa Lucia Range as a popup block. GPS data also show right-lateral shear and plate-normal convergence (DeMets, 2012; DeMets et al., 2014; Murray, 2012; Bird, 2012). Based on these GPS data, the total horizontal slip budget available for faults west of the Oceanic fault is 1–3 mm/yr [0.04–0.12 in./yr]. Plate-normal rates are significantly lower, on the order of 0.2–0.5 mm/yr [0.008–0.02 in./yr]. For comparison, horizontal slip of the San Andreas fault in central California is estimated to be 25–36 mm/yr [9.8–14.2 in./yr] (e.g., Sieh and Jahns, 1984; Titus et al., 2005; Toké et al., 2011; Titus et al., 2011).

### **3.3.2. Senior Seismic Hazard Analysis Committee Process**

The licensee developed the DCP PSHA used to develop the ground motions for reference rock conditions in two parts. The licensee used the SSHAC process to develop a site-specific SSC model based on the geological, tectonic, and seismological conditions in the central California coast region. A single GMC model was developed from the SWUS GMC model, a SSHAC study cosponsored by PG&E and APS. The licensee adjusted the SWUS GMC model using onsite strong ground motion recordings and site-specific geotechnical and geophysical measurements to develop control point hazard curves at the specified reference horizons for the DCP.

The DCP SSC and SWUS GMC SSHAC studies followed the established SSHAC Level 3 process, including three structured workshops and several formal and informal working meetings among the SSC and GMC TI Teams. Details of the DCP and SWUS GMC SSHAC studies, including the workshops, NRC observations at the workshops, and the review conducted by the SSHAC PPRP appear in the licensee's SHSR (PG&E, 2015a); SSC model report (PG&E, 2015b); the SWUS GMC report (GeoPentech, 2015); and the NRC's SA (NRC, 2016a).

### 3.3.3. Seismic Source Characterization

The SSC for the DCPD site was the first step in developing the site-specific PSHA. Specifically, the DCPD SSC was organized to identify and characterize geologic faults and areal source zones that could potentially generate earthquakes that could affect the site. To accomplish this, the DCPD SSC TI Team cataloged historical and instrumented seismicity surrounding the site and analyzed a wealth of geological, geophysical, and seismic imagery data to define and characterize the fault sources and areal source zones that encompass and surround the site. For each areal and fault source, the SSC determined the magnitude, rate, style of faulting, and relative distances from the source to the DCPD control point elevation.

One of the unique features in the DCPD SSC model was the way the SSC TI Team developed a geometric and kinematic framework to model the complexities of faulting. Earthquakes near the DCPD are the result of a combination of tectonic compression and clockwise horizontal shear, which is often referred to as dextral transpression. Earthquakes in transpressive tectonic environments often involve complex ruptures, with both dip-slip and strike-slip motions on one or more connected faults. To better understand the complex pattern of faulting at the DCPD, the SSC TI Team evaluated fault rupture patterns from nine historical earthquakes in regions with similar transpressive tectonic settings. Section 9.2.1.5 of the SSC model report (PG&E, 2015b) describes this survey of historical rupture patterns on complex transpressive faults, with a summary in Table 6.1 of the same report. This set of analog fault ruptures offered the SSC TI Team useful insights into the potential for complex fault ruptures and provided an important underlying technical basis to support the way in which these complex ruptures were characterized in the SSC model for the region surrounding the site.

#### 3.3.3.1. Data and Supporting Studies

Since licensing activities in the 1970s, PG&E has maintained an active seismic research program, working with other State and Federal agencies, including the USGS. Hence, the SSC SSHAC study is supported by an extensive database that consists of several generations of scientific and engineering technical information. This research program was developed in response to license condition 2.C.(7), which the NRC imposed on the licensee when it issued the operating license for Unit 1 in 1984. Specifically, the license condition required the licensee to reevaluate the seismic design bases of the DCPD. As part of the ensuing LTSP, PG&E committed to an ongoing effort to study seismic issues and to perform periodic seismic reviews of the DCPD (PG&E, 1991b, 1991c). To date, data acquisition for the LTSP has included (1) earthquake records from seismic monitoring, including the PG&E Central Coast Seismic Network, (2) high-resolution potential field data (magnetics and gravity), (3) seismic reflection data, and (4) topographic and bathymetric measurements.

This commitment to ongoing research and review included the Central Coastal California Seismic Imaging Project (CCCSIP) offshore and onshore studies, independent research by USGS investigators under the PG&E–USGS Cooperative Research and Development Agreement (CRADA) program, licensee-funded studies to university researchers and consultants, and independent research by university researchers and the California Geological Survey. Through the CRADA program, important geological, geophysical, and seismological data were acquired from 2008 through 2011, with an emphasis on characterizing the Shoreline fault (PG&E, 2011). In addition to recompiled and new onshore and offshore gravity and magnetic surveys, this dataset includes updates to the geological maps of the DCPD site, new high-resolution, single-channel reflection profiles (Sliter et al., 2010), and multibeam echo-sounder surveys of the seafloor bathymetry in the nearshore regions from Estero Bay to

San Luis Obispo Bay. The Seafloor Mapping Lab at the California State University Monterey Bay acquired the multibeam echo-sounder data (CSUMB, 2012).

In 2006, California Assembly Bill 1632 directed the California Energy Commission to assess the potential vulnerability of the DCPD to a major disruption due to a seismic event. To support this assessment, the licensee collected additional onshore and offshore geophysical data to reduce uncertainties in the characterization of seismic sources using current state-of-the-practice methods and approaches. This geophysical program, which operated from 2011 to 2014, included both 2D and three-dimensional (3D) seismic reflection data in the offshore and onshore regions near the DCPD (PG&E, 2014). Within this phase of data collection, the licensee collected a significant amount of new onshore and offshore seismic images from 2D and 3D low-energy seismic signals (PG&E, 2014). Specifically, the low-energy seismic signal surveys were designed to image near-surface features of the Hosgri fault north of Point Buchon and the Shoreline fault in San Luis Bay. In addition, the licensee acquired high-resolution tomographic data within a 1-km<sup>3</sup> [0.24-mi<sup>3</sup>] volume directly beneath the DCPD site. This high-resolution seismic tomographic data provide a detailed characterization of compressional-wave and shear wave velocity structure beneath the DCPD, which was used in the licensee's site response analysis (see Section 3.3.7 of this report).

In 2012, the USGS acquired additional high-resolution multibeam images of the Hosgri fault in Estero Bay (Hartwell et al., 2013). As part of this survey, the USGS remapped a linear southwest-facing bathymetric slope, which is referred to as the cross-Hosgri slope. This feature is important because it provides one of the constraints on the slip rate of the Hosgri fault. Johnson et al. (2014) interpret this feature as the shoreface of a Pleistocene<sup>7</sup> sand spit that has been offset by strike-slip motion on the Hosgri fault.

Through the CRADA program, the USGS also compiled a database of earthquake hypocenter and focal mechanism data that was used to support fault characterizations (Hardebeck, 2010, 2013). Within this set of studies, refinements were made to the locations of the earthquake hypocenters, based on an advanced technique called double-difference tomography, to develop a 3D crustal velocity model (Zhang and Thurber, 2003).

In addition to these datasets, the licensee-developed database for the SSC SSHAC study included new geologic mapping and geomorphic analysis to support the SSC TI Team's characterization of the Los Osos, Cambria, and San Luis Bay faults, including constraints on fault slip rates. These data included updates to fluvial and marine terrace characterizations, revised geologic maps, and subsurface data compiled from oil and gas wells, California Department of Transportation wells, and existing geotechnical studies. This information is detailed in the CCCSIP report (PG&E, 2014).

### 3.3.3.2. *Complex Fault Sources and Fault Ruptures*

Based on the set of fault analogs developed by the SSC TI Team, the SSC model captures the potential for multifault ruptures that explicitly account for the inherent complexities and constraints of connected fault ruptures. One of the more unique modeling approaches adopted in the SSC model is the grouping of individual faults into fault geometry models. Specifically, the licensee considered two main fault sources: (1) the Hosgri fault, with possible rupture connectivity to the San Simeon and San Gregorio faults and (2) a group of three connected faults (Los Osos, San Luis Bay, and Shoreline), which are grouped into a collective fault source

---

<sup>7</sup> Pleistocene is the geologic period between 11,500 years ago and 2.5 Ma.

known as the San Luis Pismo Block (SLPB). For the SLPB, the SSC TI Team also developed three alternative fault-geometry models (i.e., Outward Vergent, Southwest Vergent, and Northeast Vergent) to account for the alternative interpretations in how uplift of the San Luis Range occurs geologically through different combinations of thrust, reverse, and oblique strike-slip faulting. These combinations of fault sources and fault linkages for the alternative fault geometry models are shown in plates 9-1 and 9-2 of the SSC model report (PG&E, 2015b).

The SSC TI Team used the alternative fault-geometry models to account for epistemic uncertainty in the nature and style of faulting, especially the potential for a blind thrust fault beneath the Irish Hills and directly beneath the DCP. The SSC model also evaluates single fault segment ruptures, multisegment fault ruptures with a single sense of fault slip as either linked or splayed, and multisegment fault ruptures with different senses of fault slip as complex. The SSC TI Team modeled slip on these linked, splayed, or complex ruptures in terms of a slip distribution budget that is consistent with geologic and tectonic constraints on the regional deformation. Specifically, the SSC TI Team constrained the amount of slip rate based on the maximum rates that could occur given the known rates of relative plate motion between the Pacific and North American plates and the uplift rates of the Irish Hills, derived from fluvial and marine terraces near the DCP and the paleosea-level model for California terraces (e.g., Muhs et al., 2012).

#### 3.3.3.3. *Seismic Source Characterization Modeling Approach*

The SSC TI Team developed an overall logical framework to evaluate active faults and associated faulting characteristics, including fault slip, fault rupture, and faulting recurrence. It used similar logic to define the virtual faults used to account for seismicity in the areal source zones.

The SSC TI Team characterized fault sources based on their location, geometry, depth extent, slip sense, slip rate, magnitude-frequency distribution, and probability of occurrence of an earthquake within a given time period. The SSC TI Team characterized fault sources as either primary faults (Hosgri, Shoreline, Los Osos, and San Luis Bay faults) or connected faults (local and regional faults that directly connect to the primary faults as part of a potentially complex fault rupture). In this approach, the SSC TI Team considered (1) rupture of a single fault segment, (2) rupture of two or more adjacent fault segments on the same fault, or (3) rupture of adjacent primary and/or connected fault segments. These ruptures may involve a single sense of slip (e.g., all strike-slip) on all segments or different senses of slip (e.g., reverse and strike-slip) on multiple fault segments.

Based on the segments for the four primary faults defined in the fault-geometry models and the faulting characteristics of the connected faults, the SSC TI Team derived a suite of fault rupture sources to capture the full range of possible rupture scenarios. The various combinations of rupture sources with each fault-geometry model form a rupture model (i.e., the combinations of all fault segments that can rupture together within a single fault geometry model). Next, the SSC TI Team assigned slip rates to the various fault-rupture models by allocating the available fault slip, which is based on the measured slip rates for the individual faults, among the network of faults described in the fault-geometry model.

For this approach, the SSC TI Team used the slip rate determined from evidence of fault slip from geological, geophysical, or seismological information as the available slip-rate budget, which was then distributed among the various rupture sources. In this slip-rate allocation model, a slip rate for each rupture source is assigned to each fault source such that, when the

contributions from all rupture sources are summed, the combined slip rate equals the target slip-rate budget for that particular fault within that rupture model. The SSC TI Team developed magnitude distribution models for each rupture source using the fault-area scaling relationships of Hanks and Bakun (2008, 2014). The SSC TI Team also used three different probability distributions to define the magnitude frequency distribution based on the characteristic model of Youngs and Coppersmith (1985); the Wooddell, Abrahamson, Acevedo-Cabrera, and Youngs (WAACY) model (Wooddell et al, 2014); and the simple maximum magnitude model (Wesnousky et al., 1983).

The SSC TI Team defined areal sources based on source boundary,  $M_{max}$ , and magnitude-frequency distributions. Within the areal source that encompasses the DCP, the SSC TI Team used a series of virtual faults to model potential fault ruptures within the source zone. For the more distant areal source zones, the SSC TI Team modeled the occurrence of earthquakes as simple point sources. The SSC TI Team also characterized the San Andreas fault and other regional faults, including those derived from the UCERF3 model (Field et al., 2013). The SSC TI Team evaluated the occurrence of past earthquakes from four earthquake catalogs (see Appendix F to the SSC model report (PG&E, 2015b) to develop distributions of the size and frequency of earthquakes the areal source zones, with magnitudes converted to moment magnitude. In addition, the SSC TI Team used the truncated exponential (Gutenberg and Richter, 1956) magnitude frequency distribution to define the recurrence relationships for future earthquakes with a-value and b-value determined from the seismicity rates indicated by the four earthquake catalogs.

#### 3.3.3.4. *The Hosgri Fault Source*

The Hosgri fault is located just a few kilometers offshore south-central California and forms the eastern boundary of the offshore Santa Maria Basin (PG&E, 1988; Clark et al., 1991; Steritz and Luyendyk, 1994). Characterization of the fault is primarily derived from traditional marine seismic reflection data and single-channel, high-resolution sparker data. The Hosgri fault has been mapped along its entire length using petroleum industry multichannel seismic-reflection data that images the traces of the fault to a depth of 3 km [2 mi] beneath the seafloor (PG&E, 1988, 1991a; Willingham et al., 2013). Significant sections of the Hosgri fault also were remapped using single-channel, high-resolution USGS sparker data (Johnson and Watt, 2012; PG&E, 2014). In the immediate vicinity of the DCP, the Hosgri fault trends N25° to N30° W and is made up of multiple fault traces, with individual segment lengths up to 18 km [11.2 mi] that overlap en echelon, forming a fault zone up to 2.5 km [1.5 mi] wide. In the seismic reflection profiles, fault traces appear to be vertical to steeply dipping in the uppermost sedimentary section, but some of the fault traces about 1 km [0.6 mi] below ground surface appear to be subvertical or dipping steeply to the east.

The SSC TI Team modeled the Hosgri fault source with three alternative fault geometries, which were based mainly on different interpretations of the surface map traces and the down-dip profile of the fault surface based on seismic images and relocated hypocenters. The main difference in the three geometry models is the fault dip, which ranges between 75 and 90 degrees.

Much of the information the SSC TI Team used to derive the geologic ages of fault slip and associated uplift was from the detailed chronology developed in PG&E (2013). This chronology is based on evidence of the effects of sea-level changes on the geologic record that occurred in response to glacial cycles during the last several million years. In essence, sea levels fell and were low during the glacial periods, when much of Earth's water was sequestered in glacial ice.



Sea levels rose and were high during periods when the global climate warmed and these glaciers melted. The SSC TI Team relied on this chronology in two ways. First, the SSC TI Team used the relative vertical displacement of paleoshorelines preserved in the Irish Hills to determine uplift rates of the San Luis Range. Second, the SSC TI Team identified stream channels that were cut into the paleoshorelines during the lowstands (i.e., periods when sea levels were low) and were subsequently buried by sediments and preserved in the offshore sedimentary record during the next highstand (i.e., periods when sea levels were high). Some of the seismic images revealed that these paleochannels subsequently were offset by right-lateral slips on the Hosgri fault, where the paleochannels crossed the fault trace. The amount of offset of these paleochannels (either best estimate or range of best estimates) was used to quantify the cumulative amount of fault slip since the time when the paleochannels first eroded into the paleoshorelines.

The SSC TI Team determined slip rates at four locations along the Hosgri fault trace (Figure 3.3-5): (1) an offset marine terrace strandline near San Simeon (referred to as the Oso Terrace), (2) offset of a sand spit approximately 11.5 ka between Morro Bay and Point San Simeon (referred to as the Cross-Hosgri slope), (3) right-lateral separation of a buried paleochannel in Estero Bay, and (4) right-lateral separation of a buried paleochannel near Point Sal. Median slip rates based on these four offset measurements, and ages of the offset features, range between 0.8 mm/yr [0.31 in./yr] (Point Sal) and 2.5 mm/yr [0.10 in./yr] (Cross-Hosgri slope), with a weighted mean from all four sites of 1.7 mm/yr [0.67 in./yr]  $\pm$  0.7 mm/yr [0.03 in./yr] ( $\pm$  1 standard deviation).

#### *3.3.3.5. NRC Staff Independent Evaluation of the Hosgri Slip Rate*

In the SSC model, the Hosgri fault is characterized by both geometric and seismic parameters, including fault length, down-dip width, dip angle, maximum and characteristic magnitude, and the magnitude distribution model. As described in the SSC model report (PG&E, 2015b) and confirmed by the NRC staff evaluation (NRC, 2015c), the Hosgri fault slip rate or earthquake recurrence rate (and uncertainty in these values) is the dominant contributor in the SSC model to the resulting seismic hazard at the DCP. This is often the case for large fault sources because fault-slip rate results directly from the seismic moment rate and because the intensity (relative position of the hazard curve to the x-axis) scales proportionally with slip rate. Consistent with a risk-informed regulatory review, the NRC staff's evaluation of the SSC model focused on conducting an independent analysis of information that can be used to evaluate the slip-rate estimates for the Hosgri fault.

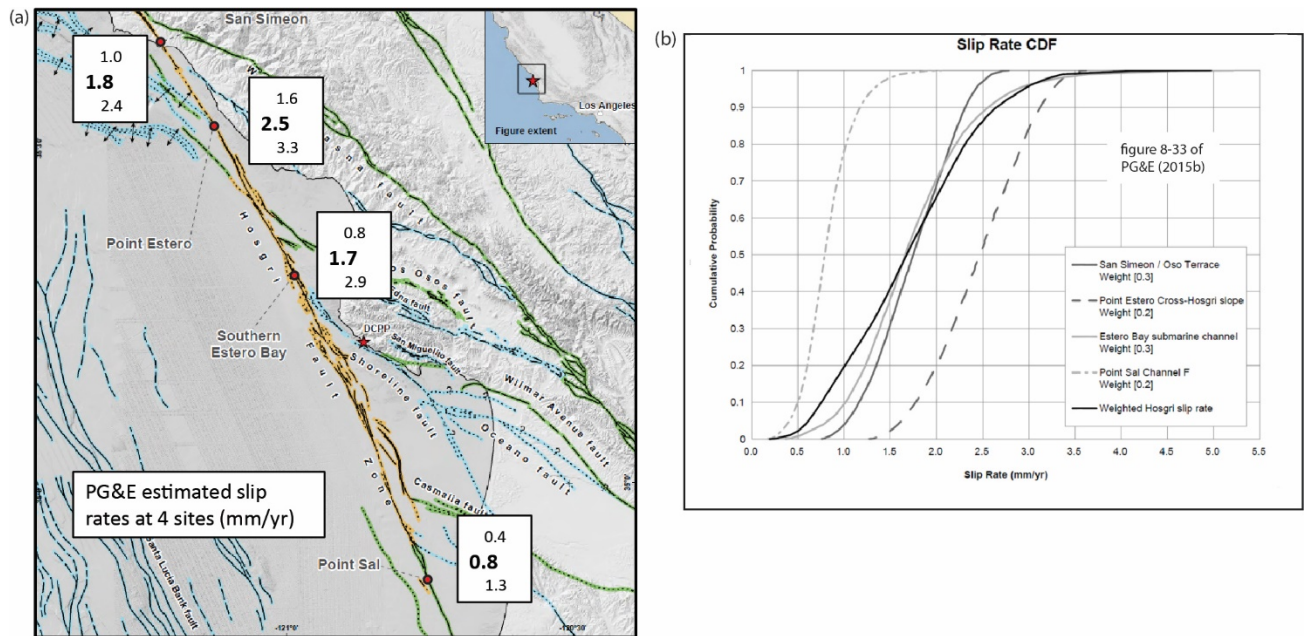


**Figure 3.3-5 Slip-Rate Estimates for the Hosgri Fault from the SSC Model Showing (a) the Locations of the Four Sites with Cumulative Slip-Rate Probabilities and (b) the Mean Cumulative Slip-Rate Curve. Both Figures were Derived from Figures 8-13 and 8-33 in PG&E (2015b)**

In reviewing offshore seismic imaging data, the NRC staff identified that this half-graben formed where displacement on the Hosgri fault appears to be transferring its slip to the San Simeon fault along a right-stepping extensional pull apart. These kinds of transtensional segments of the Hosgri fault zone offshore from Cambria—northwest of the DCP—have also been identified using analysis of high-energy, multichannel seismic-reflection data (PG&E, 1988, 1990; Willingham et al., 2013). One of these features is an extensional half-graben bounded by a 15-km [9.3-mi]-long extensional fault named the Half Graben fault (Figure 3.3-6). This half-graben and associated extensional fault zone is situated a few kilometers offshore, 23–40 km [14–25 mi] northwest of the DCP. This fault lies entirely between the traces of the Hosgri and San Simeon faults and has been interpreted as part of a pull-apart basin developed within a right step between two right-lateral strike-slip faults, the Hosgri Fault Zone to the south and the San Simeon fault to the north (DiSilvestro et al., 1990; Lettis and Hanson, 1991; Hanson et al., 2004).

As the pull-apart developed, sediments accumulated along the fault, infilling the available volume created by the extensional pull-apart. Because the relative rate of sediment accumulation within the pull-apart basin is controlled by the rate of fault slip on the bounding fault, the growth of this pull-apart, as determined from the rate of sediment growth, provides an independent estimate of the Hosgri fault slip rate (Figure 3.3-7). For the independent analysis, the NRC staff acquired two sets of seismic reflection data from the licensee, one based on the USGS 2008–2009 high-resolution sparker tracklines and one from the 1986 joint PG&E and Alaska COMAP lines. Collectively, these seismic reflection data make up 24 profiles across the Half Graben fault. McGinnis et al. (2016) provide the details of the NRC staff analysis and results.

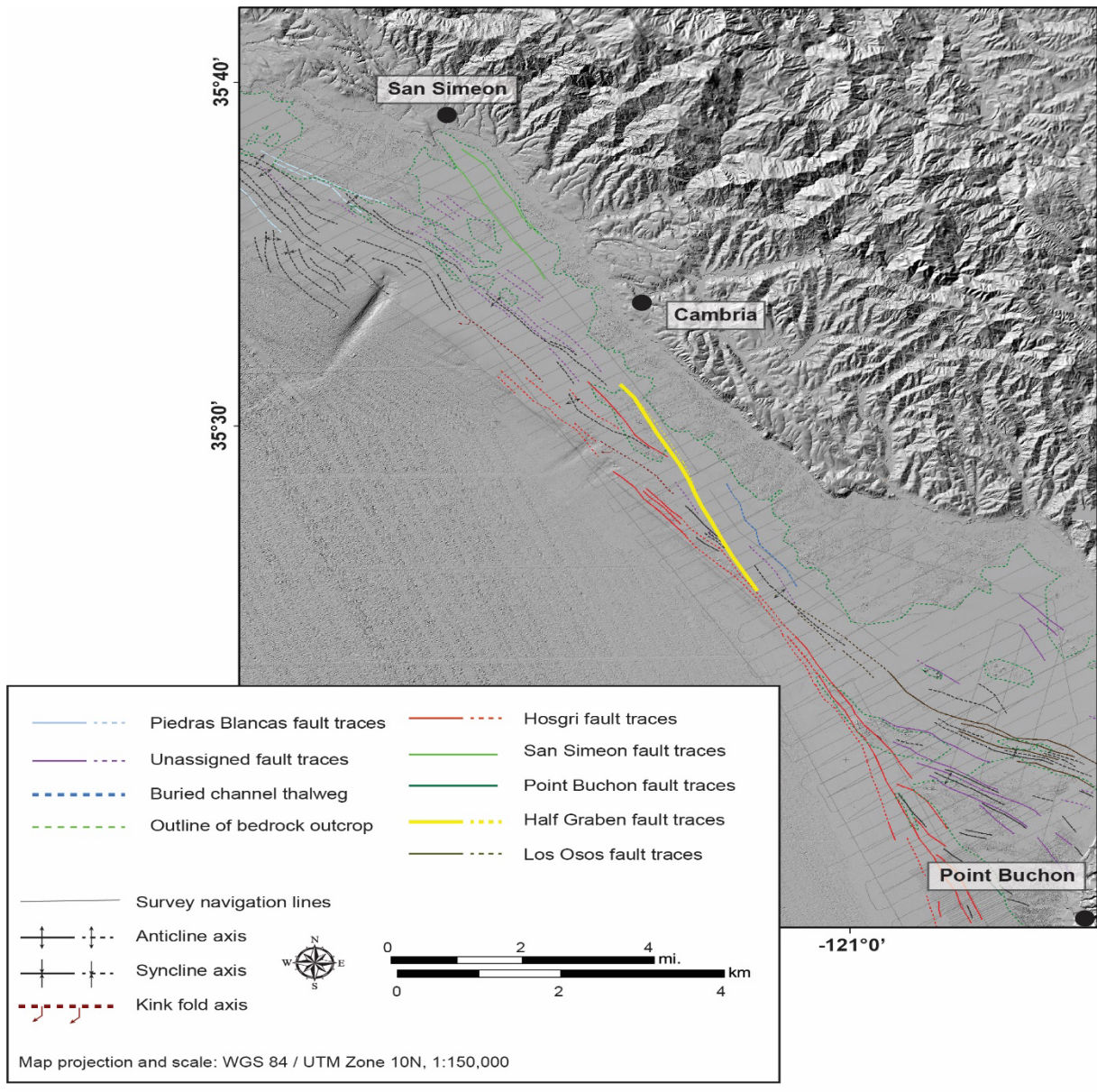


**Figure 3.3-6 Location Map of the Half Graben Fault, Modified from Figure 1.2-1 in PG&E (2014), Showing Full Trace of the Half Graben Fault with Respect to the Hosgri Fault Trace**

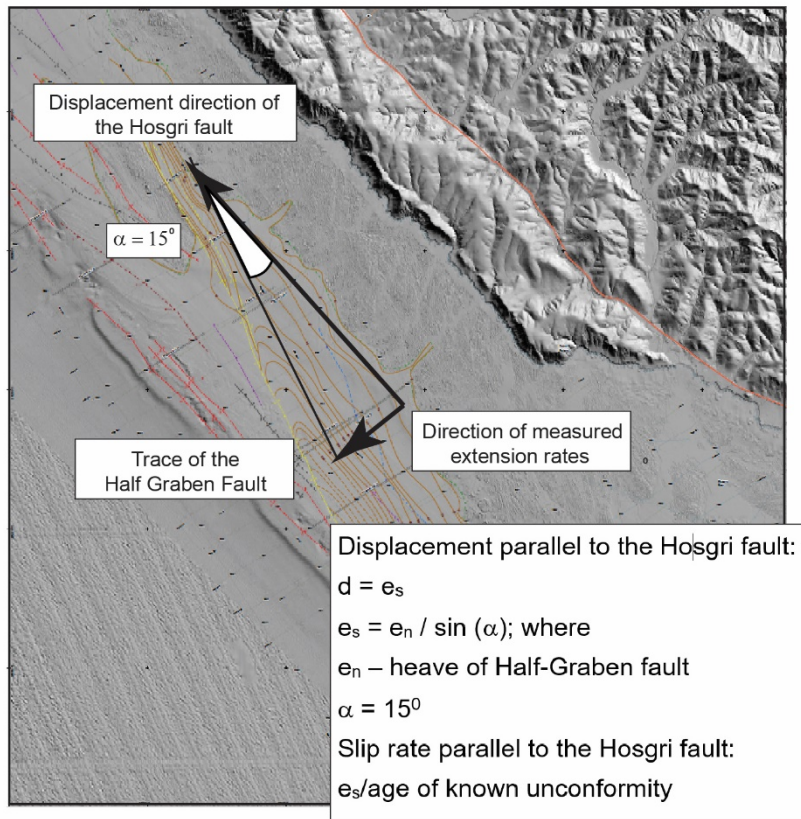


**Figure 3.3-7 Map View of the Principal Geometric Elements of the Hosgri and Half Graben Faults Showing how the Magnitude and Slip Rate of Hosgri-Parallel Slip are Calculated from the Extension with the Half Graben Pull-Apart Basin. Heave is the Measured Horizontal Offset of the Fault**

Figure 3.3-8 shows one of these seismic image profiles, and the NRC staff interpreted the images to show that the extensional pull-apart basin is asymmetric, shallowing to the northeast and containing a series of southwest-dipping reflectors. These reflectors illuminate sediment layers that thicken toward the southwest and record the progressive accumulation of sediment into the developing half-graben. With each increment of transpressional right-slip on the Hosgri fault, the half-graben basin deepens and entraps more sediment. As defined in Figure 3.3-7, this temporal record of sediment accumulation provides a measure of the past motion of fault slip and fault-slip rate. The NRC staff used these geometric relationships to derive a slip rate for the Hosgri fault.

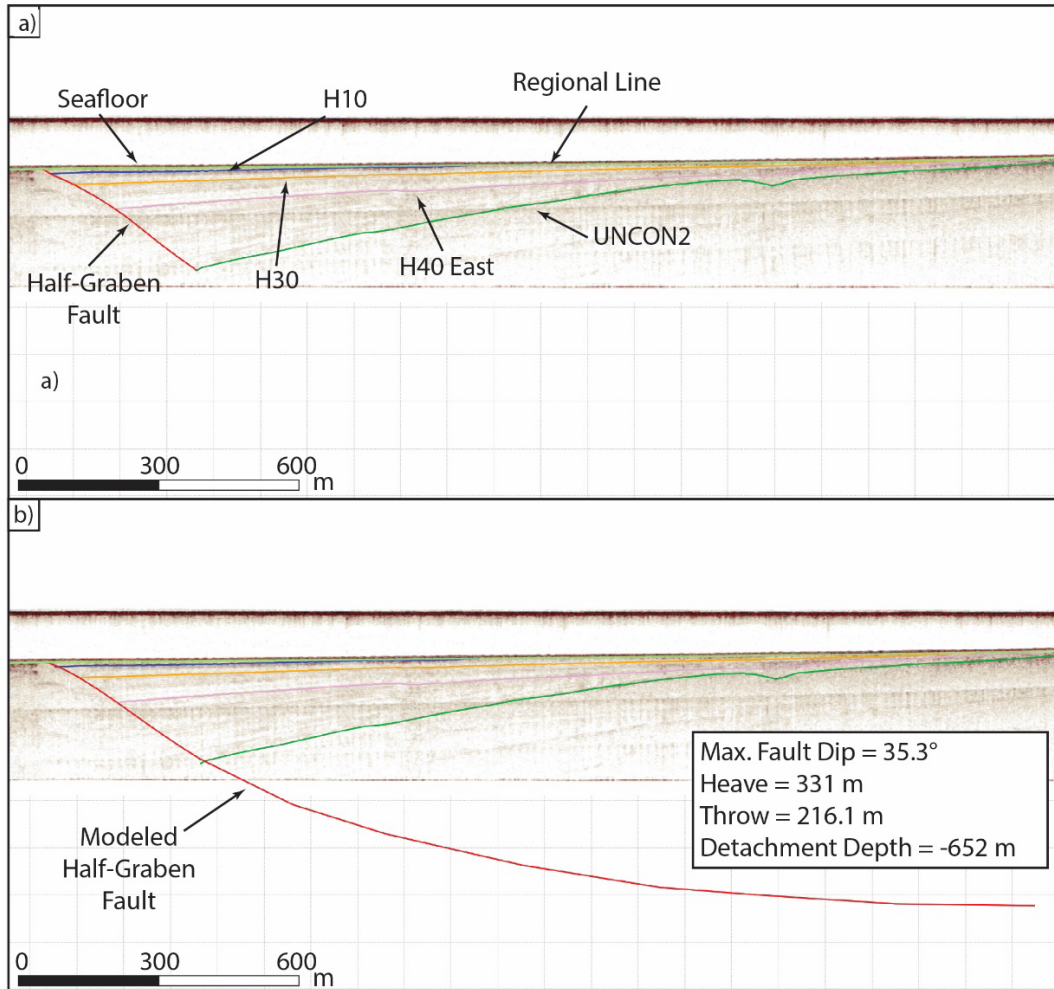


**Figure 3.3-8 An Example Seismic Reflection Line from the USGS 2008–2009 High-Resolution Sparker Tracklines, Showing (a) the Initial Unconformity Horizon and Fault Interpretations, along with the Four Regional Unconformities (H10, H30, H40 East, and UNCON2) and (b) the Modeled Half Graben Fault Geometry and Attributes**

The NRC staff observed four regional unconformities<sup>8</sup> within the seismic image profiles. The licensee identified and described these in PG&E (2014), and the SSC TI Team relied upon these unconformities to constrain geologic events in the SSC model report (PG&E, 2015b). These four unconformities are (1) Pleistocene age unconformities H10 (0.020 Ma), (2) H30 (0.135 Ma), (3) H40 East (0.625 Ma), and (4) a basal Pliocene unconformity UNCON2 (2.58 Ma).

Based on the geometric constraints of the fault system and fault growth, the NRC staff concluded that the slip rate on the Hosgri fault appears to increase from a Pliocene rate of

<sup>8</sup> An unconformity is a buried erosional or nondepositional surface-separating stratum of different ages. It indicates that sediment deposition was not continuous and that the older layer was exposed to erosion for an interval of time before deposition of the younger layer. These unconformities correspond to changes in sea level due to climate cycles

0.2 mm/yr [0.008 in./yr] to a late Quaternary rate of 2.2 mm/y [0.09 in./yr] (Figure 3.3-9). The late Quaternary rate is consistent with the median rate of 1.7 mm/yr [0.67 in./yr] derived by the SSC TI Team and is within the range of uncertainty in slip rate described in Section 3.3.3.4.

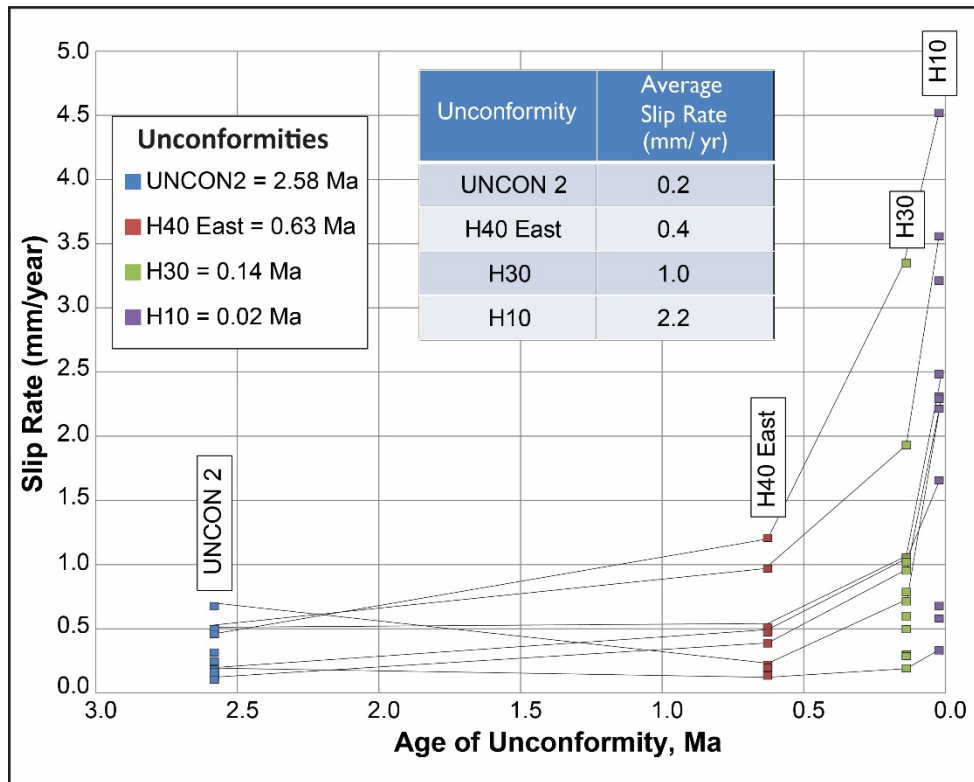


**Figure 3.3-9** Calculated Horizontal Slip Rate for the Hosgri Fault Over Time. Black Line Connects Each Slip Rate for Seismic Lines that Contain All Four Unconformities. The Inset Chart Shows the Average Slip Rate Based on Each Age Unconformity

### 3.3.3.6. Shoreline Fault

The Shoreline fault is a 16–23 km-long [10–14 mi-long] fault that bounds most of the western margin of the Irish Hills. At its closest approach, the fault is located approximately 600 m [1,969 ft] from the DCCP. The fault was identified from a number of geological and geophysical observations, including the nearly vertical alignment of earthquake hypocenters (Hardebeck, 2013) that coincides with linear magnetic anomalies revealed as part of the high-resolution aeromagnetic data (e.g., Langenheim et al., 2009).

The NRC staff also conducted a detailed review of the Shoreline fault. This fault generated significant interest among the NRC staff and the public when the licensee, working in collaboration with the USGS, identified it as a possible new fault very close to the DCCP site in 2008. In January 2011, the licensee submitted to the NRC “Report on the Analysis of the Shoreline Fault Zone, Central Coastal California: Report to the U.S. Nuclear Regulatory Commission” (PG&E, 2011). This report provided new geological, geophysical, and seismological data used to assess the potential seismic hazard of the Shoreline fault. This new

information supplements or improves the geological, geophysical, and seismological information near the DCPD site under the PG&E LTSP. The NRC staff evaluated the new information and developed a deterministic seismic hazard assessment for comparison to the existing DCPD design spectra. The results of the NRC staff analysis, which are documented in NUREG-2117 (NRC, 2012c), indicate that deterministic seismic-loading levels predicted for all the Shoreline fault earthquake scenarios developed and analyzed by the NRC are at, or below, those levels for the Hosgri earthquake and LTSP ground motions.

For the DCPD SSC SSHAC study, the licensee obtained and evaluated new offshore seismic images to further constrain the spatial extent and slip rate of the Shoreline fault. The overall results of the licensee's evaluation are consistent with earlier published results (e.g., PG&E, 2011; NRC, 2012d). The SSC TI Team also concluded that the Shoreline fault was not a significant contributor to the seismic hazard at the site, especially when compared to the Hosgri fault. Some of the new seismic reflection images provided sharp and even vivid details of fault morphology, showing a clear fault trace in the seafloor as the fault cuts across several paleochannels that are now buried on the submerged paleoterrace (Figure 3.3-10). Slip rates for the Shoreline fault, based on observed small-to-marginal displacements of these paleochannels, are similar (about 0.1 mm/yr [0.003 in./yr]) to many of the other secondary faults in the DCPD region and an order of magnitude less than the Hosgri fault.

#### 3.3.3.7. *Areal Sources*

In addition to the fault sources, the SSC TI Team developed three areal sources (regional, vicinity, and local) to model the temporal and spatial distribution of seismicity where there was little or no geologic or geophysical evidence that allowed past earthquakes to be associated with known faults. Because past hazard sensitivity analyses showed that hazard at the DCPD is dominated by ground motions caused by earthquakes occurring at close distances on the primary fault sources, the SSC TI Team used simplified approaches for modeling the areal source zones.

To develop distributions of the size and frequency of earthquakes in all three areal source zones, the SSC TI Team evaluated the occurrence of past earthquakes from the four earthquake catalogs described in Appendix F to the SSC model report (PG&E, 2015b). The SSC TI Team then used the methodology adopted in NUREG-2115 (NRC, 2012b) to develop recurrence parameters to model the seismicity in each areal source. The SSC TI Team modeled the occurrence of potential earthquakes in the regional and vicinity areal source zones as point sources. The SSC TI Team also used the gridded seismicity file developed as part of UCERF2 (Petersen et al., 2008b) as a baseline model for the areal source zones in the SSC model.  $M_{max}$  for the regional and vicinity areal source zones were modeled following the UCERF3 approach for maximum off-fault magnitude (Field et al., 2013). To model the style of faulting, the SSC TI Team included 70-percent strike-slip and 30-percent reverse-slip earthquakes, based on the relative rate of these earthquakes in the catalogs and the dominantly transpressional environment of the DCPD site.

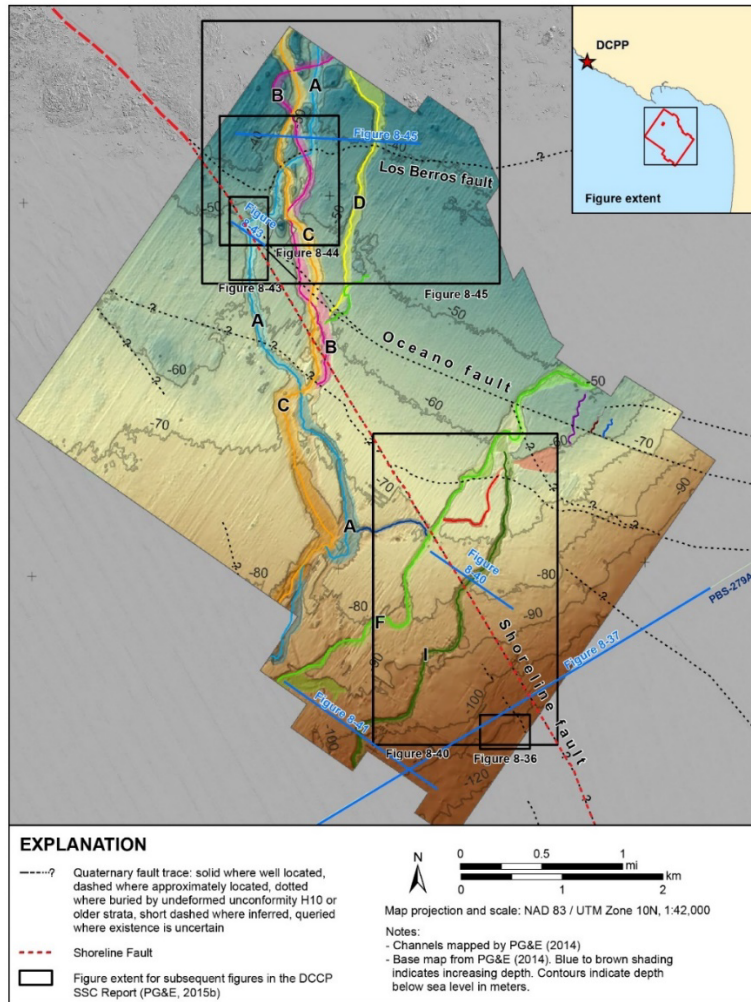


**Figure 3.3-10 Shaded Relief Image of the Bedrock Surface Interpreted from 3D Seismic-Reflection Data in the San Luis Obispo Bay Study Area. The Image Shows a Series of Paleochannels Now Buried Offshore. The Shoreline Fault Cuts Across these Paleochannels with Little or No Detectable Offset. Redrafted from Figure 8-35 in PG&E (2015b)**

For the local areal source zone, the SSC TI Team modeled earthquakes as occurring on a set of parallel virtual faults. For the local areal source zone, the SSC TI Team modeled 18 subparallel, 50-km-long [31-mi-long] faults striking N50°W, with a spacing of 1 km [0.6 mi]. The characteristics of these virtual faults were based on their fault geometry (i.e., location, strike, length, down-dip width, and dip), sense of slip, and  $M_{max}$ , including both aleatory and epistemic uncertainty. Like the regional and vicinity areal source zones, the SSC TI Team distributed the seismicity for the local source zone as 70-percent strike-slip and 30-percent reverse-slip earthquakes. The SSC TI Team based its estimates of the  $M_{max}$  values of  $M6.8$  for the virtual faults on the maximum dimensions of the virtual faults and applied the same magnitude-area scaling relationships used for the primary and connected fault sources.



### 3.3.3.8. Time Dependency Model

The SSC TI Team concluded that a growing body of seismological evidence shows that earthquake recurrence on many faults is too regular to be considered simply as a time-independent Poisson process (Biasi et al., 2002; Scharer et al., 2010; Fitzenz et al., 2010). To account for a time-dependent process, the SSC TI Team developed an equivalent Poisson ratios (EPR) approach based on recurrence models represented by multiple distributions such as log-normal, Weibull, and Brownian Passage Time distributions. The SSC TI Team applied the ratios to the primary and connected fault source rates. The SSC TI Team derived the key parameters in the EPR model from historical observations of past earthquakes and coefficients of variations based on paleoseismic records across California. One of the key data points the SSC TI Team relied on was the observation that the historic San Luis Obispo Mission has not experienced earthquake damage since it was built in 1772. The SSC TI Team also noted that by the early 1870s, road and rail connections were opened across California, and the first newspaper in San Luis Obispo was established. Because there is no historical record of a large earthquake on the Hosgri fault since the 1870s or even since 1772, the minimum time since the last medium- to large-magnitude coastal earthquake near the DCPD site was 140–242 years ago. Considering this constraint on the time since the last big coastal earthquake, the calculated recurrence interval for the Hosgri and SLPB faults, and a range of coefficients of variations based on values for best available paleoseismic records in California, the SSC TI Team derived an average EPR of 1.3 for the Hosgri fault and an average EPR of 1.1 for the SLPB faults.

### 3.3.4. Ground Motion Characterization

The GMC model is the second element required to perform a PSHA for the DCPD site. The two GMC models for the DCPD PSHA, developed by the GMC TI Team as part of the SWUS SSHAC Level 3 GMC (GeoPentech, 2015), characterize median ground motions and their associated aleatory variability (i.e., sigma)—one for nearby, and one for distant earthquakes. Specifically, the GMC models consist of two suites of GMPEs for 5-percent damped horizontal spectral accelerations at 17 spectral periods between 0.01 and 10 seconds. To capture the epistemic uncertainty in both the predicted median ground motions and the aleatory variability, the GMC TI Team developed logic trees, with each branch on the tree representing an individual GMPE with an assigned weight. The GMPEs developed by the GMC TI Team assume WUS reference baserock site conditions. The licensee subsequently adapted these median GMPEs to account for site-specific conditions at the DCPD.

The DCPD GMC models were developed for common reference site conditions of near-surface shear wave velocity ( $V_{S30}$ )<sup>9</sup> of 760 m/sec [2,500 ft/sec] and near-surface attenuation parameter (kappa) of 0.041 seconds (GeoPentech, 2015). The reference  $V_{S30}$  value of 760 m/sec [2,500 ft/sec] is lower than the estimated near-surface shear wave velocity at the DCPD site. However, the 760-m/sec [2,500-ft/sec] value is in the upper range of values that are well constrained by the available empirical seismological data. The GMC TI Team modified the reference rock ground motions to be consistent with the DCPD-specific  $V_S$  conditions through the site response analyses (see Section 3.3.7 of this report).

---

<sup>9</sup>  $V_{S30}$  is the time-averaged shear wave velocity in the top 30 m [100 ft] of soil and rock beneath a site.

### 3.3.4.1. Median Ground Motion Models

Based on previously conducted PSHA studies as well as interaction between the DCPD SSC and GMC projects, the GMC TI Team concluded that the seismic hazard at DCPD is dominated by the nearby fault and areal sources for all spectral frequencies. However, for longer period motions, the more distant plate boundary sources (i.e., San Andreas fault system) do contribute. Hence, the GMC TI Team developed two sets of median GMPEs: one for local fault sources and one for distant plate boundary sources. Each of these GMPEs predicts median spectral accelerations for magnitude, various source-to-site distance measures, depth to the top of rupture, and fault dip angle and fault type (i.e., strike-slip or reverse).

#### Local Fault Sources

To develop the two GMC models, the GMC TI Team evaluated a suite of data and models relevant to the hazard for the DCPD site. In particular, the GMC TI Team evaluated recently developed GMPEs for shallow crustal earthquakes in active tectonic regions and regional data to assess the applicability of the GMPEs. The GMC TI Team also created a finite-fault simulation dataset to augment the regional dataset. To evaluate the available GMPEs for use as inputs to the two GMC models, the GMC TI Team developed a set of objective criteria based on its assessment of best practices in ground motion modeling and also considered the predominant earthquake source mechanisms for the region surrounding the DCPD site.

The GMC TI Team used the PEER NGA-West2 database (Ancheta et al., 2014) and a database of ground motions from finite-fault simulations (Maechling et al., 2015) to evaluate the existing GMPE models relevant to the DCPD site and to develop new GMPE models. The NGA-West2 database includes worldwide ground motion data recorded from shallow crustal earthquakes in active tectonic regions. To develop a dataset to evaluate the GMPEs for the local earthquake sources, the GMC TI Team focused its selection on earthquakes with  $M > 5$  that were recorded at multiple stations (more than three recordings) within 70 km ( $R < 70$  km) [43 mi] of the epicenter. In addition, each of the recording sites has a  $V_{S30}$  greater than 250 m/s [820 ft/s]. The resulting database of earthquake recordings consists of about 200 earthquakes. To supplement this database, the GMC TI Team developed a database of ground motions from finite-fault simulations. The scenarios selected by the GMC TI Team for the simulations include (1) near-fault ground motions from larger magnitude earthquakes ( $M > 7$ ), (2) ground motions from complex ruptures (i.e., single rupture on multiple faults with more than one sense of slip on adjacent fault sections), and (3) ground motions from splay ruptures (i.e., a rupture source that includes overlapping faults that rupture simultaneously).

In addition to gathering and evaluating ground motion databases, the GMC TI Team evaluated 19 recently developed and published GMPEs for shallow crustal earthquakes in active tectonic regions. Based on its evaluations, the GMC TI Team selected all five of the NGA-West2 GMPEs (Abrahamson et al., 2014; Boore et al., 2014; Campbell and Bozorgnia, 2014; Chiou and Youngs, 2014; and Idriss, 2014) for use as seed models for characterizing the hazard for both the local and distant sources. For the local sources surrounding the site, the GMC TI Team included three additional GMPEs (Akkar et al., 2014; Zhao et al., 2006; Zhao and Lu, 2011) as seed models.

For the nearby fault sources, as well as the local areal source zone, the GMC TI Team developed a set of GMPEs by implementing a 2D visualization process, commonly referred to as Sammon's maps (Sammon, 1969). The purpose of the Sammon's map approach is to develop a continuous distribution of median GMPEs that also captures alternative

magnitude- and distance-scaling approaches and satisfies the mutually exclusive, collectively exhaustive requirement for the use of logic trees. After analysis of the eight seed models, the GMC TI Team identified a common functional GMPE form (parameterized in terms of magnitude scaling, distance scaling, and style of faulting). The GMC TI Team then fit the common-form model to the spectral acceleration results from each of the seed GMPEs, resulting in eight common-form model versions that represent the original seed models. Based on the mean and variance for each of the common-form model coefficients, as well as the covariance among the coefficients, the team developed a suite of 2,000 new candidate GMPEs that span a broad range in ground motion space. The GMC TI Team then used the Sammon's map approach to visualize this suite of new models in two dimensions, which was then discretized and resampled to produce a final GMPE for each spectral frequency. Figure 3.3-11 depicts an example of the 2,000 new models and candidate or seed models used to derive them in Sammon's map space and clearly shows the greater range in the derived models relative to the seed models.

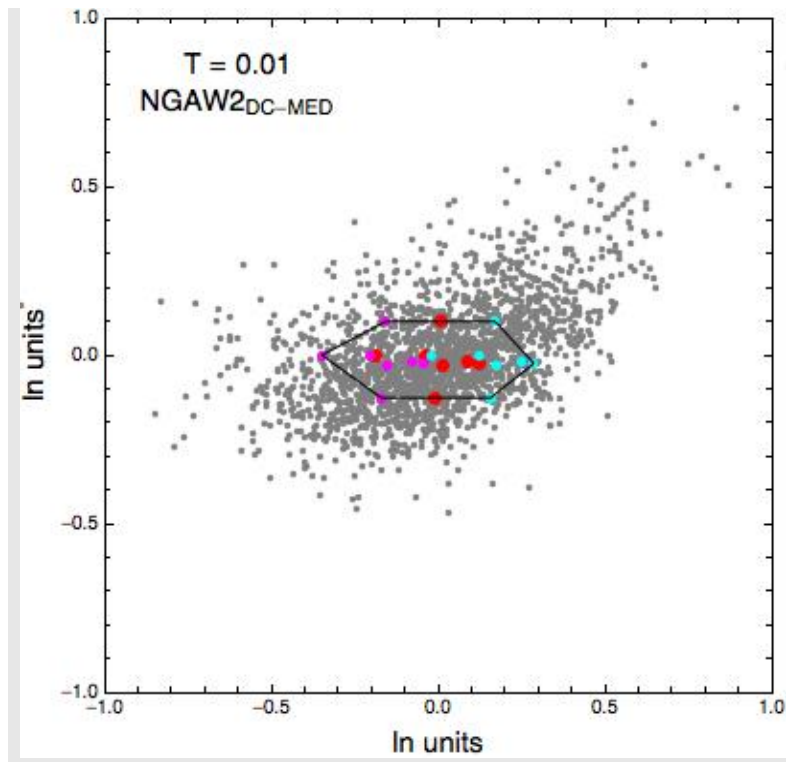


**Figure 3.3-11 Example Sammon's Map for 100 Hz Spectral Acceleration, Redrafted from Figure 6.4.4-1 of the SWUS GMC Report (GeoPentech, 2015), Showing the 2,000 Models Derived from the Common-Form Models (Gray Dots), the Common-Form Models that Fit to the Candidate or Seed GMPEs (Red Dots), and the Common-Form Models that Fit to the Candidate GMPEs, Including Plus and Minus Epistemic Uncertainty (Magenta and Cyan Dots, Respectively). The Solid Black Line Shows the Smallest Shape that Encloses these Points**

### Distant Plate Boundary Sources

The GMC TI Team determined that the Sammon's mapping approach was not necessary for the distant earthquake sources, which only impact the lower frequency hazard. For the distant fault sources such as the San Andreas fault, the GMC TI Team used the five NGA-West2 GMPEs (Bozorgnia et al., 2014), adding epistemic uncertainty to capture the potential range of motions from larger magnitude earthquakes ( $M > 7$ ) (Al-Atik and Youngs, 2014).

#### 3.3.4.2. *Ground Motion Variability*

In addition to developing GMPEs that predict median ground motions, the GMC TI Team developed models to characterize the random (i.e., aleatory) variability about the median ground motions. To develop these models, the GMC TI Team used the ground motion databases and backbone GMPEs described in Section 3.3.4.1 of this report. Because Enclosure 1 to the 50.54(f) letter (NRC, 2012a) requests that licensees perform a detailed site response analysis, the GMC TI Team first separated the residuals between the predicted and observed ground motions into their component pieces to remove the repeatable effects of site response (and avoid double-counting this source of uncertainty). The GMC TI Team then combined the standard deviations for each of the remaining components of the total residuals to produce the final aleatory standard deviation, which is referred to as "single-station sigma." In order to use the single-station sigma approach, the GMC TI Team captured the site-specific portion of the uncertainty by developing (1) a set of site terms, (2) distributions for the local site response amplification factor, and (3) a distribution for the epistemic uncertainty for single-station sigma.

The single-station sigma approach starts with separating the total residuals into between-event and within-event residual components, where the between-event and the within-event residuals have standard deviations, referred to as tau and phi, respectively. The within-event residual is then further separated into a site-term component and a site- and event-corrected residual component with their respective standard deviations. The single-station sigma approach then excludes the site term standard deviation from the total sigma and instead evaluates the site term component as epistemic uncertainty.

To develop a model for single-station sigma for the crustal earthquake GMPEs, the GMC TI Team first constructed models for the between-event standard deviation and the single-site within-event standard deviation, assuming both models depend on earthquake magnitude. The GMC TI Team developed a model for the between-event standard deviation by averaging these models from four of the five NGA-West2 GMPEs along with the Zhao et al. (2006) model. For the site- and event-corrected residual component standard deviation model, the GMC TI Team used the NGA-West2 dataset along with the Taiwanese data from Lin et al. (2011). The GMC TI Team further partitioned the NGA-West2 dataset into a California-only subset, giving this subset a higher weight (0.67) compared to the weight (0.33) for the entire NGA-West2 dataset.

In addition to developing models for each of the individual components of sigma, the GMC TI Team developed epistemic uncertainty distributions for each of these components. The GMC TI Team next combined these epistemic uncertainty distributions to develop a final continuous distribution for single-station sigma, which it represented by three discrete points selected at the 5<sup>th</sup>, 50<sup>th</sup>, and 95<sup>th</sup> percentiles (low, central, and high values).

### 3.3.5. Probabilistic Seismic Hazard Analysis

The licensee used the results of the SSC and ground motion model (GMM) to develop the baserock PSHA hazard curves, which then served as inputs to the site response analysis. For the GMC model, the licensee selected the reference baserock condition to be a soft rock with a  $V_{S30}$  value of 760 m/sec [2,500 ft/sec]. In accordance with the guidance in the SPID (EPRI, 2012) and RG 1.208 (NRC, 2007), the licensee used a minimum  $M5.0$  earthquake and included all seismic sources within 320 km [200 mi] of the site. However, only the sources within 15 km [9.3 mi] of the DCPD contribute significantly (at least 5 percent) to the total hazard at AFE of  $10^{-3}$  or smaller. Figure 3.3-12 shows the total mean site-specific rock hazard curves for seven spectral frequencies. For both the 1 Hz and 10 Hz spectral acceleration hazard curves, the hazard contribution from the Hosgri fault contributes most to the total hazard (Figure 3.3-13). Based on the deaggregation of the 1 Hz and 10 Hz hazard curves, local moderate-to-large-magnitude earthquakes on the Hosgri fault (i.e.,  $M6.0$  to  $M8.0$  at distances from 0 to 10 km [0 to 6 mi]) from the DCPD site dominate the hazard.

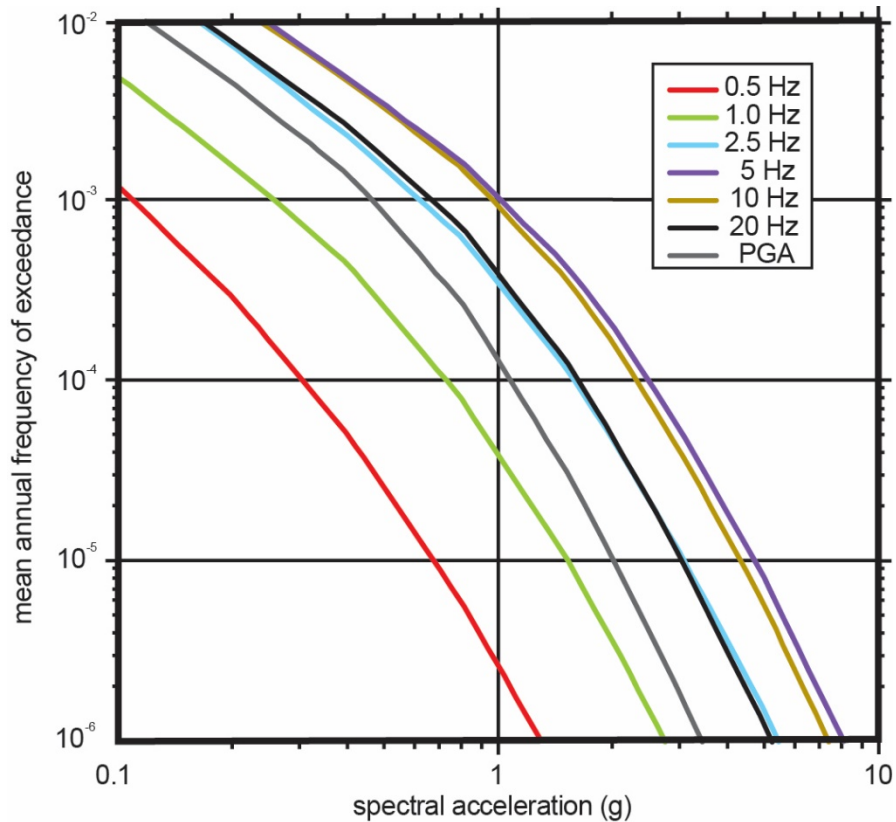
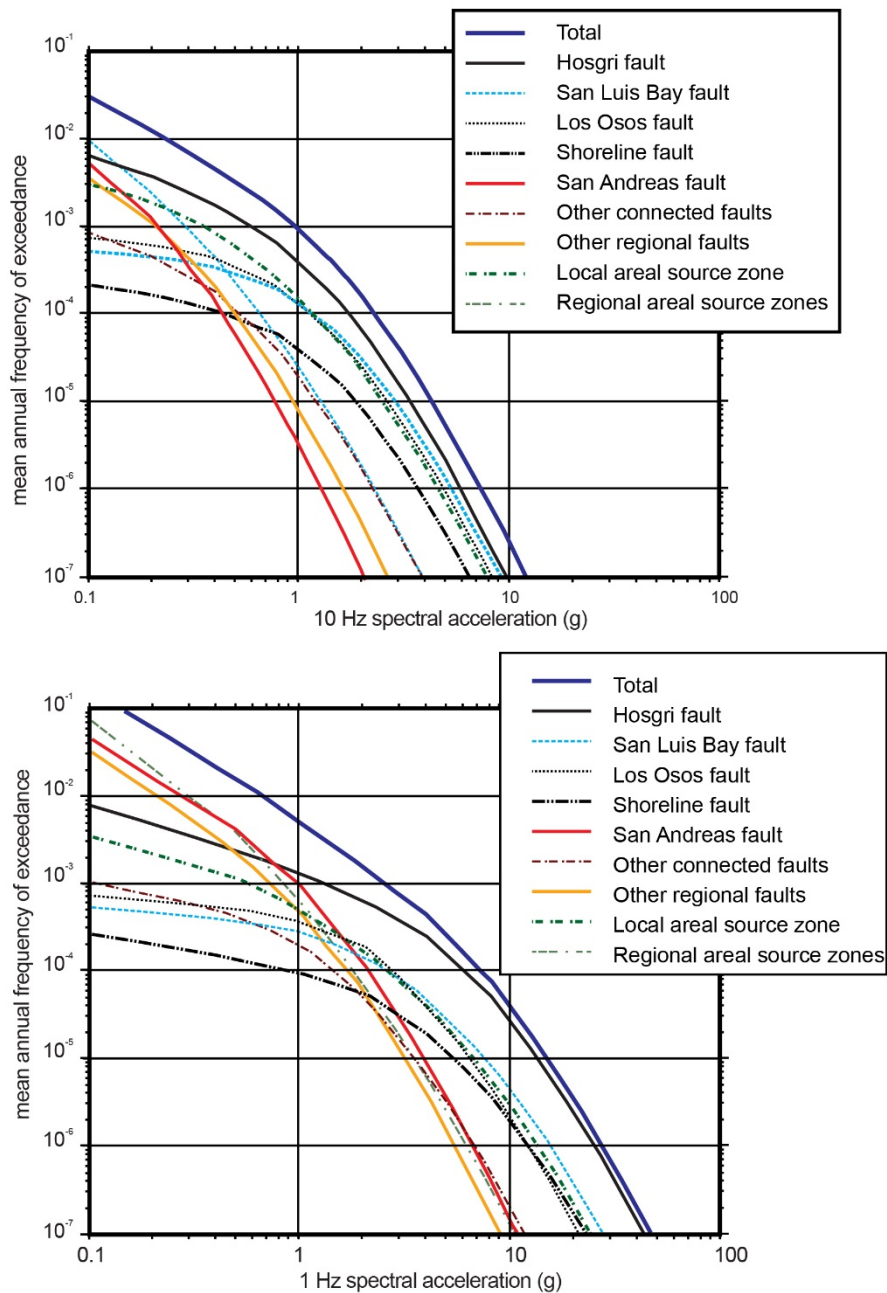


Figure 3.3-12 Total Mean Site-Specific Rock Hazard Curves for Seven Spectral Frequencies, Redrafted from Figure 2.2.2-3 in PG&E (2015a)



**Figure 3.3-13 Reference Rock Hazard by Source for 1 Hz and 10 Hz Spectral Accelerations, Redrafted from Figures 2.2.2-1 and 2.2.2-2 in PG&E (2015a)**

### 3.3.6. NRC Staff Confirmatory Evaluation of the Probabilistic Seismic Hazard Analysis

The NRC staff developed a series of confirmatory evaluations to support its review of the DCPD PSHA results. The confirmatory evaluations summarized in this report illustrate the scope and depth of the NRC evaluations and provide additional information on the current DCPD PSHA results in support of the knowledge management (KM) mission of this NUREG/KM. The NRC

staff's evaluation (NRC, 2016c) provides a complete description of all the confirmatory analyses staff relied on for its review.

For this confirmatory analysis, the NRC staff selected a subset of the SSC and GMC branches that focus on the highest weighted and most hazard significant components of the logic tree. The NRC staff selected the Hosgri and SLPB faults for its confirmatory evaluation (see Figure 3.3-3). For each of the fault sources, the staff primarily focused on either the Hosgri or the Outward Vergent fault geometry model and modeled a range of earthquake ruptures on these primary faults using the characteristic earthquake distribution (Youngs and Coppersmith, 1985). Rather than allocating the fault slip rate among the multiple rupture models developed by the SSC TI Team, the staff used the 5<sup>th</sup>, 50<sup>th</sup>, and 95<sup>th</sup> percentile slip rates for each individual fault to develop baserock 1 Hz and 10 Hz hazard curves. Figure 3.3-14 shows the NRC staff's 1 Hz and 10 Hz hazard curves for the Hosgri fault, assuming a vertical fault geometry model, a maximum magnitude of **M7.4**, a fault length of 107 km [66.5 mi], a width (seismogenic thickness) of 12 km [7.5 mi], an equivalent Poisson's ratio of 1.2, and fault slip rates of 0.7, 1.7, and 2.6 mm/yr [0.001, 0.0023, 0.006 in./yr], which correspond to the 5<sup>th</sup>, 50<sup>th</sup>, and 95<sup>th</sup> percentiles, respectively. For its confirmatory evaluation, the NRC staff used all of the 1 Hz or 10 Hz GMPEs and the central branch for single-station sigma. As shown in Figure 3.3-14, the staff's confirmatory results assume the median slip rate closely matches the licensee's results for both the 1 Hz and 10 Hz mean hazard curves at the 10<sup>-4</sup> and 10<sup>-5</sup> AFE, which were used to develop the GMRS.

Figure 3.3-15 shows the NRC staff's 1 Hz and 10 Hz hazard curves for the Shoreline fault, assuming the SSC TI Team's Outward Vergent fault geometry model, a maximum magnitude of **M6.7**, a fault length of 51 km [31.7 mi], a width of 12 km [7.5 mi], and fault slip rates of 0.03, 0.06, and 0.16 mm/yr [0.001, 0.002, and 0.63 in./yr], which correspond to the 5<sup>th</sup>, 50<sup>th</sup>, and 95<sup>th</sup> percentiles, respectively. As shown in Figure 3.3-15, the NRC staff's confirmatory results encompass the licensee's hazard results for both the 1 Hz and 10 Hz mean hazard curves. Similarly, for the Los Osos and San Luis Bay faults, the staff developed 1 Hz and 10 Hz hazard curves for the other SSC TI Team alternative Outward Vergent fault geometry models. The staff's confirmatory results for these faults are similar to the licensee's results at the 10<sup>-4</sup> and 10<sup>-5</sup> AFE even though the SSC TI Team allocated only a portion of the total fault-slip rates to these two rupture models. Additionally, the staff notes that these confirmatory calculations, like the licensee's calculations, show that the seismic hazard at the DCPD is largely controlled by the Hosgri fault. As shown in the NRC sensitive analysis, the contribution of the Shoreline fault to the total hazard is also small (less than a few percent).

The NRC staff selected the local areal source zone for its PSHA confirmatory evaluation, which, as the host source zone, contributes moderately to both the 1 Hz and 10 Hz total mean hazard for the DCPD site. For each of the virtual faults modeled in the confirmatory analysis, the NRC staff assumed a maximum magnitude of **M6.8**, a fault length of 50 km [31 mi], both reverse and strike-slip faulting, and a spatially uniform recurrence rate. Figure 3.3-16 shows the staff's 1 Hz and 10 Hz confirmatory hazard curves for each of the 18 virtual faults, along with the weighted mean hazard curve. As shown in Figure 3.3-16, the staff's confirmatory results closely match the licensee's mean hazard curves for the local areal source zone.

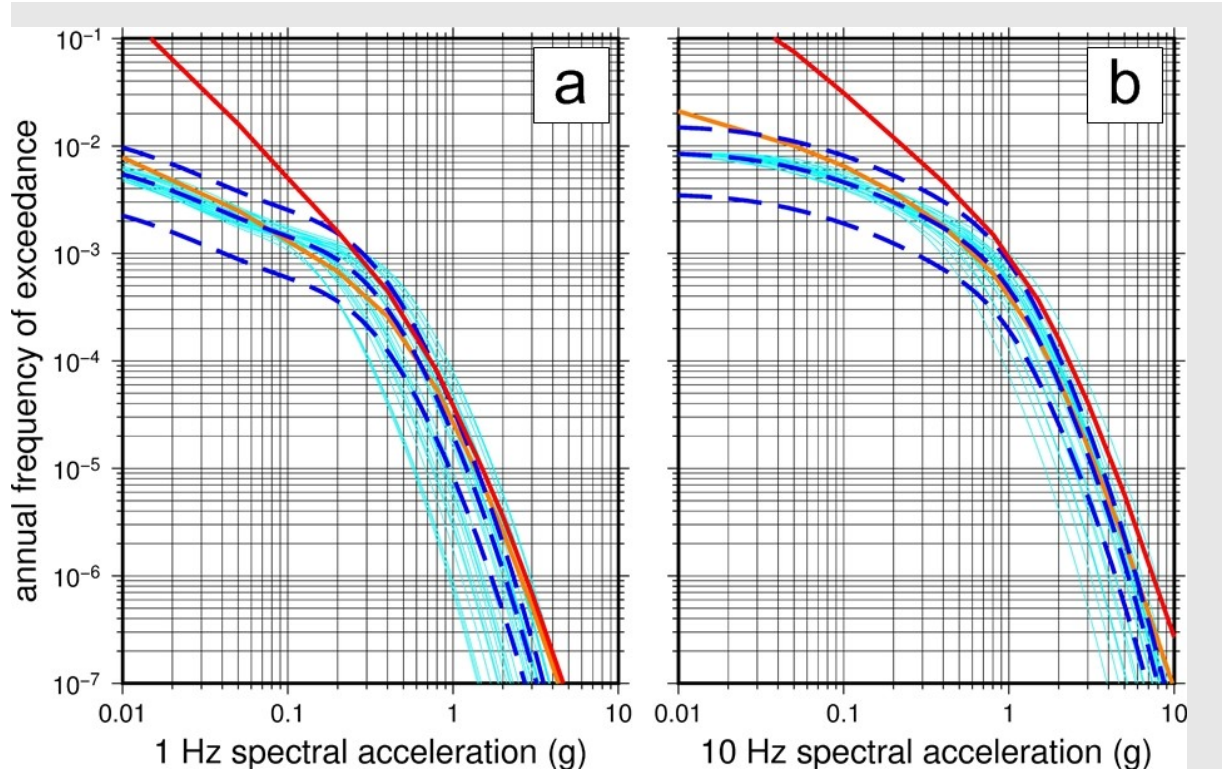


**Figure 3.3-14 Results of the NRC Staff's Confirmatory Analysis for the Hosgri Fault, Showing the Individual Analyses, Assuming Median Slip Rate, for each GMPE (Thin Light-Blue Lines); Staff Mean Confirmatory Results for Three Fault Slip Rates (Dashed Blue Lines); the Licensee's Mean Result (Orange Line); and the Licensee's Total Mean Result (Red Line)**

### 3.3.7. Site Response Analysis

The licensee used two methods to quantify the influence of the geologic profile beneath the DCPD site on the amplitude and frequency of seismic waves propagating to the profile surface. For its first approach, the licensee used site recordings of two earthquakes to adjust the median GMC models from a generic "host" condition to a site-specific "target" condition. For its second approach, the licensee developed analytical site-spectral amplification factors using the numerous geophysical and geotechnical surveys conducted both regionally and locally to determine the engineering properties of the soil and rock beneath the site. Bedrock directly beneath the DCPD site consists of the Miocene Obispo Formation, which is a 400-m-thick stratum of thinly to moderately bedded marine volcanic and volcanoclastic deposits. This bedrock is overlain by a thin veneer {1–2 m [3–6 ft] thick} of marine sands and gravels overtopping a relatively thick sequence {1 to several tens of meters thick [1 to 100 ft]} of nonmarine fluvial sands, gravel, and colluvium. The basal contact between the overlying marine sands and gravels and the underlying Obispo Formation is a gently southwest-sloping marine terrace platform that eroded during the last interglacial marine highstand about 120 ka (e.g., Hanson et al., 1994).



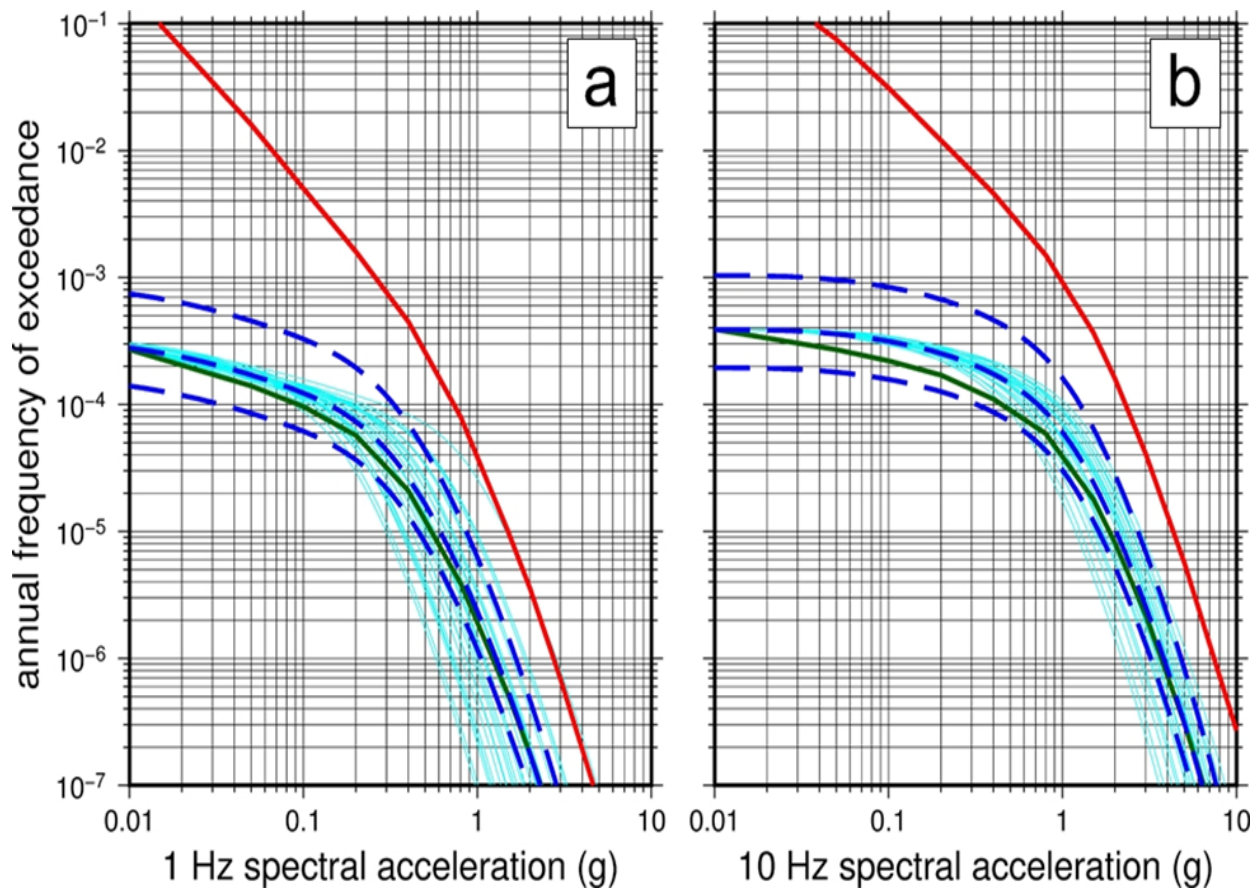


**Figure 3.3-15 Results of the NRC Staff's Confirmatory Analysis for the Shoreline Fault, Showing the Individual Analyses, Assuming Median Slip Rate, for Each GMPE (Thin Light-Blue Lines); Staff Mean Confirmatory Results for Three Fault Slip Rates (Dashed Blue Lines); the Licensee's Mean Result (Green Line); and the Licensee's Total Mean Result (Red Line)**

### 3.3.7.1. Data for Empirical and Analytical Approaches

For the empirical approach, the licensee used strong motion recordings from the **M6.5** 2003 San Simeon and the **M6.0** 2004 Parkfield earthquakes to develop the site term adjustment factors for the median GMMs. The 2003 San Simeon earthquake occurred on the central coast of California approximately 40 km [25 mi] north-northwest from the DCP site, and the 2004 Parkfield earthquake occurred on the San Andreas fault approximately 85 km [53 mi] north-northeast from the DCP site (see Figure 3.3-4). The San Simeon earthquake was recorded at station EST27, which is located to the south of the turbine building, where the  $V_{S30}$  is approximately 856 m/sec [2,808 ft/sec] (Figure 3.3-17). After the San Simeon earthquake, the licensee installed EST28, an additional station to the northeast of the turbine building, which has a  $V_{S30}$  of approximately 777 m/sec [2,550 ft/sec]. Both EST27 and EST28 recorded the 2004 Parkfield earthquake. In addition to the onsite DCP recordings, the San Simeon and Parkfield earthquakes were recorded at numerous other strong ground motion recording sites throughout the region. The licensee used a subset of the recordings of the two

earthquakes from these other regional sites to estimate the uncertainty in the event-path term for each earthquake (see Section 3.3.7.2 of report).

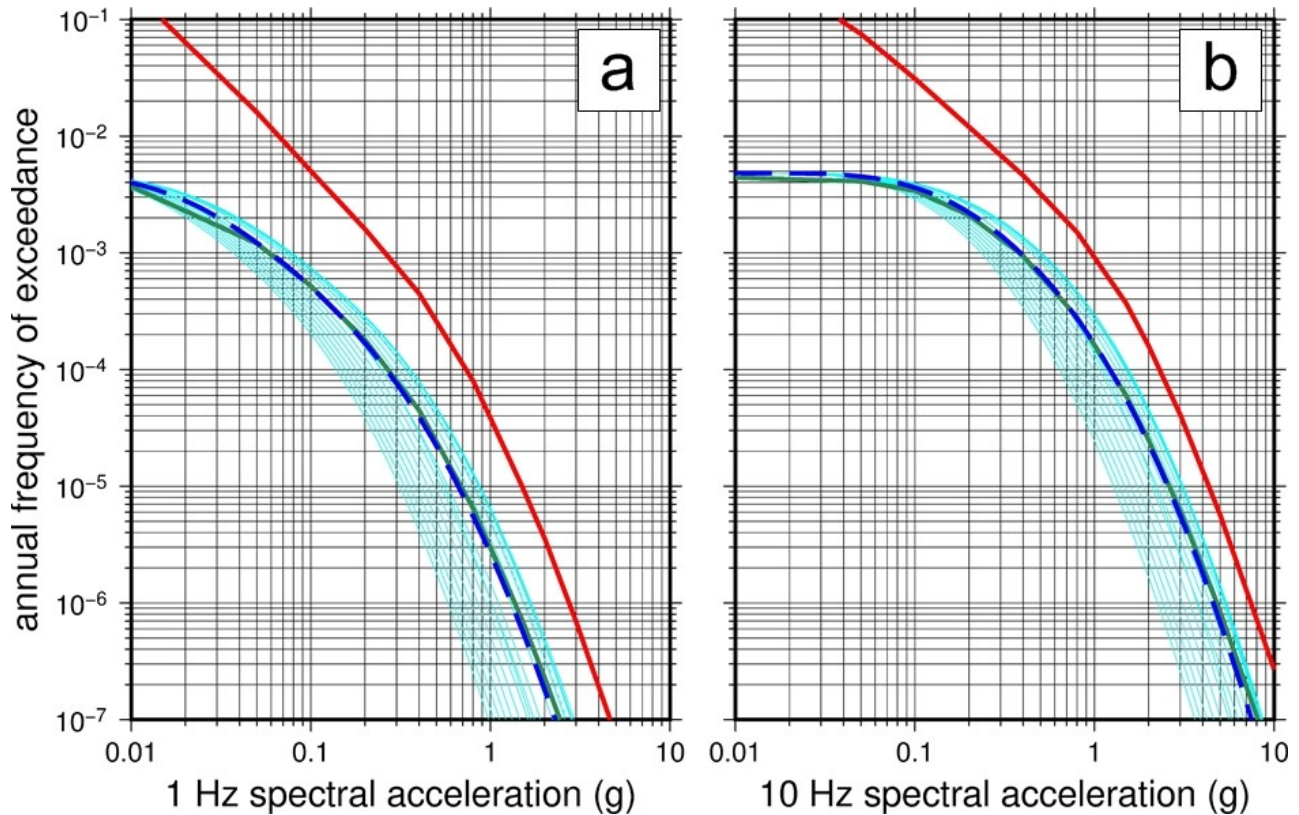


**Figure 3.3-16 Results of the NRC Staff's Confirmatory Analysis for the Virtual Faults Showing the Mean Hazard Curves for Each of the Virtual Faults (Thin Light-Blue Lines), the Overall Mean Result (Dashed Blue Line), the Licensee's Mean Result (Green Line), and the Licensee's Total Mean Result (Red Line)**

To perform an analytical site response, the licensee used onsite data from the Power Block 3D Velocity Model (Fugro Consultants, 2015), which was derived from multiple geophysical exploration techniques, including seismic reflection, surface wave dispersion, and downhole suspension logging. The final 3D velocity model combines a high-resolution 3D compressional wave velocity model derived from joint travel time-gravity tomography with an updated 3D shear wave velocity model. This model provided the licensee with a detailed 1-km by 1-km by 600-m [3,280-ft by 3,280-ft by 1,969-ft] volume of shear wave velocity values that it used for the analytical site response.



**Figure 3.3-17 Aerial View of the DCPD Site Location, Basemap (from Google Maps). Red Squares Indicate Location of ESTA27 (South of Turbine Building) and ESTA28 (North of the Turbine Building)**

### 3.3.7.2. Empirical Site Term Approach

PG&E used the three onsite earthquake recordings of the San Simeon and Parkfield earthquakes to develop a mean site term to estimate the site-specific effects on ground motions due to the local geology underlying the DCPD. The licensee isolated the site-specific effects by first removing the event-specific source and path effects from the GMPEs (which are termed event-corrected GMPEs). Then PG&E computed the within-event residuals between the event-corrected GMPEs and the onsite recordings. If the within-event residuals computed for separate events were repeatable, then the site term represents the expected deviation in site response from the baserock median GMPEs. To isolate the source and path effects relative to the baserock median GMPEs, PG&E used recordings from eight stations located within 100 km [62 mi] of the San Simeon earthquake epicenter and recordings from 16 stations located 50–150 km [31–93 mi] from the Parkfield earthquake epicenter. In addition to determining the mean site term, PG&E estimated the epistemic uncertainty in the site term, which consists of (1) the uncertainty in the estimated source and path terms for each earthquake, (2) the variability in the single-path within-event residuals, and (3) the variability in the  $V_{S30}$  values for stations ESTA27 and ESTA28. The licensee modeled the epistemic uncertainty in the site term by using a three-point weighted distribution for the 5<sup>th</sup>, 50<sup>th</sup>, and 95<sup>th</sup> percentile values and then used these three estimates to adjust the median GMC models before performing a PSHA to develop control point seismic hazard curves for the site.

### 3.3.7.3. Analytical Site Response Evaluation

The licensee also developed an analytical site response approach to provide amplification factors relative to the baserock hazard conditions defined for the SWUS GMC models. The licensee then incorporated these analytical site amplification factors directly into its PSHA used to develop a set of control point hazard curves for the site.

#### Site Basecase Profiles

The licensee used the geometric mean of the 3D shear wave velocity model at multiple points beneath the powerblock and turbine building to develop the upper part of its basecase shear wave velocity profile. The licensee's profile consists of shear wave velocities at 0.5-m [1.6-ft] intervals from the surface to a depth of 125 m [420 ft], the range over which its high-resolution geophysical data are available. The profiles were extended to a depth of 900 m [2,953 ft] based on information in Fugro Consultants (2015) and then continued to a depth of 8 km [5 mi] using reference velocity profiles from the data used to develop its GMC models. The licensee developed lower and upper basecase velocity profiles using a factor of 1.6 times the depth-dependent natural log standard deviation in order to capture the uncertainty in the basecase shear wave velocity beneath the site. For the deeper portions of the upper and lower profiles, the licensee used scale factors of 0.9 and 1.1. The licensee assigned weights of 0.6, 0.2, and 0.2, respectively, for the central, upper, and lower profiles. Figure 3.3-18(a) shows the licensee's three basecase velocity profiles for the upper 125 m [410 ft], and Figure 3.3-18(b) shows the licensee's profiles to a depth of 8 km [5 mi]. As shown in Figure 3.3-18(a), the shear wave velocities beneath the site range from 500 to 1600 m/sec [1,640 to 5,580 ft/sec] at a depth of 125 m [410 ft]. In order to incorporate aleatory variability in the site response analysis, the licensee generated 30 random velocity profiles for each of its basecase profiles such that the resulting profiles capture the range of alternative 3D velocity models across the site subsurface.

#### Dynamic Material Properties and Kappa

To model the potential nonlinear behavior in the upper 150 m [492 ft] of strata to input ground motions, the licensee used two sets of shear modulus degradation and damping curves, giving equal weight to the EPRI curves (EPRI, 1993) and the Peninsular Range curves (Silva et al., 1996, 1998) and limiting the critical damping ratio to 15 percent. In addition, the licensee added a third branch to its site response logic tree to capture the potential for linear behavior. The licensee equally weighted the linear and the two nonlinear responses over the upper 150 m [492 ft] of the profile, such that the linear model has a weight of 0.5 and the EPRI soil and Peninsular curves (Silva et al., 1996, 1998) each have weights of 0.25. Laboratory testing results (PG&E, 1988) of the soft rock at DCPD were cited as the basis for the weights for the three alternative models.

The licensee also used the spectral shape from its onsite recording of the Deer Canyon Earthquake (PG&E, 2011) to estimate a site kappa value of 0.04 second for its site response profile. To account for the epistemic uncertainty in kappa, the licensee evaluated the spectral shapes from its onsite recordings of the San Simeon and Parkfield earthquakes in order to constrain the range of kappa values from 0.03 second to 0.05 second. The licensee assigned weights for the three kappa values of 0.03 second, 0.04 second, and 0.05 second as 0.2, 0.6, and 0.2, respectively.

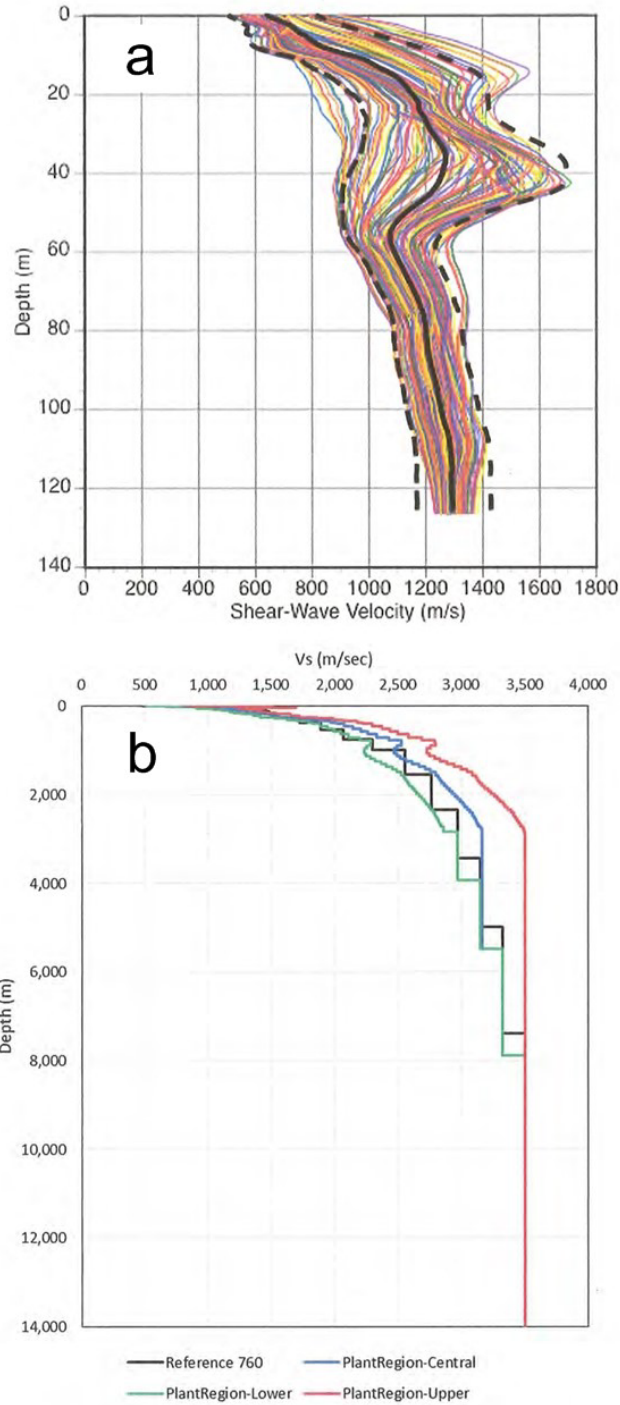


**Figure 3.3-18 (a) Shear Wave Velocity Profiles (Colored Lines) Beneath the DCPP Powerblock and Turbine Building Region. Heavy Black Curves Show the Central, Upper, and Lower Profiles from Figure 2.2 in PG&E (2015c). (b) Comparison of the Host  $V_s$  Profile (Labeled Reference 760) and the Central, Upper, and Lower Profiles for the Target, from Figure 2.3 in PG&E (2015c)**

### Site Amplification Factors

The licensee developed amplification factors for the DCPD profile relative to the surface response spectra for the SWUS baserock condition by using the RVT approach. To develop input ground motions for the site response analysis, the licensee used a point-source model for a *M*<sub>7</sub> earthquake at a depth of 8 km [5.6 mi] for a range of source-to-site distances. After developing input motions for the site response, the licensee generated 30 random shear wave velocity profiles for each of the three basecase profiles to determine the median site amplification factor and its associated log standard deviation. The site amplification factors were limited to values greater than 0.5, as recommended in the SPID (EPRI, 2012).

#### 3.3.7.4. NRC Staff Confirmatory Evaluation

##### Empirical Site Term Approach

To evaluate the reasonableness of the DCPD empirical site term, including its empirical uncertainty, the NRC staff performed a confirmatory analysis using the onsite ESTA27 and ESTA28 earthquake records of the San Simeon and Parkfield earthquakes as well as the recordings of these two earthquakes from other recording stations. As shown in Figure 3.3-19, the NRC staff's confirmatory results for the mean site term, as well as the 10- and 90-percent confidence intervals, are reasonably consistent with the licensee's results over the entire frequency range (0.1 to 100 Hz). In addition, based on a comparison of the site term residuals from the San Simeon and Parkfield earthquakes, the NRC staff observed reasonably consistent behavior for the two sets of residuals above the frequency value of 2 Hz. In the SA, the NRC staff concluded that the consistency of the site term residuals from the two earthquakes demonstrated that the licensee's use of the empirical site term approach successfully identified the site effects for the DCPD. However, as shown in Figure 3.3-19, the site term residuals from the two earthquakes do not follow a consistent trend below 2 Hz, which suggests that the site term residuals from the two earthquakes may still contain source and path effects in addition to the site effects.

##### Analytical Site Response

To perform its evaluation of PG&E's analytical site response approach, the NRC staff first developed an independent 3D seismic velocity model for the DCPD site. This model consists of both compressional and shear wave velocity structures based on the data compiled in Fugro Consultants (2015). In addition, the NRC staff used a digital elevation model and the locations of two seismic stations (ESTA27 and ESTA28) provided in PG&E (2015c) for the construction of this model. The NRC staff used Petrel software to construct its velocity models, which is a Schlumberger product commonly used by the oil and gas industry for subsurface modeling. The digital elevation model used in this analysis consisted of a regularly spaced grid of 2 m by 2 m [6.6 ft by 6.6 ft] and an elevation range between -57.08 and 426.29 m [-187.01 and 1,398.60 ft] above sea level. The NRC staff used a total of 151,003,108 data points to create the velocity models. The NRC staff's velocity model compares favorably with the velocity profiles the licensee relied on to determine the site response.

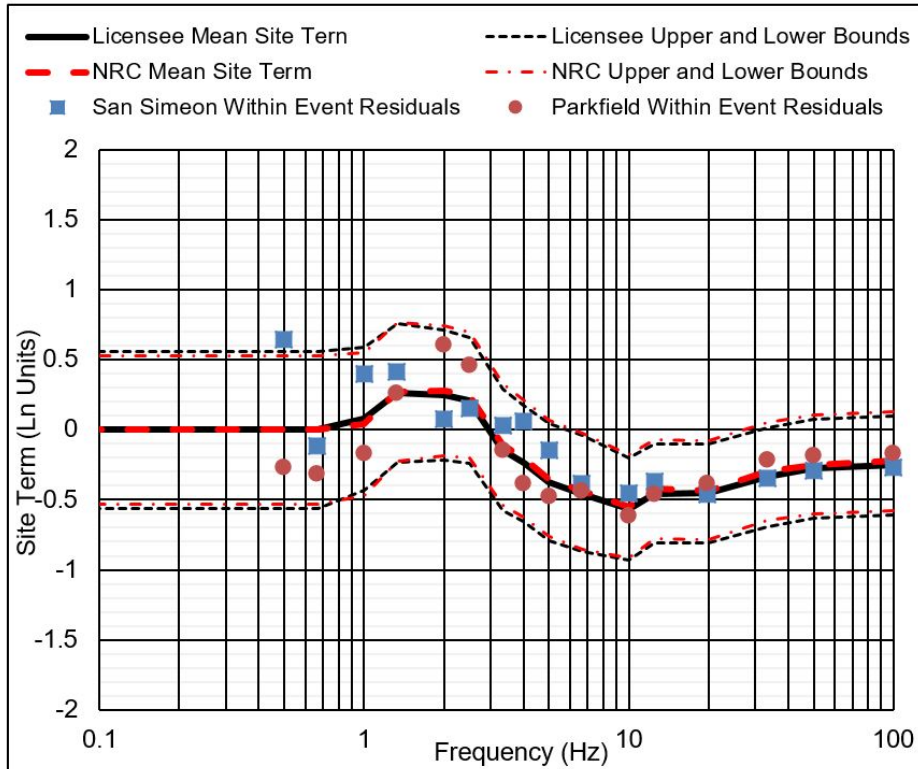


**Figure 3.3-19 Empirical Site Term for the DCPD, Showing the results of NRC Staff's Confirmatory Analyses (Red Lines) and the Licensee's Analyses in PG&E (2015c)**

Based on the similarities between velocity models developed by the licensee and the NRC staff, the NRC staff used the licensee's basecase shear wave velocity profiles for its confirmatory site response analysis of the DCPD site. In addition, because the dynamic material property curves used by the licensee are consistent with both the laboratory testing of the near-surface rock (i.e., PG&E, 1988) and the geology of the site, the NRC staff used the same dynamic material property curves for its evaluation. To evaluate the licensee's estimate of the kappa value for the site response profile, the NRC staff calculated kappa for each of the onsite DCPD earthquake recordings. Based on these confirmatory calculations, the NRC staff determined that the resulting range of kappa values is reasonable. The NRC staff also concluded that the licensee acceptably implemented the point-source model to develop input ground motions, which resulted in a wide range of input motions that appropriately capture the deaggregation results from the PSHA. Figure 3.3-20 shows that the NRC staff's confirmatory amplification factors for input PGAs of 0.2g and 1.07g closely match the licensee's results.

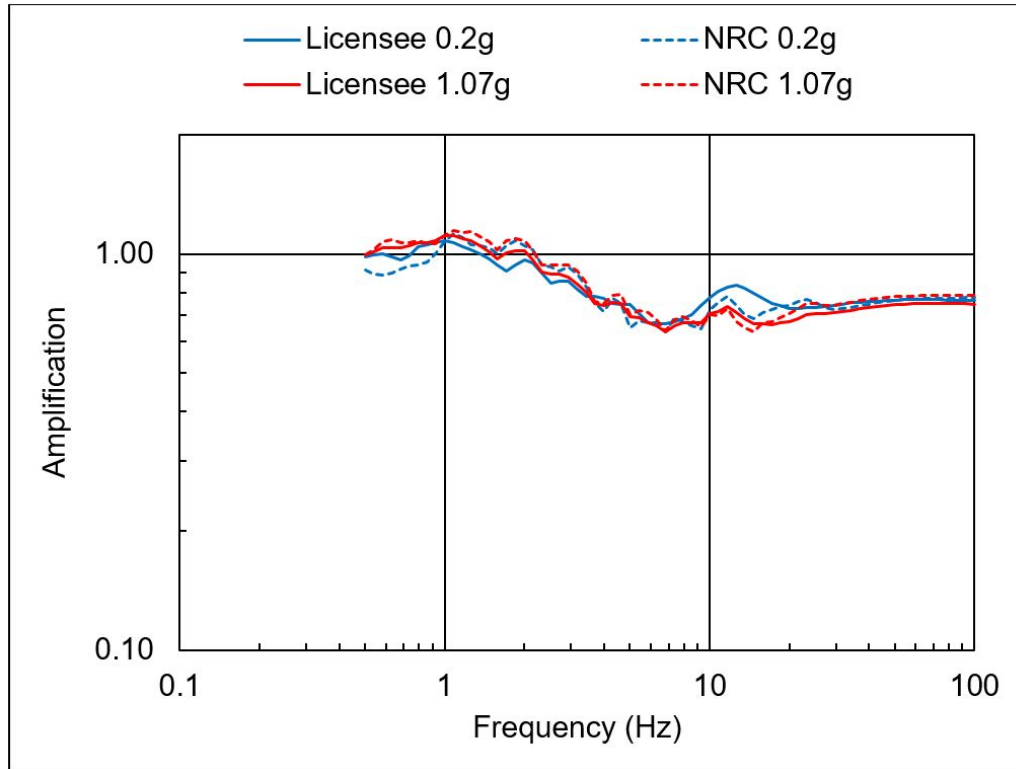


**Figure 3.3-20 Comparison of the NRC and Licensee Amplification Factors Using the Analytical Site Terms for SWUS Reference Rock {760 m/sec [2,493 ft/sec]} with 0.2g and 1.07g PGA**

### 3.3.8. Control Point Hazard

In summary, the licensee performed SSHAC Level 3 studies to develop SSC and GMC models in response to the NRC staff's 50.54(f) letter. The licensee's PSHA results demonstrate that the primary contributor to the hazard at the  $10^{-4}$  annual frequency of exceedance is the Hosgri fault. Other fault sources, such as the SLPB faults, and the local areal source zone also contribute to the hazard, but the Hosgri fault dominates the hazard because of its proximity to the site and its relatively high slip rate compared to all other fault sources.

As described in Section 3.3.7 of this report, the licensee used both empirical and analytical approaches to compute a site correction term and amplification factors to account for the nearfield site conditions for the DCPD site. For the empirical approach, the licensee used the site term to correct the median GMC models, which were then used in the PSHA to develop control point hazard curves for the site at the control point elevation. In addition, the licensee used Approach 3, as described in Appendix B to the SPID (EPRI, 2012), to implement the site amplification factors from its analytical site response analysis into the PSHA to develop an alternative set of control point hazard curves. The licensee then combined these two sets of control point hazard curves using a weight of 0.67 for the curves developed from the empirical approach and a weight of 0.33 for the curves developed from the analytical approach (see Figure 3.3-21a). The licensee gave higher weight to the empirically developed control point hazard curves because the recordings from ESTA27 and ESTA28 for the San Simeon and Parkfield earthquakes provided a direct estimate of the site response for the DCPD. Figure 3.3-21b shows the licensee-calculated GMRS for the DCPD using the uniform hazard



response spectra (UHRS) from the combined weighted control point hazard curves. The GMRS shape is dominated by energy in the 1 Hz to 10 Hz range, with a peak at 2 Hz.

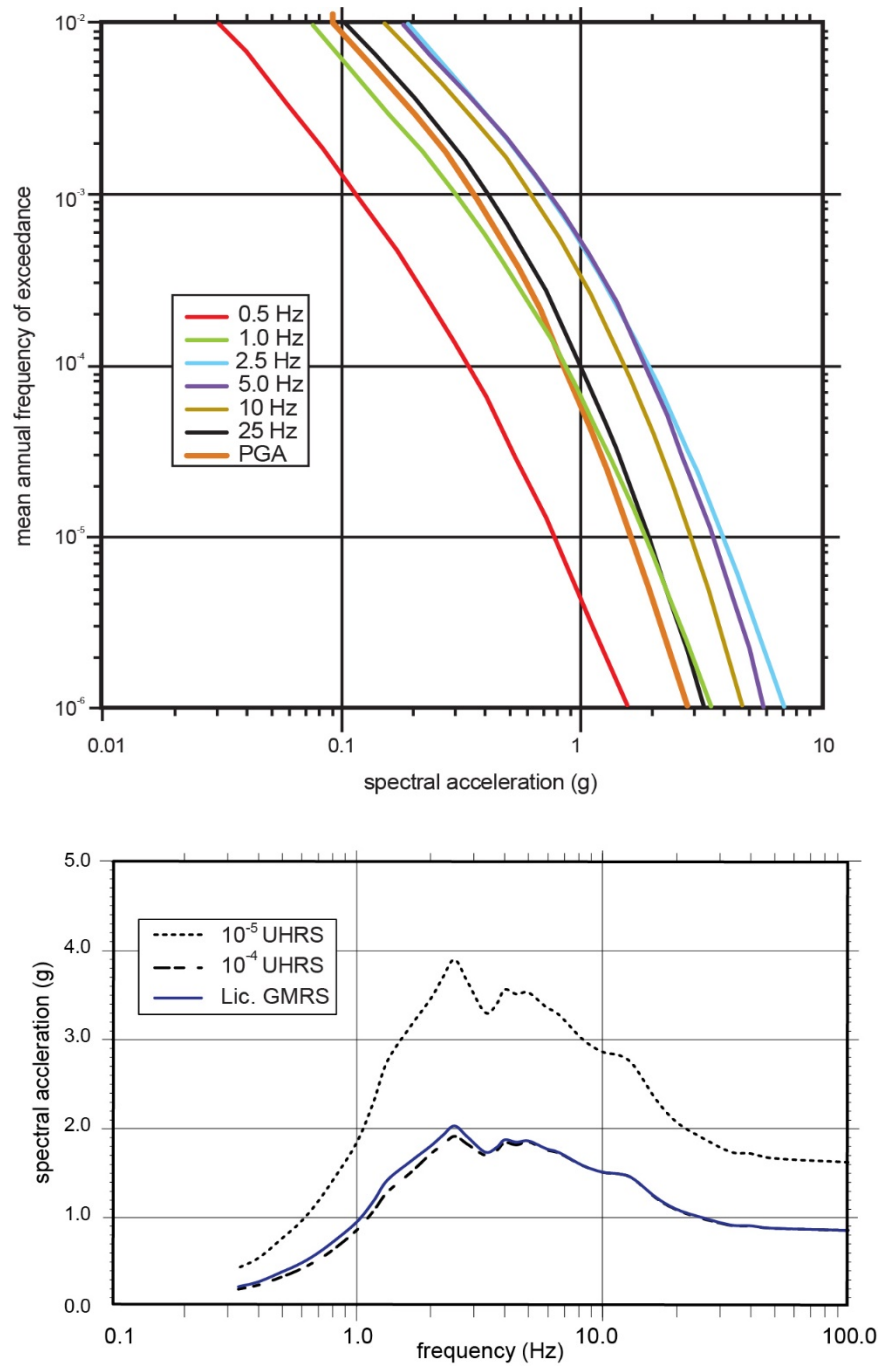


**Figure 3.3-21 (a) Total Mean Site-Specific Control Point Hazard Curves Plotted for Seven Spectral Frequencies, Based on the Data in PG&E (2015c). (b) UHRS and GMRS are Plotted Based on the Data from Table 6-1 in PG&E (2015c)**

### 3.4. Columbia Generating Station

The CGS is located on a 441-hectare [1,089-acre] site within the DOE Hanford Site, 16 km [10 mi] north of Richland, WA, and is owned and operated by Energy Northwest (hereafter referred to as “the licensee” in this subsection). The site is east of the Cascade Range in southeastern Washington within the back-arc of the Cascadia Subduction Zone (Figure 3.4-1). The site rests atop the Columbia River Basalts in the Columbia Basin. The Columbia Basin drains to the Columbia River and is characterized by steep river gorges, including the Yakima and Snake River canyons, and extensive plateaus and fault-bound ridges.

The SSE for CGS is a Newmark-Hall spectrum shape anchored at 0.25g PGA (Section 3.1 in Swank, 2015a; Swank, 2015b). The licensee stated that a PGA of 0.25g is consistent with the vibratory accelerations associated with a Modified Mercalli Intensity VIII earthquake, which is larger than any known earthquake east of the Cascades in Washington or Oregon. In the FSAR (Energy Northwest, 2013), the licensee indicated that this earthquake was assigned to the Rattlesnake-Wallula alignment, located 20 km [12.4 mi] from the site. The licensee specified that the SSE control point for the CGS site is located at the surface of the finished grade at an elevation of 134 m [440 ft] (Section 3.2 in Swank, 2015a).

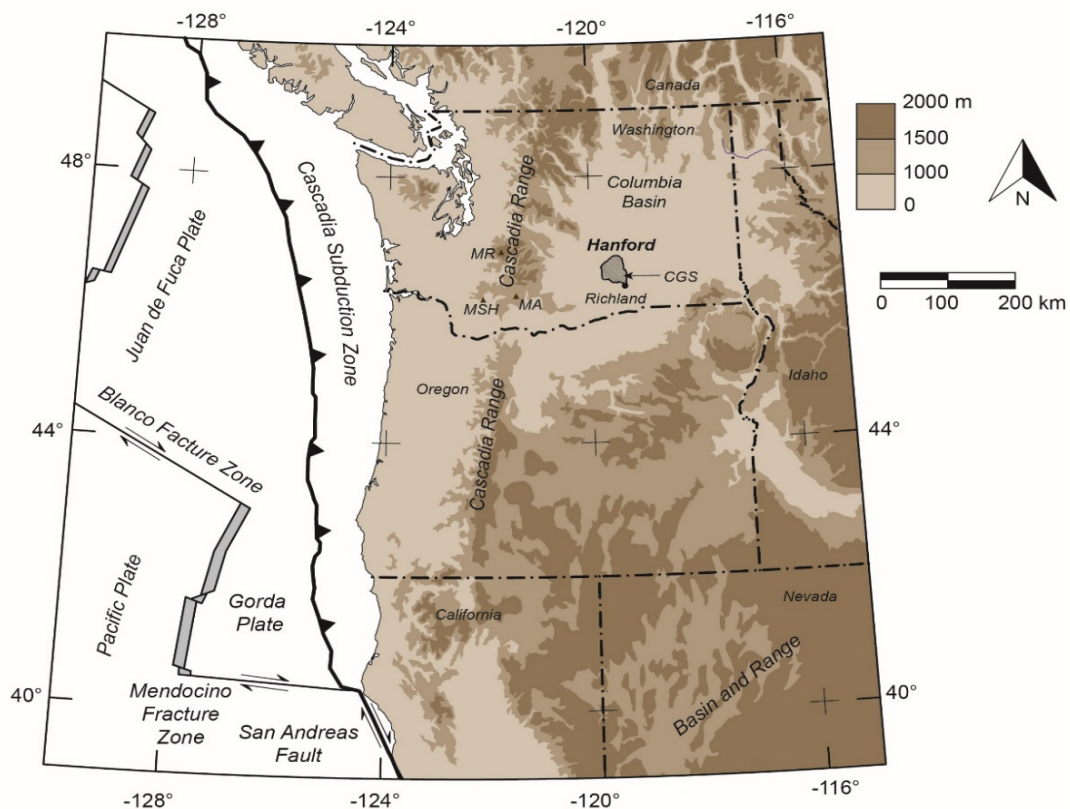


**Figure 3.4-1 Tectonic Setting of the Hanford Site Modified from Figure 1 of Blakely et al. (2014). Cascade Volcanic Peaks in Washington: Mount Rainier (MR), Mount Adams (MA), and Mount Saint Helens (MSH)**

### 3.4.1. Seismotectonic and Geologic Setting

The CGS and the DOE Hanford Site are situated in a region of active tectonics that is part of the Pacific “Ring of Fire.” The Ring of Fire is a horseshoe-shaped ribbon of active plate tectonic features that rims nearly the entire Pacific Ocean Basin, including most of eastern Asia and all of western North and South America. The dominant tectonic features in the Pacific Northwest segment of the Ring of Fire are the Cascadia subduction zone and its associated volcanic arc that together constitute the Cascade Mountain Range (Figure 3.4-1). The Cascade Range includes many large, active stratovolcanoes including Mount Rainer, Mount Adams, and Mount St. Helens. These volcanoes formed atop basement rocks that comprise a series of late Paleozoic<sup>10</sup> and Mesozoic<sup>11</sup> accreted terranes—allochthonous fragments of older tectonic orogens that were dispersed and reassembled by the tectonic forces along much of North American Cordillera.<sup>12</sup>

The Hanford Site is in the Cascadia back-arc, which developed about 40 Ma in response to subduction of the Juan de Fuca plate beneath northern California, western Oregon, and western Washington. About 18 Ma, the western edge of North America also overrode a mantle hotspot that initiated a period of intense basaltic volcanism within the Columbia River Basin. The Columbia River Basalts Province covers about 210,000 km<sup>2</sup> [88,000 mi<sup>2</sup>] of eastern Washington, western Idaho, and northern Nevada (e.g., Reidel et al., 2013). At the CGS site, the Columbia River Basalt ranges in thickness from 2 to 3 km [1.2 to 1.9 mi] and comprises four major units: the Saddle Mountain Basalt (6.0 to 14.5 Ma), Wanapum Basalt (14.5 to 15.6 Ma), Grande Ronde Basalt (15.6 to 16.5 Ma), and Imnaha Basalt (16.5 to 17.5 Ma). Some of the basalt units are massive, indicating formation through rapid or continuous eruptions. However, many Columbia River Basalt units also contain interbeds of fluvial and lacustrine sediments that were deposited onto weathered tops of the lava flows.

This Columbia River Basalt-sediment sequence is capped by several hundred meters of Pliocene and Quaternary<sup>13</sup> alluvium and colluvium that were deposited in subbasins within the Columbia Plateau. At the Hanford Site, these older rocks form a section about 4 km [2.5 mi] thick, with crystalline basement encountered at depths ranging from 7.5 to 9.0 km [4.7 to 5.6 mi]. Much of the Columbia Plateau in eastern Washington was extensively eroded by the cataclysmic Missoula Floods, which occurred about 14,000 to 30,000 years ago. Throughout the Columbia Basin, the Missoula Floods removed much of the relatively young geologic deposits, which paleoseismologists normally rely upon to develop estimates of earthquake recurrence. At the Hanford Site, the Missoula Floods removed about half of the sedimentary deposits that overlie the Columbia River Basalts.

Folding and faulting resulting from tectonic deformation is a characteristic of the region surrounding the Hanford Site and formed in response to the interaction between the North American Plate and the various Pacific Ocean plates along the Cascadia subduction zone. In eastern Washington, the Columbia River Basalt lavas and interbedded sedimentary strata are deformed by a series of generally east-trending and north-verging asymmetric anticlines that formed above reverse faults, either as fault propagation or fault bend folds. With a few exceptions, the north-verging folds have short, steep, north-dipping fore limbs and broad,

---

<sup>10</sup> The Paleozoic is the period of geologic time from 541 Ma to 251 Ma.

<sup>11</sup> The Mesozoic is the period of geologic time from 251 Ma to 66 Ma.

<sup>12</sup> The North American Cordillera is the series of mountain chains along the entire western side of the North American Continent, from Mexico to Alaska.

<sup>13</sup> The Pliocene is the period of geologic time from 5.3 Ma to 2.58 Ma. The Quaternary is the period of geologic time from 2.58 Ma to the present.

shallow, south-dipping back limbs. This folded and faulted terrain is known collectively as the Yakima Fold and Thrust Belt (YFTB). Deformation of the YFTB extends beyond the Columbia Plateau, and north-south shortening (i.e., compression) is observed to fan westward across the Cascade Range. Geodetic indicators, including GPS measurements, confirm that north-south compressional stresses continue to control tectonic deformation of the YFTB. Seismicity around the CGS site is dominated by small-magnitude reverse and strike-slip earthquakes that occur within the upper 3 km [1.8 mi] of the Columbia River Basalts, with more diffuse seismicity extending to depths of about 20 km [12.4 mi].

Seismicity in the Columbia Basin is diffuse and relatively sparse, especially when compared to concentrations of higher seismicity in other regions of the Pacific Northwest region (Figure 3.4-2). Concentrations of seismicity include earthquakes associated with the transform motion on the Blanco fracture zone, sea-floor spreading along the Gorda Ridge, and subduction of the Juan de Fuca and Gorda plates beneath North America along the Cascadia Subduction zone. The subduction zone seismicity is manifest as relatively deep earthquakes beneath the Cascade Range.

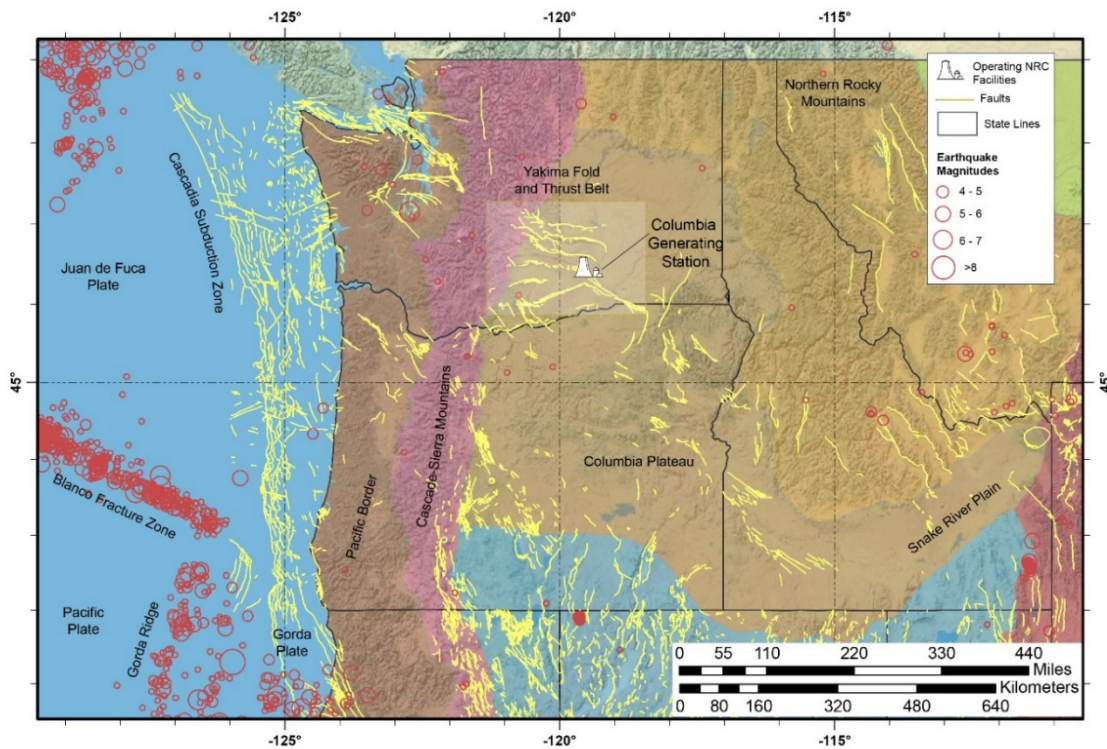


**Figure 3.4-2 Map of the Pacific Northwest Showing the Distribution of Earthquakes Relative to the Physiographic Provinces, Quaternary Faults, and Other Tectonic Features. The Earthquake Epicenters are from the USGS Advanced Nation Seismic System Catalog Spanning 1900–2018**

### 3.4.2. Senior Seismic Hazard Analysis Committee Process

The Pacific Northwest National Laboratory (PNNL) and its contractors for the DOE and licensee undertook the Hanford Site PSHA (hereafter the Hanford PSHA), in a joint sponsorship, to

provide a detailed characterization of the vibratory ground motion hazard at the Hanford Site from potential future earthquakes. The study was conducted to fulfill the requirements for DOE facilities and those for commercial NPPs. The Hanford SSHAC followed the established SSHAC Level 3 process, including holding three structured workshops and several formal and informal working meetings among the SSC and GMC TI Teams. To accomplish the PSHA, PNNL and its contractors developed a sitewide seismic model for use in the final PSHA. Site-specific analyses were then conducted to develop the final seismic hazard curves for each of the critical DOE facilities and for the control point at CGS. Details of the Hanford SSHAC, including the workshops, NRC observations at the workshops, and the review conducted by the SSHAC PPRP, appear in the DOE's PSHA report (PNNL, 2014) and the NRC's SA (NRC, 2016b).

### **3.4.3. Seismic Source Characterization**

The SSC model for the CGS site represents one stage of a PSHA. The goal of the SSC TI Team was to develop an SSC model for the PSHA based on its evaluation of available geological, geophysical, and seismological information. The SSC TI Team considered three types of seismic sources: faults, areal source zones, and the Cascadia subduction zone. The SSC TI Team derived input parameters to the SSC model for these seismic sources from (1) earthquake records, based on the instrumental and historical seismicity catalogued for the region, (2) geologic evidence of the magnitude, age, and frequency of past seismic events, and (3) geophysical evidence for crustal strain based on GPS measurements.

To develop the SSC for the Hanford site, the SSC TI Team compiled existing information from plant licensing documents, DOE reports for the Hanford Site, USGS reports, and published technical information. Based on the discussions during Workshop 1, the SSC TI Team recognized the need to conduct additional studies to improve the characterization of fault geometries in the subsurface and to develop information on Quaternary deformation and slip rates of the YFTB faults. Following SSHAC Workshop 1, the SSC TI Team conducted new studies on Quaternary geologic features and used alternative methods to analyze and relocate earthquakes in the Hanford PSHA crustal catalog.

#### *3.4.3.1. Crustal Fault Sources*

The SSC TI Team identified 20 Quaternary crustal fault sources with the potential to contribute to the seismic hazard at the Hanford Site. Nineteen of these are part of the YFTB faults (Figure 3.4-3). The twentieth is the Seattle fault, which is a thrust fault located more than 200 km [125 mi] west of the Hanford Site in the Puget Lowlands. The Seattle fault is a well-characterized Quaternary fault and has the highest slip rate of all the faults in the Puget Lowlands (JBA et al., 2012) {mean rate of 0.9 mm/yr [0.354 in./yr]}. Sensitivity analyses conducted by the SSC TI Team showed that the Seattle fault does not contribute significantly to the hazard because it is so distant from the site. The SSC TI Team included the Seattle fault in its analysis to document the limited contribution that these Puget Lowland faults make to the hazard and to justify its decision to exclude the other Puget Lowlands faults from the Hanford PSHA.

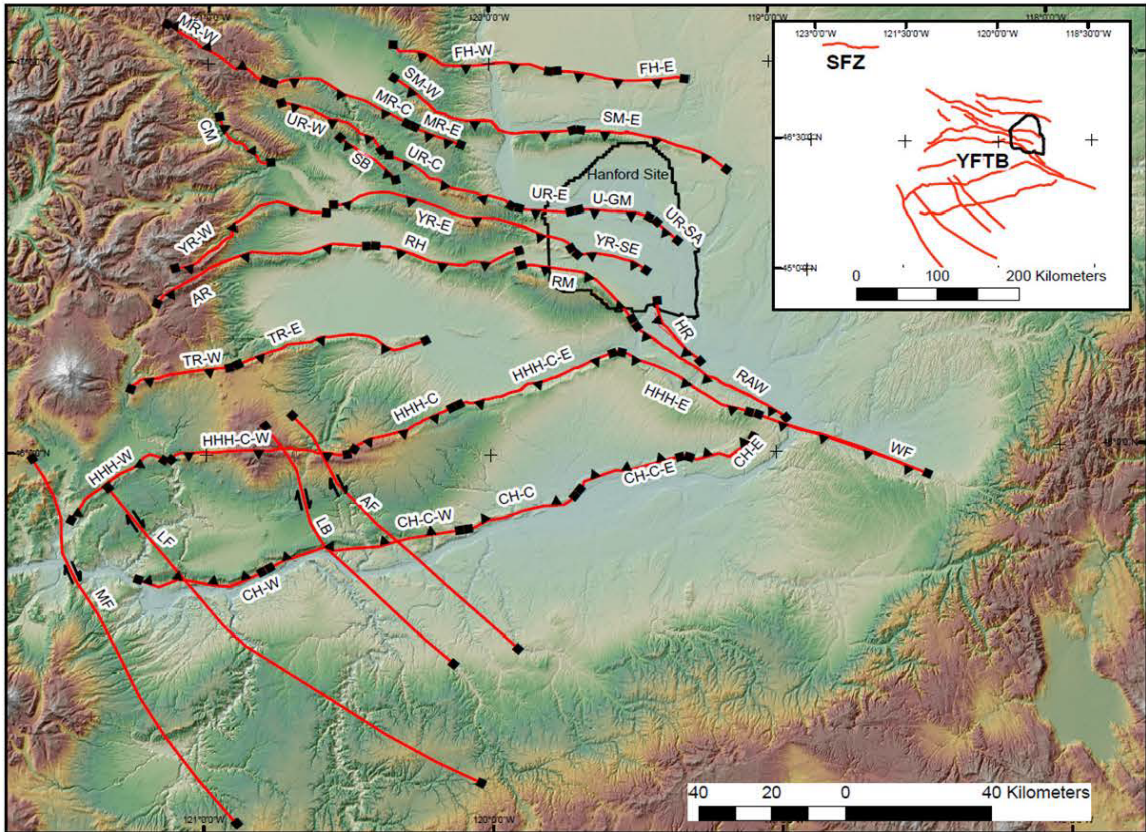


**Figure 3.4-3 The 20 Fault Sources the SSC TI Team Identified for Inclusion in the SSC Model: Ahtanum Ridge (AR), Arlington (AF), Cleman Mountain (CM), Columbia Hills (CH), Frenchman Hills (FH), Horn Rapids (HR), Horse Heaven Hills (HHH), Laurel (LF), Luna Butte (LB), Manastash Ridge (MR), Maupin (MF), Rattles of the Rattlesnake-Rallula (RAW) Alignment, Rattlesnake Hills (RH), Rattlesnake Mountain (RM), Saddle Mountains (SM), Seattle Fault Zone (SFZ), Selah Butte (SB), Toppenish Ridge (TR), Umtanum Ridge (UM), and Wallula Fault (WF). The Figure was Adapted from Figure 8.43 in PNNL (2014)**

The SSC model for fault sources is based on constructing a logic tree for each fault source, which is a standard method to account for fault source parameters and associated uncertainties in seismic hazard calculations. Nodes of the logic tree account for faulting characteristics such as the 3D fault geometry (including fault segments), style of faulting (i.e., reverse, oblique, and strike-slip), slip rate for each fault segment, characteristic magnitude ( $M_{char}$ ) and  $M_{max}$  for each fault segment, and earthquake recurrence for each fault source. Branches at each of these nodes account for the epistemic uncertainties associated with alternative interpretations or statistical distributions of these fault parameters.

The SSC TI Team based its assessments of seismic potential of the faults on (1) geologic evidence for active deformation within the contemporary tectonic regime, (2) evidence that the fault could produce an earthquake with  $M > 5$ , and (3) information indicating that the fault generated seismicity above the rate calculated for the areal seismic sources. Based on these criteria, the SSC TI Team considered the 15 reverse or reverse-oblique faults that constitute the

YFTB to be seismogenic for the following three reasons. First, deformation of the Columbia River Basalt flows by these faults, especially the resulting topographic and structural relief, is consistent with the contemporary tectonic strain field. Second, all these faults are large enough to produce earthquakes with  $M > 5$ . Third, in the few places where the Missoula Floods did not remove surficial Quaternary and Holocene deposits, geomorphic and paleoseismic evidence of active deformation is consistent with deformation observed in the underlying basalts. The remaining 4 faults in the list of 20 fault sources are strike-slip faults that the SSC TI Team considered to be either active basement reactivation faults or wrench faults that simply accommodate the growth of the anticlines and synclines in the YFTB. These criteria were used to differentiate the 19 YFTB faults included in the SSC model from all other mapped faults in the YFTB.

An important consideration in the characterization of these fault sources in the YFTB is the nature of the faults in the subsurface. Two alternative geologic models have been proposed within the geologic literature to explain the observed deformation of YFTB (e.g., Zachariassen et al., 2006; Chamness et al., 2012). The most widely accepted interpretation is the thick-skinned model, in which the reverse and thrust faults of the YFTB are considered to extend as single fault planes from the surface all the way to the base of the seismogenic crust (below this depth, the seismologists consider the crust to be too ductile for earthquakes to occur). The alternative interpretation is the thin-skinned model, in which the YFTB faults gradually become subhorizontal at an intermediate depth and terminate within one or more horizontal detachments at the base of the Columbia River Basalts or within other weak zones lower down in the crust. Other unseen faults may exist deeper in the crust beneath the detachments, but these faults are only partially coupled (or completely uncoupled) from the faults observed at the surface. Some earlier PSHAs for the Hanford region (Geomatrix, 1996; JBA et al., 2012) included both thin- and thick-skinned fault models, with model weights justified by interpretations of research available at those times. For the Hanford PSHA, the SSC TI Team evaluated the latest technical information and concluded that a thin-skinned model was not justified for the seismogenic sources under consideration.

### Fault Source Geometries

The geometric parameters of fault sources are important because they form the basis from which the SSC TI Team derived fault slip, slip rate, and the  $M_{\text{char}}$  and  $M_{\text{max}}$  for each fault source. Fault lengths (i.e., surface trace lengths of the fault) were derived from the topographic expressions of the associated YFTB folds. The SSC TI Team based its characterization of the down-dip widths (i.e., measured extent of the fault plane from the surface to the base of the seismogenic crust) on variations in fault dip and three different interpretations of the depth to the base of the seismogenic crust {13, 16, and 20 km [8.1, 9.9, and 12.4 mi]}. The SSC TI Team associated deeper seismogenic thickness values with steeper fault dips (i.e., Figure 8.75 in PNNL, 2014) and calculated a range of dips for each fault source using a range of possible geometrical relationships that were consistent with the observed features of the resulting YFTB folds, especially the medial extent of the back limb on the surface fold.

The SSC TI Team assessed the faulting style for each fault source using fault-specific geologic evidence and regional geological and geophysical data, and by considering the tectonic stress regime and other strain indicators. Based on these results, the dominant faulting style is reverse, although some of the fault segments include components of both strike-slip and reverse faulting (designated as oblique slip). The SSC model fault tree includes branches for each fault segment that incorporates the detailed assessment of faulting style. Four of the nineteen YFTB faults were identified as strike-slip faults (Arlington, Luna Butte, Laurel, and

Maupin faults). All four were characterized as northwest-trending strike-slip or wrench faults. The SSC TI Team considered two alternative models for these faults. One model assumes that the faults are independent reactivated basement faults and thus are seismogenic. The second model assumes the faults are tear faults or secondary features associated with deformation of the folds and thus are nonseismogenic. The SSC model includes both fault models, but the SSC TI Team slightly favored the nonseismogenic model (weight of 0.6).

### Fault Slip

The SSC TI Team determined the fault slip for each of the YFTB fault sources using a simple trigonometric relationship that relates net fault slip to the vertical component of fault offset, fault dip, and the relative proportion of dip-slip motion on the fault to total fault slip considering the potential for strike-slip or oblique-slip motion. To determine the vertical component of fault offset, the SSC TI Team first measured the topographic relief across the crests of the fault-cored folds. For these measurements, the ends of the topographic profiles were anchored within a common stratigraphic horizon in the Columbia River Basalts. Because there has been minimal erosion of the folded basalts, the measured topographic relief effectively quantifies the structural relief of the folds produced by faulting. Using this approach, the SSC TI Team quantified the vertical component of total fault slip that occurred since the fault became active between 6 and 10 Ma. The only exception to this analysis approach was at Rattlesnake Mountain, where the SSC TI Team was able to measure the vertical offset of Quaternary-aged material that was offset by the Rattlesnake Mountain fault.

The SSC TI Team assumed a simple kinematic model that relates fault dip to the 3D geometry of the folds at the surface to determine fault dip in the subsurface. In this kinematic model, folds observed at the surface developed in the hanging wall of a blind or emergent reverse fault. These faults are assumed to extend as planar surfaces to the base of the seismogenic crust. The model also assumes that the medial extent of the fold's back limb is related to fault dip, in which broad back-limbs indicate shallow-dipping reverse faults and narrow back limbs indicate steep-dipping reverse faults. The SSC TI Team also interpreted the reverse faults to intersect the base of the seismogenic crust along a line parallel to and directly beneath the hinge of the back limb fold (i.e., the inflection point where the basalt beds are essentially horizontal). Because the SSC TI Team derived three alternative interpretations for the thickness of the seismogenic crust {13, 16, and 20 km [8, 10, and 12.4 mi] deep}, its approach resulted in three different fault dips for each YFTB fault. Thus, in this approach, the 16 km [10 mi] and 20 km [12.4 mi] depths of the seismogenic crust yield progressively steeper fault dips compared to the 13 km [8 mi] depth. The SSC TI Team then added further epistemic uncertainty to the analysis by including varied interpretations of the location of the back limb syncline hinge relative to the fault. The SSC TI Team also multiplied the amount of dip slip by a net-slip factor to account for strike-slip or oblique motion. For pure reverse motion, this net-slip factor was 1.0. For oblique slip motion, this net-slip factor was 1.4. However, for strike-slip motion, the SSC TI Team developed two alternatives, using factors of 2.2 or 5.0, weighted equally.

### Slip Rates

Because the Missoula Floods erased much of the Quaternary geologic record in eastern Washington, the SSC TI Team concluded that the most reliable indicator of fault slip was to estimate slip rate based on long-term slip-rate averages, which were calculated by dividing the fault's total slip by the geologic age at which that fault slip was first initiated. Field geologic evidence at Saddle Mountain shows that sediments of the Ringold Formation dip less on the back limbs of the YFTB folds relative to the dip of the underlying Columbia River Basalt lavas



(e.g., an angular unconformity). The SSC TI Team interpreted this stratigraphic relationship to indicate that faulting in the YFTB began before deposition of the Ringold Formation. The geologic age of the Ringold Formation is constrained to be between 4 and 9 Ma (e.g., Lindsey and Gaylord, 1990). Based on this observed angular unconformity, the SSC TI Team used end-member ages of 6 Ma and 10 Ma to define the onset of YFTB faulting. The SSC TI Team gave these two alternatives equal weight to develop two sets of fault slip-rates.

The long-term slip rates determined by the SSC TI Team are in good agreement with slip rates derived from the limited Quaternary strata in the Hanford region. For example, Rattlesnake Mountain has a broad coalescing alluvial fan (often called a bajada in geologic terminology) that is offset by the Rattlesnake Mountain fault. The estimated age of the bajada is 425–600 ka based on thorium/uranium radiogenic analysis of the carbonate rinds on sedimentary clasts and on magnetic polarity of the sediments (Baker et al., 1991). Using this age and measured vertical separation of the bajada, the SSC TI Team determined an average slip rate for the Rattlesnake Mountain fault of 0.05 mm/yr [0.0020 in./yr]. These rates are comparatively low relative to more active tectonic regions, where slip rates typically are 1 mm/yr [0.039 in./yr] or more. The SSC TI Team also determined the average long-term slip rate of the Rattlesnake Mountain fault as 0.06 mm/yr [0.0024 in./yr] based on the offset Columbia River Basalt lavas. The SSC TI Team reached similar agreement in the Quaternary and long-term slip rates for the Manastash and Umtanum faults.

### Earthquake Recurrence

Using the slip-rate approach described above, the SSC TI Team combined information about fault slip with the seismic moment rate,  $M_{char}$ , and  $M_{max}$  to develop a magnitude-frequency distribution for each fault source. The SSC TI Team considered four alternative types of magnitude-frequency distribution models: (1) the truncated exponential (Gutenberg and Richter, 1956), (2) characteristic (Youngs and Coppersmith, 1985), (3) maximum moment (Wesnousky, 1986), and (4) WAACY (Wooddell et al., 2014). The SSC TI Team analyzed the rate of small earthquakes for each of the YFTB faults and determined that the characteristic model provided the best fit to the earthquake data over the truncated exponential or maximum moment models. Based on this analysis and analysis of Hecker et al. (2013), the SSC TI Team selected the characteristic model. The WAACY model was developed to account for large strike-slip faults that could link with nearby strike-slip faults to produce earthquakes of very large magnitude. Because the YFTB does not contain such faults, the SSC TI Team did not use the WAACY model to characterize the fault sources.

The characteristic model uses slip rate and an estimate of the magnitude of  $M_{char}$  to derive the recurrence curves for each fault source. This model defines  $M_{max}$  to be 0.25 magnitude units larger than  $M_{char}$ , and  $M_{max}$  is the largest earthquake that can occur given the area of the fault surface. To determine the magnitude of the  $M_{char}$  for the YFTB fault sources, the SSC TI Team relied on four published scaling relationships that relate fault rupture length or rupture area to magnitude: Wells and Coppersmith (1994), Wesnousky (2008), Hanks and Bakun (2008), and Stirling et al. (2008). Based on the results of these four scaling relationships and the relative weights assigned them in the logic tree, the SSC TI Team developed probability distributions of the characteristic magnitude for each fault source.

### Crustal Fault Source Characterization Summary

Table 3.4-1 summarizes the SSC TI Team's fault source characterization. The data were derived from Chapter 8 in PNNL (2014) and the hazard input document (Appendix D1 to PNNL,

2014). The fault information for the four strike-slip faults (Arlington, Laurel, Luna Butte, and Maupin) was based largely on prior seismic hazard studies (e.g., JBA et al., 2012). The SSC TI Team also considered it more likely that these faults formed as tear faults associated with folding rather than as reactivated basement faults. Because of the sparsity of Quaternary strata that can be used to constrain slip rates and the lack of reliable palinspastic markers<sup>14</sup> to constrain fault-slip history, the SSC TI Team could not determine the average net-slip rate with certainty. Thus, to account for this large uncertainty, the SSC TI Team developed slip-rate distributions for these faults that were significantly broader than the other faults included in the SSC model.

Of the 19 fault sources summarized in Table 3.4-1, the licensee identified eight as contributing more than 5 percent to the total hazard at 1 and 10 Hz, for mean AFE of  $10^{-4}$  and  $10^{-5}$  (Table 2.2.2-3 of Swank, 2015a). These eight fault sources are delineated in bold text in Figure 3.4-2. The SSC TI Team also included the Seattle fault in the SSC model; however, due to its low slip rate {about 1 mm/yr [0.04 in./yr]} and large distance from the Hanford Site {200 km [125 mi]}, the hazard contribution from the Seattle fault is small relative to other faults in the YFTB.

---

<sup>14</sup> A palinspastic marker is a geological feature that can be used to identify the original positions of layers of rock strata before fault offset.

**Table 3.4-1 Summary of Fault Characterization Data for Fault Sources in the Yakima Fold and Thrust Belt**

FAULT NAME	FAULT STYLE <sup>1</sup>	AVE. THW <sup>2</sup> (m)	AVE. HVE <sup>3</sup> (m)	AVE. RUP. LENGTH <sup>4</sup> (m)	NET SLIP. <sup>5</sup> (m)	M <sub>CHAR</sub> <sup>6</sup>			M <sub>MAX</sub> <sup>6</sup>			SLIP RATE <sup>6</sup> (mm/yr)			DST. <sup>7</sup> (km)
						L	HW	H	L	HW	H	5%	M	95%	
<b>Ahtanum Ridge</b>	R[0.9], O[0.1]	330	277	45.0	448	6.8	7.2	7.5	7.05	7.45	7.75	0.03	0.05	0.08	123
Arlington	SS[1.0]			42.5		6.6	7.0	7.3	6.85	7.25	7.55	0.01	0.05	0.10	157
Cleman Mountain	R[0.3], O[0.7]	650	545	23.0	1086	6.5	6.7	6.9	6.75	6.95	7.15	0.01	0.11	0.02	165
Columbia Hills	R[1.0]	180	151	33.5	235	6.4	7.0	7.3	6.65	7.25	7.55	0.02	0.02	0.03	74
Frenchman Hills	R[1.0]	155	130	34.6	202	6.5	6.8	7.3	6.75	7.02	7.45	0.02	0.02	0.03	42
<b>Horn Rapids</b>	R[0.6], O[0.4]	90	76	24.0	136	6.5	6.7	6.9	6.75	6.95	7.15	0.01	0.01	0.02	16
<b>Horse Heaven Hills</b>	R[0.8], O[0.2]	305	256	42.5	430	6.8	7.2	7.5	6.85	7.25	7.55	0.05	0.07	0.13	44
Laurel	SS[1.0]			42.5		6.6	7.0	7.3	6.85	7.25	7.55	0.01	0.05	0.10	222
Luna Butte	SS[1.0]			42.5		6.6	7.0	7.3	6.85	7.25	7.55	0.01	0.05	0.10	171
Manastash Ridge	R[0.9], O[0.1]	290	243	33.5	394	6.4	6.9	7.2	6.65	7.05	7.45	0.03	0.04	0.06	98
Maupin	SS[1.0]			42.5		6.6	7.0	7.3	6.85	7.25	7.55	0.01	0.05	0.10	262
Rattlesnake Hills	[0.9], O[0.1]	335	281	60.0	455	6.8	7.2	7.5	7.05	7.45	7.75	0.03	0.05	0.08	63
<b>Rattlesnake Mountain</b>	R[0.9], O[0.1]	619	519	38.0	840	6.8	7.1	7.4	7.05	7.35	7.65	0.06	0.10	0.19	27
<b>Rattles of Rattlesnake-Wallula Alignment</b>	R[0.4], O[0.6]			50.0		6.8	7.1	7.4	7.05	7.15	7.55	0.01	0.02	0.03	30
<b>Saddle</b>	R[1.0]	328	275	50.0	428	6.8	7.2	7.4	7.05	7.45	7.65	0.03	0.04	0.06	76
Selah	R[0.3], O[0.7]	460	386	22.0	769	6.5	6.6	6.9	6.75	6.85	7.15	0.05	0.07	0.12	116
Toppenish	R[0.9], O[0.1]	305	256	45.0	414	6.6	7.0	7.4	6.85	7.45	7.65	0.03	0.03	0.05	103
<b>Umtanum-Gable</b>	R[0.9], O[0.1]	215	180	33.0	292	6.4	6.9	7.2	6.65	7.15	7.45	0.03	0.03	0.05	10
Wallula	R[0.3], O[0.6], SS[0.1]	250	210	50.0	459	6.9	7.3	7.4	7.15	7.55	7.65	0.03	0.04	0.12	68
<b>Yakima Ridge</b>	R[0.9], O[0.1]	250	210	55.0	339	6.4	7.0	7.6	6.65	7.25	7.85	0.01	0.05	0.10	12

Notes:

<sup>1</sup> For fault style, reverse (R), oblique (O), and strike-slip (SS), with the weights assigned by the SSC TI Team. Values in brackets denote weighting assigned to the alternatives.

<sup>2</sup> Average throw (Thw) is the vertical component of fault slip, derived from the measure structural relief (Table 8.9 in PNNL, 2014). Strike-slip faults do not have a throw or heave component. To convert from meters to feet, multiply by 3.28.

<sup>3</sup> Average heave (Hve) is the horizontal component of fault slip, derived from the average throw by assuming a fault dip of 50°, which is the mean fault dip based on focal mechanisms (Figure 8.26 in PNNL, 2014).

<sup>4</sup> Average characteristic rupture length is based on the mapped trace of the fault (Table 8.8 in PNNL, 2014).

<sup>5</sup> Average net slip is the component of fault slip parallel to the fault plane for faults with normal and oblique slip, using the slip multipliers given in Table 8.11 in PNNL (2014). This value cannot be derived for pure strike-slip faults in the Hanford PSHA (PNNL, 2014).

<sup>6</sup> M<sub>Char</sub>, M<sub>Max</sub>, and slip rates were obtained from Microsoft Excel file attachments to Appendix D1 to PNNL (2014) and are presented as low (L), high (H), highest weight (HW), and median (M) values. All magnitudes are reported as moment magnitude (M). To convert from mm/yr to in./yr, divide by 25.4.

<sup>7</sup> Distance (Dst.) is the closest approach of the fault measured as the horizontal distance from the closest point on the fault tract to the CGS. These measures of the fault's closest approach to the CGS were obtained by using the Proximity Toolset in ArcGIS® and based on the map fault traces in Figure 3.4-3 of this report. The licensee identified the eight faults (in bold) as contributing more than 5 percent to the total hazards at the CGS site (Table 2.2.2-3 in Swank, 2015a). Divide the distances in km by 1.61 to convert to miles.

### 3.4.3.2. Cascadia Subduction Zone Sources

Although the Hanford Site is located relatively far from the Cascadia subduction zone {250–300 km [155–185 mi]}, the downgoing slab of ocean lithosphere extends beneath much of western Washington and Oregon (Figure 3.4-4). Preliminary sensitivity studies conducted by the SSC TI Team showed that earthquakes from Cascadia make a moderate contribution to the seismic hazard at the Hanford Site, mainly at lower spectral frequencies (i.e., 1 Hz and below). Thus, the SSC TI Team included the Cascadia Subduction Zone in the SSC model. Rather than develop a new SSC model, the SSC TI Team used the characterization in the BC Hydro and Power Authority SSC model (BC Hydro, 2012). The BC Hydro SSC model represents the Cascadia subduction zone as two distinct seismogenic sources: (1) an “intraslab source” within the downgoing Juan de Fuca plate (i.e., slab), which is modeled as an areal source zone, and (2) a “plate interface source” located at the interface between the Juan de Fuca and North American plates, which is modeled as a fault source (Figure 3.4-4). The SSC TI Team also determined that two important components of the BC Hydro SSC model needed to be updated for use at the Hanford Site and modified the BC Hydro (2012) source SSC model to account for the location of the Hanford Site based on the seismic, geophysical, and geodetic data reported by McCrory et al. (2006, 2014).

For characterization of the intraslab source zone, the SSC TI Team interpreted plate geometry based on the seismic, geophysical, and geodetic data reported by McCrory et al. (2006). The SSC TI Team determined that the most important parameter was the maximum depth of the plate beneath the Hanford Site, which defines the closest approach of the intraslab source zone to the site. Seismicity data in McCrory et al. (2006) indicate that the seismogenic plate only extends to depths of approximately 60 km [37 mi] at the latitude of the Hanford Site. To allow for the possibility that the seismogenic plate might be deeper at the latitude of the site, the SSC TI Team modified the weighted depth distribution centered on 90 km [56 mi] for the intraslab source zone based on seismicity patterns north and south of this latitude, which effectively extended the intraslab source zone closer to the Hanford Site.

For the plate interface source, the SSC TI Team determined that the most significant parameter was the location of the easternmost extent of the plate interface, which defines the closest approach of that source to the Hanford Site. The SSC TI Team judged that the three alternative locations (i.e., Locations A, B, and C in BC Hydro, 2012) for the landward down-dip extent of the plate interface source were still appropriate. Nevertheless, the SSC TI Team adjusted the weights of the three potential locations used in the BC Hydro model (BC Hydro, 2012), so that the weights are consistent with more recent interpretations that considered earthquakes in the area of nonvolcanic episodic tremor and slip.

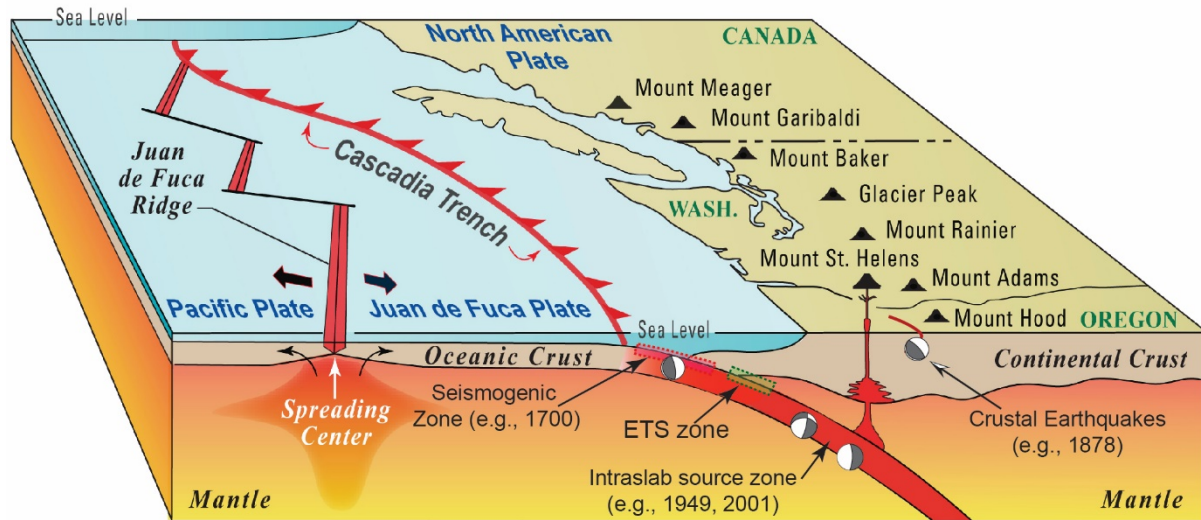


**Figure 3.4-4** Block Diagram Showing the Seismic Sources Related to the Cascadia Subduction Zone, Modified from Dzurisin et al. (2014). The Subduction Interface Source is Labeled “Seismogenic Zone.” The Episodic Tremor and Slip (ETS) Zone Approximates the Fore-Arc Mantle Corner of McCrory et al. (2014), which is the Line of Intersection of the Fore-Arc Moho with the Plate Interface. Example Focal Mechanisms for Historic Earthquakes are Identified to Represent the Kind of Seismicity Typical for Each Zone. The Volcanic Arc Forms the Axis of the Cascade Range. The CGS Site is Right (East) of the Cascade Range and would be Located Off the Image to the Right

### 3.4.3.3. Areal Source Zones

To account for potential seismic hazards from background seismicity associated with unrecognized faults, the SSC TI Team included four areal seismic source zones—Zone B, Zone C, Zone D, and the YFTB (Figure 3.4-5)—in the SSC model. The SSC TI Team developed four distinct areal source zones to account for differences in (1) earthquake recurrence rate, (2)  $M_{max}$ , and (3) expected future earthquake characteristics (e.g., style of faulting, rupture orientation, and seismogenic thickness). The SSC TI Team did not identify and characterize individual faults within Zones B, C, and D because these zones do not contribute significantly to the total hazard relative to the YFTB zone. However, the YFTB source zone encompasses the 19 individual YFTB fault sources described previously, as well as the Hanford Site. Thus, to avoid double-counting the seismicity associated with YFTB faults in the YFTB source zone, the SSC TI Team differentiated future earthquakes associated with these fault sources from the additional background seismicity within the YFTB zone.

To model the occurrence of future earthquakes within the areal source zones, the SSC TI Team used virtual faults that were randomly located within each of the zones. Earthquakes are simulated on these virtual faults based on the geological and seismological characteristics of each zone, including the orientation and style of faulting, 3D rupture geometries, magnitude-dependent rupture dimensions, thickness of the seismogenic crust, and recurrence rates based on the record of past earthquakes. The style of faulting, seismogenic thickness, and orientation of ruptures for each source zone was determined from earthquake focal mechanism information, as well as the tectonic environment of the Hanford Site region. The

SSC TI Team estimated  $M_{max}$  using the earthquake with the largest observed magnitude within each source zone and considering the  $M_{max}$  calculated from the fault-source dimensions.

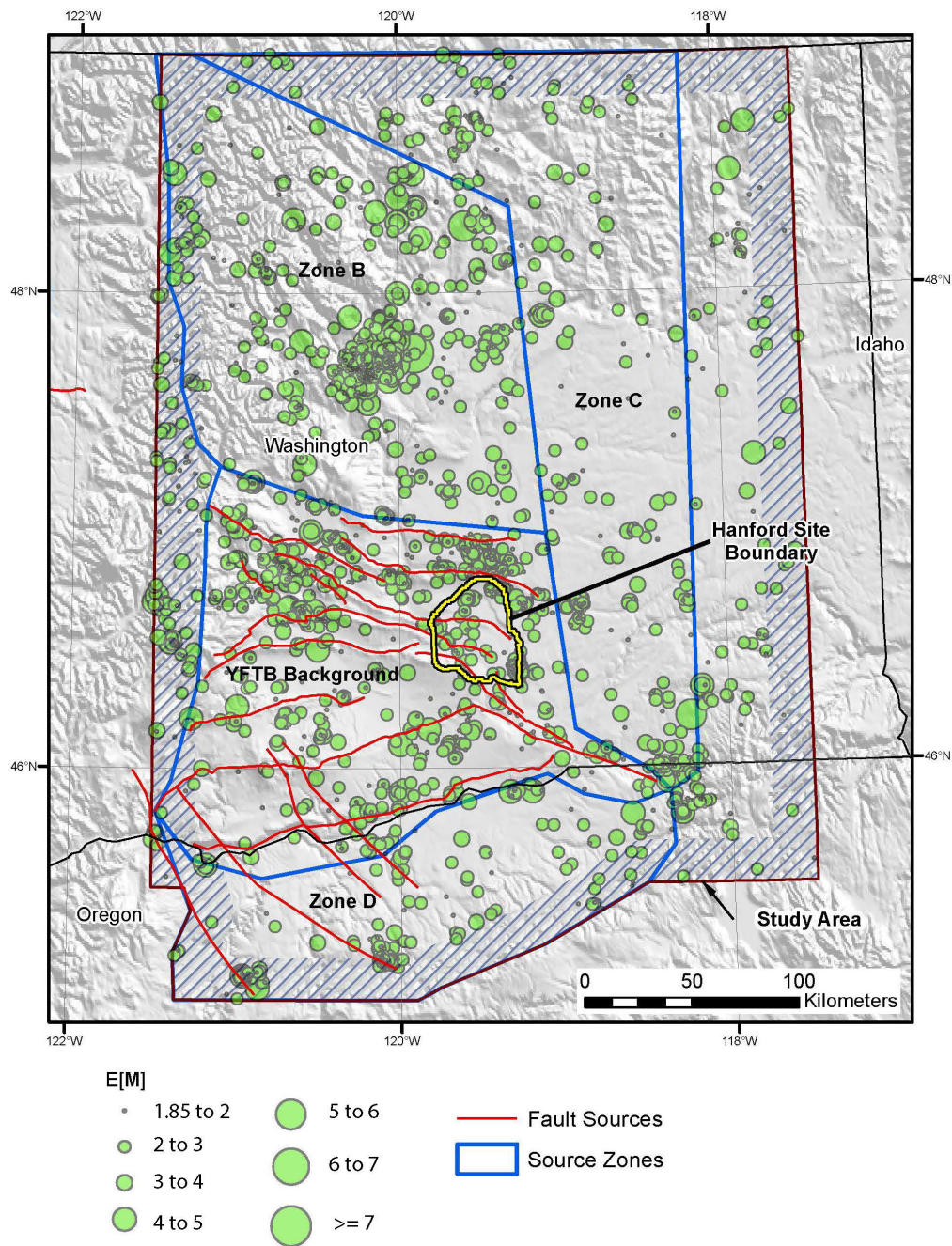


**Figure 3.4-5 Seismic Source Zones Characterized in the SSC Model and Earthquake Epicenters in the Hanford PSHA Crustal Catalog with  $M \geq 1.85$ . Red Lines Indicate Fault Sources. The Figure was Adapted from Figure 8.1 of PNNL (2014). E[M] is the Expected Moment Magnitude as Defined in NUREG-2115 (NRC, 2012b)**

The upper part of the  $M_{\max}$  distribution for the YFTB source zone is smaller than used for the other source zones because large-magnitude events associated with the known fault sources already are considered as separate seismic sources for the YFTB source zone.

To develop the boundaries of the areal source zones, the SSC TI Team primarily used the source zone boundaries developed in a previous regional seismic hazard characterization (JBA et al., 2012). In particular, the SSC TI Team defined the eastern boundary of the YFTB using deep crustal structures (Figure 8.33 in PNNL, 2014) and positioned the western boundary of the YFTB source zone to include the westernmost topographic expression of the YFTB faults and the boundary with the Cascades tectonic province. The northern boundary of the YFTB was drawn to coincide with the deeper crustal boundary identified in McCaffrey et al. (2007). The SSC TI Team placed the boundary between the YFTB and Zone D to encompass a region of lower seismicity rates that occur south of the Columbia Hills within Zone D. The boundary between the YFTB Zone and Zone D was also drawn so that a collection of faults trending north-northwest remained within the YFTB source zone.

The SSC TI Team developed a database of past earthquakes for these areal sources by compiling earthquake information from both historical and instrumental records that span the timeframe from November 1866 to April 2013. These records include regional and continental-scale earthquake catalogs, scientific literature, and preexisting earthquake catalog compilations (e.g., JBA et al., 2012; Geomatrix, 1996). The SSC TI Team combined the information from these sources and developed two catalogs: one for the distant Cascadia subduction zone and one for the continental crust beneath the CGS site region. The process the SSC TI Team used to compile the two earthquake catalogs is similar to the CEUS process described in NRC (2012b).

The SSC TI Team obtained earthquake records from the Hanford Site, Pacific Northwest Seismic Network, and USGS Advanced National Seismic System catalogs, which recorded earthquake magnitudes in either duration magnitude or coda magnitude. The SSC TI Team then converted the various magnitudes to  $M$  using the methodology recommended in NRC (2012). The SSC TI Team then used four declustering techniques to identify independent events and remove aftershocks and duplicate events from the catalogs (Gardner and Knopoff, 1974; Grünthal, 1985; Uhrhammer, 1986; EPRI, 1988). In addition, the SSC TI Team used two approaches to assess catalog completeness: the Stepp Method (Stepp, 1972) and a probability of detection methodology (Veneziano and Van Dyck, 1985). The SSC TI Team used both uniform and smoothed seismicity grids to represent the spatial density of earthquake occurrences and the distribution of earthquake recurrence within the areal source zones. Because changes in tectonics, geology, and seismicity across source zone boundaries were not sharply defined, the SSC TI Team used “leaky source zone boundaries,” which allow ruptures beginning within a source zone to propagate into adjacent source zones. Following commonly used practice, the SSC TI Team used the truncated exponential (Gutenberg and Richter, 1956) magnitude frequency distribution to define the recurrence relationships for future earthquakes within the areal source zones.

Table 3.4-2 summarizes the SSC TI Team’s areal source characterization. The data were derived from information in Chapter 8 in PNNL (2014) and the hazard input document (Appendix D1 to PNNL, 2014). According to the licensee, the YFTB is the only areal zone that contributes more than 5 percent to the total hazard at 1 and 10 Hz, for mean AFE of  $10^{-4}$  and  $10^{-5}$  (Table 2.2.2-3 in Swank, 2015a). In fact, the YFTB source zone is the dominant contributor to the total hazard at 1 and 10 Hz, for mean AFE of  $10^{-4}$  and  $10^{-5}$ .

AREAL SOURCE ZONE	SEISMO-GENIC THICKNESS (km)	FAULT STYLE <sup>2</sup>	ORIENTATION OF RUPTURES		M <sub>MAX</sub>	MAX OBS <sup>3</sup>	SPATIAL VARIATIONS <sup>4</sup>
			Strike (°)	Dip (°)			
<b>YFTB</b>	13 [0.20] <sup>1</sup> 16 [0.50] 20 [0.30]	R [0.60] N [0.20] SS [0.20]	R: 40 [0.20] 90 [0.60] 140 [0.20] N: 10 [0.20] 90 [0.60] 140 [0.20] SS: 60 [0.50] 150 [0.50]	R: 30 [0.20] 50 [0.60] 70 [0.20] N: 40 [0.20] 60 [0.60] 80 [0.20] SS: 70 [0.40] 90 [0.60]	6.5 [0.30] 6.75 [0.40] 7.0 [0.30]	<b>M4.79</b>	Uniform [0.80] A-Kernel [0.20]
<b>Zone B</b>	10 [0.20] 12 [0.50] 15 [0.30]	R [0.60] S [0.40]	Uniform 0-360	Not Modeled	6.5 [0.30] 6.75 [0.40] 7.0 [0.30] 7.25 [0.09] 7.5 [0.01]	<b>M7.06</b>	A-Kernel [1.00]
<b>Zone C</b>	13 [0.20] 16 [0.50] 20 [0.30]	R [0.60] S [0.40]	Uniform 0-360	Not Modeled	6.5 [0.30] 6.75 [0.40] 7.0 [0.30] 7.25 [0.09] 7.5 [0.01]	<b>M5.98</b>	Uniform [1.00]
<b>Zone D</b>	15 [0.20] 20 [0.50] 24 [0.30]	R [0.60] S [0.40]	Uniform 0-360	Not Modeled	6.5 [0.30] 6.75 [0.40] 7.0 [0.30] 7.25 [0.09] 7.5 [0.01]	<b>M4.80</b>	Uniform [0.80] A-Kernel [0.20]
Notes:	<sup>1</sup> Numbers inside brackets are the assigned weights. To convert kilometers to miles, divide by 1.61. <sup>2</sup> For fault style, normal (N), reverse (R), and strike-slip (SS). <sup>3</sup> Maximum Observed earthquake <sup>4</sup> Spatial variation refers to the modeling method used to smooth the spatial seismicity parameters, either as uniform distributions with the zone or with the adaptive kernel (A-Kernel) approach of Silverman (1986).						

### 3.4.4. Ground Motion Characterization

The GMC model for the CGS site represents the second element of a PSHA. The goal of the GMC TI Team was to characterize median ground motions and their associated aleatory variability (sigma) for both shallow crustal and subduction zone earthquakes. Specifically, the GMC models consist of two suites of GMPEs for 5-percent damped horizontal spectral accelerations for 20 oscillator frequencies between 0.1 and 100 Hz. Due to the limited number of strong ground motion earthquake recordings in the CGS region, the GMC TI Team used existing GMPEs developed from ground motion datasets in more seismically active regions as the basis for the GMC. The GMC TI Team implemented an approach referred to as the “scaled backbone approach” to capture the epistemic uncertainty in predicted median ground motions. This approach uses a set of weighted adjustment factors to produce a suite of GMPEs that encompass a range of ground motion amplitudes and alternative magnitude- and distance-scaling models.

#### 3.4.4.1. Median Models

For the crustal earthquakes, the GMC TI Team selected four of the five NGA-West2 GMPEs (Bozorgnia et al., 2014). To implement the scaled backbone approach, the GMC TI Team first selected a set of earthquake scenarios in terms of magnitude, source-to-site distance, fault dip



angle, and depth to the top of rupture. For each scenario, the GMC TI Team determined the median predicted ground motions from Chiou and Youngs (2014), Abrahamson et al. (2014), Boore et al. (2014), and Campbell and Bozorgnia (2014) and the residual in the predicted medians from each of the four GMPEs with respect to the model of Chiou and Youngs (2014). In order to capture the epistemic uncertainty in both the predicted median ground motions and the host-to-target adjustment factors, the GMC TI Team expanded these backbone GMPEs into multiple sets of GMPEs. The GMC TI Team centered the backbone model based on the geometric mean of the residuals from the four NGA-West2 GMPEs using a mixed-effects model. The GMC TI Team represented the uncertainty in scaling about the centered backbone with a 2D Gaussian covariance matrix, which it then sampled with a nine-point discrete distribution. As a result of using the scaled backbone approach and the four NGA-West2 GMPEs, the GMC TI Team transformed its initial single backbone based on the CY14 GMPE to nine alternative, weighted GMPEs. Figure 3.4-6 illustrates an example of this process, showing that the resulting range in predicted ground motions is broader than the range in the initial four NGA-West2 GMPEs, including significant differences in magnitude scaling.

For subduction zones, the GMC TI Team concluded that only the recently completed BC Hydro project (BC Hydro, 2012) GMPE was appropriate for use in developing a subduction-zone GMC model for the Hanford Site. However, rather than simply using the BC Hydro GMPE as the backbone model for the GMC, the GMC TI Team made several revisions to this GMPE, including adjustments to incorporate new earthquake data collected after the BC Hydro project was completed.

#### *3.4.4.2. Ground Motion Characterization Median Adjustment Factors*

Although eastern Washington is in an active tectonic belt, the GMC TI Team concluded that the region around the Hanford Site has some elements of a stable continental region given its distance from the plate boundary, its low seismic activity rates, and unique upper crustal physical properties. Thus, in order to use active-tectonic region GMPEs for the Hanford PSHA, the GMC TI Team developed an extensive set of “host-to-target” adjustment factors that consider differences between the host (i.e., seismically active regions such as California) and target (i.e., eastern Washington) regions in terms of earthquake source properties, regional path characteristics, and site conditions. For both the shallow crustal and subduction zone earthquakes, the GMC TI Team adjusted the GMPEs to characterize the hazard at the baserock horizon for the Hanford Site (i.e., the top of the Wanapum Basalt in the Columbia River Basalt). These baserock-elevation ground motions were used as input motions for the site response analysis for the CGS site.

In addition to gathering available ground motion recordings, the GMC TI Team also developed profiles of  $V_S$ , density and damping for the five recording stations near the Hanford Site. The GMC TI Team also compared values of the quality factor  $Q$  (i.e., a measure of energy loss of earthquake waves due to anelastic attenuation) for sites in Washington and California, finding moderately higher crustal  $Q$  for eastern Washington relative to coastal California. The GMC TI Team used both the estimate of local rock and soil properties for the Hanford Site and the differences in crustal  $Q$  between Washington and California to develop adjustment factors for the backbone GMPEs.

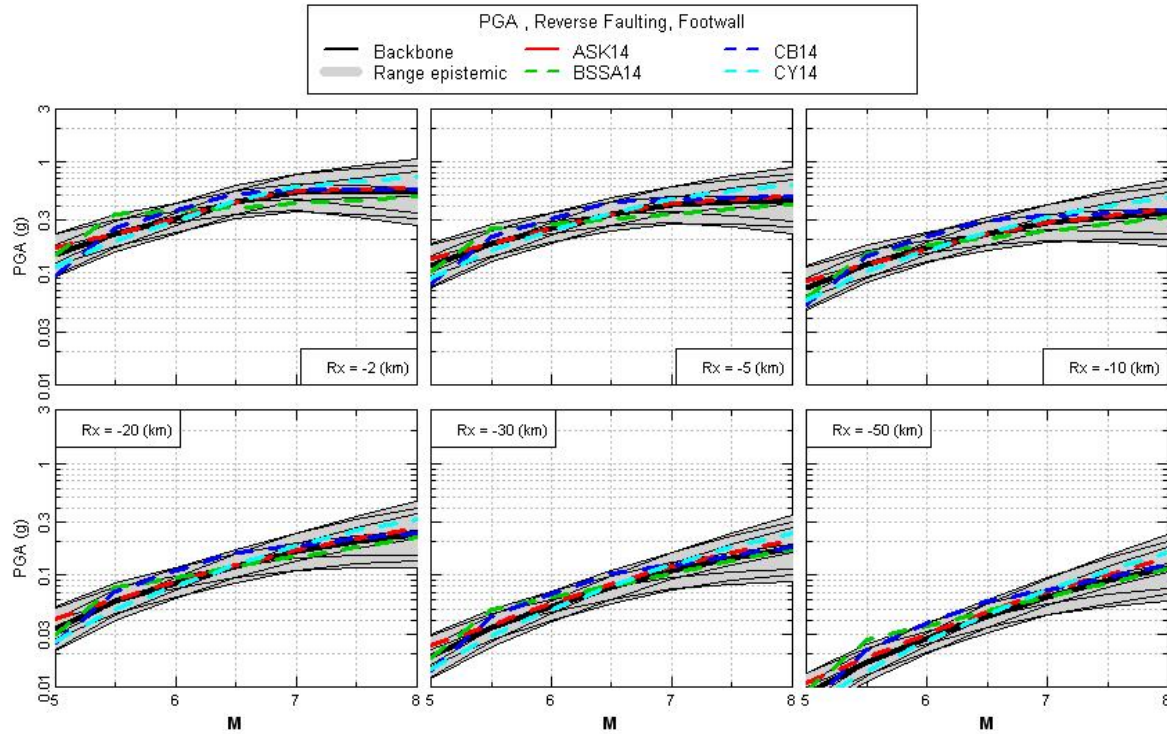


**Figure 3.4-6 Range of Magnitude Scaling Produced by Crustal Footwall GMPEs. The Illustration is for PGA, and for the Reverse Faulting Case with the Site Located on the Footwall of the Fault. The Different Site-To-Source Distances are in Terms of the Parameter Rx, which is the Perpendicular (to Fault Strike) Distance to the Site from the Fault Line (Surface Projection of Top of Rupture), Positive in the Downdip Direction (in km). The Four NGA-West2 GMPEs are Shown by Colored Lines, the Nine Scaled Backbone Models are Solid Black Lines, and the Total Range in Epistemic Uncertainty is Indicated by the Gray Shaded Area. To Convert km to Miles, Divide by 1.61**

Because the Hanford Site is located atop a sedimentary basin, the GMC TI Team also investigated whether to include an adjustment in the models to account for basin effects. Seismic waves travelling through sedimentary basins are usually amplified, and examples of this phenomena are documented worldwide. To assess the potential effects of the sedimentary basin, the GMC TI Team sponsored a study that conducted 3D seismic waveform simulations of the limited number of recorded earthquakes near the site and also modeled waveforms of larger magnitude hypothetical earthquakes in the region. Due to the inconclusive simulation results and the fact that the shallow, mostly flat-lying sediments of the basin are above the baserock horizon level for which the GMPEs are calibrated, the GMC TI Team decided that any potential basin effects at the site should be included as part of the site response analysis rather than as an adjustment factor for the GMPEs.

#### 3.4.4.3. Aleatory Variability

In addition to developing GMPEs that predict median ground motions, the GMC TI Team developed models to characterize the random (i.e., aleatory) variability about the median ground

motion. Because Enclosure 1 to the 50.54(f) letter (NRC, 2012a) requests that licensees perform a detailed site response analysis, the GMC TI Team first separated the residuals between the predicted and observed ground motions into its component pieces to remove the repeatable effects of site response. The GMC TI Team then combined the standard deviations for each of the remaining components of the total residuals to produce a partially nonergodic total aleatory standard deviation, which is referred to as “single-station sigma.”

An additional motivation for the adoption of a single-station sigma approach in the Hanford GMC study is that the value of the event-corrected single-station standard deviation (or single-station phi) has proven to be relatively constant across different regions and tectonic environments. The lack of regional dependence of the single-station phi implies that these values are more readily “exportable” to different regions and that global datasets can be used to estimate them. This was important for the Hanford study, as the available regional data were insufficient to estimate these parameters.

The Hanford GMC TI Team identified several basic requirements that need to be satisfied in order implement a partially nonergodic GMC model in the PSHA. Specifically, (1) the median value of the site term must be properly estimated for the site under analysis, (2) the epistemic uncertainty on the value of the site term must be fully accounted for, and (3) the epistemic uncertainty on the single-station sigma must be taken into account.

For the Hanford PSHA, the first requirement is satisfied because a site-specific correction is applied to the backbone GMPEs. The site term is estimated through the  $V_S$ -kappa correction and the site response calculations. The epistemic uncertainty in the site term (the second requirement) is accounted for by developing branches in the median logic tree for the  $V_S$ -kappa correction factors and by including the variability of the site amplification factor. The variability of the site amplification factor is accounted for by including uncertainty in the characterization of the Saddle Mountains Basalt stack and in the characterization of the suprabasalt sediments in the subsequent CGS-specific site response analyses. To ensure that the site amplification factors captured enough uncertainty, the GMC TI Team prescribed a minimum level of uncertainty. The third requirement was met by including alternative branches in the sigma logic tree model that represent the global epistemic uncertainty in the sigma model.

#### *3.4.4.4. Implementation in the Ground Motion Characterization Logic Tree*

To construct the GMC models for the crustal and subduction zone earthquakes, the GMC TI Team developed two logic trees with multiple nodes and branches to capture the epistemic uncertainty in the median as well as the host-to-target adjustment factors. Each of the logic trees starts with a “backbone” GMPE, which is then expanded into multiple GMPEs through three to four sets of weighted branches that capture alternative models for magnitude and distance scaling, ground motion amplitude, and host-to-target adjustment factors.

The GMC logic tree for median ground motions for the crustal earthquakes consists of a single branch for the backbone GMPE, seven alternative weighted branches to represent the differences in site conditions ( $V_S$  and site kappa) between the host and target regions, nine branches for alternative scaling and adjustments of the backbone GMPE, and three branches to account for potential differences in source properties between the host and target regions. The resulting GMC model for median motions for the crustal earthquakes consists of 189 weighted alternative GMPEs. For the aleatory variability about the median GMPEs, the GMC TI Team developed three alternative branches (low, medium, and high).

The GMC logic tree for median motions for the subduction zone earthquakes consists of a single branch for the backbone GMPE, three branches for epistemic uncertainty in the median, three branches to represent alternative magnitude scaling, two branches for alternative distance scaling, and four branches for differences in the host-to-target site conditions. The resulting GMC model for median motions for the subduction zone earthquakes consists of GMPEs with alternative weights. For the aleatory variability about the median GMPEs, the GMC TI Team developed three alternative branches (low, medium, and high).

### **3.4.5. Probabilistic Seismic Hazard Analysis**

The SSC and GMC TI Teams implemented the SSC and GMC models to develop baserock PSHA hazard curves for each of the critical DOE facility sites and the CGS site (Figure 3.4-7). The licensee then used these baserock hazard curves as inputs to the site response analysis described in Section 3.4.7 of this report. For the Hanford Site, the GMC TI Team selected the top of the Wanapum Basalt in the Columbia River Basalt Group as the reference baserock horizon (Figure 3-4.8).

After implementing the SSC and GMC logic trees to develop the baserock hazard curves at the Hanford Site, the TI Teams performed a deaggregation of the hazard for both the 1 Hz and 10 Hz spectral accelerations for  $10^{-4}$  and  $10^{-5}$  mean AFE. For 10 Hz, the TI Teams determined that local earthquakes with moderate-to-large magnitudes {i.e., *M*5–*M*7 at distances from 0 to 20 km [0 to 12.5 mi]} dominate the hazard, whereas for 1 Hz, larger distant subduction earthquakes {i.e., *M*8.5 at distances from 250 to 300 km [155 to 186 mi]} dominate the hazard.

### **3.4.6. Staff Confirmatory Evaluations of the Hanford Probabilistic Seismic Hazard Analysis**

The NRC staff performed a series of confirmatory evaluations to support its review of the Hanford PSHA results as they apply to the CGS site (Site C in PNNL, 2014). Several of these confirmatory evaluations are summarized in this report to illustrate the scope and depth of the NRC evaluations and to provide additional information on the current CGS PSHA results in support of the KM mission of this NUREG/KM. The NRC staff's evaluation (NRC, 2016b) provides a complete description of all the confirmatory analyses staff relied on for its review.

#### *3.4.6.1. Evaluation of the Baserock Probabilistic Seismic Hazard Analysis Results*

To evaluate the Hanford PSHA, the NRC staff performed a confirmatory evaluation of the seismic sources that contribute the most to the hazard at the CGS site. The purpose of the staff's evaluation was to assess the reasonableness of the 1 Hz and 10 Hz mean hazard results for the most significant seismic sources, and to assess the impact of the most significant source and ground motion parameters on the final hazard results. For this confirmatory analysis, the NRC staff selected a subset of the SSC and GMC branches that focus on the highest weighted components of the logic tree.

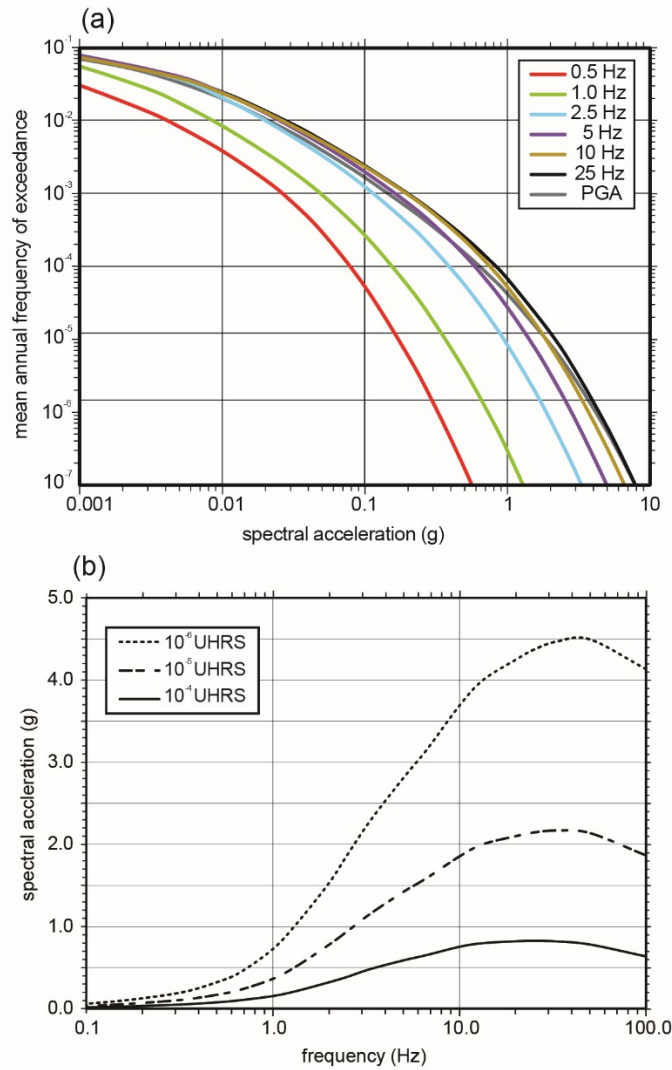


**Figure 3.4-7** (a) The Reference Baserock Probabilistic Seismic Hazard Curves for the CGS Site for PGA and Six Spectral Accelerations, Based on the Data in Table 2.2.2-2a in Swank (2015a). (b) The Mean UHRs for the  $10^{-4}$ ,  $10^{-5}$ , and  $10^{-6}$  Annual Exceedance Frequencies, Based on the Data in Table 2.2.2-1 in Swank (2015a)

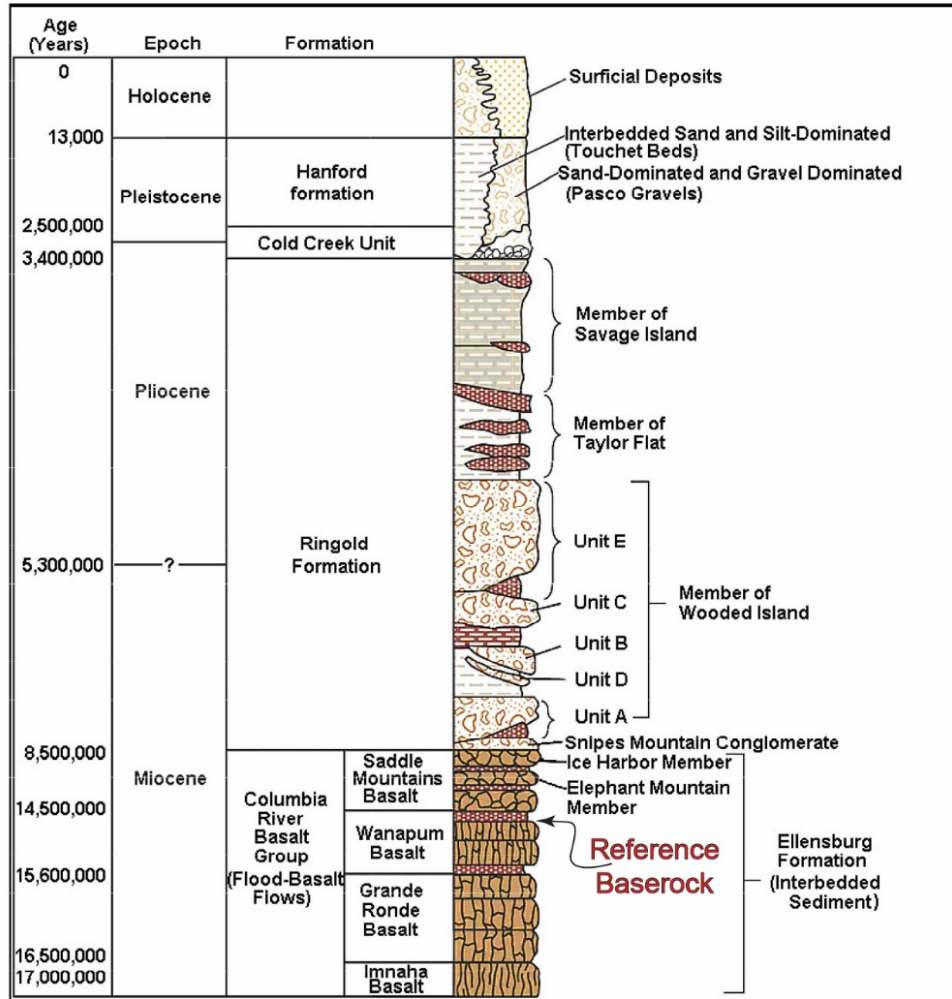


**Figure 3.4-8 Generalized Stratigraphy of the Hanford Site and Vicinity Showing the Location of the Reference Baseroack Horizon, which is Atop the Uppermost Low in the Wanapum Basalt. The Figure was Adapted from Figure 2.1 in Barnett et al. (2007)**

The staff selected four YFTB fault sources for its confirmatory evaluation: Rattlesnake Mountain, Yakima Ridge, Umtanum Ridge, and Saddle Mountain faults (Figure 3.4-9(a)). For each of the fault sources, the staff evaluated a plausible range of slip rates. Figure 3.4-9(b) and (c) also show the staff's 1 Hz and 10 Hz hazard curves for the Rattlesnake Mountain fault. For its confirmatory evaluation, the staff used 27 of the 189 crustal earthquake GMPEs, also shown in Figure 3.4-9(b) and (c). Figure 3.4-9(b) and (c) also show hazard curves resulting from using the 5<sup>th</sup> and 95<sup>th</sup> percentile slip rates for the Rattlesnake Mountain fault. Finally, this figure shows that the staff's confirmatory results closely match the PNNL (2014) results for both the 1 Hz and 10 Hz mean hazard curves. Using similar methods for the other contributing YFTB faults, the NRC staff's confirmatory evaluation similarly matched the results in PNNL (2014) for the 1 Hz and 10 Hz hazard curves.

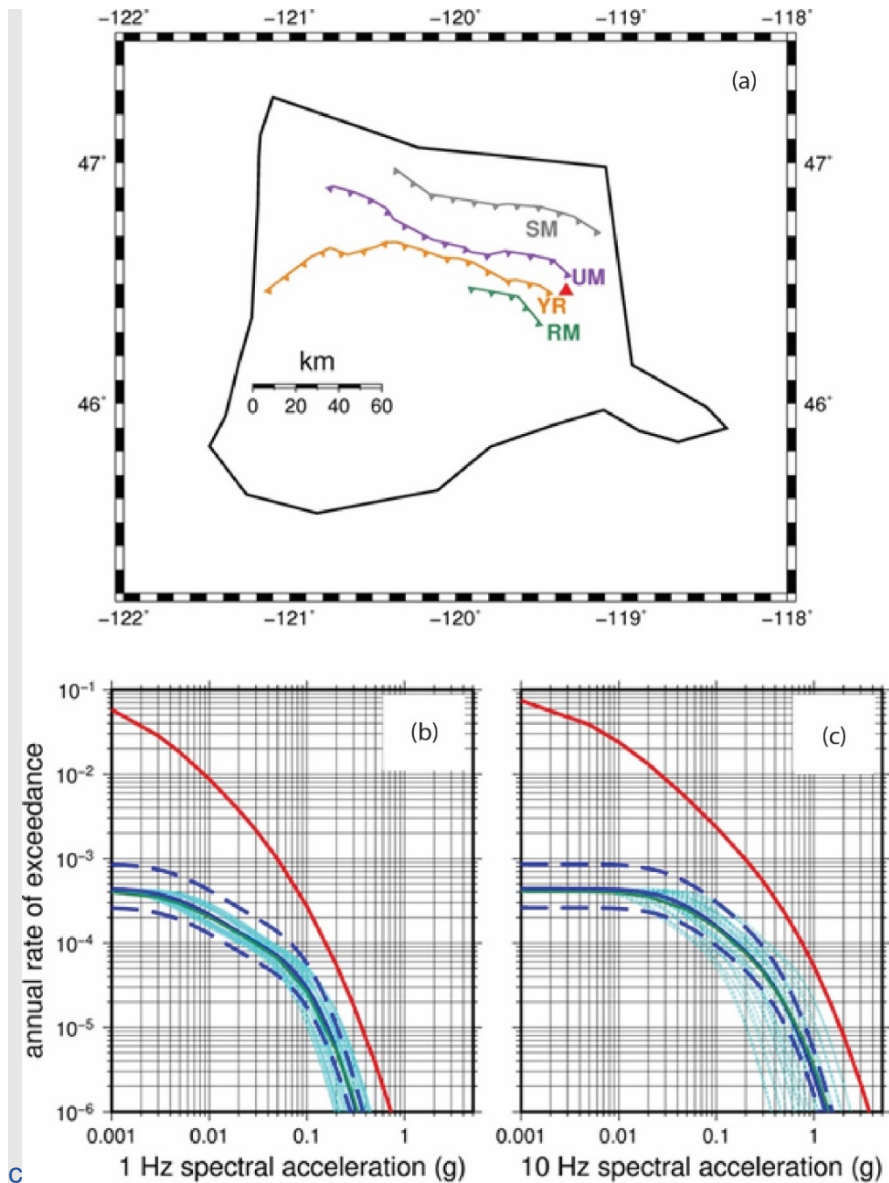


**Figure 3.4-9** (a) The NRC Staff's Confirmatory Calculation for the Rattlesnake Mountain Fault, which uses 27 of the 189 Crustal Earthquake GMPEs (Light-Blue Lines). Hazard Curves (Blue Dashed Lines) Result from Using the 5th and 95th Percentile Slip Rates for the Rattlesnake Mountain Fault. The NRC Staff's Confirmatory Results (Solid Blue Line) Closely Match the Licensee's Results (Solid Green Line), for 1 Hz (b) and 10 Hz (c)

### 3.4.6.2. Evaluation of Fault Source Geometries

To confirm that the SSC TI Team's faulting model adequately captured the appropriate range of uncertainty, the NRC staff conducted confirmatory calculations based on two alternative interpretations of the subsurface geometry of faults in the YFTB. The goal of these confirmatory studies was to evaluate whether the range of epistemic uncertainty included in the SSC model

was sufficient to ensure that the resulting hazard captured the center, body, and range of technically defensible interpretations.

In the first alternative, the NRC staff used Coulomb elastic dislocation modeling software (Lin and Stein, 2004; Toda et al., 2005) to calculate the expected topographic relief of Saddle Mountain based on the SSC TI Team's fault slip values for the Saddle Mountain fault, as given in Appendix D to PNNL (2014). Results of this calculation show that the Coulomb elastic dislocation model's calculated topographic relief of Saddle Mountain is less than the observed topographic relief (Figure 3.4-10(a)). To reproduce the topography of Saddle Mountain using the Coulomb dislocation model, the NRC staff had to increase the amount of slip by 30 to 50 percent (Figure 3.4-10(b)). The NRC staff recognizes that its elastic dislocation model does not account for elastoplastic deformation and, therefore, is a simplified representation of the topographic relief produced by fault slip. Nevertheless, results from the staff's Coulomb elastic dislocation modeling suggest that the fault-slip ranges of these faulting parameters (e.g., fault dip or fault slip) in the SSC model (PNNL, 2014) may have been too narrow.

To evaluate the significance of these modeling results on the PSHA, the staff conducted a sensitivity analysis using the PSHA confirmatory model discussed in Section 3.4.6.1 of this report. In this sensitivity analysis, the NRC staff modified the faulting parameters for the Yakima Ridge, Umtanum Ridge, Rattlesnake Mountain, and Saddle Mountain fault sources to calculate the effect on baserock hazard at the CGS site. The NRC staff's sensitivity analysis shows that these parameter changes to the YFTB faults did not significantly affect the PSHA at 1 and 10 Hz for  $10^{-4}$  and  $10^{-5}$  annual exceedance frequencies. Therefore, in its staff assessment (NRC, 2016b), the NRC staff concluded that the current epistemic uncertainty in the SSC TI Team's model is acceptable.

The NRC staff also evaluated the potential significance of including the thin-skinned fault model in the SSC model using similar weights to the thick-skinned and thin-skinned models that were applied in a recent SSC model for the Hanford Site (i.e., JBA et al., 2012). For this evaluation, the NRC staff conducted a confirmatory analysis using its PSHA model discussed in Section 3.4.6.1. The NRC staff calculated the fault areas for the YFTB faults, using the dip angles from PNNL (2014) for depths of 8 km [5 mi] representing a thin-skinned model, and depths of 16 km [10 mi] for a thick-skinned model, and incorporated these alternatives into the logic tree. The staff's sensitivity analyses showed that including the thin-skinned model into the SSC model with weights similar to those applied in JBA et al. (2012) did not significantly affect the PSHA at 1 and 10 Hz for  $10^{-4}$  and  $10^{-5}$  annual exceedance frequencies and that incorporation of the thin-skinned tectonic model would therefore not significantly affect the PSHA results.

During the course of its review, the NRC staff also reviewed a geologic publication by Casale and Pratt (2015), which used seismic reflection data to interpret YFTB faults in the subsurface in terms of a thin-skinned fault model. In the paper, Casale and Pratt indicate that their model would result in relatively high slip rates on these faults—0.10 to 0.23 mm/yr [0.004 to 0.009 in./yr]—compared to the rates derived by the SSC TI Team. The Casale and Pratt (2015) model assumes a thin-skinned interpretation of the YFTB, but it also assumes the geologic age for the onset of faulting at 3.5 Ma, which is inconsistent with the 6–10 Ma age for the onset of faulting as indicated by the unconformity observed at Saddle Mountain. Using the fault offsets determined in Casale and Pratt (2015) with the correct age of the unconformity yields a slip rate of 0.13–0.04 mm/y [0.005–0.002 in./yr], which is consistent with those developed in the SSC TI Team's model.



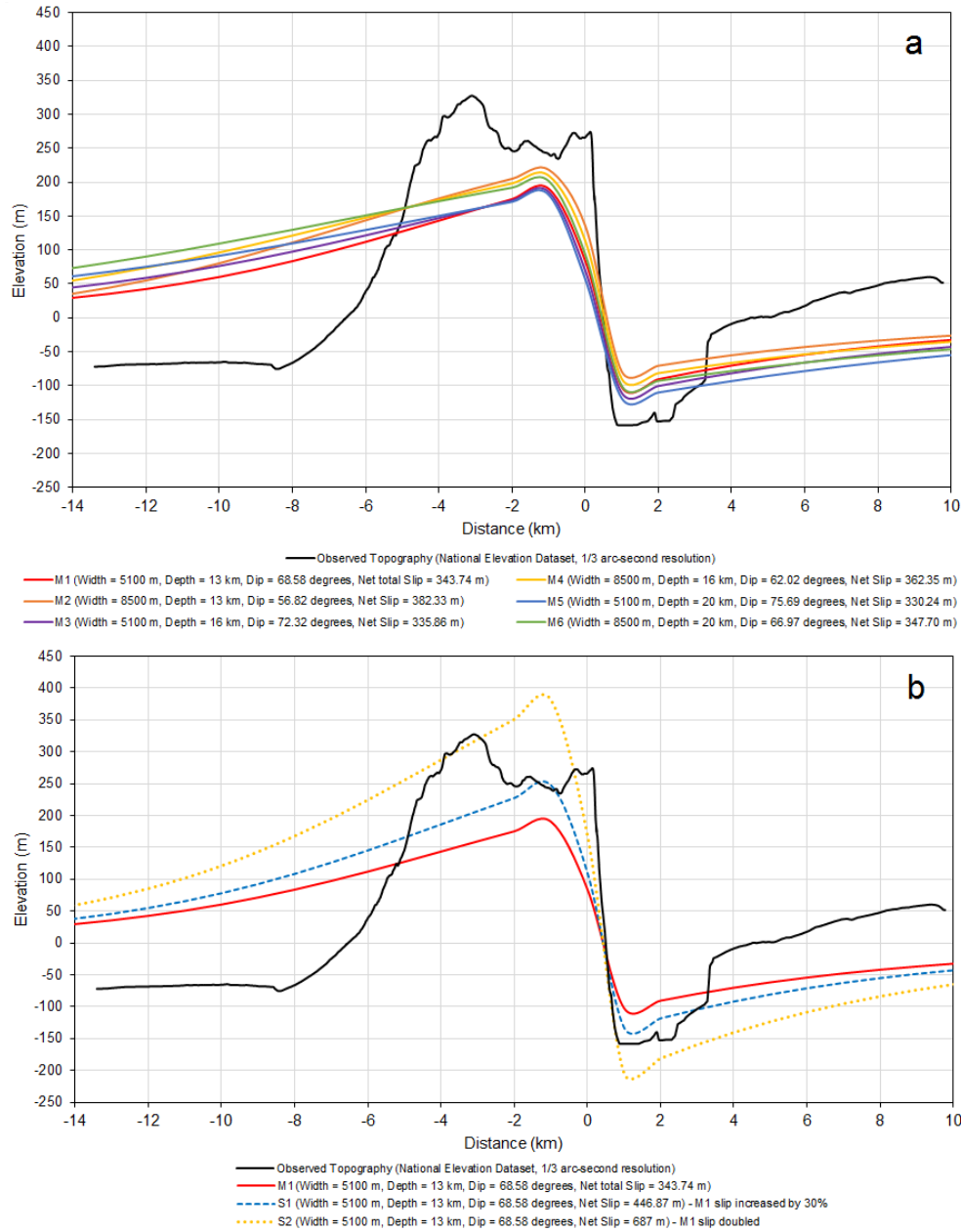


**Figure 3.4-10 (a) Observed (Black Line) and Modeled (Colored Lines) Topography Using the SSC TI Team’s Fault-Source Parameters and the NRC Staff’s Elastic Dislocation Model for the Saddle Mountain Fault. (b) Observed (Black Line) Topography and Differences in Modeled (Colored Lines) Topography Generated by Increasing the Fault Slip-Rate by 30 to 50 Percent in the Staff’s Elastic Dislocation Model**

### 3.4.6.3. Evaluation of Cascadia Subduction Zone Hazard

To confirm the relatively small contribution of Cascadia Subduction Zone seismicity to the hazard results, the NRC staff evaluated the potential ground motion at the Hanford Site from an  $M9.1$  earthquake occurring on the plate interface source. The NRC staff used the GMC model in PNNL (2014) for the Cascadia Subduction Zone to calculate 84<sup>th</sup> percentile response spectra for an  $M9.1$  earthquake occurring on the subduction interface, at distances of 320 km [200 mi] and 350 km [218 mi] from the Hanford Site. As shown in Figure 3.4-11, the calculated 84<sup>th</sup> percentile response spectra for this large earthquake scenario are significantly lower than both the SSE and operating basis earthquake for the CGS site. Thus, contributions of the Cascadia Subduction Zone seismicity to the total hazard at the Hanford Site are small.

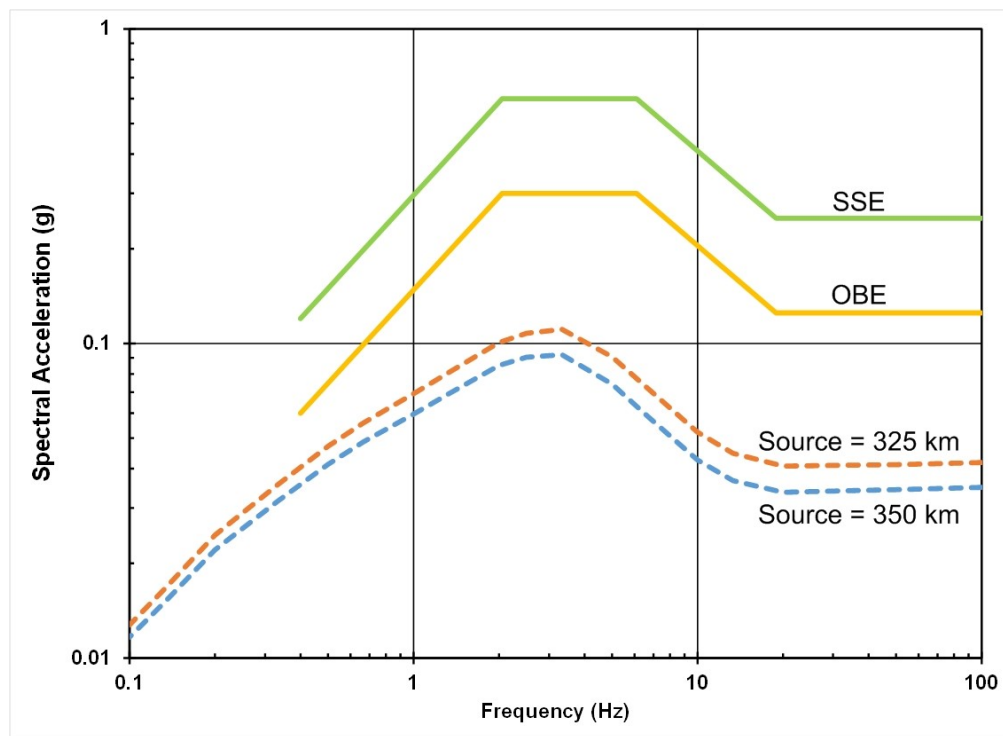


**Figure 3.4-11** The NRC Staff's Deterministic Models of the 84<sup>th</sup> Percentile Spectral Acceleration at the CGS Site from an  $M9.1$  Earthquake Occurring 320 km [200 mi] (Upper Dashed Line) and 350 km [218 mi] (Lower Dashed Line) from the Site in the Cascadia Subduction Zone, Showing a SSE and Operating-Basis Earthquake for the CGS Plant for Comparison

### 3.4.6.4. Evaluation of Areal Source Zone Hazard

The NRC staff performed a confirmatory evaluation of hazard contribution of the YFTB source zone in the PNNL PSHA (PNNL, 2014), which, as the host areal source zone, contributes significantly to both the 1 Hz and 10 Hz total mean hazard for the CGS site. Similar to the SSC TI Team's approach, the NRC staff assumed that the majority of the seismicity within the YFTB zone is not associated with YFTB faults. For this evaluation, the NRC staff developed a set of virtual faults to generate earthquakes not directly associated with known faults within the YFTB. Using the Hanks and Bakun (2008) magnitude-area scaling relationships, the staff derived the length for each of the virtual faults from the median  $M_{max}$ , faulting mechanism, dip angle, and

seismogenic thickness used in the YFTB zone logic tree. For each of the virtual faults in the YFTB zone, the staff calculated the hazard using a range of earthquake magnitudes from *M*5 to the median maximum-magnitude earthquake, which is *M*6.8. The staff developed a suite of seismic hazard curves for each of the virtual faults and then averaged the results to obtain mean 1 Hz and 10 Hz hazard curves for the YFTB source zone.

Figure 3.4-12(a) shows the location of the virtual reverse faults for the YFTB source zone. For its analysis, the NRC staff placed virtual faults more densely around the CGS site and more sparsely at distances beyond 100 km [62 mi] from the site. The NRC staff used this placement of virtual faults to adequately capture the range of significant source-to-site distances.

Each fault in Figure 3.4-12(a) is about 31 km [19 mi] long and has a down-dip width of about 20 km [24.4 mi]. To represent the predominant structural characteristics of the YFTB, the NRC staff selected fault orientations randomly between N60°W and N120°W for the reverse-faulting mechanism, consistent with the weighting used by the SSC TI Team. For the strike-slip and normal faulting mechanisms, the staff selected similar predominantly east-to-west fault orientations. Figure 3.4-12(b) and (c) shows the 1 Hz and 10 Hz hazard curves for each of the 324 YFTB virtual faults and the staff's and TI Teams' mean hazard curves, which compare favorably with those developed in PNNL (2014).

### **3.4.7. Site Response Evaluation**

To develop site-specific hazard curves at the control point elevation, the licensee performed a site-response analysis. This was done after the completion of the Hanford SSHAC study. The purpose of the site response analysis was to determine the site amplification that occurs because of baserock ground motions propagating upward through the soil/rock column to the surface. The critical soil and rock characteristics that determine the frequencies of ground motion affected by the upward propagation of baserock motions are the layering of soil or soft rock, the thicknesses of these layers, the  $V_S$  and low-strain damping of the layers, and the degree to which the shear modulus and damping change with increasing input baserock amplitude.

#### *3.4.7.1. Site Basecase Profiles*

The CGS site is located within the Pasco Basin and is underlain by approximately 160 m [525 ft] of soil and sedimentary strata that overly the Saddle Mountain Basalt, which extends to a depth of approximately 400 m [1,313 ft]. The Saddle Mountain Basalt includes sediment interbeds and is underlain by the Wanapum Basalt. Figure 3.4-13, which was developed from data in Section 3.2 in Swank (2015a), plots a profile of the strata beneath the CGS site and includes  $V_S$  and density for each layer.

Due to the amount of near-surface  $V_S$  data available for the soil and rock at the CGS site and the consistency between the velocity measurements, the licensee used a single basecase  $V_S$  profile for the soils and sedimentary strata in the upper 160 m [252 ft]. To develop two  $V_S$  profiles for the Saddle Mountain Basalt and its sedimentary interbeds, which extend from 160 m to 400 m [525 ft to 1,312 ft] below the surface, the licensee used downhole measurements and a P-S suspension log from the Waste Treatment Plant at the Hanford Site. Following the recommendation of the GMC TI Team, the licensee gave twice as much weight to the  $V_S$  profile from the downhole measurements than to the suspension log data in its site response logic tree.

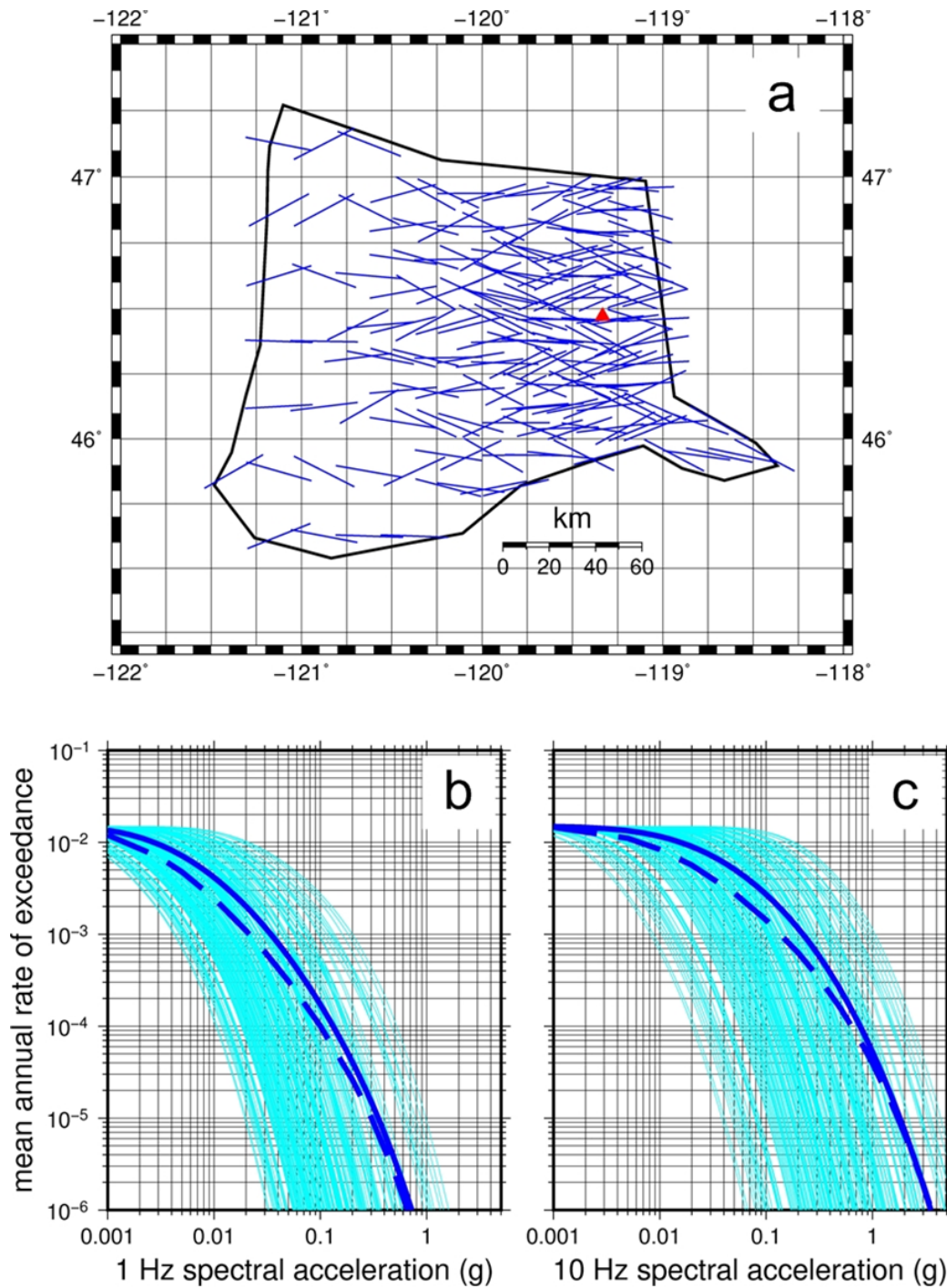
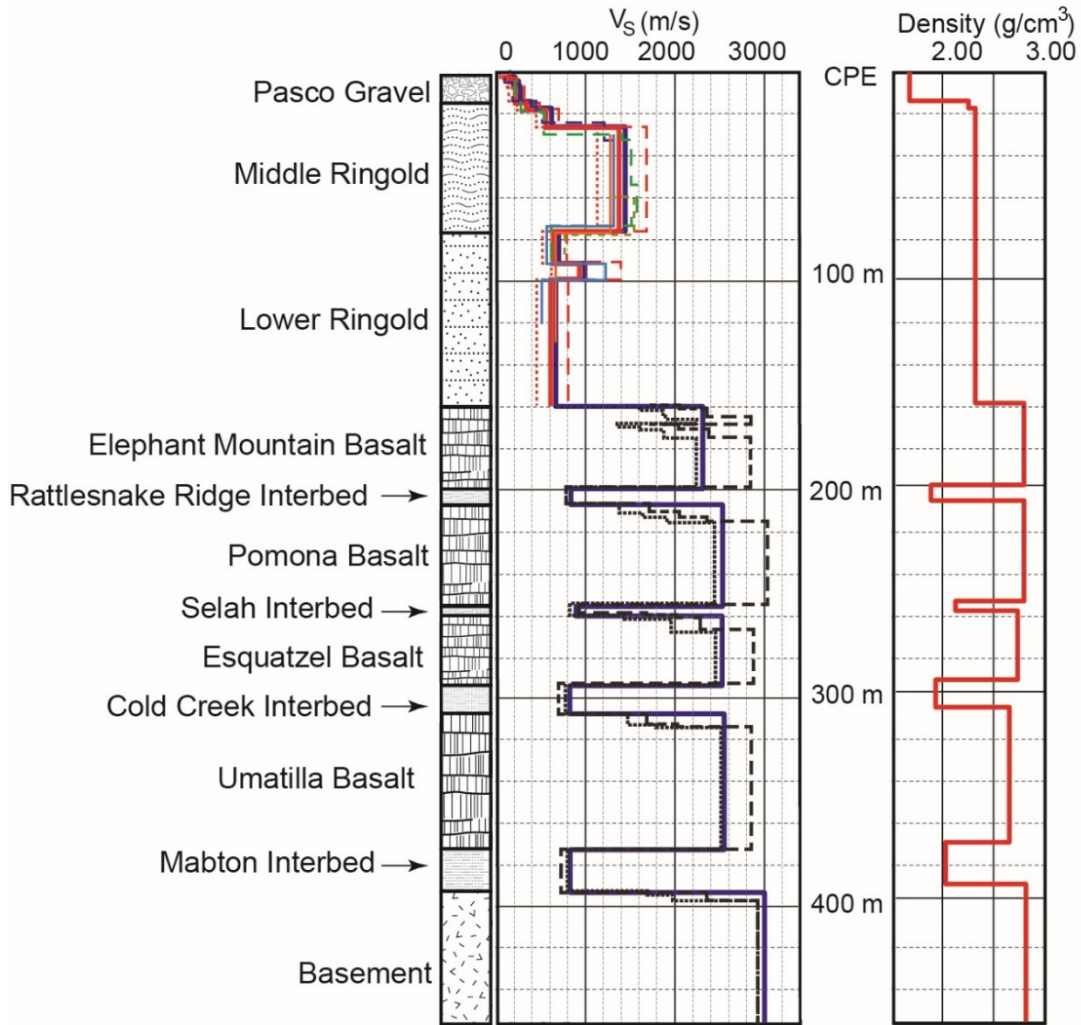


**Figure 3.4-12** (a) The NRC Staff's Confirmatory Analysis Showing the Location of Virtual Faults for the YFTB Source Zone in the Vicinity of the CGS Site (Red Triangle). The NRC Staff's Hazard Curves for Each of the 324 YFTB Virtual Faults (Light-Blue Lines) are Shown with Staff's (Thick Blue Line) and PNNL (2014) (Dashed Blue Line) Mean Hazard Curves for 1 Hz (b) and 10 Hz (c)



Base Case Soil Profile		Base Case Deep Profile	
.....	Lower Bound	.....	From Downhole Measurements
----	Upper Bound	----	From P-S Suspension Measurements
—	Base Case	—	Weighted Mean
-----	WNP-1 CH	WNP - Washington Nuclear (WNP) Public Power Supply System Nuclear Projects, Cross-Hole (CH) and Down Hole (DH) measurements.	
-----	WNP-2 CH		
-----	WNP-4 CH		
-----	WNP-1 DH		
-----	WNP-4 DH		
<i>Depths are measured as distances below the CGS Control Point Elevation (CPE) = 134 m [440 ft]</i>			

**Figure 3.4-13 Geologic Profile and Estimated Layer Thicknesses for the Strata Beneath the CGS Site, Compiled from the Data in Section 2.3 in Swank (2015a). To Convert Depth and  $V_s$  Values (m to ft), Multiply the Values by 3.28. To Convert from Density Values ( $g/cm^3$  to  $lb/ft^3$ ), Multiply the Values by 62.48**

To incorporate aleatory variability in the site response analysis, the licensee generated 60 random velocity profiles for each of its basecase profiles using log standard deviation values of 0.15 to 0.30 for the soil and sedimentary strata in the upper 160 m [525 ft] and values of 0.1 and 0.2 for the Saddle Mountain Basalt and interbeds. In addition, the licensee varied the layer thickness for each of its  $V_S$  profiles by amounts varying from  $\pm 10$  percent to  $\pm 22$  percent.

#### *3.4.7.2. Dynamic Material Properties and Site Kappa*

To model the potential nonlinear behavior in the upper 160 m [525 ft] of strata to input ground motions, the licensee used two sets of shear modulus degradation and damping curves. As recommended in the SPID (EPRI, 2012), the licensee gave equal weight to the EPRI soil and Peninsular Range curves and limited the amount of damping to 15 percent. For the basalt layers within the Saddle Mountain Basalt, the licensee assumed a linear response to input ground motions with constant damping values ranging from 0.46 to 1.03 percent. For the sedimentary interbeds within the Saddle Mountain Basalt, the licensee modeled the potential nonlinear behavior using the Darendeli (2001) shear modulus degradation and damping curves because these curves account for confining stress dependence, which is important for the depths at which the interbeds are located. For the shear modulus degradation curves, the licensee accounted for aleatory variability by randomizing about each curve using a log standard deviation of 0.15. Similarly, for the damping curves, the licensee randomized about each the curve using a log standard deviation of 0.30. In addition, the licensee randomized the constant damping values for the Saddle Mountain Basalts using a log standard deviation of 0.40. To reconcile the estimated Hanford Site kappa value ( $\kappa_0$ ) with the small strain damping used for the site response basecase profiles, the licensee evaluated the total amount of damping assumed for each of the layers. The licensee estimated  $\kappa_0$  values of 6 and 9 msec for its two alternative 160-m [525-ft] profiles above the reference horizon within the Wanapum Basalt.

#### *3.4.7.3. Site Response Method and Results*

The licensee used RVT for its site response analysis (Section 2.3.5 in Swank, 2015a); to develop input ground motions for the site response analysis, the licensee used the Conditional Mean Spectra (CMS) developed by Baker (2011). The CMS method uses the magnitude and distance pairs from the PSHA deaggregation results. For the input response spectral shape, the licensee used the Hanford GMC model developed by the GMC TI Team. After developing input motions for the site response, the licensee generated 60 random  $V_S$  profiles for each of the basecase profiles to determine the median site amplification factor and its associated log standard deviation. Based on the material properties of the interbed layers and the sharp contrasts in impedance, the licensee did not limit the site amplification factors to values greater than 0.5, as recommended in the SPID (EPRI, 2012).

In order to develop probabilistic site-specific control point hazard curves, the licensee used Approach 3, as described in Appendix B to the SPID (EPRI, 2012) and discussed in Section 2.1.5 of this report. The licensee's use of Approach 3 involved computing the site-specific control point elevation hazard curves for a broad range of spectral accelerations by combining the site-specific baserock hazard curves, determined from the initial PSHA, and the amplification factors and their associated uncertainties, determined from the site response analysis.

### 3.4.8. NRC Staff Confirmatory Evaluation of Site Response Analysis

Similar to the confirmatory evaluations developed by the NRC staff to evaluate the PNNL PSHA (PNNL, 2014) and the baserock hazard curves, the NRC staff developed a series of confirmatory evaluations to support its review of site response analysis and the control point hazard results. This report summarizes several of these confirmatory evaluations to further illustrate the scope and depth of the NRC evaluations and to provide additional information on the current CGS control point hazard results in support of the KM mission of this NUREG/KM. The NRC staff's evaluation (NRC, 2016b) provides a complete description of all the confirmatory analyses the staff relied on in its review.

The NRC staff performed confirmatory site response analyses to assess which aspects of the licensee's analysis were most significant to the resulting control point hazard results and to test whether the range of epistemic uncertainty included in the site response model was sufficient to ensure that the resulting hazard captured the center, body, and range of technically defensible interpretations. To accomplish this, the NRC staff examined (1) the effect of differing assumptions for the epistemic uncertainty and aleatory variability for the site basecase  $V_S$  profiles, (2) the sensitivity of the site amplification factors to the thickness of the interbed layers within the Saddle Mountain Basalt, and (3) the use of the Darendeli (2001) shear modulus degradation and damping curves for the sedimentary interbeds.

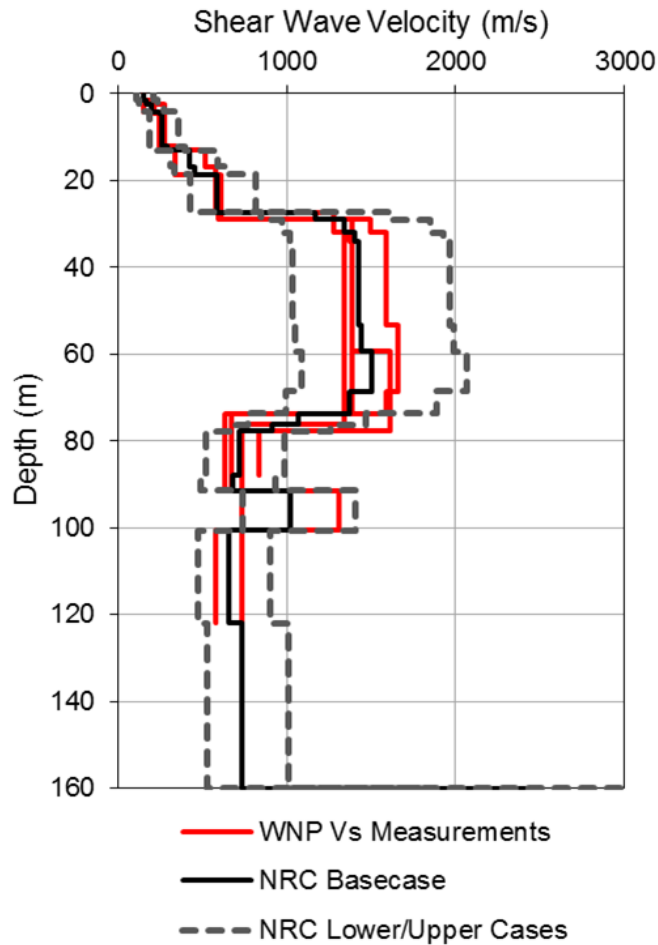
For its confirmatory evaluation, the NRC staff developed three profiles for the upper 160 m [525 ft] using a log standard deviation of 0.25 to account for epistemic uncertainty in the subsurface properties instead of using only a single basecase  $V_S$  profile. Figure 3.4-14 shows the NRC staff's basecase profiles and the recorded  $V_S$  data in the upper 160 m [525 ft]. To evaluate the sensitivity of the site amplification factors to the thickness of the interbed layers within the Saddle Mountain Basalt, the NRC staff performed its analysis by randomly removing a few of the interbed layers in the 60 randomized site profiles. The NRC staff also performed its site response analysis using either the Darendeli (2001) curves or by assuming a linear response for the interbeds.

Figure 3.4-15 shows the results of NRC staff's confirmatory analyses for the three scenarios for both 1 Hz (a) and 100 Hz (b) median amplification factors and 1 Hz (c) and 100 Hz (d) log standard deviations. As shown in Figure 3.4-15, the impact of using multiple basecase profiles, randomly varying the thickness of the interbeds, and assuming a linear response for the interbed layers does not result in significantly different amplification factors from those developed by the licensee. Similarly, Figure 3.4-16 shows that the 1 Hz and 100 Hz control point hazard curves for each of the three scenarios do not significantly differ from the licensee's hazard curves.

### 3.4.9. Control Point Hazard Results

In summary, in responding to the NRC staff's 50.54(f) letter, the licensee participated in a jointly sponsored SSHAC Level 3 study with the DOE to develop a baserock PSHA for the Hanford Site. In terms of the SSC model, the primary contributors to the hazard at the  $10^{-4}$  annual frequency of exceedance are the host YFTB areal source zone and several of the YFTB faults closest to the CGS site (Rattlesnake Mountain, Umtanum Ridge, and Yakima Ridge faults). For the GMC model, the licensee used a hybrid backbone approach to develop 189 alternative median models that were adjusted to the regional crustal properties surrounding the site. In addition, the GMC model provided six alternative aleatory variability models for the single-station standard deviation about each of the median predictions. Finally, the licensee

used a combination of previously developed geophysical surveys of the local site subsurface and borehole measurements to develop amplification factor distributions for the CGS site. The licensee then combined the results of these three models (SSC, GMC, and site response) to develop control point hazard curves and associated response spectra. Figure 3.4-17(a) shows the resulting control point hazard for the CGS site. Figure 3.4-17(b) shows the resulting control point UHRS for  $10^{-4}$  and  $10^{-5}$  AFE and the GMRS.



**Figure 3.4-14 Measured Shear Wave Velocities and the NRC Staff’s Shear Wave Profiles in Upper Strata. WNP (Red Lines) Represents  $V_s$  Measurements Made for WNP Site Investigations (PNNL, 2014). In Earlier Licensing Documentation, the CGS Plant was Referred to as the Washington Public Power Supply System Nuclear Project (WNP)**



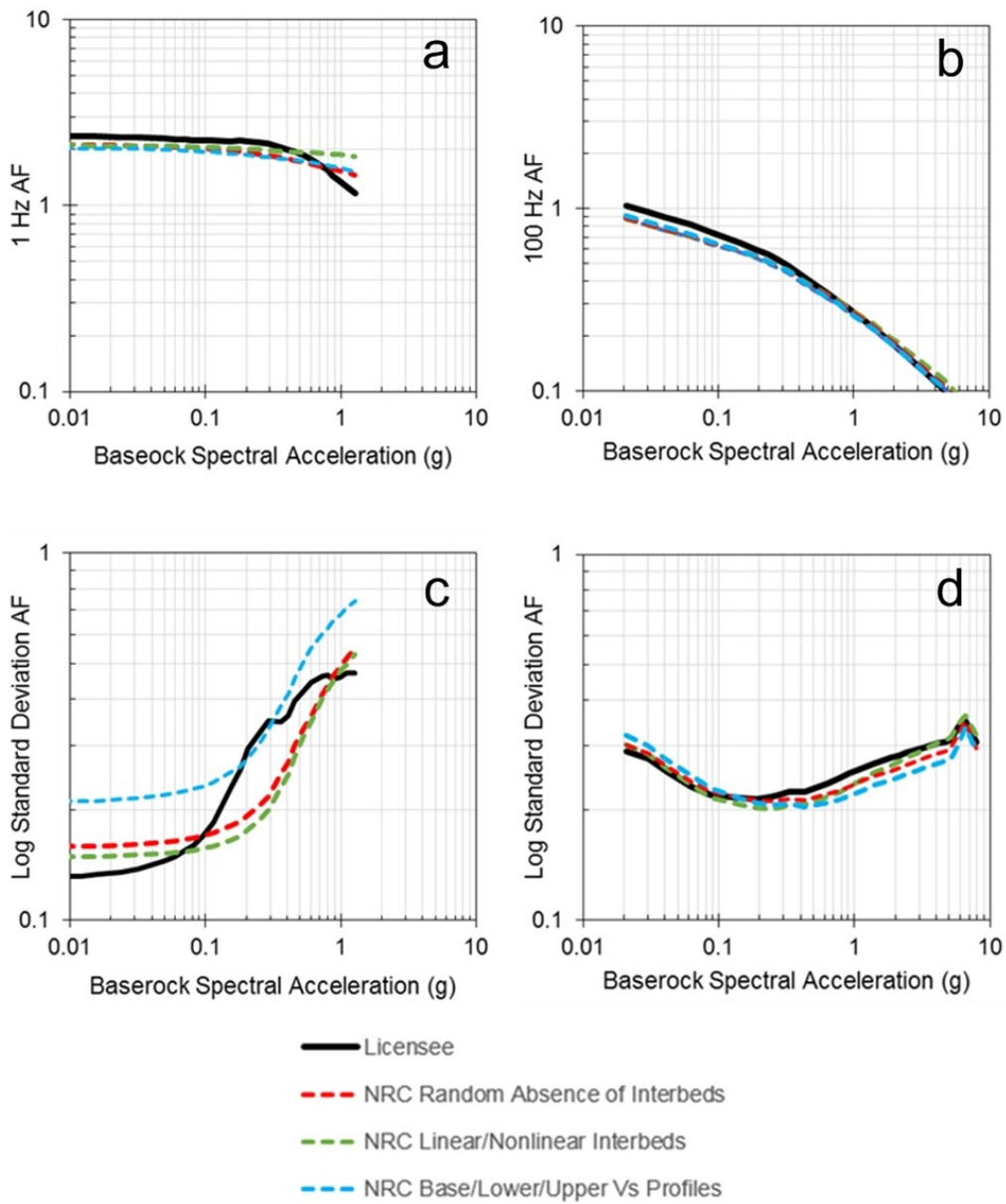


**Figure 3.4-15 Comparison of the NRC staff's Confirmatory Analyses with the Licensee's Amplification Functions and Amplification Function Log Standard Deviation for (a) 1 Hz Amplification, (b) 10 Hz Amplification, (c) 1 Hz Log Standard Deviation, and (d) 100 Hz Log Standard Deviation**

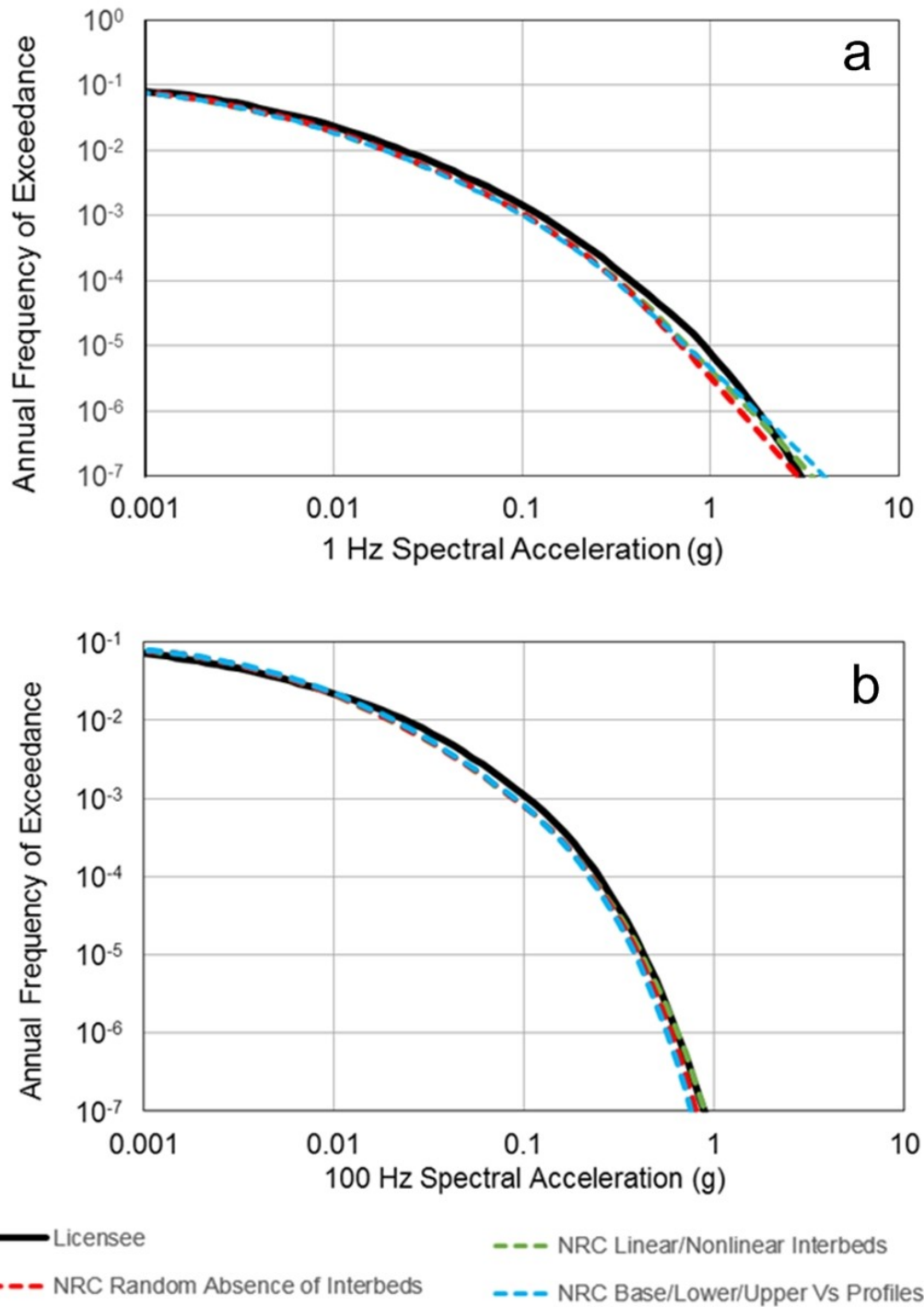


**Figure 3.4-16 Comparison of the Licensee's and the NRC Staff's Hazard Curves at (a) 1 Hz Spectral Acceleration and (b) 100 Hz Spectral Acceleration**

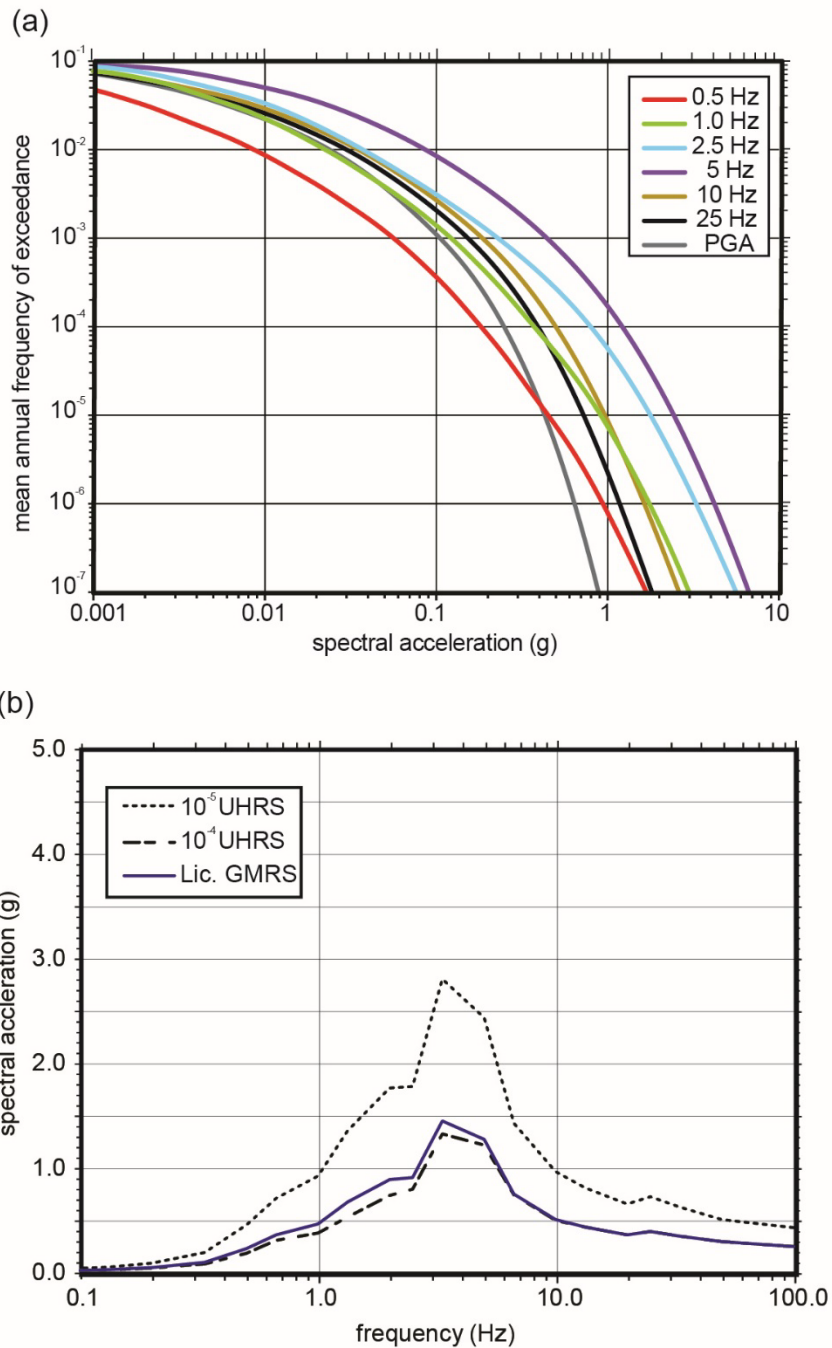


**Figure 3.4-17 (a) Total Mean Site-Specific Control Point Hazard Curves Plotted for Seven Spectral Frequencies, Based on the Data in Tables 2.3.7-1 through 2.3.7.7 in Swank (2015a). (b) Uniform Hazard Response Spectra and the GMRS are Plotted Based on the Data from Table 2.4-1 in Swank (2015a)**

### 3.5. References

Abrahamson, N.A., W.J. Silva, and R. Kamai. "Summary of the ASK14 Ground Motion Relation for Active Crustal Regions." *Earthquake Spectra*. Vol. 30, No. 3. pp. 1,025–1,055. 2014.

Abrahamson, N.A. and J.J. Bommer. "Probability and Uncertainty in Seismic Hazard Analysis." *Earthquake Spectra*. Vol. 21, No. 2. pp. 603–607. 2005.

Akkar, S., M.A. Sandikkaya, and J.J. Bommer. "Empirical Ground-motion Models for Point- and Extended-source Crustal Earthquake Scenarios in Europe and the Middle East." *Bulletin of Earthquake Engineering*. Vol. 12, No. 1. pp. 359–387. 2014.

Al-Atik, L. and R.R. Youngs. "Epistemic Uncertainty for NGA-West2 Models." *Earthquake Spectra*. Vol. 30, No. 3. pp. 1,301–1,318. 2014.

American National Standards Institute/American Nuclear Society (ANSI/ANS). "Probabilistic Seismic Hazard Analysis." ANSI/ANS-2.29-2008. La Grange Park, IL. 2008.

Ancheta, T.D., R.B. Darragh, J.P. Stewart, E. Seyhan, W.J. Silva, B.S-J. Chiou, K.E. Wooddell, R.W. Graves, A.R. Kottke, D.M. Boore, T. Kishida, and J.L. Donahue. "NGA-West 2 Database." *Earthquake Spectra*. Vol. 30, No. 3. pp. 989–1,005. 2014.

APS. "Quaternary Geologic Mapping in The Vicinity of The Palo Verde Nuclear Generating Station." Prepared by Lettis Consultants International for APS. Concord, CA. 2014.

APS. "Palo Verde Nuclear Generating Station Units 1, 2, and 3 dated Final Safety Analysis Report Revision 17." Phoenix, AZ. 2013. Agencywide Documents Access and Management System (ADAMS) Accession No. ML13214A057 (nonpublic).

Arizona Public Service (APS). "Palo Verde Nuclear Generating Station Seismic Source Characterization, Technical Report." Prepared by Lettis Consultants International for Westinghouse Electric Company. Concord, CA. 2015.

U.S. Atomic Energy Commission. "Design Response Spectra for Seismic Design of Nuclear Power Plants." Regulatory Guide 1.60. October 1973. ADAMS Accession No. ML13350A358.

Baker, J.W. "Conditional Mean Spectrum: Tool for Ground-Motion Selection." *Journal of Structural Engineering*. Vol. 137, No. 3. pp. 322–331. 2011.

Baker, V.R., B.N. Bjornstad, A.J. Busacca, K.R. Fecht, E.P. Kiver, U.L. Moody, J.G. Rigby, D.F. Stradling, and A.M. Tallman. "Quaternary Geology of the Columbia Plateau," in *Quaternary Nonglacial Geology: Conterminous U.S., The Geology of North America*, R.B. Morrison (ed.). Vol. K-2. pp. 215–250. Geological Society of America. Boulder, CO. 1991.

Barnett, D.B., B.N. Bjornstad, K.R. Fecht, D.C. Lanigan, S.P. Reidel, and C.F. Rust. "Geology of the Waste Treatment Plant Seismic Boreholes." PNNL-16407, Revision 1. Pacific Northwest National Laboratory (PNNL). Richland, WA. 2007.

BC Hydro and Power Authority (BC Hydro). "Dam Safety—Probabilistic Seismic Hazard Analysis (PSHA) Model, v.2: Seismic Source Characterization (SSC) Model." Engineering Report E65. Vancouver, Canada. 2012.

Biasi, G.P., R.J. Weldon II, T.E. Fumal, and G.G. Seitz. "Paleoseismic Event Dating and the Conditional Probability of Large Earthquakes on the Southern San Andreas Fault, California." *Bulletin of the Seismological Society of America*. Vol. 92, Issue 7. pp. 2,761–2,781. 2002.

Bird, P. "NeoKinema Fault-Based Deformation Model of the California Region for UCERF3, with Focus on the DCPD Region." Presentation at DCPD SSHAC Workshop 2, San Luis Obispo, CA, November 7, 2012.

Blakely, R.J., B.L. Sherrod, C.S. Weaver, R.E. Wells, and A.C. Rohay. "The Wallula Fault and Tectonic Framework of South-Central Washington, as Interpreted from Magnetic and Gravity Anomalies." *Tectonophysics*. Vol. 624–625. pp. 32–45. 2014.

Boore, D.M., J.P. Stewart, E. Seyhan, and G.A. Atkinson. "NGA-West2 Equations for Predicting PGA, PGV, and 5% Damped PSA for Shallow Crustal Earthquakes." *Earthquake Spectra*. Vol. 30, No. 3. pp. 1,057–1,085. 2014.

Bozorgnia, Y., N.A. Abrahamson, L. Al Atik, T.D. Ancheta, G.M. Atkinson, J.W. Baker, A. Baltay, D.M. Boore, K.W. Campbell, B.S.-J. Chiou, R. Darragh, S. Day, J. Donahue, R.W. Graves, N. Gregor, T. Hanks, I.M. Idriss, R. Kamai, T. Kishida, A. Kottke, S.A. Mahin, S. Rezaeian, B. Rowshandel, E. Seyhan, S. Shahi, T. Shantz, W. Silva, P. Spudich, J.P. Stewart, J. Watson-Lamprey, K. Wooddell, and R. Youngs. "NGA-West2 Research Project." *Earthquake Spectra*. Vol. 30, No. 3. pp. 973–987. 2014.

Cadogan, J.J., Jr. Letter from John Cadogan, Jr., Vice President Engineering, APS, to the NRC, Palo Verde, Units 1, 2, and 3, Seismic Hazard and Screening Report. March 2015a. ADAMS Accession No. ML15076A073.

Cadogan, J.J., Jr. Letter from John Cadogan, Jr., Vice President Engineering, to the NRC, Palo Verde Nuclear Generating Station (PVNGS), Units 1, 2, and 3, Supplemental Information Regarding the PVNGS Seismic Design and Licensing Basis. April 2015b. ADAMS Accession No. ML15105A076.

Campbell, K.W. and Y. Bozorgnia. "NGA-West2 Campbell-Bozorgnia Ground Motion Model for the Horizontal Components of PGA, PGV, and 5%-Damped Elastic Pseudo-Acceleration Response Spectra for Periods Ranging from 0.01 to 10 sec." *Earthquake Spectra*. Vol. 30, Issue 3. pp. 1,087–1,115. 2014.

Casale, G. and T.L. Pratt. "Thin- or Thick-Skinned Faulting in the Yakima Fold and Thrust Belt (WA)? Constraints from Kinematic Modeling of the Saddle Mountains Anticline." *Bulletin of the Seismological Society of America*. Vol. 105, No. 2A. pp. 745–752. 2015.

Chamness, M.A., K. Winsor, and S.D. Unwin. "A Summary of Coupled, Uncoupled, and Hybrid Tectonic Models for the Yakima Fold Belt—Topical Report." PNNL-17500. PNNL. Richland, WA. 2012.

Chiou, B.S.-J. and R.R. Youngs. "Update of the Chiou and Youngs NGA Model for the Average Horizontal Component of Peak Ground Motion and Response Spectra." *Earthquake Spectra*. Vol. 30, No. 3. pp. 1,117–1,153. 2014.

Clark, D.H., N.T. Hall, D.H. Hamilton, and R.G. Heck. "Structural Analysis of Late Neogene Deformation in the Central Offshore Santa Maria Basin, California." *Journal of Geophysical Research*. Vol. 96, Issue B4. pp. 6,435–6,457. 1991.

California State University, Monterey Bay (CSUMB). "Sea Floor Mapping Lab, Multibeam echosounder (MBES) data for the California Central Coast." 2012.  
<http://seafloor.otterlabs.org/index.html>

Darendeli, M.B. "Development of a New Family of Normalized Modulus Reduction and Material Damping Curves." Ph.D. Dissertation. University of Texas at Austin. 2001.

DeMets, C. "Final Report: Kinematics of Coastal California Inferred from GPS Geodesy." Unpublished technical report submitted to Pacific Gas and Electric Company (PG&E). December 2012.

DeMets, C., B. Márquez-Azúa, and E. Cabral-Cano. "A New GPS Velocity Field for the Pacific Plate – Part 2: Implications for Fault Slip Rates in Western California." *Geophysical Journal International*. Vol. 199, Issue 3. pp. 1,900–1,909. 2014.

DePolo, C.M. and J.G. Anderson. "Estimating the Slip Rates of Normal Faults in the Great Basin, USA." *Basin Research*. Vol. 12, Issue 3-4. pp. 227–240. 2000.

DiSilvestro, L.A., K.H. Hanson, W.R. Lettis, and G.I. Shiller. "The San Simeon/Hosgri Pull-Apart Basin, South-central Coastal California." *EOS, Transactions, American Geophysical Union*. Vol. 71, Issue 43. p. 1,632. 1990.

Dorsey, R.J. and P.J. Umhoefer. "Influence of Sediment Input and Plate-motion Obliquity on Basin Development Along an Active Oblique-divergent Plate Boundary: Gulf of California and Salton Trough." Busby, C. and Azor, A. (eds.). *Tectonics of Sedimentary Basins: Recent Advances*. Blackwell Publishing, Hoboken, NJ. pp. 209–225. 2012.

Dzurisin, D., C.L. Driedger, and L.M. Faust. "Mount St. Helens, 1980 to now—what's going on." Fact Sheet 2013–3014, Version 1.1. U.S. Geological Survey (USGS) and U.S. Forest Service. 2014. <https://doi.org/10.3133/fs20133014>

Energy Northwest. "Columbia Generating Station Final Safety Analysis Report, Amendment 62." Richland, WA. 2013. ADAMS Accession No. ML14010A476.

Electric Power Research Institute (EPRI). "EPRI Ground Motion Model Review Final Report." Palo Alto, CA. June 3, 2013. ADAMS Accession No. ML13155A553.

EPRI. "Seismic Evaluation Guidance, Screening, Prioritization and Implementation Details (SPID) for the Resolution of Fukushima Near-Term Task Force Recommendation 2.1: Seismic." EPRI Report 1025287. Palo Alto, CA. 2012. ADAMS Accession No. ML12333A170.

EPRI. "Methods and Guidelines for Estimating Earthquake Ground motion in Eastern North America, in Guidelines for Determining Design Basis Ground Motions." Vol. 1. EPRI TR-102293. Palo Alto, CA. 1993.

EPRI. "Seismic Hazard Methodology for the Central and Eastern United States." EPRI-NP-4726. Palo Alto, CA. 1988.

Field, E.H., G.P. Biasi, P. Bird, T.E. Dawson, K.R. Felzer, D.D. Jackson, K.M. Johnson, T.H. Jordan, C. Madden, A.J. Michael, K.R. Milner, M.T. Page, T. Parsons, P.M. Powers, B.E. Shaw, W.R. Thatcher, R.J. Weldon, II, and Y. Zeng. *Uniform California Earthquake Rupture Forecast, Version 3 (UCERF3)—The Time-Independent Model*. USGS Open-File Report 2013-1165, California Geological Survey Special Report 228, and Southern California Earthquake Center Publication 1792. 2013.

Fitzenz, D.D., M.A. Ferry, and A. Jalobeanu. "Long-Term Slip History Discriminates Among Occurrence Models for Seismic Hazard Assessment." *Geophysical Research Letters*. Vol. 37, Issue 2. L20307. 2010.

Fugro Consultants. "Update of the Three-Dimensional Velocity Model for the Diablo Canyon Power Plant (DCPP) Foundation Area." Technical Report to PG&E. May 2015.

Gardner, J.K. and L. Knopoff. "Is the Sequence of Earthquakes in Southern California, with Aftershocks Removed, Poissonian?" *Bulletin of the Seismological Society of America*. Vol. 64, No. 5. pp. 1,363–1,367. 1974.

Geomatrix Consultants, Inc. (Geomatrix). "Probabilistic Seismic Hazard Analysis, DOE Hanford Site, Washington." Technical report to Westinghouse Hanford Company, Richland, WA, under Contract WHC-SD-W236A-TI-002, Revision 1. Oakland, CA. 1996.

GeoPentech. "Southwestern United States Ground Motion Characterization SSHAC Level 3— Technical Report, Rev. 2." March 2015.

Gilbert, W.G. *Bedrock Geology of the Eastern Gila Bend Mountains, Maricopa County, Arizona*. Arizona Geological Society Open-File Report 91-05. Tucson, AZ. 1991.

Grünthal, G. "The Up-dated Earthquake Catalogue for the German Democratic Republic and Adjacent Areas-statistical Data Characteristics and Conclusions for Hazard Assessment." In *3rd International Symposium on the Analysis of Seismicity and on Seismic Risk*. Prague, Czech Republic. 1985.

Gutenberg, B. and C.F. Richter. "Earthquake Magnitude, Intensity, Energy, and Acceleration: (Second paper)." *Bulletin of the Seismological Society of America*. Vol. 46, No. 2. pp. 105–145. 1956.

Hanks, T.C. and W.H. Bakun. "M-logA models and other curiosities." *Bulletin of the Seismological Society of America*. Vol. 104, No. 5. pp. 2,604–2,610. 2014.

Hanks, T.C. and W.H. Bakun. "M-logA Observations for Recent Large Earthquakes." *Bulletin of the Seismological Society of America*. Vol. 98, No. 1. pp. 490–494. 2008.

- Hanson, K.L., W.R. Lettis, M.K. McLaren, W.U. Savage, and N.T. Hall. "Style and Rate of Quaternary Deformation of the Hosgri Fault Zone, Offshore South-central California." M.A. Keller, ed. *Evolution of Sedimentary Basins/Onshore Oil and Gas Investigations—Santa Maria Province*, USGS Bulletin 1995-BB. p. 33. 2004.
- Hanson, K.L., J.R. Wesling, W.R. Lettis, K.I. Kelson, and L. Mezger. "Correlation, Ages, and Uplift Rates of Quaternary Marine Terraces, South-Central California." I.B. Alterman, R.B. McMullen, L.S. Cluff, and D.B. Slemmons, eds. *Seismotectonics of the Central California Coast Range*, *Geological Society of America Special Paper* 292. pp. 45–72. 1994.
- Hardebeck, J.L. "Geometry and Earthquake Potential of the Shoreline Fault, Central California." *Bulletin of the Seismological Society of America*. Vol. 103, Issue 1. pp. 447–462. 2013.
- Hardebeck, J.L. "Seismotectonics and Fault Structure of the California Central Coast." *Bulletin of the Seismological Society of America*. Vol. 100, Issue 3. pp. 1,031–1,050. 2010.
- Hartwell, S.R., D.P. Finlayson, P. Dartnell, and S.Y. Johnson. *Bathymetry and Acoustic Backscatter—Estero Bay, California, U.S.* USGS Open-File Report 2013-1225. 2013.
- Hecker, S., N.A. Abrahamson, and K.E. Wooddell. "Variability of Displacement at a Point; Implications for Earthquake-size Distribution and Rupture Hazard on Faults." *Bulletin of the Seismological Society of America*. Vol. 103, No. 2A. pp. 651–674. April 2013.
- Idriss, I.M. "An NGA-West2 Empirical Model for Estimating the Horizontal Spectral Values Generated by Shallow Crustal Earthquakes." *Earthquake Spectra*. Vol. 30. pp. 1,155–1,177. 2014.
- Jack Benjamin & Associates (JBA), URS Corporation Seismic Hazards Group, Geomatrix Consultants, Inc., and Shannon & Wilson. "Probabilistic Seismic Hazard Analyses Project for the MidColumbia Dams." Final Report prepared for the Public Utility Districts of Chelan, Douglas, and Grant Counties. Chelan County Public Utility District. Wenatchee, WA. 2012.
- Johnson, S.Y. and J.T. Watt. "Influence of Fault Trend, Bends, and Convergence on Shallow Structure and Geomorphology of the Hosgri Strike-slip Fault, Offshore Central California." *Geosphere*. Vol. 8, Issue 6. pp. 1,632–1,656. 2012.
- Johnson, S.Y., S.R. Hartwell, and P. Dartnell. "Offset of Latest Pleistocene Shoreface Reveal Slip Rate on the Hosgri Strike-slip Fault, Offshore Central California." *Bulletin of the Seismological Society of America*. Vol. 104, Issue 4. pp. 1,650–1,662. 2014.
- Kishida, T., R.E. Kayen, O.-J. Ktenidou, W. Silva, R. Darragh, and J. Watson-Lamprey. "PEER Arizona Strong Motion Database and GMPEs Evaluation." PEER Report 2014/09. p. 135. Pacific Earthquake Engineering Research Center. Berkeley, CA. 2014.
- Langenheim, V.E., R.C. Jachens, and K. Moussaoui. *Aeromagnetic Survey Map of the Central California Coast Ranges*. USGS Open-File Report 2009-1044. 2009.
- Lettis, W.R. and K.L. Hanson. "Crustal Strain Partitioning; Implications for Seismic Hazard Assessment in Western California." *Geology*. Vol. 19. pp. 559–562. 1991.



- Lettis, W.R., K.L. Hanson, J.R. Unruh, M. McLaren, and W.U. Savage. "Quaternary Tectonic setting of south-central coastal California." M.A. Keller, ed. *Evolution of Sedimentary Basins/Offshore Oil and Gas Investigations—Santa Maria Province*. USGS Bulletin 1995-AA. pp. 1–21. 2004.
- Lin, J. and R.S. Stein. "Stress Triggering in Thrust and Subduction Earthquakes and Stress Interaction Between the Southern San Andreas and Nearby Thrust and Strike-slip Faults." *Journal of Geophysical Research*. Vol. 109(B2). pp. 2,156–2,202. 2004.
- Lin, P.-S., B. Chiou, N. Abrahamson, M. Walling, C.-T. Lee, and C.-T. Cheng. "Repeatable source, site, and path effects on the standard deviation for empirical ground-motion prediction models." *Bulletin of the Seismological Society of America*. Vol. 101, Issue 5. pp. 2,281–2,295. 2011.
- Lindsey, K.A. and D.R. Gaylord. "Lithofacies and Sedimentology of the Miocene-Pliocene Ringold Formation, Hanford Site, South-central Washington." *Northwest Science*. Vol. 64, No. 3. pp. 165–180. 1990.
- Maechling, P.J., F. Silva, S. Callaghan, and T.H. Jordan. "Broadband Platform: System Architecture and Software Implementation." *Seismological Research Letters*. Vol. 86, Issue 1. pp. 27–38. 2015.
- McCaffrey, R., A.I. Qamar, R.W. King, R. Wells, G. Khazaradze, C.A. Williams, C.W. Stevens, J.J. Vollick, and P.C. Zwick. "Fault Locking, Block Rotation and Crustal Deformation in the Pacific Northwest." *Geophysical Journal International*. Vol. 169, No. 3. pp. 1,315–1,340. 2007. <https://doi.org/10.1111/j.1365-246X.2007.03371.x>
- McCrory, P.A., R.D. Hyndman, and J.L. Blair. "Relationship Between the Cascadia fore-arc Mantle Wedge, Nonvolcanic Tremor, and the Downdip Limit of Seismogenic Rupture." *Geochemistry, Geophysics, Geosystems*. Vol. 15, No. 4. pp. 1,071–1,095. 2014.
- McCrory, P.A., J.L. Blair, D.H. Oppenheimer, and S.R. Walter. *Depth to the Juan de Fuca Slab Beneath the Cascadia Subduction Margin; a 3-D Model for Sorting Earthquakes*. USGS, Data Series 91. 2006.
- McGinnis, R.N., A.P. Morris, D.A. Ferrill, K.J. Smart, J.A. Stamatakos, and M R. Juckett. *Independent Evaluation of The Hosgri Fault Slip Rate Based on A Structural Analysis Of The Pull-Apart Basin Linking the Hosgri And San Simeon Fault Systems*." Center for Nuclear Waste Regulatory Analyses, Southwest Research Institute. San Antonio, TX. 2016. ADAMS Accession No. ML16334A406.
- McLaren, M.K. and W.U. Savage. "Seismicity of South-central Coastal California: October 1987 through January 1997." *Bulletin of the Seismological Society of America*. Vol. 91, Issue 6. pp. 1,629–1,658. 2001.
- McLaren, M.K., J.L. Hardebeck, N. van der Elst, J.R. Unruh, G.W. Bawden, and J.L. Blair. "Complex Faulting Associated with the 22 December 2003 Mw 6.5 San Simeon, California Earthquake, Aftershocks and Postseismic Surface Deformation." *Bulletin of the Seismological Society of America*. Vol. 98, Issue 4. pp. 1,659–1,680. 2008.

Muhs, D.R., K.R. Simmons, R.R. Schumann, L.T. Groves, D. Laurel, and J.X. Mitrovica. "Sea-level History During the Last Interglacial Complex on San Nicolas Island, California: Implications for Glacial Isostatic Adjustment Processes, Paleozoogeography and Tectonics." *Quaternary Science Reviews*. Vol. 37. pp. 1–25. 2012.

Murray, R.W. "Regional Deformation and Kinematics from GPS Data." Presentation at DCPD SSHAC Workshop 2. San Luis Obispo, CA. November 7, 2012.

<http://www.pge.com/mybusiness/edusafety/systemworks/dcpp/SSHAC/workshops/index.shtml>

U.S. Nuclear Regulatory Commission (NRC). "Updated Implementation Guidance for SSHAC Hazard Studies." NUREG-2213. Washington, DC. October 2018. ADAMS Accession No. ML18282A082.

NRC. "Palo Verde Nuclear Generating Station, Units 1, 2, and 3—Staff Assessment of information Provided Under Title 10 of the Code of Federal Regulations Part 50, Section 50.54(F), Seismic Hazard Reevaluations for Recommendation 2.1 of the Near-Term Task Force Review of Insights from the Fukushima Dai-Ichi Accident And Staff Closure of Activities Associated With Recommendation 2.1, Seismic (CAC Nos. MF5277, MF5278 and MF5279)." Washington, DC. September 13, 2016a. ADAMS Accession No. ML16221A604.

NRC. "Columbia Generating Station—Staff Assessment of Information Provided Under Title 10 of The Code of Federal Regulations Part 50, Section 50.54(F), Seismic Hazard Reevaluations for Recommendation 2.1 of The Near-Term Task Force Review of Insights from the Fukushima Dai-Ichi Accident (CAC NO. MF5274)." Washington, DC. November 4, 2016b. ADAMS Accession No. ML16285A410.

NRC. "Diablo Canyon Power Plant, Unit Nos. 1 and 2—Staff Assessment of Information Provided Under Title 10 of the Code of Federal Regulations Part 50, Section 50.54(F), Seismic Hazard Reevaluations for Recommendation 2.1 of the Near-Term Task Force Review of Insights from the Fukushima Dai-Ichi Accident (CAC Nos. MF5275 and MF5276)." Washington, DC. December 21, 2016c. ADAMS Accession No. ML16341C057.

NRC. Letter from Eric J. Leeds, Director, Office of Nuclear Reactor Regulation and Michael R. Johnson, Director, Office of New Reactors, to All Power Reactor Licensees and Holders of Construction Permits in Active or Deferred Status. Washington, DC. March 12, 2012a. ADAMS Accession No. ML12053A340.

NRC. "Central and Eastern United States Seismic Source Characterization for Nuclear Facilities." NUREG-2115. Washington, DC. January 2012b. ADAMS Accession Nos. ML12048A804, ML12048A833, ML12048A851, ML12048A858, ML12048A859, and ML12048A860.

NRC. "Practical Implementation Guidelines for SSHAC Level 3 and 4 Hazard Studies. NUREG-2117, Revision 1. Washington, DC. April 2012c. ADAMS Accession No. ML12118A445.

NRC. "Confirmatory Analysis of Seismic Hazard at the Diablo Canyon Power Plant from the Shoreline Fault Zone." Research Information Letter 12-01. Washington, DC. September 2012d. ADAMS Accession No. ML121230035.

NRC. "A Performance-Based Approach to Define the Site-Specific Earthquake Ground Motion." Regulatory Guide 1.208. Washington, DC. March 2007. ADAMS Accession No. ML070310619.

NRC. "Technical Basis for Revision of Regulatory Guidance on Design Ground Motions: Hazard- and Risk-consistent Ground Motion Spectra Guidelines." NUREG/CR-6728. Washington, DC. November 6, 2001. ADAMS Accession No. ML013100232.

NRC. "Recommendations for Probabilistic Seismic Hazard Analysis: Guidance on Uncertainty and the Use of Experts." NUREG/CR-6372, Volumes 1 and 2. Washington, DC. April 1997. ADAMS Accession Nos. ML080090003 and ML080090004.

NRC. "Safety Evaluation Report Related to the Operation of Diablo Canyon Nuclear Power Plant, Units 1 and 2." NUREG-0675, Supplement No. 7. Washington, DC. May 26, 1978.

Pearthree, P.A., C.M. Menges, and L. Mayer. "Distribution, Recurrence, and Possible Tectonic Implications of Late Quaternary Faulting in Arizona." Arizona Geological Survey Open-File Report 83-20. Tucson, AZ. p. 53. 1983.

Petersen, M.D., A.D. Frankel, S.C. Harmsen, C.S. Mueller, K.M. Haller, R.L. Wheeler, R.L. Wesson, Y. Zeng, O.S. Boyd, D.M. Perkins, N. Luco, E.H. Field, C.J. Wills, and K.S. Rukstales. "Documentation for the 2008 Update of the United States National Seismic Hazard Maps." USGS Open-File Report 2008-1128. p. 61. 2008a.

Petersen, M.D., C.S. Mueller, A.D. Frankel, and Y. Zeng. "Appendix J—Spatial Seismicity Rates and Maximum Magnitudes for Background Earthquakes." E.H. Field, T.E. Dawson, K.R. Felzer, A.D. Frankel, V. Gupta, T.H. Jordan, T. Parsons, M.D. Peterson, R.S. Stein, R.J. Weldon II, and C.J. Wills, Eds. *The Uniform California Earthquake Rupture Forecast, Version 2 (UCERF 2)*. USGS Open-File Report 2007-1437. 2008b.

PG&E. Letter from Barry Allen, Vice President, Nuclear Services, to U.S. Nuclear Regulatory Commission, Diablo Canyon Units 1 and 2 Docket Nos. 50-275 and 50-323, Response to NRC Request for Information Pursuant to 10 CFR 50.54(f) Regarding the Seismic Aspects of Recommendation 2.1 of the Near-Term Task Force Review of Insights from the Fukushima Dai-ichi Accident: Seismic Hazard and Screening Report. Avila Beach, CA. March 2015a. ADAMS Accession No. ML15071A046.

PG&E. "Seismic Source Characterization for the Diablo Canyon Power Plant, San Luis Obispo County, California." Revision A. Avila Beach, CA. March 2015b.

PG&E. Letter from L. Jearl Strickland, Director, Technical Services, to U.S. Nuclear Regulatory Commission, Diablo Canyon Units 1 and 2 Docket Nos. 50-275 and 50-323, Response to NRC Request for Additional Information dated October 1, 2015, and November 13, 2015, Regarding Recommendation 2.1 of the Near-Term Task Force Seismic Hazard and Screening Report. Avila Beach, CA. December 2015c. ADAMS Accession Nos. ML15355A550 and ML15355A551.

PG&E. "Central Coastal California Seismic Imaging Project (CCCSIP)." Report to the California Public Utilities Commission. Avila Beach, CA. 2014.  
<http://www.pge.com/en/safety/systemworks/dcpp/seismicsafety/report.page>

- PG&E. "Stratigraphic Framework for Assessment of Fault Activity Offshore of the Central California Coast between Point San Simeon and Point Sal." PG&E Technical Report GEO.DCPP.TR.13.01. Avila Beach, CA. 2013.
- PG&E. "Report on the Analysis of the Shoreline Fault Zone, Central Coastal California, Report to the U.S. Nuclear Regulatory Commission." Avila Beach, CA. 2011. ADAMS Accession No. ML110140431.
- PG&E. "PG&E Letter No. DCL-91-027, Addendum to the 1988 Final Report of the Diablo Canyon Long Term Seismic Program." Docket Nos. 50-275 and 50-323. Avila Beach, CA. February 1991a.
- PG&E. "PG&E Letter No. DCL-91-091, Benefits and Insights of the Long-Term Seismic Program." Docket Nos. 50-275 and 50-323. Avila Beach, CA. April 1991b. ADAMS Accession No. ML9104300253.
- PG&E. "PG&E Letter No. DCL-91-143, Long-Term Seismic Program—Implementation of the Results of the Program." Docket Nos. 50-275 and 50-323. Avila Beach, CA. May 1991c. ADAMS Accession No. ML9106070210.
- PG&E. "Additional Deterministic Evaluations Performed to Assess Seismic Margins of the Diablo Canyon Power Plant, Units 1 and 2." Enclosure to PG&E Letter DCL-90-226, "Long Term Seismic Program Additional Deterministic Evaluations," September 18, 1990. Avila Beach, CA. 1990.
- PG&E. "Final Report of the Diablo Canyon Long-Term Seismic Program, Report to the U.S. NRC." Docket Nos. 50-275 and 50-323. Avila Beach, CA. 1988. ADAMS Accession No. ML8803160246.
- PNNL. "Hanford Sitewide Probabilistic Seismic Hazard Analysis." PNNL-23361. Richland, WA. 2014.
- Reidel, S.P., V.E. Camp, T.L. Tolan, and B.S. Martin. "The Columbia River Flood Basalt Province: Stratigraphy, Areal Extent, Volume, and Physical Volcanology." Reidel, S.P., V.E. Camp, M.E. Ross, J.A. Wolff, B.S. Martin, T.L. Tolan, and R.E. Wells, eds. *The Columbia River Flood Basalt Province, Geological Society of America Special Paper 497*. pp. 1–43. 2013.
- Sammon, J.W. "A Nonlinear Mapping for Data Structure Analysis." *IEEE Transactions on Computers*. Vol. C-18, Issue 5. pp. 401–409. 1969.
- Scharer, K.M., G.P. Biasi, R.J. Weldon II, and T.E. Fumal. "Quasi-periodic Recurrence of Large Earthquakes on the Southern San Andreas Fault." *Geology*. Vol. 38, Issue 6. pp. 555–558. 2010.
- Scherbaum, F., N.M. Kuehn, M. Ohrnberger, and A. Koehler. "Exploring the Proximity of Ground-Motion Models Using High-Dimensional Visualization Techniques." *Earthquake Spectra*. Vol. 26, Issue 4. pp. 1,117–1,138. 2010.
- Sieh, K.E. and R.H. Jahns. "Holocene Activity of the San Andreas Fault at Wallace Creek, California." *Geological Society of America Bulletin*. Vol. 95, Issue 8. pp. 883–896. 1984.

Silva, W.J., C. Costantino, S. Li. "Quantification of nonlinear soil response for the Loma Prieta, Northridge, and Imperial Valley California earthquakes." *Proceedings of The Second International Symposium on The Effects of Surface Geology on Seismic Motion*. Irikura, Kudo, Okada & Sasatani, eds. Yokohama, Japan, December 1–3, 1998. pp. 1137–1143. 1998.

Silva, W.J., N. Abrahamson, G. Toro, and C. Costantino. "Description and Validation of the Stochastic Ground Motion Model." Report Submitted under Contract No. 770573 to Brookhaven National Laboratory, Associated Universities, Inc. Upton, New York. 1996.

Silverman, B.W. "Density Estimation for Statistics and Data Analysis." Chapman and Hall, London, England. 1986.

Sliter, R.W., P.J. Triezenberg, P.E. Hart, J.T. Watt, S.Y. Johnson, and D.S. Scheirer. "High-Resolution Seismic Reflection and Marine Magnetic Data Along the Hosgri Fault Zone, Central California, U.S." USGS Open-File Report 2009-1100, Version 1.1. 2010.

Stein, S. "Approaches to Continental Intraplate Earthquake Issues." *Geological Society of America Special Paper 425*. p. 1–16. 2007.

Stepp, J.C. "Analysis of Completeness of the Earthquake Sample in the Puget Sound Area and Its Effect on Statistical Estimates of Earthquake Hazard." In *Proceedings of the 1st Int. Conf. on Microzonation, Seattle*. Vol. 2. pp. 897–910. 1972.

Steritz, J.W. and B.P. Luyendyk. "Hosgri Fault Zone, Offshore Santa Maria Basin, California." *Geological Society of America Special Paper 292*. pp. 191–209. 1994.

Stirling, M., M. Gerstenberger, N. Litchfield, G. McVerry, W. Smith, J. Pettinga, and P. Barnes. "Seismic Hazard of the Canterbury Region, New Zealand." *Bulletin of the New Zealand Society for Earthquake Engineering*. Vol. 41, No. 2. pp. 51–67. 2008.

Swank, D.A. Letter from David Swank, Assistant Vice President Engineering, CGS, to U.S. Nuclear Regulatory Commission, Columbia Generating Station Docket No. 50-397, Seismic Hazard and Screening Report, Response to NRC Request for Information Pursuant to 10 CFR 50.54(f) Regarding Recommendation 2.1 of the Near-Term Task Force Review of Insights from the Fukushima Dai-ichi Accident. March 12, 2015a. ADAMS Accession No. ML15078A243.

Swank, D.A. Letter from David Swank, Assistant Vice President Engineering, to U.S. Nuclear Regulatory Commission, Columbia Generating Station Docket No. 50-397, Response to Request for Additional Information Associated with Near-Term Task Force Recommendation 2.1, Seismic Reevaluations. September 24, 2015b. ADAMS Accession No. ML15267A780.

Titus, S.J., C. DeMets, and B. Tikoff. "New Slip Rate Estimates for the Creeping Segment of the San Andreas Fault, California." *Geology*. Vol. 33, Issue 3. pp. 205–208. 2005.

Titus, S.J., M. Dyson, C. DeMets, B. Tikoff, F. Rolandone, and R. Bürgmann. "Geologic versus Geodetic Deformation Adjacent to the San Andreas Fault, Central California." *Geological Society of America Bulletin*. Vol. 123, Issue 5-6. pp. 794–820. 2011.

- Toda, S., R.S. Stein, K. Richards-Dinger, and S.B. Bozkurt. "Forecasting the Evolution of Seismicity in Southern California: Animations Built on Earthquake Stress Transfer." *Journal of Geophysical Research*. Vol. 110(B5). pp. 2,156–2,202. 2005.
- Toké, N.A., J.R. Arrowsmith, M.J. Rymer, A. Landgraf, D.E. Haddad, M. Busch, J. Cayan, and A. Hannah. "Late Holocene Slip Rate of the San Andreas Fault and its Accommodation by Creep and Moderate-Magnitude Earthquakes at Parkfield, California." *Geology*. Vol. 39, Issue 3. pp. 243–246. 2011.
- Uhrhammer, R.A. "Characteristics of Northern and Central California Seismicity." *Earthquake Notes*. Vol. 57, No. 1. p. 21. 1986.
- Veneziano, D. and J. Van Dyck. "Analysis of Earthquake Catalogs for Incompleteness and Recurrence Rates, Seismic Hazard Methodology for Nuclear Facilities in the Eastern United States." EPRI Research Project P101-29. Vol. 2. pp. A221–A297. EPRI. Palo Alto, CA. 1985.
- Vucetic, M. and R. Dobry. "Effects of Soil Plasticity on Cyclic Response." *Journal of Geotechnical Engineering*. American Society of Civil Engineers. Vol. 117, No. 1. pp. 89–107. 1991.
- Warren, D.H. "A Seismic-Refraction Survey of Crustal Structure in Central Arizona." *Geological Society of America Bulletin*. Vol. 80, No. 2. pp. 257–282. 1969.
- Wells, D.L. and K.J. Coppersmith. "New Empirical Relationships Among Magnitude, Rupture Length, Rupture Width, Rupture Area, and Surface Displacement." *Bulletin of the Seismological Society of America*. Vol. 84, No. 4. pp. 974–1,002. 1994.
- Wesnousky, S.G. "Displacement and Geometrical Characteristics of Earthquake Surface Ruptures: Issues and Implications for Seismic-Hazard Analysis and the Process of Earthquake Rupture." *Bulletin of the Seismological Society of America*. Vol. 98, No. 4. pp. 1,609–1,632. 2008.
- Wesnousky, S.G. "Earthquakes, Quaternary Faults, and Seismic Hazard in California." *Journal of Geophysical Research*. Vol. 91, No. B12. pp. 12,587–12,631. 1986.
- Wesnousky, S.G., C.H. Scholz, K. Shimazaki, and T. Matsuda. "Earthquake Frequency Distribution and the Mechanics of Faulting." *Journal of Geophysical Research*. Vol. 88. pp. 9,331–9,340. 1983.
- Willingham, C.R., J.D. Rietman, R.G. Heck, and W.R. Lettis. "Characterization of the Hosgri Fault Zone and Adjacent Structures in the Offshore Santa Maria Basin, South Central California." M.A. Keller, ed., *Evolution of Sedimentary Basins/Onshore Oil and Gas Investigations—Santa Maria Province*, USGS Bulletin 1995-CC. p. 105. 2013.
- Wooddell, K.E., N.A. Abrahamson, A.L. Acevedo-Cabrera, and R.R. Youngs. "Hazard Implementation of Simplified Seismic Source Characterization Allowing for Linked Faults." *Seismological Research Letters*. Vol. 85, No. 2. p. 471. 2014.

Youngs, R.R. and K.J. Coppersmith. "Implications of Fault Slip Rates and Earthquake Recurrence Models to Probabilistic Seismic Hazard Estimates." *Bulletin of the Seismological Society of America*. Vol. 75, No. 4. pp. 939–964. 1985.

Zachariassen, J., K. Berryman, R. Langridge, C. Prentice, M. Rymer, M. Stirling, and P. Villamor. "Timing of late Holocene surface rupture of the Wairau Fault, Marlborough, New Zealand." *New Zealand Journal of Geology and Geophysics*. Vol. 49, No. 1. pp. 159–174. 2006.

Zhang, H. and C.H. Thurber. "Double-Difference Tomography: The Method and Its Application to the Hayward Fault, California." *Bulletin of the Seismological Society of America*. Vol. 93, Issue 5. pp. 1,875–1,889. 2003.

Zhao, J.X. and M. Lu. "Magnitude-Scaling Rate in Ground-Motion Prediction Equations for Response Spectra from Large, Shallow Crustal Earthquakes." *Bulletin of the Seismological Society of America*. Vol. 101. pp. 2,643–2,661. 2011.

Zhao, J.X., J. Zhang, A. Asano, Y. Ohno, T. Oouchi, T. Takahashi, H. Ogawa, K. Irikura, H.K. Thio, P.G. Somerville, Y. Fukushima, and Y. Fukushima. "Attenuation Relations of Strong Ground Motion in Japan Using Site Classification Based on Predominate Period." *Bulletin of the Seismological Society of America*. Vol. 96. pp. 898–913. 2006.





## 4 SITE AMPLIFICATION FACTORS AND SPECTRAL SHAPES

### 4.1 Background

This section presents median amplification factors and response spectral shapes for each of the nuclear power plants (NPPs) in the central and eastern United States and in the western United States grouped by their National Earthquake Hazard Reduction Program (NEHRP) site classifications (BSSC, 2004). The U.S. Nuclear Regulatory Commission (NRC) staff categorized each of the NPPs into one of four NEHRP site classifications using the average shear wave velocity over the top 30 meters (m) [100 feet (ft)] ( $V_{S30}$ ) of the median basecase profile for each of the sites. As described in Sections 2 and 3 of this report, the basecase profiles extend from the control point elevation beneath the site down to the reference rock horizon. Table 4.1-1 provides the four NEHRP site classifications that apply to U.S. NPPs and associated  $V_{S30}$  ranges.

Class	Description	$V_{S30}$ (m/sec)
A	Hard rock	> 1,500
B	Firm to hard rock	760–1,500
C	Dense soil and soft rock	360–760
D	Stiff soil	180–360

#### 4.1.1 Amplification Factor Distributions

Using the site response evaluation for each of the NPPs, the NRC staff developed a set of low, medium, and high amplification factors ( $AF$ ) corresponding to the 10<sup>th</sup>, 50<sup>th</sup>, and 90<sup>th</sup> percentiles of the overall  $AF$  distribution, which is assumed to be lognormal. To determine these percentiles for each of the NPPs, the NRC staff first calculated median amplification factors ( $\bar{AF}_i$ ) and logarithmic variances ( $\sigma_{\ln AF_i}^2$ ) from the 60 randomized profiles developed for each of the combinations of three basecase profiles, site kappa ( $\kappa_0$ ) values, and two shear modulus and damping curves. Next, the NRC staff determined the overall logarithmic-weighted mean amplification factor ( $\mu_{\ln AF,T}$ ) and variance ( $\sigma_{\ln AF,T}^2$ ) for each oscillator period ( $T$ ) given by

$$\mu_{\ln AF,T} = \sum_i w_i \mu_{\ln AF_i} = \sum_i w_i \ln \bar{AF}_i \quad \text{Eq. 4-1}$$

$$\sigma_{\ln AF,T}^2 = \sigma_{\ln,ep}^2 + \sigma_{\ln,al}^2 \quad \text{Eq. 4-2}$$

where  $w_i$  is the weight for each of the unique combinations of basecase profiles and shear modulus and damping curves, and the overall logarithmic variance ( $\sigma_{\ln AF,T}^2$ ) is separated into its epistemic ( $\sigma_{\ln,ep}^2$ ) and aleatory ( $\sigma_{\ln,al}^2$ ) components. The epistemic component of the overall logarithmic variance is given by

$$\sigma_{\ln,ep}^2 = \sum_i w_i (\mu_{\ln AF_i} - \mu_{\ln AF,T})^2 \quad \text{Eq. 4-3}$$

and the aleatory component is given by

$$\sigma_{ln,al}^2 = \sum_i w_i \sigma_{ln AF_i}^2 \quad \text{Eq. 4-4}$$

To determine the 10<sup>th</sup>, 50<sup>th</sup>, and 90<sup>th</sup> percentile estimates of the overall *AF* distribution, which is assumed to be lognormally distributed, the NRC staff used the epistemic component of the overall logarithmic standard deviation

$$AF_{10} = \exp(\mu_{ln AF,T} - 1.282\sigma_{ln,ep}) \quad \text{Eq. 4-5}$$

$$AF_{50} = \exp(\mu_{ln AF,T}) \quad \text{Eq. 4-6}$$

$$AF_{90} = \exp(\mu_{ln AF,T} + 1.282\sigma_{ln,ep}) \quad \text{Eq. 4-7}$$

The figures of the amplification factor presented in the following subsections for each of the four NEHRP site classifications show the 10<sup>th</sup>, 50<sup>th</sup>, and 90<sup>th</sup> percentile estimates of the overall *AF* distributions for each of the NPP sites.

#### 4.1.2 Spectral Shapes

To determine whether there are consistent spectral shapes for the four different NEHRP classifications, the NRC staff developed normalized acceleration response spectra using the ground motion response spectrum (GMRS) for each of the NPP sites. After grouping the NPP sites into one of four NEHRP classifications (A to D) based on the site's  $V_{S30}$ , the NRC staff divided each site GMRS by its peak ground acceleration (PGA), assumed to be the spectral acceleration at 100 Hertz (Hz) ( $GMRS_{100}$ ), to develop the normalized spectral shapes. These spectra show distinct shapes that are typical for soil and rock sites and can be used to develop seismic design response spectra.

### 4.2 NEHRP Class A Nuclear Power Plant Sites

The NEHRP Class A NPP sites are hard rock sites with  $V_{S30}$  values greater than 1,500 meters/second (m/sec) [5,000 feet/second (ft/sec)] and are located in the New England, Appalachian Plateaus, Piedmont, Valley and Ridge, Interior Low Plateaus, Central Lowlands, Ouachita, and Great Plains physiographic provinces. Table 4.2-1 lists the Class A NPP sites and key site characteristics: (1) site subsurface profile description, (2)  $V_{S30}$ , (3)  $\kappa_0$ , (4) peak  $\overline{AF}$  and associated frequency ( $f$ ), (5) depth to  $V_S$  of 1,000 m/sec [3,300 ft/sec] ( $z_{1.0}$ ), (6) depth to  $V_S$  of 2,500 m/sec [8,200 ft/sec] ( $z_{2.5}$ ), and (7)  $GMRS_{100}$ . The  $V_{S30}$ ,  $\kappa_0$ ,  $z_{1.0}$ , and  $z_{2.5}$  values are based on the median basecase profiles for each of the NPP sites, and the peak  $\overline{AF}$  and associated  $f$  are based on the lowest input spectra (Level 1 of 12) used for the site response analysis.

As shown in Table 4.2-1, the  $\kappa_0$  values for the Class A NPP sites are generally less than 10 milliseconds (msec), with the exception of the deeper profile sites with lower  $V_S$  values. This result arises from the NRC staff's use of Model 1 from Campbell (2009), which estimates the effective seismic quality factor of shear waves ( $Q_{ef}$ ) for each layer based on the  $V_S$  for that layer. As described in Section 2.1.4.3, the NRC staff calculated  $Q_{ef}$  for each layer and then determined a  $\kappa_0$  value using Equations 2-3 and 2-4. Each  $\kappa_0$  value includes the reference rock value from the ground motion model.

<b>Plant</b>	<b>Profile Desc.</b>	<b><math>V_{S30}</math> (m/sec)</b>	<b><math>\kappa_0</math> (msec)</b>	<b><math>\bar{AF}</math></b>	<b><math>f</math> (Hz)</b>	<b><math>z_{1.0}</math> (m)</b>	<b><math>z_{2.5}</math> (m)</b>	<b><math>GMRS_{100}</math> (g)</b>
Arkansas	Rock	1,743	23	1.4	0.2	0	2,260	0.14
Bellefonte*	Rock	2,765	6	1.2	7.4	0	3	0.34
Browns Ferry	Rock	2,831	13	1.2	0.5	0	0	0.19
Catawba	Rock	2,501	6	1.1	25.1	0	11	0.33
Comanche Peak	Rock	1,679	19	1.8	1.6	0	1,372	0.05
Duane Arnold†	Rock	2,234	7	1.2	4.6	0	116	0.11
Ginna	Rock	1,951	8	1.3	4.3	0	0	0.13
Harris	Rock	1,781	14	1.3	0.4	0	1,128	0.10
Indian Point†	Rock	2,695	6	1.0	-	0	0	0.43
Limerick	Rock	1,639	7	1.6	6.8	0	61	0.30
McGuire	Rock	2,538	6	1.0	-	0	8	0.35
Millstone	Rock	2,275	6	1.2	17.1	0	0	0.27
Nine Mile Pt. & FitzPatrick	Rock	2,183	9	1.2	1.0	0	0	0.12
Oconee	Rock	2,615	6	1.1	18.5	0	0	0.45
Peach Bottom	Rock	1,796	6	1.2	25.1	0	20	0.50
Perry	Rock	1,526	11	1.7	1.0	0	387	0.25
Quad Cities	Rock	1,921	8	1.4	5.8	0	76	0.18
Seabrook	Rock	2,831	6	1.0	-	0	0	0.44
Sequoyah	Rock	1,909	8	1.3	0.2	0	244	0.21
Summer	Rock	2,620	6	1.0	-	0	8	0.53
Susquehanna	Rock	2,212	6	1.2	9.3	0	40	0.15
Three Mile Island†	Rock	1,524	7	1.5	2.9	0	152	0.30
Watts Bar	Rock	1,812	9	1.4	1.7	0	320	0.41
*Plant is not operational.								
†Plant was shut down or has subsequently shut down.								

Recently, Xu et al. (2020) used Kik-net<sup>1</sup> array data from Japan and six sites in California to develop a relationship between  $\kappa_0$  and both  $V_{S30}$  and  $z_{2.5}$ . Their study shows that  $\kappa_0$  increases with decreasing  $V_{S30}$  and increasing  $z_{2.5}$ , thus confirming the general trend of the NRC staff's  $\kappa_0$  estimates.

Figure 4.2-1 shows the overall low, medium, and high amplification factors ( $AF_{10}$ ,  $AF_{50}$ ,  $AF_{90}$ ) for two of the input spectra (low level and intermediate level) used for the site response analyses. As shown in Figure 4.2-1, the amplification factors for the Class A sites generally range from 1.0 to 1.5 for the low input spectrum (Level 2 of 12) and from 0.5 to 2.0 for the intermediate input spectrum (Level 6 of 12). This result demonstrates that the Class A very stiff hard rock sites do

<sup>1</sup> The Kik-net (Kiban Kyoshin) array is a Japanese network of pairs of strong-motion seismographs installed at the ground surface and in co-located boreholes.

not generate significant site amplifications or significant nonlinear behavior for higher input loading levels. Figure 4.2-2 shows the normalized GMRS for the Class A sites. The average normalized spectral shape (red curve) shows a typical hard rock spectral shape with a peak near 25 Hz.

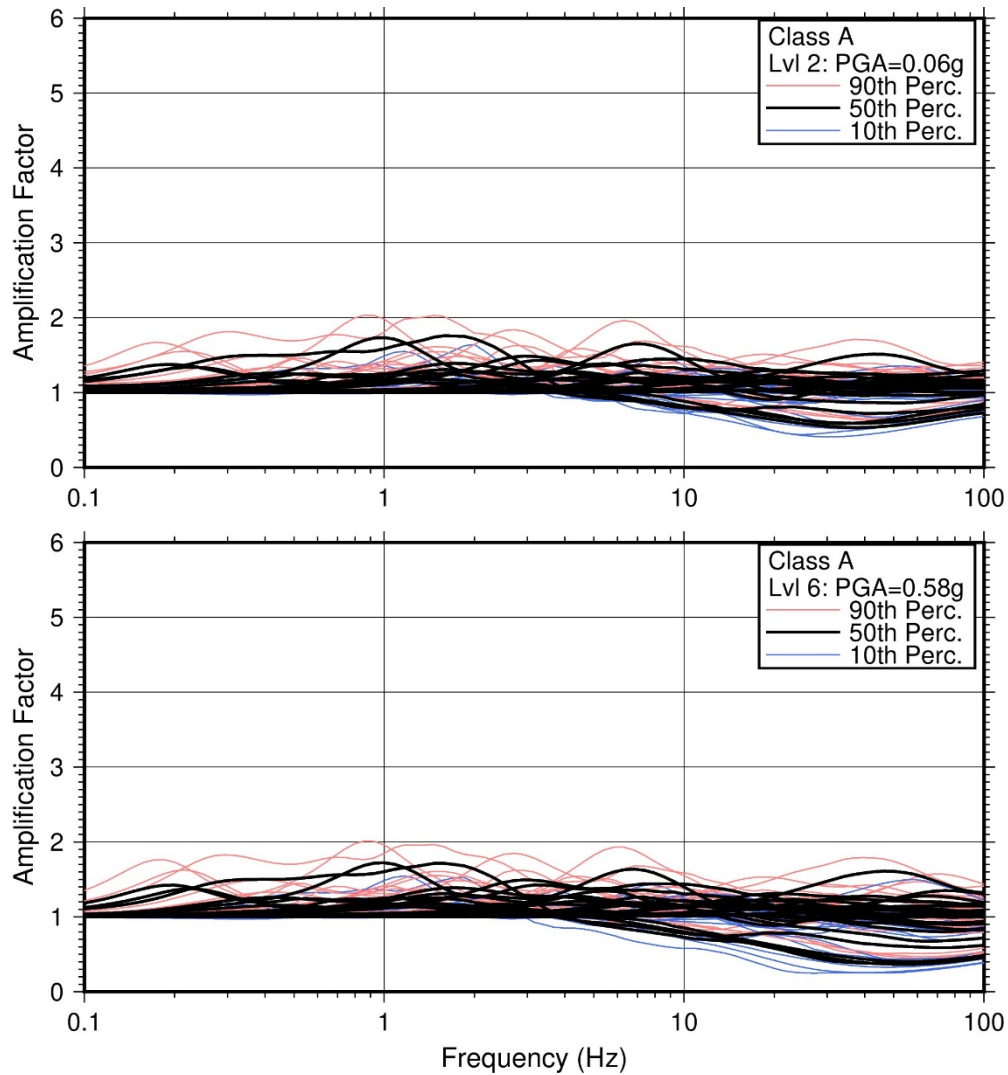


**Figure 4.2-1 Amplification Factors as a Function of Frequency for Class A NPP Sites. Upper Panel Results are for Low Input Loading Level (PGA = 0.06g), and Lower Panel Results are for Intermediate Input Loading Level (PGA = 0.58g)**

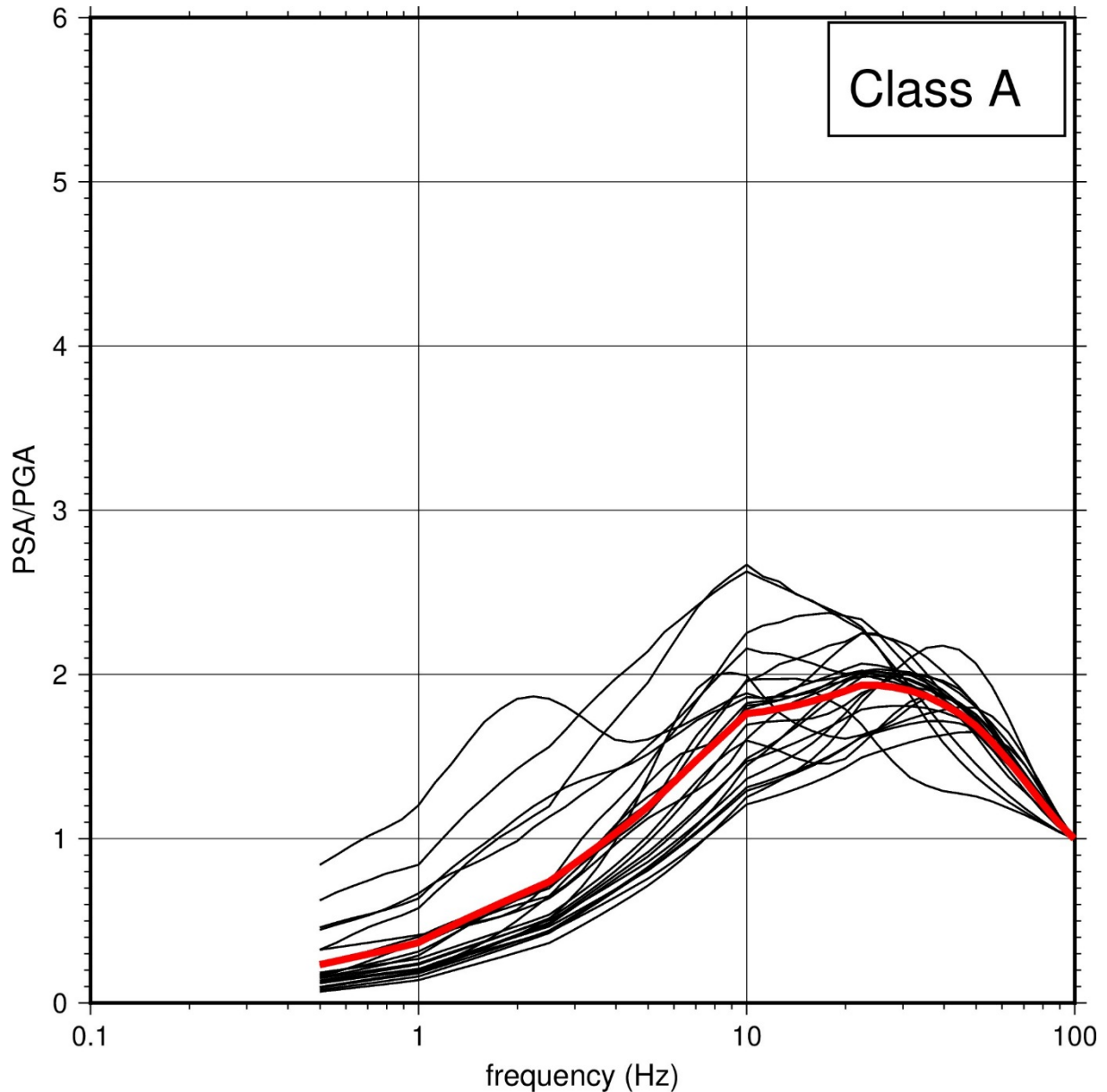


**Figure 4.2-2 Normalized GMRS Results for Class A Sites. Average Normalized Spectral Shape is Shown by Red Curve, and Individual Sites are Shown by Thin Black Lines**

### **4.3 NEHRP Class B Nuclear Power Plant Sites**

The NEHRP Class B NPP sites are either firm to hard rock sites or shallow soil over rock sites with  $V_{S30}$  values between 760 m/sec [2,500 ft/sec] and 1,500 m/sec [5,000 ft/sec]. The Class B NPP sites are located in the New England, Coastal Plain, Piedmont, Central Lowlands, and Coast Ranges physiographic provinces. Table 4.3-1 lists the Class B NPP sites and key site characteristics: (1) site subsurface profile description, (2)  $V_{S30}$ , (3)  $\kappa_0$ , (4) peak  $\bar{A}\bar{F}$  and associated  $f$ , (5)  $z_{1.0}$ , (6)  $z_{2.5}$ , and (7)  $GMRS_{100}$ .

<b>Plant</b>	<b>Profile Desc.</b>	<b><math>V_{S30}</math> (m/sec)</b>	<b><math>\kappa_0</math> (msec)</b>	<b><math>\bar{AF}</math></b>	<b><math>f</math> (Hz)</b>	<b><math>z_{1.0}</math> (m)</b>	<b><math>z_{2.5}</math> (m)</b>	<b><math>GMRS_{100}</math> (g)</b>
Braidwood	Rock	1,229	8	1.5	6.3	0	68	0.26
Brunswick	Soil over rock	866	21	2.3	0.5	7	452	0.22
Byron	Rock	1,432	7	1.6	9.3	0	35	0.30
Davis Besse	Rock	1,387	9	1.7	6.8	0	52	0.21
Diablo Canyon	Soil over rock	968	40	1.4	2.0	10	700	0.86
Dresden	Rock	1,129	8	2.0	7.4	12	12	0.30
Fermi	Rock	1,498	7	2.0	4.3	0	88	0.15
North Anna	Rock	1,464	7	1.6	10.8	0	30	0.48
Pilgrim	Soil over rock	1,018	7	2.6	10.8	13	15	0.44

As shown in Table 4.3-1, the  $\kappa_0$  values for the Class B NPP sites are generally less than 10 msec, with the exception of the deeper profile sites with lower  $V_S$  values. The overall low, medium, and high amplification factors ( $AF_{10}$ ,  $AF_{50}$ ,  $AF_{90}$ ) shown in Figure 4.3-1 for the Class B sites range from 1 to 3, with the peak value generally occurring around 10 Hz for the low input spectra (Level 2 of 12). The amplification factors for the intermediate input spectra (Level 6 of 12) show a more pronounced decrease beyond 10 Hz, which is due to nonlinear response of the soil, rock, or both to increased loading levels. Figure 4.3-2 shows the normalized GMRS for the Class B sites. The average normalized spectral shape (red curve) shows a typical firm-to-hard rock spectral shape with a peak near 10 Hz.

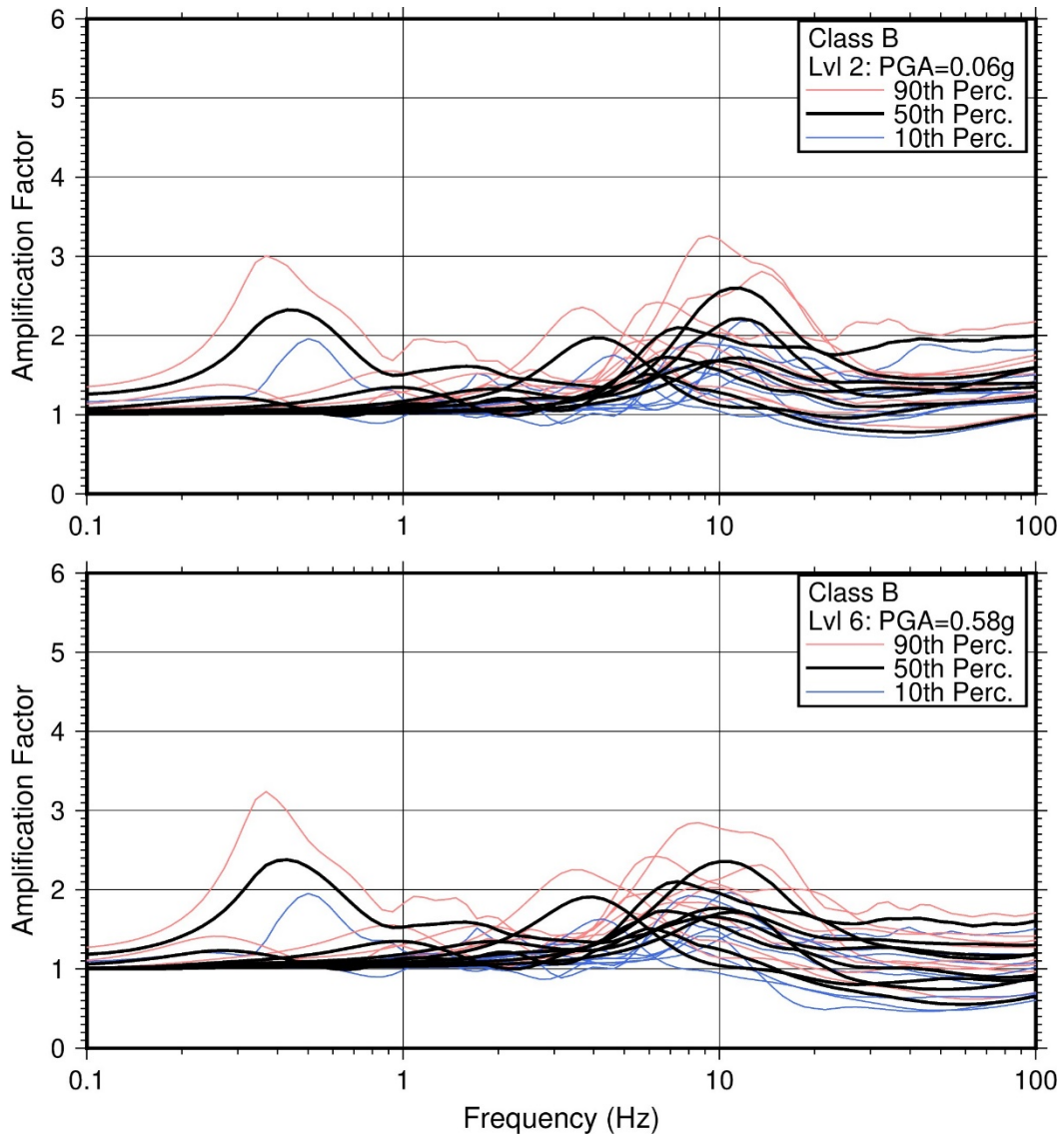


**Figure 4.3-1 Amplification Factors as a Function of Frequency for Class B NPP Sites. Upper Panel Results are for Low Input Loading Level (PGA = 0.06g), and Lower Panel Results are for Intermediate Input Loading Level (PGA = 0.58g)**

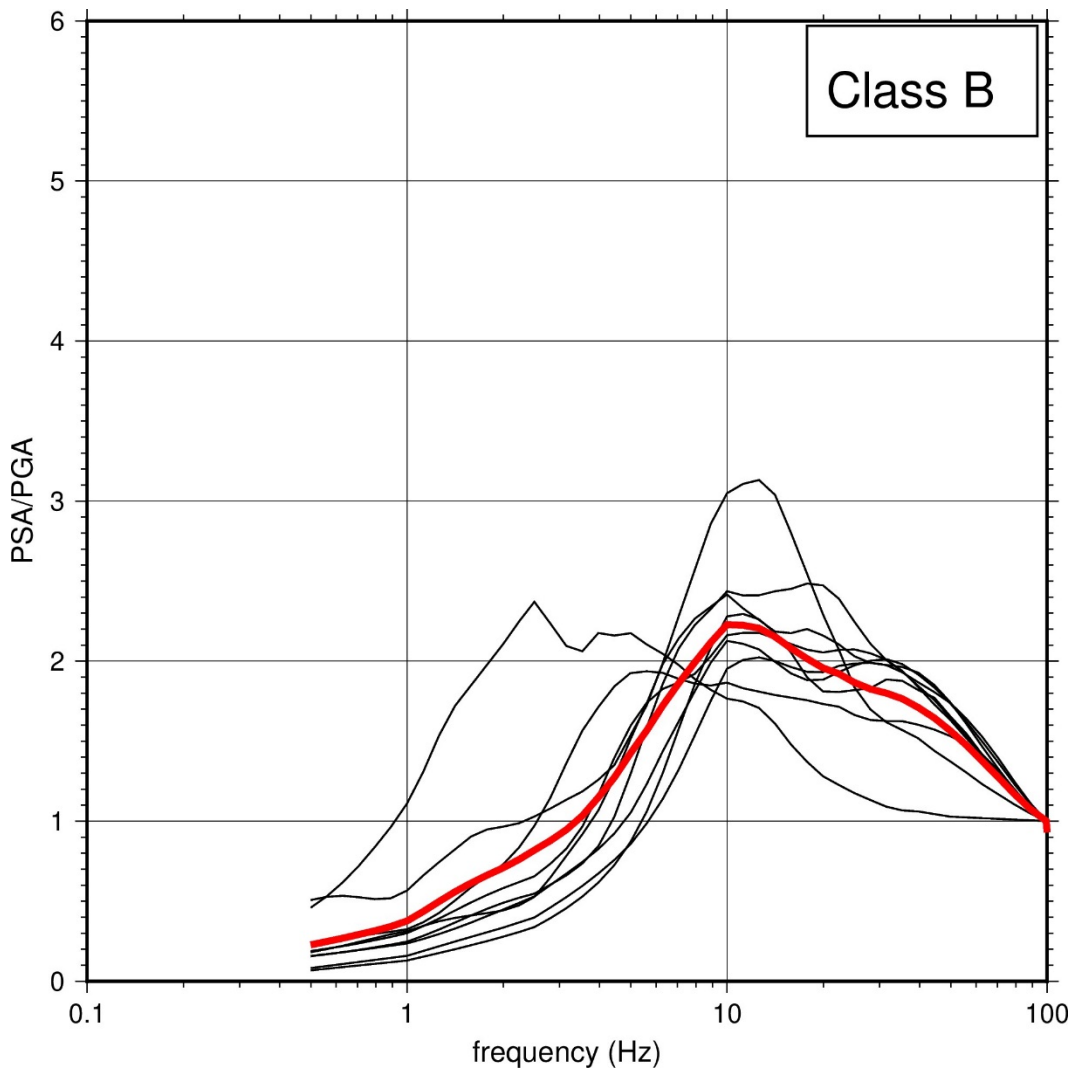


**Figure 4.3-2 Normalized GMRS Results for Class B Sites. Average Normalized Spectral Shape is Shown by Red Curve, and Individual Sites are Shown by Thin Black Lines**

#### **4.4 NEHRP Class C Nuclear Power Plant Sites**

The NEHRP Class C NPP sites are either soil, soil over rock, or soil and soft rock, with  $V_{S30}$  values between 360 m/sec [1,200 ft/sec] and 760 m/sec [2,500 ft/sec]. The Class C NPP sites are located in the Appalachian Plateaus, Coastal Plain, and Central Lowlands physiographic provinces. Table 4.4-1 lists the Class C NPP sites and key site characteristics: (1) site subsurface profile description, (2)  $V_{S30}$ , (3)  $\kappa_0$ , (4) peak  $\bar{A}\bar{F}$  and associated  $f$ , (5)  $z_{1.0}$ , (6)  $z_{2.5}$ , and (7)  $GMRS_{100}$ .



**Table 4.4-1 NEHRP Class C Nuclear Power Plant Sites**

Plant	Profile Desc.	$V_{S30}$ (m/sec)	$\kappa_0$ (msec)	$\bar{AF}$	$f$ (Hz)	$z_{1.0}$ (m)	$z_{2.5}$ (m)	$GMR_{S10}$ $o$ (g)
Beaver Valley	Soil over rock	538	19	3.1	5.0	17	1,336	0.20
Callaway	Soil over rock	610	9	3.9	7.4	17	31	0.43
Calvert Cliffs	Soil over rock	420	51	3.1	0.3	764	764	0.10
Clinton	Soil over rock	427	19	3.2	5.4	88	686	0.27
Columbia	Soil over rock	365	31	2.8	0.7	30	180	0.25
Cook	Soil over rock	367	13	3.8	3.2	39	152	0.26
Cooper	Soil over rock	420	13	3.5	4.0	29	585	0.21
Fort Calhoun*	Soil over rock	389	16	4.1	4.3	23	213	0.17
Grand Gulf	Soil	502	>65	2.8	0.2	>1220	>1220	0.10
Hope Creek & Salem	Soil	710	30	2.9	0.4	28	515	0.14
Monticello	Soil over rock	490	10	3.4	13.6	18	35	0.15
Oyster Creek*	Soil	433	>65	2.5	0.1	>1220	>1220	0.11
Prairie Island	Soil over rock	748	18	2.2	3.4	55	905	0.08
Point Beach	Soil over rock	535	11	3.2	5.8	27	41	0.14
Turkey Point	Soil and rock	614	31	3.1	0.7	9	1,128	0.06
Wolf Creek	Soil over rock	728	12	2.9	10.8	11	145	0.24

\*Plant was shut down or has subsequently shut down.

As shown in Table 4.4-1, the  $\kappa_0$  values for the Class C NPP sites vary considerably but are generally higher for the sites with deeper profiles and lower  $V_S$  values. As described in the plant-specific analyses in Section 2 of this report, for the very deep soil sites (Grand Gulf and Oyster Creek), the estimated  $\kappa_0$  values would likely exceed 65 msec had the NRC staff not terminated the basecase profiles for these sites at 1,220 m [4,000 ft]. The overall low, medium, and high amplification factors ( $AF_{10}$ ,  $AF_{50}$ ,  $AF_{90}$ ) shown in Figure 4.4-1 for the Class C sites range from 1 to 4, with the peak value generally occurring between 5 to 10 Hz for the low input spectra (Level 2 of 12). The amplification factors for the intermediate input spectra (Level 6 of 12) show a pronounced decrease beyond 10 Hz, which is due to nonlinear response of the soil, rock, or both to increased loading levels. Figure 4.4-2 shows the normalized GMRS for the Class C sites. The average normalized spectral shape (red curve) shows a fairly broad spectral shape with a peak near 7 Hz.

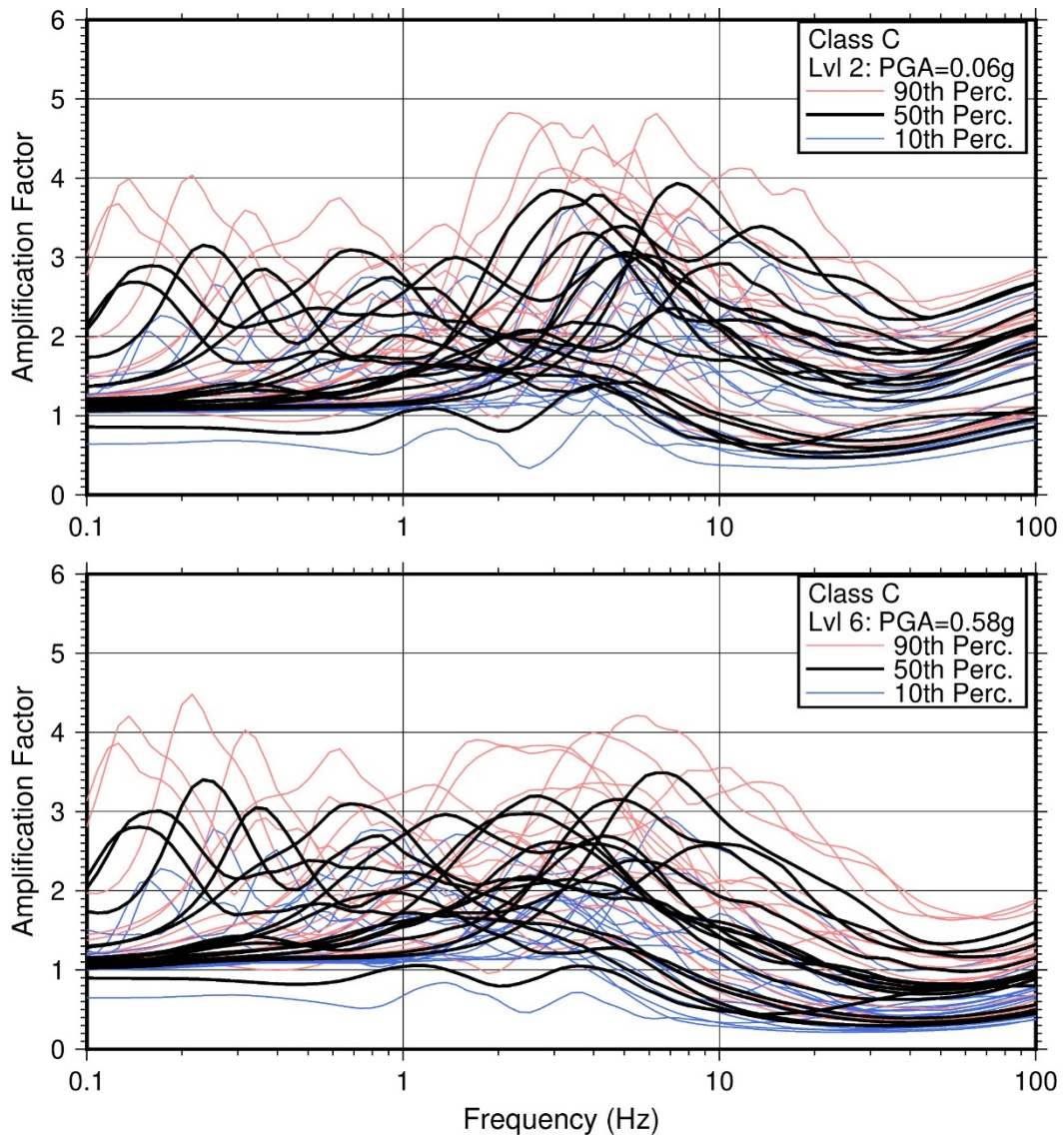


**Figure 4.4-1 Amplification Factors as a Function of Frequency for Class C NPP Sites. Upper Panel Results are for Low Input Loading Level (PGA = 0.06g), and Lower Panel Results are for Intermediate Input Loading Level (PGA = 0.58g)**

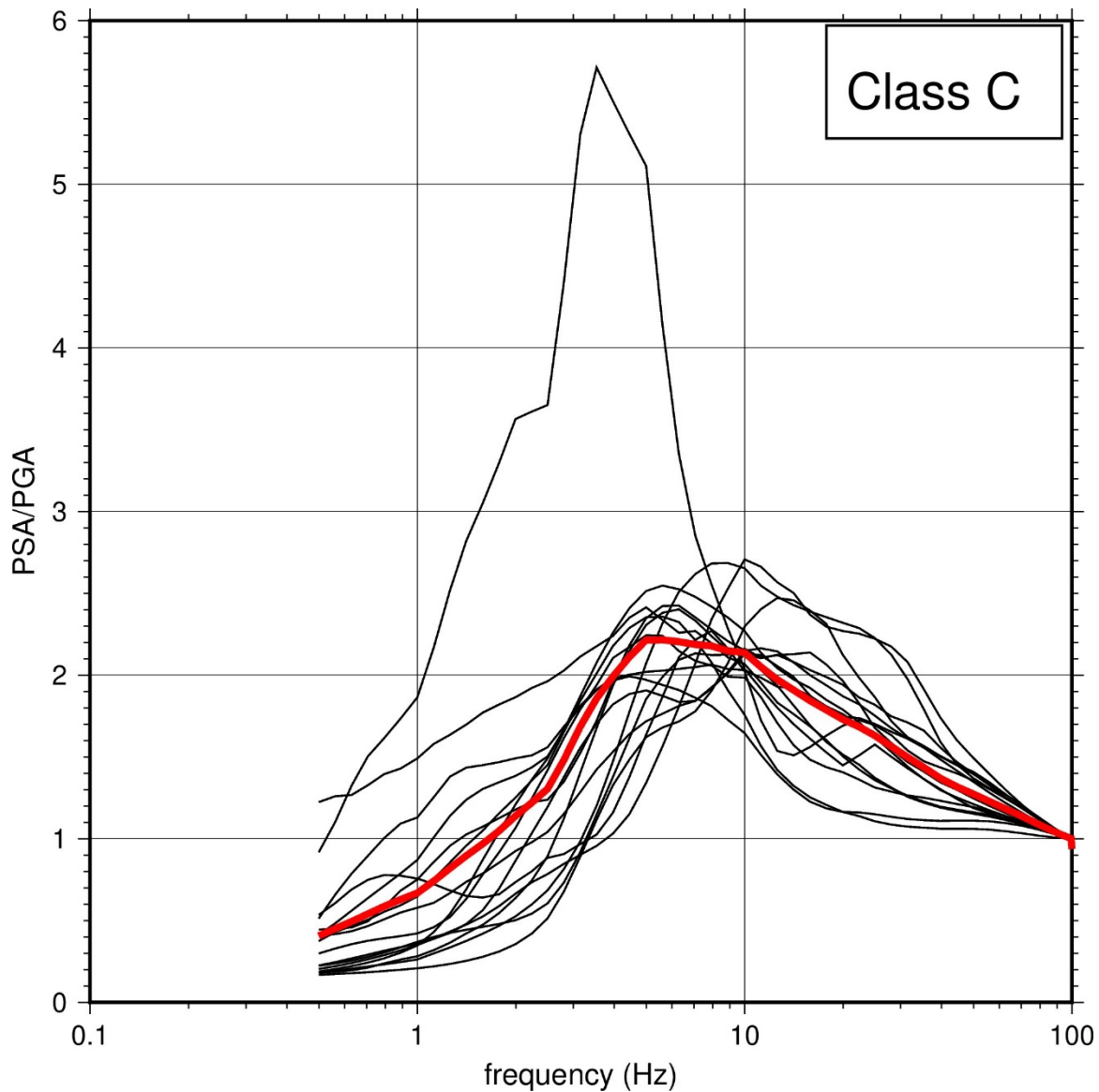


**Figure 4.4-2 Normalized GMRS Results for Class C Sites. Average Normalized Spectral Shape is Shown by Red Curve, and Individual Sites are Shown by Thin Black Lines**

#### **4.5 NEHRP Class D Nuclear Power Plant Sites**

The NEHRP Class D NPP sites are either soil, soil over rock, or soil and soft rock, with  $V_{S30}$  values between 180 m/sec [600 ft/sec] and 360 m/sec [1,200 ft/sec]. The Class D NPP sites are located in the Basin and Range, Coastal Plain, and Central Lowlands physiographic provinces. Table 4.5-1 lists the Class D NPP sites and key site characteristics: (1) site subsurface profile description, (2)  $V_{S30}$ , (3)  $\kappa_0$ , (4) peak  $\bar{A}F$  and associated  $f$ , (5)  $z_{1.0}$ , (6)  $z_{2.5}$ , and (7)  $GMRS_{100}$ .

<b>Plant</b>	<b>Profile Desc.</b>	<b><math>V_{S30}</math> (m/sec)</b>	<b><math>\kappa_0</math> (msec)</b>	<b><math>\bar{AF}</math></b>	<b><math>f</math> (Hz)</b>	<b><math>z_{1.0}</math> (m)</b>	<b><math>z_{2.5}</math> (m)</b>	<b><math>GMR_{S100}</math> (g)</b>
Farley	Soil and rock	267	37	3.6	1.8	56	1,220	0.08
Hatch	Soil and rock	318	35	3.5	1.4	134	1,246	0.18
LaSalle	Soil over rock	354	13	3.8	2.7	38	90	0.36
Palisades	Soil over rock	306	16	4.2	2.3	45	311	0.23
Palo Verde	Soil over rock	352	33	2.8	1.3	104	379	0.22
River Bend	Soil	335	>65	3.2	0.3	516	>1,220	0.09
Robinson	Soil over rock	348	16	3.4	1.7	115	125	0.34
South Texas	Soil	323	>80	3.4	0.2	943	>1,220	0.06
St. Lucie	Soil over rock	282	37	3.7	0.9	122	1,198	0.06
Surry	Soil	268	48	3.8	0.4	396	396	0.10
Vogtle	Soil over rock	334	29	3.2	0.6	323	374	0.31
Waterford	Soil	283	>65	3.3	0.8	507	>1,220	0.11

As shown in Table 4.5-1, the  $\kappa_0$  values for the Class D NPP sites vary considerably but are generally higher for the sites with deeper profiles and lower  $V_S$  values. As discussed in the site-specific analyses in Section 2 of this report, for the very deep soil sites (River Bend, South Texas, and Waterford), the estimated  $\kappa_0$  values would likely exceed the values given in Table 4.5-1 had the NRC staff not terminated the basecase profiles for these sites at 1,220 m [4,000 ft]. The overall low, medium, and high amplification factors ( $AF_{10}$ ,  $AF_{50}$ ,  $AF_{90}$ ) shown in Figure 4.5-1 for the Class D sites range from 1 to 5, with the peak value generally occurring below 3 Hz for the low input spectra (Level 2 of 12). The amplification factors for the intermediate input spectra (Level 6 of 12) show a pronounced decrease beyond 10 Hz, which is due to nonlinear response of the soil, rock, or both to increased loading levels. Figure 4.5-2 shows the normalized GMRS for the Class D sites. The average normalized spectral shape (red curve) shows a fairly broad spectral shape with a peak near 5 Hz.

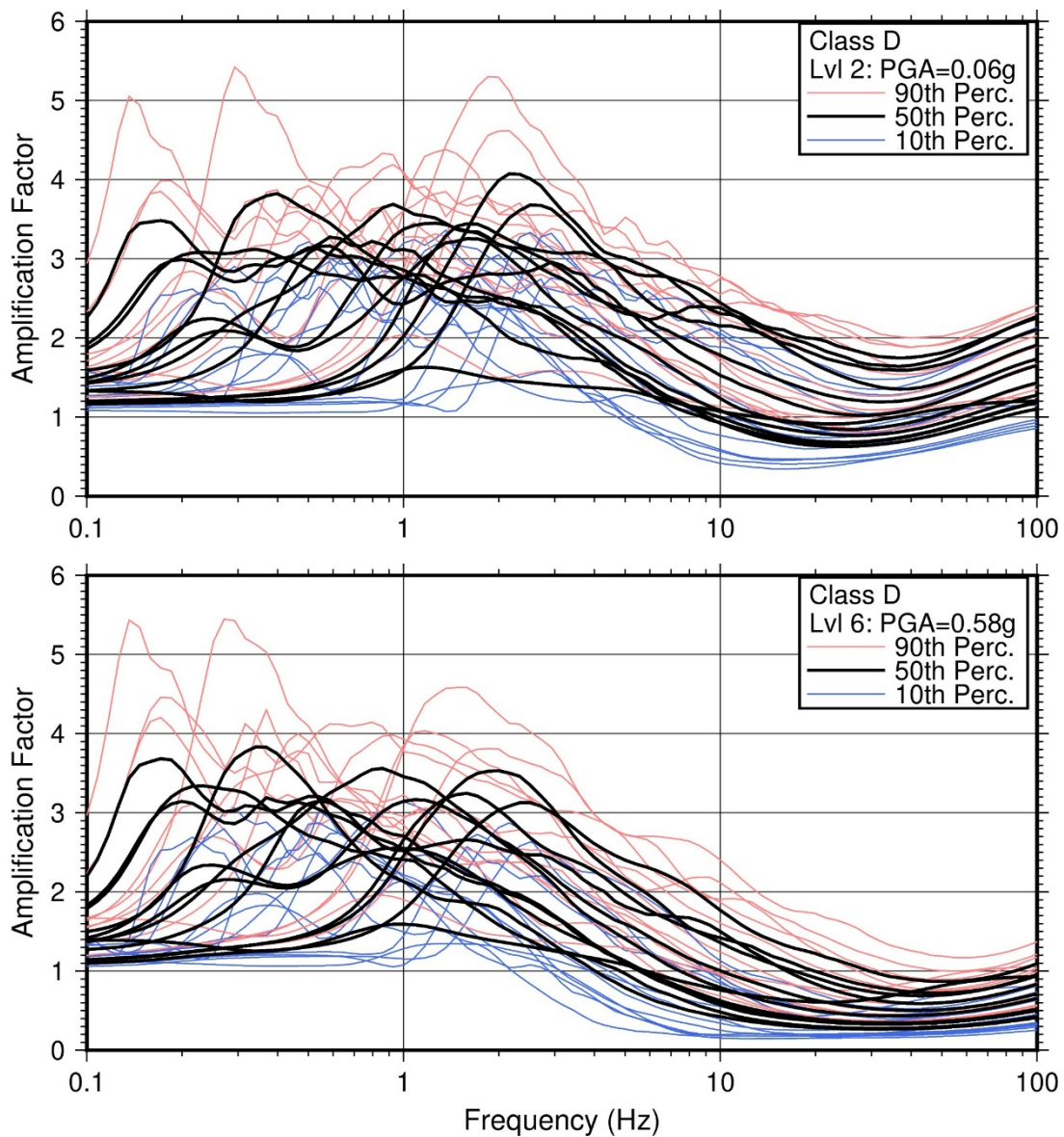


**Figure 4.5-1 Amplification Factors as a Function of Frequency for Class D NPP Sites. Upper Panel Results are for Low Input Loading Level (PGA = 0.06g), and Lower Panel Results are for Intermediate Input Loading Level (PGA = 0.58g)**

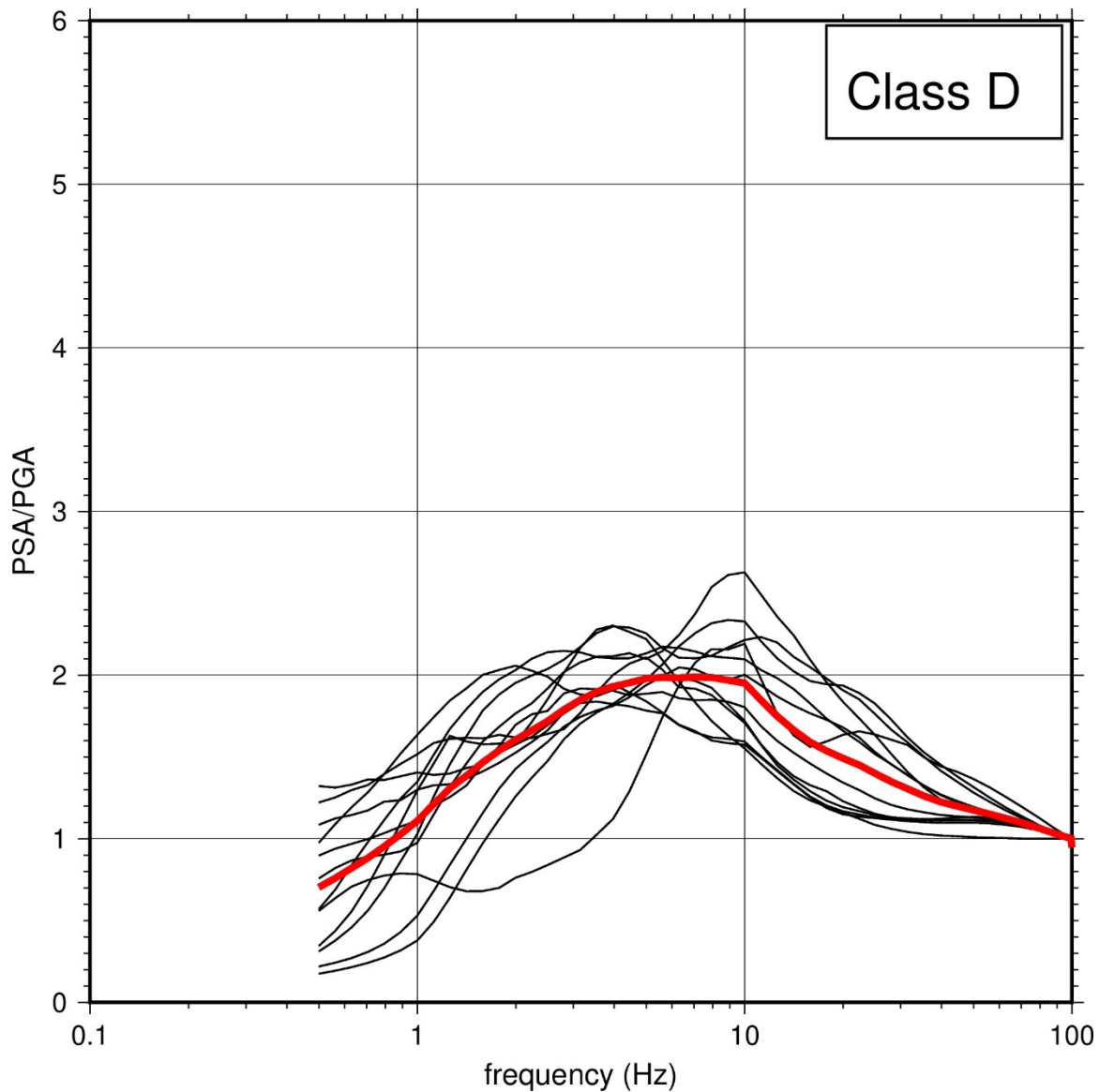


**Figure 4.5-2 Normalized GMRS Results for Class D Sites. Average Normalized Spectral Shape is Shown by Red Curve, and Individual Sites are Shown by Thin Black Lines**

#### **4.6 References**

Building Seismic Safety Council (BSSC). "NEHRP Recommended Provisions for Seismic Regulations for New Buildings and Other Structures (FEMA 450), 2003 Edition." National Institute of Building Sciences. Washington, DC. 2004.

Campbell, K.W. "Estimates of Shear-Wave  $Q$  and  $\kappa_0$  for Unconsolidated and Semiconsolidated Sediments in Eastern North America." *Bulletin of the Seismological Society of America*. Vol. 99, No. 4. pp. 2365–2392. 2009.

Xu, B., E.M. Rathje, Y. Hashash, J. Stewart, K. Campbell, and W.J. Silva. “ $\kappa_0$  for Soil Sites: Observations from Kik-net Sites and Their Use in Constraining Small-Strain Damping Profiles for Site Response Analysis.” *Earthquake Spectra*. Vol. 36, Issue 1. pp.111–137. 2020.





## 5 SUMMARY

The information compiled in this NUREG/KM represents the current best knowledge and practices for characterizing the site-specific seismic hazards for each nuclear power plant (NPP) in the United States. As more fully discussed in Section 1.2 of this report, in response to the letter issued by the U.S. Nuclear Regulatory Commission (NRC) under Title 10 of the *Code of Federal Regulations* (10 CFR) 50.54(f) [50.54(f) letter] and associated information requests (NRC, 2012), U.S. NPP licensees performed probabilistic seismic hazard analyses for the NPP sites based on Senior Seismic Hazard Analysis Committee (SSHAC) Level 3 seismic source and ground motion studies, which the NRC staff reviewed. These SSHAC Level 3 studies incorporated the latest data, models, and methods that have been developed over the past 30 to 40 years and have also systematically incorporated parametric and modeling uncertainty. For each of the sites, licensees and the NRC staff developed control point hazard curves, uniform hazard response spectra, and a representative ground motion response spectrum (GMRS) for comparison with the plant design-basis Safe Shutdown Earthquake Ground Motion (SSE). As described in the 50.54(f) letter and Section 3 of Electric Power Research Institute (EPRI) Report 1025287, “Seismic Evaluation Guidance, Screening, Prioritization, and Implementation Details (SPID) for the Resolution of Fukushima Near-Term Task Force Recommendation 2.1: Seismic,” dated November 27, 2012 (EPRI, 2012), the GMRS developed by each of the licensees were compared to the plant SSE to determine (screen) which plants needed to perform new seismic risk evaluations. The individual plant screening assessments are complete and were not redone in this NUREG/KM. Section 1 of this NUREG/KM presents the ADAMS accession numbers for the NRC staff assessments of the SHSRs for all operating U.S. NPPs and holders of construction permits in active or deferred status. All plants that screened in for further risk evaluations have completed their plant risk assessments. Section 1 also provides a list of these seismic probabilistic risk assessments (SPRAs) and NRC staff assessments. It is important to note that the results contained within this report did not change the conclusions documented in the NRC’s Staff Assessment for each NPP.

For many of the NPP sites, the NRC staff was able to gather additional geologic data subsequent to its reviews of the licensee’s 50.54(f) letter Seismic Hazard and Screening Reports (SHSRs). The NRC staff used this additional information to refine and augment its analyses and provide a more fully informed characterization of the hazard for many of the NPP sites. Even though the NRC staff was able to further refine the stratigraphic profiles for many of the plant sites based on additional research, there is still considerable uncertainty with determining the deeper portion of the site profiles beneath the plant foundations for many of the older plants. For these older plants, the geologic and geophysical investigations focused primarily on the uppermost layers and stability of the rock or soil layers supporting the plant foundations. As such, the NRC staff’s refined site geologic profiles provide a more likely but not definitive interpretation of each site’s geology. This report provides these updated hazard characterizations, and the staff will continue to use them in the future as a benchmark for the evaluation of new data, models, and methods consistent with the staff’s process for ongoing assessment of natural hazard information (POANHI) provided in Staff Requirements Memorandum (SRM)-SECY-16-0144, “Staff Requirements—SECY-16-0144—Proposed Resolution of Remaining Tier 2 and 3 Recommendations Resulting from the Fukushima Dai-ichi Accident,” dated May 3, 2017 (NRC, 2017).

This report summarizes the seismic hazard characterization for each U.S. NPP and compares the licensee’s hazard characterization and the NRC staff’s confirmatory analyses. This document also summarizes spectral shapes and amplification functions for specific site classes consistent with those used in the National Earthquake Hazards Reduction Program (BSSC,

2004). The data files developed by the NRC staff and presented in this report can be found in the NRC's Agencywide Documents Access and Management System (ADAMS) online library, along with an explanatory file (ADAMS Accession Package No. ML21133A274). Plant-specific files are also contained within that same package number and can be found individually in ADAMS as shown in Table 5.1-1.

<b>Plant Name</b>	<b>ADAMS Reference Number</b>
Arkansas Nuclear 1 and 2	ML21133A298
Beaver Valley 1 and 2	ML21133A301
Bellefonte 1 and 2*	ML21133A302
Braidwood 1 and 2	ML21133A377
Browns Ferry 1, 2, and 3	ML21133A317
Brunswick 1 and 2	ML21133A318
Byron 1 and 2	ML21133A319
Callaway	ML21133A320
Calvert Cliffs 1 and 2	ML21133A321
Catawba 1 and 2	ML21133A322
Clinton	ML21133A323
Columbia	ML21133A324
Comanche Peak 1 and 2	ML21133A325
Cooper	ML21133A326
D.C. Cook 1 and 2	ML21133A328
Davis-Besse	ML21133A327
Diablo Canyon	ML21133A330
Dresden 2 and 3	ML21133A331
Duane Arnold <sup>†</sup>	ML21133A332
Farley 1 and 2	ML21133A334
Fermi 2	ML21133A335
FitzPatrick	ML21133A336
Fort Calhoun <sup>†</sup>	ML21133A337
Ginna	ML21133A338
Grand Gulf	ML21133A339
Harris 1	ML21133A340
Hatch 1 and 2	ML21133A341
Hope Creek	ML21133A342
Indian Point 2 and 3 <sup>†</sup>	ML21133A343
LaSalle 1 and 2	ML21133A344
Limerick 1 and 2	ML21133A345
McGuire 1 and 2	ML21133A346
Millstone 2 and 3	ML21133A347
Monticello	ML21133A348
Nine Mile Point 1 and 2	ML21133A336
North Anna 1 and 2	ML21133A349
Oconee 1, 2, and 3	ML21133A350
Oyster Creek <sup>†</sup>	ML21133A351
Palisades	ML21133A352
Palo Verde	ML21133A353
Peach Bottom 2 and 3	ML21133A354

<b>Plant Name</b>	<b>ADAMS Reference Number</b>
Perry 1	ML21133A355
Pilgrim 1 <sup>†</sup>	ML21133A356
Point Beach 1 and 2	ML21133A358
Prairie Island 1 and 2	ML21133A357
Quad Cities 1 and 2	ML21133A359
River Bend 1	ML21133A360
Robinson 2	ML21133A361
Saint Lucie 1 and 2	ML21133A367
Salem 1 and 2	ML21133A342
Seabrook 1	ML21133A362
Sequoyah 1 and 2	ML21133A363
South Texas 1 and 2	ML21133A364
Surry 1 and 2	ML21133A369
Susquehanna 1 and 2	ML21133A370
Three Mile Island 1 <sup>†</sup>	ML21133A371
Turkey Point 3 and 4	ML21133A372
V.C. Summer Unit 1	ML21133A368
Vogtle 1 and 2	ML21133A373
Waterford 3	ML21133A374
Watts Bar 1 and 2	ML21133A375
Wolf Creek 1	ML21133A376
*Plant is not operational.	
†Plant was shut down or has subsequently shut down.	

## **5.1 References**

Building Seismic Safety Council (BSSC). “NEHRP Recommended Provisions for Seismic Regulations for New Buildings and Other Structures (FEMA 450), 2003 Edition.” Washington, DC. National Institute of Building Sciences. 2004.

*Code of Federal Regulations* (CFR), “Domestic licensing of production and utilization facilities.” Part 50, Chapter 1, Title 10, “Energy.” Washington, DC. September 2019.

Electric Power Research Institute (EPRI). “Seismic Evaluation Guidance, Screening, Prioritization, and Implementation Details (SPID) for the Resolution of Fukushima Near-Term Task Force Recommendation 2.1: Seismic.” EPRI Report 1025287. Palo Alto, CA. November 27, 2012. ADAMS Accession No. ML12333A170.

U.S. Nuclear Regulatory Commission (NRC). “Staff Requirements—SECY-14-0144—Proposed Resolution of Remaining Tier 2 and 3 Recommendations Resulting from the Fukushima Dai-Ichi Accident.” SRM-SECY-16-0144. Washington, DC. May 3, 2017.

NRC. Letter from Eric J. Leeds, Director, Office of Nuclear Reactor Regulation and Michael R. Johnson, Director, Office of New Reactors, to All Power Reactor Licensees and Holders of Construction Permits in Active or Deferred Status. Washington, DC. March 12, 2012. ADAMS Accession No. ML12053A340.



**BIBLIOGRAPHIC DATA SHEET**

*(See instructions on the reverse)*

**NUREG-KM 0017**

2. TITLE AND SUBTITLE

3. DATE REPORT PUBLISHED

MONTH	YEAR
<b>December</b>	<b>2021</b>

4. FIN OR GRANT NUMBER

5. AUTHOR(S)

6. TYPE OF REPORT

**Technical**

7. PERIOD COVERED (Inclusive Dates)

8. PERFORMING ORGANIZATION - NAME AND ADDRESS (If NRC, provide Division, Office or Region, U. S. Nuclear Regulatory Commission, and mailing address; if contractor, provide name and mailing address.)

9. SPONSORING ORGANIZATION - NAME AND ADDRESS (If NRC, type "Same as above", if contractor, provide NRC Division, Office or Region, U. S. Nuclear Regulatory Commission, and mailing address.)

10. SUPPLEMENTARY NOTES

11. ABSTRACT (200 words or less)

12. KEY WORDS/DESCRIPTORS (List words or phrases that will assist researchers in locating the report.)

13. AVAILABILITY STATEMENT

**unlimited**

14. SECURITY CLASSIFICATION

*(This Page)*

**unclassified**

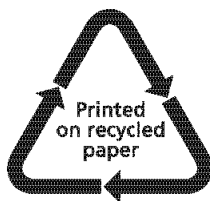
*(This Report)*

**unclassified**

15. NUMBER OF PAGES

16. PRICE





Federal Recycling Program



UNITED STATES  
NUCLEAR REGULATORY COMMISSION  
WASHINGTON, DC 20555-0001

OFFICIAL BUSINESS





**NUREG/KM-0017**

**Seismic Hazard Evaluations for U.S. Nuclear Power Plants:  
Near-Term Task Force Recommendation 2.1 Results**

**December 2021**